

**PROCEEDINGS OF THE  
INTERNATIONAL SYMPOSIUM ON  
URANIUM RAW MATERIAL FOR THE  
NUCLEAR FUEL CYCLE:  
EXPLORATION, MINING,  
PRODUCTION, SUPPLY AND DEMAND,  
ECONOMICS AND ENVIRONMENTAL  
ISSUES (URAM 2014)  
(CD-Rom)**



## TABLE OF CONTENTS

### PAPERS PRESENTED

|   |     |
|---|-----|
| Uranium supply strategy of China.....   | 1   |
| <i>S. Gao, D. Zhang, Y. Zhang</i>   |     |
| IAEA geological classification of uranium deposits.....   | 8   |
| <i>P. Bruneton, M. Cuney, F. Dahlkamp, G. Zaluski</i>   |     |
| The World Nuclear Association medium to long term outlook for uranium demand and supply .....   | 19  |
| <i>I. Emsley</i>  |     |
| Uranium potential in Greenland.....   | 22  |
| <i>N. Keulen, K. Thrane, P. Kalvig</i>  |     |
| Dynamics of uranium ore formation in the basement and frame of the Streltsovskaya Caldera .....   | 34  |
| <i>V.A. Petrov, S.I. Schukin, V.V. Poluektov, V.A. Tolstobrov</i>   |     |
| The diversity of relations between felsic magmatism and uranium deposits.....   | 44  |
| <i>M. Cuney</i>   |     |
| Central Ukraine Uranium Province: the genetic model .....   | 54  |
| <i>A. Emetz, M. Cuney</i>   |     |
| Granite-related hypothermal uranium mineralization in South China .....   | 66  |
| <i>X. Liu, J. Wu, J. Pan, M. Zhu</i>  |     |
| Uranium mine regulation and remediation in Australia's Northern Territory.....  | 69  |
| <i>P. Waggitt</i>   |     |
| Radiation requirements for uranium project approvals.....   | 74  |
| <i>J. Hondros</i>   |     |
| Risk based environmental assessment for uranium mines — the Canadian experience.....  | 84  |
| <i>M. McKee, M. Phaneuf</i>   |     |
| Calibration of a PHREEQC based geochemical model to predict surface water discharge<br>compositions from an operating uranium mill in the Athabasca Basin ..... | 94  |
| <i>J.J. Mahoney, R.A. Frey</i>  |     |
| The 'Namibian uranium mining' model.....  | 104 |
| <i>W. Swiegers</i>  |     |
| Geological 3-D modelling and resources estimation of the Budenovskoye uranium<br>deposit, Kazakhstan .....  | 112 |
| <i>A. Boytsov, T. Heyns, M. Seredkin</i>  |     |
| How effective project management will add value to your uranium asset.....  | 118 |
| <i>R. Bradford, M. Titley</i>   |     |
| International standardisation for the reporting of resources and reserves .....   | 124 |
| <i>K. Farmer, S. Hocquet</i>  |     |
| An overview of uranium, rare metal and REE mineralization in the crystallines of Sonbhadra<br>District, Uttar Pradesh, India.....                               | 130 |
| <i>P.S. Parikh</i>  |     |
| Sandstone deposits of Eurasia — from genetic concepts to forecasting and new discoveries.....   | 136 |
| <i>I.G. Pechenkin, G.A. Mashkovzhev</i>   |     |
| The outlook on potential uranium ISL mining at Nyota deposit, Tanzania .....  | 145 |
| <i>A. Boytsov, S. Stander, V. Martynenko</i>  |     |
| In-Situ Leach mining of uranium in the permafrost zone, Khiagda Mine, Russian Federation.....   | 156 |
| <i>I. Solodov</i>   |     |
| Nichols ranch In-Situ Leach (ISL) mine — a case history.....  | 162 |
| <i>G.J. Catchpole, G.C. Thomas</i>  |     |
| Development of uranium mining by In-Situ Leaching (ISL) in Kazakhstan .....   | 167 |
| <i>Yu. Demekhov, O. Gorbatenko</i>  |     |
| Thorium and uranium separation from rare earth complex minerals in Turkey.....  | 176 |
| <i>R. Uzmen</i>   |     |
| Creating a multi-national development platform: thorium energy and rare earth value chain.....  | 181 |
| <i>J.C. Kennedy, J.H. Kutsch</i>  |     |

|  |     |
|--|-----|
| The potential for thorium recovery as a co-product of processing magmatic rare earth element deposits.....   | 186 |
| <i>B.S. Van Gosen, D.B. Stoeser</i>  |     |
| Thorium: geology, occurrence, deposits and resources.....  | 193 |
| <i>F.H. Barthel, H. Tulsidas</i>   |     |
| Solvent extraction of uranium — towards good practice in design, operation and management .....  | 201 |
| <i>P. Bartsch, S. Hall, S. Ballestrin, A. Hunt</i>   |     |
| Development of the Falea polymetallic uranium project, Mali.....   | 216 |
| <i>R. Ring, P. Freeman</i>   |     |
| Metallurgical testwork to support development of the Kintyre uranium deposit.....  | 226 |
| <i>M. Maley, M. Fainerman-Melnikova, M. Ovinis, K. Soldenhoff, R. Ring, E. Paulsen, D. Maxton</i>  |     |
| Development of carbonate hosted uranium mineralization in India.....   | 236 |
| <i>D. Acharya, A.K. Sarangi</i>  |     |
| Resin-in-pulp based ion exchange separation of uranium from alkaline leach slurry.....   | 241 |
| <i>T. Sreenivas, K.C. Rajan</i>  |     |
| Uranium exploration in Mongolia: a major discovery in the Gobi desert.....   | 252 |
| <i>O. Cardon, F. Le Goux</i>   |     |
| The successful application of modern exploration techniques to previously explored areas in the Athabasca Basin, Canada.....   | 264 |
| <i>K.L. Wheatley</i>   |     |
| Uranium in phosphate rocks and future nuclear power fleets .....   | 279 |
| <i>S. Gabriel, A. Baschwitz, G. Mathonniere</i>  |     |
| Uranium from coal ash: resource assessment and outlook on production capacities.....   | 289 |
| <i>A. Monnet, S. Gabriel</i>   |     |
| Seawater uranium recovery by a polymeric adsorbent: development, characterization and economics.....   | 300 |
| <i>E. Schneider, S. Kung, P. Britt, G. Gill, G. Bonheyo, S. Dai, B. Hay, C. Janke, R. Jeters, T. Khangaonkar, L. Kuo, W. Long, R. Mayes, J. Park, L. Rao, T. Saito, C. Tsouris, T. Wang, J. Wood</i> |     |
| Uranium and rare earths recovery from florida phosphate — looking back and going forward.....  | 311 |
| <i>P. Zhang, B. Birky</i>  |     |
| Regulatory preparation towards commencement of uranium mining and processing of radioactive ores in Tanzania.....  | 324 |
| <i>M.S. Gurisha, C.L. Kim, I.S.N. Mkilaha</i>  |     |
| The last twenty years of the IAEA technical cooperation on the uranium production cycle in Argentina.....  | 329 |
| <i>L. Lopez</i>  |     |
| Uranium deposit types and resources of Argentina.....  | 332 |
| <i>L. Lopez, M. Cuney</i>  |     |
| Uranium refining by solvent extraction.....  | 339 |
| <i>J. Kraikaew, W. Srinuttrakul</i>  |     |
| Geochemical dispersion associated with uranium in sandstone roll front type deposits and its relationship to the Orinoco Oil Belt, Venezuela .....   | 351 |
| <i>J.L. Manrique</i>   |     |
| Uranium legacy sites in Portugal: environmental radioactivity and mitigation of radiological impact.....   | 355 |
| <i>F.P. Carvalho</i>   |     |
| Ensuring safe use of water in a river basin with uranium drainage.....   | 362 |
| <i>F.P. Carvalho, J.M. Oliveira, M. Malta</i>  |     |
| Radiological legacy of uranium mining — the case study of Caldas, MG, Brazil.....  | 368 |
| <i>D. De Azevedo Py Junior, J.V. Da Silva Júnior, M.V. De Almeida Dantas, R. Zafalon, T.F. De Ávila Navarro, D. De Figueiredo, J.C. Pereira Magalhães, W. Scassiotti Filho</i>                       |     |
| On-line X-ray fluorescence analysis of uranium materials in mining and processing industry .....   | 371 |
| <i>E. Hasikova, A. Sokolov, V. Titov, M. Celier, P. Nardoux, Y. Prevost</i>  |     |
| Quantitative analysis of thorium containing materials using industrial XRF analyser .....  | 378 |

|  |     |
|--|-----|
| <i>E. Hasikova, A. Sokolov, V. Titov</i>   |     |
| Brazilian uranium production and demand: scenarios for the near future .....   | 386 |
| <i>R.A.S. Villegas, L.A. Gomiero</i>   |     |
| Uranium mining and extraction industries, environmental impacts and mitigation techniques.....   | 393 |
| <i>A.A. Gadalla, M.M. El-Fawal</i>   |     |
| Environmental monitoring data review of a uranium ore processing facility in Argentina.....  | 451 |
| <i>J.P. Bonetto</i>  |     |
| Studies of the uranium pyrochlore mineral betafite [(ca,u) <sub>2</sub> (nb,ti,ta) <sub>2</sub> o <sub>7</sub> ].....                      | 409 |
| <i>S.A. McMaster, R. Ram, J. Tardio, S.K. Bhargava</i>   |     |
| The prospects for the application of the new generation neutron  |     |
| logging system developed by Rusburmash Inc. (Russian Federation) for handling  |     |
| geotechnical issues at sandstone-hosted uranium deposits .....   | 421 |
| <i>V.G. Martynenko, A.R. Minosyants, S.N. Fedyanin</i>   |     |
| Prospects for increasing uranium resources in the Khiagda ore field, Russian Federation.....   | 431 |
| <i>A.A. Novgorodtsev, V.G. Martynenko, A.V. Gladyshev</i>  |     |
| Using high temperature reactors for energy neutral mineral development processes,  |     |
| a proposed IAEA Coordinated Research Project .....   | 439 |
| <i>N. Haneklaus<sup>†</sup>, F. Reitsma, H. Tulsidas, B. Tyobeka, E. Schnug, H.-J. Allelein, B. Birk, P.F. Peterson, G. Dyck, T. Koshy</i> |     |
| Research on uranium and thorium elements exploration through the study of petrography,   |     |
| petrology and geophysical method in Saghand area (Central Iran) Islamic Republic of Iran ..  | 445 |
| <i>J. Iranmanesh, V. Fattahi, S. Raziani</i>   |     |
| Environmental geological studies of thorium and other radioactive elements in the Narigan  |     |
| area (Central Iran) Islamic Republic of Iran .....   | 454 |
| <i>J. Iranmanesh, M. Razaei, A. Noohi</i>  |     |
| Measurement of <sup>226</sup> ra and <sup>228</sup> ra in Brazilian and Israeli phosphates .....   | 462 |
| <i>A.C. Avelar, W.M. Ferreira, M.A.B.C. Menezes</i>  |     |
| A newly developed accelerator for future possible applications — to convert thorium  |     |
| to uranium-233 .....   | 466 |
| <i>T. Kamei, Y. Kokubo</i>   |     |
| Challenges of development of regulatory control for uranium mining in developing   |     |
| countries to achieve regulatory compliance — Tanzanian experience .....  | 477 |
| <i>A. Kileo, D. Mwalongo, A. Mwaipopo, S. Mdoe, I. Mkilaha</i>   |     |
| Developments in the modeling approach for radiological safety assessment of U-238 series   |     |
| radionuclides in waste disposal.....   | 486 |
| <i>D. Pérez-Sánchez, M. Thorne</i>   |     |
| Steady-state fluid flow as a complementary driver of mineralization and redistribution   |     |
| at unconformity-type uranium deposits in the Athabasca Basin,  |     |
| Saskatchewan, Canada .....   | 493 |
| <i>G. Ruhmann</i>  |     |
| Regulatory issues for safety and environmental on uranium mining and milling in Romania .....  | 503 |
| <i>L. Pop</i>  |     |
| Further new activities at uranium deposit Rozna .....  | 506 |
| <i>F. Toman, P. Vinkler</i>  |     |
| The characteristics of uranium oxide sintered pellets from phosphate fertilizer waste as a   |     |
| potential resource of uranium.....   | 510 |
| <i>A. Muchsin, R. Langenati, G.K. Suryaman</i>   |     |
| Study of geological details towards feasibility of uranium project: Indian case studies.....   | 518 |
| <i>A.K. Sarangi, K.S.V. Kumar</i>  |     |
| Ore genesis of Gogi uranium deposit in Bhima Basin, Yadgir District, Karnataka, India.....   | 523 |
| <i>M.K. Kothari, A.K. Rai, P.S. Pariha</i>   |     |
| Estimation of uranium concentration in building stones used in Jordanian buildings .....   | 540 |
| <i>H.H. Saleh</i>  |     |
| Approaches to mastering the uranium potential of Cameroon .....  | 546 |
| <i>P.J. Chakam Tagheu, A. Simo</i>   |     |

|  |     |
|--|-----|
| Uranium deposits of Madagascar.....  | 550 |
| <i>L.H. Randriamananjara</i>   |     |
| Bottle roll test for Temrezli uranium ore.....   | 557 |
| <i>K. Çetin, A.A. İsbir Turan, E. Üçgül, M.Y. Albayrak</i>   |     |
| Uranium in South Africa: exploration and supply capacity.....  | 567 |
| <i>A.O. Kenan, E. Chirenje</i>   |     |
| Geochemical model on uranium mineralizations in the rhyolite-granite complex in the<br>Jabal Eghei area, Libya ..... | 578 |
| <i>J. Kovačević, M. B. Radenković, Š.S. Miljanić, M. B. Tereesh, S. Turki</i>  |     |
| Dadag uranium deposit in Central Anatolia, Turkey.....   | 582 |
| <i>I.H. Ünal</i>   |     |

# **URANIUM SUPPLY STRATEGY OF CHINA**

S. GAO, D. ZHANG, Y. ZHANG  
China Uranium Corporation Ltd,  
China National Nuclear Corporation,  
Beijing, China.

## **Abstract**

Presently there are 28 units of Nuclear Power Plants (NPPs) under construction in China. These plants will be put into operation sequentially, mostly in the next couple of years. With the new NPPs operational, the requirement for uranium will increase substantially. As the air pollution spreads rapidly from northern part to the southern part, the choice to develop nuclear power has become a priority. Hence the uranium supply will be the key issue to support the development of nuclear power plant in the future. This paper will present the current requirement of uranium and potential demand in the future and the supply strategy envisaged.

## **1. NUCLEAR POWER STATUS**

Currently, there are 20 nuclear power reactors in operation in China. The total capacity is 17.94 GWe (Fig. 1, Table I). There are 28 nuclear power reactors which are under construction (Table II). The total capacity of Nuclear power will reach 40 GWe by the end of 2015. The aim is to have 58 GWe in operation and 30 GWe under construction by the end of 2020.

In October 2012, the State Council approved the nuclear safety planning, which strengthened the safety of nuclear power sector. The National Energy Administration is expected to approve some of the new NPP units in 2014. Construction of coastal and inland nuclear power projects are expected to proceed steadily.

TABLE I. NPPS IN OPERATION

| Index                                      | Name of nuclear power plant | Reactor | Capacity MWe | Construction | Operation  |
|--|-----------------------------|---------|--------------|--------------|------------|
| 1  | Qingshan I                  | PWR     | 310          | 1985-3-21    | 1991-4-1   |
| 2  | Daya Bay                    | No. 1   | PWR          | 984          | 1987-8-7   |
|  |                             | No. 2   | PWR          | 984          | 1988-4-7   |
| 3  | Qingshan II                 | No. 1   | PWR          | 650          | 1996-6-2   |
|  |                             |         | PWR          | 650          | 2006-4-28  |
|  |                             | No. 2   | PWR          | 650          | 1997-4-1   |
|  |                             |         | PWR          | 650          | 2007-1-29  |
| 4  | Ling'ao I                   | No. 1   | PWR          | 990          | 1997-5-15  |
|  |                             | No. 2   | PWR          | 990          | 1997-11-28 |
|  | Ling'ao II                  | No. 3   | PWR          | 1080         | 2006-6-15  |
|  |                             | No. 4   | PWR          | 1080         | 2006-6-15  |
| 5  | Qingshan III                | No. 1   | HWR          | 700          | 1998-6-8   |
|  |                             | No. 2   | HWR          | 700          | 1998-9-25  |
| 6  | Tianwan                     | No. 1   | PWR          | 1060         | 1999-10-20 |
|  |                             | No. 2   | PWR          | 1060         | 2000-9-20  |
| 7  | Hongyanhe                   | No.1    | PWR          | 1080         | 2007-8-18  |
|  |                             | No.2    | PWR          | 1080         | 2008-3-28  |
| 8  | Ningde                      | No.1    | PWR          | 1080         | 2008-2-18  |
|  |                             | No. 2   | CPR PWR      | 1080         | 2008-11-3  |
| 9  | Yangjiang                   | No. 1   | CPR PWR      | 1080         | 2008-12-16 |
| Total installed capacity of 20 units, MWe: |                             |         | 17938        |              |            |

TABLE II. NPP UNDER CONSTRUCTION

| Index        | Province  | Name of nuclear power plant | Reactor                        | Construction | Capacity MWe |       |
|--------------|-----------|-----------------------------|--------------------------------|--------------|--------------|-------|
| 1            | Fujian    | Fuqing                      | No. 1                          | PWR II       | 2008-11-21   | 1080  |
| 2            | Zhejiang  | Fangjiashan                 | No. 1                          | PWR II       | 2008-12-26   | 1080  |
| 3            | Liaoning  | Hongyianhe                  | No. 3                          | CPR PWR      | 2009-3-7     | 1080  |
| 4            | Zhejiang  | Sanmen                      | No. 1                          | AP1000 PWR   | 2009-4-19    | 1250  |
| 5            | Guangdong | Yangjiang                   | No. 2                          | CPR PWR      | 2009-6-5     | 1080  |
| 6            | Fujian    | Fuqing                      | No. 2                          | PWR II       | 2009-6-17    | 1080  |
| 7            | Zhejiang  | Fangjiashan                 | No. 2                          | PWR II       | 2009-7-17    | 1080  |
| 8            | Liaoning  | Hongyianhe                  | No. 4                          | CPR PWR      | 2009-8-15    | 1080  |
| 9            | Zhejiang  | Sanmen                      | No. 2                          | AP1000 PWR   | 2009-12-15   | 1250  |
| 10           | Guangdong | Taishan                     | No. 1                          | EPR PWR      | 2009-12-21   | 1700  |
| 11           | Shandong  | Haiyang                     | No. 1                          | AP1000 PWR   | 2009-12-28   | 1250  |
| 12           | Fujian    | Ningde                      | No. 3                          | CPR PWR      | 2010-1-8     | 1080  |
| 13           | Guangdong | Taishan                     | No. 2                          | EPR PWR      | 2010-4-15    | 1700  |
| 14           | Hainan    | Changjiang                  | No. 1                          | PWR II       | 2010-4-25    | 650   |
| 15           | Shandong  | Haiyang                     | No. 2                          | AP1000 PWR   | 2010-6-20    | 1250  |
| 16           | Guangxi   | Fangchenggang               | No. 1                          | CPR PWR      | 2010-7-30    | 1080  |
| 17           | Fujian    | Ningde                      | No. 4                          | CPR PWR      | 2010-9-29    | 1080  |
| 18           | Guangdong | Yangjiang                   | No. 3                          | CPR PWR      | 2010-11-15   | 1080  |
| 19           | Hainan    | Changjiang                  | No. 2                          | PWR II       | 2010-11-21   | 650   |
| 20           | Guangxi   | Fangchenggang               | No. 2                          | CPR PWR      | 2010-12-28   | 1080  |
| 21           | Fujian    | Fuqing                      | No. 3                          | PWR II       | 2010-12-31   | 1080  |
| 22           | Fujian    | Fuqing                      | No.4                           | PWR II       | 2012-10      | 1080  |
| 23           | Guangdong | Yangjiang                   | No.4                           | CPR PWR      | 2012-11-17   | 1080  |
| 24           | Shandong  | Rongcheng                   | No.1                           | HTGR         | 2012-12-21   | 200   |
| 25           | Jiangsu   | Tianwan                     | No.3                           | PWR          | 2012-12-27   | 1120  |
| 26           | Jiangsu   | Tianwan                     | No.4                           | PWR          | 2013-9-27    | 1120  |
| 27           | Guangdong | Yangjiang                   | No.5                           | CPR PWR      | 2013-9-18    | 1080  |
| 28           | Guangdong | Yangjiang                   | No.6                           | CPR PWR      | 2013-12-23   | 1080  |
| Total Units: |           | 28                          | Total installed capacity, MWe: |              |              | 30500 |

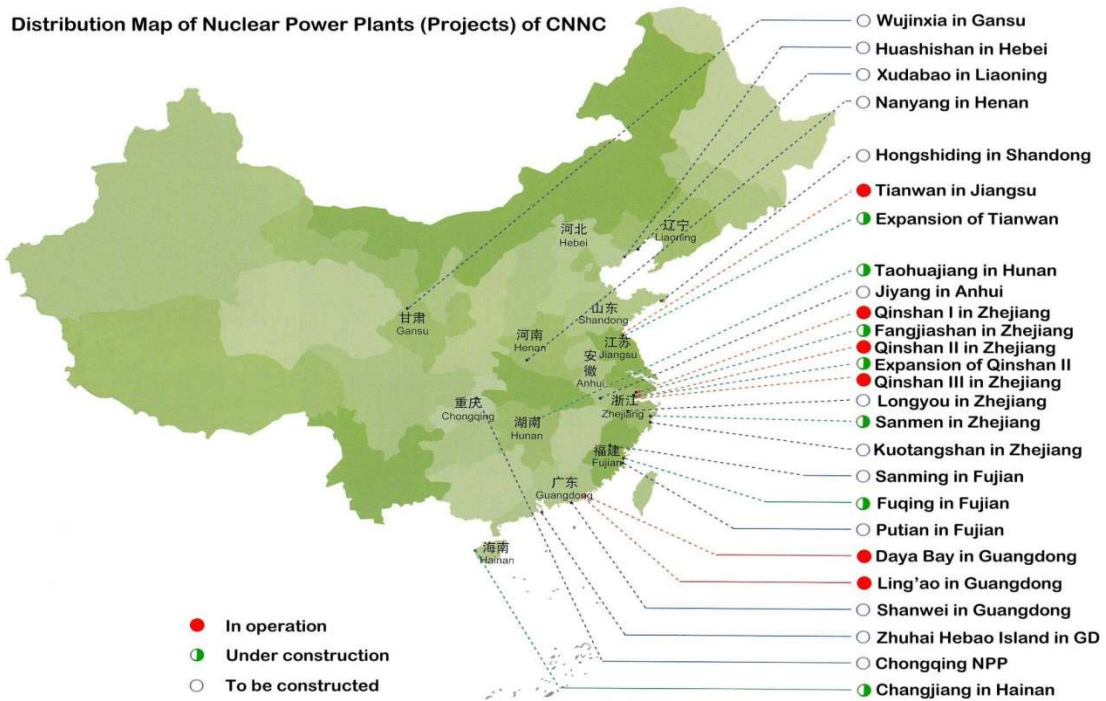


FIG. 1. The distribution map of nuclear power plants (projects) of CNNC.

## 2. URANIUM DEMAND AND SUPPLY STRATEGY

### 2.1. Uranium demand

The uranium demand is expected to reach 7400 t U by 2015, and will be 24 000 t U by 2030 (Table III).

TABLE III. URANIUM DEMAND IN CHINA

|                                     |       | 2015 | 2020  | 2025  | 2030  |
|-------------------------------------|-------|------|-------|-------|-------|
| Nuclear power development plan (GW) | China | 40   | 58    | 100   | 130   |
|                                     | CNNC  | 18   | 26    | 45    | 59    |
| Uranium demand (t U)                | China | 7400 | 11000 | 18500 | 24000 |
|                                     | CNNC  | 3300 | 4800  | 8300  | 11000 |

Based on the requirement from NPPs, uranium is expected to be supplied through three channels:

- Domestic production;
- Overseas development;
- International trade.

## **2.2. Domestic exploration**

The domestic uranium exploration and production of the whole country is carried out by China National Nuclear Corporation (CNNC) through its subsidiary, Department of Geology and Mining, which was restructured in 2011. It consists of three divisions, Bureau of Geology, China Nuclear Uranium Corporation and China Uranium Corporation Limited.

The Department of Geology and Mining, CNNC focuses on uranium exploration and production as the sole platform of Uranium exploration, mining and metallurgy in China.

The Department has about 40 subsidiaries including exploration teams, uranium mines, refineries, research institutes and engineering design companies. Currently, over 16 000 staff are employed by the department.

The exploration business of the department, started in the early 1950s. Over the past 60 years of exploration, hundreds of uranium deposits were discovered, and over 300 000 tU uranium was identified. It is estimated that additional 2 million tU potential exists in the country. The exploratory drilling capacity is over 1 million meters per year.

## **2.3. Domestic production**

There are six production centres in China: (i) Fuzhou; (ii) Chongyi, Jiangxi, East China; (iii) Lantian, Shaanxi, Central China; (iv) Benxi, Liaoning, Northeast China; (v) Shaoguan, Guangdong, South China; and (vi) Yining, Xinjiang, Northwest China (Fig. 2).

Fuzhou production centre, located in Fuzhou, Jiangxi Province, is an underground mine, which process Xiangshan volcanic type of uranium ore bodies through conventional processing method. Currently uranium mines in operation of this centre have steady capacity and several new uranium mines are under construction.

Chongyi production centre, located in Ganzhou, Jiangxi Province, is also an underground mine, which produces uranium from Ganzhou and Taoshan granite-type of ore by heap leaching. Production capacity of this centre is steady in recent years.

Yining production centre, located in Yining, Xinjiang Autonomous Region, is an in-situ leaching (ISL) uranium operation, which produces uranium from Yili and Tuha sandstone-hosted deposits. This centre has accelerated the development of the Kujieertai deposit and its adjacent ore bodies, which will improve the production significantly.

Benxi production centre, located in Benxi of Liaoning Province, is an underground mining uranium mine, which produces uranium from Benxi granite-type and Qinglong volcanic type uranium deposit by heap leaching.

Shaoguan production centre, located in Shaoguan of Guangdong Province, is an underground mining uranium mine, which produces uranium from Xiaozhuang and Zhuguang granite type uranium deposits by hydrometallurgical process of heap leaching and solvent extraction. This centre is now developing uranium resources of Guangxi Region and will increase production capacity in a phased manner.

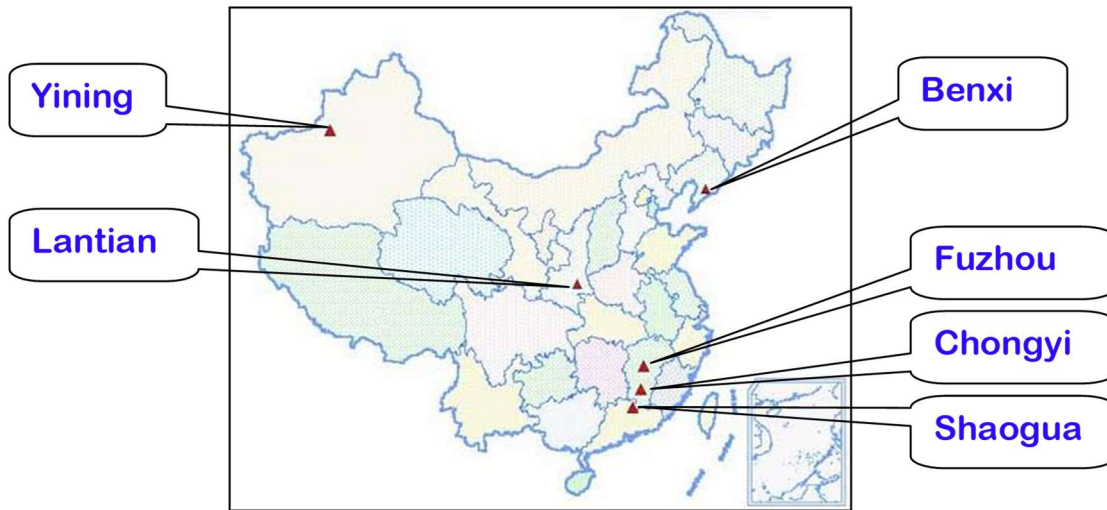


*FIG. 2. Location of the uranium production centres.*

The nominal capacity of the existing production centres are 1800 t U/a, and with potential for expansion up to 2900 t U/a.

With the intensive exploration in Northern China focused on sandstone type of uranium deposit, some significant deposits are recently discovered, such as Daying deposit. Exploration around existing mines have also made progress. Prefeasibility and feasibility study to develop these deposits are also progressing. With increased resources, expansion of old production centres will be possible, as in Fuzhou and Benxi.

Domestic development are also focused on sandstone type of deposits in Xinjiang and Inner Mongolian regions. As a number of such deposits are discovered in these regions, it may make low cost production possible.

For the existing mines, an increase the production capacity and extension of the mine life is very likely due to the newly discovered resources in the vicinity.

#### **2.4. Overseas development**

Since early 2004, CNNC has been looking for uranium development opportunities outside of China. Subsequently CGNPC also started to look for uranium assets from 2006.

CNNC acquired Azelik project in Niger in 2006 and started construction in 2008 and first barrel of product was produced in 2010. Production reached 300 t U/a currently, but the total capacity is 700 t U. The project has 13 500 t U resource and grade is 0.14% U.

CGNPC acquired Irkol and Semizbay projects in 2008, the two projects combined into Semizbay-U LLP. The total capacity of Semizbay-U is 1450 t U/a.

CGNPC acquired 100% of Husab project, Namibia from Kalahari Minerals and Extract Resources in 2012, the construction of the mine started in October 2012. It expected to start operation by the end of 2015, and reached the designed capacity of 5700 t U/a by the end of 2017.

In 2008 and 2009, CNNC acquired other Namibia, Mongolian projects. In 2009, CGNPC acquired majority shares of Energy Metals limited. All these projects are under different stages of exploration

and development. In January 2014, CNNC acquired 25% of Langer Heinrich project, Namibia from Paladin, and the annual share of production is 500 t U.

Low uranium prices at present have slowed down the development of some of the projects, but China is looking to acquire more projects abroad to fulfill the future needs of uranium.

## **2.5. Uranium trade**

Purchasing uranium from the international market is the third option. This is complementary to the supply by domestic production and overseas development

CNEIC, fully subsidiary of CNNC, has been doing uranium trade on behalf of CNNC for many years and signed some long-term contracts with uranium production entities.

CGNPC uranium corp., a newly formed uranium trader, will be doing uranium trade on behalf of CGNPC.

The uranium trade is supplementary to the domestic and overseas production to meet the requirement of NPPs in China.

## **3. CONCLUSION**

With the rapid development of Nuclear power in the next few years, uranium demand will increase accordingly.

Overseas uranium development will be the major channel to meet the future requirement of NPP demand in China.

# IAEA GEOLOGICAL CLASSIFICATION OF URANIUM DEPOSITS

P. BRUNETON\*, M. CUNEY\*\*, F. DAHLKAMP\*\*\*, G. ZALUSKI<sup>†</sup>

\* Consultant,  
Le Chalard

\*\* CNRS – GeoRessources – CREGU,  
Université de Lorraine, Nancy

France

\*\*\* Consultant<sup>1</sup>,  
Wachtberg, Germany

<sup>†</sup>CAMECO,  
Saskatoon, Saskatchewan,  
Canada

E-mail address of main author: p.bruneton@orange.fr

## Abstract

A modified and improved geological classification of uranium deposits was approved by the IAEA in 2013 and is used in the World Distribution of Uranium Deposits (UDEPO) database and the current Uranium: Resources, Production and Demand (“Red Book”) publications. Fifteen deposit types and 50 sub-types/classes have been defined and is based on over 1500 deposits/districts listed in the UDEPO.

## 1 INTRODUCTION

The previous IAEA classification, used in particular up to the 2009 version of the ‘Red Book’ [1], dates from 1993. At that time, 582 uranium deposits were recorded in the UDEPO Database [2]. In 2009, 878 deposits were present in UDEPO [3] and at the end of 2013, 1532 deposits/districts were listed in the database. The increase in the number of deposits were largely due to identifying and listing additional deposits from published and un-published reports the details of which were not known earlier. A few new deposits that were discovered in the intervening period were also added.

In 2010, a working group was created by the Agency to review the various existing uranium deposit classifications and to propose a new or a modified classification that could be used internationally. With the dramatic increase in exploration following the uranium price rise starting in 2005, abundant publications and company data have become available for expanding the database, which also provided inputs for revising the classification.

In 1993, Dahlkamp [4] in his book, *Uranium Ore Deposits*, recognizes 16 principal types of uranium deposits and occurrences based on host environment and/or geometry. In addition, more than 40 subtypes and classes were defined.

The same year, 15 main types of uranium deposits were officially adopted by the IAEA and have been used then in the Red Book publications. They were conventionally listed in decreasing order of economic importance:

1. Unconformity-related;
2. Sandstone;

---

<sup>1</sup> Deceased

3. Quartz pebble conglomerate;
4. Veins;
5. Breccia complex;
6. Intrusive;
7. Phosphorite;
8. Collapse breccia pipe;
9. Volcanic;
10. Surficial;
11. Metasomatite;
12. Metamorphite;
13. Lignite;
14. Black shale;
15. Others (limestone, bony detritus, dolomite).

Dahlkamp [5] in his book *Uranium Deposits of the World-Asia* indicates that recent information on uranium deposits, particularly in the former eastern block countries and new research data on earlier established and defined types of uranium deposits justify a rearrangement and refinement of the classification scheme which was proposed by the author in 1993. The terminology selected for types and subtypes is based primarily onto the host environments and geotectonic settings of the types. On this basis, Dahlkamp (2009) distinguishes 20 principal types of uranium deposits including some 40 subtypes and classes.

The formerly term ‘Vein type’ was removed as a principal deposit type by Dahlkamp since it causes confusion with several other deposit types. Veins may be hosted in various rock types, including granitoids, volcanic rocks, metasomatites, metasedimentary rocks and sandstones. Therefore, the term ‘vein’ is only used to describe the configuration of ore bodies in any respective geological environment.

## 2. THE 2013 IAEA GEOLOGICAL CLASSIFICATION OF URANIUM DEPOSITS

Fifteen types of deposits have been described in the new IAEA classification scheme of 2013. They are listed in order from deep primary magmatic deposits to sedimentary and surficial deposits (Fig. 1). The economic ranking used in the previous IAEA classifications has not been taken into account.

1. Intrusive;
2. Granite-related
3. Polymetallic iron-oxide breccia complex;
4. Volcanic-related;
5. Metasomatite;
6. Metamorphite;
7. Proterozoic unconformity;
8. Collapse-breccia pipe;
9. Sandstone;
10. Palaeo quartz-pebble conglomerate;
11. Surficial;
12. Lignite and coal;
13. Carbonate;
14. Phosphate;
15. Black shale.

As a revision of the 1993 IAEA classification and following Dahlkamp [5], the ‘Vein type’ has been removed. Deposits of this type have been classified mainly into ‘Granite-related’ corresponding to a new type and within ‘Metamorphite’, with a smaller proportion being assigned to other types such as volcanic-related and metasomatite. ‘Breccia complex’ has been renamed ‘Polymetallic iron-oxide breccia complex’. ‘Unconformity-related’ deposits are called ‘Proterozoic unconformity’, ‘Quartz pebble conglomerate’ has become ‘Palaeo quartz-pebble conglomerate’, and ‘Phosphorite’ deposits are renamed ‘Phosphate’ to also include continental phosphate deposits.

Most sub-types and classes defined by Dahlkamp [5] have been retained with minor modifications and some new sub-types and classes have been created. Most deposit types are named by the host rocks except for types 3, 7 and 8 which are related to structures and type 5 related to metasomatic alteration. The number of deposits for each type and sub-type is given in Table I.

However, it should be recognized that the 15 types have far greater significance than the simple names. Deposit types have fundamental characteristics and recognition criteria and in that respect, while mainly named by host rock, the types are essentially empirical models, based on observable characteristics. The numbers of deposits for each type and sub-type are presented in Table I. A diagramme showing the relationships between types is given in Fig. 1.

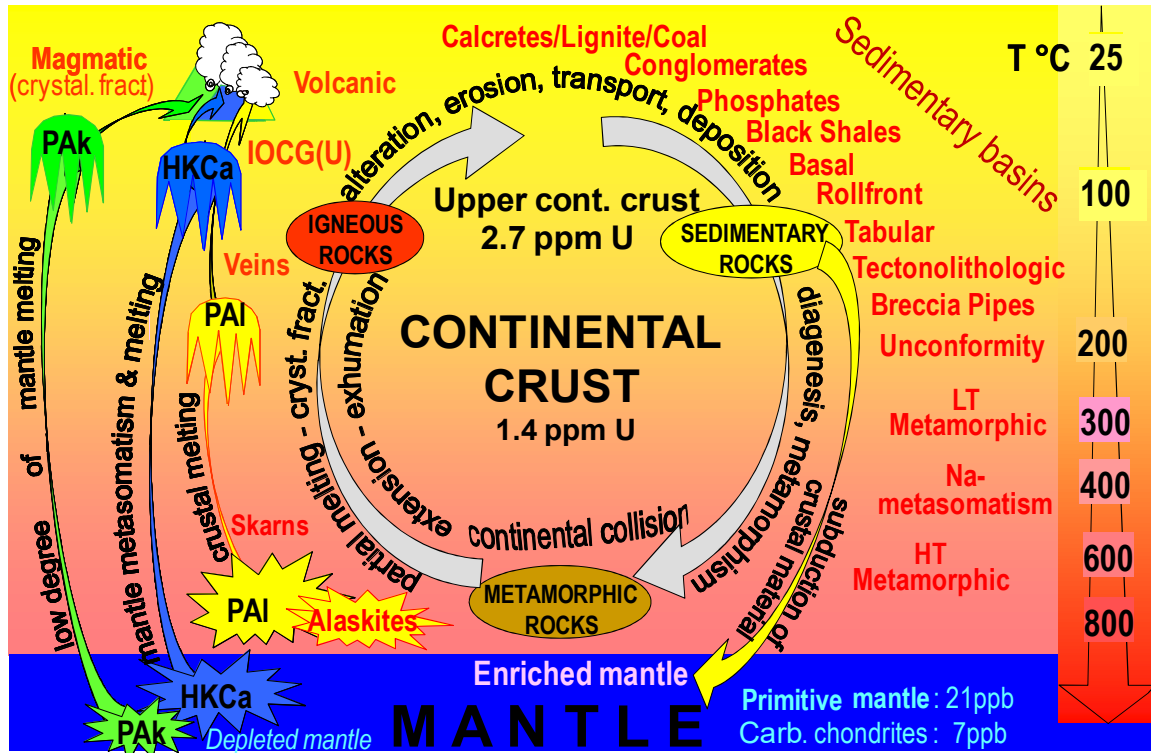


FIG. 1. Position of uranium deposit types with respect to the main fractionation processes along the geological cycle. The different types of U-rich magmas are indicated: Pak peralkaline, Kca High-K calc-alkaline, Pal peraluminous (reproduced from Ref. [6] with permission).

### 3. DETAILED CLASSIFICATION WITH TYPES, SUBTYPES AND CLASSES

#### Type 1. Intrusive

1.1. Anatetic pegmatite-alaskite (Rossing, Namibia; Bancroft district, Canada)

1.2. Plutonic

*Quartz monzonite* (Bingham Canyon, USA; Chuquicamata, Chile)

*Peralkaline complexes* (Kvanefjeld, Greenland; Poços de Caldas, Brazil)

*Carbonatite* (Palabora, South Africa; Catalao, Brazil)

#### Type 2. Granite-related

2.1. Endogranitic (La Crouzille District, France; Xiaozhuang District, China)

2.2. Perigranitic (Pribram Region, Czech Republic; Niederschlema-Alberoda, Germany)

Type 3. Polymetallic iron-oxide breccia complex (Olympic Dam, Carrapateena, Australia)

Type 4. Volcanic-related

- 4.1. Structure-bound (Streltsov-Antei, Russian Federation; Kuriskova, Slovakia)
- 4.2. Strata-bound (Dornod N° 7 ore zone, Mongolia; Maureen, Australia)
- 4.3. Volcano-sedimentary (Anderson Mine, USA; Sierra Pintada District, Argentina)

Type 5. Metasomatite

- 5.1. Na- metasomatite
  - Granite-derived* (Kirovograd District, Ukraine; Lagoa Real, Brazil; Coles Hill, USA)
  - Metasediments-metavolcanics-derived* (Krivoy Rog District, Ukraine; Michelin, Canada)
- 5.2. K-metasomatite (Elkon District, Russian Federation)
- 5.3. Skarn (Mary Kathleen, Australia; Tranomaro, Madagascar)

Type 6. Metamorphite

- 6.1. Stratabound (Forstau, Austria)
- 6.2. Structure-bound
  - Monometallic* (Schwartzwalder, USA; Ace-Fay-Verna, Canada; Rozna, Czech Republic)
  - Polymetallic* (Shinkolobwe, Democratic Republic of Congo; Port Radium, Canada; Jaduguda, India)
- 6.3. Marble-hosted phosphate (Itataia, Brazil; Nuottijarvi, Finland)

Type 7. Proterozoic unconformity

- 7.1. Unconformity-contact (Cigar Lake, Key Lake, McArthur River, Canada)
- 7.2. Basement-hosted (Jabiluka, Ranger, Australia; Eagle Point, Millennium, Canada)
- 7.3. Stratiform fracture-controlled (Lambapur, Chitrial, India)

Type 8. Collapse-breccia pipe (Arizona Strip, USA)

Type 9. Sandstone

- 9.1. Basal channel (Dalmatovskoye, Russian Federation; Beverley, Australia)
- 9.2. Tabular (Arlit District deposits, Niger; Ambrosia Lake District deposits, USA)
  - Continental fluvial, U associated with intrinsic reductant* (Arlit type, Niger)
  - Continental fluvial, U associated with extrinsic humate/bitumen* (Grants type, USA)
  - Continental fluvial vanadium-uranium* (Salt Wash type, USA)
- 9.3. Rollfront (Wyoming Province, USA; Chu-Sarysu Basin, Kazakhstan)
  - Continental basin, U associated with intrinsic reductant* (Wyoming type, USA)
  - Continental to marginal marine, U associated with intrinsic reductant* (Chu-Saryisu type, Kazakhstan)
  - Marginal marine, U associated with extrinsic reductant* (South Texas, USA)
- 9.4. Tectonic-lithologic (Lodève Basin, France; Franceville Basin, Gabon)
- 9.5. Mafic dykes/sills in Proterozoic sandstone (Westmoreland District, Australia; Matoush, Canada)

Type 10. Palaeo quartz-pebble conglomerate

- 10.1. U-dominant (Elliot Lake District, Canada)
- 10.2. Au-dominant (Witwatersrand Basin, South Africa)

Type 11. Surficial

- 11.1. Peat-bog (Kamushanovskoye, Kyrgyzstan; Flodelle Creek, USA)
- 11.2. Fluvial valley (Yeelirrie, Australia; Langer Heinrich, Namibia)
- 11.3. Lacustrine-playa (Lake Maitland and Lake Way, Australia)
- 11.4. Karst cavern (Tyuya-Muyun, Kyrgyzstan, Pryor-Little Mtns, USA)
- 11.5. Pedogenic and fracture fill (Beslet, Bulgaria)

Type 12. Lignite and coal

- 12.1. Stratiform (Koldzhat, Kazakhstan; North Dakota, USA)
- 12.2. Fracture-controlled (Freital, Germany; Turakavak, Kyrgyzstan)

Type 13. Carbonate

- 13.1. Stratabound (Tumalappalle, India)
- 13.2. Cataclastic (Mailuu-Suu, Kyrgyzstan; Todilto District, USA)
- 13.3. Palaeokarst (Sanbaqi, China)

Type 14. Phosphate

- 14.1. Organic phosphorite (Mangyshlak, Kazakhstan; Ergeninsky Region, Russian Federation)
- 14.2. Minerochemical phosphorite (Phosphoria Formation and Florida land pebble formation, USA)
- 14.3. Continental phosphates (Bakouma District, Central African Republic)

Type 15. Black shale

- 15.1. Stratiform (Haggan, Sweden; Chattanooga Shale Formation, USA)
- 15.2. Stockwork (Ronneburg District, Germany; Dzhantuar, Uzbekistan)

TABLE I. NUMBER OF DEPOSITS FOR EACH DEPOSITS TYPE AND SUB-TYPE (UDEPO 2013)

|    | Deposit type                            | Number of deposits | Deposit sub-type   | Number of deposits          |
|----|---|--------------------|--|-----------------------------|
| 1  | Intrusive                               | 83                 | 1.1. Anatectic<br>1.2. Plutonic  | 51<br>32                    |
| 2  | Granite-related                         | 129                | 2.1. Endogranitic<br>2.2. Perigranitic   | 80<br>49                    |
| 3  | Polymetallic iron-oxide breccia complex | 15                 |  | 15                          |
| 4  | Volcanic-related                        | 124                | 4.1. Structure-bound<br>4.2. Strata-bound<br>4.3. Volcano-sedimentary                                      | 103<br>18<br>3              |
| 5  | Metasomatite                            | 76                 | 5.1. Na-metasomatite<br>5.2. K-metasomatite<br>5.3. Skarn  | 54<br>17<br>4               |
| 6  | Metamorphite                            | 106                | 6.1. Strata-bound<br>6.2. Structure-bound<br>6.3. Marble-hosted  | 5<br>92<br>9                |
| 7  | Proterozoic unconformity                | 84                 | 7.1. Unconformity-contact<br>7.2. Basement-hosted<br>7.3. Stratiform fracture-controlled                   | 36<br>43<br>5               |
| 8  | Collapse breccia pipe                   | 16                 |  | 16                          |
| 9  | Sandstone                               | 627                | 8.1. Basal channel<br>8.2. Tabular<br>8.3. Rollfront<br>8.4. Tectonic-lithologic<br>8.5. Mafic dykes/sills | 76<br>294<br>231<br>18<br>8 |
| 10 | Palaeo quartz pebble conglomerate       | 69                 | 10.1. U-dominant<br>10.2. Au-dominant  | 26<br>43                    |
| 11 | Surficial                               | 65                 | 11.1. Peat-bog<br>11.2. Fluvial valley<br>11.3. Lacustrine-playa<br>11.4. Pedogenic/fracture-fill          | 2<br>39<br>21<br>3          |
| 12 | Lignite-coal                            | 33                 | 12.1. Stratiform<br>12.2. Fracture-controlled  | 31<br>2                     |
| 13 | Carbonate                               | 10                 | 13.1. Stratabound<br>13.2. Cataclastic<br>13.3. Palaeokarst  | 1<br>7<br>2                 |
| 14 | Phosphate                               | 49                 | 14.1. Organic phosphorite<br>14.2. Phosphorite<br>14.3. Continental phosphate                              | 7<br>38<br>4                |
| 15 | Black shale                             | 45                 | 15.1. Stratiform<br>15.2. Stockwork  | 26<br>19                    |
|    |   | 1532               |  | 1532                        |

## 4. DESCRIPTION OF THE DEPOSITS TYPES

### Type 1 – Intrusive

Deposits included in this type are hosted in intrusive rocks of many different petrochemical compositions. Two main subtypes are recognized which are: 1.1.) **intrusive anatectic** deposits associated with partial melting processes and contained in granite-pegmatite (Rössing and Husab, Namibia, and deposits in the Bancroft area, Canada) and 1.2.) **intrusive plutonic** deposits related to magmatic differentiation processes and subdivided into three classes: *quartz monzonite* (Bingham Canyon, USA; Chuquicamata, Chile), *peralkaline complexes* (Kvanefjeld, Greenland; Pocos de Caldas, Brazil) and *carbonatite* (Palabora, South Africa; Catalao, Brazil).

### Type 2 – Granite-related

Deposits related to granite include 1) classical veins composed of ore and gangue minerals in granite or adjacent (meta-) sedimentary rocks and 2) disseminated mineralization in granite as episyenite bodies. Uranium mineralization occurs within, at the contact or peripheral to the intrusion. In the Hercynian Belt of Europe and other parts of the world, these deposits are generally associated with large, peraluminous, two-mica granite complexes (leucogranites). Resources range from small to large and grades vary from low to high. Two subtypes are distinguished based on their spatial setting with respect to the granitic pluton and country rocks, endogranitic deposits and perigranitic deposits

### Type 3 – Polymetallic iron-oxide breccia complex

This type of deposits has been attributed to a broad category of iron-oxide-copper-gold deposits from around the world. Olympic Dam (Australia) is the only known representative of this type with significant by-product uranium production. The deposit contains the world largest uranium resources with more than 2 Mt of uranium at low grade (230 ppm). Deposits of this group occur in haematite-rich granite breccias (Olympic Dam, Gawler Craton) or meta-sedimentary-meta-volcanic breccias (Salobo, Carajas District, Brazil) and contain low grade disseminated uranium in association with copper, gold, silver and rare earth elements.

### Type 4 – Volcanic-related

Uranium deposits of this type are located within and near volcanic calderas filled with mafic to felsic volcanic lavas or more commonly pyroclastic rocks and intercalated clastic sediments. Uranium mineralization is preferentially controlled by structures as veins and stockworks (structure-bound deposits), but may also be found as disseminations and impregnations in permeable flows and volcanoclastic sediments (stratabound deposits). This mineralization occurs at several stratigraphic levels of the volcanic and sedimentary units and may extend deeply into the underlying basement. Uranium minerals (pitchblende, coffinite, U<sup>6+</sup> minerals and less commonly brannerite) are associated with Mo-bearing sulphides and pyrite. Associated gangue minerals consist of violet-coloured fluorite, carbonates, barite and quartz. The most significant deposits are located within the Streltsovskaya Caldera in the Russian Federation. Other examples are known in China (Xiangshan District), Mongolia (Dornot and Gurvanbulag Districts), USA (McDermitt Caldera), Peru (Macusani District) and Mexico (Peña Blanca District). Uncommon volcano-sedimentary deposits consist of peneconcordant, low-grade carbonaceous lacustrine sediments with an important tuffaceous component (Anderson Mine, USA).

### Type 5 – Metasomatite

Deposits of this type are generally confined to Precambrian shields (an exception being Coles Hill, USA) in orogenic belts affected by intense Na-metasomatism or K-metasomatism which produced albited or illitized rocks along deeply-rooted fault systems. In Ukraine, these deposits are developed within a variety of basement rocks, including granite, migmatite, gneiss and ferruginous quartzite which produced albitite, aegirinite and alkali-amphibolite. Principal uranium phases are uraninite, brannerite and other Ti-U-bearing minerals, pitchblende, coffinite and hexavalent uranium minerals. The resources

range from medium to very large. Examples include the Michurinskoye, Vatutinskoye, Severinskoye, Zheltorechenskoye, Novokonstantinovskoye deposits (Ukraine), deposits of the Elkon District (Russian Federation), Espinharas and Lagoa Real (Brazil), Valhalla (Australia), Kurupung (Guyana), Coles Hill (USA), Lianshanguan (China), Michelin (Canada) and several small deposits of the Arjeplog region, northern Sweden. Three subtypes of metasomatite deposits are distinguished on the basis of precursor rock lithology and the type of metasomatism: Na-metasomatite, K-metasomatite and skarn.

### Type 6 – Metamorphite

These deposits consist of disseminations, impregnations, veins and shear zones within metamorphic rocks of various ages with no relation to granitic intrusions. These deposits are highly variable in size, resources and grades. Two sub-types are recognized, stratabound deposits which are uncommon (Forstau, Austria; Nuottijarvi and Lampinsaari, Finland), structure-bound deposits which are well represented (Schwartzwalder, USA; Ace-Fay-Verna, Canada; Kamyshevoye, Kazakhstan) (Shinkolobwe, Democratic Republic of the Congo; Port Radium, Canada; Jaduguda, India) and marble-hosted phosphate deposits (Itataia, Brazil; Zaozernoye, Kazakhstan).

### Type 7 – Proterozoic unconformity

Unconformity-related deposits are associated with and occur immediately below, above, or spanning an unconformable contact that separates Archean to Palaeoproterozoic crystalline basement from overlying, red bed clastic sediments of Proterozoic age. In most cases, the basement rocks immediately below the unconformity are strongly hematized and clay altered, possibly a result of palaeo-weathering and/or diagenetic/hydrothermal alteration. Deposits consist of pods, veins and semi-massive replacements consisting mainly of pitchblende. Strong quartz dissolution is generally associated with them. They are preferentially located in two major districts, the Athabasca Basin (Canada) and the Pine Creek Orogen (Australia). The Proterozoic unconformity deposits include three sub-types of variable importance, *unconformity-contact* deposits which all occur in the Athabasca Basin (Canada), basement-hosted deposits such as Kintyre, Jabiluka and Ranger (Australia), Millennium and Eagle Point in the Athabasca Basin and Kiggavik and Andrew Lake in the Thelon Basin (Canada) and stratiform structure-controlled deposits (Chitrial and Lambapur, Cuddapah Basin, India).

### Type 8 – Collapse breccia pipe

Deposits in this type occur in sedimentary basins within cylindrical, vertical breccia pipes within sedimentary basins. The collapse breccia pipes contain down-dropped fragments from overlying lithological units filling karst dissolution cavities developed in the underlying, thick carbonate layers. The uranium is concentrated as primary, tetravalent uranium minerals, mainly pitchblende, in the permeable breccia matrix, and in the arcuate, ring-fracture zone surrounding the pipe. The pitchblende is associated with numerous sulphide and oxide minerals containing Cu, Fe, V, Zn, Pb, Ag, Mo, Ni, Co, As and Se. Type examples are the deposits of the Arizona Strip north of the Grand Canyon and those immediately south of the Grand Canyon of the United States. Resources are small to medium (300–2500 t) with relatively high grades around 0.20–0.80%.

### Type 9 – Sandstone

Sandstone-hosted uranium deposits occur in medium- to coarse-grained sandstones deposited in continental fluvial or marginal marine sedimentary environments. Volcanic-ash may represent a major uranium source within the sandstone in some regions (Niger; Lodève, France; Wyoming, USA). Uranium is precipitated by reduction processes caused by a variety of possible reducing agents within the sandstone. These include carbonaceous material (mainly detrital plant debris), sulphides (pyrite), ferro-magnesian minerals (chlorite), bacterial activity, migrated fluids from underlying hydrocarbon reservoirs, and others. Sandstone uranium deposits can be divided into five main sub-types with frequent transitional types between them.

**9.1 – Basal channel** deposits consist of wide channels filled with thick, permeable alluvial-fluvial sediments. The uranium is predominantly associated with detrital plant debris, forming ore bodies that display, in a plan view, an elongated lens or ribbon-like configuration and, in a section-view, a lenticular or, more rarely, a roll-shape. Individual deposits may range from several hundred to 20 000 t of uranium, at grades ranging from 0.01% to 3%. Examples are the deposits of Dalmatovskoye (Transural Region) and Khiagdinskoye (Vitim District) in the Russian Federation and Beverley (Australia).

**9.2 – Tabular** deposits consist of uranium matrix impregnations that form irregularly shaped lenticular masses within reduced sediments. The mineralized zones are largely oriented parallel to the depositional trend. Individual deposits may contain several hundred to 150 000 tonnes of uranium, at average grades ranging from 0.05% to 0.5%. Examples of deposits include Hamr-Stráz (Czech Republic), Akouta, Arlit, and Imouraren (Niger) and those of the Colorado Plateau (USA).

**9.3 – Roll-front** deposits: the mineralized zones are convex in shape, oriented down the hydrologic gradient. They display diffuse boundaries with reduced sandstone on the down-gradient side and sharp contacts with oxidized sandstone on the up-gradient side. The mineralized zones are elongated and sinuous along strike and perpendicular to the direction of deposition and groundwater flow. Resources range from a few hundred tonnes to several thousand tonnes of uranium, at grades averaging 0.05% to 0.25%. Examples are Budenovskoye, Tortkuduk, Moynkum, Inkai and Mynkuduk (Kazakhstan) and Crow Butte and Smith Ranch (USA).

**9.4 – Tectonic-lithologic** deposits are discordant to strata. They occur in permeable fault zones and adjacent sandstone beds in reduced environments created by hydrocarbons and/or detrital organic matter. Uranium is precipitated in fracture or fault zones related to tectonic extension. Individual deposits contain a few hundred tonnes up to 5000 tonnes of uranium at average grades ranging from 0.1–0.5%. Examples include the deposits of the Lodève District (France) and of the Franceville Basin (Gabon).

**9.5 – Mafic dykes/sills in Proterozoic sandstones:** mineralization is associated with mafic dykes and sills that are concordant with or crosscut Proterozoic sandstone formations. Deposits may be subvertically oriented along the dyke's margins (Matoush, Otish Basin, Canada), or hosted within the dykes, or stratabound within the sandstones along lithological contacts with mafic sills (Red Tree, Westmoreland District, Australia). Deposits are small to medium (300–10 000 t) with low to medium grades (0.05–0.40%).

#### Type 10 – Palaeo quartz-pebble conglomerate

Detrital uranium oxide ores are found in quartz pebble conglomerates deposited as basal units (Elliot Lake District, Canada) or intraformational conglomerates (Witwatersrand Basin, South Africa) in fluvial to lacustrine braided stream or lacustrine systems older than 2400–2300 Ma. The conglomerate matrix is pyritic, and gold, as well as other accessory and oxide and sulphide detrital minerals, are often present in minor amounts. Examples include deposits of the Witwatersrand Basin, South Africa, where uranium is mined as a by-product of gold as well as deposits in the Blind River/Elliot Lake area of Canada. Two economic subtypes are distinguished:

- *U-dominant* deposits: uranium dominant with REE and Th (Elliot Lake District, Canada);
- *Au-dominant* deposits: Au with uranium as a by-product (Witwatersrand Basin, South Africa) ± REE and thorium.

#### Type 11 – Surficial

Surficial uranium deposits are broadly defined as young (Tertiary to recent), near-surface uranium concentrations in sediments and soils. The largest of the surficial uranium deposits are found in calcretes (calcium and magnesium carbonates). These calcrete-hosted deposits mainly occur in valley-fill sediments along Tertiary drainage channels (Yeelirrie, Australia and Langer Heinrich, Namibia) and in

lacustrine-playa sediments (Lake Way, Lake Maitland, and Centipede, Australia) in areas of deeply weathered, uranium-rich granites. Carnotite is the main uraniferous mineral. Surficial uranium deposits also occur less commonly in **peat bogs** (Kamushanovskoye, Kyrgyzstan), and soils (Beslet, Bulgaria).

#### Type 12 – Lignite-coal

Elevated uranium contents occur in lignite or coal mixed with mineral detritus (silt, clay), and in immediately adjacent carbonaceous mud and silt/sandstone beds. Pyrite content is high. Lignite-coal seams are often interbedded or overlain by felsic pyroclastic rocks. Examples are deposits of the southwestern Williston Basin, North and South Dakota (USA), Koldjat and Nizhne Ilyskoe (Kazakhstan), Freital (Germany) and Ambassador (Australia). Two sub-types are recognized, **stratiform** lignite-coal deposits (North and South Dakota, USA; Ambassador, Australia) and **fractured-controlled** lignite-coal deposits (Cave Hills and Slim Buttes, USA and Freital, Germany).

#### Type 13 – Carbonate

Deposits are hosted in carbonate rocks (limestone and dolostone). Mineralization can be syngenetic and stratabound or more commonly structure-related within karsts, fractures, faults and folds. Three types of carbonate-hosted uranium deposits are recognized: **stratabound carbonate** deposits (Tumalappalle, India), **cataclastic carbonate** deposits (Mailuu-Suu, Kyrgyzstan; Todilto District, USA), and **karst** deposits (Bentou-Sanbaqi, China; Tyuya-Myuyun, Kyrgyzstan; Pryor-Little Mountains District, USA).

#### Type 14 – Phosphate

Phosphate deposits are principally represented by marine phosphorite of continental-shelf origin containing syn-sedimentary, stratiform, disseminated uranium in fine-grained apatite. Phosphorite deposits constitute large uranium resources (millions of tonnes), but at very low grade (0.005–0.015%). Uranium can be recovered as a by-product of phosphate production. Examples include the Land Pebble District, Florida (USA), Gantour (Morocco) and Al-Abiad (Jordan). Another type of phosphorite deposits consists of organic phosphate such as argillaceous marine sediments enriched in fish remains that are uraniferous (Melovoe, Kazakhstan). Deposits in continental phosphates are not common. Three subtypes of uranium-bearing phosphate deposits are identified: *minerochemical phosphorite deposits* (Land Pebble District, Florida and Phosphoria Formation, Idaho and Montana, USA), *organic phosphorite deposits* (Melovoe, Mangyshlak District Kazakhstan; Ergeninsky Region, Russia), and *continental phosphate deposits* only known in the Bakouma District (Central African Republic).

#### Type 15 – Black shale

Black shale-related uranium mineralization includes marine, organic-rich shale and coal-rich pyritic shale, containing synsedimentary, disseminated uranium adsorbed onto organic material and clay minerals, and fracture-controlled mineralization within or adjacent to black shale horizons. Examples include the uraniferous alum shale in Sweden and Estonia, the Chattanooga shale (USA), the Chanziping deposit (China), and the Gera-Ronneburg deposit (Germany).

### 5. CONCLUSIONS

The classification of uranium deposits presented in this paper was initiated by the IAEA and is based largely on the work of F. Dahlkamp over the past 40 years. It compiles the flurry of new information published by exploration and mining companies since 2005. It is essentially a geological classification with 15 deposit types and 50 sub-types/classes and covers all of more than 1500 deposits/districts listed in the IAEA UDEPO Database. The classification and the description of about 50 selected deposits will be presented in 2015 in a new IAEA publication [7].

## REFERENCES

- [1] OECD NUCLEAR ENERGY AGENCY, INTERNATIONAL ATOMIC ENERGY AGENCY, Uranium 2011: Resources, Production and Demand, A joint report by the OECD/NEA and IAEA, OECD, Paris (2012).
- [2] INTERNATIONAL ATOMIC ENERGY AGENCY, Guidebook to accompany IAEA map: World Distribution of Uranium Deposits, IAEA, Vienna (1996).
- [3] INTERNATIONAL ATOMIC ENERGY AGENCY, World Distribution of Uranium Deposits (UDEPO) with Uranium Deposit Classification, IAEA-TECDOC-1629, IAEA, Vienna (2009) 117.
- [4] DAHLKAMP, F.J., Uranium Ore Deposits, Springer-Verlag Berlin-Heidelberg (1993) 460.
- [5] DAHLKAMP, F.J., Uranium Deposits of the World—Asia. Springer-Verlag Berlin-Heidelberg (2009) 493.
- [6] CUNNEY, M., Felsic magmatism and uranium deposits, Bulletin de La Société Géologique de France 185 (2) (2014) 75–92.
- [7] INTERNATIONAL ATOMIC ENERGY AGENCY, Geological Classification of Uranium Deposits with Description of Selected Examples, IAEA-TECDOC-1842, IAEA, Vienna (2018).

# **THE WORLD NUCLEAR ASSOCIATION MEDIUM TO LONG TERM OUTLOOK FOR URANIUM DEMAND AND SUPPLY**

I. EMSLEY

World Nuclear Association,  
London, United Kingdom

## **Abstract**

This paper gives World Nuclear Association (WNA) views on nuclear capacity additions to 2030 and the likely adequacy of the fuel supply chain to meet the nuclear fleet's uranium requirements, as presented at the URAM-2014 symposium. A scenario approach is adopted resulting in three capacity projections based on the outlook for existing and new nuclear countries. Uranium resource estimations are taken from the OECD-NEA/IAEA Red Book and the prospects for new and existing mines assessed on a site-by-site basis. Both prospective uranium requirements and primary uranium supply have decreased since the WNA's previous 2011 report, the latter markedly so from the mid-2020s. Secondary supply is also projected and expected to remain high to 2030.

## **1. INTRODUCTION**

Rapid growth in the world demand for electricity has provided a strong market for the development of nuclear power over the past 30 years, and it now contributes over 12% of world supply. Electricity demand growth today is relatively low in most of the countries where nuclear power is well-established, but remains rapid in many developing countries. Nuclear is an essential element in any credible strategy to combat carbon emissions, while also contributing to energy security of supply.

In both established and potential markets, nuclear power faces an increased competitive challenge from other modes of generation, while continuing to face regulatory and political hurdles. The scenarios for nuclear generating capacity in individual countries and areas have been revised and the prospects of nuclear power extending into many new countries are examined, but it remains the case that nuclear fortunes in a relatively small number of countries, notably the United States, China, Japan, India and Russia, will be crucial in determining its overall contribution to world electricity supply.

Until the Fukushima accident in Japan in March 2011, the outlook for nuclear power around the world was improving. Despite the setback that Fukushima represents, countries are putting more emphasis on satisfying environmental and security of supply objectives in their energy strategies and the prospects for new reactor build continue to be strong in China, India and the Republic of Korea as well as a number of countries in the EU and the Middle East.

Three scenarios for world nuclear generating capacity up to 2030 have been prepared, referred to as the reference, upper and lower scenarios. These range from strongly positive to slightly negative growth of nuclear power over the projection period. At mid-2013, world nuclear capacity was 370 GWe which includes all Japanese reactors except Fukushima Daiichi 1–4. In the reference scenario this is expected to rise to 433 GWe by 2020 and to 574 GWe by 2030. The annual average rate of growth over the whole period is 2.6%, sufficient to maintain the nuclear share of world electricity at close to the current 12% level to 2030. In the upper scenario, the equivalent figures are 466 GWe in 2020 and 700 GWe in 2030. In the lower scenario, nuclear generating capacity effectively stagnates in the period to 2020 and then drops away with many reactor closures in the period to 2030.

Within the global picture, there are some significant changes at the country level. The most obvious feature is the increasing prominence of China, which currently has 40 per cent of the reactors under construction around the world.

The WNA reactor requirements model has been updated, with a reassessment of the various factors affecting nuclear fuel demand, such as enrichment levels, cycle lengths and fuel burn-ups. Questionnaires sent to nuclear utilities throughout the world provided useful information to both inform and supplement the model.

Secondary supplies of nuclear fuel have been an important source in satisfying reactor requirements over the past thirty years. There are several separate elements and, contrary to the opinion of some commentators, these will remain important in the period to 2030.

World reactor requirements for uranium in 2012 are estimated at about 62 000 tU equivalent. In the reference scenario, these are expected to rise to 78 000 t U in 2020 and 97 000 t U in 2030. In the upper scenario, uranium requirements are expected to be 87 000 in 2020, and 119 000 t U in 2030.

By comparison with the 2011 Market Report, both the upper and reference scenario uranium requirements are significantly lower in the period to 2030, but the lower scenario is overall little changed.

World known resources of uranium are more than adequate to satisfy reactor requirements to well beyond 2030. World uranium production has continued rising steadily and reached 58 344 t U in 2012. The generally higher uranium prices apparent since 2003 (compared with the period before) have greatly encouraged exploration and future production plans which in a number of cases have been implemented. The decline of uranium prices since 2007 has resulted in the cancellation or deferment of a number of projects.

Three scenarios for uranium production have been developed by evaluating expected mine production capabilities. Assumptions have been made to generate three scenarios for likely uranium production in the period to 2030. It is expected that production will rise over the next ten years in both reference and upper scenarios. In the reference case, world uranium production is expected to reach 67 000 t U in 2020 before declining to 53 000 t U by 2030. In the upper case, the equivalent figures are 77 000 t U and 60 000 t U respectively. These projections represent a significant downward revision from their equivalents in the 2011 Market Report. This revision reflects the project cancellations and deferments noted above, but also the new more objective project category definitions now employed in the current report. Many former ‘Planned’ and ‘Prospective’ projects have now been placed in the ‘Supply Pipeline’ category.

Secondary supplies of uranium are gradually playing a diminishing role in the world market, but will continue to be important over the entire period to 2030. There remain uncertainties about the magnitude and character of Russian inventories and stockpiles and it is unclear where they will be consumed and how long they will last.

Combining all primary and secondary sources suggests that the uranium market should be adequately supplied in the period to 2025, provided that all mines currently under development enter service as planned. Beyond 2025, further uranium mines will be required if the reference and upper demand scenarios are to be satisfied.

The uranium conversion sector is characterized by a small number of companies producing UO<sub>2</sub> for those reactors fuelled with natural uranium and UF<sub>6</sub> for those using enriched uranium. The market in the immediate future has an adequate supply base but new investment will be required thereafter.

The most significant feature of the uranium enrichment sector is the now almost complete replacement of the old gaseous diffusion plants by new ones employing centrifuge technology. A shift in the utilisation of excess Russian capacity, driven by wider market access and the ending of the Russia-US HEU Agreement, is matched by an expansion of new and more efficient Western supply sources to meet additional utility demand.

The fuel fabrication market differs from the others in that it supplies a highly differentiated product, rather than a commodity or simple service. Current capacities are more than sufficient to cover anticipated demand for both first cores and reloads, but new investments will be required if the upper scenario is realised.

There have always been significant risks for the nuclear power industry in over-reliance on supplies from secondary sources, as additional primary supplies can only be brought on line with some delay. This is now, at last, beginning to happen, but projects continue to face many challenges in entering production and, on current plans, mine production is expected to decline in the late 2020s.

## BIBLIOGRAPHY

ORGANISATION FOR ECONOMIC CO-OPERATION AND DEVELOPMENT NUCLEAR ENERGY AGENCY, INTERNATIONAL ATOMIC ENERGY AGENCY, Uranium 2011: Resources, Production and Demand, OECD, Paris (2012).

WORLD NUCLEAR ASSOCIATION, The Nuclear Fuel Report Global Scenarios for Demand and Supply, World Nuclear Association, London (various editions).

# URANIUM POTENTIAL IN GREENLAND

N. KEULEN, K. THRANE, P. KALVIG

Geological Survey of Denmark and Greenland (GEUS),  
Department of Petrology and Economic Geology,  
Copenhagen, Denmark

## Abstract

The uranium potential in Greenland is considered high with several known uranium occurrences. South Greenland is the largest uranium province in Greenland, containing the Kvanefjeld REE-U-Zn-F deposit, the Motzfeldt Centre and the Grønnedal-Ika complex, which are all large Mesoproterozoic alkaline Gardar intrusions. In West Greenland, several large carbonate intrusions (e.g. Sarfartoq and Qaqqaarsuk) contain elevated uranium concentrations. In East Greenland, mineralised zones are located in volcanic and granitic rocks of Devonian age at Randbøldal, Foldaevl and Moskusokseland. Given the very limited uranium exploration carried out in Greenland to date, a greater potential is presumed to exist based on spot observations and the knowledge of favourable geological environments. The highest potential for undiscovered uranium in Greenland is expected for sandstone type, unconformity type, vein type and intrusion type deposits in the well-known uranium province in South Greenland, in sandstones, veins and intrusions in West and East Greenland, and in the Mesoproterozoic-Neoproterozoic Thule Supergroup in North-West Greenland.

## 1. INTRODUCTION

### 1.1. Geology of Greenland in a uranium context

Greenland is endowed with several large uranium deposits, in various geological settings [1, 2]. Here, we discuss the general geology of Greenland for both the areas, where actual uranium occurrences have been recognised, and areas with a potential to host uranium deposits. The largest deposits by far are hosted in peralkaline intrusions related to the Gardar intrusive complex in South Greenland, encompassing the deposits around Kvanefjeld and Motzfeldt Sø (Fig. 1). The Mesoproterozoic Gardar province in South Greenland is an intracratonic rift province consisting of sandstones, and a variety of volcanic and plutonic igneous rocks of alkaline and peralkaline affinity [3, 4]. The Gardar rift province has been formed in the Ketilidian orogen of South Greenland. This orogen consists of Palaeoproterozoic reworked and juvenile rocks on the northern and southern side of the orogen and the large mainly granitic Julianehåb batholith [5, 6]. The southern side of the complex comprises, among others, the highly metamorphosed sandstones of the psammite zone (the area around the occurrence at Illorsuit in Fig. 1).

The northern part of the Ketilidian orogen reworks the North-Atlantic Craton of Southern West Greenland and southern East Greenland. This craton mainly consists of high-grade Archaean orthogneisses with smaller units of intrusive and supracrustal rocks. The northernmost areas of the North-Atlantic Craton were reworked during other Palaeoproterozoic orogenic events [7]. Within the orthogneisses of the North-Atlantic Craton a number of carbonatite-associated uran deposits occur, most notably the Sarfartoq Carbonatite Complex and Qaqarssuk carbonatite, both in southern West Greenland [8] (Fig. 1).

In North-West Greenland the Thule Supergroup, a sedimentary-volcanic succession, was deposited at middle Mesoproterozoic-late Neoproterozoic times. The Thule Basin is an intracratonic fracture basin characterised by block faulting and basin sagging formed during an extensional tectonic regime in the North Greenland Precambrian Basement [9, 10].

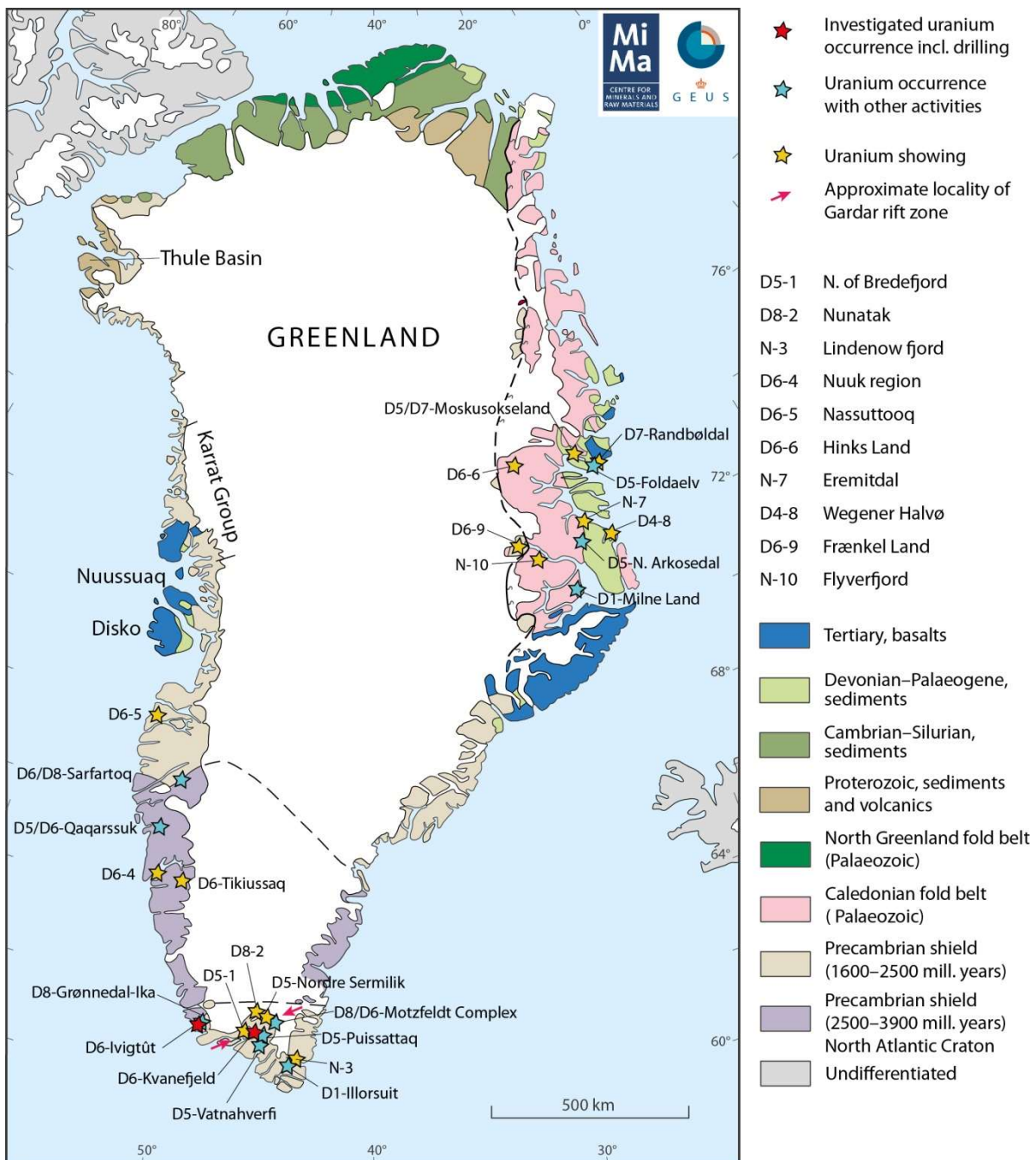


FIG. 1. Simplified geological map of Greenland indicating the exploration activity on previously investigated uranium occurrences. Occurrences with drilling activity, with other investigations than drilling, and with only little investigations are shown. Labels refer to the deposit classification scheme described in the main text. Occurrences labeled with N are of an unknown deposit type. Figure modified from [1].

Central East Greenland was affected by several orogenic events, including the Caledonian orogeny, and hosts a range of felsic to alkaline intrusive complexes, volcanic rocks and veins that range from Proterozoic to Palaeogene in age [11–14]. Central East Greenland also hosts a thick series of sediments that were formed during the opening of the northern Atlantic between the Triassic and Palaeogene [7, 15]. A smaller series of Cretaceous and Palaeogene sediments is observed in Central West Greenland on Nuussuaq and Disko island, related to extensional tectonics in the Davis Strait [16].

## 1.2. Assessment of the uranium potential in Greenland

The focus of the current contribution will be two-fold. We will start with providing a description of the known uranium occurrences in Greenland in Section 2. These serve as an aid to illustrate the possibilities of finding other uranium deposits in the larger area and will help establish an overview of the potential to host an hitherto undiscovered uranium deposit. The potential to find new uranium deposits will be discussed in Section 3. In the remaining part of this contribution, all known uranium showings, occurrences and deposits will be referred to as occurrences, regardless of size.

### 1.2.1. Classification of uranium deposit types

This contribution applies the principal uranium deposit types and the associated subtypes defined by the International Atomic Energy Agency (IAEA) in combination with the criteria from the genetic and fluid- and process-oriented classification schemes [17–20]. Table I gives an overview over the observed and most relevant potential uranium deposit types in Greenland. From the 15 types of deposits, only sandstone (D1); unconformity (D2); quartz-pebble conglomerate (D4); vein (D5); intrusion (D6); volcanic (D7); metasomatites (D8); and metamorphic (D13) deposits are relevant in a Greenlandic context.

## 2. AREAS WITH KNOWN URANIUM OCCURRENCES

Nearly 30 uranium occurrences are known in Greenland. These are shown in Figure 1, where they are classified by the amount of information that is available on these occurrences. Most occurrences are either showings with only little exploration activity, or areas where more investigations, like geological mapping or trenching, have been performed. Drilling for uranium as a product or by-product has only been executed in Ivittuut and Kvanefjeld. The Sarfartoq carbonatite has been drilled, but with the aim to investigate the niobium potential of the intrusion. The occurrences have been classified according to the uranium deposit type classification described above. The most important occurrences will be discussed in more detail below, starting with Kvanefjeld and moving around the Greenlandic coast in a roughly clockwise manner.

### 2.1. Kvanefjeld (Kuannersuit) (D6)

The 150 km<sup>2</sup> Ilímaussaq alkaline complex of South Greenland hosts the REE-U-Zn-F deposit referred to as Kvanefjeld. It is intruded into the Palaeoproterozoic Julianehåb batholith and the unconformably overlying Mesoproterozoic Eriksfjord formation comprising sandstone and basalt. Kvanefjeld represents the top of the Ilímaussaq intrusion and is composed of hyper-agpaitic lujavrites and naujaite. The last intrusive phase, the lujavrite, has an average U concentration of 273 ppm. Most of the radioactive minerals are complex silicates and phosphates with rare earth elements, niobium, tantalum, zirconium and iron. Steenstrupine, a sodium-cerium-silico-phosphate is an important carrier of uranium (0.2–1.5% U). The thorium-silicate thorite (3.1% U) occurs only in the late stage differentiate lujavrite. In other rock types, eudialyte, a sodium-calcium- and iron-silicate with zirconium, is the dominant uranium- and thorium-bearing mineral. The Kvanefjeld uranium deposit is unique in Greenland and has been described in great detail. Geological mapping and radiometric acquisition have been carried out from 1956 to 1985, and 12 455 metres of core were drilled and a 1 km long adit was constructed [4, 21].

Since 2007, Greenland Minerals and Energy Ltd. [22] has conducted REE-exploration activities in the Kvanefjeld area, including the drilling of an additional 57 710 meters of core. GME reports that the overall resource inventory for Kvanefjeld (150 U<sub>3</sub>O<sub>8</sub> ppm cut-off) is 619 Mt of ore containing 350 Mlbs U<sub>3</sub>O<sub>8</sub> and 6.55 Mt TREO including 0.24 Mt heavy REO. Additional resources exist in Zone Sørensen and Zone 3.

TABLE I. KNOWN GLOBAL AND GREENLANDIC URANIUM OCCURRENCES CLASSIFIED BY DEPOSIT TYPE

| Uranium deposit type                        | Commodities (potential by-products)                      | Subtypes  | Global examples   | Greenlandic examples   |
|---|--|---|---|--|
| D1<br>Sandstone deposits                    | U<br>(V, Cu)   | 1. Roll-front deposits<br>2. Tabular deposits<br>3. Basal channel               | • Colorado Plateau, USA<br>• Grants, USA  | 1)<br>• Illorsuit<br>2)<br>• Milne Land<br>3) No known examples  |
| D2<br>Unconformity-related deposits         | U<br>(Au, Ni)  | 1. Unconformity contact deposit<br>2. Sub-unconformity-post-metamorphic deposit | • Rabbit Lake, Canada<br>• Cluff Lake, Canada<br>• Key Lake, Canada<br>• Jabiluka, Australia<br>• Ranger, Australia   | No known examples  |
| D4<br>Quartz-pebble conglomerate deposits   | U, Au, PGE   | 1. Monometallic<br>2. Polymetallic  | • Blind River/Elliot Lake, Canada<br>• Witwatersrand, South Africa  | 1)<br>• Wegener Halvø<br>2)<br>No known examples   |
| D5<br>Vein type (granite-related deposits)  | U<br>(Ni, Co, As, Bi, Cu, Pb, Zn, Mn, Se, V, Mo, Fe, Ag) |   | • Ace Fay-Verna and Gunnar, Saskat-chewan, Canada<br>• Millet Brook, Nova Scotia, Canada<br>• Schwartzwader, Colorado, USA<br>• Xiazhuang district, China<br>• La Crouzille area, Massif Central, France<br>• Jachymov, Czech Republic  | • Nordre Sermilik<br>• North of Bredefjord<br>• Puissattaq<br>• Vatnaverfi<br>• Moskusokseland<br>• Nedre Arkosedal<br>• Foldaelv<br>• Qaqarssuk carbonatite |
| D6<br>Intrusive deposits                    | U, REE<br>(F, Zr, Nb, Ta, Cu)                            | 1. Anatectic deposits<br>2. Plutonic deposits                                   | 1)<br>• Rössing, Namibia<br>• Bancroft area, Ontario, Canada<br>• Campbell Island Mine, Ontario, Canada<br>2)<br>• Bingham Canyon, Utah, USA<br>• Kvanefjeld and Motzfeldt, Greenland<br>• Pilanesberg, South Africa<br>• Araxa, Brazil | 1)<br>• Naassuttooq<br>• Hinks Land<br>2)<br>• Kvanefjeld<br>• Motzfeldt<br>• Ivigtût<br>• Sarfartoq<br>• Tikiussaq<br>• Qaqarssuk<br>• Frænkel Land         |
| D7<br>Volcanic and caldera-related deposits | U<br>(Mo, F, REE)  | 1. Structure-bound<br>2. Strata-bound<br>3. Volcano-sedimentary deposits        | • Streltsovsk district, Russian Federation<br>• Dornot Complex, Mongolia  | 1) and 2)<br>No known examples<br>3)<br>• Randbøldal<br>• Moskusokseland   |

| Uranium deposit type         | Commodities (potential by-products) | Subtypes   | Global examples   | Greenlandic examples  |
|------------------------------|-------------------------------------|--|---|---|
| D8<br>Metasomatite deposits  | U                                   | 1. Na-metasomatite deposits<br>2. K-metasomatite deposits<br>3. Skarn deposits | 1)<br>• Kirovograd district, Ukraine<br>2)<br>• Krivoi Rog Basin, Ukraine<br>3)<br>• Elkon Horst Deposits, Russian Federation<br>• Mary Kathleen, Queensland, Australia | 1)<br>• Motzfeldt<br>• Grønnedal-Ika<br>2)<br>• Sarfartoq<br>• Nunatak north of Nordre Sermilik<br>• 3) No known examples |
| D13<br>Metamorphite deposits | U<br>(Th, Cu, REE)                  | 1. Strata-bound deposits<br>2. Structure-bound deposits                        | 1)<br>• Forstau, Austria<br>2)<br>• Nuottojarvi. Lampinsaari, Finland<br>• Schwartzwalder, USA<br>• Ace-Fay-Verna, Canada<br>• Kamyshevoye, Kazakhstan                  | No known examples   |

Table modified from Keulen et al. [1].

## 2.2. Motzfeldt complex (D6/D8)

The 45 km<sup>2</sup> Mesoproterozoic Motzfeldt Centre within the Igaliko alkaline intrusive complex is part of the Gardar Province. It is made up of multiple intrusions of syenite and nepheline syenite and was emplaced as two main igneous episodes into the Proterozoic Julianehåb batholith and the unconformably overlying Gardar supracrustal rocks. It contains an extensive U-Nb-Ta-Zr-REE mineralisation that was discovered by the reconnaissance surveys of the Syduran project [23]. The coarser syenitic rocks are intruded by sills or sheets of microsyenite in the north and northeast part of the Motzfeldt Centre. Uranium is hosted in pyrochlore, which is concentrated in a 200 – 300 m wide zone along the outer margin of the intrusion. The mineral is hosted in both peralkaline microsyenite and altered syenite [24]. The micro-syenite contains 100 – 500 ppm U. Metasomatic processes enriched uranium in zones to concentrations larger than 500 ppm. The zones extend over several 100 meters. The width of most zones lies in the range several meters to 100 m, but few are wider than 100 m. The altered rocks are also enriched in Zr, Nb, Ta, REE and Th. Pyrochlore contains 3 – 9% UO<sub>2</sub> [25]. Presently, RAM Resources Ltd. has licensed the area and undertakes exploration for REE, Nb and Ta.

## 2.3. Veins related to the formation of the Gardar province (D5)

The Gardar province of southern Greenland is an area where multiple known uranium-enriched veins occur. Most veins occur in the Julianehåb batholith, but are related to Gardar province events of c. 1300 to c. 1120 Ma. The batholith forms the basement for the Gardar province and was emplaced between 1868 and 1796 Ma in a sinistral transpressive setting [5, 6]. Apart from the two occurrences described below, other uranium-bearing occurrences have been reported north of Bredefjord [26].

### 2.3.1. Vatnahverfi (including Eqaluit) and Puissattaq

This area in the Julianehåb batholith covers the region south of Igaliko Fjord, east of Equaluit and SSW of the settlement Igaliuk. Geochemical stream sediment surveys proved anomalously high uranium concentrations in the area. In 1982, a great number of faults and fractures in the basement were checked for radioactivity covering an area about 200 km<sup>2</sup>, and many radioactive mineral occurrences were found. Exposure is rather poor, but several radioactive localities have been found to extend 50–150 m along a

fault zone near Vatnahverfi. In several fault zones, pitchblende has been found as veins or irregular bodies of up to 1.5 m long and is 1–2 cm wide. In Puissattaq, pitchblende accumulation and veinlets were already found in several places. The veins were not exposed, but were found by tracing radioactive boulders, often below the soil, with a scintillometer back to their source. Then veins were exposed after trenching and blasting. Vein samples assayed by gamma-spectrometry contain from 0.7 to 6.3% U and very little thorium. Besides pitchblende, brannerite is the most common U-mineral in the area. The distribution and the mineral genesis suggest that hydrothermal fluids circulated in the many fractures [26, 27].

### 2.3.2. *Nordre Sermilik (Qingua and Ulungarssuaq)*

The area, consisting of granites of the Julianehåb batholith, was investigated in 1980 [26, 27]. Uranium occurrences are common and are especially related to faults and fractures. In Qingua, in a WNW trending fault, pitchblende is found in thin smears along the related fractures. In the part of the fault where the pitchblende occurs, the granite wall rock has been chloritised and laced with haematite, giving it a dark red colour. Radioactive hematitic and carbonate material occur in the same fault. No pitchblende is found, but samples yield over 1000 ppm U [26]. Several NNE reverse faults occur between Ulungarssuaq and Qingua. The eastern most faults can be traced for over 10 km; veins rich in uranium are present at a number of places along this fault. Pitchblende has been identified in one locality, and samples contain up to 3000 ppm U. Uranium is also disseminated in the sandstone overriding the fault — which contains up to 600 ppm [26].

## 2.4. **Illorsuit (D1)**

This locality is part of the psammite zone, in the Ketilidian orogenesis supracrustal rocks. Illorsuit is situated on a cliff face 500 m above sea level on the eastern side of the fjord. Regional mapping showed that it was the largest and richest of over 35 similar uranium occurrences scattered over the hillside in a large xenolith enclosed within the rapakivi granite the area [28]. The main uranium-bearing mineral is uraninite, which is disseminated as fine grains through certain strata or concentrated as medium-sized grains along fractures and associated breccias. The main mineralisation was found to extend 125 m with a width of 1–5 m and it occurs exclusively in fine grained, granular textured meta-arkosic units surrounded by rapakivi granite. The average grade is 0.3% uranium with highs up to 7% uranium. The uraninite crystals formed during the cooling phase of the intruding rapakivi granite at 1730 Ma [29]. If the surface dimensions are projected 60 m down dip, based on the distribution of the supracrustal units, this would give a tonnage of c. 50 tonnes of uranium [28]. The license for the area is currently held by Samarium Group Corporation, who are exploring for Au.

## 2.5. **Grønnedal-Ika (D8)**

The Grønnedal-Ika intrusion is an intensively faulted centre of nepheline syenite penetrated by a central plug of carbonatite, and it is the oldest of the Gardar intrusive centres (1299 Ma). The radioactivity of the carbonatite intrusion due to U is low (< 60 ppm). However, minor areas of U-rich, Na-metasomatised syenite occurs around the intrusion. Due to poor exposure the extent of this type of alteration is not known in detail. The radioactive syenite contains cracks filled with carbonate, iron oxides and pyrochlore, yielding U concentrations up to 1000 ppm. It is probable that the metasomatism and mineralisation is controlled by fault and fracture zones with are abundant in the intrusion [30].

An airborne gamma-spectrometer survey, as well as a reconnaissance exploration survey using stream sediments samples yielded elevated U values in the Ivittuut-Grønnedal-Ika area [31], but these might also be related to the nearby Ivigtût Granite. Rimbal Pty. Ltd has currently licensed both areas and are exploring for carbonate and REE in Grønnedal-Ika and for ultra-pure quartz in the Ivigtût Granite.

## 2.6. **Ivigtût Granite and associated cryolite body (D6)**

The Ivigtût intrusion (1250 Ma) is one of the most evolved granite complexes in the Gardar Province. The unique cryolite body of the intrusion was mined from 1854 to 1984 by the Kryolitselskabet Øresund

A/S, who also carried out the first investigations around the cryolite mine to look for radioactivity. The main U occurrence was associated with columbite in marginal areas of the cryolite body. The main cryolite body has been mined today, and the mine abandoned; some remaining tailings are stored adjacent to the mine site. The majority of the tailings have been reprocessed. A halo of radioactivity around the Ivigtût intrusion has been recognised and investigated; it contains 50–100 ppm U in the highly altered granites [32].

## 2.7. Qaqarssuk carbonatite complex (Qeqertaasaq) (D5/D6)

The 15 km<sup>2</sup> Qaqarssuk carbonatite complex, east of Maniitsoq, southern West Greenland, was found in 1965 by Kryolitselskabet Øresund A/S [33]. The carbonatite intruded into the Archaean basement as dykes and veins over several generations during the Jurassic ( $165.7 \pm 1.9$  Ma) [8, 34]. Ca. 15% of the area consists of largely concentric steeply outward-dipping ring-dykes. The outermost carbonatite ring-dyke in the complex contains fine-grained dolomite carbonatite. Radioactive, narrow ferrocarbonatite dykes (beforsite) and vents, rich in altered basement fragments, are found in the highly altered basement, often located in shear zones with a higher radioactivity. The ring-dykes are cut by coarse-grained late stage sövite and REE carbonatite veins. Pyrochlore occurs in these late stage sövite veins, which are locally enriched in U, Ta, Ba and REE. Pyrochlore-enriched in U and uranopyrochlore also occur in the fenite zone [35]. The average values in the sövitic carbonatite are 1 ppm U, but close to the southern margin values up to 180 ppm U occur. Currently, NunaMinerals A/S is holding the license for the area.

## 2.8. Sarfartoq carbonatite complex (D6)

The 90 km<sup>2</sup> Sarfartoq carbonatite complex, southern West Greenland, was found by airborne radiometric surveys carried out in 1975–76 by the Geological Survey of Greenland. The carbonatite was emplaced at  $560 \pm 13$  Ma in a zone of weakness in the Precambrian shield [8, 34]. It comprises a core area of carbonatite and Na-fenite (15 km<sup>2</sup>), mantled by a marginal zone of hydrothermally altered gneisses (K-fenite) with carbonatite dykes (beforsite). The carbonatite rocks of the core occur as concentric sheets dominated by rauhaugite and sövite occurs only occasionally in schlieren. Pyrochlore occurs both sporadically in the core sövite with peak values up to 400 ppm U as disseminated accumulation within the marginal zone with uranium values up to 1%. Pyrochlore veining and brecciation are also found as 1–5 m wide monomineralic veining [36]. At the end of the carbonatite activity, hydrothermal activity apparently reached the surface, and hot circulating water locally dissolved the carbonatite and remobilised the uranium [8]. Hudson Resources Inc. currently has licenced the area and are investigating the REE, Nb, and Ta potential.

## 2.9. Volcanism in central East Greenland (D7)

Volcanism in East Greenland has been reported as late-syn to post-orogenic stage of the Caledonian orogeny in the latest Silurian and Devonian. The magma is mainly rhyolitic and contains enhanced levels of uranium in several places [13, 14]. Steenfelt [14] advocates a genetic model, in which Devonian magmas enriched in uranium and fluorine reacted with circulating meteoric water in the Post-Devonian Main Fault, and proposed an epigenetic model in which uranium was remobilised and introduced postmagmatically. Vein-type uranium deposits (D5) occur as well in the same area, and some are related to the same event. The main occurrences related to volcanism are described below. In addition, uranium occurrences are described in Foldaelv, Gauss Halvø [37].

### 2.9.1. Moskusokseland (D5/D7)

Minor uranium mineralisation was discovered near Hochwacht [38]. The mineralisation is associated with Devonian acid volcanics. Scattered pitch-blende and beta-uranophane occur in veinlets and disseminated in the volcanics at several localities, but only in negligible amounts. Selected samples contain up to 1% U [14, 39]. ARC Mining holds the license for this area and for Randbøldal.

### 2.9.2. *Randbøldal, Gauss Halvø (D7)*

Outcropping uranium-enriched rocks were located in Randbøldal by the Geological Survey of Greenland [40]. The area comprises Devonian porphyritic rhyolites locally overlain by pyroclastic rocks and Devonian molasse sediments. Intensely altered and limonite-stained radioactive mineralisation is located within ca. 1 km<sup>2</sup> of the rhyolites close to the boundary of the overlying pyroclastic rocks. Individually mineralised outcrops are concentrated along faults and shear zones. They can rarely be traced for more than 20 m, and contain on average 500–700 ppm U. Selected samples contain up to 0.2% U [39]. Most of the uranium is hosted in uraniferous hydrocarbons (carburan), which occur disseminated and in veinlets; other identified uranium minerals are surface weathering minerals as barian wölsendorfite [41].

### 2.9.3. *Nedre Arkosedal (Stauning Alper) (D5)*

The uranium mineralization is located in a major fault zone forming the contact between the Caledonian terrane of Mesoproterozoic migmatitic rocks intruded by Caledonian granite and the Lower Permian continental clastics of the Jameson Land basin [42]. The locality was first observed in 1956 by the Lauge Koch Expeditions. Reinvestigations in 1970 revealed high uranium concentrations. Uranium found in two veins displaying distinct yellow, limonitic zones. The main uranium mineralisation is restricted to brecciated and mylonitised granite and occurs as fine-grained pitchblende in fluorite. 251 surface samples have an average of 252 ppm U with maximum of 3427 ppm. A smaller vein is c. 40 m long; the best 2 m of this section average 3100 ppm U. Selected samples from the smaller vein contain up to 2.3% U [39]. Avannaa Exploration Ltd. is currently holding the licence for the area. They are investigating for Zn, Cu, and Sr.

## 2.10. Milne Land (D1)

The Mesozoic sediments of east Milne Land, central East Greenland, form a fossil placer that was first discovered in 1968, due to high Zr, REE, and Th anomalies detected from pan samples. In 1970s, a number of additional Th anomalies were detected [43, 44] and followed up with ground surveys in 1971 – 1972 [45]. The basal unit of the placer is ca. 20 m thick and comprises among others unconsolidated heavy mineral sands rich in garnet, ilmenite, rutile, zircon and monazite, which interfinger with the arkosic sandstone. The heavy mineral sands occur as irregularly distributed 10 – 40 cm thick lenses within the unit. Uranium is mainly hosted in the monazite, and samples from trenches yield 190 – 640 ppm U [37, 45]. CGRG Ltd. currently has the license for the area and is exploring for Mo-Zr-REE-Ti.

## 3. AREAS IN GREENLAND WITH A HIGH POTENTIAL TO HOST A URANIUM DEPOSIT

The selection of the potential areas is mainly based on the available geological information on the area and follows loosely the method of the USGS global mineral resource assessment program (but without a panel and quantified estimations; see [46–48] for details). More information on the individual deposits can be found in [1]. The amount of available information varies considerably within Greenland, and consequently the potential cannot be assessed with the same amount of confidence in all areas. This section is structured according to the different deposit types, and not according to the economic potential of the areas. Only the areas with a high or very high potential to host a uranium deposit are described below. Details on areas with a medium or low potential are found in [1].

For *sandstone deposits*, the areas with the highest potential are found in the Mesoproterozoic-Neoproterozoic Thule Supergroup in North-West Greenland and in the psammite zone with high metamorphic grade sandstones in South Greenland. The feldspar-bearing sediments at the base of the Thule Supergroup were derived from a Precambrian basement and deposited in an intracratonic basin with block faulting. Evidence for reduction near the unconformity with the basement has been observed [9, 10]. The Palaeoproterozoic psammite zone, the area near the known occurrence Illorsuit (Fig. 1), shows a very high potential to host a uranium deposit. The area was uplifted during the Ketilidian orogeny and the sediments are rich in feldspathic minerals. The rocks are locally strongly migmatised

due to low pressure-high temperature metamorphism, at upper amphibolite facies to granulite facies conditions and are no longer typical sandstones [5]. Steenfelt and Armour-Brown **Error! Reference source not found.** assume that the volcanic rocks and sediments are the source of the uranium, while concentration of the uranium occurred during metamorphism or during synsedimentary and diagenetic processes. The Cretaceous to Palaeogene Nuussuaq Group sandstones in central West Greenland and Devonian to Palaeocene sandstones in the basins in central East Greenland also show a high potential. The known placer deposit on Milne Land is located in the latter area. The presence of coal and investigations for oil in these areas prove that plant debris has been deposited in the area where the rocks are permeable, and that reducing conditions prevailed.

Two areas have a very high potential to host an *unconformity-related uranium deposit*. These are the base of the Thule Supergroup, which overlies Precambrian basement, and the base of the Eriksfjord Formation in the Gardar Province in South Greenland. The Eriksfjord Formation sandstones are preserved in an ENE trending fault-bounded basin formed during the Gardar rifting episode. The sediments were derived from the Julianehåb batholith, which was uplifted during the Ketilidian orogeny. The sandstones have been deposited under a high rate of tectonic activity and under constant subsidence of the area [49]. Another high potential unconformity-related target could be the Kome Formation at the base of the Nuussuaq Group.

The Palaeoproterozoic *conglomerates* of Grænseland and Midternæs in South Greenland [50], of the Karrat Group in central West Greenland and North-West Greenland [51] and the Archaean and Palaeoproterozoic conglomerates on southern Nuussuaq and in the Ataa domain immediately south of Nuussuaq [52] all have a high potential to host a uranium deposit. In all three areas the conglomerate contains quartz-pebbles, is derived from nearby Precambrian basement and is deposited near the boundary with the Archaean craton (Fig. 1).

There is a high potential for *vein-related deposits* in several areas in Greenland. The highest potential is probably found associated with the veins related to the Gardar province in South Greenland (Fig. 1). A high potential is present in the areas around two known vein deposits in the Gardar Province: in the Nordre Sermilik region (Qingua and Ulungarssuaq) and in Vatnaverfi/Puissattaq, where more vein-type deposits are most likely present. Also, the veins in central East Greenland have a high potential to host further uranium deposits. In the latter area the potential is illustrated by two known occurrences with a high potential: Moskusokseland on Wollaston Forland and Nedre Arkosdal in the Stauning Alper. In both areas, South and East Greenland, vein formation occurred together with tectonic activity and highly evolved magma activity in the area [3, 14, 26, 39].

For the *intrusion deposits* the highest potential to find an undiscovered uranium deposit occurs in the Gardar province in South Greenland [3, 26] and in the Neoproterozoic Sarfartoq carbonatite complex [36]. Several occurrences are already known in the Gardar province, including the Kvanefjeld and Motzfeldt, both with a high potential [23, 24]. More intrusion-type uranium deposits might be present in the Gardar area. A large number of granite intrusions occur in central East Greenland and North-East Greenland, of these the 950–900 Ma granites and the Caledonian granites in central East Greenland have a good potential. The former is anatetic leucocratic muscovite-biotite granites associated with partial melting of the Krummedal supracrustal succession [11], the latter are felsic granites, derived from partially molten crust and intruded in an extensional setting during the latest phase of orogenesis [13].

Central East Greenland also has a high potential to host a *volcanic uranium-deposit*. Volcanism in the area has been reported as late-syn to post-orogenic stage of the Caledonian orogeny in the latest Silurian and the Devonian [13, 14]. In this context the occurrences on Moskusokseland and in Randbøldal are mentioned again as a known example with a high potential [39].

## ACKNOWLEDGEMENTS

Comments by A. Steenfelt and K. Secher on earlier versions of MiMa report 2014/1, which formed the basis for this contribution, are highly appreciated. This paper is published with permission of the Geological Survey of Denmark and Greenland (GEUS).

## REFERENCES

- [1] KEULEN, N., THRANE, K., STENSGAARD, B.M., KALVIG, P., “An evaluation of the potential for uranium deposits in Greenland”, Geological Survey of Denmark and Greenland, Center for Minerals and Materials, MiMa report **2014/1** (2014) 87, [mima.geus.dk/mima\\_rapport\\_2014-1.pdf](http://mima.geus.dk/mima_rapport_2014-1.pdf).
- [2] STEENFELT, A., “Uranium data for Greenland registered by GEUS: data acquisition, coverage and spatioal uranium variation”, Danmarks og Grønlands Geologiske Undersøgelse Rapport **2014/28** (2014) 5.
- [3] UPTON, B.G.J., EMELEUS, C.H., “Mid-Proterozoic alkaline magmatism in southern Greenland: the Gardar province”, Alkaline igneous rocks (FITTON, J.G., UPTON, B.G.J. Eds), Geological Society Special Publication, London **30** (1987) 449–471.
- [4] SØRENSEN, H., The Iliausaaq alkane complex, South Greenland: status of mineralogical research with new results, Geology of Greenland Survey Bulletin **190** (2001) 167.
- [5] CHADWICK, B., GARDE, A.A., “Palaeoproterozoic oblique plate convergence in South Greenland: a reappraisal of the Ketilidian Orogen”, Precambrian Crustal Evolution in the North Atlantic Region (BREWER, T.S., Ed.), Geological Society Special Publication **112** (1996) 179–196.
- [6] GARDE, A.A., HAMILTON, M.A., CHADWICK, B., GROCOTT J., MCCAFFREY K.J.W., The Ketilidian orogeny of South Greenland: geochronology, tectonics, magmatism, and fore-arc accretion during Palaeoproterozoic oblique convergence, Canadian Journal of Earth Sciences **39** (2002) 765–793.
- [7] HENRIKSEN, N., HIGGINS, A.K., KALSBECK, F., PULVERTAFT, T.C.R., Greenland from Archaean to Quaternary, Descriptive text to the 1995 Geological map of Greenland 1:2 500 000, 2nd edn, Geological Survey of Denmark and Greenland Bulletin **18** (2009) 126.
- [8] SECHER, K., HEAMAN, L.M., NIELSEN, T.F.D., JENSEN, S.M., SCHJØTH, F. AND CREASER, R.A., Timing of kimberlite, carbonatite, and ultramafic lamprophyre emplacement in the alkaline province located 64° – 67°N in southern West Greenland, Lithos **112** (2009) 400–406.
- [9] DAWES, P.R., The Proterozoic Thule Supergroup, Greenland and Canada: history, lithostratigraphy and development, Geology of Greenland Survey Bulletin **174** (1997) 150.
- [10] DAWES, P.R., Explanatory notes to the Geological map of Greenland, 1:500 000, Thule, Sheet 5, Geological Survey of Denmark and Greenland Map Series **2** (2006) 97.
- [11] KALSBECK, F., THRANE, K., NUTMAN, A.P. AND JEPSEN, H.F., Late Mesoproterozoic to early Neoproterozoic history of the East Greenland Caledonides: evidence for Grenvillian orogenesis? Journal of the Geological Society, London **157** (2000) 1215–1225.
- [12] NIELSEN, T.F.D., “Tertiary alkaline magmatism in East Greenland: a review” Alkaline Igneous Rocks (FITTON, J.G., UPTON, B.G.J., Eds), Geological Society Special Publication **30** (1987) 489–515.
- [13] STRACHAN, R.A., MARTIN, M.W. AND FRIDERICHSEN, J.D., Evidence for contemporaneous yet contrasting styles of granite magmatism during extensional collapse of the northeast Greenland Caledonides, Tectonics **20** (2001) 458–473.
- [14] STEENFELT, A., Uranium and selected trace elements in granites from the Caledonides of East Greenland, Mineralogical Magazine **46** (1982) 201–210.

- [15] SURLUYK, F., The Jurassic of East Greenland: a sedimentary record of thermal subsidence, onset and culmination of rifting, Geological Survey of Denmark and Greenland Bulletin **1** (2003) 659–722.
- [16] DAM, G., PEDERSEN, G.K., SØNDERHOLM, M., MIDTGAARD, H.H., LARSEN, L.M., NØHR-HANSEN, H., PEDERSEN, A.K., Lithostratigraphy of the Cretaceous-Paleocene Nuussuaq Group, Nuussuaq Basin, West Greenland, Geological Survey of Denmark and Greenland Bulletin **19** (2009) 171pp.
- [17] DAHLKAMP, F.J., Uranium ore deposits, Berlin: Springer-Verlag (1993) 460.
- [18] INTERNATIONAL ATOMIC ENERGY AGENCY, World Distribution of Uranium Deposits (UDEPO) with Uranium Deposit Classification, IAEA-TECDOC-1629, IAEA, Vienna (2009).
- [19] PLANT, J.A., SIMPSON, P.R., SMITH, B., WINDLEY, B.F., “Uranium ore deposits - products of the radioactive earth”, Uranium: Mineralogy, Geochemistry and the Environment (BURNS, P.P., FINCH, R. Eds), Reviews in Mineralogy and Geochemistry **38** 1 (1999) 255–319.
- [20] SKIRROW, R.G., JAIRETH, S., HUSTON, D.L., BASTRAKOV, E.N., SCHOFIELD, A., VAN DER WIELEN, S.E., BARNICOAT, A.C., “Uranium mineral systems: Processes, exploration criteria and a new deposit framework”, Geoscience Australia Record **2009/20** (2009) 44.
- [21] ROSE-HANSEN, J., SØRENSEN, H., WATT, W.S., Inventory of the literature on the Ilmaussaq alkaline complex, South Greenland, Danmarks og Grønlands Geologiske Undersøgelse Rapport **2001/102** (2001) 42pp.
- [22] GME: Greenland Minerals and Energy homepage, <http://www.ggg.gl/>
- [23] ARMOUR-BROWN, A., TUKAINEN, T., WALLIN, B., “The South Greenland uranium exploration programme”, Final report, Grønlands Geologiske Undersøgelse (1982) 95 (unpublished report).
- [24] THOMASSEN, B., “The Motzfeldt 87 Project”, Final report, Open file Series Grønlands Geologiske Undersøgelse **88/1** (1988) 81.
- [25] TUKAINEN, T., “Pyrochlore in the Motzfeldt centre of the Igaliko nepheline syenite complex, South Greenland”, Final report, internal GGU report (1986) 98 (unpublished).
- [26] ARMOUR-BROWN, A., TUKAINEN, T., NYEGAARD, P., WALLIN, B., “The South Greenland regional uranium exploration programme”, Final report of progress 1980-1983, Geological Survey of Greenland (1984) 110 (unpublished report).
- [27] NYEGAARD, P., ARMOUR-BROWN, A., “Uranium occurrences in the Granite Zone. Structural setting - genesis - exploration methods”, The South Greenland exploration programme 1984-1986, Report No.1, Open File Series Grønlands Geologiske Undersøgelse **1** (1986) 138.
- [28] ARMOUR-BROWN, A., “Geology and evaluation of the uranium mineral occurrence at Igdlorssuit, South Greenland”, The South Greenland Exploration Programme 1984 - 1986, Report No. 2, Open File Series Grønlands Geologiske Undersøgelse **2** (1986) 60.
- [29] STEENFELT, A., ARMOUR-BROWN, A., “Characteristics of the South Greenland uranium province”, Tech. Comm. Mtg on Recognition of Uranium Provinces, Panel Proceedings Series, IAEA, Vienna (1988), 305–335.
- [30] ARMOUR-BROWN, A., TUKAINEN, T. WALLIN, B., Pitchblende vein discoveries in the Proterozoic Ketilidian granite of South Greenland, Geologische Rundschau **71** (1982) 73–80.
- [31] ARMOUR-BROWN, A., STEENFELT, A., KUNZENDORF, H., Uranium districts defined by reconnaissance geochemistry in South Greenland, J. Geochemical Exploration **19** (1983) 127–145.
- [32] PAULY, H., Det Radioaktive Mønster om Ivigtut, GEUS Report File no **21546** (1960).
- [33] GOTHENBORG, J., PEDERSEN, J.L., Exploration of the Qaqarssuk carbonatite complex 1975, Part II, Kryolitselskabet Øresund A/S (1975) (unpublished company report).
- [34] LARSEN, L.M., REX, D.C., SECHER, K., The age of carbonatites, kimberlites and lamprophyres from southern West Greenland: recurrent alkaline magmatism during 2500 million years, Lithos **16** (1983) 215–221.

- [35] KNUDSEN, C., Petrology, geochemistry and economic geology of the Qaqarssuk carbonatite complex, Southern West Greenland, Monograph Series on Mineral Deposits **29** (1991) 1–110.
- [36] SECHER, K., LARSEN, L.M., Geology and mineralogy of the Sarfartoq carbonatite complex, southern West Greenland, *Lithos* **13** (1980) 199–212.
- [37] THOMASSEN, B., Prospecting for Cu-Pb-Zn-Au-Ag in the Clavering Ø, Giesecke Bjerge and Canning Land areas, Internal NM-report **1/81** (1982) 59.
- [38] STEENFELT, A., Uranium exploration in northern East Greenland, Grønlands Geologiske Undersøgelse Rapport **80** (1976) 110–112.
- [39] HARPØTH, O., PEDERSEN, J.L., SCHØNWANDT, H.K., THOMASSEN, B., The mineral occurrences of central East Greenland. *Meddelelser om Grønland, Geoscience* **17** (1986).
- [40] NIELSEN, B.L., STEENFELT, A., “Distribution of radioactive elements and the recognition of uranium mineralizations in East Greenland”, *Recognition and Evaluation of Uraniferous Areas, IAEA-TC-25/3*, IAEA, Vienna (1977) 87–105.
- [41] SECHER, K., Airborne radiometric survey between 66° and 69°N, southern and central West Greenland, Grønlands Geologiske Undersøgelse Rapport **80** (1976) 65–67.
- [42] HALLENSTEIN, C., Uranium and thorium prospecting in Nordmine concession, East Greenland, Internal NM-report **4/76** (1977) 109.
- [43] HINTSTEINER, E.A., et al., Uran. Internal NM-report **SP1/70** (1970).
- [44] NIELSEN, B.L., LØVBORG, L., Radiometric survey between Scoresby Sund and Hold with Hope, central East Greenland, Rapport Grønlands Geologiske Undersøgelse **76** (1976) 44.
- [45] SCHATZLMAIER, P., SCHÖLLNBERGER, W., THOMASSEN, B., Untersuchung des Vorkommens von Zirkon und seltenen Erden auf Kote 800 Milneland, Internal NM-report **4/72** (1973) 91.
- [46] BRISKEY, J.A., SCHULZ, K.J., USGS Mineral Resources Program, The Global Meneral Resource Assessment Project, USGS Fact Sheet **5303** (2003) 2.
- [47] SINGER, D.A., Basic concepts in three-part quantitative assessments of undiscovered mineral resources, *Nonrenewable Resources* **2** (1993) 69–81.
- [48] SINGER, D.A., MENZIE, W.D., Quantitative mineral resource assessments, New York, Oxford University Press (2010) 219.
- [49] TIRSGAARD, H., ØXNEVAD, I.E.I., Preservation of pre-vegetational mixed fluvio–aeolian deposits in a humid climatic setting: an example from the Middle Proterozoic Eriksfjord Formation, Southwest Greenland, *Sedimentary Geology* **120** (1998) 295–317.
- [50] BONDESEN, E., The stratigraphy and deformation of the Precambrian rocks of the Grænseland area, South-West Greenland, *Bulletin Grønlands Geologiske Undersøgelse* **86** (1970) 210 (also *Meddelelser om Grønland* **185(1)**).
- [51] HENDERSON, G., PULVERTAFT, T.C.R., Descriptive text to geological map of Greenland 1:100 000, Mårmorilik 71 V.2 Syd, Nügâtsiaq 71 V.2 Nord and Pangnertôq 72 V.2 Syd, Geological Survey of Greenland, Copenhagen (1987) 72.  
GARDE, A.A., STEENFELT, A., Precambrian geology of Nuussuaq and the area north-east of Disko Bugt, West Greenland, *Geology of Greenland Survey Bulletin* **181** (1999) 6–40.

# DYNAMICS OF URANIUM ORE FORMATION IN THE BASEMENT AND FRAME OF THE STRELTSOVSKAYA CALDERA

V.A. PETROV\*, S.I. SCHUKIN\*\*, V.V. POLUEKTOV\*, V.A. TOLSTOBROV\*\*

\* Institute of Geology of Ore Deposits, Petrography,  
Mineralogy and Geochemistry (IGEM), Russian academy of sciences,  
Moscow, Russian Federation

\* Priargunsky Mining and Chemical Operation (PPGHO),  
Krasnokamensk, Russian Federation

## Abstract

Spatiotemporal pattern of uranium mineralization formation in the basement and frame of the Streletssovskaya caldera is generalized on the basis of previous and newly received geological, geophysical, palaeogeodynamics, mineralogical, geochemical, isotope, and geochronological data. Main occasions for uranium mineralogenesis in the context of tectonomagmatic cycles (Proterozoic, Caledonian, Variscan, and Late Mesozoic) of the territory evolution and activation of fluid-conducting fault zone network on the basis of seismic cycle model for fluid-saturated rock massifs of the upper seismogenic crust are distinguished. Directions for further investigation and areas, that are perspective for prospecting works on identification of uranium mineralization in the basement and frame of the caldera are determined.

## 1. INTRODUCTION

The Streletssovskoe orefield (SOF) in the Krasnokamensk area of Transbaikalia, Russian Federation consists of 19 uranium deposits which are classified as caldera related volcanic deposits [1]. SOF is the most important examples of type of caldera-related volcanic deposits, along with the Dornot orefield in Mongolia, Xiangshan orefield in China, Michelin deposit, Labrador in Canada, Nopal-Peña Blanca in Mexico and McDermitt in USA.

The Streletssovskaya caldera with dimensions of about  $15 \times 15$  km is located at the intersection of the regional north-east-trending Urulunguy (including N- and S-Urulunguy faults) and Argun fault zones with submeridional Dalainor-Gazimur (including Chindachin, Talan-Gozogor, Meridionalny, Central, Shirondukuy faults) zone (Fig. 1).

Geological structure of the caldera is created by prolonged and intensive tectonic activity and characterized by combination of Proterozoic-Palaeozoic basement (lower structural stage) and Late Mesozoic cover (upper structural stage) [2, 3]. The lower structural stage is composed of Proterozoic and Early Palaeozoic metamorphic rocks (schist, gneiss, amphibolite, marmorized limestone) originated and transformed during the Proterozoic tectonomagmatic cycle (TMC) as well as Palaeozoic granitoids which were formed during Caledonian and Variscan TMC. Caledonian granitoids dominate in the western and northwestern parts of the caldera whereas Variscan granitoids occupy its eastern part. These rocks were subsequently transformed during the Late Mesozoic tectonothermal activation (TTA) of the region. In the process of the Late Mesozoic TTA, the caldera was formed and filled by Late Jurassic-Early Cretaceous sedimentary and volcanic rocks of upper structural stage. The thickness of the stage is about 1000 m of alternating conglomerate, gravel, sandstone and siltstone horizons and basalt, trachybasalt, trachydacite and rhyolite sheets consisting of tuffs, lavas, lava-breccias. This sequence also includes subvolcanic intrusive bodies composed of granosyenite and rhyolite porphyries. Volcanic rocks were formed from 170–160 Ma to 145–142 Ma, whereas age of intrusive rock formation is 141–128 Ma [4, 5].

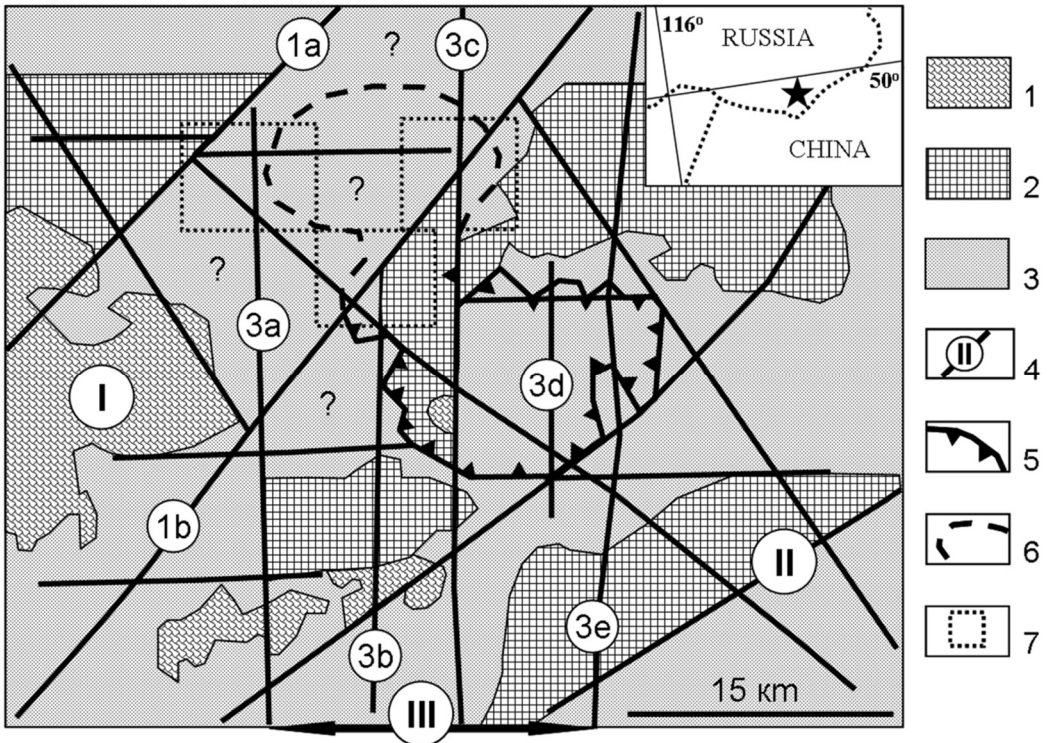


**FIG. 1.** Superposition of the Streltsovskaya caldera edges on regional fault network without Late Mesozoic volcano-sedimentary cover. 1 – Proterozoic schists and marbles, 2 – Proterozoic-Early Palaeozoic granite gneiss, 3 – Palaeozoic granitic rocks, 4 – main transblock and intrablock faults and zones (numerals in figure): I – Urulunguy (1a – N-Urulunguy, 1b – S-Urulunguy), II – Argun, III – Dalainor-Gazimur (3a – Chindachin, 3b – Talan-Gozogor, 3c – Meridionalny, 3d – Central, 3e – Shirondukuy), 5 – main caldera, 6 – northwestern extension of the caldera under the Sukhoy Urulunguy depression, 7 – areas for further prospecting activity.

Original resources within the SOF totaled approximately 245 000 t U. Since the discovery of the orefield in 1963, nineteen deposits have been brought into exploration: seventeen deposits in Late Mesozoic volcano-sedimentary cover and two deposits (Antei and Argunskoe) in the Proterozoic-Palaeozoic basement of the caldera [6]. Among the largest deposits in the cover are Streltsovskoe ( $> 60\,000$  t U), Tulukuyevskoye ( $> 35\,000$  t U), Oktyabrskoe ( $> 15\,000$  t U), Krasniy Kamen (5000 t U) and other deposits, which original resources ranging between 5000 and 15 000 t U. The Antei ( $> 35\,000$  t U) and Argunskoe ( $> 35\,000$  t U) deposits in the basement comprise approximately one third of the orefield total resources. Herewith the Streltsovskoe deposit is a continuation of the Antei deposit from basement to the cover. However, it should be noted that most of survey, exploration and exploitation activities were concentrated on uranium resources in the volcano-sedimentary cover of the caldera. Thus the resource potential of the basement is not completely evaluated.

In this context, the main aim of the contribution is to combine data on the consecutive stages of deformation, inflow and migration of palaeofluids and accumulation of mineral filling with uranium traces within the faulted-fractured environment of the Streltsovskaya caldera. The object of the examination is a framework of fault-fracture zones transecting the Proterozoic-Palaeozoic granitic unit into the frame (Urtuy Massif at the north-western flank and Bambakay Massif at the south-eastern flank) and basement of the caldera (Antei and Argunskoe deposits). Considerations of stress- and permeability-time relationships in faulted-fractured zones were taken with account of stress and strain dependencies within fluid saturated rock massifs at crustal seismogenic level [7, 8]. Stress-time consecution of fault zone permeability and mineral accumulation was developed using a set of fieldwork and lab tests. Some aspects and results were previously published [9, 10]. New isotopic chronological data on granitoids [11] and dispersed uranium mineralization [12] are considered. In addition, new chronological data on age formation of granitic rocks within the frame ( $806 \pm 19$  Ma for Urtuy Massif and  $745 \pm 33$  Ma for

Bambakay Massif) and the basement ( $242 \pm 20$  Ma for Antei deposit) are utilized. These data were obtained by Dr Marion Tichomirowa, TU Bergakademie Freiberg, Germany, using a method of  $^{207}\text{Pb}/^{206}\text{Pb}$  age investigations of zircons on double-filament thermal ion source. Perspective areas for prospecting works within the SOF are indicated.

## 2. FLUID-CONDUCTING STRUCTURES

The evaluation of mineral resources in crystalline rocks directly depends on the identification of the most probable pathways of fluid flow in connection with spatial-temporal evolution of radionuclide transport conditions. In the general case, it is suggested [13, 14] that in fluid-saturated rocks of the upper crust the deformation develops in the framework of a seismic cycle consisting of four stages: (a) preseismic, when stresses accumulate steadily against the background of nonlinear deformation of rocks; (b) coseismic, when deformation occurs immediately after relaxation of stresses (an earthquake); (c) postseismic, with nonlinear deformation of rocks during some time after stress relaxation; (d) interseismic (the stage of seismic quiescence), when the deformation is close to linear.

During the progressive deformation over the stages, essential modifications in fluid flow regimes occur. However, the main phase of hydrothermal fluid inflow into the discontinuities, which are optimally oriented in the stress field, is connected with the coseismic and postseismic stages of stress relaxation. In contrast, deposition of the main volume of mineral assemblages occurs during interseismic stage of short-term and low-amplitude displacements in enabling structural, lithological, tectonophysical and physicochemical environment [15].

Furthermore, at the interseismic stage, the fault cores undergo less dilatancy and are less permeable in comparison with the zones of their dynamic effect, where fluids accumulate and slowly diffuse. At the coseismic stage, a considerable volume of these fluids is squeezed out from the compressed fractures and leaks into the disturbed core of the fault, where favorable conditions are created for drainage and circulation of solutions and precipitation of solid matter. Against this background when in a local domain of the geological medium the fluid pressure approaches threshold level, the tensile cracks develop along heterogeneities favorably oriented (plane  $\sigma_1\sigma_2$ ) in the stress field. The spatiotemporal cyclic relationships between pore pressure and favored paths of fluid flow are considered in the fault valve (pumping) model [16, 17], which causes step-by-step formation of mineral assemblages in the process of solid matter deposition. The efficiency of the fault valve mechanism is determined by the geometry of pore-fracture space, stressed-strained state of the rocks, physicochemical parameters (composition) of solutions and their equilibrium with host rocks.

It must be emphasized, that first successful attempts to link hydraulically active fracture formation and fluid flow state during tectonic events were made in the University of Lorraine, France. It was suggested [18, 19] to use fluid inclusions in minerals (mainly quartz) as markers of thermobaric and physicochemical conditions of fluid migration, and fluid inclusion planes (FIPs) as structural indicators of changes in geometry of fluid-conducting fractures and geotectonic setting of permeability. FIPs start to form as tensile microcracks (mode I crack) which change orientation in response to rearrangement of the stress field. They are oriented perpendicular to the least compression axis  $\sigma_3$  while vector of maximum permeability lies in plane  $\sigma_1\sigma_2$  forming direction of dominant fluid migration [20]. The new tectonic setting gives rise to a new stage of deformation that is inevitably reflected in the orientation of FIPs of the second generation, etc.

Model of short-term (in geologic time scale) seismic cycle in the first approximation could be applied to long-term tectonomagmatic (tectonothermal) evolution of geological structures due to the seismic cycle sketches the broad outline of main tendencies in formation, development, transition to latent state and reactivation (if happen) of the structures. Herewith three complementary aspects were taken into account during consideration of stress- and permeability-time relationships for fault zones:

- a) Deformation of fluid saturated rock massifs within crustal seismogenic level is essentially non-linear during tectonic events and variation of stressed-strained states and temperature impacts;

- b) There is coupling between main phases of fluid inflow into and mineral accumulation in by different domains of fault zones due to fault valve (pumping) effect against the backdrop of seismic deformation cycle leads to formation of thermo-convective cell with mixture of hydrothermal and meteoric solutions;
- c) Local mineral associations into fault zones do not have univocal correlation due to various  $P$ - $T$  conditions in distant domains (dilational jogs vs frictional fault planes) along even single fault zone.

The issue of stress- and permeability-time relationships in fault zones within the Streletsovskaya caldera frame and basement was realized by fieldworks and lab tests. The fieldwork procedures consisted of structural-geological and mineral-petrographic survey of the main fault zone domains, their architecture, morphology, component strikes, dips, mineral filling, etc; determination of the mean principal stresses orientation, fault kinematics (dextral or sinistral displacements), and faulting regime (normal, strike-slip, and thrust) using fault slip data analysis; sampling of positioned lumps for studying rock mineral-chemical composition, FIPs characterization and fission-track radiography (FTR) analysis.

The lab tests included optical microscopy and mineral-chemical studies (XRF and ICP-MS) of rock varieties, nature and intensity of hydrothermal-metasomatic alteration and oxidizing transformation; microfracture space digitalization for distinguishing stress dependent FIPs and open micro discontinuities; evaluation of content and specific features of uranium distribution in rock varieties using FTR data.

### 3. SEQUENCE OF TECTONOMAGMATIC EVENTS AND URANIUM FORMATION

Geological history of the Streletsovskaya caldera area is divided on two main periods: pre-ore preparation and ore-forming tectonomagmatic (tectonothermal) activation. Period of pre-ore preparation comprises Late Proterozoic-Early Palaeozoic (PR3-PZ1) and Middle-Late Palaeozoic (PZ2-3) stages. Period of ore-forming activation consists of Middle-Late Jurassic (J2-3), Late Jurassic-Early Cretaceous (J3-K1) and Early Cretaceous (K1) stages. Beyond Early Cretaceous the territory was developed in platform conditions. It is possible to find data on geodynamic regimes of the ore-forming activation period in published materials [2], which emphasize linkage between the pre-ore preparation events and superimposed ore-forming TTA processes resulting in caldera formation and localization of numerous uranium deposits inside. Admittedly, modelling of tectonomagmatic events and uranium formation in the course of the pre-ore preparation period were distinguished with lesser attention.

Reconstruction of geodynamic circumstances throughout Pre-Mesozoic pre-ore preparation period and Mesozoic ore-forming tectonothermal events shows that activation (reactivation) of interblock regional fault zones occurred on a step-by-step basis during succeed TMCs: Proterozoic (terminated about 600 Ma), Caledonian (~520 – 430 Ma), Variscan (~360 – 210 Ma), and Late Mesozoic (~160 – 100 Ma) [10]. Preferred faulting regimes of TMCs were indicated on about 40 fault zones using fault slip data analysis technique [21] combined with palaeogeomorphological analysis technique [22] and data on relative age of fault infill.

#### 3.1. Proterozoic tectonomagmatic cycle

The beginning of PR3-PZ1 stage in the region was connected with folding and localization of concomitant fault systems. Within the caldera area the most ancient Proterozoic complex of terrigenous and effusive rocks metamorphized in amphibolite stage composes major anticline fold. The core of the fold later on but during Proterozoic was subject for granitization (Urulunguy complex of Late Riphean of 804–784 Ma [11]) with formation of granitic-gneissic cupola (so-called Zaurulunguevsky Massif). It was founded that magmatic body formation took place in regime of general tension with complementary component of submeridional compression. The main indicator of this regime is original magmatic foliation of the granitic rocks around the caldera.

Based on discrimination criteria of Rb-(Y+Nb) [23] granitoids of Urulunguy complex (Urtuy and Bambakay Massifs in the frame of caldera) belong to syn-collisional type. It is important to note that

new geochemical and geocronological data show, that granitoids of the Urtuy Massif should be ranged to Late Riphean and not to Early Palaeozoic as before.

The initial uranium mineralization occurs inside some blocks of the granitic-gneissic cupola. For example, within the Urtuy Massif the NE-trending fault zone of initial ductile deformation was discovered and studied [10]. The main peculiarity of this zone of about 10 km length and 10 m width is ductile rock deformation stated in schistosity, blastic elongation of quartz and feldspar grains into the mylonite quartz-chlorite-carbonate matrix. Dispersed uranium mineralization  $783 \pm 26$  Ma (U-Pb age) was found in the core of the zone [12].

### **3.2. Caledonian tectonomagmatic cycle**

During Early Palaeozoic (Caledonian TMC) the cupola cores were again exposed to granitization. Caledonian formations consist of plagiogranites and variously gneissic quartz diorites and granites. They form cores of large Argunskiy, Marguek-Klickinskiy and a number of small cupolas within SE Transbaikalia. Large-size plutons of granodiorites of Gazimurskiy complex of Ordovician-Silurian age [24] terminated Caledonian cycle of tectogenezis.

During Caledonian TMC ( $\sim 520 - 430$  Ma) the principal axes of stress  $\sigma_1$  and  $\sigma_3$  were subhorizontal while the principal axis of stress  $\sigma_2$  was oriented in subvertical direction. This is characteristic feature of the strike-slip faulting regime.

There are fragmentary data on uranium mineralization (REE-Th-uraninite and Y-uraninite) of Early Palaeozoic ( $520 - 420$  Ma) at different occurrences located north-eastward and north-westward from the Streltsovskaya caldera [3].

### **3.3. Variscan tectonomagmatic cycle**

The main phase of structure creation of Middle-Late Palaeozoic (PZ2-3) stage (Variscan TMC) is connected with intrusion new portions of gabbro, diorites, granodiorites, biotite-hornblende and biotite granites to the cores of cupolas. Beginning with Early Permian the intracontinental volcanic activity evolved. Subvolcanic bodies and dykes of granosienite and granosienite-porphyre of Undinskiy complex were formed. Time of emplacement of these granitoids resides in diapason of  $254 - 245$  Ma, that corresponds to Late Permian-Early Triassic. Based on discrimination criteria of Rb-(Y+Nb) the granitoids of Undinskiy complex (at the Antei deposit) rank to volcanic arc geodynamic setting. Formation of the Antei deposit host rocks corresponds with time of attenuation orogenic processes in Central Asia and passing on regime of Pacific subduction [25].

As is shown in [26] the significant events of uranium concentration in the Streltsovskaya caldera basement took place. It is supposed, that intrusion of granitoids of Undinskiy complex leads to violation of U-Pb isotopic system in ancient ( $783 \pm 26$  Ma) uraninite of the Urtuy Massif and generation of redeposited uranium phase with age of  $262 \pm 34$  Ma. This age is simultaneous with U-Pb age of zircons from the Undinskiy complex granitoids ( $244 \pm 2$  and  $255 \pm 1$  Ma) [11] within limits of accuracy. There is supplementary information that the uranium mineralization (Th-Y-uraninite and Y-uraninite) of Late Palaeozoic ( $320 - 250$  Ma) occurs in the vicinity of the Streltsovskaya caldera [3].

During Variscan TMC previous strike-slip faulting regime was gradually changed by normal faulting regime with ENE-WSW direction of general tension axis. However, at the time border between Palaeozoic and Mesozoic eras, probably during T3 – J2 time [27], all geological structures in SE Transbaikalia underwent inversion of tectonic movements due to global reorganization of the stress-strain field. In this connection the strike-slip faulting regime (transpression,  $\sigma_v = \sigma_2 \approx \sigma_3$ ) prevailed. As a result most intensive strike-slip displacements and shearing were developed along NNE-submeridional and WNW-latitudinal fault zones.

### 3.4. Late Mesozoic tectonothermal activation

Outset of activation of tectonomagmatic (tectonothermal) processes at the territory could be fitted to Middle-Late Jurassic (J2 – 3) stage. At this time in SE Transbaikalia a range of rock formation were originated: rhyolite-granite and andesite-granodiorite volcano-plutonic series (Shachtaminskiy and coeval Amudzikan-Sretenskiy complexes) as well as Li-F granites of Kukulbeiskiy complex. The age of Shachtaminskiy complex (U-Pb zircon dates) varies from  $161.7 \pm 1.4$  to  $155.0 \pm 1.7$  Ma [28]. Herewith age of granodiorite-porphyry of Amudzikan intrusions within the Darasun Au-ore field is  $160.5 \pm 0.4$  Ma [29]. According to I.V. Chernyshev and co-authors this age could be interpreted as principal mark in geological history of SE Transbaikalia. In the context of the geologic time scale [30], this is border of Middle and Late Jurassic, which corresponds to completion of collision between East Siberian and Mongol-Chinese continents and starting point to post-orogenic (intraplate) evolution of Mongol-Okhotsk folded belt and adjacent territories of Central Asia. Inside of the Streltsovskaya caldera the rocks of this age are trachybasalts and trachydacites of Priargunskaya series [3].

The age of granitic-leucogranitic intrusions of Kukulbeiskiy complex varies in wide range from 145 to 120 Ma [4]. It is supposed [3], that within the Streltsovskaya caldera the analogues of Kukulbeiskiy complex are acid effusives of Turginskaya series (felsites, rhyolites, glasses) with elevated (15 – 25 ppm) content of uranium. However, it should be noted that geochemical characteristics of rocks of Kukulbeiskiy complex and Turginskaya series differ whereas data on chronology coincide. These rocks concurrent only in high content of uranium. Furthermore, effusives of Turginskaya series are expanded in rift zone with NE-trending chain of volcanic structures (Streltsovskaya, Kuytun, Kuladjin, Engershank-Tsav, and Dornot calderas) while granites of Kukulbeiskiy complex are emplaced within neighboring consolidated blocks penetrated by multiple-aged intrusions. The issue on time relationships of Mesozoic post-orogenic and anorogenic ore-bearing intrusions requires solution.

During J3 – K1 stage the Streltsovskaya caldera forms with bimodal basalt-rhyolite volcanic units. The trend of volcanic processes in cross-section of the caldera (Priargunskaya and Turginskaya series) is as follow: outflow of basic lava (basalts, andesite-basalts, dacites) substituted by formation of ignimbrite and acid tuff section, and again changed by lavas of basic composition. Sequence of effusive rocks is penetrated by stocks and dykes of felsites and quartz porphyrites. In the course of J3 – K1 time the economic uranium ores of the SOF were deposited. The age of the ores is  $136 \pm 3$  Ma [12, 26].

During K1 stage of TTA a number of small covers of basalts were formed within the coal-bearing sediments (Kutinskaya series) of compensatory basins in the frame of the caldera. These coal-bearing rocks are characterized by elevated content of uranium in many cases.

Reconstruction of dynamics of tectonic processes at the Streltsovskaya caldera area during Late Mesozoic reasonably start from T3 – J2, when inversion of tectonic movements occur due to global rearrangement of the field of stresses and strains [27]. The reorientation of lateral compression axis  $\sigma_1$  from near-meridional to near-latitudinal direction resulted in right-lateral normal-strike slip displacements along the Urulunguy and Argun transblock fault zones accompanied by development of the structural kinematics assembly. As this mechanism came about, stresses concentrated in an interfault block (transform valley). The displacements along coplanar planes of the echeloned intrablock faults and the capture of stresses at their terminations resulted in the formation of a pull-apart depression (graben). Development of the pull-apart structures goes during three main stages: initial, early, and mature [31]. The master boundary and intradepression normal faults of the initial stage; the nearly parallel shears (Meridionalny, Central, Shirondukuy fault zones) perpendicular to the walls of depression formed during the early stage; and a system of strike-slip and normal faults and oblique ruptures formed during the mature stage are distinguished. Volcanoes were formed in the axial zone of the depression (for example, Krasnokamenskiy palaeovolcano) during the mature stage, probably during Middle-Late Jurassic, against the background of a local dome related to the increase in volume of the upper crustal magma chamber. In the Late Jurassic-Early Cretaceous, these volcanoes acted as eruption centres of bimodal basalt-rhyolite lavas that filled the Streltsovskaya caldera. The sequence of events (magma chamber exhaustion, origination of concentric faults (Ring fault), subsidence of central part of

the dome, development of concentric dike complex along the framing normal faults) is consistent with tectonophysical models of concentric structure formation and volcanic caldera collapse [32].

The economic vein, stockwork and stratiform uranium orebodies of the SOF were formed in the Late Jurassic-Early Cretaceous [2], to be more exact  $136 \pm 3$  Ma [26]. The evolution of the Streletsovskaya caldera was completed by formation of the compensation Sukhoy Urulunguy depression filled with Late Cretaceous coal-bearing sedimentary rocks and Quaternary sediments.

Hence, during period of pre-ore preparation the geological block of the Streletsovskaya caldera developed in the regime of cupola. The tectonophysical conditions surerimposed for forming depression in pull-apart regime within the core of the cupola by the beginning of Middle-Late Jurassic. During Middle-Late Jurassic to Late Jurassic-Early Cretaceous stages of the regional ore-forming TTA the volcanic activity was concentrated along the axis of the depression. This volcanic activity was complited by the caldera subsidence in respect to ring faults deriving from the boarding normal faults. It is apparently that the depth of the main magma chamber was about 5–6 km from palaeosurface bearing in mind mechanism of caldera formation and level of erosional truncation.

Furthermore, the geophysical data [33] show that to the north-west direction from the main caldera a geological block delineated by closed contour lines of negative gravity anomaly is situated. Dimensions of this block is equivalent to the main caldera. The modeling of fault kinematics [34] indicates that within this block a depression as an echelon relative to the main caldera was formed in Late Triassic-Middle Jurassic. According to geological and geophysical data, this depression is bounded by NE-trending and sublatitudinal long-living fault zones. The sites of long-term circulation of hydrothermal solutions marked by telescoping hydrothermal metasomatic alteration [35] and structural-lithologic traps favorable for depositing of uranium mineralization were formed into the fault intersections. The preservation of ores was ensured here by subsidence and reductive hydrogeochemical conditions over a long time after ore-forming processes waned.

#### 4. CONCLUSIONS

Thus, the example of granitic environment of the basement and frame of the Streletsovskaya caldera shows long-term circulation of uranium-bearing hydrothermal solutions within the fault zone network from Late Proterozoic and Palaeozoic to Mesozoic and probably Cenozoic. The periodicity of the solutions in flowing into the fault zones is connected with alternative repulsion phases of structural and deformation processes during tectonomagmatic cycles. Four main cycles characterizing by inherent stressed-strained state of the rock massifs were identified namely Proterozoic, Caledonian, Variscan, and Late Mesozoic. The generation and activation (reactivation) of interblock regional fault zones occurred on a step-by-step basis during these cycles. The most long-living fluid-conducting structures are interblock NE-SW, NNE-submeridional, NW-SE and, probably, WNW-sublatitudinal faults. The oldest NE-SW faults and schistosity zones were formed during Proterozoic TMC with reactivation in T3-J2 stage due to global reorganization of stress field and reactivation of tectonic movements. The NNE-submeridional and NW-SE faults were extended with increased fluid permeability during Caledonian and Variscan TMCs (Fig. 2). They also were reactivated during Late Mesozoic TTA. Thus, already at early stages of geotectonic evolution within the knots of NE-SW and NNE-submeridional faults the areas of increased fluid and magmatic activity were formed.

The dynamics of fault formation in the basement and frame of the Streletsovskaya caldera and its volcano-sedimentary cover differs. The NE-SW, NNE-submeridional and NW-SE faults are interblock structures of the I rank in the basement and granite framework. Their knots formed areas of long-term circulation of hydrothermal solutions and telescopic appearance of multiage metasomatites that created conditions for localizing of vein-stockwork mineralization [36]. In volcano-sedimentary cover the NE-SW and NNE-submeridional faults should be considered as interblock structures of the I rank which knots provided inflow of ore-bearing solutions and their redistribution within the cover. Here the main ore distributing role belongs to NW-SE shears. They are intrablock II rank structures which were formed due to dextral strike-slip displacements along interblock faults during Late Mesozoic TTA. Within the

knots of NW-SE shears with stratified low-angle faults the conditions for forming of bedded deposits were created [35].

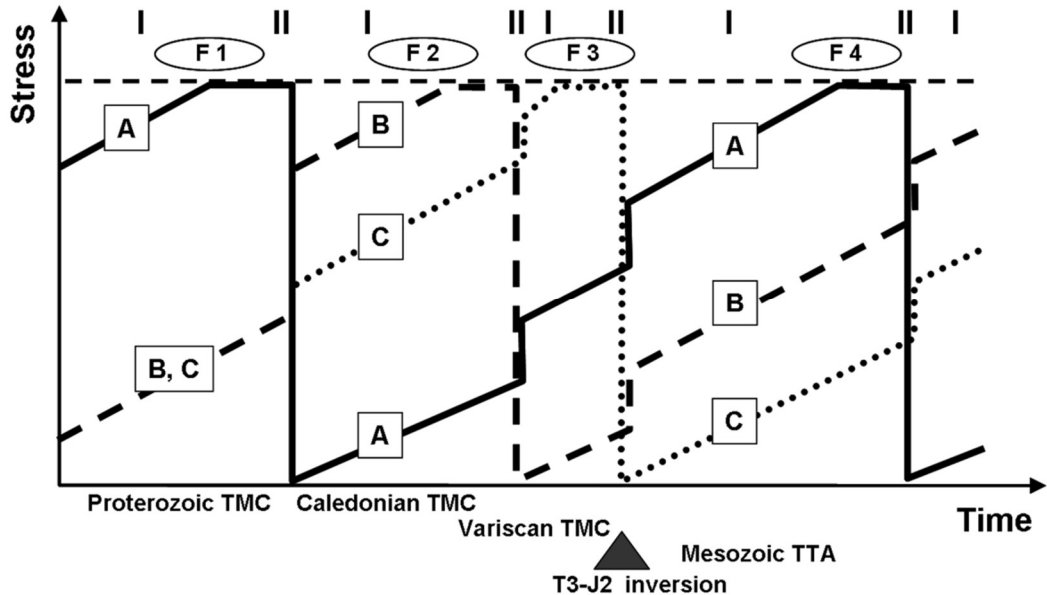


*FIG. 2. Stress-time dependence of fluid permeability for the fault zones in the basement and frame of the Streltsovskaya caldera: A – NE-SW, B – NNE-submeridional, C – NW-SE. Periods of stress accumulation (I) and relaxation (II) are accompanied by inflow of multiple-aged fluid portions committed to fluid inclusion generations (from F1 to F4) during various tectonomagmatic cycles (TMC) and regional tectonothermal activation (TTA).*

At the Palaeozoic and Mesozoic border (T3–J2) into the caldera north-western frame the pull-apart structure was developed. Dimension of the caldera and structure is comparable, and the latter is now hidden under K1-Q sediments of Sukhoy Urulunguy depression. Combination of palaeotectonic analysis and data on dynamics of ore-forming processes and fluid-conducting fault zone formation allows us to allocate three most perspective areas for carrying out prospecting activity (see Fig. 1). Two of them are located in Sukhoy Urulunguy depression in knots of NE-trending S-Urulunguy fault with submeridional Talan-Gozogor and Meridionalny faults. The areas have prerequisites for detecting hidden Late Mesozoic mineralization both in volcanosedimentary cover and basement. The third area is located in knot of NE-SW N-Urulunguy fault with meridional Chindachin fault where prerequisites for detecting mineralization in Proterozoic-Early Palaeozoic basement were found. It is supposed that these areas are mostly required for further prospecting activity and identification of additional uranium resources within the Streltsovskoe ore field.

#### ACKNOWLEDGEMENTS

We are hearty grateful to M. Lespinasse (University of Lorraine, France), J. Hammer (Federal Institute for Geosciences and Natural Resources, Germany), A. Burmistrov (Moscow State University), and R. Nasimov (Institute of Physics of the Earth, RAS) for long-standing collaboration. These studies were supported by the Presidium of RAS (programme no. 4), Division of Earth Sciences of RAS (program no. 2), and the Russian Foundation for Basic Research (project no. 12-05-00504-a).

## REFERENCES

- [1] INTERNATIONAL ATOMIC ENERGY AGENCY, World Distribution of Uranium Deposits (UDEPO) with Uranium Deposit Classification, IAEA-TECDOC-1629, IAEA, Vienna (2009).
- [2] ISHCHUKOVA, L.P. et al., Uranium Deposits of the Strel'tsovka Ore Field in Transbaikal Region, Geologorazvedka, Irkutsk (2007) (in Russian).
- [3] LAVEROV, N.P., VELICHKIN, V.I., VLASOV, B.P., ALESHIN, A.P., PETROV, V.A., Uranium and molybdenum-uranium deposits in regions of continental intracore magmatism development: geology, geodynamic and physical-chemical conditions of formation, IFZ RAS-IGEM RAS, Moscow (2012) (in Russian).
- [4] ANDREEVA, O.V., et al., Evolution of Mesozoic magmatism and ore-forming metasomatic processes in the south-eastern Transbaikal region, Russia, *Geol. Ore Deposits* **38** 2 (1996) 101–113.
- [5] SHATKOV, G.A., et. al., U-Pb (SIMS SHRIMP-II) age of volcanic rocks from the Tulukuev caldera (Streltsov uranium-ore cluster, Eastern Trasbaikalia), *Doklady Earth Sciences* **432** 1 (2010) 587–592.
- [6] DALHKAMP, F.J., *Uranium Deposits of the World: Asia*, Springer-Verlag Berlin Heidelberg (2009).
- [7] COX, S.F., Coupling between deformation, fluid pressures, and fluid flow in ore-producing hydrothermal systems at depth in the crust, *Econ. Geol.* **100** (2005) 39–75.
- [8] SIBSON, R.H., Earthquakes and rock deformation in crustal fault zones, *Ann. Rev. Earth Planet. Sci.* **14** (1986) 149–175.
- [9] PETROV, V.A., et. al., “Uranium mineralization in oxidized fractured environment of the giant volcanic-related uranium field from the Krasnokamensk area”, Proc. Int. Symp. on Uranium Production and Raw Materials for the Nuclear Fuel Cycle – Supply and Demand, Economics, the Environment and Energy Security, Proceedings Series, IAEA-CN-128, IAEA, Vienna (2006) 260–264.
- [10] PETROV, V.A., et. al., Stress-time context of fault permeability at the Krasnokamensk Area, SE Transbaikalia, *J. Physics: Conference Series* **416** (2013) doi:10.1088/1742-6596/416/1/012018.
- [11] GOLUBEV, V.N., et al., The Streltsovka uranium district: Isotopic geochronological (U-Pb, Rb-Sr, Sm-Nd) characterization of granitoids and their place in the formation history of uranium deposits, *Geol. Ore Deposits* **52** 6 (2010) 496–513.
- [12] GOLUBEV, V.N., Age of dispersed uranium mineralization in rocks of the framework of the Streltsovka uranium ore field and the Yamsky site, Eastern Transbaikal region, *Geol. Ore Deposits* **53** 5 (2011) 401–411.
- [13] SCHOLZ, C.H., *The Mechanics of Earthquakes and Faulting*, Cambridge Univ. Press, Cambridge (1990).
- [14] WOOD MUIR, R., Earthquakes, strain cycling and the mobilization of fluids, *Geofluids, Origin, Migration and Evolution of Fluids in Sedimentary Basins*, Geol. Soc. Spec. Publ. **78** (1994) 85–98.
- [15] PETROV, V.A., LESPINASSE, M., HAMMER, J., Tectonodynamics of fluid-conducting Structural elements and migration of radionuclides in massifs of crystalline rocks, *Geol. Ore Deposits* **50** 2 (2008) 89–111.
- [16] COWIE, P.A., A healing-reloading feedback control on the growth rate of seismic faults, *J. Struct. Geol.* **20** 8 (1998) 1075–1087.
- [17] NGUYEN, P.T., HARRIS, L.B., POWELL, C.McA., COX, S.F., Fault-valve behaviour in optimally oriented shear zones: An example at the Revenge Gold Mine, Kambalda, Western Australia, *J. Struct. Geol.* **20** 12 (1998) 1625–1640.
- [18] LESPINASSE, M., CATHELINÉAU, M., Fluid percolations in a fault zone: A study of fluid inclusion planes (F.I.P.) in the St. Sylvestre Granite (NW French Massif Central), *Tectonophysics* **184** (1990) 173–187.
- [19] LESPINASSE, M., Are fluid inclusion planes useful in structural geology?, *J. Struct. Geol.* **21** (1999) 1237–1243.

- [20] LESPINASSE, M., DESINDES, L., FRATCZAK, P., PETROV, V., Microfissural mapping of natural cracks in rocks: Implications on fluid transfers quantification in the crust, *Chemical Geology Spec. Issue* **223** (2005) 170–178.
- [21] ANGELIER, J. Tectonic analysis of fault slip data sets, *J. Geophys. Res.* **89 B7** (1984) 5835–5848.
- [22] MERCIER, J.L., CAREY-GAILHARDIS, E., SEBRIER, M., Palaeostress determinations from fault kinematics: application to the neotectonics of the Himalayas-Tibet and the Central Andes (WHITMARSH, R.B., BOTT, M.H.P., FAIHEAD, J.D., KUSZNIR, N.J. Eds), *Tectonic Stress in the Lithosphere*, *Philos. Trans. R. Soc. London* **337** (1992) 41–52.
- [23] PEARCE, J.A., HARRIS, N.B.W., TINDLE, A.G., Trace element discrimination diagrams for the tectonic interpretation of granitic rocks, *Journal Petrology* **25** (1984) 956–983.
- [24] RUTSHTEIN, I.G., CHABAN, N.N. (Eds), Geological structure of Chita region. Explanatory note to the geological map of scale 1:500000, Chita, SGUE Chitageolsyomka (1997) (in Russian).
- [25] WU, F.-Y., et. al., Geochronology of the Phanerozoic granitoids in northeastern China, *J. Asian Earth Sciences* **41** (2011) 1–30.
- [26] CHERNYSHEV, I.V., GOLUBEV, V.N., The Streltsovskoye deposit, eastern Transbaikalia: Isotope dating of mineralization in Russia's largest uranium deposit, *Geochem Intern.* **34** 10 (1996) 834–846.
- [27] DELVAUX, D., MOEYS, R., STAPEL, G., MELNIKOV, A., ERMIKOV, V., Palaeostress reconstructions and geodynamics of the Baikal region, Central Asia, Part I. Palaeozoic and Mesozoic pre-rift evolution, *Tectonophysics* **252** (1995) 61–101.
- [28] BERZINA, A.P., et. al., The Shakhtama porphyry Mo ore-magmatic system (eastern Transbaikalia): age, sources, and genetic features, *Geology and Geophysics* **54** 6 (2013) 764–786 (in Russian).
- [29] CHERNYSHEV, I.V., et. al., Age of granodiorite porphyry and beresite from the Darasun gold field, Eastern Transbaikal Region, Russia, *Geol. Ore Deposits* **56** 1 (2014) 1–14.
- [30] GRADSTEIN, F.M., OGG, G., The geologic time scale, *The Timetree of Life* (HEDGES, S.B., KUMAR, S., Eds), Oxford University Press (2009) 26–34.
- [31] RAHE, B., FERRILL, D.A., MORRIS, A.P., Physical analog modeling of pull-apart basin evolution, *Tectonophysics* **285** (1998) 21–40.
- [32] WALTER, T.R., TROLL, V.R. Formation of caldera periphery faults: an experimental study, *Bull. Volcanol.* **63** (2001) 191–203.
- [33] SHUMILIN, M.V., On the possibility of new discoveries in the Streltsovka ore field, *Geol. Ore Deposits* **49** 5 (2007) 413–415.
- [34] PETROV, V.A., SIM, L.A., NASIMOV, R.M., SHCHUKIN, S.I., Fault tectonics, neotectonic stresses, and hidden uranium mineralization in the area adjacent to the Strel'tsovka caldera, *Geol. Ore Deposits* **52** 4 (2010) 279–288.
- [35] ANDREEVA, O.V., GOLOVIN, V.A., PETROV, V.A., Wall-rock argillic alteration and uranium mineralization of the northwestern Strel'tsovka caldera, *Geol. Ore Deposits* **52** 1 (2010) 32–45.
- [36] PETROV, V.A., ANDREEVA, O.V., POLUEKTOV, V.V., Effect of petrophysical properties and deformation on vertical zoning of metasomatic rocks in U-bearing volcanic structures: a case of the Strel'tsovka caldera, Transbaikal Region, *Geol. Ore Deposits* **56** 2 (2014) 81–100.

# THE DIVERSITY OF RELATIONS BETWEEN FELSIC MAGMATISM AND URANIUM DEPOSITS

M. CUNÉY

GéoRessources, CNRS, CREGU,  
Vandoeuvre les Nancy Cedex, France

## Abstract

The strongly incompatible behaviour of uranium in silicate magmas results in its concentration in the most felsic melts and a prevalence of granites and rhyolites as primary U sources for the formation of U deposits. Despite the incompatible behavior of uranium, U deposits directly related to magmatic processes are quite rare. Generally, U is mobilized by hydrothermal fluids or ground water well after the emplacement of the igneous rocks. Only a few granite or volcanic rock types, have U contents and physico-chemical properties that permit the crystallization of accessory minerals from which U can be leached for the formation of a large diversity of U deposits. Four types of granites or rhyolites can be sufficiently enriched in U to represent a significant source for the genesis of U deposits: peralkaline, high-K metaluminous calc-alkaline, L-type peraluminous, and anatectic pegmatoids. The evaluation of the potentiality for igneous rocks to represent an efficient U source represents a critical step during the early stages of exploration. A wider use of magmatic inclusions to determine parent magma chemistry and its U content is of utmost interest to evaluate the U source potential of sedimentary basins that contain a felsic volcanic acidic tuff contribution.

## 1. INTRODUCTION

Uranium in silicate magmas exhibits a strongly incompatible behaviour because of its large ionic radius and high valence which prevents its incorporation into the structure of the main rock forming silicates. As a result, during partial melting and crystal fractionation, U is preferentially fractionated into silicate melts. Such a behaviour has several major geochemical, geophysical and metallogenetic consequences:

- 1) Through geological time U has been continuously transferred from the mantle to the Earth crust, and within the continental crust towards its upper part together with other incompatible elements and more particularly Th and K;
- 2) Consequently, radiogenic heat production is maximized in the upper crust, and thus radiogenic heat flux production distribution may be used to delineate radioelement enriched crustal blocks;
- 3) The most felsic melts tend to be the most enriched in U;
- 4) Granites and rhyolites represent the primary sources of uranium for the formation of U deposits. However, despite, the strongly incompatible behaviour of U, deposits dominantly resulting from magmatic processes are rare. In an average granitoid, with a U enrichment of 3 to 4 ppm, uranium is dominantly held within the crystal structure of accessory minerals [zircon, apatite, monazite, titanite, xenotime ...] from which U cannot be leached by most geological fluids. Only some specific granites have higher U contents permitting the crystallization of other types of accessory minerals from which U can be more or less easily leached for the formation of U deposits. On this basis [1] was the first to define the notion of "fertile granites", which has been very fruitful for U exploration.

## 2. THE DIFFERENT TYPE OF URANIUM-RICH MAGMATIC ROCKS

The three main types of magmatic rocks which can be enriched in U above their Clarke values, are distinguished according to in the A/CNK–A/NK plot [2]. They are the peralkaline, metaluminous, and peraluminous felsic magmatic rocks (Fig. 1). The use of an Al saturation index is particularly relevant for understanding the behaviour of U and associated incompatible elements such as Th, Zr, REE... in magmatic rocks because the fractionation of these elements is controlled by the solubilities of the accessory minerals such as monazite, zircon, uraninite, which in turn depend on the degree of Al

saturation of the silicate melt [2–5], as well as of temperature and volatile element content. The A-B diagram of [6] is also used to further refine the distinction between the different types of magmatic rocks, and to track the evolution of the Al saturation index during magmatic fractionation. Each of these rock types is characterized by a specific magmatic fractionation of Th and U and a specific accessory mineral paragenesis [7]. The distribution of U between the different accessory minerals is of critical importance for the genesis of U mineralization. A fourth type of magmatic rock enriched in U corresponds to weakly peraluminous granitoid rocks occurring in migmatitic domains. They are generally referred to as alaskite or anatetic pegmatoid.

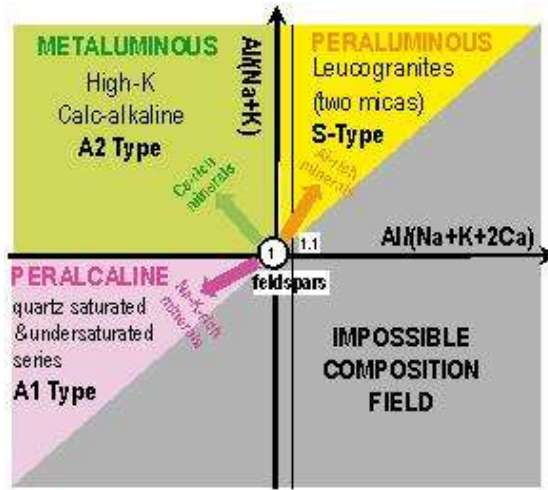


*FIG. 1. Diagram discriminating peraluminous, metaluminous and peralkaline igneous rocks [2]. Only the U-rich igneous rocks are indicated with their corresponding designation in the alphabetic classification. The arrows indicate the effect of an increasing abundance of the minerals at the origin of the Al, Ca and Na-K excess with respect to their ratios in feldspars.*

## 2.1. Peralkaline magmatic rocks

These rocks are characterized by an excess of alkalis, either Na or K, with respect to the amount Al bound to the feldspars (Fig. 1) and they are always enriched to variable degrees in high field strength elements and especially in U. They can be quartz saturated [peralkaline granites or rhyolites] or undersaturated (syenites or trachytes).

## 2.2. Metaluminous high-K calc-alkaline magmatic rocks

Certain metaluminous calc-alkaline magmatic rock family are enriched in K and other incompatible elements. Such magmatic rocks are called high-K calc-alkaline (HKCa) granite or shoshonitic granite when K-enrichment reaches levels above 5 – 6 wt%. These rocks are metaluminous because of an excess of Ca not balanced by Al as in the plagioclase structure. This Ca is hosted by Ca-rich minerals devoid of, or poor in Al, such as clinopyroxene, amphibole, titanite and allanite.

## 2.3. Peraluminous magmatic rocks

All magmatic rock with an A/CNK index greater than 1.1 have been defined as S-type by [8], because of their presumed derivation from the melting of metasedimentary rocks. However, in the A-B plot of [6] (Fig. 2) several types of contrasting fractionation trends can be differentiated within the peraluminous field composition: S-type granites [8] with a positive trend, Guéret-type granites (G-type) [9] with a negative trend, metaluminous calc-alkaline magmatic rocks also with a negative trend but rooted in the metaluminous field, L-type magmatic rocks corresponding either to biotite+muscovite±garnet±cordierite leucogranites, as exemplified by the peraluminous leucogranite complexes of Limousin (French Massif Central) [10] or the felsic volcanic rocks of Macusani in Peru [11].

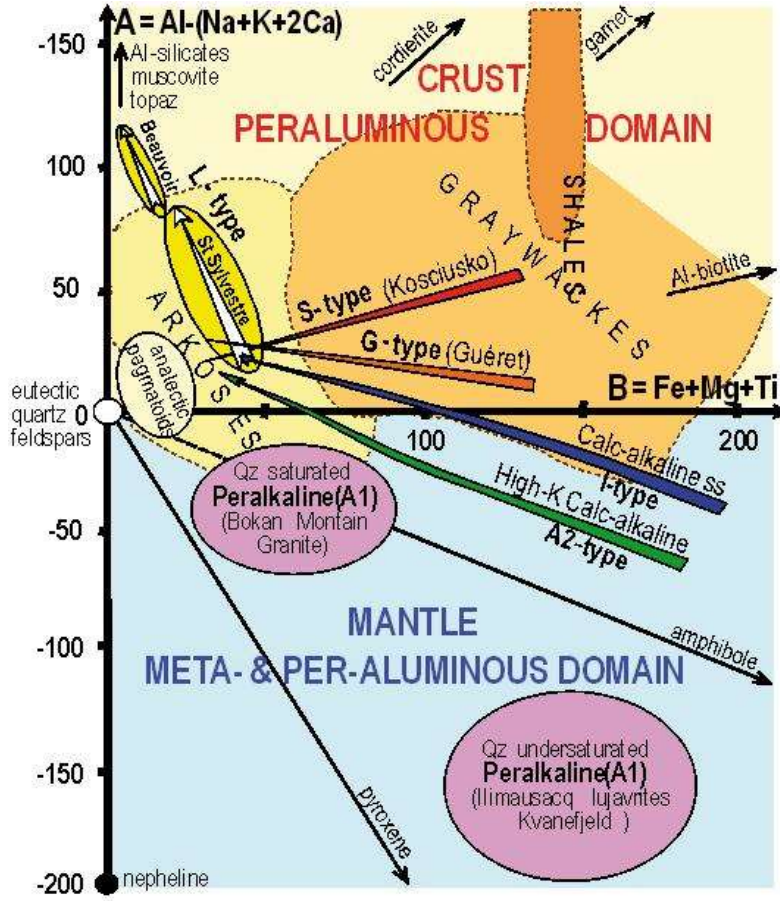


FIG. 2. Peraluminous [ $A = Al - [Na + K + 2Ca]$ ] versus differentiation [ $B = Fe + Mg + Ti$ ] indices diagram [6], discriminating various magmatic fractionation trends for igneous rocks. Composition fields of the major types of sedimentary rocks are represented. And = Andalusite, Sill = Sillimanite, Mus = Muscovite, Qz = Quartz, F[K] = K-feldspar, Plg = Plagioclase, Hyp = Hypersthene, Mgt = Magnetite, Ilm = Ilmenite, Hnb = Hornblende. Modified from [20].

#### 2.4. Anatectic pegmatoids

They always occur in high grade metamorphic rocks submitted to partial melting, generally injected as dykes of various size, more or less conformable with the foliation of the enclosing metamorphic rocks, with variable grain size and occur commonly as coarse grained unzoned pegmatoids. At Rössing in Namibia, they are referred to as alaskites. They are commonly weakly peraluminous due to their composition dominated by quartz and feldspars [12].

### 3. RELATIVE URANIUM FERTILITY OF U-RICH MAGMATIC ROCKS

Despite their U-enrichment, the magmatic rocks described above have not all the same potential to represent an efficient source of U for the genesis of U deposits.

#### 3.1. Peralkaline magmatic rocks

In peralkaline melts the excess of alkalis with respect to Al ( $Na + K/Al > 1$ ) and their high temperature, favor a strong melt depolymerization and consequently a high solubility of the incompatible elements, such as U, Th, Zr, Nb, Ta, REE [3–5]. Hence, U is continuously enriched with the other incompatible elements during magma fractionation, which all reach the highest concentrations in the most fractionated peralkaline melts. Typically, in peralkaline complexes Th (as well as Zr, REE) is positively correlated with U and their Th/U ratios remain close to the average crustal ratio during fractionation (Fig. 3). When crystallizing highly fractionated peralkaline plutons, abundant and complex Zr, REE, Th, Nb, and Ta minerals form with U as a minor element substituted in all these minerals [7]. Uraninite is generally not

able to crystallize despite the strong enrichment in U of these melts. Extreme fractional crystallization of peralkaline melts may lead to U, Th, Zr, and REE concentrations in the silicate melts up to several hundreds to thousands of ppm and more rarely up to several wt%. However, as U is hosted in accessory minerals it cannot be leached by fluids, and they do not represent a favourable U source. However, fractionated peralkaline rocks may represent significant U sources when the U hosting silicate minerals become metamict.

By contrast, peralkaline felsic volcanic rocks are excellent U sources, because most of the U is in the glass. When the glass is devitrified during alteration, U can easily be mobilized.

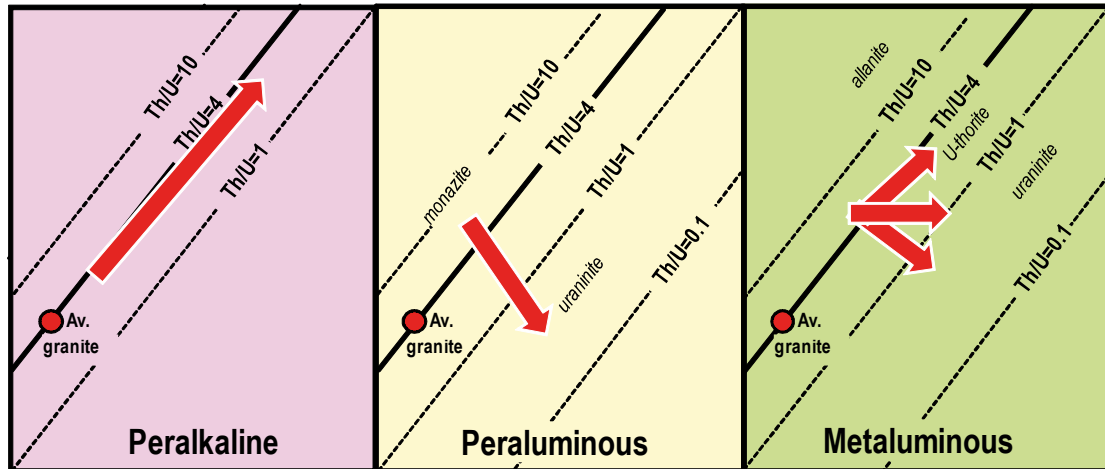


*FIG. 3. Evolution of Th and U contents and Th/U ratios during fractionation in U-rich peralkaline, peraluminous and metaluminous HKCa igneous rocks. Main U-bearing minerals specific of each igneous rock type are indicated according to their average Th/U ratio.*

### 3.2. High-K calc-alkaline magmatic rocks

HKCa magmas have intermediate to high temperatures and metaluminous to slightly peraluminous compositions which confer them variable degree of polymerization. Consequently, the solubility of Th-, Zr-, and REE-bearing accessory minerals is variable and the behaviour of Th, Zr and REE relatively to U will likewise vary (Fig. 3). Because of the high CaO contents of HKCa magmas, Ca-rich minerals such as amphibole, titanite and allanite crystallize. These minerals incorporate REEs as well as minor quantities of Th and U, that substitute easily for Ca together with in their structure. In a melt with a Th/U ratio close to 4, most of the U will be incorporated in the structure of uranothorite [13, 7]. This mineral, being refractory, U will not be leached by fluids circulating soon after the granite emplacement and thus will not represent a source for U deposits [7]. However, uranothorite and other Th- and U-rich silicate phases may become efficient U sources during later fluid circulation events when their structure becomes metamict [13, Error! Reference source not found.]

Allanite is the main U bearing host for high REE/Th ratios in HKCa melts, whereas Nb and Nb-Ti oxides become the main U bearing mineral for high Nb/Th ratios. When the Ca-content of HKCa melts is sufficiently low, monazite become stable and uraninite may crystallize. However, the proportion of uraninite is generally small and such fractionated granites generally represent only small volumes of HKCa complexes.

In conclusion, U-rich high-K calc-alkaline granites may become a significant U source for the formation of U deposits, when their U-bearing accessory minerals have become metamict or when they contain a significant proportion of uraninite. High-K calc-alkaline volcanic rocks may represent a significant U source if the magmas are fractionated and if the U is dominantly hosted by the glassy matrix rather than in accessory minerals.

### **3.3. Peraluminous magmatic rocks**

Peraluminous magmatic rocks cover a wide spectrum of magmas generated in different conditions. They can be distinguished in a A-B chemical-mineralogical diagram (Fig. 2).

#### *3.3.1. S-type peraluminous magmatic rocks*

S-type peraluminous magmatic rocks derive from high degrees of melting of source rocks which do not permit selective partial melting of protolith(s) enriched in U above the crustal Clarke value. During restite unmixing and magma fractionation, decreasing temperature leads to the fractionation of the U-bearing accessory minerals. Consequently, the enrichment in U in the residual melts is moderate, to a level insufficient to crystallize a significant proportion of uraninite. This type of granite is not known to be associated with U deposits.

#### *3.3.2. G-type magmatic rocks*

For G-type magmatic rocks, even if the crustal protolith undergoing partial melting was enriched in U, the U content of the melt will decrease because of its mixing with a metaluminous melt poor in U. Such granite is not known to be associated with U deposits.

#### *3.3.3. L-type magmatic rocks*

When enriched in U, they represent highly favorable U sources because U is dominantly hosted in Th-poor uraninite, easily leachable by hydrothermal fluids or ground waters. Crystallization of U – dominantly as uraninite – results from a succession of processes:

- 1) The protoliths submitted to melting have to be enriched in U significantly above the Clarke value for the upper continental crust [ $> 2.7 \text{ ppm}$ ], in order to have a large proportion of U hosted outside the structure of the accessory minerals;
- 2) The degree of partial melting has to remain low, to have preferential melting of quartz-feldspar-rich lithologies [meta-arkoses, felsic magmatic rocks] which are the ones the most likely enriched in U;
- 3) During fractional crystallization Th, REE and Zr contents decreases because of monazite and zircon fractionation. As these minerals incorporate only minor amounts of U, U continues to be enriched during fractionation until Th-poor uraninite crystallizes [7]. Uraninite represents a very easily leachable source of metal. In a Th [Zr, REE] versus U diagram, these elements are reversely correlated (Fig. 3), and the Th/U ratio of such granite decreases during fractionation.

Felsic highly peraluminous volcanic rocks equivalent to two-mica peraluminous leucogranites are rare. A typical example is the U-rich pyroclastic tuffs at Macusani in Peru [11]. They represent a very good source of U via devitrification of the glass by oxidizing fluids.

## **4. RELATIONS BETWEEN U DEPOSITS AND FELSIC MAGMATIC ROCKS**

U can be enriched either by magmatic processes, or by a variety of hydrothermal processes disconnected with the magmatic activity, or by a combination of magmatic and hydrothermal processes, as well as by leaching by ground waters at low temperature. These relations are reviewed following the genetic classification proposed by Cuney [14, 15].

### **4.1. Magmatic deposits**

#### *4.1.1. Fractional crystallization*

Peralkaline magmas lead to formation of the only type of U deposit related to extreme magmatic fractionation. Such an association can be extended to carbonatites such as Palabora, South Africa [16]. The U mineralization always occurs within the most fractionated intrusions of the peralkaline

complexes, located in their apical part or at their margins. These deposits may represent very large, low-grade U and Th resources, such as the Kvanefjeld deposit at Ilímaussaq, Greenland ( $> 250\,000$  t U at 200 ppm) [17, 18]. However, even if the U content of some deposits of this type are relatively high, they are not mined because of the high U extraction cost from refractory minerals. Locally, U, Th, and the REE may be transported by hydrothermal fluids up to several kilometres [Th veins, USA] from the intrusion.

#### *4.1.2. Partial melting*

Low degrees of partial melting of U-rich metasediments or felsic meta-magmatic rocks leads to the formation of anatetic pegmatoids with disseminated uraninite associated with highly variable amounts of other U-bearing accessory minerals. The type example is the Rössing deposit in Namibia (246 500 t U at 300 ppm) whose mineralization is hosted by granitic pegmatite sheets and small plutonic bodies, called alaskites [19, 20].

### **4.2. Hydrothermal deposits**

#### *4.2.1. Hydrothermal granitic U deposits*

They derive their U mostly from L-type peraluminous leucogranites [21]. The European Variscan Belt which extends for over 2000 km is the largest province of this type is with U deposits associated with Carboniferous leucogranites. Similar U provinces are known in southeastern China and in Argentinia. The U deposits are dominantly located within the granites in the French Variscides, or in their enclosing metamorphic rocks, in the Erzgebirge district. They occur as veins or as disseminations in de-quartzified granite (episyenite) [22].

HKCa granites may also represent a major source of U for hydrothermal deposits. At Hotagen, in Sweden, U-deposits occur within a Palaeoproterozoic HKCa granite but where U was subsequently precipitated during a Caledonian tectonic-hydrothermal event [23]. The large time difference between granite emplacement and hydrothermal circulations resulted in metamictization of uranothorite, the main U-bearing mineral, which becomes an easily leachable source of U. The U sources for the Olympic Dam deposit in Southern Australia are the host HKCa granites and overlying synchroneous HKCa volcanic rocks [24].

#### *4.2.2. Hydrothermal volcanic uranium deposits*

They are mostly related to peralkaline volcanic rocks. The world largest U district of this type [280 000 t U at 0.2%] is the late Jurassic Stretsovskoye caldera in Transbaikalia, Russian Federation. The exceptional size of the resources results from the juxtaposition of 4 main U sources:

- 1) Liparitic tuffs which represent 30 to 35 vol% of the volcanic pile;
- 2) Variscan U-rich high-K calc-alkaline granitoids in the basement [25];
- 3) Ordovician U mineralization in the basement [26];
- 4) Fluids expelled from the volcanic melts or from underlying magma chamber. A quantitative estimate of the amount of U liberated by the liparites is obtained from mass balance calculations between the U content of the melts inclusions from quartz trapped in the liparites and the average present U content of these rocks [25].

HKCa volcanic rocks are generally a less favorable U source because a significant portion of the U in these rocks tends to be trapped in accessory minerals [27]. Most deposits related to this type of volcanism have a relatively small size.

Highly peraluminous acidic volcanics, mineralized in U are known in the Macusani district, Peru. Pitchblende and autunite occur in fractures in Pliocene tuffs. A resource of 30 000 t U has been estimated for the whole Macusani district at an average grade of 0.1% U [28].

#### *4.2.3. Hydrothermal diagenetic U deposits od tabular or tectonolithologic type*

They may derive a large part of their U from volcanic tuffs, commonly of peralkaline origin, deposited within continental sandstone units of sedimentary basins and leached by diagenetic fluids as in the Arlit-Akouta U district in Niger with more than 100 000 t U at 0.3 % [29].

#### *4.2.4. Hydrothermal diagenetic U deposits with basement/basin redox control*

They are generally called unconformity related deposits They are characterized by large resources [631 000 t U] and comprised the highest-grade U deposits in the world. The source of U for these deposits is debated. For the Athabasca, it is proposed that U is derived either from the sandstone basin [30] or from the basement lithologies and especially the abundant U-rich peraluminous granites and pegmatites [31, 32]. Other possible sources include U-rich HKCa granites mainly emplaced in Talton Belt, to the west of the Athabasca Basin. It has been shown that, highly saline, acidic, and oxidizing hydrothermal diagenetic fluids [33, 34], were able to liberate U from a refractory mineral like monazite [35].

#### *4.2.5. Hydrothermal metasomatic U deposits*

Na-metasomatic U deposits are associated to regional scale alteration characterized by dequartzification, albitization and later Ca- and K-metasomatism [36]. The largest resources of this type are located in central Ukraine (280 000 t U at 0.08 to 0.13 %). The alteration may affect HKCa granites as at Lagoa Real in Brazil [100 000 t U at 0.12%] [37] and at Kurupung in Guyana [38], or HKCa metavolcanics in Labrador [36 800 t U at 840 ppm], Canada [39].

#### *4.2.6. Hydrothermal metasomatic U deposits associated with skarns*

In the Mary Kathleen U-REE deposit, Australia (8550 t U at 0.11%), the skarns result from an interaction between the U-Th-rich HKCa Burstall Granite ( $1737 \pm 15$  Ma) and enclosing calc-silicates, involving highly saline fluids derived from evaporites [40].

#### *4.2.7. Olympic Dam, a iron oxide-copper-gold [IOCG-U] deposit*

This is by far the world's largest U resource [2 200 000 t U at 230 ppm]. The deposit occurs in the highly fractionated HKCa Roxby Downs granite (1.59 Ga) emplaced at a very shallow structural level [41]. U source is probably the Roxby Downs granite and the Gawler Range volcanic rocks of similar geochemistry and age. However, the genetic model for the genesis of the U mineralization in the Olympic Dam deposit is still not very well understood, but the most likely U source is the enclosing granite and overlying volcanic rocks.

### **4.3. Other deposit types**

The first U deposits of the Earth, the Archean to Early Palaeoproterozoic Quartz Pebble Conglomerates [QPC] of the Dominion Reef and the Witwatersrand Basin in South Africa and the Elliot Lake district in Canada, derive their uraninite crystals of detrital origin, from Archean HKCa granites and pegmatites [42].

Many other types of U deposits may derive their U from spatially related U-rich granites or volcanic rocks. Such an origin is proposed for many roll front deposits from the Wyoming district, with an U derived either from U-rich Archean HKCa granites [43] or from interstratified volcanic ash [44]. Similar processes apply to the calcrete hosted deposits formed by evapotranspiration processes, with the type example represented by the Yeelerie deposit in Western Australia [45]. The relation between granites is still more direct in the palaeovalley U deposit type from the Vitim district in the Russian Federation which occur in organic matter bearing sandstone deposited in narrow valleys directly incised into HKCa granites [46].

For other U deposit types their relation with a magmatic U source is more tenuous. Large U grade differences exist between black shales and phosphorite-hosted deposits over the world. The high U content of the Cambrian Alum shale of Sweden [47], compared to other occurrences, may be explained from a provenance comprising the alteration of the U-rich Svecofennian granitic basement. Similarly, the high U content of the Moroccan phosphorites may derive from the presence of U-rich Hercynian granite in their source area. However, no specific study has yet been carried out to confirm such relationships.

## 5. CONCLUSIONS

U deposits may derive directly and dominantly from magmatic processes in the case of deposits related to extreme fractional crystallization of peralkaline rocks, or to partial melting of U-rich crustal protoliths. However most deposits are related to U leaching by hydrothermal and surficial fluids, much later than the emplacement of the U-rich magmatic rocks. U enrichment above the Clarke value is necessary for a granitic or volcanic rock to represent a viable U source for the formation of U deposits, but is not sufficient. In addition, U has to be hosted in a site from which it can be leached by oxidized hydrothermal fluids or ground waters. Uraninite represent the most easily leachable U source occurring mainly in highly fractionated peraluminous leucogranite and related pegmatites, in weakly peraluminous anatetic pegmatoids and less commonly in highly fractionated high K metaluminous granite and related pegmatites. U hosted in silicates, such as uranothorite, allanite, U-rich zircon and Nb-Ti-oxides can be leached easily only when the structure of these minerals is metamict.

## REFERENCES

- [1] MOREAU, M., et al., L'uranium et les granites, *Chron. Mines Rech. Min.* **350** (1966) 47–51.
- [2] SHAND, S.J., *Eruptive Rocks: Their Genesis, Composition, Classification, and Their Relation to Ore-Deposits*, John Wiley & Sons, New York (1943).
- [3] PEIFFERT, C., et al., Uranium in granitic magmas. 2. Experimental determination of U solubility and fluid-melt partition coefficients in the uranium oxide- haplogranite-H<sub>2</sub>O-NaX [X = Cl, F] system at 770°C 2 kbar, *Geochim. Cosmochim. Acta* **60** (1996) 1515–1529.
- [4] MONTEL, J.-M., A model for monazite/melt equilibrium and application to the generation of granitic magmas, *Chem. Geol.* **110** (1993) 127–146.
- [5] WATSON, E.B., HARRISON, T.M., Zircon saturation revisited: temperature and composition effects in a variety of crustal magma types, *Earth Planet. Sci. Lett.* **64** (1983) 295–304.
- [6] DEBON, F., LEFORT, P., A cationic classification of common plutonic rocks and their magmatic associations: principles, method, applications, *Bull. Minéral.* **111**(1988) 493–510.
- [7] CUNNEY, M., FRIEDRICH, M., Physicochemical and crystal-chemical controls on accessory mineral paragenesis in granitoïds, Implications on uranium metallogenesis, *Bull. Minéral.* **110** (1987) 235–247.
- [8] WHITE, A.J.R., CHAPPELL, B.W., Ultrametamorphism and granite genesis, *Tectonophysics* **43** (1977) 7–22.
- [9] STUSSI, J.M., CUNNEY M., Modèles d'évolution géochimique de granitoïdes peralumineux. L'exemple du complexe plutonique varisque du Millevaches [Massif central français], *Bull. Soc. Géol. France* **164** (1993) 585–596.
- [10] CUNNEY, M., et al., Metallogenesis in the French part of the Variscan orogen, Part I: U-preconcentrations in the pre-Variscan and Variscan formations - A comparison with Sn, W and Au, *Tectonophysics* **177** (1989) 39–57.
- [11] PICHAVANT, M., et al., The Mio-Pliocene Macusani volcanics, SE Peru II: geochemistry and origin of a felsic peraluminous magma, *Contrib. Mineral. Petrol.* **100** (1988) 325–338
- [12] CUNNEY, M., The extreme diversity of uranium deposits, *Miner. Dep.* **44** (2009) 3–9.
- [13] ALEXANDRE, P., Mineralogy and geochemistry of the sodium metasomatism-related uranium occurrence of Aricheng South, Guyana, *Mineral. Dep.* **45** (2010) 351–367.
- [14] CUNNEY, M., Evolution of uranium fractionation processes through time: driving the secular variation of uranium deposit types, - *Econ. Geol.* **105** (2010) 449–465.

- [15] CUNNEY, M., Uranium and Thorium Resources and Sustainability of Nuclear Energy, Uranium: Cradle to Grave (BURNS, P., Ed.), MAC Short Course Series **43** (2013) 417–438.
- [16] VERWOERD, W.J., “Mineral deposits associated with carbonatites and alkaline rocks”, Mineral Deposits of Southern Africa. Vol. 2. Geological Society of South Africa, Johannesburg (1986) 2173-2191.
- [17] SØRENSEN, H. (Ed.), The Ilímaussaq complex, South Greenland: status of mineralogical research with new results, Geol. Greenland Surv. Bull. **190** (2001) 167.
- [18] STEENFELT, A. On the behavior of uranium during crystallization of magmas – with special emphasis on alkaline magmas, in Formation of Uranium Ore Deposits: Proceedings of a Symposium on the Formation of Uranium Ore Deposits, Organized by the International Atomic Energy Agency and Held in Athens, Greece, Vol. 374 (1974). International Atomic Energy Agency.
- [19] BERNING, J., COOKE, R., HIEMSTRA, S.A., HOFFMAN, U., The Rössing uranium deposit, South West Africa. Econ. Geol. **71** (1976) 351–368.
- [20] CUNNEY, M., KYSER, K., Recent and not-so-recent developments in uranium deposits and implications for exploration, Mineral. Assoc. Canada, Short Course Series **39** (2008) 257.
- [21] FRIEDRICH, M., CUNNEY, M., POTY, B., Uranium geochemistry in peraluminous leucogranites, Uranium **3** (1987) 353–385.
- [22] LEROY, J., The Margnac and Fanay U deposits of the La Crouzille district [Western Massif Central, France], geologic and fluid inclusion studies, Econ. Geol. **73** (1978) 1611–1634.
- [23] TRÖENG, B., WILSON, M.R., “Geological setting of uranium mineralization in the Hotagen area, central Swedish Caledonides”, Geology of Vein- and Similar type Uranium Deposits, Panel Proceedings Series, IAEA, Vienna (1981) 65-85.
- [24] HITZMAN, M.W., VALENTA, R.K., Uranium in Iron Oxide-Copper-Gold [IOCG] systems, Econ. Geol. **100** (2005) 1657–1661.
- [25] CHABIRON, A., CUNNEY, M., POTY, B., Possible uranium sources for the largest U district associated with volcanism: the Steltsovka caldera (Transbaïkalie, Russia), Mineral. Dep. **38** (2003) 127–140.
- [26] CHERNYSHEV, I.V., GOLUBEV V.N., The Strel'tsovskoe deposit, Eastern Transbaikalia: isotope dating of mineralisation in Russia's largest U deposit, Geokhim. **10** (1996) 924–937 (in Russian).
- [27] LEROY, J., GEORGE-ANIEL, B., Volcanism and uranium mineralisations: the concept of source rock and concentration mechanism, J. Volcan. Geotherm. Res. **50** (1992) 247–272.
- [28] OECD NUCLEAR ENERGY AGENCY, Forty Years of Uranium Resources, Production and Demand in Perspective “The Red Book Retrospective”, OECD/NEA, Paris (2006)
- [29] FORBES, P., PACQUET, A., CHANTRET, F., OUMAROU, J., PAGEL, M., Marqueurs du volcanisme dans le gisement d'uranium d'Akouta (République du Niger), C. R. Acad. Sci., Paris **298** (1984) 647–650.
- [30] FAYEK, M., KYSER, K., Characterization of multiple fluid events and rare-earth-element mobility associated with formation of unconformity- type uranium deposits in the Athabasca Basin, Saskatchewan, Canad. Mineral. **35** (1997) 627–658.
- [31] ANNESLEY, I.R., MADORE, C., Leucogranites and pegmatites of the sub-Athabasca basement, Saskatchewan: U protore?, Mineral Deposits: Processes to Processing (STANLEY C.J. et al., Eds), Balkema **1** (1999) 297–300.
- [32] MERCIADER, J., ANNESLEY, I.R., MCKECHNIE, C.L., BOGDAN, T.S., CREIGHTON, S., Magmatic and metamorphic uraninite mineralization in the western margin of the Trans-Hudson Orogen (Saskatchewan, Canada]: major protores for unconformity-related uranium deposits, - Econ. Geol. **108** 5(2013) 1037-1065.
- [33] DEROME, D., CATHELINÉAU, M., CUNNEY, M., FABRE, C., LHOMME, T., Evidences of brine mixing in the McArthur River unconformity-type uranium deposit (Saskatchewan, Canada], Implications on genetic models. Econ. Geol. **100** 8 (2005) 1529–1545.
- [34] RICHARD, A., et al., Giant uranium deposits originate from exceptionally U-rich brines, Nature Geosci. **5** 2 (2012) 142–146.
- [35] HECHT, L., CUNNEY, M., Hydrothermal alteration of monazite in the Precambrian basement of the Athabasca Basin: implications for the genesis of unconformity related deposits, Mineral Dep. **35** (2000) 791–795.

- [36] CUNNEY, M., EMETZ, A., MERCADIER, J., MYKCHAYLOV, V., SHUNKO, V., YUSLENKO, A., U deposits associated with sodium metasomatism from Central Ukraine: a review of some of the major deposits and genetic constraints, *Ore Geology Review* **44** (2012) 82–106.
- [37] TURPIN, L., MARUEJOL, P., CUNNEY, M., Comparative U-Pb, Rb-Sr and Sm-Nd chronology of granitic basement, hydrothermal albitites and uranium mineralization (Lagoa Real, South-Bahia, Brazil), *Contrib. Mineral. Petrol.* **98** (1988) 139–147.
- [38] ALEXANDRE, P., Mineralogy and geochemistry of the sodium metasomatism-related uranium occurrence of Aricheng South, Guyana, *Mineral. Dep.* **45** (2010) 351–367.
- [39] GHANDI, S.S., Geological setting and genetic aspects of uranium occurrences in the Kaipokok Bay-Big river area, Labrador. *Econ. Geol.* **73** (1978) 1492–1522.
- [40] OLIVER, N.H.S., PEARSON, P.J., HOLCOMBE, R.J., ORD, A., Mary Kathleen metamorphic hydrothermal uranium - rare-earth element deposit: ore genesis and numerical model of coupled deformation and fluid flow, *Austral. J. Earth Sci.* **46** (1999) 467–484.
- [41] CREASER, R.A., Petrogenesis of a Mesoproterozoic quartz latite-granitoid suite from the Roxby Downs area, South Australia, *Precamb. Res.* **79** (1996) 371–394.
- [42] FRIMMEL H.E., et al., The formation and preservation of the Witwatersrand goldfields, the largest gold province in the world, *Economic Geology* **100** (HEDENQUIST, J.W., THOMPSON, J.F.H., GOLDFARB, R.J., RICHARDS, J.P., Eds) (2005) 769–797.
- [43] STUCKLESS, J.S., NKOMO I.T., Uranium-lead isotope systematics in uraniferous alkali-rich granites from the Granite Mountains, Wyoming: implications for uranium source rocks, *Econ. Geol.* **73** (1978) 427–441.
- [44] ZIELINSKI, R.A., Tuffaceous Sediments as Source Rocks for Uranium - A Case Study of the White River Formation, Wyoming, *J. Geochem. Explor.* **18** (1983) 285–306.
- [45] CARLISLE, D., MERIFIELD, P.M., ORME, A.R., KOHL, M.S., KOLKER, O., LUNT, O.R., The distribution of calcrites and gypcretes in southwestern United States and their uranium favorability based on a study of deposits in Western Australia and South West Africa (Namibia), US Dept. of Energy. Open File Rpt GJBX-29 (1978).
- [46] KONDRAT'EVA, I.A., MAKSIMOVA, I.G., NAD, G.I., Uranium Distribution in Ore-Bearing Rocks of the Malinov Deposit: Evidence from Fission Radiography, *Litholog. Mineral. Res.* **39** (2004) 333–344.
- [47] ANDERSSON, A., DAHLMAN, B., GEE, D.G., SNÄLL, S., The Scandinavian Alum Shales, *Sveriges Geolog. Unders., Serie Ca: Avhandlingar och Uppsatser I A4 NR56* (1985) 1-50.
- [48] PAGEL, M., The mineralogy and geochemistry of uranium, thorium, and rare-earth elements in two radioactive granites of the Vosges, France, *Min. Mag.* **46** (1982) 152–163.

# CENTRAL UKRAINE URANIUM PROVINCE: THE GENETIC MODEL

A. EMETZ\*, M. CUNEV\*\*

\*Institute of Geochemistry,  
Mineralogy and Ore Formation of NASU,  
Kyiv, Ukraine

\*\*GeoRessources, Nancy-Université, CNRS, CREGU,  
Vandoeuvre les Nancy, France

## Abstract

This paper presents a descriptive genetic model of the Central Ukraine Uranium Province (CUUP), the largest U Province related to Na-metasomatism around the world. It is located in the Palaeoproterozoic metamorphic-magmatic complexes of the Ukrainian Shield. Na-metasomatic alterations are fault-controlled, regionally extended along crustal scale tectonic fault structures. Economic U-mineralization follows brittle deformations in extensive areas of multistage metasomatites spatially controlled by ductile to brittle deformation structures. The Na-metasomatism model suggests interaction of the host rocks with heated marine water infiltrating along the structures. U mineralization is related to later percolation of hydrothermal fluids resulting in Ca- and K-metasomatic alterations.  $^{87}\text{Sr}/^{86}\text{Sr}$ ,  $\delta^{13}\text{C}$  and  $\delta^{18}\text{O}$  isotopic data characterize a deep crustal source for the mineralizing hydrothermal fluids related to the crust dehydration during metamorphism. An enrichment in HFSE and LILE may indicate their derivation from the last stage granitic melts enriched in incompatible elements and reflecting melting within zones of contrasting thickness in the lithosphere induced by a mantle plume and evidenced by successive magmatic events from regional injection of basic dyke swarms to decompression melting with emplacement of a large A-type granitic batholith.

## 1. INTRODUCTION

U deposits related to sodium metasomatism are found throughout the world [1, 2], but the largest, and most intensely explored deposits occur in Ukraine where this type of deposit was first recognized about 65 years ago [3]. Presently, the Ukraine U mining industry produces 1100 t U per year from the Central Ukraine U Province (CUUP) which includes the Kirovograd and Kryvy Rig U districts comprising about 20 U deposits and numerous U showings related to the Palaeoproterozoic Na-metasomatism [1]. Geoenvironmental and modern geochemical-mineralogical review of Na-metasomatites in Ukraine was reported in [1] whereas early research results on the CUUP are mostly summarized in [3].

Large U resources in Na-metasomatites are also presently mined in the Palaeoproterozoic terrains of Brazil [4]. Besides, U mineralization associated with Na-metasomatism developed in metamorphic, granitic or volcanic rocks was documented worldwide [1] and may represent large resources as in Ukraine (over 300 000 t U), Brazil (over 100 000 t U) and Canada (50 000 t U) [5, 6]. However, the processes controlling the localization of U mineralization in Na-metasomatites are poorly known [2]. This paper proposes a model for the development of Na-metasomatism and U-mineralization in the CUUP, starting from general structural, tectonic and geological position, using mineral and whole rock geochemistry. The proposed model provides new tools for the delineation of prospective territories having a potential to host U deposits associated with Na-metasomatites.

## 2. REGIONAL ENVIRONMENT

The CUUP extends W-E over about 150 km across the Ingul Megablock of the Ukrainian Shield (Fig. 1). The metamorphic and magmatic rocks in the CUUP are covered by up to several tens meters of the Cenozoic sediments.

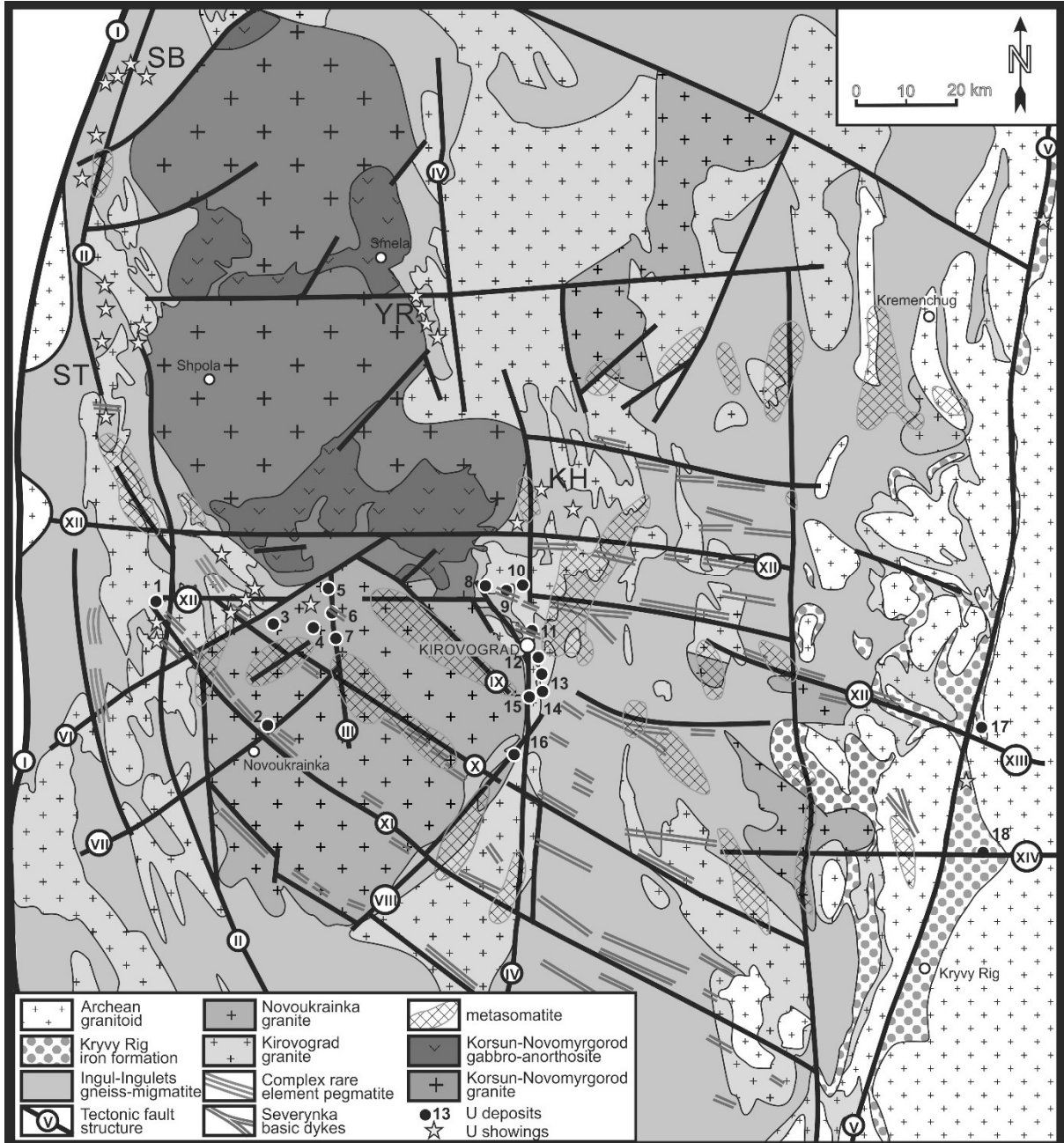


*FIG. 1. The central Ukrainian province in the frame of the geological map of the Ingul megablock. Tectonic structures: (I) Golovanivsk–Yadlov–Traktemyriv; (II) Zvenygorod – Bratsk; (III) Novokostantynivka; (IV) Kirovograd; (V) Kryvy Rig – Kremenchug; (VI) Glodosk, (VII) Adabash, (VIII) Maryivska, (IX) Krupska, (X) Anikeyevka, (XI) Novoukrainka, (XII) Subotin – Mashorin, (XIII) Spasivska, (XIV) Devladivska. U deposits: (1) Vatutinske, (2) Partyzanske, (3) Kvitneve, (4) Lisne, (5) Novokostantynivka, (6) Litne, (7) Dokuchayivka, (8) Schorsivska, (9) Pidgaytsi, (10) Severynivske, (11) Central, (12) Michurinske, (13) Northern Konoplanka, (14) Southern Konoplanka, (15) Western Konoplanka, (16) Yuryivske, (17) Zhovta Richka, (18) Pervomayske. U showing fields: ST – Stetsivske; SB – Steblivske; KH – Kohanivske; YR – Yarovske.*

## 2.1. Regional geological position

The Ingul megablock is the central one of the five megablocks constituting the Ukrainian Shield [7]. It consists of Archean to Palaeoproterozoic metamorphic and magmatic complexes. To the west, it is bounded by the Golovanivsk–Yadlov–Traktemyriv crustal scale shear zone marking the contact between the Ingul megablock and the Bila Tserkva–Mid Bug megablock composed of the Mesoarchean supracrustal domains (Fig. 1). The eastern margin of the Ingul Megablock consists of the Mesoarchean

granitic basement and Lower Palaeoproterozoic granite-gneiss units (Fig. 1). The N-S striking Kryvy Rig — Kremenchug crustal scale fault marks the eastern border of the Ingul megablock and the western side of the Fore – Mid-Dnieper megablock of Mesoarchean age (3.0 to 2.8 Ga) [8].

## 2.2. Major rock complexes

The Ingul-Ingulets gneiss series and Kirovograd, Novoukrainka and Korsun-Novomygorod granitoid complexes are dominant in the Ingul megablock. The Kryvy Rig series fills a range of linear synclines along the Kryvy Rig — Kremenchug shear zone and represents coastal facies of the Ingul-Ingulets series [1]. Basic and rare earth pegmatite dykes widely occur in the CUUP.

*The Kryvy Rig series* are folded and thrusted and consists of the following units (from the base to the top): (i) New Kryvy Rig (mainly metabasaltic rocks) covering the Mesoarchean granitoids, (ii) Skelevatsk (siliciclastic metasedimentary rocks), (iii) Saxagan (schists, iron quartzites and hornfels) and (iv) Gdantsi (graphite schists, calcsilicates and marbles).

*The Ingul-Ingulets series* comprises para- and orthogneisses derived from terrigenous-volcanogenic strata accumulated at 2.3 – 2.1 Ga and metamorphosed at ~2.0 Ga into biotitic gneisses with different proportions of amphibole, pyroxene, garnet, cordierite and graphite under P-T condition of amphibolite to granulite facies [1]. The gneisses are migmatized and folded with a general N-S strike. Their total thickness exceeds 10 km in the central parts of the Ingul megablock. In the eastern margin of the Ingul megablock, the series includes layers of iron quartzite correlated with the iron formations of the Kryvy Rig area [1].

*The Kirovograd granitoid complex* is composed of grey to rose-grey, fine- to medium-grained and porphyritic mostly peraluminous S-type granitoids [9] forming plutonic bodies, up to  $80 \times 30$  km in size (Fig. 1). Many Kirovograd granite bodies present a gradual transition from migmatized gneisses to granitoids. They were derived from melting of the host gneisses at  $2060 \pm 42 - 2026 \pm 46$  Ma [10] and were preferentially injected along N-S structures in the Ingul-Ingulets strata.

*The Novoukrainka granitoid complex* which covers an area of  $\sim 3500$  km $^2$ , was emplaced at  $2039 \pm 6 - 2025 \pm 48$  Ma [10]. Smaller intrusions occur in the eastern part of the Ingul megablock (Fig. 1). The complex consists mainly of red porphyritic coarse-grained garnet-biotite granites and adamellites (70 – 80% of the complex) and of quartz diorites and quartz monzonites [9]. The granitoids exhibit a strong magmatic foliation defined by the alignment of large K-feldspar megacrysts, suggesting about magma crystallization at regional stress [11]. Drilling shows the dominance of grey orthopyroxene granitoids at depth. Geochemically, the Novoukrainka granitoids vary between S-type peraluminous and A-type metaluminous granites [9]. Deep seismic survey indicates the floor of the batholith at a depth of 15 – 20 km [12]. The similar ages of the Novoukrainka and Kirovograd granitoids suggest their synchronous emplacement, but the Novoukrainka melt should derive from deeper crust.

*Rare element pegmatites* of petalite and spodumene subtypes occur as swarms of veins and dykes, up to 30 – 50 m in thickness, injected along N-S trending faults intersecting the Ingul-Ingulets gneisses and Kirovograd granitoids. They are mostly found along the Zvenygorod–Bratsk tectonic zone in the Vatutynske and Stankovatske Li – rare element ore fields (Fig. 1). Numerous pegmatite veins in this zone occur along the faults controlling the Vatutynske U deposit. A K/Ar age of  $1800 \pm 35$  Ma has been obtained on a muscovite from the Polohivske Li-pegmatites of the Vatutynske field [13]. The spodumene ( $\pm$  pollucite) granite pegmatite veins, up to 5 – 8 m thick, are also known in the Zhovta Richka U deposit.

*The Severynka basic dykes* occur along NW-SE and W-E trending tectonic structures. They crosscut U deposits and thus at least in part are younger than U-mineralized albites. U-Pb ages of  $1774.3 \pm 7.4$  Ma has been obtained on zircons from a dyke striking E-W along the Subotin-Mashorin tectonic zone [14]. Zircons from NW-SE dolerite dykes were dated at  $1800 \pm 30$  Ma and  $1760 \pm 40$  Ma [15].

*The Korsun-Novomygorod granitoid complex* covers an area of  $\sim 5000 \text{ km}^2$ . It consists of anorogenic A2-type rapakivi granites [9] and associated anorthositic rocks and mafic intrusions injected within the crust during decompression melting at  $1754 \pm 4 - 1725 \pm 11 \text{ Ma}$  [10, 16]. In contact with the batholith, the host rocks including U-mineralized albitites were metamorphosed.

## 2.3. Geotectonic environment

The regional, deposit-scale and local-scale environments of Na-metasomatites and U ores of the CUUP are similar. All the deposits are fault-controlled both regionally and locally, and present a range of similarities in relation to tectonic structures.

### 2.3.1. Regional tectonic control

At a regional scale, the CUUP extends W-E along the Subotin-Mashorin crustal scale tectonic structure (Fig. 1). However, the location of the major U deposits is strongly controlled by four crustal scale tectonic structures trending N-S, which are from west to east: the Zvenygorod–Bratsk, Novokostantynivka, Kirovograd, and Kryvy Rig–Kremenchug structures (Fig. 1). Several U deposits and numerous fields of barren metasomatites are also controlled by the NW-SE and SW-NE tectonic systems in the Kirovograd ore district (Fig. 1). The W-E and NW-SE structures also control the Severynka dyke injections (Fig. 1). The tectonic structures are well identified from seismic and gravimetric data [12]. They consist of en echelon or parallel second-order faults developed alongside the major structures. These tectonic zones have had a protracted activity, from high temperature ductile regimes to lower temperature brittle deformation regimes [1]. The earliest extreme deformations have led to the formation of bodies of blastomylonites, up to several tens meters in thickness.

*The Kryvy Rig–Kremenchug tectonic structure* strikes N-S over 230 km through the Ukrainian Shield. It comprises a synclinorial linear structure, up to 10 km wide, filled with the Kryvy Rig metamorphic strata. The western side of the syncline is bordered by the first order Kryvy Rig crustal-scale fault dipping  $60-70^\circ$  west and separating the 47–53 km thick crust of the western margin of the Fore–Mid-Dnieper megablock from the 40–43 km thick crust of the Ingul megablock **Error! Reference source not found.**. Second order structures dipping mostly west include both thrusts and normal faults. Na-metasomatites are common in the Kryvy Rig strata. In the Kryvy Rig ore district, two U deposits are known in the metasomatites of the Pervomaysk (the Pervomaysk U deposit) and Zhovta Richka (the Zhovta Richka U deposit) synclines, at the intersection between the Kryvy Rig–Kremenchug faults and the Devladivska and Spasivska sublatitudinal fault structures, respectively (Fig. 1).

*The Kirovograd tectonic structure* is up to 25 km wide, dips  $60-80^\circ$  E and trends N-S over 200 km. It borders the Novoukrainka and Korsun-Novomygorod batholiths to the east. A sharp offset of 5–10 km of the Moho depth is visible beneath the Kirovograd structure along the seismic profile “IV” (Fig. 2). It separates the eastern thinner crust of the Ingul megablock from the thickened crust beneath the Novoukrainka batholiths. 22 km northward, along the profile “XXV”, the Kirovograd tectonic structure marks a 2-km reverse offset of thinned crust of the Korsun-Novomygorod batholith. Alongside the Novoukrainka batholith, the Kirovograd structure controls numerous fields of Na-metasomatites including most U deposits recently found in the CUUP and located in the Michurynske, Lelekivske and Kompaniyivske U ore fields (Fig. 1). To the north, close to the Korsun-Novomygorod batholith, the structure controls the Kohanivske and Yarovske U showings (Fig. 1).

*The Novokostantynivka tectonic structure* is several hundred meters to 1.5–2 km wide, trends N-S over  $\sim 25$  km and divide the Novoukrainka batholith into two parts. The fault zone dips  $45-55^\circ$  E and is well recognized as a range of linear magnetic and gravimetric anomalies [9]. The Korsun–Novomygorod batholith crosscuts the Novokostantynivka faults to the north. In the central northern part of the Novoukrainka batholith it controls the Novokostantynivka field of U deposits (Fig. 1).

*The Zvenygorod–Bratsk tectonic structure* is up to 10 km wide, deeps  $50-70^\circ$  E and trends submeridionally over  $\sim 250$  km along the western border of the Novoukrainka and Korsun–Novomygorod batholiths **Error! Reference source not found.**. It corresponds to a sharp distortion of

the seismic reflectors with no clear offset. The structure controls the Vatutynske U ore field located to the north-west of the Novoukrainka batholith, and numerous fields of albitization including Stetsivske and Steblivske U showings beside the Korsun-Novomygorod batholith.

*The Subotin-Mashorin tectonic structure* represents a 20–30 km wide fault zone, trending W-E over ~200 km across the Ingul megablock with a 70–80° S dip (Fig. 1). It separates the Novoukrainka and Korsun-Novomygorod batholiths and displaces the Moho down from ~40 km beneath the Korsun-Novomygorod batholith to 43–46 km beneath the northern side of the Novoukrainka batholith.

### 2.3.2. Mantle related constraints

The Subotin-Mashorin structure confines the northern slope of the W-E extended Moho depression found beneath the northern side of the Novoukrainka batholith [12, 17] and reflecting the crust thickening from overall of 40–42 km up to 43–46 km (Fig. 2). Most U deposits and complex rare element pegmatites of the Kirovograd U district are located along its northern margin beside the younger Korsun-Novomygorod batholith and only a few deposits are found along the southern margin (Fig. 2). The Kryvy Rig U district is also located at the western margin of the thicker crust block along the Kryvy Rig–Kremenchug fault zone (Fig. 2). Thus, the location of the U deposits of the CUUP are constrained by the Moho offsets inducing lateral changes of heat flow, P-T parameters and therefore representing the ‘weakness’ zones favorable for reworking of tectonic fault structures and crustal melting, and circulation of deeply derived fluids.

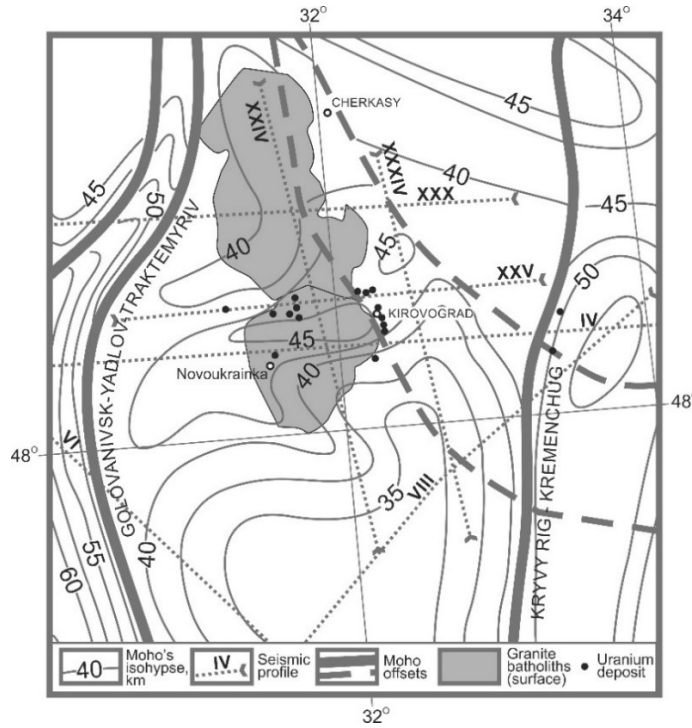


FIG. 2. Moho depth in the Ingul megablock from deep seismic survey data (modified after [17]).

### 2.3.3. Local structural position

The metasomatites intermittently follow the major tectonic fault structures for up to several kilometers. The strike of the structures undulates, especially at the intersection with other tectonic structures. In such places, the major faults ramify into an echelon and flower-like strike slip structures consisting of second and third order faults, and the host metamorphic and magmatic rocks are extensively fractured and brecciated. These structures are intensively metasomatized and locally control a single or few U ore zones following brittle deformations in Na-metasomatites. Locally, the brittle deformations controlling the metasomatic alterations follow bedding and layering of the metamorphic strata as in the Vatutynske

and Zhovta Richka U deposit. Structure-controlled morphology ranges from the gently dipping ore zones of the Partyzanske U deposit, to steep and nearly vertical ore zones in other U deposits.

#### 2.3.4. Shape and size

Shape and size of the metasomatic bodies vary significantly, reflecting structural control of the hydrothermal activity. The metasomatic bodies may reach several hundred meters in intensively fractured and brecciated structures. They form massive zones of irregular alteration, plate-like and complex shaped bodies controlled by tectonic faults. U-mineralized bodies are also fault-controlled and form lense-, pipe-, plate-like and complex shaped bodies within Na-metasomatites. With depth, metasomatic alterations gradually pinch out. U deposits in the CUUP have been partly eroded and weathered. Presently, vertical extent of the U mineralization varies from several hundred meters (the Michurynske and Vatutynske deposits) to more than one kilometer in some deposits (the Novokostantynivka, Zhovta Richka and Severynivske U deposits).

### 3. ORE CHARACTERISTICS

#### 3.1. Grade and tonnage

Average grade of U deposits in the metasomatites of the CUUP varies from 0.05 to 0.20 wt% U. U reserves in the deposits are large and reach 93 600 t U in the largest Novokostantynivka U deposit (mining commenced in 2008). Also, mining is presently active in the Michurynske (26 800 t U), Centralne (60 000 t U) and Vatutynske (26 000 t U) U deposits of the Kirovograd U district. Other deposits of similar grade and tonnage are expected to be mined in future. The Zhovta Richka (18 900 t U) and Pervomaysk (11 000 t U) U deposits of the Kryvy Rig U district discovered in 1945–1946 were mined out several decades ago [3]. All the deposits are/were mined by underground technique. U-ore dressing and production in Ukraine is actually provided by the Eastern ore dressing and processing enterprise (S'hidGZK) located in Zhovti Vody city, Dnipropetrovsk region. For the total period of mining the Ukrainian U industry produced ~50 000 t U.

#### 3.2. Gangue mineralogy variance

The mineralogical characteristics of the metasomatites from the Kirovograd and Kryvy Rig ore districts differ [1]. Metasomatites of the Kirovograd ore district occur as episyenites and albitites whereas the Kryvy Rig metasomatites correspond to albitites, aegirinites and riebeckitites. U ore bodies are mostly localized in albitites. According to femic mineral composition, albitites are classified into aegirine, riebeckite, garnet-epidote, actinolite, phlogopite-biotite and chlorite-epidote albitites. Mixed varieties of albitites are common. Phlogopite-biotite albitites contain most U ores and do not occur in barren metasomatites mostly composed by aegirine, riebeckite and/or chlorite-epidote albitites. At the contact with the Korsun-Novomygorod batholith (Andriyivske and Kohanivske U showings) the albitites have been metamorphosed, the diopside-hornblende-actinolite paragenesis replaces the previous femic minerals [3].

##### 3.2.1. Mineral associations

Mineral associations corresponding to five successive stages of hydrothermal alteration are observed in the mineralized metasomatites of the CUUP: (i) dequartzification; (ii) Na-metasomatism; (iii) Ca-metasomatism; (iv) K-metasomatism; (v) chloritization-epidotization [1, 20].

*Dequartzified rocks* result from selective quartz leaching from the host rocks before Na-metasomatism to give the so called episyenites [1]. Dequartzified rocks surround or occur within the Na-metasomatites. Minor development of riebeckite and partial albitization of feldspar are common in episyenites.

*Na-metasomatites* mineral composition depends on the chemical composition of the host rocks [1]. Quartz-feldspar gneiss and granite of the Kirovograd ore district were altered to aegirine and riebeckite

albitites. In the Kryvy Rig ore district, mineralogically contrasting beds of the Kryvy Rig series were altered into aegirine and riebeckite albitites, aegirinites and riebeckitites.

*Ca-metasomatites* fill new zones of brittle deformations within Na-metasomatites after their ductile deformations. Femic minerals of Na-metasomatites (aegirine and riebeckite) were in part to completely replaced by the andradite–titanite–epidote–actinolite–calcite paragenesis. The new mineral paragenesis also includes hydrothermal apatite, tourmaline and irregular U-mineralization.

*K-metasomatites* occur after some cooling of the hydrothermal solutions [1]. Widespread calcite–phlogopite paragenesis indicates gradual transitions between the Ca- and K-alteration events. Laminar phlogopite and biotite are major minerals of the K-metasomatites. Adularia is rare. Calcite–phlogopite albitites correspond to the major U-ores, associated with hydrothermal zircon and minor sulphides of Fe, Cu and Ni.

*Chorite–epidote* albitites correspond to the last stage with crystallization of disseminated epidote ( $\pm$  calcite,  $\pm$  barite) veinlets and chloritization of femic minerals. Chloritization is superimposed on all earlier metasomatite types. Chlorite–epidote albitites are widespread in barren metasomatite fields. U was remobilized and in part redeposited.

### 3.3. Uranium minerals

Uranium mineralogy in the deposits of the CUUP is uniform. Major minerals are U-titanates (davidite and brannerite) and uraninite which occur as disseminations, rarely as veinlets. Visible uraninite and brannerite occur only locally. Uraninite replaces U-titanates and forms single microcrystals, microcrystalline aggregates, or pitchblende spherolites. Both U-titanates and uraninite commonly replace Fe-minerals (magnetite, ilmenite, Fe-amphiboles, aegirine–augite). Coffinite occurs locally. Hexavalent U-minerals (uranophane and boltwoodite) were formed during oxidation of U-ores by meteoric water infiltration [1].

#### 3.3.1. Age of mineralization

TIMS and SIMS U-Pb dating of U-minerals of the CUUP embraces ages from 1820 to 1750 Ma [3, 21, 22]. The oldest uraninite was found in the Partyzanske deposit ( $1810 \pm 5$  Ma) [3] and Novokostantynivka deposit ( $1822 \pm 12$  Ma) [22]. These dates are close to the age of the Severynka basic dykes injected at  $1774.3 \pm 7.4$  Ma [14],  $1800 \pm 30$  Ma and  $1760 \pm 40$  Ma [15] and intersecting the metasomatites. The injection of complex rare element pegmatite dikes of the Vatutynske ore field, dated by K/Ar TIMS at  $1800 \pm 35$  Ma [13] may represent another magmatic event related to the U-mineralization.

## 4. ELEMENT AND ISOTOPIC GEOCHEMISTRY

Major element transfer during the mineral alteration stages is well illustrated on the P-Q diagram [20] (Fig. 3): (i)  $\text{SiO}_2$  loss = quartz leaching; (ii)  $\text{Na} \rightarrow \text{K}$  exchange = conversion of granite or episyenite into aegirine–riebeckite albitite; (iii) crystallization of Ca-silicates and calcite with dissolution of Na-minerals; (iv)  $\text{K} \rightarrow \text{Na}$  exchange = replacement of Na-silicates by phlogopite/biotite. As demonstrated using Grant's isocone diagrams [1, 20], trace elements were significantly transferred only during Na-, Ca- and K-metasomatism stages.

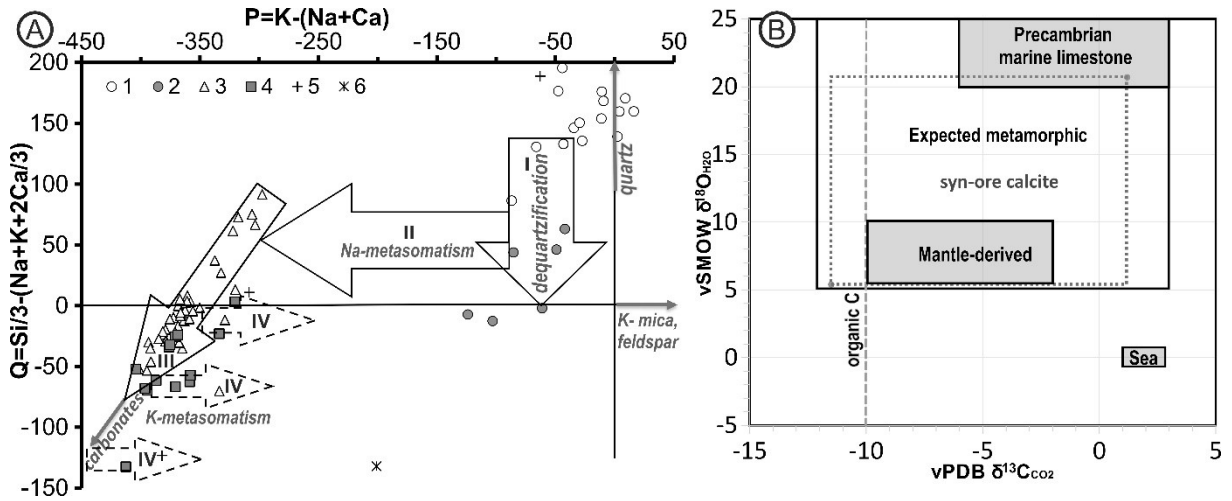


**FIG. 3.** (A)  $Q - P$  diagram for the host rocks and metasomatites of the CUUP. 1: host granites and gneiss; 2: episyenites; 3-4: albrites; 3: < 0.2 wt % U; 4: > 0.2 wt % U; 5: aegirinites and riebeckitites; 6: U-mineralized iron-calcareous metasomatite of the Zhovta Richka deposit. Arrows: I: dequartzification; II: albitization; III: Ca-metasomatism; IV: K-metasomatism. (B) Isotopic characteristics of syn-ore calcite.

#### 4.1. Sodium metasomatism

Na-metasomatism resulted in element transfer of only a few elements [1, 20]: Na, Ca and V were deposited and Si, K, Rb, Ba and Cs were removed.  $\text{Fe}^{2+}$  minerals were converted into  $\text{Fe}^{3+}$ -minerals, suggesting oxidative properties of the incoming fluids.

Summary data on  $\delta^{18}\text{O}$  in albite from the U deposits (3.5 to 8.2‰) [1], and  $\delta^{18}\text{O}$  and  $\delta\text{D}$  in fluid inclusions from albite of the Novokostantynivka deposit (−3.1 to 0.7‰ and −38 to −180‰, respectively) [1] characterize meteoric fluids in part equilibrated with the host rocks during infiltration.

#### 4.2. Calcium metasomatism

Ca-metasomatism resulted in dissolution of Na-silicates with removal of Na, Si, Al and V, and accumulation of Ca, Sr, Mg,  $\text{Fe}^{2+}$  and U [1, 20].

Calcite has a broad range of  $\delta^{13}\text{C}$  (from −0.8 to −13.5‰) and  $\delta^{18}\text{O}$  (from 10.7 to 26.0‰) which might reflect diverse metamorphic sources (Fig. 3B). Initial  $^{87}\text{Sr}/^{86}\text{Sr}$  ratio in calcite ( $0.7152 \pm 2$  to  $0.7271 \pm 2$ ) [23] indicates fluids derived from  $^{87}\text{Sr}$  rich source. The lowest  $^{87}\text{Sr}/^{86}\text{Sr}$  ratio of 0.7092 detected in apatites from the mineralized albrite of the Dokuchayivka deposit [24], exceeds the values characterizing either the 1.8 Ga mantle or oceanic water [25]. The  $^{87}\text{Sr}/^{86}\text{Sr}$  ratios are mostly lower than the  $^{87}\text{Sr}/^{86}\text{Sr}$  ratio of  $0.72409 \pm 2$  of the apatites from the host Novoukrainka granites [24], and thus indicate fluids derived from lower to upper crustal sources less enriched in radiogenic  $^{87}\text{Rb}$  in comparison with the Novoukrainka granite.

#### 4.3. Potassium metasomatism

K-metasomatism is associated with the removal of Na, Si, Al, V, Fe whereas Ca, K, Mg, Rb, Cs, F, U, Zr, Th, Y and REE are enriched [20]. These elements may derive from fluids expelled from highly fractionated granitic melts. New crystallization of hydrothermal zircon with suprachondritic Zr/Hf ratio reflects infiltration of Hf-poor solutions that may derive from Zr-Hf fractionation during felsic pegmatitic melt evolution [20].

#### 4.4. P-T conditions

Maximum temperature during Na-metasomatism was estimated up to 450 – 500°C from the temperature regime required for ductile deformation of albite and from riebeckite thermometry [1]. These temperatures correspond to a pressure of  $250 \pm 20$  MPa using a geothermal gradient of 50°C/km [26], typical of geothermal fields ( $\sim 9.5 \pm 0.8$  km in lithostatic pressure conditions). Maximum temperature of Ca-metasomatism is constrained by andradite crystallization, which is estimated from its occurrence in modern geothermal fields (300–360°C) [1]. A pressure of  $180 \pm 20$  MPa is obtained using the same lithostatic geothermal gradient. Temperature of K-metasomatism was estimated from homogenization temperatures of fluid inclusions in calcite crystals syngenetic with laminar phlogopite of the Novokostantynivka deposit at  $180 \pm 30$ °C [1] corresponding to  $50 \pm 10$  MPa for hydrostatic geothermal gradients of 50 to 30°C/km.

### 5. REGIONAL MODEL

#### 5.1. Na-metasomatism

##### 5.1.1. Regional tectonic regime

Regional-scale development of Na-metasomatites along diversely trending tectonic structures requires a large-scale tectonic process providing the hydrothermal activity through the entire Ingul megablock. As demonstrated above, they preceded or were in part synchronous with the Severynka basic dyke injections occurring prior an emplacement of the Korsun-Novomygorod anorogenic rapakivi granite – gabbro-anorthosite complex. These successive magmatic events followed Na-metasomatism and are interpreted as reflecting the evolution of a mantle plume during extensional tectonic regime inducing decompression melting: from flowing out flood basalts to the emplacement of A-type granitic batholith. Thus, Na-metasomatism occurred during the early stages of the regional extension.

##### 5.1.2. Source of mineral forming solutions

Uniform regional-scale mineral alterations of the host rocks during Na-metasomatism resulted in exchange of Si, Fe<sup>2+</sup>, K, Rb, Ba and Cs by Na, Ca, Fe<sup>3+</sup> and V by oxidizing hydrothermal fluids.  $\delta^{18}\text{O}$  and  $\delta\text{D}$  isotopic values of these fluids indicate a surficial origin. These data suggest host rock interaction with hot marine waters convecting along permeable fault zones, induced by an increased heat flow event (Fig. 4).

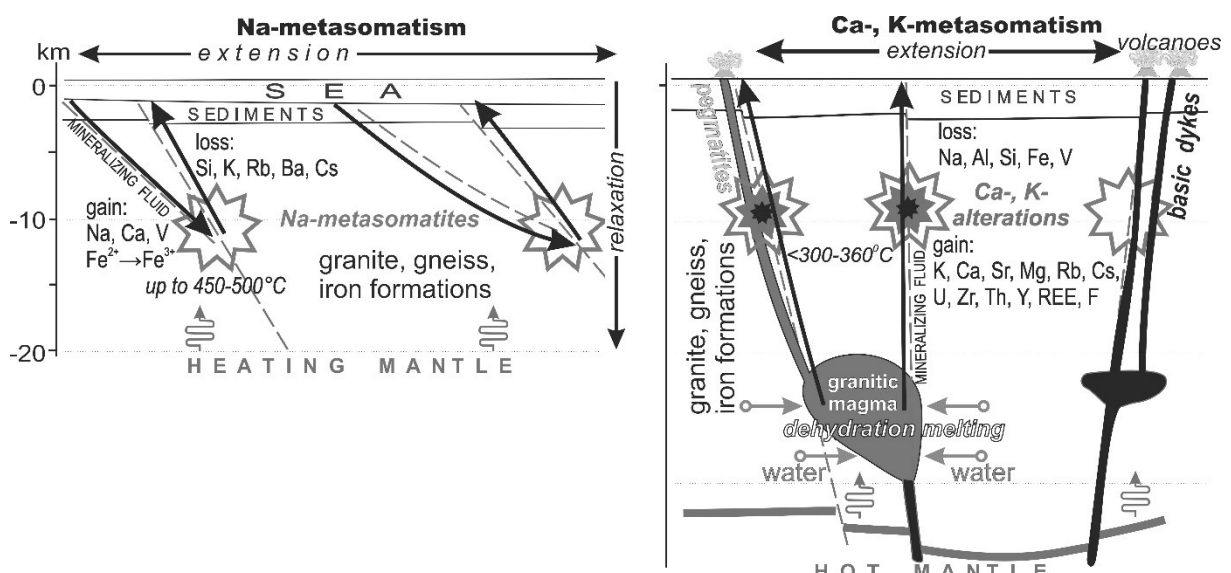


FIG. 4. Models of metasomatic alteration and plume-related dyke magmatism in the Ingul megablock.

## **5.2. Ca- and K-metasomatism, and U-mineralization**

### *5.2.1. Tectonic regime*

Both the Kirovograd and Kryvy Rig U ore districts are constrained by several kilometres vertical offsets of the mantle, which correspond to the Moho depression beneath the Kirovograd ore district and the tectonic margin between the Fore-Mid-Dnieper and Ingul megablocks (Fig. 2). They indicate crustal-scale tectonic faulting with rapid changes of the P–T parameters along the crustal-mantle boundaries, inducing crustal melting in response to increased heat flow. This may also explain the injections of rare metal pegmatites along the Zvenygorod-Bratsk tectonic structure. The several kilometres offset of the Moho induces difference of heat flow in the adjacent blocks, resulting in contrasting thermal expansion during plume-related heating [27]. This may have reactivated crustal scale tectonic structures in the Ingul megablock providing the channels for the fluids responsible for the formation of the metasomatites (Fig. 4). The renewed hydrothermal activity resulted in Ca- and K-metasomatism stages associating with U ore deposition.

### *5.2.2. Source of mineral forming solutions*

Calcite precipitation during Ca-metasomatism demonstrates a broad range of carbon and oxygen isotopic ratios that comply with variable metamorphic source of CO<sub>2</sub> and H<sub>2</sub>O. The depth of such source was varying from upper to lower crust as suggested by wide variations in the enrichment of hydrothermal calcite and apatite in radiogenic <sup>87</sup>Sr implying K(<sup>87</sup>Rb)-mineral abundance in the source. The hydrothermal solutions delivered Ca, Sr, Mg and Fe<sup>2+</sup>, which may reflect dissolution of metasedimentary carbonates during crust dehydration initiated by the increased heat flow. Fluid inclusion data indicate that the transition from Ca-metasomatism to K-metasomatism occurred under gradual collapse and concomitant cooling of the hydrothermal systems. HFSE (U, Zr, Th, Y and REE), LILE (K, Rb and Cs) and F may have been derived from the fluids expelled from highly fractionated granitic melt similar to the rare element granite pegmatites of the Vatutynske ore field. Such magmatic sources may have formed through high-temperature dehydration (biotite, amphiboles) melting of the deep-seated metamorphic rocks poor in chalcophile elements (Fig. 4). The Novoukrainka batholith provides a sheet in the upper crust, which would stimulate the crustal melting during injections of the mantle magma. With cooling and solidification, the magmas were fractionated, saturated by water and eventually emanated the mineralizing hydrothermal solutions which tunnelled the crustal scale tectonic fault zones and reacted with chemically contrasting Na-metasomatites (Fig. 4).

### *5.2.3. U transport and deposition*

The richest U mineralization was precipitated during formation of phlogopite-calcite paragenesis. U-minerals were deposited during the crystallization of F-bearing minerals (phlogopite, biotite, tourmaline) but the richest U ores are enriched in Th and other HFSE that can be transported by fluorine complexes. These data suggest that carbonate-uranyl and carbonate-fluorine-uranyl complexes were the major transport medium for U in mineralizing solution. Replacement of Fe-bearing minerals by the reduced U-minerals and common haematite pigmentation of the mineralized rocks suggest that the oxidation of Fe<sup>2+</sup> was responsible for the reduction of uranyl ions:  $U^{6+}_{\text{solution}} + 2Fe^{2+}_{\text{mineral/solution}} = U^{4+}_{\text{mineral}} + 2Fe^{3+}_{\text{solution/mineral}}$ .

## **ACKNOWLEDGEMENTS**

Authors thank to the Chief Geologists of S'hidGZK Vereschagin O., Sinchuk V. and Yuslenko A. for helps in sampling and field works. A. Emetz thanks to IAEA for a grant enabling him to participate to the URAM 2014 Symposium.

## REFERENCES

- [1] CUNNEY, M., EMETZ, A., MERCADIER, J., MYKCHAYLOV, V., SHUNKO, V., YUSLENKO, A., Uranium deposits associated with Na-metasomatism from central Ukraine: A review of some of the major deposits and genetic constraints, *Ore Geology Reviews* **44** (2012) 82–106.
- [2] WILDE, A., Towards a model for albitite-type uranium. *Minerals* **3** (2013) 36–48. ANDERSON, Y.B., TARHANOV, A.B., ZASLAVSKY, V.G., Age interrelations of uranium ore formation and regional metamorphism in Zhovta Richka deposit, *Sovetskaya Geologiya* **12** (1987) 64–69 (in Russian).
- [3] BELEVTSOV, Y.N. et al., Genetic types and regularities in placement of uranium deposits of Ukraine, Naukova Dumka press, Kiev (1995) (in Russian).
- [4] LOBATO, L.M., FYFE, W., Metamorphism, metasomatism and mineralisation at Lagoa Real, Bahia, Brazil, *Econ. Geol.* **85** (1990) 968–989.
- [5] RUHLMANN, F., et al., Un exemple de metasomatisme alcalin albite uranium dans le bassin des Monts Otish Quebec, *Can. J. Earth Sci.* **23** (1986) 1742–1752.
- [6] KISH, L., CUNNEY, M., Uraninite–albite veins from the Mistamisk Valley of the Labrador Trough. *Québec. Mineralog. Mag.* **44** (1981) 471–483.
- [7] GLEVASSKI, E.B., KALAYEV, G.I., Precambrian tectonics of the Ukrainian Shield, *Mineral. J.* **22** (2000) 77–79 (in Russian).
- [8] SCHERBAK, N.P., et al., Geochronology of Early Precambrian of the Ukrainian Shield, Archean. Naukova Dumka Press, Kiev (2005) (in Russian).
- [9] EMETZ, A., et al., Petrology, tectonogenesis and dating of the Paleoproterozoic granite magmatism and alkali metasomatism of the Ukrainian Shield, Sc. report No 0112U008169, IGMOF NASU, Kiev (2012) (in Ukrainian).
- [10] CUNNEY, M., et al., Petrological and geochronological peculiarities of Novoukrainska massif rocks and age problem of uranium mineralisation of the Kirovograd Megablock of the Ukrainian Shield, *Mineral. J.* **2** (2008) 5–17.
- [11] PATERSON S.R., et al., A review of criteria for the identification of magmatic and tectonic foliations in granitoids, *J. Struct. Geol.* **11** (1989) 349–363.
- [12] STAROSTENKO, V.I., et al., Kirovograd ore district: Deep structure, Tectonophysical analysis, Deposits of ore minerals, Prastyi Ludy, Kiev (2013) (in Russian).
- [13] NECHAYEV S.V., Mineralogical zoning of the central part of Ukrainian Shield and some general geological consequences of its investigations, Collections of Sci. Works of UkrSGRI 2 (2012) 38–57.
- [14] SHUMLYANSKY, L., et al., “Isotope systematics of the Ukrainian shield kimberlites”, Alkaline Rocks: Petrology, Mineralogy, Geochemistry (Abstract Conf. Kiev, 2010), IGMOF, Kiev (2010).
- [15] SAVITSKY, A.V., KAZANSKY, V.I., “Results of petrophysical investigations of ore-bearing faults of crystalline basement”, Internal Structure of the Ore-bearing Precambrian Faults (TOMSON, I.N., Ed.), Nauka Press, Moscow (1985) 48–73 (in Russian).
- [16] SHUMLANSKY, L., et al., U–Pb zircons isotopic age of the Korsun–Novomyrgorod anorthosite–rapakivi–granite pluton, *Geol. Ukraine* **1–2** (2008) 77–85 (in Ukrainian).
- [17] SOLOGUB, V.B., Lithosphere of Ukraine, Naukova Dumka Press, Kiev (1986) (in Russian).
- [18] KOMAROV, A.N., “Tectonic-magmatic zones of the Ukrainian Shield, their structural position and forming conditions”, *Ore Formation and Metallogeny* (BELEVTSOV, Y.N., Ed.), Naukova Dumka Press, Kiev (1981) 45–53 (in Russian).
- [19] STAROSTENKO, V.I., et al., From superficial structures to integral deep model of the Kirovograd ore district (Ukrainian Shield), II, *Geophysical J.* **5** (2011) 5–18.
- [20] CUNNEY, M., EMETZ, A., The Novokostantynivka U deposit: geology, mineralogical composition and geochemical constraints, *Econ. Geol.* (in review).
- [21] EMETZ, A., et al., “Chemical Composition and age of uraninite of the Zhovta Richka uranium deposit (Ukraine)”, International Congress on Applied Mineralogy (Proc. Cong. Trondheim, 2011) (BROEKMAN, A.T.M.M., Ed.), Springer, Berlin Heidelberg (2012) 153–161.
- [22] EMETZ, A., et al., Chemical composition and age of uraninite of the Novokostantynivka uranium deposit (Ukraine) (in preparation).

- [23] SCHERBAK, D.N., Conditions of formation of uranium-bearing albitites of the Novokostantynivka zone, PhD Thesis, IGFM, Kiev (1981) (in Russian).
- [24] STEPANIUK, L.M., et al., Source of sodium and uranium of uranium-bearing albitites (by example of the Dokuchayivka deposit of the Ingul megablock of the Ukrainian Shield), *Geochemistry and Ore Formation* **31-32** (2012) 99–104.
- [25] FLAMENT, N., COLTICE, N., REY, P.F., The evolution of the  $^{87}\text{Sr}/^{86}\text{Sr}$  of marine carbonates does not constrain continental growth, *Precambrian Research* **229** (2013) 177–188.
- [26] SANDIFORD, M., HAND, M., MCLAREN, S., High geothermal gradient metamorphism during thermal subsidence, *Earth Planet. Sci. Lett.* **163** (1998) 149–165.
- [27] DUESTERHOEFT, E., BOUSQUET, R., WICHURA, H., OBERHÄNSLI, R., Anorogenic plateau formation: the importance of density changes, *J. Geophys. Res.* **117** (2012) 1–13.

# GRANITE-RELATED HYPOTHERMAL URANIUM MINERALIZATION IN SOUTH CHINA

X. LIU, J. WU, J. PAN, M. ZHU

Key Laboratory of Nuclear Resources and Environment,  
Ministry of Education,  
East China Institute of Technology, Nanchang,  
Jiangxi, China

## Abstract

As one of the important geological types, granite-related uranium deposits account for about 29% of the total discovered natural uranium resources in China. Most of the granite-related uranium deposits are located in Taoshan-Zhuguang uranium metallogenic belt, South China. In addition to the typical pitchblende vein type uranium mineralization of epithermal metallogenic system, a new type of granite-related uranium mineralization with characteristics of hypothermal metallogenic system was discovered in South China by current studies. However, hypothermal is a relative term when contrasted to epithermal mineralization and not the conventional intrusive high temperature mineralization. Hypothermal uranium mineralization is presented by disseminated uraninite or pitchblende stockwork in fissured granites normally with extensive alkaline alteration. The high temperature mineral assemblage of uraninite associate with scheelite and tourmaline was identified. Fluid inclusion studies indicated middle to high temperatures ( $> 250^{\circ}\text{C}$ ) with the evidence of mixing of ore forming solutions derived from deep levels. The boiling and mixing of ore forming solution are regarded as the dominant mineralization mechanism for the precipitating of uranium. In contrast to the mineralization ages of 67 Ma to 87 Ma for typical pitchblende vein type mineralization of epithermal metallogenic system, the mineralization age is older than 100 Ma for hypothermal uranium mineralization in granite. In the Shituling deposit in Xiaozhuang uranium ore field, uraninite and pitchblende micro veins with extensive potassic alteration, chloritization and sericitization are hosted in fissured Indo-Chinese epoch granites with the uranium mineralization age of 130 Ma to 138 Ma and the mineralization temperature of  $290^{\circ}\text{C}$  to  $330^{\circ}\text{C}$ . More examples sharing the similar characteristics of hypothermal uranium mineralization have been recognized in Taoshan, Xiaozhuang and Nanxuiyang areas, South China. Detailed geodynamic studies reveal that hypothermal uranium mineralization in granites occurs in the areas with lithospheric extension in crust thickening geological setting. This new type of uranium mineralization in granite is now considered as the new target for future exploration.

## 1. DISTRIBUTION OF GRANITE-RELATED URANIUM DEPOSITS IN CHINA

According to the geological setting and the spatial distribution of different type uranium deposits, the new subdivisions for uranium deposits in China were divided into Palaeo-Asian, Qin-Qi-Kun, Marginal-Pacific and Tethys 4 uranium metallogenic domains with 11 uranium provinces and 49 metallogenic regions/belts [1]. While granite-related uranium deposits, such as the well known Zhuguang and Xiaozhuang granite-related uranium ore fields, mainly distributed in Taoshan-Zhuguang and Chenzhou-Qinzhou metallogenic belts, South China uranium province. Most of the discovered typical pitchblende veins granite-related uranium deposits in South China have the mineralization ages less than 100 Ma with the ages of 60 Ma to 90 Ma in the main uranium mineralization stage.

## 2. GENERAL CHARACTERISTICS OF GRANITE-RELATED HYPOTHERMAL URANIUM MINERALIZATION

Current studies on granite-related type uranium deposits in south China reveal that, in addition to the typical pitchblende vein granite-related uranium deposits, a new pattern of the uranium mineralization characterized by relatively higher mineralization temperature with extensive alkaline alterations in fissured granites have been recognized in south China [2–4]. Such as the hypothermal uranium mineralization in Shituling deposit, Xiaozhuang granite-related uranium ore field. Uranium mineralization is dominated by coffinite micro-veins or disseminated uraninite in fissured biotite monzogranite with extensive potassic alteration, chloritization and sericitization (Fig. 1). The isotopic age for host granite is of  $238 \pm 2.3$  Ma, while the mineralization ages by U-Pb dating method for uranium minerals range from 130 Ma to 138 Ma. Results of fluid inclusion studies indicated that the temperature

for uranium mineralization in this deposit ranges from 290°C to 338°C. Another typical hypothermal mineralization example is presented by Lanhe granite-related deposit in north Guangdong province, which shares similar characteristics to Shituling deposit that pitchblende micro-veins or stockworks distributed in potassic alteration granite (Fig. 2).

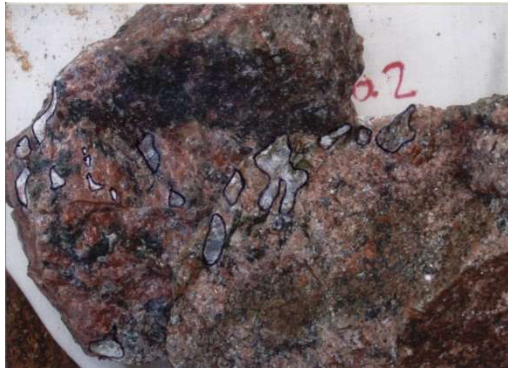


*FIG. 1. Uranium ore in Shituling deposit. Coffinite micro-veins or disseminated uraninite in fissured granite with extensive potassic alteration, chloritization and sericitization [2].*



*FIG. 2. Uranium ore in Lanhe deposit. Pitchblende micro-veins in potassium alteration granite.*

Because the characteristics of hypothermal uranium mineralization in granites are different from the general characteristics of conventional vein type uranium deposit, epithermal mineralization system for typical vein type granite-related deposits and hypothermal mineralization system for this new mineralization pattern have been proposed recently [3]. Table I summarizes the general characteristics both for granite-related epithermal and hypothermal uranium mineralization.

TABLE I. GENERAL CHARACTERISTICS OF EPITHERMAL AND HYPOTHERMAL URANIUM MINERALIZATION

| General characteristics  | Epithermal mineralization  | Hypothermal mineralization   |
|--------------------------|--|--|
| Type of ore              | Vein   | Disseminated/stockwork in fissured granites  |
| Alterations              | Silicification, fluoritization                                       | Alkaline metasomatism (potassic alteration), beresitization  |
| Major uranium minerals   | Pitchblende  | Uraninite, coffinite   |
| Mineralization T (°C)    | < 250°C  | >250°C   |
| Mineralization age (Ma)  | < 100 Ma   | >100 Ma  |
| Mineralization mechanism | Mixing of ancient meteoric water with underground circulation fluids | Boiling/mixing of fluids with ore forming solution derived from deep, might related to small porphyry. |

### 3. DISCUSSION

With the further exploration and studies on granite-related uranium deposits in south China currently, increasing evidence indicates that hypothermal uranium mineralization is characterized by relatively high temperature mineral assemblages in fissured granites with extensive potassic alteration. The “hypothermal mineralization” is not the typical intrusive high temperature mineralization, as seen in “epithermal mineralization”. Preliminary studies suggested that hypothermal uranium mineralization priority occurred in the areas with lithospheric extension in crust thickening geological setting and the mineralization mechanism dominated by boiling and mixing of ore forming solution. However, detail studies on ore controlling factors, mineralization ages, alterations and fluid inclusions for hypothermal uranium mineralization are needed to evaluate the importance of this new pattern of granite-related uranium mineralization for future exploration and to reveal the relations of hypothermal uranium mineralization to late epithermal uranium mineralization in south China.

### REFERENCES

- [1] ZHANG, J., LI, Z., CAI, Y., GUO, Q., LI, Y., HAN, C., The Main Advance and Achievements in the Potential Evaluation of Uranium Resource in China, *Uranium Geology* **28** (2012) 321–326.
- [2] DU, L., WANG, W., New exploration target for granite type uranium deposit in South China — A case study on uranium mineralization of sericitic alteration, *Uranium Geology* **25** (2009) 85–90.
- [3] LIU, X. et al., Metallogenesis studies on uranium deposits in China in Mesozoic-Cenozoic epoch, Unpublished Annual Report (2012).
- [4] FAN, H., HE, D., XU, H., LI, J., SUN, Y., et al., The potential evaluation of granite type uranium resources in China, *Uranium Geology* **28** (2012) 335–341.

# URANIUM MINE REGULATION AND REMEDIATION IN AUSTRALIA'S NORTHERN TERRITORY

P. WAGGITT

Northern Territory Department of Mines and Energy,  
Darwin, Northern Territory, Australia

## Abstract

The Northern Territory of Australia (NT) has a long association with uranium mining extending back over 70 years. Although currently there is only one active mine, the Ranger Uranium Mine, owned and operated by Energy Resources of Australia, there is plenty of uranium-related activity with several on-going exploration operations and a number of remediated and legacy sites. The regulation of Ranger is complex as it involves both NT and Australian Federal Governments in addition to other significant stakeholders and consideration of exacting, site specific, administrative requirements. The paper describes the current regulatory systems for Ranger and the other uranium operations in the NT, including the recent changes to the remediation security bonding process and the concurrent introduction of a remediation levy on all aspects of the NT mining industry. The paper also reports briefly on the progress of remediation at some significant former uranium mine sites in the NT, including the major project at the former Rum Jungle mine site.

## 1. INTRODUCTION

The Northern Territory of Australia (NT) has long been associated with uranium mining. The first probable reference dates from 1869 and refers to a discovery of a green mineral “*that was not copper*” by a survey party lead by a Mr Goyder. The discovery was in the vicinity of what later became known as the Rum Jungle mine. In 1912, the Government geologist Dr H.L. Jensen reported the presence of uranium, again in the area known as Rum Jungle [1]. There was a small amount of copper mining activity after this but the main discovery was by a Mr Jack White in 1949. The Australian Government had offered a considerable reward in the post war era, payable to the first person to discover a commercial uranium deposit. Mr White was paid the reward, eventually. Further uranium discoveries within the feature known as the Pine Creek Geosyncline followed at locations that included the South Alligator River Valley, Adelaide River township and near Pine Creek township itself [2]. More modern exploration resulted in the discoveries in the 1960s at Ranger, Nabarlek, Koongarra and Jabiluka. Thus, the NT has been associated with uranium mining more or less continuously since the early 1950s.

## 2. URANIUM MINING TODAY

Only the Ranger Uranium Mine (RUM), operated by Energy Resources of Australia (ERA), continues to operate in the NT today, although the mine’s recent production is low following two significant enforced stoppages in production in the past three years and the cessation of open pit mining in late 2013. Ranger has operated since 1981 with a total production of over 100 000 t U<sub>3</sub>O<sub>8</sub> (84 800 tU) since then. However, a very high rainfall in the wet season (October to April) in 2010–11 resulted in production being suspended for 6 months due to the water level in the tailings storage facility coming close to the maximum operating level whilst further significant rain could be expected. The second incident was the catastrophic failure of a leach tank in December 2013 when the regulators shut down production until ERA could provide assurances that changes to the procedures on site had been implemented that would preclude a repetition of the event. The facility was allowed to restart after about 6 months but full production capability was only restored in September 2014. Consequently, output has been severely reduced in recent times; varying from 5678 t U<sub>3</sub>O<sub>8</sub> in 2008–9, to 4262 t in 2009–10, 2677 t in 2010–11, 3284 t in 2011–12, 4313 t in 2012–13 and 1113 t in 2013–14 [3] (4815, 3614, 2270, 2785, 3657 and 943.8 t U respectively). It should also be noted that open pit mining ceased in December 2012 when mining in Pit 3 ceased. The current production is from existing stockpiles of generally lower grade material. However, the Ranger Three Deeps Project (R3D) is currently undergoing an environmental assessment process as well as a Prefeasibility Study. ERA is targeting late 2015 for the commencement

of production from R3D assuming the mine is proved viable and all regulatory approvals have been obtained. The R3D mineralised zone has been estimated to contain over 34 000 t of U<sub>3</sub>O<sub>8</sub> (~29 000 tU).

There is also a considerable amount of exploration work ongoing related to uranium in the NT, although the level of activity has begun to slow down over the past couple of years. At the end of 2014 there were 58 authorisations issued in relation to uranium mining within the NT, although it is considered that only about 60% are truly active. Several “junior explorer companies” originally started up following the U<sub>3</sub>O<sub>8</sub> price spike of 2007 and many have now exhausted their initial funding. Following the global financial crisis many smaller exploration companies have found it virtually impossible to obtain additional investor funding for any mineral exploration, especially uranium, in this time of depressed mineral commodity prices. Whilst the majority of the uranium exploration effort is located in the West Arnhem area at the eastern end of the Pine Creek geosyncline, there is ongoing activity and interest in uranium throughout the NT, including at various project locations where some resources have already been identified including Napperby (3362 t U<sub>3</sub>O<sub>8</sub>, 2851 t U), Angela/Pamela (10 200 t U<sub>3</sub>O<sub>8</sub>, ~8650 t U) and Bigryli (7270 t U<sub>3</sub>O<sub>8</sub>, 6165 tU) [3]. The Jabiluka project (67 700 t U<sub>3</sub>O<sub>8</sub>, ~57 400 t U), 20 km north of RUM and also owned by ERA is currently under long term care and maintenance with all previous infrastructure removed and the site being revegetated. However, none of these is thought likely to be developed soon given the present state of the uranium market. There are also some rare earth and phosphate deposits under development which have small amounts of associated uranium mineralisation; but again, funds for capital expenditure to finance development are not freely available at present, thus development is moving slowly.

### 3. REGULATION

Uranium mining in the NT is primarily undertaken by the Mines Directorate within the Department of Mines and Energy (DME) of the NT Government (NTG). The principle pieces of relevant legislation are the Mineral Titles Act covering all aspects of tenure relating to mining activity, administered by the Titles Division and the Mining Management Act which deals with all matters of environmental protection on every mining tenement for all activities (mining, exploration and extractive minerals) and is administered by the Mining Compliance Division, with extra technical support provided by staff of the Mining Remediation Division. Other NTG agencies involved include: the Environmental Protection Authority (NTEPA) who are responsible for the environmental impact assessment process, waste discharge licences for off-site discharges of water; NTWorkSafe which administers matters of worker safety and transport of radioactive materials; and the Department of Health which regulates radiation protection and supply of information to the National Dose Rate Register for uranium miners. The Australian Government is also involved as uranium mining is a matter of national environmental significance under the federal Environment Protection and Biodiversity Conservation Act (EPBC Act), administered by the Department of the Environment; the Ranger Uranium Mine was also set up on a special project area granted through an agreement under section 41 of the Atomic Energy Act which is administered by the Department of Industry, although the day-to-day regulation has been delegated to the DME through a Memorandum of Understanding and associated working arrangements. These arrangements also specify that the Australian Government’s Supervising Scientist shall have an oversight role and work with the DME and stakeholders to ensure protection of the environment of the Alligator Rivers Region from adverse impacts of uranium mining in that region. Elsewhere in the NT uranium mining activities are, at present, regulated by the DME alone.

In the case of RUM the operation is regulated through an authorisation document issued by the NT Minister for Mines and Energy after consultation with the Australian (federal) Government Minister administering the Atomic Energy Act. Amendments to the authorisation have to be agreed to by all major stakeholders and both Ministers before they can be authorised. The site is inspected very month by a combined team including representatives of the DME, the Supervising Scientist, the Gundjeihmi Aboriginal Corporation (representing the specific local Aboriginal Traditional Owners of the land) and the Northern Land Council — an organisation having responsibilities to oversee all activities on aboriginal land, including mining. These same four organisations are members of the Minesite Technical Committee (MTC) which is chaired by DME and meets every two months. The MTC is the forum where amendments to the authorisation or the on-site work programme are discussed prior to approval. RUM

is required to submit comprehensive monitoring reports at weekly, monthly and other periodic intervals in relation to water quality on and around the site. This is important as the site is surrounded by the World Heritage listed Kakadu National Park, an area listed for both cultural and natural values. In addition, the RUM authorisation contains a schedule for reporting on all other environmental matters including radiation protection, water management and progressive remediation. ERA is also required to submit an Annual Plan of Rehabilitation which includes detailed costs of the rapid remediation of the whole project area should the operation cease at short notice for any reason. Once the plan and costings have been agreed by the MTC parties and the Department of Industry ERA must ensure that the appropriate sum of money is lodged with the Australian Government in an acceptable form (cash or unconditional bank guarantee) which would enable the site to be remediated without recourse to public funds.

For all other mining operations in the NT, including uranium mining, the operator must first have a legal mining title issued under the Mineral Titles Act that is appropriate to the type of activity planned. Once a title has been granted the operator may apply for an authorisation to carry out the specific mining activity. These activities must be set out in a comprehensive document called the Mining Management Plan (MMP) which has to be approved before an authorisation can be issued. The form and content of an MMP should be in accord with guidelines set down by the DME and published on the DME website. In addition to the approved MMP an operator must also deposit with the DME a financial security which has been calculated for that specific MMP. The security is calculated using a spreadsheet tool provided by the DME on their website at: [http://www.nt.gov.au/d/Minerals\\_Energy/index.cfm?header=Mining](http://www.nt.gov.au/d/Minerals_Energy/index.cfm?header=Mining).

The same page also includes guidelines on various activities and the security calculation tools and operational advice on leading environmental management practices. The security has to be deposited either as cash or an undated unconditional bank guarantee drawn on an Australian licenced deposit holding financial institution. The final sum deposited is also the basis of a mining remediation levy of 1% of the lodged security amount. This levy is payable annually on the balance of security money held against each operation or authorisation as at 1 July each year. The funds collected are used to finance a small Legacy Mines Unit within the Mining Remediation Division, to fund some additional compliance activities related to improving environmental management standards in mines and at least 33% is put aside towards DME carrying out remediation works on a small scale at genuine legacy sites. The level of unfunded mining legacy liability in the NT in 2011 was estimated to be about AUD 1 billion<sup>2</sup>. The mining security fund currently holds about AUD 750 million and so the legacy fund presently has an annual income of approximately AUD 7.5 million. It is expected this will increase with inflation and increased levels of mining disturbance leading to increased security deposits as developments proceed. As mine sites are remediated and security deposits are returned the fund will decrease by that amount but no major projects are anticipated to close in the next 5 years.

The regulatory process is straightforward. The MMP and amendment documents are assessed and approved in an iterative process and the authorisation issued for 12 months in the first instance. Once an operator has applied for a renewal after that time the updated MMP may be approved for up to four years with an annual progress report and future plan being required on the intermediate anniversary dates. This is being introduced to reduce the workload for operators in preparing full MMP every year and to allow Mining Officers more time to undertake field investigations and regulatory visits. Each major site can expect to be audited against the MMP or an environmental audit site-specific protocol annually. Depending on the complexity of the site, the assessed environmental risks of the operation and the performance of the operator additional inspections may be undertaken at any time throughout the year. In general, every mining operation will be audited at least once per year and exploration operations generally inspected at the same frequency. Extractive operations are often visited more frequently as they tend to be relatively short lived and close out or remediation completion inspections may be called for more frequently.

---

<sup>2</sup> All currency quoted in Australian Dollars (AUD)

#### 4. URANIUM MINE REMEDIATION

There have been a number of significant uranium mining operations that have reached the end of mine life in the NT since 1950 and some of these have been remediated and some remain as either part or whole legacy sites. The regulation of mining remediation really only commenced with the introduction of the remediation security in 2006. Bonds held before that time did not represent 100% of the estimated remediation costs, except in the case of RUM, and in that case the money is held by the Australian Government Minister not the NT Minister.

The NT Government seeks to have remediation carried out using leading practice at all mine sites. In the case of uranium mines within the Alligator Rivers Region, including RUM and Nabarlek, it is a legal requirement that all mill tailings are disposed of below ground level. At Nabarlek the ore body had been mined out in one campaign in 1978 and tailings went directly to the mined-out pit until the end of operations in 1988 [4]. The processing plant was decommissioned in the wet season of 1994–5 and earthworks for remediation were completed in January 1995 [4]. The final closure of the site has yet to be confirmed by the regulators and stakeholders with revegetation progressing steadily.

At Ranger Pit 1 was mined from 1981 to 1994 and tailings were deposited in an above ground 1 km square tailings storage facility (TSF). A trial relocation of 1 million cubic metres of tailings from the TSF using a dredger was undertaken in 1996 to gather data for remediation studies. Also, tailings from the mill were redirected to Pit 1 from August 1996 until the maximum permitted level was reached in December 2008. ERA is currently working to cover the tailings as the initial stage of remediation. Mining in Pit 3 started in 1995 and was completed in December 2013. The pit was prepared to receive tailings with the installation of over 30 million t of waste rock and drainage systems. This work was completed in December 2014 and tailings from the mill will go directly to the new repository starting in February 2015, transfer of tailings from the TSF with a new, custom built, dredge will commence in the middle of 2015. This transfer is planned to be completed by 2021 the date at which ERA is due to end processing operations under current agreements. The full remediation of the site is due to be completed by 2026.

Elsewhere in the NT the site at Rum Jungle is perhaps one of the best-known uranium legacy sites in the NT. It has been the subject of many papers and became well known for the excessive damage caused to wild life in and around the adjacent Finni River as a result of acid metalliferous drainage (AMD) leaving the site. The site has been the subject of several remediation programmes but none to date has proved to be sustainable. The site operated as a copper-uranium mine from 1949–1970s and was not fully remediated at the initial relinquishment. A more comprehensive remediation was completed in 1986 but this too failed to be sustainable and so a new programme of works was commenced in 2009. Under that programme work has begun to prepare a comprehensive remediation plan of works. In the first phase (2009–13) a National Partnership Agreement between the Australian and NT Governments saw studies undertaken and extensive stakeholder consultation resulting in an agreed conceptual plan for remediation being selected from a number of options. The second phase agreement, from 2013 to 2016, relates to the development of the final design and tender documentation to prepare for the implementation of the chosen plan. The projects are funded by the Australian Government Department of Industry but undertaken by a dedicated team located within the NT DME Mines Directorate. Full details of the programme can be seen at:

<http://www.nt.gov.au/d/rumjungle/index.cfm?header=Rum%20Jungle%20Home>.

Some of the uranium mine legacy sites have been remediated in recent years. In the late 1980s and early 1990s the Australian Government undertook an inventory of all known NT uranium legacy sites which was used to implement a “hazard reduction” programme at several locations. The aim was to reduce radiological and physical risks to an acceptable level at sites that were easily accessible to the public. Most of the effort was focussed in the South Alligator Valley (SAV) which had been included in stage 3 of an expanded Kakadu National Park. The story of that programme has been described elsewhere [6] and will not be repeated here. After further discussions with the Aboriginal Traditional Owners the SAV sites were all finally remediated in a programme that was undertaken using Australian Government

funds between 2002 and 2009 [7]. Remaining uranium legacy sites are to be included in the inventory of all legacy sites being prepared by the Legacy Mines Unit.

## 5. FUTURE DEVELOPMENTS

As noted earlier, the present combination of a low price and depressed market for uranium is likely to make most new developments less attractive to investors for the immediate future. The possible expansion of production at RUM through development of the R3D project will be the exception if a positive investment and development decision is made in 2015. Other projects are either ‘on standby’ or proceeding slowly. Whenever the market changes the regulatory regime will be in place to respond appropriately and quickly.

The NT regulatory regime is robust but flexible, and has been proven able to cope not only with the past 30 years or more with the complex of legal, technical and stakeholder issues that surround the Ranger Uranium Mine, including specially the multitude of Agencies and government and stakeholder organisations involved; but also with the day-to-day needs of mines (including uranium) outside the Alligator Rivers Region. Various components within the regime, such as the MTC and the stakeholder committees, have been examined in many other locations and even adopted and adapted in some cases to meet local needs. The future for uranium mining globally may be less bright than it was before the Fukushima accident in 2011 but demand for the fuel for nuclear power plants continues and the NT will continue to play its part in the uranium production cycle for some time to come.

## REFERENCES

- [1] BARRIE, D.R., *The Heart of Rum Jungle*, Dominion Press, Hedges and Bell, Australia (1982).
- [2] ANNABEL, R., *The Uranium Hunters*, Rigby Limited, Adelaide, Australia (1971).
- [3] WORLD NUCLEAR ASSOCIATION, Australia’s Uranium Deposits and Potential Mines, (accessed Dec. 2014), <http://www.world-nuclear.org/info/Country-Profiles/Countries-A-F/Appendices/Australia-s-U-deposits-and-Prospective-Mines/>.
- [4] WAGGITT, P.W., “Nabarlek Uranium Mine: From EIS to Decommissioning”, Proc. Uranium 2000, Canadian Institute of Mining Metallurgy and Petroleum, Quebec, Canada (2000) 631–642.
- [5] PAULKA, S., WAGGITT, P., Nabarlek – The history of a modern uranium mine, AusIMM Bulletin No. 3 Australasian Institute of Mining and Metallurgy, Melbourne (June 2013) 52–53, 55
- [6] WAGGITT, P., Uranium mine rehabilitation: the story of the South Alligator Valley intervention, J. Environ. Radioact. **76** 1-2 (2004) 51–66.
- [7] FAWCETT, M., WAGGITT, P., “Remediating the South Alligator Valley uranium mining legacy”, Uranium 2010 (Proc. Conf. Saskatoon, Canada, 2010) Metallurgical and Materials Society, Canadian Institute of Mining, Metallurgy and Petroleum, Quebec **2** (2010) 495-506.

# RADIATION REQUIREMENTS FOR URANIUM PROJECT APPROVALS

J. HONDROS  
JRHC Enterprises, Stirling,  
South Australia, Australia

## Abstract

Uranium mining projects are required to be approved under state and national laws based on impact assessments. The process may take a number of years, involving government and public consultation and scrutiny. The impact assessment is broad and usually covers; environmental, social and economic aspects. Information provided in the approvals documentation needs to be presented in a credible and understandable manner for all audiences. For uranium projects, along with other projects involving radioactive materials, such as minerals sands and rare earths, radiation and its impacts usually draw a disproportionate amount of both government and public scrutiny compared to its actual risk. It is therefore important that radiation assessments are properly performed and results presented and communicated with sufficient detail for stakeholders to make informed decisions. This paper outlines a structure for a simple radiation impact assessment based on practical experience, which aims to ensure the right balance between scientific fact, digestible information and demonstrable competence.

## 1. INTRODUCTION

All new mining or mineral processing projects require some form of regulatory approval which is generally based on economic, social and environmental impact assessments (for example Toro Energy 2011[1]). Experience shows that the approval process can be long and complex, involving many studies and taking many years.

For a project that involves the mining or processing of radioactive material, the approvals process is usually more complicated and an assessment of the radiological impacts must be conducted. For radiation, the assessment must be technically and scientifically accurate and at the same time recognise that there are varying perceptions of radiation.

In practice, radiation assessments can be exhaustive and complex studies which aim to categorically show that the actual impact is low. However, these studies sometimes have the side effect of overemphasising the importance of radiation in the overall impact assessment and can also be very difficult to understand. On the other hand, some assessments try to underestimate the radiological impact, and focus solely on the actual risk and impact, which is usually very low and much lower than other impacts. While this may be technically correct, this can be interpreted as the proponent being not interested or not competent in the radiation assessment.

A balance is needed to show that the radiation impact has been competently assessed, to a satisfactory level, and that the proponent is sensitive to the stakeholder perceptions of radiation. Most importantly, the results of the assessment must be clearly communicated to ensure that any reader of the impact assessment is able to understand it.

This approach is true for all types of projects containing radioactive materials, including uranium related projects and non-uranium projects, such as rare earths projects or projects with NORM.

This paper provides a practical approach to undertaking radiological assessments for new projects involving radioactive material and draws on actual project assessments. The focus in this paper is the environmental impacts rather than the occupational exposure aspects, but it is noted that potential impacts to workers can be assessed using the approach outlined. The potential areas of environmental impacts include; members of the public, the broad environment and standard species of flora and fauna.

## 2. APPROVALS

The approvals phase is generally the first time that a company places detailed information about the proposed project onto the public record, therefore making it available for public and regulatory review and scrutiny. At this stage, it is important for the project proponent to demonstrate that it:

- Understands the project risk;
- Is addressing those risks in a responsible manner;
- Is competent at managing the risks.

The approval process is complex and detailed for new projects and is only one aspect of bringing a new operation to life.

Other aspects include:

- Technical feasibility of the project;
- Financial and investment of the project;
- Environmental impact assessment;
- Land use access agreements;
- Government approval (note that this is usually based on the previous two points);
- Board approval;
- Ongoing secondary licences and approvals.

The radiation assessment is only one part of the Environmental Impact assessment, and therefore it is important to maintain perspective across the approval and wider project startup processes.

When considering approvals alone, there are generally three main interconnected aspects that have to be addressed. These are; technical competency, public perception and government acceptance.

- The technical aspects are relatively straightforward and involve good competent science and engineering;
- The public perception is based on the expectation that the company understands its impacts and is able to competently demonstrate this. It is usual during an approval processes for communities to have their say. For radiation, the views can be biased, distorted and based on incomplete or incorrect information;
- The government needs to be satisfied with the assessment undertaken by the proponent and that the level of impact is acceptable. This may result in requests for additional assessment work or consideration of other options in order for an informed decision to be made. Whether the assessment is satisfactory or not may sometimes depend upon a number of non-technical factors.

### 3. RADIATION ASSESSMENT FRAMEWORK

To undertake the radiological assessment in a simple and effective way, a practical framework consisting of four steps has been developed. The main steps in the framework are as follows:

- Characterise the existing radiological environment (the ‘background’);
- Quantify the incremental radiological concentrations due to the project (the ‘project increment’);
- Determine the impact of any increment (the ‘impact’);
- Outline the control measures (the ‘controls’).

Details on each of the steps are described below.

#### 3.1. Characterising the existing radiological environment

The existing radiological conditions are sometimes known as baseline or background environmental radiation levels, although care should be exercised when using these terms as they may have specific meanings in different contexts. Regardless, the overall aim is to identify and quantify the environmental radiation concentrations that exist in the region of the proposed project and this is important for the following reasons:

- It provides confidence for stakeholders (including the government and the public) that the company is able to monitor radiation and understands the pre-existing radiation levels in the areas where they are working;
- It provides a quantified measure of the natural levels and the natural variation in radiation levels in space and time;
- It is important for determining the requirements for project closure, and the levels for rehabilitation.

Radiological conditions can be obtained from a range of sources, including published data or existing company or project data, such as geological information or water quality information. An important consideration when using existing information is to ensure that the results have come from reputable sources and that the monitoring techniques used to obtain the original information are valid and proper.

It is more than likely that information about the existing environment will be obtained from a dedicated monitoring program. Experience shows that monitoring should be conducted for a period of up to 2 years to ensure that seasonal variations are considered and are included in the final characterisation. Often a monitoring program is established in the very early phases of a project, for example during the project exploration stage, when little information on the project may be known. These programs are often designed with little thought given to the long term nature of such a program and are usually based on compliance monitoring requirements for the particular work being undertaken.

For a new project, there are a number of radiological parameters that should be monitored, and these include:

- Gamma radiation;
- Radon and radon decay product (note that for the particular project, this might include either or both of  $^{222}\text{rn}$  and  $^{220}\text{rn}$ );
- Radionuclides in dust;
- Radionuclides in soils and water;
- Radionuclides in flora and fauna.

Monitoring locations should be carefully selected, taking into account such factors as; natural features, wind direction, the infrastructure of the proposed future project and access to power. The environmental monitoring locations should be seen as long term investments for the project that provide information

prior to and during the operations. The locations should have a range of radiation monitors which are appropriate for the various radiological parameters being monitored.

Radiation monitoring must be undertaken in accordance with scientific procedures and with calibrated equipment and can be undertaken in a number of ways as shown in Tables I and II.

TABLE I. MONITORING TYPES

| Monitoring type | Description   | Characteristics  |
|-----------------|---|--|
| Passive         | Monitors are placed in the field and radiation levels are detected passively (without moving parts or electronics).   | Relatively inexpensive;<br>Can place many samplers into the field;<br>Provides average level over the sampling period;<br>Not as sensitive as active samplers;<br>Detectors need to be later analysed. |
| Active          | Monitor actively samples, (for example, a powered air sampler).   | Costly;<br>Requires power (batteries).   |
| Real Time       | Monitor actively samples and reports or stores information in real time.  | Costly;<br>Can be sensitive equipment;<br>Requires power (batteries).  |
| Continuous      | A monitor which samples continuously;<br>Collects a sample over an extended period and provides an average or result;<br>May also be a real time sampler;<br>May also be a passive sampler. | Able to collect data over an extended period;<br>Costly;<br>Requires power (mains power if large like a high volume sampler).  |

TABLE II. RADIATION MONITORING METHODS

| Radiation                   | Typical monitoring devices  |
|-----------------------------|---|
| Gamma radiation             | Thermo luminescent detectors (TLD badges);<br>Handheld gamma monitor;<br>Aerial radiometric survey.   |
| Radon                       | Track etch detectors (radon cups);<br>Radon Gas Monitor;<br>Lucas Cells;<br>Accumulator drum (for radon exhalation).  |
| Radon Decay Products (RnDP) | Spot sampling (Rolle, Environmental Rolle method);<br>Real time RnDP samplers.  |
| Radionuclides in dusts      | Personal dust pumps (low volume);<br>Medium and high volume air sampler (run from either mains power or batteries).   |
| Radionuclide deposition     | Dust deposition gauges.   |
| Radionuclides in soils      | Different types of soils and different depths).   |
| Radionuclides in water      | Surface water and groundwater from different aquifer).  |
| Radionuclides in flora      | Different species – perennial and ephemeral;<br>Different species – growing in different soil types;<br>Different species – for human consumption;<br>Align with soil and water sampling. |
| Radionuclides in fauna      | Different species and different organs.   |

Radiological information can be obtained in conjunction with other monitoring that is occurring. For example; groundwater monitoring is usually conducted as part of resource monitoring, and uranium, radium and radionuclide analysis can be included in this.

A poorly planned or executed monitoring program can result in delays in the approvals process due to insufficient characterisation of the existing radiological environment and the requirement to obtain more information, or it can lead to closure constraints for the project (for example a poorly defined baseline can lead to overly restrictive closure criteria).

### **3.2. Quantify the incremental radiological concentrations due to the project (the ‘project increment’)**

The aim of this step in the framework is to accurately determine the radionuclide releases from the project in order to calculate any change in environmental radiation concentrations. In this framework, this is known as the ‘increment’, and this ‘increment’ is used in the next step of the framework to make an assessment of the ‘impact’ of the releases.

In many cases, environmental assessments are undertaken very early in project development, for example, during the pre-feasibility stage. Care must be taken at this stage because, often, the project is not completely defined, and designs can change significantly as the processing or mining project variables are better defined.

In a practical sense, determining the increment involves:

- Understanding the project design and where emissions occur;

- Estimating the potential emissions from the various project components;
- Determining how the emissions result in changes in environmental levels.

The first aspect of increment assessment is to have a good and complete understanding of the proposed project to accurately identify the potential sources of emissions. This includes such aspects as understanding where radionuclide might accumulate in the process which create potential sources, through to understanding the effectiveness of the built-in controls such as ventilation systems in a mine and the project design criteria.

Once the details of the proposed project are understood and sources of emissions determined, the emissions can be quantified by using standard emission factors or experimentally determined factors. For example:

- The dust emissions from a stockpile can be estimated from standard dust lift off factors;
- The emissions of radon from an extraction ventilation shaft involves estimating the radon emission from the various rock surfaces in the mine and calculating the subsequent radon concentrations in air;
- Emissions to groundwater can be calculated by understanding the permeability of a lining system for a water or tailings retention system.

The usual approach is to be conservative when assessing emissions.

To complete the project increment quantification, non-radiological information such as surface and ground water flow rates and aquifer descriptions, and general meteorological information, such as wind direction, are required and input into a range of calculated methods, including:

- Direct modelling which use the emission rates (such as air quality modelling and fate and transport modelling);
- Use of first principles or ‘rules of thumb’;
- Consideration of other similar processes or projects (for example; emission rates from similar equipment used in other projects).

The methods provide a measure of the change in existing concentrations of the emissions at various locations, for example:

- The project design may have an open-air uranium ore stockpile. The design provides the size and surface area of the stockpile and the average uranium grade. The emission of radon can be calculated from the surface area and the unit radon emission rate (which can be a reference figure inferred from the uranium grade or experimentally determined) and then the emission rate is input into air quality modelling to show the incremental radon concentration at various locations around the project.

### **3.3. Determine the impact of any increment**

The third step in the framework is the assessment of impacts from the project emissions. The main impacts occur to people, the environment and plants and animals.

### *3.3.1. People*

As noted earlier, this paper refers to non-occupational exposures and therefore focuses on members of the general public.

The impacts to people are determined through standard dose assessment (ARPANSA 2005[2]). This involves identifying the potential exposure pathways and modelling exposure and dose from the project increment (this excludes the dose received from the naturally occurring environmental background radiation). The main exposure pathways are as follows;

- Irradiation by gamma radiation;
- Inhalation of the decay products of radon;
- Inhalation of radionuclides in dust;
- Ingestion of radionuclides in flora, fauna and water.

To assess impacts to the public, it is usual to identify a reference person, either hypothetical or real and calculate the radiation dose that they would receive. The hypothetical person is useful for situations where the project is in a remote location and can be used to provide a worst-case assessment of impact. If it can be shown that the dose in a worst-case situation is very low or negligible, then there is a high degree of confidence that doses to people further away will be much lower. Alternatively, the potential dose to a real resident of local community can be calculated.

Doses are assessed for each of the pathways, as follows, and summed to determine the total dose from which impact can be determined.

- Gamma radiation exposure to the public is usually negligible. This is mainly because sources of gamma radiation are usually well within the project boundary where access by members of the public is restricted. A potential source of gamma radiation outside the project area is from the transport of radioactive materials and exposures from this should be taken into account in the assessment;
- For emissions of airborne radionuclides, the air quality modelling provides a project increment at various locations including the location of the reference person. Standard dose assessment methods can be used to calculate the inhalation dose;
- To determine the exposure from the decay products of radon, an additional step in the assessment is required. The air quality modelling generally provides contours of radon concentrations rather than radon decay product concentrations. Since the dose comes from the decay products, the radon concentrations at the location of the reference person need to be converted to radon decay product concentrations. There is a standard conversion factor for this, based on an equilibrium ratio (UNSCEAR 2000[3]). The radon decay product impact is usually very low, mainly due to the dilution of the radon emissions that occur and the distances from the sources to the exposure locations;
- For assessment of the impact from the ingestion pathway, the output of the dust deposition modelling from the air quality modelling is used. The modelling provides project increment contours, usually as dust mass per unit area per unit time. An assumption about the radionuclide content of the dust can be made, which can be used to convert the mass deposition to a radionuclide deposition. This can then be used with various uptake factors for both flora and fauna and then combined with assumptions about consumption to provide and intake, which is then converted to a potential dose using standard ingestion dose conversion factors;
- For water, the project increment can be estimated from either deposition information or water release information and an exposure scenario developed to assess the potential doses from ingestion of the water.

### *3.3.2. Non-human biota*

In recent years, the protection of plants and animals from radiation has taken on a higher level of importance. The earlier approach was based on the assumption that if humans were protected, then plants and animals would also be protected. The ICRP revised this approach in ICRP 2003[4] and a more detailed level of assessment is required.

The recognized process for assessing the impact to non-human biota revolves around the ERICA assessment software. The ERICA software uses changes in media radionuclide concentrations as inputs to calculate a risk quotient for a range of standard species. It also provides the ability for the user to enter species specific data. A tiered assessment process is used, with higher levels of assessment occurring, if necessary, and taking into account species and situation specific information.

The changes in media concentrations can be determined from the dust deposition contours from the air quality modelling.

### *3.3.3. Environmental changes*

Environmental changes, such as increases in groundwater radionuclide concentrations, are sometimes considered to be ‘impacts’ and may need to be reported. These changes in environmental concentrations are determined from deposition and emission data as previously discussed.

Care should be taken when reporting such results as ‘impacts’ as there may be no measurable biological or physical change as a result of increased radionuclide concentrations. Baseline data is useful in providing perspective on the magnitude of the changes.

## **3.4. Outline the control measures (the ‘controls’)**

The assessment of impact is usually made against a set of standards, such as legislative limits. Where the standards have not been met, or the impact is deemed to be unacceptable, then either the original design is modified or specific controls are implemented and the impact re-assessed.

The final step in the framework is therefore the description of management controls.

Once the impacts have been determined, it is important to describe what will be done to manage and control the impacts of radiation. While impacts might comply with the relevant standards, it is important to outline clearly what the company is doing to ensure that the impacts are controlled, stay controlled and are monitored. An important aspect of this section is the ALARA description – which needs to be described as part of the management measures.

Usually this section of the approvals process involves a description of the control measures that were part of the project design and also any administrative controls measure that may be part of the overall management systems.

These measures are usually described in more detail in the project radiation management plan.

## **4. DISCUSSION**

The radiation impact assessment for new projects can be overly complicated and inconsistent with the magnitude of the actual risk, mainly due to the perceived risk of the radioactive material. By providing a clear and logical step by step process, some of the mystery around radiation and the impact process can be removed. The aim of the proposed framework is to do this in a logical and clear manner.

From a practical perspective, there are some additional aspects that assist in delivering a balanced radiological impact assessment.

#### **4.1. Understand the project**

The assessment process depends critically on understanding the details of the project that is to be impact assessed. Reading documentation is a start, however, discussion with key technical personnel, such as design engineers, mining engineers and the process metallurgists provides insights on the way certain things have been done or why certain processes have been followed. This also enables the opportunity for detailed radiation protection input in the design of the project.

#### **4.2. Understanding ALARA**

ALARA is as much a way of doing things as it is an outcome. Having a project team that understands radiation protection, and includes it as part of the design of the project is an advantage. For new projects, the ALARA component is generally more important than compliance with the dose limits.

#### **4.3. Ensure that radiation remains in perspective**

It is easy for the stakeholders to focus on perceived risks rather than actual risks and therefore over emphasize the radiological risk. However, a key task is to ensure that risks remain in perspective. It is highly unlikely that radiation is a significant factor in project development and approvals, however this needs to be clearly demonstrated and external stakeholders have to have confidence that the company is serious about radiation.

#### **4.4. Provide information in documentation rather than just data**

Radiation is a “data rich” area and it can be difficult turning data into information that can be readily understood. The challenge in any approval process is to make sure that the balance between data and information is maintained. The radiation assessment needs to be technically competent and understandable at the same time.

### **5. CONCLUSIONS**

This paper has provided a simple framework for the assessment of the radiological impacts for a new project. The radiation assessment is part of the overall impact assessment, which itself is part of the broader approvals project. The radiological assessment framework has four steps:

- Characterise the existing radiological conditions;
- Quantify the incremental radiological concentrations due to the project;
- Determine the impact of any increment;
- Outline the control measures.

However, the framework is incomplete without adequately and succinctly describing the process and findings so that all stakeholders have a good level of understanding.

## **REFERENCES**

- [1] TORO ENERGY, Wiluna Uranium Project, Environmental Review and Management Programme (ERMP) EPA Assessment No 1819 (July 2011).
- [2] AUSTRALIAN RADIATION PROTECTION AND NUCLEAR SAFETY AGENCY, Radiation Protection and Radioactive Waste Management in Mining and Mineral Processing. ARPANSA Radiation Protection Series **9**, Canberra, (2005).
- [3] UNITED NATIONS SCIENTIFIC COMMITTEE ON THE EFFECTS OF ATOMIC RADIATION, UNSCEAR 2000, Annex B: Exposures from natural radiation sources, UN, New York (2000).
- [4] INTERNATIONAL COMMISSION ON RADIOLOGICAL PROTECTION, A framework for assessing the impact of ionising radiation on non-human species, ICRP Pub. 91, Ann. ICRP **33** 3 (2003).

# RISK BASED ENVIRONMENTAL ASSESSMENT FOR URANIUM MINES — THE CANADIAN EXPERIENCE

M. MCKEE\*, M. PHANEUF\*\*

\* Canadian Nuclear Safety Commission,  
Ottawa, Ontario, Canada

\*\* International Atomic Energy Agency,  
Vienna, Austria

## Abstract

The Canadian *Nuclear Safety and Control Act (NSCA)* requires the prevention of unreasonable risk to, and adequate provision for, the protection of, the environment and the health and safety of the public. Canada has developed a regulatory framework emphasising the importance of human health risk assessments (HHRA) and ecological risk assessments (EcoRA) as core tools for ensuring protection of the public and the environment. The value of such an approach is presented as well as the evolution of environmental risk assessment (ERA: HHRA + EcoRA) from its original application for assessing the environmental acceptability of a new project to its present application throughout the life-cycle of a facility.

## 1. INTRODUCTION

Environmental Risk Assessment (ERA) provides a framework for identifying interaction(s) between an ‘activity’ and the environment, the assessment of ‘effects’ arising from interaction(s), the identification of possible mitigative options, and the design of monitoring programs to assess the adequacy of mitigative actions and the accuracy of the effects assessment in support of adaptive management. The complexity of an ERA should be commensurate with the risks associated with the activity and thus may range from simple screening assessments to complex quantitative ERAs incorporating environmental dispersion, transport, exposure and effects models. One of the major drivers for undertaking ERA is to allow the ranking of potential effects, such that effort — such as mitigative measures and monitoring — can be concentrated on important risks.

This paper discusses how the Canadian Nuclear Safety Commission (CNSC) has formally incorporated ERA within its regulatory framework for the nuclear fuel cycle with particular application to uranium mining.

## 2. EVOLUTION OF ERA IN CANADIAN NUCLEAR REGULATION

The role of ERA within the CNSC environmental protection framework has evolved over time. It is now being formally incorporated within regulatory documents and standards for application throughout the complete regulatory life-cycle of a facility. To understand this evolution, it is necessary to start with some background on the regulatory history of the nuclear fuel cycle in Canada, and the significant role of ERA in uranium mining and milling regulation.

The role of ERA within the regulation of nuclear activities has gone through four phases:

- 1990s: ERA used as a risk assessment tool within the overall environmental impact assessments (EIAs) completed under Canadian environmental assessment legislation (i.e. the *Canadian Environmental Assessment Act: CEAA*);
- 2000–2006: ERA adopted by the CNSC as a tool for assessing new projects under EA legislation (CEAA) as well as the adequacy of environmental monitoring programs for existing facilities under the NSCA;
- ~ 2006–present: ERA used by CNSC staff to independently assess facility specific emerging environmental issues (presented as case studies);

- 2010–present: ERA formally being adopted within Standards and Regulatory documents under the NSCA.

The modern concept of ERA was initially applied in the 1990s in support of a series of EIAs submitted to a joint federal-provincial panel<sup>3</sup> conducting public reviews on a number of proposed uranium mining and milling operations in northern Saskatchewan, Canada. This involved the traditional application of ERA as a planning and management tool for identifying the potential risks of an activity to the environment and public; determination of appropriate mitigation activities; followed by a final assessment of residual risk after mitigation and a determination whether or not the activity could be carried-out in a responsible, safe manner. ERAs were conducted using frameworks developed for non-nuclear applications (c.f. US EPA [1]).

The next phase in the evolution of the role of ERA in the Canadian regulation of uranium mining arose as a result of the coming into force of a new modern act and accompanying regulations for the nuclear industry in Canada. In 2000, the Atomic Energy Act (established in 1946) and the associated regulatory body the Atomic Energy Control Board (AECB) were replaced by the *Nuclear Safety and Control Act* (NSCA) [2]. The NSCA created the Canadian Nuclear Safety Commission (CNSC), whose mission is to protect the health, safety and security of persons and the environment; and to implement Canada's international commitments on the peaceful use of nuclear energy.

Amongst the new responsibilities in the NSCA were two key changes with respect to environmental protection: 1) the specific responsibility for radiological protection of the environment in and of itself (rather than relying on the previous international position that if humans were protected the environment was protected); and 2) the mandate for managing hazardous substances as well as nuclear substances released by a facility. This essentially placed the CNSC in a position to regulate the full range of risks associated with nuclear fuel cycle activities using an ecosystem approach to environmental protection.

The NSCA placed specific obligations on the CNSC to regulate nuclear licensees in order to:

- Prevent **unreasonable risk** to the environment and to the health and safety of persons;
- Disseminate objective scientific, technical and regulatory information to the public concerning the activities of the commission and the effects, on the environment and on the health and safety of persons.

The NSCA also placed specific obligations on the licensees themselves to:

- Take all **reasonable precautions** to protect the environment and the health and safety of persons;
- Take all reasonable precautions to control the release of radioactive nuclear substances or hazardous substances within the site of the licensed activity and into the environment as a result of the licensed activity.

To enforce its new mandate, the CNSC determined that the terms ‘unreasonable risk’ to the health and safety of persons and ‘reasonable precaution’ to control releases should be interpreted in a manner respecting other existing Canadian environmental protection legislation such as the Canadian Environmental Protection Act (CEPA 1999) [3], the Canadian Environmental Assessment Act (CEAA 2012) [4], the Species at Risk Act (SARA 2002) [5], the Fisheries Act (FA 1995) [6], the Metal Mining Effluent Regulations (MMER 2002) [7] and the Migratory Birds Convention Act (MBCA 1994) [8].

The application of the CEPA principle of ‘Pollution Prevention’ for hazardous substances was adopted as a counterpart to the As Low As Reasonably Achievable (ALARA) principle applied to nuclear substances. The terms ‘unreasonable risk’ and ‘reasonable precaution’ are essentially risk-based concepts and the specific environmental requirements identified in regulations are elements associated

---

<sup>3</sup> <https://www.ceaa-acee.gc.ca/default.asp?lang=en&n=76C904A0-1>

with the ERA methodology. Consequently, ERA was considered the logical core framework for meeting the new environmental protection mandate of the NSCA (Table I).

TABLE I. RELATIONSHIP BETWEEN GENERAL ENVIRONMENTAL RELATED REGULATORY REQUIREMENTS AND AN ENVIRONMENTAL RISK ASSESSMENT

| Licensing requirements   | Relationship to ERA   |
|--|---|
| Environmental baseline characteristics   | Environmental characterization is one of the initial steps for an ERA and necessary to determine environmental transport and exposure pathways as well as receptors to be assessed / protected. |
| Description of releases of nuclear and hazardous substances: points of release, quantities, concentrations, volumes and flow rates | ERA input parameters. For ERA predictions to be applicable facility must be assessed / licensed against these predicted releases.   |
| Predicted effects on the environment   | Predicted effects on the environment are the final output of the ERA  |
| Environmental Management System (EMS) (EP Policies, Programs and Procedures)   | ERA identifies the “environmental aspects” (ISO 14001 parlance) which become the focus of continuous improvement activities for the EMS.  |
| Effluent monitoring program (releases to atmosphere, surface and ground waters)  | Monitoring program should meet relevant regulations and be designed to demonstrate that releases are within the range of those assessed in the ERA.   |
| Environmental monitoring program   | Monitoring program should be designed to demonstrate environmental effects are within the range of those predicted in the ERA   |

### 3. APPLICATION OF ERA UNDER THE NSCA

The initial application under the NSCA was to require those licensed facilities that had not completed an ERA as part of an overall EIA (i.e. during the project proposal stage) to complete a site-specific ERA to confirm that existing mitigation measures and monitoring programs were adequate to ensure that the environment was protected from discharges of hazardous and nuclear substances (i.e. radiological protection of non-human biota). This resulted in CNSC staff identifying a number of emerging issues, primarily associated with hazardous substances. CNSC staff assessments served as the technical documents supporting site-specific licence conditions requiring additional mitigative action by a licensee. This is briefly presented in the summarized case studies following this section.

These assessments demonstrated the value of ERAs as a means of assessing actual operational performance rather than restricting them to the initial environmental impact assessment phase of a facility. From this experience, the CNSC has now integrated ERAs as the core element of the environmental protection framework for application throughout the life-cycle of a facility.

As demonstrated in Figure 1, the role of ERA in licensing commences with the initial environmental assessment required for a new facility or for a new activity at an existing facility. The objective is to

determine the potential risks to human health and the environment and ensure the implementation of adequate mitigation measures. The ERA should be used to identify necessary mitigation technologies (e.g., water treatment systems, filters, liners, covers) or practices (e.g., dust control, silt barriers, revegetation). The purpose is to determine whether the proposed activity is planned and designed in a manner demonstrating adequate precaution to protect the environment and in a manner ensuring the health and safety of the public. If this is demonstrated the facility can be considered for licensing under the NSCA.

In many jurisdictions, both in Canada and internationally, pre-project environmental assessment and operational licensing and regulatory oversight are often managed by different regulatory agencies. This can result in a disconnect between EA assessment predictions, commitments of the proponent and the operational regulatory compliance oversight<sup>4</sup>. To address this, the CNSC incorporates the ERA documentation and the associated performance predictions directly within the licence as part of the ‘licensing basis’ within which the facility is expected to operate. This formalizes the initial ERA predictions as a basis for benchmarking environmental performance. This requires that the release (atmosphere and liquids) and receiving environment monitoring programs be designed to test the facilities environmental performance against the site-specific predictions. It also serves to encourage the application of an initial conservative approach (i.e. not overly optimistic) to risk and impact predictions and selected mitigative measures while emphasizing the value of pre-planning for additional mitigative options/actions should there be deviations in facility environmental performance.

The next significant step in the evolution of ERA’s role within the environmental protection framework was the addition of the concept of periodic updates to the ERA. This concept requires that a licensee periodically revisit and re-run their ERA on a five-year cycle using the accumulated site-specific data from the facility’s monitoring programs and incorporating any new developments in environmental science and/or modelling that may have occurred during the cycle. This serves as the means to test performance against predictions as well as the opportunity to update predictions with respect to environmental performance for continued operations. In this manner the ERA evolves from a conservative one-off predictive performance tool to a more realistic and site-specific tool allowing for the application of an adaptive management approach to environmental protection. The integration of all these elements is shown in Figure 1.

---

<sup>4</sup> An Environmental Assessment, especially one completed under CEAA, may address elements outside of environment health and safety such as socio-economic issues which are not within the mandate of the CNSC. Thus the ERA, not the complete EA is carried forward into licencing under the NSCA as it specifically addresses issue of environment, health and safety.

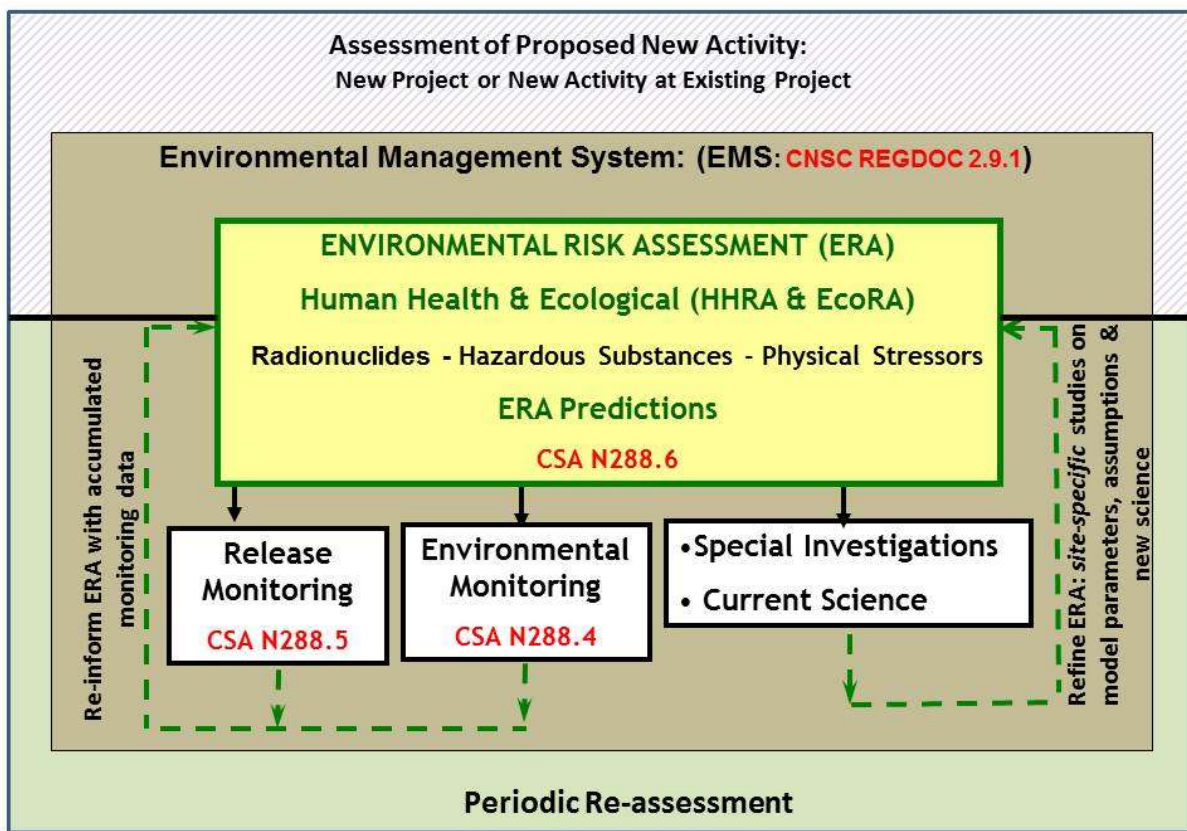


*FIG. 1. Role of environmental risk assessment (ERA) in the licensing life-cycle of a facility.*

In recent years the CNSC has worked on formally documenting this framework and has published regulatory document REGDOC-2.9.1 on Environmental Protection Policies Programs and Procedures addressing environmental management systems ([9]; currently being updated) and three environmental protection standards with the Canadian Standards Association (CSA): N288.4 Environmental Monitoring Programs [10], N288.5 Effluent Monitoring Programs [11] and N288.6 Environmental Risk Assessments [12], all of which are applicable to Class I facilities and uranium mines and mills (Fig. 1). The CSA standards are formally reviewed on a five-year basis allowing lessons learned and new science to be incorporated to ensure that they are based on best practice and modern knowledge.

#### 4. SUMMARIZED CASE STUDIES

The uranium mines and mills in northern Saskatchewan have been implementing comprehensive environmental monitoring programs since the late 1990s. In addition to the ERAs completed by licensees, a number of initiatives have resulted in risk assessments completed by CNSC staff. The results of these assessments are summarized here to demonstrate the role of a weight of evidence ERA based assessment approach combined with risk management decision making as it was applied to three different contaminants (uranium, molybdenum and selenium). The final outcome for all three of these contaminants was to require installation of additional water treatment systems.

Table II summarizes the weight of evidence used to determine whether environmental effects were occurring and the magnitude and spatial extent of any effects. The weight of evidence approach involved the completion of assessments based on various site-specific abiotic media and biological receptors. This tiered assessment approach commenced with determining whether the contaminant of concern (COC) was in the receiving environment and finishing with an assessment of the likelihood and magnitude of harm at the population or community level of organization.

Some of the questions posed are summarized in Table II starting simply with determining whether the COC was in the receiving environment at levels of potential concern (e.g. comparisons to available abiotic quality guidelines for water and sediment), and if so was the COC bioavailable (e.g., measurable in biological tissues) and at levels of concern to the organisms or to biota feeding on these organisms (comparisons to available tissue toxicity or consumption criteria). The higher assessment levels involved determining the extent of potential risk amongst multiple species and trophic levels, considering whether the magnitude and/or spatial extent of the exposure posed a population or higher level of risk to species or communities and whether field or laboratory studies indicated a cause and effect relationship to impaired reproduction or mortality (e.g. [13–15]).

TABLE II. WEIGHT OF EVIDENCE ASSESSMENT FOR THREE CONTAMINANTS OF CONCERN

| Weight of evidence considerations   | ERA conclusions        |                 |                 |
|---|------------------------|-----------------|-----------------|
|   | U                      | Mo              | Se              |
| Have effluent licence limits been exceeded?   | No                     | NA <sup>1</sup> | NA <sup>1</sup> |
| Are any available abiotic media quality guidelines exceeded                                       | Yes <sup>2</sup>       | Yes             | Yes             |
| Are any available guidelines or literature criteria exceeded for biological tissues? <sup>3</sup> | Yes                    | Yes             | Yes             |
| Are hazard quotients >1 for multiple species at multiple trophic levels?                          | Yes                    | Yes             | Yes             |
| Potential for population level effect?  | Yes (BI <sup>4</sup> ) | No              | Yes (Fish)      |
| Is there field evidence of cause effect relationship for impaired reproduction or mortality?      | Yes (BI)               | No              | Yes (Fish)      |

<sup>1</sup> Not applicable. No regulatory effluent limit available in either provincial or federal legislation at the time of assessment.

<sup>2</sup> U surface water quality objective for aquatic life was only recently developed relative to the operating life-span of the mine.

<sup>3</sup> No available provincial or federal guidelines. Requires specialist review of available scientific literature.

<sup>4</sup> BI = benthic invertebrates

With the completion of the ERA the process moves into the risk management phase to determine whether the predicted or confirmed effects are at levels that merit regulatory action. This could range from increased monitoring or oversight to requiring the installation of additional mitigative technology or ultimately, cessation of the activity. For the three contaminants discussed above, the level of effect was assessed relative to specific Canadian environmental legislation as shown in Table III as well as the specific requirements of the NSCA.

TABLE III. RISK MANAGEMENT CONSIDERATIONS

| Risk management consideration   |   | U   | Mo    | Se    |
|---|---|-----|-------|-------|
| Canadian Environmental Protection Act (CEPA)  |   |     |       |       |
| • Could the contaminant be classified as CEPA toxic?  | Yes   | No  | Yes   |       |
| Fisheries Act (FA)  |   |     |       |       |
| • Could the contaminant be considered a deleterious substance under the FA?                       | No  | No  | Yes   |       |
| Migratory Birds Act   |   |     |       |       |
| • Could the release be considered to be the deposition of a substance harmful to migratory birds? | No  | No  | Yes   |       |
| Species at Risk Act   |   |     |       |       |
| • Does the release pose a risk to identified species at risk?                                     | No  | No  | No    |       |
| Nuclear Safety and Control Act  |   |     |       |       |
| • Protect the environment   | As determined relative to Canadian environmental legislation (See above)  | Yes | No    | Yes   |
| • Reasonable risk   | Should the precautionary principle be applied?  | Yes | Yes   | Yes   |
| • Control releases  | Is there an absence of control(s) specific to this contaminant?   | Yes | Yes   | Yes   |
|   | Pollution Prevention: Is there a demonstrated control technology in application within the industry (BPT or BATEA)? | Yes | Yes   | ---   |
| Is the facility within its environmental licensing basis?   | Do measured abiotic and biotic effects exceed those predicted in the ERA forming the licensing basis?               | NA* | Yes** | Yes** |

--- Difficult to identify a treatment technology that can manage these low-level releases. Specific receiving ecosystem very sensitive to selenium.

\* NA. Old facility with long operating history. Original risk assessment was simple and involved a limited list of potential contaminants.

\*\* Advances in ecological and toxicological science and accumulation of site-specific monitoring data over operational history increased our understanding of the risks.

It was determined that all three contaminants merited regulatory action. The Commission added licence conditions requiring the identification and installation of additional water treatment system/processes. The risk management decisions and selected actions were unique for each contaminant and associated facility. They are summarized below.

#### 4.1. Uranium

The uranium assessment indicated a potential risk (i.e. exceedance of media guidelines and hazard quotients), supported by demonstrated changes in the benthic invertebrate community composition [16]. The conclusion was later further supported by *in situ* field toxicity assays [13]. Substantial improvements in effluent quality was possible with modernization and optimization of the water treatment system using standard chemical treatment technology. The associated regulatory decision was to require treatment on the basis of reasonable precaution to protect the environment and to control

releases (NSCA). Documentation of uranium risk management activities is available on the CNSC website [17–20].

#### **4.2. Molybdenum**

The molybdenum assessment indicated potential risk, predominantly to ruminants such as moose, with no demonstrated field effects [21]. It was determined that a practicable treatment technology was available and capable of eliminating the potential risk (substantial reduction in releases). The regulatory decision was to require treatment on the basis of reasonable precaution to protect the environment and to control releases (NSCA) as well as on the CEPA precautionary principle and pollution prevention.

#### **4.3. Selenium**

The selenium assessment indicated a potential risk to multiple species at multiple trophic levels confirmed through field studies directly linking selenium to teratogenesis in fish with the potential for population level effects [14, 15, 21]. The regulatory decision was to require additional treatment. However, due to the sensitivity of the receiving environment and the accumulation over time, achieving the necessary level of treatment is challenging. The decision was 1) require the installation of the best practicable treatment technology determined adequate to stabilize or promote slow recovery in the ecosystem; 2) complete studies to address uncertainty in the risk assessment; and 3) design and implement a specialized selenium monitoring program to assess potential recovery. Selenium reduction in effluent is specifically targeted for continuous improvement within the EMS.

#### **4.4. Additional regulatory requirements**

In addition to the necessary upgrades to the treatment systems, the licensees were also required to:

- 1) Establish action and administrative levels on their water treatment systems to ensure consistent treatment performance of these COCs;
- 2) Update the facility ERAs accounting for changes in the treatment system, the accumulated site-specific environmental knowledge and new science;
- 3) Re-evaluate and adjust as necessary effluent and receiving environment monitoring programs taking into account the results from the updated ERA.

### **5. CONCLUSIONS**

The role of ERA as an environmental protection instrument in the Canadian nuclear fuel cycle has substantially evolved over time. From its early limited application as a tool to assess the environmental acceptability of a proposed project it has now become a core regulatory requirement used to continuously assess performance of a facility throughout its life-cycle. The use of ERA in this manner provides the means of incorporating the learning principle of adaptive management within the regulatory framework where predictions related to environmental performance are tested, assessed and responded to as necessary. This approach provides the enhanced predictive power of site-specific models as they are refined over time. EAs for future proposed projects will also be more rigorous as a result of the lessons learned from the site-specific application of ERAs.

## REFERENCES

- [1] US ENVIRONMENTAL PROTECTION AGENCY (USEPA), Framework for ecological risk assessment, EPA/630/R-92/001, Risk Assessment Forum, U.S. Environmental Protection Agency Washington, DC (1992), <http://www.epa.gov/raf/publications/framework-eco-risk-assessment.htm>.
- [2] NUCLEAR SAFETY AND CONTROL ACT (NSCA), SC1977, c9, Minister of Justice (Canada) (Consolidated version current to Dec 10, 2014), <http://laws-lois.justice.gc.ca/eng/acts/N-28.3/>.
- [3] CANADIAN ENVIRONMENTAL PROTECTION ACT (CEPA), 1999. S.C. 1999, c. 33, Minister of Justice (Canada) (Consolidated version current to December 10, 2014), <http://laws-lois.justice.gc.ca/eng/acts/c-15.31/>.
- [4] CANADIAN ENVIRONMENTAL ASSESSMENT ACT (CEAA) 2012. S.C. 2012, c19s.52, Minister of Justice (Canada) (Consolidated version current to Dec 10, 2014), <http://laws-lois.justice.gc.ca/eng/acts/C-15.21/index.html>.
- [5] SPECIES AT RISK AC (SARA), 2002. S.C. 2002, c. 29, Minister of Justice (Canada) (Consolidated version current to Dec 10, 2014), <http://laws-lois.justice.gc.ca/eng/acts/S-15.3/>.
- [6] FISHERIES ACT, 1985. R.S.C., 1985, c. F-14, Minister of Justice (Canada) (Consolidated version current to Dec 10, 2014), <http://laws-lois.justice.gc.ca/eng/acts/f-14/>.
- [7] METAL MINING EFFLUENT REGULATIONS (MMER), 2002. SOR/2002-222, Minister of Justice (Canada) (Consolidated version current to Dec 10, 2014), <http://laws-lois.justice.gc.ca/eng/regulations/sor-2002-222/index.html>.
- [8] MIGRATORY BIRDS CONVENTION ACT (MBCA), 1994. S.C. 1994, c. 22. Minister of Justice (Canada) (Consolidated version current to Dec 10, 2014), <http://laws-lois.justice.gc.ca/eng/acts/M-7.01/>.
- [9] CANADIAN NUCLEAR SAFETY COMMISSION (CNSC), Environmental Protection: Policies, Programs and Procedures, Regulatory Document REGDOC-2.9.1, Canadian Nuclear Safety Commission, Ottawa (2013), <http://nuclearsafety.gc.ca/eng/acts-and-regulations/regulatory-documents/history/regdoc2-9-1.cfm>
- [10] CANADIAN STANDARD ASSOCIATION (CSA), Environmental monitoring programs at Class I nuclear facilities and uranium mines and mills, CSA N288.4-10 (2010), <https://community.csagroup.org/community/login.jspa?referer=%252Fcommunity%252Fnu> clear.
- [11] CANADIAN STANDARD ASSOCIATION (CSA), Effluent monitoring programs at Class I nuclear facilities and uranium mines and mills, CSA N288.5-11 (2011) <https://community.csagroup.org/community/login.jspa?referer=%252Fcommunity%252Fnu> clear
- [12] CANADIAN STANDARD ASSOCIATION (CSA), Environmental risk assessments at Class I nuclear facilities and uranium mines and mills, CSA N288.6-12 (2012), <https://community.csagroup.org/community/login.jspa?referer=%252Fcommunity%252Fnu> clear.
- [13] ROBERTSON, E.L., LIBER, K., Bioassays with caged *Hyalella azteca* to determine *in situ* toxicity downstream of two Saskatchewan, Canada, uranium operations, Environ. Toxicol. Chem. **26** 11 (2007) 2345–2355.
- [14] MUSKATELLO, J.R., BENNETT, P.M., HIMBEAULT, K.T., BELKNAP, A.M., JANZ, D.M., Larval deformities associated with selenium accumulation in northern pike (*Esox lucius*) exposed to metal mining effluent, Environ. Sci. Technol. **40** 20 (2006) 6506–6512.
- [15] MUSKATELLO, J.R., BELKNAP, A.M., JANZ, D.M., Accumulation of selenium in aquatic systems downstream of a uranium mining operation in northern Saskatchewan, Canada, Environ. Poll. **156** 2 (2008) 387–393.
- [16] CANADA GAZETTE, Publication of final decision on the assessment of a substance - Releases of radionuclides from nuclear facilities (impact on non-human biota) specified on the Priority Substances List (subsection 77(6) of the Canadian Environmental Protection Act, 1999). Canada Gazette **140**. 35 (2 Sep. 2006), <http://canadagazette.gc.ca/partI/2006/20060902/html/notice-e.html>.

- [17] CANADIAN NUCLEAR SAFETY COMMISSION (CNSC), ENVIRONMENT CANADA, Risk Management of Uranium Releases from Uranium Mines and Mills 2007 Annual Report, published by the Canadian Nuclear Safety Commission, catalogue number: INFO-0771 (2009), <http://www.nuclearsafety.gc.ca/eng/resources/publications/reports/uranium/2007-annual-report-on-uranium-management-activities.cfm>.
- [18] CANADIAN NUCLEAR SAFETY COMMISSION (CNSC), ENVIRONMENT CANADA, 2009 Annual Report on Uranium Management Activities, published by the Canadian Nuclear Safety Commission, catalogue number: INFO-0812 (2010), <http://www.nuclearsafety.gc.ca/eng/resources/publications/reports/uranium/2009-annual-report-on-uranium-management-activities.cfm>.
- [19] CANADIAN NUCLEAR SAFETY COMMISSION (CNSC), ENVIRONMENT CANADA, 2008 Annual Report on Uranium Management Activities, published by the Canadian Nuclear Safety Commission, catalogue number: INFO-0807 (2010), <http://www.nuclearsafety.gc.ca/eng/resources/publications/reports/uranium/2008-annual-report-on-uranium-management-activities.cfm>.
- [20] CANADIAN NUCLEAR SAFETY COMMISSION (CNSC) ENVIRONMENT CANADA, 2010 Annual Report on Uranium Management Activities, published by the Canadian Nuclear Safety Commission, catalogue number: INFO-0830 (2012), <http://www.nuclearsafety.gc.ca/eng/resources/publications/reports/uranium/2010-annual-report-on-uranium-management-activities.cfm>.
- [21] CANADIAN NUCLEAR SAFETY COMMISSION (CNSC), Key Lake Present Operations Cumulative Effects: CNSC Staff Determination of Environmental Risk. (WISMER, D., MCKEE, M., preparers) Directorate of Environmental Risk Assessment, Environmental Assessment and Protection Division (EAPD), Directorate of Nuclear Cycle and Facilities Regulation (DNCFR) (2006).

# CALIBRATION OF A PHREEQC BASED GEOCHEMICAL MODEL TO PREDICT SURFACE WATER DISCHARGE COMPOSITIONS FROM AN OPERATING URANIUM MILL IN THE ATHABASCA BASIN

J.J. MAHONEY\*, R.A. FREY\*\*

\* Mahoney Geochemical Consulting LLC,  
Lakewood, Colorado, USA

\*\* AREVA Resources Canada, Inc., Saskatoon,  
Saskatchewan, Canada

## Abstract

AREVA Resources Canada, Inc. has developed a predictive geochemical model of the surface water discharge system for their McClean Lake Operation. The Sink Vulture Treated Effluent Management System discharges treated waters through Sink Reservoir, followed by flow into Vulture Lake and finally into McClean Lake. Waters from two treatment plants, the dewatering of the JEB Tailings Management Facility, surface runoff, and rain and snow that falls onto the lakes make up the overall water balance. The source fluxes are converted into mixing proportions for use in the geochemical modelling program PHREEQC, which performs mixing calculations followed by evapoconcentration, equilibration with the atmospheric gases, mineral precipitation and surface complexation reactions. Strong agreement between observed and modelled concentrations was noted for many elements including sodium, potassium, chloride and magnesium. For these parameters simple mixing and dilution explain the downstream concentrations. Calcium and sulphate are generally conserved. However, discharges oversaturated with gypsum appear to rapidly precipitate gypsum. Similarly, powellite precipitation may lower molybdenum concentrations in some cases. Arsenic and uranium undergo attenuation due to surface complexation onto ferrihydrite. The agreement between observed and modelled concentrations demonstrates that this approach will provide robust predictions for the range of conditions expected at the McClean Lake Mill.

## 1. INTRODUCTION

AREVA Resources Canada, Inc. operates the McClean Lake Mill in northern Saskatchewan, Canada. The mill processes a wide variety of uranium ores; of which treated tailings are disposed in the JEB tailings management facility (TMF) [1]. The Tailings Preparation process was designed to treat arsenic and other metal concentrations in mill waste streams, resulting in trace concentrations in the tailings pore water. Water from the TMF is collected through an underdrain system. It is mixed with additional waters from the TMF surface pond and processed through a three-stage water treatment plant to meet surface water discharge standards. The water treatment plant provides secondary treatment to the entirety of milling wastes treated through the tailings preparation process. Ground water from the dewatering of the JEB TMF perimeter and treated effluent from the SUE mining operation provide additional sources that are discharged to the Sink Vulture Treated Management Effluent System (SVTEMS) (Fig. 1). These waters are first discharged to Sink Reservoir then into Vulture Lake and finally to McClean Lake.

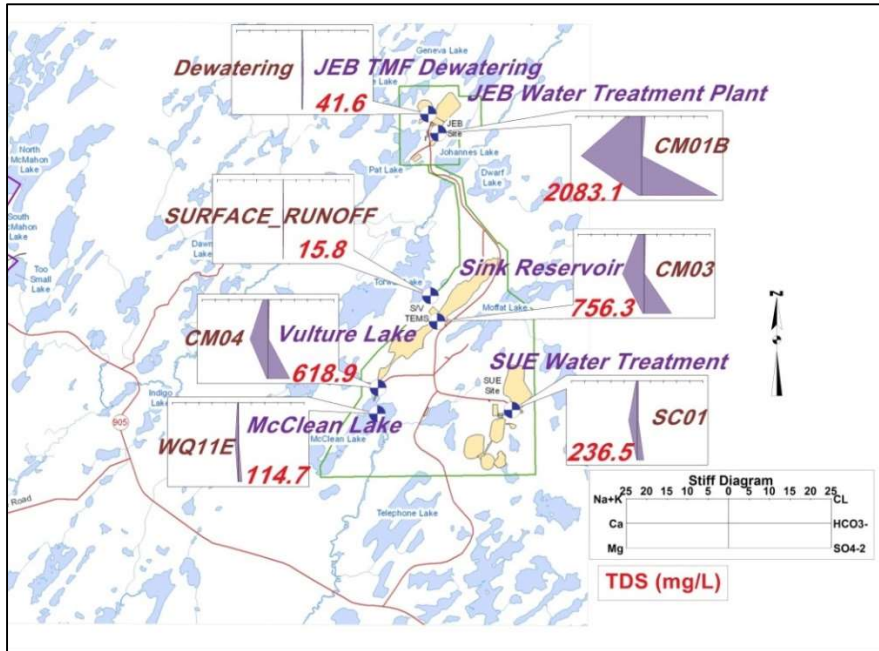


FIG. 1. Site layout of the SVTEMS with Stiff diagrams for the major water sources and total dissolved solids concentrations.

Figure 1 shows the average total dissolved solids (TDS) concentrations and Stiff diagrams for these source term waters. The figure indicates that the JEB Water Treatment Plant (JWTP) has the highest TDS concentration at more than 2000 mg/L. The JWTP also provides the greatest load of dissolved constituents to the SVTEMS. The JWTP discharge normally makes up about 30 percent of the annual water balance to Sink Reservoir. The JEB water is classified as a calcium sulphate dominated solution. The same fingerprint, albeit more diluted, is still observed as the water migrates to Sink Reservoir and then to Vulture Lake. Another water source that primarily enters Vulture and McClean Lakes is surface runoff. The model also includes a contribution of precipitation (rain and snow) that falls directly on the lake surfaces.

Throughout the last 15 years, the McClean Lake Mill has processed various uranium ores. The mill has also upgraded the water treatment system. System upgrades and ore process optimizations have produced a wide range of source term concentrations. Given the variability of the source waters it was decided that a model that relied primarily upon geochemical processes would be an improvement over one that used statistical analyses of previously reported lake data. A model that uses the site water balance and measured concentrations from the major sources, coupled with the various geochemical processes of equilibration with gases, mineral precipitation, evapoconcentration and surface complexation provides a robust predictive model that can evaluate changes in ores, processing operations, changes in water sources and water balance, and changes to the water treatment operations. PHREEQC version 3 [2] was selected because it is a public domain program that can perform all the required model calculations. The program is supported through the US Geological Survey. The SVTEMS model is primarily a batch mixing model, with mineral precipitation and surface complexation reactions that attenuate trace metals. Each set of calculations represents a single year, there is no year-to-year carry over in the annual models. Measured concentrations were generally based upon the average of 11 or 12 samples per year.

## 2. UPDATE OF THERMODYNAMIC DATABASE

The thermodynamic database included with PHREEQC [2] was updated and corrected. The original database was the WATEQ4F.dat database included with PHREEQC version 2. Updates included:

- For Uranium – Replaced constants in WATEQ4f.dat with the OECD NEA [3] selected complexes and values to define uranyl complexes. Replaced the two diffuse layer model constants for uranyl surface complexation onto hydrous ferric oxide (HFO) estimated by Dzombak and Morel [4] with the four surface complexes reported by Mahoney et al. [5]. Added the divalent uranyl carbonate complexes as reported by Dong and Brooks [6]. Removed the  $\text{UO}_2(\text{HPO}_4)_2^{2-}$  and  $\text{UO}_2(\text{H}_2\text{PO}_4)_3^-$  complexes per discussions in Grenthe et al. [7];
- For Arsenic – Included the metal arsenic complexes reported in Langmuir et al. [8] and additional complexes reported by Marini and Accornero [9, 10]. Replaced the diffuse layer surface complexation constants for arsenic onto HFO reported by Dzombak and Morel [4] with revised reactions and constants by Gustafsson and Bhattacharya [11];
- For Molybdenum – Replaced the surface complexation reactions reported by Dzombak and Morel [4] for HFO with the reactions and constants reported by Gustafsson [12].

### 3. MODEL SETUP

Water balance information (Table I) and water compositions for the source terms and compliance points were provided by AREVA Resources Canada. The water balances were recalculated in EXCEL to provide the mixing proportions required by PHREEQC. Precipitation rates were based upon annual measured rainfall/snow amounts at the site and the surface area of each water body.

TABLE I. SUMMARY OF WATER BALANCE, CALCULATIONS IN 1000 M<sup>3</sup>/YEAR. NO SURFACE RUNOFF WAS NOTED FOR SINK RESERVOIR FOR THE 12 YEARS LISTED BELOW

| Year | Direct sources   |       |      | Precipitation |         |         | Surface runoff |         |
|------|------------------|-------|------|---------------|---------|---------|----------------|---------|
|      | Dewatering wells | CM01B | SC01 | Sink          | Vulture | McClean | Vulture        | McClean |
| 2000 | 2110             | 1548  | 1075 | 90            | 270     | 823     | 1773           | 42030   |
| 2001 | 2329             | 1477  | 1303 | 109           | 326     | 996     | 1987           | 40741   |
| 2002 | 1315             | 1301  | 263  | 163           | 489     | 1494    | 901            | 64639   |
| 2003 | 1591             | 1562  | 59   | 165           | 495     | 1511    | 1301           | 82452   |
| 2004 | 1619             | 1559  | 980  | 85            | 254     | 777     | 1542           | 34705   |
| 2005 | 1461             | 1635  | 2537 | 187           | 562     | 1717    | 1823           | 66191   |
| 2006 | 818              | 1294  | 1182 | 171           | 512     | 1563    | 1701           | 47065   |
| 2007 | 1119             | 1335  | 1092 | 126           | 379     | 1157    | 1782           | 41052   |
| 2008 | 1026             | 1672  | 917  | 91            | 272     | 831     | 1945           | 51066   |
| 2009 | 837              | 1592  | 291  | 136           | 408     | 1245    | 1218           | 112457  |
| 2010 | 636              | 1447  | 0    | 139           | 418     | 1277    | 697            | 38632   |
| 2011 | 521              | 958   | 170  | 121           | 364     | 1110    | 1132           | 40846   |

Evaporation rates were based upon the surface area of each lake. Rates were determined from environmental monitoring programs conducted at the time of facility licensing. Another contribution to the mixing calculations, not listed in Table I, was residual water in each lake. These volumes were determined from topographical surveys at the time of initial facility licensing.

The steps of the annual PHREEQC models were:

- 1) The CM01B (JWTP) solution composition is printed out for reference, and user defined equilibrium phases were allowed to precipitate, these phases may include gypsum, powellite, or ferrihydrite. Surface complexation reactions can be included based upon the amount of ferrihydrite that precipitates, final models did not include surface complexation at this step;
- 2) The Sink Reservoir mixing process is the next step. The CM01B, TMF dewatering waters, SUE treated water, direct rain/snow precipitation and any residual water in Sink Reservoir are mixed. Evaporation is included in the next step, and a correction term is included to bring the volume of water back to 1 litre for use in later mixtures. Equilibrium phases are allowed to precipitate. These phases may include ferrihydrite. Surface complexation reactions can be included based upon the amount of ferrihydrite that precipitates in the mixed water;
- 3) The Vulture Lake composition is defined by mixing the Sink Reservoir water with surface water runoff, as well as an initial volume of water in the lake and additional rain/snow precipitation. Evaporation, equilibration with minerals and surface complexation reactions are allowed; in general, the solutions are too dilute for mineral precipitation reactions to proceed;
- 4) The McClean Lake composition is estimated by mixing the previously estimated Vulture Lake water with added runoff, rain/snow precipitation and any water in the lake. Evaporation, equilibration with minerals and surface complexation reactions are allowed; in general, the waters in McClean Lake are too dilute for mineral precipitation reactions to proceed.

Each subsequent annual model repeats the same sequence.

#### 4. MODEL RESULTS

##### 4.1. Conservative species

The agreement between the measured and modelled concentrations shows that many of the major ions are conserved, and the concentration changes along the flow path are due solely to mixing with other waters and evaporation. Elements that display this behaviour include sodium, chloride, (Figs 2 and 3), potassium, and magnesium. The downstream samples in Sink Reservoir, as well as Vulture and McClean Lakes show good agreement between the measured and modelled concentrations. Figure 2 shows some elevated concentrations of sodium in the JWTP water in 2008 and 2009. This is related to regeneration of the solvent used in the ore recovery process. This spike is readily seen in the model in the Sink Reservoir and Vulture Lake samples. Chloride also shows good agreement in the downstream lakes. There is a slight positive bias in the Sink Reservoir samples, but the modelled concentrations in Vulture Lake show better agreement. A similar pattern was observed in the potassium data, where modelled concentrations tended to be greater than observed values in Sink Reservoir, but showed near concurrence in Vulture Lake. The modelled magnesium concentrations provide good matches to the observed concentrations. Aluminium also appears to be conserved. Models that allowed for the precipitation of gibbsite  $[Al(OH)_3]$  or boehmite ( $AlOOH$ ) showed significantly poorer fits. Intra-year variations in pH may have some influence on this parameter.

The agreement between the measured and model predicted concentrations of these species indicates that the water balances for the twelve years of sampling provide reasonable fits. Further adjustments to the water balances are not required. Differences between observed and modelled concentrations may be caused by mineral precipitation or surface complexation.

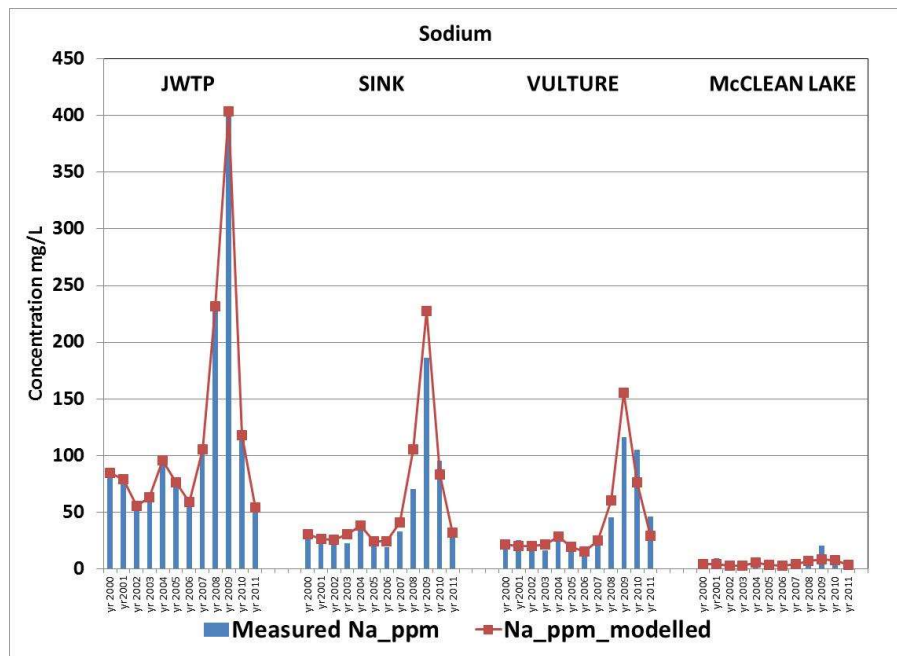


*FIG. 2. Comparison of measured and modelled sodium concentrations in the SVTEMS. The vertical lines represent the annual concentrations for years 2000 to 2011 for the JWTP discharge and the downstream Sink Reservoir followed by Vulture and McClean Lakes.*

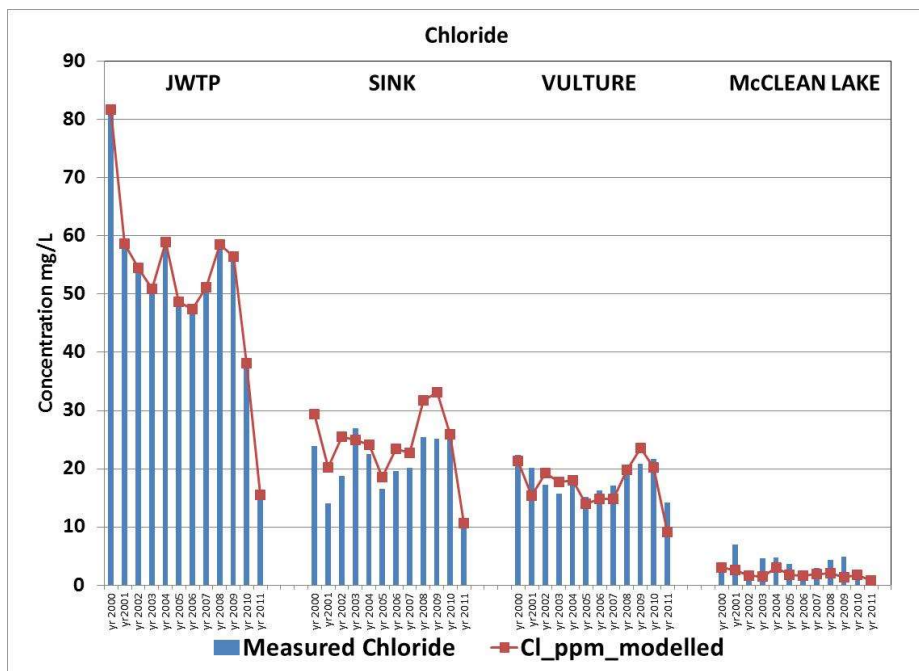


*FIG. 3. Comparison of measured and modelled chloride concentrations in the SVTEMS.*

For most years, calcium and sulphate (Figs 4 and 5) act as conservative elements. But in the years where the JWTP samples are oversaturated with respect to gypsum ( $\text{CaSO}_4 \cdot 2\text{H}_2\text{O}$ ) a slightly better fit is noted if gypsum is allowed to precipitate. The figures show two different models, the first model did not allow for the precipitation of gypsum (open triangles). The second model (filled squares) did allow for precipitation, and samples from the years 2007, 2008, and 2009 were determined by PHREEQC to be oversaturated. The removal of calcium and sulphate from these three samples improved the overall fit

of the model. The solubility product constant had a  $\log K_{sp}$  value of -4.58, and it was not adjusted to improve the fit.

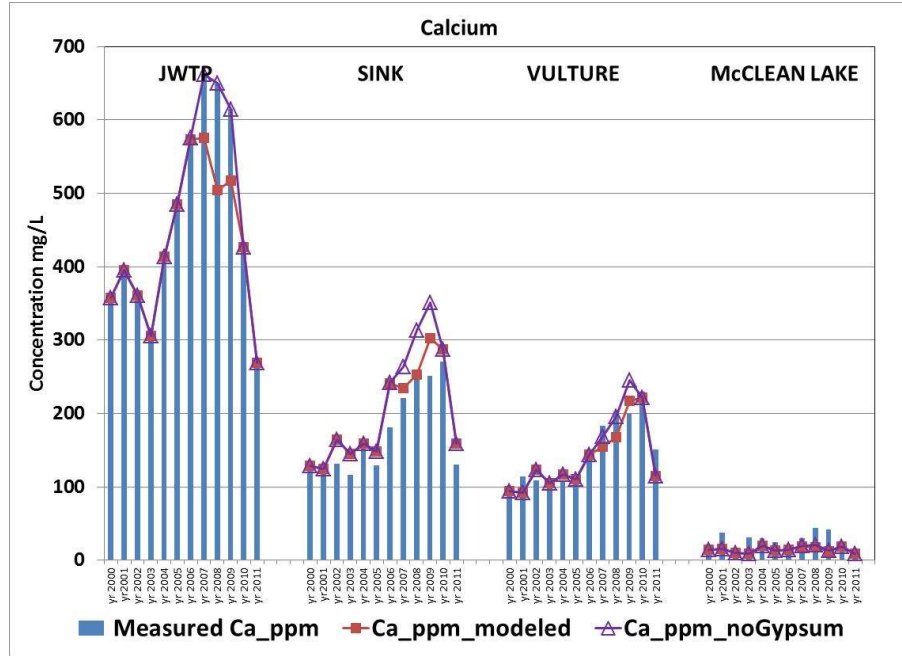


FIG. 4. Comparison of measured and modelled calcium concentrations in the SVTEMS. The figure shows two different models related to gypsum precipitation.

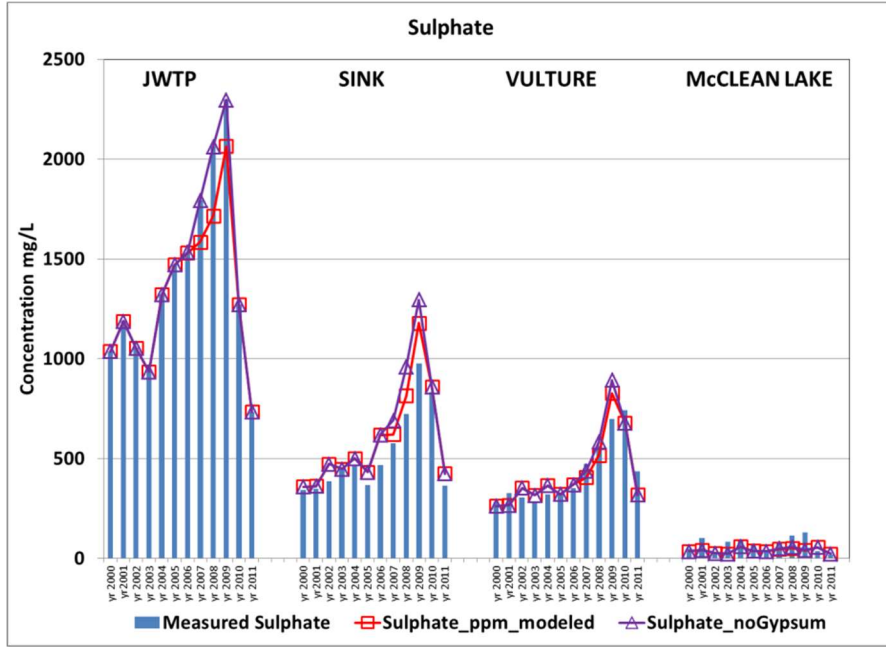
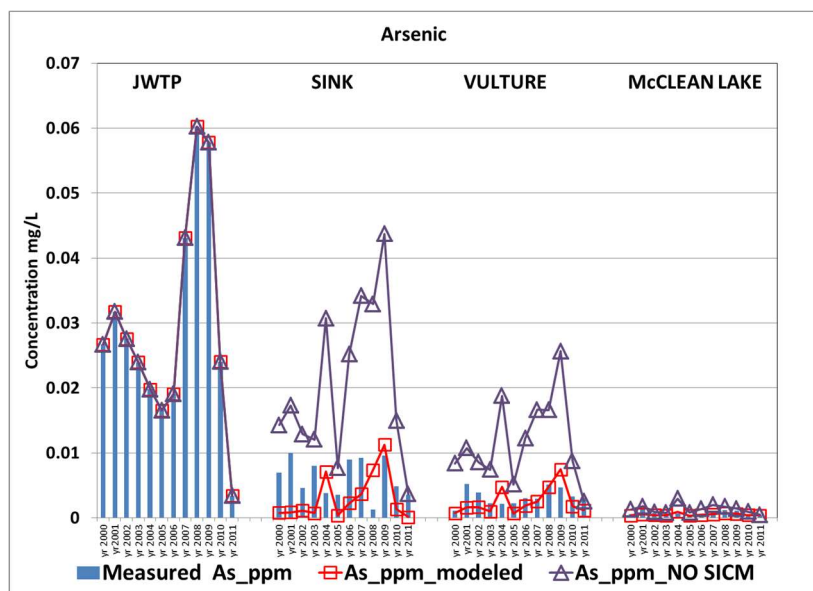


FIG. 5. Comparison of measured and modelled sulphate concentrations in the SVTEMS. The figure shows two different models based upon gypsum precipitation.

## 4.2. Arsenic and uranium – Attenuated species

The behaviour of arsenic is one of the most interesting processes identified. Arsenic concentrations are significantly lower than would be calculated if arsenic was solely retained (conserved) in the aqueous phase (Fig. 6). Concentrations in the source waters are too low to suggest the precipitation of solids such as ferric arsenate or scorodite [8]. Surface complexation onto the iron from the JWTP and dewatering wells discharges appears to be the most reasonable process. Iron precipitates as ferrihydrite [ $\text{Fe(OH)}_3$ ], also known as HFO. To better quantify the surface reactions, a series of calculations were run using PhreePlot [13]. This program uses all the features of PHREEQC, but it allows for adjustment of parameters to optimize the fit between observed and modelled concentrations. PhreePlot calculates the weighted residual sum of squares (WRSS) between the observed and modelled concentrations. The optimization routine changes user defined parameters to minimize the WRSS. In these models the surface site density function changes as the program optimizes the fit between the measured and modelled concentrations for the 36 arsenic data points in the three water bodies. Arsenic was selected for calculations because in many pit lake models [14] it tends to show the greatest amount of surface complexation for models that use default site densities per mole of ferrihydrite formed. The resultant concentrations tend to be unrealistically low. However, most pit lake models do not have the detailed observational data that is available from the McClean Lake operation so for most models the default, rather than fitted surface site density values are used.

The PhreePlot fitting calculations were set up in the following manner. After mixing the source waters in Sink Reservoir, the model is allowed to precipitate ferrihydrite. The amount precipitated is based upon the amount of iron in the JWTP and the TMF dewatering discharges. The concentration of sorption sites is proportional to the amount of ferrihydrite formed. Dzombak and Morel [4] defined the weak site ( $\text{Hfo\_wOH}$ ) concentration to be 0.2 moles of surface sites per mole of ferrihydrite available and strong sites ( $\text{Hfo\_sOH}$ ) are 0.005 moles/mole. These are the default values used in many geochemical models. Arsenic only forms surface complexes with weak sites, simplifying the fitting calculations. For our discharge model, PhreePlot estimated a value of 0.09 moles/mole for the first six years and 0.129 moles/mole for the final six years. The strong site density was calculated as the fitted weak site density divided by 40, this maintains the proportion of weak to strong sites reported by Dzombak and Morel. These modelled values are conservative as the fitted site densities are lower than the laboratory estimated values. Surface complexation reactions were not identified in Vulture or McClean Lake as all the excess iron is precipitated in the upper mixing region of Sink Reservoir.



*FIG. 6. Comparison of measured and modelled arsenic concentrations in the SVTEMS. The figure shows two different models. The open triangles assumed no surface complexation, the filled squares assumed surface complexation onto hydrous ferric oxide.*

Uranium (Fig. 7) also appears to be attenuated through surface complexation processes. Preliminary models confirmed this, but if site concentrations were adjusted to optimize the uranium data, then the modelled arsenic concentrations would be lowered significantly. Current models show only slight amounts of uranium attenuation due to surface complexation. It was decided that overestimating the modelled uranium concentrations and not underestimating arsenic concentration was the more reasonable approach and it produced a model that used conservative assumptions (that tend to increase modelled concentrations so are more protective of the environment) in its predictions.

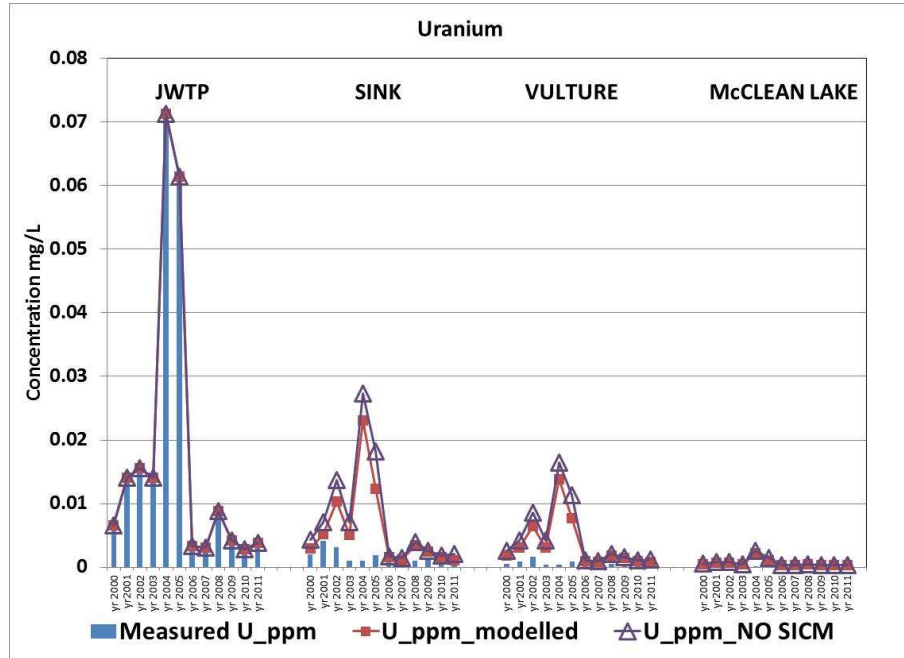


FIG. 7. Comparison of measured and modelled uranium concentrations in the SVTEMS. The figure shows two different models. Open triangles assumed no surface complexation. The filled squares assumed surface complexation onto hydrous ferric oxide based upon PhreePlot fitting of the arsenic data to estimate the surface site density function.

#### 4.3. Molybdenum

Molybdenum (Fig. 8) behaved somewhat similarly to calcium and sulphate. Figure 8 shows the results of three models. The first model did not allow for the precipitation of powellite ( $\text{CaMoO}_4$ ), and those models overestimate molybdenum concentrations in Sink Reservoir and Vulture Lake for years 2001, 2002 and 2003. The second model allowed for powellite precipitation if the solution was oversaturated with respect to that solid. The results of those calculations under estimate molybdenum concentrations during those three years. Finally, models were prepared that adjusted the solubility product constant of powellite. A trial and error model increased the  $\log K_{sp}$  to -7.65 and it produced an intermediate fit (not shown on Fig. 8).

The final model used PhreePlot and the optimized  $\log K_{sp}$  value was -7.67 (Xs in Fig. 8). The final model  $\log K_{sp}$  value is close to the trial and error value. The greater solubility of this phase may reflect a less stable amorphous solid with a greater solubility or more likely it reflects incomplete precipitation caused by a combination of slow precipitation kinetics and short residence time during transit to Sink Reservoir. It is unlikely that molybdenum concentrations at values high enough to allow for powellite formation will be observed in future JWTP discharges. In 2004, additional treatment efforts were implemented to lower molybdenum concentrations in the JWTP discharge to levels that are significantly below the solubility limit ( $\log K_{sp} = -7.95$ ). The current model allows for surface complexation, but the amount of surface complexation for these later samples is slight and not readily visible on the figures.

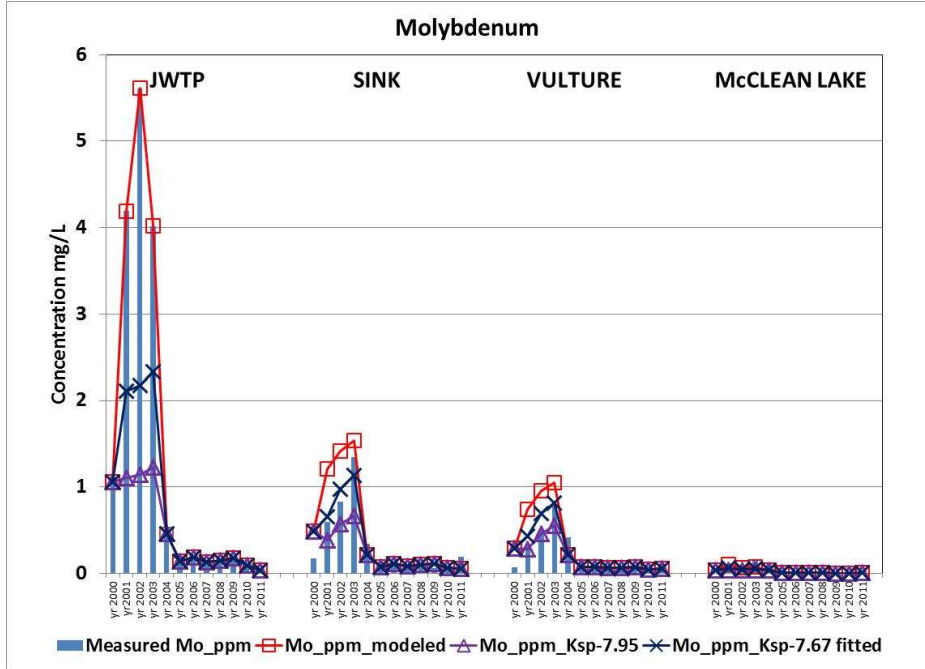


FIG. 8. Comparison of measured and modelled molybdenum concentrations in the SVTEMS.

#### 4.4. Other parameters

Several other parameters also demonstrate attenuation along the discharge flow path. Modelled ammonia concentrations tend to be consistently greater than observed values suggesting that ammonia is apparently undergoing partial nitrification. In the initial models because the model assumes oxygenated conditions the modelled ammonia converts to nitrate and the pH drops significantly. This great a pH change is not observed; therefore, ammonia was decoupled with nitrate. This is a common practice and PHREEQC has a special database for this eventuality.

Modelled selenium is also lower than measured selenium and a possible redox process is under consideration. Surface complexation reactions of selenate onto HFO are too small to have any significant impact.

Iron requires additional evaluation. Poor fits are observed in Sink Reservoir. However, better agreements are noted in Vulture Lake. Additional samples that should show seasonal effects are being evaluated and it is hoped that a better understanding of redox processes will be developed.

#### 5. CONCLUSIONS

The PHREEQC based model of the SVTEMS has provided numerous insights into the geochemical conditions within the Sink Reservoir and the downstream lakes. Dilution plays an important role in the attenuation of all components. But simple geochemical processes can, depending upon initial concentrations, attenuate calcium, sulphate, arsenic, uranium, molybdenum, selenium and ammonia. The deeper understanding of the processes demonstrates that for arsenic and uranium, much of the attenuation capacity can be provided by the residual iron released from the JWTP and dewatering discharges.

The inclusion of PhreePlot as part of the modelling protocol provides an additional tool to develop rigorously fitted parameters for surface complexation and solubility product calculations. Additional evaluations of more seasonal (three samples per year) and/or monthly data are underway and it is expected that future models will incorporate at least one redox based process.

The goal of preparing a simple model that includes pertinent geochemical processes has been achieved. This model provides a valuable methodology to assist in evaluating the downstream impacts caused by possible changes to the mill and water treatment operations over the short and long term. This quantitative model will also help in further evaluations of the detailed geochemical processes throughout the SVTEMS.

## REFERENCES

- [1] MAHONEY, J., SLAUGHTER, M., LANGMUIR, D., ROWSON, J., Control of As and Ni releases from a uranium mill tailings neutralization circuit: Solution chemistry, mineralogy, and geochemical modeling of laboratory study results, *Applied Geochemistry* **22** 12 (2007) 2758-2776.
- [2] PARKHURST, D.L., APPELO, C.A.J., PHREEQC version 3 — A computer program for speciation, batch-reaction, one-dimensional transport, and inverse geochemical calculations, U.S. Geological Survey (2013).
- [3] GUILLAUMONT, R. et al., Update on the Chemical Thermodynamics of Uranium, Neptunium, Plutonium, Americium and Technetium, Elsevier, Amsterdam (2003).
- [4] DZOMBAK, D.A., MOREL, F.M.M., Surface complexation modelling: hydrous ferric oxide. Wiley-Interscience, New York (1990).
- [5] MAHONEY, J.J., CADLE, S.A., JAKUBOWSKI, R.T., Uranyl adsorption onto hydrous ferric oxide – an-evaluation for the diffuse layer model database, *Env. Sci. Technol.* **43** 24 (2009) 9260-9266.
- [6] DONG, W., BROOKS, S.C., Determination of the formation constants of ternary complexes of uranyl and carbonate with alkaline earth metals ( $Mg^{2+}$ ,  $Ca^{2+}$ ,  $Sr^{2+}$ , and  $Ba^{2+}$ ) using anion exchange method, *Environ. Sci. Technol.* **40** (2006) 4689-4695.
- [7] GRENTHE, I. et al., Chemical Thermodynamics of Uranium, (1992) (2004 reprint available from NEA OECD).
- [8] LANGMUIR, D., MAHONEY, J., ROWSON, J., Solubility products of amorphous ferric arsenate and crystalline scorodite ( $FeAsO_4 \cdot 2H_2O$ ) and their application to arsenic behavior in buried mine tailings, *Geochim. Cosmochim. Acta* **70** (2006) 2942-2956.
- [9] MARINI, L., ACCORNERO, M., Prediction of the thermodynamic properties of metal arsenate and metal–arsenite aqueous complexes to high temperatures and pressures and some geological consequences, *Environ. Geol.* **52** (2007) 1343-1363.
- [10] MARINI, L., ACCORNERO, M., Erratum to: Prediction of the thermodynamic properties of metal–arsenate and metal–arsenite aqueous complexes to high temperatures and pressures and some geological consequences, *Environ. Earth Sci.* **59** (2010) 1601-1606.
- [11] GUSTAFSSON, J.P., BHATTACHARYA, P., “Geochemical modeling of arsenic adsorption to oxide surfaces” (Chapter 6), Arsenic in Soil and Groundwater Environment (BHATTACHARYA, P., MUKHERJEE, A.B., BUNDSCHUH, J., ZEVENHOVEN, R., LOEPPERT, R.H., Eds), Trace Metals and other Contaminants in the Environment, Elsevier, **9** (2007) 159–206.
- [12] GUSTAFSSON, J.P., Modeling molybdate and tungstate adsorption to ferrihydrite, *Chem. Geol.* **200** (2003) 103-115.
- [13] KINNIBURGH, D.G., COOPER, D., PhreePlot - Creating graphical output with PHREEQC (2014), available at <http://www.phreeplot.org/>.
- [14] DUTHE, D.M., MAHONEY, J.J., SHCHIPANSKY, A.A., TERRELL, C.L., “Assessment of the Process of Pit Lake Formation and Associated Geochemistry in Open Pits – Mupane Gold Mine, Botswana”, Mine Water - Managing the Challenges (Proc. Int. Mine Water Assoc. Congress 2011, Aachen, Germany) (RUDE, R.T., FREUND, A., WOLKERSDORFER, C., Eds). (2011) 511-515.

## **THE ‘NAMIBIAN URANIUM MINING’ MODEL**

W. SWIEGERS

Namibian Uranium Institute,  
Swakopmund, Namibia

### **Abstract**

Namibia has implemented mutually-beneficial partnerships to ensure that adequate capacity exists. Voluntary product stewardship schemes have arisen out of the need for the industry to balance their pursuit of economic gain with environmental and social concerns. Industry has built on World Nuclear Association standards in developing voluntary product stewardship schemes to gain majority sector participation.

### **1. INTRODUCTION**

This paper examines the challenges the uranium industry faces in ensuring responsible exploration and production of uranium in Africa and the complexities associated with the development of a responsible and sustainable programme based on the guidelines provided by the World Nuclear Association (WNA). It describes the uranium industry’s voluntary initiatives which are underpinned by a developing regulatory safety net to ensure leading practice and sustainability.

### **2. CONTEXT**

Namibia has extensive deposits of low-grade uranium and is regarded as a region of global importance for this source of energy. Namibia also has a long history of uranium mining, dating back to 1976, when Rio Tinto’s Rössing uranium mine opened. In 2007, a second uranium mine was opened, Paladin’s Langer Heinrich Mine. Namibia is currently the world’s fifth largest producer of uranium, but is set to move up the third spot by 2015.

During the period 2007 until 2011, the world experienced increased demands for uranium resulting in a ‘uranium rush’ in Namibia’s uranium province, the Erongo region. The genesis of the uranium industries involvement and the creation of a Namibian Uranium Institute, stemmed from the realization that the uncoordinated ‘uranium (exploration) rush’ posed a significant risk to the industry itself and was originally set up in an environment with little regulation relating to the uranium industry. This forced the Chamber of Mines (CoM), as the official representative body of the mining industry, to focus heavily on the need for self-regulation and the immediate needs of its members.

In 2011 the Fukushima Daichi nuclear-power station accident changed the nuclear industry’s reputation worldwide and the ‘aftershocks’ are still being felt today. This has had major implications for the uranium industry. It has set public confidence in nuclear power back to levels not seen since the aftermath of the Chernobyl or Three Mile Island disasters.

### **3. SUSTAINABLE DEVELOPMENT**

There is only one secure path for Namibia to address inequality and poverty in the long term and that is to develop a sustainable economy. Key is our commitment to successfully manage the balance between economic, social and ecological issues. We believe mining can play an important role in this regard. Namibia needs jobs and the mines can provide them without repeating the mistakes of the past and need to continuously improve work practises.

The Namibian Government’s position on uranium mining is clear. His Excellency Hifikepunye Pohamba, President of the Republic of Namibia, reaffirmed that “Namibia’s mineral resources (including uranium) are to be strategically exploited and optimally beneficiated, providing equitable opportunities for all Namibians to participate in the industry, while ensuring that environmental impacts are minimized and investments resulting from mining are made to develop other sustainable industries

and human capital for long-term national development". The concept of sustainable development is one of the cornerstones on which Namibia's National Constitution and National Development Plan is built. Namibia also committed itself internationally to a sustainable future, by adopting the United Nations Agenda 21 principles which cut across all sectors — social, economic and ecological.

### **3.1. Sustainable development advisory council**

In 2013 the Sustainable Development Advisory Council was appointed under the Environment Management Act, which is administered by the Ministry of Environment & Tourism. It is tasked to strike a balance between the country's development and environmental protection. It needs to mobilise resources and guide policy formulation to achieve strategic development objectives and goals as outlined in the fourth National Development Plan (NDP4) and Vision 2030 respectively. The Council promotes cooperation and coordination between states and civil society and nurtures partnerships between different branches of government with private sector, non-governmental organizations, community-based organizations and the international community. There is no doubt that the formation of these institutions has added significant value to the industry.

## **4. MINING IN NATIONAL PARKS**

Namibia is a world-famous tourist destination. Most of the uranium exploration and mining activities occur in the Central Namib, an ecologically-sensitive area containing parts of the Namib Naukluft National Park and Dorob National Park. Continued uranium exploration and mining could have a considerable effect on the natural environment as well as a cumulative impact on water and energy requirements, transportation, housing, schooling, and medical services.

Although mining and the relevant developments are vital for the growth of the economy, Namibia recognized that uncontrolled prospecting and mining activities might undermine the country's ecology and tourism potential. Namibia must reconcile development objectives and mineral exploitation with environmental protection for the country's long-term socio-economic growth and stability. Clearly, an integrated approach is required so that development of one resource will not jeopardize the potential of another.

The Policy for Mining and Prospecting in Protected Areas and National Monuments that was originally published in 1999 was amended to strengthen the conditions under which mining and prospecting might be permitted in protected areas and to ensure application of environmental best practice to promote sustainable development.

## **5. LEGISLATIVE DEVELOPMENT**

Namibia is party to the Nuclear Non-Proliferation Treaty and has had a comprehensive safeguard agreement in force since 1998. In 2012 it also ratified the Additional Protocol to the Safeguards Agreement and the Pelindaba Treaty. The Namibian Government has taken important steps in responding to the dearth of adequate legislation with the promulgation of The Minerals (Prospecting & Mining) Act, No 33 of 1992, the Minerals Policy (2005), Atomic Energy and Radiation Protection Act, 5 of 2005 and the Environmental Management Act, 7 of 2007.

An Atomic Energy Board has been established along with a National Radiation Protection Authority (NRPA). Finland's Radiation & Nuclear Safety Authority (STUK) furthermore assisted the Namibian authorities to develop a Nuclear Fuel Cycle Policy to ensure policy directive on the beneficial, safe and secure exploitation of uranium resources. A significant advance was made with the appointment of an Environmental Commissioner in 2012 to ensure environmental sustainability. As part of the Ministry of Environment and Tourism's national restructuring exercise, the Department of Environmental Affairs now falls under the Environmental Commission. Since the Namibian Government put in place a moratorium in 2007, no Exclusive Prospecting Licenses (EPL) applications have been accepted, although a number of EPL applications that were submitted prior to the moratorium, were processed.

## **6. THE DEVELOPMENT OF URANIUM STEWARDSHIP IN NAMIBIA**

The development of the Rössing Uranium mine in the mid-1970s saw massive investment into the local community and was very much at the forefront of modern corporate social responsibility. In response to the country's rapidly growing uranium industry, Rössing Uranium Limited, Langer Heinrich Uranium Mine and AREVA Resources championed the need for the Chamber of Mines of Namibia to develop minimum standards for occupational health and environmental management for uranium exploration and mining activities in Namibia to complement the emerging regulatory framework and protect the Namibian Uranium brand. Many others, notably Bannerman Resources and Swakop Uranium soon joined.

Through its membership, the Chamber of Mines turned to the WNA for assistance and adopted the WNA policy document “Sustaining Global Best-Practices in Uranium Mining and Processing: Principles for Managing Radiation, Health and Safety, Waste and the Environment” as an official guiding document in January 2008. This policy covers aspects of Sustainable Development, Uranium Stewardship and Corporate Social Responsibility (CSR) and endorses the WNA Charter of Ethics and the ICMM Sustainable Development Principles. This concept of self-regulation has expanded and developed in recent years to the point where Namibia is an outstanding proponent of Uranium Stewardship.

Central to the programme is the acceptance of Uranium Stewardship as an important pillar that supports the overarching concept of sustainable development. Its role is to ensure that business management focuses simultaneously on economic development, environmental impacts and the fulfilment of social responsibilities. Stewardship needs an integrated programme of actions aimed at ensuring that all materials, processes, goods and services are managed throughout the life cycle in a socially and environmentally responsible manner. Measures to address the cumulative socioeconomic impacts of mining and future mine closure cannot be successful if adopted by one mining company only. Decisions and actions must be aligned with each other and with national, regional and local development plans.

### **6.1. Implementing the WNA sustainability policy**

The natural resource industry has played a major role in the advancement of society’s needs and well-being and the economic growth and industrialization of many countries. Its acceptance is neither automatic nor unconditional. The need to gain and maintain the support of the people that live and work in the area of impact and influence of any given project is paramount. Failure to gain and maintain this ‘social license’ can lead to conflict, delays or costs for the proponents of a project. The social license is therefore seen as a dynamic, on-going relationship between the company and its stakeholders.

Building on the WNA policy, “Sustaining Global Best Practices in Uranium Mining and Processing — Principles for Managing Radiation, Health and Safety, Waste and the Environment”, the members of the Uranium Stewardship Committee (USC) agreed to implement the WNA’s “Standardization of the Sustainable Development (SD) performance reporting (between utilities-miners) for uranium mining and processing sites” (henceforth referred to as the WNA Checklist) and to continue promoting the WNA policy for uranium mining.

A significant milestone was achieved in 2008 when the Namibian Stock exchange (NSX) agreed that uranium exploration and mining companies would not be listed on the NSX unless they were good standing members of the Chamber of Mines of Namibia. All Chamber members are bound by the constitution and the Chamber’s Code of Conduct that commits them to upholding the Namibian Uranium brand, whilst ensuring the highest standards of environmental and radiation safety management.

### **6.2. The Uranium Institute (UI)**

The CoM’s established the Chamber of Mines Uranium Institute (UI) in the coastal town of Swakopmund (the main base of operations for most uranium companies) at the end of 2009. The UI aims to promote and protect the Namibian Uranium brand and coordinate occupational health, radiological safety/security and environmental management issues. The UI is dedicated to the cause of

bringing first-world standards to the operation of all aspects of the uranium industry in Namibia and to promote product Stewardship.

As well as providing advocacy and guidance, the UI facilities include a Uranium Information Centre, a Uranium Training Centre, Medical Centre and conference rooms. Its website ([www.namibianuranium.org](http://www.namibianuranium.org)) provides detailed information on uranium industry participants, government regulation, environmental and safety aspects of uranium mining and exploration. The UI was financially supported by Rössing Uranium, Langer Heinrich Uranium and Areva Resources Namibia in addition to contributions from the five emerging companies Swakop Uranium, Bannerman Resources, Valencia Uranium, Reptile Uranium and Zhonghe Resources.

### **6.3. The Strategic Environmental Assessment (SEA)**

The Namibian Uranium Association (NUA) supports a coordinated strategic approach by industry and government to ensure successful economic development in the Erongo Region. In conjunction with a number of other interested parties, the uranium industry identified the urgent need for a strategic environmental assessment of the uranium industry in the Central Namib in 2007 to better understand the vulnerabilities and opportunities to which the region might be exposed to as a result of multiple uranium mines developing in a relatively short space of time. To this end, the Chamber and the Ministry of Mines and Energy (MME), in cooperation with the German Federal Institute for Geosciences and Mineral Resources (BGR), commissioned the world's first strategic environmental assessment (SEA) for a mining area. The Southern African Institute for Environmental Assessment was selected to do the study in an independent and scientific manner. It was monitored by external assessors and the final draft was released in 2011.

This ground-breaking report is being translated into a Strategic Environmental Management Plan (SEMP) which provides a comprehensive annual monitoring framework to assist the Government in responsibly managing the uranium industry. The SEMP is guided by a multisectoral steering committee and run by MME, which is in the final stages of completing the first annual SEMP report. The Strategic Environmental Management Plan (SEMP) is an over-arching framework and roadmap for addressing the cumulative impacts of a suite of existing and potential developments linked to uranium mining. The Government takes overall responsibility for implementing the SEMP through a close partnership between Ministry of Mines and Energy (MME) and Ministry of Environment and Tourism (MET). This is done through a broad-based steering committee that oversees the functioning of a small SEMP secretariat based at the Geological Survey within the MME. Implementation of the SEMP began in earnest in 2011 and culminated in the preparation of the first draft Annual SEMP monitoring Report, which was published in early 2013.

### **6.4. The Namib Environmental Restoration and Monitoring Unit (NERMU)**

NERMU was established to function as a key monitoring agent for the SEMP, to drive restoration research and implementation and to develop skills in critical environmental management-related fields. The Ministry of Mines and Energy (MME) worked with their German Partners to secure funding for this unit, which led to the establishment of NERMU at Gobabeb. The German Federal Ministry for Economic Cooperation and Development, through the Technical Cooperation Project between the German Federal Institute for Geosciences and Natural Resources (BGR) and the Geological Survey of Namibia (GSN), provided seed funding in 2011 and awarded a grant for 2012–2013.

## **7. THE POST FUKUSHIMA ERA**

The nuclear world changed dramatically with the Fukushima accident. Post Fukushima, the broader uranium mining industry is facing increasing expectations from governments and communities regarding safety, occupational health and corporate social responsibility obligations. The shape of the local industry in Namibia is still in a state of flux, with existing operations and projects under severe economic pressure, whilst others are moving from exploration to start up.

## **7.1. The Namibian Uranium Association (NUA)**

In 2013 the Chamber of Mines identified a pressing need to review the current arrangement with the view of establishing a fit for purpose and sustainable management and service delivery arrangement that will effectively address the key issues facing the uranium industry. A **Strategic review** was conducted with member company representatives and subsequent detailed discussions with the Chamber of Mines of Namibia.

The net effect of the Chamber's recommendations was to morph the Chambers subcommittee into the Namibian Uranium Association (NUA) as the representative point of contact for the Namibian uranium industry. This has the effect of consolidating internal and external communications and response unequivocally in one central point. This revised approach combines a high degree of autonomous profiling for the NUA with CoM and Government support. In short, as the report urges, there is now 'a public, well-understood and memorable face' for the uranium industry.

While still expanding, the Association's membership (22-member companies at present) includes all the Namibian uranium mining operations and most of Namibia's leading exploration companies and associated contractors. The NUA enables the senior executives in Namibia's uranium industry to shape the context in which their industry operates. It argues for policy change that will let uranium compete on its merits as an energy source appropriate for the needs of the twenty first century through research, factual information and advocacy.

## **7.2. The sustainable development committee of the NUA**

A piece-meal and uncoordinated approach to sustainable development will not result in sustainable growth, effective protection of fragile ecosystems or the conservation of scarce water resources. It is no longer feasible to assess potential impacts on the basis of a single operation, nor can cumulative impacts be assessed on the basis of one operation's activity. The assessment of combined impacts, which might differ from those the individual mines are assessing, and of which one at this stage might not even know about — need to take place.

As a very first step the NUA formed a consultative Sustainable Development committee to address the key issues relevant to the Uranium Mining industry in the Erongo Region. Amongst other objectives, the SD committee re-evaluates minimum standards on health, safety and environment issues. It is also working towards developing a better understanding of the cumulative issues associated with numerous uranium companies operating in the Region and is coordinating efforts to find a constructive, sustainable way forward.

The aims of SD committee are to:

- Provide a systematic means of identifying, describing, evaluating and reporting on the regional environmental, health and social impacts of plans, procedures and strategies of uranium exploration and mining in the Erongo region;
- Develop standards for radiation protection, occupational health, occupational hygiene, environmental rehabilitation, mine closure and after care as recommendation for incorporating these into the regulations under the Minerals Act and other relevant legislation; and
- To achieve these goals, the SD committee has established technical advisory working groups, constituting members of the public, government and non-governmental organizations.

## **7.3. The Namibian Uranium Institute (NUI)**

The UI is a recognized training facility and has successfully initiated many projects around Safety, Health, Environment, Risk and Quality (SHERQ) and assisted with the creation of recommendations on legislation. In line with the recommendations of the Strategic review, the Uranium Institute was renamed as the Namibian Uranium Institute (NUI). It is now aligned with the Governments vision in terms of

national training and occupational health service delivery. It thus became a national asset to build capacity in specialized skills in the fields of health, environmental management and radiation safety with close academic ties to the Polytechnic of Namibia (soon to be rebranded as the **Namibian University for Science and Technology**) and Governments new **Namibian Energy Institute**.

The NUI continues to support and expand the competitive growth of the Namibian mining and export industry, through the continuous development of safety, health and environmental best practice, accessible research, comprehensive training, social responsibility and community upliftment. The NUI fully subscribes to objective, scientific and independent third-party review by credible institutions such as Gobabeb/Namib Ecological Restoration and Monitoring Unit (NERMU) and the International Atomic Energy Agency (IAEA).

#### **7.4. Stakeholder engagement towards environmental management**

Nuclear energy remains a highly emotive word which attracts a variety of views nationally and internationally. Naturally, there is public concern about possible radiation emanating from the exploration and mining of a radioactive mineral like uranium. While there is much public debate around health and environmental impacts of uranium mines, such impacts are not radically different from those associated with other metal mines and in many low grade uranium mines, radiation levels are close to the public exposure.

Public interpretation is however often based on perceptions rather than facts, and those perceptions sometimes relate to views shaped by events some decades ago. Whatever the perceptions are, imaginary or real, the fact is that ‘No mine is sustainable, only its legacy’. Consequently, the acid test to be met is whether adequate legislation is in place to effectively monitor the environmental impacts and to rehabilitate the areas affected by exploration and mining when the mines close.

As it is sometimes difficult to separate rhetoric from scientific information, one of the main goals of the NUA’s website is to provide transparent scientific information regarding uranium exploration and mining. This will assist thoughtful people too identify misinformation and provide accurate, scientific information, not to advocate for or against mining.

#### **7.5. Corporate social responsibility**

The uranium industry accepts corporate social responsibility as a core business interest and not a philanthropic corporate commitment. The member companies continue to invest directly in education, training, youth support and economic upliftment for socially-disadvantaged Namibians. Through its bursary schemes, members support young Namibians to undertake additional studies, especially in engineering fields and in-service development of recently qualified graduates.

Both the Rössing Foundation and the newly formed Swakop Uranium Foundation are members of the Erongo Development Foundation (EDF). The EDF was established in 1996 as an independent and financially prudent community organisation which has broad community and political support and visibility. It is a registered company not for gain, managed by a Board of Trustees.

The primary goal of the EDF is to advance funding to projects that have quantifiable social, cultural and economic benefits to residents and communities in Erongo Region. The NUA recognises the enhanced positive impact that joint initiatives (involving other mining companies and industry) under the EDF banner can deliver.

### **8. HOW CAN LESSONS LEARNED BE APPLIED ELSEWHERE IN AFRICA?**

Uranium exploration in Africa is struggling and faces major reputational and economic challenges. Given the environmental impact of uranium mining and the unique challenges associated with uranium safety and security, the industry’s credibility is at stake at a time when dissemination of information is more effective than ever before. There are a number of challenges to the long term expansion of the

nuclear power industry and the rebuilding of its reputation as a clean and safe industry. Those pertinent to this discussion include the following:

- Health risks must be considered in the context of complex scientific concepts which are often displaced by myths or generalisations;
- A proper understanding of radiation risks requires a strong educational foundation, which is inaccessible to the vast majority of African people;
- Exploration for and mining of uranium must be undertaken by companies with experience in the field of radiation management;
- Whole-cycle scrutiny of environmental and social impacts of uranium mining is increasing in importance;
- Complex political sensitivities surround the end use of uranium, including sovereign independence and security issues;
- Effective regulation of radiation risks requires bureaucratic sophistication ranging from the formation of policy to drafting of legislation to enforcement and prosecution of contraventions;
- Anti-nuclear groups enjoy an exceptional level of sophistication and financial support and can access incredible leverage from modern information dissemination such as YouTube, Twitter, Facebook, etc.

## 9. CONCLUSION

The regulatory environment in Namibia has made substantial progress and, most of the gaps that were filled by self-regulations are now closed. In fact, in many instances industry standards are forming the basis for regulations, with the benefit that law-makers adopt a system that has been tested and companies need to make limited adaptations once standards become law.

Accordingly, Namibia is viewed as a country with a secure and comprehensive regulatory safety net — which has been bridged by industry co-operation. In the absence of Uranium Stewardship, one might expect it to take years to develop effective and sustained enforcement capability. However, with an industry that values Namibian Uranium's reputation — with buyers, politicians and international communities alike — we have seen effective self-enforcement bridging the gap.

Clearly, the positive example of Uranium Stewardship demonstrated in Namibia could be applied elsewhere in Africa. Beyond ensuring that Namibian Uranium retains its premium brand status, Uranium Stewardship in Namibia has resulted in far reaching benefits, including:

- Maintaining broad social and governmental support for uranium mining in Namibia;
- Ensuring industry prescribed minimum standards (which generally exceed regulatory standards) are observed by all industry participants;
- Generating a co-operative approach amongst the industry participants, resulting in joint initiatives on infrastructure development, community engagement, etc.;
- Delivering industry standardised training;
- Centralising public relations and community awareness functions.

The author believes that leadership must be generated by both the Government and the uranium industry as a whole. This article highlights one way that this can be realistically achieved in the context of myriad challenges. Nonetheless, debate and discussion is essential, given the risks that inappropriate activities in uranium production can pose to the continued future growth of the nuclear fuel industry.

## BIBLIOGRAPHY

ATOMIC ENERGY BOARD OF NAMIBIA, Annual Review 2012–2013, Windhoek, Namibia (2013).

CHAMBER OF MINES OF NAMIBIA, Constitution — Code of Conduct and Ethics, Windhoek, Namibia (2008).

CHAMBER OF MINES OF NAMIBIA — URANIUM INSTITUTE, Annual Review 2012–2013, Windhoek, Namibia (2013).

MINISTRY OF MINES AND ENERGY, Strategic Environmental Assessment for the Central Namib Uranium Rush, Windhoek, Namibia, MME (2010).

NAMIBIAN URANIUM ASSOCIATION, Good Practice Health, Environment, Radiation Safety and Security (HERSS) Standards, Swakopmund, Namibia (2014).

HERSS Guidelines and Toolkit, Swakopmund, Namibia (2014).

OFFICE OF THE PARLIAMENT, “Government Gazette of the Republic of Namibia”, Promulgation of Atomic Energy and Radiation Protection Act, 2005, Number 50, Windhoek, Namibia (2005).

“Government Gazette of the Republic of Namibia”, Promulgation of Environmental Management Act, 2007, Number 3966, Windhoek, Namibia (2007).

OFFICE OF THE PRIME MINISTER, “Government Gazette of the Republic of Namibia”, Promulgation of Minerals (Prospecting and Mining) Act, 1992 (Act 33 of 1992), of the National Assembly, 1992, Number 564, Windhoek, Namibia (1992).

WORLD NUCLEAR ASSOCIATION, WNA Policy Document — Sustaining Global Best Practices in Uranium Mining and Processing — Principles for Managing Health and Safety, Waste and the Environment, WNA London, (2007).

Working Group on Uranium Mining Standardization, Internationally Standardized Reporting (Checklist) on the Sustainable Development Performance of Uranium Mining and Processing Sites, WNA (2011).

## WEBSITES

CHAMBER OF MINES OF NAMIBIA, [www.chamberofmines.org.na](http://www.chamberofmines.org.na), accessed on 21 May 2014.

GOBABEB RESEARCH AND TRAINING CENTRE, <http://www.gobabebtrc.org/>, accessed on 20 May 2014.

INTERNATIONAL ATOMIC ENERGY AGENCY, [www.iaea.org](http://www.iaea.org), accessed on 23 May 2014.

MINISTRY OF MINES AND ENERGY — GEOLOGICAL SURVEY, <http://www.mme.gov.na/gsn/>, accessed on 15 May 2014.

MINISTRY OF MINES AND ENERGY, Strategic Environmental Management Plan (SEMP) for the Central Namib Uranium Province 2012 Annual Report

[http://www.mme.gov.na/gsn/pdf/Annual\\_SEMP\\_Report\\_2012\\_released.pdf](http://www.mme.gov.na/gsn/pdf/Annual_SEMP_Report_2012_released.pdf), accessed on 19 May 2014.

NAMIB ECOLOGY RESTORATION AND MONITORING UNIT (NERMU), [http://www.gobabebtrc.org/index.php?option=com\\_content&view=article&id=139&Itemid=136](http://www.gobabebtrc.org/index.php?option=com_content&view=article&id=139&Itemid=136), accessed on 24 May 2014.

NAMIBIAN URANIUM ASSOCIATION, <http://namibianuranium.org/>, accessed on 01 June 2014.

WORLD NUCLEAR ASSOCIATION, <http://www.world-nuclear.org/>, accessed on 20 May 2014.

# **GEOLOGICAL 3-D MODELLING AND RESOURCES ESTIMATION OF THE BUDENOVSKOYE URANIUM DEPOSIT, KAZAKHSTAN**

A. BOYTSOV\*, T. HEYNS\*, M. SEREDKIN\*\*

\* Uranium One Inc, Toronto,  
Ontario, Canada

\*\* CSA Global Pty. Ltd., Perth,  
Western Australia, Australia

## **Abstract**

The Budenovskoye Deposit is the biggest sandstone-hosted, roll front type uranium deposit in Kazakhstan and in the world. Uranium mineralization occurs in the unconsolidated lacustrine-alluvial sediments of Late Cretaceous Mynkuduk and Inkuduk horizons. It is currently under commercial production by Karatau and Akbastau ISL mines, both owned by Kazatomprom and Uranium One in equal shares. The latest geological modelling and resource estimation done shows a significant increase in total uranium resource tonnage at both mines when compared to the March 2012 NI 43-101 resource estimate: at Karatau Measured and Indicated resources increased from 11 695 tonnes of U to 63 839 tonnes of U while at Akbastau from 13 598 tonnes of U to 47 292 tonnes of U. It has also added 55 766 tonnes of U to the Karatau Inferred Mineral Resource category. The updated mineral resource estimate is the result of having available an extensive database, adding latest exploration results, and applying 3-D modelling techniques. The modelling of roll front type uranium deposits, specifically aimed at ISL mining, has accounted for its own specific requirements. Mineral resources estimation was based on 0.04 m% grade  $\times$  thickness cut-off. The relationships between geophysical logging data and laboratory analyses were identified in order to define resource estimation parameters based on gamma log, electrical logging methods and disequilibrium studies.

## **1. INTRODUCTION**

Roll-front sandstone uranium deposits can be extracted using in situ leaching (ISL), also known as in situ recovery (ISR) method with low operational costs. The production share from the Kazakhstan roll-front sandstone-hosted uranium deposits mined using the ISL method comprised 36% of the world total in 2013. South Kazakhstan hosts a number of large unique roll-front sandstone type uranium deposits including Budenovskoye, Inkai, Mynkuduk, Akdala, Kanzhugan, Moinkum, Uvanas, Kharasan, Karamurun, Irkol, Zarechnoye.

CSA Global has completed modelling and resource estimation of Budenovskoye deposit for Uranium One Inc. The methodology of modelling these types of roll-front uranium deposits has been substantially improved.

## **2. GEOLOGICAL FEATURES OF ROLL-FRONT URANIUM DEPOSITS IN SOUTH KAZAKHSTAN**

Roll-front sandstone-hosted uranium mineralisation in South Kazakhstan is spatially and genetically associated with the pinch-out boundary of a regional reduction/oxidation zone of strata bound oxidation in permeable sediments. The mineralisation is associated with significant thicknesses (10–50 m) of highly permeable horizons, which are continuous over tens to hundreds of kilometres.

In plan, the uranium deposits present as weaving ribbons of various widths and lengths as controlled by the interface between oxidized and reduced sediments (Fig. 1), also known as the redox zone. Multi-stage bodies and extended limbs consisting of a number of mineralized lenses, which are also found in abundance between the limbs, are typical of the deposit structure and reflect the complexity of the enclosing rock sequence [1, 2].

Each of the identified uranium deposits are located within a single sedimentary horizon, which can be correlated between vertical sections. The mineralized bodies consist of several morphological elements (Fig. 1), including [1, 2]:

- The main roll-front with well-distinguished ‘nose’ parts;
- Mineralized ‘wings’ (or ‘limb’) elements;
- ‘Satellite’ or ‘residual’ bodies located in the rear of the main rolls.

An important feature of uranium-mineralized bodies is the change in the proportion of uranium and radium relative to its position in the roll shape ore body (Fig. 1). Uranium concentration dominates in the nose parts and decreases in the wings, and radium dominates in the residual bodies and forms radium halos (which show as anomalies containing no uranium based on gamma-ray logging results). Radium and uranium ratio is described by the radioactive equilibrium factor (REF).

Sometimes the mineralized bodies show increased carbonate grade (to 3%), which results in extra acid consumption.

All mentioned geological features of deposits should be taken into account for modelling.

### 3. MODELLING ROLL-FRONT URANIUM DEPOSITS

A serious challenge in estimating grades in roll-front deposits is identifying variable radiological responses influenced by the position of the mineralized interval relative to the redox front and to what extent disequilibrium is present within the deposit.

The initial downhole geophysical data is recorded at 10 cm increments. These intervals are too narrow for radiological factors determination and to do effective modelling. To negate this issue, intervals were composited over the full thickness of the mineralisation with division into sands and clays.

Modelling divided the bodies into mineralized horizons based on the geometry of the mineralisation (noses, wings, and roll residuals) and whether the mineralisation occurs within permeable sands or clays, where mineralisation is non-extractable by ISL methods.

It is important to determine the radium cut-off grade for different geochemical zones and quantify a REF for conversion of apparent radium grade  $\times$  thickness (GT) into uranium contents.

Lastly, for ISL deposits, the depletion of Mineral Resources is measured not by how much rock is removed, as is the case with most traditionally mined resources, but rather by lowering of the uranium grade and productivity.

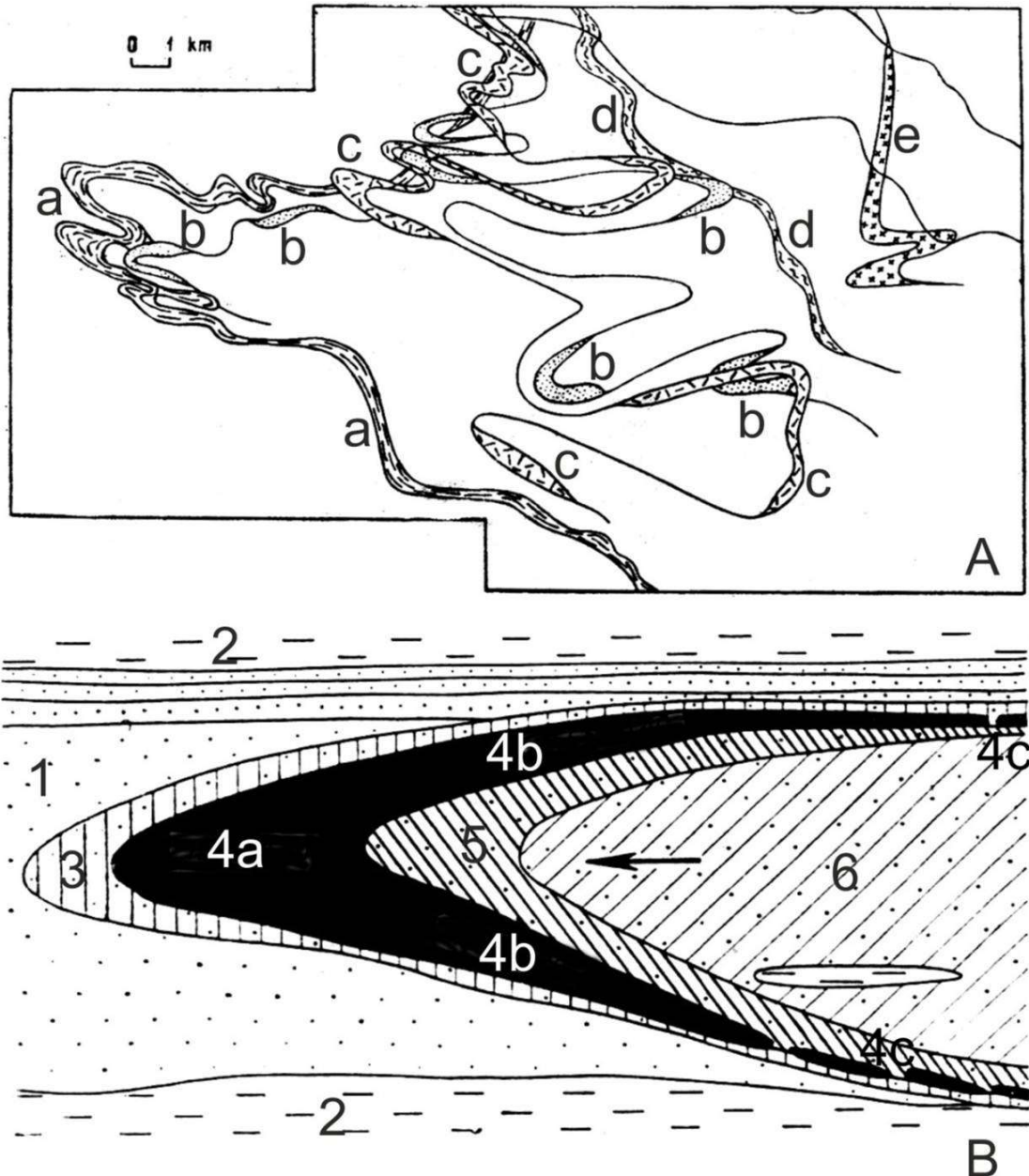


*FIG. 1. Geological features of roll-front uranium deposits in South Kazakhstan in plan (A) and section (B)[1]): a–e: weaving ribbons of roll fronts on the different levels; 1: reduced penetrable sediments (mainly sands); 2: impenetrable sediments (mainly clays); 3: diffuse radium halo; 4: uranium mineralized body (4a – nose part, 4b – wing parts, 4c – residual parts); 5: remaining radium halo; 6: oxidized penetrable sediments; arrow: direction of solutions flow.*

#### 4. DELINEATION OF MINERALIZED INTERVALS

Geophysical data (i.e. wireline logging) is the primary means of defining uranium mineralized intervals. The uranium values need to be corrected using number of modifications, which are determined according to the standard operating procedure of JSC Volkovgeologiya (see details and references in [3, 4]) including corrections for:

- Thorium and potassium (usually constant and low for South Kazakhstan deposits);
- Radon (radioactive equilibrium between radium and radon), usually constant;
- Radium (disequilibrium – REF), usually quite variable in South Kazakhstan deposits.

REF is defined in two steps:

- Definition of cut-off grades for radium equivalent to 0.01% U for establishing of boundaries of mineralized intervals. It depends of geochemistry of host sediments: oxidized or reduced;
- A correction for  $\text{REF} = \frac{\text{C}(\text{radium})}{\text{C}(\text{uranium})}$  is introduced to calculate uranium grade after establishing mineralized interval boundaries and calculation of average radium grade. It depends on the morphology of mineralized bodies — whether noses, wings, or residuals.

## 5. GEOLOGICAL INTERPRETATION

Interpretation of roll-front style uranium deposits (amenable to in situ leaching) has specific requirements, which are listed below:

- Modelling of mineralized horizons by creating surfaces;
- Defining mineralized intervals using gamma-logging that takes into consideration radium cut-off grades, which are also dependent on the location of the mineralized intervals in the oxidized or reduced sediments;
- Division of interpreted mineralized bodies into nose, wing and residual parts accounting for the geochemical composition of the host sediments; and
- Interpretation of clay horizons, in order to define mineralisation that cannot be extracted by ISL methods.

The interpreted mineralized envelopes are then divided into morphological elements – i.e., nose, wing, and residual parts as well as into mineralized horizons as follows:

- Intervals where mostly reduced rocks are developed both in the mineralized interval and above and below are attributed to the nose zone;
- Intervals where reduced rocks are developed in the mineralized interval and mainly on one of its sides (either above or below) are attributed to the limb; and,
- Intervals where there are mainly oxidized rocks developed above or below the mineralized interval are attributed to the residual part; the mineralized interval itself can be represented both by reduced and oxidized rocks.

The roll nose parts define the redox front location. The definition of redox fronts is very important for understanding the geological structure of a deposit. The wing and residual parts of rolls are located in the rear part of redox fronts. Mineralisation ends abruptly in the frontal part of the redox fronts usually. Radium halos can be distributed deep into the rear parts of roll fronts — exhibiting gamma activity but no uranium mineralisation. Prompt fission neutron (PFN) logging is used for direct uranium measurement and can be useful for exploration of these parts.

The interpretation of clay horizons is usually carried out after interpretation of the mineralized envelopes. This interpretation is based on core logging and electrical methods — resistivity logging and spontaneous polarisation logging. Clay horizons should be subconcordant with mineralisation. Sometimes it is necessary to correct the mineralized bodies after lithological interpretation.

## 6. BLOCK MODELLING

Industry standard approaches of geostatistical analysis, compositing, block modelling and grade estimation are used for the roll-front uranium deposits in South Kazakhstan. The uranium and carbonate grades as well as REF are estimated for the block model (also other minor elements such as Se, Sc, Re, REE and others. can be estimated).

There is one important feature in the methodology of resource estimation for these deposits.

For ISL deposits it is important to use a metal accumulation index (grade  $\times$  thickness or GT) to define the cut-offs for resource estimation, whereas the classical approach is to only use grade cut-offs in resource estimation. For example, the mineralized interval with U grade 0.04% and 10 m thickness (GT = 0.4 m%) is better for ISL than mineralized interval with U grade 0.10% and 3 m thickness (GT = 0.3 m%).

A gridded model is generated for each wireframe in order to estimate GT, based on block models. The vertical extent of the cells of the gridded model depends on the thickness of mineralisation. GT is calculated by multiplying the vertical size of the cells by the uranium grade. Gridded models are two-dimensional. In order to estimate the GT in three-dimensional space, it is necessary to compare each cell of the gridded model with a column of cells in the original (classical) block model. This was completed by indexing of the block model cells by comparison with the cells of the gridded model.

Lower and upper wings are estimated separately due to different wireframe modelling nose and wing parts of rolls.

## 7. ACCOUNTING FOR DEPLETION IN ISL MINING

In conventional open pit or underground mining, the depleted volume of ore can be physically surveyed. In ISL operations, the host rock remains undisturbed while uranium mineralisation is dissolved by the leaching solution. Leaching contours and the dynamics of uranium leaching process can be determined by creating a model that describes solution hydrodynamics and dissolution of uranium.

For the purposes of producing a global Mineral Resource estimate for a mine it is considered sufficient to volumetrically delineate contours of production blocks and to deduct the depleted metal (recovery and in situ loss) from the Mineral Resources. Grades and GT will decrease proportionally because the volume of rock mass remains.

Delineation of the production blocks is completed in plan projection using the location plans of production wells. The vertical boundaries of the production blocks are determined using the intervals of setting screens in the production wells.

## 8. MINERAL RESOURCES

Table I shows the recent estimate of the Mineral Resources for the Budenovskoye deposit, as of 30 June 2013.

TABLE I. ESTIMATE OF MINERAL RESOURCES FOR THE BUDENOVSKOYE DEPOSIT, AS OF 30 JUNE 2013

| Category             | Volume              | Tonnes  | GT productivity |                     | Grade |                                   | Mineral resources |                                    |
|----------------------|---------------------|---------|-----------------|---------------------|-------|-----------------------------------|-------------------|------------------------------------|
|                      | '000 m <sup>3</sup> | '000 t  | m $\times$ %    | kg / m <sup>2</sup> | U, %  | U <sub>3</sub> O <sub>8</sub> , % | Tonnes U          | M lb U <sub>3</sub> O <sub>8</sub> |
| Measured             | 43 227              | 73 487  | 0.46            | 7.8                 | 0.072 | 0.085                             | 52 646            | 136.88                             |
| Indicated            | 38 692              | 65 777  | 0.46            | 7.8                 | 0.088 | 0.104                             | 58 485            | 152.06                             |
| Measured & Indicated | 81 919              | 139 264 | 0.46            | 7.8                 | 0.080 | 0.094                             | 111 131           | 288.94                             |
| Inferred             | 58 177              | 98 901  | 0.37            | 6.2                 | 0.095 | 0.111                             | 93 623            | 243.42                             |

Note:

1. Mineral Resources based on 0.04 m% (grade × thickness) cut-off per hole.
2. Mineral Resources categories are based on CIM (Canadian Institute of Mining, Metallurgy and Petroleum) definition [5].
3. Depletion estimated using losses of 10%.
4. Measured Mineral Resources based on exploration drilling density of 50 m × 200 m (excluding residual mineralized bodies).
5. Indicated Mineral Resources based on exploration drilling density of 50–100 m × 400 m (excluding residual mineralized bodies) and 50 m × 200 m for residual mineralized bodies.

The presented geological modelling and resource estimation resulted a significant increase in total uranium resources tonnage at both mines when compared to the March 2012 NI 43-101 [5] resource estimate: at Karatau measured and indicated resources increased from 11 695 tonnes of U to 63 839 tonnes of U while at Akbastau from 13 598 tonnes of U 47 292 tonnes of U. It has also added 55 766 tonnes of U to the Karatau Inferred Mineral Resource category. The updated mineral resource estimate is the result of having available an extensive database, adding latest exploration results and applying 3-D modelling techniques.

## 9. CONCLUSION

Roll-front uranium deposits are quite difficult to model due to complicated mineralized bodies shapes and radiological complexity. The method of modelling discussed above allows creation of relevant geological models for the largest sandstone hosted deposit in the world. The average differences between resource estimates based on exploration drill holes and from production wells are less than 5% in this approach. A significant positive economic impact from using geological model and improved resource estimation approach is expected.

## REFERENCES

- [1] BROVIN, K., GRABOVNIKOV, V., SHUMILIN, M., YAZIKOV, V., Prediction, research, exploration and resource estimation of uranium deposits for in-situ recovery, Gylim, Almaty (1997) (in Russian).
- [2] INTERNATIONAL ATOMIC ENERGY AGENCY, Manual of Acid In Situ Leach Uranium Mining Technology, IAEA-TEDOC-1239, IAEA, Vienna (2001).
- [3] SEREDKIN, M., BERGEN, D., Technical NI 43-101 report for Akbastau Uranium Mine designed for Uranium One Inc., CSA Global Pty. Ltd., Perth, Vancouver (2013).
- [4] SEREDKIN, M., BERGEN, D., Technical NI 43-101 report for Karatau Uranium Mine designed for Uranium One Inc., CSA Global Pty. Ltd., Perth, Vancouver (2013).
- [5] National Instrument 43-101 Standards of disclosure for mineral projects, Canadian Institute of Mining, Metallurgy and Petroleum, Westmount, Quebec (as updated from time to time).

# HOW EFFECTIVE PROJECT MANAGEMENT WILL ADD VALUE TO YOUR URANIUM ASSET

R. BRADFORD\*, M. TITLEY\*\*

\* Jem-Met, Perth,  
Western Australia, Australia

\*\* CSA Global UK Head Office,  
London, UK

## Abstract

Up until the Fukushima incident in March 2011 project activity in the uranium sector was driven by high uranium prices and merger and acquisition corporate activity. Soon after the incident, project development in the uranium sector collapsed and capital slowly dried up as uranium prices dropped. Uranium projects, like all other commodities, have a critical ‘to do list’ which is part of project feasibility and is essential to complete in order for these assets to be packaged as desirable world class projects ready for construction. This paper presents experience based on case studies from a number of recent uranium projects in Australia, Africa and Europe, either developed through to construction or at different phases of feasibility. The presentation will focus on the experience gained and the lessons learnt when managing the development of these uranium projects. Other examples will demonstrate where projects have exceeded expectations and delivered exceptional value, due to factors which are often underrated or ignored in the management of the exploration and mine development work cycle.

## 1. INTRODUCTION

As part of the process in developing a mining project there are a significant amount of activities and tasks which need to be coordinated. The main task of any project manager is the requirement to put together these tasks with appropriate start and end times which will all feed into a project master schedule. These activities need to be motivated through a technical scope of works and one on one sessions between the technical consultant and the project manager. As part of the kick-off phase of any project this process is critically important so as to ensure scope is well defined, understood and captured through each individual schedule and with an agreed budget. Any creep in either parameter would require agreed authorization prior to the execution.

The detail of what needs to be included in a scope of works for an individual consultant is dependent on a number of factors. These may include the mineral being studied for extraction, what phase the project feasibility is currently in, what is the required legislation in the country where the mineral deposit is located, what season will the work be done and even what is the available budget from the owner of the deposit. Often a capital constraint can influence the content which a scope of work can be put together and executed. This scope definition phase is important, it is equally important that the consultant has the opportunity to compete the work required so he can confidentially sign off a phase of work, at the appropriate phase of the feasibility or detailed engineering.

Often this process of scope definition can create an impression that either the client would like to reduce as much work as possible, mainly for cost saving or reduction in schedule and time or the consultant has overloaded the scope requirement to make sure no stone is unturned – because of the Competent Person sign-off requirement<sup>5</sup>.

The paper discusses some points and examples of how through experience certain situations have either helped the project set up or have added significant value to the company.

---

<sup>5</sup> A ‘Competent Person’ is defined and their involvement in reporting by publicly listed companies is required in some jurisdictions such as Canada or Australia.

The paper discusses some points and examples of how through experience certain situations have either helped the project set up or have added significant value to the company.

## 2. PROJECT LIFE CYCLE

**Exploration** — Field work, drilling, and resource definition are the major aspects taken up in this phase. The cost of this activity is dependent on the amount of resource definition needed, which takes place during feasibility work to create a large enough resource so that a reserve can be declared which is required as part of a feasibility study. This cost can be at least US \$5 million or could be more than US \$20 million depending on the style of mineralisation.

**Feasibility development work** — Scoping study, pre-feasibility and bankable feasibility work are carried out in this phase. Included in this phase is the compilation of the Environmental and Social Impact Assessment (ESIA). It is important that this document incorporates all the documented technical discussion from at least the pre-feasibility document and avoids contradicting the technical findings in these documents. These costs can be in the range of US \$5–15 million based on the content and complexity of feasibility work requirements.

**Construction** — Detailed design will be conducted to assist in final approval for construction. This cost is dependent on issues such as location, infrastructure and size of the plant. However, this cost will be at a minimum of 5 times the amount spent to date and can run into hundreds of millions of dollars.

**Production** — Dry and wet commissioning and ramp up of production to the point the designed mine based on all the work described has to achieve the nameplate capacity in this phase.

The project life cycle has a few key points that need to be understood by any developer. The first one will be timing to start a mine. Once a mineral deposit has been found in the ground it will take a developer a minimum of four years, as a best case scenario, to bring this opportunity into production. Another important point is the cost of doing this type of work. Costs included are for drilling, feasibility studies, testwork, owners' team costs, in country environmental and social studies and company marketing costs. Over this time period it is expected that a company would spend a minimum of US \$20 million, which, unless raised internally, should be raised in the market without compromising existing shareholders growth position. Another key point which can often hinder development is the team that have found the deposit may not necessarily be the right team for developing the project and in turn the technical developers may not necessarily be the right group to go and market the project to the investor institutions.

A successful project development life cycle has to ensure all these points are addressed at the appropriate time. If this does not happen there is a high chance of the project failing due to lack of funds, wrong technical interpretation or failing to meet production targets. Developers of projects have an obligation to ensure in their best professional capacity that shareholders' and all stakeholders' interests are addressed.

As previously mentioned a project developer needs to appreciate the mineral they are working with. Each has unique properties and certainly all have their own challenges. During any project development it is important to investigate and design to the appropriate safety standards so no harm is directly put onto any person involved in either building or operating the designed asset. It would be completely unacceptable for any company to ask a person to work in an environment which causes harm to any individual.

## 3. PROJECT CONSIDERATIONS

Working with uranium and developing uranium projects has certain requirements to be addressed and met as a minimum due to its radioactivity and potential risks associated with coming into contact with radioactive minerals. However, other considerations should be understood and followed as part of the project life cycle and this paper will discuss some of those aspects. The paper will address these points

under three key areas: (i) working with uranium; (ii) who should be involved and when; and (iii) project development.

Points will be discussed around these three key points based on previous experience working on uranium projects in various locations around the world over the last seven years for “junior” companies and major producers in the uranium sector.

#### 4. WORKING WITH URANIUM

During the feasibility stage a considerable amount of sample movement will be required as part of the requirements around laboratory investigations, geotechnical investigations or environmental work. It is important, before committing to a facility to do this work and a country where this facility is situated, that the developer understands the legislative requirements for working with uranium samples in such a facility and jurisdiction. Situations have occurred where a facility has not allowed uranium samples to leave their facility due to uranium legislation stipulating service providers should do all sample studies at one facility. Any equipment used in the testing has to be either decontaminated or remain the property of the facility. Transporting uranium-bearing samples by road through borders also creates issues with paperwork and delays at customs, which can significantly affect the project schedule. Both these issues have cost and time implications which should be factored into the project schedule.

During the engineering phase of the feasibility consideration is given to design of piping, valve positions, open tanks, tailings dam position and other aspects. Before committing to either detailed design and definitely to construction the developer should ensure that engineering has been done to facilitate all safety requirements around uranium processing. This can often be done by a consultant, taking into account recommendations by groups such as the IAEA but in particular national regulations; regulators should review any proposed design prior to commitment for construction, as their early comments can greatly assist in later approval applications. Manning levels require a review based on maintenance schedules, particularly around areas of the plant that are located in high levels of uranium concentration.

As part of the final product flowsheet development, it is very important that the metallurgical team understand what is going to be produced. Unlike certain commodities such as gold, uranium can be produced in a number of oxide complexed forms, such as uranium peroxide  $\text{UO}_4 \cdot n\text{H}_2\text{O}$ , ammonium diuranate  $(\text{NH}_4)_2\text{U}_2\text{O}_7$  or sodium diuranate  $\text{Na}_2\text{U}_2\text{O}_7 \cdot 6\text{H}_2\text{O}$  and even uranium oxide  $\text{U}_3\text{O}_8$  can be produced, but potentially may not be able to be processed through a particular type of refining facility. This can create significant issues relating to getting your product to market due to lack of access to a port facility within your region or a misunderstanding that a particular refinery can process your final product.

Often discussion occurs with developers on the cost of transportation of final product and the opportunity to dry yellow cake at a much higher temperature (greater than  $400^\circ\text{C}$ ) to achieve more uranium metal mass per drum. The risk associated with drying uranium at these elevated temperatures may outweigh any potential benefit and create additional complexity to the flowsheet which should be reduced to a practical minimum, particularly during ramp up. Reports from a number of uranium producers have been made public through technical papers on the pressurization of final product drums and the blowing off of drum lids. These types of risks can close your operation until such deviations have been addressed and demonstrated to work.

#### 5. WHO SHOULD BE INVOLVED

During the project life cycle, it is important, as previously mentioned, that the developer appreciates a certain skill set is required at a particularly point in time. As an example, why would a developer bring on board a construction manager during a scoping study phase or ensure the correct support staff are engaged to help administrate the project. We recommend that it is equally important, however, that during the Scoping and Pre-feasibility that the specialist skills required are contracted in on a task basis to reduce overheads at a corporate level. Once the Pre-feasibility study is completed the technical and

economic findings would be presented to the board, potentially demonstrating the economic and technical viability of the project. Once the board has approved the next phase of the project, the bankable feasibility, as part of this phase it is important an owner's team is compiled, consisting of the main skills required to oversee and sign off all work related with this phase. These positions include a Manager Mining, Manager Process, Manager Engineering and a Manager Finance. Other positions maybe considered but a 'buy-in' culture needs to be developed. This can occur through many ways but such activities as role description, short term and long term incentives (STIP, LTIP) and Manager Once Removed (MoR) review and discussion all assist in developing a culture of effort and reward, through alignment of the strategy of the company broken down into individual tasks and with an understanding of resource requirements.

Consistently we hear of projects either being delayed or cancelled due to poor stakeholder engagement. A significant part of any uranium development is stakeholder engagement. This can be at various levels from the President in certain countries to local communities or even the press at a appropriate time. It should never be underestimated that uranium will always carry a negative sentiment until effective education and a communication plan is implemented. Below (Fig. 1) is an example of a typical stakeholder engagement sheet which shows not only the position of the person in the communication work stream, but also defines what was discussed when and clearly defines when a follow up meeting will take place. The importance of the responsibility to continually meet, communicate with and educate the individuals on such a list should never be underestimated and should be open and transparent with all stakeholders identified. This workstream is the most important workstream in the entire project life cycle. To engineer a process flowsheet may take months, convincing a local community a certain uranium project is good for their well being and social and economic development can take years.

| TARGET  | GENERAL INFORMATION | ENVIRONMENTAL IMPACT ASSESSMENT | SPECIAL MINING LICENCE | URANIUM REGULATIONS | FINANCE | EMPLOYMENT | INFRASTRUCTURE | LAND | HEALTH | EDUCATION | POWER | WATER | MEDIA AND EDUCATION | SITE VISIT | DATE OF LAST MEETING | DATE OF LAST CORRESPONDENCE |  |
|---|---------------------|---------------------------------|------------------------|---------------------|---------|------------|----------------|------|--------|-----------|-------|-------|---------------------|------------|----------------------|-----------------------------|--|
|   |                     |                                 |                        |                     |         |            |                |      |        |           |       |       |                     |            |                      |                             |  |
| MINISTER AND DEPUTY MINISTERS                 |                     |                                 |                        |                     |         |            |                |      |        |           |       |       |                     |            |                      |                             |  |
| MEMBERS OF PARLIAMENT                         |                     |                                 |                        |                     |         |            |                |      |        |           |       |       |                     |            |                      |                             |  |
| PERMANENT SECRETARIES/ASSISTANT PS            |                     |                                 |                        |                     |         |            |                |      |        |           |       |       |                     |            |                      |                             |  |
| COMMISSIONERS/DEPUTY COMMISSIONERS            |                     |                                 |                        |                     |         |            |                |      |        |           |       |       |                     |            |                      |                             |  |
| PRIVATE SECRETARIES                           |                     |                                 |                        |                     |         |            |                |      |        |           |       |       |                     |            |                      |                             |  |
| TAEC  |                     |                                 |                        |                     |         |            |                |      |        |           |       |       |                     |            |                      |                             |  |
| BUSINESS PARTNERS                             |                     |                                 |                        |                     |         |            |                |      |        |           |       |       |                     |            |                      |                             |  |
| MINISTRY OF NATURAL RESOURCES AND TOURISM     |                     |                                 |                        |                     |         |            |                |      |        |           |       |       |                     |            |                      |                             |  |
| MINISTRY OF WATER                             |                     |                                 |                        |                     |         |            |                |      |        |           |       |       |                     |            |                      |                             |  |
| INTERSECTORAL COMMITTEE - URANIUM REGULATIONS |                     |                                 |                        |                     |         |            |                |      |        |           |       |       |                     |            |                      |                             |  |
| PARLIAMENTARY MINING COMMITTEE                |                     |                                 |                        |                     |         |            |                |      |        |           |       |       |                     |            |                      |                             |  |
| POTENTIAL INVESTORS                           |                     |                                 |                        |                     |         |            |                |      |        |           |       |       |                     |            |                      |                             |  |
| OTHER REGIONAL AND DISTRICT COMMISSIONERS     |                     |                                 |                        |                     |         |            |                |      |        |           |       |       |                     |            |                      |                             |  |
| REGIONAL AND DISTRICT EXECUTIVES              |                     |                                 |                        |                     |         |            |                |      |        |           |       |       |                     |            |                      |                             |  |
| MINING INTERSTAKEHOLDERS FORUM                |                     |                                 |                        |                     |         |            |                |      |        |           |       |       |                     |            |                      |                             |  |
| ENVIRONMENTAL BODIES                          |                     |                                 |                        |                     |         |            |                |      |        |           |       |       |                     |            |                      |                             |  |
| BASELINE STUDIES                              |                     |                                 |                        |                     |         |            |                |      |        |           |       |       |                     |            |                      |                             |  |
| PRESS   |                     |                                 |                        |                     |         |            |                |      |        |           |       |       |                     |            |                      |                             |  |

FIG. 1. Stakeholder engagement (typical example).

During any project development, particularly during more complex projects such as uranium it is important that as much as possible you start to understand the people in the industry. Uranium conferences often provide the opportunity to network with other developers and producers. Without getting involved in potential company Intellectual Property it is important that people in the industry share success and failures with fellow colleges through discussions regarding successful service providers, experiences with working in particular countries or even discussions about market conditions.

Unlike other industries or commodities if a mistake is made by a uranium producer it often has massive ramification for everyone in the industry.

## 6. PROJECT DEVELOPMENT

During the feasibility phase of the project, work will be done to clearly define the flowsheet and eventual size of the processing plant. This however may change as a result of an increase in resource which plays a vital role in increasing a market value of a company. This is very important in any strategy during the development phase, it is the only area a company asset can grow and actually create value. There will be a time in the feasibility phase where capital for future and continued project development will be required so resource growth is important. This, however, may affect not only the size and position of key assets such as tailings dams and plant sites, but may change economics through increased throughput or potentially higher grade being fed into the plant. As a project manager it is important that flexibility is maintained during this resource growth but a critical size based on risk profile matching be understood.

As part of the flowsheet development time should be invested in selecting samples around appropriate mining schedules and material type. Mineralogy work can help justify why a suggested flowsheet has been considered and investigated.

As an example, the slide in Fig. 2 shows the uranium particle well liberated but associated with clay. This could very early suggest free milling may be considered but clay may cause rheology issues at a particular density.

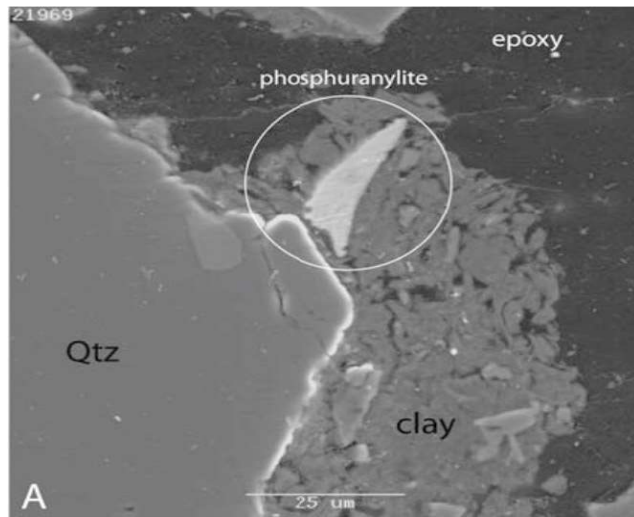


FIG. 2. Mineralogy (example).

Once various bench scale testwork has been done the opportunity to stick the entire flowsheet together and create an integrated flowsheet should always be considered. To understand lock cycle streams and impurity deportment particularly in final product should always be considered as part of a company's development. During integrated piloting at facilities such as ANSTO<sup>6</sup> opportunities arise to show potential investors live performance of the flowsheet. Significant information is also gathered for

---

<sup>6</sup> Australian Nuclear Science and Technology Organisation  
<http://www.ansto.gov.au/BusinessServices/ANSTOMinerals/index.htm>.

detailed engineering around materials of construction through the use of corrosion and abrasion coupons (Fig. 3) which will help to justify if and why expensive steels may be required.

Process design information developed from any test campaign should be carefully used in any final detailed design and appropriate scale up factors should be used. Often in heap leach projects the recoveries achieved during a particular time frame will not be achieved on a full scale basis due to the difference in flow dynamics associated with columns as opposed to actual heaps. Residence times on many flotation circuits should be scaled up correctly to factor froth factors and gravity flow. Often these scale up factors are not only calculated but are refined based on individuals industrial experience.



*FIG. 3. Corrosion coupon.*

Finally, a point to note is the development of a financial model. Even at an early stage of development of the project a financial model should be constructed and reviewed by a third party independent expert. The model should be easily operated and clearly show the sensitivities and cost drivers in the development of the project. This information should be shared with the team during project meetings as new completed tasks are reported and fed into the model. A significant output from any model is the cash-flow requirements during start up as revenue coming from the sale of uranium has a long lead time and this needs to be considered in any financial planning and requirements when approaching the market for construction funding and working capital.

## 7. CONCLUSION

In today's economic client capital funding for project development is becoming more and more limited and potential investors are becoming more diligent. Gone are the days when easy capital is available for potential projects. More and more capital investment institutions are implementing significant screening and technical due diligence prior to any allocation of funds. Part of this Due Diligence process particularly in uranium will touch on many topics covered in this paper and presentation. In order to have success in your project some of the points discussed in this paper may be adopted as part of your journey developing your uranium asset.

## ACKNOWLEDGEMENTS

The authors would like to acknowledge the permission granted by Uranium One to present some aspects of this paper.

## BIBLIOGRAPHY

Uranium 2010 The future is U (Proc. 3rd Int. Conf. on Uranium, Saskatoon, 2010), The Canadian Institute of Mining, Metallurgy and Petroleum, Westmount, Quebec (2010).

# **INTERNATIONAL STANDARDISATION FOR THE REPORTING OF RESOURCES AND RESERVES**

K. FARMER, S. HOCQUET  
AREVA, Paris, France

## **Abstract**

The mining industry is a vital contributor to national and global economies and yet it is very different from other industries. It is based on depleting finite mineral resources, the knowledge of which is imperfect prior to the commencement of mining or extraction. It is an industry with a colourful history of success and failure, entrepreneurs and opportunists, visionaries and short sightedness. These aspect or traits were both positive, it fostered innovation, and negative for the industry. Negative in that the merit of certain projects or results was difficult to assess, it created a credibility issue and consequently investment in the industry was impacted. Mineral Resource and Ore Reserve codes are the basic building block underpinning the confidence required for investment in the mineral resources sector. They are the basis for our decisions when evaluating ore resources and reserves. The mining industry is a key contributor to the world economy; however, its role in national economies varies significantly. In contrast with most other industries it is based on depleting finite mineral resources, the knowledge of which is imperfect prior to the commencement of mining or extraction operations. Mineral resource and ore reserve codes are the basic building block underpinning the confidence required for investment in the exploration and mining sector.

## **1. INTRODUCTION**

The CRIRSCO (Committee for Mineral Reserves International Reporting Standards<sup>7</sup>) family of codes is widely used for the reporting of mineral resources and ore reserves and will be the subject of this paper. CRIRSCO's members are national reporting organisations responsible for developing mineral reporting codes or standards and guidelines. Namely: Australasia (JORC<sup>8</sup>), Canada (CIM<sup>9</sup> Standing Committee on Reserve Definitions), Chile (National Committee<sup>10</sup>), Europe (PERC<sup>11</sup>), Russia (NAEN<sup>12</sup>), South Africa (SAMCODES<sup>13</sup>) and USA (SME<sup>14</sup>).

The combined value of mining companies listed on the stock exchanges of Australasia, Canada, South Africa, Chile, Europe and the USA, according to CRIRSCO figures account for more than 80% of the listed capital of the mining industry.

## **2. HISTORY**

The mining industry has a colourful history it is littered with stories of success and failure; of entrepreneurs, opportunists, visionaries and short sightedness. These traits have had both positive and negative effects. On the positive side it has fostered innovation but on the negative side it has attracted some people that may not have been exactly honest. The latter resulted in a credibility issue for the industry which in turn impacted both investment and the ability to raise funds.

In the early 1900s professional organisations and industry professionals themselves were publishing guidelines or recommendations for the reporting of mineral occurrences. It is interesting to note that Herbert C. Hoover, a renowned mining engineer who worked as far afield and Australia and China

---

<sup>7</sup> <http://www.crirsco.com/welcome.asp>.

<sup>8</sup> Joint Ore Reserves Committee <http://www.jorc.org/>.

<sup>9</sup> Canadian Institute of Mining and Metallurgy <http://www.cim.org/>.

<sup>10</sup> Institute of Mining Engineers of Chile (Instituto de Ingenieros de Minas de Chile) <http://www.iimch.cl/>.

<sup>11</sup> Pan European Reserves and Resources Reporting Committee [www.PERCstandard.eu](http://www.PERCstandard.eu).

<sup>12</sup> National Association for Subsoil Use Auditing <http://naen.ru/>.

<sup>13</sup> South African Mining Codes <http://www.samcode.co.za/>.

<sup>14</sup> Society for Mining Metallurgy and Exploration <http://www.smenet.org/>.

before becoming the 31<sup>st</sup> President of the United States of America, wrote a book in 1909 entitled “Principles of Mining” [1]. He promoted terminology such as proved, probable and prospective ore with definitions linked to the perceived level of risk on the continuity of mineralisation.

The mining industry with its cycle of boom and bust recognised that its long term sustainability was linked to both investor confidence and the ability to attract investment. Self regulation was tried but it proved to be insufficient.

In 1971 the Joint Ore Reserves Committee (JORC) was established in Australia, the group published several reports with recommendations on the classification and public reporting of ore reserves. In 1989 the first edition of the JORC Code was released. There were two critical points about this code that distinguished it from previously published material:

- It was immediately incorporated into Australian Stock Exchange (ASX) listing rules, thereby becoming binding on companies listed on the ASX;
- It was also immediately adopted by The AusIMM (Australasian Institute of Mining and Metallurgy) as an Institute Code, and therefore became binding on members of The AusIMM.

CRIRSCO was formed in 1994 under the auspices of the Council of Mining and Metallurgical Institutes (CMMI) and included representative bodies from Australasia, Canada, South Africa, USA and UK. The primary objective of the group was to develop a set of international standard definitions for Reporting Mineral Resources and Mineral (Ore) Reserves based on the evolving JORC Code definitions. In 1997 a provisional agreement, known as the Denver accord, was reached by the five original members on the standard definition for mineral resources and mineral (ore) reserves and their respective sub-categories Measured, Indicated and Inferred for Resources and Proven and Probable for Reserves.

CMMI was disbanded in 2002 but CRIRSCO remained as a separate entity. In 2006 CRIRSCO released the CRIRSCO International Reporting Template and in 2007 became a task force of the International Council on Mining and Metals (ICMM). Today National Reporting Organisations (NROs) that are members of the CRIRSCO family include: JORC (Australasia), CIM (Canada), IMEC (Chile), PERC (Europe), NAEN (Russia), SAMCODES (South Africa) and SME (United States of America). Collectively these will be referred to as “the Codes”. CRIRSCO is not strictly a code, which implies that it has legal or regulatory force, it is a Template for countries wanting to develop their own codes. Where national codes already exist, these take precedence. The template has however been adopted widely through national reporting codes and standards by bodies that do have legal and regulatory power to enforce it.

The CRIRSCO template is applicable to all solid minerals, including diamonds, gemstones, industrial minerals, stone, aggregates and coal. The template has been mapped to the petroleum (PRMS) classification system however it should be noted that the petroleum industry in general has not adopted the CRIRSCO template for reporting.

### 3. CRIRSCO TEMPLATE AND THE CODES

The fundamental principles governing the codes are Transparency, Materiality and Competence.

Transparency requires that the reader of a Public Report is provided with sufficient information, the presentation of which is clear and unambiguous, so as to understand the report and not to be misled.

Materiality requires that a Public Report contains all the relevant information which investors and their professional advisers would reasonably require, and reasonably expect to find in a Public Report, for the purpose of making a reasoned and balanced judgement regarding the Exploration Results, Mineral Resources or Mineral Reserves being reported.

Competence requires that the Public Report be based on work that is the responsibility of suitably qualified and experienced person(s) who is a minerals industry professional (the relevant National Reporting Organisation to insert appropriate membership class and organisation including Recognised Professional Organisations) with enforceable disciplinary processes including the powers to suspend or expel a member. A Competent Person must have a minimum of five years relevant experience in the style of mineralisation or type of deposit under consideration and in the activity which that person is undertaking.

The Codes set out the framework for classifying tonnage and grade estimates to reflect different levels of geological confidence and different degrees of technical and economic evaluation. Mineral Resources can be estimated mainly on the basis of geological information with some input from other disciplines. Mineral Reserves, which are a modified sub-set of the Indicated and Measured Mineral Resources (shown within the dashed outline in Fig. 1), require consideration of the Modifying Factors affecting extraction, and should in most instances be estimated with input from a range of disciplines [2]. Inferred resources can not, under any circumstances, be converted to reserves.

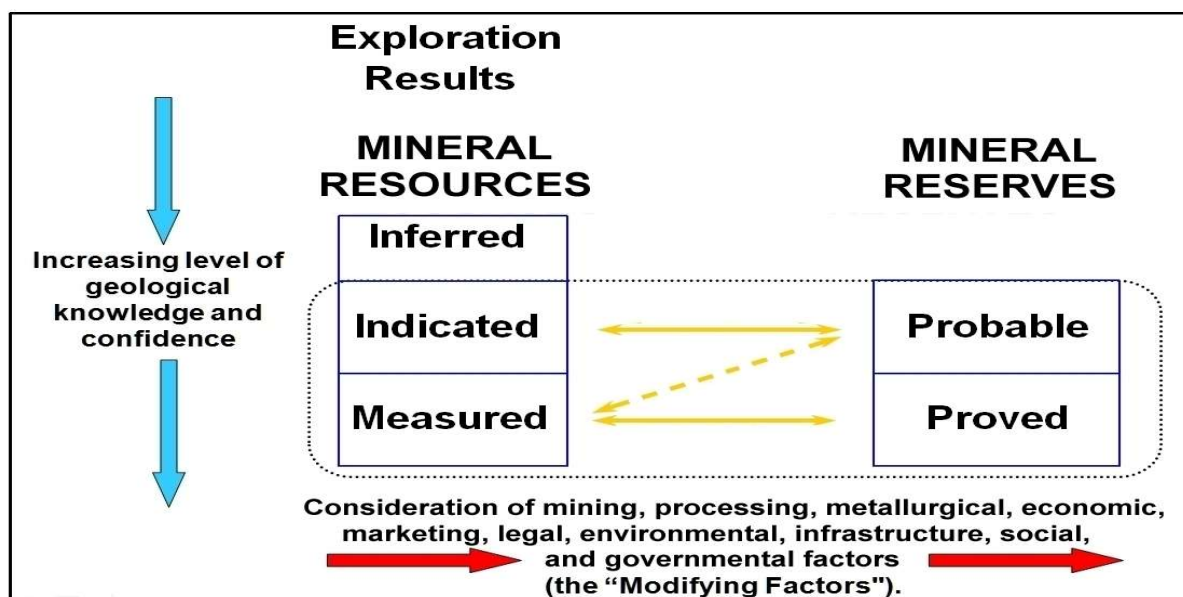


*FIG. 1. Relationships between mineral resources and ore reserves with different levels of confidence and considering modifying factors. Reproduced with permission from Ref. [2].*

Exploration Results do not form part of the declaration of either mineral resources or ore reserves although they may be quoted as a range of tonnes and of grade or quality. The reporting of exploration results has often been considered open to abuse or some artistic licence. To reduce this some Codes have adopted more stringent requirements than those outlined in the CRIRSCO template. For example, the 2012 JORC code [3] demands that — “if a Public Report includes an Exploration Target, the proposed exploration activities designed to test the validity of the exploration target must be detailed and the timeframe within which those activities are expected to be completed must be specified”.

A Mineral Resource can be subdivided, in order of geological confidence as inferred, indicated and measured. The definition of these terms is provided in the Template which is essentially the same as the definitions under the codes. Data integrity aside a key to classification is the notion of geological and grade continuity. These two variables can be interdependent or independent however undoubtedly the terms are not interchangeable. Geological continuity in the context of resource modelling and estimation usually refers to the lithological (+/- structural) features that define the ore zone with a defined consistency. Value or grade continuity is the degree of consistency with which the value of

mineralization is consistent within a particular deposit. Value speaks of grade, thickness and can be extended to geo-metallurgical consistency (the continuity of similar mineralogy). The concept of continuity can be summarised as follows:

- Implied continuity – inferred resources;
- Assumed continuity – indicated resources;
- Confirmed continuity – measured resources.

In all cases resources are not an inventory of all mineralisation drilled or sampled irrespective of cut of grade or other defining factors such as continuity or orientation of mineralisation or likely mining dimensions. By definition mineral resources must have a “reasonable expectation for eventual economic extraction” There is a certain degree of judgement by the competent person as to the technical and economic factors likely to impact economic extraction.

Mineral (Ore) reserves are subdivided in descending confidence as proven or probable. Conversion from either measured to proven or probable or indicated resources to probable requires modifying factors are assessed including but not limited to metallurgical, mining, processing, economic, marketing, legal and social.

The template however goes further and connects resource — reserve conversion to technical studies that is to say a conversion to reserves must be supported by either a Pre-feasibility or feasibility study. Essentially the difference between the studies is that a pre-feasibility assesses a range of options for the technical and economic viability and has a financial analysis based on reasonable assumptions. Whilst a feasibility study is a comprehensive technical and economic study of the selected development option for a mineral project with a detailed financial analysis. The result of a feasibility study may reasonably serve as the basis for a final decision by a proponent or financial institution to develop or fund the project.

For completeness it should be noted that the template provides a definition for a thirds type of technical study referred to as a scoping study. This study is an order of magnitude technical and economic assessment, ore reserves cannot be declared on the basis of this type of study.

Born from necessity the CRIRSCO template and family of codes have ensured that the mining industry has a yardstick by which to transmit information in the public arena. The widespread acceptance of the CRIRSCO family of codes is a positive for investors and companies but it is not a panacea. Keeping in mind that resources are the basic building block for reserves and that exploitation of reserves and return on investment is the aim, the industry does not have the best track record.

It has been estimated that only about 10 to 20 percent of all mining projects produce the return on the investment and the net present value (NPV) that was projected by their feasibility study [4].

In 2013, Peter McCarthy from AMC Consultants did a presentation to the AusIMM Melbourne branch titled “Why Feasibility Studies Fail” [5]. Some interesting statistics to come from his presentation included:

- A US study comparing the final feasibility study production rate with the average sustained production rate for 60 steeply dipping deposits found that 35% of the mines did not achieve their planned production rate [6];
- A 2003 study of 41 underground mines showed that 60% of ore reserve estimates fell outside the expected range, with some very seriously in error [7, 5].

These figures are worrisome to say the least - the obvious questions are why does this situation exist and what are the causes?

The four major causes and relative frequency are [5]:

- Mine design and scheduling 32%;
- Geology, resource and reserve estimation 17%;
- Metallurgical test work, sampling and scale up 15%;
- Process plant equipment design and selection 12%.

In the case of geology and resources the most serious sources of the problems relate to insufficient geological support, inadequate attention to local variability and deficient data integrity. Resource domaining is one of the most important steps in the estimation process, and for this, robust geological models are required. The blind or untethered use of Geostatistics at the expense of good input data and geology is a recipe for failure. This is best summarised in a quote from Jacqui Coombes [8] “without an intelligent handle on geology, geostatistical analysis is reduced to alchemy in a mathematical fantasyland”.

Ore reserve estimations and the three other major factors are interlinked. Ore reserves require the completion of a technical study, either pre-feasibility or feasibility. These studies are obligatory under most if not all the codes however whilst there is a definition of the various studies there is no prescriptive or enforceable standard as to what is required therefore internal or external factors, such as budget constraints, management pressure etc, may result in the work not being completed to the level required to truly understand risk and the potential impact on the viability of the project.

“Why has such a tremendous effort been put forth to greatly improve the quality and standards of the resource and reserve classifications, but with little or no effort to improve the detailed definition of that which determines whether or not a resource will move from a resource to a reserve classification” [9].

This is an interesting quote, it is clear that a minimum prescriptive standard for a pre-feasibility or feasibility study needs to be implemented and adopted by the regulatory bodies responsible for mineral resource and mineral (ore) reserve reporting. Without such a standard the reliability of reserve declarations in particular will remain a grey area.

## ACKNOWLEDGEMENTS

A version of this article in the French language appeared in 2014 [10].

## REFERENCES

- [1] HOOVER, H., Principles of Mining, Hill, New York, USA (1909).
- [2] COMMITTEE FOR MINERAL RESERVES INTERNATIONAL REPORTING STANDARDS (CIRSCO), International reporting template for the public reporting of exploration results, mineral resources and mineral reserves. Committee for Mineral Reserves International Reporting Standards (November 2013) <http://www.cirisco.com/welcome.asp>.
- [3] JOINT ORE RESERVES COMMITTEE, The Australasian Code for Reporting Exploration Results, Mineral Resources and Ore Reserves (The JORC Code), Australasian Institute of Mining and Metallurgy / Australian Institute of Geoscientists and Minerals Council, Melbourne, Australia (2012).
- [4] ADDISON, D., See How They Run (Project Cost and Schedule Overruns), Pincock Perspectives, Pincock, Allen & Holt, Lakewood, CO, USA, Issue **86** (2007) 1–4.
- [5] MCCARTHY, P., Why feasibility studies fail, Powerpoint presentation, Australasian Institute of Mining and Metallurgy Melbourne Branch (2013)
- [6] [https://www.ausimm.com.au/content/docs/branch/2013/melbourne\\_2013\\_02\\_presentation.pdf](https://www.ausimm.com.au/content/docs/branch/2013/melbourne_2013_02_presentation.pdf).
- [7] TATMAN, C.R., Production Rate Selection for Steeply Dipping Tabular Deposits, Mining Engineering **53** 10 (2001) 62–64.
- [8] TATMAN, C.R., Ore Reserve Accuracy, pers. comm. (7 April 2003), cited in MCCARTHY (2003).
- [9] COOMBES, J., The art and science of resource estimation, Coombes Capability, Perth, Western Australia (2008).
- [10] BULLOCK, R. L., Accuracy of feasibility study evaluations would improve accountability, Mining Engineering **63** 4 (2011) 78–85.
- [11] FARMER, K., HOCQUET, S., Les estimations et calculs des Ressources et Réserves minières: Standards internationaux de l'Industrie, Géologues **181** (June 2014) 60–63.

# **AN OVERVIEW OF URANIUM, RARE METAL AND REE MINERALIZATION IN THE CRYSTALLINES OF SONBHADRA DISTRICT, UTTAR PRADESH, INDIA**

P.S. PARIHAR

Atomic Minerals Directorate for Exploration and Research,  
Department of Atomic Energy, Begumpet,  
Hyderabad, India

## **Abstract**

Extensive exploration carried out in the north-western extension of Chotanagpur Granite Gneiss Complex (CGGC) has established a potential province for U, Nb-Ta and REE mineralization over 350 km<sup>2</sup> in the Son Valley area, Sonbhadrā district, Uttar Pradesh, India. Consistent uranium mineralization has been established at Naktu, Kudar, Lakhar, Sirsoti, Nawatola, Dhanbadua, Kudri and Anjangira, where the host rock is essentially albite-rich pegmatoid leucosome mobilizate (PLM) and to a lesser extent, melanosome mobilizate (MM). The anorogenic alkali feldspar granites within Mahakoshal supracrustals at Kundabhati, Sonwani and Chitwar also host uranium mineralization. Three major types of uranium mineralization are identified based on the host-rock characteristics, viz. (a) pegmatoid leucosome mobilizate (PLM) and biotite melanosome (BMM) hosted mineralization, (b) potassic granite/episyenite hosted mineralization and (c) magmatic pegmatite hosted mineralization. Uraninite, samarskite, fergusonite and xenotime are identified in the PLM and BMM hosted mineralization. The present geological milieu in the Son Valley area has the imprints of repeated thermal, tectonic and metamorphic reactivation.

## **1. INTRODUCTION**

The Proterozoic Chotanagpur Granite Gneiss Complex (CGGC), occurring as a linear mobile belt, constitutes an integral crustal segment in the east and central India, lying between Narmada-Son-Brahmaputra lineament designated as Central Indian Tectonic Zone (CTZ) in the north and the Central Indian Suture Zone (CIS) to the south [1, 2]. Uranium mineralization hosted by varied lithounits in the Son valley area is identified within the north-western extension of CGGC. Exploration activities by Atomic Minerals Directorate for Exploration and Research (AMD) has established a potential province for a polymetallic (U-Nb-Ta-REE) mineralization in the Son Valley [3–5], which has a complex history of geological evolution of migmatites.

## **2. GENERAL GEOLOGY**

Son valley area exhibits a wide variety of lithounits belonging to contrasting geo-environs, and include rocks of CGGC Mahakoshal supracrustals, sediments of the Vindhyan Supergroup in the north and Gondwana Supergroup in the south (Fig.1). The craton had undergone repeated rifting, giving rise to intracratonic rift basins for the development of cover rock sequences of arkosic to psammo-pelitic metasediments [6, 7], which now occur as migmatites comprising pegmatoid leucosomes and biotite melanosomes and associated mesosomes.

The CGGC rocks are oldest and exhibit evidences of multiple phases of tectonism which have resulted in a complex geology in the region [8–10]. The litho-units include schist, gneiss, amphibolites, and migmatites. Tectonic imprints in the area are reflected in the form of E-W, NE-SW and NW-SE faults and fractures. The youngest among them is E-W trending system which is sympathetic to major Son-Narmada rift, and the country rocks have undergone intense fracturing, brecciation and mylonitisation resulting in the development of dilated cataclastic breccia. These intracratonic zones are parallel to the Lower Proterozoic Mahakoshal supracrustals. Anorogenic rift related plutons of alkali granite of middle Proterozoic age are seen emplaced within Mahakoshal supracrustals, which at places like Kundabhati and Sonwani are episyenitized.

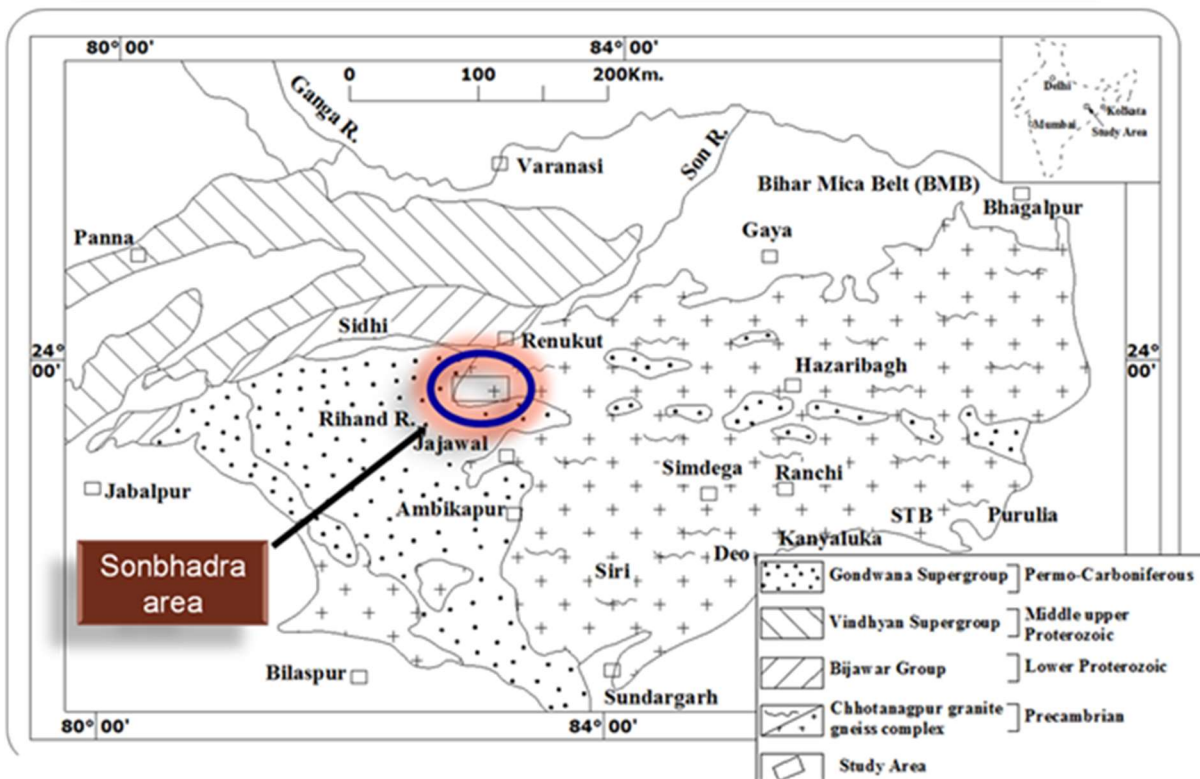


FIG. 1. Regional geology of Sonbhadrā area.

Migmatites in the area are megascopically banded rocks of composite nature, broadly consisting of alternating leucocratic quartzo-feldspathic and melanocratic biotite rich bands. They are composed of the palaeosome, i.e. the unaltered or only slightly modified parent rock and the neosomes, of which two types are distinguishable viz. the leucosome and the melanosome. Leucosome in general have hypidiomorphic texture, and comprises leucocratic minerals like quartz, microcline and albite with minor biotite and accessory amounts of zircon, apatite, sphene, hornblende and garnet. Medium to coarse grained quartz-rich leucocratic suite with pegmatoidal characteristics constitute the pegmatoid leucosome mobilizate (PLM). The PLM in general show hypidiomorphic and myrmekitic texture and is constituted by quartz, sodic plagioclase, microcline, perthite and biotite, with accessory amounts of zoned zircon, muscovite, apatite, purple fluorite, garnet and pyrite. The melanosome, on the other hand, is constituted mainly by biotite and hornblende, with occasional quartz, microcline, plagioclase and graphite. The metabasic sills (palaeosome) occurring within the migmatitic column show effects of retrograde alteration to chlorite schist. These portions host profuse sulphide mineralization as seen in borehole cores of Naktu, Kudar, Kudri and other areas. The migmatite complex show phelbitic, stromatic, ptygmatic, and occasionally agmatic and schlieren structures in two main stretches namely Naktu-Kudar tract and Kirwil-Kudri-Anjangira tract.

### 3. URANIUM MINERALIZATION

Occurrence of uranium from the area was first reported at Asnazar in brecciated granite gneisses in 1977–78. The multi-disciplinary survey and exploration since 1988–89 has resulted in locating at least 55 uranium occurrences spread over about 350 km<sup>2</sup> area. Consistent uranium mineralization has been delineated at Naktu, Kudar, Lakhar, Sirsoti, Nawatola, Dhanbadua, Kudri and Anjangira, where the host rock is essentially albite-rich pegmatoid leucosome mobilizate (PLM) and to a lesser extent, biotite melanosome/melanosome mobilizate (MM). The mineralization is lensoidal and disposed in en-echelon manner with variable dimensions up to 1800 m along the strike and 80 to 120 m along dip, with grade varying from 0.01–1.00% eU<sub>3</sub>O<sub>8</sub>. Development of thick PLM is observed in Naktu-Kudar tract, whereas the migmatites at Kirwil-Kudri-Anjangira tract occur as thin veneer over basement and contain thin

PLM bands. The anorogenic alkali feldspar granites within Mahakoshal supracrustals at Kundabhati, Sonwani and Chitwar also host uranium mineralization (Fig. 2).

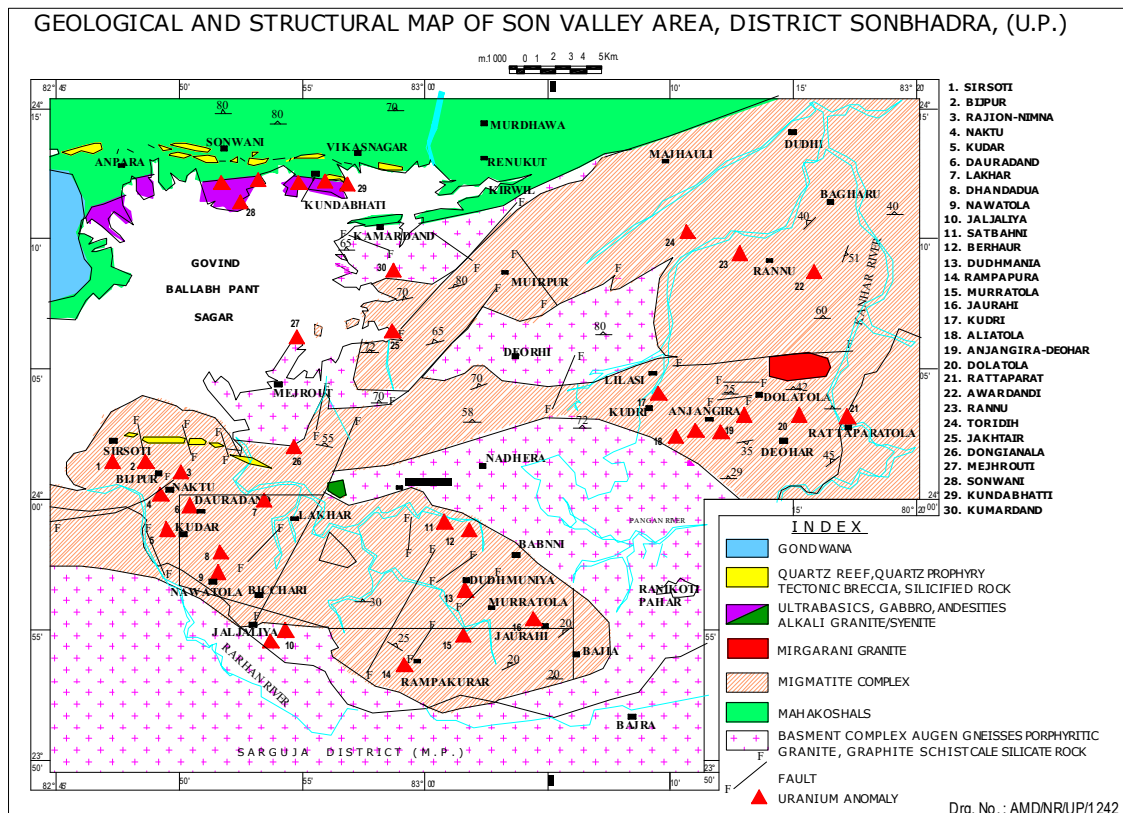


FIG. 2. Geological and structural map of Son Valley area.

#### 4. TYPES OF MINERALIZATION

Uranium mineralization within Son Valley area can be grouped under two main categories, viz.: (a) Mineralization within CGGC; and (b) Mineralization within Mahakoshals. The mineralization within the CGGC include:

- 1) Pegmatoid leucosome loblizite (PLM) hosted mineralization at Naktu, Kudar and Kudri;
- 2) Mineralization associated with surface breccias developed over migmatites at Kudar;
- 3) U-Nb-Ta-REE mineralization associated with pegmatitic injections within granitoid such as Jaurahi and Jura.

The mineralization within Mahakoshals include those associated with anorogenic ‘A’ type high potassic granite and episyenites as at Kundabhati, Sonwani, etc.

Based on the petromineralogical characteristics of the host rocks, four major types can be visualized in the area:

- 4.1. Pegmatoid leucosome mobilizate (PLM) and biotite melanosome mobilizate (BM) hosted, with ubiquitous soda-metasomatism and associated uranium-rare metal mineralization;
- 4.2. Potassic granite and syenite hosted mineralization, associated with rift-related anorogenic granites with episyenitisation and extreme K-metasomatism;
- 4.3. Breccia hosted mineralization;
- 4.4. Pegmatite hosted mineralization, which are rare-metal (Nb-Ta) and REE bearing.

#### 4.1. Pegmatite leucosome (PLM) and biotite melanosome (BMM) hosted mineralization

The mineralization at Naktu and Kudri belong to this type. Soda metasomatism in the form of albite replacing the alkali feldspars is ubiquitously seen. Uraninite, uranophane, coffinite, samarskite, fergusonite are the uranium-REE minerals. Trace amounts of xenotime also is recorded. Two types of uraninite are identified, viz. (a) rounded and euhedral crystals along biotite-albite interface and (b) as inclusions within albite and quartz. Compositional characterizations of the uraninite by EMP studies indicate upto 82% U<sub>3</sub>O<sub>8</sub> and 5 to 11% ThO<sub>2</sub>. The metallogeny in this type of deposits is caused by the remobilization and concentration of the intrinsic uranium in the antecedent sediments through anatetic processes during migmatisation.

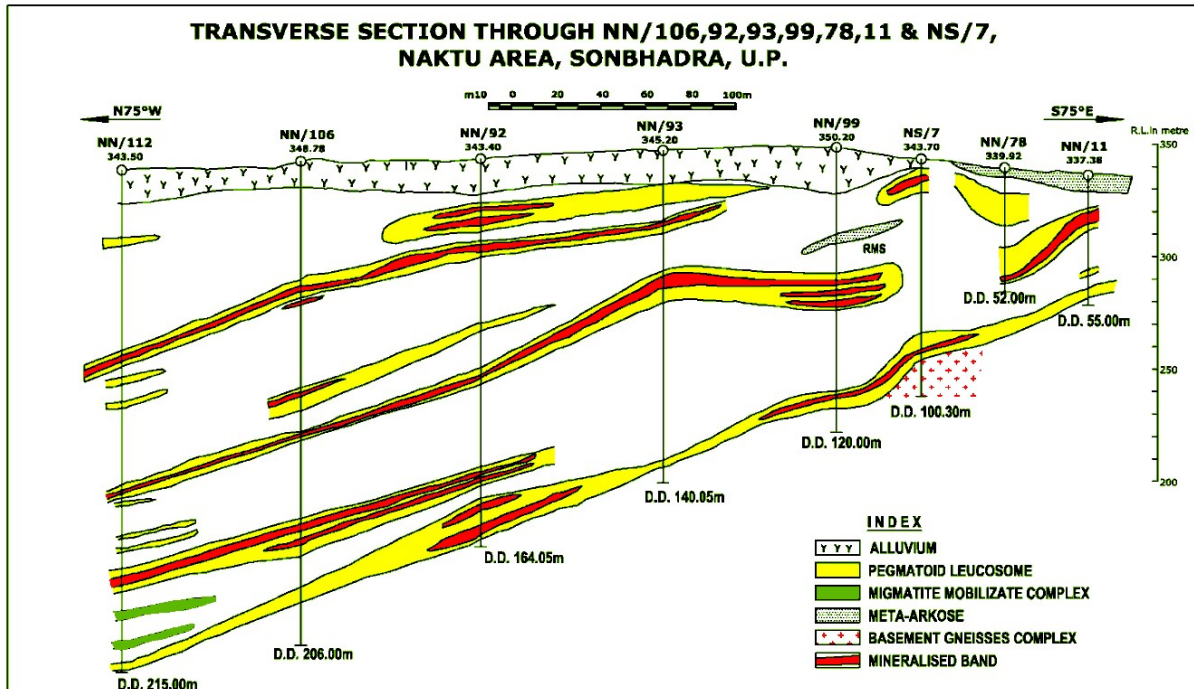


FIG. 3. A typical transverse section through Naktu deposit.

Among the mineralization along Son Valley, Naktu has the best correlatable mineralization over substantial dimension (radioactive zone of 2200 m of 0.50–8.0 m width) and occurs as lenticular bands, disposed in en-echelon pattern, with frequent pinching and swelling. The mineralisaion of 0.020–0.050% U<sub>3</sub>O<sub>8</sub> of 1.20–1.50m thickness are intercepted in the boreholes, in two main mineralized blocks. The northern block consists of only the mainly lode, intercepted at a vertical depth of 5–70m and extends over a strike-length of 400 m. On the other hand, in the southern block, main lode (5–150 m vertical impact) with additional lodes on FW and HW side are intercepted (Fig. 3). In the Naktu-Kudar sector, large thickness of migmatite is intercepted, with development of thick PLM bands, whereas in the Kirwil-Kudri-Anjangira sector, thin veneer of migmatite is observed over the basement, with thin PLM bands.

#### 4.2. Potassic granite and syenite hosted mineralisation

The mineralisation at Kundabhati, Sonwani, Chitwar and Balsotha belong to this category. These mineralizations are associated with the rift-related anorogenic granites emplaced within the Mahakoshal supracrustals along the Son-Narmada fault. Alkali feldspar granites and episyenites formed by the dequartzification and accompanying K-Fe metasomatism, are the host rocks. Extreme K-metasomatism, desilicification and concomitant release of iron renders the radioactive rock a deep red colouration. Uranoophane is the major uranium mineral identified.

Petromineralogical characteristics indicate two types of mineralization at Kundabhati. The earlier one is attributed to intrinsic radioelemental concentration, and is characterized by the presence of thorite and aeschenite. Later epigenetic mineralization is seen preferentially in episyenites, a product of desilicification of alkali granite and K-metasomatism along the brecciated zone. The brecciated zones along the E-W fault/shear zones appear to have provided the channel-ways for the hydrothermal fluids carrying uranium to form the epigenetic deposits.

#### **4.3. Breccia hosted mineralisation**

Breccia-hosted mineralisation is reported from Nawatola and Kudar. The mineralised breccias zones cut across the migmatites, and are conspicuously ferruginous, silicified and zeolitised. The iron-oxide coated breccias contain stilbite, secondary silica, chert and occasional calcite veins. Coffinite, uraninite and pitchblende are the uranium phases identified. Other ore minerals include molybdenite, pentlandite, chalcopyrite, pyrrhotite and pyrite, occurring either along the foliation or along oblique fractures. Sulphides are widespread occurring either along the folia or along oblique fractures supporting remobilization. The main lithic units are breccia and migmatite. Evidences of hydrothermal alteration are also widespread indicated by the presence of fluorite. Rocks also show retrograde alteration evidenced by presence of chlorite at the expense of biotite.

#### **4.4. Magmatic pegmatite hosted mineralisation**

Rare earth and rare metal bearing pegmatite injections are found to be associated with granitoids, as at Jaurahi. Columbite, samarskite, aescheynite, thorite are found to occur as segregations in such pegmatites. Fluorite, fluorapatite, zircon are the other associated minerals in these coarse-grained quartz-rich pegmatites.

### **5. CONCLUSION**

The present geological milieu in the Son Valley area has the imprints of repeated thermal, tectonic and metamorphic reactivation, where low-grade low-tonnage uranium deposits have been delineated at Naktu and Kundabhati. The presence of associated rare-metal and REE minerals add to the economic potential in the area. The profuse occurrence of migmatites is the resultant product of ultra-metamorphism of arkosic to psammopelitic sequence deposited in ensialic extensional basins. Thermal regime in the course of ultra-metamorphism leading to anatexis had led to the remobilization of intrinsic uranium in sediments and subsequent concentration within the albite rich pegmatoid leucosome and biotite rich melanosome. Syn-tectonic plutonic activity also has contributed towards the mobilization and subsequent concentration of U. The mineralized episyenites are the product of shearing, brecciation and desilicification of the anorogenic alkali granites, and associated metasomatism. The multimetal-mineralisation associated with magmatic pegmatites has resulted due to pneumatolytic/metasomatic activity at a later stage.

## REFERENCES

- [1] RADHAKRISHANA, B.P., RAMAKRISHNA, M., Archaean-Proterozoic boundary in India. *J. Geol. Soc. India* **32** (1988) 263–278.
- [2] RAMAKRISHNAN, M., VAIDYANADHAN, R., *Geology of India: Vol. 1 & 2*, Geological Society of India, Bangalore (2008).
- [3] BHATTACHARYA, A.K., et al., Uranium mineralisation hosted by migmatite mobilizes and associated breccia zone in northwestern parts of Chhotanagpur Granite Gneiss Complex, Rihand valley, Sonbhadra district, U.P. *Indian Jour. Geol.* **64** 3 (1992) 259–275.
- [4] DHURANDHAR, A.P., SAXENA, D.N., Integrated airborne gamma ray spectral and satellite data analysis for U and REE mineralization-A case study from north Sagobandh area, District Sonbhadra, Uttar Pradesh, India, *J. Indian Soc. Remote Sensing* **27** 1 (1999) 43–57.
- [5] MAHENDRA KUMAR, K., BHATTACHARYA, A.K., GORIKHAN, R.A., MATHUR, D.K. SENGUPTA, B., Uranium mineralisation hosted by albite-rich leucosomes in the migmatised early Proterozoic metasedimentary rocks around Naktu, Son Valley, Sonbhadra district, Uttar Pradesh, India, *EARFAM* **11** (1998) 55–60.
- [6] ACHARYYA, S.K., ROY, A., Tectonothermal history of the Central Indian Tectonic Zone and reactivation of major faults/shear zones, *J. Geol. Soc. India* **55** (2000) 239–256.
- [7] ROY, A., HANUMA PRASAD, M., Tectonothermal events in Central Indian Tectonic Zone (CITZ) and its implications in Rodinian crustal assembly, *J. Asian Earth Sci.* **22** (2003) 115–129.
- [8] GHOSE, N.C., Chhotanagpur Gneiss-Granulite Complex, Eastern India: Present status and future prospect, *Indian Jour. Geol.* **64** 1 (1992) 100–121.
- [9] MAJI, A.K., et al., Proterozoic polyphase metamorphism in the Chhotanagpur Gneissic Complex (India), and implication for trans-continental Gondwanaland correlation, *Precambrian Research* **162** (2008) 385–402.
- [10] SINGH, C.K., SRIVASTAVA, V., Morphotectonics of the Area Around Renukoot, district Sonbhadra, U.P. Using Remote Sensing and GIS Techniques, *J. Indian Soc. Remote Sensing* **39** 2 (2011) 235–240.

# SANDSTONE DEPOSITS OF EURASIA — FROM GENETIC CONCEPTS TO FORECASTING AND NEW DISCOVERIES

I.G. PECHENKIN, G.A. MASHKOVZEV

All-Russian Scientific-Research Institute of Mineral Resources,  
Moscow, Russian Federation

## Abstract

Along the southern borders Eurasian continent lie uranium ore provinces and regions controlling medium-sized and, on rare occasions, large sandstone deposits. A common criterion has been established for all deposits of the sandstone type, located in sedimentary basins — the zone of interlayer or ground-interlayer oxidation, controlling uranium mineralization. After examining the southern extremities of the Eurasian continent, in the region of the collision of the Indian Plate, a distinct similarity can be perceived between the location of infiltration uranium deposits of the Tien Shan megaprovince and the pattern of development of the Pacific Plate subduction. In both cases young sandstone deposits tend to be situated close to the zone of subsiding geodynamic activity. Endogene uranium bodies can be found near the contact area of collision plates. The size of both endogene and exogene deposits in the south and east of the Eurasian Plate differ considerably. The given material bears evidence of a close spacial connection between part of sandstone uranium deposits and endogene uranium deposits. Both types of uranium deposits belong to the same ore metallogenetic zoning which is entirely dependent on the global geodynamic processes taking place in the crust and mantle on the fringes of the Eurasian continent.

## 1. INTRODUCTION

In the past 60 years, sandstone uranium deposits have been discovered and studied on the margins of the Eurasian continent. Along its southern borders lie uranium ore provinces and regions controlling medium-sized and, on rare occasions, large sandstone deposits. Central French, Bohemian, Eastern Rhodope and other regions are known in the west. Large uranium ore provinces were discovered in the south of the Turan Plate and in the depressions of South Kazakhstan, viz. Central Kyzyl Kum, Syr Darya, Chu Sarysu (Fig. 1). The discovery of uranium deposits of a new genetic type, sandstone, in sedimentary rocks in Central Asia and Southern Kazakhstan in the mid-20th century made us pay serious attention to them. The interest in these objects was determined by their large and unique proportions, the convenience and economic benefits of processing using the method of in-situ leaching and the polycomponent composition of ores, which included uranium, selenium, molybdenum, rhenium, scandium and other elements.

## 2. THE CENTRAL KYZYL KUM URANIUM PROVINCE

Drawing on the example of Central Kyzyl Kum province, it can be seen how important geological discoveries can quite literally happen in a vacuum. Thus begins vigorous development of lifeless territories. A new genetic type of deposits becomes the main industrial type and a standard for geologists involved in forecasting and research. The unique sedimentary deposit in Uchkuduk became such a facility. Its discovery in 1952 turned the idea of the future of sandstone deposits upside down and set their systematic study in motion.

### 2.1. The Uchkuduk deposit

The study of the deposit can be divided into several stages. In 1952, a powerful aero anomaly was discovered. It was connected with near-surface concentration of uranophane both in the weathering mantle of Palaeozoic granites and in Cretaceous formations. In 1954, at a depth of 30 m, a primary pitchblende-oxide mineralization was discovered. In 1955 it was traced by means of trenching for 9 km with the width up to 400 m. Vladimir Mazin and Gertrud Pechenkin noted that the mineralization was confined to permeable sandstone horizons and tended always to be situated on the boundaries between

yellow (oxidized) and grey (unchanged) rocks. In 1956 they created the first maps of the distribution of limonitization in Cretaceous formations and showed that all ore bodies are controlled by the boundary between oxidized and unoxidized rocks [2]. The deposit in terms of its geological type was unprecedented on a world-wide scale. Many specialists were inclined to believe that this was a syngenetic mineralization. In 1958, the issues of the genesis of the Uchkuduk deposit were being discussed. After the meeting, the majority was of the opinion that the object was epigenetic and had been formed as a result of uranium precipitation from down-percolating oxygen-containing stratal water. In 1960, the deposit was taken over by a production facility. Effectively, the development of the facility began eight years after its discovery.

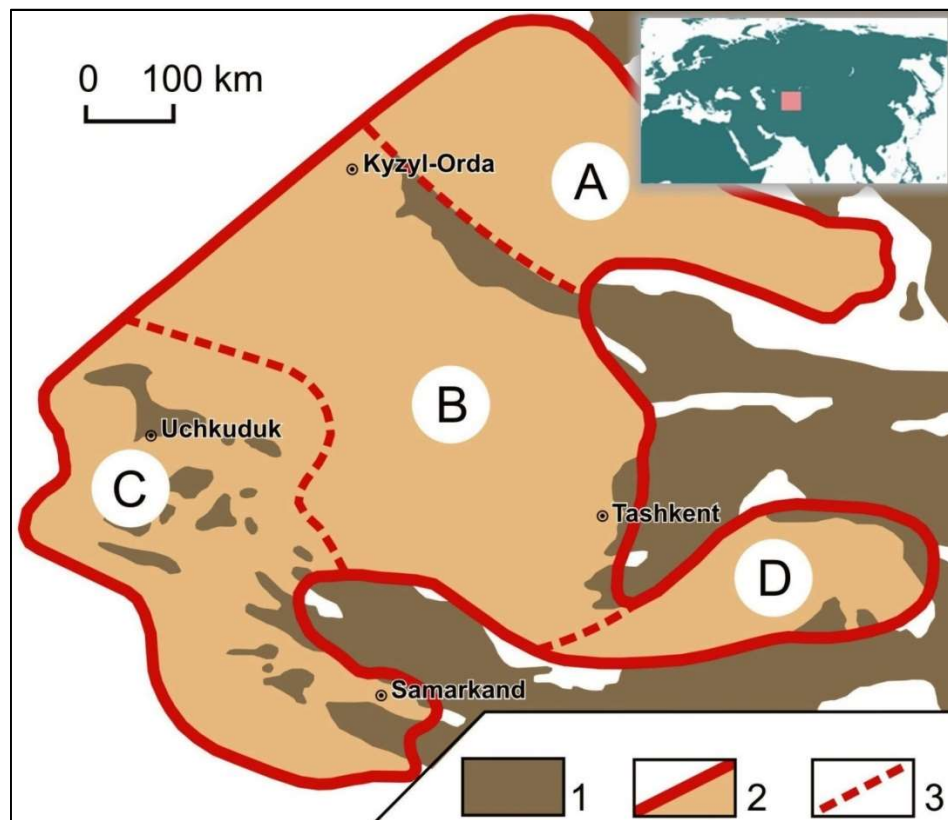


*FIG. 1. Metallogenic division of the Tien Shan uranium ore mega province [1].*

1. Exposures of crystalline basement rocks; Boundaries of: 2. Tien Shan mega province; 3. Uranium ore provinces: A – Chu Sarysu; B – Syr Darya; C – Central Kyzyl Kum; D – Fergana uranium ore region.

## 2.2. Features of sandstone deposits in Central Kyzyl Kum

In subsequent years in Central Kyzyl Kum province there were discovered over twenty deposits of this genesis. These discoveries, beginning with the unique deposit of Uchkuduk, became possible owing to the cooperation of geologists from the industry and scientific workers from a number of scientific research institutes. They developed a theoretical basis for the formation of such objects, the characteristics of ore zonality and the concept of geochemical barriers. A common criterion has been established for all objects of the sandstone type — the oxidation of tabular or ground-tabular strata, controlling uranium mineralization (Fig. 2). A single source of uranium has been suggested for the large majority of the deposits — local regions of supply of the adjacent mountain structures [1, 3]. The complex analysis of ore-bearing capacity of oil-and-gas bearing basins was being actively carried out. The study of epigenetic processes of both reduction and oxidation series holds a special place. The processes play an important role in decoding the direction and sequence of ore genesis. In the first stages

it was already established that ore deposits are often situated on the margins of oil-and-gas bearing basins and have a number of distinctive characteristics.

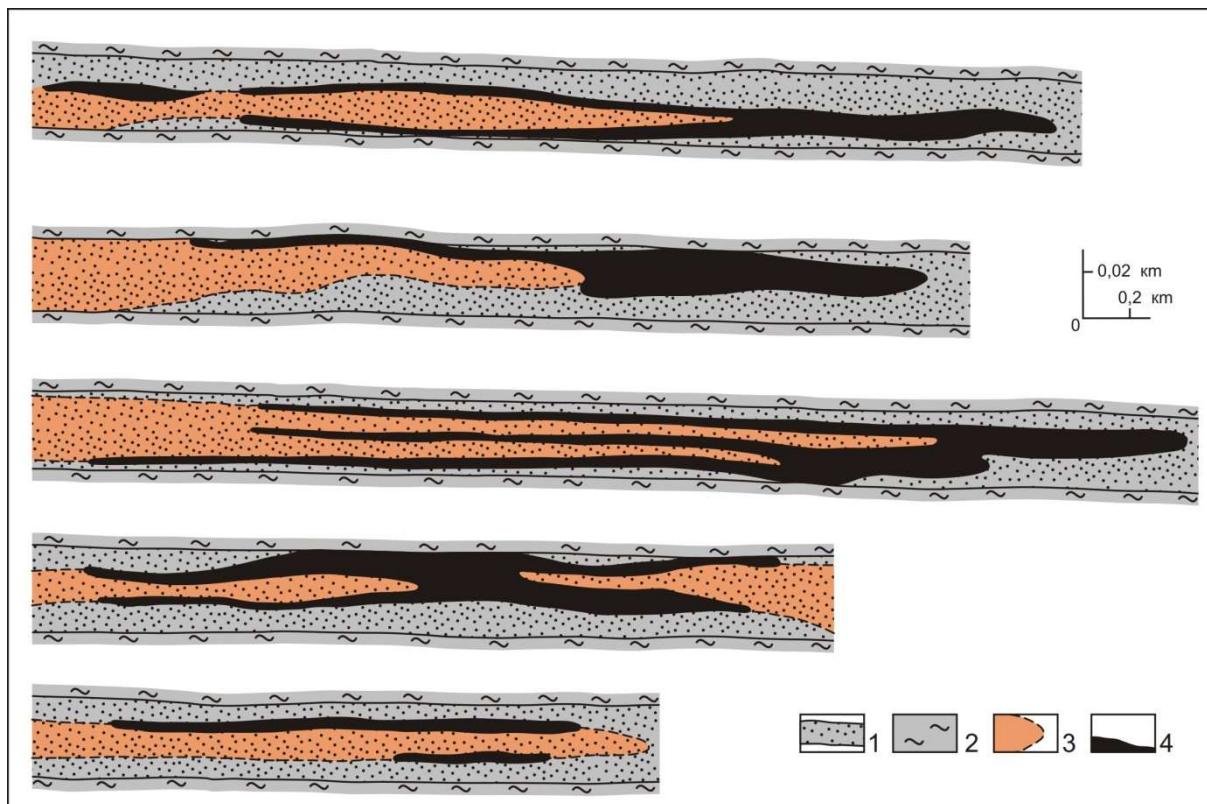


*FIG. 2. Ore-forming oxidized zone (examples of ore bodies morphology at Uchkuduk).*

1&2 – Primary grey-coloured rock: sand (1), clay (2); 3 – Secondarily oxidized rock; 4 – Finely dispersed oxide uranium ore in sandstones after Refs [1, 3].

### 3. FORECASTING SANDSTONE URANIUM DEPOSITS IN OIL-AND-GAS BEARING BASIN

#### 3.1. The Maylisay deposit

In the 1950s in the Maylisay deposit in the Fergana Valley a study of the relationship between reduction and oxidation processes was conducted in the carbonate rocks of Palaeogene age. The presence of pre-ore and post-ore epigenesis of petroleum series was established. Part of uranium mineralization was found to be submerged by liquid petroleum. A panel of experts led by Vladimir Kholodov was able to defend the view of epigenetic formation of uranium ore against the syngenetic hypothesis of ore genesis, prevailing at the time and espoused by leading scientists. Later it became apparent that their genesis was the same as that at the Uchkuduk deposit.

#### 3.2. The Sabrysay deposit

In the mid-1960s in the Sabrysay deposit in Uzbekistan there were studied pre-ore reduction changes in primary red continental sediment of Cretaceous age. They were instrumental in forming an economical uranium mineralization on a contrasting geochemical barrier. Further research showed that multidirectional epigenetic processes changed repeatedly. The study of ore zonality of the Sabrysay deposit revealed that during the process hydrocarbons and products of their alteration play an important role.

### **3.3. Role of reducing agents of petroleum series**

The most favourable conditions for contrasting ore genesis are to be found in stable zones of basins where oil and gas fluids are released. This process contributes to increased reduction capacity of formations of various primary geochemical types. In margins of basins reduction epigenesis extends aerially. Its role diminishes the further it is from the areas of oil and gas genesis. These principles have been established drawing on the example of the Central Kyzyl Kum. Reducing agents of petroleum series play the central role in the Sabrysay deposit. They are of the least importance at the Uchkuduk deposit. Formation of a new mineralization sometimes occurs after reduction [3]. The complexity of the processes is determined by the dual role of hydrocarbon fluids and their alteration products. On the one hand, the bituminization of permeable rocks as well as related pyritization, chloritization, dolomitization and other changes create a favourable geochemical environment of a reductive nature for subsequent concentration of uranium. On the other hand, introduction of bitumen and its fragmentation in the zone of aeration leads to the burial of the previously formed mineralization and to the disappearance of all traces of its formation, i.e. epigenetic oxidation zonality. This hampers prediction of the mineralization and subsequent reconnaissance studies. Over the locally collapsing hydrocarbon deposits generally fields distinguished by reductive geochemical conditions are formed. As a result, red sandstone-siltstone rocks take on blue, green and whitish hues. Sandstones are prone to intensive dolomitization. Subsequent passing of oxygenated infiltration waters with higher concentrations of uranium and other elements through these transformed masses complex epigenetic ores are formed. [4, 5].

### **3.4. Komsomol show of ore**

The research conducted at the ore showing in Komsomol, Tajikistan, located in Neogene primary red molasses, proved the possibility of geologically young mineralization which have been subjected to reduction. Previously such sedimentary formations were regarded as showing little promise. Red rocks took on light grey and blue hues. At the centre of the area all the rocks were reduced. On the margins red relicts persisted. A zone of strata oxidation developed along reduced mineralization. Uranium, molybdenum, yttrium and silver were concentrated in its attenuation.

### **3.5. The Benavides deposit**

Later, in the 1970s, American geologists studying uranium deposits on the oil-and-gas bearing Texas plain reached similar conclusions. In the Benavides deposit, in their view, the main mineralization tends to be situated closer to the boundary of the attenuation of the zones of strata oxidation, developing in epigenetically reduced rocks. In a number of deposits, a second, post-ore reduction was noticed [6].

## **4. METHODS OF MAPPING OF EPIGENETIC CHANGES**

### **4.1. Essence of this method**

The sequence of formation of superimposed changes of reduction and oxidation series and their interrelations is one of the main factors which influence the distribution of polymineral mineralization. In 1960–70s the scientists from All-Russian Scientific-Research Institute of Mineral Resources (Moscow) developed and introduced the methods of studying the sequence of epigenetic changes in sedimentary rocks. The latest changes in sedimentary rocks are visible in the most water-permeable parts of sections, such as sands, gravelite and conglomerates. Early processes can leave their traces in siltstone and clay parts of sedimentary rocks. It becomes apparent in the appearance of coloured borders of various origins. The further from the aquifer the border in the aquitard, the earlier superimposed change it corresponds with (Fig. 3). Various minerals typical of certain processes and the cementation of previously water-permeable rocks with the products of epigenesis serve as additional diagnostic indications of the completion of the changes. The established sequence of epigenetic changes makes it possible to carry out special charting of promising areas with a view to revealing hidden parts of epigenetic oxidation zonality and ‘buried’ mineralization [7, 8].

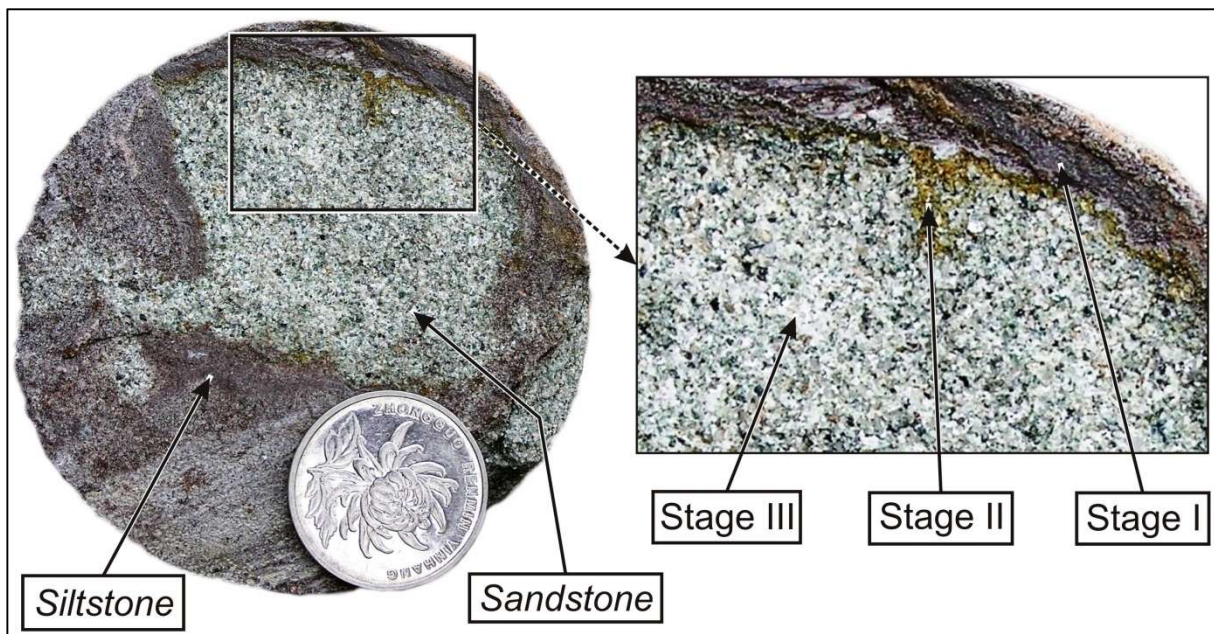


FIG. 3. An Example of a reduction-oxidation sequence.

*Stage I – Primary red rock; Stage II – Secondarily oxidized rock (relict); Stage III – Reduction after oxidation.*

#### 4.2. The Dunshen deposit as an example of mapping

Such work has been carried out within the confines of Ordos's oil-and-gas bearing basin at the Dunshen deposit. Here the zone of oxidation by means of introduction of reducing agents changed its colour from yellow and reddish-yellow to green and greyish-green. It was brought about due to the formation of epigenetic chlorite. The oxidation was preserved in the relicts. A complex of palaeographic maps and cross-sections of the Ordos basin and adjacent structures was created. They reflect the interrelations between the reactions of oxidation and reduction throughout the duration of the large stages of the region's geological history. A model of the formation of the Dunshen deposit was created using this data. The history of its development can be divided into four main stages, the first being the pre-ore stage. The second is the ore stage, with the formation of uranium mineralization. The third is the period of the 'conservation' of the mineralization. The fourth and final stage is the development of a zone of ground oxidation devoid of ore (Fig. 4). The model proves that the deposit is of a typical sandstone variety. The methods of studying epigenetic changes in rocks of oil-and-gas bearing sedimentary basins were successfully applied during forecasting research on the margins of oil-and-gas bearing basins of the Asian continent [4, 8, 9]. They helped carry out metallogenic uranium zoning and the forecasting of a large area, assessing thereby the role of hydrocarbons.

#### 5. METHODS OF PROSPECTING AND EXPLORATION OF SANDSTONE DEPOSITS IN SEDIMENTARY BASINS

This method is based on their characteristics, first established at the Uchkuduk deposit. They are located in soft formations of aquifers and as a rule are not exposed at the surface. The mineralization is localized in pitch-out limits of strata oxidation zones. Core drilling is implemented at each stage of the study of a deposit [2].

##### 5.1. Geological forecasting

Predictive assessment of the prospects of uranium-bearing capacity of large areas is undertaken prior to drilling. An exploration model of a prospective ore-bearing area is created. This permits singling out potential exploration areas. The presence of the requirements for the formation of mineralization is established. These are regional criteria: climatic, hydrodynamic and geotectonic. Also, local criteria:

geological and structural, litho-facial, litho-chemical. Then verification drilling is carried out. A geological predictive model of a deposit is created, and speculative resources are assessed on its basis.

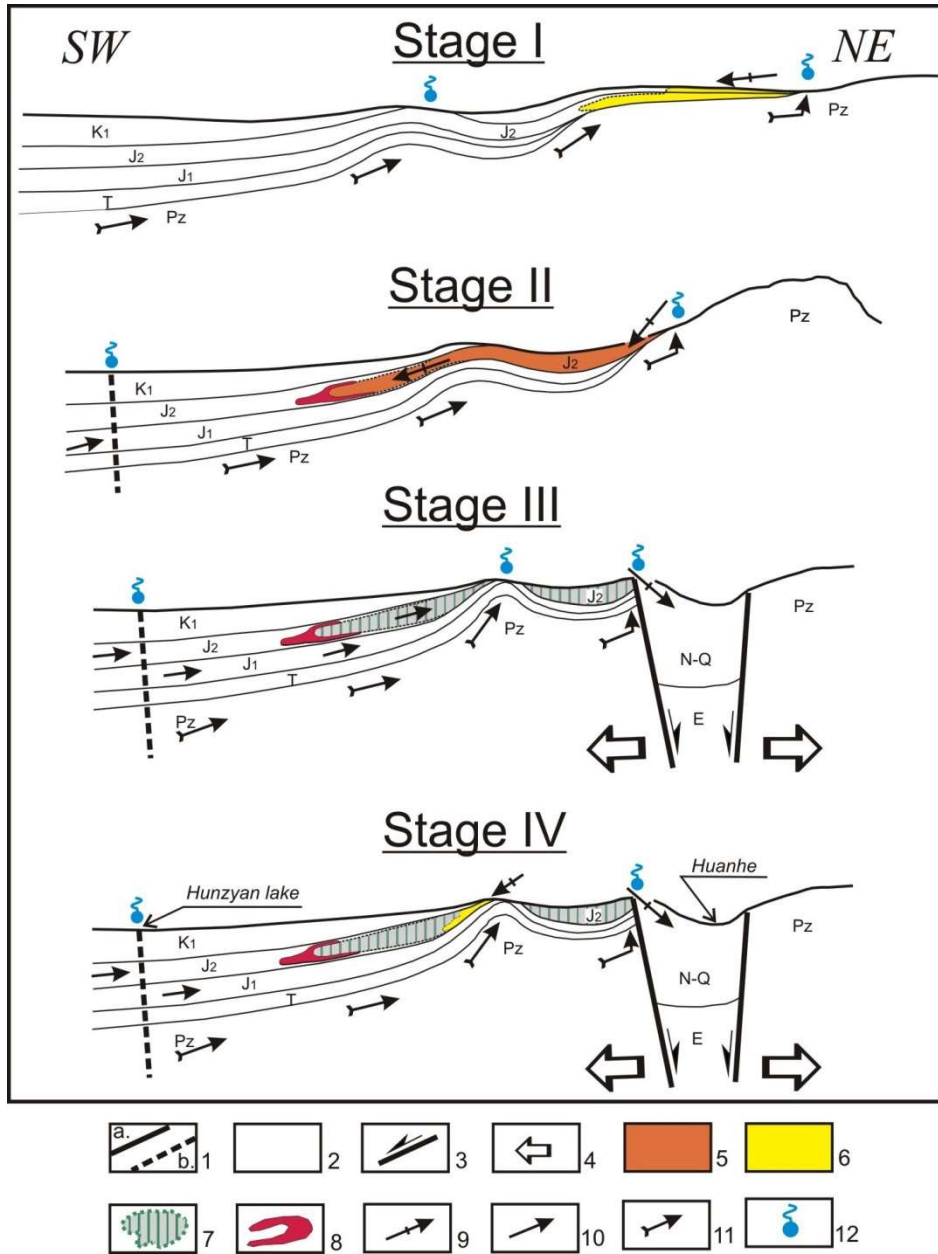


FIG. 4. A model of the formation of the Dunshen deposit.

1 – faults: a. main, b. alleged; 2 – primarily (unchanged) rocks; 3 – wrench fault; 4 – direction of tectonic stress; 5 – interlayer oxidation zone; 6 – groundwater oxidation zone; 7 – area development reduced rocks; 8 – uranium ore. Direction of movement: 9 – oxidized water; 10 – reducing agent in Mesozoic rocks; 11 – reducing agent in Palaeozoic rocks; 12 – region of fluid relieving; 13 – area of development of reduced rocks.

## 5.2. Exploration work

Prospecting begins with the creation of a grid. Then profile drilling is implemented, making it possible to pinpoint the location of the mineralization in the pinch-out of the strata oxidation zone, and preliminary establish its parameters. Following detailing helps determine the conditions of the position of the mineralization, its morphology and quality. Geotechnological laboratory experiments are carried out. It affords an opportunity to convert part of Speculative resources into Prognosticated resources.

### **5.3. Exploration and assessment**

Prospecting and assessment include the creation of a more detailed grid. Then profile drilling and detailed survey are implemented up to 50 m. Thus, the assessment of the prognosticated resources of the whole deposit and the conversion of part of them into inferred resources becomes possible. On the basis of this stage the profitability of the development of the deposits is established.

### **5.4. Prospecting**

The objectives of preliminary prospecting include delineation of ore reserves and conversion of all resources into inferred resources. In detailed survey areas some of them are transformed into Reasonably Assured resources. A reliable estimate of the possibility of ore-processing using in-situ leaching (ISL) is conducted. During detailed exploration experimental production operations on ISL are carried out. The specifics of geotechnology of the ores in the deposits are determined. Conversion of all inferred resources into reasonably assured resources is conducted. This operating sequence enables us to carry out the job with minimum time and money, though it might seem to require long time and resources.

## **6. GLOBAL GEODYNAMIC PROCESSES AND METALLOGENY OF URANIUM**

Over the last decades attention was drawn to a close spatial connection and interdependence of large ore-bearing continental blocks, which also contain deposits of sandstone type with most recent plate tectonic processes. In 2003 we were able to justify the concept that the formation of giant deposits in Chu Sarysu province was caused by the collision between the Indian Plate and the southern part of the Eurasian continent. A hypothesis was put forward in this regard, to the effect that the metal could arrive from an internal deep-seated source, from the area of maximum stress conditions, emerging in points of active contact of collision plates, as represented by the Pamir ‘wedge’ [4, 8].

### **6.1. The Pacific ore belt**

In the last years we have extended the predictive estimate for sandstone uranium deposits over the eastern part of the Eurasian continent. A close spatial connection has been noticed between these deposits and the Pacific ore belt. According to a number of researchers, the formation of the latter was caused by the subduction of the Pacific Plate, which captured vast areas on the continent. As a result, during the Mesozoic era large blocks of the eastern part of Eurasia underwent radical tectonic changes. Numerous ore-bearing deposits were formed as a consequence, among them those bearing iron, copper, tin, tungsten and uranium. All of them are united into an extensive Pacific ore belt, pointed out by Sergey Smirnov as early as 1944. It must be emphasized that due to the subduction of the Pacific Plate the eastern part of the Eurasian Plate changed from the depth of 500 to 1000 km [10].

#### *6.1.1. Endogenic uranium deposits*

Within the limits of this belt there is a zonal distribution of ore deposits. Run-of-mine mineralization is drawn towards its eastern fringe: gold, tin, copper, tungsten etc., while uranium is localized in its eastern part. Within the activated zone of the plate there are areas with continental rifting and passive margin. Volcanic and tectonic structures of central type and of Mesozoic age are located further west, from the north to the south, and these are large calderas — Streltsovskaya, Dornot, Sian Shan, controlling endogene deposits of uranium and other minerals, which are large and unique in scale.

#### *6.1.2. Exogenetic uranium deposits*

In the far west, in the region of subsiding tectonic tensions in the passive margin of the continental block young Neogene-Quaternary basalt magmatism is intensely manifested. Sandstone uranium ore deposits in Trans-Baikal, Mongolia and the western margin of the South China Plate are spatially connected to it. It should be pointed out that sandstone deposits of Vitim region are adjacent to endogene deposits of Streltsov region in the southern-easterly direction. To the east of the deposits of Yunnan and at the same latitude lies the Sian Shan caldera with geothermal deposits of uranium and other metals. We combined

them into the unified submeridional *Baikal-Southern China uranium ore belt* [8, 10]. Lack of sandstone uranium ore deposits within the Aldan shield and Sino-Korean craton can be accounted for by the old age of intensively transformed Archaean strata, exhibiting resistance to the advancement of the mantle slab of the Pacific plate. Consequently, within the limits of the mantle of the Sino-Korean craton, in the Ordos basin and the Eren depression in China, sandstone uranium ore deposits were discovered which bear no relation to young volcanism. Most probably, the majority of the deposits discovered in these structures were formed from local regions of supply.

## 6.2. Connection between sandstone and endogene uranium deposits

The data presented here bears evidence to the existing zonality in the localization of ore deposits within the Pacific belt which spans the eastern margin of Eurasia. The scale of the deposits of sandstone type in the Baikal-South China uranium-bearing belt doesn't exceed the average yet, but a considerable number of them suggest great prospects for this extensive structure. After examining the southern extremities of the Eurasian continent, the region of the collision with the Indian Plate, a distinct similarity can be perceived between the location of sandstone uranium deposits of the Tian Shan megaprovince and the pattern of development of the Pacific plate subduction. In both cases young sandstone deposits tend to be situated close to the zone of subsiding geodynamic activity. Endogene uranium deposits can be found near the contact area of collision plates. The size of both endogene and exogene objects in the south and east of the Eurasian plate differ considerably [10]. The scale of the sandstone deposits in the Tian Shan megaprovince is an order of magnitude greater than that of the deposits in the Baikal-Southern China ore belt. It can be explained by wide zones of transit and multilayered geochemical barriers, conducive to the localization of uranium from acidized uranium-rich waters moving through Cretaceous and Paleogene rocks of the Turan plate and large depressions of South Kazakhstan. However, the endogene uranium deposits of the Tian Shan are considerably smaller in scale than the large uranium deposits of caldera and fracture types in the Pacific ore belt dating from Mesozoic age. The causes of these phenomena warrant further study.

## 7. CONCLUSION

In it should be pointed out that the exogene metallogeny of uranium has been evolving separately from the endogene metallogeny for many years. The aforementioned data bears witness to a close spatial connection between part of sandstone uranium deposits and the endogene uranium deposits concurrent with volcanogenic and tectonic structures. Both types of uranium deposits fall into a single ore metallogenic zonality which is wholly due to global geodynamic processes going on in the mantle and the margins of Eurasia. Such an approach makes it possible to examine the principles of localization and the interrelations between uranium deposits of different genesis. This makes it possible to increase the prospects for the future of many parts of the world.

## REFERENCES

- [1] MASHKOVZEV, G.A. (Ed.), Geological-minable types of uranium deposits in the CIS, VIMS, Moscow (2008) (in Russian).
- [2] KARIMOV, Kh.K., et al., Uranium Deposits of the Uchkuduk Type in the Republic of Uzbekistan, FAN, Tashkent (1996) (in Russian with English Summary).
- [3] PECHENKIN, I.G., PECHENKIN, V.G., Evolution of sedimentary ore forming in fluvial paleo-systems, VIMS, Moscow (2008) (in Russian with English Summary).
- [4] GRUSHEVOY, G.V., PECHENKIN, I.G., Metallogeny of Central Asian uranium-bearing sedimentary basins, VIMS, Moscow (2003) (in Russian with English Summary).
- [5] PECHENKIN, I.G., PECHENKIN, V.G., Models of ore formation in various geostructural settings, Uranium geochemistry 2003, Uranium Deposits – Natural Analogs – Environment, Nancy – France. Unite Mixte de Recherche CNRS (2003) 285-288.
- [6] GOLDHABER, M.B., REYNOLDS, R.L., RYE, D.R., Origin of a South Texas uranium deposit; II, Sulfide petrology and sulfur isotope studies, Econ. Geol. **73** (1978) 1690-1705.
- [7] PECHENKIN, I.G., SCHETOCHKIN, V.N., Features of forecasting of exogenic uranium deposits in oil-and-gas bearing basins, Ores and Metals **3-4** (2011) 135-136 (in Russian with English abstract).
- [8] PECHENKIN, I.G., “Minerageny of the sedimentary basins of the Central Asia. Problems and solutions”, Int. Conf. on Geology, Tectonics and Minerageny of Central Asia, St. Petersburg (2011) (CD-ROM file Pechenkin\_IG).
- [9] XIANG, Weidong, et al., Uranium ore formation in fluvial paleo-system of Ordos basin, North China, 12th Quadrennial IAGOD symposium, Moscow (2006) (CD-ROM file 288).
- [10] PECHENKIN, I.G., GRUSHEVOY, G.V., “Position of infiltration uranium deposits within the Pacific ore belt”, Proc. 2nd Int. Symp. on Uranium: Resources and Production, Moscow (2009) 262-264 (in Russian).

# THE OUTLOOK ON POTENTIAL URANIUM ISL MINING AT NYOTA DEPOSIT, TANZANIA

A. BOYTSOV\*, S. STANDER\*\*, V. MARTYNENKO\*\*\*

\* Uranium One Inc,  
Toronto, Ontario, Canada

\*\* Mantra Resources,  
Dar Es Salaam, Tanzania

\*\*\* Rusburmash,  
Moscow, Russian Federation

## Abstract

The Nyota deposit, located in the Karoo sedimentary basin in South Western Tanzania, is the subject of a detailed feasibility study. The Nyota deposit has JORC compliant resources of 152 Mlbs of U<sub>3</sub>O<sub>8</sub> (~58 466 tU) at an average grade of 286 ppm U<sub>3</sub>O<sub>8</sub> (~243 ppm U). The mining and extraction philosophy is based on an open cast mining operation. Approximately one third of the resource both within and outside the current pit designs, are situated in permeable sediments below the groundwater level and potentially amenable to ISL. A preliminary hydrological study, conducted in 2012, demonstrated that the major geological, hydrological and technical parameters are favourable for ISL mining. This was followed up with a very successful Push-Pull test, conducted in 2013, which revealed the suitability of the mineralisation to leaching with sulphuric acid solutions. Commercial grade uranium content was obtained in the solutions which ranged from 30 to 124 mg/L U. The planned follow-up work consists of an ISL specific resource estimate, a more advanced hydrological study and a 5-spot ISL field leaching trial. The concept of ISL at Nyota is not without its technical, environmental and approvals challenges. Should ISL prove to be viable, it holds the potential to unlock the region as an ISL production centre.

## 1. THE MKUJU RIVER PROJECT — GENERAL INFORMATION

The Mkuju River Project is a uranium development project located in southern Tanzania, approximately 470 km southwest of Dar es Salaam (Fig. 1). Uranium One is the operator of the Mkuju River Project. It is a Canadian-based company and a wholly owned subsidiary of the Russian State Corporation Rosatom. Uranium One is a world top five uranium producer, with attributable 2013 production of 5140 tonnes U. All the uranium is produced via in situ leaching (ISL), which has resulted in average production cash cost of US \$16 per pound U<sub>3</sub>O<sub>8</sub> (US \$ 42 per kg U) sold in 2013 [1], making it one of the lowest cost producers in the industry. The development of the Mkuju River Project forms a major component of the future planned production growth for Uranium One and Rosatom.

Within Tanzania, the Mantra portfolio consists of a number of tenements. The Mkuju River Project tenements are the core assets, with the project area containing the large Nyota deposit. The project is the subject of a definitive feasibility study (DFS) and current activity is focused on licensing and permitting. In this regard, a Special Mining License (SML) has been secured and the UNESCO World Heritage Committee approved an application by the Tanzanian Government for a minor adjustment to the boundary in order to exclude the project from the Selous Game Reserve.

## 2. GEOLOGY AND MINERAL RESOURCES OF THE NYOTA DEPOSIT

The Mkuju River project is located within the Selous Sedimentary Basin, which forms part of the greater Karoo Basin (Fig. 1). The Nyota deposit, which is the key asset, occurs in the Triassic Mkuju Series and the major lithologies are felspathic sandstones, arkose sands and gritstone. The host rocks are braided fluvial sediments consisting of grits, sandstones and siltstones; with inter-bedded shale and mudstone horizons. The sediments are soft, barely consolidated and sub- horizontal. The typical Nyota cross section (Fig. 2) demonstrates the shallow depth of mineralization and lateral continuity of horizons.

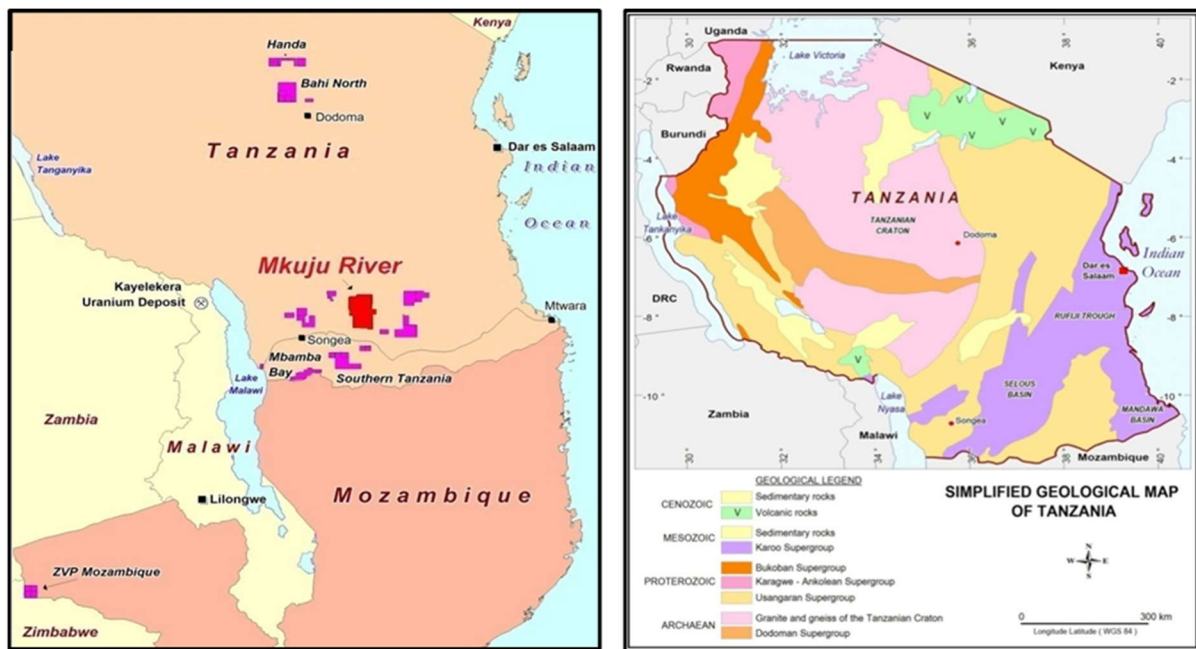
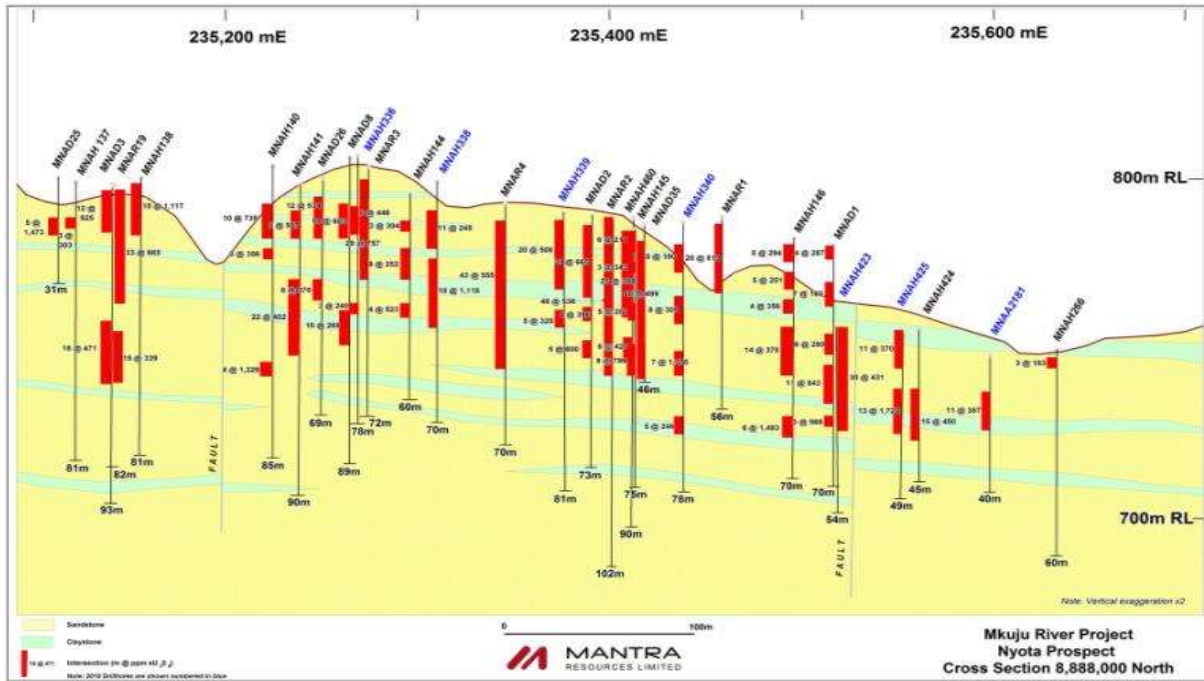


FIG. 1. Location of the Mkulu river project and simplified geological map of Tanzania.

Uranium mineralisation at Nyota is almost entirely developed within oxidised sediments, and often confined by aquiclude horizons of mudstone/claystone that are well identified as planar, thin sheets. Uranium distribution is seen to ‘cascade’ from upper hosting sedimentary cycles down into lower cycles where the lower confining aquiculides are breached by interpreted scouring or abrupt facies changes. Nyota is considered a tabular deposit where uranium precipitated under reducing conditions, caused by a variety of reducing agents within the sandstone including: carbonaceous material, ferric oxides, sulphides, hydrocarbons.



*FIG. 2. A typical Nyota cross section, showing drill hole traces and economic mineralisation intercepts, demonstrating the shallow depth of mineralization and lateral continuity of horizons (courtesy of Mantra Resources Ltd).*

To date, only secondary or hexavalent uranium minerals have been recognised; i.e. predominantly uranyl phosphates — phosphuranylite and meta-autinite, occurring interstitial to sedimentary grains (Fig. 3).

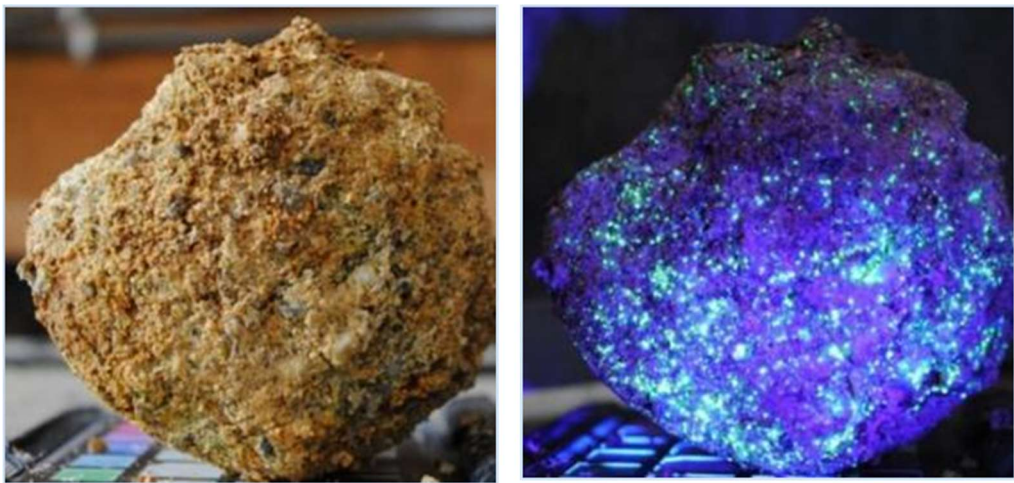


**FIG. 3.** Nyota mineralised samples under normal and ultraviolet light, highlighting the occurrence of uranium secondary minerals in the ore.

Systematic exploration drilling has resulted in continued growth in the mineral resource since the maiden mineral resource estimate in 2009. Current resources stand at 152.1 Mlbs U<sub>3</sub>O<sub>8</sub> (58 504 t U), including 124.6Mlbs (47 927 t U) in the Measured and Indicated categories. This represents a 4.2-fold increase in total, and a 7.3-fold increase in the measured and indicated (M+I) resources since inception; and a

28% growth in total resource (33% growth in M+I resources) since 2011 (Fig. 4). Significant exploration potential remains at the Nyota deposit.

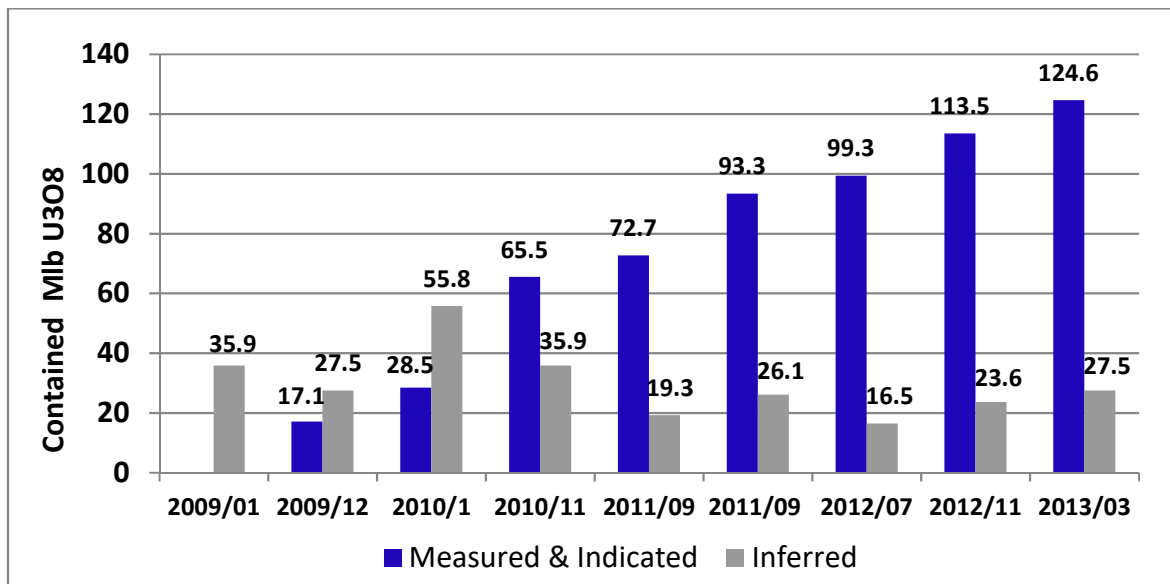
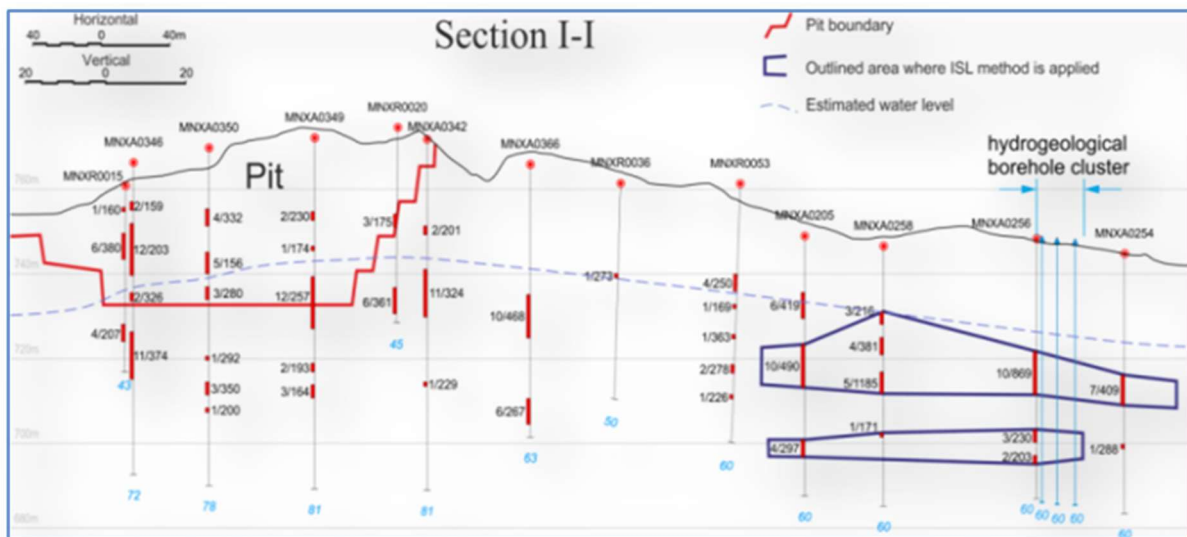


FIG. 4. Nyota mineral resource growth over time.

### 3. THE KEY MOTIVATION FOR INVESTIGATING ISL

One of the highlights of the feasibility study has been the fact that approximately 35% of the total mineral resource falls outside the economic open pit mine designs. These are parts of the ore body which are either too deep, too low grade or too small to be extracted economically via open cast mining methods under current market conditions.

In addition, a detailed 3D groundwater surface model was constructed which highlighted that approximately one third of the total mineral resources respectively occurs below the ground water table (Fig. 5). In total, a below ground water table resource of approximately 50 Mlb exists, which has led to the consideration and investigation of ISL as an alternative or additional extraction method (Fig. 6).



*FIG. 5. Cross section, showing resources location outside current pit designs and below water table, potentially amenable to ISL.*

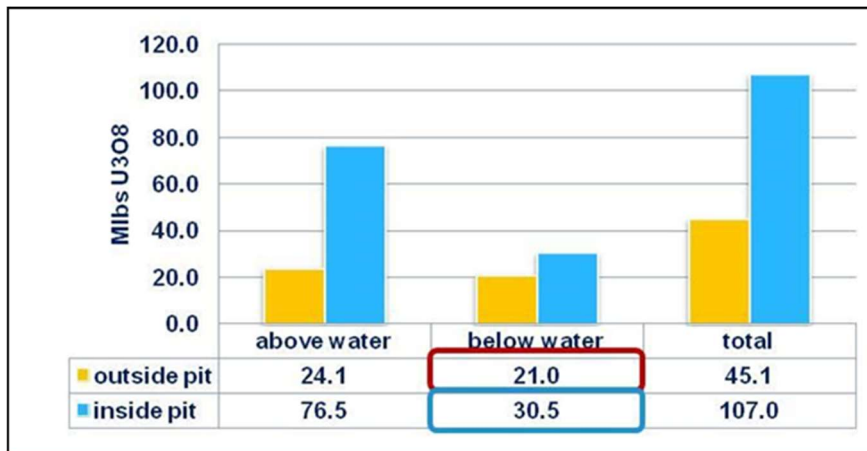


*FIG. 6. Summary of mineral resources relative to the pit designs and groundwater table (total 51.5 Mlbs U<sub>3</sub>O<sub>8</sub>).*

High level financial modelling, based on a conservative estimate of mineral resources outside the current pit design, have highlighted that considerable value can be added to the project if ISL can be proven to be a technically viable extraction method. The main advantages of ISL over conventional mining are the lower CAPEX and OPEX costs, as well as a lower environmental impact. As a result, Mantra Tanzania has embarked on a toll gated Research and Development (R&D) program into the feasibility of ISL at the Mkuju River Project.

#### 4. WORK COMPLETED AND RESULTS TO DATE

Some of the geological and hydrogeological conditions that must be present, to a more or lesser degree, for ISL to be feasible are listed below:

- Mineralization to occur below the natural ground water table;
- Mineralization must be restricted or confined to a fairly continuous, horizontal zone;
- The horizon must be highly permeable and porous to allow leaching fluids to be circulated through it and for it to come in contact with the mineralisation;
- The mineralized horizon must be sufficiently confined by less permeable rocks to facilitate the channelling and control of the leaching fluids;
- The mineralisation must be easily dissolvable into solution by the leaching chemicals;
- The natural groundwater quality should not impact negatively on the leaching process.

These conditions are often found in classical roll-front deposits, as exploited by Uranium One in Kazakhstan, the USA and Australia. The Nyota deposit is not a classical roll-front type deposit, and early work was aimed at establishing the presence of some of these conditions.

During 2012, a hydrogeological test was conducted on a selected area of the resource. This was conducted on a cluster of three closely spaced holes, and delivered the results in Table I.

TABLE I. SUMMARISED RESULTS OF THE 2012 HYDROGEOLOGICAL STUDY VERSUS FAVOURABLE ISL PARAMETERS [2]

| Factors affecting ISL process                   | Favourable parameters          | Obtained parameters                            | Factor |
|---|--------------------------------|--|--------|
| Hydraulic conductivity (permeability factor)    | 1–5 m/day                      | 1.8–5.1 m/day                                  | +      |
| Transmissivity of ore horizon                   | 10–100 m <sup>2</sup> /day     | 18.7–34.3 m <sup>2</sup> /day                  | +      |
| Depth of mineralization                         | <200                           | 26–56 m  | ++     |
| Carbonate content (CO <sub>2</sub> )            | 1–2%                           | 0.7%   | ++     |
| Mineral composition of ore                      | Disseminated uranium oxides    | Secondary uranium mineralization               | +      |
| Ore productivity                                | 1–5 kg/m <sup>2</sup>          | 1.2–18 kg/m <sup>2</sup>                       | +      |
| Water confining beds in the aquifer top, bottom | Stable water confining beds    | Local clay beds<br>0.4 m to 3.5 m thick        | + -    |
| Depth of underground water                      | 10–100 m                       | 21.8–24 m                                      | +      |
| Ground waters mineralization TDS                | <1 g/dm <sup>3</sup>           | <1.0 g/dm <sup>3</sup>                         | ++     |
| Water abundance (specific yield)                | 0.1–0.5 l/sec                  | 0.1 l/sec                                      | + -    |
| Thickness of productive aquifer                 | 10–30                          | Over 30 m, local to 1.5 m thick confining beds | - +    |
| Mineralization location in aquifer              | In the middle and bottom parts | In the upper and middle part                   | + -    |
| Temperature of ground waters                    | 10–30°                         | 26°  | +      |

The results highlighted some favourable conditions (such as mineralised thickness, low carbonate content, total dissolved solids (TDS), depth), but also some areas for further investigation, such as the thickness of the productive aquifer, specific yield and uncertainty around the presence of sufficient confining beds.

On balance, the success and positive indicators achieved with the preliminary hydrological test warranted further investigation, as per the toll-gated approach. As a result, the next logical step in the investigation, a field trial ISL Push-Pull test, was designed and conducted in 2013. The test was performed on mineralization within area MNX of the Nyota Prospect; at the site of the preliminary hydrological investigation. All the necessary governmental approvals were obtained prior to the test.

The purpose of the test was to study the possibility of recovering uranium in situ via solution leaching. Specialist technical guidance and support was provided under contract by the Russian company Rusburmash Inc. Rusburmash has worldwide experience in conducting ISL test work, most notably in operations in Russia, Kazakhstan and Uzbekistan.

The main objective of this test was to evaluate the principal amenability of the mineralization to ISL operations, with a specific focus on the effectiveness of various leaching reagents, the hydraulic conductivity, transmissivity and specific yield of the aquifer.

At the test site, the depth of mineralisation started at approximately 26 m and was about 8 m thick. The ore is hosted in sandstone, primarily composed of quartz and feldspar. Uranium is contained mainly in hexavalent uranium minerals. Uranium grade in the ore averaged 1260 ppm U<sub>3</sub>O<sub>8</sub>. Two recovery wells, five monitoring wells and one disposal well were completed, as depicted in Figs 7 and 8.

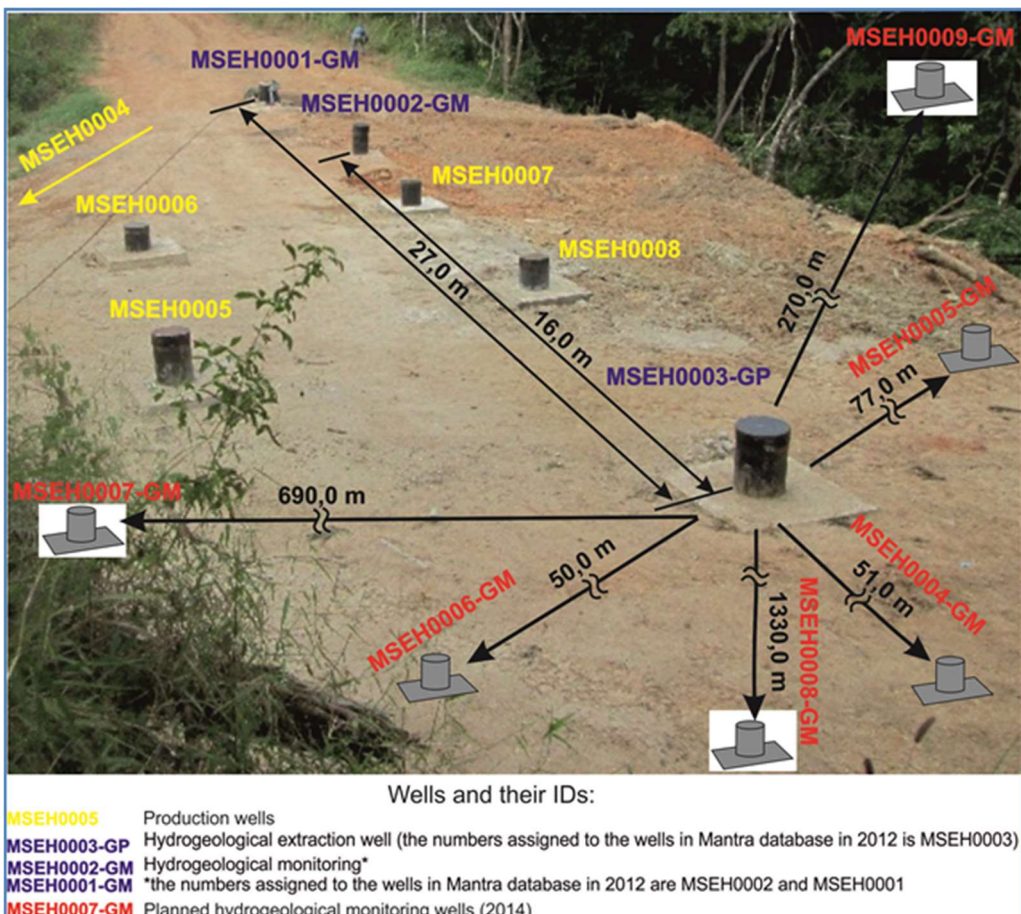


FIG. 7. Schematic well lay-out for the Push Pull test.

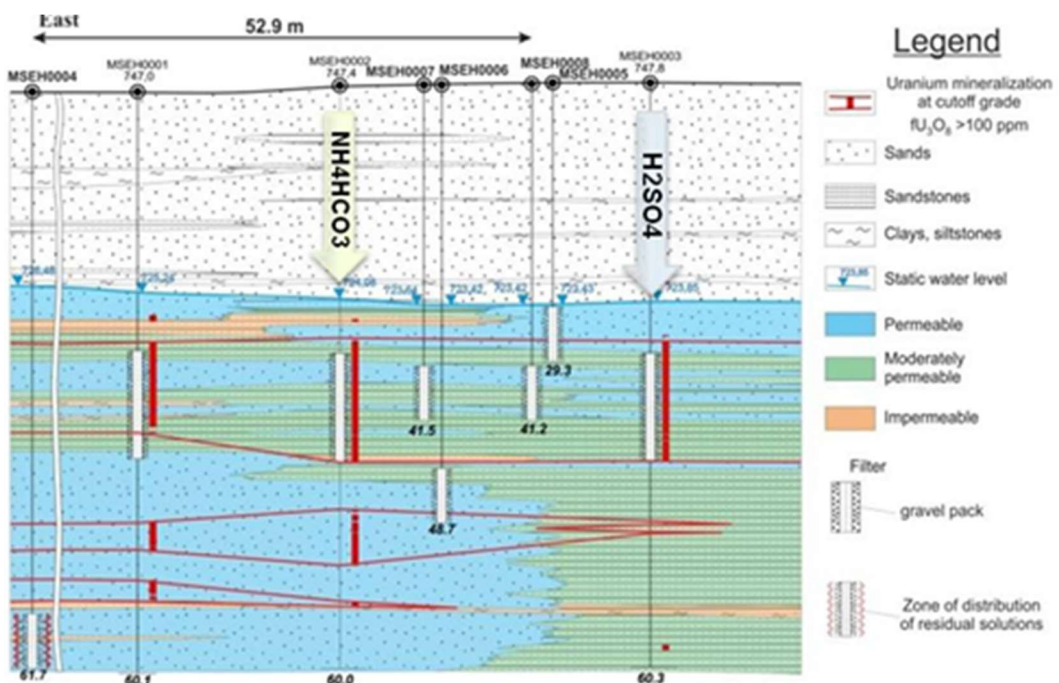


FIG. 8. Illustrative cross section lay-out of geology and the Push Pull test wells.

Water and core sample testing revealed that the carbonate content of the ore within the site is low (0.7%), which is favourable for sulphuric acidic in-situ recovery processes. The ground water aquifer that hosts the uranium bearing ore starts at 23–24 m from surface. The water of the aquifer is fresh and of type sodium bicarbonate. Water transmissivity is 18.7–34.3 m<sup>2</sup>/day; hydraulic conductivity is 1–5 m/day; specific discharge – 0.1 l/sec/m and the ground water temperature –26°C.

The following types of reagents were tested:

- NH<sub>4</sub>HCO<sub>3</sub>, with a concentration of 1, 5 g/L and 10 g/L (with and without + H<sub>2</sub>O<sub>2</sub> –2 g/L);
- H<sub>2</sub>SO<sub>4</sub>, with a concentration of 5, 10 and 20 g/L.

The two recovery wells were used for these purposes, each dedicated to one of these reagents. A total of 17 injection/extraction cycles were performed, of which 8 cycles were with sulphuric acid with exposure periods of 1, 2 and 3 days. A total of 262 groundwater and solution samples were analysed at a temporary field chemical laboratory, constructed at site during the test.

On completion of the exposure periods, water was pumped out and samples were continuously taken and tested for pH, Eh and concentrations of uranium, HCO<sup>3-</sup>, SO<sub>4</sub><sup>2-</sup>, Fe<sup>2+</sup> and Fe<sup>3+</sup>. Sampling continued until conditions of sub-commercial uranium values (0.5-1.5 mg/L) were obtained, after pumping out at least six volumes compared to that which was originally injected.

From an economic perspective, the three critical variables monitored were as follows:

- The concentrations of uranium in the leaching solutions;
- The concentration and type of leaching reagent;
- The time it took to leach uranium from the ore body.

Uranium leaching with NH<sub>4</sub>HCO<sub>3</sub> (with and without peroxide) demonstrated low potential for uranium recovery. The maximum content of uranium in the extracted solutions amounted to 4.5 mg/L, with the content during pumping ranging from 0.5 to 4.5 mg/L, which is five times less than the threshold values for commercial production of uranium. In total, 45.6 g of uranium were recovered to solution.

Uranium leaching by H<sub>2</sub>SO<sub>4</sub> with concentrations ranging from 5 to 20 g/L and exposure periods from 1 to 3 days (18–69 hours) demonstrated good leaching kinetics. All the solutions managed to recover commercially significant concentrations of uranium into solutions in short timeframes (Fig. 9).

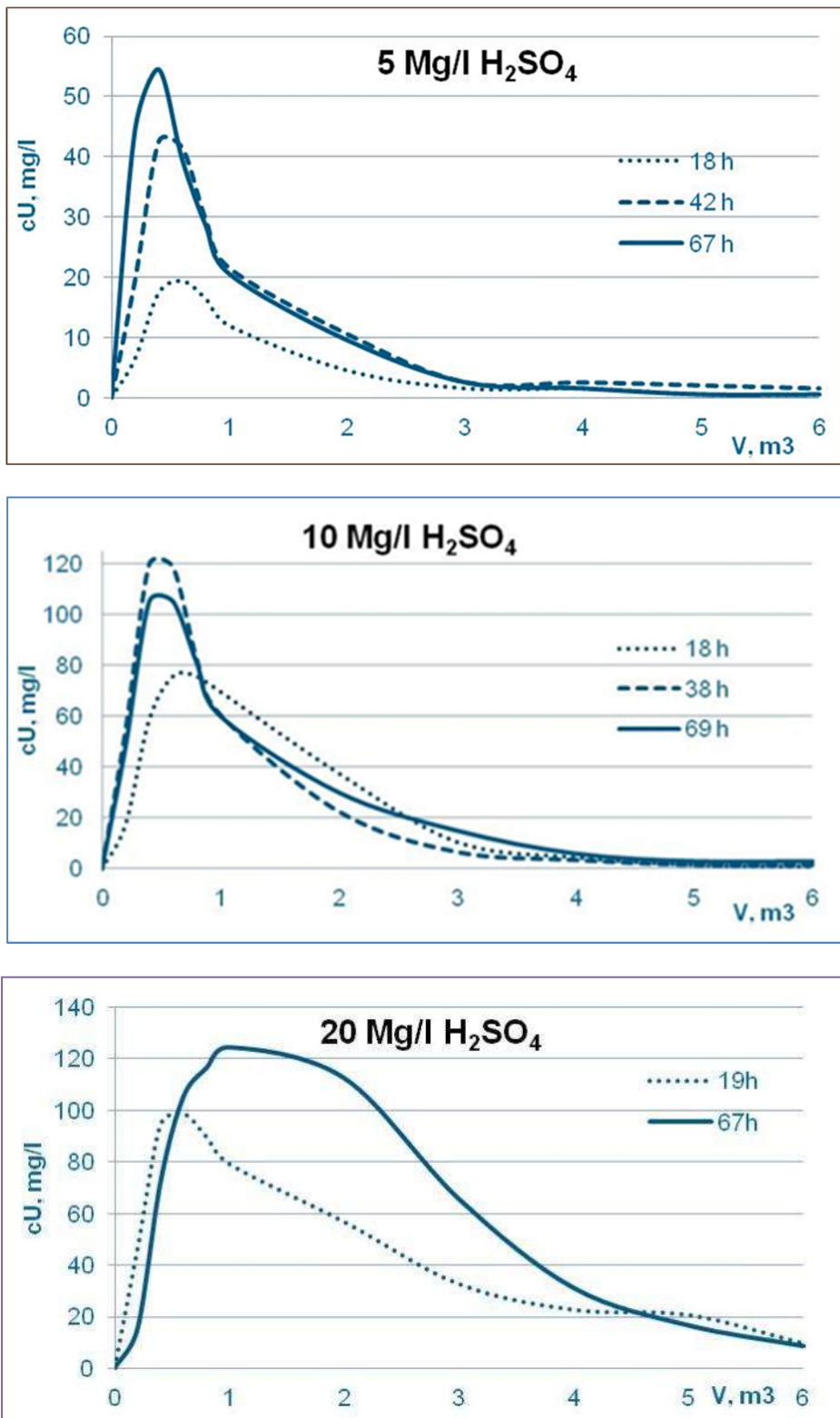


FIG. 9. Uranium leaching by  $H_2SO_4$  concentration of 5, 10 and 20 mg/L.

The uranium content, by leaching cycle, averaged between 20–90 mg/L, with an extraction rate of 9.1%, a liquid/solid ratio of 1.14 and a specific acid consumption of 70 kg/kgU. The most significant uranium content in pregnant solutions (119 and 124 mg/L) was obtained at sulphuric acid concentrations of 10 and 20 g/L respectively. The amount of uranium extracted to solution seems directly related to the time of exposure by solutions. Specifically, leaching with 5 g/L acid produced 125 g of uranium, 10 g/L – 374 g, and leaching with acid concentration of 20 g/L produced 544 g.

During the acid cycles, express laboratory analysis revealed the presence of ferric iron in solutions at concentrations varying from 5 to 220 mg/L; and V<sub>2</sub>O<sub>5</sub> up to 73.8 mg/L. V<sub>2</sub>O<sub>5</sub> has the potential to adversely affect the kinetics of the uranium pregnant solutions during commercial development. This fact was confirmed by a decrease in Eh (from 495 to 468 mV) and an increase in pH (from 1.47 to 1.57) in the solutions. One of the probable reasons for this may be that the higher acid concentrations results in interactions with the clay components of the hosting sediments.

The purpose of the Push-Pull test was achieved, and as a result it has become necessary to move to the next step along the toll-gated path of testing the Nyota ore body for ISL amenability.

## 5. FUTURE TEST WORK PLANNED

The next stage of testing has been planned and will include the following components: A hydrological study, a Five spot pattern ISL field test with subsequent aquifer demineralisation test; and an ISL specific resource estimate. The proposed work will likely stretch over two years and the outcome will serve as input for a decision on progressing to an ISL pre-commercial test and pre-feasibility study.

The hydrological study will determine the direction and speed of groundwater flow; the hydraulic connection between the ore bearing aquifers and the surface streams; how solutions will spread through the strata; the size of the groundwater depression cone; and the probable impact on the surface stream flows.

The five-spot field ISL test will determine the degree of mineralization and the ISL process parameters which will be used for ISL process modelling. The test duration is one year. The demineralization test will show how the aquifer can be restored after ISL completion and will enable the estimation of certain input data for an environmental impact assessment (EIA).

The aim of the ISL specific resource estimate is to re-estimate the resource based on specific ISL criteria (productivity, permeability, ground water level, etc.).

## 6. KEY CHALLENGES: COMMERCIAL, TECHNICAL, SAFETY, HEALTH ENVIRONMENTAL AND QUALITY

In moving forward with the toll gated approach to ISL feasibility testing, a number of key challenges must be overcome. On the technical side, challenges remain to establish suitably confined aquifer zones, as well as areas with sufficient water yield. The practicality of fairly shallow ISL in the hilly terrain must also be proved.

Should ISL prove to be technically feasible, the optimum commercial solution must be determined. A number of technical alternatives will have to be weighed up which will include decisions on which part of the sub-water level resource to extract via ISL; what the optimum sequencing will be between open pit and ISL; and how capital-intensive items, such as the plant, can be shared between the extraction methodologies.

One of the principal risks to the execution of the proposed program of works, as well as any future ISL mining, is gaining regulatory approval. The project is situated in an environmentally sensitive area with pristine ground water quality which sustains a large local wildlife population.

To date, through pro-active engaging of the authorities, responsible work practices, and comprehensive monitoring, reporting and feedback, the necessary approvals for the work completed were obtained. The planned five spot test constitutes a significant step up from the Push-Pull test in that it will require the use of much larger quantities of acid, with a potential larger environmental impact. Tanzania (and the entire Africa) has no experience in ISL and it is expected that significant effort will have to be invested to cooperate with the regulators and wider stakeholder groups on ISL best practices.

Sound environmental management practices will have to be applied throughout the test campaign. Best practices such as keeping a balance between injection and recovery volumes and making use of groundwater monitoring wells will be non-negotiable. Ultimately, aquifer restoration, be it post testing or post full scale ISL, will have to be done thoroughly. Restoration methodologies such as natural attenuation, forced demineralisation and residual solution in situ neutralisation will all have to be evaluated and tested to ensure the optimum solutions are found.

## 7. CONCLUSION

The Nyota deposit is a world class deposit, which holds approximately 50 Mlb which is potentially amenable to ISL. Initial ISL testing has yielded encouraging results, which should be followed up. The ISL project is currently at the research and development stage, and the next steps have been identified and planned. Uranium One will continue to investigate the ISL potential via a responsible, toll gated approach.

Although a number of technically, regulatory and Safety, Health, Environmental, Quality (SHEQ) risks related have been identified that must be addressed before ISL can be considered feasible at Nyota, it represents a first mover advantage opportunity within a highly prospective regional basin.

If Uranium One can demonstrate the feasibility of ISL at Nyota, it has the potential to unlock the new region by focusing further exploration on tabular uranium mineralisation below the groundwater level.

## REFERENCES

- [1] URANIUM ONE INC., News release, March 31, 2014.
- [2] INTERNATIONAL ATOMIC ENERGY AGENCY, Manual of Acid In Situ Leach Uranium Mining Technology, IAEA-TECDOC-1239, IAEA, Vienna (2001).

# **IN-SITU LEACH MINING OF URANIUM IN THE PERMAFROST ZONE, KHIAGDA MINE, RUSSIAN FEDERATION**

I. SOLODOV

JSC Atomredmetzoloto,  
Moscow, Russian Federation

## **Abstract**

The ‘Khiagda’ mine in the Republic of Buryatia is the only ISL mine in the world where ore mining is performed in a permafrost region. The uranium resources of the Khiagdinsky ore field deposits amount to 48 000 t. The ore field is a part of the Vitimsky Uranium ore district with 100 000 t resources. This is the most promising region in Russia where the deposits may be extracted by the ISL technique. Throughout a year, the air temperature varies from +35 to -45°C. Permafrost zone is developed to a 90-m depth. The Khiagdinsky ore field includes 8 deposits. Mineralization hosting sediments occur below the basalt sheet cover at a depth of 90 to 280 m. The rigorous climatic conditions, high degree of reduced uranium, complicated hydrogeological conditions and high viscosity of a very cold groundwater caused low uranium recovery at the initial stage of development. The carried out extensive scientific and research works and in particular, the use of an oxidant, made it possible, to increase significantly the uranium concentration in the productive solutions, which is currently comparable to world best examples.

## **1. THE KHIAGDA URANIUM FIELD, GEOLOGY AND MINERALIZATION**

Khiagda mine is developing uranium deposits of the Khiagda ore field which is a part of Vitimsky Uranium district, located about 140 km north of the Chita city in the north-east part of Buryatia Autonomous Republic of Russia. The area is characterized by rigorous climate. In summer time, the air temperature rises up to +35°C, and it falls down in winter up to -45°C. The yearly average temperature is -6°C. The permafrost is developed everywhere to a depth of 90 m.

Known resources of the Vitimsky Uranium district are estimated at 56 000 t U, while exploration potential is in the order of 100 000 tU.

Khiagda uranium field (Fig. 1) is the most prospective uranium region in Russia. It contains 8 close located deposits with 48 000 t U of known resources amenable for In-Situ Leach (ISL) mining. The distance between deposits is 1.5 to 6.0 km. Mineralization occurs in permeable low consolidated Neogene fluvial sediments, which fill palaeovalleys of relatively narrow tributaries (sandstone basal channel type). The basement is presented by Palaeozoic granite. Ore hosting sediments are overlapped by Neogene to Quaternary basalt. The mineralization occurs at the depths 90 to 280 m (average is 170 m) in lense, lenticular and ribbon-like ore bodies. Single ore bodies are 850 to 4100 m long, 15 to 400 m wide, 1 to 20 m thick.

ISL mining has been carried out under complicated hydrogeological environment as the water table is not stable and the mineralization is poorly and irregular saturated.

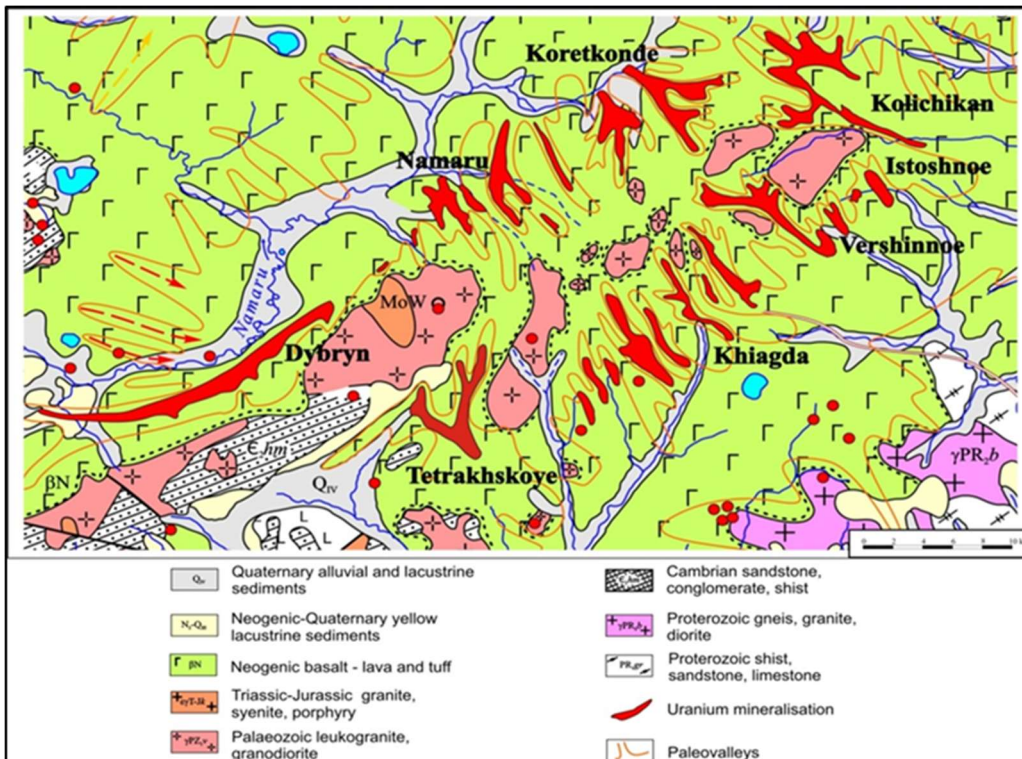


FIG. 1. Khiagda Uranium field geological map.

The main technical parameters of the Khiagda ISL mine are presented in Table I.

TABLE I. KHIAGDA MINE – MAIN CHARACTERISTICS

|  |                             |
|--|-----------------------------|
| Life of mine                                       | 2002 to 2036                |
| 2013 production                                    | 440 tU                      |
| Production capacity                                | 1000 tU/year from 2018      |
| Leaching agent                                     | Sulphuric acid              |
| Average recovery rate                              | 80%                         |
| Acid concentration in pregnant solutions (average) | 12 g/L                      |
| Average flow rate of recovery well                 | 4.6 m <sup>3</sup> per hour |
| Average uranium content in pregnant solutions      | 90 mg/L                     |
| Wellfield patterns shape                           | hexagon, row                |
| Distance between wells                             | 35 m                        |
| Ratio between recovery and injection wells         | 2.3                         |

## 2. MAIN AREAS OF ISL INTENSIFICATION

The uranium production ( $D$ ) is equal to the product of recovered pregnant solutions volume (wells flow rate  $Q$ ) and uranium content in pregnant solutions ( $C_U$ ) or  $D = Q \times C_U$ . Intensification of ISL means

increase of these main parameters ( $Q$  and  $C_U$ ) using the same amount of exploitation wells (Capex factor) and not exceeding planned sulphuric acid consumption (Opex factor)

Potential increase of recovery wells flow rate  $Q$  is limited by ore hosting sediments permeability and by the condition, when the speed of the leaching solution movement within the ore hosting aquifer is lower or equal to the chemical reaction rate.

ISL intensification for the Khiagda mine was focused on two issues:

- How to decrease leaching solution's viscosity?
- And how to oxidize uranium?

## 2.1. Decrease of leaching solutions viscosity

Khiagda has the lowest recovery wells flow rate ( $4.6 \text{ m}^3/\text{h}$ ) in comparison to ISL mines in Kazakhstan ( $5.4\text{--}9.3 \text{ m}^3/\text{h}$ ). Three main factors impact low flow rate  $Q$  capacity:

- Irregular and generally poor water abundance the ore-bearing horizons;
- Low sediments permeability;
- High viscosity of leaching solutions.

The Khiagda ground water temperature is  $1\text{--}4^\circ\text{C}$ , at Dalur it is  $16\text{--}22^\circ\text{C}$ , while at Kazakhstan deposits it is much higher  $25\text{--}45^\circ\text{C}$  (Fig. 2). Viscosity of ground water depends significantly on water temperature, slightly depends on TDS for solutions containing solids below  $50 \text{ g/L}$  and practically not depends on pressure. Solutions viscosity at Khiagda ( $1.75 \text{ cP}$ ) is 2.5 times higher than at Kazakhstan ( $0.7 \text{ cP}$ ) due to low temperature (Fig. 2).

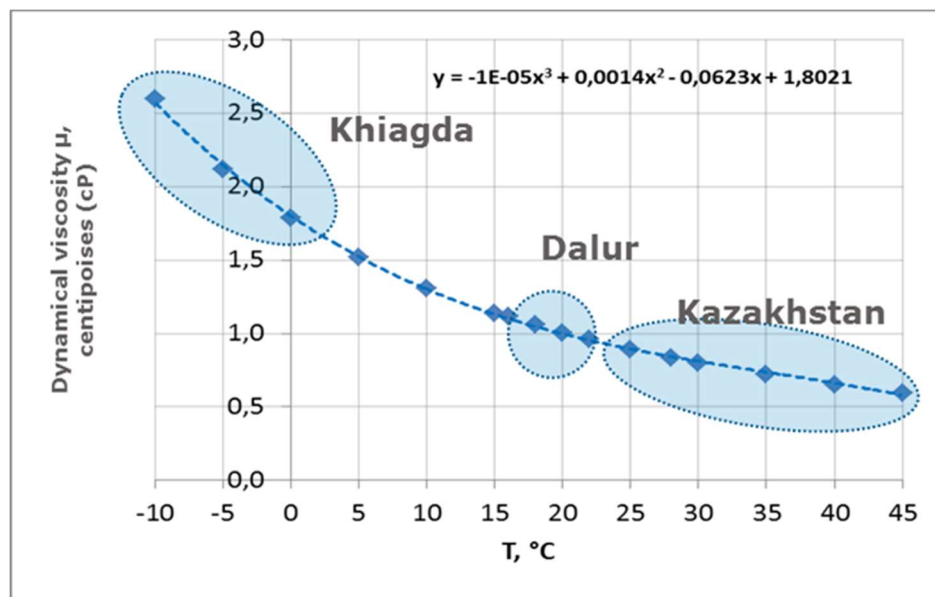


FIG. 2. Leaching solutions viscosity.

During winter time, when air temperature goes down to  $-45^\circ\text{C}$ , the temperature of acid solutions in pipelines may decrease to  $-10^\circ\text{C}$  (close to electrolytes freezing point). Viscosity of cold solutions grows up to  $2.6\text{--}2.9 \text{ cP}$ , and hydraulic resistance at the aquifer entrance through injection wells screens rises sharply.

Low permeability factor ( $K_f$ ) of the ore-hosting sediments varies from 1.4 to 3.7 m/day with the mean value 2.1 m/day. Permeability factor depends not only on sediments porosity but also on liquid properties and mainly on solutions dynamical viscosity ( $\mu$ ), while solutions density ( $\rho$ ) practically does not influence on permeability factor because it is rather stable. The transmissivity factor ( $K_p$ ) represents a rock property, and it does not depend on solutions properties. The  $K_f$  value for the normal temperature (20°C) should vary between 2.5–6.4 m/day with the mean value 3.6 m/day.

Theoretically it is possible to increase recovery wells  $Q$  flow rate to 7 m<sup>3</sup>/h compared to the actual rate 4.6 m<sup>3</sup>/h and thus to increase uranium recovery speed in 1.5 times.

Under high viscosity of solutions, the hexagonal development pattern is the most effective one. It gives highest ratio between injection and recovery wells.

Heating of all leaching solutions from 4°C to 20°C is technically impossible due to extremely high thermal capacity of ore horizon. However local heating of the leaching solutions in the surface pipelines close to injection wells may slightly decrease solutions viscosity.

The most promising way to decrease leaching solution viscosity is surfactants adding as they lower surface tension between two liquids or between a liquid and a solid.

## 2.2. Uranium oxidation

The ore bearing sands are silica-alumina (SiO<sub>2</sub> – 74.2%, Al<sub>2</sub>O<sub>3</sub> – 13.4%), with low content of iron (2%), and practically no carbonate (CO<sub>2</sub> < 0.3%). Sands are composed by two main minerals: feldspar and quartz. The content of iron disulphide is 0.4%; plant detritus is up to 1% of C<sub>org</sub>.

The main uranium mineral is ningyoite. Ningyoite is a tetravalent uranium phosphate CaU<sub>4</sub><sup>+</sup>(PO<sub>4</sub>)<sub>2</sub> × 2H<sub>2</sub>O. The following conditions are needed for Ningyoite formation: slightly acidic (pH 5.5–6.5) and strongly reduction (Eh –50 to –400 mV) environment, presence of phosphorus-containing organics and hydrogen-producing micro flora. All these conditions are typical for Khiagda ore-bearing aquifers (Fig. 3).

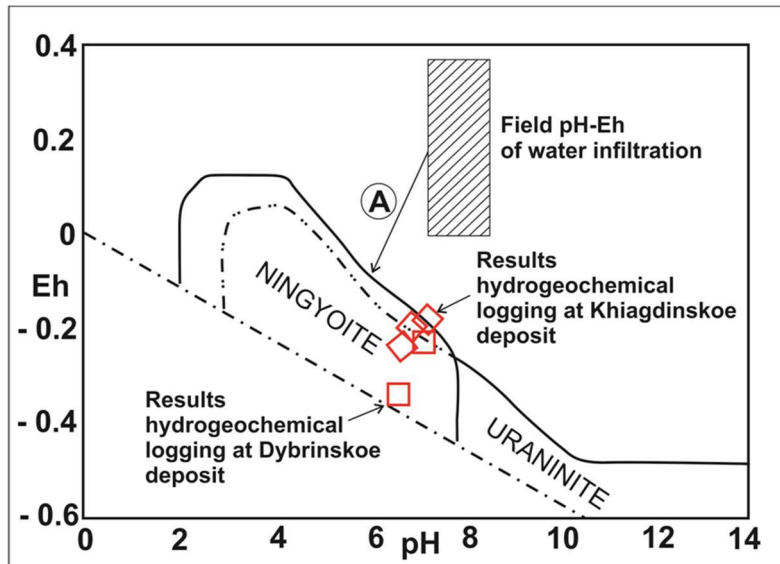


FIG. 3. The results of in situ pH and Eh measurements of on a diagram of the stability fields of ningyoit and uraninite, based on [1] and [2].

The bulk of high grade uranium mineralization (up to 3% of U) is located in the meander stream facies of the palaeochannels. This confirms rather sharp redox front conditions for uranium precipitation.

The geochemical properties of Khiagda mineralisation are characterised by:

- High reduction degree of uranium and iron;
- The share of reduced uranium IV is 90–100%;
- Deficit of soluble trivalent iron in host sediments which is a natural oxidant –  $\text{Fe(III)}_{\text{kp}} = 0$  to 15% from total iron ( $\text{Fe}_2\text{O}_3 = 0.73 - 1.76\%$ );
- The reduction environment has been created by hydrogen-producing bacteria. Vital biochemical activity of sulphate reducing bacteria, which is typical for Kazakhstan, is suppressed;
- Low redox potential Eh –440 to –150 mV is typical for the hydrogen reduce environment formed by underground micro flora.

The uranium extraction from Khiagda deposits in these conditions is of very low effectiveness, and oxidant addition is required.

Studies of U(IV) phosphates solubility in hydrochloric acid solutions (see Table II) has shown that commercial uranium concentration ( $> 10 \text{ mg/L}$ ) appear in highly concentrated solutions with  $\text{pH} < 0.4$ .

Uranium leaching tests of Khiagda ores in filtration columns has shown very slow recovery without oxidant (Fig. 4). The required recovery was reached under liquid to solid ratio 8–9. The uranium concentration was 50 mg/L.

TABLE II. THE SOLUBILITY OF URANIUM IV PHOSPHATES IN HYDROCHLORIC ACID

|            | pH    | 4.1      | 1.8      | 1.3      | 0.7      | 0.45     | 0.3      | 0 (1N HCl) |
|------------|-------|----------|----------|----------|----------|----------|----------|------------|
| Solubility | Mol/L | 2.10E-07 | 2.10E-08 | 4.00E-06 | 2.60E-05 | 6.40E-05 | 1.60E-04 | 6.40E-04   |
|            | mg/L  | 0.0499   | 0.0499   | 0.95     | 6.19     | 15.23    | 38.1     | 152.3      |

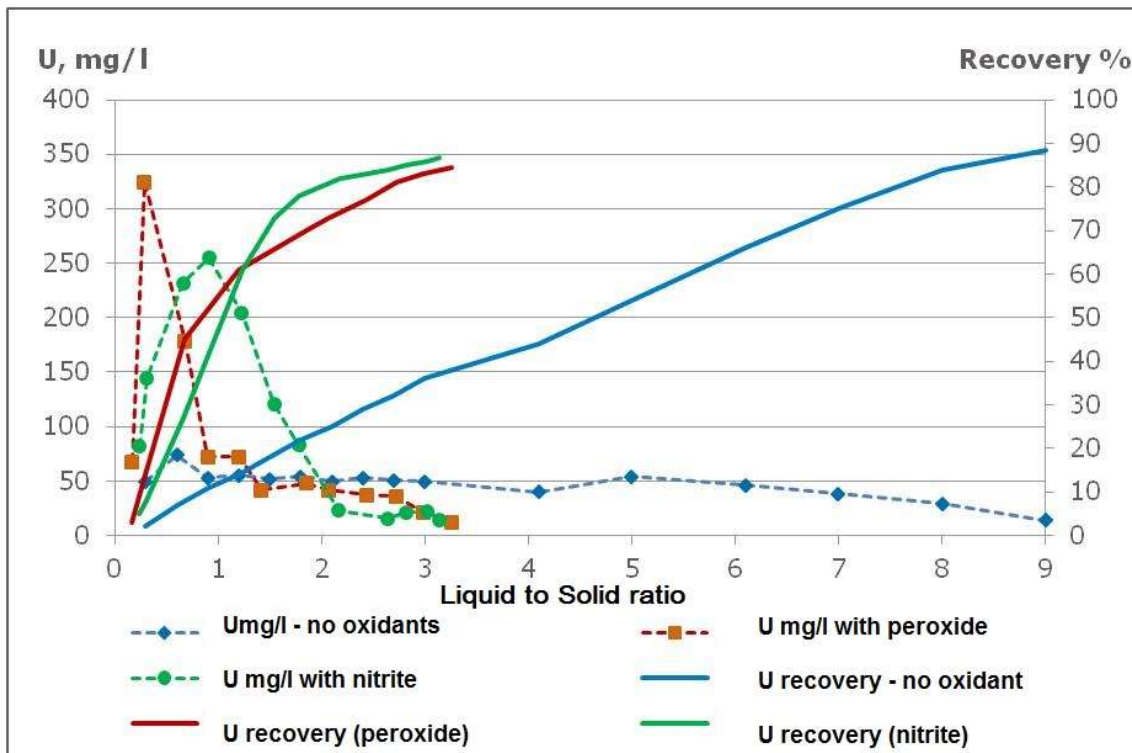


FIG. 4. Uranium leaching tests in filtration columns.

Oxidants (hydrogen peroxide or nitrite) addition increased uranium concentration to 250–325 mg/L and recovery speed thrice. The required recovery occurs under liquid to solid ratio at about 3.

### 3. CONCLUSIONS

High viscosity of leaching solutions is caused by very low underground water temperature (1–4°C) as a permafrost zone effect and negatively impacts on injection and recovery wells productivity and flow rate. It is possible to increase recovery wells flow rate up to 1.5 times by leaching solutions viscosity reduction.

Major uranium mineralisation is represented by ningyoite (a tetravalent uranium phosphate), which is sparingly soluble in diluted sulphuric acid solutions. Oxidants (hydrogen peroxide or nitrite) addition to acid solutions increases uranium recovery speed in three times.

### ACKNOWLEDGEMENTS

I would like to express my very high appreciation to A. Boytsov for his valuable and constructive contribution in the paper drafting and editing.

### REFERENCES

- [1] SOLODOV, I.N., VELICHKIN, V.I., RUBTSOV, M.G., et al., Hydrogeochemical logging: theory and practice, Moscow, Editorial URSS (2005) 320.
- [2] KAJITANI, K., A Geochemical study on the genesis of ningyoite, the special calcium uranium phosphate mineral, Economic Geology **65** (1970) 470–480.

# **NICHOLS RANCH IN-SITU LEACH (ISL) MINE — A CASE HISTORY**

G.J. CATCHPOLE, G.C. THOMAS  
Uranerz Energy Corporation,  
Casper, Wyoming, USA

## **Abstract**

The Nichols Ranch ISL Uranium Mine is located in the Powder River Basin of Wyoming, USA. The mine is owned and operated by Uranerz Energy Corporation (Uranerz); a U.S. corporation headquartered in Casper, Wyoming. Nichols Ranch started operations in April 2014 and is the newest uranium mine to go into production in the United States. The uranium being extracted is hosted in a sandstone, roll-front deposit at a depth ranging from 122 to 244 m (400 to 800 feet). The In-Situ Leach (ISL) mining method is employed at the Nichols Ranch mine which is the method currently being utilized at most uranium mines in the United States. Environmental permit applications for the Nichols Ranch mine were submitted to the appropriate regulatory agencies in late 2007. It required more than three and a half years to review and approve all the permits and licenses necessary to start construction of the mine. Construction of the mining facilities and the first wellfield started in late 2011 and was completed in late 2013. Mining results to date have been better than anticipated and Uranerz expects to reach its 2014 production target.

## **1. INTRODUCTION**

The Nichols Ranch In-Situ Leach<sup>15</sup> (ISL) uranium mine is located in the central Powder River Basin in the state of Wyoming, USA. The mine started extraction operations on 15 April 2014 after some three and half years to get through the permitting and licensing stage plus two years to get through the construction stage. The Nichols Ranch sandstone, roll-front hosted deposit was first discovered in the 1970s. Uranerz Energy Corporation (Uranerz or the Company) is a publicly traded United States corporation with 100% ownership of the Nichols Ranch ISL Uranium mine. The Uranerz headquarters are located in Casper, Wyoming, USA. The senior professional staff at Uranerz has over 100 years of combined ISL mining experience.

## **2. COMPANY HISTORY**

The Company was incorporated in 1999 under the name Carleton Ventures and changed its name to Uranerz Energy Corporation in 2005 when it became focused on acquiring uranium properties and becoming a uranium producer. The business model for the Company is to acquire quality uranium properties that have the potential of being mined using the ISL extraction method with the objective of achieving commercial uranium production as soon as practical. The primary target areas for property acquisitions were in the states of Texas and Wyoming with the latter receiving the most emphasis since Wyoming is the largest producer of uranium in the 50 states (all by the ISL mining method) and has the largest uranium reserves of all 50 states according to the U.S. Energy Information Agency. Within Wyoming, Uranerz focused its property acquisition efforts on the Powder River Basin where almost all uranium produced in that state is mined. Uranium mining first started in the Powder River Basin in the mid-1950s.

## **3. PROPERTY ACQUISITION HISTORY**

By the year 2008, Uranerz had acquired 54 000 hectares (132 000 acres) of mineral properties in Wyoming spread out among 36 identified mineral properties. Some properties are 100% owned by

---

<sup>15</sup> Editor's note: in the USA and Australia, the term In-Situ Recovery is often used.

Uranerz and some are in a joint venture where Uranerz is the 81% owner and the operator. The acquisition methodology included:

- Staff historical knowledge and private data collections;
- Purchase of historical data bases;
- Joint ventures with companies with data bases and Uranerz as operator;
- Advanced exploration (mainly with drill holes) by Uranerz' experienced exploration team;
- Purchase of uranium properties from third parties.

The current key Uranerz properties in the Powder River Basin of Wyoming include the following:

- Nichols Ranch;
- Hank;
- Jane Dough;
- Reno Creek;
- West North-Butte.

#### 4. DEVELOPMENT HISTORY

In 2006, following initial orebody delineation drilling, Uranerz management decided that the Nichols Ranch and Hank properties would be the first two properties to develop into commercial ISL uranium mines. The collection of environmental baseline data and the preparation of the environmental license applications started in mid-2006. These applications were submitted in late 2007 to the federal and state agencies that regulate uranium mining in Wyoming. The major environmental and safety licenses required for a new uranium mine in Wyoming are:

- Wyoming Department of Environmental Quality Permit to Mine;
- Federal Nuclear Regulatory Commission Source Material License;
- Wyoming Department of Environmental Quality Deep Disposal Wells Permit.

The state Permit to Mine was received in December 2010, the federal Source Material License was received in July 2011 and the Deep Disposal Wells Permit was received in October 2012. The environmental permits and licenses allow for the Nichols Ranch mine to produce up to 770 tU/yr (2 Mlbs/yr as U<sub>3</sub>O<sub>8</sub>).

#### 5. CONSTRUCTION

The Nichols Ranch ISL uranium mining license allowed Uranerz to build a full central processing plant at the Nichols Ranch unit capable of producing dried natural uranium (yellowcake) and build a satellite ion-exchange plant at the Hank unit. Midway through the design process for the Nichols Ranch ISL project, Uranerz decided to build just a satellite plant at the Nichols Ranch unit and ship uranium loaded resin to a third-party for toll processing into dried and drummed yellowcake. At the same time, a decision was made to temporarily defer building a satellite plant at the Hank unit. Uranerz signed a toll processing agreement with Cameco Resources for toll processing at their Smith Ranch — Highland ISL uranium mine located in the Powder River Basin of Wyoming. The decision was made to go ahead and construct the plant building large enough to accommodate a full processing plant when needed and to pour the concrete foundations and tank pedestals for the full plant.

Construction of the Nichols Ranch highly automated ion-exchange and lixiviate makeup facility that also includes the waste water disposal circuit was completed in late 2013. Uranerz went with a highly automated processing facility to reduce labour costs during operations, to provide for early warning of

possible upset conditions in the plant and wellfields, and to assist with keeping operating parameters in compliance with license conditions.

## 6. MINE STARTUP AND OPERATIONS

Mining operations at the Nichols Ranch ISL uranium mine started on 15 April 2014 with the addition of oxygen to the injection side of the circulating groundwater. Before mining operations could start at Nichols Ranch mine the facilities had to be audited by a team of inspectors from the Nuclear Regulatory Commission and Uranerz had to receive written communications from that same agency approving startup. The inspection results were positive and authorization to startup was received on 15 April 2014.

The Nichols Ranch ISL mine consists of the ion-exchange processing plant with a lixiviate makeup circuit, a water filtration and recycling circuit, and a waste water disposal circuit. The mining orebody is divided into two wellfield production areas designated as PA 1 and PA 2. Mining started in PA 1 and when ISL mining is complete in that area mining operations will shift to PA 2, and groundwater restoration will commence in PA 1. The current maximum authorized wellfield flow rate is 818 m<sup>3</sup>/hr (3600 gallons per minute). The production goal for the Nichols Ranch ISL uranium mine for the partial production year of 2014 is 115 to 154 tU (300 000 to 400 000 lbs as U<sub>3</sub>O<sub>8</sub>). The plan is to ship the Nichols Ranch mine production to the Converdyn conversion facility in Illinois where it will be sold to our two U.S. nuclear utility customers. A photo of the processing facilities and a diagram of PA 1 and PA 2 follow this page.

At the time of the URAM–2014 conference held in Vienna, Austria in late June 2014, the Nichols Ranch ISL mine had been conducting mining operations for approximately two and a half months and as such was still in the commissioning phase. Minor startup issues included fine tuning of the automated controls and warning system by making adjustments to some of the computer algorithms, and making adjustments to the oxygen addition system. Both individual well flow rates and the recovery wells headgrades (concentration of uranium in the recovery solution) are within expected ranges.

## 7. SUMMARY

The Nichols Ranch ISL uranium mine located in Wyoming, USA, started mining operations on 15 April 2014 as the newest producing uranium mine in North America. Startup went smoothly and the mine is now producing at the target levels. Development of future wellfields is continuing. The Company is looking forward to delivering product to its two US customers. The biggest obstacle to getting the Nichols Ranch ISL mine into production was the excessive length of time required to get all the required regulatory approvals. The uranium mining companies active in Wyoming are working with the appropriate regulatory agencies to find ways to reduce the time it takes to review and approve uranium mining license applications.

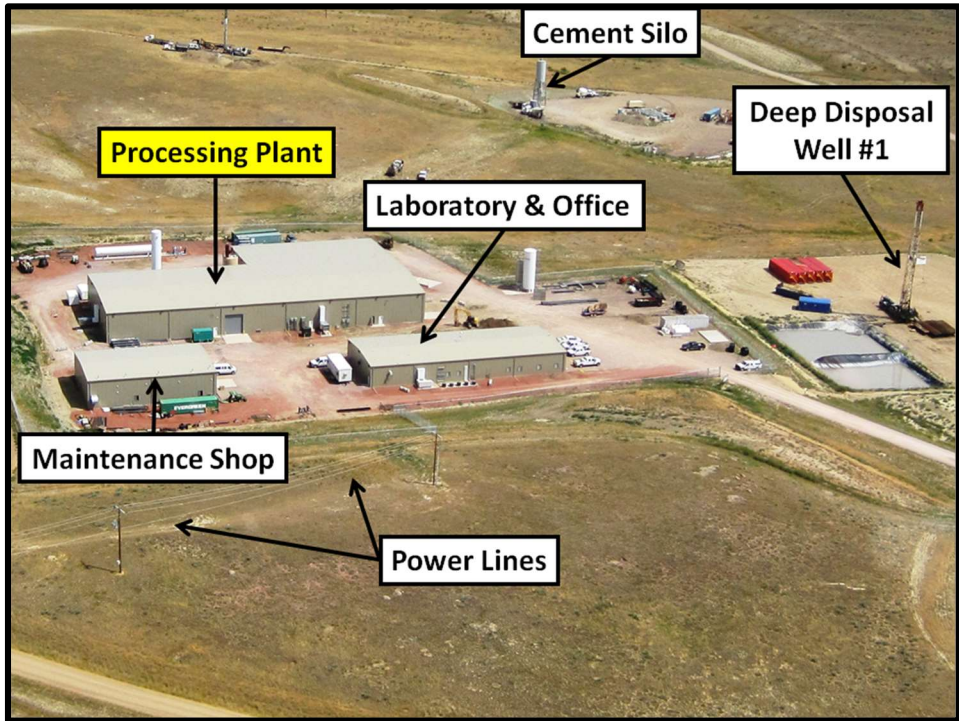


*FIG. 1. Nichols Ranch ISL uranium mine processing and support facilities.*

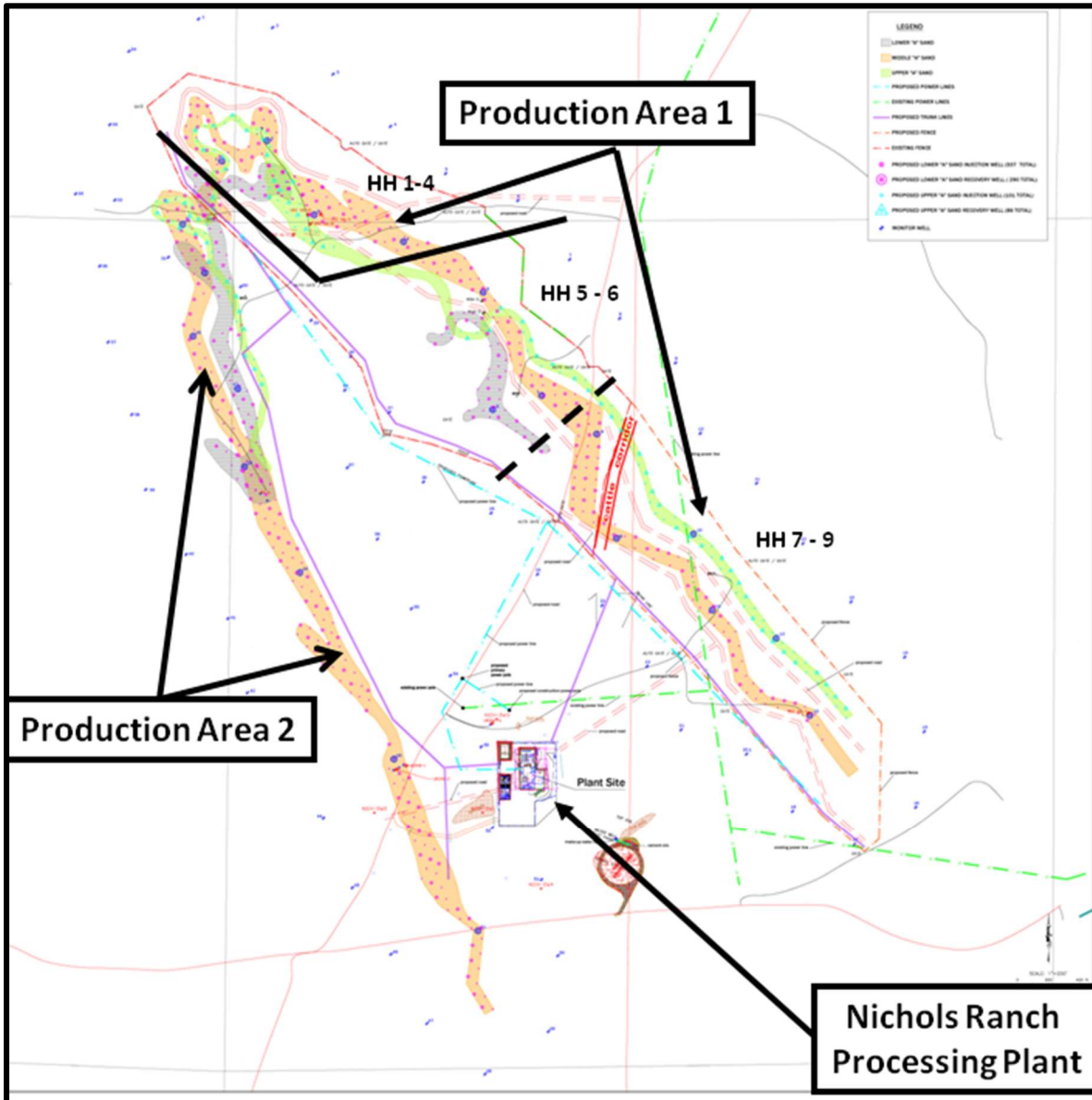


*FIG. 2. Nichols Ranch ISL uranium production areas.*

## REFERENCES

- [1] URANERZ ENERGY CORPORATION, Web Site (2015), [www.uranerz.com](http://www.uranerz.com).
- [2] URANERZ ENERGY CORPORATION, Resources & Technical Reports, Powder River Basin Uranium Resources<sup>16</sup> (2014), [http://www.uranerz.com/s/Technical\\_Reports.asp](http://www.uranerz.com/s/Technical_Reports.asp).

<sup>16</sup> Please also refer to the accompanying Cautionary Statement provided on the web site.

# **DEVELOPMENT OF URANIUM MINING BY IN-SITU LEACHING (ISL) IN KAZAKHSTAN**

YU. DEMEKHOV, O. GORBATENKO

National Atomic Company Kazatomprom,  
Astana, Kazakhstan

## **Abstract**

Kazakhstan has not only a tremendous resource base, but also the modern technology of uranium mining and processing, and goes forward to the full nuclear fuel cycle market. Since the first *In Situ Leach* (ISL) site launch, ISL technology and processing are being improved constantly. Today the exploitation of uranium deposits is associated with a set of complex technological solutions.

## **1. INTRODUCTION AND BACKGROUND**

In the second half of the 1960s, the feasibility of Uranium production from low-grade ores by ISL was proved. This radically changed the situation in the raw material base in Kazakhstan. Rapid development of uranium mining by ISL in Kazakhstan was possible because of the availability of large sandstone type uranium deposits.

As of 1 January 2014, the identified and undiscovered *in situ* uranium resource in Kazakhstan was about 1.7 million tonnes of uranium, with 77% available for ISL production.

In Kazakhstan, exploration and prospecting are continuously carry out to expand the resource base of uranium. In 2011 and 2012 uranium resources increased by more than 110 000 tU and 40 690 tU was mined. Resource growth was 2.5 times higher than the depletion. Since 2012, Kazatomprom has been prospecting for new uranium sandstone deposits in southern Kazakhstan by the efforts Volkovgeologiya, a national geological service, and at their own expense. The program lasts until 2030. Prior to 2015, allocated more than 20 M U.S. dollars in prospecting works. In near future is expected discovery of new deposits.

Kazakhstan has become the world leader in uranium ISL mining technology. For the current moment in Kazakhstan, uranium mining is conducted at 22 sites. During last 10 years, uranium production in Kazakhstan has increased 6 times and reached 22 500 t U in 2013 (Fig. 1).

This has led to a stronger position of Kazatomprom on the global uranium market. Approximately 64% of the total supplied volume goes (through the mechanism of joint ventures) to China, South Korea, and Japan. The volume of uranium deliveries to the USA are around 14.6% from the total sales of uranium by Kazatomprom, and 19.8% is sold to Europe.

In Kazakhstan, Kazatomprom performs uranium production by sulphuric acid leaching method (Fig. 2.). ISL method is chemical treatment of ores 2% solutions of sulphuric acid ( $H_2SO_4$ ) in the place of their natural occurrence and transfer of the useful component in another form and chemical status, in this case into a productive (pregnant) solution containing uranium as uranyl sulphate salts ( $UO_2(SO_4)_3$ ).

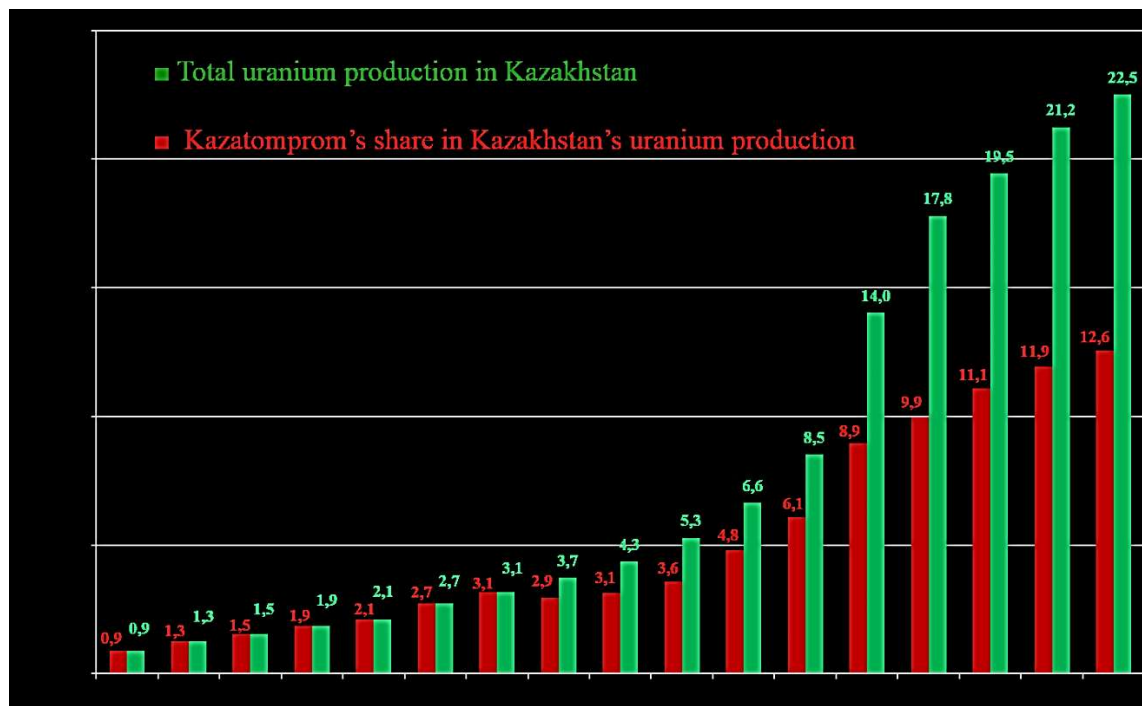


FIG. 2. Uranium production in Kazakhstan for the period from 1997 to 2013.

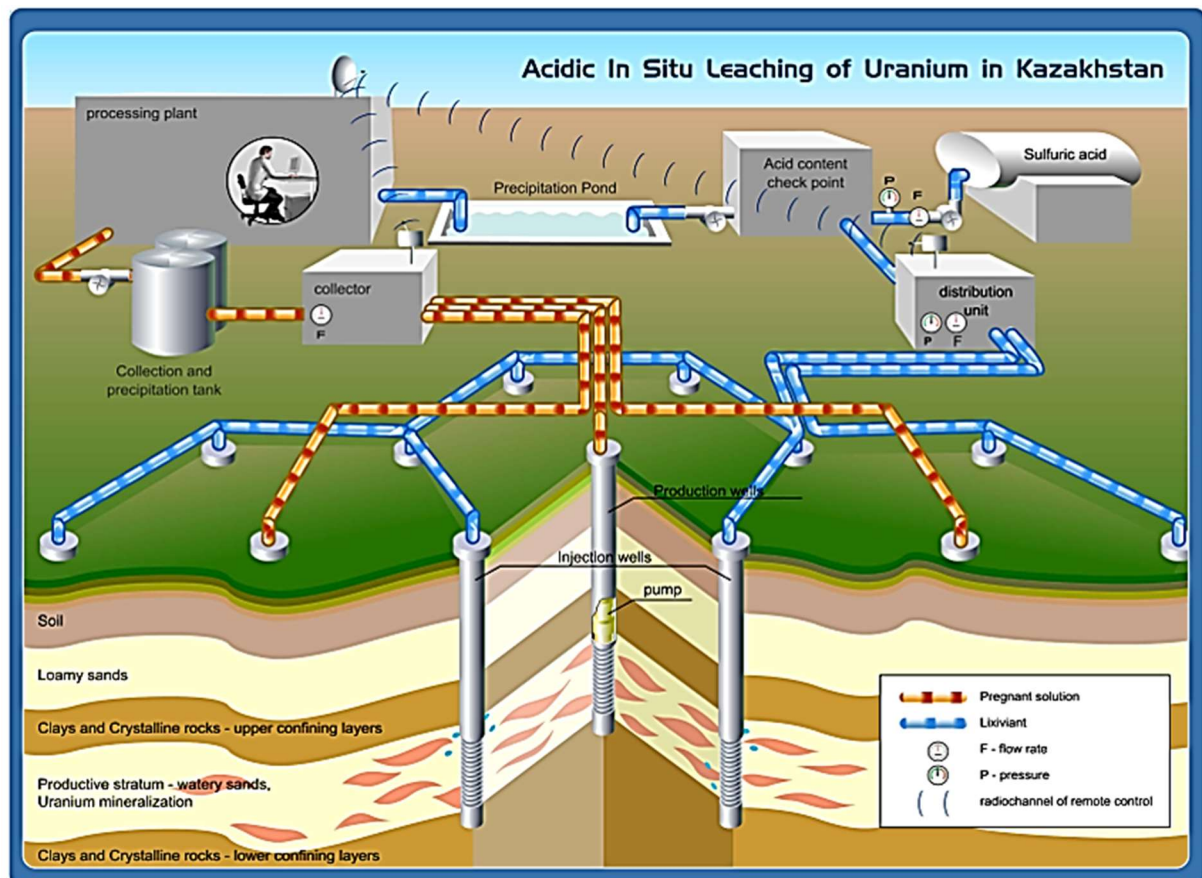


FIG. 2. ISL uranium production in Kazakhstan (courtesy Kazatomprom, reproduced with permission).

Delivery of sulphuric acid solution is performed in ore body through a network of injection wells. Passing through the ore solution dissolves the uranium minerals, forming a pregnant solution. Then the pregnant solution is pumped up to the surface through the production wells (Fig. 2). Uranium-containing solution on the surface is processed to ‘yellow cake’ and / or  $\text{U}_3\text{O}_8$ .

ISL eliminates any dust emission sources, and reduces ten times the release of radioactive substances into the atmosphere. Unlike alkaline ISL (used in the USA), acid ISL is characterized by the combined action to extract into solution more elements of ore and rock. Sulphuric acid leaching has a more intensive kinetics and high recovery than alkaline.

The concentration of radioactive elements in pregnant solution is low. For example, an amount of radium in solution is not more than 2% of the total content of the ores. It migrates at short distances (a few tens of meters), because the presence of the  $\text{SO}_4^{2-}$  ion in water leads to the formation of slightly soluble gypsum, and practically insoluble sulphates (barium, lead, strontium), which causes the co-precipitation of radioactive elements.

The sulphuric acid leaching of uranium is controlled to cause the least damage to groundwater. Working in balanced mode of ISL, high contamination does not happen. The halo of contamination reaches a distance of 50 m from the outer wells. Chemical interaction solutions with the rock minerals, neutralization, ion exchange processes, sorption, and diffusion lead to reduce the concentration of contaminants. All harmful components are deposited on the geochemical barrier at higher pH. Uranium mobilized by alkaline leaching may migrate over long distances, as uranium carbonate complexes are stable in neutral and alkaline media.

More and more complicated deposits are being involved to mine requiring a new approach to fields design and screen positions. New methods for modelling and forecasting of uranium mining are being successfully implemented.

Kazakh experts are the only in the world who successfully mine, by ISL, suspended ore bodies of uranium (not having lower aquitard), and deposits with uranium occurring at more than 700 m depth, and herewith minimal ore mining mass volumes are leached.

The gained extensive experience in the application of advance (passive) acidification (leaching solutions are injected to the ore body without pumping) it gives the opportunity to get rich uranium-containing solution at an early stage of production, shortens the time of mining, as well as reducing clogging. Solutions for advanced acidification in new mining blocks come from blocks at the final stage of production, allowing the start of aquifer remediation.

## 2. MUDDING AND REHABILITATION WORK IN WELLS

ISL mining of deposits with the depth of the ore body of over 700 m requires improved methods of well completion, combating mudding and technology for rehabilitation work in wells. Rehabilitation work (RW) in wells is performed to restore the productivity of technological wells reduced due clogging of the screen and pre-screen area, deformation of columns wells, as well as to eliminate sand plugs, reducing the addition of sand, etc.

The main types of RW are: air-lift pumping, flushing, sand plugs removal, pneumatic impulse treatment, chemical treatment and combined methods. For the moment, Kazatomprom and AREVA are conducting research to study of mudding and factors affecting the amplification of this phenomenon. In the future, we plan to develop new methods for removing and preventing clogging.

## 3. PLASMA-PULSE ACTION

Under Professor A.A. Molchanov’s leadership, the uranium companies successfully conduct research to use ***plasma-pulse action***. In the well is created a powerful impulse effect by using the electrohydraulic

discharge, which cleanses from plugging screen and penetrates deep into the sheet deposit, creating undamped fluctuations [1].

The penetration depth of the elastic energy due to the directional radiation reaches 50 m or more (depending on the condition of the well). Therefore, the elastic waves are perceived by neighbouring production wells, which also begin to work with a high flow rate. Figure 3 shows monitoring well flow rate after plasma-pulse treatment in days at the ISL site.

Research on the use of plasma-pulse action to intensify the output of uranium.

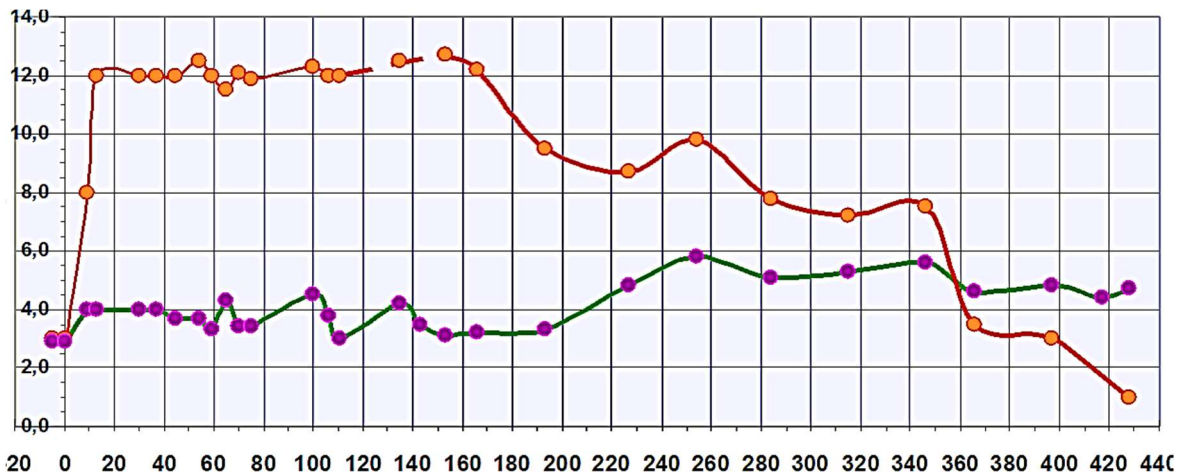


FIG. 3. Monitoring well flow rate ( $m^3/hour$ ) after plasma-pulse treatment in days.

#### 4. PROMPT FISSION NEUTRON LOGGING

Solving the problem of the direct determination of uranium offered by prompt fission neutrons (PFN) logging that expands the scope of application of the method for the quantitative determination of uranium *in situ*.

Under Professor A.G. Talalay's leadership, the group of companies 'Nedra' and Kazatomprom developed the theory, geophysical instrumentation and **double neutron logging device measurement method** of uranium mineralization (moisture, clay content and porosity, coefficient of radioactive equilibrium and direct determination of uranium) *in situ* [2–7].

Figure 4 shows block diagram of equipment complex PFN.

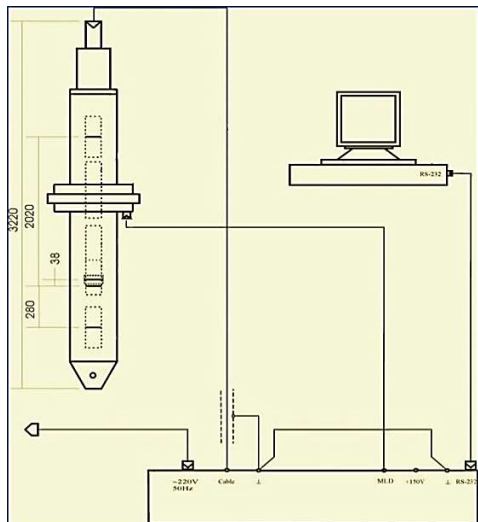


FIG. 4. Block diagram of equipment complex PFN.

Figures 5 and 6 show comparing of two methods of the single and double neutron logging device.

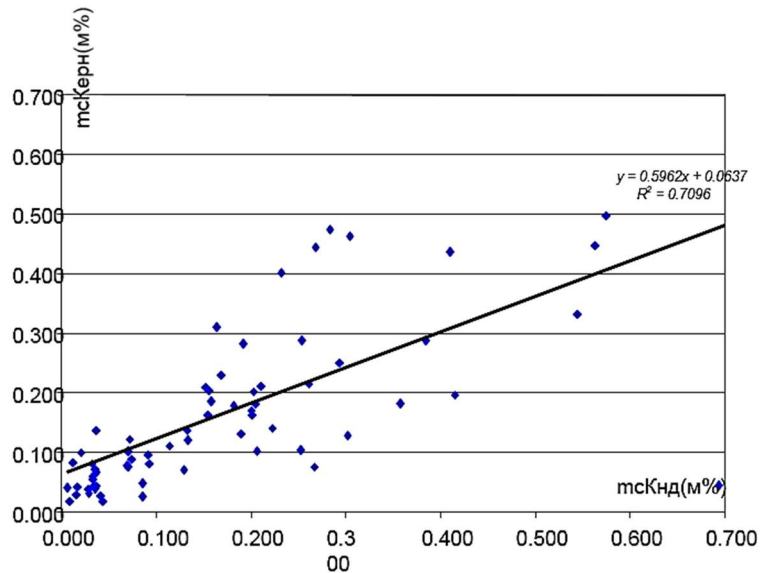


FIG. 5. The comparison between the results of interpretation of the single neutron logging device and the results of core analysis.

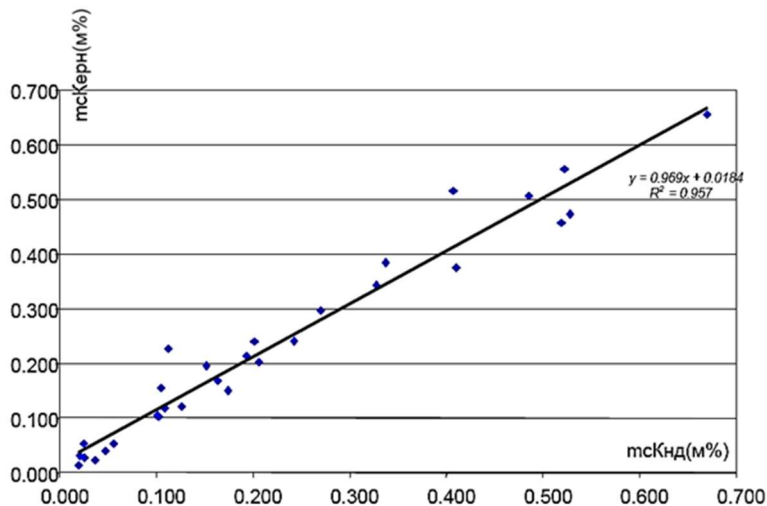


FIG. 6. The comparison between the results of interpretation of the double neutron logging device and the results of core analysis.

## 5. 4D MONITORING OF ISL DEVELOPMENT OF URANIUM DEPOSITS

Successfully Kazatomprom develops and applies new methods of research to control and optimize uranium production.

Introduction of new methods of geophysical research can solve the problem of modelling the dynamics of the ISL process using radio wave method “**4D monitoring of ISL development** of uranium deposits” by Dr V.A. Istratov. The method allows monitoring the spatial distribution of acidic solutions in time and managing the process of in-situ leaching for full mining of uranium ores and reducing acidification of the host rocks [8–10].

Figures 7 and 8 show monitoring result before and after acidification at depths 205, 207, and 212 m by method “4D monitoring of ISL development of uranium deposits” at sandstone deposit.

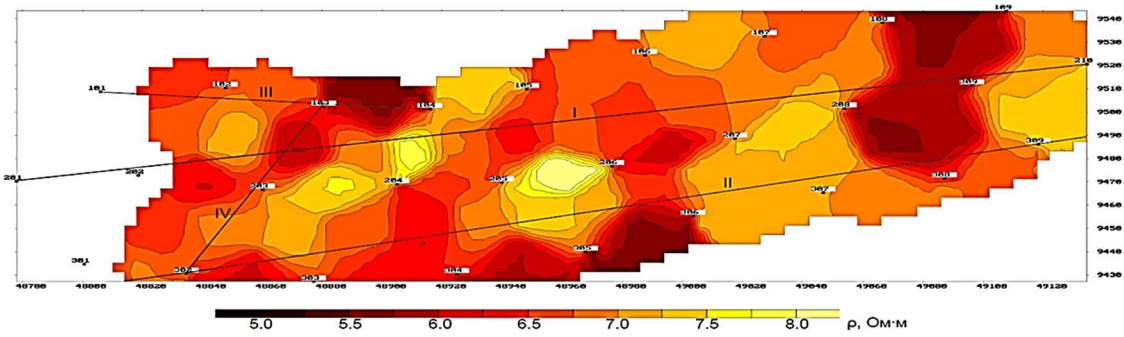
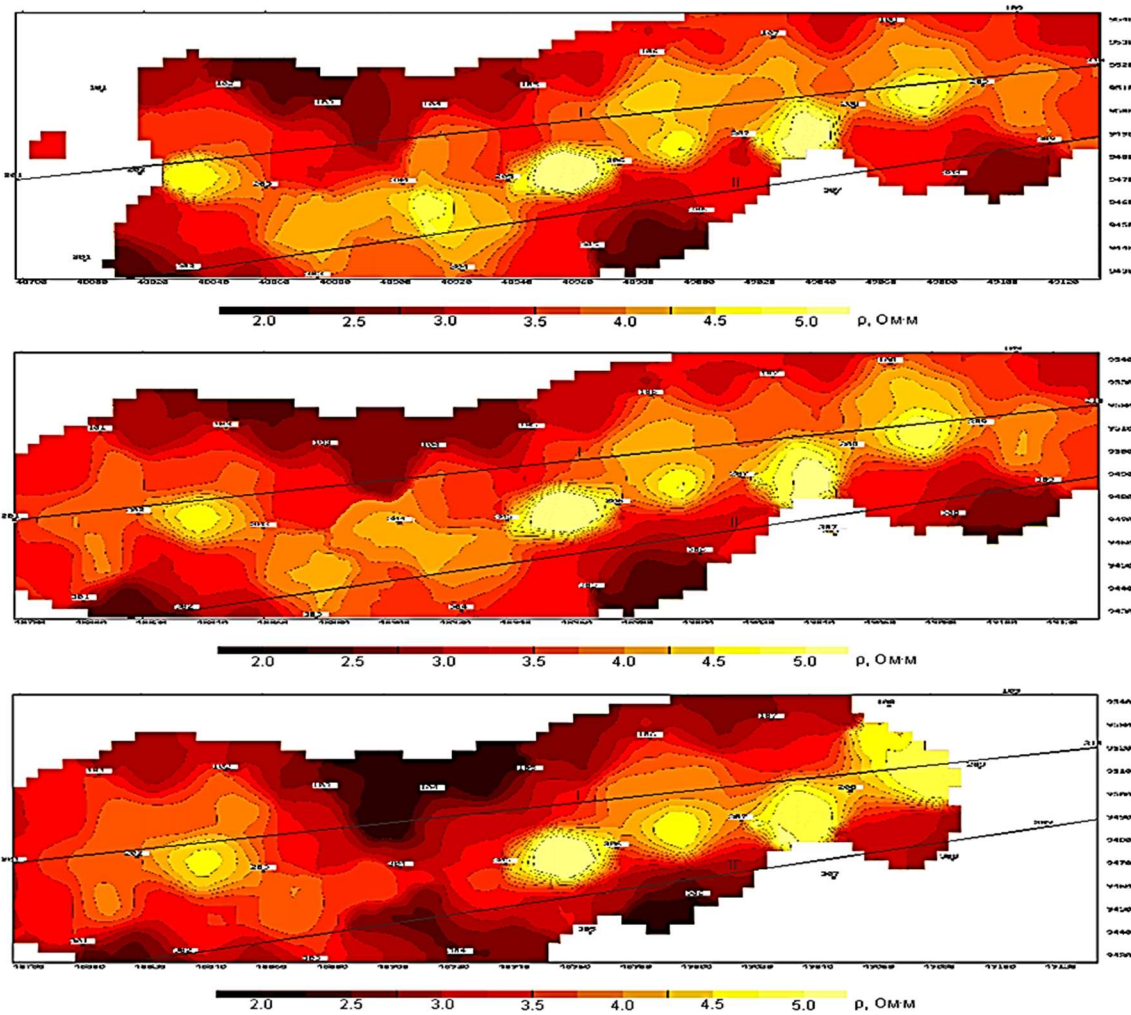


FIG. 7. Monitoring result before acidification.



*FIG. 8. Monitoring result after acidification at depths 205, 207, 212 m.*

## 6. NEW MATERIALS AND EQUIPMENT

Successfully introduced new polymeric and fiberglass materials for manufacturing storage equipment and pipe products, which improves the tightness and reduce contamination of the surface of the earth to a minimum. The use of such materials in piping blocks allows mining of the deposit with significant groundwater pressure above the surface (i.e. artesian conditions).

Technological know-how has enabled uranium mining to start in record time during the year.

The use of U-shaped sorption-desorption column has allowed a radical change the approach to the design of the processing complex. Designed modules consist of one U-shaped column and three sorption columns. The modular approach to the design and construction allows of processing capacity expansion stage-by-stage and increase the capacity of processing complex to 2 000 tU/yr and more.

## 7. SORPTION-PRECIPITATION TECHNOLOGY OF CHEMICAL NATURAL URANIUM CONCENTRATE PRODUCING WITH HIGH QUALITY

For several years, the Institute of High Technologies, owned by Kazatomprom, has conducted research work for the peroxide precipitation of uranium regenerates. The developed method for producing uranium concentrates allowed the improvement the currently applying flow sheet and reduce processing.

The results indicate the possibility of obtaining stable uranium concentrates corresponding international standard ASTM C 967-87, without the current extraction method.

## 8. ION EXCHANGE RESINS

Kazakhstan is working with leading manufacturers of ion exchange resins to optimize kinetic and physical properties of the resin, followed by their adaptation to the characteristics of each deposit:

- Dow Chemical (USA);
- Cybber (China);
- AMII (Ukraine);
- Purolite (England);
- Lunxess (Germany);
- Elbrise (Switzerland);
- Resindion (Italy).

## 9. CREATION OF EXPERIMENTAL TEST SITE

On the basis of Stepnoe Mining Group, an experimental technological test site was created, which provides facilities to carry out pilot tests of new materials, innovative technologies, devices and equipment for the intensification of technological processes, improve quality and reduce the cost of the uranium concentrates and related (rare earth metals) goods in the enterprises of Kazatomprom.

Test site activities are aimed at:

- Developing the state of the art scientific and technical technology in the extraction and processing of natural uranium with the issue of technological specifications and other regulatory documents;
- Technical and economic assessment of the use of the latest developments in order to increase profitability;
- Training and professional development of engineers and technical workers.

## 10. SMART MINE

Based on the results already obtained work conducted at the experimental technological test site Kazatomprom is considering the issue of the creation of a pilot intellectual new generation mine — **SMART MINE**.

The project to create a ‘SMART MINE’ suggests:

- Creation, testing and implementation of advanced technological innovations in various production processes (geological modelling, combined methods of leaching uranium ores, complex processing of pregnant solutions);
- Use of modern energy and resource saving materials and equipment;
- Use of complex processing of components;
- Training and retraining of technical and engineering personnel to work on advanced technology and equipment;
- Environmental safety;
- Creation of intangible assets intellectual property rights for their commercial use.

## 11. PARTICIPATION ON THE MARKET FOR RM AND REM

Years of experience in the study and exploitation of uranium deposits by ISL shows that in many cases the deposits are complex and in addition to uranium contain other beneficial ingredients: selenium, molybdenum, vanadium, yttrium, scandium, rhenium, rare earths, gold, silver, etc. Further development of geotechnical mining methods opens up new possibilities for a more complete work on the deposits  
**Error! Reference source not found..**

## REFERENCES

- [1] MOLCHANOV, A.A., DMITRIEV, D.N., SEDOROV, V.V., Applying of plasma-pulse technology to improve the efficiency of uranium mining on the sandstone-type deposits, developed by ISL, (*Herald Karotazhnik No. 4*), Tver (2014) (in Russian).
- [2] DEMEKHOV, Yu.V., DAVYDOV, Yu.B., MASHKIN, A.I., PERELYGIN, V.T., RUMYANTSEV, D.R., TALALAY, A.G., Fission neutron logging for the determination of uranium in wells at sandstone deposits for ISL mining, *Education News, Mining Journal*, Ekaterinburg (2010) 106–113 (in Russian).
- [3] DEMEKHOV, Yu.V., RUMYANTSEV, D.R., SAVIN, E.A., TALALAY, A.G., “Prompt fission neutron logging PFN-M for the direct quantitative determination of uranium in the well, Oil & gas and mining” (Proc. 4th National Conf., 16-18 November 2011), Perm (2011) (in Russian).
- [4] DEMEKHOV, Yu.V., DAVYDOV, YU.B., RUMYANTSEV, D.R., TALALAY, A.G., D.R., MAZUR, C.V., MASHKIN, A.I., PERELYGIN, V.T., SAVIN, E.A., “Direct determination of the uranium content in the wells” (Proc. Int. Symposium, UMGU), Ekaterinburg (2012) 133–138 (in Russian).
- [5] DEMEKHOV, Yu.V., GLUSHKOVA, T.A., MAZUR, C.V., MASHKIN, A.I., PERELYGIN, V.T., SAVIN, E.A., TALALAY, A.G., Application of prompt fission neutron logging tools in the exploration and exploitation of uranium, *Education News, Mining Journal*, Ekaterinburg 3 (2012) 165–169 (in Russian).
- [6] DEMEKHOV, Yu.V., GORELOV, I.G., MAKAROV, V.V., RUMYANTSEV, D.R., SAVIN, E.A., TALALAY, A.G., “Assessment of the degree of heterogeneity and permeability reservoirs in the construction of 3D models based on analysis of actual results logging properties” (Proc. 11th Ural Mining Decade UMGU), Ekaterinburg (2013) 104–105 (in Russian).
- [7] DEMEKHOV, Yu.V., RUMYANTSEV, D.R., SAVIN, “Equipment direct determination of uranium in wells PFN” (Proc. 11th Ural Mining Decade UMGU), Ekaterinburg (2013) 112–113 (in Russian).
- [8] ISTRATOV, V.A., SKRINNIK, A.B., PEREKALIN, S.O., New equipment for radio wave geointroscopy rocks in the inter-well space ‘RWGI-2005’, *Devices and systems of exploration geophysics* No. 1/2006. EGEA, Saratov (2006) 20–26 (in Russian).
- [9] ISTRATOV, V.A., KOLBENKOV, A.B., LYAKH, E.V., PEREKALIN, S.O., Radio wave method of monitoring processes in the inter-well space, (*Herald KRAUNTS, Geosciences*, No. 2, issue 14), Petropavlovsk-Kamchatsky (2009) 59–68 (in Russian).
- [10] ISTRATOV, V.A., KOLBENKOV, A.V., PEREKALIN, S.O., SKRINNIK, A.V., Radio wave method for monitoring the process for in-situ leaching uranium deposits. *Geophysics*, No. 4/2010, EGEA (2010) (in Russian).
- [11] SHOKOBAEV, N.M., BOUFFIER, C., DAULETBAKOV, T.S., Rare earth metals sorption recovery from uranium in situ leaching process solutions, *Rare Metals* 33 6 (2014) 40–47.

# THORIUM AND URANIUM SEPARATION FROM RARE EARTH COMPLEX MINERALS IN TURKEY

R. UZMEN

AMR Metalurji Ltd.,  
Istanbul, Turkey

## Abstract

In the southern part of Turkey there is a minerals deposit complex which contains rare earth elements (REEs), titanium, zirconium, uranium and thorium. Physical beneficiation operations and hydrometallurgical processes allow the separation of U along with Zr and Ti. The obtained [REEs and Th] oxalate concentrate is submitted to metathesis in order to convert oxalates to their respective hydroxides. The hydroxides cake is dissolved in acid and thorium is separated firstly by pH regulation, then peroxide precipitation is applied for the final purification of thorium.

## 1. INTRODUCTION

The AMR ore mineral deposit in the southern part of Turkey contains allanite-chevkinite and titanite as rare earth containing minerals. Thorium and in lesser extent uranium are also present along with the rare earth minerals and they are upgraded during the physical enrichment operations of the ore (Table I).

TABLE I. MINERALOGY OF THE GRAVITY CONCENTRATE

| Component     | Element,<br>Wt. % | Oxide, Wt.<br>% | Mineral               | Minerals, Wt. % |
|---------------|-------------------|-----------------|-----------------------|-----------------|
| Rare earths   | 1.86              | 2.17            | Allanite-Chevkinite   | 4–5             |
| Zircon        | 8.17              | 11              | Zircon                | 20              |
| Titanium      |                   | 8.02            | Titanite              | 20              |
| Thorium       | 0.19              | 0.22            | Thorite               | 0.3             |
| Niobium       | 0.1               | 0.14            | Betafite              | 0.3             |
| Uranium       | 0.05              | 0.06            | Betafite-Uranothorite | 0.3             |
| Hafnium       | 0.1               | 0.12            | Zircon                | 20              |
| Iron oxide(s) | 18.77             | 18.77           |                       |                 |

[Source: AMR Mineral Metal Inc., NI 43-101 Report, May 2013, reproduced with permission]

Since it is not possible to obtain a higher concentrate (i.e. more than 20%) of rare earth elements (REEs) by using the ore dressing techniques on AMR ore, chemical processes should be applied after flotation (Table II) in order to obtain a chemical concentrate of REEs.

TABLE II. AMR FLOTATION CONCENTRATE FOR HYDROMETALLURGICAL PLANT

| Element                            | % or ppm | Element | % or ppm |
|------------------------------------|----------|---------|----------|
| Fe <sub>2</sub> O <sub>3</sub> [%] | 14.5     | Sm      | 583      |
| TiO <sub>2</sub> [%]               | 13.4     | Eu      | 110      |
| Zr                                 | 4854     | Gd      | 352      |
| Th                                 | 1496     | Tb      | 39       |
| U                                  | 416.1    | Dy      | 173      |
| Y                                  | 787      | Ho      | 32       |
| La                                 | 7735     | Er      | 87       |
| Ce                                 | 12698    | Yb      | 92       |
| Pr                                 | 1407     | Tm      | 14       |
| Nd                                 | 4542     | ΣREEs   | ~2.9%    |

[Source: AMR Mineral Metal Inc., NI 43-101 Report, May 2013, reproduced with permission]

The predominant constituent of almost all valuable elements in the concentrate is silicate, which renders difficult the cracking and getting the elements into solution. So, caustic cracking has been applied to the concentrate by using sodium hydroxide at 600°C followed by water leaching which separates the greatest part of silicate as water soluble sodium silicate and transform the valuable elements (Zr, Ti, REEs, Th, U as well as Fe, etc.) to their hydroxides. Metal hydroxides, as well as untransformed gangue minerals are filtered off and washed for removing any residual sodium hydroxide solution. The dried cake is then treated with hydrochloric acid to dissolve the metal hydroxides for further separation operations. Due to the relatively low concentration values of REEs in the solution an oxalate precipitation has been envisaged [1]. But, high concentration of iron, as well as zirconium interfering during the oxalate precipitation, dissolved iron (III) chloride is first removed by TBP solvent extraction (the composition of a typical chloride solution after Fe removal is given in Table III), followed by Zr, Ti and U separations by a chemical precipitant.

TABLE III. TYPICAL COMPOSITION OF IRON-FREE CHLORIDE SOLUTION

| Element | mg/L   |
|---------|--------|
| Ti      | 3126   |
| Zr      | 1561   |
| U       | 85     |
| Th      | 133.5  |
| Y       | 64.6   |
| La      | 710.7  |
| Ce      | 1257.2 |
| Pr      | 87.8   |
| Nd      | 287.7  |

[Source: AMR Mineral Metal Inc. Project Report, Star Earth Minerals Private Ltd. Hyderabad-India, reproduced with permission]

## 2. EXPERIMENTAL DATA

### 2.1. Zr, Ti and U separation

Pre-prepared hot phthalic acid (or ammonium phthalate) solution is gently added into the hot (~100°C) iron-free chloride solution. After thorough precipitation the slurry is filtered and Ti, Zr and U phthalates cake is separated and transferred to the metathesis tank, in which 10% NaOH or NH<sub>4</sub>OH solution reacts with phthalate cake allowing to the transformation metal phthalates to their respective hydroxides. While phthalate solution is recycled for next precipitation, the hydroxide cake of Ti, Zr and U is treated with 3M HNO<sub>3</sub> and a nitrate solution is obtained. This solution is subjected to solvent extraction by using TBP (tri-n-butyl phosphate) which extracts Zr and U in organic phase, leaving Ti in aqueous raffinate. Ti containing raffinate is then precipitated by ammonia solution to get titanium hydroxide, which is to be filtered off, dried and calcined to obtain finally titanium oxide [2].

TBP organic phase is subjected to selective zirconium strip by using acidified water. Zirconium nitrate solution free of U and Ti is obtained and zirconium hydroxide is precipitated by using ammonia solution.

After Zr removal TBP organic phase is stripped by dilute sulphuric acid to get aqueous uranyl sulphate solution and ammonium diuranate (ADU – yellow cake) is precipitated from this solution.

### 2.2. Oxalate precipitation

In order to obtain a concentrate of REEs, oxalic acid precipitation method is preferred which is a widely used method and has been industrially applied for a long time, especially for the leaching solutions in which the REEs concentration is not so high for solvent extraction. Oxalic acid precipitation requires careful adjustment of pH or acidity, temperature control and mixing conditions. But thorium having similar chemical properties to that of REEs completely precipitates along with REEs and further separation of thorium becomes necessary [3]. A strong solution of oxalic acid is added by continuous stirring to the chloride solution of REEs+Th obtained after Fe, Zr and Ti removal and heated at 80°C till complete precipitation. The oxalate precipitate should be filtered without allowing the slurry to cool down. Oxalate precipitate is washed thoroughly by hot water (60–70°C) and final precipitate is dried at 100°C for analysis at ICP-MS. The composition and relative percentage of each element in dry oxalate concentrate is shown in Table IV.

TABLE IV. TYPICAL COMPOSITION OF [REES+TH] OXALATE

| Element                                | Y    | La    | Ce    | Pr   | Nd    | Sm   | Eu         | Gd   | Tb              |
|--|------|-------|-------|------|-------|------|------------|------|-----------------|
| Mass [mg]                              | 4.13 | 29.46 | 69.29 | 7.03 | 27.74 | 3.18 | 0.6        | 2.02 | 0.22            |
| Relative concentration of elements [%] | 0.98 | 7.00  | 16.47 | 1.67 | 6.59  | 0.76 | 0.14       | 0.48 | 0.05            |
| Element                                | Dy   | Ho    | Er    | Tm   | Yb    | Lu   | <b>Th</b>  | Sc   | $\Sigma$ REE+Th |
| Mass [mg]                              | 0.97 | 0.16  | 0.52  | 0.08 | 0.53  | 0.06 | <b>8.6</b> | 2.73 | 157.32          |
| Relative concentration of elements [%] | 0.23 | 0.04  | 0.12  | 0.02 | 0.13  | 0.01 | 2.04       | 0.65 | 100.00          |
|  |      |       |       |      |       |      |            |      | Oxalate         |

### 2.3. Metathesis

The separation of rare earth elements as smaller groups or from each other by solvent extraction has been largely developed in recent years. Phosphonic acid esters have been found more selective for the separation of heavy rare earths from light rare earths in chloride medium. This is also preferred as an

extractant for the separation of individual rare earth elements due to the high separation factors between any two adjacent rare earth elements [4]. Since the phosphonic acid esters usage is envisaged for further steps, the conversion of REEs concentrate into their hydroxides for easy dissolution in HCl and recovery of oxalic acid as sodium oxalate, the metathesis operation is preferred.

Approximately 100 g (dry basis) of above produced REEs+Th oxalate precipitate is heated with 500 mL of 60% NaOH (w/v) with continuous stirring for not allowing the precipitate to settle down. Metathesis operation is conducted at 100°C for about 4 hrs. The slurry is left for ageing at 60°C for 4 hr and filtered. Washing operation which is conducted with hot water should be maintained till the pH of filtrate remains around 7. Filtrate which contains mainly excessive NaOH and sodium oxalate is sent to sodium oxalate and hydroxide recovery by evaporation.

Wet hydroxide cake is dissolved in diluted HCl (5–6 N) at 35–40 °C (reaction heat) and chloride solution (final pH ≈ 0) is collected for Th separation.

#### **2.4. Thorium separation and purification**

The fact that Th(IV) hydroxide solubility decreases sharply by increasing pH even in acidic region [5] is put to use and pH regulation is used to precipitate almost completely Th as its hydroxide from above obtained  $\text{RECl}_3$  and  $\text{ThCl}_4$  solution. 5 M NaOH (or  $\text{NH}_4\text{OH}$ ) solution is added drop by drop to mixed chloride solution and the precipitation ends at  $\text{pH} \approx 4.2$ –4.5. The precipitation yield of thorium is found as high as 99%. But inevitably appreciable amount of Ce and other light REEs come along with thorium and they represent 40–45% of crude Th hydroxide precipitate.

For further purification of thorium and reclaiming mixed rare earths, crude Th hydroxide cake (3~4 g) is completely dissolved in concentrated nitric acid and traditional separation technique of thorium peroxide precipitation is applied to the nitrate solution. The optimum Th peroxide formation is found at pH between 0.9–1.2 which is adjusted by ammonia solution at 60°C. In our case thorium precipitation yield is about 98%. Thorium precipitate should be thoroughly washed with 2%  $\text{NH}_4\text{NO}_3$  solution and the filtrate containing REEs can be recycled to feed REEs+Th chloride solution.

When dried the thorium peroxide cake contains about 96% of  $\text{ThO}_2$  (other REEs in which Ce is predominant represent about 4% of the total), but for storing safely the thorium, the wet cake is subjected to be dissolved in nitric acid, purified, if necessary, by SX and converted (a) to thorium nitrate crystals or (b) ignited to  $\text{ThO}_2$  powder.

### **3. CONCLUSION**

The study shows the possibility of uranium and thorium separation from a REEs solution. In this case the solution is in a chloride medium where conventional and simple processes is adopted. The main advantage of this method is the complete separate of uranium (about 75% yield) and thorium (around 99%) which are undesirable elements due to their radioactive properties in the different REEs group or individual REE. A relatively easy and reliable method is used, avoiding complicated solvent extraction operations. Separation of thorium before any other step of REEs group or individual element separation is crucial, because without previous thorium separation, there is always risk of contamination of this radioactive element to the other REEs since their chemical properties are more or less similar to those of REEs.

### **ACKNOWLEDGEMENTS**

During the laboratory research of chemical separation of thorium and ICP-MS analysis of the samples I would like to thank to L. Güreli and to my other colleagues from Nuclear Fuel Technology Department, Çekmece Nuclear Research and Training Centre, Istanbul, as well as to B. Bukka, Star Earth Minerals Private Limited, Mumbai, India for the works conducted at his plant in Hyderabad for micro pilot plant tests for AMR ore concentrate.

## REFERENCES

- [1] PASCAL P., Nouveau traité de chimie minérale, Vol. 7.1, Masson, Paris (1966) 187.
- [2] RAMSEY, J.W., WHITSON, W.K., Jr., Production of Zirconium at Y-12, Y-817, USAEC, Oak Ridge, TN (1951).
- [3] PASCAL P., Nouveau traité de chimie minérale, Vol. 7.1, Masson, Paris, (1966) 190–192.
- [4] GUPTA C.K., KRISHNAMURTHY, N., Extractive Metallurgy of Rare Earths, CRC press (2005) 184–189.
- [5] NECK, V., et al., Solubility of amorphous Th (IV) hydroxide—application of LIBD to determine the solubility product and EXAFS for aqueous speciation, *Radiochimica Acta* **90** (2002) 485–494.

# **CREATING A MULTI-NATIONAL DEVELOPMENT PLATFORM: THORIUM ENERGY AND RARE EARTH VALUE CHAIN**

J.C. KENNEDY\*, J.H. KUTSCH\*\*

\* ThREE Consulting LLC,  
St. Louis, Missouri,

\*\* The Thorium Alliance,  
Harvard, Illinois,

United States of America

## **Abstract**

Rare earths and thorium have become linked at the mineralogical and geo-political level. Regulatory changes pertaining to thorium contributed to excessive market concentration in rare earths. This has resulted in economic dislocation and national security issues in many countries. United States Senate Bill S. 2006 and House Bill H.R. 4883 are designed to overcome this ‘market failure’ by establishing a federally chartered multi-national rare earth value chain cooperative and a federally chartered multi-national thorium storage, energy and industrial products corporation. Participation in both entities is open to sovereign states, sovereign funds and the users and consumers of such products.

## **1. INTRODUCTION**

Rare earths and thorium are linked at the mineralogical level and at the geo-political level. International regulations pertaining to thorium have played a significant role in today’s ‘out sized’ market distortions related to rare earths. The resulting market concentration has caused severe economic dislocation and national security problems for the United States of America, Japan, Republic of Korea, the European Union, and other nations. A solution to this problem is required.

Private interests have invested around US \$6 billion in an effort to challenge China’s market dominance in REEs. The Japanese, Indian and Korean governments have made direct investments into this sector also. These efforts have largely failed.

What was the cause of this market failure?

## **2. REGULATIONS AND UNINTENDED CONSEQUENCES**

Thorium-bearing Rare-Earth Element Phosphate ores (Th-REE-P), principally monazite, were the primary commercial source of rare earths until the mid-1960s. From 1965 to 1984 these Th-REE-P materials supplied nearly half of the world’s rare earth requirements, and nearly 100% of the non-Chinese heavy rare-earth elements. Th-REE-Ps are mineralogically superior to low thorium bearing ores like bastnaesite because they typically contain recoverable quantities of all 16 naturally occurring rare earth elements (one other REE, Pm does not exist in the Earth’s crust). These materials were also typically a low cost (or no cost) by-product of some other commodities, such as titanium, zircon, iron ore or phosphates.

The proliferation of regulations reflecting international standards regarding the definition of ‘source material’ eliminated these high value rare earths from the value chain for most of the world. Beginning around 1980 refineries no longer wanted to accept Th-REE-Ps to avoid accumulating thorium. Under the governing laws the material itself constituted ‘source material’ and the traditional producers of these

valuable Th-REE-P by-products began ‘blending’ the Th-REE-P ore back into the recently depleted ore-body or dumping it into tailings lakes.

U.S. Regulations 10 CFR 40 states that:

“Atomic Energy Act (AEA) and the U.S. Nuclear Regulatory Commission (NRC) refer to ‘source material’:

*Per the Atomic Energy Act of 1954, as amended by the Uranium Mill Tailings Radiation Control Act of 1978, generated through the Cooperative, consistent with the regulations in Title 10 Code of Federal Regulations Parts 20, 40, Appendix A to Part 40 (as in effect on the date of the enactment of this Act).*

The following definitions apply to ‘source material’:

US Atomic Energy Act (AEA) Section 11.z. The term ‘source material’ means: (1) uranium, thorium, or any other material which is determined by the Commission (i.e., the US NRC) pursuant to the provisions of section 61 to be source material; or (2) ores containing one or more of the foregoing materials, in such concentration as the Commission may by regulation determine from time to time

Title 10, Code of Federal Regulations Part 40, Section 40.4 (10 CFR 40.4) – Definitions:

‘Source material’ means: (1) uranium or thorium, or any combination thereof, in any physical or chemical form; or (2) ores which contain by weight, one-twentieth of one percent (0.05%) or more of: (i) uranium, (ii) thorium or (iii) any combination thereof;

10 CFR 40.13(c) – Exemptions for low Thorium-bearing ores:

Any person is exempt from the regulation in this part and from the requirements for a license set forth in section 62 of the Act to the extent that such person receives, possesses, uses, or transfers: (1) (vi) rare earth metals and compounds, mixtures, and products containing not more than 0.25 percent by weight thorium, uranium, or any combination of these”.

The exemptions above fit nicely with the only remaining U.S. producer of rare earths - the Mountain Pass mine in California. The primary ore of this deposit has very low levels of thorium, but also lacked recoverable heavy rare earths (Tb, Dy, Ho, Er, Tm, Yb, Lu, Sc).

With its higher mining cost and lower value resources the mine struggled to compete (most of China’s rare earth production is a by-product of iron ore mining). It was eventually closed down due to a tailings discharge that included ‘concentrated levels’ of thorium in 2002. The mine was recently re-opened. All thorium bearing monazites, the primary source of thorium, are cemented in an on-site tailings impoundment. Its mining operations incur substantial losses.

Being no longer able to utilize these far superior Th-REE-P resources, USA, Japanese and European value chains were disadvantaged. Over the next two decades most of these refineries and metallurgical facilities were closed or fell into a state of underinvestment.

The Chinese market was unconstrained by these regulations and filled the breach. The government elected to actively support the development of its rare-earth industry as a National Industrial Policy (Program 863 and 973). China’s forward-thinking industrial policy included direct and indirect investment and support for rare-earth related enterprises, including research and development. General Motors sold Magnequench, the world’s leading rare earth magnet manufacturing facility to Chinese companies with close ties to the government. As its rare earth market concentration increased, most of the world’s leading technology companies moved to China.

### 3. LIFE WITHOUT THORIUM

Rare-earth ores like bastnaesite that did not meet the source material threshold have many disadvantages. The most problematic is the corollary relationship between thorium and the high value heavy rare earths: low thorium levels equated to low heavy rare earths concentrations. The next problem is that these ores are directly mined, so all of the mining cost must be covered from the extracted rare earths. The third problem with these ores is that the typical distribution of rare earths is disproportionately apportioned to the elements with the lowest economic value (typically +80% Ce and La).

The USA has a rare-earth mine where the ore does not meet the defining threshold level of thorium to be considered source material. This is the Molycorp, Mountain Pass deposit in California. As a precaution U.S. law specifically exempted this mine's ore from source material classification. Despite its exemption, and all of its mineralogical disadvantages, it was a tailings pipeline discharge of thorium that caused this mine to close in 2002.

Today this mine and other deposits that are being financed and developed or re-developed are selected for their low thorium content. This is not a viable answer to the problem, because these types of deposits cannot produce the full spectrum of rare earths (typically only 8 of 16 elements). The economic prospects are not good. The disadvantages listed above are reason enough for caution. The complete lack of fully integrated refining assets and expansive rare-earth value chain outside of China is another (Malaysia, India, Russia, South Africa and Estonia all have limited refining capacity, but none have a fully developed rare earth value chain).

The other recently financed rare-earth mining company, Lynas, constructed a rare-earth refinery in Malaysia. Again, the thorium problem prevented it from initiating production for a number of months. This action caused the company to burn through its cash reserves. The company was then forced to raise additional financing during this troubling period, thereby undermining its capital structure. In the end, the high cost of directly mining a relatively low value ore and then shipping it across the ocean for refining may prove too much. As of this writing (May 2014) the company had about 70 days of operating cash and its overall production costs are about 30% higher than the market. However, the company did recently complete a secondary offering (selling new shares of stock), but losses will continue until the prices for abundant light rare earths move higher.

### 4. RARE-EARTH INDEPENDENCE

The resulting economic dislocation and national security concerns have forced the U.S. Congress to consider ways of overcoming this 'market failure'. The U.S. Congress has considered a number of legislative changes that would reduce mine permitting and environmental standards for rare-earth mines, incorrectly believing that mine production is the problem.

The Californian Molycorp mine ships all of its most valuable rare earths to China for refining and value adding. The protracted financial problems of Lynas' investment in a refining facility (costing more than US \$800 million) demonstrates that the cost and financial risks associated with refining rare earths are too great for any one company. Any new producer will most likely follow Molycorp's example and ship their concentrates to China for refining and value adding into metals, alloys, magnets and industrial components.

Recklessly opening new mines with lower environmental standards is not a solution. An alternative to lowering environmental standards is to employ well-established practices such as the formation of a cooperative, specifically designed to overcome 'market failures,' spread financial risk, gain access to low-cost capital, expanded markets and utilize the lowest cost and highest value resources available.

### 5. SOLUTION

Historically the USA has looked to cooperatives as a way to overcome market failure as it relates to high capital cost, low margin businesses like farming. Before the wide-spread use of farmer-owned grain

elevators all of the farm's production hit the market at the same time. Merchant speculators, who controlled grain elevators would pay next to nothing for grain during the harvest season and sell off the grain throughout the year — maximizing profits. Many farmers starved or went bankrupt. Cooperatives offered a solution.

A farmer-owned cooperative spreads the capital cost among its many owners and suppliers, thus spreading the risk. Large grain elevators attracted rail lines, greatly increasing market access and allowing timely sales of grain, including into forward markets. The cooperatives, owned by their suppliers (the farmers), were able to rationalize grain prices across markets and time. Profits were distributed to the owners, and consumers benefited from more stable food prices at the retail level.

By creating an old-fashioned cooperative, the USA can solve a very modern problem. Rare-earth end-users from around the world can directly invest in a cooperative value chain. This cooperative would produce exactly what it's owners need (oxides, metals, alloys, standardized components, etc.). The owner end-users would initially purchase their value added rare earth goods at market prices. Excess inventory, not utilized by the owners, would also be sold at market prices to non-owners. Profits, if any, would be redistributed back to the owners. As owners of the cooperative, all members would ultimately acquire their value added rare earths goods at cost (free of price manipulation and speculators).

By utilizing abundant and available Th-REE-P resources, the need to make massive investments into low thorium/low value rare-earth mines is eliminated. Because the Th-REE-P is typically a by-product of some other commodity, its production cost is near zero.

Today the US mining industry could meet 50% of global rare-earth demand with Th-REE-P by-products if the thorium problem was resolved. The management and safe storage of thorium does not pose any technical challenges. The economic challenge of long term thorium storage can be overcome by sharing the cost with the many end-user members.

The cost of long-term thorium storage would amount to a fractional surcharge on the rare earths produced and sold. The thorium storage facility would take ownership of the material and be given Congressional authority to develop industrial uses and markets for thorium, including energy. The commercial prospects should be adequately compelling to attract the level of investment necessary to create new uses for thorium, including energy products and systems.

Recently introduced bills in the United States Congress, H.R. 4883 and S. 2006, would resolve the 'thorium problem'. The legislation is designed to induce a fully integrated rare-earth value chain structured as a multi-national rare-earth cooperative, which is owned and controlled by the end users of rare earths.

"The National Rare Earth Cooperative Act (NRECA—H.R. 4883 & S. 2006)" is designed to:

- 1) Utilize existing and available Th-REE-P resources within a Federally Chartered Rare Earth Cooperative (and Thorium Corporation) that would serve as a fully integrated value chain for rare-earth materials;
- 2) Be owned and funded by multi-national corporations, defence contractors, sovereign nation agencies, sovereign wealth funds, end-user organizations and suppliers who commit capital.

More importantly, the bills also create a federally chartered Thorium Energy and Industrial Products Corporation that will take all liability and physically hold and safely store all thorium and associated actinide liabilities from the Rare Earth Cooperative.

The Thorium Corporation will be given Congressional authority to establish a multi-national corporate platform:

- 1) To develop industrial uses and markets for Thorium (including decay products), that include:
  - a) Alloys;
  - b) Catalysts;
  - c) Medical isotopes;
  - d) And other uses.
- 2) And for the commercial development of thorium energy systems, that include:
  - a) Solid fuels from thorium;
  - b) Solid-fuel reactor technology;
  - c) Beam / accelerator driven reactors;
  - d) Liquid-fuel reactor technology, to include:
    - i) Electric power;
    - ii) Thermal energy;
    - iii) Synthetic liquid fuel production;
    - iv) Desalination;
    - v) Nuclear waste reduction (actinide burners);
    - vi) Hardened and deployable energy systems.

The Thorium Energy Corporation is required to seek out direct investment from sovereign entities (and the users and consumers of energy). The successful deployment of next generation thorium based reactors could greatly augment the declining economic status of sovereign states around the world. The potential for future revenues from the successful deployment of next generation reactors could help offset declining corporate tax receipts, which is a global phenomenon that undermines state sovereignty.

Various configurations of high-temperature liquid-fuelled reactors (molten salts or metals) or beam/accelerator driven reactors have better safety feature than the current generation Liquid Water Reactors (LWRs). High-temperature thorium liquid-fuelled reactors can eliminate the risk of widespread radiation release (water/hydrogen event) and greatly reduce issues related to long-lived spent fuel and the proliferation of weapon-grade material. The potential benefits of eliminating and/or offsetting greenhouse gas emissions and ocean acidification are greater still.

## 6. CONCLUSION

The timing of this multi-national platform coincides with enhanced concerns for safety of the traditional LWR technology, which could conflict with the monumental and intractable costs required to avert climate change and oceanic acidification.

The status quo is not tenable. Biosphere-altering problems related to climate and ocean deviation require an aggressive solution, something beyond renewables. A solution, an ‘acceptable alternative’, is needed in short order.

High temperature, thorium liquid fuelled reactors and beam/accelerator driven reactors are technologically obtainable and may be the ‘acceptable alternative’ and a viable solution to our energy and environmental needs.

These technologies can be developed by one nation or many. If they become the *accepted alternative* the humanitarian benefits are boundless, but the economic benefits must also balance.

Broad international support and participation must be the centrepiece of this effort. It is only through collective action that the benefits can be shared.

# THE POTENTIAL FOR THORIUM RECOVERY AS A CO-PRODUCT OF PROCESSING MAGMATIC RARE EARTH ELEMENT DEPOSITS

B.S. VAN GOSEN, D.B. STOESER

U.S. Geological Survey (USGS),  
Colorado,  
United States of America

## Abstract

Thorium (Th) can be obtained as a co-product of processing deposits of rare earth elements (REEs). The REEs and Th are chemically associated in magmas that form REE-rich alkaline intrusive rocks and carbonatites. An example is the Mountain Pass mine and ore processing operations of MolyCorp, Inc., in South-eastern California, which is the only active REE mine in the United States. The ore is a carbonatite containing an average REE oxide content of 7.98 percent. Monazite is an accessory mineral, giving the ore a Th content of about 0.025%. After ore processing to capture the REEs, Th is carried with other residues into the tailings impoundment. A second example is the Bear Lodge REE project of Rare Element Resources in North-eastern Wyoming. The deposits occur in an altered carbonatite-alkaline intrusive complex. The ore averages 3.11% REE oxides and about 0.12% Th. The company stated their processing will “selectively isolate and economically remove thorium.” As a third example, UCore Rare Metals plans to mine REE-rich, thin vein-like dikes at the Bokan Mountain alkaline intrusive complex on Prince of Wales Island in South-eastern Alaska. The ‘vein-dike’ deposits average 0.65% REEs; about 40% are the heavy REEs. A U.S. Geological Survey study during 2013 and 2014 by the authors found Th in thorite and  $Ti \pm Nb \pm Y$  oxide minerals in these vein-dikes. Bulk sampling revealed Th contents of about 0.06 to 0.07%. The three REE ore bodies examined herein as case studies display the potential for Th as a co-product, but presently considered a waste product that will be either lost or difficult to recover.

## 1. INTRODUCTION

In magmatic systems, the large sizes of the rare earth element ions (<sup>+3</sup>) and thorium ions (<sup>+4</sup>) impede their ability to fit into the structure of the common rock-forming minerals, which have coordination sites best suited for smaller cations. Elements such as the REEs that do not tend to participate in the early mineral formation processes are referred to as incompatible elements or high-field strength elements. In magmatic systems, the incompatible elements can also include zirconium (Zr), hafnium (Hf), niobium (Nb), tantalum (Ta), titanium (Ti), phosphorus (P), scandium (Sc), and uranium (U). As a result, when common silicate minerals crystallize — feldspars, pyroxenes, olivine, and amphiboles — most of the rare earth elements (REEs) and thorium (Th) tend to preferentially remain in the melt. These elements concentrate in differentiated magmas, such as melts that form alkaline intrusions and carbonatites, which are the most common hosts for REEs. Successive generations of this process, referred to as crystal fractionation, increase concentrations of REEs and Th in the remaining melt until individual REE- and Th-rich minerals crystallize. Thus, high-grade Th deposits are often high-grade REE deposits.

Due to above normal concentrations of Th in REE ore bodies, Th can be considered as a co-product of developing REE deposits, that is if a market emerges for Th as a nuclear fuel. Currently, Th within REE deposits in the United States is treated as a radioactive contaminant, not as a potential commodity. Separation and stockpiling of Th from the residue streams of REE production provide a possible method to economically obtain Th, if it becomes a viable commodity.

This paper evaluates the Th content in three REE deposits in the United States; these include one deposit that is actively mined and processed for recovery of REEs (Mountain Pass, California) and two projects with plans to produce REEs in the foreseeable future (Bear Lodge project, Wyoming, and Bokan Mountain project, Alaska). Currently, these three projects focus on REEs as their economic commodity. This paper estimates the amounts of Th that could be recovered as a co-product commodity during the processing of the deposits for REEs.

## 2. CASE STUDIES

### 2.1. Mountain pass mine, California

The Mountain Pass operation of MolyCorp, Inc., in South-eastern California is the only active REE mine and processing facility in the United States (Fig. 1, <http://www.molycorp.com>). The mine reopened in late 2010 after an eight-year hiatus. The orebody is a massive carbonatite intrusion — the Sulphide Queen carbonatite — that reportedly contains 16.7 million metric tonnes of proven and probable reserves averaging 7.98% total REE oxides [1]. This carbonatite is thought to be the largest REE resource in the United States. The Sulphide Queen is a calcite-dolomite-barite-strontianite carbonatite [2, 3]. The primary ore mineral is bastnaesite  $[(\text{REEs})\text{CO}_3\text{F}]$ , forming 10–15% of the carbonatite ore body, plus lesser REE contributions from the mineral parisite  $[\text{Ca}[(\text{REEs})_2(\text{CO}_3)_3\text{F}_2]]$  [2, 3]. The Sulphide Queen is the only known carbonatite where the REE ore minerals — bastnaesite and parisite — are interpreted to have crystallized directly from the magma, thus representing primary magmatic mineralization [4]. In the other carbonatites, the REE-bearing minerals are interpreted to have formed by secondary processes, such as hydrothermal events (as displayed by the next case study — the Bear Lodge carbonatite-intrusive complex).

Monazite  $[(\text{REEs})\text{Th}(\text{PO}_4)]$  is an accessory mineral in the Sulphide Queen carbonatite, varying in amounts from a trace mineral to locally abundant within the ore body; the monazite gives the ore a Th content of about 0.025%. In 2011, bulk sampling (about 1 metric tonne) of high-grade REE carbonatite ore collected in the mine by the U.S. Geological Survey (USGS) found an average Th content of about 0.025% (elemental weight percent) (unpublished author data). This estimate of Th content is nearly identical to the thorium concentrations found in an earlier geochemical study of this carbonatite [5].

Applying an estimated Th concentration of 0.025% within the Sulphide Queen carbonatite, this suggests that each metric tonne of ore mined and processed at Mountain Pass contains, on average, about 0.25 kg of Th. This estimate of Th content in the Sulphide Queen orebody is certainly an approximation based on limited sampling; monazite concentrations may prove to vary considerably across the carbonatite as mining progresses. At the time of writing (2014), when the carbonatite of Mountain Pass is mined, processed, and the REEs are separated, the Th moves with other residues into the tailings impoundment. Thus, it would require further processing of the tailings in order to recover the Th in the future.

### 2.2. Bear lodge project, Wyoming

The Bear Lodge project of Rare Element Resources Ltd is located in the Bear Lodge Mountains near Sundance in North-eastern Wyoming. This project is currently in an advanced stage of permitting for their proposed REE mine and processing plant (<http://www.rareelementresources.com/>). Based on considerable exploratory drilling over the last several years, the company reports total measured and indicated resources of 15.2 million metric tonnes of ore averaging 3.11% total REE oxides in the district. Within this total REE resource they identified a high-grade zone of 5.4 million metric tonnes containing 4.72% total REE oxides, applying a cut-off grade of 3% total REE oxides [6].

The Bear Lodge REE deposits occur in hydrothermal alteration of an Eocene carbonatite-alkaline intrusive complex [7]. The REE deposits are hosted by diatremes composed of fragmented, highly altered trachyte and phonolite intrusive rocks, which are cross cut by carbonatite and siliceous carbonatite dikes, veins, and stock work veinlets [6]. The primary REE ore minerals are aenylite and REE-fluorocarbonates of the bastnaesite group, and important Th-bearing accessory minerals are monazite and cerianite  $[(\text{Ce},\text{Th})\text{O}_2]$  [6, 7].

In 2011, Rare Earth Elements permitted the USGS to sample an exploration trench excavated into ore at the site of the proposed open pit mine (Fig. 2). The sampling found Th concentrations that average about 0.11–0.12 percent (elemental weight percent). Although this sampling must be considered a reconnaissance investigation, it suggests that each metric tonne of ore material in the upper part of the deposit contains about 1 kg of Th.



FIG. 1. The Mountain Pass mine of Molycorp, Inc., in South-eastern California. This is the only active REE mine in the United States (in 2014). The ore body is a carbonatite intrusion, thought to represent the largest REE resource in the United States. The mine is located at latitude 35.47853 North, longitude 115.53181 West (datum, WGS84).

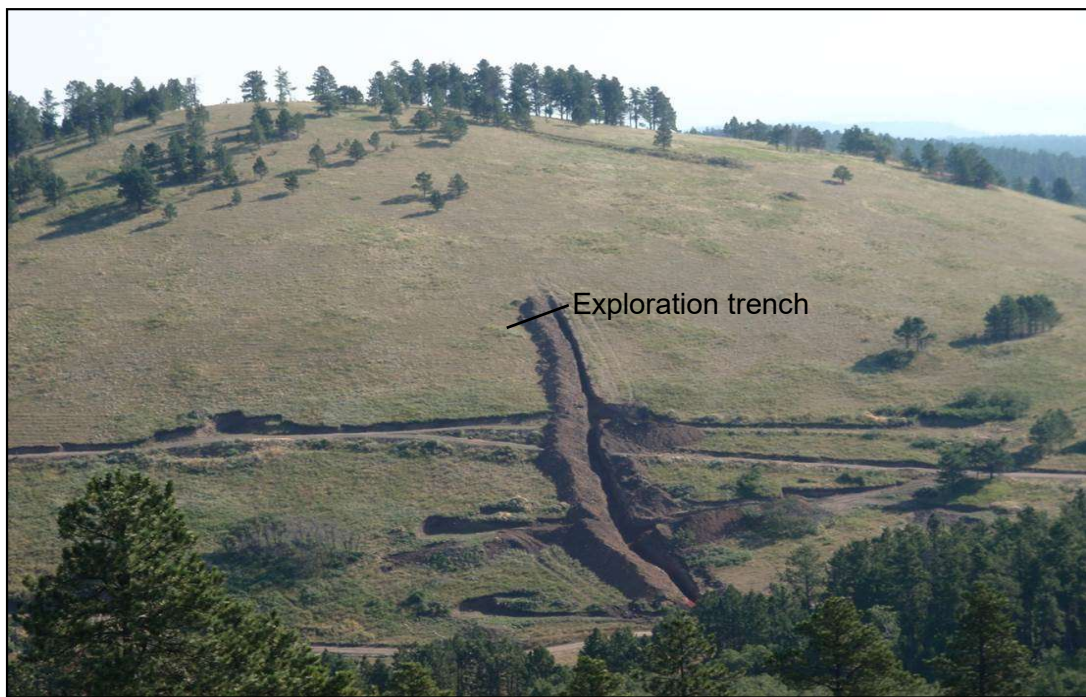


FIG. 2. Bull Hill in the Bear Lodge Mountains, near Sundance, North-eastern Wyoming. Bull Hill is composed of REE-mineralized, hydrothermally altered diatreme breccia in the upper part of an alkaline–carbonatite intrusive complex. The hill is the site of the proposed open pit REE mine planned by Rare Element Resources. The exploration trench is located at latitude 44.48983 North, longitude 104.44525 West (datum, WGS84).

In a press release of 21 January 2014, the company announced that pilot testing of their proposed ore processing technology identified a process to “selectively isolate and economically remove thorium”. Their proposed processing procedures were filed as a utility patent application with the U.S. Patent and Trademark Office; the patent currently (July 2014) awaits evaluation and approval. Separation and capture of Th from their waste stream was designed into their ore processing plan due to concerns of radioactivity generated by Th-bearing waste materials. The company states the Th will be disposed of by a third party, in an unspecified manner. Thus, the segregated Th may become either unavailable or difficult to obtain in the future.

### 2.3. Bokan mountain, South-eastern Alaska

As a third example of coexisting REEs and Th, the exploration company UCore Rare Metals Inc. (<http://ucore.com/>) plans to mine REE-Th-rich, vein-like dike deposits associated with the Jurassic Bokan Mountain alkaline intrusive complex in southern Prince of Wales Island in South-eastern Alaska (Fig. 3) [8]. The ore target is a series of thin, REE-rich dikes that crop out along Dotson Ridge on the southeast flank of Bokan Mountain. The ore zone is formed by numerous alkaline dikes exposed side-by-side across a zone about 50 m wide. Individual vein-like intrusions (thin dikes) occur either as closely spaced sets that are a few millimeters to 50 cm wide, or as single dikes that are individually 40 cm to several metres thick; these intrusions are separated by earlier-formed, unaltered Silurian–Ordovician quartz monzonite (Fig. 4), granite, quartz diorite, and diorite. The REE-bearing dikes of Dotson Ridge follow a linear shear zone along its strike for a distance of at least 1 km [8, 9]. These REE-rich intrusions are informally described by the company as ‘vein-dikes’ due to their vein-like appearance. These vein-dikes are particularly enriched in the heavy REEs, which compose about 40% of the total REEs. Based on a multi-year drilling program, UCore Rare Metals reports inferred resources for the Dotson Ridge vein-dike zone of 5.2 million metric tonnes averaging 0.65% total REE oxides (<http://ucore.com/>). The company plans to exploit only the REE resources with no plans to recover the Th.

The vein-dike features of Dotson Ridge show evidence of early alkaline magmatic injection with subsequent orthomagmatic hydrothermal alteration [8]<sup>17</sup>. As a result, the vein-dikes contain a complex ore mineralogy with evidence of hydrothermal overprinting of primary magmatic phases; more than 30 REE-Y-bearing minerals representing multiple generations have been identified [8, 9]<sup>18</sup>. Detailed mineralogical study of the Dotson Ridge vein-dike system by the USGS revealed that Th and U are dominantly sited in thorite and a complex suite of  $Ti \pm Nb \pm Y$  oxide minerals, including fergusonite, polycrase, and aeschynite. These oxide minerals along with Y-silicates are the primary heavy REE-bearing minerals of the deposit.

Limited bulk sampling (about 1 metric tonne) of the Dotson Ridge ore zone by the USGS in 2011 revealed Th contents of about 0.066% (elemental weight percent), which includes barren rock between the mineralized veins. Although only an approximate estimate, the USGS sampling suggests that each metric tonne of ore mined and processed from the deposit would contain, on average, about 0.66 kg of Th. To address environmental concerns of radioactivity, the company suggests in their proposed plan of operations that the mine waste materials will be encased in concrete, which will be used to backfill the mine openings after mining is completed.

## 3. DISCUSSION

In the ore processing and waste disposal procedures for the three REE development projects described above, Th and its radioactivity must be addressed due to environmental permitting requirements.

---

<sup>17</sup> Including unpublished author studies

<sup>18</sup> Including unpublished author studies

However, in the operational design for two of these projects, the companies dilute the Th with waste products, thereby adding complexity to recovering the Th in the future.

Stockpiling of Th in the United States is not occurring today for at least a couple of reasons:

- Presently there is no significant market for Th as a commodity. For example, according to the USGS, in 2013 in the United States “the estimated value of thorium compounds imported for consumption by the domestic industry was [only] US \$54 000” [10];
- The stockpiling of Th in the United States requires special permits and licenses; these difficult-to-obtain permits are required in order to store radioactive materials, including Th-rich materials. Thus, companies have little incentive at this time to stockpile Th-oxide or Th-rich wastes while waiting for a Th market to arrive.

In the future, separation of Th from the residue streams of REE mining and ore processing provides a possible economic solution to obtaining Th resources for nuclear fuels. As shown by the three case studies described above, Th is available for recovery from magmatic REE deposits. If a need and associated market should develop for Th, then the co-production of Th from the development of REE deposits provides a means for Th supply.

#### 4. ACKNOWLEDGEMENTS

The authors thank MolyCorp, Inc., Rare Element Resources Ltd., and UCore Rare Metals Inc. for the opportunities to visit and sample their deposits. Any use of trade, product, or company names is for descriptive purposes only and does not imply endorsement by the U.S. Government.



*FIG. 3. Bokan Mountain is the core of the Jurassic Bokan Mountain peralkaline granite complex, southern part of Prince of Wales Island, South-eastern Alaska. A REE-rich vein-dike system, about 50 meters in total width, occupies a linear shear zone along Dotson Ridge. Bokan Mountain is located at latitude 54.9159 North, longitude 132.1548 West (datum of WGS84).*

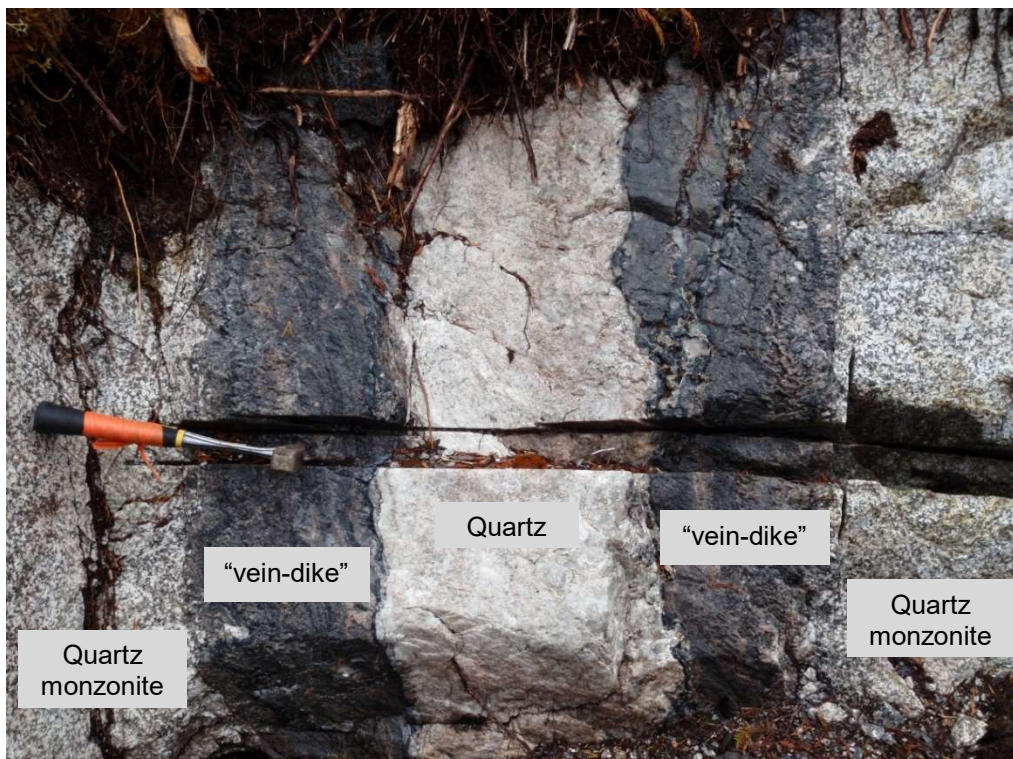


*FIG. 4. Example of REE-rich vein-dikes within the Dotson Ridge deposit, Bokan Mountain, Alaska. These altered intrusions contain more than 30 REE-Y-bearing minerals, and at least 7 Th-bearing phases. This deposit has been explored and drilled recently by UCore Rare Metals.*

## REFERENCES

- [1] MOLYCORP, INC., Molycorp's rare earth reserves at Mountain Pass increase by 36%, Molycorp, Inc., press release, 9 April 2012.
- [2] CASTOR, S.B., et al., "Mountain pass rare earth deposit, California", Betting on Industrial Minerals, Proceedings of the 39th Forum on the Geology of Industrial Minerals, Reno/Sparks, Nevada, May 18–24, 2003 (CASTOR, S.B., et al., Eds), Nevada Bureau of Mines and Geology Special Publication **33** (2004) 68–81.
- [3] CASTOR, S.B., The Mountain pass rare-earth carbonatite and associated ultrapotassic rocks, California, *The Canadian Mineralogist* **46** 4 (2008) 779–806.
- [4] MARIANO, A.N., "Economic geology of rare earth elements, Chapter 11", *Geochemistry and Mineralogy of Rare Earth Elements* (LIPIN, B.R., et al., Eds), Washington, D.C., The Mineralogical Society of America, *Reviews in Mineralogy* **21** (1989) 309–337.
- [5] STAATZ, M.H., et al., Thorium Resources of Selected Regions in the United States, U.S. Geological Survey Circular 824 (1980) 32pp.
- [6] RARE ELEMENT RESOURCES, Bear Lodge Project, Rare Element Resources company website (2014), <http://www.rareelementresources.com/>.
- [7] ANDERSEN, A.K., et al., "Rare earth element zonation and fractionation at the Bear Lodge REE deposit", Wyoming, *Geological Society of America Abstracts with Programs* **45** 5 (2013) 42.
- [8] DOSTAL, J., et al., The early Jurasic Bokan Mountain peralkaline granitic complex (southeastern Alaska), *Geochemistry, Petrogenesis and Rare-metal Mineralization, Lithos* **202–203** (2014) 395–412.
- [9] BARKER, J.C., VAN GOSEN, B.S., Alaska's rare earth deposits and resource potential, *Mining Engineering* **64** 1 (2012) 20–32.

- [10] GAMBOGI, J., Thorium, U.S. Geological Survey Mineral Commodity Summaries (2014) 166–167, <http://minerals.usgs.gov/minerals/pubs/commodity/thorium/>.

# THORIUM: GEOLOGY, OCCURRENCE, DEPOSITS AND RESOURCES

F.H. BARTHEL\*, H. TULSIDAS\*\*

\* Private Consultant,  
Weissstein, Germany

\*\* International Atomic Energy Agency,  
Vienna, Austria

## Abstract

The average content in the upper crust of the earth reaches 6–10 g/t Th. Thorium occurs in oxides, silicates, phosphates, and other minerals. Deposits can be classified into placers, carbonatites, veins and alkaline rocks. Placers are formed by weathering, transportation and wave action. The main Th-mineral is monazite, with generally less than 10% Th, from which Th can be extracted as by-product. Carbonatite rocks are of magmatic origin (> 50% carbonate minerals) often enriched in magnetite, apatite, fluorite and accessory Nb–Ta minerals, containing Th and may be recovered as by-product. Vein-type deposits occur close to igneous rocks, often related to carbonatites. They are frequently polymetallic. Th minerals are thorium oxide and thorium silicate. Alkaline rocks are characterized by high amount of alkali feldspar. Alkaline and peralkaline rocks can be spatially related to carbonatites. Thorium resources can be classified according to confidence in estimates of tonnages. Official figures are frequently not available or not in agreement with standards. World estimates indicate more than 6.2 Mt Th reported from 35 countries. About 35% of identified resources are located in placer deposits, 29% in carbonatites and 25% in vein-type deposits. The rest may be assigned to alkaline rocks and others. Major resources are: India (846 500 t), Brazil (632 000 t), USA (595 000 t), Egypt (380 000 t), Turkey (374 000 t), Venezuela (300 000 t), Canada (172 000 t), and South Africa (148 000 t). No official figures are available for the Russian Federation and China. 28 countries have less than 100 000 t Th. Present thorium demand is limited, production is reported from Brazil and India. Placers might be a future source, when thorium is required as an alternative or substitute to uranium.

## 1. INTRODUCTION

The collection of data on thorium deposits, their resources as well as on its geology was undertaken by IAEA during the 1980s and reassessed recently [1, 2]. Thorium resource estimates were published by the OECD Nuclear Energy Agency (OECD/NEA) and International Atomic Energy Agency (IAEA) in its Red Books [3]. In the 21st century a renewed interest in thorium can be observed [4–6]. A detailed collection of material on deposits and resources of thorium is presented in a document of the IAEA and this paper summarizes the results [7].

## 2. GEOLOGICAL FEATURES

### 2.1. General remarks

Thorium was discovered 1828 by the Swedish chemist Berzelius, and named it after Thor, the Germanic god of thunder. It has the atomic number of 90 and an atomic weight of 232. In nature thorium exists mainly as a single isotope Th-232. Thorium is radioactive, has a half-life time of ~14 billion years, and decays in several stages to its lead-208 [5].

Thorium may be used as an alternative or substitute to uranium in nuclear power reactors in the future, thus an early collection of relevant data seems to be useful. The first experimental and prototype reactors using thorium as nuclear fuel were developed in several countries during the 1960s and 1970s and some continued in later years, however this technology was not continued due to various reasons, and reactors were shut down. Thorium based reactors had some challenges compared to uranium based reactors and

the technology could not compete with the advancing uranium reactor technology in view of the vast uranium resources that were discovered in the 1970s and 1980s.

## 2.2. Thorium minerals

Thorium is not observed in its metallic form in nature. The element is forming chemical compounds with oxygen. The common oxide is  $\text{ThO}_2$  — thorianite — mainly accompanied by uranium. Another thorium mineral is the silicate thorite —  $\text{ThSiO}_4$ . Thorium is found as a radioactive component of the Ce and rare earth elements phosphate monazite, containing from a few ppm (parts per million) up to several percent Th [1, 8]. Thorium can occur in other oxides, silicates, phosphates and carbonates. More than 60 minerals are reported to contain thorium in various concentrations (few ppm to several %).

## 2.3. Geochemical behaviour

Thorium exists under natural conditions as  $\text{Th}^{4+}$  and has a similar geochemical behaviour as  $\text{U}^{4+}$ . Its ionic radius is about  $10^{-7}$  mm, which explains why thorium substitutes with similar cations, e.g. rare earth elements (REE), U, Zr, etc. [8].

Thorium is enriched during magmatic differentiation (metal fractionation). This explains why concentrations increase from less than 0.05 ppm in ultrabasic rocks to about 3.5 ppm in basic rocks and to about 12 ppm in granites [8], compared to uranium at 0.01 ppm, 0.5 ppm, 3–4 ppm respectively. The average content in the upper crust of the earth reaches 6–10 ppm, about 3–4 times that uranium.

## 2.4. Geological remarks

Due to limited commercial demand, thorium publications dealing with geological features of thorium were mostly concerned with scientific considerations. The radioactivity of thorium and its close geological association to uranium however has resulted in a number of papers explaining the geological association of this element to various rock types, thus enabling to draw to some extent conclusions, which are far from final. It can be stated that most knowledge on thorium is a ‘fall out’ of uranium. During exploration for uranium, thorium also responds to measurements of radioactivity, and in case of using spectrometric instruments or by chemical analysis, the presence of thorium and its concentrations will be recorded. Due to this this knowledge on thorium gradually increased, leading to the present understanding. Though, in general thorium is described to occur jointly with uranium, however under special circumstances thorium may be present without uranium. Scientific publications therefore are mostly pertaining to situations where both elements occur together. Publications describing thorium geology are limited and mostly are concerned with deposit types, which will be described in the following part.

# 3. THORIUM DEPOSITS

Despite its abundance in the crust of the earth — especially in the lithosphere — scientific interest in thorium deposits has been less attractive, compared to uranium, due to limited commercial demand. Thus, attempts to classify thorium deposits are fewer. When commercial interest for thorium as a nuclear fuel started in the 1960s and 1970s, some scientific publications appeared with attempts to classify thorium deposits, e.g. [1] in 1991, mostly based on geological aspects. A description of thorium deposits and a classification used in the former Soviet Union was published in 1997 [9]. A classification using genetic aspects was propagated by Cuney [10, 11]. A simplified version of the classification of thorium deposits is in use by the joint publication of OECD/NEA–IAEA in the Red Book [12], giving a description into four major types: Carbonatite, Placer, Vein-type, Alkaline rocks, accounting for more than 95 % of the world known deposits. The classification is descriptive and can assist for general information and is in, most case, sufficient. In 2012, IAEA called a Consultancy Meeting in which experts attempted to refine the classification and to draft a tentative classification for further discussion [7]. The tentative classification proposed considers genetic aspects of the deposits known today. In general, a subdivision is given into: igneous syngenetic and epigenetic deposits, deposits occurring as the result of metasomatic and metamorphic processes and finally a suit of sedimentary deposits led by

placers. The simplified classification of four major deposit types is presented to describe major characters of the different deposit types.

### **3.1. Deposits of magmatic origin**

#### *3.1.1. Carbonatites*

Carbonatites are intrusive or extrusive rocks of igneous origin, consisting to more than 50% of magmatic carbonate minerals (e.g. calcite, dolomite, ankerite). Carbonatites are very common. Many of them show elevated contents of magnetite, apatite, fluorite, rare earth elements, niobium, tantalum, thorium minerals and others. In some cases, mineral contents can reach economic concentrations, thus bringing carbonatites into commercially used deposits. The concentration of thorium minerals rarely reaches economic grade, however, when e.g. niobium/tantalum minerals are mined, thorium would be a possible by-product, if commercially required.

#### *3.1.2. Vein-type deposits*

This type is of hydrothermal origin or a result of metasomatic or metamorphic processes. Veins occur in or close to intrusive or extrusive igneous rocks. Veins carrying thorium minerals can occur in close connection to carbonatites. The configuration of veins can vary and appear thin shape of lenses or sheet, filling joints and fissures in the surrounding rocks. Many veins are polymetallic and some contain thorianite and/or thorite.

#### *3.1.3. Deposits in alkaline rocks*

Alkaline rocks are classified as magmatic rocks with a high amount of alkali feldspar. Typical examples are alkali granites, alaskites, alkali syenites. In many cases a strict separation to peralkaline rocks is not given or is being neglected. Peralkaline rocks are typified by the excess of alkalis (Na, K) in relation to aluminium, commonly expressed as the agpaitic index  $\text{Na} + \text{K}/\text{Al}$ . The rocks of alkaline/peralkaline composition are often observed in association to carbonatites.

## **3.2. Sedimentary deposits**

#### *3.2.1. Palaeo placers*

Palaeo-placers are presented by Archean quartz-pebble conglomerates (QPC) of the Witwatersrand in South Africa, mined for gold, with uranium as by-product. The deposit contains associated thorium, which is presently not used, as well as thorium in the now dormant QPC mines in the Elliot Lake area of Ontario, Canada.

#### *3.2.2. Tertiary to recent placers*

Tertiary and recent placers are also called black sands or heavy mineral sands, indicating both the colouration as well as their composition. Placers are characterized by its unconsolidated material at beaches, shores, dunes, along rivers or streams, resulting from weathering of rocks in the hinterland. The prime economic interest is on the heavy minerals ilmenite, rutile, magnetite, garnet, zircon, sillimanite cassiterite, monazite, xenotime and others. For thorium the Ce-rare earth phosphate monazite is of interest, in which the thorium content varies from less than 1% to less than 10%, rarely reaching as much as more than 20%.

#### *3.2.3. Other sedimentary deposits*

Apart from sedimentary enrichment of thorium in placer deposits thorium may be present to interesting amounts in hard coal and lignite as well as in phosphate rocks. These are rather exceptions, however occasionally of some interest.

Thorium may be enriched during weathering of underlying rocks, resulting in residual deposits. It occurs that thoraniferous deposits are exposed to weathering during which the weathered part remains on top or close to the deposit considered. Thus, thorium minerals may be enriched to economic interesting grades. Such examples occur, e.g. in Venezuela (Cerro Impacto) and other countries. Residual enrichments of thorium are mentioned in laterites, which preferentially are developed under tropical climate. In few cases thorium is reported from coal, lignite and in phosphates. In general, concentrations are low and are currently not of economic relevance.

#### 4. RESOURCE CLASSIFICATIONS

Beside of national regulations to estimate mineral resources, e.g. the Australian JORC Code, Canadian NI 43-101, United States Geological Survey (USGS) guidelines for estimation of mineral resources, efforts were made to develop uniform, world-wide accepted systems such as the United Nations Framework Classification (UNFC-2009).

##### 4.1. OECD/NEA–IAEA classification

For uranium, IAEA in collaboration with the Nuclear Energy Agency of OECD, has agreed to introduce resource categories and cost classes. The definitions have been refined over the years, and are presently following:

- **Reasonably Assured Resources (RAR)**, are in detailed explored deposits or in parts of them, have high assurance of existence. Size, grade and configuration are known. Resources are recoverable;
- **Inferred Resources (IR)**, are in addition to RAR, based on geological evidence, in extension of well-explored deposits. Details are less known as RAR. Resources are recoverable;
- **Prognosticated Resources (PR)**, are in addition to IR. Expected to occur, mainly indirect evidence. Resource in situ;
- **Speculative Resources (SR)**, are in addition to PR. Thought to exist based on indirect evidence. Expected in a geological explored area. Resources in situ.

In lack of specific guidelines for thorium resource estimations national or international organizations prefer to apply existing regulations. Thorium resources were reported by OECD/NEA–IAEA as for uranium [3].

Cost classes used for thorium resources are not in agreement with those for uranium. Resources recoverable up to US \$80/kgTh and total thorium resources were reported only.

##### 4.2. United Nations Framework Classification–2009 (UNFC–2009)

Discussions on the harmonization of resource terminologies used by national or international organizations have been conducted during last decades and finally taken forward by the United Nations Economic Commission for Europe as the UN Framework Classification (UNFC). It is desirable to assess thorium resources accordingly, however national estimates are either old and/or not in agreement with the requirements of UNFC-2009, the current version. UNFC-2009 uses three major classes E, F, and G [14].

- E describes the economic state of project development, where E1 refers to resources economically viable under current market conditions, E2, E3 ff are of lower or nil current economic interest;
- F determine the degree of feasibility, where F1 stands for confirmed feasibility, F2, F3 ff have gradually lower degrees of feasibility;
- G characterizes the geological knowledge of resources. G1 stands for estimates with high level of confidence, and consequently G2, G3 ff are of lower levels of confidence.

It is desirable to assess thorium resources accordingly; however, national estimates are either old and/or not in agreement with the requirements of UNFC–2009.

## 5. THORIUM RESOURCES

OECD/NEA-IAEA started in 1965 with the collection of thorium resource data and continued to report with interruptions until recently [3]. Independent, resource data were reported by [1] and [2]. A renewed interest for resource data was initiated by the IAEA in 2010 with a Consultancy Meeting [15]. Together with a database on World thorium deposits and their characteristics (ThDEPO), a publication was launched in order to compile available information [7]. World total thorium resources were estimated in 2014 at more than 6.2 million t Th. An overview of geographic areas is given in Table I.

TABLE I. TOTAL THORIUM RESOURCES OF THE WORLD (1000 T TH)

| Region       | Resources | Percentage |
|--------------|-----------|------------|
| Asia         | > 2 500   | > 40       |
| America, N+S | 1 700     | 27         |
| Europe       | 720       | 12         |
| Africa       | 650       | 10         |
| Australia    | 595       | < 10       |
| Total        | > 6 200   | ~100       |

Figures in Table I represent total thorium resources, regardless of category or cost class mentioned in Sections 4.1 and 4.2.

In Table II, total resources for major countries is provided.

TABLE II. MAJOR THORIUM RESOURCES (1000 T TH)

| Country      | Resources | Percentage<br>(% of total) |
|--------------|-----------|----------------------------|
| India        | 846.5     | 13.6                       |
| Brazil       | 632       | 10.2                       |
| USA          | 595       | 9.5                        |
| Australia    | 595       | 9.5                        |
| Egypt*       | 380       | 6.1                        |
| Turkey*      | 374       | 6.0                        |
| Venezuela*   | 300       | 4.8                        |
| Canada       | 172       | 2.8                        |
| South Africa | 148       | 2.4                        |
| Total        | 6 212     | 100.0                      |

\* Historical estimates

## 6. RECOVERABLE RESOURCES

For the estimation of recoverable resource data published in the RED BOOK 2009, category Reasonably Assured Resources (RAR), recoverable at less than US \$80/kg Th, can be used. If available, updates were included in the estimates, however not all data were updated recently. Considering inaccuracies, the world total in the category RAR is estimated at 829 000 t Th for 7 countries specified. Others, not specified are included.

The majority of resources in this category was reported 2009 for India at 319 000 t Th, occurring mostly in placer deposits. A recent information [16] reported identified resources of about 260 000 t Th, contained in monazite of placer origin, grading between 0.02 and up to 5% Th. Additionally about 160 000 t Th were reported in monazite low grade (~ 0.02% Th and below). Amounts of recoverable thorium were not reported.

In 2009, USGS reported updated figures on thorium resources [17] of about 170 000 t Th as ‘reserves’, without cost classes. About 2/3 are located in vein-type deposits. It is not mentioned whether the term ‘reserve’ is used to determine the recoverability and their costs.

In an update, Australia has reported in 2009 reasonably assured resources recoverable at less than US \$80/kgTh at 46 000 t Th [RB 2009] to 76 000 t Th [19], the majority in placer deposits at different locations and with different size.

Brazilian recoverable resources are estimated both for carbonatites and placers, as well for other types [20]. Depending on the type, recovery of thorium will as a by-production. Thus, the estimates vary between 172 000 and 300 000 t Th.

Taking the recently estimated resources of the four countries above, which are classified here as identified they amount to 650 000 to 800 000 t Th.

Estimates of resources expected to be recoverable under assumptions of the categories used by IAEA are presented in Table III.

TABLE III. EXPECTED RECOVERABLE RESOURCES (1000 T TH)

| Country      | Resources<br>(1000 t Th) |
|--------------|--------------------------|
| India        | 260, identified          |
| USA          | 170                      |
| Brazil       | 170–300                  |
| Australia    | 76                       |
| Russian Fed. | 75*                      |
| Greenland    | 54                       |
| South Africa | 18                       |
| Others       | 23                       |
| Total        | 846–976                  |

\* estimated

## 7. THORIUM PROVINCES

More than 90% of world total thorium resources are attached to four major deposit types, carbonatites, veins, alkaline/peralkaline rocks and placers. The first three types often occur together in magmatic rock provinces, leaving placers as a separate, sedimentary type. Placers are in most cases geographically not related to the other three types, however minerals of economic importance in placers derive from magmatic and or metamorphic rocks in the hinterland.

### 7.1. Provinces in magmatic associations

Carbonatites, peralkaline/alkaline rocks and associated veins are characteristic for silica-undersaturated magmatic provinces. Carbonatites are defined as magmatic rocks with more than 50% carbonate minerals (calcite, dolomite, ankerite and others), formed by complex processes. Peralkaline rocks are characterized by the ratio  $(\text{Na}_2\text{O} + \text{K}_2\text{O})/\text{Al}_2\text{O}_3 > 1$ . A common feature of carbonatite and peralkaline/alkaline rocks is the enrichment of minerals of the rare-earth elements group (REE), Y, Nb, Ta, Zr, Th, U, and other minerals, however not all have economic grades. A similar composition may occur in veins, related spatially and possibly genetically to the above rocks. A common feature for the occurrence of carbonatite, peralkaline/alkaline rocks and veins is their association to geological shields of alkaline character. In a Consultancy Meeting of the IAEA in September 2013 [21] some characteristics of thorium provinces have been reviewed. A preliminary compilation shows for the association of carbonatites, peralkaline/alkaline rocks and associated veins areas e.g. on the Fennoscandian Shield (Norway, Sweden, Finland, western part of the Russian Federation [Kola Peninsula]), Greenland, western part of the Canadian Shield, Rocky Mts Province, Brazilian Shield, Guiana Shield, West African Craton, East African Shield, and Shield areas in Australia. An example of vein-type deposits occurs in South Africa, and possibly other vein-type.

### 7.2. Provinces in the sedimentary environment

Sedimentary provinces for thorium deposit occur preferential in coastal areas of the continent, characterized by thorium in placer deposits. Examples are Coastal India, coastal areas in Australia, Brazil, Atlantic coastal plains of the United States, Nile river delta in Egypt, various coastal areas in Asia. Other sedimentary occurrences, such as coal, lignite, phosphate etc are scattered and may not regarded as accumulations in provinces.

## 8. FINAL REMARKS

Although knowledge on thorium resources is less confident compared to other minerals, it seems to be worthwhile to report information scattered in various papers. Present demand for thorium is low and certainly will remain on low levels until commercial requirement for nuclear reactors arises. Requirement for thorium can mainly be satisfied by recovering the metal as a by-product of other minerals/elements. In the first instance requirement would be covered if thorium is extracted chemically from monazite, a product of placer mining. Production of monazite is not difficult and requires dredging of heavy mineral sands, physical separation of mineral components and refining to clean monazite. Thorium extraction from monazite however requires several chemical processes using sulphuric acid at elevated temperatures, and separation by organic compounds. Production of the refined end product is costly. At present thorium is extracted from monazite in few countries only. At the beginning of the 21st century the extraction of around 6000 to more than 7000 t of monazite annually is reported, with India being the largest producer. The theoretical content of thorium in monazite mined is estimated between 300 and 600 t Th annually. If this amount would be extracted it would be sufficient for initial fuel loading of 6–12 thorium operated nuclear reactors. Known total resources of more than 6 million t Th are far beyond of any optimistic demand. Even estimated resources, expected to be economic under present conditions (RAR <US \$80/kgU), amounting between 600 000 and 800 000 t Th [7], are sufficient for expected future requirement.

## REFERENCES

- [1] BARTHEL, F.H., DAHLKAMP, F.J., Thorium deposits, Gmelin Handbook of Inorganic and Organometallic Chemistry; Suppl. Vol. A1b, Springer (1991) 345–432.
- [2] BARTHEL, F.H., DAHLKAMP, F.J., “Thorium deposits and their availability”, New developments in uranium exploration, resources, production and demand, IAEA-TECDOC-650, IAEA, Vienna (1992) 104–115.
- [3] ORGANISATION FOR ECONOMIC CO-OPERATION AND DEVELOPMENT NUCLEAR ENERGY AGENCY, INTERNATIONAL ATOMIC ENERGY AGENCY, Uranium Resources Production and Demand, OECD, Paris, editions 1970-1986, 2009 and 2011.
- [4] BARTHEL, F.H., "Thorium and unconventional uranium resources", Fissile material management strategies for sustainable nuclear energy (Proc. Tech. Mtg Vienna 2007), STI/PUB/1288, IAEA, Vienna (2007) 199-215.
- [5] WORLD NUCLEAR ASSOCIATION, Thorium, <http://www.world-nuclear.org/info/current-and-future-generation/thorium/>.
- [6] World Thorium Resources, IAEA Tech. Mtg, Thiruvananthapuram, India (2011).
- [7] INTERNATIONAL ATOMIC ENERGY AGENCY, World Thorium Occurrences, Deposits and Resources, IAEA, Vienna (in preparation).
- [8] CUNNEY, M., Genesis of thorium deposits, paper presented at IAEA Tech. Mtg on World Thorium Deposits, Thiruvananthapuram, India, 2011.
- [9] KOTOVA, V.M., SKOROVAROV, J.I., “Thorium Deposits in the Commonwealth of Independent State and their prospective characteristics”, Changes and Events in Uranium Deposit Development, Exploration, Resources, Production and the World Supply-Demand Relationship, IAEA-TECDOC-961, IAEA, Vienna (1997) 213–220.
- [10] CUNNEY, M., Uranium and Thorium: The Extreme Diversity of the Resources of the World’s Energy Minerals, Non-Renewable Resources Issues, Geoscientific and Societal Challenges, (SINDING-LARSEN, R., WELLMER, F.W., Eds), Springer (2012) 91-129.
- [11] CUNNEY, M., Univ. Lorraine, Une classification genetic des gisements de thorium, written communication, unpublished manuscript, 2011.
- [12] ORGANISATION FOR ECONOMIC CO-OPERATION AND DEVELOPMENT NUCLEAR ENERGY AGENCY, INTERNATIONAL ATOMIC ENERGY AGENCY, Uranium 2011: Resources, Production and Demand, 2012, OECD, Paris (2011).
- [13] GREAVES, E.D., “Impacto, Venezuela’s Thorium Deposit”, paper presented at IAEA Tech. Mtg on World Thorium Deposits, Thiruvananthapuram, India, 2011.
- [14] UNITED NATIONS FRAMEWORK CLASSIFICATION FOR FOSSIL ENERGY AND MINERAL RESOURCES, ECE Energy Series No. 39, UN, New York and Geneva (2010).
- [15] Development of an Information System on World Thorium Resources (ThDepo), IAEA Consultancy Mtg, IAEA, Vienna, 2010.
- [16] CHANDRASEKARAN, S., “India’s strategy for thorium utilization”, paper presented at IAEA Consultancy Mtg on ThDepo, Vienna, 2012, Vienna.
- [17] VAN GOSEN, B.S., GILLERMAN, V.S., ARMBRUSTMACHER, T.J., Thorium Deposits of the United States – Energy Resources for the Future?, USGS Circular 1336 (2009).
- [18] ORGANISATION FOR ECONOMIC CO-OPERATION AND DEVELOPMENT NUCLEAR ENERGY AGENCY, INTERNATIONAL ATOMIC ENERGY AGENCY, Uranium 2009: Resources, Production and Demand, OECD, Paris (2010).
- [19] MIEZITIS, Y., Thorium, Australian Mines Atlas Geoscience Australia, Canberra (2009).
- [20] VILLAS-BOAS, R., Centre for Mineral Technology, Brazil, Thorium in South America, personal communication, 2011.
- [21] Consultancy Mtg and Tech. Mtg on Thorium Resources and Provinces, IAEA, Vienna, (2013).

# **SOLVENT EXTRACTION OF URANIUM — TOWARDS GOOD PRACTICE IN DESIGN, OPERATION AND MANAGEMENT**

P. BARTSCH\*, S. HALL\*\*, S. BALLESTRIN\*\*\*, A. HUNT\*\*\*

\* Alchemides Pty Ltd,  
Mile End, South Australia,

\*\* Uranium South Australia,  
Norwood, South Australia,

\*\*\* Uranium One Australia Pty Ltd,  
Adelaide, South Australia,

Australia

## **Abstract**

Uranium solvent extraction (USX) has been applied commercially for recovery and concentration for over 60 years. Uranium in acidic leach liquor can be treated through a sequence of operations; extraction-scrubbing-stripping, to obtain purified strip liquor, and hence precipitation of marketable products, e.g. converter grade yellowcake or Uranium Ore Concentrate. The practices of design and operation of USX facilities has found renewed interest as new mines are developed following decades of industry dormancy. Development of the Olympic Dam and Honeymoon operations in Australia has led to innovative design and operation of pulsed columns technology in applications of solvent extraction. This article seeks to outline principles of design and operation from the practitioner's perspective. The discussion also reviews historical developments of USX applications and highlights recent innovations. This review is hoped to provide guidance for technical personnel who wish to learn more about good practices that leads to reliable USX performance.

## **1. INTRODUCTION**

This paper provides a brief summary of practical knowledge and lessons learnt in the field of uranium recovery by solvent extraction, (SX) from testwork, through design to production. These suggestions, clarifications and observations are offered on the basis of the authors' experience which are hoped to encourage constructive discussions in the hydrometallurgical community, and thereby improve solvent extraction performance in current and future facilities.

## **2. FOUNDATION CHEMISTRY**

Uranium solvent extraction (USX) involves exchange of dissolved metals, as complex ionic components, from an aqueous phase into an organic phase or solvent. The organo-metal complexes may be purified by scrubbing, before they are subsequently stripped into a more pure, concentrated aqueous phase. The soluble, metal complex, or ion-pair, is chemically loaded by an extractant, which is dissolved in a hydrocarbon diluent [1] which together form the solvent. An exchange of metal ion pairs will allow a charge balance to be maintained across the transfer interface (cations or anions will be exchanged depending on the selected extractant). Interested readers can learn more detailed chemistry of USX in useful texts [2–5].

## **3. SX FEED CONTROL**

The most important feature for good SX practice is stable stream flow, particularly pregnant leach solution, (PLS) and hence steady process chemistry. Every effort of designers, and the eternal vigilance of operators, must be aimed at consistent rates and composition of feed streams, and thereby internal and recycle streams. Realistic sizing of PLS storage, as well as sensible make-up capacity for reagent streams are essential aspects for reliable performance of a SX facility. Operators must expect that crud,

which is a generic term for dispersed solid phases that accumulate in settlers, [6] will occur. Adequate systems and procedures must be installed and maintained to collect and treat this nuisance material so that reliable flows and hence performance can be maintained.

The relative performance of extraction, scrubbing and stripping can be characterized by coefficients for uranyl complexes which will shift with the overall sulphate and chloride concentrations in the respective aqueous phase [7]. Testwork for process specification must be conducted with representative solutions' chemistry and temperatures, and transfer results interpreted for process criteria. Interpretation of kinetic and equilibrium effects will be important. For example, SO<sub>4</sub> levels in PLS may rise to over 100 g/L [8], while few uranium leaching operations have operated with 'high' Cl concentrations, e.g. above 5 g/L. The Honeymoon Project [9] has operated in-situ recovery in a saline aquifer with about 8 g/L Cl in PLS, and use solvent extraction for uranium purification [10].

PLS may contain significant nitrate which can depress uranium transfer. Nitrosyl in sulphuric acid, (NOHSO<sub>4</sub> reported as NO<sub>x</sub>) at levels of above 50 ppm may be present in delivered acid that is manufactured from smelter gases [11]. Hydrolysis to nitrates, together with contamination from residual explosives in mined ore means nitrates can accumulate in PLS depending on the closure of the process water balance [12].

For each impurity that is partially transferred through various scrubbing or stripping stages selective precipitation, or re-leach, can be investigated as potential flowsheet additions to ensure the specifications of customers, (i.e. uranium converters) are met for marketed products [13]. In this respect detailed quantification of PLS chemical speciation is interesting for process optimization, but largely superfluous compared to the leach chemistry in respect to selecting an economic or preferred flowsheet, unless precipitate specifications are threatened.

#### 4. PROCESS STAGES — EXTRACTION, SCRUBBING AND STRIPPING

##### 4.1. Solvent extraction

Cationic or neutral extractants, i.e. long-chain alcohol, phosphoric derivatives, were first proposed for uranium recovery from PLS, [14] but were superseded by amines due to greater selectivity. These reagents are no longer used alone for uranium recovery from PLS, but are popular for yellowcake purification at converter operations. Organic phosphate derivatives are commonly used for purification of uranium concentrates or oxides following digestion with nitric acid where the purpose is the removal of anion impurity fractions, e.g. silicates, sulphate and zirconia.

Mixed solvent, i.e. cationic and anionic extractants applied in the same transfer stage, was first described in reports from Colorado [15]. Operations at the Durango facility with mixed solvent were described. Application of mixed solvent, together with a neutral modifier, (tri-butyl phosphate, TBP or di-butyl-butyl phosphonate, DBBP) were investigated at Honeymoon for treating PLS that contains elevated Cl in process waters [16]. The Honeymoon project has included the first application of solvent extraction combined with in-situ leaching for recovery of uranium [17], but was under 'care and maintenance' at the time of writing.

Anionic extractants such as proprietary tertiary amines, (i.e. organic, nitrogen compounds with three alkyl chains in liquid form) have become favoured for uranium recovery from acidic PLS because base metal impurities are efficiently rejected into raffinate. Silica and halides, (F, Cl, Br) can form simple anions, and some transition metals form soluble complexes, e.g. V or Mo as oxy-anions, Co as cyanide, Bi as oxy-chloride, or Fe in the presence of chloride, are also extracted by amines [18].

Certain additives tend to inhibit third phase formation that can arise as semi-miscible fluids of extractant-metal salts which separate and accumulate at the phase interface within settlers [19]. Solvents that contain amines often utilize modifiers such as long chain alcohols, iso-decanol or tri-decanol, at about half the extractant concentration, (%v/v).

Dosing the solvent with mixed polarity modifiers can influence the uranium extraction co-efficient, hence lowering extraction of uranium in amine systems. Modifiers in cationic solvents include TBP and DBBP, which can have synergistic influence to improve uranium extraction [20]. Appearance of a third phase is more prevalent during high extractant or uranium concentration due to the potential formation of organo-metallic salt.

Management of solvent degradation can become an operational challenge in SX circuits with high nitrate or ferric concentrations in PLS. Declining extraction performance, or extended phase break time are indicators that solvent properties require improvement. Where SX facilities have high organic entrainment in raffinate, or include solvent bleed streams that dispose of excess crud, the degradation products may not reach nuisance levels. In this respect the control of PLS chemistry is a good strategy, while uranium leaching rates and extent are managed, with acid and oxidant dosing for pH and Eh control, to reach economic levels. Alternatively, PLS treatments to lower its chemical potential are also available, e.g. dosing with metallic iron or sparging with pure SO<sub>2</sub> gas.

Bisulphate loading at high PLS acid level can suppress uranium extraction when leaching solution contains above 10 g/L free acid in SX feed. Controlled acid in PLS will offer benefits of economic leaching and SX performance [21]. Lower acid levels for leaching are recommended, consistent with reaching uranium dissolution and mass transfer targets, as well as balancing silica dissolution, and accounting for downstream PLS and raffinate or tailings treatment costs.

Given the rapid kinetics of sulphate, bisulphate and uranyl sulphate exchange on solvent in the extraction stage, the relative loadings of U will quickly reach equilibrium. While the PLS has pH between 1.5–2.5 the stage-wise extraction equilibrium is usually available within 1–2 minutes of mixer retention, depending on mixer box design and mass transfer gap [22]. Stage design with twin or triple sequenced mixer boxes may be cost effective to obtain efficient mass transfer and adequate residence time distribution with low temperature PLS.

Loading and distribution of uranium on amine extractant will generally improve with increasing acidity of PLS. Adjustment of PLS with dilute sulphuric acid to lower pH to improve extraction performance has been mentioned at ERA's Ranger operation [23]. The solvent performance can also shift with PLS sulphate and chloride concentration. Each system must determine the competition of uranium and other anions in highly saline PLS with operating solvent, and allow for cost of reagent inputs.

#### **4.2. Solvent scrubbing**

Solvent scrubbing can be applied advantageously between extraction and stripping to displace anionic impurity from amine based solvents, or metal cations from phosphate based solvents. Water scrubbing can wash out entrainment of PLS from the advancing solvent.

The number of scrub stages and make-up of scrub liquor will depend on the impurity type and relative loading on solvent compared to uranium. Dilute sulphuric acid, low chloride water, or strip liquor bleed, i.e. ammonium sulphate solution, can be used in 2 or 3 sequential scrub stages [24].

Generally, spent scrub liquor will be recycled to the PLS pond, or directly into the extraction feed stream, to permit recovery of the contained uranium. Process stability and entrainment are also important criteria for the choice of scrub stages and stream recycle destinations.

#### **4.3. Solvent stripping**

Strong ammonium or acid sulphate solutions, ca > 150–300 g/L SO<sub>4</sub> can be used for uranium stripping from tertiary amine extractants [3]. In this process step the sulphate concentration is the dominant chemical which displaces the uranyl sulphate into the aqueous phase, while ammonia gas or solution is applied to regulate pH. Stripping with strong sulphate solution is preferred above dosing with ammonium hydroxide, (aqua-ammonia) due to more stable operation. Sulphate strip chemistry can avoid

localized, high pH which can cause premature precipitation of yellowcake in settlers and hence subsequent crud generation.

Stripping kinetics can be accelerated at marginally higher pH or increased solution temperature. Stage-wise control of pH rise across the stripping must be graduated. Tightly regulated stripping chemistry may be countered by pH regulation difficulties, or the presence of excessive crud.

Stripping with strong ammonium sulphate solution is preferred if the yellowcake precipitation process uses ammonia gas to make ammonium di-uranate as a marketable product. Residual ammonium in tailings liquor, which arises from the stripping process, cannot be released off the mine site. Hence ammonia recycle via lime boiling, or production of ammonium sulphate from evaporation, will be a necessary flowsheet inclusion.

Strong acid stripping can be attractive for flowsheets where acid, and caustic or magnesia for neutralization, are low cost and high quality. Acid stripping can avoid the need for a solvent regeneration stage and potentially simplify the overall SX circuit design. Carbonate stripping will be preferred when uranyl peroxide is the desired form of yellowcake or sulphate stripping is undesirable for environmental reasons [25]. The maximum uranyl concentration in strip liquor will be determined by the extractant concentration, and impurity loading, to ensure product specification, or avoid third phase formation in the strip stage.

## 5. PROCESS STABILITY

SX facilities will meet the design criteria when the feed flow and concentrations, particularly the uranium tenor, have low variability. Changes to PLS flow control set-point once per day are recommended, while efforts to minimize swings in uranium and impurity tenors, and hence mass rates, will be beneficial to overall production. Otherwise the SX operator will need to vary the PLS flow proportionally to the uranium tenor to maintain productivity, i.e. constant ‘metal’ feed rate.

PLS, scrub or strip aqueous phase flow variations will induce the respective settler interface level to rise or fall progressively through the sequence of settlers. A stepped flow increase can displace crud from the settler interface to the next mix box where more crud will be generated due to the turbulent intensity at the impeller tip. The transmission of excess crud in sequential mix boxes can promote crud generation through the entire system, i.e. ‘crud begets crud’.

Large storage volume can subdue fluctuations of PLS uranium tenor. An added benefit of thoughtful design will be suspended solid removal, which can be available from a generously sized PLS pond. Minimization of PLS storage volume is poor design practice that is often driven by misguided efforts of project managers to cut facility capital costs prior to startup, without accounting for overall life-cycle costs of the asset. Zealous cost cutting can also compromise equipment selections for cleaning PLS such as filters or clarifiers. Dynamic process simulation can be helpful to optimized sizing of process storages for hydrometallurgical facilities [26].

Stable PLS tenor is an important ally for operators to control impurity transfer. If the loaded solvent carries high impurity loads then scrub liquor concentrations can be adjusted to suit anion transfer rates. Progressive process startup, shut-down and changes to phase ratios of each stage can be managed carefully to avoid unplanned crud displacement, and transient impurity transfer though to final product.

For high uranium concentration in PLS, the SX plant could be run with alternative series-parallel extraction configuration, while the raffinate is recycled to ore leach. This design option will be determined by mine plans but is unlikely to become favoured for new plants that have low ore grade and do not recycle process waters or discharge raffinate to tails.

## 6. SX EXCHANGE EQUIPMENT

Process engineers will apply results from relevant extraction, scrubbing and stripping investigations to prepare ‘isotherms’ which are derived from shake-out test data, or pilot plant testwork, and obtained with varying ratios of PLS and solvent. The relevant test techniques and interpretation procedures are generally known in technical literature [27].

McCabe-Thiele diagrams are constructs of uranium distribution or concentration profiles across various ratios of equilibrated aqueous and organic phases, using results from laboratory or pilot tests run at pre-determined conditions and constant temperature, i.e. graphical isotherms [28]. Such interpretations are used to generate process criteria, e.g. flow ratios of solvent to aqueous. Design criteria can then be specified and applied to equipment sizing and selection, including mixer-settler units or columns for extraction [29].

Initial SX investigations for pre-feasibility, and consequent preliminary designs may be done with synthetic solutions. Experimental programs based on actual leach solutions can be used for confirmation of process criteria during the various study stages, and hence detailed plant design. Fresh solvents can be used for preliminary shake-out tests, but aged or used solvent is recommended when process designs are used for final feasibility studies. The choice to run continuous mini-rig or pilot solvent extraction investigation will depend on the degree of innovation of process chemistry, flowsheet, equipment or unusual impurity occurrence. Testwork must be conducted by experienced technicians, and guided by practitioners who can translate the isotherms into design criteria and equipment sizing.

Two major types of equipment are used for extraction of uranium from PLS; namely mixer-settlers and agitated columns. Materials of construction for hydrometallurgical plants and equipment include lined or stainless steel or lined concrete [30]. Fibre reinforced plastic bodies and linings have become popular for small mixer settlers, as well as columns for primary uranium extraction applications.

Columns evolved from designs in the nuclear industry for purification of numerous metals including uranium [31]. Column size and capacity have increased in recent installations, e.g. Olympic Dam. Columns are suited to multiple stages of extraction in a single unit consisting of active section with top and bottom decanters, and throughput is limited by hold-up of the dispersed phase. Columns can provide effective performance when mass transfer of uranium is relatively rapid, e.g. in extraction stages. Multiple columns, which operate in parallel, to accommodate larger flows, can be installed as determined by total flux, i.e. total PLS feed plus advance organic flow rates per unit area of cross section. Columns may also be advantageous in comparison to mixer settlers due to lower, overall solvent inventory, or when advance phase ratios are widely different [32].

Mixer settlers were also originally developed in the nuclear industry [33], while design improvements and scale-up was driven by copper extraction. These units have become popular for all transfer stages during the late 20th century [34].

For extraction mixers the turn-down ratio of organic recycle over a wide range is useful for maintaining organic phase continuity. Likelihood of phase inversion arises if the mixer O:A occurs below 0.9:1.0 for extended durations. The authors experience suggests that organic continuity in extraction mixers is essential for management of emulsion break time and maintaining lower solvent losses by entrainment, i.e. avoidance of phase inversion. The effect of phase ratios and continuity on transfer of anions can be optimized with trials during commissioning and operation, and will depend on mixer retention time and potential for unwanted transfer by entrainment.

Overall process operation, and interface control in columns, can be easier than mixer settlers, particularly with respect to flow regulation and crud removal. Metal loading characteristics of columns in terms of approach to equilibrium are usually rapid following changes to PLS metal inputs. Operators’ control of uranium loading in columns, or control of O:A holdup, have little influence on uranium transfer kinetics or equilibrium if the columns designs and scale-up are reasonable.

Extraction columns may run at O:A phase ratio at up to 1:10, whilst maintaining organic continuity of the hold-up emulsion, depending on PLS conditions, particularly suspended solids and temperature. Above this phase ratio ‘inversion’ of the emulsion continuity may occur, or carry-over of solvent into raffinate may become excessive or intolerable. Operators’ immediate response to changes of PLS flow or tenor in columns will be startup or shutdown of individual columns.

Columns can be idled while full to permit rapid re-start and avoid excess tank inventory of solvent. Sufficient solvent storage is needed outside the columns to allow individual column drainage of fluids for maintenance.

Columns for extraction will generally use more power than mixer settler configurations for the same duty if agitation is driven by pulse air, although direct comparison will depend on location and design criteria for the proposed operation [35]. The installed power for mixer impellers is more efficient than supply of pulsing air from blowers, but the number of mixers is often more than the number of blowers. Mechanical or hydraulic agitation designs for columns are not commercially available for PLS applications, but smaller installations for yellowcake purification and nuclear fuel reprocessing are available.

Columns are designed as closed vessels, (except for pulse air vents), with low roof space. Given good design columns can have greater fire suppression attributes, particularly if solvent purge or dump is arranged with due consideration of piping corridors. Columns will require more attention to piping detail during design to ensure adequate support and maintenance access are installed.

## 7. SOLVENT CONDITION

A separate protonation or acidification stage is redundant while SX feed contains about 5–10 g/L acid. The recycle of spent scrub liquor to join PLS will lower its pH, which will assist process control if the upstream leach conditions are variable. In-line dosing of recycle or acid streams are a design opportunity if intermediate, sectional storages are available. Direct dosing of ‘neat’ acid into solvent streams must be avoided due to localized over-heating and oxidation.

Mass transfer of uranium through solvent scrubbing and stripping also tend to be relatively rapid, but retention may be dictated by dispersion and stability of reagent dosing for pH control. Equilibrium transfer of impurities during stripping can require 1–5 minutes retention per stage depending on solution chemistry, temperature and mass transfer gap.

Regeneration of solvent is recommended if degradation products or interfering long-chain organic anions, e.g. carboxylates, accumulate in the running solvent. Such contaminants can be scrubbed from solvent in a separate stage with highly alkaline liquor, ca > pH 10 [36].

The effectiveness of regeneration can vary with the recipe of the wash liquor, which will depend on contaminant type and load, by systematic experimentation. Strength of the regeneration liquor and campaign intensity will depend on extent of solvent deterioration as measured by break time. The Olympic Dam facility applied a three-component mix [37], but operators will necessarily develop or procure their own recipe.

A routine, laboratory, maximum-loading test can assess the capability limit of the working solvent. Such tests which trend solvent performance over extended time frames. Tracking phase break results from regular testing of the plant solvent are useful to determine when regeneration is required.

## 8. PHASE DISENGAGEMENT

The specific settling rates for uranium solvent extraction plant design are determined by design SX feed and solvent flow rates, with an allowance for crud interference. Experimental tests on pure fluids tend to overestimate the rate of phase break. Useful methods to assess phase disengagement in operating

plants includes regular, standardized break tests, e.g. separation of emulsion in 1L cylinder, on loaded and stripped solvent during each shift. A simple procedure can be established for use by plant personnel.

Specific rates for conventional settlers are generally set at 3–5 m<sup>3</sup>/m<sup>2</sup>/hour depending on extractant concentration, ionic strength, solvent temperature and expectation of crud make and accumulation, [38]. Recent settler designs are proposed to enhance specific flow rates up to 5–15 m<sup>3</sup>/m<sup>2</sup>/hour, but potential for increased entrainment losses are not quantified. The flow pattern of emulsion from the mixer overflow to the settler will influence separation and solvent circulation. Installation of ‘picket’ fences within the settler box, located in proximity to the incoming flow, which spreading of organic-continuous emulsion from the mixer overflow into the solvent layer, are recommended.

Specific settling rates for pulse columns, when treating ‘clean’ PLS can be between 20–50 m<sup>3</sup>/m<sup>2</sup>/hour for the active, pulsing section. The total flux will depend on extractant concentration, solvent condition and system temperature.

Without diligent or automated crud removal a conservative settling rate is recommended. Recent design for scrub and strip stages have applied comparatively low settler rates due to the prevailing high crud content. Scrub and strip settlers do not generally receive suspended ore particles and silica solids, so crud management, and hence design settling rates will depend on precipitation of silica, zirconia or other impurities as observed during pilot trials.

## 9. CRUD FORMATION AND HANDLING

Suspended solids in PLS will enter USX following poor clarification of PLS. Dissolved species, such as silica and zirconia, have the potential to generate crud during solvent extraction processes.

Soluble silica in PLS becomes a problem when it polymerizes and converts to sub-micron colloidal, or larger particulate form [39] which can carry into the extraction, scrubbing and stripping sections. The silica colloids change in size as the silica polymerises and different size colloids can cause crud generation problems in different parts of the SX circuit [6].

Slimed ore particles and floating floccules from clarification can contribute to PLS solids loading and hence crud make in extraction settlers. These colloids and particles will tend to build up at the settler fluid interface, which causes stable emulsion build-up, and can restrict hydraulic throughput or lead to increased solvent losses [40].

Silica content of PLS, as a forward measure of potential crud make, can be determined quantitatively by laboratory filtering at defined filter pore sizes. Visual field observation of PLS solids, e.g. sighting in a clarity wedge, can be useful for rapid operator intervention. Field operators can collect ‘dip’ samples from each settler with a clear plastic tube, and thereby track crud build-up.

Maintenance of organic phase continuity in all SX mixers for uranium will limit crud formations and so limit crud build-up in settlers. In extreme circumstances bulk crud flows between settler banks can occur, otherwise known as ‘crud-runs’, which leads to higher solvent losses and poor metallurgical control.

Crud handling and treatment is important to recover solvent and lower metal losses [41]. All uranium SX plants will experience crud formation and good plant designs will accommodate its removal and treatment. The design philosophy for PLS preparation as SX feed can best focus on prevention as compared to cure or remedial action. While less silica is dissolved during lower intensity leaching, and if more silica is precipitated and flocculated during PLS clarification, then less crud can be expected to accumulate in extraction settlers. Crud in downstream scrub or strip settler is often related to impurity transfer during unstable pH control.

Careful observation and impurity tracking during pilot testing can help designers and operators gain control of anion transfer and set stage pH targets. Preventative measures to avoid the deleterious effects of silica and crud include:

- a) Control leach temperature, retention and acidity:
  - Extended retention time at lower temperature can ensure effective uranium dissolution;
  - Higher acid levels will tend to dissolve more silicate minerals and consume more acid;
  - Two stage leaching can keep final leach temperature down and conserve acid but at higher capital cost for installation of a second leach thickener or cyclone bank;
- b) Minimize slime formation during grinding particularly of ores with clays or foliated silicates;
- c) Operate effective PLS clarification; note that one stage of sedimentation will have difficulty reaching below 50–100 ppm suspended solids in SX feed when process upsets occur. A second clarifier with steady flow and deep bed operation can polish PLS to about 20–50 ppm;
- d) Provide a PLS pond with large retention volume; e.g. one day minimum, (not recommended), three days is good practice while one week will be preferred by operators. Capability to remove settled or flocculated particulates from floor of pond will provide benefits by lower solvent losses;
- e) Heat the clarified PLS before SX feed to remove super-saturation of silica and gypsum. Direct steam injection of PLS, or allow heating of the recycled, spent scrub liquor will tend to re-dissolve colloidal silica.

Silica polymerization and aggregation can be modified by anion or cation concentrations in PLS [42]. Many solutes will form ion-pairs, e.g. Al and F, which can influence the relative effects of dissolved species including silica. Variable solute concentrations in PLS can complicate diagnosis of silica deportment and subsequent clarification and crud control measures.

## 10. MOST RECENT USX PROJECT — HONEYMOON URANIUM

Solvent extraction was chosen as the preferred uranium recovery technology at Uranium One's recently operated Honeymoon Project in South Australia. The Honeymoon project was discovered in the 1970s, and field leaching trials were conducted in two campaigns; 1982 [9] and 1998 [43]. Industrial scale production eventually started in 2011, but was shut down and placed on care and maintenance in 2013 due to low uranium prices. The flowsheet is unique due to the coupling of solvent extraction with in situ leaching, and was chosen to mitigate the effect of high salinity of the leach solutions, > 5000 mg/L chloride content [44].

### 10.1. Honeymoon USX process description

The Honeymoon Project was designed with a capacity to enable production of 400 tonnes per annum (tpa) U<sub>3</sub>O<sub>8</sub> equivalent, (as uranium peroxide (UO<sub>4</sub>.2H<sub>2</sub>O)). The uranium peroxide produced at Honeymoon is obtained through conventional in-situ recovery (ISR) methods of the Honeymoon wellfields, followed by a solvent extraction (SX) plant to concentrate and purify the uranium contained in solution. The uranium in the SX plant loaded strip solution is precipitated in the peroxide form to produce yellowcake slurry which is then de-watered via thickening in the precipitation and thickening (P&T) area. Thickened slurry is further washed and dried in the drying and packing plant (D&P) where moisture is removed by indirect heating using thermal oil with the final product packaged into 205L drums capable of containing approximately 300 kg of final uranium oxide concentrate (UOC) product. The process plant is intended to operate at 96% availability for 365 days a year, based on two 12-hour operating shifts per day.

The SX plant at Honeymoon receives feed solution containing uranium and other impurities (chloride and iron) from the PLS pond which has a capacity representing < 1-day surge capacity. The PLS is fed at a nominal flow rate 690 m<sup>3</sup>/hr to the extraction stage comprising two Pulsed Columns operating in parallel at a volumetric A:O phase ratio of 20:1 and a design U<sub>3</sub>O<sub>8</sub> recovery of 93%.

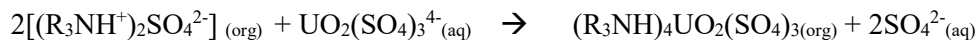
The SX process uses a unique combination of organic reagents to extract uranium from the PLS, including approximately; 2% (v/v) Di-2-Ethyl Hexyl Phosphoric Acid (DEHPA), 2% (v/v) Alamine® 336, and 3% (v/v) Tri-Butyl Phosphate (TBP); all diluted in a suitable organic diluent, in this case Shellsol® 2046. Due to the presence of iron and chloride impurities in the PLS, the combination of all three organic reagents is required for uranium extraction at Honeymoon.

DEHPA is an acidic extractant, exchanging protons for metal-bearing cations (cation exchange process) and is capable of extracting uranyl cation on its own, as below:



Unfortunately, since DEHPA also extracts iron (as ferric,  $\text{Fe}^{3+}$ ), uranium extraction is less selective in the presence of soluble iron of which Honeymoon has in abundance in the PLS, partly as ferric ions.

The tertiary amine, Alamine 336, a common uranium extractant, undertakes anion exchange, rather than the cationic exchange of the DEHPA, as below with the sulphate anion exchanging with the uranyl sulphate anion:



Unfortunately, in the presence of competing anions such as chloride, tertiary amines are less selective for uranium and like ferric iron, Honeymoon also has an abundance of chloride (8–9 g/L).

Fortunately, at Honeymoon the combination of the two extractant types performs in synergy, extracting the uranium whilst leaving the majority of the iron and chloride in the raffinate phase. The exact loading mechanisms involved are unknown, but according to the stoichiometry it appears that the majority of uranium is loaded on the DEHPA, whilst the amine prevents significant levels of iron extraction.

The third component of the organic phase is TBP. This organic phosphate can also extract uranium according to a solvation reaction. However, in the case of Honeymoon it is thought that TBP mainly acts as a third-phase modifier.

Following the extraction stage, loaded organic exiting the Pulsed Columns is contacted with the scrub aqueous flow stream in a two-stage, hybrid, cross-flow, counter-current configuration using mixer-settlers. This scrub system removes impurities such as iron, silica and zinc from the loaded organic co-extracted upstream in the Pulsed Columns. Removal of these impurities reduces crud generation in the scrub and strip units, and also limits impurity contamination of the yellowcake product.

Scrub aqueous solution flow rate is controlled to maintain a volumetric A:O phase ratio of 1:10, based on total organic feed to extraction, and is comprised of: diluted sulphuric acid solution for pH adjustment; and sodium meta-bisulphite (SMBS) for adjustment of the ORP (Oxygen Reduction Potential), which chemically reduces soluble iron.

The cross-flow, counter-current configuration allows for maximum flexibility with either acidified SMBS solution or separate streams of dilute sulphuric acid and SMBS added to either stage. SMBS reduces iron on the loaded organic from the ferric to the ferrous state by dropping the ORP of the emulsion in the mixer compartment. Since ferrous is not extracted by DEHPA, and so iron transfers from the organic phase into the aqueous phase. Here, the addition of acid ensures iron and other scrubbed metals remain solubilised and not be precipitated, as hydrolyzed metal hydroxides will form a stable crud.

Scrubbed organic is passed to the strip circuit where uranium is stripped with the strip aqueous flow stream in a two-stage counter-current flow arrangement using mixer-settlers similar to the scrub system. The loaded strip liquor is dosed to the second stage strip mixer at a volumetric A:O phase ratio of about 1:10, then proceeds to thickening and precipitation, whilst the stripped organic returns to the Pulsed Columns for extraction.

Stripping is accomplished by adjustment of the mixer emulsion pH in Strip 1 to the region of 8.3 to 8.6, progressing to a more alkaline pH reading of 9.6 to 9.8 in Strip 2 using sodium carbonate solution (50–55 g/L) addition to the mixer, as shown below.



The uranium is stripped from the organic as a sodium uranyl carbonate complex, leaving the DEHPA present as the sodium form, which then returns to extraction for re-loading with uranium.

Crud is removed from the Pulsed Columns by gravity and from the settlers using an air diaphragm pump and flexible snorkel. In particular the strip stage settlers precipitate iron as a hydrated species when the organic is contacted with carbonate solution, and this ‘iron crud’ tends to follow the loaded strip liquor. Crud is first treated with the addition of reagents (sulphuric acid, diluent and clean water) intended to enhance phase separation. The mixed crud phase is pumped to a tricanter centrifuge designed for the continuous separation of two liquids with different specific gravities and one intermediate solid phase.

## 10.2. Commissioning and ramp-up

SX process commissioning began in July 2011 following the successful water treatment and the subsequent commencement of uranium leaching in the Honeymoon wellfields. By early September 2011, the first dried UOC product from Honeymoon was produced and by late September, two wellfields had commenced uranium mining and the operation of one Pulsed Column had begun to reach design volumetric flow-rates and exceeding design metallurgical recovery.

Initially the availability of wellfields was impacted by pre-treatment of the wellfield aquifer to remove calcium to levels below saturation for gypsum precipitation. The slower than planned ramp-up in the drying and packaging sections throughout October to November 2011 combined with the wellfield availability prevented the commissioning of the second pulse column. Throughout the period from December 2011–March 2012, reliable SX operations were affected by unplanned downtime due to losses of mains power and downstream equipment restrictions.

Two Pulsed Column operations commenced in February and by April 2012 flow throughput and metallurgical recovery was approaching nominal design rates with the highest  $\text{U}_3\text{O}_8$  mass transfer rates achieved in May 2012 since the commencement of the Honeymoon operation.

Several issues were prevalent in the initial twelve months of SX process commissioning including:

- Organic entrainment caused by crud generation in Pulsed Columns;
- High volumes of aqueous entrainment in the barren organic leaving strip settler no.2;
- Presence of a third phase typically in strip settler no. 2;
- High phase disengagement times in strip mixers.

Organic entrainment in the raffinate exiting each Pulsed Column is minimised by maintaining organic phase continuity within the column, which also optimises mass transfer and phase separation rates and minimises crud generation. Organic entrainment can be separated into two main forms; insoluble — which is characterised as a thin film observed on the surface of an aqueous solution, soluble — dissolved organic not visible by the naked eye with composition determined by analysis typically using gas chromatography equipment.

Insoluble organic entrainment was very rarely observed and only ever resulted from upset Pulsed Column conditions, particularly as a result of increased crud generation in the lower decanter. High pH conditions caused by increases in entrainment of alkaline aqueous solution (sodium carbonate) leaving the final strip stage (strip settler 2) generated crud which required regular draining. Operational improvements to mitigate the risk of insoluble organic entrainment in raffinate were:

- Increasing the frequency of removal of aqueous entrainment from barren organic tanks prior to being sent to the Pulsed Columns;
- Acidification of aqueous within the barren organic tank;
- Installation of acid addition to the PLS pond to maintain a constant pH in PLS feed to extraction at the range of 2.0–2.1.

Aside from above-mentioned upset conditions, all plant organic entrainment data collected and analysed leaving the SX plant averaged 7–10 mg/L, well below the design of 50 mg/L.

The presence of high aqueous entrainment in the barren organic leaving Strip 2 settler was also regularly evident in the stripped organic leaving the upstream strip settler 1. This increase impacted the physical performance of the stripping circuit, exceeding the design flow of aqueous in pipe-lines, and hence causing flow restrictions. These flow restrictions in turn caused difficulty in maintaining recommended levels of aqueous and organic in the strip settlers eventually leading to plant downtime. Throughout these periods of high aqueous entrainment, high phase disengagements within strip mixers were also observed, often exceeding 5 minutes.

Several investigations were conducted to determine the cause of high phase disengagements as resolving this issue would mitigate, if not reduce periods of high aqueous entrainment hence reduce the likelihood of crud generation in Pulsed Columns and further organic entrainment in the raffinate. Some possible causes of high phase disengagement time in strip mixers were:

- Acid base reaction releasing CO<sub>2</sub> within the mixer;
- Generation of iron precipitates;
- Unstable mixer inflows caused by upstream plant instability;
- Operating mixers in organic continuity as opposed to aqueous continuity.

Test-work concluded that phase disengagement in strip was highly dependent on pH and the concentration of the third phase modifier, TBP. The optimal pH range was 8.3 to 8.6 for Strip 1. Increasing the fresh sodium carbonate solution (strip) flow to Strip 2 could achieve the desired pH in Strip 1, but undesirably led to the generation of a third phase forming in the Strip 2 settler, especially when the pH exceeded 10.0 in Strip 2. A disadvantage of using a carbonate strip is the formation of a third phase due to the poor solubility of the sodium salt of DEHPA in the diluent [20, 4].

Successful plant trials were conducted in February 2012 which determined that the desired pH in Strip 1 could be achieved by the addition of strip flow directly to the Strip 1 mixer. This addition was not included in the design and construction of the Honeymoon SX plant and was retro-fitted following the February trials. This proved beneficial for reducing phase disengagement times especially when operating two Pulsed Columns due to increased throughputs of both organic and aqueous flows. Further improvements were required in subsequent months to improve the pH control in Strip 1 and 2 including additional pH measurement and flow control however, phase disengagement times less than five minutes could now be obtained.

The presence of a DEHPA rich third phase within the Strip 2 settler would also dramatically affect uranium recovery in the extraction circuit. As DEHPA is the main driver of uranium recovery in the synergistic reagent system, a small quantity of DEHPA retained within the Strip 2 settler as a third phase would decrease DEHPA concentrations below that required to maintain the desired uranium recovery. Third phase was so detrimental that within 6–12 hours of operators observing a third phase in Strip 2, uranium recovery results would begin to drift.

The presence of third phase was easily overcome through the addition of TBP. A preventative TBP addition regime was chosen as on-site analysis was not capable of producing real-time feedback of TBP concentration for process control. A certain proportion of reagents were added weekly to maintain levels above critical concentrations at which the third phase phenomena could occur. The small, regular additions were successful in increasing reliability of operations and were based upon several months historical data, combining monthly external analysis results with the volumes of TBP added to the SX plant organic inventory.

Further work commenced to define conditions at which TBP losses were most prevalent in the Honeymoon SX process and to better prevent the formation of a third phase. On-site analysis of TBP was not possible given that additional instrumentation was required (e.g. GC-MS: gas chromatography

– mass spectrometry). A wet chemistry method, as used for Alamine and DEHPA concentrations, was not successful for TBP determination and external analysis methods were able to provide repeatable data despite the long turn-around time.

External analysis showed reductions in TBP concentrations above that predicted by design however aligns with reported literature suggesting that TBP solubility is above 400 mg/L in aqueous solutions. Analysis also showed that the highest proportion of TBP was solubilised in the loaded strip solution, contributing to organic transfer to downstream operational areas.

### 10.3. Lessons learned

Commissioning and ramp-up of the Honeymoon SX plant provided metallurgical improvement opportunities for operational staff.

Key areas of future focus at Honeymoon SX areas can be utilized in future USX plant designs similar to Honeymoon include:

- Pulsed Column organic entrainment performance was better than design, which benefits from operator vigilance and stable organic phase continuity;
- The solubility of organic reagents is important in controlling entrainment in raffinate, and can be determined for design in SX plants;
- Metallurgical recovery met expectation and is dependent on maintaining target organic conditions, in particular active extractant and modifier concentrations;
- Aqueous entrainment leaving the strip circuit may affect uranium recovery; frequent draining or acidification of the barren organic tanks leads to lower disengagement times;
- Additional organic re-protonation may depend on pH of PLS, an organic wash with acid solution (e.g. HCl solution) may be utilized;
- Sodium carbonate is an effective stripping agent for DEHPA extractant but solubility of third-phase must be managed by control of relative concentration;
- Infrequent off-site TBP analysis for determining concentrations caused operational difficulties;
- The addition of fresh strip solution to Strip 1, was a significant improvement in the control of pH which lowered phase disengagement time and lowered entrainment;
- Recent test-work concluded that operating Strip 2 with aqueous continuity could improve phase disengagement times by 25%, hence is recommended for future operations;
- Further consideration of alternatives to TBP as a third phase modifier due to its solubility should be considered for future operations, e.g. Di- Butyl- Butyl Phosphonate.

## 11. TOWARDS THE FUTURE OF USX

Solvent extraction has dominated the uranium production industry for over 50 years, but during the hiatus in new uranium projects, the technology did not advance [45]. USX is currently utilised in Australia's two largest uranium mines, as shown in Table I. The future of USX will reflect the expected trends of new projects that include lower grade ores, tighter controls on water supply or discharge. The trend of higher proportion of production via in-situ recovery will increase the application of ion exchange technology. To remain competitive USX will need to achieve greater stage recovery, lower solvent losses, and higher tolerance of salinity.

TABLE I. AUSTRALIAN URANIUM EXTRACTION PLANTS AT MARCH 2014

*Projects with feasibility study ongoing or complete at the time of writing are shown in italics*

| Operation and location | Ranger,<br>Northern<br>Territory | Olympic Dam,<br>South<br>Australia | Beverley<br>South,<br>Australia  | Honeymoon,<br>South<br>Australia | <i>Four Mile,<br/>South<br/>Australia</i> <sup>19</sup> |
|------------------------|----------------------------------|------------------------------------|----------------------------------|----------------------------------|---|
| Ore category           | Unconformity                     | Breccia                            | Sandstone                        | Sandstone                        | <i>Sandstone</i>  |
| Leach chemistry        | Acid sulphate                    | Acid sulphate,<br>3 g/L chloride   | Acid sulphate,<br>4 g/L chloride | Acid sulphate,<br>8-9 g/L Cl     | <i>Acid sulphate</i>                                    |
| Recovery technique     | Amine SX                         | Amine SX                           | Strong base IX                   | Mixed SX                         | <i>Strong base<br/>IX</i>                               |
| Nominal capacity, tU   | 4660                             | 3820                               | 850                              | 340                              | <i>1150</i>   |

| Operation and location | <i>Kintyre,<br/>Western<br/>Australia</i> | <i>Wiluna, Western<br/>Australia</i> | <i>Yeelirrie, West<br/>Australia</i> | <i>Lake Maitland<br/>West Australia</i> | <i>Ranger<br/>Underground</i> |
|------------------------|---|--------------------------------------|--------------------------------------|---|-------------------------------|
| Ore category           | <i>Unconformity</i>                       | <i>Surficial/calcrete</i>            | <i>Surficial/calcrete</i>            | <i>Surficial/calcrete</i>               | <i>Unconformity</i>           |
| Leach chemistry        | <i>Acid sulphate</i>                      | <i>Alkali carbonate</i>              | <i>Alkali carbonate</i>              | <i>Alkali carbonate</i>                 | <i>Acid sulphate</i>          |
| Recovery technique     | <i>Direct<br/>precipitation</i>           | <i>Direct<br/>precipitation</i>      | <i>Direct<br/>precipitation</i>      | <i>Direct<br/>precipitation</i>         | <i>Amine SX</i>               |
| Nominal capacity, tU   | 2000                                      | 680                                  | 3000                                 | 850                                     | <i>TBC</i>                    |

## REFERENCES

- [1] BOSMAN, R.J., Practical considerations in diluent selection for hydrometallurgy, Symposium for Ion Exchange and Solvent Extraction, S. African Institute Mining Metallurgy, Randberg, South Africa, 7-8 February (1980).
- [2] INTERNATIONAL ATOMIC ENERGY AGENCY, Uranium Extraction Technology, Technical Reports Series No. 359, IAEA, Vienna (1993).
- [3] RITCEY, G.M., ASHBROOK, R.A, Solvent extraction: principles and applications to process metallurgy, Elsevier (1979 and 1984).
- [4] MERRITT R.C., The Extractive Metallurgy of Uranium, Colorado School of Mines Research Institute No. 389, Golden, Colorado, USA (1971).
- [5] BROWN, K.B., COLEMAN, C.F., CROUSE, D.J., BLAKE, C.A, RYON, A.D., “Solvent extraction processing of uranium and thorium ores”, Proceeding of Second United Nations International Conference on the Peaceful Uses of Atomic Energy, Geneva, 3, Processing of Raw Materials (1958) 472–487.
- [6] RITCEY, G.M., Crud in solvent extraction processing - A review of causes and treatment, Hydrometallurgy 5 2 (1980) 97–107.
- [7] SOLDENHOFF, K., DAVIDSON, J., “Uranium recovery from highly saline in situ leach solutions by ion exchange”, (Proc. First Extractive Metallurgy Operators Conf., Brisbane), Australasian Institute of Mining and Metallurgy, Melbourne (2005) 47–51.

<sup>19</sup> Production commenced on 14 April 2014 (Ed.).

- [8] THIRY, J., ROCHE, M., “Recent process developments at the Cominak uranium mill”, Uranium 2000 (Proc. Int. Symp. on the Process Metallurgy of Uranium), MetSoc, Canadian Institute of Mining Metallurgy and Petroleum (2000) 209–223.
- [9] DOBROWOLSKI, H.J., “The Honeymoon Project – An alternative method of uranium mining”, Uranium Technology in South Australia (Proc. Symp. Adelaide, Australia) Australian Mineral Foundation, Adelaide, Australia (1983).
- [10] MAYFIELD ENGINEERING PTY LTD, AKER KVAERNER AUSTRALIA, Honeymoon Uranium Project, Summary of Feasibility Study (2006).
- [11] LYNE, E.G., BERRYMAN, A.B., EVANS, C.M., SAMPAT, S., JENSEN-HOLM, H., “Advances in NO<sub>x</sub> removal in smelter acid plants”, Proc. Int. Seminar for New Initiatives in the Mining Sector Chilean Copper Commission, Santiago (2002).
- [12] MUNYUNGANO, B., FEATHER, A., VIRNIG, M., “Degradation problems with the solvent extraction organic at Rössing uranium”, Proc. ISEC 2008 Solvent Extraction: Fundamentals to Industrial Applications (Proc. Int. Solvent Extraction Conf., September, Tucson, AZ) (2008) 296–274.
- [13] BELLINO, M., MACKENZIE, J.M.W., “Solvent extraction of uranium-impurity transfer and phase separation” (Proc. Third Int. Conf. on Uranium, Saskatoon, Canada), Canadian Institute of Mining Metallurgy and Petroleum (2010) 685–697.
- [14] GRINSTEAD, R.R., SHAW, K.G., LONG, R.S., “Solvent extraction of uranium from acid leach slurry and solution”, Peaceful Uses of Atomic Energy (Proc. United Nations Int. Conf., Geneva), Production Technology **8** (1958) 71–76.
- [15] ROSENBAUM, J. B, BORROWMAN, S. R, CLEMMER, J. B., “Solvent Extraction for Recovery of Uranium and Vanadium from Salt Roast Process Solutions”, Peaceful Uses of Atomic Energy (Proc. Second United Nations Int. Conf., Geneva) Processing of Raw Materials **3** (1958) 505–509.
- [16] PHILLIPS, R., Honeymoon Uranium Project, Metallurgical Testing – Laboratory and Plant Trials, 1998 to 2000, Southern Cross Resources Pty Ltd (May 2001).
- [17] LABROOY, S., SPRATFORD, D., MIDDLIN, B., OTTO, K., “Differentiating the honeymoon uranium process flowsheet”, ALTA (Proc. Conf., Perth, Australia) (2009)
- [18] BENDER, J., VIRNIG, M., NISBETT, A., CRANE, P., MACKENZIE, M., DUDLEY, K., “Uranium solvent extraction circuits; operational challenges and adjusting to unique process conditions”, (Proc. Third Int. Conf. on Uranium, Saskatoon, Canada), Canadian Institute of Mining Metallurgy and Petroleum (2010) 675–684.
- [19] KERTES, A.S., The chemistry of the formation and elimination of a third phase in extraction systems, Solvent Extraction Chemistry of Metals, MacMillan, London, UK (1966) 377–400.
- [20] BLAKE, C.A., BAES, K.B., COLEMAN, C.F., WHITE, J.C., “Solvent extraction of uranium and other metals by acidic and neutral organic phosphorus compounds”, Oak Ridge National Laboratories (prepared for the Proceeding of Second United Nations International Conference on the Peaceful Uses of Atomic Energy, Geneva (1958) Paper P/1550.
- [21] GEORGE, D.R., ROSS, J.R., “Recovery of uranium from mine waters and copper ore leaching solutions”, Processing of Low-Grade Uranium Ores (Proc. Panel on Low Grade Uranium Ore, Vienna, 1966), IAEA, Vienna (1967) 227–234.
- [22] FAURE, A., TUNLEY T.H., “Uranium Recovery by Liquid-Liquid Extraction in South Africa”, The Recovery of Uranium (Proc. Symp. Sao Paulo, Brazil, 1970), IAEA, Vienna (1971) 241–251.
- [23] NICE, R.W., BANACZKOWSKI, M., “Expansion of the ore treatment plant at Ranger uranium mines”, Uranium 2000 (Proc. Int. Symp. on the Process Metallurgy of Uranium), MetSoc, Canadian Institute of Mining Metallurgy and Petroleum (2000) 163–180.
- [24] HARDY, H.J., The chemistry of uranium milling, Radiochimica Acta **25** 3-4 (1978) 121–134.
- [25] EDWARDS, C.R., Uranium extraction process alternatives, CIM Bulletin **85** 958 (1992) 112–136.
- [26] SMITH, H., “Process simulation and modelling”, Advances in gold ore processing (ADAMS, M., Ed.), Developments in Mineral Processing **15**, Elsevier (2005) 109–121.
- [27] GUPTA, C.K., SINGH, H., Uranium Resource Processing Secondary Resources, Springer Verlag, Berlin, Germany (2003) 172–175.

- [28] INTERNATIONAL ATOMIC ENERGY AGENCY, Manual on Laboratory Testing for Uranium Ore Processing, IAEA-TRS-313, IAEA, Vienna (1990) fig. 27.
- [29] BARTSCH, P.J., LAWSON, B., “Confirmation of process criteria for pulse column plant expansion”, ALTA (Proc. Conf., Perth, Australia) (2003).
- [30] ROBINSON, T., SANDOVAL, S., COOK, P., World copper solvent extraction plants; Practices and design. JOM (Journal of the Minerals, Metals and Materials Society) **55** 7 (2003) 24–46.
- [31] DESSON, M., DUCHAMP, C., HENRY, E., JOUIN, J.P., MICHEL, M., “Industrial experience with pulse columns in the processing of uranium ores”, AIChE Symposium Series **80** 238 (1983) 162–169.
- [32] MOVSOWITZ, R.L., KLEINBERGER, R., BUCHALTER, E.M., GRINBAUM, B., “Comparison of the performance of full scale pulsed columns vs. mixer-settlers for uranium solvent extraction”, Uranium 2000 (Proc. Int. Symp. on the Process Metallurgy of Uranium), MetSoc, Canadian Institute of Mining Metallurgy and Petroleum (2000) 181–192.
- [33] ROYSTON, D., BURWELL, A., The design and performance of pump-mix and gravity flow mixer settlers, Australian Atomic Energy Commission, Lucas Heights (1972).
- [34] GLASSER, D., ARNOLD, D.R., BRYSON, A.W., VIELLER, A.M.S., “Aspects of Mixer Settler Design”, Minerals Science and Engineering **8** 1 (1976) 23–45.
- [35] TAYLOR, A., “Review of mixer-settler types and other possible contactors for copper SX”, ALTA (Proc. Conf. Perth, Australia) (2007).
- [36] MACDONALD, J.B., MATTISON, P.L., MACKENZIE, J.M.W., “Technical service in uranium solvent extraction”, Practical problem solving in South Africa and the United States, Henkel Corporation Guidebook (1978).
- [37] HALL, S, REED, M, “Cross contamination of ODC solvent extraction circuits”, Preprints SME Annual Meeting, Phoenix, AZ (1996).
- [38] CHENG, C.Y., BUJALSKI, J.M., SCHWARZ, M.P., Mixer-Settlers; Theory, Design, Modelling and Application, Report for AMIRA Project P706 (2004).
- [39] MOYER, B.A., McDOWELL, W.J., Factors influencing phase-disengagement rates in solvent-extraction systems employing tertiary amine extractants, Separation Sci. Technol. **16** 9 (1981) 1261–1289.
- [40] SARUCHERA, T., JARVI, J., MOLDOVAN, B., “Crud separation and SX optimization at Key Lake”, Proc. Third Int. Conf. on Uranium, Saskatoon, Canada, Canadian Institute of Mining Metallurgy and Petroleum (2010) 731–740.
- [41] HARTMANN, T., “Crud treatment with 3 phase centrifuge in heap leach uranium process”, ibid., 741–749.
- [42] TERRY, B., The acid decomposition of silicate minerals part II, Hydrometallurgical applications, Hydrometallurgy **10** 2 (1983) 151–171.
- [43] BUSH, P.D., “Development considerations for the Honeymoon ISL uranium project”, Uranium 2000 (Proc. Int. Symp. on the Process Metallurgy of Uranium), MetSoc, Canadian Institute of Mining Metallurgy and Petroleum (2000) 257–280.
- [44] BALLESTRIN, S., LOW, R., RAYNAUD, G., CRANE, P., “Honeymoon Mine Australia; Commissioning and Operation of the Process Plant Using a Novel Solvent Extraction Reagent Mixture in a High Chloride Environment”, ALTA Uranium REE (Proc. Conf., Perth, Australia) (2014).
- [45] RITCEY, G.M., “State of the art and future directions in solvent extraction”, Proc. third Int. Solvent Extraction Workshop, Digby, Nova Scotia, Canada (2003).

# **DEVELOPMENT OF THE FALEA POLYMETALLIC URANIUM PROJECT, MALI**

R. RING, P. FREEMAN  
ANSTO Minerals, ANSTO,  
Lucas Heights, New South Wales,  
Australia

## **Abstract**

The Falea uranium deposit is located in south western Mali, West Africa and was owned by Denison Mines Corporation at the time of writing. The current resource estimate is approximately 45 million pounds of U<sub>3</sub>O<sub>8</sub> (~17 000 t U) at an average grade of ~ 0.07% U<sub>3</sub>O<sub>8</sub> (~ 0.06% U). The deposit also contains ~37 million ounces Ag (~1000 t) and ~70 000 t Cu. The dominant uranium mineral is uraninite, of copper chalcopyrite, and silver occurs mainly as argentite and as native silver. The polymetallic nature of the Falea deposit dictates that there are a range of flow sheet options. The ore contains both carbonate and sulphide mineralizations, which have potential impacts on acid and alkaline leaching respectively. Two primary flow sheet options were considered: 1) acid leach of ore to recover uranium/flotation of leach residue to recover a sulphide concentrate, treatment of concentrate for Cu and Ag recovery; 2) flotation of ore/alkaline leaching of flotation tails to recover uranium and treatment of flotation concentrate for Cu and Ag recovery. This paper presents an overview of the various flow sheet options, an outline of the preferred flow sheet, and the results and conclusions of on-going engineering and laboratory/pilot studies to refine the preferred flow sheet.

## **1. INTRODUCTION**

The Falea uranium, silver, copper deposit is located in south western Mali, West Africa and was owned by Denison Mines Corporation at the time of writing. The current resource estimate was approximately 45 million pounds of U<sub>3</sub>O<sub>8</sub> (~17 000 t U) at an average grade of ~ 0.07% U<sub>3</sub>O<sub>8</sub> (~ 0.06% U). The deposit also contains ~ 37 million ounces (~1000 t) Ag and ~ 70 000 t Cu, which makes it different to most other uranium deposits. The dominant uranium mineral is uraninite, copper is present mainly as chalcopyrite and silver mainly as argentite and in its native form. Only 5% of the property has been explored to date, and all zones remain open.

## **2. LOCATION AND PROJECT BASICS**

Figure 1 shows the location of the deposit. The Falea ore body is located in south west Mali, near the intersection of the Guinea and Senegal borders. Uranium was initially found near Falea in the late 1970s by COGEMA. Mali is an established mining region, mainly for gold, and has the third highest gold production in Africa after South Africa and Ghana. The Falea deposit is located on a plateau, which makes it favourable for an underground operation. Figure 2 shows the mineralised regions located to date.

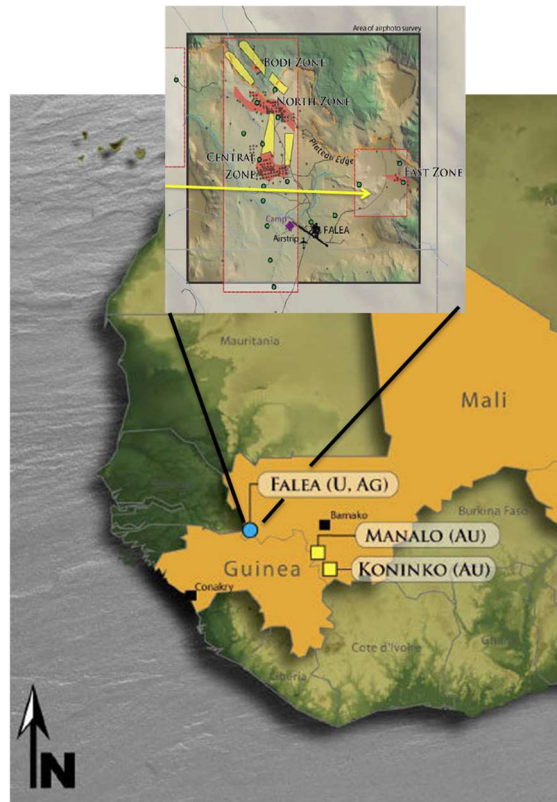


FIG. 1. Falea location (courtesy of Denison Mines Corporation).

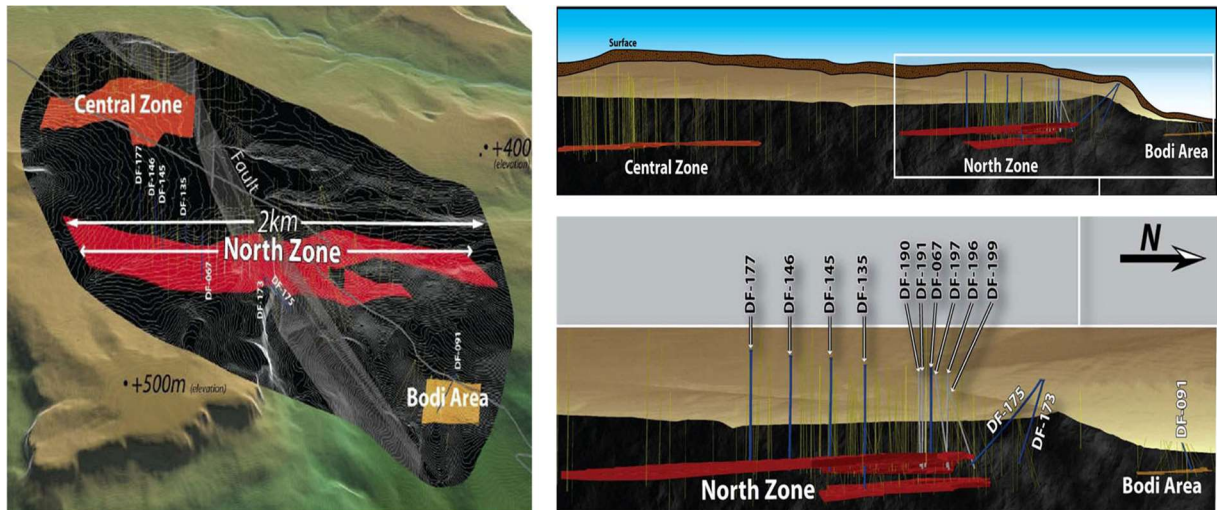


FIG. 2. Falea ore body (courtesy of Denison Mines Corporation).

There are three main zones, Central, North and Bodi, with two new areas discovered only recently. Work to date has been on ore from the North zone.

### 3. RECENT PROCESS DEVELOPMENT

In 2010, preliminary test work was conducted at SGS Lakefield in South Africa. This test work included acid leaching of uranium, sulphide flotation and mineralogy. This preliminary test work yielded some promising results showing that high uranium extractions were possible for acid leaching of ore and that it was feasible to separate out the copper and silver in a sulphide concentrate, which also contained the native silver.

In March 2011, the first phase of the ANSTO Minerals test work commenced. This test work included the following:

- Acid and carbonate leaching;
- Solid / liquid separation;
- Flotation of the ore and the residue from acid leaching of ore.

From this phase of test work potential flow sheets were identified, which are discussed in more detail below.

In November 2011, phase 2 commenced. This consisted of a comprehensive test program to generate data for the economic evaluation of alternative flow sheets. The economic evaluation was conducted by DRA (an engineering company based in South Africa), in close collaboration with ANSTO Minerals. When the preferred process route was identified, a further work program was undertaken by ANSTO Minerals to refine the preferred option. This work included pilot milling and flotation of ore to produce a copper/silver rich concentrate, concentrate leach optimisation, options for silver recovery and radionuclide deportment in the process flow sheet.

The refinement program led to the final phase of work which covered IX recovery of uranium, production of a uranyl peroxide product, enhancing copper and silver recovery, radiometric sorting and environmental test work on tailings.

#### 4. MINERALOGY

Mineralogical studies have been a key tool in understanding the drivers for recovery and reagent consumption in the flowsheet development programs. These studies have included examination of ore, flotation concentrates and tailings, and leached residues. Table I summarises the mineralogy of Falea ore and a corresponding acid leached residue.

TABLE I. FALEA MINERALOGY\*

| Mineral                              | Chemical formula  | Ore  | Leach residue | Level of attack                  |
|--------------------------------------|---|------|---------------|----------------------------------|
| Quartz                               | SiO <sub>2</sub>  | 70   | 76            | Very low                         |
| Muscovite                            | KAl <sub>2</sub> (AlSi <sub>3</sub> O <sub>10</sub> )(OH) <sub>2</sub>                              | 11.9 | 13.6          | Low                              |
| Clinochlore                          | (Mg,Fe) <sub>6</sub> (Si,AL)4O <sub>10</sub> (OH) <sub>8</sub>                                      | 6.6  | 5.7           | Medium                           |
| Dolomite                             | CaMg(CO <sub>3</sub> ) <sub>2</sub>   | 3.3  | nd            | Complete                         |
| Calcite                              | CaCO <sub>3</sub>   | 1.8  | nd            | Complete                         |
| Albite                               | NaAlSi <sub>3</sub> O <sub>8</sub>  | 2.2  | 0.6           | High                             |
| Riebeckite                           | (Na,Ca) <sub>2</sub> (Fe,Mg,Al) <sub>5</sub> (Si,Al) <sub>8</sub> O <sub>22</sub> (OH) <sub>2</sub> | 0.8  | 0.4           | Formed from calcite and dolomite |
| CaSO <sub>4</sub> .xH <sub>2</sub> O | CaSO <sub>4</sub>   | 0.8  | 2.1           |                                  |
| Apatite                              | Ca <sub>5</sub> (PO <sub>4</sub> ) <sub>3</sub> (OH,F,Cl)   | 0.7  | 0.3           |                                  |
| Haematite                            | Fe <sub>2</sub> O <sub>3</sub>  | 0.6  | 0.4           |                                  |
| Pyrite                               | FeS <sub>2</sub>  | 0.6  | 0.5           |                                  |
| Chalcopyrite                         | CuFeS <sub>2</sub>  | 0.6  | 0.3           |                                  |
| Rutile                               | TiO <sub>2</sub>  | 0.5  | 0.2           |                                  |
| Microline                            | KAlSi <sub>3</sub> O <sub>8</sub>   | 0.3  | 0             |                                  |

\* Leach conditions were 45°C, pH 1.8, oxidation/reduction potential (ORP) 500 mV, P<sub>80</sub> 75 µm, 24 hours.

The major minerals in the Falea ore are quartz, muscovite and clinochlore. The main acid consumers are carbonates (calcite and dolomite), chlorite, feldspars (albite and microline), apatite and chalcopyrite. In carbonate leaching, the main carbonate consumers are the sulphide minerals.

The uranium is mostly present mainly as uraninite ( $\text{UO}_2$ ), with coffinite ( $(\text{USiO}_4)_{1-x}(\text{OH})_{4x}$ ) and brannerite ( $(\text{U,Ca,Ce})(\text{Ti,Fe})_2\text{O}_6$ ) also present. Other uranium minerals, eg uranophane, are present at low concentrations.

The copper is mainly present as chalcopyrite ( $\text{CuFeS}_2$ ), with silver as argentite ( $\text{Ag}_2\text{S}$ ) (50–70%), tennantite, and in its native form (10%).

## 5. FLOW SHEET DEVELOPMENT AND TEST WORK RESULTS

Due to the polymetallic nature of the Falea ore, a range of flowsheet options were considered. The considerations were carbonates in acid leaching, sulphides in carbonate leaching and the need to also recover silver and copper. From the initial test work two potential flow sheets were identified and are given in Figs 3 and 4.

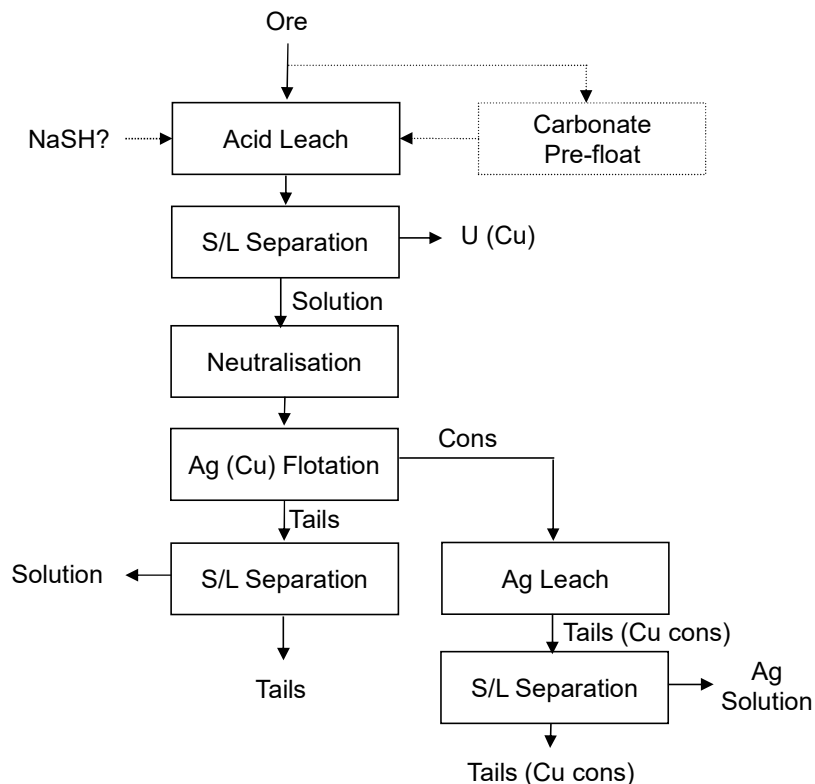


FIG. 3. Acid leach/flotation flow sheet.

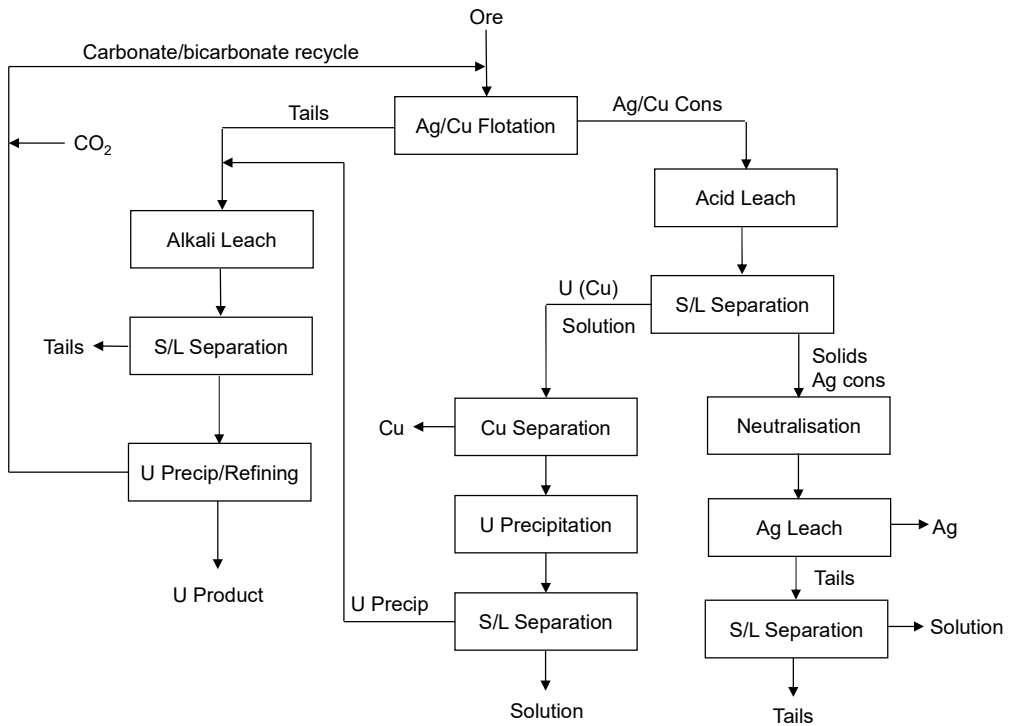


FIG. 4. Flotation/carbonate and acid leach flow sheet.

### 5.1. Flow sheet comparison

Flow sheet 1 (Fig. 3) is the simplest of the two flow sheets, it has an acid leach of ore (a low temperature leach is preferred as copper dissolution and acid consumption are minimised) followed by flotation of the washed leach residue to produce a copper/silver concentrate, and subsequent cyanide leaching of the concentrate to recover silver. The uranium is recovered in a single acid leach (carbonate leaching of the ore was tested and rejected due to excessive carbonate and oxidant consumption by sulphides). The major drawbacks to this flow sheet are twofold:

- 1) The acid consumption is relatively high (51 kg/t at pH 1.8–2.0), even at low temperature (45°C);
- 2) As the acid leach cannot be economically conducted at high temperatures due to excessive acid consumption, the silver present as argentite is not oxidised to silver sulphate and is therefore refractory in the subsequent acid leach.

Flow sheet 2 (Fig. 4) is rather more complex as it incorporates two leaching stages, an acid leach on the flotation concentrate and an atmospheric carbonate leach on the flotation tails. Both the flotation tails and concentrate have to be leached for uranium recovery as about 15–20% of the uranium reports to the flotation concentrate, which is about 3.5% of the mass of the ore. However, it has the following significant benefits:

- 1) Preliminary flotation of the sulphides practically eliminates carbonate consumption in the subsequent carbonate leach on the flotation tails;
- 2) High temperature acid leaching of the flotation concentrate oxidises the argentite, thereby rendering more silver amenable to subsequent cyanide leaching;
- 3) High temperature oxidative leaching of the concentrate also maximises copper and uranium extractions.

This circuit is similar to that used at the Beaverlodge uranium mill in Canada, which operated successfully from 1953 to 1982 [1].

### *5.1.1. Flow sheet performance comparison*

Similar uranium extractions were obtained in the primary leach steps of both flowsheets, although the atmospheric carbonate leach rate at 90°C was slightly slower than the acid leach, as shown in Fig. 5. Originally flow sheet 1 incorporated a carbonate float with the intention of rejecting carbonates prior to leaching to reduce acid consumption. Although the flotation was successful, it also floated excessive quantities of all the valuable metals and was therefore not considered further.

The overall uranium extraction from flow sheet 2 was found to be greater than flow sheet 1 as the conditions adopted for the acid leach of the float concentrate (80°C, pH 1.2, ORP 450 mV, P<sub>80</sub> 23 µm — as received, ≤ 24 h) yielded a greater extraction of uranium (and copper) than the primary leaches. The high copper extraction also reduced cyanide consumption in the subsequent silver recovery step.

High recoveries of copper and silver to the flotation concentrate (> 90%) were achieved for both flotation of ore (flowsheet 2) and flotation of acid leach residue (flowsheet 1). Extraction of silver by cyanide leaching of the acid leached residue was found to be problematic. The more favourable conditions (for silver sulphate oxidation) used in the acid leach in flow sheet 2 yielded better silver extractions than for flow sheet 1, but extractions were still less than 70%.

At this stage of either flowsheet development, the simplification of selling a copper/silver sulphide concentrate, after uranium removal, was considered as an option. However, despite the leaching of uranium (and <sup>230</sup>Th) from the concentrate in the sulphuric acid leach, the residual leach residue would be classified as a radioactive material due to the concentrations of the uranium chain daughter radionuclides. A variety of leaching reagents, and thermal treatment, were therefore tested to remove radionuclides from the copper/silver concentrate. Despite moderate success and achieving relatively low residual radionuclide concentrations, some radionuclides still remained above the regulatory criteria of 1 Bq/g per radionuclide. This option was therefore discounted.

### *5.1.2. Flow sheet selection*

Both flow sheets were subjected to an economic evaluation by DRA. Flow sheet 2 was selected as the most favourable flow sheet, and several options and areas for refinement were identified.

After the DRA evaluation, further test work was conducted by ANSTO Minerals to investigate processes to improve silver recovery, and to also evaluate the options of incorporating some variations to flow sheet 2, such as radiometric sorting, ion-exchange (IX) to recover uranium, and copper recovery.

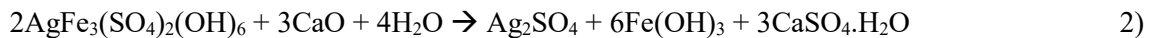
## **5.2. Optimisation test work**

The first stage of this test work was to conduct pilot flotation on a bulk sample of Falea ore. About 3 tonnes of ore was prepared as feed to a continuous grinding and flotation plant at SGS Lakefield in Perth. The piloting confirmed high recoveries of silver and copper to the flotation concentrate, with mineralogical examinations on several samples from the continuous flotation circuit, and confirmatory batch tests, revealing only one liberated particle of silver and very few liberated particles of copper in the flotation tailings. The flotation tails and concentrate were used in optimisation test work by ANSTO Minerals.

The major priority was to improve the recovery of silver recovery from the flotation concentrate. The highest silver extraction achieved before the optimisation test work commenced was 65–70% from cyanide leaching of the residue from acid leaching of flotation concentrate. The reason for the relatively poor silver extraction was thought to be due to the formation of some silver jarosite (argentojarosite) in the acid leach stage by reaction 1.



Jarosites are relatively refractory in cyanide leaching. Therefore, test work was conducted to attempt to break down the argentojarosite prior to cyanide leaching [3, 4]. A high temperature lime boil is one way to decompose jarosites, see reaction 2.

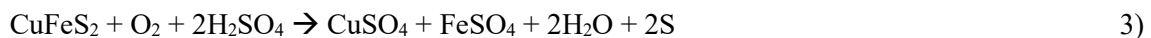


Initial lime boils were conducted at 90°C and pH 10.5. The subsequent cyanide leach extracted ~96% of the silver, however the lime consumption in the lime boil was >700 kg/t feed, thus rendering it uneconomic. Several variations of the lime boil were tested to improve lime utilisation, including reducing the lime boil pH, controlling the lime addition to stoichiometric requirements and an attrition lime boil to improve lime utilisation [5, 6]. Only the attrition lime boil showed any promise, either the lime consumption remained high, or the silver extraction in cyanide leaching decreased significantly in the other variations. However, the attrition lime boil was conducted over 6 hours, and this would need to be reduced by a factor of at least 12 to be economically attractive.

As elemental sulphur consumes cyanide, flotation test work was also conducted to remove the sulphur formed during the oxidative leach, prior to cyanidation. Unfortunately, significant quantities of silver also reported to the sulphur concentrate and it was impossible to obtain a clean split between silver and elemental sulphur.

Pressure oxidative (POX) leaching of the concentrate was also tested, both at 105°C, with a fine grind (Activox® conditions) and at higher temperatures, 150 to 220°C [2]. The aim of the pressure oxidative leaching was twofold; to leach the concentrate in a range in which silver jarosite does not form, and to generate data for conducting an economic comparison of POX versus atmospheric leaching.

One major benefit of high temperature POX leaching is that acid is generated in situ, see reaction 4, whereas atmospheric leaching requires acid, see reaction 3. However, the saving in acid is offset by the higher oxygen consumption in converting the sulphides through to sulphate. Another major benefit of high temperature POX leaching is that the reaction kinetics are significantly faster than under atmospheric conditions.



The Activox® leach gave relatively poor extractions of both uranium and copper, and the silver extraction in the subsequent cyanide leach was also poor, so this option was not considered for any further test work. The high temperature POX leaches resulted in copper and uranium extractions of > 95% with fast reaction kinetics. However, the silver extractions in cyanide leaching were poor and the higher the POX leach temperature, the lower the subsequent silver extraction in cyanide leaching. The reason for this was almost certainly the formation of silver alunite, which is more readily formed at the higher temperatures, see reaction 5.



Lime boils were tested on the POX residues to attempt to decompose the alunite, but it was stable under lime boil conditions.

Two oxidative roasting tests were conducted on flotation concentrate, with the aim of converting argentite to silver oxide and to also oxidise any other sulphides through to oxides. It was hoped that this would render all the silver amenable to cyanide leaching. Unfortunately, oxidative roasting rendered all the three major components refractory, < 3% of the copper and only 28–30% of the uranium leached in an acid leach at pH 1.5, and < 30% of the silver leached in the subsequent cyanide leach. The poor copper extraction was not a surprise as thermodynamic modelling had shown that copper was very likely to form iron spinels ( $\text{CuO} \cdot \text{Fe}_2\text{O}_3$ ) under the selected roasting conditions. Due to the poor silver and uranium extractions, no further roasting tests were conducted.

As a result of this test work, further optimisation work on silver recovery concentrated on optimizing the atmospheric oxidative leach conditions with respect to minimising the formation of silver jarosite. As other jarosites readily form under atmospheric leach conditions, some more readily than argentojarosite, the preferential formation of non-silver jarosites was pursued. Recovery of the carbonate used in carbonate leaching is critical for this type of circuit. This requires the recycle of carbonate solutions to milling and therefore flotation. Consequently, the flotation concentrate for acid leaching will contain sodium ions. Therefore, concentrate leaching was conducted in a solution containing 20 g/L sodium ions as sodium sulphate. The subsequent silver extraction increased to  $\geq 84\%$ , showing that the addition of sodium ions preferentially promoted the formation of sodium jarosite, although some silver jarosite still formed. In a further test, potassium ions were added. As potassium forms a more stable jarosite than sodium it was hoped that this would further increase the subsequent extraction of silver, which did improve to  $> 85\%$ . It is expected that the silver extraction can be further increased with more optimisation test work.

The copper in the concentrate leach solution was successfully recovered by cementation with iron. The copper can also be recovered by solvent extraction; this option has not been tested to date, but is a standard plant practice. After copper removal, over 99.8% of the uranium in the concentrate leach solution was precipitated by addition of magnesium hydroxide. Uranium in the precipitate was recovered by leaching under the primary carbonate leach conditions for the flotation tails, which yielded a uranium extraction of 99.3%.

As an alternative to SDU precipitation, test work was successfully conducted to recover the uranium by IX using a strong base resin. The aim of the IX was to increase the uranium concentration of the feed to sodium diuranate (SDU) precipitation. As the excess sodium hydroxide in solution ( $\sim 6$  g/L) is required to achieve complete SDU precipitation, a higher U:NaOH ratio reduces the cost of NaOH/kg U. The uranyl peroxide product produced from the redissolved SDU met converter specification for all elements.

Studies have been conducted to determine the deportment of radionuclides in alternative processes for recovery of silver from CN liquor. Radionuclide deportment to a silver/zinc cement product was not encouraging as the product contained sufficient  $^{226}\text{Ra}$ , and possibly  $^{210}\text{Pb}$  to be classified as radioactive. However, there is potential to reprecipitate both lead and radium prior to silver precipitation. An alternative and promising approach under consideration is to process silver through to a pure metal by smelting the cement product, AM's experience has shown that radium, lead, uranium and thorium typically report to the slag in such operations. The carbon in pulp route is also being investigated as it has also been shown to provide rejection of radionuclides.

A small sighter program utilising counting of individual rocks was conducted to assess the potential for radiometric sorting as a means of upgrading the ore and waste. The radiometric sorting test work on ore gave very promising results, with 94–96% of the uranium reporting to 54–60% of the mass, along with 88% of the silver, as shown in Fig. 5 for two rock sizes.

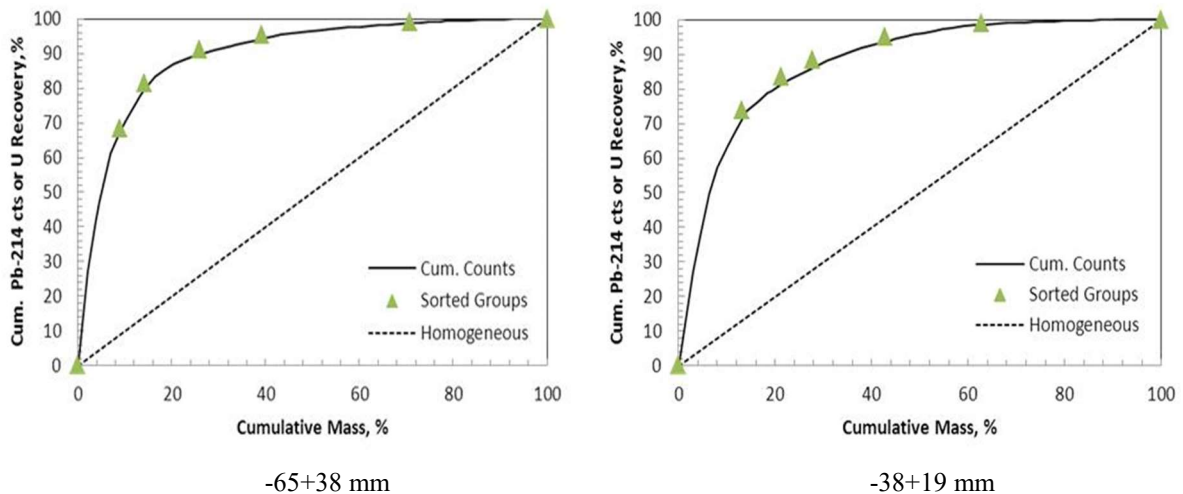


*FIG. 5. Potential upgrade in ore by radiometric sorting.*

## 6. CURRENT STATUS

The current flow sheet has been developed from the results of the test work detailed in this paper and the techno-economic evaluation by DRA. The current proposed flow sheet is given in Fig. 6.

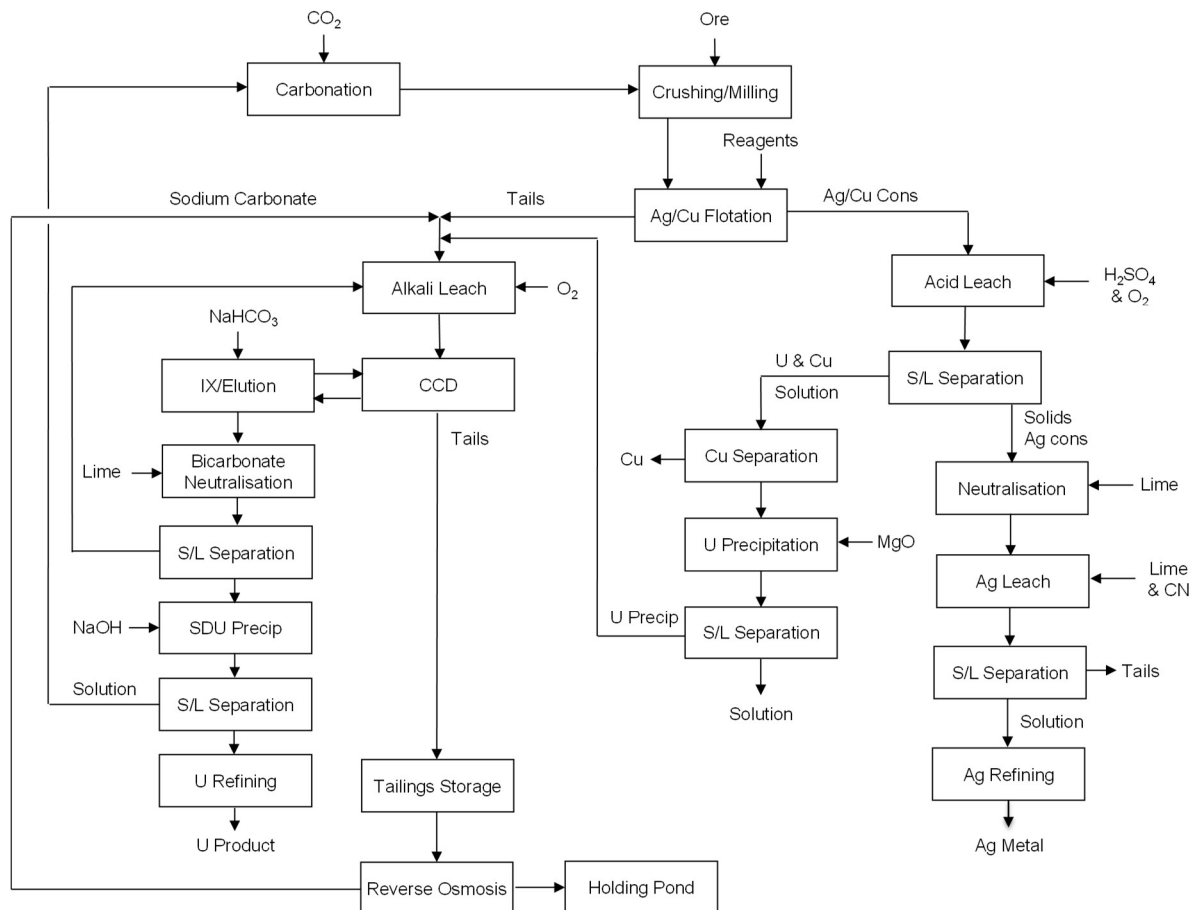


*FIG 6. Current proposed flow sheet.*

It is a closed circuit flow sheet as the recycle of the reagents is critical to economic viability. In a closed circuit the water balance is critical and the addition of fresh solution to the circuit needs to be minimised. Reverse osmosis (RO) has been incorporated, and serves two complimentary functions by concentrating the ions in the tailings pond return solution. This allows a more concentrated feed to leach, thereby increasing the solids loading in the leach section and the RO permeate can be used for wash water and reagent make-up, thereby minimising the fresh water addition and maintaining the plant water balance. A further issue with closed circuit carbonate leach circuits is the potential to generate what has been termed a ‘soda spiral’. This is partly a misnomer, as the real issue is if the addition of sodium ions is greater than the outlet of sodium ions, resulting in a sodium spiral. The sodium concentration in this circuit is controlled by the sodium bleeds from the circuit, which are sodium locked in the tailings and also sodium precipitated as jarosite in the acid leach.

The next steps in the process development are production of a final silver product and conduct variability test work from a range of ore types.

## ACKNOWLEDGEMENTS

The authors would like to thank Denison Mines for permission to publish this paper. The authors would also like to acknowledge to contributions of DRA staff, S. Lawrence, V. Coetzee, J. Du Toit and S. Archer to this work.

## REFERENCES

- [1] FEASBY, D.G., Eldorado Beaverlodge Operation, Canadian Mining Journal (June 1980) 75–149.
- [2] MCDONALD, R.J., MUIR, D.M., Pressure oxidation leaching of chalcopyrite, Part 1. Comparison of high and low temperature reaction kinetics and products, Hydrometallurgy **86** (2007) 191–205.
- [3] CATALAN, L.L.J., BUSET, K.C., YIN, G., Reactivity of oxidised sulphidic mine tailings during lime treatment, Environ. Sci. Technol. **36** (2002) 2766-2771.
- [4] REYNOLDS, G.A., The Jarosite Group of Compounds – Stability, Decomposition and Conversion, MSc Thesis, University of Newcastle, NSW, Australia (July 2007).
- [5] JOHNSON, G.D., ZHUANG, Y., Ammonia Recovery – Patent, International Publication Number WO 00/41967 (July 2000).
- [6] NEL, G.J., van den BERG, D.A., “Novel design aspects of the Tati Activox® Project Ammonia Recovery Circuit”, Proc. The South African Institute of Mining and Metallurgy Base Metals Conference (2009) 201–213.

# METALLURGICAL TESTWORK TO SUPPORT DEVELOPMENT OF THE KINTYRE URANIUM DEPOSIT

M. MALEY\*, M. FAINERMAN-MELNIKOVA\*,  
M. OVINIS\*, K. SOLDENHOFF\*, R. RING\*,  
E. PAULSEN\*\*, D. MAXTON\*\*

\* ANSTO Minerals,  
Lucas Heights, New South Wales,  
  
\*\* Cameco Australia,  
Osborne Park, Western Australia,  
  
Australia

## Abstract

The Kintyre uranium deposit is located in the Pilbara region of Western Australia and is jointly owned by Cameco and Mitsubishi Development. The current indicated resource estimate is approximately 55 million pounds U<sub>3</sub>O<sub>8</sub> at an average grade of 0.58% (~21 kt U at an average grade of 0.49%). Due to the high levels of carbonates in the deposit, alkaline leaching was considered as an option to the usually preferred acid route. Following a detailed assessment, the acid option was chosen, with the flowsheet involving acid leaching, solvent extraction and precipitation. ANSTO Minerals performed an extensive work program for Cameco, examining numerous aspects of the proposed flowsheet. This included a leach optimisation program, followed by a study determining the effects of sample variability in leaching. Settling, filtration and rheology work on slurries and tailings was performed, as well as work concerning neutralisation, precipitation and radionuclide deportment. An extensive laboratory and solvent extraction mixer-settler mini-pilot plant campaign was also performed to compare the performance of ammonia stripping and the less common strong acid strip using leach liquor generated from Kintyre ore. The pilot plant involved two campaigns of three days operation using each stripping system, with > 99.3% uranium recovery achieved in each campaign.

## 1. INTRODUCTION

The Kintyre uranium deposit is located at the western edge of the Great Sandy Desert in Western Australia, approximately 80 km south of the town of Telfer. The deposit was discovered in 1985 by CRA (now known as Rio Tinto) and was acquired by Cameco and Mitsubishi Development in a 70/30 joint venture in 2008. The indicated resource estimate is 55 Mlb U<sub>3</sub>O<sub>8</sub> at an average grade of 0.58% U<sub>3</sub>O<sub>8</sub>, or ~21 kt U at an average grade of ~0.49% U.

The uranium in the ore is present mainly as uraninite (UO<sub>2</sub>), with lesser amounts of coffinite ((USiO<sub>4</sub>)<sub>1-x</sub>(OH)<sub>4x</sub>). The ore also contains large concentrations of carbonate minerals, primarily ankerite (Ca(Fe,Mg,Mn)(CO<sub>3</sub>)<sub>2</sub>) and dolomite (CaMg(CO<sub>3</sub>)<sub>2</sub>), meaning that in an acid leaching processing route the reagent consumptions would be high. This was shown in an acid leach pilot plant operated at ANSTO in 1997, using feed that had been upgraded to approximately 2% U<sub>3</sub>O<sub>8</sub> (1.7% U) by radiometric sorting. The pilot plant was operated over seven campaigns and direct precipitation of uranium peroxide from the liquor yielded an on-specification product [1].

Due to the highly acid consuming nature of the ore, the Cameco/Mitsubishi Development joint venture partners investigated the potential of an alkaline leaching flowsheet, however following economic analysis and detailed risk assessment the acid route was selected as the preferred processing route. In order to better define this process, ANSTO Minerals was engaged by Cameco to perform an extensive metallurgical testwork program. This involved optimisation of acid leaching conditions, assessment of leaching of a variety of samples taken from throughout the deposit, and settling, filtration, neutralisation and rheology of leach slurries. An assessment of solvent extraction was also performed, using both ammonia and strong acid stripping, along with subsequent uranium precipitation work. In addition,

testwork with regards to radionuclide behaviour was also performed, including the radionuclide deportment and long-term stability in tailings and an assessment of radium removal from liquors.

The focus of this paper is on the leaching and solvent extraction testwork, including the results from the small-scale laboratory leach optimisation program and the results from a solvent extraction mini-plant operated to assess the ammonia and strong acid stripping systems.

## 2. LEACHING TESTWORK

A composite sample was prepared from samples taken from throughout the Kintyre orebody, with the blend aiming to match the global average of uranium and carbonate in the orebody. The composition of the sample is summarised in Table I. All leaches were performed at a set pH and oxidation-reduction potential (ORP)<sup>20</sup> in temperature controlled 2 L baffled tanks at a solids density of 50 wt% for 18 hours (based on the results from previous testwork), using 40 wt% NaMnO<sub>4</sub> solution as an oxidant. In practice permanganate would not be used due to its cost and a cheaper oxidant such as pyrolusite (MnO<sub>2</sub>) would most likely be utilised. However, the faster reacting sodium permanganate solution allows much better control of the ORP and permanganate consumptions can readily be converted to equivalent pyrolusite additions. Samples were taken from the leaches after 1, 2, 4, 8, 12 and 18 hours. A summary of the variables and the ranges investigated is given in Table II.

TABLE I. SUMMARY OF KINTYRE COMPOSITE SAMPLE USED FOR LEACH OPTIMIZATION TESTWORK

| Species                       | wt%  |
|-------------------------------|------|
| CO <sub>3</sub>               | 9.55 |
| Ca                            | 3.03 |
| Fe                            | 8.2  |
| Mg                            | 7.3  |
| Si                            | 25.6 |
| U <sub>3</sub> O <sub>8</sub> | 0.52 |

TABLE II. VARIABLES INVESTIGATED IN THE KINTYRE LEACH OPTIMIZATION PROGRAM

| Variable    | Range tested |
|-------------|--------------|
| Temperature | 35–65 °C     |
| pH          | 1.8–2.5      |
| ORP         | 450–550 mV   |

<sup>20</sup> In this paper, all ORP values are quoted relative to an Ag/AgCl reference electrode filled with 3 mol/L KCl.

The plots in Figs 1, 2 and 3 show the impact of the varying selected leach parameter on uranium extraction and reagent addition. As each point on the line represents a sampling time, the lower the point on the vertical axis, the greater the uranium extraction. Presenting the leach data in this way allows the identification of optimum leach conditions to be performed more easily than by simply plotting the uranium extraction vs time.

The impact of temperature was investigated by a series of leaches performed on the composite sample ground to P<sub>80</sub> 500 µm at pH 1.8 and an ORP of 500 mV. The results from these tests shows that although increased leach temperature increased the rate of uranium extraction, acid addition also increased due to a greater amount of the gangue minerals dissolving (Fig. 1). In addition, final uranium extractions were similar after the 18-hour leach period at all temperatures studied, between 95.5 and 98.7%. Based on these results, 55°C was selected as the optimum leach temperature, as the final uranium extraction of 98.3% was close to the maximum result achieved at 65°C (98.7%), however the acid addition was significantly lower (175 kg/t compared to 195 kg/t).

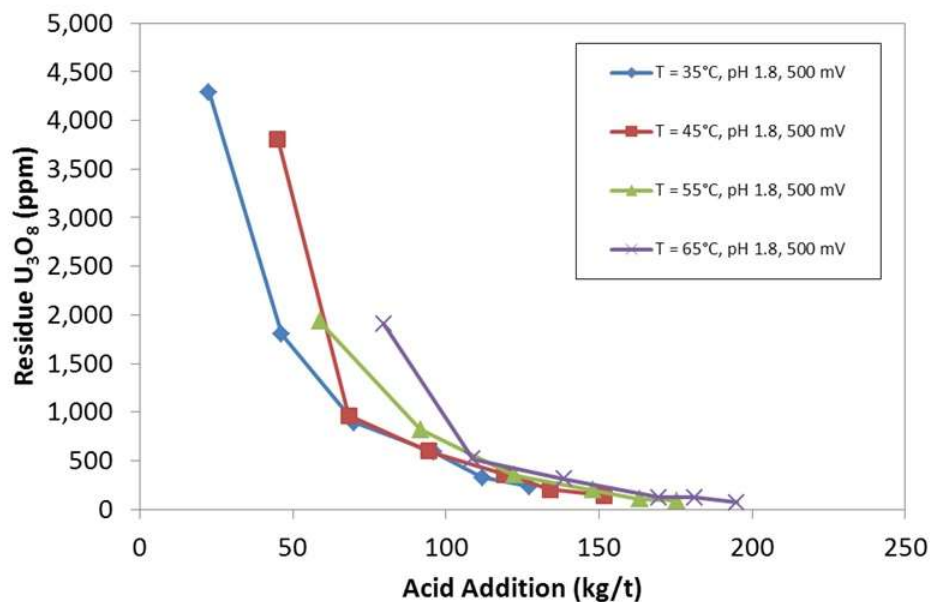


*FIG. 1. Effect of leach temperature on uranium leaching rates and acid addition for leaches on the Kintyre composite sample.*

Following identification of the optimal leach temperature, a series of tests was performed on the same sample at 55°C and varying pH setpoints. The results from these leaches showed that although the rate of uranium leaching increased with decreasing pH, at the conclusion of the leach period the uranium extractions were all very similar for tests between pH 1.8 and 2.2 (97.8–98.5%). The leach at the highest pH, 2.5, yielded a significantly lower uranium extraction most likely due to the reduced solubility of Fe<sup>3+</sup> at this pH. The final concentrations of Fe<sup>3+</sup> in the leach liquors were between 1200 and 4700 mg/L for leaches performed between pH 1.8 and 2.2, whilst in the leach performed at pH 2.5 the final concentration was 540 mg/L. The impact of Fe<sup>3+</sup> concentration on uranium leaching for this sample is discussed further below.

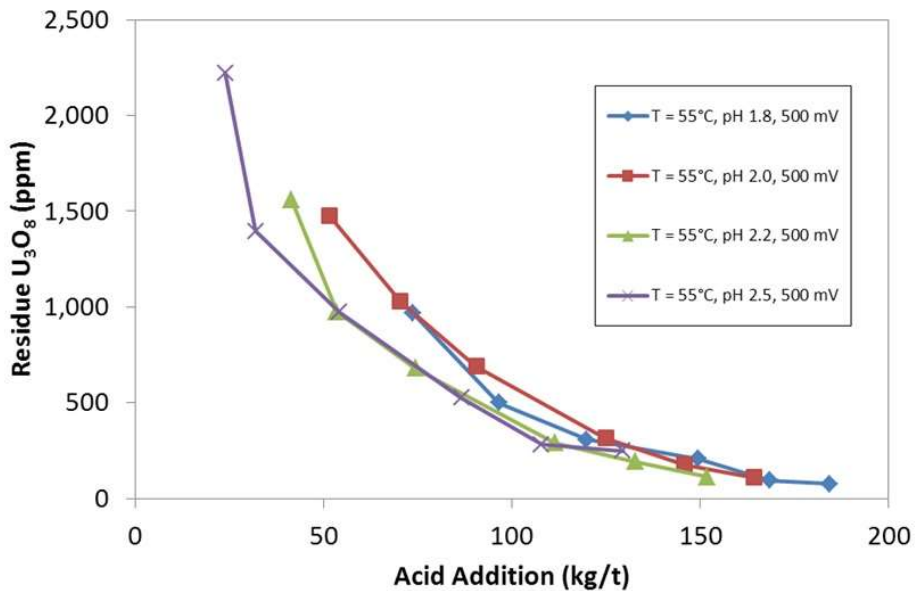


*FIG. 2. Effect of leach pH on uranium leaching rates and acid addition for leaches on the Kintyre composite sample.*

The leach ORP setpoint was optimised by performing a series of leaches on the P<sub>80</sub> 500 µm composite sample at the identified optimum conditions of 55°C and pH 2.2. The initial rate of uranium extraction was faster for the leach performed at 550 mV, however the final extractions in each of the three tests were virtually identical at the conclusion of the leach period, between 97.7 and 97.9%. As expected, oxidant addition increased with ORP setpoint due to the greater amount of Fe<sup>2+</sup> oxidised. An ORP setpoint of 450 mV was therefore selected as the optimum, as this yielded effectively the same uranium extraction as the higher ORP tests whilst minimising the oxidant addition.

The results for tests at varying ORP can be explained by the impact of Fe<sup>3+</sup> concentration on the dissolution of uraninite, the dominant uranium mineral present in the ore. The kinetics of uraninite leaching are known to be directly proportional to the Fe<sup>3+</sup> concentration [2] however ultimately if the Fe<sup>3+</sup> concentration is sufficiently high, about 1–2 g/L, the uraninite will readily leach to the extent allowed by the particle size and porosity of the ore particles [3]. As shown in Fig. 4, the Fe<sup>3+</sup> concentrations in the leaches matched the trend with initial uranium extraction rate, however as the concentrations throughout the leaches was greater than 1 g/L, the maximum uranium extraction was achieved in each leach within the 18-hour leach period. It is likely that an ORP setpoint lower than 450 mV would result in a decreased uranium extraction for this sample as the Fe<sup>3+</sup> concentration in solution would decrease to levels too low for effective uraninite leaching.

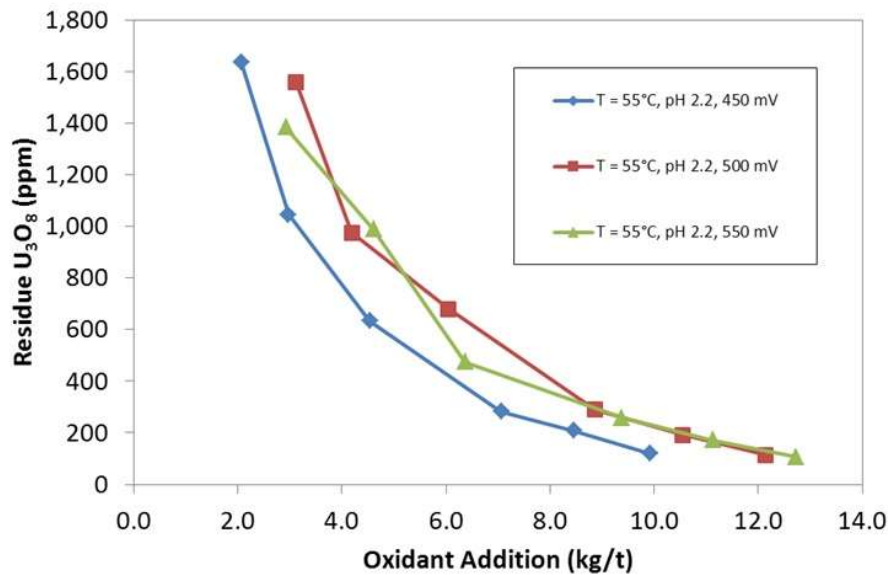


FIG. 3. Effect of leach ORP on uranium leaching rates and oxidant addition for leaches on the Kintyre composite sample.

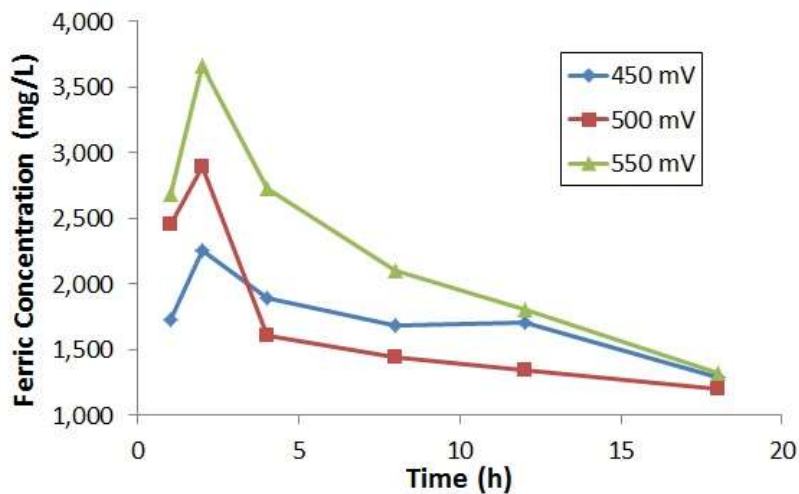


FIG.4. Effect of leach ORP on  $Fe^{3+}$  concentration for leaches on the Kintyre composite sample.

Following the leach optimisation study, a variability study was performed using a selection of 34 samples taken from throughout the Kintyre orebody. Each sample was ground to  $P_{80}$  500  $\mu m$  and leached at pH 2.2, ORP 450 mV and 55°C at a solids density of 55 wt% with a residence time of 18 hours. The results from these leaches are summarised in Table III. A strong correlation was also observed between head calcium concentration and acid addition, representing the ankerite and dolomite content in the samples (Fig. 5). Although the acid addition to the leaches was high, averaging 187 kg/t, the relatively high uranium grade means that the reagent costs are offset.

TABLE III. SUMMARY OF RESULTS FROM LEACHES PERFORMED ON KINTYRE VARIABILITY SAMPLES

|         | U <sub>3</sub> O <sub>8</sub> grade (ppm) | U extraction (%) | Acid addition (kg/t) | Equivalent MnO <sub>2</sub> addition (kg/t) |
|---------|---|------------------|----------------------|---|
| Maximum | 9210                                      | 99.2             | 432                  | 22.3  |
| Minimum | 1630                                      | 86.2             | 42                   | 2.8   |
| Average | 4378                                      | 95.5             | 187                  | 11.1  |

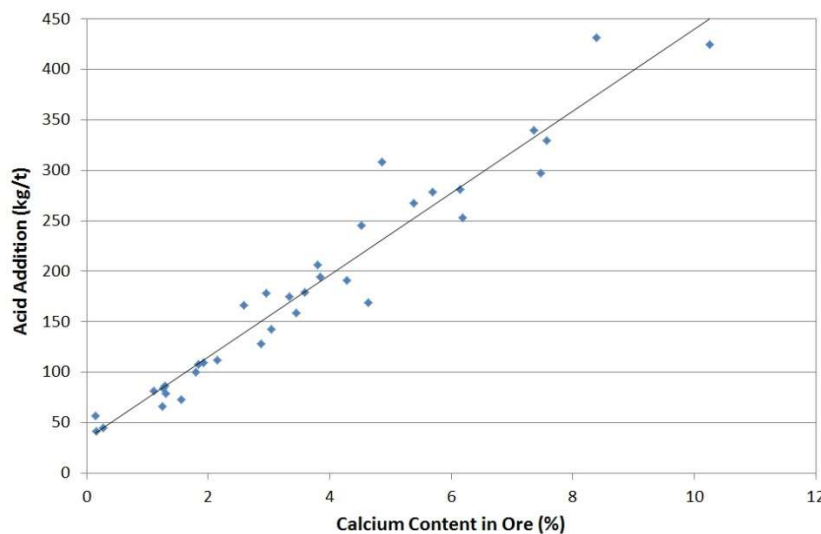


FIG. 5. Acid addition vs. head calcium content for leaches on Kintyre variability samples.

### 3. SOLVENT EXTRACTION MINI-PLNT

A bulk leaching campaign processing a total of 2000 kg of Kintyre ore was performed to generate approximately 1000 L of pregnant leach solution for solvent extraction work, with the composition of the liquor summarised in Table IV. The pH of the liquor was adjusted to 1.8 and the ORP of the bulk liquor was 420 mV (at ambient temperature). This liquor was then processed in a mini-plant for two lots of 72 hours continuous runs (a total of 144 h), with each run evaluating a different stripping method, conventional ammonia stripping using NH<sub>4</sub>OH / (NH<sub>4</sub>)<sub>2</sub>SO<sub>4</sub> and strong acid stripping using ~400 g/L H<sub>2</sub>SO<sub>4</sub>.

TABLE IV. COMPOSITION OF FEED LIQUOR FOR SOLVENT EXTRACTION MINI-PLANT

| Element | g/L   | Element | g/L | Element | g/L  | Element | g/L    |
|---------|-------|---------|-----|---------|------|---------|--------|
| Al      | 1.6   | Fe      | 1.5 | Na      | 1    | U       | 2.7    |
| As      | 0.002 | Mg      | 25  | Ni      | 0.02 | V       | <0.001 |
| Ca      | 0.57  | Mn      | 16  | S       | 53   | Zn      | 0.03   |
| Cu      | 0.02  | Mo      | 1   | Si      | 0.3  | Zr      | 0.01   |

Conventional extractant, Alamine 336 (5 vol.%) in Shellsol 2046, with isodecanol phase modifier (2.5 vol.%), was used in both campaigns.

A simplified flowsheet for each process is shown in Figs 6 and 7. The SX mini-plant comprised a battery of variable sized mixer-settlers (Table V). The solvent extraction circuits for both ammonia and acid stripping processes included a total of 13 stages: four extraction, three scrub, five uranium strip and single reprotoonation or wash stage. The main plant operating parameters are presented in Table VI.

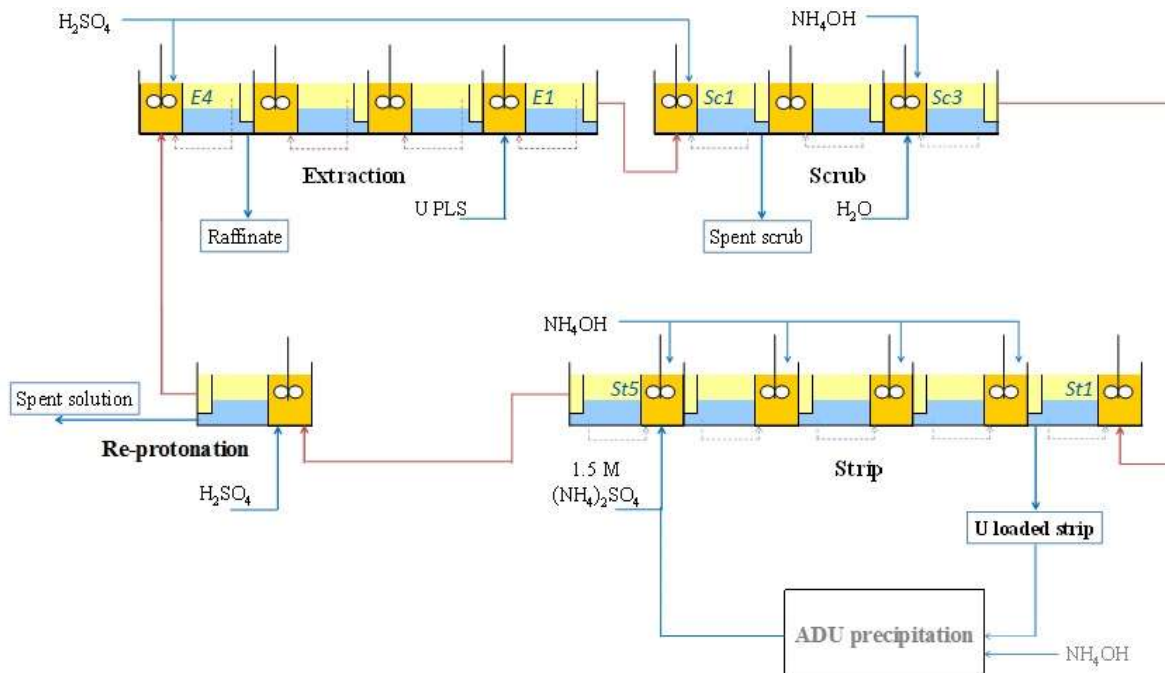


FIG. 6. Simplified ammonia stripping solvent extraction mini-plant flowsheet.

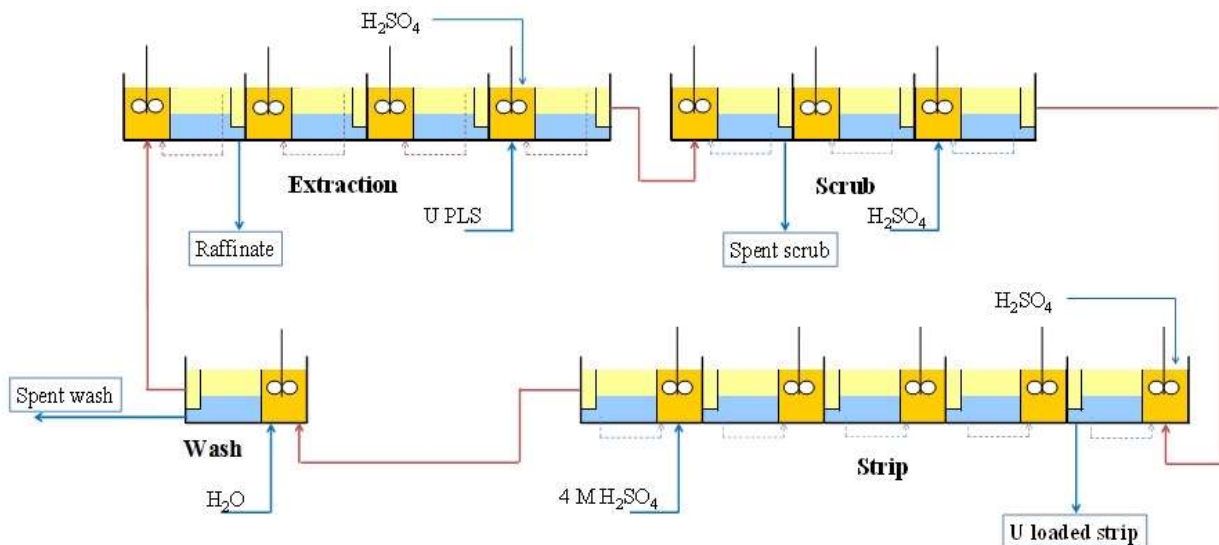


FIG. 7. Simplified strong acid stripping solvent extraction mini-plant flowsheet.

TABLE V. MIXER-SETTLER PARAMETERS

| Circuit                          | Mixer volume (mL) | Settler volume (mL) |
|----------------------------------|-------------------|---------------------|
| Extraction                       | 473               | 922                 |
| Scrub, strip, reprotonation/wash | 136               | 343                 |

TABLE VI. MINI-PLANT OPERATING PARAMETERS

| Circuit         | O/A flow ratio<br>(advanced flows) | Phase continuity in<br>mixer | Temperature (°C) |
|-----------------|------------------------------------|------------------------------|------------------|
| Extraction      | 0.65                               | organic                      | 35–50            |
| Scrub           | 10                                 | organic                      | 30–40            |
| Strip (ammonia) | 5                                  | organic                      | 30–40            |
| Strip (acid)    | 10                                 | organic                      | 30–40            |

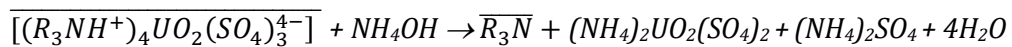
The extraction circuit was operated at an organic to aqueous ratio (O/A) of 0.65. To prevent operational problems associated with the poor phase disengagement, organic continuity was maintained in the extraction circuit mixers by partial recycling of solvent from the adjacent settlers.

The pH gradient in the extraction circuit was between 1.9–2.1 in the aqueous after the extraction stage 1 and 1.6–1.8 in the raffinate (extraction stage 4). Concentrated H<sub>2</sub>SO<sub>4</sub> was used to control the pH in the extraction circuit. Uranium extraction was very high, between 99.7 and 99.96%, yielding U concentrations of approximately 4.3 g/L in the loaded solvent and <10 mg/L in the raffinate.

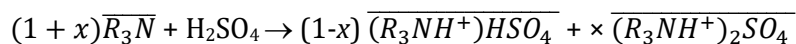
A three-stage scrub at O/A ~ 10 was employed for both processes. Two sets of scrubbing conditions were tested: scrubbing with water using the pH gradient from 1.5 in scrub stage 1 to 2.5 in scrub stage 3 (the ammonia strip campaign) and scrubbing with dilute sulphuric acid with the acidity in the scrub stages at pH ~1.6–1.7 (acid strip campaign). Scrubbing successfully removed > 50% entrained Mg and Mn from the solvent. However, regardless of the scrubbing conditions, only negligible amounts of As, Ca, Cu, Si and Zr were rejected. Scrubbing of loaded uranium was minimal, with 0.1–0.3% removed.

The ammonia strip process was performed at O/A = 5, using 1.5 mol/L (NH<sub>4</sub>)<sub>2</sub>SO<sub>4</sub>, with a pH gradient maintained between ~3 in the strip stage 1 (uranium product stream) and ~5 in the strip stage 5 (stripped organic out) by ammonia addition. In the ammonia strip process higher pH facilitates uranium stripping from the amine extractant. However, at pH > 5 ammonium diuranate (ADU) precipitate starts to form. To avoid ADU precipitation/crud formation in the continuous process, lower pH (~3) is maintained in the first strip stages, where the uranium concentration is high in both the organic and aqueous phases. On the other hand, higher pH is used in the last strip stages, aiming to maximise recovery of uranium and minimise its recycling to the extraction circuit. Maintaining of the constant pH gradient in the strip circuit is the main operational challenge of the ammonia stripping process.

Uranium stripping with NH<sub>4</sub>OH/(NH<sub>4</sub>)<sub>2</sub>SO<sub>4</sub> occurs predominantly in the following reaction:



When contacted with sulphuric acid, free amine, R<sub>3</sub>N, gets reprotonated:



To minimize sulphuric acid consumption in PLS for solvent reprotoonation and, hence, to alleviate the pH control in the extraction circuit, a reprotoonation stage was introduced in the ammonia strip process.

The strong acid stripping circuit was operated at O/A = 10, with ~400 g/L H<sub>2</sub>SO<sub>4</sub>. Because of the higher O/A ratio, the U concentration in the product stream (at ~40 g/L) was more than twice as high as the U concentration in the ammonia strip liquor (18 g/L). However, the former solution contained a proportionally higher sulphate concentration and was highly acidic.

A comparison of the results from the two campaigns shows that both the ammonia and strong acid systems were effective for stripping of uranium from the solvent, with > 99.3% uranium recovery achieved (Table VII). The uranium recovery was marginally higher using strong acid stripping, with uranium recoveries between 99.6 and 99.8%.

TABLE VII. COMPARISON OF PERFORMANCE OF AMMONIA AND STRONG ACID STRIPPING SYSTEMS

| Circuit              | Product stream<br>U conc. (g/L) | Product stream<br>S conc. (g/L) | Stripped<br>solvent stream<br>U conc. (g/L) | Stripped<br>solvent S conc.<br>(g/L) | % U<br>stripped |
|----------------------|---------------------------------|---------------------------------|---|--------------------------------------|-----------------|
| Ammonia strip        | 18                              | 54                              | 0.03  | —                                    | 99.3            |
| Strong acid<br>strip | 41                              | 126                             | 0.015                                       | 3.7                                  | 99.6–99.8       |

A summary of the compositions of the product streams for each of the methods, presented in Table VIII, shows that the strip liquors were low in impurities, with only the Zr concentration above the limit without rejection for the strong acid strip liquor. However, in practice the presence of Zr would not pose a problem as it would be not precipitated with the uranyl peroxide.

TABLE VIII. SUMMARY OF IMPURITIES IN AMMONIA AND STRONG ACID STRIP PRODUCT STREAMS

| Element | % of U in<br>ammonia strip<br>liquor | % of U in acid strip<br>liquor | Maximum limit without<br>rejection* |
|---------|--------------------------------------|--------------------------------|-------------------------------------|
| As      | 0.03                                 | 0.02                           | 0.1                                 |
| Ca      | 0.16                                 | 0.29                           | 1.0                                 |
| Fe      | 0.04                                 | 0.01                           | 1.0                                 |
| Mg      | 0.07                                 | <0.002                         | 0.5                                 |
| Mo      | <0.03                                | <0.01                          | 0.3                                 |
| Si      | <0.03                                | <0.01                          | —                                   |
| V       | <0.03                                | <0.01                          | 0.3                                 |
| Zr      | 0.06                                 | 0.15                           | 0.1                                 |

\* ASTM C967-13 Standard specification for uranium oxide concentrate.

The results from the solvent extraction mini-plant indicate that both of the stripping methods are effective and would be suitable for use for the Kintyre project, with each of the methods having its own advantages and disadvantages. The primary advantage of the strong acid stripping route is the simplicity in controlling the strip circuit as no pH or acidity control is required. The higher O/A in the acid strip circuit means that a higher uranium concentration can be achieved in the strip liquor compared to ammonia stripping, whilst the acidic liquor affords a greater number of options for the precipitation of the uranium product. However, the use of a high concentration of acid means that neutralisation costs before uranium precipitation will be high due to the large amount of lime required, resulting in large amounts of gypsum to be washed to recover entrained uranium and be disposed of. The ammonia stripping route is a well-known technology with a liquor that allows simpler recovery of the uranium, however careful pH control of the circuit is necessary to ensure that the uranium does not precipitate, and crud is more likely to form in the circuit. In addition, the use of ammonia requires an ammonium sulphate bleed which must be treated to avoid environmental contamination. A comprehensive comparison of the two technologies has been performed by van Tonder and Edwards [4].

#### 4. CONCLUSIONS

A series of leach optimization tests performed on a composite sample from the Kintyre deposit identified pH 2.2, ORP 450 mV, 55 °C, P<sub>80</sub> 500 µm and an 18-hour residence time as the conditions for maximum uranium extraction whilst minimizing reagent addition. A selection of samples taken from throughout the deposit were leached under these conditions, with uranium extractions between 86.2 and 99.2%, averaging 95.5. Due to the high ankerite and dolomite contents in the deposit, acid addition was high for these samples, averaging 187 kg/t. However, the reagent costs are outweighed by the relatively high uranium concentration in the deposit of 0.58%.

A fully integrated uranium solvent extraction mini-plant was operated continuously for a total of 144 h, processing liquor generated from bulk leaches on Kintyre ore. As part of the mini-plant operation, two stripping processes, conventional ammonia and strong acid stripping with 400 g/L H<sub>2</sub>SO<sub>4</sub>, were tested in separate 72-hour campaigns. Both stripping methods were demonstrated to be equally effective, achieving > 99% uranium recovery from the solvent and yielding liquors with compositions indicating the generation of on-spec uranium products. The simplicity of operation is the primary advantage of the strong acid strip method, there are costs associated with neutralisation. The ammonia route is a well-established technology. However, control of the stripping circuit is more challenging and the ammonia sulphate bleed must be treated.

#### ACKNOWLEDGEMENTS

The authors would like to thank Cameco and Mitsubishi Development for their permission to publish this work.

#### REFERENCES

- [1] MACNAUGHTON, S.J., COLLIER, D., TAPSELL, G., RING, R.J., HAWLEY, B., BELLINGHAM, A., "Pilot plant scale production of yellowcake from the Kintyre uranium deposit using a direct precipitation process", Chemeca 98 (Proc. 26<sup>th</sup> Australasian Chem. Eng. Conf., Port Douglas, Australia), Institution of Chemical Engineers (IEAust) (1998).
- [2] NICOL, M.J., NEEDES, C.R.S., FINKELSTEIN, N.P., "Electrochemical model for the leaching of uranium dioxide – acid media", Leaching and Reduction in Hydrometallurgy (BURKIN, A.R., Ed.), The Institution of Mining and Metallurgy, London (1975).
- [3] RING, R.J., Ferric sulphate leaching of some Australian uranium ores, Hydrometallurgy **6** (1980) 89–101.
- [4] VAN TONDER, D., EDWARDS, C., "Strong acid versus ammonia strip in uranium SX circuits", ALTA Uranium Sessions (Proc. Conf., Perth, Australia, 2012) ALTA Metallurgical Services, Melbourne (2012).

# **DEVELOPMENT OF CARBONATE HOSTED URANIUM MINERALIZATION IN INDIA**

D. ACHARYA, A.K. SARANGI  
Uranium Corporation of India Ltd,  
Singhbhum East, Jharkhand,  
India

## **Abstract**

India, the second-most populous country of the world with a population of more than 1.2 billion has been registering accelerated agricultural and industrial growth for about a decade. This has posed a serious challenge of meeting the quantitative demand of secure and affordable energy. This vibrant development process is also resulting in a shift from the use of non-commercial energy sources to commercial energy sources, particularly electricity. The problem is all the more acute in the light of recent developments of global measures to cut emission and emphasis on producing electricity in environmentally benign means. In this context of India's planned electricity generation, expansion of nuclear power capacity occupies a special standing towards energy independence of the country. It has also been established and appreciated in many countries of the world that nuclear power is the reliable, environmentally superior and economically viable source of energy. Accordingly, India is on the preferred path of generating nuclear power with the use of its indigenous atomic mineral resources. Some multiplying capacity generation is though expected through the import of fuel as a result of recently concluded India-specific international agreement on nuclear co-operation, the indigenous production of atomic fuel continues to expand with vigour.

## **1. SIGNIFICANCE OF URANIUM TOWARDS ENERGY SECURITY**

Uranium and thorium are the two chiefly known naturally occurring atomic minerals considered as sources of energy. Of the two, only uranium is fissionable and considered as the primary source for production of electricity. Thorium is a fertile material. Its use in the process of fission and potential production of electricity is linked with the technological development of transmutation and its industrial application. Presently, natural uranium is considered as the only source of power in nuclear power plants all over the world.

The core consideration of India's nuclear power programme is the fact that the country has moderate uranium reserves but abundant thorium. The programme is geared towards maximizing the utilization of scarce uranium and to aim for conversion of thorium to fissile  $^{233}\text{U}$ . The Indian nuclear programme is based on distinctive sequential three stages and allied technologies intending to optimally utilize the indigenous nuclear resource i.e. moderate Uranium and abundant Thorium. Accordingly, the three-stage program is called 'closed fuel cycle', where the spent fuel of one stage is reprocessed to produce fuel for the next stage. The first stage comprises of Pressurized Heavy Water Reactors fuelled by natural uranium which undergoes fission releasing energy and fissile element  $^{239}\text{Pu}$ . The second stage, comprising of Fast Breeder Reactors (FBRs) are fuelled by mixed oxide of  $^{238}\text{U}$  and  $^{239}\text{Pu}$ , recovered from first stage. In FBRs,  $^{239}\text{Pu}$  undergoes fission producing energy and also producing more  $^{239}\text{Pu}$  by transmutation of  $^{238}\text{U}$ .  $^{232}\text{Th}$ , abundantly available in India, is not fissile and can be converted by transmutation in a fast breeder reactor in third stage to a fissile material,  $^{233}\text{U}$ . The closed fuel cycle thus multiplies the energy potential of the fuel manifold and greatly reduces the quantity of waste.

Development of indigenous uranium reserve is the vital link for operation of Pressurized Heavy Water reactors (PHWRs) and thorium based reactors in future.

## **2. INDIA'S URANIUM RESOURCES**

Uranium exploration activities in India carried out since 1951, has established moderate low grade mineralization in different geological basins of India. Of the total resources identified so far, Proterozoic basins of the country account for about 85% whereas remaining 15% are located in Phanerozoic basins. Indian uranium deposits are of medium size and the country has a modest uranium resource. The known

Proterozoic basins with significant uranium finds are: a) Cuddapah basin; b) Singhbhum shear zone; c) North Delhi fold belt; and d) Bhima basin. Of the above basins, Cuddapah basin in southern part of India accounts for 52% of Indian uranium resources and a lion's share of it (about 80%) lies in carbonate hosted rock around Tummalapalle in the State of Andhra Pradesh.

### 3. URANIUM MINERALIZATION AROUND TUMMALAPALLE

Geologically, Tummalapalle area is in the south-western part of the Cuddapah basin, close to the Archean basement. A thick pile of carbonate rock (Vempalle formation) is the host to uranium mineralization in this area which consists of purple shale, massive limestone, intra-formational conglomerate, dolostone (uraniferous), shale and cherty limestone. The impersistent conglomerate and a purple shale band occurring immediately below and above the mineralized rock respectively, serve as the marker horizons. The general strike of the formation is WNW-ESE with the amount of dip varying between  $15^\circ$  to  $17^\circ$  due N $22^\circ$ E.

The ore lenses are fairly continuous over the entire strike length of 6.6 km and extending down-dip at  $15^\circ$  to  $18^\circ$  up to a depth of 275m. Two parallel ore bands, designated as Hangwall Lode and Footwall Lode with average width of 3.2 m and 2.5 m respectively (Fig. 1) are considered for mining. The two bands are tabular, stratabound and non-transgressive in nature with little variation in grade and thickness along strike and dip. These two bands are separated by a lean zone of 1.5 m to 3 m width. 70% of the total reserves is confined to Hangwall Lode of the deposit. In general, the host rock is quite competent. But the Hangwall Lode is overlain by a layer of shale which is fractured and weak. Fairly extensive continuation of mineralization along strike and down-dip has been confirmed through surface exploration around Tummalapalle.

The radioactive minerals identified in the ore zone are pitchblende, coffinite, U-Ti complex. Pitchblende, which is the major contributor of radioactivity, occurs as fine grained aggregates intimately associated with pyrite in carbonate and phosphatic matrix. Coffinite is fine grained and associated with pyrite. Other associated minerals are pyrite, chalcopyrite, molybdenite and collophane. The gangue minerals are dolomite, quartz and microcline.

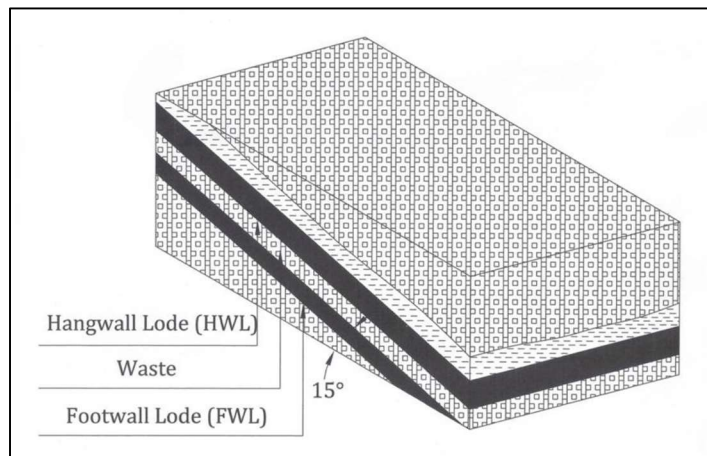
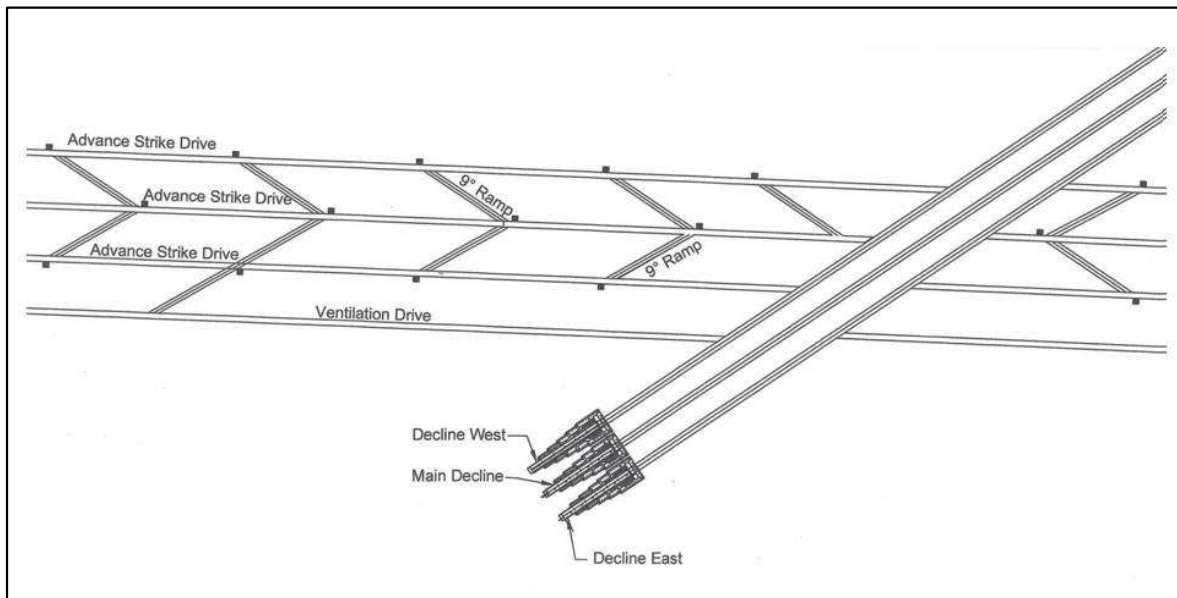


FIG. 1 Ore bands at Tummalapalle.

### 4. MINING AT TUMMALAPALLE

Several studies were made to develop the orebody at Tummalapalle with an aim to produce the ore at an early date, minimise the cost of production and dilution through optimum level of mechanization and maximize the ore recovery. The entry into the mine has been established through a central decline at  $9^\circ$  gradient along the apparent dip of orebody. Two more declines, 15 m apart on both sides and parallel to the central decline are also developed (Fig. 2). The central decline is provided with a conveyor for ore

transport and other two parallel declines are used as service path for movement of men and materials. All declines, developed following the orebody have helped in generating the ore at an early stage.



*FIG. 2 Mine development at Tummalapalle.*

Mine development at Tummalapalle mainly includes progress of Advance Strike Drives (ASDs) in the strike direction from both the service declines till the extreme limits of the orebody. As all the developmental works are in the ore lenses, the dilution has been kept to minimum. The ramp has been developed connecting two ASDs driven in apparent dip of  $9^\circ$  to facilitate manoeuvring of the underground equipment. Advance Strike Drives (ASDs) developed along the orebody have crown pillars of  $5\text{ m} \times 5\text{ m}$  along the full strike length. The inclined distance between ASDs is 39 m. Length of each panel is 120 m along strike direction followed by 10 m wide rib pillar. Ramps are driven between ASDs (level to level) at  $9^\circ$  gradient for movement of vehicles and transporting the ore to the conveyor. The equipment under use for development includes low profile jumbo drill, rock bolter, low profile loader, dozer and dump truck.

While opening the mine, very poor strata condition was encountered in the roof of the Hang Wall Lode resulting in a number of roof collapses and it was found unsafe to continue working in this lode. Presently, mining of ore at Tummalapalle is confined to narrower Footwall Lode. Effective mine planning has ensured adequate production from the mine establishing a large stock-pile. However, exclusive mining of narrower ore body in the Footwall Lode has resulted in higher dilution. It has been realized that it is necessary to mine Hangwall Lode safely and efficiently to meet the projected goals with respect to tonnage, quality of ore and cost. Accordingly, reputed mining research institutes of the country are engaged to devise a newer development method / sequence to enable opening of Hangwall Lode for commercial scale mining.

After development of the panel, open stoping method will be practiced with pillars for support of stopes. No back filling is being carried out at this stage. However, provision has been made for delayed filling of the stopes with de-slimed mill tailings. The normal sequence of stoping is to extract from top to bottom and away from declines, towards strike boundary. Ore, after primary crushing (to  $< 4$  inch ( $\sim 100$  mm) size) will be brought to plant in conveyor through main decline.

Top most ASDs in eastern and western side of the mine are serving as ventilation drives. Other ASDs and ramps are serving as network for return path of air exhausting to surface through four ventilation shafts.

## 5. PROCESSING TECHNOLOGY

In India, the operating plant at Jaduguda and plants planned at other places are designed with acid leaching technology. The host rock composition at Tummalapalle, as shown in Table I does not favour the conventional processing of acid leaching because of high carbonate content. A great deal of laboratory and pilot plant studies were conducted to develop the process flow sheet on alkali leaching and finalise the process parameters.

TABLE I. COMPOSITION OF HOST ROCK AT TUMMALAPALLE

| Constituent       | %      |
|-------------------|--------|
| Carbonates        | 83.2   |
| Quartz + Feldspar | 11.3   |
| Collophane        | 4.3    |
| Pyrite            | 0.47   |
| Chalcopyrite      | 0.05   |
| Magnetite         | 0.15   |
| Ilmenite          | 0.25   |
| Iron-hydroxide    | 0.27   |
| Galena            | Traces |

The mined ore, after conventional crushing and grinding (80% passing 74 micron) are thickened, repulped and subsequently subjected to alkali leaching by sodium carbonate and sodium bicarbonate solution. Leaching is carried out in autoclaves in series with a nominal residence time of 6.5 hrs at 130°C and 6.0–8.0 kg/cm<sup>2</sup> pressure. The leached slurry is then filtered in Horizontal Belt Filter (HBF) and the desired concentration leached liquor is achieved through repeated recirculation and washing. The washed cake in the form of slurry is disposed in tailings impoundment facility. The leached filtrate, after clarification and pre-coat filtration is subjected to precipitation with the addition of sodium hydroxide. The final product, at a pH of 12 or above is precipitated as sodium di-uranate (SDU). A study to treat the barren liquor to regenerate sodium carbonate and sodium hydroxide before recycling has been taken up. The plant is designed to process 3000 tonnes of ore per day. It will also produce sodium sulphate as by-product.

## 6. FUTURE POTENTIAL

The exploration around Tummalapalle area has established large resources in recent years. The resources known so far in this area, account for about 45% of the total Indian uranium resources. New mines and plants have been envisaged to be taken up in coming years as the operations at Tummalapalle stabilize. The operations at Tummalapalle have been taken up for expansion to mine and process additional 1500 tonnes of ore per day. Pre-feasibility study for a large underground mine and plant at Kanampalle shall be taken up soon.

Multi-disciplinary research is in progress to establish appropriate mining technology for the Hangwall Lode of area which is underlain by poor rock strata (shale). Mining of the Hangwall Lode shall substantially improve the Run-of-Mine grade ore to the plant. Pilot plant studies are in progress to improve leaching and precipitation efficiency of the plant. New equipment is being introduced in the process stream. Recovery of re-agents is expected to bring in substantial financial benefit to the operations in coming years.

The area around Tummalapalle has the vast potential for multiplying uranium production to support indigenous nuclear power programme of the country.

## 7. CONCLUSION

Mining and processing of carbonate hosted uranium mineralization is not a very favored practice in the world. In the past, many operators have closed the operations prematurely due to various difficulties. Some of the operations are also on hold now due to adverse economics.

In India, carbonate hosted mineralization accounts for lion's share of uranium inventory. The success of this extraction technology is significant towards multiplying the uranium production from indigenous resources which will help in long term energy security of the country. Therefore, many innovative practices through in-house research are under implementation to overcome the hurdles of present mining and processing at Tummalapalle.

## BIBLIOGRAPHY

GUPTA, R. SARANGI, A.K., A new approach to mining and processing of a low-grade uranium deposit at Tummalapalle, Andhra Pradesh, India, paper presented at IAEA Tech. Mtg on Uranium Small-Scale and Special Mining and Processing Technologies Vienna, 2007.

— Overview of Indian uranium production scenario in coming decades, Energy Procedia 7 (2011) 146–152.

SARANGI, A.K., Geological characteristics of Indian uranium deposits influencing mining and processing techniques, Book of Abstracts, International Symposium on Uranium Raw Material for Nuclear Fuel Cycle: Exploration, Mining, Production, Supply and Demand, Economics and Environmental Issues (URAM-2009), Vienna (22-26 June 2009) 143.

— “Uranium exploration, resources and production in India”, Geo-resources, Scientific Publishers, India, Vol. II-25 (2014) 253–263.

SARANGI, A.K., KRISHNAMURTHY, P., Uranium metallogeny with special reference to Indian deposits, Trans. Mining Geological and Metallurgical Institute of India, **104** 1–2 (2008) 19–54.

SARANGI, A.K., YADAV, D.S., “Uranium Resources of India and Potential for Development”, Proc. 17th convention of the Indian Geological Congress and International Conference on New Paradigms of Exploration and Sustainable Mineral Development: Vision 2050 (NPESMD 2011), 2011, Dhanbad, India (2011) 99–110.

SURI, A.K., Innovative process flowsheet for the recovery of Uranium from Tummalapalle Ore, Bhabha Atomic Research Centre (BARC) Newsletter **317** (Nov.-Dec. 2010) 6–12.

SURI, A.K., et al., Process development studies for low grade uranium deposit in alkaline host rocks of Tummalapalle, paper presented at IAEA Tech Mtg on Low Grade Uranium Deposits, Vienna, 2010.

# **RESIN-IN-PULP BASED ION EXCHANGE SEPARATION OF URANIUM FROM ALKALINE LEACH SLURRY**

T. SREENIVAS, K.C. RAJAN

Mineral Processing Division, Bhabha Atomic Research Centre,  
AMD (Atomic Minerals Directorate for Exploration & Research) Complex,  
Begumpet, Hyderabad, India

## **Abstract**

Some of the prominent low-grade uranium ore deposits in India are hosted in acid consuming gangue matrix. This paper describes the results of the resin-in-pulp (RIP) studies on very-fine grained alkaline leach slurry using various commercially available strong base anionic exchange resins. Parametric variation studies were conducted to establish the ideal conditions for maximum sorption, kinetics and elution using ‘resin-in-solution’ technique. Based on these results, semi-continuous ‘resin-in-pulp’ experiments on ‘carousel’ mode were carried out. The results indicate superiority of gel type polystyrene based resins grafted with quaternary ammonium ion in comparison to the macro-porous resins. Semi-continuous counter-current extraction and elution tests indicated that about 98% of the dissolved uranium values can be recovered during the loading process and practically the entire loaded uranium can be eluted using NaCl eluant. Integration of the RIP followed by precipitation of dissolved uranium as uranium peroxide helps in overcoming processing difficulties associated with slimy diuranate precipitate.

## **1. INTRODUCTION**

Per-capita energy consumption is a critical indicator of societal development in any nation. The growing energy demand in developing countries with dense population like India or China calls for a holistic approach in choosing the energy sources. Nuclear energy fits the bill as the carbon foot-print of this source is very minimal [1]. The basic fuel element in a nuclear power reactor is uranium, either natural or enriched [2]. Conventional ore deposits constitute the main source of uranium. The milling of uranium ores and refining of the yellow cake product consist of a series of hydrometallurgical operations [3, 4]. Of the two stages in the production of uranium metal, the milling stage is very important as it generally involves handling of huge volumes of material, particularly for lean tenor ores.

The stages in uranium milling include comminution aimed at liberation or release of mineral phases from the host matrix, dissolution, separation of uranium laden solution, purification and precipitation of dissolved uranium. Amongst these, the comminution and filtration unit processes are very cost intensive [4, 5]. Sustained research towards improving the efficiency of cost-intensive operations is in vogue in several laboratories to improve the process recovery and lower the cost of production [6–8]. This is very important when the uranium prices are low.

Nuclear energy constitutes an important component of overall energy mix planned for futuristic requirements. At present reports indicate that 10% of the nuclear power reactors under construction world-wide are from India [9, 10]. The fuel requirements for these reactors consist of indigenous sources and from imports. Some of the prominent low-grade uranium ore deposits in India which are part of the fuel supply-chain are the Tummalapalle in Andhra Pradesh and Gogi in Karnataka [11]. Both the ores are hosted in acid consuming gangue matrix. These ore deposits necessitate fine grinding and application of alkaline conditions for the dissolution of uranium values [12, 13].

Solid-solution separation of post-leach slurry is one critical issue in their processing in spite of using well acclaimed horizontal belt filters with counter-current wash facility, all under moderately hot conditions. Continuous research is being carried out for identifying alternative technologies for maximal and efficient recovery of uranium laden solution from the inert solids. This paper gives the results of the investigations on application of resin-in-pulp technique on leach slurry generated from brecciated limestone type uranium ore of southern India.

Filtration separation of uranium bearing solution from leach slurry containing very-fine size solids in highly viscous liquor is a challenging task [3, 4]. In view of the slow rate of filtration occurring in above-said slurries several developments aimed at circumventing the associated process problems have come-up which include flocculant aided high rate thickeners for use in counter-current decantation (CCD) and that of resin-in-pulp process [14–24]. Though the CCD process is a simple operation it always leads to dilution of the concentrate assay. Thus, application of CCD on low-grade ores or lean grade liquors is not favoured. Unlike CCD, the resin-in-pulp (RIP) process is ideal in many respects. The RIP process yields purified and enriched pregnant eluate like in conventional static-bed ion exchange (SBIX) process. It bestows additional advantage of eliminating the steps of primary filtration and clarification which generally precedes the SBIX stage.

RIP is more attractive option for ores of very-fine grinds which are difficult to thickening or filtration. The use of resin-in-pulp (RIP) for the recovery of gold, uranium or base metals was in practise in United States, France, China and erstwhile USSR during 1950s and 1960s [25]. One of the major reasons for discontinuation of RIP in uranium industry has been the potential resin loss or consumption on a full-scale operation. In earlier days the RIP process was carried out in USA on reciprocating basket RIP system for de-sanded slimes [25]. The CSIRO jiggled bed RIP system was piloted at Rum Jungle, Australia in 1958, but was not commercialized. The screen-mix RIP systems were used in USA in late 1950s and later in Spain, USSR, and Eastern Europe.

In recent times, all the major resin manufacturers have made significant technological advances resulting in a number of durable, commercially available, RIP-grade strong-base resins for the recovery of uranium [26, 27]. This has renewed interest in RIP as a potential economically attractive processing route for the recovery of valuable metals from low grade slurries. Besides synthesizing resins of mechanically strong chemical structure developments were also made towards efficient resin transfer technologies to avoid wear and tear of resins during counter-current flow or transportation. This includes Kemix and AAC Pumpcell, Clean Teq Clean-iX® and MeTRIX system of Mintek and Bateman of South Africa [25].

RIP technology is included in various feasibility studies and commercial applications including Paladin's Kayelekera Project, Malawi; Toro Energy's Lakeway-Centipede Project in Western Australia; Kiggavik project, Michelin Project (Labrador) in Canada; Guezouman conglomeration in Niger; Gold Fields Limited Driefontein and Kloof operations, South Africa, to name a few [20, 23, 25, 26].

## 2. MATERIALS AND METHODS

The materials and experimental methods described below extend the work documented in broad sense in [27].

### 2.1. Leach slurry

The leach slurry for the experimental test work was obtained using a medium grade uranium ore ( $U_3O_8$  0.18%) from a brecciated lime-stone deposit of southern India. The main constituents (by weight) in the ore are calcite 62%, quartz 13%, micaceous minerals 6% and the sulphides of iron 0.6%. Since the carbonate minerals form the major gangue phase, alkaline leaching using reagent combination of  $Na_2CO_3$  –  $NaHCO_3$  – Air was used for dissolution of uranium values from ground ore. The  $d_{50}$  and  $d_{80}$  size of the ground ore is 34 and 75  $\mu m$  respectively. The partial chemical composition of the leach slurry was,  $U_3O_8$  0.7 g/L,  $Na_2CO_3$  36 g/L,  $NaHCO_3$  15 g/L,  $Na_2SO_4$  15 g/L and total dissolved solutes (TDS) 46 g/L.

### 2.2. Resins

Various commercially available strong base anion exchange (SBA) resins of both macro-porous and gel type were evaluated for their efficacy in selective sorption of uranium values from the carbonate medium [27]. This include PFA460/4783 and PFA600/ 4740, A500/2788 (Purolite, France), Ambersep<sup>(TM)</sup> 400SO4, 920USO4, 920UHCSO4, 920UCl, Amberlite IRA910UCl (Rohm and Haas, UK), Ambersep

(<sup>TM</sup>)4400 HCO<sub>3</sub>, and Indion ARU 103 (Ion Exchange India). The functional group for all the resins is quaternary ammonium ions excepting Ambersep (<sup>TM</sup>)4400 HCO<sub>3</sub> which consists of tertiary ammine. The average bead size of gel-type resins was 550 µm while that of macro-porous variety was 850 µm.

### 2.3. Other reagents

All the other chemicals used in the test work are of A.R. Grade. De-ionized water was used for resin preparation and making of stock solutions of various reagents.

### 2.4. Resin in solution/pulp test work

The resins obtained from various manufacturers were used without any chemical pre-treatment. The beads were soaked in de-ionized water overnight at *insitu* pH. Known volume of the wet settled resin (w.s.r.) was taken-out from the stock regularly and added to the leach solution or pulp. The optimum conditions arrived from the resin-in-solution (RIS) experiments was used for the resin-in-pulp (RIP) test work. The mixing in ‘resin-in-solution’ tests was carried out by shake-flask technique while overhead stirrer was used in the ‘resin-in-pulp’ experiments. Semi-continuous RIP tests were carried out in carousel model arrangement (Fig. 1).



FIG. 1. Carousel model RIP set-up.

The carousel model resin-in-pulp equipment used for the test work consists of 5 reactors of 900 mL volume (total 4.5 L). In a carousel type RIP circuit, the slurry and resin contact was achieved through mechanical agitation using a paddle type impeller. The resin was retained in each stage with the screens while the slurry flows to the downstream stage by gravity. After a pre-defined time period sufficient for saturation loading of the resin in the first reactor the feed flow was interrupted.

The slurry and resin mixture of first reactor was drained over a screen to separate the loaded resin from the partially metal depleted slurry and the slurry is recycled to a collection tank. In the intervening gap the feed flow was directed to second reactor and at this point an extra reactor with the recycled resin comes online at the back of the cascade. The loaded resin from the first reactor was transferred to the

elution circuit and washed with de-ionized water to remove the adhered ore particles followed by elution of uranium species. After elution and re-washing, the resin was recycled to the back-end of the adsorption circuit during the subsequent transfer.

Elution was carried out by downward flow of the eluant at a pre-defined flow-rate in a 15-mm diameter and 400 mm height glass column using different eluants. The eluant solution was collected periodically and analysed for uranium and other constituent ions. All the experiments were conducted at ambient temperature (about 25°C).

### 3. CHEMICAL AND DATA ANALYSIS

The metallurgical accounting in all the experiments was based on wet chemical analysis of uranium and other species in various streams. The uranium concentration in the aqueous phase was determined by liquid fluorimetry (ELICO Model SL 174). The relative standard deviation (RSD) in the uranium analysis was  $\pm 2\%$ . Carbonate, bicarbonate, phosphate and chloride was determined by titrimetry while the sulphate analysis was carried out using the gravimetric technique. The loading of uranium on the resin phase is expressed as grams of  $\text{U}_3\text{O}_8$  per litre of wet settled resin (w.s.r.) and calculated as given in equation 1.

$$\text{Loading Capacity} = \frac{C_F - C_B}{V_R} \times V_L \quad (1)$$

where,  $C_F$  and  $C_B$  are concentration of  $\text{U}_3\text{O}_8$  in grams per litre,  $V_R$  and  $V_L$  are volumes of wet settled resin and feed solution respectively in litres. Repeatability of the data was ensured such that the maximum standard deviation observed between the reported experimental values never exceeded  $\pm 3\%$ .

### 4. RESULTS AND DISCUSSION

The preliminary experiments in resin-in-pulp separation studies was focused on evaluation of various strong base anion exchange resins with respect to their affinity for anionic uranyl carbonate species over the other anions present in the leach solution. The test results indicate higher loading of uranium on gel-type resins in comparison to the macro-porous type resins (Table I).

Saturation loading of about 65–70 g of  $\text{U}_3\text{O}_8$  /L of w.s.r. was obtained with all the gel type resins tested excepting the ARU 103 resin, which gave about 55 g  $\text{U}_3\text{O}_8$ /L of w.s.r. only. Unlike the gel-type resins, the macro-porous resins gave maximum loading of 40–55 g  $\text{U}_3\text{O}_8$  /L of w.s.r. The lesser number of functional groups in macro-porous resins in comparison to the gel type variety for a given unit weight is responsible for the observed difference in the loading capacity between the two [28]. Based on the screening results, PFA460/4783 resin was taken for all the other process parametric variation tests.

#### 4.1. Parametric variation studies with PFA460/4783

##### 4.1.1. Saturation loading capacity

The saturation loading of uranyl carbonate anions on PFA460/4783 resin was carried out in shake-flasks agitated under constant shear as per the following test conditions: Resin to leach solution volume ratio 1:50; number of stages 6; contact time per stage 2 h; temperature ambient. The cumulative loading profile over each stage is illustrated in Fig. 2. About 31 g of  $\text{U}_3\text{O}_8$ /L of w.s.r. was loaded in the first stage and it enhanced progressively to about 68 g/L of w.s.r by fourth stage.

Further equilibration did not show any noticeable additional sorption. Though the concentration of  $\text{U}_3\text{O}_8$  was relatively lower in the leach solution, about 730 mg/L in comparison to other competing ions particularly  $\text{CO}_3^{2-}$ ,  $\text{HCO}_3^-$  and  $\text{SO}_4^{2-}$ , (Sec.2.1), the affinity of uranium bearing species for the exchangeable sites on the resin was more than the other ions. This is mainly due to the higher electrostatic affinity between  $[\text{UO}_2(\text{CO}_3)_3]^{4-}$ , the predominant uranium bearing species in the pH range of 9–10, and the functional site on the resin over the other bivalent or mono-valent anions [29, 30].

#### 4.1.2. Effect of contact time

The kinetics of uranium loading on PFA 460/4783 resin was determined by equilibrating the resin and leach solution in the ratio of 0.4:100 at ambient temperature for over 6 hours. Solution samples were withdrawn periodically (every  $\frac{1}{2}$  h) for estimating the depletion of uranium concentration due to sorption on the resin. The kinetic profile indicated rapid uptake, about 52 g/L  $\text{U}_3\text{O}_8$  of w.s.r in the initial phase of 45 minutes and remained sluggish thereafter. The sorption level observed during 2<sup>nd</sup> to 6<sup>th</sup> cumulative hour of contact was 53 to 57 g/L of  $\text{U}_3\text{O}_8$ .

The results obtained in the kinetic experiments fitted with good correlation coefficient ( $R^2$  0.99) with the pseudo-second order sorption kinetic model, implying that the rate-controlling step in the exchange process between anionic uranyl carbonate in solution and quaternary ammonium ions on the resin is of chemisorptive nature [31].

TABLE I. SORPTION OF URANYL CARBONATE SPECIES FROM ALKALINE LEACH SOLUTION: LOADING CAPACITY OF OBSERVED WITH DIFFERENT COMMERCIAL RESINS

| Name of resin (gel type)   | ARU 103 | PFA 4740  | PFA 4783 | 400SO4                   |
|--|---------|-----------|----------|--------------------------|
| Loading capacity<br>grams of $\text{U}_3\text{O}_8$ per<br>litre of w.s.r. | 55.6    | 74.6      | 70       | 68.5                     |
| Name of resin<br>(macroporous type)  | 920USO4 | 920UHCSO4 | 920UCl   | IRA 910 478    A500/2788 |
| Loading capacity<br>grams of $\text{U}_3\text{O}_8$ per<br>litre of w.s.r. | 48      | 49        | 35       | 48    57                 |

(Resin to leach solution ratio 1:100; Contact time 12 h; Temp. ambient; pH 9.5)

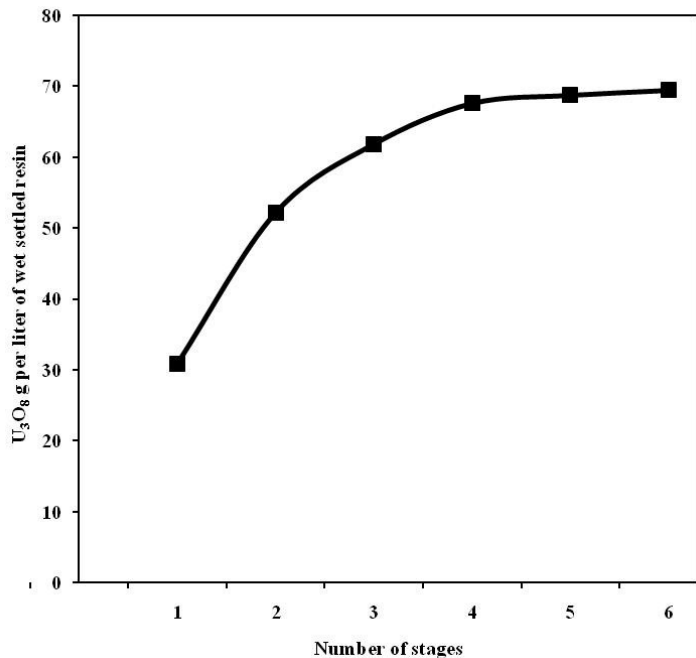


FIG. 2. Cumulative loading of uranyl carbonate on a strong base anion exchange resin.

#### 4.1.3. Resin to leach solution ratio

The objective in these experiments were to achieve maximum loading with minimum resin inventory. The optimal ratio of resin and leach solution was elucidated by varying the volume of resin, PFA 4783, for fixed quantity of leach solution. The resin volume was varied from 0.5 mL to 15 mL keeping the volume of leach solution constant at 100 mL ( $U_3O_8$  700 mg/L). The contact time in all the single-stage loading experiments was 100 minutes and the reaction was carried out at ambient temperature. The extent of depletion of uranium in the leach solution with various ratios is given in Table II.

About 60% of the uranium values in the leach solution were adsorbed on the resin, when the ratio was 1:100. The uptake increased to 80% when the resin content is increased to 2 mL for every 100 mL of leach solution and the sorption reached maxima in the ratio range of 1:33 to 1:6.5. Results of the single-stage extraction tests indicate that the resin to leach solution volume ratio of 1:50 to 1:33 as ideal for maximum loading of uranyl carbonate with minimum resin inventory.

The number of theoretical mass-transfer steps necessary for maximum loading of uranyl carbonate anions on the resin in continuous counter-current mode was determined from the McCabe Thiele plot constructed using the data given in Table II. The working line in the plot (Fig. 3) was obtained by joining the coordinates corresponding to 80% loading capacity of the uranium species on the resin (56 g of  $U_3O_8$  per L of w.s.r) and the point that represent the practical  $U_3O_8$  concentration in the exit stream, about 15 mg/L. About 98% of the uranium values could be extracted in 4 stages of equilibration.

#### 4.2. Resin-in-pulp extraction with PFA460/4783 for alkaline leach slurries

Based on the data generated from the ‘resin-in-solution’ test work, necessary experimental conditions for carrying out semi-continuous counter-current ‘resin-in-pulp’ experiments were developed. The RIP experiments were carried out with alkaline leach slurry containing about 30% solids by weight (pulp density 1.2 kg/L) at pH of about 9.5 at ambient temperature. Five reaction vessels containing 0.9 L of the leach slurry and 7.3 mL of resin in each reactor were agitated gently using an overhead paddle type stirrer at a peripheral speed of 0.5–0.7 m/sec.

TABLE II. SORPTION OF URANYL CARBONATE ON A STRONG BASE ANION EXCHANGE RESIN AT DIFFERENT RESIN TO SOLUTION VOLUME RATIO

| Resin to leach liquor volume ratio                           | 0.5:100 | 1:100 | 2:100 | 3:100 | 5:100 | 10:100 | 15:100 |
|--|---------|-------|-------|-------|-------|--------|--------|
| U <sub>3</sub> O <sub>8</sub> depleted from leach liquor (%) | 44      | 62    | 81    | 91    | 93    | 96     | 95.7   |

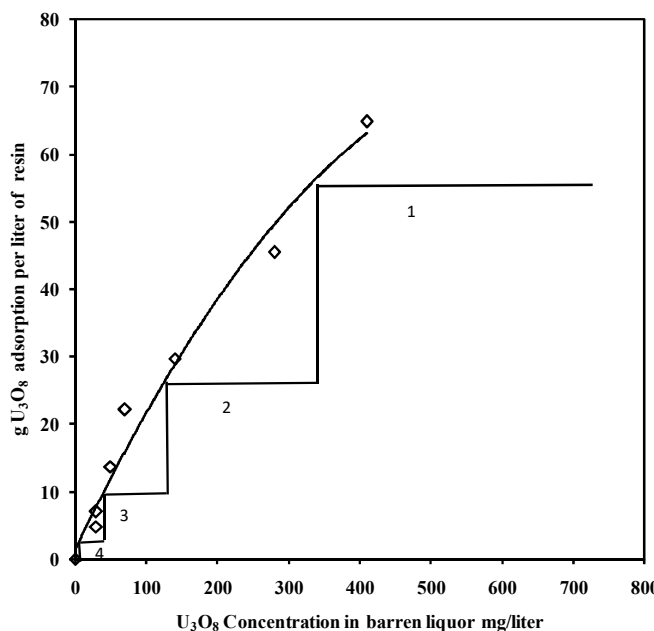


FIG.3. McCabe Thiele Plot of uranyl carbonate sorption on a strong base anion exchange resin (adapted from [27]).

TABLE III. RESIN-IN-PULP SORPTION OF URANYL CARBONATE ON A STRONG BASE ANION EXCHANGE RESIN. PARTIAL CHEMICAL COMPOSITION OF LEACH SOLUTION

| U <sub>3</sub> O <sub>8</sub> | Na <sub>2</sub> CO <sub>3</sub> | NaHCO <sub>3</sub> | Na <sub>2</sub> SO <sub>4</sub> | TDS  |
|-------------------------------|---------------------------------|--------------------|---------------------------------|------|
| Grams per litre               |                                 |                    |                                 |      |
| 0.84                          | 16.7                            | 19.4               | 2                               | 24.8 |

The flow-rate of slurry and resin was 4.25 and 0.0345 l/h respectively. The reactor contents were separated manually using a 35# size (Tyler) screen. The screen over size (resin) and the undersize (pulp) were moved in counter-current directions in carousel mode. After each stage of equilibration, a small volume of leach solution was drawn and analysed for extent of depletion of U<sub>3</sub>O<sub>8</sub> concentration. The composition of solution phase of the leach slurry is given in Table III.

About 80% of the uranium values were extracted in the initial two reactors and it attained about 96.3% in stage 4. Continuing equilibration for two more stages improved the extraction efficiency to 97% only.

The system attained steady state after three cycles (Fig. 4) and the average  $\text{U}_3\text{O}_8$  content in the barren solution was about 18 mg/L after 5<sup>th</sup> stage, which implies an extraction efficiency of about 98%.

#### 4.3. Resin-in-pulp studies with PFA460/4783 for alkaline leach slurries – Elution

Elution of loaded uranyl carbonate species and other ions from the resin was carried out in a water-jacketed glass column at ambient temperature using different eluants like  $\text{NaCl}$ ,  $\text{Na}_2\text{CO}_3$ ,  $\text{NaHCO}_3$  and  $\text{Na}_2\text{SO}_4$ , all at 1M strength dissolved in 0.1M  $\text{Na}_2\text{CO}_3$ . The pH of the eluate solution was 9.5 and the flowrate was 2.5 BV/h (residence time 10 min). Samples of eluate were taken every 3–5 BV fraction and analysed for uranium content. The results of the elution experiments are given in the Fig. 5. Faster and complete elution, about 98% of sorbed uranyl carbonate anions, was achieved with  $\text{NaCl}$ . The maximum concentration of uranium as  $\text{U}_3\text{O}_8$  in the eluate obtained with  $\text{NaCl}$  was 10 g/L (Tab. IV). Both  $\text{NaHCO}_3$  and  $\text{Na}_2\text{SO}_4$  were both able to dislodge the loaded uranium species to the same extent as  $\text{NaCl}$ , but the kinetics was far inferior. In contrast to these eluants,  $\text{Na}_2\text{CO}_3$  was totally ineffective for this system.

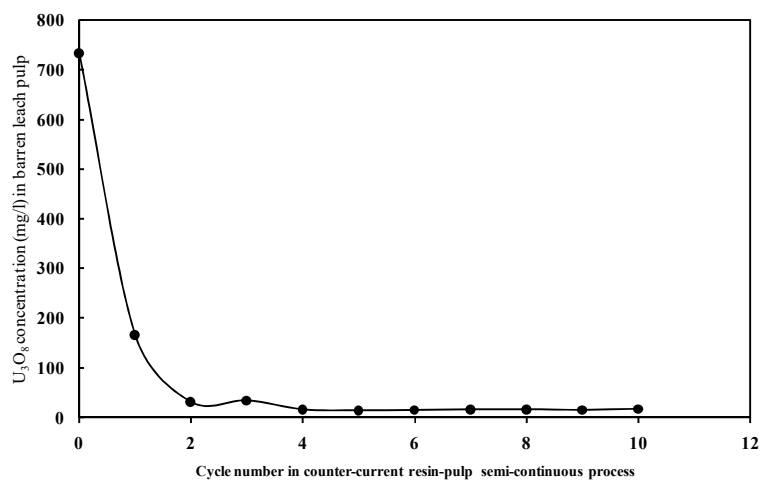


FIG. 4. Resin-in-pulp studies on uranium bearing alkaline leach slurry with strong base anion exchange resin. Uranium content in the exit after of uranium. Depletion of uranium in leach solution after 5 stages.

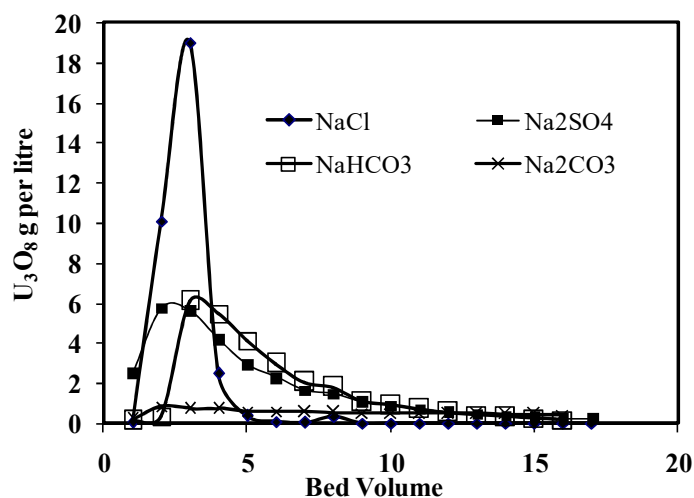


FIG.5. Resin-in-pulp separation of uranium from alkaline leach slurry using strong base anion exchange resin. Elution profile with different eluants.

TABLE IV. RESIN-IN-PULP SEPARATION OF URANIUM FROM ALKALINE LEACHATE WITH STRONG BASE ANION EXCHANGE RESIN (ADAPTED FROM [27])

| $\text{U}_3\text{O}_8$ | $\text{Na}_2\text{CO}_3$ | $\text{NaHCO}_3$ | $\text{Na}_2\text{SO}_4$ | TDS |
|------------------------|--------------------------|------------------|--------------------------|-----|
| Grams per litre        |                          |                  |                          |     |
| 10                     | 3                        | 25               | traces                   | 70  |

Partial chemical composition of eluate with NaCl.

## 5. CONCLUSIONS

A strong base anion exchange resin was used for resin-in-pulp mode separation of dissolved uranyl carbonate species from an alkaline leach slurry. The granulometry of the solid particles is very-fine in nature, the  $d_{80}$  size being 74  $\mu\text{m}$ .

The total dissolved solutes (TDS) in the leach liquor was about 47 g/L consisting of predominantly  $\text{Na}_2\text{CO}_3$  and  $\text{NaHCO}_3$  and minor levels of  $\text{Na}_2\text{SO}_4$ . The uranium assay in the leach liquor was 700 to 750 mg/L.

Loading capacity observed with various commercially available SBA resins (quaternary ammonium ion on polystyrene crosslink with divinyl benzene (DVB)) showed relatively better performance with two commercial resins — PFA 4740 and 4783. About 65 g of  $\text{U}_3\text{O}_8$  was sorbed per litre of wet settled resin.

Semi-continuous counter-current RIP tests indicated loading to the tune of 98% in 4 stages with overall contact time of 100 minutes at a resin to leach slurry volume ratio of about 1:100. Practically the entire uranium values loaded on the resin were eluted using NaCl.

## ACKNOWLEDGEMENTS

The Authors are thankful to G. K. Dey, Director, Materials Group, Bhabha Atomic Research Centre, Mumbai, for his encouragement and interest in the investigations. They also express their sincere thanks to R.R. Venkatkrishnan and G. Rama Devi for analytical support.

## REFERENCES

- [1] INTERNATIONAL ATOMIC ENERGY AGENCY, Judge Nuclear on Its Merits (2012), <http://www.iaea.org/OurWork/ST/NE/judge-nuclear.html>.
- [2] GIRALDO J.S., GOTHAM, D.J., NDERITU, D.G., PRECKEL, P.V., MIZE, D.J., Fundamentals of Nuclear Power, State Utility Forecasting Group, West Lafayette, IN (2012). <https://www.purdue.edu/discoverypark/energy/assets/pdfs/SUFG/publications/SUFG%20nuclear%20report.pdf>.
- [3] MERRITT, R.C., The Extractive Metallurgy of Uranium. Colorado School of Mines, Johnson Publishing Co., Boulder, CO (1971).
- [4] INTERNATIONAL ATOMIC ENERGY AGENCY, Uranium Extraction Technology, IAEA Technical Report Series No. 359, IAEA, Vienna (1993) 157-226.
- [5] VAN TONDER, D., Comparison of resin-in-pulp and direct precipitation for recovery of uranium in alkaline leach circuits, CIM Journal 3 2 (2012) 131-139.
- [6] TAYLOR, A., “Innovations and trends in uranium ore treatment”, Proc. ALTA 2007 Uranium Conference, Perth, Australia, ALTA Metallurgical Services, Melbourne (2007).

- [7] CARR, J., ZONTIV, N., YAMIN, S., "Meeting the future challenges of uranium industry", Proc. ALTA 2008 Uranium Conference, Perth, Australia, ALTA Metallurgical Services, Melbourne (2008).
- [8] BROWN, J., GOODE, J.R., FLEMING, C., "Re-emergence of resin in pulp with strong base resins as a low cost, technically viable process for the recovery of uranium", SGS Minerals Services Tech. Paper 2010-02 (2010).
- [9] World Nuclear Power Reactors & Uranium Requirements (June 2014), <http://www.world-nuclear.org/info/Facts-and-Figures/World-Nuclear-Power-Reactors-and-Uranium-Requirements>.
- [10] JAIN, S.K., Inevitability of Nuclear Power in the Asian Region, Energy Procedia 7 (2011) 5-20.
- [11] GUPTA, R., SARANGI, A.K., Overview of Indian Uranium Production Scenario in coming Decades, Energy Procedia 7 (2011) 146-152.
- [12] SURI A.K., et al., Process development studies for the recovery of uranium and sodium sulphate from a lowgrade dolostone hosted stratabound type uranium ore deposit, Mineral Processing and Extractive Metallurgy (Trans. Inst. Min. Metall. C) 123 2 (2014) 104–115.
- [13] SURI, A.K., et al, "Process development studies for low-grade uranium deposit in alkaline host rocks of Tummalapalle", paper presented at the IAEA Tech Mtg on Low-grade Uranium Deposits at Vienna, 29-31 March 2010.
- [14] McKEVVIT, B., DREISINGER, D., "Lessons from the Past: A literature review of resin-in-pulp process in uranium industry", Uranium 2010 The Future is U (Proc. 3<sup>rd</sup> Int. Conf. on Uranium, Saskatoon, 2010) (LAN, E.K., RAWSON, J.W., OZBERK, E., Eds), The Canadian Inst. of Mining, Metallurgy and Petroleum, Westmount, Quebec, Vol. II (2010) 3-14.
- [15] MIRJALILI, K., ROSHANI, M., Resin-in-pulp method for uranium recovery from leached pulp of low-grade uranium ore, Hydrometallurgy 85 (2007) 103-109.
- [16] MIKHAYLENKO, M., VAN DEVENTER J., "Notes on practical application of ion exchange resins in uranium extractive metallurgy", Proc. ALTA Uranium Conference 2009, Perth, Australia, ALTA Metallurgical Services, Melbourne (2009).
- [17] YAHORAVA, V., KOTZE, M. H., SCHEEPERS, J., AUERSWALD, D., "Evaluation of Various durability tests to assess resins for in-pulp applications", Proc. Fifth Southern African Base Metals Conference 2009, Kasane, Botswana, The South African Inst. Min. Metall. (2009) 341-358.
- [18] YAHORAVA, V., SCHEEPERS, J., KOTZE, M.H., "Comparison of various anion exchange resin for the recovery of uranium by means of RIP", Proc. ALTA Uranium Conference 2009, Perth, Australia, ALTA Metallurgical Services, Melbourne (2009).
- [19] UDAYAR, T., KOTZE, M.H., YAHORAVA, V., "Recovery of uranium from dense slurries via resin-in-pulp", Proc. 6th Southern African Base Metals Conference 2011, The Southern African Inst. Min. Metall. (2011) 49-64.
- [20] KOTZE, M., "The resurrection of hydrometallurgy's own RIP van Winkle: Uranium", presented at Mintek 75 (Proc. Conf. Randburg, South Africa 2009)
- [21] THULARE, T., VOS, P., PHIRI, C., VAN HEDGE, B., "Developments in Resin In Pulp (RIP) for uranium recovery in Africa", Proc. Int. Uranium Conf. ALTA 2008, Perth, Australia, ALTA Metallurgical Services, Melbourne (2008).
- [22] AUERSWALD, D., UDAYAR, T., KOTZE, M., SCHEEPERS, J., "Operation of a resin-in-pulp (RIP) demonstration plant for recovering uranium from a South African gold pulp", Proc. ALTA Uranium Conference, Perth, Australia, ALTA Metallurgical Services, Melbourne (2011) 103-115.
- [23] LING, Y., DURUPT, N., BANTON, N., "RIP studies at AREVA: R & D and applications for Niger and Canada projects", Proc. 3<sup>rd</sup> Int. Conf. on Uranium, Saskatoon, 2010 (LAN, E.K., RAWSON, J.W., OZBERK, E., Eds), The Canadian Inst. of Mining, Metallurgy and Petroleum, Westmount, Quebec Vol. II (2010) 27-38.
- [24] PANTURU, E., FILIP, S., PETRESCU, G., GEORGESCU, D., RADULESCU, R., "Researches concerning the Purolite assimilation for use within the uranium separation-concentration resin in pulp process", Proc. 9<sup>th</sup> Int. Conf. on Tailings and Mine Waste, Fort Collins, CO (2002) 361.

- [25] TAYLOR, A., “Review of CIX and RIP systems for uranium extraction”, Proc. ALTA 2008 Uranium Conf., Perth, Australia, 2008 ALTA Metallurgical Services, Melbourne (2008).
- [26] BROWN, J., GOOD, J.R., FLEMING, C., The re-emergence of resin in pulp with strong base resins as a low cost, technically viable process for the recovery of uranium, 42nd Annual Meeting of the Canadian Mineral Processors, 2010, Ottawa, (2010) (as reprinted, SGS Mineral Services Technical Paper 2010-10).
- [27] SREENIVAS, T., RAJAN, K.C., Studies on the separation of dissolved uranium from alkaline carbonate leach slurries by resin-in-pulp process, Separation and Purification Technology **112** (2013) 54-60.
- [28] ABRAMS, I.M., MILLAR, J.R., A history of the origin and development of macroporous ion-exchange resins, Reactive and Functional Polymers **35** 1-2 (1997) 7-22.
- [29] BOTHA, M., BESTER, L., HARDWICK, E., “Removal of uranium from mine water using ion exchange at Driefontein Mine”, Proc. Int. Mine Water Conf., 2009, Pretoria, Water Institute of Southern Africa and International Mine Water Association (2009) 382-391.
- [30] McGARVEY, F.X., UNGAR, J., The influence of resin functional group on the ion-exchange recovery of uranium, J. South African Institute of Mining and Metallurgy **81** 4 (1981) 93-100.
- [31] RAHMATI, A., GHAEMI, A., SAMADFAM, M., Kinetic and thermodynamic studies of uranium (VI) adsorption using amberlite IRA 910 resin, Annals of Nuclear Energy **39** (2012) 42-48.

# **URANIUM EXPLORATION IN MONGOLIA: A MAJOR DISCOVERY IN THE GOBI DESERT**

O. CARDON, F. LE GOUX  
COGEGOBI LLC / AREVA Mongol LLC,  
Ulaanbataar, Mongolia

## **Abstract**

During the last decade, the exploration efforts carried out in Mongolia have resulted into the discovery of two new uranium roll-front type deposits in the Sainshand basin of the Gobi Desert: Dulaan Uul and Zoovch Ovoo deposits. These discoveries resulting from a new exploration approach of the wide distal Cretaceous sedimentary basins, reach more than 60 000 tU in the Upper Sainshand formation and the potential for new discoveries is still open. A successful ISR technology test has been carried out during 6 months on Dulaan Uul deposit and another test is planned in the coming years to evaluate the recoverability of Zoovch Ovoo ore. The work carried out to convert the Dulaan Uul and Zoovch Ovoo resources into a minable product is ongoing and could lead to an ISR production after 2020, with an output capacity of 2000 t of uranium per year for Zoovch Ovoo only, which could place Mongolia as one of the world major uranium producer.

## **1. INTRODUCTION**

Mongolia has a long history in uranium exploration. The first prospection started just after the second world war with joint Russian and Mongolian geological endeavours. The exploration targets were mainly focused on the eastern part of the country where some uraniferous lignite occurrences had been firstly discovered. From 1970 to 1990, a systematic geological exploration, carried out by the Mongolian Geological Survey, was conducted all over the country to identify the most favourable areas for uranium deposit (and other metals). Based on the results of the survey, the country was classified into four uranium provinces: Mongol-Priargun, Gobi-Tamsag, Khentei-Daur and Northern Mongolian [1].

Each of these provinces has a distinct geology, hosts different deposit types or mineral associations, with varied ages of mineralization. Within these provinces, more than 1600 uranium showings or radioactive anomalies and about 100 uranium occurrences related to different deposit types were identified: volcanic, sandstone, lignite, phosphoric, metasomatite, intrusive, vein and structure controlled type. These extensive exploration works resulted in the discovery of several volcanic type deposits in the Dornod province as well as the Kharaat sandstone-hosted deposit, along with several occurrences in the Choir Basin within cretaceous proximal sedimentary basins.

After the 1990s, foreign companies came in Mongolia to develop the identified prospective occurrences and to invest in exploration of new fields with new concepts, leading to the discovery of new world class size uranium deposits.

## **2. A NEW EXPLORATION APPROACH FOR NEW PROSPECTS**

The French company COGEMA (former name of AREVA Mines company) started up uranium exploration in Mongolia in 1997 by opening its Mongolian subsidiary called COGEGOBI. After assessment and general investigations of various uranium deposit types, the objective was quickly focused on the prospection for sandstone-hosted uranium deposits in major distal cretaceous sedimentary basins of the East Gobi region. Most of the known uranium occurrences discovered until then were located in small proximal sedimentary basins enclosed into uranium rich volcanic and/or intrusive basement.

Following some attempts on proximal occurrences in the shallow part of the Sainshand basin (Nars deposit – Inginsky sector) and on the Uneget sub-basin northern edge, both situated not far from Sainshand city, the attention then turned to more distant targets. The innovative strategy developed by Cogegobi was to believe in a different approach of the mineralizing process. The idea was to not only

focus on the source of uranium and search for a deposit in the surrounding basins fringe, but to look for wider and more distal sedimentary basins allowing to develop larger size deposits, even if these basins were located far from the known uranium sources.

Driven by this evolution of the exploration approach, Cogegobi has undertaken exploration works for the past 14 years in the Dornogovi Province, in the eastern part of the Gobi Desert, approximately 550 km southeast of Ulaanbaatar, in the Uneget and Zuunbayan sub-basins (Fig. 1), in which Cogegobi has discovered two deposits in the Sainshand formation (Upper Cretaceous). The first one is the Dulaan Uul deposit located in the Uneget basin, a typical roll-front type deposit with 6500 t of uranium resources at 150 ppm U average grade, officially registered by the Mongolian authorities in 2011. The second one, located about 20 km East in the Zuunbayan basin, is the Zoovch Ovoo deposit with 54 500 t of uranium resources at 223 ppm U, registered in 2013 (both based on a 75 ppm U cut-off).

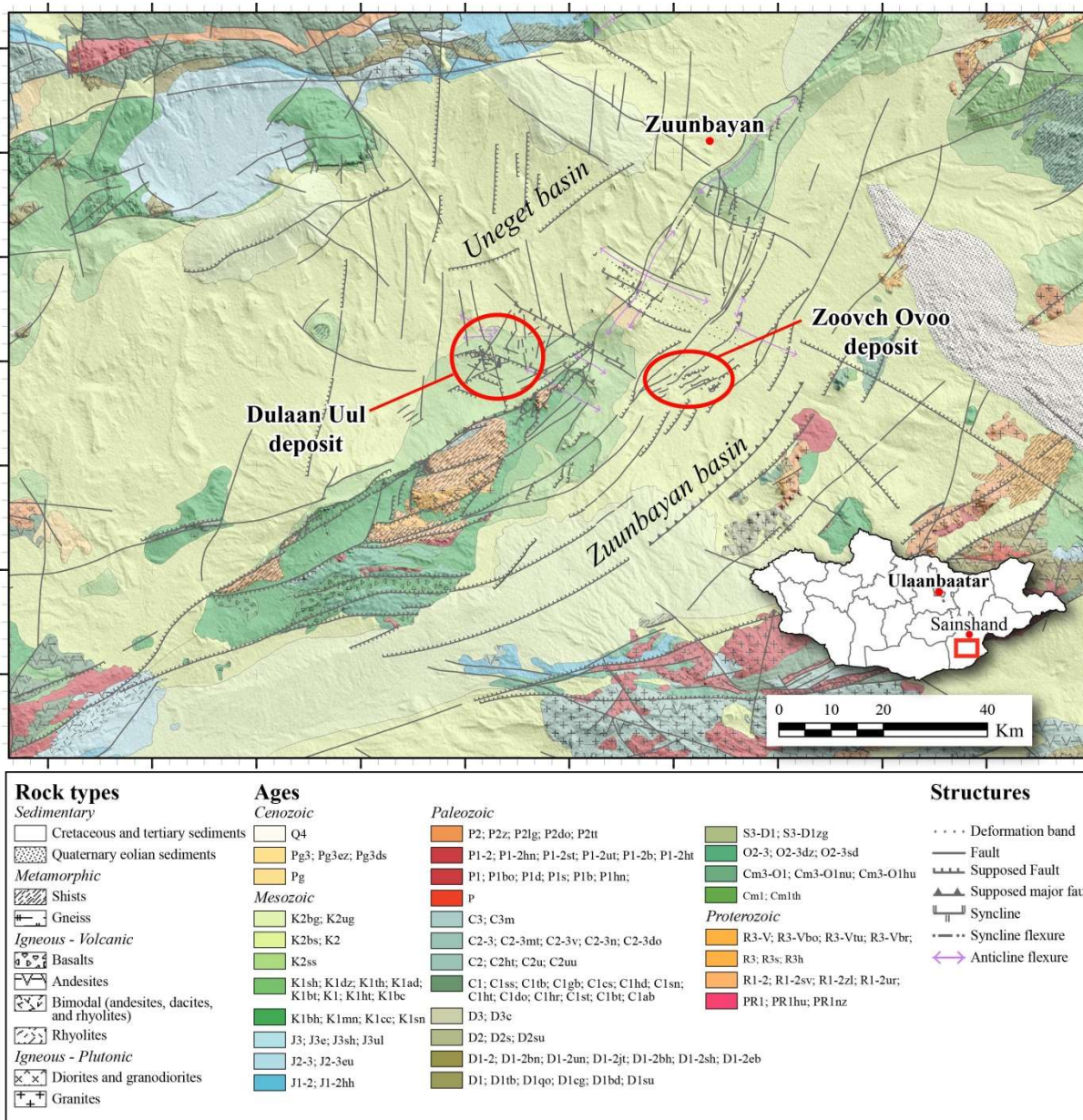


*FIG. 1. Geological map of the Uneget and Zuunbayan sub-basins, and location of the Dulaan Uul and Zoovch Ovoo uranium deposits.*

### 3. METHODOLOGY

#### 3.1. Preliminary to detailed exploration

The exploration methodologies used by COGEGOBI are quite conventional for the exploration of sandstone-hosted roll-front uranium deposits. The first stage is the acquisition of an accurate and detailed geological map to get from the surface the best understanding of the basin geology, especially its structural features. In some cases, a detailed ground radiometric survey is also performed to identify and delineate potential surficial radiometric anomalies.

The second stage of the exploration mainly consists of drilling and downhole logging operations, with subsequent geological observations of cores. During the first years of exploration, the drilling operations used to be conducted with Russian ZIF rigs, either by destructive rotary or simple tube coring mud drilling. In order to improve both the recovery rate and the core quality, the drilling equipment has been progressively replaced by Korean Hanjin<sup>©</sup> Power rigs using triple tube coring tools (HQ size). To improve the mud quality and minimize the environmental impact (water consumption, footprint of the drilling pad, water truck movements), each operating rig is now systematically equipped with a recycling system of drilling mud

Depending on the exploration stage, the level of geological knowledge, and the size of the targets investigated in the prospective area, the drilling grid, the core ratio and the kind of studies conducted on the samples are variable:

- Reconnaissance drilling: large scale profiles are made in the basin and a high proportion of core drilling is used for each borehole (75 to 100% of core) in order to assess the presence or absence and the depth of the different members of the reference stratigraphic series, to define the nature of the sediments filling the basin, to identify permeable levels, and potentially locate a reduced pole;
- Detailed exploration stage: once both reduced and oxidized poles are identified, drilling profiles are placed perpendicularly to the presumed oxidization front orientation, with a spacing between the lines ranging from 400 m to 3200 m, iteratively tightening up the drillholes on the lines towards the main redox contrasts until the front(s) is(are) reached. When a mineralization is identified on the redox front, it is then searched for on the neighbouring lines. Each borehole is sampled and the cored intervals are focused on the oxidoreduction contrast levels (30 to 75% of core);
- Finally, when a significant and continuous mineralization is discovered, the potential deposit enters into a first development phase and the drilling grid is tightened to a 200 × 200 m down to a 100 × 50 m grid, locally 25 m on some parts of the deposits. The cored intervals are focused on the mineralized levels and on the levels in which the oxidoreduction state of the rocks remains uncertain, possibly hosting other undefined mineralized sections (10 to 30% of core).

#### 3.2. Geological studies

From the reconnaissance drilling to the development phase of the deposits, each borehole drilled is cored (except in some local very tight grid at 25 m spacing) and is logged with geophysical probes (natural gamma ray, calliper, mud level, resistivity, spontaneous polarization, and verticality continuous measurements). In addition to the geological description of the cores, regular geochemical sampling is done to define the chemical grade of uranium in order to assess the equilibrium state of the mineralization, to measure and precise the nature of the clay content of the sand host of the mineralization, and to analyse the content in other significant elements (Fe, CO<sub>2</sub>, etc.).

Selective sampling is also conducted to carry out petrographic and mineralogical studies of the mineralization and of the host rocks, granulometry analyses, and palynology dating. In parallel, specific sedimentology, structural, and basin geology studies are also implemented for a more general and conceptual understanding of the metallogenic model.

### **3.3. Deposit modelling**

Based on the data collected during the successive exploration and development campaigns, a 3D model is built for each deposit using Micromine software<sup>21</sup>. The model gives the main host rock type of the mineralization with specific envelopes for the permeable layers (sand) and for the non-permeable layers (clay, silt, carbonate-cemented levels), the oxidization front, and the ore body itself at a given grade cutoff.

This model allows to better visualize and understand the complexity of the geology in the close vicinity of the mineralization, to delimit the volume used for the resources estimation, but also to discriminate the mineralization contained in the non-permeable layers (not recoverable), the mineralization located in the permeable oxidized environment (with a negative disequilibrium), and the recoverable mineralization in the reduced environment.

### **3.4. Resources estimation**

The resources estimation results presented in this paper were calculated in Mongolia by MGCE LLC, an independent consultant in charge of the estimations studies used by the Mongolian authorities for the official classifications and registrations. In parallel, internal estimations are conducted by the Geosciences Direction of AREVA Mines in France.

In both cases, estimations are based on systematic cross-section of the deposits made by the geologists in accordance with the established genetic model, 3D model envelopes (see above), systematic in-situ radiometric measurements, and chemical assays for the definition of empirical radiometry-grade conversion laws and/or the assessment of the impact of local disequilibrium. The resources issued by these two different technical entities are similar.

## **4. URANIUM DEPOSITS IN THE SAINSHAND REGION**

### **4.1. Geological context of the mineralization**

#### *4.1.1. Tectonic history of the sedimentary basins*

Uranium mineralization of the Dulaan Uul and Zoovch Ovoo deposits is located in the Jurassic-Cretaceous basin of Sainshand, respectively in the Uneget and Zuunbayan sub-basins. The structural evolution of these basins can be summarized in four main tectonic events:

- Jurassic rifting: extension and syn-tectonic sedimentation in a graben and half-graben system;
- Lower Cretaceous uplift: erosion and alteration;
- Lower to Upper Cretaceous subsidence: basin unconformity and new syn-tectonic sedimentation;
- End of Mesozoic – beginning of Cenozoic transgression: tectonic reactivation of the main faults, deformation of the Cretaceous series on the edges of the basins.

As a result of their structural history, the basins are structured by a ENE–WSW to NE–SW fault network parallel to the basement outcrops constituted by Jurassic to ante-Mesozoic intrusive and metasedimentary rocks. The Uneget and Zuunbayan sub-basins are separated by a regional NE–SW left strike slip fault named the Zuunbayan Fault (Fig. 1).

---

<sup>21</sup> KATAN 3D Resources and Reserves module of Micromine©

#### 4.1.2. Stratigraphy and paleoenvironment of the sedimentation

The stratigraphy of the main sedimentary formations of the upper part of the Sainshand basins is the following, from the base to the top:

- Tsagantsav (Jurassic, 50 to 100 m thick): syn-rifting volcano-sedimentary formation which consists of an alternance of breccia, basalt flows, and thin grey ashes layers;
- Zuunbayan K1Dz (Lower Cretaceous, > 150 m thick): post-rifting formation, mainly consisting of clay and silt of lacustrine to palustrine origin, with rare sandy channels, in the distal position. The proximal term of the formation is made of red breccia corresponding to alluvial fans, and sand to silt dominated alternations from lacustrine delta systems, in the intermediate position;
- Sainshand K2Ss1 & K2Ss2 (Cenomanian to Turonian, 150–300 m thick): formation consisting of sequences of unconsolidated, mostly sand-dominated fluvial and shallow lacustrine sediments (conglomerates, sands, silts, clays) with disseminated organic matter content, oxidoreduction contrasts, and rare disseminated sulphides and carbonaceous cementations, separated from the Zuunbayan formation by an unconformity;
- Bayanshiree K2Bs (Upper Cretaceous, > 200 m thick): oxidized sands, sandstones and clays (the clay proportion increasing towards the top of the formation) from meandering river systems separated from the Sainshand formation by an unconformity.

#### 4.1.3. Mineralization occurrences

Uranium mineralization that occurs in the sand layers is preferentially located in the Upper Sainshand formation K2Ss2. This formation can be divided into four stratigraphic units: U1, U2, U3, U4 for the Uneget basin, and U0, U1, U2, U3 for the Zuunbayan basin. All the K2Ss2 units contain mineralized bodies in the Dulaan Uul deposit. In Zoovch Ovoo, the main part of the mineralized bodies is hosted by the Unit 2 and Unit 1 reservoirs and some small occurrences can be found in the Unit 0 (Fig. 2). Until now, no direct correlation has been established between the stratigraphic units described in the Uneget basin and the ones described in the Zuunbayan basin.

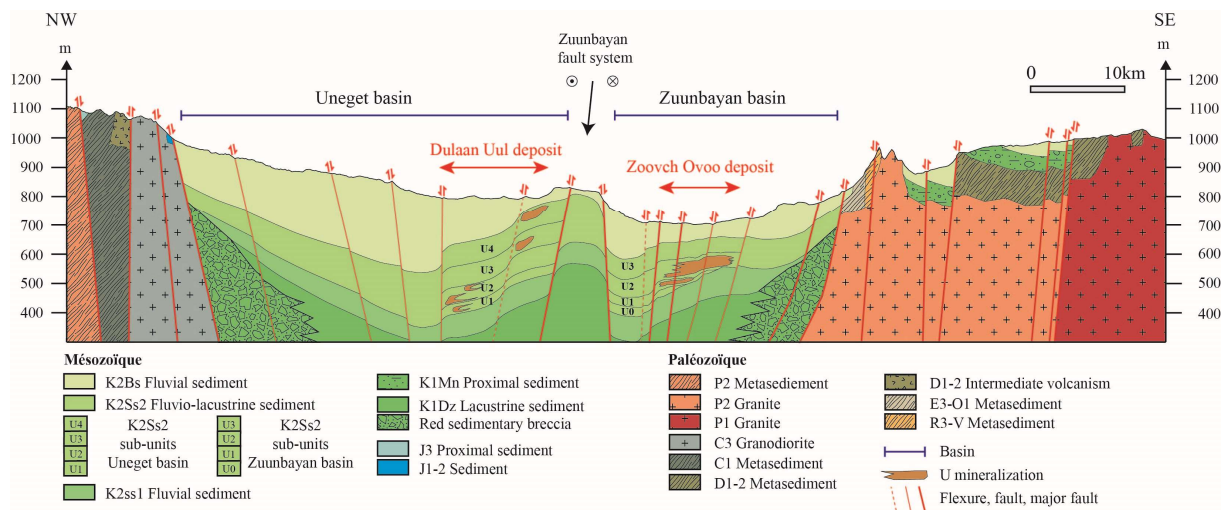


FIG. 2. Schematic NW-SE cross-section of the Sainshand basin showing the Uneget and Zuunbayan sub-basins general morphology and the location of the mineralizations of the Dulaan Uul and Zoovch Ovoo deposits.

## 4.2. Dulaan Uul deposit

### 4.2.1. History of the discovery

In 1982, Russian geologist teams identified significative surficial airborne radiometric anomalies and confirmed the existence of very shallow uranium concentrations and visible native selenium from trenches and small holes in the southern part of the Uneget basin. At that time, the geologists did not consider that this area was worth further investigations. Based on these historical uranium indications and following the resumption by Cogegobi of the exploration activities in the Sainshand area in 1999, the first drilling operations were carried out on the Dulaan Uul area in 2002, quickly identifying reduced sand levels along with several underground anomalies, and as soon as 2003 the first significative mineralized impacts of the Dulaan Uul deposit were intersected in drillholes. The continuity and significant extension of this mineralization were later confirmed by the 2004 campaign.

### 4.2.2. Morphology of the deposit

The Dulaan Uul deposit is a sedimentary-hosted uranium deposit, roll-front type, developed on several levels and multiple sub-rolls inside the four local stratigraphic units of the Upper Sainshand Formation (K2Ss2) at the contact between oxidized and reduced sands.

The sand reservoirs of the K2Ss2 stratigraphic units hosting the mineralization significantly deepen from the south to the north, with the base of the K2Ss2 being found at less than 150 m depth at the southern end of the deposit area and at more than 300 m at the northern end of the Western Fronts. The global thickness of the Upper Sainshand formation and the thickness of each stratigraphic unit of the K2Ss2 are very stable in this part of the Uneget basin, except in the southern half of the deposit area, in which the upper stratigraphic units (U4 and U3) are partly or completely eroded.

The depth of the mineralization ranges from a few meters up to 300 m, depending of the mineralized unit considered and the location inside the deposit. However, the depth of the condensed central orebodies does not exceed 120 m.

There are two main morphologies for the orebodies of the Dulaan Uul deposit (Fig. 3):

- Massive orebodies located, from the top to the bottom, in the units U4, U3 and the upper part of U2. Five main mineralized bodies have been discovered: Myagmar, Umnut NW, Umnut, SW, Umnut E and Australiens, with extension ranging from 1.5 to 2.5 km long by 0.3 to 1 km wide. In some local parts of the orebodies where the structural control is very strong (mineralization lined up with water flow screening faults) and in the shallowest parts in which sub-surface phenomena have affected the mineralized levels, the classical superimposed roll-front morphologies are modified. This leads to more complex detailed mineralization geometries and patterns, but also to the more condensed aspect of the central orebodies;
- Ribbon-shaped mineralization in the units U2 and U1. This group of typical roll-front-shaped mineralized bodies called Western Fronts consists in narrower elements compared to the mineralization in the units U4 and U3, but much more stretched and almost continuous along 20 km of superimposed oxidization fronts (two different ones in the Unit 1, and four in the Unit 2). The mineralization thickness varies depending on the sector and the stratigraphic unit considered, but ranges in average from 5 to 15 m. The main orientation of the orebody is N-S on the northern half of the deposit and NE-SW in the southern half. NNW-SSE secondary direction is also visible on some sections of the fronts (central area and southern end).

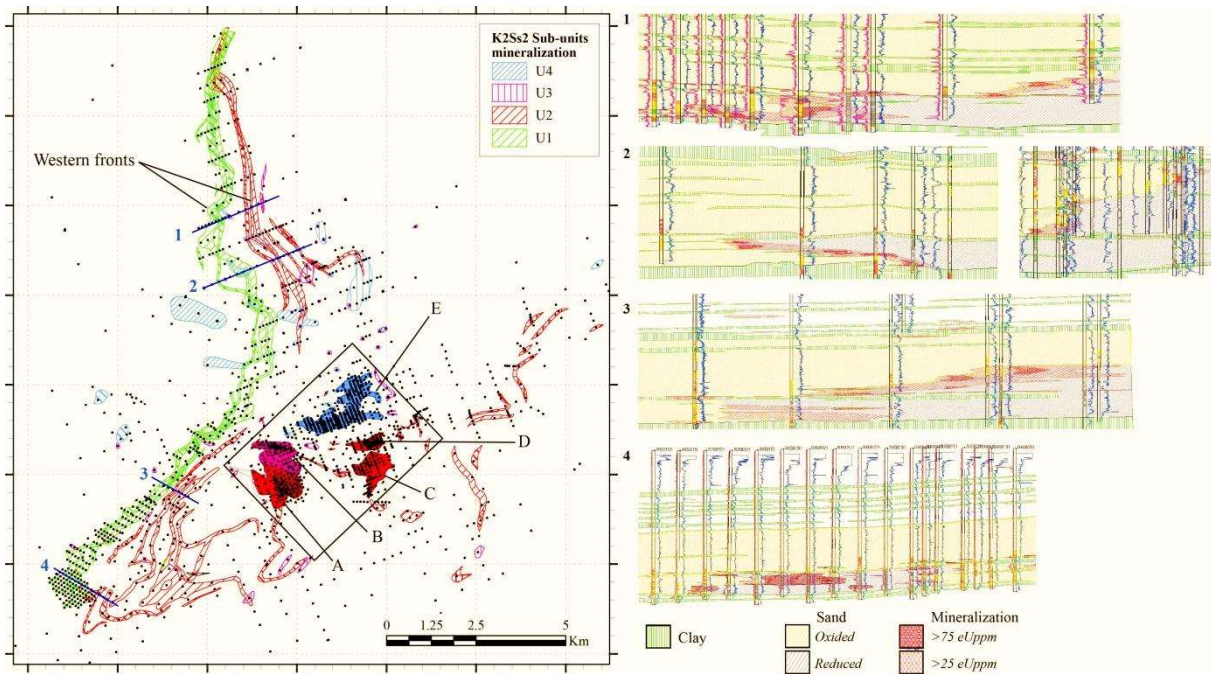


**FIG. 3.** Map and cross-section of the Dulaan Uul deposit. The orebodies taken into account for the resources estimation are located on the map inside the black rectangle. A: Umnut south-west; B: Umnut north-west; C: Umnut east; D: Australiens and E: Myagmar. The location of the cross-sections on the right of the figure is indicated by the blue lines numbered on the map.

#### 4.2.3. Mineralization

The Dulaan Uul mineralization consists mainly of coffinite and uranium oxides associated with finely crystallized pyrite. The richest mineralization is associated with pyritized fragments of lignite. The mineralization situated close to the surface is made of complex oxidized species (yellow products).

#### 4.2.4. Resources estimation and geological potential

A resources estimation was conducted in 2011 on the massive orebodies located in the upper K2Ss2 units. The calculation was based on a  $200 \times 50$  m down to a  $100 \times 25$  m drilling grid in this sector and gave a result of 6260 t of recoverable uranium in the sand. 70% of these resources – 4481 t – have been classified as indicated and 30% – 1779 t – as inferred (categories B and C according to the Mongolian classification). The average grade of the mineralization is 233 ppm for the indicated resources and 201 ppm for the inferred ones, based on a 75 ppm U cut-off.

The Western Fronts mineralization has not been estimated yet because the exploration works are still active today on the corresponding orebodies, and the mineralized area remains open. According to the results obtained until now, the expected additional potential of this mineralization is between 6000 and 10 000 t of uranium.

### 4.3. Zoovch Ovoo deposit

#### 4.3.1. History of the discovery

After the Dulaan Uul deposit, Zoovch Ovoo is the second major discovery of Cogegobi in the Sainshand region.

Before the effective beginning of the exploration works in 2008, no special chemical or radiometric anomaly at the surface was predicting the presence of a mineralization in depth. The works began with the drilling of large scale profiles across the Zuunbayan basin. The first mineralized impacts have been

discovered as soon as 2009, and 30 km of oxidoreduction front have been delineated. The continuity and substantial extension of the mineralization identified was then confirmed in 2010. In 2011 and 2012, an extensive further exploration and first stage development campaign was performed on the whole mineralized orebodies, covering the considered area with a  $200 \times 200$  m down to  $100 \times 100$  m drilling grid, and a local 25 m spaced drillholes cross, in order to quickly be able to assess the potential of this new deposit.

In 2013, the development works have been dedicated to some specific studies (see Section 5.2), more focused on the characterization of the ore properties and the analysis of the deposit hydrogeological parameters. Since the acquisition of the exploration licence of Zoovch Ovoo by Cogegobi, 1136 boreholes, representing 237 930 m of drilling, have been performed (Fig. 4).

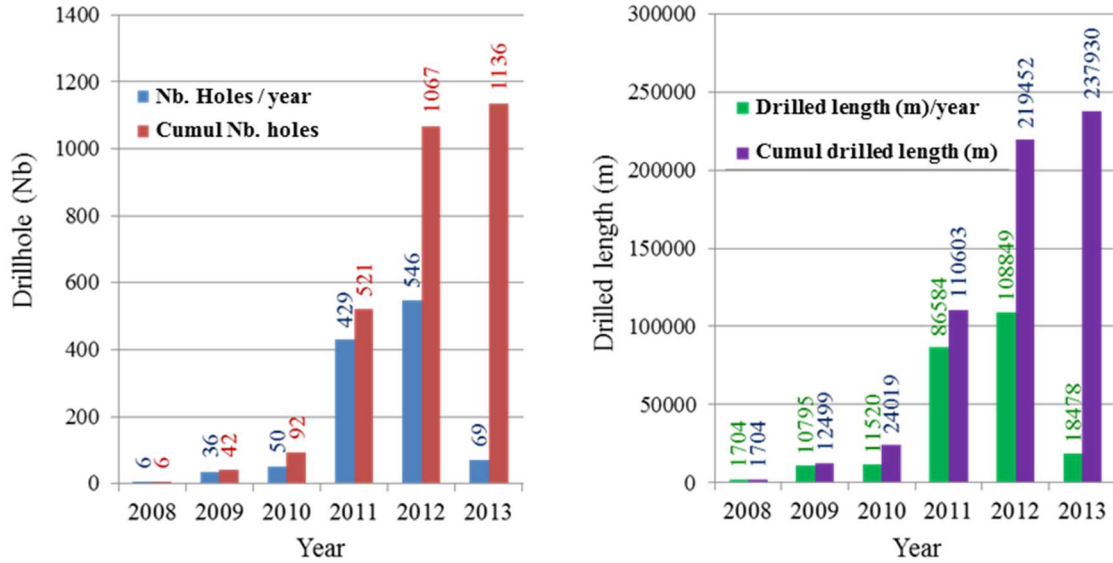


FIG. 4. Bar diagram of the number of drillholes and drilled length per year since the acquisition of the Zoovch Ovoo licence by Cogegobi.

#### 4.3.2. Morphology of the deposit

The Zoovch Ovoo deposit is a major high tonnage low grade sedimentary-hosted roll-front type under cover deposit. It consists of a complex system of partly over-imposed elementary sub-rolls of irregular shapes that built a quite atypical sub-massive tabular looking orebody.

The thickness of the sand reservoir hosting the mineralization ranges from approximately 60 m to a 100 m, as it is slightly and continuously increasing towards the north and the northwest, along with the gentle deepening of all the K2Ss2 stratigraphic units (the base of the K2Ss2 formation is at less than 170 m south of the deposit and more than 230 m in its northern end). This reservoir is confined at its base by thick non-permeable layers (mostly red clay and silt dominated) of the undifferentiated Lower Cretaceous.

The recognized mineralization, comprising three main enriched blocks (South-East, North and West), covers a WNW-trending area of approximately  $8 \text{ km} \times 3.5 \text{ km}$  (Fig. 5), and ranges from 4 m up to 40 m thick, with an average thickness of about 15 m of continuous mineralization (Fig. 6). It occurs at depths ranging from 100 m to 230 m below the surface. Most of the mineralization is located in the stratigraphic units U2 and U1 of the Upper Sainshand (K2Ss2).

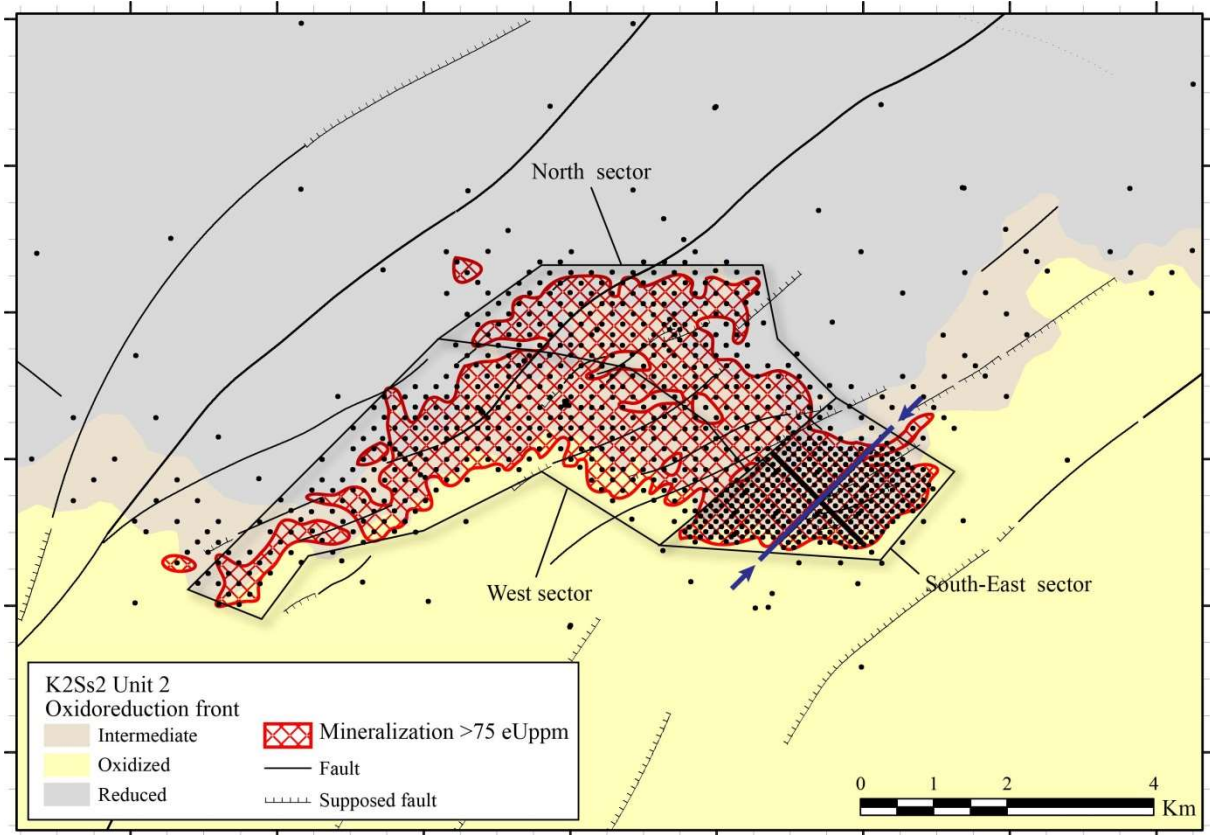


FIG. 5. Zoovch Ovoo deposit map. The three main mineralized sectors are localized on the map. The blue line with the arrows indicates the location of the cross-section presented in Fig. 6.

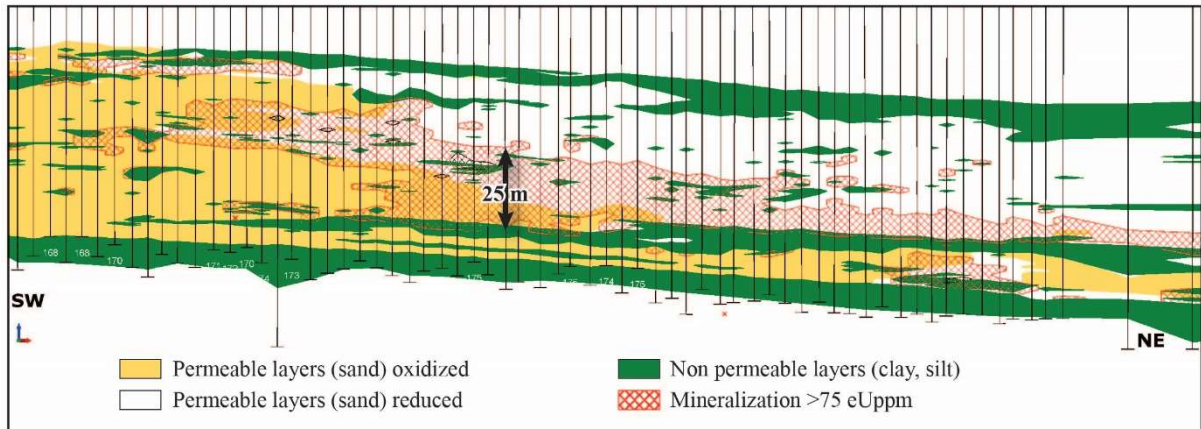


FIG. 6. SW-NE cross-section along the 25-m spacing cross located in the south-eastern sector of Zoovch Ovoo deposit. The cross-section is extracted from the Micromine© 3D model of the deposit.

#### 4.3.3. Structural control of the deposit

The deposit is affected by a flexural deformation probably associated with a network of minor normal faults with the same N60 – N70° orientation as the main fault system structuring the basin. These faults are poorly expressed in the observed cores and probably essentially accommodated by the non-consolidated sediments. This flexure-type deformation and diffuse faulting seem not to significantly affect or control the geometry and internal grade distribution of the orebodies. Nevertheless, they are

suspected to constrain the circulation of the oxidizing fluid flows coming from the south, therefore controlling the general morphology of the deposit (Fig. 5).

#### 4.3.4. Mineralization

The mineralization consists of uranium oxides, coffinite, phosphocoffinite, and uranothorite. The mineralization can be associated with automorphous or framboidal pyrite, ilmenite or titaniferous magnetite. The mineralization is localized at the contact between the oxidization front and the reduced sands. The disequilibrium values and distribution are typical of a roll-front deposit, indicating a strong disequilibrium in disfavour of the uranium in the oxidized zone and, in the reduced zone, an equilibrium state of the mineralization, to a slightly uranium favourable disequilibrium.

Due to the recent discovery of this deposit some of the studies are ongoing, and the detailed nature and preponderance of the reducing agents trapping the mineralization are still to be fully understood. The prevailing hypothesis remains the primary reduction of the K2Ss2 sediments due to their disseminated organic matter content, and to the anoxic conditions of the fluvio-lacustrine paleoenvironment. Besides, the migration of deep basin reducing fluids and gas from hydrocarbons source rocks could account for some of the massive enrichment of Zoovch Ovoo compared to the Dulaan Uul scattered orebodies, and for second order unexplained mineralization morphologies and distributions inside the deposit.

#### 4.3.5. Resources estimation and geological potential

A resource estimation was conducted in 2012 and published in 2013. The calculation was based on the results obtained at the end of the 2011 exploration and development campaign. The drilling grid taken into account ranges from a  $200 \times 200$  m down to a  $200 \times 100$  m. A large cross with a 50-m spacing between the drillholes, conducted on the south-eastern part of the deposit in order to evaluate the short-range variability of the mineralization and the oxidoreduction state of the host sediments, was also involved in the estimation process. The calculation made from these data gave a result of 54 640 t of recoverable uranium in the sand. 20% of these resources – 12 510 t – have been classified as indicated and 80% – 42 130 t – as inferred (categories B and C according to the Mongolian classification). The average grade of the mineralization is 233 ppm, based on a 75 ppm U cut-off.

The results of this estimation are based on the 2011 exploration results. yet in 2012 the exploration works have identified and fully investigated extensions of the deposit in the Unit 2, and identified some new mineralization in the Unit 1 stretching deeper and remaining open at depth towards the north and the northwest. The forecast additional geological resources reach more than 10 000 t U.

### 5. FROM THE GEOLOGICAL OCCURENCES TO THE MINING OPERATIONS

#### 5.1. First recovery test in the Sainshand basin: Umnut technological test (Dulaan Uul)

In order to assess the technical feasibility of a uranium In Situ Recovery (ISR) in the context of the K2Ss2 formation sedimentary-hosted deposits, to appraise the economic parameters of this exploitation methodology, and to evaluate the needs of the future site remediation, an ISR test has been conducted on the southern part of the Umnut orebody, representative of the central Dulaan Uul deposit. The test was designed based on two combined hexagonal cells composed of two production wells — one in the centre of each cell — and a total of 10 injection wells (two injection wells being shared between the two cells).

The distance between the injection and the production wells is 15 m. In addition to this setup, 12 piezometers were placed inside and outside the cells, but also under, inside, above and downstream the mineralized aquifer in order to monitor the environment of the cells and the evolution of the physical and chemical parameters on the test area and around it, during the ISR operations and in the short, medium and long term after the end of it.

The test was operated over a 6 months period, from December 2010 to June 2011. The method evaluated in this test was an acidic leaching using sulphuric acid ( $H_2SO_4$ ) to locally bring the pH of the aquifer down to 1.5. The total amount of uranium recovered from the test is 2876 kg, which is estimated to represent a recovery rate of 79%.

### **5.2. Preparing the future for Zoovch Ovoo uranium recovery**

In 2013, as a first step of the ISR pre-feasibility study phase, 30 dedicated boreholes were drilled following a  $400 \times 400$  m grid and covering the entire Zoovch Ovoo deposit in order to get cored samples representing all types of host-sediment characteristics (stratigraphic units, grain size distribution, redox condition) in relation with different grades of uranium mineralization (from barren rocks to highest uranium grade category) on the different sectors of the deposit.

A total of 6200 m was drilled, allowing the recovery of more than 1680 m of cores. 1791 samples were collected, and 278 representative samples (512 kg) were selected and sent to AREVA Mines assay and process laboratory in France for dynamic and column leaching tests. These Zoovch Ovoo ore leaching tests are still in progress.

The results expected from the column leaching tests are to provide the best parameters to realize an ISR pilot test for the extraction of the uranium from the Zoovch Ovoo deposit. The technical characteristics of this future ISR pilot test are not yet defined at the time of the writing of this paper, but as of now the construction of the pilot is planned to start in 2015.

## **6. CONCLUSION: MONGOLIA A NEW PLAYER IN THE URANIUM WORLD MARKET**

The exploration efforts based on the review of the historical data and Cogegobi new geological approach of the targets have been successful, and the added uranium resources of the resulting new deposits is now estimated to reach more than 60 000 tU, without taking into account the 10 000 to 20 000 t of expected additional resources not yet formally estimated, in the extension of the already classified orebodies.

This world class size discovery has revealed a new sedimentary-hosted uranium district. Since their official classification, the Dulaan Uul and Zoovch Ovoo deposits put together represent more than half of the classified uranium resources of the country, which takes Mongolia into the top ten countries in the world in terms of inferred uranium resources (cost range < 130 US\$/kgU). In addition, these exploration successes demonstrate the potential of the wide distal basins, allowing to expect much larger geological resources lying into the ground, from the possible future discoveries in all the under-explored cretaceous basins of the country.

In the past, Mongolia produced a total of 535 t of uranium from the Dornod open-pit mine located in the Mardai Gol district from 1989 to 1995 [2]. Currently, there is no operating uranium mine in the country. The work carried out to convert the Dulaan Uul and Zoovch Ovoo resources into a minable product is ongoing and could lead to an ISR production after 2020, with an output capacity of 2000 t of uranium per year for Zoovch Ovoo only, which would place Mongolia as one of the major uranium producers in the world behind Kazakhstan, Canada, Australia, Niger, Namibia, and the Russian Federation.

## **ACKNOWLEDGEMENTS**

The achievements hereby described are the results of the work of all the teams of Mongolian and several nationalities expatriate collaborators who have shaped the story of Areva's subsidiary Cogegobi for the past 17 years. This paper is dedicated to them, as their conviction, passion, and sustained efforts throughout these years allowed the following of the trail, the discovery, the exploration, development, and the official classification of the Dulaan Uul and Zoovch Ovoo deposits.

## **REFERENCES**

- [1] DAHLKAMP, F.J., Uranium Deposit of the Wold: Asia, Springer, Berlin (2009).
- [2] OECD NUCLEAR ENERGY AGENCY, INTERNATIONAL ATOMIC ENERGY AGENCY, Uranium 2011: Resources, Production and Demand, OECD, Paris (2012).

# THE SUCCESSFUL APPLICATION OF MODERN EXPLORATION TECHNIQUES TO PREVIOUSLY EXPLORED AREAS IN THE ATHABASCA BASIN, CANADA

K.L. WHEATLEY  
Forum Uranium Corp.,  
Vancouver, British Columbia,  
Canada

## Abstract

Several project areas within the Athabasca Basin of northern Saskatchewan, Canada, that were explored in the 1970s and 1980s have had recent discoveries due to the application of modern exploration techniques and the evolution in the understanding of unconformity uranium deposit models. The Griffith showings of the Maurice Bay area and the Patterson Lake deposit on the west side of the basin, and the Roughrider and Phoenix deposits on the east side of the basin are all relatively recent discoveries in areas that were explored in the past. This paper describes the exploration methods that were used to locate “new” mineralization within previously explored areas.

## 1. INTRODUCTION

Exploration for unconformity uranium deposits in the Athabasca Basin of northern Saskatchewan, Canada, has been underway for approximately 40 years. The original exploration models used during the 1950s through to the early 1970s were for basement lithology hosted vein-type deposits or sandstone hosted ‘roll-front’ deposits. The discoveries of the ‘D’ deposit at Cluff Lake [1] and the Key Lake deposits [2], led to the development of a model based on uranium mineralization being located at the unconformity of the Athabasca sandstones with the underlying basement lithologies, typically overlying a graphitic horizon in the basement (an electro-magnetic (EM) conductor), and bordering an Archean antiform [3, 4]. Based on this model, numerous deposits were found in the late 1970s and early 1980s (Midwest, McLean, Dawn Lake, Collins Bay/Eagle Point and Cigar Lake). As exploration continued, further mineralization was found in the late 1980s to early 1990s (McArthur, La Roque, Sue A-E and Shea Creek). The original Rabbit Lake deposit was located in the basement and not recognized as an unconformity deposit until well after its discovery. McArthur was located along a faulted contact with a thick quartzite unit rather than an Archean antiform, providing a slight variation of the model [5]; both the quartzite and the Archean antiform provide a competency contrast that provides a focus for faulting.

In 1997, a showing was discovered wholly situated in the basement lithologies approximately 3 km east of the Key Lake deposits along a north-south EM conductor, the P-trend. The showing was aptly named the P Patch and was characterized by ‘clean’ mineralization with little to no associated sulphides with a grade of uranium averaging 1%  $\text{U}_3\text{O}_8$  [ $\sim 0.85\%$  U] and associated lead and boron (in dravite clay) within a bleached zone underlying fresh basement rocks. The alteration of the basement lithologies produced a gravity low around the mineralization, and a strong boron anomaly was present in the overlying altered sandstones. Three years later in 2000, the Millennium deposit was found on another north-south conductive trend approximately thirty kilometres north of Key Lake. It is also located wholly within the basement lithologies and is characterized by a bleached alteration halo around the mineralization with associated lead and boron enrichment and a ‘clean’ mineralogy. Millennium (68 Mlb U [ $\sim 26\,000$  tU] at 4.16%) has become the type exploration model for this variation on the unconformity deposits in the Athabasca [6].

The Millennium and McArthur models have been recently used by exploration companies to successfully find uranium mineralization in areas that were previously explored in the 1970s and 1980s for the ‘standard’ unconformity deposit model (Forum at Maurice Bay, Hathor/Rio at Roughrider and Denison at Wheeler River). Fission’s discovery at Patterson Lake South has followed the more traditional unconformity exploration model — drilling EM conductors up-ice from a substantial

radioactive boulder field. However, modern techniques of improved radon detection and airborne geophysical surveys have aided in quickly locating and delineating the mineralization along this trend.

## 2. DESCRIPTIONS OF FOUR RECENT URANIUM DISCOVERIES IN THE ATHABASCA BASIN

Four relatively new discoveries of uranium mineralization in the Athabasca Basin are discussed. These are located in four different areas of the basin (Fig. 1).

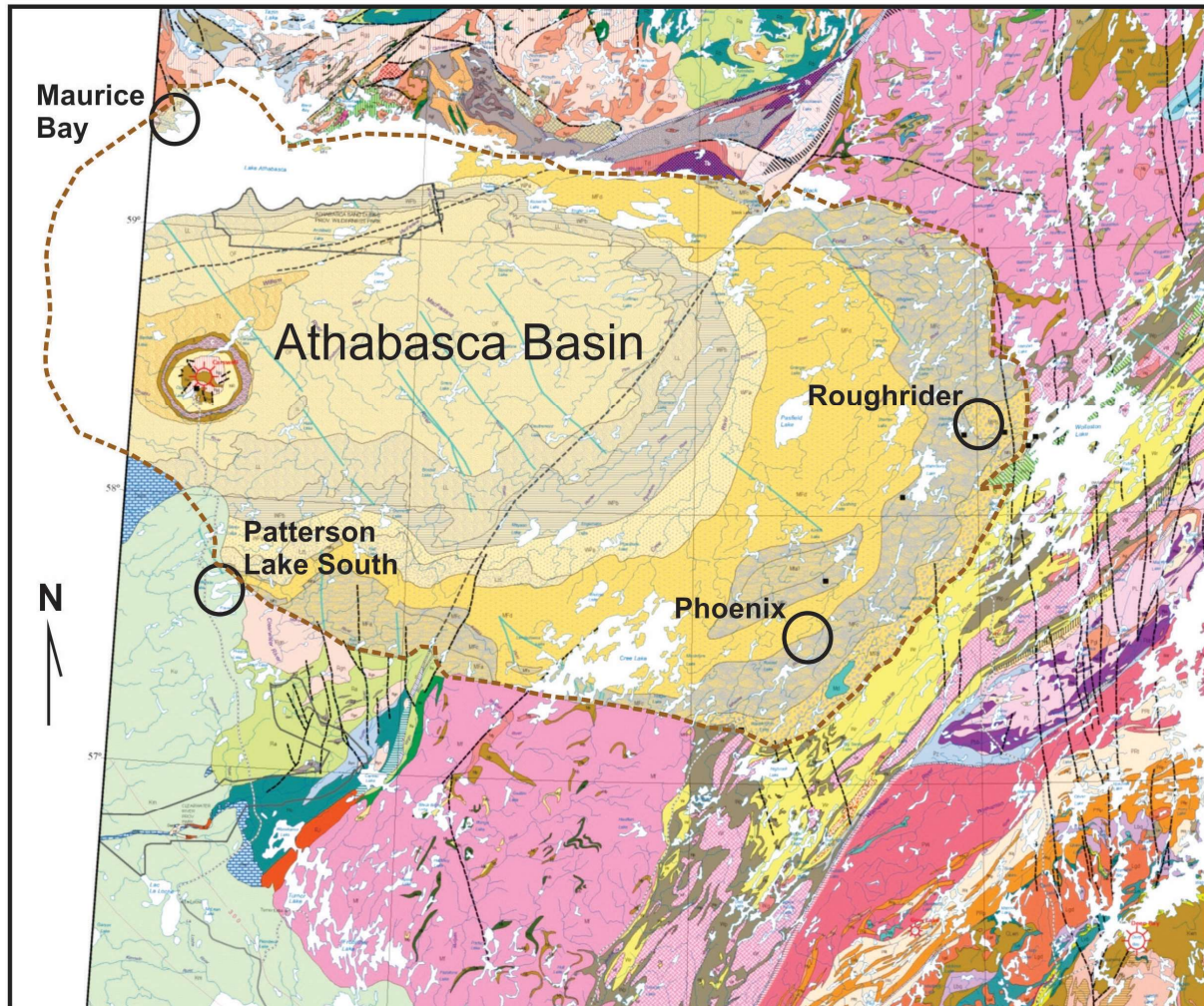


FIG. 1. Location map of new discoveries in the Athabasca Basin, northern Saskatchewan. Geology in background, modified from the Saskatchewan Geological Survey geology map.

### 2.1. The Griffith Showings, Maurice Bay

Uranerz Exploration and Mining Ltd successfully explored the Maurice Bay area in the mid to late 1970s and discovered the Maurice Bay showing (1.5 Mlb U [ $\sim 580$  tU] at 0.6%) and several other unconformity hosted showings (F-subcropping and Maurice Creek) plus two basement hosted showings (Zone 1A and Zone 2A), both located wholly in the basement as vein-type mineralization of very limited extent but with good grades (6.0 m at 5.65% U and 8.5 m at 5.68% U respectively). Exploration in the area was mothballed in the early 1980s and left mostly untouched until the mid-2000s. Cameco Corporation commenced exploration with a series of airborne and ground geophysical surveys (magnetic (mag) and EM) culminating in a 10-hole drill program in 2008 which tested some of the EM conductors but with little success, partially due to a very cold winter and limited access to preferred targets. Unlike the east side of the Athabasca Basin, EM conductors are relatively weak due to the lack of well-connected and graphite rich horizons that occur in the basal Wollaston Group meta-sediments.

Forum Uranium Corp. assumed operatorship in 2011 and completed an extensive ground gravity survey (Fig. 2) to test for areas of alteration. This ground gravity survey had been used extensively on Forum's Nunavut project around AREVA's Kiggavik project, and successfully identified basement hosted zones of alteration in areas with no sandstone cover. The Maurice Bay area lies on the north-western border of the Athabasca Basin and the sandstone cover varies from 0 to 200 m, allowing the gravity survey to easily 'see' through to the basement lithologies and detect any density differences. Both fresh and altered samples of sandstone and basement lithologies were sampled for density measurements, with the following results:

|                           |                          |                          |                          |
|---------------------------|--------------------------|--------------------------|--------------------------|
| Fresh sandstone density   | = 2.42 g/cm <sup>3</sup> | Fresh basement density   | = 2.71 g/cm <sup>3</sup> |
| Altered sandstone density | = 2.06 g/cm <sup>3</sup> | Altered basement density | = 2.29 g/cm <sup>3</sup> |

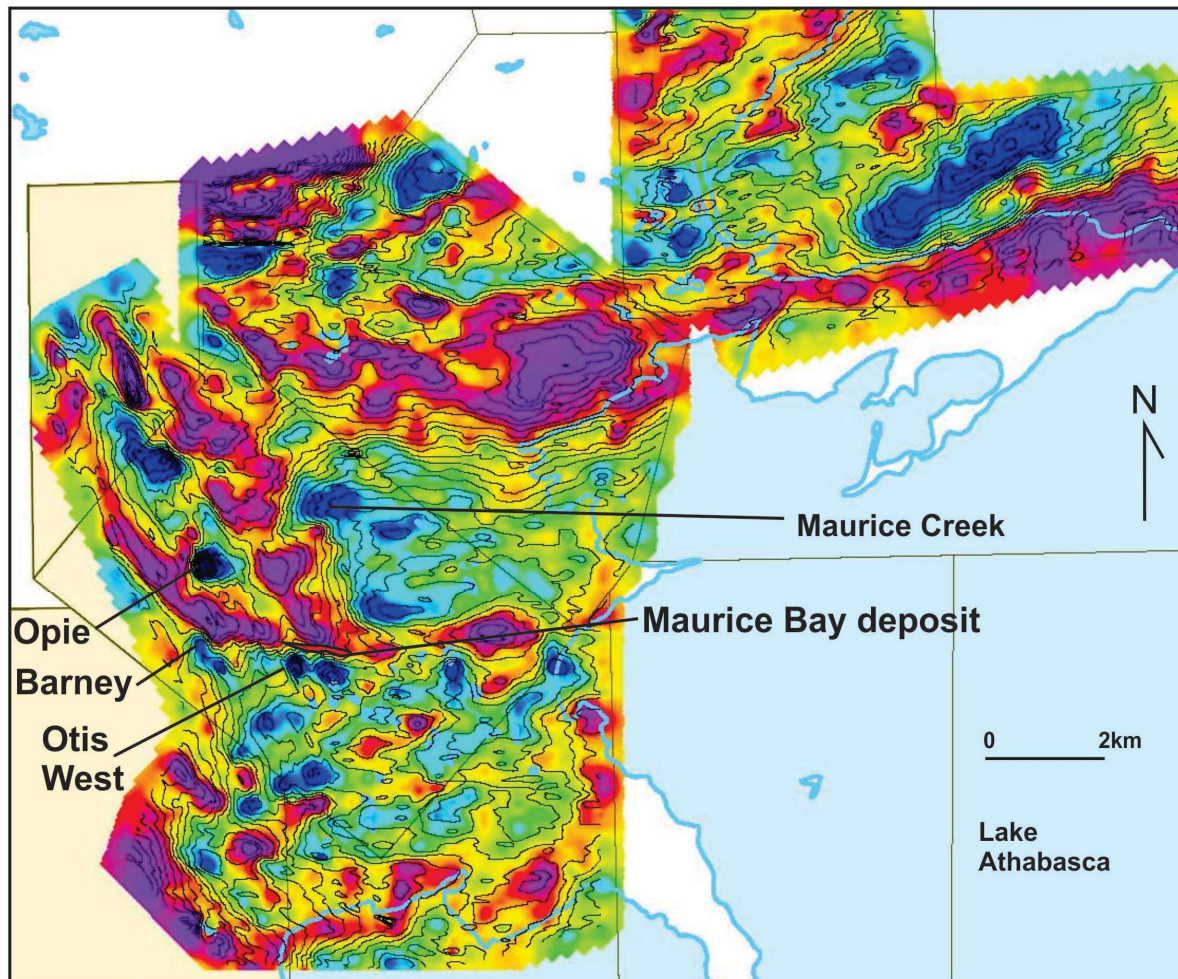


FIG. 2. Filtered ground gravity survey on the Maurice Bay project [7]. Blue colours are gravity lows, red colours are gravity highs. The Maurice Bay showing lies along the southern border of a gravity high.

This large variation in density was easily measured and a map prepared for the following drill programs with a total of 19 distinct gravity low anomalies. Due to the large number of targets generated by the survey, a naming system was derived based on the name of one of the two creeks on the project: Griffith Creek. Targets explored within the first two years were named Opie, Barney and Otis, with Andy, Aunt Bea and Goober to be explored at a later date.

The first target to be tested was the Opie zone because it was the strongest anomaly and several historic holes by Uranerz situated on the border of the anomaly were strongly bleached. Uranium mineralization was intersected in several holes located at the centre of the gravity low in conjunction with a weak NNW trending EM conductor. The mineralized zone strikes N110°E for 50 m and dips -70° to the south, is approximately 10 m thick and approximately 30 m in horizontal extent; the zone has not been completely drilled yet so exact dimensions are not known. The mineralization is 40 to 70 m below surface.

The second target was the Barney zone, where uranium mineralization was also intersected in the centre of the northern gravity low in conjunction with a weak EM conductor that trends NNW. The mineralization strikes approximately 30 m on an east-west axis, has a vertical extent of about 30 m and varies from 1 to 10 m in thickness. It lies approximately 120 m below surface.

The third target area was the Otis West zone, where uranium mineralization was also intersected in the centre of the gravity low, associated with a NW trending EM conductor and directly linked to a N110°E trending normal fault with an associated unconformity offset of about 20 m, parallel to another unconformity offset approximately 100 m to the north that controls the Maurice Bay showing. The Otis mineralization strikes N100°E and is approximately 50 m in strike length, 40 m thick, up to 100 m in vertical extent and varies from 75 to 175 m below surface (Fig. 3).

The similar characteristics of the three mineralized zones are as follows: a) they are located at relatively shallow depths entirely within the basement rocks under the Athabasca sandstones; b) they lie within a hydrothermal haematite alteration halo within a larger bleached alteration halo; c) they are orientated at N090°E to N110°E and dip to the south; d) they lie within a distinct gravity low caused by the bleached zone and are typically associated with a weak EM conductor orientated NW to NNW; and e) they are associated with a very strong boron signature (up to 1% B) in the overlying sandstone, associated with dravite clays. The average uranium grades are low (0.1% U<sub>3</sub>O<sub>8</sub> [ $\sim$ 0.085%U]) compared to the typical Athabasca unconformity deposits, and currently of limited extent; further exploration is required to fully delineate these showings.

An interpretation, based on the surrounding geology, structure and alteration, is that this mineralization has been remobilized into place at a later date (possibly 1.1 Ma) than the main uranium mineralization event at approximately 1.5 Ma. The main secondary mineralization event at 1.35 Ma introduced sulphides [8] that both contaminated and diluted the initial high-grade mineralization and probably formed the Maurice Bay showing. The Griffith showings are both lower grade and have little in the way of sulphides, suggesting they were formed at a date later than the 1.35 Ma mineralization event. Mylonites and healed breccias on a large scale in the Maurice Bay area, combined with post-Athabasca faulting, widespread mineralization of several types (unconformity, vein-type and the Griffith showings) suggest that this has been a structurally active zone since the Trans-Hudson and Taltson orogenies.

Plans are to continue with exploration in this area by following up the remaining gravity targets. An attempt will be made to try to prioritize the remaining 15 gravity lows by sampling the overburden immediately down-ice from each anomaly and analysing for boron, the strongest indicator element in the overlying sandstones.

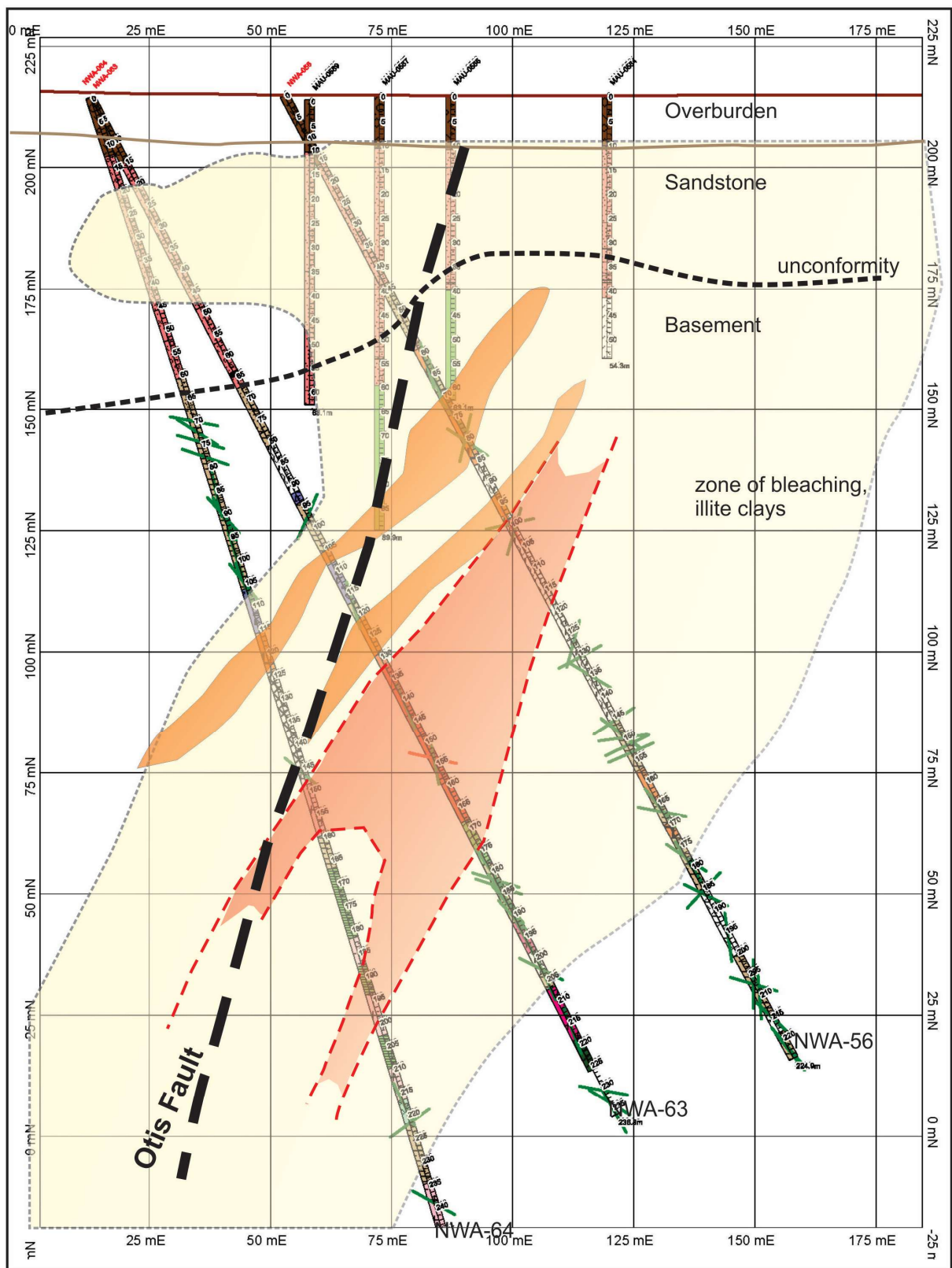


*FIG. 3. Cross-section of the Otis West mineralized zone [7]. The red dashed line with red fill is the zone of hydrothermal haematite and uranium mineralization. The orange elongated zones are pegmatites within pelitic to psammo-pelitic gneiss metasediments. The thin black dashed line shows the unconformity contact which is offset down to the south by the Otis fault (normal fault), the thick black dashed line.*

## 2.2. The Roughrider deposit

The Roughrider deposit was found in early 2008 by Hathor Exploration Ltd., which has since been bought out by Rio Tinto. The deposit was found by following up on alteration noted in historic drill holes that were completed in the late 1970s by Asamara along the northern extent of the Midwest Lake structure. Improved geochemical techniques in clay identification allowed for hydrothermal illite identification in the sandstone in the old holes, and the recent discovery of the Midwest 'A' deposit (originally called the Mae Zone) by AREVA Resources Canada Ltd. along strike to the SSW (Fig. 4) showed that the N030°E striking Midwest structure was fertile beyond the Midwest deposit itself. EM, resistivity, gravity and magnetic (mag) surveys and a structural interpretation aided in locating the mineralization. Depth to basement in the project area is approximately 200 m.

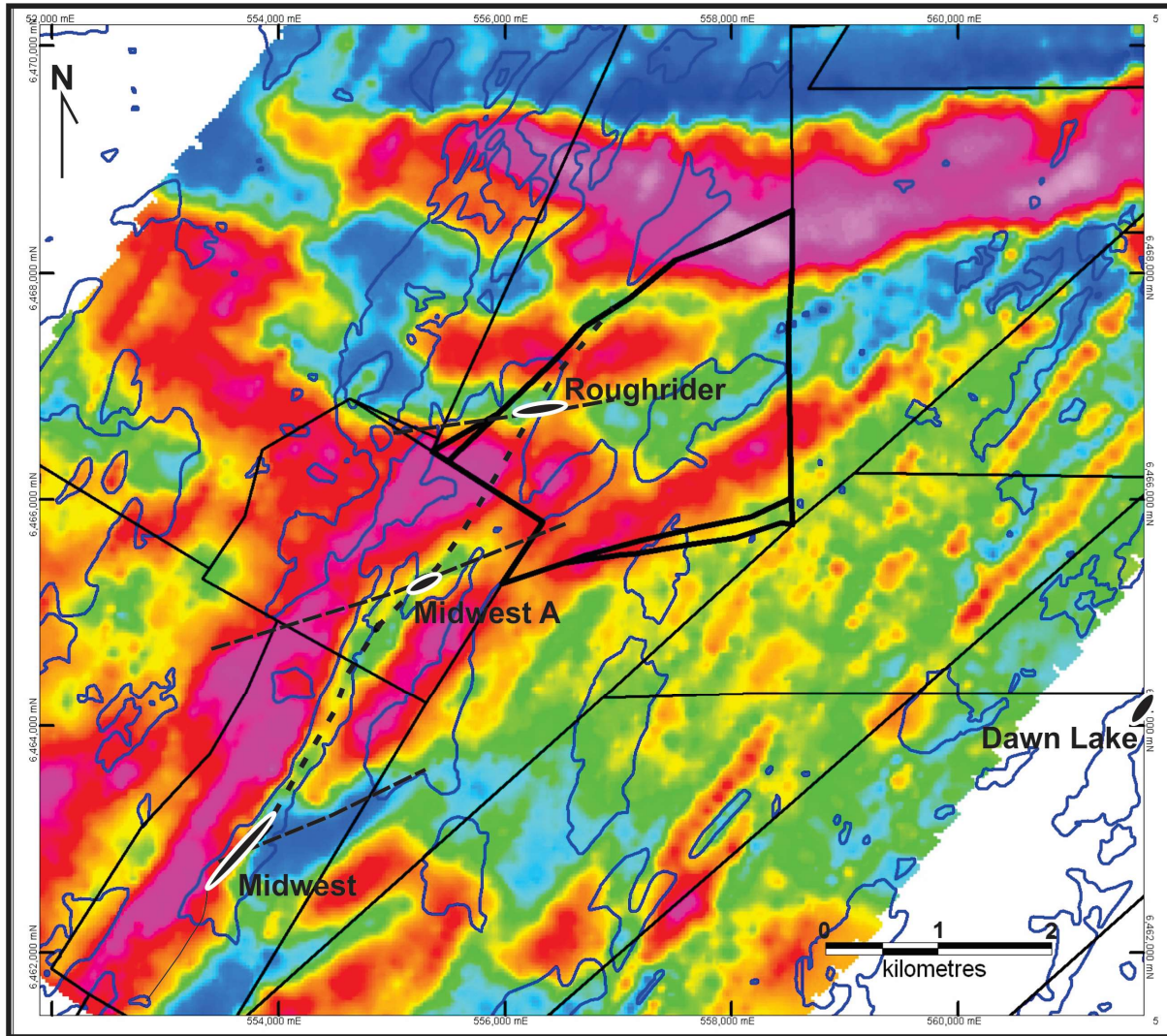


FIG. 4. The location of the Roughrider deposit. The background of the map is the regional magnetic signature and the straight black lines show the local claim boundaries. Mineralized zones are named and shown by black ellipses with white outlines. Black dashed lines are major faults along the Midwest trend. Modified from [9].

Exploration work between 2005 and 2009 on the Roughrider Project included electromagnetic, magnetic, gravity, seismic and resistivity surveys, re-logging of historic drill core and diamond drilling [9, 10]. An airborne electromagnetic (TEMPEST) and magnetic gradiometer survey was completed in 2007. A one-kilometre wide region of early channel conductivity was identified that coincided with a group of low resistivity zones from a series of six ground surveys. At mid-sandstone depths (74 m to 136 m) an east-west trending corridor of low resistivity has been interpreted to represent alteration in the sandstone associated with the underlying mineralization. The following descriptions are summarized from [10].

In 2007 and 2008, several ground gravity surveys were completed in the immediate vicinity of the Roughrider deposit which identified numerous gravity lows, also interpreted to be due to alteration effects in the underlying rocks. One of these is located over the West Zone pod of mineralization. In 2007, a detailed three dimensional ('3D') seismic reflection survey was completed. 3D analysis of the data identified major structural features, mostly oriented at 65°, as well as zones of intense alteration. A helicopter-borne time-domain electromagnetic ('VTEM') survey was carried out in 2008 to locate bedrock conductors on the Roughrider Project, but none were detected. In summary, the Roughrider deposit lies in an area distinguished by a resistivity low, a gravity low, a magnetic low and a structurally complex area as defined by the seismic survey. It lies at the intersection of a cross-cutting east-west structure with a regional-scale fertile N030°E trending structure that hosts two other deposits.

The Roughrider deposit comprises of three zones, Roughrider West, East and Far East Zones. The Roughrider West Zone was discovered during the winter drilling program of February 2008. A hydrothermal clay alteration system was intersected in drill hole MWNE-08-10, and then high-grade uranium mineralization (5.29% U<sub>3</sub>O<sub>8</sub> [ $\sim$ 4.49%U] over 11.9 m) was intersected in drill hole MWNE-08-12. The Roughrider West Zone has a northeast-southwest strike length of approximately 200 m with a width of 100 m. Uranium mineralization occurs at depths of 190 m to 290 m below surface and is hosted predominantly within basement rocks. Only minor amounts of uranium occur at or above the unconformity.

The Roughrider East Zone was discovered in September 2009. Hydrothermal alteration was intersected in a number of earlier drill holes and then high-grade mineralization (12.71% U<sub>3</sub>O<sub>8</sub> [ $\sim$ 10.8%U] over 28 m) was intersected in drill hole MWNE-10-170. The best intersection to date was obtained in drill hole MWNE-10-648 (7.75% U<sub>3</sub>O<sub>8</sub> [ $\sim$ 6.57%U] over 63.5 m). The Roughrider East Zone is approximately 120 m long striking northeast and has a width of up to 70 m. The mineralization has a vertical extent of up to 80 to 100 m, starting at depth approximately 250 m from surface, and 30 m to 50 m below the unconformity (Fig. 5).

Roughrider Far East Zone was discovered in February 2011. The discovery drill hole intersected 1.57% U<sub>3</sub>O<sub>8</sub> [ $\sim$ 1.33%U] over 37.5 m. The best intersection to date is drill hole MWNE-11-715, which intersected 7.91% U<sub>3</sub>O<sub>8</sub> [ $\sim$ 6.71%U] over 27.0 m. The West Zone occurs as a number of high grade lenses (>3.0% U<sub>3</sub>O<sub>8</sub> [ $\sim$ 2.5%U]) mantled by an envelope lower grade mineralization. The mineralization plunges moderately to the north or northwest. The contacts between the mineral lenses are sharp.

Uranium mineralization is highly variable in thickness and style with high-grade mineralization occurring primarily as medium- to coarse-grained, semi-massive to massive pitchblende with 'worm-rock' texture. This mineralization is locally associated with red to orange coloured iron oxides and yellow secondary uranium minerals that are locally present as veinlets or filling voids within the high grade primary mineralization. Lower grade mineralization occurs as disseminated grains of pitchblende, fracture-fills or veins of pitchblende.

Mineralization is mostly mono-metallic in composition, but nickel-cobalt sulpharsenides are locally present in the West Zone. The presence of nickel–cobalt sulpharsenides is rare in the East Zone, but significant levels of copper mineralization are present; atypical of most uranium deposits in the Athabasca Basin.

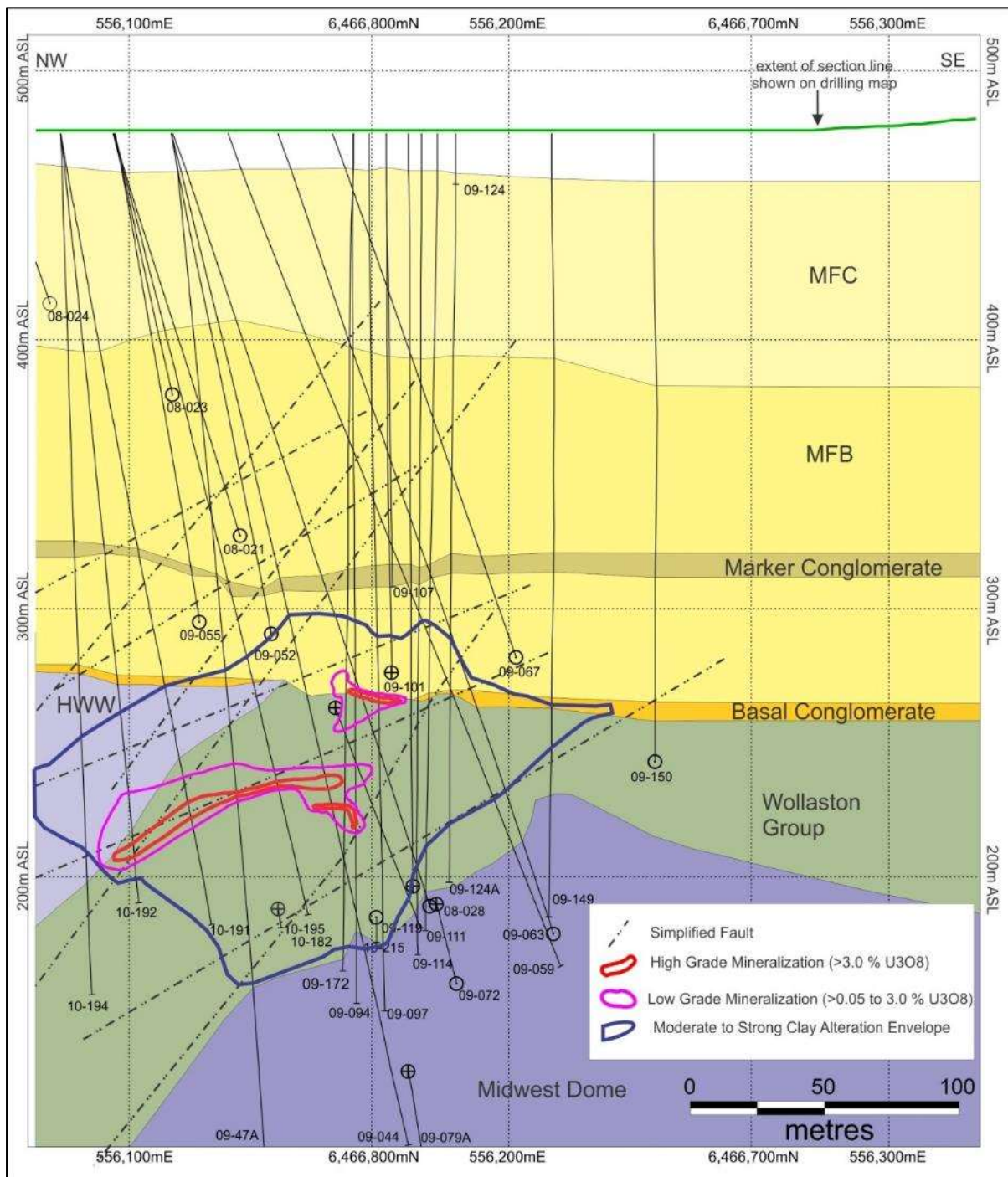


FIG. 5. Cross-section of the Roughrider deposit [9]. The Athabasca Group is shown in yellow colours, Wollaston Group meta-sediments are in green and the Midwest Dome, a mix of fresh granitic to dioritic orthgneiss, is in purple. The HWW is the hanging wall wedge.

The basement lithologies are structurally complex, comprising of steeply dipping Wollaston Group metasediments interlayered with Archean granitic to granodioritic orthogneisses. Several basement packages are located in the area of the deposit: the Wollaston Group, a hanging wall wedge (HWW), a foot wall wedge (FWW) and the 'Midwest Dome'. The deposit is situated within basement rocks belonging to the basal part of the Wollaston Group, composed of garnet and cordierite pelitic gneisses with lesser amounts of graphitic pelitic, psammopelitic and psammitic gneisses. The FWW and HWW are comprised of granitic to tonalitic orthogneiss and the MWD is composed of well-foliated granitic to dioritic orthogneiss. It also contains younger 'Hudsonian' pegmatites, leucogranites and microgranites, probably derived by partial melting of the host rock. The basement rocks and overlying Athabasca

sandstones have been subjected to several episodes brittle reactivation of older ductile shear zones, a typical feature of the Athabasca unconformity deposits.

The latest estimate of ore reserves released by Rio Tinto is 57.9 Mlb U<sub>3</sub>O<sub>8</sub> at a 4% average grade [~22 300 tU at average ~3.4%U] [10]. Rio Tinto has continued with substantial drill programs on this deposit so this number may change.

### 2.3. The Phoenix deposit

The Phoenix deposit was discovered by Denison Mines in 2008 on the Wheeler River JV Project [11]. This very large property was explored almost continually since 1978 (192 drill holes) and a number of showings were discovered, such as the M and O Zones in 1986 and the K Zone in 1988. Rare earth element mineralization was also discovered in the MAW Zone in 1982. Depth to basement (thickness of sandstone) ranges from 170 m in the south, to 760 m in the northwest. The project hosts many graphitic EM conductors and several large meta-quartzite ridges in the centre of the property.

Denison became operator of this project in 2004 and it took them four years and approximately 50 drill holes to find the Phoenix deposit. The deposit was found by changing the key exploration parameters from the standard Key Lake unconformity model (EM conductor, U, Ni, As anomaly, bordering an Archean antiform) to the McArthur River model (EM conductor, boron anomaly, bordering meta-quartzite ridge). Exploration switched to targeting boron haloes in altered sandstone overlying a meta-quartzite ridge contact, preferably combined with a resistivity low and an EM conductor. The following descriptions are summarized from [11, 12].

Denison carried out property-wide airborne GEOTEM and gravity surveys with subsequent ground TEM grids over the resulting anomalies in 2004. In 2007 an IP and MT survey using Titan 24 DC (direct current) resistivity technology was used to survey the K and M zones plus an area that had potential for a McArthur or Millennium style deposit. The results showed that the resistivity was very high over the meta-quartzite rock but two well-defined resistivity lows were present in areas where previous drill holes had been lost due to alteration/tectonization of the sandstone. Drilling in 2007 on several resistivity anomalies did not discover any mineralization, but the holes proved that the resistivity survey did locate alteration in the sandstones. This alteration consists of bleaching, silicification, desilicification, drusy quartz-lined fractures, secondary haematite, dravite, and/or clay minerals.

In 2008, the resistivity survey data was reinterpreted and three drill targets were developed. These targets were composed of resistivity lows located adjacent to the meta-quartzite in areas where diamond drilling could not reach the unconformity and showed anomalous boron values. Drill hole WR-249 in 2008 is considered to be the discovery hole for the Phoenix deposit. In summary, the Phoenix deposit lies on an EM conductor within a resistivity low due to alteration and tectonic activity, with anomalous boron values along a lithological contact (meta-quartzite) that provides a competency contrast and focus for repeated faulting.

The local geology is illustrated in Fig. 6.

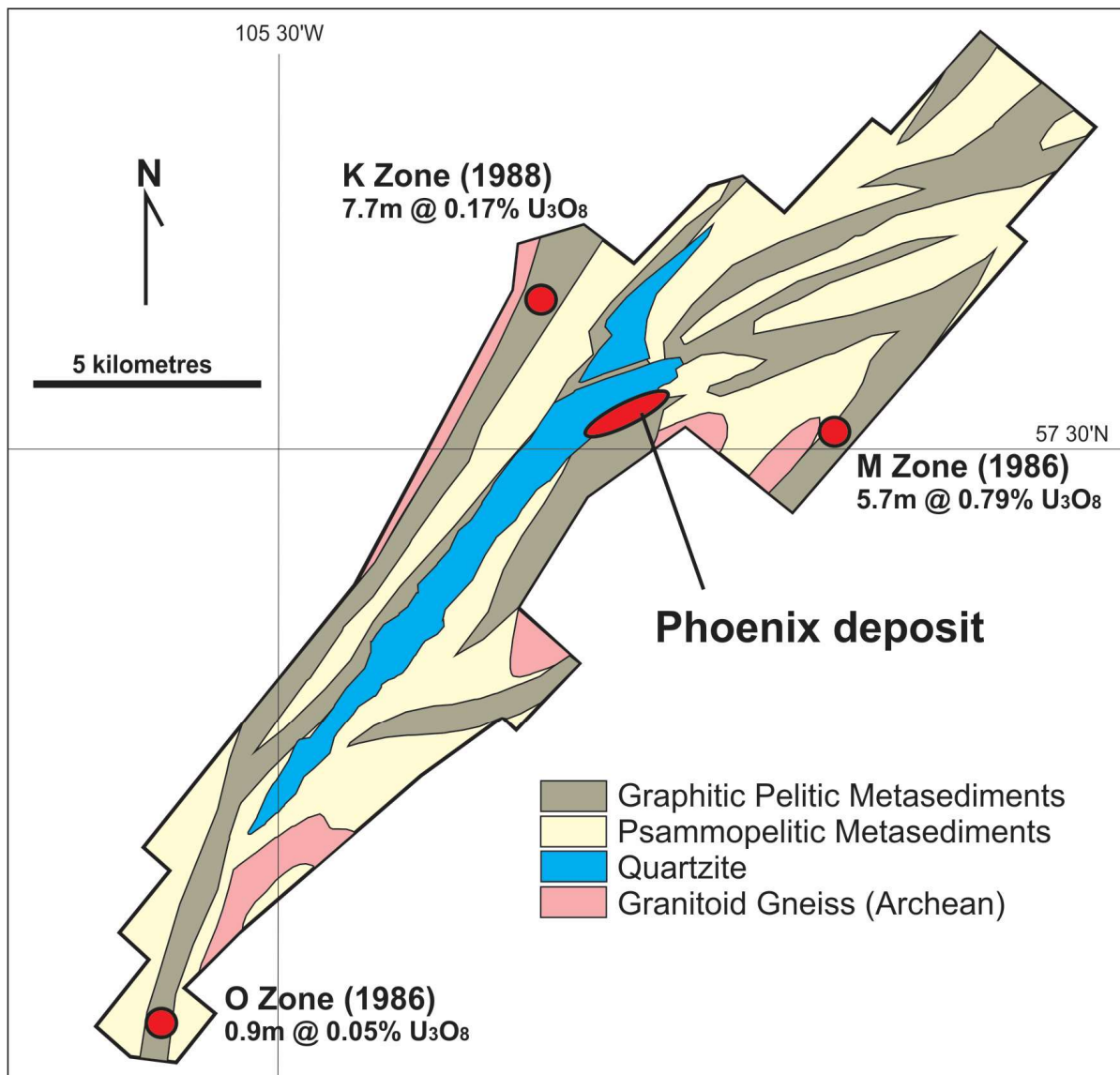


FIG 6. Geology and showings on the Wheeler River Project, modified from [11]. The overlying Athabasca sandstone is transparent to show the basement geology

The Phoenix deposit is an unconformity-type uranium deposit located at the south-eastern border of a meta-quartzite palaeotopographic ridge with graphitic pelitic metasediments, lying mostly within the Athabasca sandstones immediately above the unconformity. The deposit is located at a depth of approximately 400 m below the surface. The majority of the mineralization occurs in the Athabasca sandstones with a minor amount located within fractures in the basement. The uranium occurs as uraninite/pitchblende ( $\text{UO}_2$ ). Other metals, such as nickel, arsenic and cobalt which are typically associated with unconformity deposits in the Athabasca basin, compose only a very minor part of the deposit: values range in the 100s of ppm. The sandstones are altered for as much as 200 m above the unconformity, and exhibit varying degrees of silicification and desilicification, as well as dravitzation, chloritization, illitization and hydrothermal haematite. This alteration also occurs, to a much lesser extent, in the basement rocks.

The deposit strikes northeast for a distance of approximately 1100 m, varies from a few metres to 40 m wide and in thickness from 1 to 10 m thick, with intersections of up to 62.6%  $\text{U}_3\text{O}_8$  [ $\sim 53.0\%$  U] over 6 m (Fig. 7). The current resources are estimated at 70.2 Mlb at an average grade of 19.13%  $\text{U}_3\text{O}_8$  [ $\sim 27\,000$  tU at an average  $\sim 16.2\%$  U] [12].

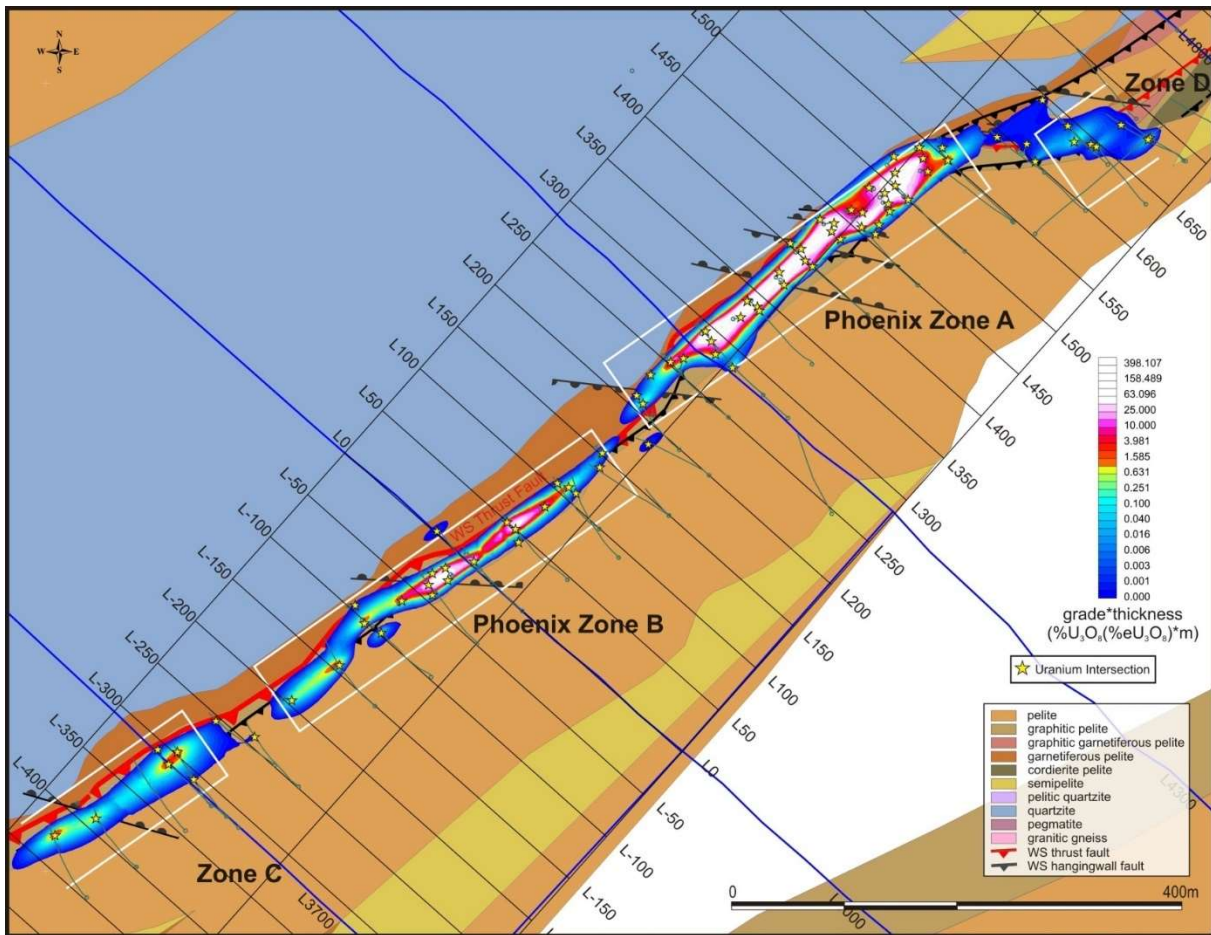


FIG. 7. Plan map of the Phoenix deposit [12].

Basement rocks beneath the Phoenix deposit are comprised of metasedimentary and granitoid gneisses of the basal Wollaston Group. The metasedimentary rocks include graphitic and non-graphitic pelitic and psammo-pelitic meta-sedimentary gneisses, meta-quartzite and feldspathic granitoid gneisses. Pegmatitic segregations and intrusions are common in all units. The meta-quartzite unit provides both a competency contrast and a hydrothermal barrier, forms the footwall to the mineralization and dips to the southeast at about 50°. This is overlain by a garnetiferous meta-pelitic gneiss, (7–60 m thick), then a graphitic meta-pelitic gneiss (5–70 m thick) with 1% to 40% graphite, and lastly a massive, non-graphitic, unaltered meta-pelitic gneiss (unknown thickness).

A major structural feature at the Phoenix deposit is the WS reverse fault (N055 azimuth, 55° dip to SE) that lies within or at the base of the graphitic meta-pelitic gneiss near the south-eastern border of the meta-quartzite ridge. The WS fault exhibits both ductile shearing and brittle fracturing.

Continued drilling on the project has led to the discovery of two further mineralized zones, the 489 Zone and the Gryphon zone.

#### 2.4. The Patterson Lake South deposit

The Patterson Lake South deposit was discovered by Fission Uranium in 2012. Fission has bought out previous partner Alpha Minerals portion and now owns the project 100%. This property lies in the southwest part of the Athabasca Basin, just outside the limit of the sandstone and straddles the former road to the Cluff Lake mine site (Fig. 8). The property hosts numerous east-northeast trending EM conductors, very few of which have been tested by drilling. This property saw minor exploration in the 1970s and early 1980s, but mostly left untouched until the 2000s. The discovery of this deposit followed the more traditional lines of exploring up-ice from a mineralized boulder train (Key Lake, Cluff Lake, Maurice Bay, etc.) along an EM conductor. However, more advanced techniques in airborne EM, mag

and radiometric surveys, ground radon, resistivity and EM surveys aided in finding the deposit much quicker and more efficiently than using the older technologies.

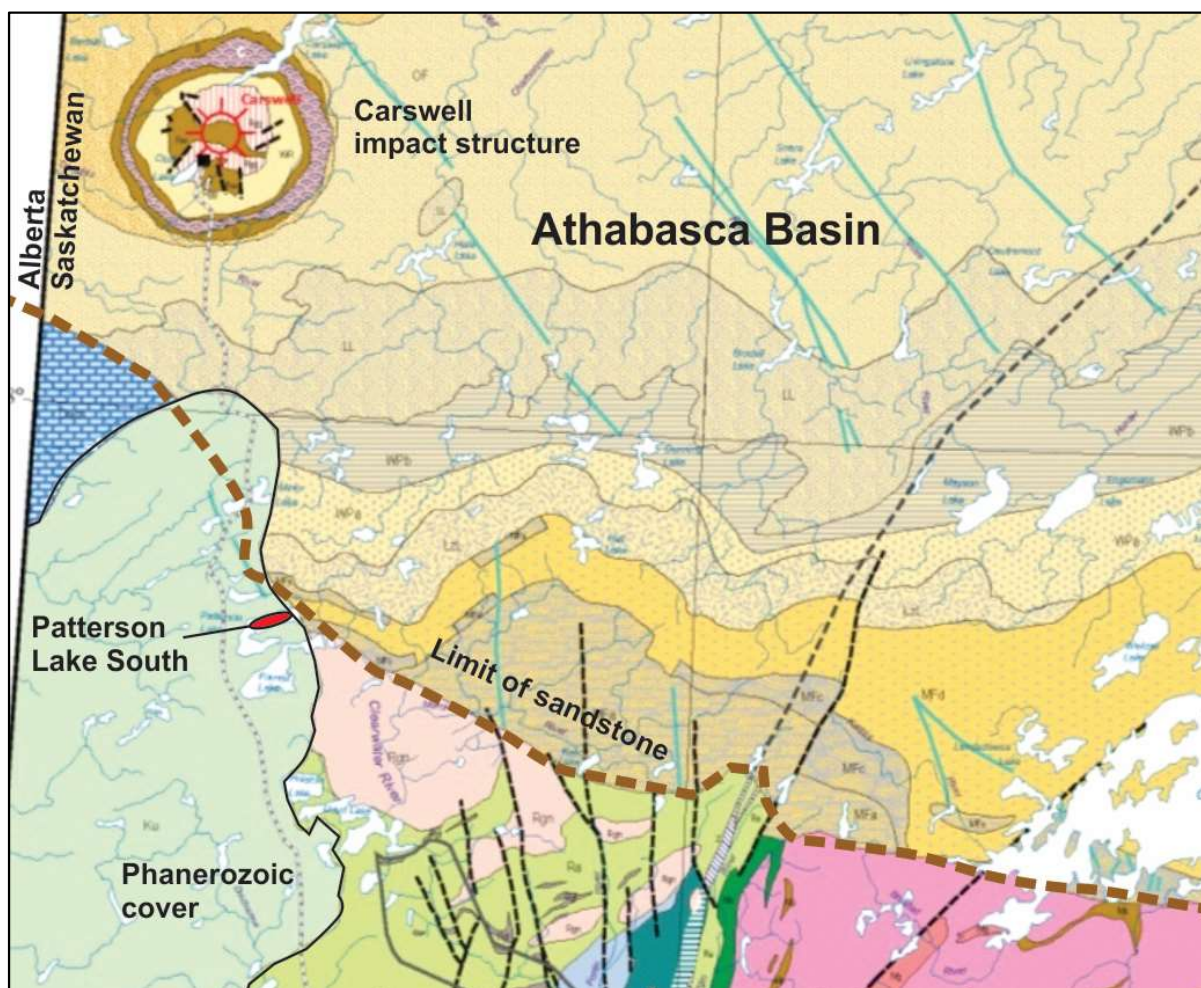


*FIG 8. Patterson Lake South location map. Modified from the Saskatchewan Geological Survey geology map.*

Early exploration (using alpha meters) identified an area of high radon and airborne radiometric values west of the Cluff Lake road in the Patterson Lake area in 1977. Several uraniferous pebbles were found by prospecting, but they were described as being ‘exotic’ and interpreted as not being locally derived (as explained to the author while working in the Cluff Lake camp in the 1980s). A few drill holes were located in the area, but the difficult ground conditions caused by approximately 70 m of overburden and another 70 m of incompetent Manville Formation overlying the basement rocks halted the programs after the drop in uranium prices in 1982. The area was left mostly unexplored for the next 35 years. The following description is summarized mostly from [13].

Exploration was restarted in 2007 with a mixture of airborne radiometric, magnetometer and EM surveys, followed by ground prospecting surveys and mapping of both outcrop and glacial material [13]. The radiometric spectrometer survey identified a 4 km by 1.4 km wide area of anomalous gamma radiation located about 2 km west of the Cluff Lake road. Follow-up prospecting in 2011 discovered numerous pitchblende boulders within the area, returning grades of up to 39.6% U<sub>3</sub>O<sub>8</sub> [ $\sim$ 33.5%U]. The boulders were soft, angular and of basement composition, suggesting that the source was within the property boundaries.

A seven-hole diamond drill program was started at the end of 2011 and intersected favourable geology, alteration and structure. In 2012, an airborne VTEM survey was completed, along with a DC resistivity survey (Fig. 9) and a SML (Small Moving Loop) TEM survey. A sixteen-hole winter drill program was completed with further intersections of favourable geology (graphite, pyrite and strong structure), alteration (hydrothermal haematite, chlorite and bleaching), and increased uranium geochemistry with values of up to 0.5 m of 0.1% U<sub>3</sub>O<sub>8</sub> [~0.085%U].

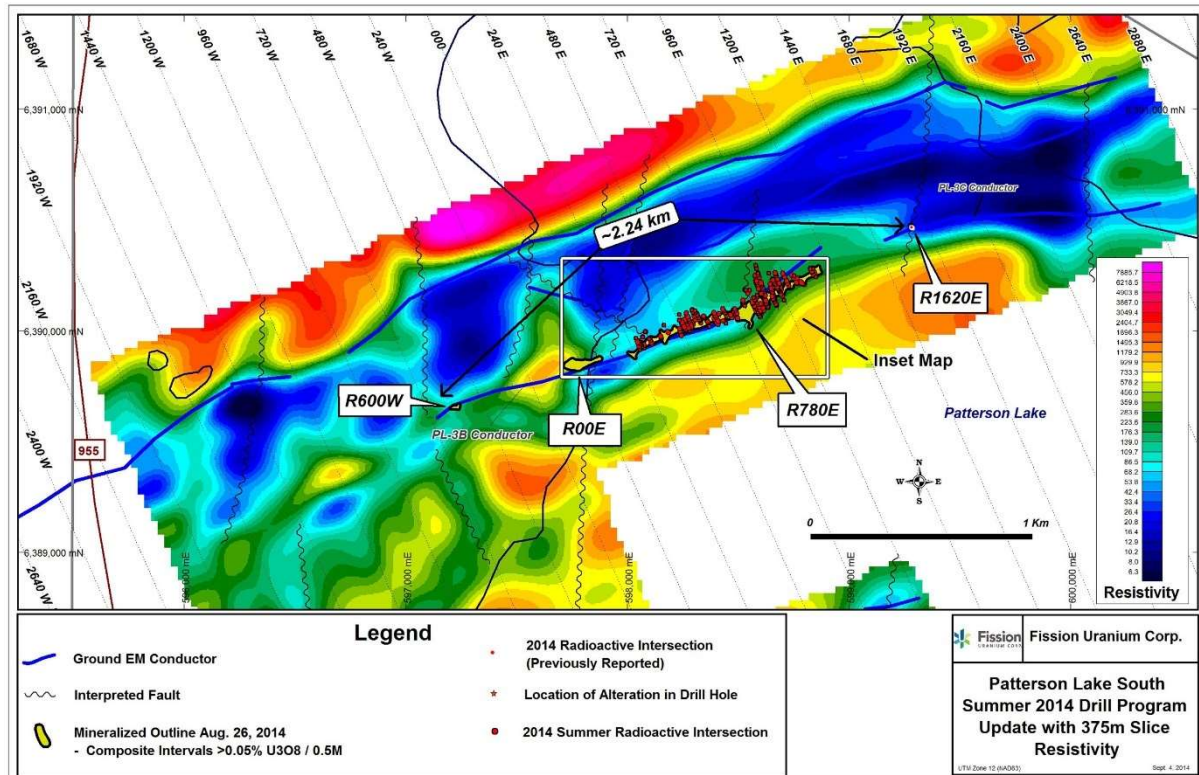


FIG 9. Plan map of the Patterson Lake South deposit with resistivity background [14].

A fall drill program in 2012 intersected mineralization in the four last holes, with 8.5 m of 1.07% U<sub>3</sub>O<sub>8</sub> [~0.91%U] in the discovery hole (PLS12-022) and up to 18 m of 1.78% U<sub>3</sub>O<sub>8</sub> [~1.51%U] in hole PLS12-024. Continued drilling in 2013 and 2014 has delineated mineralization in four distinct zones over a strike length of approximately 2.24 km. In summary, this deposit lies along an EM conductor, within a resistivity low and at the interpreted intersections of north-south structures with the main east-northeast trending conductive system. The mineralization lies wholly within the basement rocks and is located mostly within graphitic-pelitic metasediments that dip steeply to the south. This is bounded to the south by silicified psammopelitic gneisses and both units are located within a larger unit of psammopelitic gneisses.

A resource evaluation has been completed as of January 2015 with an estimate of 79.61 Mlbs U<sub>3</sub>O<sub>8</sub> indicated at 1.58% [~30 600 tU at ~1.34%U], and 25.884 Mlbs U<sub>3</sub>O<sub>8</sub> inferred at 1.3% using a cut-off grade of 0.1% U<sub>3</sub>O<sub>8</sub> [~9 960 tU at ~1.1% U, cut-off 0.085%U] [14]. This deposit has since been renamed the Triple R deposit.

## ACKNOWLEDGEMENTS

All information on the Griffith showings is original and is taken from Forum Uranium assessment reports, submitted by the author and Forum Uranium exploration crew. Information on the remainder of the deposits is a summary of public information: The Roughrider deposit is from Rio Tinto's website, from a PowerPoint presentation by A. McCready that was completed when the project was still operated by Hathor and a consultant's report (SRK). Information on the Phoenix deposit is taken from the Denison website, a 43–101 technical report (RPA) and from a PowerPoint presentation provided by L. Forand. Information on the Patterson Lake South deposit is from information provided on the Fission Uranium website, including a 43–101 report by A. Armitage and a 43–101 report by Roscoe Postle Associates Inc.

The author would like to acknowledge permission to present and write on the Griffith showings by Cameco Corp., AREVA Resources Canada Ltd. and by NexGen Energy Ltd., and acknowledge the efforts put into the discovery of new uranium mineralization by the exploration teams at Forum, Denison, Hathor (now Rio Tinto), and Fission (+ Alpha).

## REFERENCES

- [1] TONA, F., ALONSO, D., SVAB, M., “Geology and mineralization in the Carswell Structure — a general approach”, *The Carswell Structure Uranium Deposits, Saskatchewan* (LAINE, R., ALONSO, D., SVAB, M., Eds), Geological Association of Canada Special Paper **29** (1985).
- [2] GATZWEILER, R., SCHMELING, B., TAN, B., “Exploration of the Key Lake uranium deposits, Saskatchewan, Canada”, *Uranium Exploration Case Histories*, (Proc. Advisory Group Mtg, Vienna, 1979), IAEA and NEA (OECD) Panel proceedings series (STI/PUB/584) IAEA, Vienna (1981) 195–220.
- [3] HOEVE, J., SIBBALD, T., On the genesis of Rabbit Lake and other unconformity-type uranium deposits in northern Saskatchewan, Canada, *Economic Geology* **73** (1978) 1450–1473.
- [4] JEFFERSON, C.W., THOMAS, D.J., GANDHI, S.S., RAMAEKERS, P., DELANEY, G., BRISBIN, D., CUTTS, C., PORTELLA, P., OLSON, R.A., “Unconformity-associated uranium deposits of the Athabasca Basin, Saskatchewan and Alberta”, *EXTECH IV: Geology and Uranium EXploration TECHnology of the Proterozoic Athabasca Basin, Saskatchewan and Alberta*, (JEFFERSON, C.W., DELANY, G., Eds), Geological Survey of Canada Bulletin **588** (2007) 23–67.
- [5] MCGILL, B., MARLATT, J., MATTHEWS, R., SOPUCK, V., HOMENIUK, L., HUBRECHTSE, J., The P2 North uranium deposit Saskatchewan, Canada, *Exploration Mining Geology* **24** (1993) 321–331.
- [6] ROY, C., HALABURDA, J., THOMAS, D., HIRSEKORN, D., “Millennium deposit — basement-hosted derivative of the unconformity uranium model”, *Uranium Production and Raw Materials for the Nuclear Fuel Cycle: Supply and Demand, Economics, the Environment and Energy Security*, IAEA Proceedings Series, Vienna, Austria (2006) 111–121.
- [7] WHEATLEY, K., WILLIAMSON, A., TAN, B., HARMESON, B., Northwest Athabasca Project: 2013 Winter Exploration Assessment Report, submitted to the Saskatchewan Geological Survey (2014).
- [8] ALEXANDRE, P., KYSER, K., POLITO, P. “Geochronology of the Paleoproterozoic basement-hosted unconformity-type uranium deposits in northern Saskatchewan, Canada”, *Uranium Geochemistry 2003* (Proc. Int. Conf., 2003), (CUNY, M. Ed.), Unite Mixte de Recherche CNRS 7566 G2R, Université Henri Poincaré, Nancy, France (2003) 37–40.
- [9] HATHOR EXPLORATION LIMITED, Hathor Explorations’ Roughrider Zone: The new high-grade discovery in the Athabasca Basin, Canada. RRZ talk SGA (2009) (PowerPoint presentation).
- [10] SRK CONSULTING REPORT, Preliminary Economic Assessment Technical Report for the East and West Zones Roughrider Uranium Project, Saskatchewan (2011).

- [11] DENISON MINES LTD., The Discovery of the Phoenix: New High-Grade, Athabasca Basin Unconformity Uranium Deposits, Saskatchewan Canada (2010) (PowerPoint presentation).
- [12] ROSCOE, W., Technical Report on a Mineral Resource Estimate Update for the Phoenix Uranium Deposit, Wheeler River Project, Eastern Athabasca Basin, northern Saskatchewan, Canada by RPA Inc. for Denison Mines Corp. (2014).
- [13] ARMITAGE, A., Technical Report on the Patterson Lake South Property, Northern Saskatchewan, for Alpha Minerals Inc. 43-101 (2013) (from Fission Uranium website).
- [14] FISSION URANIUM website, <http://www.fissionuranium.com/>.

# URANIUM IN PHOSPHATE ROCKS AND FUTURE NUCLEAR POWER FLEETS

S. GABRIEL, A. BASCHWITZ, G. MATHONNIERE  
CEA, DEN/DANS/I-tésé,  
Gif sur Yvette, France

## Abstract

According to almost all forward-looking studies, the world's energy consumption will increase in the future decades. The effort to contain global warming makes it hard to exclude nuclear energy from the global energy mix. Current Light Water Reactors (LWR) burn fissile uranium (a natural, finite resource), whereas some future Generation IV reactors, as Sodium fast reactors (SFR), starting with an initial fissile load, will be capable of recycling their own plutonium and already-extracted depleted uranium. This makes them a feasible solution for the sustainable (a few thousand years) development of nuclear energy. Nonetheless, a sufficient quantity of plutonium is needed to start up an SFR, with the plutonium already being produced in LWR. The availability of natural uranium therefore has a direct impact on the capacity of the reactors (both LWR and SFR) that we can build. This paper discusses the correspondence between the resources and the nuclear power demand as estimated by various international organizations.

## 1. INTRODUCTION

The production of carbon-free energy is a key issue in the fight against global warming. Future energy demand scenarios elaborated by international organizations tend to be ambitious in terms of the installed nuclear power capacity.

Current Light Water Reactors (LWR) use thermal neutrons and burn uranium (a natural, finite resource), whereas some future Generation IV reactors using fast neutrons, such as Sodium Fast Reactors (SFR), (starting with an initial fissile load) will be capable of recycling their own plutonium and already-extracted depleted uranium (self-sufficient or breeder fast reactors). Nonetheless, a sufficient quantity of plutonium is needed to start up an SFR, with the plutonium already being produced in LWRs. The availability of uranium therefore has a direct impact on the capacity of the reactors that we can build. It is therefore important to have an accurate estimate of the available uranium resources in order to plan for the world's future nuclear reactor fleet.

This paper aims at examining the differences between the resources (uranium and plutonium) and the nuclear power demand as estimated by various international organizations, with an emphasis on uranium resources associated with phosphates and phosphoric acid production.

Uranium is currently produced from conventional sources. The estimated quantities of uranium evolve over time in relation to their rate of extraction and the discovery of new deposits. In addition to conventional resources, unconventional resources also exist. These resources are more uncertain both in terms of their quantities and the feasibility of recovering them.

After having reviewed current knowledge on conventional uranium resources, the first part of this paper focuses on unconventional resources such as those potentially recovered from phosphate rocks.

In line with these considerations and taking into account different assumptions on the limited quantities of available uranium, this paper examines the correspondence between the estimated resources and the forecast energy scenarios. The second part of this paper first examines the current type of light water reactors which 'burns' uranium, before examining a mixed fleet with both light water reactors and fast reactors which use plutonium and uranium-238.

## 2. PRIMARY SUPPLY OF URANIUM

### 2.1. Data sources

Since the mid-1960s, with the cooperation of their Member States, the OECD Nuclear Energy Agency (OECD/NEA) and the International Atomic Energy Agency (IAEA) have jointly updated their report which summarises the current status of uranium exploration, resources and production, as well as nuclear power plant requirements. This report is based on the declarations made by the Member States and on recommendations issued by the Uranium standing group of experts. Released in 2012, a recent version of this report, dubbed the ‘Red Book’, is titled “Uranium 2011: Resources, Production and Demand” [1]. This is the only easily accessible source of information on the worldwide uranium resources which is published every two years, and has been used as a source of information in this paper.

Resource assessments in the Red Book are divided into distinct categories that stand for different degrees of geological certainty concerning the indicated amounts. The resources are subdivided into ranges on a production cost basis, i.e. the cost of recovered uranium at the ore processing plant.

So-called ‘conventional resources’ are those that allow uranium to be recovered as a primary product, a co-product or a major by-product (e.g. in copper or gold mines). ‘Unconventional resources’ are very low-grade resources and those from which uranium is only recoverable as a minor by-product. Uranium is therefore a secondary product and its recovery is not subjected to most of extraction costs. The boundary between conventional and unconventional resources is not clear-cut, and rather exists as a kind of transition zone.

### 2.2. Conventional resources

Conventional resources consist of ‘identified resources’ (7.1 MtU recoverable at costs lower or equal to US \$260/kg U) and ‘undiscovered resources’ (10.4 MtU) [1]. The information on resources cited can change as uranium resource figures are dynamic and depend on the market prices. On the one hand, high prices give rise to optimistic forecasts, whereas low prices result in more pessimistic assessments. Nonetheless, market prices determine prospecting expenditure as well as cutoff grades and other parameters used in resource calculations. Therefore, uranium resource figures are a ‘snapshot’ of the available information on resources of economic interest; they are not an inventory of the total amount of recoverable uranium in the earth’s crust. When the market conditions are favourable and boost prospecting activities, additional discoveries may be expected, just as in past periods of heightened prospecting activity.

### 2.3. Unconventional resources

#### Seawater

Uranium is found in seawater in very small concentrations (3–4 µg/L [1]), which nonetheless represents almost 4.5 billion tonnes of uranium considering the volume of the oceans and seas. The very low concentration of uranium in seawater requires processing enormous volumes of water to recover significant quantities of uranium. Only processes using strong natural currents without pumping would be energetically viable.

A number of industrial extraction models have been developed since the 1950s. The extraction technology has been validated on a laboratory scale but there is currently no industrial or semi-industrial application. Most of the teams have stopped their research, though Japan hopes to reach a production cost of about US \$300/kgU [2]. This figure is based on a set of very optimistic assumptions and is probably unrealistic. New efforts are underway in the United States to assess recovery costs using improved new systems [3]. Even if it is technically possible to extract uranium from seawater, the current cost estimates are such that an industrial application is hardly possible except in the case of a major technical breakthrough.

## Phosphate rock deposits

Among unconventional resources, uranium from phosphate rocks might shelter the highest economic potential. According to the 2011 'Red Book' [1], 7 to 22 MtU could be recovered from the phosphate reserves which exceeds the amount of identified resources below US \$260/kgU, i.e. 7.1 MtU.

This section deals with uranium reserves contained in phosphate rocks, production capacities as a by-product of phosphoric acid and the potential cost as a primary product. Uncertainties about phosphate reserves and their uranium content have been taken into account (see also [4]).

### 3. ZOOM ON PHOSPHATE-BASED URANIUM RESOURCES

#### 3.1. Assessment of uranium reserves contained in phosphates

Phosphate rocks are a source of phosphorus, a vital element for plants and the raw material used mainly in the manufacture of fertilizers, but also for food supplements, drinks and others industrial products. Phosphate deposits may be sorted into two classes: igneous phosphate rocks (87%) and sedimentary phosphate rocks (13%) [5]. An assessment of available uranium reserves in phosphate deposits first requires accurately determining the phosphate reserves and then the content of uranium in these deposits.

##### 3.1.1. *Uncertainty of phosphate reserves*

For the phosphate reserves, various figures are provided by the US Geological Survey (USGS) [6]: 65 Gt, the International Fertilizer Development Center (IFDC) [7]: 60 Gt, and by a rather dated American report (De Voto & Steven, 1979) **Error! Reference source not found.**. This last report assumed 223 Gt of recoverable phosphate rocks, but this assessment was only for the USA and it went up to 293 Gt when it was extended to the "Free World". Obviously, the global figure of 65 Gt for the USGS is radically different from the 293 Gt and this latest figure is surely out of date and can be excluded.

##### 3.1.2. *Causes of the uncertainty on the available amount of uranium*

The uranium content in phosphate deposits varies within a deposit but also between different deposits. Several studies have reported an average concentration of uranium close to 100 ppm (parts per million) in phosphate rocks [5], [10–12]. However, the actual concentration is quite contrasted with considerable range scaling from 23 to 220 ppm. Igneous phosphates seemingly contain, on average, less uranium than sedimentary phosphates (59 instead of 96 ppm) but the concentration distribution is more heterogeneous and can reach 200 ppm or more; e.g. this had been found in some Brazilian areas.

Concerning the uranium reserves in phosphate rocks, several estimations are cited by the Red Book to reflect the uncertainties of all these estimations:

- 22 MtU based on the De Voto and Steven report **Error! Reference source not found.**;
- 9 MtU in an IAEA report [9];
- 7.3–7.6 MtU reported in 1965–1993 Red Books.

The 22 MtU from De Voto and Steven [8] is often given as the upper limit for the uranium contained in the phosphate reserves, but this estimation is the most questionable because it is based on a recoverable phosphate rock estimation of 223 Gt, a figure which is largely out of date.

Furthermore, the IAEA hosts a database called UDEPO **Error! Reference source not found.**, which references the majority of uranium deposits with a tonnage superior to 300 tonnes of uranium. The total uranium content is estimated to be 13.6 MtU.

Keeping in mind all the uncertainties on the phosphate rock reserves and their uranium concentration, the uranium recoverable from phosphate reserves is assessed in this paper. Assuming the global phosphate rock reserves are 65 Gt [6] and based on the assumption of an average 100 ppm uranium concentration in phosphate rocks [5], **Error! Reference source not found.**, 6.5 MtU is contained in phosphate rocks. It is very close to the last Red Book figures at 7.3–7.6 MtU, but different from the 9 MtU cited in the 2001 IAEA assessment [9]. Nonetheless, this figure ignores inevitable losses due to the imperfection of many processes. The uranium contained in phosphate rocks can only be recovered through the use of phosphoric acid which is a by-product of the wet phosphoric acid process and the first step to produce fertilizers. When the phosphate rocks are dissolved with sulphuric acid, it generates both phosphoric acid and phosphogypsum. The majority of uranium passes into the phosphoric acid (93%) and only a negligible portion goes into the phosphogypsum **Error! Reference source not found.**. In addition, only 72% of phosphate rocks are used to produce phosphoric acid **Error! Reference source not found.** [16]. Finally, the rate of uranium recovery from the phosphoric acid can reach 90% with the DEHPA-TOPO process **Error! Reference source not found.** Considering all these losses, we could expect to recover 3.9 MtU from the 6.5 MtU contained in the phosphate reserves. In fact, this figure could fall to 3.4 MtU when excluding igneous phosphates rocks (13% of the global phosphate rock reserves) which are known to obtain a lower uranium concentration and could be unprofitable.

### 3.2. Uranium recovery from phosphates

#### 3.2.1. The future of uranium as a primary product of phosphates

Despite a significant supply of 10.6 ktU/y, phosphates would not provide more than 17% of the current world demand (63.9 ktU/y [1]). To get around this limited production and meet the world demand at the same time, uranium should be recovered from phosphate rocks as a primary product. In this case, uranium could be considered to be bearing all the costs: extraction, phosphoric acid production and uranium recovery.

A study by the British Sulphur Consultants [19] describes the cost of a phosphoric acid plant with its breakdown. According to the BSC, the total production cost of one tonne of phosphoric acid reaches US \$203 (2003), actualised at US \$257 (2011) with the producer price index. To estimate the cost of uranium as a primary product, the assumptions below have been made:

- Phosphoric acid production: 500 kt/y;
- Average uranium concentration: 100 ppm (0.01%);
- Global recovery rate: 90%;
- Uranium extraction cost: us \$130 /kgU.

The first three of these assumptions lead to a uranium production of 45 tU/y. If uranium is a primary product of phosphates, it could be considered to bear both the production cost of phosphoric acid (US \$128.5 M) and the cost of recovery from the phosphoric acid (US \$5.85 M), i.e. US\$134.35 M; in which case **its unit cost (pessimist case) is around US \$3000/kgU** (in practice income from the sale of phosphoric acid would slightly reduce this unit cost). This magnitude is also in the report of De Voto and Steven **Error! Reference source not found.** which provides a cost range between US \$455–650 (1979)/kgU equivalent to US \$1162–1660 (2011)/kgU actualised for uranium as a primary product.

Regardless of the assumptions — more or less optimistic — the price of uranium recovered as a primary product of phosphates could be so high that it questions its contribution to nuclear electricity competitiveness.

#### 4. DEVELOPING NUCLEAR POWER WITH LIMITED URANIUM RESOURCES

In the energy sector, the demand must be estimated several years or even several decades in advance. The construction of power plants cannot be improvised because of the duration of the construction works and the time needed to obtain the various authorisations and licences. This is particularly true when it comes to planning the production of nuclear power.

Energy scenarios are only uncertain estimates of what the future electricity market may become; they are an estimate of what may happen based on current knowledge of how the world is evolving, on demographics, the GDP, the energy intensity, and political decisions made by the different countries. These scenarios can be used to analyse the construction of different types of reactor technologies and to determine the related requirements in resources (uranium and plutonium).

This paper aims at assessing the impact of limited quantities of available uranium on these scenarios. Case studies are used to illustrate the uranium requirements according to the different global nuclear power growth scenarios and to stress the fact that more resource-saving reactor technologies must be deployed to ensure the sustainable development of the industry.

##### 4.1. Energy scenarios

For several reasons explained in **Error! Reference source not found.**, we have chosen to work with the IIASA scenarios from 1998 for this study (see FIG. 1 using data from IIASA [21]). These scenarios consider a strong increase in the world demand in primary energy. Even if the share of nuclear power is less than 20% of the total, it supposes a quite significant increase in the installed nuclear power capacity.

**Scenario A2** is a strong global growth scenario, of around 2.7% per year, with a short-term preference for the use of oil and gas resources. Nuclear energy accounts for 4% of world energy demand in 2050 and 21% in 2100.

**Scenario A3** is also a strong global growth scenario with an earlier, more gradual introduction of nuclear energy than in scenario A2; nuclear energy represents around 11% of world energy demand in 2050 and 22% in 2100.

**Scenario B** is a business as usual world growth scenario during the 21st century (around 2% per year).

**Scenario C2** corresponds to a strong will to protect the environment against global warming. Nuclear energy represents around 12% of world demand for primary energy in 2050; this is close to twice as much as it represents today.

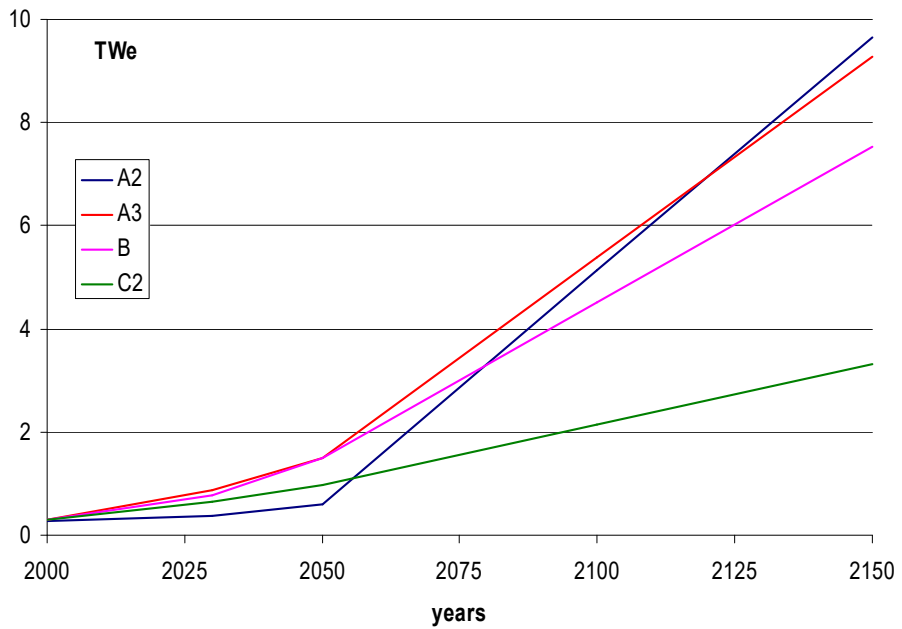


*FIG. 1. IIASA scenarios of requested nuclear power (based on Error! Reference source not found.).*

#### 4.2. Reactor technologies

This study takes into consideration Pressurised Water Reactors (PWR), representative of the LWR currently operating throughout the world today, European Pressurised (or Evolutionary Power) Reactors (EPR), representative of what is currently being built or scheduled for construction throughout the world and Fast Reactors (FR) which use plutonium as fissile material (see also Error! Reference source not found.).

#### 4.3. Limits of available uranium reserves

As mentioned earlier in this paper, it turns out that the unconventional uranium resources recovered from phosphate rocks are not as significant as first estimated, and that the recovery costs could prove to be very high. Actually, it is not possible to say how much uranium might be available for mining in the coming years. So we have chosen four limits of available uranium resources as hypotheses that can be used to make a sensitivity analysis.

- 7 Mt, which represents the quantity of identified conventional uranium resources;
- 21 Mt, which comprises 17 Mt of both identified and undiscovered conventional uranium resources, together with 4 Mt from phosphate rocks;
- 39 Mt, which comprises 17 Mt of both identified and undiscovered conventional uranium resources, together with 22 Mt from phosphate rocks (former optimistic estimate);
- 90 Mt, which takes into account the hope that mining exploration will find substantial new resources; this Figure is a case study rather than an evaluation.

We do not consider uranium extracted from seawater because of its expense, would could render LWRs uncompetitive compared to other power plants.

The quantity of uranium consumed during the lifetime of the reactor is called ‘engaged uranium’. An EPR is only built if there is some foresight on the availability of uranium resources. In modelling, when the consumed and engaged uranium exceeds one of the above-mentioned limits, it will be impossible to build a new reactor requiring uranium and to provide uranium for all its life expectancy (60 years). The

only reactors that would be built once this limit has been reached are fast reactors that operate with plutonium. Considering that plutonium has to be produced and is not available in unlimited quantities, it will become possible one day that we cannot build enough plutonium-producing reactors and thus no longer match supply to demand for fast reactors.

#### 4.4. Exclusive deployment of EPRs

Our first calculations are based on the assumption that only EPRs can be built and that fast reactors will never become available. FIG. 2 illustrates the demand and production of nuclear power (in TWh) for the A3 and C2 scenarios.

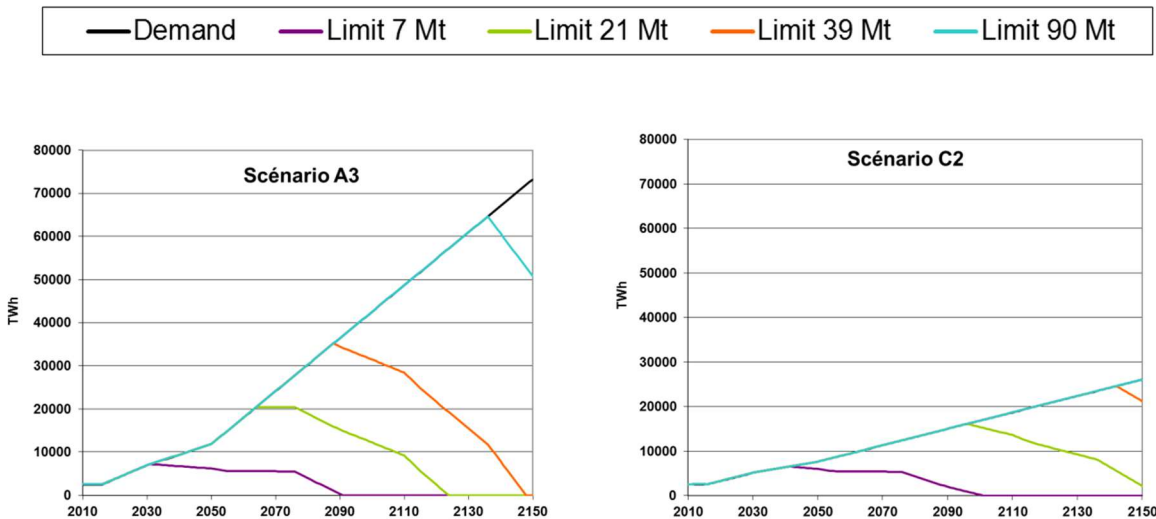


FIG. 2. Light water reactors only — Demand and power production according to the natural uranium limit (TWh).

When no other reactor can be built for lack of uranium, the installed power starts to drop and it no longer meets demand since the reactors at the end of their lifetime cannot be replaced. The very ambitious A3 scenario shows that EPRs do not meet the entire nuclear power demand even with a uranium limit of 90 Mt (as noted above, this excludes possible extraction from seawater). With only 7 Mt available, the problem of a shortage of resources arises in less than 20 years. The C2 scenario represents the slowest growth of nuclear power with less pressure on the uranium resources. Nonetheless, only the uranium limit of 90 Mt will meet the nuclear power demand up to 2150.

With 21 Mt, the uranium shortage would arise in the 2060s for the three scenarios with the highest demand (A2, A3 and B), i.e. between 25 and 30 years earlier than with a 39 Mt limit. For the C2 scenario, the uranium shortage arises at the end of the century with 21 Mt, and 45 years later with 39 Mt. These results stress the need to develop fast reactors in order to ensure the sustainable future of nuclear power.

#### 4.5. Possible deployment of FRs from 2040

From 2040, we assume in our calculations that building fast reactors (self-sufficient reactors or breeder reactors with a breeding gain (BG) of 0.3 if necessary) will be given a top priority. We suppose that all the spent fuel can be reprocessed and that the reprocessing capacities are adapted to needs. There is no geopolitical consideration; we take the world as a whole unit which of course is a hypothetical case. However, if there is an insufficient stock of available plutonium (which we demonstrate in [22]) but still a sufficient supply of uranium, EPRs will be built. If both uranium and plutonium are lacking, no reactors would be built and it will be impossible to meet the demand. FIG. 3 shows the possible nuclear power

production for the A3 and C2 scenarios based on the availability of plutonium and the uranium limit taken into consideration (PWR and FR production).

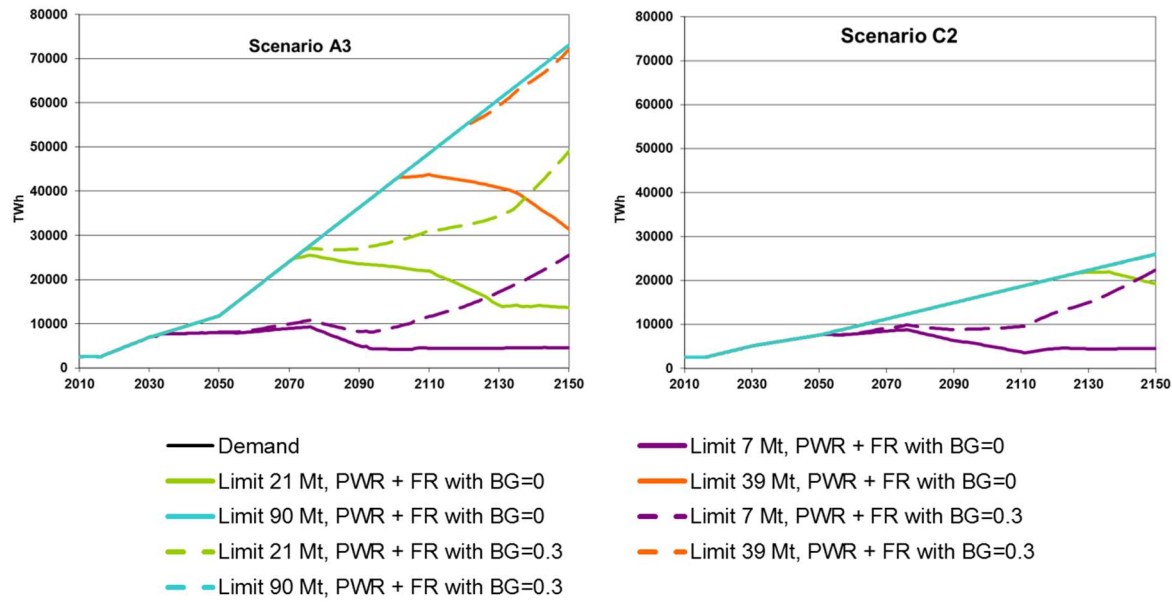


FIG. 3. Light water reactors and fast reactors – Demand and power production according to the natural uranium limit (TWh).

For the C2 scenario with limited nuclear power growth, only the very restrictive limit of 7 Mt curbs the deployment of nuclear energy. Fast reactors with a breeding gain are necessary when the uranium limit is 21 Mt. Considering the availability of plutonium and the limit in uranium, it is not possible to build as many EPRs and FRs as intended in the other scenarios. It can be seen that a stable installed nuclear power capacity is reached with fast reactors when the latter are self-sufficient. Globally, 1 million tonnes of natural uranium used in PWRs would make it possible to produce enough plutonium to generate 85 GWe using fast reactors. The quantity of plutonium is not only distributed in the fast reactor cores, but also in the fuel cycle facilities. Breeder reactors would make it possible to increase the total of installed nuclear power, though with certain uranium limits, we still remain below the estimated power requirements.

## 5. CONCLUSION

The large-scale deployment of nuclear reactors on an international level will require more uranium in the more-or-less long term. Knowledge of the uranium resources is a prerequisite to studying nuclear power deployment scenarios. These resources are nevertheless ascertained with more or less uncertainty in terms of costs and quantities. Their estimates evolve as mining exploration progresses or as the economic conditions change.

Recovering uranium from seawater would ensure a practically infinite resource of nuclear fuel, but its technical and economic feasibility have yet to be confirmed.

The largely quoted estimate of 22 Mt of uranium recovered for phosphate rocks can be seriously downscaled. Based on our current knowledge of phosphate resources, 4 Mt of recoverable uranium already seems to be an upper bound value. The recovery of uranium from phosphate rocks will only ensure a limited resource.

Mineral exploration is therefore essential in the hope of discovering new sources of uranium. It is also essential to examine how we can optimise the use of uranium. This raises the question of deploying fast reactors.

Given the various categories of resources and the uncertainties on each of them, it is wiser to take into account several different estimates of the available uranium quantities when studying global scenarios of the nuclear power demand since they reflect a more or less optimistic view of our future resources.

Considering light water reactors exclusively, 7 Mt and 21 Mt of uranium are required for the least ambitious C2 scenario up to 2042 and 2097 respectively when it will no longer be possible to build EPRs. However, it is possible to reach the end of the century with 39 Mt.

For the three other scenarios with higher demand, 39 Mt would allow for the construction of PWRs up to the end of the century, whereas construction would come to an end 20 or 30 years earlier with only 21 Mt.

The deployment of fast reactors and the recycling of materials therefore prove to be necessary, which is all the more true for scenarios with high growth. Their deployment is nonetheless restricted by the availability of plutonium and they do not meet the energy demand in all the scenarios. Self-sufficient reactors would make it possible, it generates a stable installed power capacity equivalent to about 85 GWe per million tonnes of available uranium. Breeder reactors would significantly improve the situation since they would enable the nuclear fleet to continue its development. In any case, fast reactors make it possible to at least double the nuclear power production by 2150.

## REFERENCES

- [1] OECD NUCLEAR ENERGY AGENCY, INTERNATIONAL ATOMIC ENERGY AGENCY, Uranium 2011: Resources, Production and Demand, OECD, Paris (2012).
- [2] TAMADA, M., Current status of technology for collection of uranium from seawater, Erice Seminar (2009),  
[http://nuclearinfo.net/twiki/pub/Nuclearpower/WebHomeAvailabilityOfUsableUranium/2009\\_Tamada.pdf](http://nuclearinfo.net/twiki/pub/Nuclearpower/WebHomeAvailabilityOfUsableUranium/2009_Tamada.pdf).
- [3] AMERICAN CHEMICAL SOCIETY, Advances in decades-old dream of mining seawater for uranium (2012), [http://www.eurekalert.org/pub\\_releases/2012-08/acs-aid072612.php](http://www.eurekalert.org/pub_releases/2012-08/acs-aid072612.php).
- [4] GABRIEL, S., BASCHWITZ, A., MATHONNIÈRE, G., FIZAINE, F., ELEOUET, T., Building future nuclear power fleets: the available uranium resources constraint, *Resources Policy* **38** 4 (2013) 458–469.
- [5] VAN KAUWENBERGH, S.J., Cadmium and other minor elements in world resources of phosphates rocks. *The Fertilizer Society, Proceeding* **400** (1997).
- [6] UNITED STATES GEOLOGICAL SURVEY, USGS Database of phosphates, Mineral commodity summaries, (2011),  
[http://minerals.usgs.gov/minerals/pubs/commodity/phosphate\\_rock/index.html#mcs](http://minerals.usgs.gov/minerals/pubs/commodity/phosphate_rock/index.html#mcs) accessed on January 2012.
- [7] INTERNATIONAL FERTILIZER DEVELOPMENT CENTER, IFDC Report Indicates Adequate Phosphorus Resources Available to Meet Global Food Demands 2011, [http://www.ifdc.org/media\\_center/press\\_releases/september\\_2010/ifdc\\_report\\_indicates\\_adequate\\_phosphorus\\_resource](http://www.ifdc.org/media_center/press_releases/september_2010/ifdc_report_indicates_adequate_phosphorus_resource) accessed on January 2015.
- [8] DE VOTO, R.H., STEVEN, D.N. (Eds), Uraniferous phosphate resources and technology and economics of uranium recovery from phosphate resources, United States and Free World. US DOE Report GJBX-110, 3 volumes, Earth Sciences Inc, Golden, CO (1979).
- [9] INTERNATIONAL ATOMIC ENERGY AGENCY, Analysis of Uranium supply to 2050, STI/PUB/1104, IAEA, Vienna (2001).
- [10] KENNEDY, R.H., Recovery of uranium from low-grade sandstone ores and phosphate rock, Proc. Processing of low-grade uranium ores, IAEA Panel Proc. Series, IAEA, Vienna (1967) 216–225.
- [11] KRATZ, S., SCHNUG, E., “Rock phosphates and P fertilizers as sources of uranium contamination in agricultural soils”, *Uranium in the Environment* (MERKEL, B.J., HASCHE-BERGER, A., Eds), Springer, (2006) 57–67.

- [12] BARTHEL, F.H., "Thorium and unconventional uranium resources", Fissile Material Management Strategies for Sustainable Nuclear Energy, Proc. Tech. Mtg, Vienna, STI/PUB/1288, IAEA, Vienna (2007) 199-215.
- [13] INTERNATIONAL ATOMIC ENERGY AGENCY, About UDEPO, <https://infcis.iaea.org/UDEPO/About.cshtml> (accessed on January 2015).
- [14] GUIDA, J.W., ROYSTER, D., Phosphoric Acid and Uranium Recovery, Arab Fertilizer Association, November 10–12 (2008).
- [15] VAN KAUWENBERGH, S.J., World Phosphate Rock Reserves and Resources. Presented at Center for Strategic and International Studies, 22 September 2010 (2010), [http://csis.org/files/attachments/100922\\_Kauwenbergh\\_Presentation\\_0.pdf](http://csis.org/files/attachments/100922_Kauwenbergh_Presentation_0.pdf) (accessed on June 2015).
- [16] BIRKY, B., HILTON, J., MOUSSAID, M., STANA, R., "Uranium and phosphorus: a cooperative game for critical elements in energy and food security", presented at IAEA Tech. Mtg. on Uranium Recovery from Unconventional Resources, Vienna 2009.
- [17] MCCARN, D.W. Uranium by-product recovery from phosphoric acid production: methodology and cost, IPI consulting, (1998).
- [18] WALTERS, M., BAROODY, T., BERRY, W. "Technologies for uranium recovery from phosphoric acid", Annual International Phosphate Fertilizer & Sulfuric Acid Techno Conference (AIChE) (June 2008), <http://www.aiche-cf.org/Clearwater/2008/Paper1/8.1.4.pdf>.
- [19] BRITISH SULPHUR CONSULTANTS, The competitiveness of phosphate fertilizer producers to 2020: coping with changing production costs, resource availability and market structures, CRU group (2003).
- [20] GABRIEL, S., BASCHWITZ, A., MATHONNIÈRE, G., ELEQUET, T., FIZAINE, F., A critical assessment of global uranium resources, including uranium in phosphate rocks, and the possible impact of uranium shortages on nuclear power fleets, Annals of Nuclear Energy **58** (2013) 213–220
- [21] INTERNATIONAL INSTITUTE FOR APPLIED SYSTEM ANALYSIS, GGI Scenario Database (accessed January 2015), <http://www.iiasa.ac.at/web-apps/ggi/GgiDb/dsd?Action=htmlpage&page=series>.
- [22] BASCHWITZ, A., LOAËC, C., FOURNIER, J., DELPECH, M., LEGÉE, F., "Long term prospective on the electronuclear fleet: from GEN II to GEN IV", Proc. of the GLOBAL 2009 Congress, Paris, (2009).

# URANIUM FROM COAL ASH: RESOURCE ASSESSMENT AND OUTLOOK ON PRODUCTION CAPACITIES

A. MONNET, S. GABRIEL

I-tésé / Nuclear Energy Division,  
CEA (French Alternative Energies and Atomic Energy Commission),  
Gif-sur-Yvette, France

## Abstract

Sixty years after first investigations on producing uranium from coal ash, this uranium source of supply has regained a strong interest. While the world consumption of coal keeps rising, several papers tackle radiological health issues. Besides, uranium-bearing coal deposits are sometimes mentioned as a potential source of supply for the nuclear fuel. While uranium production from coal ash has remained sub-economic for decades, the emergence of new projects begs the questions again. How much coal ash do we have? Are the coal deposits all rich in uranium? Can we produce them all? The present study gives an estimation of both the world resources and the production capacities of uranium as a by-product of coal. It shows that there are significant quantities of technically accessible uranium in the world coal reserves. Yet, most of these quantities correspond to very low-grade ores. Potential reserves should be less than 200 ktU. In terms of production capacities, a realistic potential should not exceed 700 tU/year, that is approximately 1% of current needs.

## 1. INTRODUCTION

Uranium as a by-product of coal used to remain sub-commercial but recent news releases mention the promising pre-feasibility achievements of Sparton Resources Inc. [1]. This Canadian company and its Australian competitor Wildhorse Energy Ltd [2] could start operating the first ash leaching plants in over 40 years. Sparton announced that the Yunnan Chinese region could produce 150 tU a year from three coal-fired power plants [1]. Although these three coal power plants could almost be enough to supply a nuclear one, it is hard to tell how many of the 2300 world coal power stations could provide uranium.

IAEA provides a large database on uranium deposits called UDEPO [3]. This database gives a resource assessment on most known deposits. It is based on available information and may not always be JORC/NI 43–101 compliant. The database classifies the deposits based on their geological type. For instance, if one is interested in the world known uranium resources associated with coal, so called ‘lignite-coal’ category, these are said to represent up to 400 ktU at grades above 400 ppm. These are only the most promising deposits. That is why UDEPO provides a good tool to follow rising projects in which uranium can be produced from coal as a primary product or a co-product. Though, if one wants to assess resources in a prospective approach, the whole resource must be considered (meaning also uranium that can potentially be produced as a by-product, with grades potentially below 400 ppm). For these reasons, our study focuses on uranium production from coal ash, that is when uranium is considered as a by-product of coal. As for any by-product, the production capacities are limited by the primary product, which is why our study also focuses on production limits when producing uranium from coal ash.

Besides, in the ‘lignite-coal’ category, UDEPO reports quantities of uranium that may not always be in the coal itself. Indeed, in some deposits, uranium lies in sandstone layers, in between the coal layers (case of the Springbok Flats and Letlhakane deposits [4, 5]). For these reasons, this study is rather based on coal databases (mainly USGS [6] and Enerdata [7]) instead of uranium databases.

Section 2 of this paper summarizes the main actual and historical issues and challenges about uranium production from coal ash. Section 3 presents the key parameters in detail. Section 4 describes the methodology of assessing the whole quantities of uranium in the world coal resources. After introducing technical and economic constraints, it leads to potential reserves assessment. Based on the same methodology, Section 5 presents additional results in terms of production capacities.

## 2. CONTEXTUAL BACKGROUND

### 2.1. Past production

Uranium has already been produced from coal ash in the past. It is important to notice that it occurred in very specific historical situations, mostly due to the Cold War context. For instance, the United States produced 380 tU in the 1960s by milling coal-ash [8] (and more than 1000 tU until 1995 [9]). Yet, at that time, uranium was not a by-product of coal: no electricity was produced, there was no coal powerplant, and brown coals were just burnt in place to recover the ashes. The grades were probably rather high (0.1 to 10%U according to Hurst [8]) and at the same time the United States produced 17 times more uranium from phosphates [9].

Finally, two other countries are known to have produced uranium from coal in the past, but there is less information about these projects (2 sites in China and 3700 tU produced in East Germany from 1947 to 1955 and from 1968 to 1989[10]).

### 2.2. Issues and challenges

Before assessing the resources, it is important to stress some strong implications of uranium production from coal ash. These are mainly strategic challenges.

#### 2.2.1. Strategic challenges

First, we should wonder if coal-ash can be considered as a significant source of uranium for the future. As stated in the previous paragraph, it produced small amounts of uranium when demand was high, but for the 21st century, the question is: can it be significant in case of new tensions on global supply?

The second important challenge is for China and other big coal producers and big uranium consumers (United States or Russia for instance). China is the world's first producer of coal with approximately 50% of the total global production. Chinese uranium demand and their imports are already growing. In 2010, the uranium needs were up to 3900 tU while domestic production was about 1300 tU [11]. Plus, the challenge there is not only to increase domestic production but also how fast they can move on to higher production. The equation is: in 2030, demand could be up to 16 000 tU/year [11], while a typical mine (about 1000 tU/year) needs around 10 years to be developed and start producing. As a comparison, ash leaching plants (about 150 tU/year) are said to be operational in 3 years [9]. They could probably take advantage of this fast lead time, as did the in-situ leaching facilities in Kazakhstan.

#### 2.2.2. Health and environmental issues

To finish with issues and challenges, there are also important environmental and health concerns when dealing with milling coal ash. This study does not cover them (the reader can refer to [12, 13] among others) but it is interesting to mention that milling coal ash can also have environmental benefits. Though, we do not believe that these benefits can be a trigger to start a massive uranium production. Strategic challenges would certainly be stronger incentives. In fact, coal ash milling roughly faces the same issues as conventional mining and we expect it to have the same Health, Safety and Environment (HSE) constraints as any other new project.

### 2.3. Milling process flow

As illustrated on Figure 1, the milling process of ash leaching is based on two ideas.

First, unless coals have really significant uranium grades (similar to conventional ores), it is more interesting to mill the ashes rather than feed coal. The reason is simple: uranium is concentrated in the ashes when the coal is burnt and as a result, grades can be up to 10 times higher in the ashes [12]. This way, a feed coal at 40 ppm may sometimes be enough to provide ash ores at 400 ppm.

The second idea is to use the flue gases from the thermal coal powerplants. The more sulphur dioxide the gases contain, the better their leach reagent properties. Thus, the recovery of sulphuric acid from flue gases can reduce the global reagent consumption. In Section 4.3.1, we will see that this recovery process is often necessary to reach commercial feasibility.

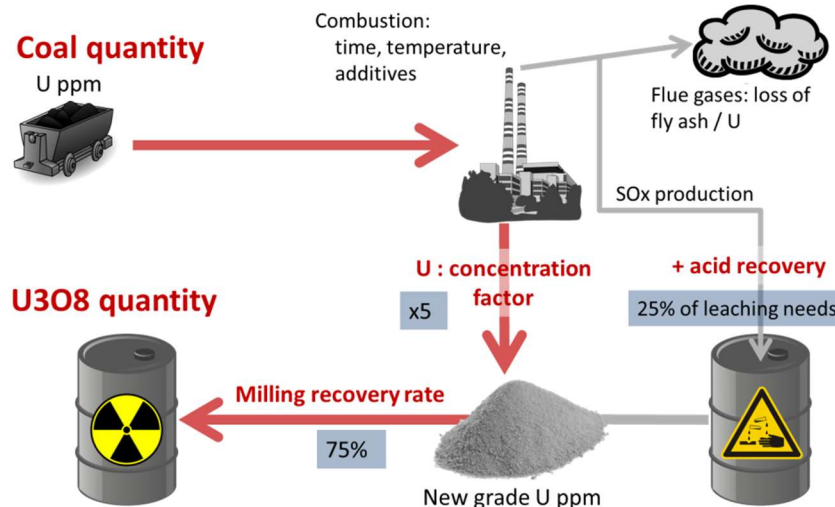


FIG. 4. Process flow and key parameters of milling coal ash for uranium recovery.

### 3. KEY PARAMETERS

This paragraph gives a review of ash-leaching key parameters. These are either process parameters, as presented in Section 3.1 or bottlenecks at a global level, as presented in Section 3.2.

#### 3.1. Process parameters

The first important parameter in the process flow is the **uranium grade** of feed coal. The assumptions we make for this parameter are detailed in Section 4.1. As stated before, uranium is concentrated in the ashes when the coal is burnt. This **concentration ratio** is the second most important parameter. The review of literature shows that it could vary from 2 to 10 [1, 8, 12, 14, 15]. For the purposes of this study, a mean value of 5 is considered as a first approximation. But we should keep in mind that the concentration ratio depends on various parameters, such as combustion conditions or combustion additives. Though, we have not managed to establish a clear relation between these factors.

The **milling recovery rate** is obviously another important parameter. It greatly depends on coal quality and acid consumption but we assume it to be 75%. Our review of literature makes us believe it is a good first approximate value [8, 16].

As part of the other key parameters, we assume the loss of uranium through the flue gases to be negligible, which is verified for modern powerplants (1% losses according to [13]). Though, the most important about flue gases is the production of SO<sub>x</sub> and the **possibility to recover sulphuric acid**. We estimate this potential up to 25% of the final leaching reagent consumption. Yet, this is an optimistic potential, and depending on coal quality, it can be much lower. A focus needs to be presented on this estimation since the literature gives no single approach.

This study includes an estimation of the acid savings based on real samples from literature: 4 from Turkey [15], 2 from Spain and Croatia [14] and 12 from United States [8].

All samples have their uranium grades  $U_{ppm}$  and their sulphur contents  $S$  reported (both for feed coal and coal ash). Final uranium recovery rate  $\rho$  and final acid consumption  $Real\ consumption_{H_2SO_4}$  (in kg H<sub>2</sub>SO<sub>4</sub> per kg of recovered U) are also input experimental data. Provided that a method is available to estimate the quantity of sulphur  $S_{recov}$  (in kg S per kg of burnt coal) that can be recovered, the percentage of savings can be computed as follow:

$$\text{Savings (\%)} = \frac{S_{recov} \times (M_{H_2SO_4}/M_S) \times \frac{1}{(U_{ppm,in\ coal} \times \rho)}}{Real\ consumption_{H_2SO_4}}$$

Two methods have been reviewed to estimate the sulphur recovery potential and finally our own estimation has been defined. The first method comes from “Les Techniques de l’Ingénieur” [17]. A massic 80 to 95% (we assume 85%) of sulphur present in coal is said to be transferred into the flue gases. We assume these quantities to be fully recovered as sulphuric acid while the experimental conversion rates are said to be 95% for regenerative fume treatments (as opposed to treatment processes which produce solid waste or gypsum). We derive:

$$S_{recov} = 0.85 \times S_{in\ coal}$$

The second method corresponds to Hurst’s estimation [8]: the average savings would be 300 lbs (136 kg) of sulphuric acid per ton of coal ash. Thus, in this case, it was not necessary to compute  $S_{recov}$  and we directly computed the saving percentage by considering this same mean value for every sample.

Our own estimation is based on the mass balance of element sulphur: the quantity of sulphur that can be recovered is the difference between the sulphur content of feed coal and the sulphur content of ashes. The uranium element is almost completely transferred to the ashes. Therefore, the concentration ratio that is computed from input experimental data corresponds to the loss of mass between the feed coal state and the coal ash state. Thus,  $S_{recov}$  can be derived as:

$$S_{recov} = \text{Max} \left( 0; S_{in\ coal} - S_{in\ ash} \times \frac{U_{ppm,in\ coal}}{U_{ppm,in\ ash}} \right)$$

Finally, the results of these estimations are summarized in Table I. It turns out that potential savings seem much lower than estimated by Hurst. Their great variability is the second conclusion even though it is not meaningful in method 2 (since it uses Hurst’s mean estimation instead of the sulphur content from experimental data).

TABLE I. ESTIMATIONS OF REAGENT SAVINGS FROM SULPHURIC ACID RECOVERY

| Method                       | Average percentage of savings<br>on final acid consuption | Max/min percentage of savings<br>on final leaching needs |
|------------------------------|---|--|
| 1. Techniques de l’ingénieur | 6%  | From <1% to 23%  |
| 2. Hurst’s mean estimation   | 49%   | From <1% to >99%   |
| 3. Mass balance estimation   | 4%  | From <1% to 25%  |

### 3.2. Global parameters

At the global supply level, there are other important parameters, which include:

- The reserves of coal;

- The coal consumption in energy sector (this one is because when the coal is used for coking, the residues become refractory and therefore much more difficult to mill for uranium recovery);
- The part of coal-ash that remains available for milling (this one is because a percentage from 40% in the us to 66% in china is re-used in the building industry [18, 19]);
- The capital costs, the operating costs and the cut-off grade compared with other types of uranium production.

## 4. RESOURCE ASSESSMENT

This Section aims to present the first results of our resource assessment. At first, the whole uranium quantities which are contained in coal resources is considered. This is the first step of the procedure that is followed to lead to technically accessible. Sections 4.1 to 4.3 also aim at describing this step-by-step procedure for a better understanding of the production capacities assessment (Section 5) which is based on the same method.

### 4.1. Global uranium quantities

#### 4.1.1. *From coal resources*

Let's start with total uranium quantities. To assess this resource category, assumptions on global coal reserves and their mean grade in uranium are necessary. The references on which these assumptions are based are mainly:

- Enerdata [7] and German Federal Institute for Geosciences [20] for the coal reserves;
- USGS World Coal Quality Inventory Database [6] and Yang [21] for the uranium grades.

The USGS database shows a significant difference between the mean grade of brown coal samples and higher quality coal samples. This database gathers more than a thousand coal samples from many countries. Yet, it misses some information from some big coal producers such as Russia, Germany or Australia. Besides, the literature gives no clue that uranium grade is really correlated with coal quality and another USGS database [22] shows that lignite and other coals have the same mean grade based on US samples. That is why we present results where coal and lignite are considered together but also separately.

From these data, the total uranium quantities can be derived by multiplying the coal resources by their uranium mean grade. The main results are presented below:

- There would be around 4–5 MtU in the 2012 world coal reserves and up to 1 MtU in the Chinese coal reserves (Table II);
- If we consider coal resources, including undiscovered resources, the corresponding uranium quantities can go up to 100 MtU (Table III). Though, this figure is not meaningful in terms of prospective.

TABLE II. ASSESSMENT OF URANIUM QUANTITIES IN THE WORLD AND CHINESE COAL AND LIGNITE RESERVES (2012)

| Primary product                                      | World          |                |                | China            |
|--|----------------|----------------|----------------|------------------|
|  | Coal           | Lignite        | Coal + lignite |                  |
| Reserves (Gt)  | 690–750        | 150–280        | 840–1030       | 115–418          |
| Mean grade in U (ppm)                                | 3.4            | 12.0           | 4.7            | 2.31             |
| <b>Uranium quantities (MtU)</b>                      | <b>2.4–2.6</b> | <b>1.8–3.4</b> | <b>4.0–4.9</b> | <b>0.26–0.97</b> |
| Technically accessible resources, 75% recovery (MtU) | 1.8–2.0        | 1.4–2.5        | 3.0–3.7        | 0.20–0.70        |
| Percentage > 40 ppm                                  | 1%             | 7%             | 2%             | –                |
| <b>Potential reserves (ktU)</b>                      | <b>15–20</b>   | <b>95–180</b>  | <b>60–70</b>   | –                |

TABLE III. ASSESSMENT OF URANIUM QUANTITIES IN THE WORLD COAL AND LIGNITE ADDITIONAL RESOURCES

| Primary product                 | Coal            | Lignite         | Coal + lignite   |
|---------------------------------|-----------------|-----------------|------------------|
| Additional resources (Gt)       | 610–17 120      | 170–4 150       | 780–21 270       |
| Mean grade in U (ppm)           | 3.4 ppm         | 12.0 ppm        | 4.7 ppm          |
| <b>Uranium quantities (MtU)</b> | <b>2.1–58.2</b> | <b>2.0–49.8</b> | <b>3.6–100.0</b> |

#### 4.1.2. *From coal-ash piles*

Not only accessible from in-place coal resources, uranium is also concentrated in existing coal-ash piles. Since the 1970s, around 150 Gt of coal have been burnt in the energy sector [4]. Taking into account the re-use rate of coal-ash in the US over the period 1970–2010 **Error! Reference source not found.** (and assuming the concentration factor equals 5), there would be around 21 Gt of coal ashes that could have been stored in piles around the world since the 1970s.

To estimate the amount of uranium concentrated in these stock piles, the same coal grades are considered and converted to ash grade through the concentration factor. Based on these assumptions, there could be from 190 to 500 ktU in the existing coal-ash piles. This amount is actually rather low compared with the amount of uranium remaining in coal reserves.

This calculation introduces additional uncertainties compared with the first estimation from coal reserves:

- The main additional uncertainty deals with the concentration factor. The latter is poorly known and varies widely (from 2 to 10);
- The mean grade is estimated by multiplying the feed coal grade by the concentration factor (which is equivalent to the mass ratio between ash and feed coal since the losses of uranium through the flue gasses is negligible). But some anthropogenic parameters may change the mean

grade of ashes. For instance, one may think that the building industry gives a priority to re-use low-grade ashes first, therefore increasing the global uranium mean grade;

- On the contrary, when power plants proceed to homogenization of their feed coals from different supply sources, they tend to mix low-grade coal with higher-grade coals. This does not affect the global mean grade but it affects the grade distribution by decreasing the share of high-grade ashes.

## 4.2. Technically accessible resources

Now that the total quantities of uranium have been assessed, we can estimate the technically accessible part of these quantities. For that purpose, we simply apply the 75% leaching recovery rate which was discussed in Section 3.1. The technically accessible resources are presented in Table II. No detailed analysis of these figures is given here since they do not include any constraints on minimum grades and economic issues. They are a good order of magnitude of the global accessible quantities but they are far from the quantities which could potentially be produced.

## 4.3. Economic constraints and potential reserves

### 4.3.1. Cut-off grade assumptions

In order to assess potential reserves (that is quantities which could become commercial projects), it is necessary to introduce some economics. For that purpose, we decide to compare uranium production from coal ash with other technics based on their acid consumption<sup>22</sup>. Actually, the capital cost (capex) of ash leaching is lower than in other applications [9, 23–25], but the operating costs of milling (opex) are certainly higher. In ash leaching, the reagent consumption is a big part of the opex and it is actually bigger than for in-situ recovery or most typical heap leaching projects [26–31]. This is what comes out of Fig. 2, built from ash leaching experiments found in the literature [8, 14, 15].

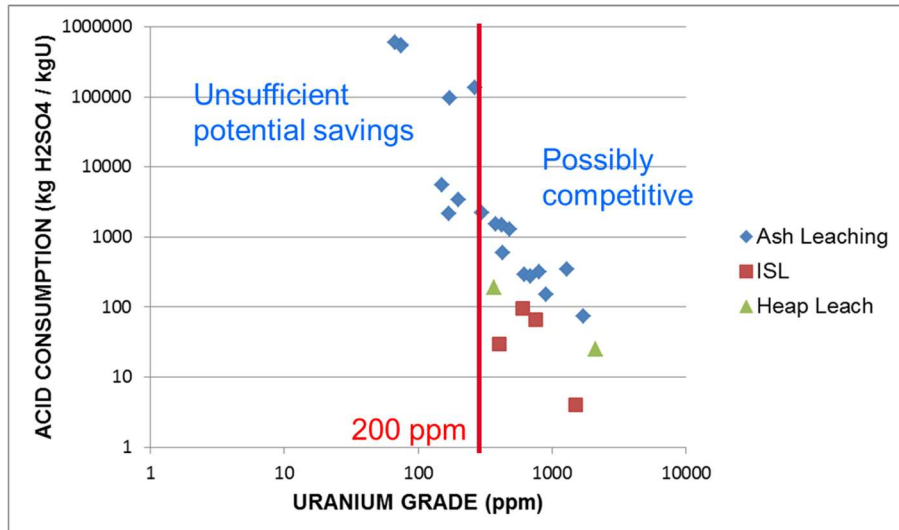


FIG. 5. Acid consumption for three uranium production technics based on the ore grade.

Though, as stated in Section 3.1, coal-ash milling can make potential savings by recovering acid reagent from coal combustion gases. If optimistic savings of 25% of reagent consumption are applied to ash

---

<sup>22</sup> Although comparing acid consumption is not equivalent to comparing production costs of each technique, it may provide a first approximate picture of the relative competitive positions.

leaching on Fig. 2, we can derive a minimum grade of 200 ppm. Below this grade, the potential acid savings are not enough to make ash leaching possibly competitive with the other technics.

This result is based on the assumption that acid consumption only depends on ore grade which, in reality, is not completely true. But out of the little available information, we have decided to assume a cut-off grade at 200 ppm to conduct further calculations.

#### 4.3.2. *Extrapolation of coal quality database*

Now that an assumption has been made for the cut-off value of ore grades, it is necessary to assess the percentage of resources that is above this limit. Basically, if we assume a concentration ratio of 5, the 200-ppm cut-off for the ashes is equivalent to 40 ppm for the feed coal. Thus, we need to look for the percentage of coals with grades higher than 40 ppm and this can be obtained by extrapolating the USGS database [6]. Here, the main assumption is that the USGS samples are representative of the actual volumes of coal. In other words, we assume that if 2% of the USGS samples have grades higher than 40 ppm, then 2% of the global coal reserves have grades higher than 40 ppm. This is probably the main uncertainty of our study. According to the USGS database, 7% of the world lignite reserves have grades higher than 40 ppm and only 1% of higher-quality coals do so. When coal and lignite are considered together, only 2% of reserves are over the cut-off limit.

#### 4.3.3. *Corresponding potential reserves*

To derive uranium potential reserves from technically accessible quantities, we simply multiply the latter by the above-mentioned percentage. The results are presented in detail in Table II. While there is no big difference in assessing total quantities of uranium from coal and lignite together or separately, the difference is significant when assessing potential reserves. The corresponding potential reserves are either 70 (together) or 200 kt of uranium (separately). Yet, the order of magnitude does not change and the main uncertainty we identify is more directly related to the extrapolation of USGS database.

### 5. PRODUCTION CAPACITIES

The uranium resources we are trying to assess in this study are only by-products of coal. Therefore, the available quantity of uranium is not the only constraint to production. The production of uranium by ash leaching is also constrained in terms of capacities by coal production and coal consumption in the energy sector. To estimate the capacity limitations, we follow the same kind of procedure as before:

- We first estimate the maximum theoretical production capacity (that is when all coal powerplants around the world start leaching the ashes they produce). Unlike for the resource assessment, this step already takes the 75% recovery rate into account;
- Then a more ‘realistic’ potential is estimated by introducing the above-mentioned cut-off limit.

The assumptions we make are the same as for the resource assessment but we use coal consumptions in energy sector [7] as input data instead of coal reserves and resources. The main results are gathered in Table IV. Thus, we derive a maximum production of 9 or 13 ktU/year. Yet, this amount of production will never happen unless the world starts leaching the ashes of all its powerplants. The second result is certainly more realistic: even in an optimistic approach, production should not exceed 700 tU/year (approximately 1% of current needs).

TABLE IV. ESTIMATION OF THEORETICAL AND REALISTIC CAPACITIES IN PRODUCTION OF URANIUM FROM COAL ASH

| Primary product                                | World  |             |                | China |
|--|--|-------------|----------------|-------|
|  | Coal   | Lignite     | Coal + lignite |       |
| Mean grade in U (ppm)                          | 3.4  | 12.0        | 4.7            | 2.31  |
| 2012 consumption in energy sector (Mt)         | 5120   | 880         | 6000           | 2600  |
| Available part of coal-ash*                    | Assumed 33%  | Assumed 60% | 33–60%         | 33%   |
| Max theoretical production capacity (ktU/year) | 4.3  | 4.7         | 7–13           | 1.5   |
| Percentage > 40 ppm                            | 1%   | 7%          | 2%             | -     |
| Available part of coal-ash*                    | 100% of high-grade coal-ash is made available for U production |             |                |       |
| ‘Realistic’ production potential (tU/year)     | 150  | 550         | 400            | -     |

\* The estimation of theoretical production takes into account the percentage of ashes that is re-used in the building industry (see Section 3.2). Since they have higher mean grade than other coals, lignites are given a lower re-use percentage when both are considered separately. On the other hand, the ‘realistic’ potential calculation does not take into account any re-use percentage: since it only considers high grade ashes, we assume that no industry would have used these ashes anyway.

## 6. CONCLUSION

To conclude, this study recalls that uranium production from coal-ash is technically feasible. In some situations, it could reach commercial development and in such cases, the fast lead time of this technique will be a plus. Lignites seem to have higher uranium reserves and production potentials than higher-quality coals but this result is one of the main uncertainties of this study: the statistical significance of USGS samples. Further work would be necessary to confirm this point. In terms of resource assessment, the main results of this study are:

- Firstly, the significant amount of technically accessible resources (1.1 to 4.5 MtU);
- Secondly, since most of these are low grade resources, no more than 200 ktU could become reserves one day.

In terms of production capacities, a realistic potential should not exceed 700 tU/year, that is approximately 1% of current needs. This estimation is already rather optimistic and even if production constraints are released (for example if coal consumption keeps rising), coal-ash could be a supplementary rather than a significant source of uranium for the 21st century.

## REFERENCES

- [1] SPARTON RESOURCES, Sparton locates major source of high uranium coal ash for its non-conventional uranium program in China, news release (2006),  
<http://www.spartonres.ca/pressreleases/PR2006Dec19.htm>.
- [2] WILDHORSE ENERGY, WildHorse signs MOU to recover uranium from coal ash in Europe, company announcement (25 May 2007).
- [3] INTERNATIONAL ATOMIC ENERGY AGENCY, World distribution of Uranium Deposits (UDEPO) with Ureanium Deposit Classification, 2009 Edition, IAEA-TECDOC-1629, IAEA, Vienna (2009).
- [4] BARKER, O., “CBM in the Springbok flats coalfield: a major untapped source of energy”, presented at the Limpopo Coal Conference, Limpopo (2012).
- [5] CAP RESOURCES LTD, 2013 Annual Report (2013) <http://acap.com.au>.
- [6] UNITED STATES GEOLOGICAL SURVEY, Chemical Analyses in the World Coal Quality Inventory, Version 1, Open-File Report 2010-1196 (2011).
- [7] ENERDATA, Enerdata Website (2012), <http://www.enerdata.net/>.
- [8] HURST, F.J., Recovery of Uranium from Lignites, Hydrometallurgy 7 4 (1981) 265–87.
- [9] WORLD FINANCE, “Rethinking uranium” (2010),  
<http://www.worldfinance.com/markets/equities/rethinking-uranium>.
- [10] ORGANISATION FOR ECONOMIC CO-OPERATION AND DEVELOPMENT NUCLEAR ENERGY AGENCY, Forty Years of Uranium Resources, Production and Demand in Perspective, OECD, Paris (2006).
- [11] ORGANISATION FOR ECONOMIC CO-OPERATION AND DEVELOPMENT NUCLEAR ENERGY AGENCY/INTERNATIONAL ATOMIC ENERGY AGENCY, Uranium 2011: resources, production and demand, OECD, Paris (2012).
- [12] UNITED STATES GEOLOGICAL SURVEY, Radioactive Elements in Coal and Fly Ash: Abundance, Forms, and Environmental Significance, Fact Sheet FS-163-97 (1997).
- [13] PANDIT, G.G., SAHU, S.K., Natural radionuclides from coal fired thermal power plants – estimation of atmospheric release and inhalation risk, Radioprotection 46 6 (2011) 173–179.
- [14] INTERNATIONAL ATOMIC ENERGY AGENCY, Advances in uranium ore processing and recovery from non-conventional resources, Proc. Tech. Comm. Mtg, Vienna, 1983, Panel Proceedings Series, IAEA, Vienna (1985).
- [15] USLU, I., GOKMESE, M., Coal an impure fuel source: radiation effects of coal-fired power plants in Turkey, Hacettepe J. of Biol. Chem. 38 4 (2010) 259–268.
- [16] WINNING, D., Out of the ashes, The Wall Street Journal 255 42 (2010).
- [17] CORNILLOT, J., Combustibles solides: charbon, de l'extraction à la combustion, Techniques de l'Ingénieur, BE8533 (2007).
- [18] AMERICAN COAL ASH ASSOCIATION, American CAA website, “CCPs Production & Use Charts” (2013), <http://www.acaa-usa.org/Publications/ProductionUseReports.aspx>.
- [19] ASIAN COAL ASH ASSOCIATION, Asian CAA website, “Fly Ash Utilization in China: Market Landscape and Policy Analysis” (2010), <http://www.asiancoalash.org/>.
- [20] FEDERAL INSTITUTE FOR GEOSCIENCES AND NATURAL RESOURCES, Energy Study 2012 Reserves, Resources and Availability of Energy Resources, Hannover (2012).
- [21] YANG, J., Concentration and distribution of uranium in Chinese coals, Energy 32 3 (2007) 203–12.
- [22] UNITED STATES GEOLOGICAL SURVEY, USGS Website, US Coal Quality Database, <http://energy.er.usgs.gov/coalqual.htm> (1998).
- [23] CRU INTERNATIONAL, “An Overview of the Uranium Mining Industry of Kazakhstan”, presented at the Kazakhstan Business Forum (2010).
- [24] GOVERNMENT OF SOUTH AUSTRALIA, Uranium in South Australia, paper presented at the Invest in Australia Conference, Adelaide (2012).
- [25] URANIUM ONE, “Creating a Globally Diversified Uranium Producer”, corporate presentation (2012).
- [26] INTERNATIONAL ATOMIC ENERGY AGENCY, Manual of Acid in Situ Leach Uranium Mining Technology, IAEA-TECDOC-1239, IAEA, Vienna (2001).

- [27] MAERTEN, H., "Advancements in Uranium ISL Technology", paper presented at IAEA Technical Meeting on Optimization of In Situ Leach (ISL) Uranium Mining Technology, Vienna (2013).
- [28] DAHLKAMP, F.J., Uranium Deposits of the World: Asia, Springer, Heidelberg (2009).
- [29] FYODOROV, G.V., "Uranium production and the environment in Kazakhstan", The Uranium Production Cycle and the Environment, IAEA C&S Papers Series No. 10/P, IAEA, Vienna (2002) 191-198.
- [30] GOMIERO, L.A., "Uranium Production in Caetité, Brazil", Uranium Exploration, Mining, Production, Mine Remediation and Environmental Issues (Proc. of the Regional Tech. Mtg, Mendoza, Argentina, 2006), IAEA, Vienna.  
<https://www.iaea.org/OurWork/ST/NE/NEFW/documents/RawMaterials/TC%20BRA/24%20Caetite%20Mining%20&%20Milling%20-%20Brazil.pdf>
- [31] SCHEFFEL, R.E., "Heap Leach Design for Success", paper presented at IAEA Technical Meeting on Low Grade Uranium Ore, Vienna, 2010.

# **SEAWATER URANIUM RECOVERY BY A POLYMERIC ADSORBENT: DEVELOPMENT, CHARACTERIZATION AND ECONOMICS**

E. SCHNEIDER<sup>+</sup>, S. KUNG\*\*\*, P. BRITT\*, G. GILL\*\*,  
G. BONHEYO\*\*, S. DAI\*, B. HAY\*, C. JANKE\*, R. JETERS\*\*,  
T. KHANGAONKAR\*\*, L. KUO\*\*, W. LONG\*\*, R. MAYES\*,  
J. PARK\*\*, L. RAO<sup>++</sup>, T. SAITO\*, C. TSOURIS\*, T. WANG\*\*, J. WOOD\*\*

\* Oak Ridge National Laboratory,  
Oak Ridge, Tennessee

\*\* Pacific Northwest National Laboratory,  
Marine Sciences Laboratory,  
Sequim, Washington

\*\*\* US Department of Energy,  
Office of Nuclear Energy,  
Germantown, Maryland

<sup>+</sup> The University of Texas at Austin,  
Nuclear and Radiation Engineering Program,  
Austin, Texas

<sup>++</sup> Lawrence Berkeley National Laboratory,  
Berkeley, California

United States of America

## **Abstract**

Seawater contains more than 4 billion metric tonnes of dissolved uranium. This unconventional uranium resource, combined with a suitable extraction cost, can potentially meet the uranium demands for centuries to come. The challenge, however, is the low concentration of uranium in seawater — approximately 3.3 ppb. A multidisciplinary team from the U.S. national laboratories, universities, and research institutes has been assembled to address this challenge. Polymeric adsorbents materials containing amidoxime ligands, developed at the Oak Ridge National Laboratory (ORNL), have demonstrated great promise for the extraction of uranium from seawater. These ORNL adsorbents showed adsorption capacities for the extraction of uranium from seawater that exceed 3 mg U/g adsorbent in testing at the Pacific Northwest National Laboratory Marine Sciences Laboratory. A key component of this novel technology lies in the unique high surface-area polyethylene fibers that considerably increase the surface area and thus the grafting yield of functional groups without compromising its mechanical properties. Economic analyses have been used to guide the technology development and highlight parameters, such as capacity, recyclability, and stability, which have the largest impact on the cost of extraction of uranium from seawater.

## **1. INTRODUCTION**

For nuclear power to remain a sustainable energy source, there must be assurance that economically viable nuclear fuel is available. Currently, the primary natural resource for nuclear energy production is uranium, and almost all the commercial reactors in the world operate with a uranium fuel cycle. One goal of the US Department of Energy (DOE), Office of Nuclear Energy (NE) is to develop sustainable nuclear fuel cycles that improve uranium resource utilization, maximize energy generation, minimize waste generation, improve safety, and limit proliferation risk. Thus, the availability of fuel resources for each potential fuel cycle and reactor deployment scenario must be well understood. This area is most relevant for once-through approaches, but even full-recycle strategies will require comparable levels of natural resources for the foreseeable future. As stated in the US DOE NE Roadmap, the most appropriate

place for federal involvement in this area would be research and development (R&D) to support investigation of long-term, ‘game-changing’ approaches, such as recovering uranium from seawater.

The world’s oceans represent a vast and as yet untapped source of uranium at approximately 3.3 ppb. Since seawater is slightly basic ( $\text{pH } 8.1 \pm 0.2$ ), uranium exists primarily as  $[\text{UO}_2(\text{CO}_3)_3]^{4-}$ . It is estimated that the total sum of uranium in seawater is approximately 4.5 billion metric tonnes. This reserve, combined with a suitable production cost for the extraction of uranium, can contribute to the growing international nuclear industry. Researchers in many countries have been inspired to develop adsorbents to recover this untapped supply of uranium contained in world’s oceans since the 1960s.

It was clear to scientists 60 years ago, just as it is today, that to exploit the ocean’s reserves of uranium, a high-performance adsorbent was needed. A successful cost-effective extractant must have a very high distribution coefficient, very high selectivity, high loading capacity, rapid adsorption and elution kinetics, low losses of extractant, and low cost. Thus, solvent extraction is not considered to be suitable for large-scale extraction of uranium from seawater because of the complex and expensive engineering aspects, the large amounts of chemicals and volatile solvents needed, and the loss of reagents by entrainment and dissolution. Extractants based on solid-state adsorbents appear to be the most promising, but they need to be stable at slightly basic pH and high ionic strength, and they need to be extremely insoluble and durable in seawater.

In the early 1980s, scientists at the Nuclear Research Center in Jülich, Germany, conducted a systematic evaluation of 200 ion-exchange resin materials [1]. The resins were tested at both laboratory scale and large field scale (100 g sorbent) with seawater (German North Sea and in the Gulf Stream near Miami). The team found that among all the materials tested, only amidoxime-based compounds, specifically cross-linked poly(acrylamidoximes), met the requirements for chemical stability and selective uptake of uranium under typical marine conditions. The uranium could be eluted from the poly(acrylamidoximes) resin by 1M HCl, but the uranium uptake decreased (ca. 6%) with increasing sorption-elution cycles. Although a number of other uranium extraction materials and methods have been studied, their various shortcomings have kept the focus on amidoxime-based adsorbents.

For the last three decades, Japan has been a leader in the extraction of uranium from seawater using amidoxime-based polymeric adsorbents, and it has conducted both laboratory and marine experiments in the Pacific Ocean. Seko, Tamada, and coworkers [2] developed a braided adsorbent; fashioning long seaweed-like braids of amidoxime-functionalized polyethylene fiber and attached the braids via remotely controlled fasteners to anchors that were lowered to the ocean floor. The 60 m amidoxime functionalized braided adsorbent was evaluated in marine tests in the Okinawa area of Japan, and it was found that the average adsorbent collected was 1.5 g of uranium per kg of sorbent in 30 days. Thus, it was concluded that the braided-type adsorbent had a higher ability to adsorb uranium than the stacks of nonwoven fabric owing to the better contact between the seawater and the adsorbent.

Economic analysis is key to determining the feasibility of technologies for uranium recovery from seawater. Several studies have reported economic analyses of actively pumped systems and passive, current-driven system [3–5]. Passive, current-driven system designs have come to be viewed as desirable due to their lower operating cost and simplicity compared to the actively pumped schemes. An extended economic analysis of the production cost for the extraction of uranium from seawater, based on the amidoxime braided fiber system described above, was developed by the Japan Atomic Energy Agency (JAEA). This analysis [2] confirmed that increased adsorption capacity is one of the most important factors in decreasing uranium costs. In addition to adsorption capacity, the recycling frequency and the number of recycles are important parameters for reducing cost. These economic analyses provided motivation to develop robust adsorbents of high capacity, which can be regenerated and recycled many times.

The availability of terrestrial ores may diminish over time, should new discoveries of accessible, secure, environmentally tenable deposits not keep pace with extraction. Uncertainty in the sustainability of the conventional resource base can erode confidence in the long-term viability of the energy source, especially given the very long capital plant lifetimes that are in other respects a strength of the nuclear

power industry. Nuclear fuel cycle research and development decision makers consider even longer time scales and are consequently strongly hampered by uncertainties surrounding the long term availability of the resource. Taken together, these factors imply that the costs — in nuclear build decisions not taken due to uncertainty around security of uranium supply and in research and development (R&D) pursued as a hedge against scarce, expensive uranium — of not knowing how much uranium is available and at what cost are high. For its potential to eliminate this uncertainty and secure an indefinite supply of uranium at moderate cost, technology for the recovery of uranium from seawater will play a vital role in securing future energy resources. Furthermore, an effective uranium-recovery technology from seawater, based on selective adsorbents, can be extended to obtain other valuable materials present in seawater.

Research and development efforts on uranium uptake technologies from seawater have progressed during the past six decades. However, for these efforts to lead to a viable technology for the production of uranium from seawater, additional breakthroughs are needed. Economic viability requires the development of the next generation of adsorbents that will exhibit higher adsorbent capacity, faster loading kinetics, and lower degradation over multiple loading/elution cycles. Equally important, uncertainties surrounding the performance and environmental impact of the technology must continue to be reduced. Both experimentation and modeling/simulation have a role to play in developing the technology to the point where its credibility as a viable large-scale source of uranium is beyond doubt.

## 2. ADSORBENT DESIGN AND DEVELOPMENT

Although amidoxime-based adsorbents have been studied extensively for the extraction of uranium from seawater, the coordination mode of the amidoxime ligand to the uranyl ion,  $\text{UO}_2^{2+}$ , had not been identified. There are multiple possible binding motifs for the amidoxime ligand including monodentate binding to either the oxime oxygen or the amine nitrogen, bidentate binding through the oxime oxygen and the amine nitrogen, or  $\eta^2$ -binding through the N-O bond. Density functional theory calculations was used to evaluate the possible binding motifs for a series of  $[\text{UO}_2(\text{AO})_x(\text{OH}_2)]^{2-x}$  ( $x = 1-3$ ) complexes. It was determined that  $\eta^2$  motif was the most stable form [6] (Fig. 1). This prediction was confirmed by single-crystal X-ray diffraction of three different uranyl-amidoximate complexes which all displayed the  $\eta^2$ -binding [6, 7]. This information is now being used in *de novo* structure-based design methods to design new, more selective bis(amidoxime) ligands [8]. This method computationally screened millions of potential structures and identified the best bis(amidoxime) ligands, i.e., those with the lowest ligand strain energy upon metal complexation, to be synthesized.

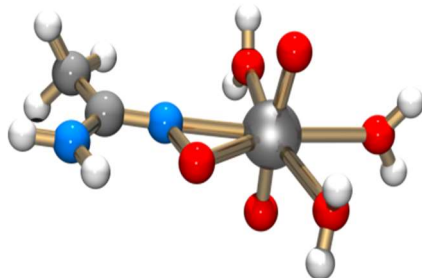


*FIG. 1.  $\eta^2$ -binding of amidoxime ligand to uranyl ion.*

In addition to coordination modes, a better fundamental understanding of the thermodynamics and kinetics of amidoxime binding with the uranyl ion is needed to improve the extraction efficiency and selectivity. Potentiometric and spectrophotometric titrations were jointly used to determine the stability constants of the complexes between  $\text{UO}_2^{2+}$  and the two structurally related amidoxime ligands: glutarimidedioxime (the cyclic imidedioxime H<sub>2</sub>A) and glutardiamidoxime (the open-chain bis-amidoxime H<sub>2</sub>B). The data indicates that the cyclic imidedioxime (H<sub>2</sub>A) is a stronger ligand than the open-chain diamidoxime (H<sub>2</sub>B) [9]. Microcalorimetric titrations were conducted to determine the enthalpy of complexation between  $\text{UO}_2^{2+}$  and amidoxime-related ligands (H<sub>2</sub>A and H<sub>2</sub>B). Based on the

thermodynamic parameters on the speciation of carbonate, the cyclic imidedioxime ligand and its complexes with U(VI), the dominant species under seawater pH, are  $\text{HCO}_3^-$ ,  $\text{H}_2\text{A}$ ,  $\text{UO}_2(\text{CO}_3)_3^{4-}$ , and  $\text{UO}_2(\text{HA})\text{A}^-$ , respectively. Therefore, the major overall reaction can be written as



Using the enthalpy values from the literature and this work, the enthalpy of reaction (1) is calculated to be +16.7 kJ/mol [10]. This means that the overall binding of uranyl tricarbonate from seawater by the cyclic imidedioxime ligand is *endothermic*, and that the efficiency of sequestration should be enhanced at higher temperatures.



FIG. 2. Optical microscopy images of non-round shaped polyethylene fibers produced by Hills, Inc. (from left) hollow gear, flower, solid gear, and caterpillar shapes.

Over the last three years, we have focused on increasing the adsorption capacity of amidoxime-based polymeric adsorbents by the radiation-induced graft polymerization (RIGP) on high surface-area polyethylene fiberous trunk materials. The hypothesis is that the adsorption capacity could be increased by increasing the fiber surface area. High surface area high-density polyethylene fibers were fabricated through an ‘islands-in-the-sea’ fiber-spinning method, which can considerably enhance the surface area of the fiber without compromising its mechanical properties. Fiber shapes that we have studied include solid or hollow flower shape, solid or hollow gear shape, solid or hollow trilobal shape, solid trilobal gear shape, and others (Fig. 2). The Brunauer–Emmet–Teller (BET) surface areas of our high-surface-area fibers ranged from 0.36 to 11.5 m<sup>2</sup>/g versus 0.18 m<sup>2</sup>/g for the standard 20-micron-diameter round fiber.

Amidoxime-based polymeric adsorbents are prepared by radiation-induced graft polymerization (RIGP) which involve four processing steps [11]: electron beam irradiation of high-surface-area polyethylene fibers; co-grafting polymerizable monomers containing nitrile groups and hydrophilic groups to form grafted side chains throughout the fiber; conversion of nitrile groups to amidoxime groups; and alkaline conditioning of the grafted fibers. The resulting adsorbents are then tested for their capacity to bind uranium from seawater (as discussed below).

The four processing steps discussed above have many parameters that can influence the uranium adsorption capacity; therefore, effort was focused on systematically investigating the large number of experimental variables and preparing hundreds of adsorbent samples to determine which parameters were the most important. These parameters included trunk polymer fiber type, fiber diameter, fiber morphology, fiber surface area, and crystallinity. Irradiation conditions included dose, dose rate, irradiation time, atmosphere, and temperature. Graft conditions included solvent, co-monomers, concentration, co-monomer ratio, additives, and reaction temperature and time. Amidoximation conditions included solvent, solvent concentration, hydroxylamine concentration, and reaction temperature and time. Alkaline conditions included alkaline concentration and reaction temperature and time. Based on these results, additional experiments were conducted to better understand and optimize the key parameters in order to continuously improve the uranium adsorption capacity. Currently, the best adsorbents are produced from the hollow gear fiber with amidoxime ligands with either methacrylic acid (38H) or an alternative acid (AF1) to enhance the hydrophilicity of the polymer.

Batch and flow-through laboratory experiments have also been conducted to investigate the uranium adsorption kinetics and equilibrium by amidoxime-based polymeric adsorbents with the objectives to determine the rate-limiting mechanism for uranium adsorption. Different mathematical models based on liquid film mass transfer, diffusion, or reaction kinetics were evaluated. Overall, it was shown that, for 5-gallon batch experiments with real seawater, uranium binding is the rate limiting step compared to diffusion [12].

### 3. MARINE TESTING AND CHARACTERIZATION

The marine testing and characterization program is being conducted at the Marine Sciences Laboratory (MSL), a part of the Pacific Northwest National Laboratory (PNNL) with the objective to evaluate advanced adsorbent materials for the extraction of uranium using natural seawater. Adsorbent materials undergoing testing were provided principally by Oak Ridge National Laboratory (ORNL). The MSL has a specialized ambient seawater delivery system for material testing and specialized analytical capabilities for determination of trace elements in natural seawater at part per trillion levels. Marine testing of adsorbent fibers is being conducted in packed columns using flow-through filtered natural seawater. Braided adsorbent material are being tested in flumes. In both test systems, temperature and flow-rate (linear velocity) are controlled at realistic marine conditions.

Determination of uranium and other elements in adsorbent materials was conducted by Inductively Coupled Plasma Optical Emission Spectrometry (ICPOES) and Inductively Coupled Plasma Mass Spectrometry (ICPMS) following digestion of the adsorbent material in a 50% aqua regia solution for 3 hours at 80°C. Natural uranium in seawater was determined without preconcentration using a variation of the method of standard additions. Determination of selected trace elements in seawater was conducted using borohydride reduction precipitation preconcentration from a mixture of Fe/Pd and ammonium pyrrolidine dithiocarbamate (APDC).

Measurements of the adsorption of uranium and other elements from seawater as a function of time onto the adsorbent materials are used to determine the adsorbent capacity and adsorption rate (kinetics) of uranium and other elements. Illustrated in Fig. 3 are the results obtained with multiple time series experiments using the ORNL amidoxime-based polymeric adsorbent material 38H produced in 2012 and an improved adsorbent, AF1, produced in 2013. The 38H adsorbent had a 56 day adsorption capacity of  $3300 \pm 680 \mu\text{g U/g adsorbent}$  (normalized to a salinity of 35 psu). Applying a one-site ligand saturation model predicts a saturation adsorption capacity of  $4890 \pm 830 \mu\text{g U/g}$  of adsorbent material (normalized to a salinity of 35 psu) and a half-saturation time of  $28 \pm 10$  days. The AF1 adsorbent material had a 56 day adsorption capacity of  $3850 \pm 200 \mu\text{g U/g}$  adsorbent material (normalized to a salinity of 35 psu), a saturation capacity of  $5300 \pm 200 \mu\text{g U/g}$  adsorbent material (normalized to a salinity of 35 psu) and a half saturation time of  $21 \pm 2$  days.

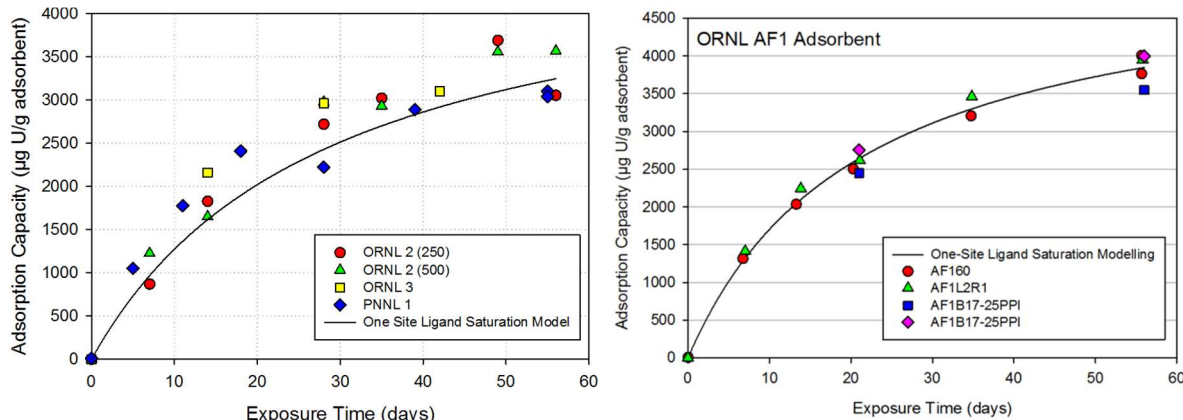


FIG. 3. Time-series measurements of the adsorption capacity of the ORNL amidoxime-based adsorbent materials 38H (left) and AF1 (right).

The amidoxime-based adsorbent materials are not specific for uranium, but also adsorb other elements from seawater. Shown in Table I, in order of adsorption capacity, are the elements which were absorbed by a sample of the ORNL AF1 adsorbent material. Note that the major doubly charged cations in seawater (Ca and Mg) account for a majority of the cations adsorbed (53% by mass and 59% by molar percent). For the AF1 adsorbent material, uranium is the 5<sup>th</sup> most abundant element adsorbed by mass and 8<sup>th</sup> most abundant by molar percentage.

TABLE I. RELATIVE ABUNDANCE OF ELEMENTS ABSORBED BY THE ORNL AMIDOXIME-BASED ADSORBENT MATERIAL AF1. ADSORPTION CAPACITY IS EXPRESSED IN UNITS OF  $\mu\text{G}$  (ELEMENT)/G ADSORBENT ON THE LEFT PANEL AND  $\mu\text{MOL}$  (ELEMENT)/G ADSORBENT IN THE RIGHT PANEL

| Element | Adsorption capacity<br>(mg/g adsorbent) | % of total<br>(by mass) | Element | Adsorption capacity<br>( $\mu\text{mol/g}$ adsorbent) | % of total<br>(by mass) |
|---------|---|-------------------------|---------|---|-------------------------|
| Mg      | 24 302                                  | 27                      | Mg      | 1000  | 37                      |
| Ca      | 23 664                                  | 26                      | Ca      | 590   | 22                      |
| Na      | 16 266                                  | 18                      | Na      | 708   | 26                      |
| V       | 14 918                                  | 17                      | V       | 293   | 11                      |
| U       | 3949                                    | 4.4                     | Fe      | 34.9  | 1.3                     |
| Fe      | 1949                                    | 2.2                     | Zn      | 24.3  | 0.89                    |
| Zn      | 1589                                    | 1.8                     | K       | 20.5  | 0.75                    |
| Cu      | 1035                                    | 1.2                     | U       | 16.6  | 0.61                    |
| K       | 800                                     | 0.89                    | Cu      | 16.3  | 0.60                    |
| Ni      | 392                                     | 0.55                    | Ni      | 8.37  | 0.31                    |
| Sr      | 197                                     | 0.22                    | Sr      | 2.25  | 0.083                   |
| Ti      | 117                                     | 0.13                    | Ti      | 2.45  | 0.090                   |
| Cr      | 33                                      | 0.037                   | Cr      | 0.631   | 0.023                   |
| Co      | 31                                      | 0.034                   | Co      | 0.520   | 0.019                   |
| Mn      | 24                                      | 0.026                   | Mn      | 0.431   | 0.016                   |
| Mo      | 11                                      | 0.013                   | Mo      | 0.119   | 0.004                   |
| Sum     | 89 376                                  | 100                     | Sum     | 2718  | 100                     |

Thermodynamic modeling predicts the interaction between the uranyl ion ( $\text{UO}_2^{2+}$ ) and the amidoxime binding ligand to be endothermic in seawater; hence higher temperatures should yield enhanced adsorption capacity [10]. Direct evidence for this thermodynamic prediction is shown in Fig. 4 using the ORNL amidoxime-based adsorbent AF160. The adsorption capacity observed after 56 days of exposure at 20°C (~3900  $\mu\text{g}$  U/g adsorbent) is approximately 2.9 times higher than that observed at after 56 days of exposure at 8°C (~1350  $\mu\text{g}$  U/g adsorbent).

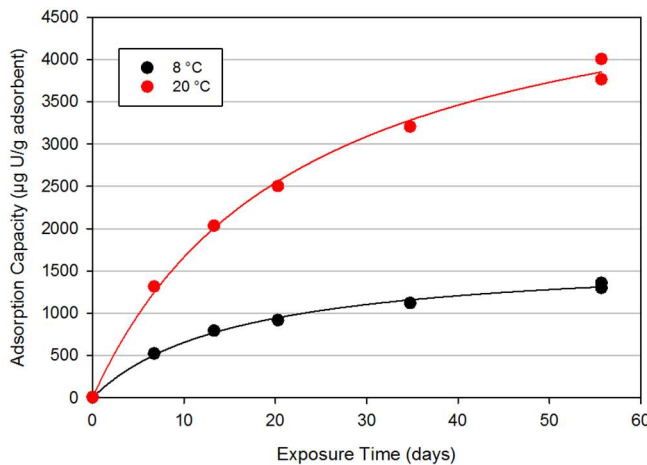


FIG. 4. Effect of temperature on adsorption capacity using the ORNL adsorbent AF160.

Mining the sea for uranium at viable scales will require deployment of expansive ‘farms’ of adsorbent material that must be shown not to harm marine biota and the marine ecosystem. This program has been investigating two issues: toxicity of adsorbent material and reduction in ocean currents from deployment of a farm of ‘kelp-like’ adsorbent material. Toxicity testing is being conducted with the ‘Microtox®’ aquatic toxicity test on solid adsorbents and column effluents containing adsorbent. No toxicity was observed with column effluents of any adsorbent materials tested to date. Toxicity could be induced with some non amidoxime-based adsorbents only when the ratio of solid adsorbent to test media was increased to highly unrealistic levels. Concern about reduction in coastal currents is being addressed by assessing the form drag from a braid adsorbent farm using hydrodynamic modelling. Applying the model to an 670 km<sup>2</sup> adsorbent farm with a spacing density of 0.00178 moorings/m<sup>2</sup> results in the reduction in ambient currents of 4–10%. This reduction is fairly minor compared to the reduction in currents through a kelp forest (up to 50%) and is not anticipated to have significant impact in the open ocean.

#### 4. ECONOMICS

The uranium production process is based upon the braided adsorbent system pioneered by JAEA [2] and consists of three basic steps: adsorbent synthesis, adsorbent deployment, and uranium elution and purification (Fig. 5). The adsorbent material is reusable, though not indefinitely so, and undergoes multiple deployment and elution cycles.

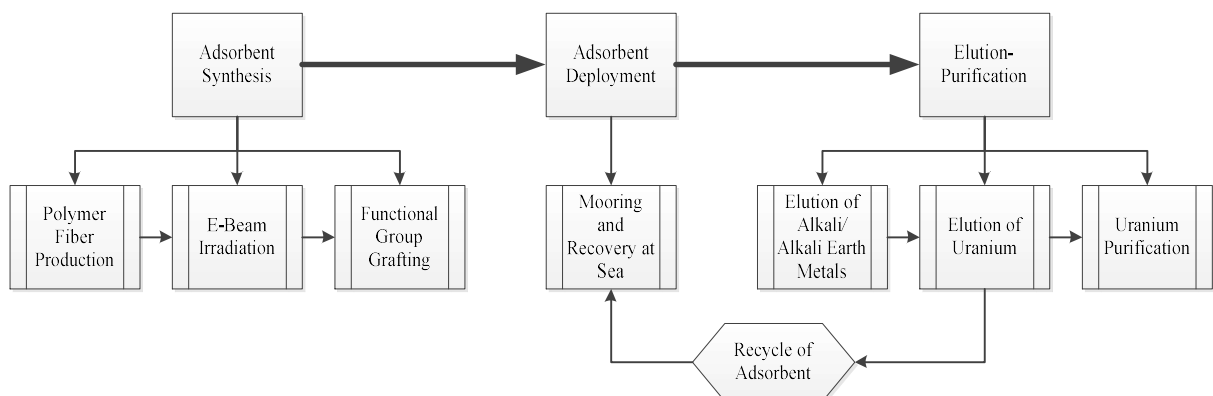
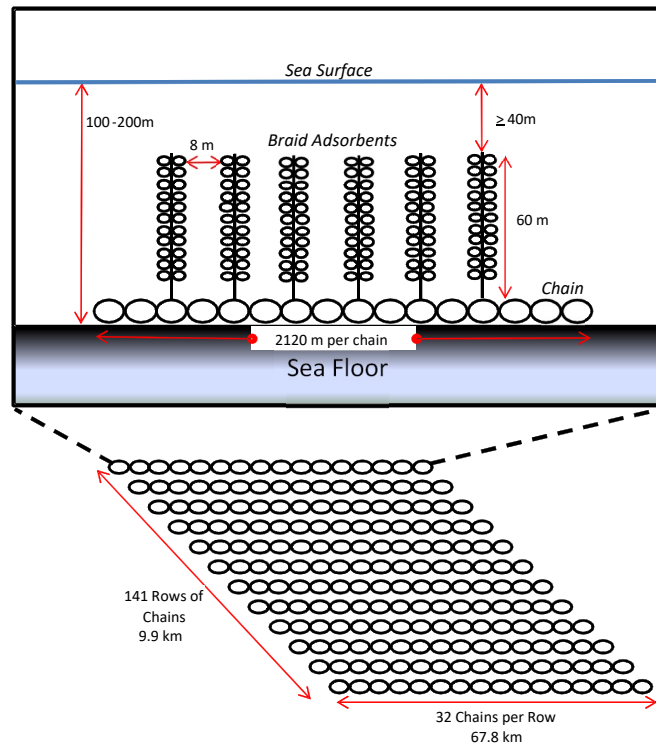


FIG. 5. Process overview.

There are several components to each major step. Fiber production requires purchase of the high-density polyethylene (HDPE) base polymer and its melt spinning and extrusion into fibers. The fibers are irradiated to open grafting sites for amidoxime and hydrophilic functional groups. The chemicals used in the grafting process represent a significant part of overall system costs.

The fibers are braided around a low-density core to create positively-buoyant braids approximately 60 meters in length. The material is carried to the deployment site by workboats and moored to the ocean floor with anchor chains as depicted in Fig. 6. At the end of the mooring period, the boats winch up the chains to recover the adsorbent material. The material is then returned to shore or a centrally-located mother ship for recovery of uranium. The adsorbent performance is characterized by capacity (kg U/tonne adsorbent), which in turn is a function of time immersed and temperature of the seawater. Both capacity and durability — number of adsorbent uses prior to disposal, extent of capacity retention with reuse — are important drivers of the uranium production cost.



*FIG. 6. Braid adsorbent and mooring system.*

The life cycle discounted cash flow (LCDCF) approach is used to synthesize the system component costs into a uranium production cost in US\$/kg U. This widely-used methodology is described in the Generation IV International Forum Economic Modeling Working Group (EMWG) cost estimation guidelines [13] and its application to the uranium recovery system is fully documented in [3].

Table II lists the key parameters defining the reference system for the cost analysis. The annual uranium production affects scale economies, with a larger adsorbent field leading to somewhat reduced costs. The value given in the table was chosen for comparability with the JAEA cost estimate [2] and leads to a field with an undersea footprint of 670 km<sup>2</sup>, as depicted in Figure 6. The uranium uptake in seawater, currently 3.33 g U/kg adsorbent if the material is immersed for 60 days, was measured through an extensive marine testing program described in this paper.

TABLE II. TOP LEVEL PARAMETERS OF REFERENCE SYSTEM

| Parameter                       | Value | Unit              |
|---------------------------------|-------|-------------------|
| Annual uranium production       | 1200  | tonnes/year       |
| Uranium uptake                  | 3.33  | g U/ kg adsorbent |
| Length of mooring campaign      | 60    | days              |
| Adsorbent uses                  | 6     | N/A               |
| Uranium uptake degradation rate | 5%    | per reuse         |

Based upon these parameters, the cost of producing uranium from seawater is estimated to be US \$606/kg U. There are uncertainties associated with input costs and system design (e.g., chemical and commodity costs) as well adsorbent performance (fresh capacity, durability). These give rise to a 95% confidence interval of [US \$420/kg U, US \$1000/kg U]. The uncertainties and their propagation are discussed fully in [3].

Table III provides a breakdown of the US \$606/kg U cost by category and type of expense. Adsorbent production system operating costs are the largest cost component at US \$290/kg U. Chemicals and materials contribute 75% of this component cost; major expense items include hydroxylamine, acrylonitrile, methacrylic acid, and high density polyethylene. Capital and operating costs associated with the deployment and mooring of the adsorbent at sea account for another US \$223/kg U of the total. Capital costs arise from work boat and chain/rope anchor system purchase, while operations are driven by boat running costs.

TABLE III. MAJOR COST COMPONENTS

|                          | Capital investment<br>Contribution to cost (US \$/kg U) | Operations<br>Contribution to cost (US \$/kg U) |
|--------------------------|---|---|
| Adsorbent production     | 58  | 290   |
| Mooring and deployment   | 102   | 121   |
| Elution and purification | 13  | 22  |
| Total                    | 173   | 433   |

Figure 7 shows that adsorbent capacity is the most crucial driver of uranium production cost. To generate the figure, capacity and recycle number were varied without modifying the adsorbent production process or other inputs. Marine tests described elsewhere in this paper indicate that a 60-day loading of 4.0 g U/kg adsorbent is within reach, and novel elution and adsorbent regeneration processes are being developed that will limit the rate at which the adsorbent loses capacity when it is reused. If the adsorbent can also retain its full capacity over many recycles, the U production cost would be cut by almost half to ca. US \$350/kg U.

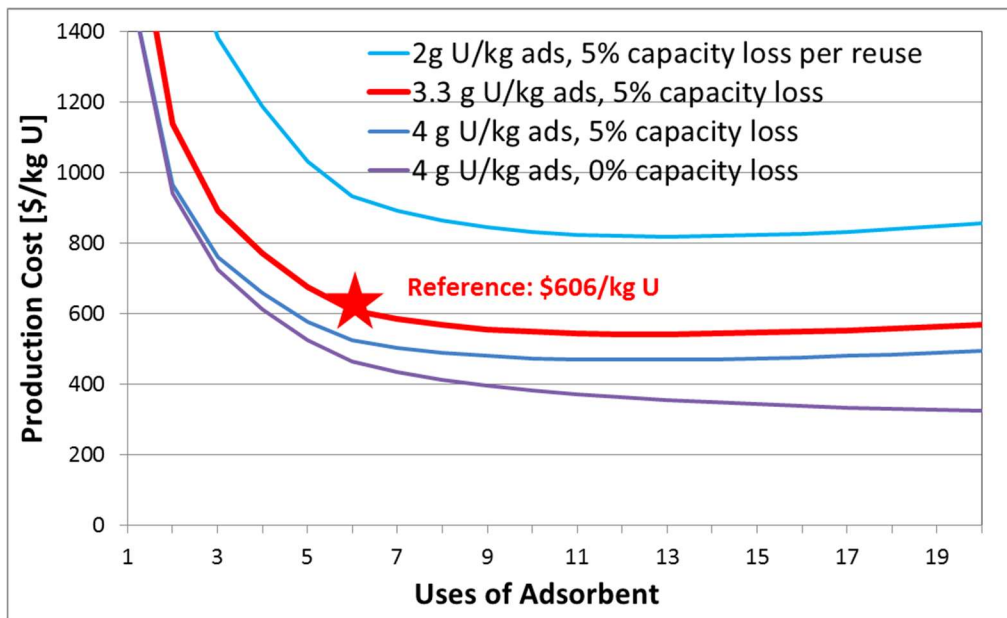


FIG. 7. Uranium production cost sensitivities.

## ACKNOWLEDGEMENTS

The authors wish to acknowledge the support of the United States Department of Energy Office of Nuclear Energy.

## REFERENCES

- [1] BITTE, J., KELLER, A., LUDWIG, K.P., “Comparison of different extraction concept for the recovery of uranium from seawater”, Proc. IMRUS 83: International Meeting on Uranium Recovery from Seawater, Tokyo, 1983 (1984).
- [2] TAMADA, M., SEKO, N., KASAI, N., SHIMIZU, T., Cost Estimation of Uranium Recovery from Seawater with System of Braid Type Adsorbent, Transactions of the Atomic Energy Society of Japan **5** 4 (2006) 358–363.
- [3] SCHNEIDER, E.A., SACHDE, D.J., The Cost of Recovering Uranium from Seawater by a Braided Polymer Adsorbent System, Science and Global Security **21** (2013) 134–146.
- [4] FORBERG, S., LAGSTROM, G., VALLA, P., “Recovery of uranium from seawater using an appraisal from Novel Sorbent Data”, Proc. IMRUS 83: International Meeting on Recovery of Uranium from Seawater (1983).
- [5] SUGO, T., TAMADA, M., SEGUCHI, T., SHIMIZU, T., UOTANI, M., KASHIMA, R., Recovery system for uranium from seawater with fibrous adsorbent and its preliminary cost estimation, J. Atomic Energy Society of Japan **43** 10 (2001) 1010–1016.
- [6] VUKOVIC, S., WATSON, L.A., KANG, S.O., CUSTELCEAN, R., HAY, B.P., How amidoximate binds the uranyl cation, Inorg. Chem. **51** (2012) 3855–3859.
- [7] BARBER, P.S., KELLY, S.P., ROGERS, R.D., Highly selective extraction of uranyl ion with hydrophobic amidoxime-functionalized ionic liquids via  $\eta^2$  coordination, RSC Advances **12** (2012) 8526–8530.
- [8] VUKOVIC, S., HAY, B., De Novo Structure-based design of bis-amidoxime uranophiles, Inorg. Chem. **52** (2013) 7805–7801.
- [9] TIAN, G., TEAT, S.J., RAO, L., Thermodynamic studies of U(VI) complexation with glutardiamidoxime for sequestration of uranium from seawater, Dalton Trans. **42** (2013) 5690–5696.

- [10] TIAN, G., TEAT, S.J., ZHANG, Z., RAO, L., Sequestering uranium from seawater: Binding strength and modes of complexation with glutarimidedioxime, *Dalton Trans.* **41** (2012) 11579–11586.
- [11] KIM, J., TSOURIS, C., MAYES, R.T., OYOLA, Y., SAITO, T., JANKE, C.J., DAI, S., SCHNEIDER, E.A. SACHDE, D., Recovery of uranium from seawater: A review of current status and research needs, *Separation Science Technology* **34** (2013) 367–387.
- [12] KIM, J., OYOLA, Y., TSOURIS, C., HEXEL, C.R., MAYES, R.T., JANKE, C.J., DAI, S., Characterization of uranium uptake kinetics from seawater in batch and flow-through experiments, *Ind. Eng. Chem. Res.* **52** (2013) 9433–9440.
- [13] THE ECONOMIC MODELING WORKING GROUP OF THE GENERATION IV INTERNATIONAL FORUM, Cost Estimating Guidelines for Generation IV Nuclear Energy Systems, Technical report, OECD/NEA, Paris (2007).

# **URANIUM AND RARE EARTHS RECOVERY FROM FLORIDA PHOSPHATE — LOOKING BACK AND GOING FORWARD**

P. ZHANG, B. BIRKY

Florida Industrial and Phosphate Research Institute,  
Bartow, Florida,  
United States of America

## **Abstract**

Uranium recovered during the production of phosphoric acid represents a significant source of nuclear fuel as the gap between uranium supply and demand is expected to grow. The phosphate industry in Florida supplied uranium to both the defense and energy sectors in the past, but market conditions ended the recovery process. Currently, the uranium is retained in the phosphoric acid and the granulated fertilizer products, primarily diammonium and monoammonium phosphate, and dispersed on farm fields as a trace element in blended fertilizers. This represents a loss to the nuclear fuel cycle that will never be recovered. In an era of heightened awareness of sustainability and increasing pressure to reduce greenhouse gas emissions, market conditions and social factors may converge to create favorable conditions for uranium recovery to resume. However, the future may not resemble the past as uranium concentrations are lower in the newer mining areas and ion exchange challenges solvent extraction for the extraction technology of choice. New factors will also influence both the economic decision to resume recovery operations, as well as the recovery technology. Rare earth elements (REE) are also present in the processing streams at recoverable levels, and can be co-extracted with uranium using the proven solvent extraction method. REE are vital to the phosphor industry, green energy development, and technology advances in many fields. However, the world has limited REE resources, and the recovery of REE from many of these resources is both economically challenging and environmentally troublesome. Phosphate as a secondary REE resource has a great potential to fill this gap. World annual phosphate rock production has surpassed 200 million tons, representing 60 000 tons of unrecovered REE assuming an average concentration of 300 ppm. In the case of Florida, REE in the phosphate ore reports to four mining and processing streams, with approximately 10% to flotation tailings, 30–40% to waste clay, 35–40% to phosphogypsum (PG), and 15–20% to phosphoric acid. Due to the concern about disposal of thorium-containing wastes, the Florida phosphate industry stepped back from their effort to recover REE from flotation tailings in the past. Now there is even greater concern about potential disruption of the REE supply, such that the government, industry, and academia are partnering to develop economical extraction technologies. At the same time, we must develop recovery flowsheets that adhere to the regulatory framework of the US EPA for phosphogypsum management due to its radium content, and the US Nuclear Regulatory Commission for uranium as U<sub>3</sub>O<sub>8</sub> prior to enrichment, and thorium that could approach or exceed the concentrations meeting the ‘source material’ definition.

## **1. INTRODUCTION**

It is well known that phosphate is a non-renewable resource essential for plant growth and crop production, and it is, therefore, vital to feeding the fast-growing population of the world. But there is a lack of general awareness of many other valuable elements in phosphate ore, which may play significant roles in the development of future energy, particularly green energy, high tech equipment, and advancement of various key technologies. These elements include rare earths, uranium and thorium. Uranium in phosphate accounts for more than 80% of the world’s unconventional uranium resources, while rare earth elements in the world’s annual production of phosphate rock (about 200 million tons) total about 100 000 tons<sup>23</sup>, assuming an average REE concentration of 500 ppm. If U is not recovered during phosphate mining and processing, in the majority goes into the fertilizers and is ultimately spread on farm lands, making it impossible to ever recover. Except for the two ‘waves’ of uranium recovery from phosphoric acid due to government defense and nuclear power demands, millions of tons of these critical elements have been discarded with fertilizers and other processing streams.

---

<sup>23</sup> 1 ton = 907 185 kg (0.907 185 tonne)

## 1.1. Synopsis of phosphate mining and processing

According to the most recent estimates by the US Geological Survey and the International Fertilizer Development Center, the world's remaining phosphate reserves range from 60 and 67 billion tons, while the phosphate resources total approximately 300 billion tons. These tons are assumed to contain about 30% P<sub>2</sub>O<sub>5</sub>. In a descending order, the following countries hold most of the phosphate resources on the planet: Morocco, China, Algeria, Syria, Jordan, South Africa, the US, and Russia.

Worldwide phosphate rock production reached 200 million tons in 2011 and will likely stay at or above this level in the future. As is shown in Table I, China, Morocco and the US are the top three phosphate rock producers in the world.

Over 90% of the phosphate rock is consumed for manufacturing phosphate fertilizer mainly through the 'wet process' used to make phosphoric acid. Since 1950, the 'wet process' has quickly overtaken the thermal method as the primary technology for manufacturing phosphoric acid. Today, more than 70% of the world's phosphate rock is used to produce phosphoric acid. The primary chemical reaction in the 'wet acid' process may be expressed in the following equation using fluorapatite as the phosphate mineral and sulphuric acid as the reactant [1]:



Depending on the value of n, the process is defined as Dihydrate (n=2) process, Hemihydrate (n=1/2) process, or Anhydrate process. The term CaSO<sub>4</sub>•nH<sub>2</sub>O in the above equation is called phosphogypsum (PG). The majority of today's phosphoric acid plants is based on either the dihydrate or hemihydrate processes, with the dihydrate being more widely used.

TABLE I. PHOSPHATE ROCK PRODUCTION IN '000 TONS

| Country      | 2007    | 2008    | 2009    | 2010    | 2011    | 2012    |
|--------------|---------|---------|---------|---------|---------|---------|
| Finland      | 831     | 780     | 658     | 817     | 870     |         |
| Russia       | 10 937  | 9 810   | 9 538   | 10 844  | 10 304  | 11 300  |
| USA          | 30 231  | 30 850  | 26 609  | 25 244  | 27 619  | 29 200  |
| Brazil       | 6 095   | 6 344   | 5 949   | 5 693   | 6 094   | 6 300   |
| Peru         |         |         |         | 791     | 2 544   | 2 560   |
| Egypt        | 2 504   | 3 179   | 3 708   | 3 435   | 4 746   | 3 000   |
| Morocco      | 27 638  | 24 198  | 18 163  | 25 655  | 27 821  | 28 000  |
| South Africa | 2 553   | 2 287   | 2 237   | 2 499   | 2 468   | 2 500   |
| Tunisia      | 8 005   | 7 623   | 7 298   | 8 132   | 2 510   | 6 000   |
| Israel       | 3 050   | 3 034   | 2 530   | 3 078   | 3 118   | 3 000   |
| Jordan       | 5 546   | 6 148   | 5 271   | 6 529   | 7 589   | 6 500   |
| Saudi Arabia |         |         |         | 121     | 1 068   | 1 700   |
| Syria        | 3 678   | 3 221   | 2 147   | 3 765   | 3 542   | 2 500   |
| India        | 1 507   | 1 485   | 1 588   | 2 000   | 1 910   | 1 260   |
| China        | 62 666  | 61 800  | 64 500  | 69 100  | 73 000  | 89 000  |
| Australia    | 2 174   | 2 492   | 2 113   | 2 095   | 2 519   | 2 600   |
| Others       | 10 312  | 11 163  | 12 052  | 14 812  | 13 234  | 14 580  |
| Total        | 176 220 | 175 010 | 162 733 | 182 111 | 190 957 | 210 000 |

## 1.2. Uranium in phosphate

Uranium content in world's phosphate rock products ranges from 50 to 200 ppm averaging about 100 ppm (Tab. II). Worldwide, unrecovered U from phosphate totals about 20 million kg (based on 200 Mt rock production) per year. Using the same average uranium concentration of 100 ppm, total U in the world's 290 billion tons of phosphate resources amounts to 29 billion kg. Florida phosphate ranks near the top in terms of uranium content, which was one reason why past uranium extraction plants from phosphoric acid were built mostly in Florida. The next generation uranium extraction plants may also start in Florida.

A majority (about 65%) of the uranium in sedimentary phosphate exists in the tetravalent state in isomorphous substitution with calcium ion, because the ionic radius of  $\text{U}^{4+}$  is very close to that of  $\text{Ca}^{2+}$ , which are 0.97 Å and 0.99 Å, respectively. Uranium in hexavalent (+6) state is held by chemisorption on the phosphate surface as  $\text{UO}_2 \cdot \text{HPO}_4$ . Some U in phosphate, particularly in igneous phosphate, is associated with rare earth elements and thorium.

Wherever there are rare earth-containing minerals, there is usually thorium. Thorium is detected in nearly all phosphate ores, though at low levels. Some scientists have long believed that thorium could provide the world with an ultra-cheap and environmentally safe source of nuclear power. This approach is gaining momentum in recent years, particularly in India and China. The recently formed Weinberg Foundation in the United Kingdom also plans to push the promise of thorium nuclear energy into the mainstream political discussion of clean energy and climate change. According to Evans-Pritchard, "if China can crack thorium, it will have clean energy for 20 000 years" [2]. In his Sydney Morning Herald article titled "Safe nuclear power not a pipedream", Evans-Pritchard also talked in some detail about China's thorium program with a startup budget of \$350 million<sup>24</sup> and a staff of 140 full-time scientists at the Shanghai Institute of Applied Physics, with a plan to increase the staff to 750 people by 2015.

TABLE II. ANALYSIS OF URANIUM AND THORIUM IN PHOSPHATE ROCK FROM DIFFERENT SOURCES [3–4]

| Sample                         | Number of samples | Median content of element, ppm |         |
|--------------------------------|-------------------|--------------------------------|---------|
|                                |                   | Uranium                        | Thorium |
| Florida, USA pebble, 1926–1935 | 11                | 208                            | 14      |
| Florida, USA pebble, 1946–1955 | 14                | 148                            | 13      |
| Florida, USA pebble, 1959–1964 | 12                | 127                            | 17      |
| Florida, USA Pebble, 1994      | 3                 | 95                             | –       |
| North Carolina, USA, 1957–1964 | 3                 | 79                             | 9       |
| Utah, USA, 1936–1961           | 9                 | 128                            | 7       |
| Idaho, USA                     | 5                 | 151                            | 8       |
| Peru, washed rock, 1961–1964   | 7                 | 106                            | 8       |
| Morocco, 1937–1943             | 5                 | 141                            | 8       |
| Tunisia, 1927–1955             | 6                 | 48                             | 23      |
| Jordan, 1956–1963              | 6                 | 48                             | 0       |
| Egypt, 1936–1937               | 6                 | 122                            | 6       |
| Senegal                        | 6                 | 107                            | 17      |

<sup>24</sup> All monetary values given as US \$.

### 1.3. Rare earth elements in phosphate

Rare earth elements (REE) have very specific critical uses in a multitude of markets. Many of these applications have no substitute materials and the move to green technologies has dramatically increased their demand. Table III summarizes various REE applications.

Rare earth elements have earned their reputation for being ‘rare’ not because they are scarce in the Earth’s crust but because they ‘rarely’ exist in mineral forms that can be mined and extracted. For example, the average concentration of the rare earth elements in the Earth’s crust (ranging from 150 to 220 ppm) is much higher than that of copper (55 ppm).

TABLE III. VARIOUS USES OF RARE EARTH ELEMENTS

| Field             | Uses   |
|-------------------|--|
| Green energy      | Rechargeable batteries; electric motors; fuel cells; solar cells; wind, hydro and tidal power turbines   |
| Electronics       | Computers; fiber optics; cell phones; digital cameras; DVD and CD players; lasers  |
| Defense           | Satellite communications; night vision gear; jamming devices; predator unmanned aircraft; tomahawk cruise missile; smart bombs; bunker buster smart bomb; precision guided weapons; long range acoustic device and area denial systems |
| Magnetics         | Computer hard drives; disk drive motors; headphones and speakers; microphones; refrigeration; electric motors, anti-lock brakes  |
| Medical equipment | MRI machines; X-ray imaging; surgical lasers; surgical tools; computed tomography; electron beams  |
| Glass & ceramics  | Polishing powders; pigments and coating; tinted glasses; photo-optical glass; UV resistant glass   |
| Chemical          | Petroleum refining; catalytic converters; fuel additives; hydrogen storage; water filtration; air pollution controls; chemical processing  |
| Lighting          | LED lighting; colour TV; flat screen displays; cell phone displays; fluorescent lighting   |

Although there are over 200 minerals known to contain appreciable amounts of rare earth elements, only three of them are economically significant, they include bastnaesite, monazite and xenotime, with bastnaesite and monazite accounting for about 95% of the current sources for light rare earths. Some rare-earth-bearing clays are also significant sources for REE. Xenotime is the primary mineral for heavy REE and yttrium.

Rare earth elements may also be extracted as a by-product from processing of minerals, such as copper, gold, uranium, and phosphate ores, with phosphate having a great potential. Certain phosphate deposits, specifically the fluorapatite ores, contain significant amounts of the rare earths [5–7]. Table IV shows lanthanide content in some phosphate rock [8, 9].

TABLE IV. LANTHANIDE CONTENT IN SELECTED PHOSPHATE ROCK

| Phosphate rock source | Ln <sub>2</sub> O <sub>3</sub> (%) |
|-----------------------|------------------------------------|
| Kola, Russia          | 0.8–1.0                            |
| Florida, USA          | 0.06–0.29                          |
| Algeria               | 0.13–0.18                          |
| Morocco               | 0.14–0.16                          |
| Tunisia               | 0.14                               |

Some phosphate ores or processing streams contain much higher REE than what is shown in Table IV. A Canadian phosphate deposit near Quebec, for example, contains about 1800 ppm of rare earth elements. In some recently discovered phosphate deposits in northern China [10], REE concentration (total R<sub>2</sub>O<sub>3</sub>) ranges from 1.5%~6.41%.

#### 1.4. Fate of U in the acidulation process

In the phosphoric acid manufacturing process using the dihydrate process, about 90% of the uranium in the phosphate rock feed reports to phosphoric acid and 10% ends up in phosphogypsum, versus 80% and 20% using the hemihydrate process, respectively. Therefore, the dihydrate process favors uranium recovery. Indeed, past uranium recovery plants all used phosphoric acid produced from dihydrate based acid plants.

#### 1.5. Rare earth elements in Florida phosphate

The Florida phosphate ore (matrix) is mined in open pits using large draglines. Phosphate matrix is first transported to the beneficiation plant, and after several washing and separation steps, is turned onto four streams, pebble product, flotation concentrate product, sand tailings, and waste clay. In the chemical processing plant, the combined pebble/concentrate rock product is reacted with sulphuric acid producing a relatively concentrated phosphoric acid and phosphogypsum by-product.

Published analyses, decades old, of trace elements in Florida phosphate rock have shown that many of the vital rare earth elements are present. Though only present in trace amounts, because of the tonnage of phosphate produced, these elements are still significant in aggregate mass and have not been recovered.

A comprehensive investigation of REE in Florida phosphate was conducted by Kremer and Chokshi [11] of Mobil Research & Development Corporation. The total REE in Florida phosphate matrix analysed 282 ppm (88 ppm neodymium, 68 ppm cerium, 57 ppm yttrium, and 49 ppm lanthanum, accounting for 90%). Distributions of REE in the mining and chemical processing streams were also determined, showing 40% in waste clay, 37.5% in PG, 12.5% in phosphoric acid, and 10% in sand tailings. Data further indicated that REEs were concentrated in fine phosphate particles, as the pebble product analysed 284 ppm REE versus 575 ppm in the flotation concentrate. The high REE concentration (336 ppm) in waste clay is another evidence of REE concentrating in fine phosphate particles.

Another set of data [8] showed that Florida phosphate rock contained about 500 ppm REE, with 150 ppm lanthanum, 120 ppm cerium and 110 ppm yttrium. According to a report by the former USBM [12], Florida phosphogypsum contained 300 ppm REE, with 130–170 ppm gadolinium, 49 ppm cerium and 39 ppm lanthanum.

The most recent characterization of REE in Florida phosphate was conducted by the Florida Industrial and Phosphate Research (FIPR) Institute [13]. In this study, two sets of samples were collected from two operating mines, with each set consisting of eight samples, including fine flotation feed, coarse flotation feed, flotation concentrate, pebble product, fatty acid flotation tails, amine flotation tails, waste clay (primary slime), and phosphogypsum. Total REE concentrations in various samples are listed in Table V. REE mass balance was calculated based on chemical analysis and plant mass flow rates. For Plant A, mass balance analysis shows the following REE distributions: 61.9% in rock product, 19.6% in waste clay, and 18.2% in flotation tailings. These distributions add up to 99.7%. For the Plant B samples, mass balance analysis shows the following REE distributions: 53.19% in rock product, 39.83% in waste clay, and 8.5% in flotation tailings. These distributions add up to 101.25%.

TABLE V. TOTAL REE CONTENT IN TWO SETS OF FLORIDA SAMPLES

| Sample ID         | Total REE |         |
|-------------------|-----------|---------|
|                   | Plant A   | Plant B |
| Final concentrate | 608       | 901     |
| Pebble product    | 163       | 262     |
| Flotation feed    | 160       | 209     |
| Cleaner tails     | 153       | 335     |
| Rougher tails     | 40        | 20      |
| Waste clay        | 102       | 346     |
| Phosphogypsum     | 118       | 112     |

## 2. HISTORICAL OVERVIEW OF U EXTRACTION FROM PHOSPHORIC ACID IN FLORIDA

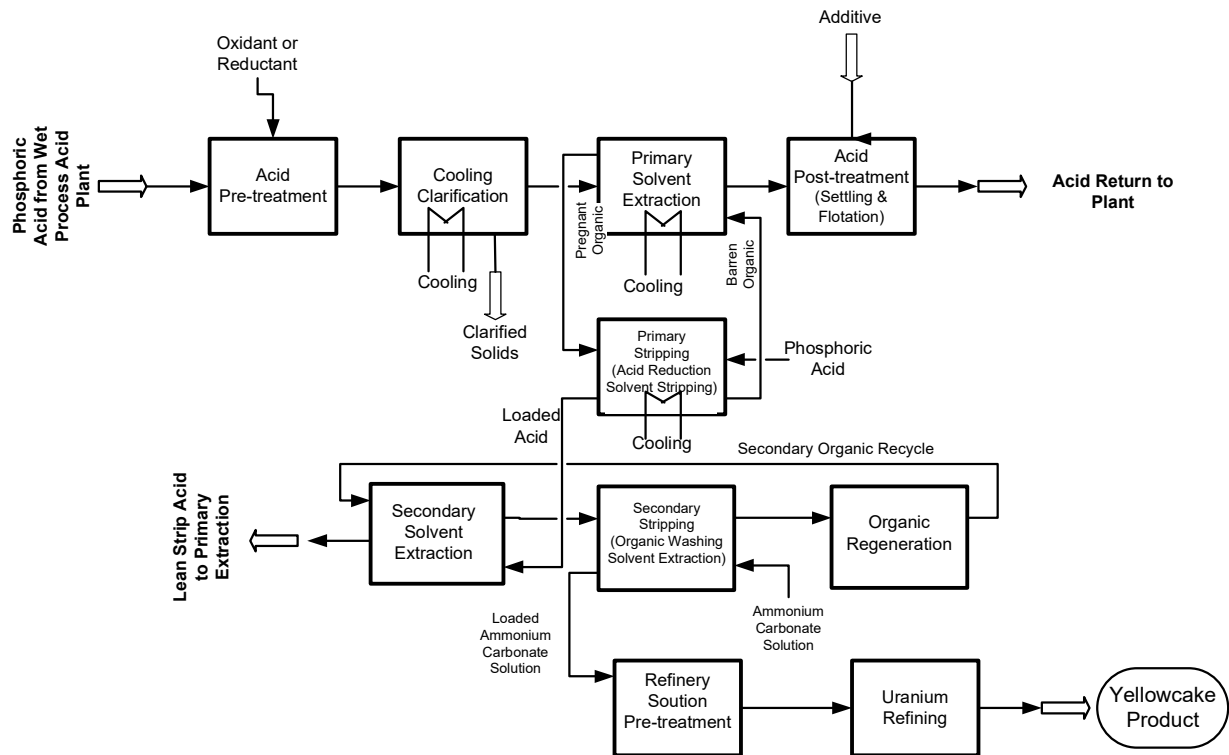
As is shown in Table VI, in the dihydrate process, uranium content in the rock feed to the wet process is very close to that in the product phosphoric acid. These results show a clear advantage of the Florida phosphate industry over other world's major phosphate producers in terms of U recovery from phosphoric acid.

TABLE VI. URANIUM IN SELECTED PHOSPHATE ROCK AND PHOSPHORIC ACID SAMPLES (PPM)

| Location | U <sub>3</sub> O <sub>8</sub> in phosphate rock | U <sub>3</sub> O <sub>8</sub> in phosphoric acid (30% P <sub>2</sub> O <sub>5</sub> ) |
|----------|---|---|
| Algeria  | 110–140   | 130   |
| Brazil   | 80  | 80  |
| Israel   | 50–150  | 165   |
| Jordan   | 120–150   | 165   |
| Morocco  | 90–140  | 140   |
| Tunisia  | 50–100  | 80  |
| Florida  | 150–180   | 190   |

The race for nuclear weapon supremacy in the 1950s prompted research and technology development for recovering uranium from phosphoric acid. In 1952, the first commercial plant was built in the US. This plant was operated by the Blockson Chemical Co. in Joliet, IL, and it used a chemical precipitation technique to recover the uranium as uraniferous phosphate [14–17]. Two other plants started operating in Florida in 1955 and 1957, one operated by International Minerals & Chemicals Corporation (IMC) at Bartow, and another by Gardiner near Tampa. This time, a solvent extraction technique was used to recover uranium. An inexpensive solvent, octyl-pyro-phosphoric acid (OPAP) was used. These uranium recovery plants were operated only for several years, because they could not compete with inexpensive sources of uranium from traditional uranium mines.

In the early 1970s, scientists at the Oak Ridge National Laboratory made great contributions to the science and art of uranium extraction from phosphoric acid [18–20]. The popular DEPA/TOPO and octyl phenyl acid phosphate (OPAP) solvent systems were optimized during this period. DEPA stands for di(2-ethylhexyl) phosphoric acid while TOPO represents trioctyl phosphine oxide. A typical overall flowsheet for extracting uranium from phosphoric acid is shown in Fig. 1 [14].



*FIG. 1. Overall process for uranium recovery from phosphoric acid, after [14].*

In the meantime, the price of uranium rose due to the rapid expansion of nuclear energy. It became particularly extractive to recover uranium from phosphoric acid in the United States. As a result, nearly all major phosphoric acid plants had a uranium plant attached, totaling eight uranium plants during peak years. Table VII shows a list of the major uranium recovery plants. These uranium recovery plants stayed quite profitable for 10–15 years. During these years they were able to improve the process economics and efficiency. The depressed uranium price eventually drove all the uranium recovery plants out of business and all of them were completely dismantled. At the time of writing there were no operating plants commercially recovering uranium from phosphoric acid in the world.

TABLE VII. URANIUM RECOVERY FROM PHOSPHORIC ACID FACILITIES [21]

| Acid producer | Location           | Capacity U <sub>3</sub> O <sub>8</sub><br>(lbs/year) | Process   | Operating period |
|---------------|--------------------|--|-----------|------------------|
| Farmland      | Pierce, FL         | 400 000  | DEPA-TOPO | 1978–81          |
| Freeport      | Uncle Sam, LA      | 690 000  | DEPA-TOPO | 1978–99          |
| Agrico        | Donaldsonville, LA | 420 000  | DEPA-TOPO | 1981–98          |
| IMC           | New Wales, FL      | 800 000  | DEPA-TOPO | 1980–92          |
| CF Industries | Bartow, FL         | 600 000  | DEPA-TOPO | 1981–85          |
| CF Industries | Plant City, FL     | 600 000  | DEPA-TOPO | 1980–92          |
| W. R. Grace   | Bartow, FL         | 330 000  | OPAP      | 1976–80          |
| Gardinier     | East Tampa, FL     | 420 000  | OPPA      | 1979–82          |
| Western Coop. | Calgary, Canada    | 120 000  | OPAP      | 1981–87          |
| Chemie Rupel  | Purrs, Belgium     | 150 000  | DEPA-TOPO | 1980–98          |

As is indicated in the table above, all uranium extraction from phosphoric acid was done using the solvent extraction technology. A generic uranium recovery plant involves the following steps:

- 1) Acid pre-treatment;
- 2) First cycle solvent extraction;
- 3) First cycle stripping;
- 4) Second cycle solvent extraction;
- 5) Second cycle stripping;
- 6) Acid uranium solution oxidation/precipitation;
- 7) Calcination to produce the product ‘yellow cake’.

The acid pre-treatment serves three major purposes: lowering acid temperature to allow precipitation of Na<sub>2</sub>SiF<sub>6</sub> and CaSO<sub>4</sub> for more efficient solvent extraction; bringing uranium to the appropriate valence state (U<sup>+6</sup> or U<sup>+4</sup>) for the specific solvent by either oxidation or reduction; and removing suspended solids and organics thus reducing ‘crud’ formation. As one can see, pre-treatment could be quite elaborate and expensive.

The first cycle stripping is carried out using concentrated phosphoric acid so that uranium is transferred into a smaller volume of acid.

In the secondary stripping, the pregnant secondary organic containing the U is contacted with an alkaline solution in a mixer/settler system. Here the U is stripped from the organic solvent and transferred to the alkaline solution in a more concentrated form. The secondary strip solution is then treated to neutralize the alkali and produce an acidic uranium solution.

For production of the final product, the acid uranium solution may be oxidized in the following manners:

- 1) With hydrogen peroxide to form uranyl peroxide UO<sub>4</sub>·nH<sub>2</sub>O;
- 2) With ammonia to form ammonium diuranate (ADU), (NH<sub>4</sub>)<sub>2</sub>U<sub>2</sub>O<sub>7</sub>;

- 3) With ammonium carbonate (or ammonia+CO<sub>2</sub>) to form ammonium uranyl tricarbonate (AUT), (NH<sub>4</sub>)<sub>4</sub>U<sub>2</sub>O<sub>7</sub>(CO<sub>3</sub>)<sub>3</sub>.

The final product is produced by thickening, washing, drying and calcining the above products to produce U<sub>3</sub>O<sub>8</sub> yellow cake.

Each of the uranium recovery plants started in the 1970s had their advantages and disadvantages, presenting many opportunities for improving efficiency in designing the third-generation plants. For example: the pre-treatment costs for the past plants ranged from \$0.5 to \$9 per kilogram of U<sub>3</sub>O<sub>8</sub>; solvent loss varied between \$4 and \$12 per kg; capital costs had a low of \$25 million and high of \$67 million; and total operating costs varied from \$24 to \$40 per kg.

### 3. GOING FORWARD

Although there is no uranium recovery plant in operation today, research and pilot testing efforts are intensive worldwide, which is particularly enhanced by the UxP (Uranium eXtraction from Phosphates and Phosphoric Acid) program lead by the International Atomic Energy Agency (IAEA) and Aleffgroup, with several other contributors [22–25].

#### 3.1. Recent developments in uranium recovery from phosphoric acid

Perhaps the most significant development in uranium extraction from phosphoric acid is the advancement of the ion exchange technology. Recently, Uranium Equities successfully completed another round of pilot scale demonstration of U recovery from phosphoric acid based on the patented PhosEnergy (ion exchange) technology in two acid plants in the US [26]. Uranium Equities estimates the cash operating cost of uranium production using the PhosEnergy Process to be \$20–25/lb U<sub>3</sub>O<sub>8</sub>, with a capital cost of \$100/lb U<sub>3</sub>O<sub>8</sub>. Also, a Florida engineering firm has recently manufactured and shipped a few modular ion exchange plants to different clients. The ion exchange method does not have three of the vexing problems associated with the solvent extraction technology: emulsion, solvent loss, and crud formation. In addition, the phosphate producers prefer not to handle and store flammable solvents.

Under the phosphate project of the Critical Materials Institute (CMI), the Oak Ridge National Laboratory (ORNL) of the US and the Florida Industrial and Phosphate Research (FIPR) Institute teamed up to conduct advanced beneficiation and extraction studies on recovery of uranium and rare earths from phosphate. Since the official beginning of the CMI program on 1 July 2013, this team has made significant progress both in concentrating REE-containing minerals from various phosphate processing products and extraction of REE/U from leach solutions as well as phosphoric acid.

Research efforts in this area have intensified recently worldwide, both on lab and pilot scales. Ongoing pilot scale investigations are conducted in Egypt, Tunisia, Morocco, Jordan, and the US. Commercialization efforts will likely pick up, as fears of further nuclear power accidents ease. Reuters reported on 30 June 2014 that “China was set to beat its 2020 targets for nuclear power, after getting back on track with projects that had been halted after Japan's Fukushima disaster”. Beijing is undertaking the world's biggest expansion of civilian nuclear power as the government aims to increase its use of cleaner energy. India is also moving ahead with its planned nuclear power projects. As the carbon footprint becomes a more and more critical global warming issue, nuclear power could become the energy technology of choice rather than an underutilized option.

#### 3.2. Recovery of rare earth elements from phosphate and phosphoric acid

Until recently, research efforts to recover rare earth elements from phosphate had been sporadic, and had not been put on the agenda of the research community, the industry or any governments. That lack of conviction was mainly attributed to the fact that in the wet phosphoric acid manufacturing process, only about 30% of the rare earth elements in the feed rock reported in the acid phase, with the rest ending up in the large volume of stockpiled phosphogypsum. However, a good case can be made about the

potential and viability of recovering rare earths from phosphate, not only from phosphoric acid, but also from other processing streams. This case can be built using Florida as an example. Fig. 2 is a graphic demonstration of REE distribution in the four major phosphate mining and processing streams.

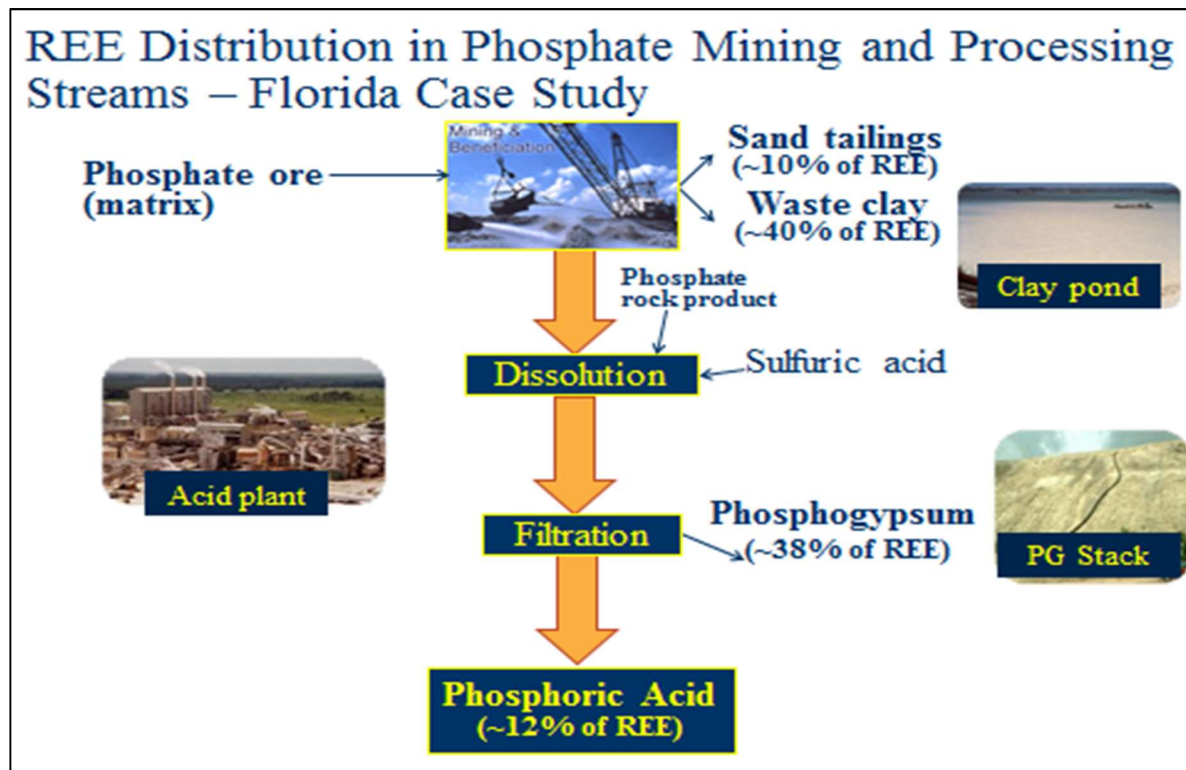


*FIG. 2. REE Distribution in different phosphate mining and processing streams.*

Figure 2 indicates that every processing stream is worth pursuing for REE recovery. In January 2014, the Critical Materials Institute (CMI) and the Florida Industrial and Phosphate Research (FIPR) Institute co-organized a workshop on uranium and rare earths in phosphate. At the workshop, both industry representatives and scientists endorsed four ‘swim lanes’ for CMI and FIPR to move forward with their efforts to recover U and REE, including flotation tailings, phosphoric acid, waste clay and phosphogypsum.

### 3.3. Pre-concentration of U and REE from different streams

Since REE content in any of the phosphate streams is very low, pre-concentration is necessary prior to acid leaching for their recovery. Otherwise, acid consumption and handling of large amounts of materials would make any extraction approach economically prohibitive. Previous analysis showed that both U and REE strongly correlate with phosphate. Therefore, the first step towards economic recovery of U and REE from many of the streams is to concentrate phosphate using inexpensive beneficiation techniques.

#### 3.3.1. Waste clay

The waste clay contains up to 50% clay minerals. In order to concentrate the phosphate, it is necessary to remove most of the clay minerals. Clay particles are extremely fine ( $\pm 1$  micron), and can be separated from other minerals using hydrocyclone, an inexpensive method for separating particles in slurry form without chemicals. After clay removal, phosphate can be further upgraded using flotation.

### *3.3.2. Amine tails*

REE in this stream exists in three major forms, in monazite, heavy minerals (such as zircon) and calcium substitution in phosphate crystals. The major gangue mineral is quartz. With a specific gravity of 2.6, quartz can be separated using gravity separation methods from other heavier minerals: phosphate (specific gravity 3.2), monazite (specific gravity 5.0–5.3), and zircon (specific gravity 4.6–4.7). Gravity separation testing using a shaking table concentrated the REE minerals in about 13% of the original mass, achieving over 60% recovery of all the major REE.

### *3.3.3. Phosphoric acid*

The easiest and perhaps the most economical way of recovering the REE from phosphate is to extract them from the phosphoric acid. The key to success for this approach is to increase REE enrichment in the acid phase. Research work by the National Engineering Research Center for Rare Earth Materials of China [27] showed that REE leaching efficiency into the phosphoric acid phase could be increased to 75% by three methods: lowering leaching temperatures, reducing the solid/liquid ratio in the reactor, and adding surfactant to enhance gypsum crystal growth thus reducing REE adsorption. Of course, any change in operating parameters for REE recovery must be easy to implement, and have minimal impacts on phosphoric acid production.

### *3.3.4. Phosphogypsum (PG)*

PG holds nearly 40% of the REE in the original phosphate ore. In the ‘wet process’ for phosphoric acid manufacturing, roughly five tons of PG are produced for each ton of P<sub>2</sub>O<sub>5</sub> product. The large volume of PG makes it challenging to recover the REE from it economically. However, if REE could be shifted to the acid phase, this would not be a problem. Nevertheless, some studies for REE recovery from PG achieved promising results. A Russian company was even talking about commercializing a process for REE recovery from PG.

## **3.4. Simultaneous recovery of U and REE**

The best approach to recover REE from phosphate is to combine it with uranium recovery. In their 1976 US patent, Wamser and Bruen [28] disclosed a method for simultaneous recovery of fluorine, uranium and rare earth metal from phosphoric acid. Although the patent is based on phosphoric acid production by leaching phosphate minerals by hydrochloric acid, the approach may be applied to sulphuric acid leaching. As a matter of fact, some researchers have attempted to recover both uranium and rare earths from phosphoric acid made by sulphuric acid leaching [29–31].

Recent CMI research discovered promising reagent systems for simultaneous recovery of U and REE while leaving a majority of the thorium behind.

## **4. CONCLUSIONS**

Florida phosphate has the potential to become a vast resource for both uranium and rare earths.

Past experiences in uranium recovery from phosphoric acid in Florida are valuable for designing more efficient, third generation U recovery plants.

Simultaneous recovery of U and REE enhances each other’s economic and environmental viability.

## **ACKNOWLEDGEMENTS**

This research was funded by the Florida Industrial and Phosphate Research Institute under contract FIPR #12-02-186. The authors want to thank V. Astley and R. Stana for their contribution to this paper.

## REFERENCES

- [1] UNITED NATIONS INDUSTRIAL DEVELOPMENT ORGANIZATION (UNIDO) AND INTERNATIONAL FERTILIZER DEVELOPMENT CENTER (IFDC), editors, *Fertilizer Manual*, Kluwer Academic, The Netherlands (1998).
- [2] EVANS-PRITCHARD, A., Safe nuclear power not a pipedream, Sydney Morning Herald (8 January 2013).
- [3] MENZEL, R., Uranium, radium, and thorium content in phosphate rocks and their possible radiation hazard, *J. Agricultural and Food Chemistry*, **16** 2 (1968) 231–234.
- [4] EL-SHALL, H., BOGAN, M., Characterization of future Florida phosphate resources, Final Rep., FIPR Publication No. 02-082-105 (1994).
- [5] JORJANI, E., et al., Prediction of Yttrium, Lanthanum, Cerium, and Neodymium Leaching Recovery from Apatite Concentrate Using Artificial Neural Networks, *J. Univ. Science and Technology Beijing* **15** 4 (2008) 367–374.
- [6] BECKER, P., *Phosphates and Phosphoric Acid: Raw Materials, Technology, and Economics of the Wet Process*, Marcel Dekker, New York (1983).
- [7] PRESTON, J.S., COLE, P.M., CRAIG, W.M., FEATHER, A.M., The recovery of rare earth oxides from a phosphoric acid by-product. Part 1 Leaching of rare earth values and recovery of a mixed rare earth oxide by solvent extraction, *Hydrometallurgy* **41** (1996) 1–19.
- [8] ALTSCHULER, Z.S., et al., Rare Earths in phosphorites – geochemistry and potential recovery, Intermountain Assoc. Petrol. Geol. Ann. Conf. Guidebook No. 15 (1967) 125–135.
- [9] BLISKOVSKIY, V.Z., MINEYEV, D.A., KHOLODOV, V.N., The lanthanide composition of phosphorites, *Doklady Akad Nauk SSR*. **186** (1969) 230–234.
- [10] XIA, X.H., “The distribution characteristics and potential of endogenous phosphate rock in north China”, Proc. Conf. Beneficiation of Phosphates VI, Kunming, China (2011).
- [11] KREMER, R.A., CHOKSHI, J.C., Fate of rare earth elements in mining/beneficiation of Florida phosphate rock and conversion to DAP fertilizer, Research Report, Mobil Mining and Minerals Company, Nichols, Florida (1989).
- [12] MAY, A., SWEENEY, J.W., Evaluation of radium and toxic element leaching characteristics of Florida phosphogypsum stockpiles, USBM Report of Investigation #8776 (1983).
- [13] ZHANG, P., “Recovery of critical elements from Florida phosphate: Phase I. Characterization of rare earths,” Proc. ECI Int. Conf. Rare Earth Minerals/Metals – Sustainable Technologies for the Future, San Diego (2012).
- [14] ASTLEY, V., STANA, R., “Recovery of uranium from phosphoric acid: history and present status,” *Beneficiation of phosphates: new thought, new technology, new development*, (ZHANG, P., MILLER, J., EL-SHALL, H., Eds), Society for Mining, Metallurgy, and Exploration, Inc., Englewood, CO (2012).
- [15] RING, R.J., Recovery of byproduct uranium from the manufacture of phosphatic fertilizers, *Atomic Energy* (1977) 12–20.
- [16] BRITISH NUCLEAR FUELS LTD., By-product uranium from phosphoric rock (1976).
- [17] The recovery of uranium from wet-process phosphoric acid – part 1. *Phosphorous & Potassium* **111** (1981) 31–34.
- [18] HURST, F.J., “Recovery of uranium from wet process phosphoric acid by solvent extraction,” paper presented at AIME Annual Meeting, Las Vegas, NV 1976, AIME preprint 76-B-66 (1976).
- [19] HURST, F.J., CROUSE, D.J., Oxidative stripping process for the recovery of uranium from wet-process phosphoric acid, US Patent 3,835,214A (1974).
- [20] HURST, F.J., CROUSE, D.J., BROWN, K.B., Recovery of uranium from wet phosphoric acid”, *Ind. Eng. Chem. Process Des. Develop.* **11** (1972) 122–128.
- [21] POOL, T., “Uranium from phosphoric acid: is it time (again)?”, *Beneficiation of Phosphates: Technology and Sustainability*, (P. ZHANG ET AL., Eds), Society for Mining, Metallurgy, and Exploration, Inc. Littleton, CO (2006) 69–78.
- [22] MOUSSAID, M., UxP - Uranium eXtraction from phosphates and phosphoric acid. [www.uxponline.com/Home.aspx](http://www.uxponline.com/Home.aspx). Accessed October 2012.

- [23] ZHANG, P., “Sustainable, comprehensive utilization of phosphate resources”, paper presented at IAEA Regional Training Workshop: Uranium Resources Assessment and Recovery from Phosphate and Rare Earth Elements Ores, Cairo, 2012.
- [24] CHTARA, M.C.,“Rare earth elements in Tunisian phosphate and phosphoric acid”, paper presented at IAEA Regional Training Workshop: Uranium Resources Assessment and Recovery from Phosphate and Rare Earth Elements Ores, Cairo, 2012.
- [25] GADO, H.S., “The Egyptian experiment for the uranium extraction from phosphoric acid”, paper presented at IAEA Regional Training Workshop: Uranium Resources Assessment and Recovery from Phosphate and Rare Earth Elements Ores, Cairo, 2012.
- [26] URTEK, PhosEnergy Demonstration Plant Update, [http://www.urtekllc.com/fileadmin/news/20120919\\_Phosphoric\\_Acid\\_Demonstration\\_Plant\\_Update.pdf](http://www.urtekllc.com/fileadmin/news/20120919_Phosphoric_Acid_Demonstration_Plant_Update.pdf), Accessed 1/26/2013.
- [27] WANG, L., et al., Recovery of rare earths from wet-process phosphoric acid, *Hydrometallurgy* **101** (2010) 41–47.
- [28] BUNUS, F., “Uranium and rare earth recovery from phosphate fertilizer industry by solvent extraction,” *Mineral Processing and Extractive Metallurgy Review* **21** (2000) 381–478.
- [29] WAMSER, C., BRUEN, C., “Recovery of Fluorine, Uranium and Rare Earth Metal Values from Phosphoric Acid By-product Brine Raffinate,” US patent 3,937,783 (1976).
- [30] WETERINGS, K., JANSSEN, J., recovery of uranium, vanadium, yttrium and rare earths from phosphoric acid by a precipitation method, *Hydrometallurgy* **15** 2 (1985) 173–190.
- [31] BUNUŞ, F., DUMITRESCU, R., Simultaneous extraction of rare earth elements and uranium from phosphoric acid, *Hydrometallurgy* **28** 3 (1992) 331–338.
- [32] BUNUŞ, F., MIU, I., DUMITRESCU, R., Simultaneous recovery and separation of uranium and rare earths from phosphoric acid in a one-cycle extraction-stripping process, *Hydrometallurgy* **35** 3 (1994) 375–389.

# **REGULATORY PREPARATION TOWARDS COMMENCEMENT OF URANIUM MINING AND PROCESSING OF RADIOACTIVE ORES IN TANZANIA**

M.S. GURISHA\*, C.L. KIM\*, I.S.N. MKILAHA\*\*

\* Department of NPP Engineering,  
KEPCO International Nuclear Graduate Schools,  
Ulsan, Republic of Korea

\*\* Tanzania Atomic Energy Commission,  
Arusha, United Republic of Tanzania

## **Abstract**

The regulatory preparatory work undertaken by the government of United Republic of Tanzania through Tanzania Atomic Energy Commission (TAEC) following the Mkuju River Uranium Project definitive feasibility study is discussed. The project, which has been taken over by ARMZ Uranium One, acquired a construction permit in April 2013, where by 345 km<sup>2</sup> of land inside the 50 000 km<sup>2</sup> world heritage Selous Game Reserve was allocated for the purpose. The project has been realized through the government effort to strengthen the regulatory framework via the revised Atomic Energy Act No. 7 of 2003, preparations of Radiation Safety in Mining & Radioactive Ores Regulations of 2011, and the human resource capacity development in areas related to inspection and licensing. Sample collection in Bahi and Manyoni areas in the central part of the country to investigate Uranium uptake from the plants and radioactivity from water and plant samples is ongoing. The regulatory preparatory work will provide an opportunity to the public to comprehend the measures undertaken by TAEC to protect human health and the environment.

## **1. INTRODUCTION**

Uranium (chemical symbol U) is a naturally occurring radioactive element. In its pure form it is a silver-coloured heavy metal, similar to lead, cadmium and tungsten. Like tungsten it is very dense, about 19 grams per cubic centimetre, 70% more dense than lead. It is so dense a small 10-centimetre cube would weigh 20 kilograms. In its natural state, it consists of three isotopes (U-234, U-235 and U-238). Other isotopes that cannot be found in natural uranium are U-232, U-233, U-236 and U-237 [1].

Uranium mineralization in Tanzania was first discovered in follow-up exploration to country wide airborne radiometric surveys completed in the late 1970s [2]. Uranium deposit types in Tanzania are sandstone hosted (oxidizing reducing conditions in sandstones) with examples of similar deposits at Beverley Australia and Inkai in Kazakhstan. The most significant deposits of this type are contained within permeable sandstones. Mineralization occurs when oxidizing fluids transport the uranium into sandstone, where it is deposited under reducing conditions. The uranium deposits of Tanzania are of such type potentially suitable for in-situ leaching ore extraction, so the mining company ARMZ's Uranium One preparing to exploit the same technology at its Mkuju River deposit [3].

The technology is only feasible for permeable ore bodies such as sandstone-hosted deposits. The greatest advantage of in-situ leaching (Fig. 1) is that the host rock is relatively undisturbed, with no open pits or waste tailings to deal with. The largest uranium mining operations currently using the in-situ leach method are in Kazakhstan.

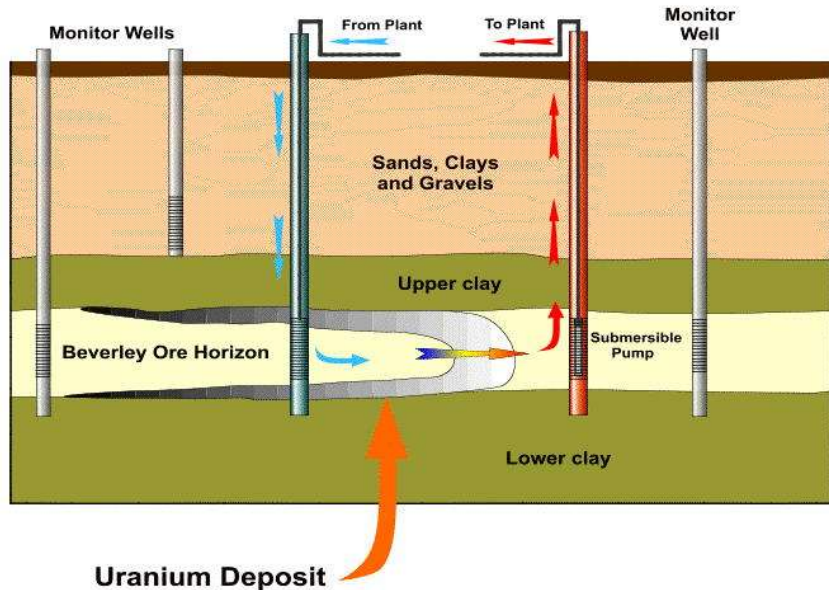


*FIG. 1. In situ leaching uranium mining (courtesy Heathgate Resources).*

Though Tanzania's government appears to be determined to take part in the lucrative mining business, however, the public is still reluctant and facing anxiety towards operations of mining. The nervousness has been accelerated by the NGOs from outside and within the country which have been actively promoting opposition to uranium mining in Tanzania. Beyond that, some nations are starting to phase out the nuclear option and there is increasing pressure by the people of the world for a complete abolition of nuclear weapons [4]. On the other hand, distrust from the public toward uranium projects was magnified by the nuclear reactor catastrophes that most recently took place in Fukushima Daiichi in Japan. The regulatory preparatory work therefore will provide an opportunity to the public to comprehend the measures undertaken by TAEC to protect their health and environment, and finally compromise with the government decision towards mining radioactive ores.

## 2. LOCATION OF MKUJU RIVER PROJECT

Uranium One/Mantra's Mkuju River Project (MRP) is located in southern Tanzania, about 470 km southwest of Dar es Salaam. The Project comprises twenty-six contiguous tenements covering an area of over 3250 km<sup>2</sup>. Mantra, through its wholly owned subsidiaries, controls 100% of the Project area, including the Nyota Prospect. Nyota falls on Prospecting License No. PL 4700/2007. The Prospecting License was granted by the Ministry of Energy and Minerals to Mantra Tanzania Limited on 18 September 2007 and tenement PL 4700/2007 is subject to a Special Mining License application [2, 3].

The MRP area falls along a spine of the roughly north-south oriented ridges along the Mbarangandu and Luwego River drainage divide. Natural weathering over the Mkuju Series topographical units has resulted in the development of steep sided, incised valleys and generally narrow, prominent ridge crests. Large, cliff faces, 20–40 m high, have developed in certain areas, with circular slumping also prevalent in the soft, weakly consolidated sedimentary rocks.

## 3. REGULATORY FRAMEWORK

Discovery of uranium mining in Tanzania has led to the increased in number of mineral types found in the country. However, mining and processing of radioactive ores is a big challenge to the government, and therefore triggering a special call for its management. In view of that, the United Republic of Tanzania (URT) through the Tanzania Atomic Energy Commission (TAEC) has exerted itself to strengthen the regulatory framework to overcome the major challenging issues, topmost being public health and environmental safety. TAEC was established as the regulatory body on 1 July 2004, replacing

the previous National Radiation Commission (NRC) [5]. A new regulatory body which is the official government body responsible for all atomic energy matters in Tanzania, was established by the Tanzania Atomic Energy Act No. 7 of 2003. The Commission took over all the responsibilities and functions of the former National Radiation Commission that was earlier established from the Protection from Radiation Act No. 5 1983 but with some added responsibilities and functions. The main functions and responsibilities of the Commission (TAEC) are to:

- Be responsible for all matters relating to the safe and peaceful use of atomic energy and nuclear technology including radioactive materials and radiation devices, with a view to ensuring the promotion of their applications and protection of workers, patients and the public generally from harm resulting from radiation;
- Establish and operationalize or implement a system for the control and authorization through registration and licensing of the importation, exportation, movement, possession or use of atomic energy and radiation sources;
- Carry out regulatory inspections and ensure that corrective actions are taken if unsafe or potentially unsafe conditions are detected.

In 2011, the URT government through TAEC revised the Atomic Energy Act No. 7 of 2003 to accommodate the uranium mining and milling activities which were not reflected in the legislation. This assignment was followed by the development of Radiation Safety in Mining and Processing of Radioactive Ores Regulations of 2011 for the promulgation, monitoring, and enforcement of the Act [6]. The process was initiated by creating a draft of regulation which was revised by the regulatory staffs and then an IAEA expert through a expert mission followed by stakeholder discussions, agreement on the draft and finally the regulation was endorsement by the government Authority. The process of developing the guidance documents such as inspection and enforcement manuals, authorization and license procedures is ongoing at the Commission level.

#### 4. THE ROLE OF IAEA

The government of URT is constantly receiving support from the IAEA through the Technical Cooperation programme to continue the strengthening of regulatory framework through training programs on uranium mining and processing activities, expert missions and scientific visits. The support has been realized through regional and interregional projects RAF3007 and INT2016 respectively. Moreover, further supports are anticipated from the newly approved national project URT9006. Through this project more data will be collected from the uranium mining and exploration vicinity such as Bahi and Manyoni in central Tanzania to predict, assess, and mitigate environmental impacts on the communities surrounding these sites and to build capacity to conduct systematic and continual monitoring of biophysical and human environments.

#### 5. PUBLIC AWARENESS

The Tanzania Atomic Energy Commission (TAEC), as the government body responsible for Atomic Energy Matters in the country, is liable with the provision of awareness training to the public as part of its mandate. The training has been delivered through different approaches such as seminars in the mining locality to stimulate occupational understanding on uranium mining and safety related issues. Emphasis was also given to indigenous stakeholders, and therefore a number of seminars were conducted to local leaders and communities surrounding the mining site to alleviate fears and to minimize negative impacts (Fig. 2). Health effects related to radioactive materials were also highlighted during the sessions. The radio and TV documentary has been prepared by the regulatory staffs and air time has been provided to them to educate the public. Furthermore, special training courses were organized for the government officers from Ruvuma, Dodoma and Singida region and Members of Parliament as well.

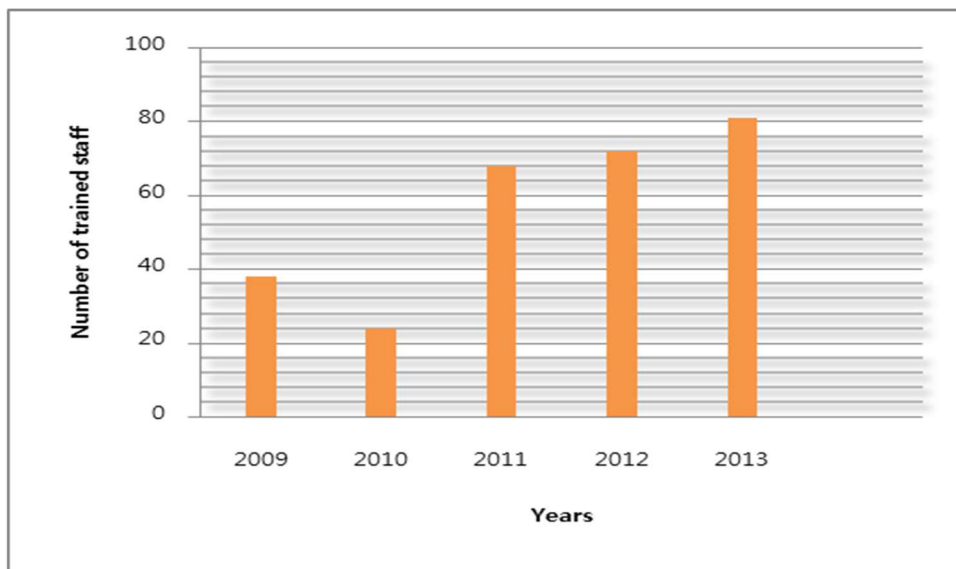


*FIG. 2. Trends of training/seminars delivered to public as from 2009.*

## 6. HUMAN RESOURCE CAPABILITY DEVELOPMENT

TAEC has a training programme, which is reviewed continuously based on funds availability and time demand. Currently the Commission is facing a big challenge on how to regulate the uranium mining activity. However, more resources have been invested to train TAEC staffs in different fields including uranium. At this point in time, the emphasis has been kept in the area of inspection, licensing, and monitoring of biophysical and human environments. In recent years (starting from 2009) a number of TAEC staff have been enrolled into different postgraduate studies such as MSc and PhD in different Universities locally and abroad to study, among other topics, Nuclear Physics specialized in Uranium Mining, NORMs and Environmental Management (UM), Nuclear Medicine, Medical Imaging, (MD) Nuclear Engineering (NE), Non Ionizing Radiation (NI), and Radiation Protection (RP) (Fig. 3).

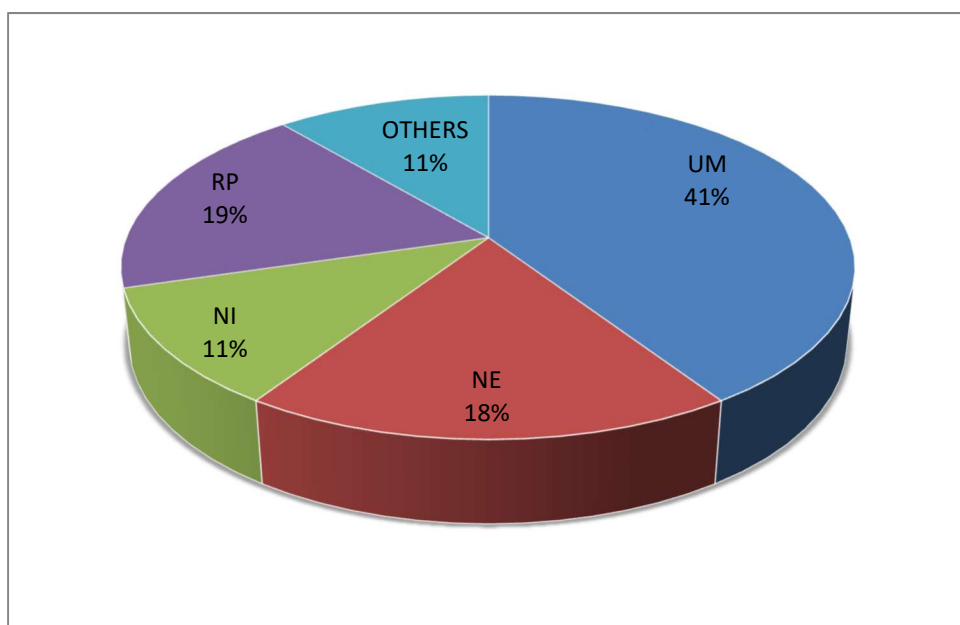


*FIG. 3. Number of TAEC staff trained in different area of specialization as from 2009.*

## 7. CONCLUSION AND RECOMMENDATIONS

From the beginning of the uranium exploration projects, TAEC has been pushing all the way using the available capability to make sure that uranium mining activities are conducted in a safe way according to the international regulatory standards. However, some drawbacks are always on the sideways of the better plan. Lack of enough funds to train enough staff and a lack of competent training institute within the country have been a dragging force constraining the necessary effort of the country to achieve the human resources capacity development plan.

On-the-job training/fellowships from the uranium mining developed countries like Australia, Canada, South Africa and Namibia are highly recommended to TAEC staff to allow them to acquire enough exposure on how to inspect, license and to develop guidance documents such as inspection and enforcement manuals as well as authorization procedures. The arrangement can be made in collaboration with URT government and the IAEA through its Technical Cooperation programme [7].

Uranium mining is new to URT and inevitably, the regulator will be inexperienced for sometimes compared to the operator in certain specialist respects. However, in the case where there is a deficit in specialist knowledge and experience, the deficit can be managed and progressively eliminated with foresight and planning. Over time the regulator will extend existing capabilities into this new area and learn the uranium specific aspects. Working with a responsible operator the regulator can learn and develop these capabilities without compromising regulatory control. Improving regulatory competence by defining competency criteria and training are also proposed.

## ACKNOWLEDGEMENTS

The authors would like to express their gratitude to the International Atomic Energy Agency (IAEA) and KEPCO International Nuclear Graduate School (KINGS) for the provision of assistances and allow an author to participate in the URAM-2014 International Symposium. The authors are also indebted to the Tanzania Atomic Energy Commission (TAEC) for granting permission to publish this information.

## REFERENCES

- [1] [SOUTH AFRICAN] NATIONAL NUCLEAR REGULATOR COMMUNICATIONS AND STAKEHOLDER RELATIONS OFFICE, Fact Sheet Depleted Uranium (2012).
- [2] KAROO EXPLORATION CORP, Why Tanzania (2013),  
<http://www.karooexploration.com/why-tanzania/ID567741>.
- [3] BOYTSOV, A., STANDER, S., MARTYNENKO, V., “The outlook on potential uranium ISL mining at Nyota Deposit (Tanzania)”, Proc. Int. Symp. on Uranium Raw Material for the Nuclear Fuel Cycle: Exploration, Mining, Production, Supply and Demand, Economics and Environmental Issues (URAM-2014), 2014 IAEA, Vienna (these proceedings).
- [4] Uranium Mining - Impact on Health and Environment, (Proc. Int. Conf., Dar es Salaam 2013), Rosa Luxemburg Stiftung, Dar es Salaam (2014).
- [5] UNITED REPUBLIC OF TANZANIA, the Atomic Energy Act. No.3 of United Republic of Tanzania (2003).
- [6] UNITED REPUBLIC OF TANZANIA, Radiation Safety in Mining and Processing of Radioactive Ores Regulations of (2011).
- [7] UNITED REPUBLIC OF TANZANIA, Radiation and Waste Safety Infrastructure Profile (RaWaSIP) (2012).

# **THE LAST TWENTY YEARS OF THE IAEA TECHNICAL COOPERATION ON THE URANIUM PRODUCTION CYCLE IN ARGENTINA**

L. LOPEZ

National Atomic Energy Commission (CNEA),  
Buenos Aires, Argentina

## **Abstract**

During the last two decades, the National Atomic Energy Commission of Argentina (CNEA) has been involved in several IAEA Technical Cooperation Projects at interregional, regional and national levels, covering different aspects of the Uranium Production Cycle. This has aided the design of programs in the country that consider a more sustainable use of uranium resources for nuclear power generation.

## **1. INTRODUCTION**

Since 1993, the National Atomic Energy Commission of Argentina (CNEA) has been involved in several IAEA Technical Cooperation Projects at interregional, regional and national levels, covering different aspects of the uranium production cycle which can be listed as follows [1, 2]:

- INT 2/015 "Supporting Uranium Exploration Resource Augmentation and Production Using Advanced Techniques" (2012–Present) [3, 4];
- RLA 3/006 - 010 "Upgrading of Uranium Exploration, Exploitation and Yellowcake Production Techniques taking Environmental Problems into Account" (2007–Present) [5];
- ARG 2/014 "Development and Strengthening of the Uranium Mining Cycle Human Resources" (2012–Present) [6];
- ARG 3/012–014 "Geology favourability, production feasibility and environmental impact assessment of uranium deposits exploitable by the in situ leaching technology (ISL)" (2007–Present) [7];
- ARG 3/009 "Development and use of biological techniques for uranium production (ARG 3/009)" (2003–2006) [8];
- ARG 3/008 "Prospection of uranium and other elements using gamma-ray spectrometry surveys" (2001–2005) [9];
- ARG 3/007 "Uranium Favourability and Exploration in Argentina" (1993–1997) [10].

## **2. DESCRIPTION**

The project activities were carried out by the Raw Material Exploration and Production Branches of the CNEA, which have Regional Offices in the central, northern, southern and western parts of the country and a Mining–Milling Complex in the province of Mendoza.

The IAEA Technical Cooperation programme supported interaction with specialized uranium technology organizations from Australia, Brazil, Canada, Czech Republic, France, Kazakhstan and USA.

The technology transfer was carried out through three lines of action:

- Development and strengthening of human resources in the uranium mining cycle fulfilled through the implementation of expert missions, scientific visits, training courses both overseas and in-country, and through participation in national and international meetings;

- Operational capabilities acquired to support the exploration activities, emphasizing innovative technology (GIS, magneto telluric techniques, well logging geophysics, and gamma ray spectrometry) and concepts (U unconventional resources, ISL mining, comprehensive extraction, UNFC-2009 [11], social licensing, stakeholder communication);
- A high degree of efficiency was achieved due to a large extent to the fact that at the same time as the technology transfer, within the framework of institutional goals and public investment projects dedicated to nuclear raw materials, the CNEA has been carrying out different projects in different geological domains with the aim of defining new uranium resources and its production feasibility.

The logical framework matrix for the TC projects involved the following outputs: uranium favourability and exploration, production feasibility, environmental impact assessment, regulatory issues, development of human resources programmes, and the purchase and startup of new equipment. As part of the purchasing procedure for relevant equipment, on-site training courses on installation and operation were implemented by the provider, which was beneficial and expedient for the working groups.

### 3. FINAL CONSIDERATIONS

The TC projects contribute to develop the uranium potential of the country and the knowledge of state of the art of the uranium production cycle constitutes a baseline for building a uranium mining strategy, by gathering examples of both good and bad practices implemented in the past.

In addition to the direct benefits for the CNEA, the results of the TC projects help the design of future programs in the country that consider a more sustainable use of uranium resources for nuclear power generation.

### ACKNOWLEDGEMENTS

This contribution attempts to sum up in a few words several activities that were conducted with funding from the International Atomic Energy Agency and the National Atomic Energy Commission (Argentina). The author is grateful to both institutions for allowing its presentation.

### REFERENCES

- [10] INTERNATIONAL ATOMIC ENERGY AGENCY, Technical cooperation programme, <https://www.iaea.org/services/technical-cooperation-programme> .
- [2] LOPEZ, L., FERREYRA, R., “Overview of the IAEA national technical cooperation projects on uranium exploration in Argentina”, Proc Int. Symp. Uranium raw material for the nuclear fuel cycle: exploration, mining, production, supply and demand, economics and environmental issues (URAM–2009)”, IAEA–TECDOC–1739, IAEA, Vienna (2014) Appendix, TC workshop.
- [3] TULSIDAS, H., ZHANG, J., “Enabling sustainable uranium production in a global context”, paper presented at IAEA INT0085 Best Practices Dissemination Mtg, Vienna, 2014.
- [4] LOPEZ, L., IAEA TC Project INT/2/015, Country Report, Argentina, internal report (2013).
- [5] CASTILLO, A., IAEA TC Project RLA/3/006-010 — Country Report — Argentina, IAEA–CNEA internal reports (2007-2013) unpublished.
- [6] LOPEZ, L., Project Progress Assessment Report, TC Project ARG/3/012-014, IAEA internal reports (2012–2014) unpublished.
- [7] LOPEZ, L., SLEZAK, J., Technological transfer on in situ leaching (ISL) mining: A more sustainable alternative for uranium production in Argentina, paper presented at IAEA INT0085 Best Practices Dissemination Mtg, Vienna, 2014.
- [8] SILVA PAULO, P., et al., “Evaluation of microbial leaching of uranium from Sierra Pintada ore, preliminary studies at laboratory scale”, paper presented at IAEA Tech. Mtg Uranium Exploration, Mining, Production and Mine Remediation and Environmental Issues, Mendoza, Argentina, 2006.

- [9] LOPEZ, L., GASTY, R., PEÑALVA, G., Carbone gamma ray spectrometry test survey in Argentina, Status of Radioelement Mapping Towards a Global Radioelement Baseline (Proc. Tech. Meeting 2003, Golden, CO), IAEA Nuclear Energy Series No. NF-T-1.3, IAEA, Vienna (2010) Appendix C.
- [10] FERREYRA, R., IAEA TC Project ARG/3/007, IAEA–CNEA internal reports (1993–1997) unpublished.
- [11] UNITED NATIONS ECONOMIC COMMISSION FOR EUROPE, United Nations Framework Classification for Fossil Energy and Mineral Reserves and Resources 2009 (UNFC–2009), UNECE, Geneva (2009).

# URANIUM DEPOSIT TYPES AND RESOURCES OF ARGENTINA

L. LOPEZ\*, M. CUNAY\*\*

\* National Atomic Energy Commission (CNEA),  
Buenos Aires, Argentina

\*\* Université de Lorraine, Géoressources CREGU,  
Nancy, France

## Abstract

Several geological types of uranium deposits have been discovered in Argentina. The current uranium identified resources are 31 685 t U and belong to volcanic-related, sandstone-hosted and surficial models.

## 1. INTRODUCTION

The uranium related activities in Argentina began in the 1950s and, as a result of the systematic exploration, several types of deposits have been discovered since then: volcanic-related, sandstone-hosted, granite-related, surficial and intrusive [1, 2].

In recent years, an increase in exploration efforts has led to a significant increase in uranium resources and their level of knowledge, especially in the Patagonia region.

This paper briefly describes some examples of uranium deposits and their contribution to the uranium resources of the country taking into consideration both conventional and unconventional sources [3, 4].

## 2. DESCRIPTION OF THE MAIN TYPES OF URANIUM DEPOSITS

Figure 1 shows the location of the main Argentinean uranium deposits/ districts, which are described in the following paragraphs, while in Fig. 2 different pictures of selected uranium deposits are exhibited.

### 2.1. Intrusive

In this category, it can be mentioned the Rodeo de los Molles deposit (San Luis Province) which correspond to a carbonatite and associated alteration mineralisations hosted in the Las Chacras batholith (174 Ma). The main mineral potential of this deposit is related to REE and the speculative resources are 177 600 t REO at 2.52%, while associated uranium resources are approximately 950 t U at a grade of 0.017% U [5].

Another example of this geological type is given by some granites with elevated uranium contents of the Pampean Ranges (NW Argentina) like as La Chinchilla stock with zinnwaldite, fluorite and occasionally beryl of Lower Carboniferous age ( $354 \pm 3.9$  Ma), in the Sierra de Velasco (La Rioja Province). They are emplaced during the late stages of the Famatinian orogeny. The La Chinchilla stock (about 2.8 km<sup>2</sup>) is the most fractionated intrusion of the Huaco high K calcalkaline granite, where the mineralization is mainly represented by uranophane. In the complex U content ranges from 75 to 260 ppm and prognosticated resources are under evaluation [6].

### 2.2. Granite-related

La Estela deposit (San Luis Province) corresponds to the endogranitic type and is located in the Cerro Aspero-Alpa Corral batholith (358 Ma). The mineralization is in veins (pitchblende, uranophane, autunite, gummite) hosted by high K calcalkaline granites with 3–4 ppm U contents. This deposit was mined in the past with a production of 36 t U [7].

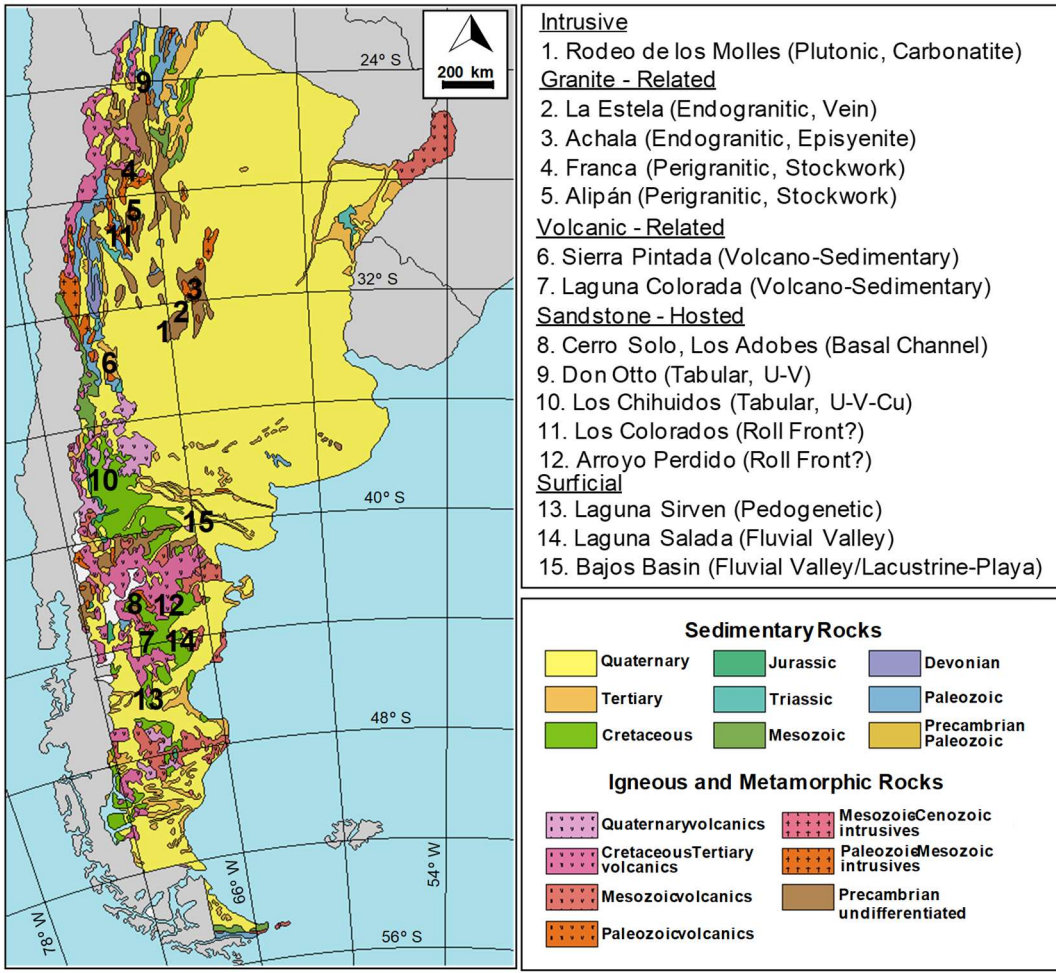


FIG. 1. Location of the main Argentinean uranium deposits/distRICTS.

The episyenites with disseminated U mineralization hosted by the peraluminous leucogranites of the Achala batholith (Cordoba Province) represent another type of endogranitic deposit. These granites are Devonian – Carboniferous and the related deposits are comparable to those from the Middle European Variscan chain [8–10].

There is also the vein/ stockworks subtype located in the metamorphic basement enclosing high potassium calcalkaline granites. An example of this type of deposit is the Franca deposit (Catamarca Province), located in periphery of the Los Ratones granite (335–340 Ma) in the Sierra de Fiambala (North-western Pampean Ranges). The mineralisation is mainly controlled by north to north-east fractures zones to the west and north-west border of the pluton, and dominantly consists of pitchblende and hexavalent uranium minerals. The speculative resources have been evaluated at 1500 t U at a grade of 0.3% U [11][12]. This perigranitic subtype is also represented by the Alipán deposit, hosted by the Velasco Ranges granitoids (350–358 Ma), which correspond to the most recent discovery by the CNEA [13].

### 2.3. Volcanic-related

The deposits that have been the focus of the most important uranium exploitations are the ones that belong to the volcaniclastic type. These mineralisations (uraninite, brannerite, coffinite, uranophane, Fe and Ti oxides) are localized in Permian formations associated with synsedimentary acid volcanism in the Sierra Pintada district (Mendoza Province). From this deposit 1600 t U were mined, and the current identified resources are 10 010 t U recoverable at a production cost below US \$130/Kg U [14–16]. The volcanic-related type is also present in the Laguna Colorado deposit (Chubut Province) located in the San Jorge basin (Cretaceous) with evaluated resources of 160 t U at 660 ppm U [17].

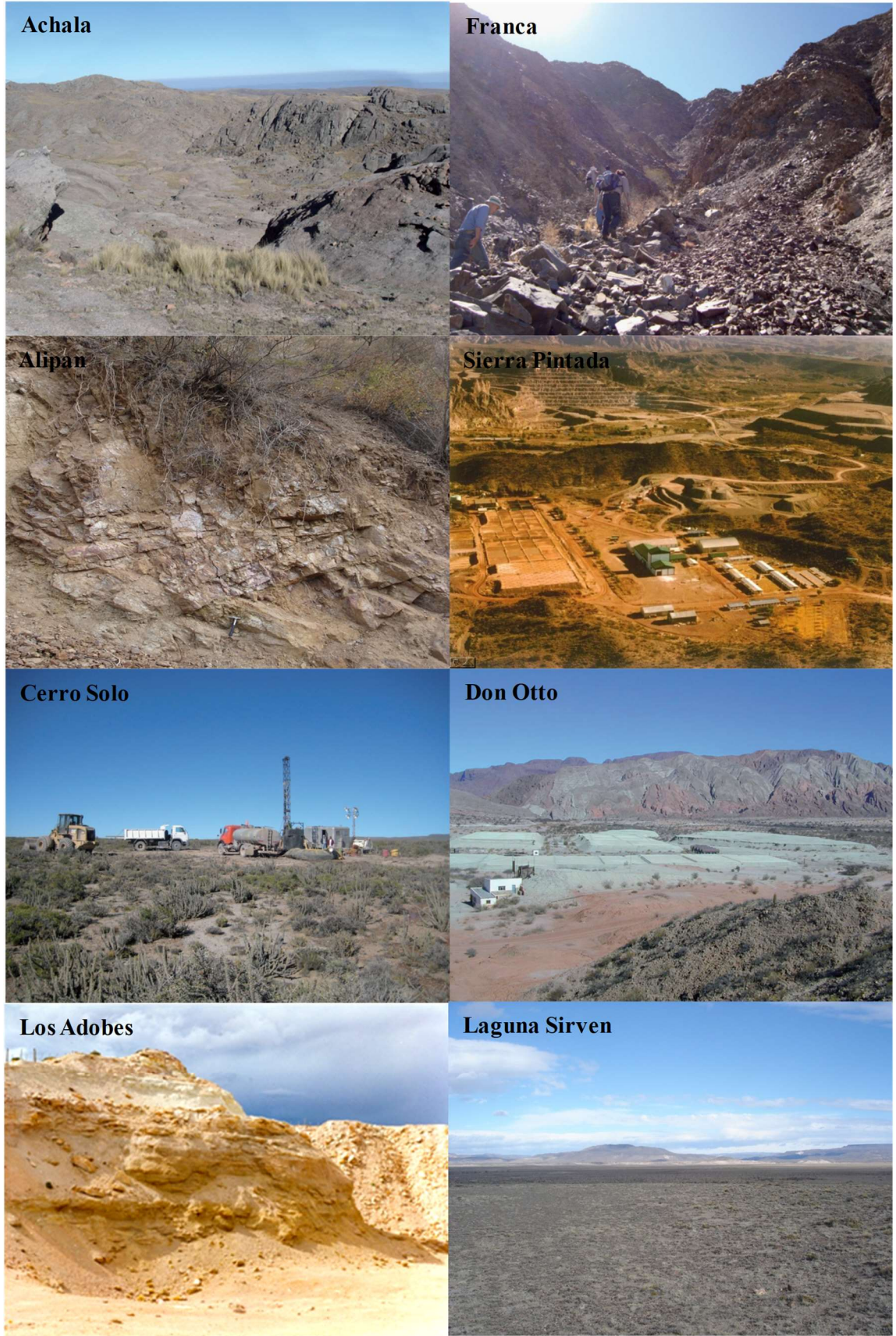


*FIG. 2. Pictures of selected Argentinean uranium deposits.*

## **2.4. Sandstone-hosted**

In the Chubut Province, the San Jorge Basin extends over about 180 000 km<sup>2</sup>, contains Jurassic and Cretaceous continental sediments, hosting not only important uranium deposits, but also oil and gas resources. Several important uranium mineralisations have been identified in Cretaceous fluvial sandstones and conglomerates of the Los Adobes Formation belonging to the Chubut Group, among which the most relevant is the Cerro Solo deposit. In this palaeochannel structure, the mineralised levels (uraninite, pitchblende, uranopilitic, coffinite) are 0.5–6 m wide and 50–130 m deep. The identified resources are 9230 t U at approximately 0.2 % U, included in the < US \$130/kg U production cost category [18–20]. Besides, in the vicinity of Cerro Solo, approximately 8000 t U of identified resources at the same cost category, have been reported regarding the Meseta Central project [21]. In the region, two small sized uranium deposits were mined in the 1970s: Los Adobes and Cerro Condor.

Other subtypes of sandstone models have been studied. For instance, the Salta Basin (Salta Province), covering approx. 150 000 ha, is known for its uranium, oil and gas resources. The Don Otto deposit, located in the Cretaceous Yacoraite Formation of the Salta Group, belongs to the tabular U-V subtype. This deposit was in operation from 1963 to 1981 and produced 275 t of U at 0.1%–0.2% U grade [22, 23]. In the Neuquina basin, also known for its oil and gas potential, the prevalent typology that has been identified is the U-Cu-V one as described in Los Chihuidos district (Cretaceous) located in the Neuquén Province [24].

The roll front subtype can also be found in the Los Mogotes Colorados deposit (La Rioja Province) which is hosted by Carboniferous continental sandstones [25]. The Arroyo Perdido mineralisations (Chubut Province) might be also associated to a redox front and would correspond to a more recent system hosted in Cretaceous fluvial sandstones of confined aquifers [26, 27].

## **2.5. Surficial**

Uranium deposits of the calcrete type have been discovered in the modern covered area of Laguna Sirven (Santa Cruz Province). Mineralized levels (uranophane) are 30 cm wide and are placed 20 cm from the surface. The length of the associated radioactive anomaly is kilometric and the speculative resources there are about 1000–1500 t U at 200 ppm U [28].

The Laguna Salada project (Guanaco and Laguna Salada deposits) in the Chubut Province is a surficial uranium-vanadium deposit. Mineralization occurs within 3 m from surface in soft, unconsolidated gravel. Identified resources have been evaluated at 3 890 t U at grades ranging between 55 and 72 ppm U [29].

In the Bajos Basin (Eastern Rio Negro Province) three mineralized areas (Santa Barbara, Anit and Ivana) are hosted in unconsolidated grits sedimentary strata of possible late Tertiary or Pleistocene age. They correspond to an enclosed internal drainage system in an area of ephemeral streams and playa lakes mineralized with carnotite. At the Anit occurrence the mineralized fluvial channel is 6 km long, 1.97 m thick in average and 40 to 480 m wide at an average grade of 337 ppm U and 594 ppm V. The Ivana occurrence contains carnotite hosted in fine well-layered claystone and fine sand likely belonging the Middle Miocene Bajo del Gualicho Formation. The environment at Ivana appears to be a low-energy flood-plain or lacustrine (playa) environment [30].

## **3. URANIUM IDENTIFIED RESOURCES**

In 2011, CNEA reported about 20 000 t U as Identified Resources (Reasonably Assured Resources + Inferred Resources) for the production cost category <130 US \$/kgU [31]. In addition, about 11 000 t U of Canadian National Instrument 43–101 (NI 43-101) certified resources have been reported in recent years by public/ private mining companies [21, 29]. The total uranium resources of Argentina are thus around 32 000 t U in the aforementioned Identified Resources category as shown in Table I [32].

Table I. Uranium Identified Resources in Argentina according to the NEA/OECD – IAEA Classification Scheme [21, 29, 31, 32]

| <i>Deposit</i>                 | <i>Type</i>      | <i>Reasonably Assured Resources (tU)<br/>≤ US \$130/kgU</i> | <i>Inferred Resources (tU)<br/>≤ US \$130/kgU</i> |
|--------------------------------|------------------|---|---|
| Sierra Pintada (CNEA)          | Volcanic-related | 3900  | 6110  |
| Cerro Solo (CNEA)              | Sandstone        | 4420  | 4810  |
| Don Otto (CNEA)                | Sandstone        | 130   | 300   |
| Laguna Colorada (CNEA)         | Volcanic-related | 100   | 60  |
| Laguna Salada (U3O8 Corp)      | Surficial        | 2430  | 1460  |
| Meseta Central (UrAmerica Ltd) | Sandstone        | -   | 7965  |
| Sub Total                      |                  | 10 980 tU   | 20 705 tU   |
| Total                          |                  | 31 685 tU   |   |

#### 4. FINAL CONSIDERATION

It can be pointed out that the existence of favourable basins and different uranium mineralisation models configure promising conditions to develop new uranium resources. In this general context, the uranium deposit types related to continental sandstones, volcanic-related, granite-related and surficial appear as the most interesting exploration targets.

#### ACKNOWLEDGEMENTS

This contribution attempts to sum up in a few words several studies that were conducted with funding from the National Atomic Energy Commission (Argentina) and the International Atomic Energy Agency. The authors are grateful to both institutions for allowing its presentation. A very special thank goes out to H. Tulsidas and P. Woods for encouraging the participation of Argentina in URAM-2014. An earlier discussion on the uranium geology of Argentina was given in [33].

#### REFERENCES

- [1] DAHLKAMP, F.J., Uranium ore deposits, Springer-Verlag, Berlin (1993).
- [2] INTERNATIONAL ATOMIC ENERGY AGENCY, World Distribution of Uranium Deposits (UDEPO) with Uranium Deposit Classification 2009 Edn IAEA-TECDOC-1629, Vienna (2009),.
- [3] LÓPEZ, L, Uranium Deposits and Resources in Argentina in the Framework of the UDEPO Classification 2013, Paper presented at IAEA Tech. Mtg on Classification of World Uranium Deposits with a Focus on Volcanic-related Deposits, Vienna 2013.
- [4] LÓPEZ, L., CUNAY, M., “Les principaux types de minéralisations uranifères en Argentine”, 22ème Réunion des Sciences de la Terre, Fédération Française de Géologie et de la Société Géologique de France, 2008, Nancy, Recueil des Résumés: 577 (2008).
- [5] VIÑAS, N, Exploración de subsuelo mediante sondeos y laboreos mineros en la anomalía La Juli, yacimiento Rodeo de los Molles. Cálculo de reservas, Michelotti e Hijos SRL, internal report (1999) 52 (unpublished).

- [6] SALVATORE, M., PARRA, F., SÁNCHEZ, D., ÁLVAREZ, J., BELLO, C., ZARCO, J., “Mapeo detallado de facies graníticas en el stock uranífero La Chinchilla, Sierra de Velasco, provincia de La Rioja”, Proc. XVIII Congreso Geológico Argentino, Neuquén, 2011.
- [7] BLASÓN, R., Yacimiento La Estela, distrito uranífero Comechingones, San Luis, Recursos Minerales de la República Argentina, Anales N° 35 SEGEMAR (ZAPPETTINI, E., Ed.), (1999) 621–624.
- [8] CUNHEY, M., GAGNY, C., The uranium potential of the Achala batholith (Argentina); Proposed exploration strategy, (1994) unpublished report.
- [9] ZARCO, J., Estudio de los controles estructurales y magmáticos de indicios intragraníticos del batolito de Achala (Córdoba), Comisión Nacional de Energía Atómica internal report, (2005), unpublished.
- [10] ZARCO., J, ÁLVAREZ, J., Trabajos de prospección realizados en los indicios intragraníticos del batolito de Achala (Córdoba), Comisión Nacional de Energía Atómica internal report (2005), unpublished.
- [11] GUIDI, F., “Geoquímica y ambiente tectónico del granito Los Ratones, Catamarca”, Proc. 14º Congreso Geológico Argentino, Salta, 1999, Vol 2 (1999) 163–166.
- [12] FERREIRA, L., ÁLVAREZ, J., GUIDI, F., SOLER, R., Geología del área del área del depósito de uranio Las Termas, provincia de Catamarca, Proc. 16º Congreso Geológico Argentino, La Plata, 2005) (2005) CD-ROM.
- [13] NORIEGA, J., ANZIL, P., ZARCO, J., “Evolución estructural tentativa y su relación con la mineralización uranífera para el área de Alipán, provincia de La Rioja”, Proc. XVIII Congreso Geológico Argentino, Neuquén, 2011.
- [14] KLEIMAN, L., Mineralogía y petrología del volcanismo permo-triásico del Bloque San Rafael en el área de Sierra Pintada, provincia de Mendoza, y su relación con las mineralizaciones de uranio, PhD Thesis, Univ. of Buenos Aires (1999).
- [15] SALVARREDI, J., Yacimiento Doctor Baulés y otros depósitos del distrito uranífero Sierra Pintada, Mendoza, Recursos Minerales de la República Argentina, Anales N° 35 SEGEMAR (ZAPPETTINI, E., Ed.), (1999) 895–906.
- [16] SARDIN, P., URQUIZA, L., Tabulación de Recursos Uraníferos en Argentina, Comisión Nacional de Energía Atómica internal reports (2009 - 2013) (unpublished).
- [17] FUENTE, A., GAYONE, M., Distrito uranífero Laguna Colorada, Chubut. Recursos Minerales de la República Argentina, Anales N° 35 SEGEMAR (ZAPPETTINI, E., Ed.), (1999) 1253–1254.
- [18] BENÍTEZ, A., FUENTE, A., MALOBERTI, A., LANDI, V., BIANCHI, R., MARVEGGIO DE BIANCHI, N., GAYONE, M., “Evaluación de la Mina Nuclear Cerro Solo, Prov. del Chubut”, Proc. XII Congreso Geológico Argentino, (1993) 272–278.
- [19] FUENTE, A., GAYONE, M., “Distrito uranífero Pichiñán, yacimientos Los Adobes, Cerro Cóndor y Cerro Solo, Chubut”. Recursos Minerales de la República Argentina, Anales N° 35 SEGEMAR (ZAPPETTINI, E., Ed.),(1999) 1255–1259.
- [20] BIANCHI, R., PÁEZ, M., Tipificación y distribución de depósitos de uranio en la cuenca del Golfo de San Jorge, Proc. 16º Congreso Geológico Argentino, La Plata (Argentina), 2005 (CD-ROM).
- [21] URAMERICA LIMITED, <http://www.uramerica.co.uk> (2014).
- [22] GORUSTOVICH, S., Metalogénesis del uranio en el Noroeste Argentino, PhD Thesis, Univ. of Salta (1989).
- [23] ROMANO, H., Distrito Uranífero Tonco Amblayo, Salta, Recursos Minerales de la República Argentina, Anales N° 35 SEGEMAR (ZAPPETTINI, E., Ed.), (1999) 959-970.
- [24] ROJAS, G., Distrito Uranífero Los Chihuidos — Las Cárcel, Neuquén, Recursos Minerales de la República Argentina, Anales N° 35 SEGEMAR (ZAPPETTINI, E., Ed.), (1999) 1143–1146.
- [25] BELLUCO, A, NORIEGA, C., BRAGANTINI, J., Yacimiento Los Mogotes Colorado, distrito uranífero Los Colorado, La Rioja, Recursos Minerales de la República Argentina, Anales N° 35 SEGEMAR (ZAPPETTINI, E., Ed.) (1999) 767–772.
- [26] BENÍTEZ, A, MARVEGGIO, N., Presencia de CO<sub>2</sub> en el distrito uranífero Pichiñán Este, Chubut: un proceso de lixiviación natural, Proc. 16º Congreso Geológico Argentino, La Plata, 2005 (CD-ROM).

- [27] LÓPEZ L., Perspectives of ISL/ ISR uranium mining in Argentina (IAEA TC Project ARG 3012/3014), Paper presented at IAEA Tech. Mtg on the Optimization of In Situ Leach (ISL) Uranium Mining Technology, Vienna 2013.
- [28] PÁEZ, M., BENÍTEZ, A., Informes de avance – Proyecto Laguna Sirven – Provincia de Santa Cruz, Comisión Nacional de Energía Atómica internal reports, (2004 – 2007) unpublished.
- [29] U3O8 CORPORATION, <http://www.u3o8corp.com> (2014).
- [30] BLUE SKY URANIUM CORPORATION, <http://www.blueskyuranium.com> (2014).
- [31] ORGANISATION FOR ECONOMIC CO-OPERATION AND DEVELOPMENT NUCLEAR ENERGY AGENCY/INTERNATIONAL ATOMIC ENERGY AGENCY, Uranium 2011: Resources, Production and Demand, OECD, Paris (2012).
- [32] LÓPEZ, L., TULSIDAS, H., Case studies and testing of the United Nations Framework Classification for Fossil Energy and Mineral Reserves and Resources 2009, Considerations related to the application of UNFC-2009 to uranium resources in Argentina, ECE/ENERGY/GE.3/2014/5, Geneva (2014).
- [33] LÓPEZ, L., The main geological types of uranium deposits in Argentina, Proc. Int. Symp. Uranium raw material for the nuclear fuel cycle: exploration, mining, production, supply and demand, economics and environmental issues (URAM-2009), IAEA-TECDOC-CD-1739, IAEA, Vienna (2014), Appendix, Session 3.

# URANIUM REFINING BY SOLVENT EXTRACTION

J. KRAIKAEW<sup>25</sup>, W. SRINUTTRAKUL<sup>26</sup>

Chemistry and Material Science Research Program,  
Office of Atoms for Peace  
Bangkok, Thailand

## Abstract

The solvent extraction process to produce higher purity uranium from yellow-cake, which uranium purity is around 70% and the main impurity is thorium, was studied in laboratory scale. This yellow-cake was obtained from a monazite processing pilot plant. The extractant chosen was tributylphosphate (TBP) in kerosene and the aqueous feed was uranyl nitrate in nitric acid. It was found that the optimum TBP concentration in kerosene was 10% and the optimum nitric acid concentration in uranyl nitrate feed solution was 4 N. The equilibration study of  $\text{UO}_2(\text{NO}_3)_4/4\text{N HNO}_3$ –10%TBP/kerosene was also investigated. By graphical method, two extraction stages were calculated from 100 g/L uranium input with 90% extraction efficiency and the flow ratio of aqueous to organic was adjusted to 1.0. Furthermore, thorium scrubbing conditions was studied and the results showed that the optimum nitric acid concentration to scrub thorium should not less than 1 N and the diluted nitric acid or the de-ionized water was suitable to strip uranium from organic phase in the final refining process.

## 1. INTRODUCTION

Uranium is a chemical element in the periodic table that has the symbol U and atomic number of 92. Its two principal isotopes are  $^{235}\text{U}$  and  $^{238}\text{U}$ . The isotope  $^{235}\text{U}$  is important for both nuclear reactors and nuclear weapons because it is the only isotope existing in nature that is fissile. The isotope  $^{238}\text{U}$  is also important because it absorbs neutrons to produce a radioactive isotope that subsequently decay to the  $^{239}\text{Pu}$  (plutonium) which is also fissile [1].

Production of high purity yellow cake in Thailand was studied in both laboratory and semi-pilot scales at Office of Atomic Energy for Peace, Bangkok, from 1977 to 2007, around 30 years, together with the research studies of production of thorium (Th) and individual rare earths (RE). Uranium extraction was performed by monazite processing with caustic soda. Monazite is the economic rare earth phosphate mineral which is obtained as a by-product of tin-mining in the South of Thailand. Between 1971–1989, production of monazite was 6368 tonnes [2]. Thai monazites contain U and Th in the ranges of 0.3–0.8 and 5–10%, respectively [3].

Uranium and thorium from monazite are precipitated together as hydroxide. The precipitate is dissolved with nitric acid and uranium in the aqueous solution obtained is separated from thorium by a liquid-liquid extraction process. 5% tributylphosphate (TBP) in kerosene is used as the organic extractant. Uranium is precipitated as ammonium diuranate or yellow-cake by ammonia solution. The best yellow-cake purity obtained from uranium re-extraction process semi-pilot plant is 90.32%  $\text{U}_3\text{O}_8$  but there are many impurities that were not analysed at that time because of the limited efficiency of analytical techniques [4]. No attempt is made to refine uranium to nuclear grade.

From the success of monazite processing semi-pilot plant, the Rare Earth Research and Development Center (RRDC) was established at Pathumthani province by Office of Atomic Energy for Peace, around 20 years ago. The operation of this pilot plant was started around year 2000 and approximate 300 tonnes

---

<sup>25</sup> Present address: Nuclear Non-Proliferation Center, Bureau of Technical Support for Safety Regulation, Office of Atoms for Peace, Bangkok, Thailand.

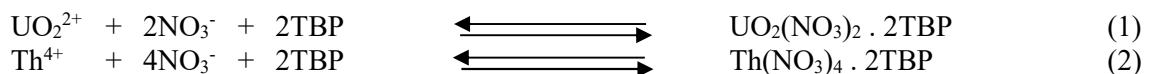
<sup>26</sup> Present address: Thailand Institute of Nuclear Technology (Public Organization) Bangkok, Thailand.

of monazite per year was processed to achieve the products, i.e. yellow cake, thorium oxide, and mixed rare earths hydroxide. Uranium and thorium were aimed to be the raw materials for nuclear fuel research and development. Rare earths were expected to be sold for the income to support RRDC.

However, there are so many problems in this centre until it was changed to be the small part of Thailand Institute of Nuclear Technology, around 7 years ago up to now. The monazite processing was stopped but the research and development was still continued. Their yellow-cake product, which uranium purity is around 70% and the main impurity is thorium [5], was used for this uranium refining study in laboratory scale at Office of Atoms for Peace, Bangkok.

Actually, uranium refining by the TBP process has been accomplished in several countries, i.e. Pakistan, Australia, India and China [6]. The purification of crude uranium recovered from its ores at plant-scale using TBP started in the early 1950s in Canada and the U.K., then in the U.S. in 1953 **Error! Reference source not found.**

The equilibrium constants of the extraction reactions of uranium and thorium in nitric acid aqueous phase by organic TBP, are shown as Eqs(1) and (2), respectively [11, 12]:



It is the fact that uranium is much more readily extracted by TBP than thorium due to the great different between their respective distribution coefficients. As a result, thorium can be scrubbed selectively by nitric acid solution from TBP extract leaving the uranium behind, which can later be recovered by stripping with water **Error! Reference source not found.**

This solvent extraction research was carried out in laboratory scale. Yellow-cake or ammonium diuranate from RRDC, which uranium purity is around 70% and the impurities are thorium and small amount of rare earths, was dissolved in nitric acid to prepare aqueous feed. The extractant used was organic TBP in kerosene. The optimum conditions of uranium re-extraction, which is a part of uranium refining by solvent extraction were studied. The equilibrium of the  $\text{UO}_2(\text{NO}_3)_2 / 4\text{N HNO}_3 - 10\%$ -TBP/kerosene system was investigated. The distribution coefficients and the number of extraction stages were determined as well as thorium scrubbing optimum conditions. Variations of rare earth concentrations were also analysed.

Actually, this work was planned to improve uranium refining process at RRDC but this plant was closed after that. Nevertheless, these investigation results are still available and are expected to serve as the operational experience and technical know-how to develop the similar processes for the refining of yellow-cake.

## 2. EXPERIMENTAL

### 2.1. Chemicals

98% TBP (BDH) was used as the extractant. Kerosene (Jet A-1, Shell) was employed as organic diluent. Uranyl nitrate feed solution was prepared from yellowcake, provided from RRDC. BDH supplied the AR grade 69%  $\text{HNO}_3$ .

### 2.2. Apparatus

A Gerhardt laboratory shaking machine, type LS 5, was used to mix aqueous and organic solutions. An inductively coupled plasma atomic emission spectrometer, ICP-AES (Spectro Analytical Instruments, Spectroflame M Type FMVO5) was used for the uranium, thorium, and rare earth analysis. Free acidity of uranyl nitrate feed solution was analysed using a pH meter Model 250, Denver Instruments.

### 2.3. Analysis

Each experimental condition was repeated twice and two samples were obtained. Each sample was analysed by ICP-AES in duplicate. Their concentrations in the samples were determined using the standard calibration curves. The results of each condition were determined from the average values of two samples or four ICP-AES analysis.

The pH measurement was applied to determine the free acidity of uranyl nitrate feed solution **Error! Reference source not found.**. The pH of  $(\text{NH}_4)_2\text{SO}_4$  solution containing nitric acid with known pH, volume and normality was measured. The uranyl nitrate was added into this  $(\text{NH}_4)_2\text{SO}_4$  solution and then its pH was re-measured. The free acidity of the sample was calculated from the difference of the two pH measurements.

The concentration of the stock TBP was analysed by equilibration with 8N  $\text{HNO}_3$  **Error! Reference source not found.**. The organic solution obtained after equilibration was titrated with standard  $\text{NaOH}$  solution. The exact concentration of TBP was determined from nitric acid normality in the organic solution and the calculated result was 80.81%.

### 2.4. Procedure

#### 2.4.1. Effect of TBP concentration in kerosene

Yellowcake was dissolved in conc.  $\text{HNO}_3$  and undissolved precipitate was filtered off. The acidity of  $\text{HNO}_3$  in uranyl nitrate feed solution was adjusted to 4 N (the analytical value was 4.1681 N). Two samples of feed solution were taken for U, Th, and RE analysis by the ICP-AES. The average concentrations of U, Th, and RE in feed solution are shown in Table I. The concentrations of TBP in kerosene were prepared as 3, 5, 8, 10, 13, 15, 18 and 20%, respectively, to use for uranium extraction from feed solution.

TABLE I. AVERAGE CONCENTRATIONS OF U, TH, AND RE IN FEED SOLUTION (EXPERIMENT 1)

| Composition         | U    | Th  | La   | Ce   | Pr   | Nd   | Sm   | Eu  | Gd   | Y   | Dy  | Yb  |
|---------------------|------|-----|------|------|------|------|------|-----|------|-----|-----|-----|
| Concentration (ppm) | 9457 | 543 | 12.8 | 17.4 | 91.9 | 23.0 | 18.2 | 2.5 | 18.3 | 2.5 | 5.1 | 2.5 |

The extraction was performed at an average temperature of 30°C by equilibration equal volume (25 mL) of both phases in a separating funnel by the laboratory shaking machine at 200 rpm for 10 minutes. Both phases were allowed to stand for 10 minutes after mixing. After phase separation, the raffinate was collected for U, Th, and RE analysis by the ICP-AES. Each experimental condition was run in duplicate and each sample was also analysed in duplicate.

#### 2.4.2. Effect of $\text{HNO}_3$ concentration in feed solution

Uranyl nitrate stock solution was prepared by yellow-cake dissolution with concentrated  $\text{HNO}_3$  and undissolved precipitates were filtered off. The 25 mL volume of feed solution was pipetted 8 times and each was added to each of 100 mL volumetric flasks. Feed stock solution was collected for ICP-AES analysis and the concentration obtained was divided by four to be the concentration of feed solution.  $\text{HNO}_3$  concentration of each feed solution in each of 100 mL volumetric flask was adjusted to 1, 2, 3, 4, 5, 6, 7 and 8 N respectively, by conc.  $\text{HNO}_3$ . By using pH measurement technique, the analytical  $\text{HNO}_3$  concentration values were 0.95, 1.96, 3.19, 3.98, 5.13, 6.23, 7.37 and 8.64 N respectively. The average concentrations of U, Th, and RE in feed solution are shown in Table II.

TABLE II. AVERAGE CONCENTRATIONS OF U, TH, AND RE IN FEED SOLUTION (EXPERIMENT 2)

| Composition         | U*     | Th  | La  | Ce   | Pr    | Nd   | Sm   | Eu  | Gd   | Y   | Dy  | Yb  |
|---------------------|--------|-----|-----|------|-------|------|------|-----|------|-----|-----|-----|
| Concentration (ppm) | 12 460 | 772 | 8.0 | 18.7 | 119.1 | 31.0 | 20.9 | 2.2 | 23.1 | 1.7 | 6.1 | 3.3 |

\* rounded.

By the same method as experiment 1, the extraction was performed at the average temperature of 29.5°C by equilibration equal volume (25 mL) of 8 concentrations of the HNO<sub>3</sub> in uranyl nitrate feed solution and 10%TBP in kerosene in a separating funnel. After phase separation, the raffinates were collected for U, Th, and RE analysis by the ICP-AES. Each experimental condition was run in duplicate and each sample was also analysed in duplicate.

#### 2.4.3. Equilibrium study of UO<sub>2</sub>(NO<sub>3</sub>)<sub>2</sub> / 4N HNO<sub>3</sub> — 10% TBP / kerosene system

Uranyl nitrate stock solution was prepared by dissolving the yellow-cake in conc. HNO<sub>3</sub> and undissolved precipitate was filtered off. The acidity of HNO<sub>3</sub> in uranyl nitrate was adjusted to 4 N (the analytical value was 3.9641 N). This stock solution was made to 8 feed concentrations by pipetting 80, 60, 40, 20, 10, 5, 2.5 and 1 mL of stock solution and added to eight of 100 mL volumetric flasks, respectively, then diluted to 100 mL by 4 N HNO<sub>3</sub> (the analytical value was 3.9443 N). Therefore, there were 9 concentrations of feed solutions, including undiluted stock solution. Two samples of each feed solution were collected to analyse for U and Th by the ICP-AES. Each sample was analysed in duplicate. The average concentrations of U and Th in these feed solutions are shown in Table III. The extractant was also prepared by diluting TBP with kerosene to a concentration of 10%.

TABLE III. AVERAGE CONCENTRATIONS OF U AND TH IN 9 FEED SOLUTIONS (EXPERIMENT 3)

|          |       |       |       |       |       |       |      |      |      |
|----------|-------|-------|-------|-------|-------|-------|------|------|------|
| U (g/L)  | 230.2 | 191.1 | 132.8 | 88.64 | 44.48 | 19.86 | 6.08 | 3.19 | 1.22 |
| Th (g/L) | 12.91 | 10.77 | 7.01  | 4.89  | 2.48  | 1.08  | 0.34 | 0.16 | 0.07 |

An equilibrium study was performed by extracting uranium from 9 concentrations of feed solution with 10%TBP / kerosene at an average temperature of 30.1°C. The equilibration was run in duplicate with the same method as experiment 1. After phase separation, two samples of raffinate were collected for U and Th analysis by the ICP-AES. Each sample was analysed in duplicate.

#### 2.4.4. Thorium scrubbing study with low concentration nitric acid

Stock solution of uranyl nitrate in approximate 4 N nitric acid was prepared from yellow cake by the same method as experiment 1. By equilibration method, some uranium and thorium were loaded from uranyl nitrate stock solution to 10%TBP in kerosene. The calculated U and Th concentrations in organic phase, 10%TBP in kerosene, were 42.35 and 8.44 g/L, respectively. Various low concentrations of nitric acid (0.5, 1, 1.5, and 2 N) were prepared.

Thorium scrubbing experiment was performed at an average temperature of 30°C by equilibration equal volume of U-Th loaded organic phase and each concentration of nitric acid, i.e. 0, 0.5, 1, 1.5, and 2 N, in a separatory funnel with the same method as experiment 1. After phase separation, the raffinates were collected for U and Th analysis by the ICP-AES. Each experimental condition was run in duplicate and each sample was also analysed in duplicate.

#### 2.4.5. Calculation

Uranium, thorium and rare earth extraction efficiency were calculated to illustrate the effect of the % TBP / kerosene and the effect of the HNO<sub>3</sub> concentration. The following equations were applied:

$$\text{Uranium extraction efficiency (\%)} = \frac{([U]_F - [U]_R)}{[U]_F} \times 100 \quad (3)$$

$$\text{Thorium extraction efficiency (\%)} = \frac{([Th]_F - [Th]_R)}{[Th]_F} \times 100 \quad (4)$$

$$\text{Rare Earth extraction efficiency (\%)} = \frac{([RE]_F - [RE]_R)}{[RE]_F} \times 100 \quad (5)$$

where

[U]<sub>F</sub>, [Th]<sub>F</sub> and [RE]<sub>F</sub> are the concentrations of U, Th, and RE in feed, respectively (g/L),  
 [U]<sub>R</sub>, [Th]<sub>R</sub> and [RE]<sub>R</sub> are the concentrations of U, Th, and RE in raffinate, respectively (g/L),

In order to study the distribution of U and Th, their concentrations in organic phase were calculated from the following equations:

$$[U]_{\text{org}} = [U]_F - [U]_R \quad (6)$$

$$[Th]_{\text{org}} = [Th]_F - [Th]_R \quad (7)$$

where

[U]<sub>org</sub> is the concentration of uranium in organic phase (g/L),  
 [Th]<sub>org</sub> is the concentration of thorium in organic phase (g/L),

Then, the distribution coefficient, K<sub>d</sub> **Error! Reference source not found.**, was calculated as follows:

$$K_{d,U} = \frac{[U]_{\text{org}}}{[U]_R} \quad (8)$$

$$K_{d,Th} = \frac{[Th]_{\text{org}}}{[Th]_R} \quad (9)$$

K<sub>d,U</sub> and K<sub>d,Th</sub> were plotted as the functions of the concentration of uranium and thorium in feed solutions, respectively. The equilibrium line between the concentration of uranium in aqueous phase (raffinate) and the concentration of uranium in organic phase was constructed. The operating line at the ratio of feed to extractant of 1.0 was created and the number of extraction stage was determined.

In order to investigate optimum nitric acid concentration to scrub thorium, concentrations of U and Th in raffinates were analysed and their concentrations in organic phase were calculated by Eqs (6) and (7), respectively. Their K<sub>d</sub> were also calculated using Eqs (8) and (9), respectively. The results obtained were interpreted graphically at various nitric acid concentrations to optimize for thorium scrubbing conditions.

### 3. RESULTS AND DISCUSSION

#### 3.1. Effect of TBP concentration in kerosene and effect of HNO<sub>3</sub> concentration in feed solution

Because thorium is the main impurity in yellow-cake obtained from monazite processing, so it is necessary to consider it together with uranium extraction. Plots of U and Th extraction efficiency vs %TBP/kerosene and vs nitric acid concentration are shown in Figs 1 and 2, respectively. Heavy and light rare earth extraction efficiencies are also plotted vs %TBP/kerosene and vs nitric acid concentration as in Figs 3 and 4, respectively.

It is found that at 10%TBP in kerosene, 91.1%U is extracted to organic phase while Th extraction efficiency is 57.3%. When the concentration of TBP in kerosene is higher than 10%, U extraction efficiency is almost constant while Th extraction efficiency is increasing. However, % extractions of RE are almost constant when %TBP in kerosene is higher than 10%. Because the amounts of RE in feed solution (Tables I and II) are very low, then the extracted RE in organic are lower and they can be

scrubbed easily in the next process. As a result, 10%TBP in kerosene is selected to be the extractant. It is also found that U and Th extraction efficiency are almost constant if the nitric concentration is higher than 4 N. At a  $\text{HNO}_3$  concentration of 4 N, 89.7%U is extracted where as that of Th is 61.1%. Therefore, nitric acid concentration of 4 N is selected to be the optimum acidity of the feed solution (Fig. 2).

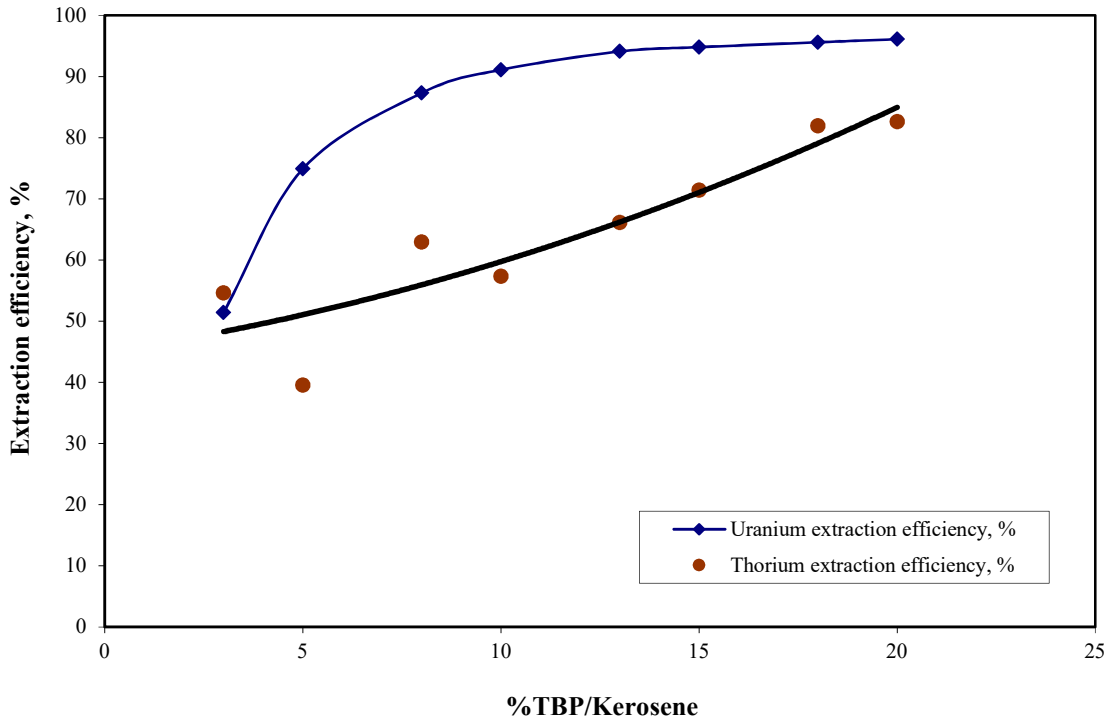


FIG. 1. Uranium and thorium extraction efficiency as a function of % TBP in kerosene.

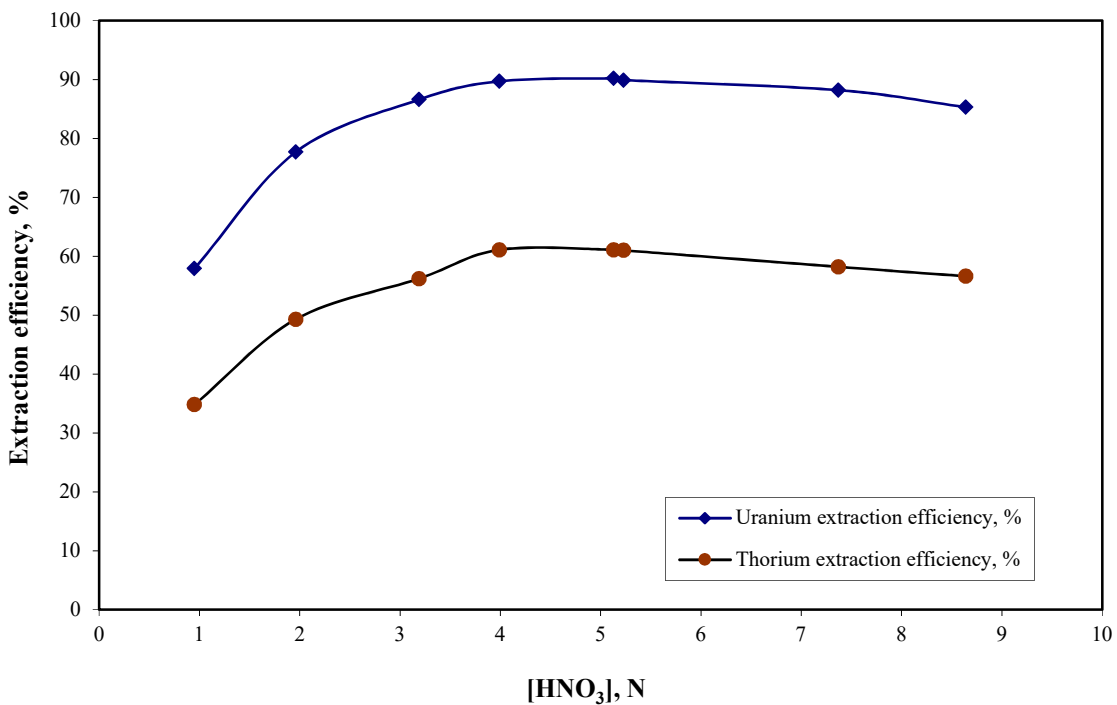


FIG. 2. Uranium and thorium extraction efficiency as a function of  $\text{HNO}_3$  normality.

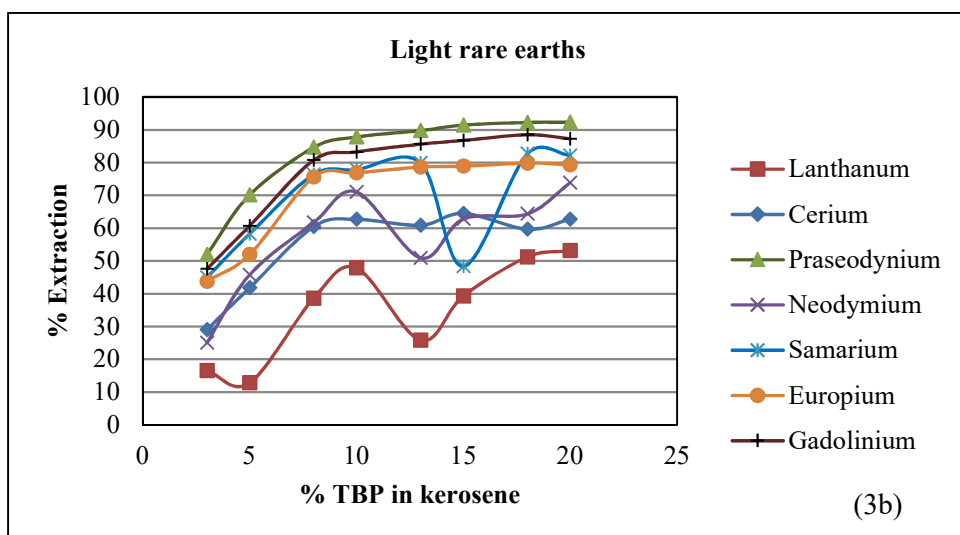
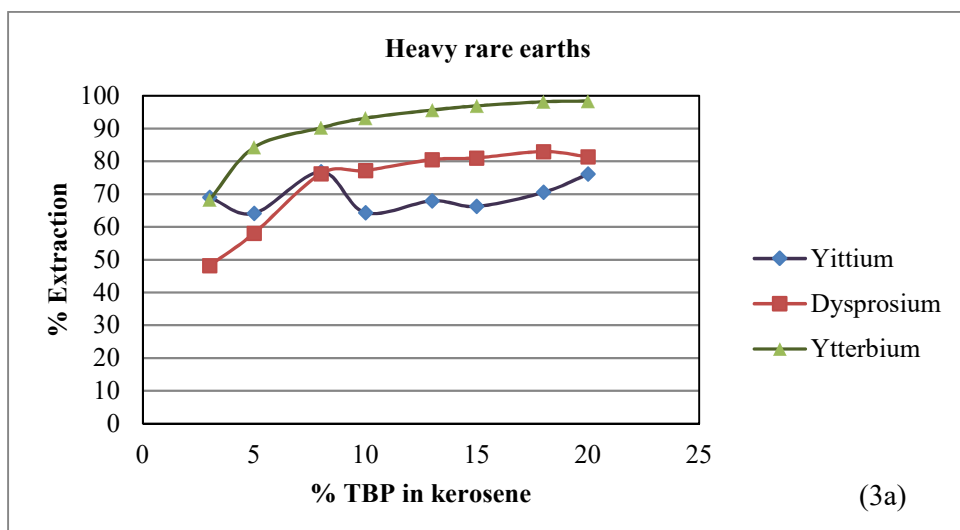


FIG. 3(a, b). Rare earth extraction efficiency as a function of %TBP in kerosene.

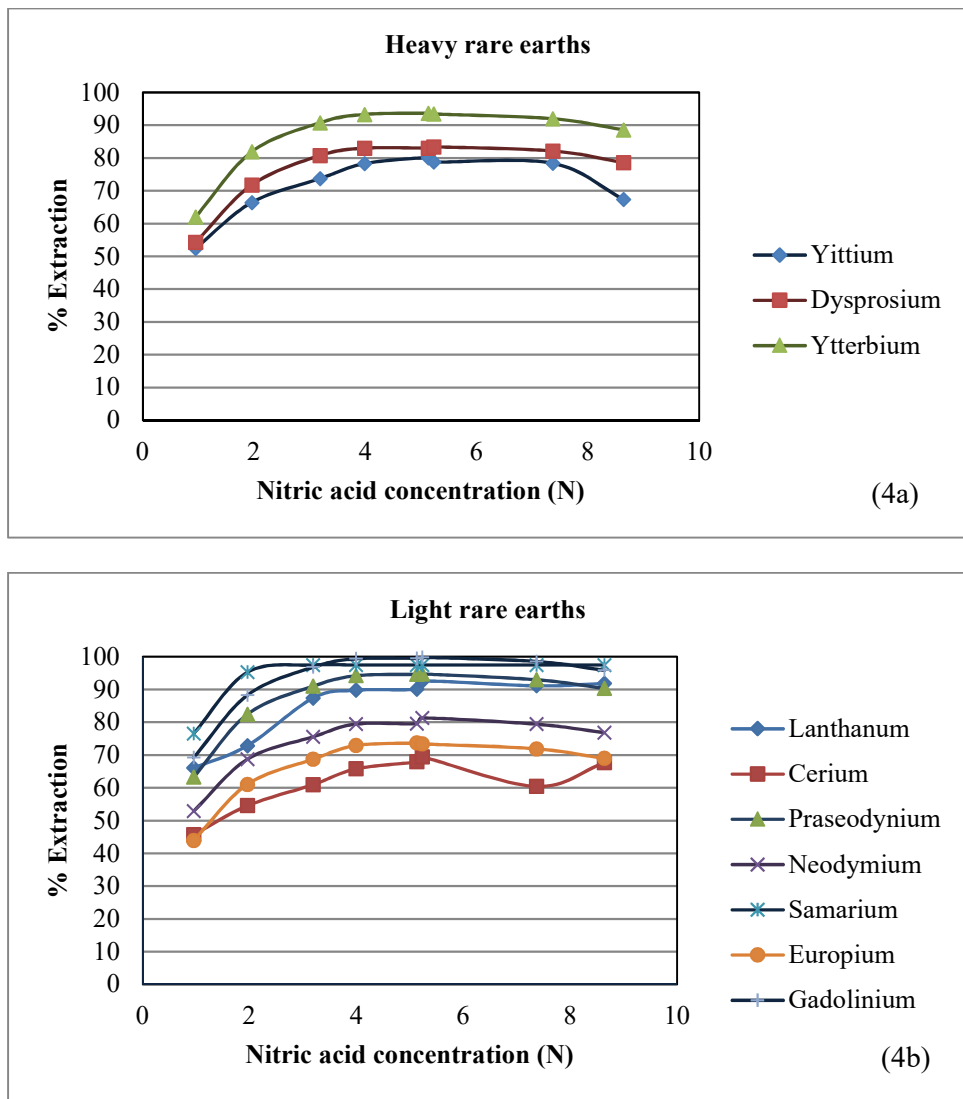


FIG. 4(a, b). Rare earth extraction efficiency as a function of  $\text{HNO}_3$  normality.

### 3.2. Equilibrium study of $\text{UO}_2(\text{NO}_3)_2 / 4\text{N HNO}_3 - 10\% \text{TBP} / \text{kerosene}$ system

Plots of uranium distribution coefficient,  $K_{d,U}$ , and thorium distribution coefficient,  $K_{d,Th}$ , vs concentrations of U and Th in feed solution are illustrated in Figs 5 and 6, respectively.  $K_{d,U}$  is apparently higher than  $K_{d,Th}$  and thus U is preferentially extracted into 10%TBP. However,  $K_{d,U}$  and  $K_{d,Th}$  decrease with the increasing of U and Th concentrations, respectively, in the feed solution. In other words, an increasing in the concentration of U and Th in feed solution will result in a decrease in the distribution of U and Th into 10%TBP in kerosene.

Uranium equilibrium line of  $\text{UO}_2(\text{NO}_3)_2/4\text{N HNO}_3 - 10\% \text{TBP}/\text{kerosene}$  system is plotted as shown in Fig. 7. The operating line is created with an extraction efficiency of 90%. The flow ratio of aqueous phase to organic phase in this experiment is set to 1.0 with uranium feed at a concentration of 100 g/L. It is found graphically that the number of extraction stage required for these uranium extraction conditions is only 2 stages to render 10 g/L U in barren solution.

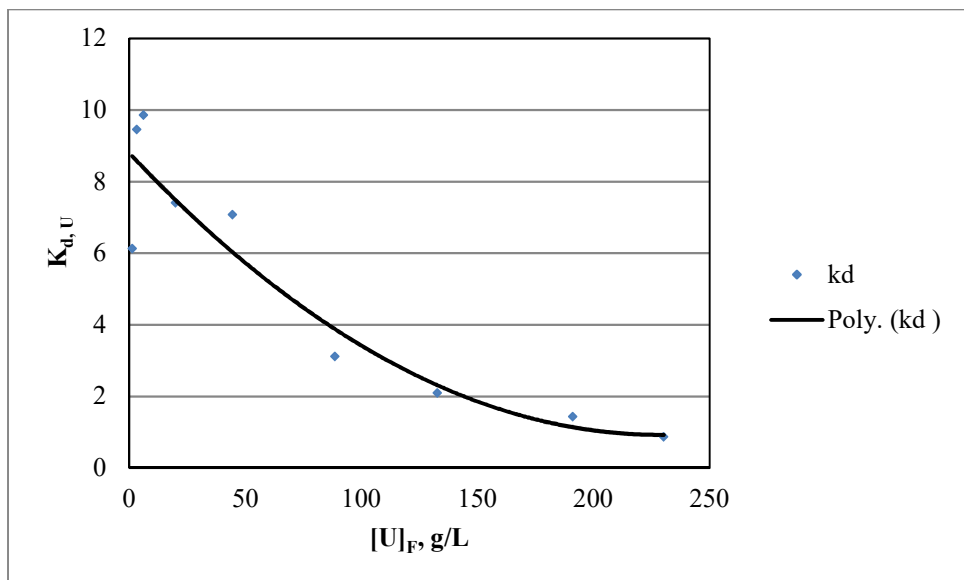


FIG. 5. Distribution coefficient of uranium as a function of uranium concentration in feed.

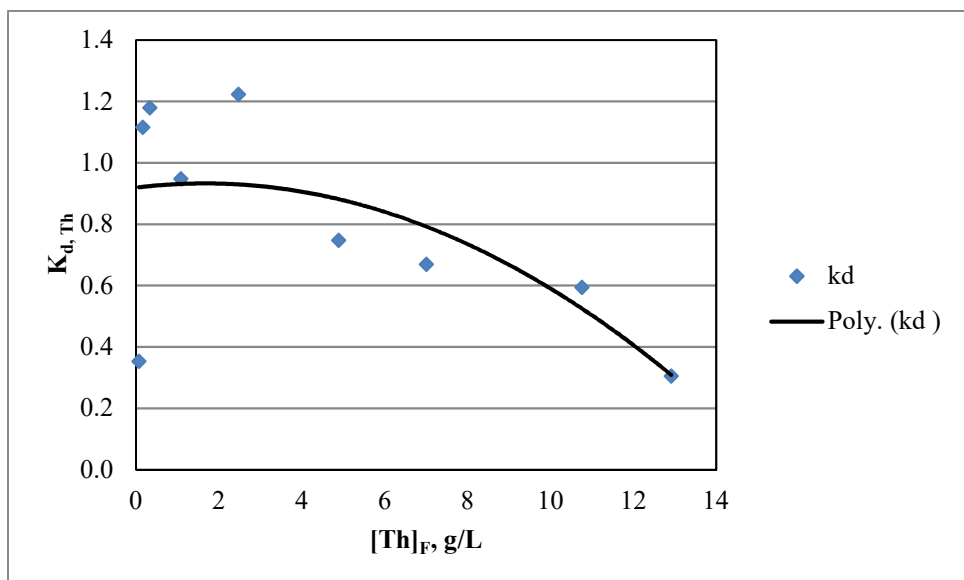


FIG. 6. Distribution coefficient of thorium as a function of thorium concentration in feed.

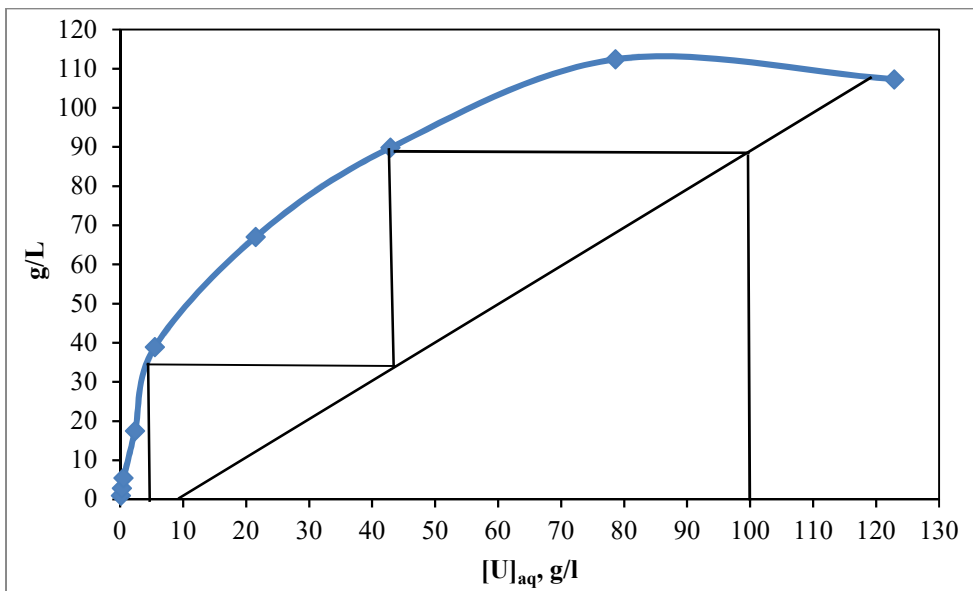


FIG. 7. Stage calculation of  $\text{UO}_2(\text{NO}_3)_2$  / 4 N  $\text{HNO}_3$  – 10% TBP / kerosene system.

### 3.3. Thorium scrubbing study with low concentration nitric acid

Plots of U and Th concentrations that are scrubbed to aqueous phase vs nitric acid normality are illustrated in Fig. 8. It is found that at nitric acid normality is less than 1 N, the distribution of U to nitric acid aqueous phase increases sharply while Th concentration increases slightly. Therefore, the scrubbing nitric acid concentration should not less than 1 N and the diluted nitric acid or de-ionized water is suitable to strip uranium from organic phase. In nuclear fuel cycle, this stripping solution will be reacted with ammonium hydroxide to precipitate as ammonium diuranate or yellow cake **Error! Reference source not found.**. At present, yellowcake means a fine uranium powder, ranging in colour from yellow to black or  $\text{U}_3\text{O}_8$ , not necessarily ammonium diuranate as before [17, 18].

Uranium distribution coefficient,  $K_{d,\text{U}}$ , and thorium distribution coefficient,  $K_{d,\text{Th}}$ , are compared together at various nitric acid concentrations as shown in Fig. 9. It is found that Th prefers to be in organic phase. When nitric concentration is higher, the distributions of U and Th into nitric acid scrubbing solution decrease.  $K_{d,\text{U}}$  increases slightly when nitric acid concentration is higher than 1 N. In order to keep most of U in organic phase, 1 N nitric acid is selected to be Th scrubbing solution.

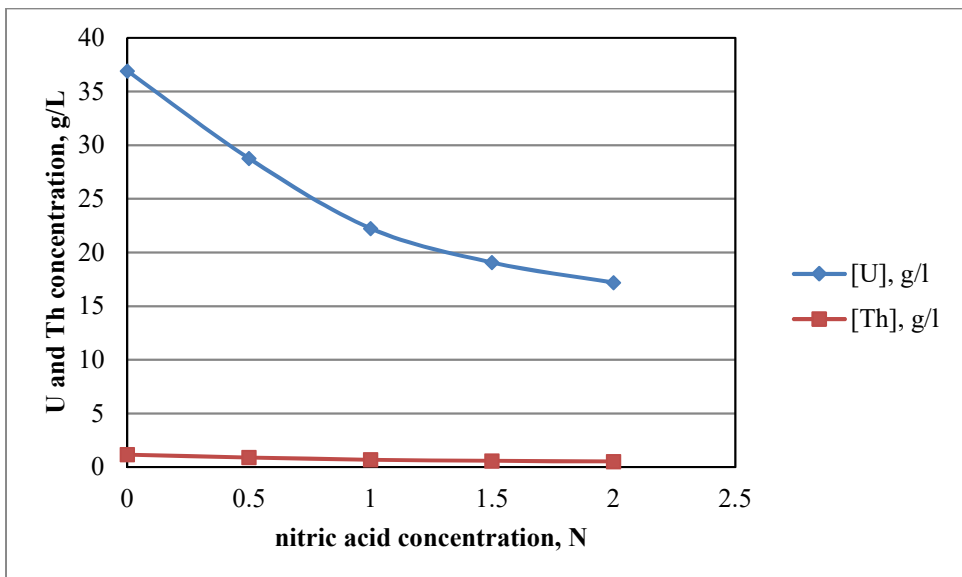


FIG. 8. Concentrations of scrubbed U and Th in aqueous phase as a function of  $HNO_3$  normality.

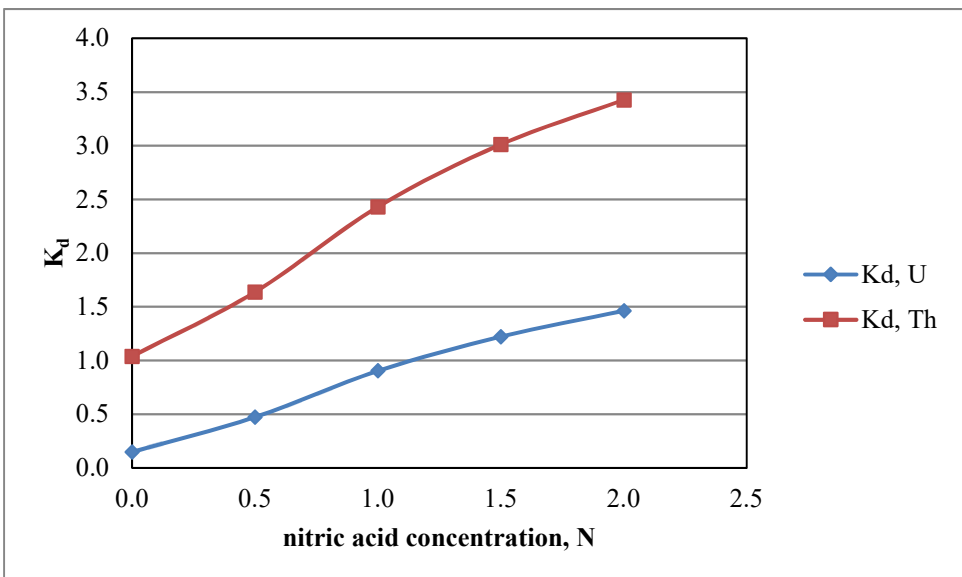


FIG. 9. Distribution coefficients of U and Th as a function of  $HNO_3$  normality.

#### 4. CONCLUSIONS

The yellow-cake obtained from monazite processing is applied to prepare feed input. The optimum concentration of TBP in kerosene for uranium refining is %10 and the optimum nitric acid normality in feed solution input is 4N. At this condition, uranium is extracted into this extractant higher than thorium. However, when concentrations of uranium and thorium in feed solution are higher, the distribution of both elements to this extractant decreases. By means of a graphical method, with set-up conditions, i.e. %90 extraction efficiency, uranium concentration input of 100 g/L in feed solution, and flow of aqueous to organic ratio of 1.0, only two extraction stages are required for uranium re-extraction. It is also found that the optimum concentration of nitric acid to scrub thorium from this extractant, which is loaded with uranium and thorium, is 1N. Furthermore, in order to strip uranium from organic phase in the final refining process, the diluted nitric acid or the de-ionized water was available.

## ACKNOWLEDGEMENTS

The lead author would like to thank IAEA for their grant award given to her to present this research work in URAM–2014 at Vienna, Austria. Support of ICP–AES and yellow-cake from Rare Earth Research and Development Center are also appreciated. Furthermore, the lead author would like to express her deep thanks to K. Sirisena, former Director of Chemistry Division (Office of Atomic Energy for Peace), for her guidance and valuable support in the past.

## REFERENCES

- [1] Uranium-Element information, properties and uses/Periodic Table, <http://www.rsc.org/periodic-table/element/92/uranium>.
- [2] UNITED NATIONS, Mineral Resources of Thailand, Atlas of Mineral Resources of the Escap Region **16** (2001).
- [3] LAOWATTANABANDIT, P., PICHESTAPONG, P., Thailand and Uranium Deposits, paper presented at IAEA UNFC Workshop, Santiago, Chile, 2013.
- [4] KRAIKAEW, J., Uranium refining by solvent extraction, INIS-TH-006, Proc. 6<sup>th</sup> Nuclear Science and Technology Conference, Bangkok, 1996, Office of Atomic Energy for Peace, Bangkok (1996) 293–304.  
**Error! Hyperlink reference not valid..**
- [5] OFFICE OF ATOMIC ENERGY FOR PEACE, Rare Earth Research and Development Center, OAEP Annual Reports 2544–2547, OAEP, Bangkok (2001–2004) (in Thai).
- [6] YUNUS, M., MUZAFFAR, A., QURESHI, M.I., QAZI, N.K., KHAN, J.R., CHUGHTAI, N.A., ZAIDI, S.M.H., “Refining of yellow cake by solvent extraction, Pakistan status report”, Proc. Advisory Group Meeting on Production of Yellow Cake and Uranium Fluorides, Paris, 1979, Panel Proc. Series, STI/PUB/553, IAEA, Vienna (1980) 329–339.
- [7] ALFREDSON, P.G., CHARLTON, B.G., RYAN R.K., VILKAITI V.K., Development of processes for pilot plant production of purified uranyl nitrate solutions, AAEC/E-344, Australian Atomic Energy Commission Research Establishment, Lucas Heights (1975).
- [8] ROY, S.B., SINGH, H., KUMAR, K., MEGHAL, A.M., KRISHNAN, V.N., KOPPIKER, K.S., “Operating experience in the refining of uranium by solvent extraction using mixer-settler”, Proc. Int. Symp. on Uranium Technology, Bombay, 1989, Bhabha Atomic Research Centre; Bombay, **2** (1991) 653–658.
- [9] HUANG-LUNGUANG, ZHUANG-HAIXING, NIU-YUQING, “Technical improvement of uranium purification”, Proc. Int. Conference on Uranium Extraction, Beijing, 1996h, China Nuclear Information Centre, Beijing (1996) 54–64.
- [10] SCHULZ, W.W., NAVRATIL, J.D., (Eds), Science and Technoly of Tributylphosphate, V.II, Selected Technical and Industrial Uses, Part A, Florida (1987).
- [11] STAS, J., DAHDOUH, A., SHLEWTT, Extraction of uranium (VI) from nitric acid and nitrate solutions by tributylphosphate / kerosene, Periodica Polytechnica Ser. Chem. Eng. **49** 1 (2005) 3–18.
- [12] RABIE, K.A., ABDEL-WAHAB, S.M., MAHMOUD, K.F., HUSSEIN, A.E.M., ABD EL-FATAH, A.I.L., Monazite-uranium separation and purification applying oxalic-nitrate-TBP extraction, Arab Journal of Nuclear Science and Application **46** 1 (2013) 30–42.
- [13] ZHI-REN, L., YOUN-HUAI, X., CHENG-FA, Determination of free acidity in uranyl nitrate by pH measurement, J. Radioanal. Nucl. Chem. **81** 1 (1984) 15–19.
- [14] KRAIKAEW, J., Analysis of tributylphosphate in kerosene, OAEP Annual Report **2522**, OAEP, Bangkok (1979) (in Thai).
- [15] CUSACK, R.W., FREMEAUX, P., GLATZ, A fresh look at liquid-liquid extraction, Chem. Eng. **98** 2 (1991) 66–76.
- [16] SEIDEL, D.C., Extracting uranium from its ores, IAEA Bulletin **23** 2 (1980) 24–28.
- [17] Nuclear Fuel Cycle, AFN Environmental Stewardship (information sheet) (undated) [www.afn.ca/uploads/files/env/nuclearfuelcycle.pdf](http://www.afn.ca/uploads/files/env/nuclearfuelcycle.pdf).
- [18] SETTLE, F., Nuclear Chemistry Uranium Production (undated) (general chemistry case study) <http://www.chemcases.com/nuclear/nc-06.htm>.

# GEOCHEMICAL DISPERSION ASSOCIATED WITH URANIUM IN SANDSTONE ROLL FRONT TYPE DEPOSITS AND ITS RELATIONSHIP TO THE ORINOCO OIL BELT, VENEZUELA

J.L. MANRIQUE<sup>27</sup>

Instituto de Ciencias de la Tierra,  
Universidad Central de Venezuela,  
Caracas, Venezuela

## Abstract

In Venezuela there is a potential for the formation of uranium deposits in areas such as the Guiana Shield, the south of Eastern Basin, the Andes, and the massif of Baúl, among other areas. Of especially great interest is the exploration for uranium redox interface type (roll front) deposits in areas such as the southern part of the Orinoco Oil Belt, and north and northwest of the Guiana Shield, where groundwater-uranium weathered from the shield flows northward in the sandstones and mudstones which constitute the southern boundary of the Eastern Basin of Venezuela. The presence of gas, crude oil, bitumen and lignite of the Orinoco Oil Belt can be an effective barrier for uranium in solution, which may have precipitated at the redox interface of this groundwater. This work was based on a qualitative model describing geochemical dispersion associated with uranium deposits in sandstone, roll front type, which indicates that the daughter isotopes  $^{238}\text{U}$  which can migrate extensively are:  $^{222}\text{Rn}$ ,  $^4\text{He}$ , and smaller proportion:  $^{226}\text{Ra}$  and  $^{222}\text{Rn}$  daughters ( $^{214}\text{Bi}$ ,  $^{210}\text{Pb}$ ). The main exploration methods were established, which can be applied in areas of the Orinoco Oil Belt, north of the Guiana Shield, and areas west of there.

## 1. INTRODUCTION

The uranium deposits in sandstones of the ‘roll front’ type, consist of areas or arched bodies or matrix impregnations of uranium, which cut across the stratification of the sandstones that contain limited at the top and bottom by beds less permeable. The mineralized zones consist of elongated and sinuous bands approximately parallel to the direction of stratification and perpendicular to the direction of sedimentation and groundwater flow. The redox interface controls the environment and configuration of these areas [1]. In the present study are considered favorable areas for the formation of these deposits, especially the south area of the Eastern Basin, the area comprising the Orinoco Oil Belt and west of it [2], so is recommended that a plan of uraniferous exploration in this area, because it has favorable characteristics to host uranium deposits and other elements, such as vanadium. A proposed exploration plan which is primarily a combination of geochemical, geological and geophysical methods, which allow detection of anomalous areas with emphasis on surface measurements and obtaining profile information oil wells in the area of interest. These methods are proposed according to a model of geochemical dispersion associated with this type of deposits, which is considered the most mobile elements within the  $^{238}\text{U}$  decay series [3].

## 2. GEOCHEMICAL DISPERSION OF ELEMENTS OF INTEREST

In the radioactive series  $^{238}\text{U}$ , several elements with different chemical characteristics are formed, which are dispersed in different ways, according to their chemical and physical properties. In particular, the  $^4\text{He}$  and  $^{222}\text{Rn}$  are highly mobile and tend to escape while  $^{226}\text{Ra}$ ,  $^{234}\text{U}$ ,  $^{210}\text{Pb}$  and  $^{206}\text{Pb}$  can migrate under certain conditions in which the (Eh and pH mainly) system is. By contrast,  $^{234}\text{Th}$ ,  $^{230}\text{Th}$  and  $^{234}\text{Pa}$  are extremely immobile and can stay with their daughters for significant periods of time, indicating the

---

<sup>27</sup> Present address: Univ. Técnica Particular de Leja, San Cayetano Alto s/n, Loja, Ecuador.

former presence of uranium or its proximity to the host rock of the mineralization. There are also elements associated with theuranium, with similar geochemical properties (V, Se, Mo, As); see Fig. 1.

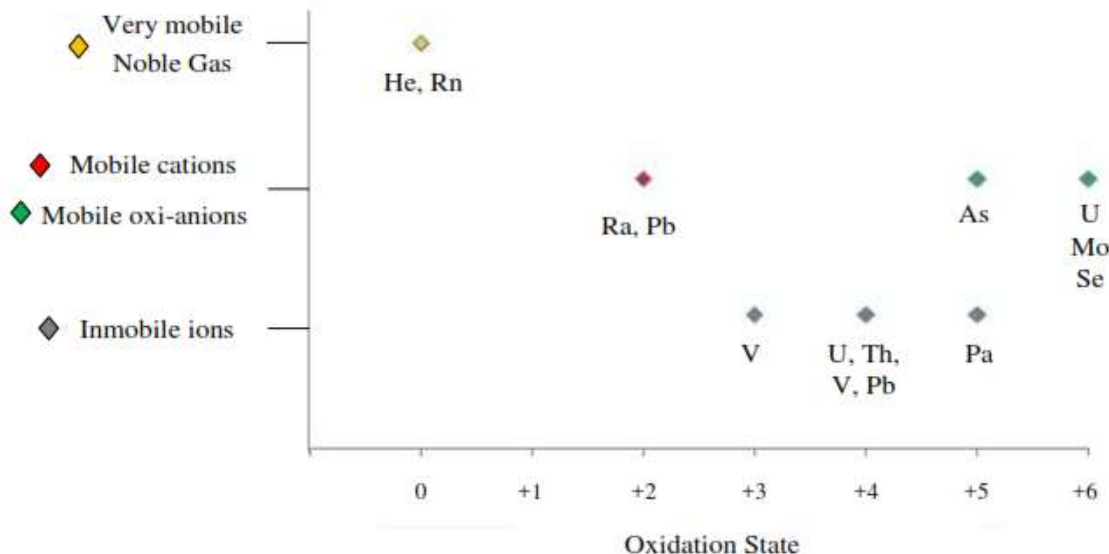
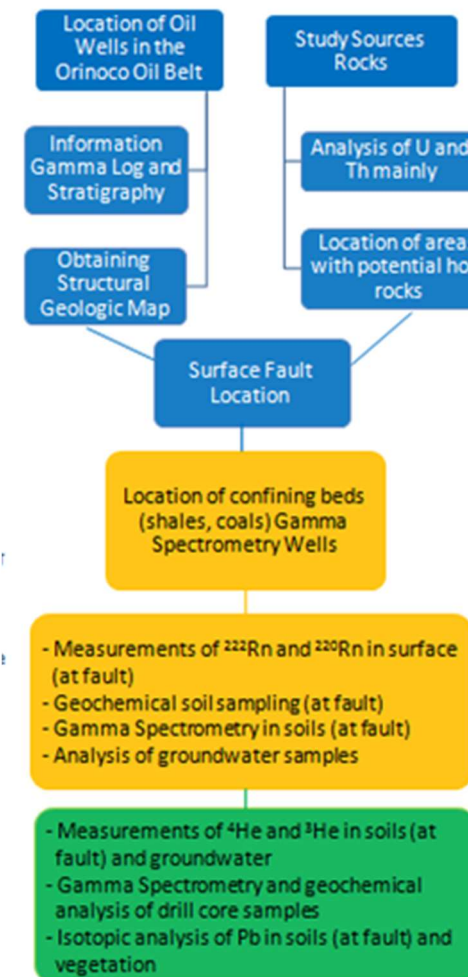


FIG. 1. Chemical mobility of various elements  $^{238}\text{U}$  series and other elements associated in the deposits (adapted from Smith and Huyck, 1999 [4]).

### 3. EXPLORATION METHODS

The suggested exploration area is located in the south of the Eastern Basin, north of the Guiana Shield, whose uranium source rocks are thought to be system first geological Province Imataca (Guiana Shield) formed by granitic gneisses, granites and felsic granulites of Archean age and secondly the Caicara Formation of Pre-Cambrian age (1736 My), composed primarily of acid volcanic rocks [5]. The transport of uranium may have been through surface waters by rivers flowing from south to north, which may have led uranium as uranyl ion and/or absorbed in inorganic and organic colloids. Subsequently uranium may have been infiltrated by groundwater aquifers in the Eastern Basin. Host mineralization rocks may be the Cretaceous–Tertiary Formations, which are composed of sandstones, shales, siltstones, coal, oil and gas. These formations were deposited in transitional fluvial-deltaic environments which are conducive to host uranium deposits in sandstones (e.g. uranium deposits, South Texas [6]). This plan is set out in Fig. 2.

The main exploration methods have been established, which can be applied in areas of the Orinoco Oil Belt, north of the Guiana Shield, and areas west of this. Among the most important are: soil measurements of radon and helium near faults, sampling soils with gamma spectrometry analysis, log interpretation of oil wells in the area of interest to establish gamma–lithological anomalies, ground water analysis of uranium, radon, radium, helium, vanadium, selenium, molybdenum, analysis of samples oil drilling cores to locate anomalous stratigraphic levels.



*FIG. 2. Plan for uranium exploration in the Orinoco Oil Belt.*

#### 4. CONCLUSIONS

There is good potential to host uranium deposits in sandstone type roll front, in areas of the Eastern basin (Orinoco Oil Belt), since according to this model may have the formation suitable for geological and geochemical conditions, source rock uranium, uranium transport, precipitation and preservation.

The study of geochemical dispersion associated with uranium deposits of this type, describes as the behavior of each of the elements in the  $^{238}\text{U}$  decay series, which have different chemical-geochemical behaviors and different half-life times, leading to different geochemical dispersion in the source rock, during transport in surface water-groundwater and mineralization.

An exploration plan was established which includes: obtaining information from PDVSA (Petróleos de Venezuela S.A.) regarding the locations of wells in the Orinoco Oil Belt, structural geological map, location of potential source rocks and exploration areas, location of fault surfaces, location of confining beds, stratigraphy; measurements of  $^{222}\text{Rn}$  and  $^{220}\text{Rn}$  in surface (at faults), geochemical soil sampling (at faults), gamma spectrometry in soils (at faults), and analysis of groundwater samples.

## ACKNOWLEDGEMENTS

To do this research with the collaboration of the following organizations and institutions: Internacional Atomic Energy Agency (IAEA), Instituto de Ciencias de la Tierra de la Facultad de Ciencias de la Universidad Central de Venezuela (Earth Sciences Institute, Faculty of Sciences, Universidad Central de Venezuela), Laboratorio de Física Nuclear de la Universidad Simón Bolívar (Laboratory of Nuclear Physics, Universidad Simón Bolívar), Ministerio del Poder Popular para la Energía Eléctrica.

## REFERENCES

- [1] DAHLKAMP, F., Uranium deposits of the world, Part I Typology of uranium deposits: Asia. Springer-Verlag, Berlin Heidelberg (2009) 1–492.
- [2] PASQUALI, J., SIFONTES, R., Exploración de uranio en Venezuela, Proc. IX Congreso Geológico Venezolano (IX Venezuelan Geological Congress), Universidad Central de Venezuela, GEOS **39** (2007) 74–75 (English abstract).
- [3] MANRIQUE, J., Dispersión geoquímica asociada a yacimientos de uranio del tipo interfase oxidación-reducción, Masters Thesis, Universidad Central de Venezuela (2014).
- [4] SMITH, K.S., HUYCK, H.L., An overview of the abundance, relative mobility, bioavailability, and human toxicity of metals, Reviews in Economic Geology **6A**, The Environment Geochemistry of Minerals Deposits, Ch. 2, An overview of the abundance, relative mobility, bioavailability, and human toxicity of metals (1999) 29–70.
- [5] MENDOZA, V., Geología de Venezuela, Evolución Geológica, Recursos Minerales del Escudo de Guayana y Revisión del Precámbrico Mundial, Tomo 1, Gran Colombia Gold Corp., Bogotá (2012) 1–364.
- [6] HODBAY, D.K., GALLOWAY, W.E., Groundwater processes and sedimentary uranium deposits, Hydrogeol. J. **7** (1999) 127–138.

# URANIUM LEGACY SITES IN PORTUGAL: ENVIRONMENTAL RADIOACTIVITY AND MITIGATION OF RADIOLOGICAL IMPACT

F.P. CARVALHO

Laboratório de Protecção e Segurança Radiológica/  
Instituto Superior Técnico (LPSR/IST),  
Universidade de Lisboa,  
Bobadela LRS, Portugal

## Abstract

Uranium legacy sites in Portugal include milling tailings, mining waste, old infrastructures, and acid mine drainage with elevated radioactivity concentrations that in some areas could represent a radiation hazard to public health. A national programme was approved for remediation of abandoned and degraded mine areas. Remediation work was carried out in several mine sites already, including Urgeiriça and Cunha Baixa. Radiation exposure and environmental contamination at several sites is described, contrasting the situations before and after site remediation and identifying radiation protection enhancements and socioeconomic gains achieved.

## 1. INTRODUCTION

Mining of radioactive ores in Portugal was carried out from 1908 to 2001, initially for producing radium and after 1944 for producing uranium. Sixty uranium deposits were exploited and the ore was processed in milling facilities, generally near the mines [1]. After cessation of mining and milling activities the industrial legacy included about 160 Mt of mining waste and 13 Mt of milling waste, most of the last one disposed near the facilities of Urgeiriça mine, in the centre-North of the country. After closure of the mining company Empresa Nacional de Urânia (ENU), concerns of populations and local administrations about the fate and impact of uranium residues on public health, led the Parliament to approve in 2001 a recommendation for assessment of environmental and public health impact in those areas. National Laboratories for Public Health, Geological Survey, and Nuclear Technology Institute (ITN) worked together in assessing the impact of uranium residues (MinUrar Project). Based on the reports produced, recommendations were made for cleanup and environmental remediation of contaminated sites [2, 3]. Although the issue of radioactive and environmental impact of this mining industry has long been debated and the need for environmental remediation perceived, such recommendations contributed to support the approval in 2004 of a remediation plan for abandoned mines initiated thereafter to mitigate radioactive and environmental impacts [4–6]. Herein, environmental radioactivity information gathered over several years through the monitoring carried out by Laboratório de Protecção e Segurança Radiológica (LPSR)/IST (former ITN) is briefly reviewed and the outcome of remediation work in enhancing radiation protection is succinctly summarized.

## 2. WORK PERFORMED

The evaluation of contaminated and radioactive waste of uranium mines was extensively carried out by LPSR (ex-ITN) from 2000 to 2002, with field work in all old mine and milling sites. Abandoned mines, old facilities, and waste piles were identified, visited, geo referenced, monitored for ambient radiation dose, and samples of waste collected for determination of activity concentration of radionuclides by radioanalytical techniques in the laboratory [7–9].

The risk assessment requested by the Government in 2001 from National Laboratories, enabled an in depth study of selected uranium sites (MinUrar project). Several mine sites were selected to represent the most contaminated areas (those with old milling facilities and milling tailings besides uranium mines), areas with old mines and mining waste but no milling tailings, and reference areas in the same region (i.e., without mines and without mining and milling waste). These sites were investigated for radioactive and stable metal contamination and, furthermore, an epidemiological study was carried out

on the resident population applying a careful study design. Results were reported to the Government and Parliament and made available to the public [2, 3].

Decision on environmental remediation and proper decommissioning of abandoned and degraded mine areas was approved by the Government and entrusted to the mining State holding Empresa de desenvolvimento Mineiro (EDM). EDM initiated remediation works in 2005. During 2006–2008 the main site with mining and milling tailings at Urgeiriça, was clean up and waste removed and concentrated in two previously existing dump areas, Barragem Velha and Barragem Nova. Barragem Velha was reshaped and covered with a multilayer cap. A drainage system was built to collect mine water and seepage into an automatic water treatment plant [6]. Remediation of other uranium mine sites is currently in progress or planned. Until 2014 were cleaned and remediated the uranium mine sites of Urgeiriça, Valinhos, Abrutiga, Espinho, Cunha Baixa, Senhora das Fontes, and Bica mines, most of them with milling tailings and acid mine drainage.

As by law LPSR/IST (formerly ITN) is in charge of the environmental radioactivity monitoring and implementation of the EURATOM Treaty article 35, the assessment of radioactivity in regions of remediated sites and not yet remediated sites is regularly carried out and results reported to the Government, to the CEC, and to the public [10]. Sites that had not been assessed in the framework of MinUrar project have gradually been assessed, radioactivity measured, and risks evaluated and reported.

### 3. RESULTS AND DISCUSSION

A detailed account of environmental radioactivity and radiation issues in all sites could not be reported here. Instead, some selected sites are presented.

The Urgeiriça mine and milling site is located in Viseu county. Mine operation started in 1913, and a chemical treatment plant was added in 1944 for production of uranium concentrates. When facilities were closed in 2001, there were two main milling tailings dump areas, Barragem Nova and Barragem Velha, plus mining waste and low grade ore in other locations inside the mining area facilities. The mine and mill facilities are located in the urban perimeter of Urgeiriça village, but over the years the area was surveyed by ENU company and the access restricted to employees. With the company shut down, waste piles could become areas of public access and contaminated materials could be dispersed. Figure 1 gives an aerial view of the rehabilitated site taken in 2007.



FIG. 1. The milling tailings waste pile Barragem Velha, at Urgeiriça, after placement of the multilayer cap (Aerial view, 2007).

External radiation doses on the top of milling tailings averaged  $7.5 \mu\text{Sv/h}$  with a maximum of about  $12 \mu\text{Sv/h}$ , and radon exhalation from tailings averaged  $3.5 \text{ Bq m}^{-2} \text{ s}^{-1}$  with a maximum of about  $7 \text{ Bq m}^{-2} \text{ s}^{-1}$  [10, 11]. External radiation, re-suspension of tailings' radioactive dust, radon emanation, and dispersal of tailings' materials by landslides, surface runoff, and leaching of radionuclides by rainwater were of environmental concern. Furthermore, the work carried out in the framework of MinUrar project identified high radioactivity levels in seepage from tailings piles, mine water, and surface runoff that were of radiological concern. The epidemiological study carried out concluded that population living near the milling tailings had seen their health condition diminished in comparison with the reference groups, and analysis of  $^{210}\text{Po}$  in human hair and radiation induced chromosome damage in blood cells indicated higher accumulation of uranium daughters in the body and enhanced radiation exposure than in reference population groups [3].

The cleaning of mining and milling facility areas in Urgeiriça, with disposal of waste from facility areas on top of milling tailings piles followed by the placement of a multilayer cap totalizing 1 m thickness, was carried out from 2006 to 2008 (25 months' work). A drainage system was built and an existing water treatment station improved and automated. The waste dump Barragem Nova, that received contaminated mud and sludge from mine water treatment was also re shaped and covered with shielding layers and soil after 2008.

The outcomes of these works were the reduction of ambient radiation dose on top of Barragem Velha to about 5% of previous dose rate, i.e., down to  $0.30 \mu\text{Sv/h}$  (natural background dose rate in the area is  $0.2\text{--}0.4 \mu\text{Sv/h}$ ), the elimination of re suspension of radioactive waste particles into the atmosphere, and the reduction of radon exhalation to near background levels ( $0.2 \text{ Bq m}^{-2} \text{ s}^{-1}$ ).

Radioactivity in the stream Ribeira da Pantanha, receiving process water from milling tailings for decades was, in 2005, at  $22.6 \pm 0.8 \text{ Bq/L}$  of dissolved  $^{238}\text{U}$  and  $0.247 \pm 0.016 \text{ Bq/L}$  of dissolved  $^{226}\text{Ra}$ , while in 2012 it was of  $0.782 \pm 0.024 \text{ Bq/L}$  and  $0.065 \pm 0.003 \text{ Bq/L}$  for the same radionuclides, respectively [11, 12]. Sediments from the bed of this stream displayed very high concentrations in the past and are gradually diminishing now. Radionuclides in horticulture products grown on the banks of Ribeira da Pantanha using stream water for irrigation were also often higher than in reference areas [11–14]. With the cleanup of the area and contaminated water treatment, radionuclide concentrations are expected to decrease.

The clean-up of the Urgeiriça mine area and confinement of milling tailings and other contaminated waste in Barragem Vellha corresponds to securing a waste volume of  $1.6 \times 10^6 \text{ m}^3$ . This was performed in 25 months, with a cost of 6 million Euros from public funds. With this remediation work there were gains in radiation protection of the public, environmental clean-up of a stream basin, reduction of the contamination of agriculture and pasture lands in the vicinity of tailings and along the stream, and reduction of contaminated discharges into River Mondego. Furthermore, there were gains also achieved with the decontamination of property (buildings, industrial area, machinery, lands) that can be now released and sold by the mine holding company.

Cunha Baixa mine near the city of Mangualde, is another major uranium mine site located in the village with the same name [15]. Besides the usual impacts of external radiation dose, dust resuspension and radon, in this area contaminated acid mine water from underground mine spread into groundwater and reached the wells of agriculture properties in a field located at altitude lower than the mine. For example, concentrations of dissolved radionuclides in the water of a well in this zone were, in 2007,  $4176 \pm 280 \text{ mBq/L}$  of  $^{238}\text{U}$  and  $184 \pm 40 \text{ mBq/L}$  of  $^{226}\text{Ra}$  (water pH = 3.88) and, in 2012, concentrations were of  $4983 \pm 222 \text{ mBq/L}$  and  $552 \pm 33 \text{ mBq/L}$  (water pH = 4.12) for the same radionuclides respectively, and showing no improvement. Since mine closure, chemical processing of acid mine water from the underground mine did not help much to reduce radioactivity in the water of those irrigation wells. These contaminated wells were recently sealed and a surface water reservoir was built in terrains of the former mine concession for supplying clean irrigation water to farms in this valley. Views of the water treatment station and a recreational area created by the rehabilitation are shown in Figs. 2 and 3.

The survey of radioactivity in horticulture products from this area was performed several times over the years and radionuclide concentrations were above average natural background radioactivity in comparison areas of the region. Internal radiation dose to members of the public in Cunha Baixa village, consuming horticulture products from their farms, were higher than the EU recommended dose limit for members of the public, 1 mSv/h [12]. This radiation exposure through intake of radionuclides with the diet is expected to decrease with the use of clean water in irrigation. Furthermore, the treatment of Cunha-Baixa contaminated and acid mine water was modified with the introduction of a passive treatment in constructed wetlands and using the chemical treatment as a second resource in mine water treatment.



*FIG. 2. Partial view of the old uranium mine site of Cunha Baixa, with the new water treatment station, water reservoir for irrigation, and passive water treatment ponds in first plane (View from the village, 2014).*



*FIG. 3. Partial view of the small lake and leisure area of the remediated former uranium mine site of Valinhos, near Canas de Senhorim (2014).*

Major remediation works were carried out in other mine sites. Many of the former uranium mine sites have no milling tailings and some of them have mining waste that actually contains radioactivity at about background level. Two sites with such features were Valinhos and Espinho mines, in the regions of Urgeiriça and Cunha Baixa, respectively. In both sites did existed flooded open pits and piles of mining waste. Contaminated materials were removed and sites were cleaned, including scrapping of surface ground, and landscape re shaped to adapting for new uses. The Valinhos mine site was transformed in a leisure park, with picnic areas and a fishing pond with facilities for using small boats. Espinho mine site was re-naturalized, keeping the 35 m deep open pit as a water pond used for sports fishing and as water source for firefighting. External radiation and radioactivity levels in environmental materials of these sites are at the level of regional background. For example, in Valinhos area the external radiation dose was determined at  $< 1\mu\text{Sv/h}$  and radioactivity in the water pond at about background values for natural waters. These environmentally remediated sites, after due clearance by radiation protection authorities, could be used for other societal purposes soon. The challenge is the suitable transfer of site property along with responsibilities on surveillance, maintenance and proper use, to new owners.

Many former uranium sites were not remediated yet. Some of them are of more concern because of radioactive materials and potential for environmental radioactive contamination. For example, some open pit mines such as Mondego Sul, Boco, and Murtorios, contain large volumes of contaminated water and are located near surface water streams, such as the River Mondego, and are of strategic value as sources of drinking water [13, 16]. Adequate action shall be taken in the future, expectedly to ensure suitable water quality and radiation protection to population.

These sites, especially those with large quantities of milling tailings and high radionuclide concentrations, are deemed to be kept isolated from biosphere by multilayer caps placed on tailings and by drainage systems [15]. Such engineered waste management solutions are adequate but will not stand alone and require maintenance in the future and continued radiological monitoring and surveillance. In particular, water, surface air and food chains will continue to require radioactivity monitoring to ensure that radiation dose to members of the public is in compliance with European Union directives and radiation dose limits, as well as international standards [17].

The environmental remediation program for abandoned mine sites, was started in 2005 and the cost so far is of 145 MEuros (of which about 70 MEuros for radioactive mines) for a total of near 30 mine sites remediated or in course of remediation. The remediation program identified 175 degraded and abandoned mine sites and amongst them 61 uranium/radium mine sites [6]. The investment made in remediation of abandoned mine sites (radioactive and non-radioactive) is aimed at protecting public health and environment, and preserving the territory and natural resources for future generations. Remediation works implemented contributed already to a significant abatement of radiation exposure allowing for safer implementation of economic activities, such as agriculture, grazing, and tourism in the surroundings of legacy sites. Environmental remediation contributed also to re build confidence in mining activities and improved life quality in the region.

#### 4. CONCLUSIONS

Research and monitoring of environmental radioactivity at old uranium mine sites and in their surrounding environment allowed identifying existing exposures to ionizing radiation from uranium waste and identifying pathways of radionuclides' transfer in the environment leading to enhanced exposure of population members to ionizing radiation. In the terrestrial environment at these mine sites, besides the direct exposure to external radiation that more easily could be controlled using multilayer caps as a shielding, the main challenge are environmental pathways that may transfer radionuclides from uranium waste to humans. Amongst radionuclides of the uranium family, radium-226 usually is the most water soluble and mobile [18]. Control of water pathways and radium transfer to plants, cattle, and humans may provide control on this major component of radiation exposure of local population

members. On the long run, the confinement of residues to isolate them from water cycle and from the food chains may ensure environmental health and radiation safety to population.

## REFERENCES

- [1] CARVALHO, F.P., "Past uranium mining in Portugal: legacy, environmental remediation and radioactivity monitoring", The Uranium Mining Remediation Exchange Group (UMREG) Selected Papers 1995–2007, STI/PUB/1524 IAEA, Vienna (2011) 145–155.
- [2] MARINHO FALCÃO, J., CARVALHO, F.P., LEITE, M.M., ALARCÃO, M., CORDEIRO, E., RIBEIRO, J., MinUrar-Minas de Urânia e seus Resíduos. Efeitos na Saúde da População, Relatório Científico I, Publ. INSA, INETI, ITN (2005) (in Portuguese).
- [3] MARINHO FALCÃO, J., CARVALHO, F.P., LEITE, M.M., ALARCÃO, M., CORDEIRO, E., RIBEIRO, J., MinUrar-Minas de Urânia e seus Resíduos, Efeitos na Saúde da População. Relatório Científico II. Publ. INSA, INETI, ITN (2007) (in Portuguese).
- [4] NERO, J.M., DIAS, J.M., TORRINHA, A.J., NEVES, L.J., TORRINHA, J.A., "Environmental evaluation and remediation methodologies of abandoned radioactive mines in Portugal", Proc. Int. Workshop on Environmental Contamination from Uranium Production Facilities and Remediation Measures, Lisbon, 2004, Proceedings Series, IAEA, Vienna (2005) 145–158.
- [5] SANTIAGO BATISTA, A., "The programme for remediation of contaminated sites: its regulation and follow-up in Portugal", Proc. Int. Workshop on Environmental Contamination from Uranium Production Facilities and Remediation Measures held in Lisbon, 2004, Proceedings Series, IAEA, Vienna (2005) 223–232.
- [6] EMPRESA DE DESENVOLVIMENTO MINEIRO, The Legacy of Abandoned Mines, Empresa de Desenvolvimento Mineiro, Lisbon (2011).
- [7] CARVALHO, F.P., OLIVEIRA, J.M., LOPES, I., BATISTA, A., Radionuclides from past uranium mining in rivers of Portugal, *J. Environ. Radioact.* **98** (2007) 298–314.
- [8] CARVALHO, F.P., OLIVEIRA, J.M., FARIA, I., Alpha Emitting Radionuclides in Drainage from Quinta do Bispo and Cunha Baixa Uranium Mines (Portugal) and Associated Radiotoxicological Risk, *Bull. Environ. Contam. Toxicol.* **83** (2009) 668–673.
- [9] CARVALHO, F.P., MADRUGA, J.M., REIS, M.C., ALVES, J.G., OLIVEIRA, J.M., GOUVEIA, J., SILVA, L., "Radioactive survey in former uranium mining areas in Portugal", Proc. Int. Workshop on Environmental Contamination from Uranium Production Facilities and Remediation Measures held in Lisbon, 2004, Proceedings Series, IAEA, Vienna (2005) 29–40.
- [10] CARVALHO, F.P., The National Radioactivity Monitoring Program for the Regions of Uranium Mines and Uranium Legacy Sites in Portugal, *Procedia Earth and Planetary Science* **8** (2014) 33–37.
- [11] CARVALHO, F.P., OLIVEIRA, J.M., MALTA, M., Analyses of radionuclides in soil, water and agriculture products near the Urgeiriça uranium mine in Portugal, *J. Radioanal. Nucl. Chem.* **281** (2009) 479–484.
- [12] CARVALHO, F.P., OLIVEIRA, J.M., MALTA, M., Radioactivity in Iberian Rivers with Uranium Mining Activities in their Catchment Areas, *Procedia Earth and Planetary Science* **8** (2014) 48–52.
- [13] CARVALHO, F.P., OLIVEIRA, J.M., MALTA, M., Intake of Radionuclides with the Diet in Uranium Mining Areas, *Procedia Earth and Planetary Science* **8** (2014) 43–47.
- [14] CARVALHO, F.P., OLIVEIRA, J.M., MALTA, M., Radioactivity in Soils and Vegetables from Uranium Mining Regions, *Procedia Earth and Planetary Science* **8** (2014) 38–42.
- [15] PEREIRA, R., BARBOSA, S., CARVALHO, F.P., Uranium mining in Portugal: a review of the environmental legacies of the largest mines and environmental and human health impacts, *Environ. Geochem. Health* **36** (2014) 285–30.
- [16] CARVALHO, F.P., OLIVEIRA, J.M., MADRUGA, M.J., LOPES, I., LIBANIO, A., MACHADO, L., "Contamination of hydrographical basins in uranium mining areas of Portugal", *Uranium in the Environment: Mining Impacts and Consequences* (MERKEL, B.J., HASCHE-BERGER, A., Eds), Springer-Verlag Berlin Heidelberg (2006) 691–702.

- [17] INTERNATIONAL ATOMIC ENERGY AGENCY, Release of sites from Regulatory Control on Termination of Practices, IAEA Safety Standards Series No. WS-G-5.1., IAEA, Vienna (2006).
- [18] INTERNATIONAL ATOMIC ENERGY AGENCY, The Environmental Behaviour of Radium: Revised Edition, Tech. Rep. 476, IAEA, Vienna (2014).

# **ENSURING SAFE USE OF WATER IN A RIVER BASIN WITH URANIUM DRAINAGE**

F.P. CARVALHO, J.M. OLIVEIRA, M. MALTA  
Laboratório de Protecção e Segurança Radiológica/  
Instituto Superior Técnico (LPSR/IST),  
Universidade de Lisboa, Portugal

## **Abstract**

In the catchment basin of Mondego River, centre of Portugal, there is a significant legacy of uranium mining and milling sites that in the past discharged untreated contaminated waters into Mondego tributaries. This river basin is an important agriculture and livestock region with industrial forest areas and artificial lakes, such as the Aguiaria Dam, that supply drinking water to the centre of the country. A radioactivity monitoring programme currently ensures radioactivity surveillance of this river system. The water from Aguiaria Dam on the River Mondego has been, over the last years, consistently in compliance with the EU drinking water quality standards, and radioactivity levels are comparable to natural levels in other rivers with no uranium mines. Environmental remediation of old mine sites is in progress, and continued environmental radioactivity monitoring is needed to confirm its effectiveness and to demonstrate radiation safety to the population.

## **1. INTRODUCTION**

Uranium mining legacy in the catchment basin of River Mondego, centre of Portugal, includes twelve old uranium mine sites, three of them having been uranium milling sites also. This river basin is an important agriculture and livestock production region, with industrial forest used for paper pulp production. In the river basin were built four dams for electricity production, two of them with large artificial lakes that supply drinking water to three million people and irrigation water for crops.

In past decades, wastewater discharges from uranium milling and acid mine drainage caused significant contamination in streams affluent to River Mondego [1, 2]. Environmental remediation works were implemented recently, especially at the milling tailings dump site of Urgeiriça mine and in other major mine sites, which reduced radioactive discharges into Mondego tributaries (Fig. 1) [3].

The Mondego basin has been monitored for radioactivity, especially in water, suspended matter, and sediments in order to assess radionuclide concentrations and the radiological quality of water. Results of recent radioactivity surveys are reported and discussed herein in the perspective of public health and radiation exposure.

## **2. MATERIALS AND METHODS**

Sampling of water and sediments was carried out in November 2012, during high river water flow. Water samples of 10 L were filtered on site through 0.45 µm membrane filters to analyse dissolved and particulate fractions separately. Sediment samples were collected with a hand operated sampler. Sediments were sieved and the sediment fraction < 63 µm analysed for radionuclides of natural decay series.

Analyses of samples were carried out by complete dissolution of sample materials followed by radiochemical separation of radionuclides and electrodeposition on metal discs. Determination of radionuclide activity concentrations was performed by measurement of alpha radiation using an OCTECTEplus spectrometer (ORTEC-EG&G). Radiochemical procedures and quality assurance applied in analytical work were described in detail elsewhere [4–6]. Results are expressed in activity concentrations for the main alpha emitting radionuclides of uranium decay chain.

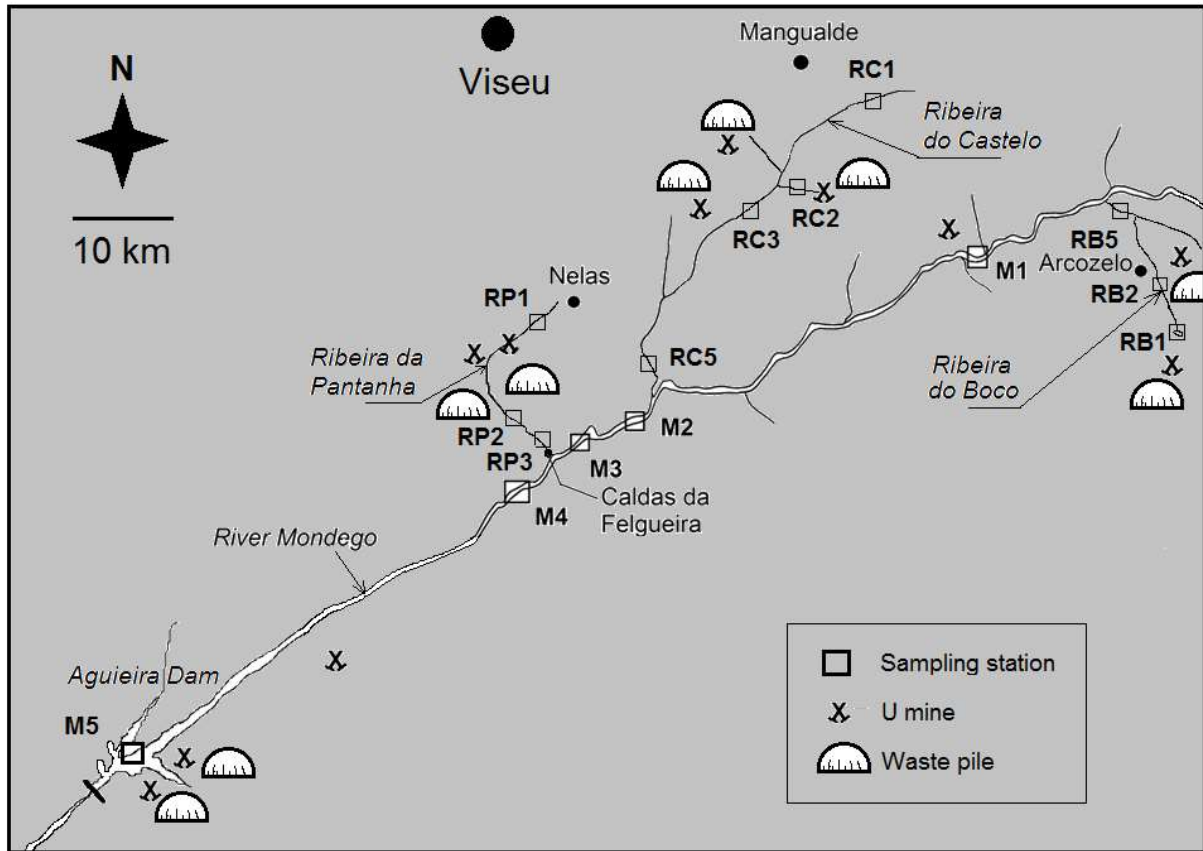


FIG. 1. River Mondego basin and old uranium mine sites.

### 3. RESULTS AND DISCUSSION

Analysis of milling tailings and mining waste dumped in Urgeiriça area had been performed in previous years, before the start of remediation works in this area. Results showed that radionuclide concentrations were very high in solid waste materials and in seepage from the tailings, thus being a source of radioactive contamination to neighbor environment and, in particular, to water streams. For example, solid materials in the milling tailings waste pile contained activity concentrations of  $2500 \pm 100$  Bq/kg of  $^{238}\text{U}$ ,  $25\,000 \pm 2000$  Bq/kg of  $^{226}\text{Ra}$ , and  $20\,400 \pm 700$  Bq/kg of  $^{210}\text{Po}$  [1]. Acidic seepage from Barragem Velha milling tailings contained  $36 \pm 1$  Bq/L of  $^{238}\text{U}$ ,  $1.84 \pm 0.03$  Bq/L of  $^{226}\text{Ra}$  and  $0.70 \pm 0.04$  Bq/L of  $^{210}\text{Po}$  in the dissolved phase and much higher concentrations in the particulate phase, and this seepage was directly released into the stream Ribeira da Pantanha [1, 2]. Surface runoff from waste piles and seepage from other mines in the basin were likely to contribute to contamination of River Mondego also (Fig.1).

Determinations of radionuclides in stream water sampled at several sampling points in three tributaries and in River Mondego are shown in Tab. I and activity concentrations in suspended particulate matter in Tab. II. Results indicated that old mine sites and mine water discharges were the sources of radioactive contamination in the streams, namely Ribeira do Boco (RB), Ribeira do Castelo (RC), and Ribeira da Pantanha (RP). The discharge of these streams into River Mondego caused enhanced concentrations particularly of uranium ( $^{238}\text{U}$ ) decay series radionuclides. This was measurable in the tributary streams, where radionuclide concentrations in dissolved and particulate phases were higher downstream mine discharges (Tables I and II). With high water flow in the River Mondego, the radioactivity in the tributaries' discharge was diluted rapidly with the increasing water volume (M1 to M5) and in the artificial lake of Aguiaria Dam (M5) radionuclide concentrations were  $9.1 \pm 0.3$  mBq/L,  $4.6 \pm 0.3$  mBq/L, and  $3.1 \pm 0.2$  mBq/L for uranium ( $^{238}\text{U}$ ), radium ( $^{226}\text{Ra}$ ) and polonium ( $^{210}\text{Po}$ ), respectively.

These radionuclide concentrations in water from Aguieira Dam were comparable to naturally occurring levels in other rivers of the region with no drainage from uranium mines [1, 7, 8].

TABLE I. ACTIVITY CONCENTRATION (MBq/L) OF RADIONUCLIDES IN DISSOLVED PHASE OF RIVER WATER

| Sampling station |                     | $^{238}\text{U}$ | $^{226}\text{Ra}$ | $^{210}\text{Pb}$ | $^{210}\text{Po}$ |
|------------------|---------------------|------------------|-------------------|-------------------|-------------------|
| RP1              | Ribeira da Pantanha | 19.5±0.7         | 13±1              | 10.1±0.8          | 7.0±0.3           |
| RP2              | Ribeira da Pantanha | 370±10           | 65±3              | 7.5±0.5           | 8.4±0.4           |
| RP3              | Ribeira da Pantanha | 780±20           | 29±2              | 4.8±0.4           | 9.1±0.5           |
| RC1              | Ribeira do Castelo  | 22.8±0.7         | 30±3              | 11.4±0.7          | 27±1              |
| RC2              | Ribeira do Castelo  | 2400±100         | 250±20            | 77±4              | 9.4±0.4           |
| RC3              | Ribeira do Castelo  | 90±3             | 86±8              | 11.1±0.7          | 7.5±0.5           |
| RC5              | Ribeira do Castelo  | 58±2             | 25±2              | 3.2±0.2           | 4.5±0.3           |
| RB1              | Ribeira do Boco     | 132±3            | 18±1              | 18±1              | 14.5±0.7          |
| RB5              | Ribeira do Boco     | 24.1±0.6         | 15±1              | 5.4±0.3           | 8.9±0.3           |
| M1               | River Mondego       | 14.9±0.6         | 7.8±0.9           | 3.4±0.3           | 25±1              |
| M2               | River Mondego       | 13.7±0.4         | 15±1              | 5.0±0.3           | 5.2±0.3           |
| M3               | River Mondego       | 12.7±0.4         | 4.5±0.4           | 4.9±0.3           | 23±1              |
| M4               | River Mondego       | 23.0±0.5         | 5.1±0.4           | 5.3±0.3           | 14.2±0.7          |
| M5               | River Mondego       | 9.1±0.3          | 4.6±0.3           | 1.7±0.1           | 3.1±0.2           |

Undetermined amounts of milling tailings materials and contaminated process water were discharged over decades by these mines into the surface streams. Radionuclide concentrations in riverbed sediments were determined in the past [1]. Current radionuclide concentrations in river bed sediments were still relatively high in the streams near mine discharges (Tab. III). For example, at RC2 in Ribeira do Castelo  $^{238}\text{U}$  was  $5200 \pm 200$  Bq/kg, which is much higher than naturally occurring concentrations,  $329 \pm 10$  Bq/kg at the reference station RC1. Concentrations in sediments decreased also with distance from mine discharges and they point out to input of contaminated solid materials from mining and milling waste as a source of sediment contamination. In aqueous media under oxic conditions some radionuclides, such as uranium and radium, likely will dissolve from riverbed sediments with time while others, such as thorium and polonium, will remain mostly in the solid fraction [8-15].

Radionuclide concentrations in the tributary streams Ribeira da Pantanha and Ribeira do Castelo (Tabs I and II) were now lower than recorded in 2006, before the implementation of remediation measures in these areas [1, 7]. The collection of mine drainage and seepage for chemical treatment contributed to decrease radioactive contamination, allowing for the partial recovery of these streams from mine impact.

TABLE II. ACTIVITY CONCENTRATION (BQ/KG DRY WEIGHT) OF RADIONUCLIDES IN SUSPENDED PARTICULATE MATTER OF RIVER WATER

| Sampling station | $^{238}\text{U}$ | $^{226}\text{Ra}$ | $^{210}\text{Pb}$ | $^{210}\text{Po}$ |
|------------------|------------------|-------------------|-------------------|-------------------|
| RP1              | 13903±387        | 76113±4183        | 69286±3261        | 69380±2560        |
| RP2              | 28199±1462       | 350±17            | 820±45            | 528±21            |
| RP3              | 12945±396        | 1188±78           | 1830±111          | 2794±112          |
| CB1              | 984±27           | 939±45            | 1322±56           | 1235±58           |
| CB2              | 67225±2081       | 2958±119          | 10793±477         | 5254±296          |
| CB3              | 4199±108         | 2492±153          | 2119±106          | 1330±82           |
| CB5              | 3293±102         | 2724±182          | 1855±101          | 1964±128          |
| RB1              | 2814±72          | 952±61            | 2384±126          | 2148±74           |
| RB5              | 2403±55          | 1565±70           | 2519±141          | 3278±103          |
| M1               | 9018±240         | 3562±228          | 7604±297          | 7775±338          |
| M2               | 2346±63          | 940±88            | 2462±113          | 2634±120          |
| M3               | 9729±314         | 4100±396          | 5740±307          | 8702±422          |
| M4               | 2866±73          | 912±40            | 2212±97           | 2750±127          |
| M5               | 1646±44          | 692±35            | 1563±70           | 1254±62           |

TABLE III. ACTIVITY CONCENTRATION (BQ/KG DRY WEIGHT) OF RADIONUCLIDES IN RIVER BED SEDIMENTS (< 63  $\mu\text{m}$  FRACTION)

| Sampling station | $^{238}\text{U}$ | $^{226}\text{Ra}$ | $^{210}\text{Pb}$ | $^{210}\text{Po}$ |
|------------------|------------------|-------------------|-------------------|-------------------|
| RP1              | 540±20           | 4900±450          | 7600±400          | 7600±400          |
| RC1              | 330±10           | 260±25            | 260±10            | 260±10            |
| RC2              | 5200±200         | 2700±200          | 2700±160          | 2700±160          |
| RC3              | 1440±40          | 1980±270          | 700±40            | 700±40            |
| RB1              | 1060±30          | 710±60            | 960±40            | 960±40            |
| RB2              | 600±20           | 1100±100          | 750±30            | 750±30            |
| M1               | 410±10           | 390±30            | 370±20            | 370±20            |
| M2               | 520±20           | 350±40            | 310±20            | 310±20            |
| M3               | 630±20           | 260±20            | 440±30            | 440±30            |
| M5               | 143±6            | 390±40            | 124±6             | 124±6             |

Current radionuclide concentrations in water from the artificial lake of Aguiéira Dam were under the limits recommended for radioactivity in drinking water, 1.0 Bq/L for total beta and 0.5 Bq/L for total alfa radioactivity, and WHO guideline for uranium in drinking water, < 15 µg/L [16, 17].

In spite of progress made in uranium legacy control and site remediation, including waste management and radioactive mine drainage treatment, not all mine sites in the Mondego basin were cleaned-up and remediated so far. Some of them are of concern from the radiological point of view and represent a threat to water quality, in particular due to its proximity to this river (Fig. 1). Therefore, monitoring of radioactivity in terrestrial and freshwater ecosystems of this river basin is deemed essential to ensure radiological protection to the public.

#### 4. CONCLUSIONS

Current levels of radionuclides in stream waters were moderately low despite many years of untreated process water and mine water discharges into tributaries to Mondego River. Compared with past years, there was a decrease in water radioactivity in these streams and an improvement in water quality has been observed since water treatment and site remediation were implemented at Urgeiriça and Cunha Baixa mine sites.

Radioactivity levels in River Mondego water, particularly from the artificial lake of Aguiéira Dam, were below recommended limits for uranium as well as total alpha and total beta radioactivity limits recommended by the European Union for drinking water.

Due to the importance of water resources of Mondego basin, radioactivity monitoring is periodically carried out to ensure radiological protection of the population and safety for economic activities of this region.

#### REFERENCES

- [1] CARVALHO, F.P., OLIVEIRA, J.M., LOPES, I., BATISTA, A., Radionuclides from past uranium mining in rivers of Portugal, *J. Environ. Radioact.* **98** (2007) 298–314.
- [2] CARVALHO, F.P., OLIVEIRA, J.M., MADRUGA, M.J., LOPES, I., LIBANIO, A., MACHADO L., “Contamination of hydrographical basins in uranium mining areas of Portugal”, *Uranium in the Environment: Mining Impacts and Consequences* (MERKEL, B.J., HASCHE-BERGER, A. Eds), Springer-Verlag Berlin Heidelberg (2006) 691–702.
- [3] CARVALHO, F.P., Uranium legacy sites in Portugal: Environmental radioactivity and mitigation of radiological impact (these proceedings).
- [4] CARVALHO, F.P., MADRUGA, J.M., REIS, M.C., ALVES, J.G., OLIVEIRA, J.M., GOUVEIA, J., SILVA, L., “Radioactive survey in former uranium mining areas in Portugal”, Proc. Int. Workshop on Environmental Contamination from Uranium Production Facilities and Remediation Measures, Lisbon, 2004, Proceedings Series, IAEA, Vienna (2005) 29–40.
- [5] OLIVEIRA, J.M., CARVALHO, F.P., “A sequential extraction procedure for determination of uranium, thorium, radium, lead and polonium radionuclides by alpha spectrometry in environmental samples”, Proc. 15th Radiochemical Conference, Czechoslovak Journal of Physics **56** (Suppl. D) (2006) 545–555.
- [6] CARVALHO, F.P., OLIVEIRA, J.M., Performance of alpha spectrometry in the analysis of uranium isotopes in environmental and nuclear materials, *J. Radioanal. Nucl. Chem.* **281** (2009) 591–596.
- [7] Drainage from Quinta do Bispo and Cunha Baixa Uranium Mines (Portugal) and Associated Radiotoxicological Risk, *Bull. Environ. Contam. Toxicol.* **83** (2009) 668–673.
- [8] CARVALHO, F.P., OLIVEIRA, J.M., MALTA, M., Analyses of radionuclides in soil, water and agriculture products near the Urgeiriça uranium mine in Portugal, *J. Radioanal. Nucl. Chem.* **281** (2009) 479–484.

- [9] CARVALHO, F.P., OLIVEIRA, J.M., MALTA, M., Radionuclides in plants growing on sludge and water from uranium mine water treatment, *Ecological Engineering* **37** (2011) 1058–1063.
- [10] CARVALHO, F.P., The national radioactivity monitoring program for the regions of uranium mines and uranium legacy sites in Portugal, *Procedia Earth and Planetary Science* **8** (2014) 33–37.
- [11] CARVALHO, F.P., OLIVEIRA, J.M., MALTA, M., Radioactivity in Iberian rivers with uranium mining activities in their catchment areas, *Procedia Earth and Planetary Science* **8** (2014) 48–52.
- [12] CARVALHO, F.P., OLIVEIRA, J.M., MALTA, M., Radioactivity in soils and vegetables from uranium mining regions, *Procedia Earth and Planetary Science* **8** (2014) 38–42.
- [13] CARVALHO, F.P., OLIVEIRA, J.M., MALTA, M., Intake of radionuclides with the diet in uranium mining areas, *Procedia Earth and Planetary Science* **8** (2014) 43–47.
- [14] FESENKO, S., CARVALHO, F.P., MARTIN, P., MOORE, W.S., YANKOVICH, T., Radium in the environment, *The Environmental Behaviour of Radium: Revised Edition*, Tech. Rep. 476, IAEA, Vienna (2014) 33–105.
- [15] CARVALHO, F. P., CHAMBERS, D., FESENKO, S., MOORE, W.S., PORCELLI, D., VANDENHOVE, H., YANKOVICH, T., Environmental pathways and corresponding models, *The Environmental Behaviour of Radium: Revised Edition*, Tech. Rep. 476, IAEA, Vienna (2014) 106–172.
- [16] WORLD HEALTH ORGANIZATION, Guidelines for drinking water quality, 3<sup>rd</sup> edn, **I**. Recommendations, ISBN 92 4 1546387, WHO, Geneva (2004).
- [17] EUROPEAN UNION, COUNCIL DIRECTIVE 98/83/EC of 3 November 1998 on the quality of water intended for human consumption (OJ L 330, 5.12.1998) (1998) 32.

# RADIOLOGICAL LEGACY OF URANIUM MINING — THE CASE STUDY OF CALDAS, MG, BRAZIL

D. DE AZEVEDO PY JUNIOR, J.V. DA SILVA JÚNIOR,  
M.V. DE ALMEIDA DANTAS, R. ZAFALON,  
T.F. DE ÁVILA NAVARRO, D. DE FIGUEIREDO,  
J.C. PEREIRA MAGALHÃES, W. SCASSIOTTI FILHO  
Indústrias Nucleares do Brasil,  
Caldas, Minas Gerais, Brazil

## Abstract

The Brazilian uranium mine of Caldas, Minas Gerais (MG), produced 1030 tonnes of uranium, during twenty years of operation, from 1977 to 1997. Currently the mine and the mill are deactivated and the decommissioning process is in course. The total mass of ore tailings produced is equal to 108 Mt and the mass of milling solid waste is equal to 2.4 Mt. The ore tailings are distributed through several piles placed near the mine pit and the milling wastes are deposited in the waste dam. The mine pit and two of the tailing piles generate acid water which requires treatment before the environmental standards are achieved and the water is liberated to the environment. The waste dam also liberates treated water to the environment. This work presents data, discussions and main conclusions of radiological monitoring of the water liberated by Caldas uranium mine to the environment during the last four years, from 2010 to 2013. All the calculated annual doses of members of the public, from 2010 to 2013, are above the annual dose constraint but are below the annual dose limit.

## 1. INTRODUCTION

The 2013 annual environmental monitoring program of the Brazilian uranium mine of Caldas, MG, has required 1689 surface water samples; 39 underground water samples; 17 sediment samples; 5 soil samples; 7 farm products and fish samples; and 1728 direct measurements of pH, temperature, dissolved oxygen, turbidity and salinity. The stable parameters determined in water samples are:  $Mg^{2+}$ ,  $Ca^{2+}$ ,  $Cr^{n+}$ ,  $Cu^{n+}$ ,  $Ni^{2+}$ ,  $Zn^{2+}$ ,  $Ba^{2+}$ ,  $Mn^{n+}$ ,  $Fe^{n+}$ ,  $Al^{3+}$ ,  $SiO_2$ ,  $SO_4^{2-}$ ,  $F^-$ ,  $Na^+$ ,  $K^+$ ,  $P$ ,  $Cl^-$ ,  $NO_3^-$ , and  $N$ . The radionuclides determined in all samples are: U-238, Th-230, Ra-226, Pb-210, Th-232 and Ra-228.

The objective of this work is to interpret the registered results from 2010 to 2013 at the Caldas uranium mining and milling site monitoring program in terms of estimates of the public exposure to radiation.

## 2. SENSITIVITY OF THE ANALYTICAL METHOD

Uranium is analysed by spectrophotometry after arsenazo addition and uranium chemical isolation in the sample volume of 2 L. The minimum detectable concentration is equal to 0.01 becquerels per litre (Bq/L).

## 3. COMPARISON OF MONITORING RESULTS WITH PERMITTED UPPER LIMIT FOR DISCHARGE INTO THE ENVIRONMENT

Figure 1 shows the visual comparison of uranium concentrations measured during the last four years in the critical liquid effluent release point with the permitted upper limit for discharge. Uranium concentrations are represented by the curve adjusted through the measured concentrations and the horizontal line represents the upper limit for discharge.

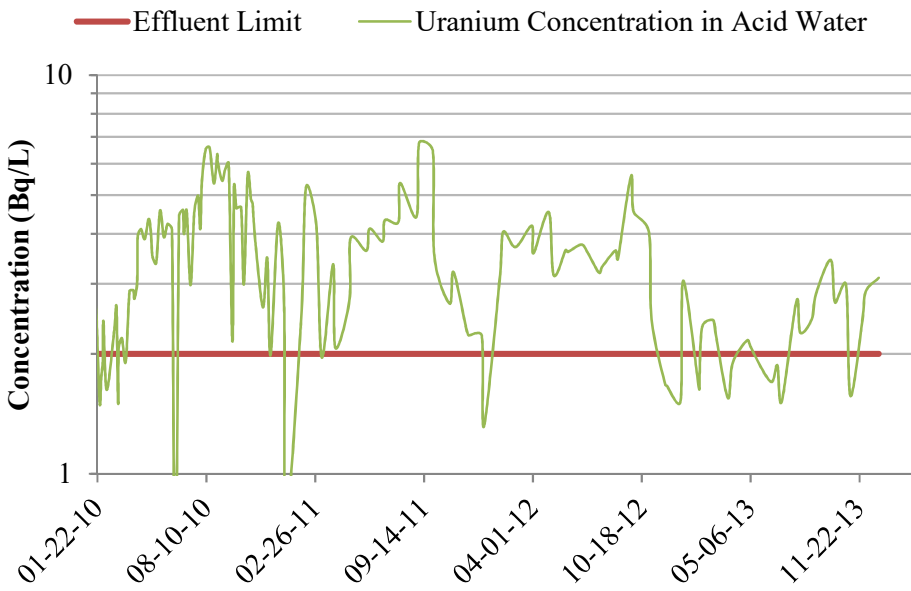


*FIG. 1. Uranium monitoring in water.*

The annual means of uranium concentration from 2010 to 2013 are all above the permitted upper limit for discharge. Actions for the mitigation radiological impacts due to acid water releases into the environment are being taken, such as waterproofing of waste pile surfaces and channels used for collecting precipitation water.

#### 4. RADIOLOGICAL IMPACT CALCULATION

The doses to members of the public were calculated considering that the fraction of annual mean of uranium concentration in water and the respective permitted upper limit is equal to the fraction of annual dose and the annual dose constraint of 0.3 mSv/y. Figure 2 shows the annual dose limit, the calculated annual doses, the annual dose constraint and the annual rainfall.

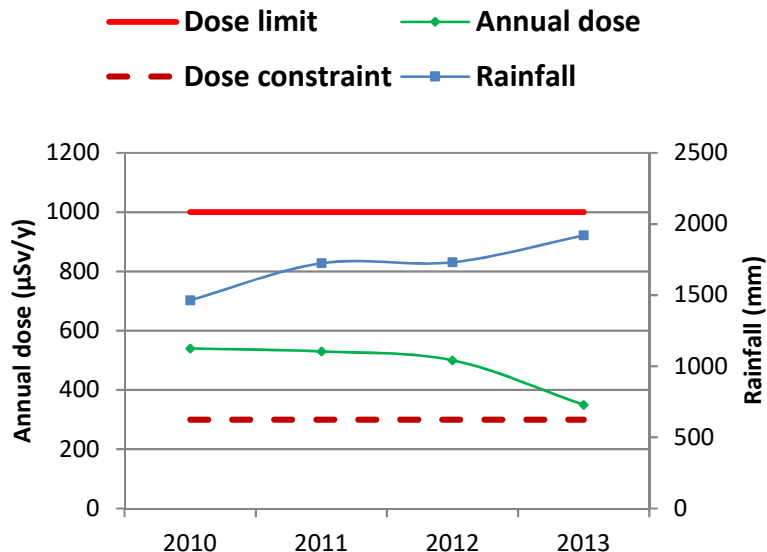


*FIG 2: Annual dose and rainfall.*

All the calculated annual doses, from 2010 to 2013, are above the annual dose constraint and are below the annual dose limit. Compared with annual rainfall, annual dose shows some inverse correlation, although it is not a controlled process.

## 5. CONCLUSIONS

These studies were part of investigations for the solution of the acid water drainage problem — prior to the discovery of this problem, uranium concentrations were lower than now, and annual doses were below the dose constraint. To address the problem a new water basin was constructed in 2012, in order to collect and to pump acid water into the treatment plant. In February 2012 the conceptual decommissioning plan was finished, including a hydrogeological study, aiming to establish the guidance for additional remediation works. Besides the maintenance works, there are new structures being implemented, aiming to minimize rain water drainage entering the tailing piles.

## REFERENCES

- [1] COMISSÃO NACIONAL DE ENERGIA NUCLEAR, Princípios Básicos de Proteção Radiológica, Norma CNEN 3.01, Rio de Janeiro, (2011) (in Portuguese).
- [2] COMISSÃO NACIONAL DE ENERGIA NUCLEAR, Programa de Proteção Radiológica Ambiental, Norma CNEN 3.01, Posição Regulatória PR 3.01/008, Rio de Janeiro, (2011) (in Portuguese).
- [3] COMISSÃO NACIONAL DE ENERGIA NUCLEAR, Modelo para Elaboração de Relatórios de Programa de Proteção Radiológica Ambiental, Norma CNEN 3.01, Posição Regulatória PR 3.01/009, Rio de Janeiro, (2011) (in Portuguese).
- [4] INDÚSTRIAS NUCLEARES DO BRASIL, Programa de Monitoração Radiológica Ambiental, PMRA Revisão 06 (2004) (in Portuguese).

# ON-LINE X-RAY FLUORESCENCE ANALYSIS OF URANIUM MATERIALS IN MINING AND PROCESSING INDUSTRY

E. HASIKOVA\*, A. SOKOLOV\*, V. TITOV\*,  
M. CELIER\*\*, P. NARDOUX\*\*, Y. PREVOST\*\*

\* Baltic Scientific Instruments,  
Riga, Latvia

\*\* Areva Mines,  
Bessines-sur-Gartempe, France

## Abstract

Application of on-line X-ray fluorescence (XRF) analysis in the mining and processing industry of uranium (U) can improve the representativeness and speed of analysis and lower costs. Potential applicability of the industrial XRF analyser CON-X series is demonstrated for continuous measurement of uranium content in various uranium-bearing materials (heavy mineral sands, phosphate rock and fertilizers, U ore residues after heap-leaching, monazite ore etc.) and at wide ranges of U concentrations (from 100 ppm up to tens of percent). In addition to the physical components required to perform on-line XRF measurements, analyser design and analytical method can be customized to the requirements of specific field or process. The dynamic laboratory simulation of on-line measurement of uranium in ground N-P-K fertilizers indicates statistically acceptable correlation with routine analysis. Estimated detection limit (DL) obtained with replicate measurements is 25–50 ppm depending on the type of phosphate material. On-site test of the CON-X analyser for continuous analysis of uranium in ore residues after heap-leaching showed that the difference between on-line and laboratory results was within 10% relative at the level of 100 ppm U. DL is estimated at 30–50 ppm in 5-minute measurements depending on interfering elements. Advantages and limitations of CON-X analyser for on-line analysis of uranium in solid materials transported by the conveyor are also discussed.

## 1. INTRODUCTION

Baltic Scientific Instruments develops and manufactures highly sensitive and accurate uranium and thorium (U and Th) XRF industrial on-line analyser CON-X series for mining operators, prospectors and concentrator plants [1]. The expected detection limit (DL) for U analysis is under 30–50 ppm (depending on the type of matrix) which we have already achieved in our laboratory application studies.

The on-line analysers are based on the non-destructive XRF technology (X-ray fluorescence) and one version of the analyser is mounted directly above a conveyor belt to measure and analyse crushed ore or any solid flows in real time. Another on-stream version of the analyser measures slurry flows between the process units to enable the production of high grade uranium leaching solutions.

Yet more version of the U analyser is under development, i.e. drill core analyser that is capable to follow the drilling equipment and make precise measurement and U grade analysis on-site. Accurate knowledge of the uranium content in ore, heap or in-situ leaching solutions enables optimizing the yield of U production process and gives great monetary savings by reducing the consumption of energy, raw materials, chemicals and water in mines and plants.

Results of online analysis are not to be affected by variation of external parameters: temperature and humidity of material and industrial environment, variation of the material lump size, variation in the height of flow, etc. X-ray fluorescence analyser CON-X series has been designed and manufactured accounting for these features [1]. Specially designed software uses X-ray spectra to account for changes in distance to measured material, which provides the user with accurate results irrespective of the material flow rate.

## 2. POTENTIAL APPLICATIONS OF ANALYSER IN MINING AND PROCESSING

Potential applicability of conveyor XRF analyser CON-X series for on-line analysis of U content in process materials is discussed in this article. Here we present the results confirming that CON-X analyser is applicable starting with the primary enrichment (sorting and rejection of uranium ore) to the final control of the content of uranium residues after heap-leaching process. In 2011, 30% of the world U was produced by underground mining, 17% was the share of open pits, in-situ leaching technology share accounted for 45% and the remaining was a by-product extracted from unconventional resources [2].

Uranium residues ( $\leq 100$  ppm), phosphate rock and fertilizers (50–200 ppm), rutile and zircon heavy mineral sands (50–350 ppm), monazite concentrate (0.2%  $U_3O_8$ ) and others were the objects of the study.

Figure 1 demonstrates CON-X02 analyser operating on the industrial conveyor.



FIG.1. XRF on-line analyser CON-X02 installed on the industrial conveyor to analyse traces of iron in quartz sand.

### 2.1. Uranium residues after heap leaching process

On-site test of the CON-X analyser for on-line measurement of uranium in ore residues after heap-leaching was implemented on the pilot conveyor at Areva Mines. The study showed that U may be determined in the matrix containing a number of interfering elements (rubidium, molybdenum and zircon) with accuracy  $\leq 10\%$  ( $2\sigma$ ) at measurement time of 5–10 min. The range of U concentrations studied was 30–200 ppm.

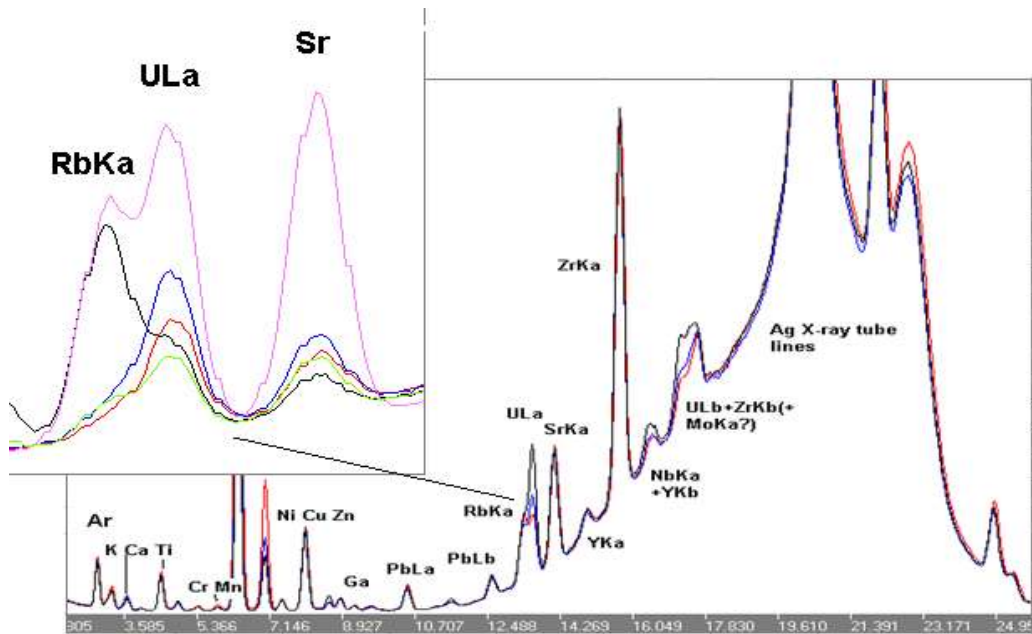


FIG. 2. Overview of the spectra of uranium ore residues. Parameters of measurement: Ag X-ray tube voltage 36 kV, current 500  $\mu$ A, 100  $\mu$ m thick Ag filter of primary radiation, measurement time 600 s.

An overview of XRF spectra of uranium ore residues after heap-leaching is shown on Fig. 2: U La and Lb lines are proportional to U concentration. This means that depending on the material composition analyser can be calibrated by either U La or U Lb line intensities.

Detection limit (DL) is estimated at 30–50 ppm in 5-minute measurements depending on interfering elements.

Dedicated software BSIKit based on the Method of Fundamental Parameters was successfully used to solve the problem of the overlapping lines Rb Ka and U La. Due to this it successfully calculates uranium concentrations in the solid residues after heap-leaching process with accuracy  $\leq 10\%$ .

Concentration trend of real dynamic measurements of uranium in residues on the pilot conveyor is shown on Fig. 3 below:

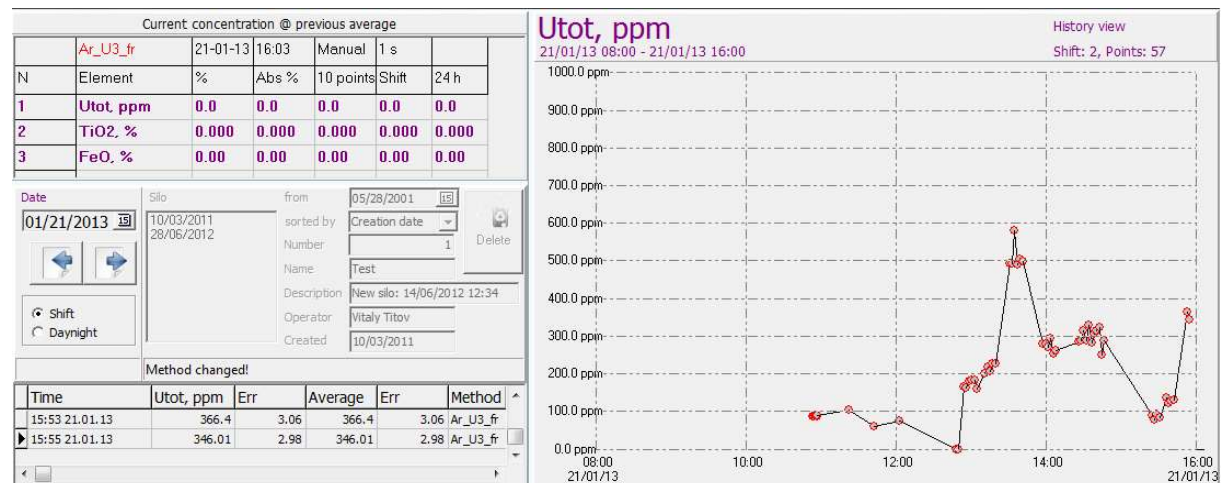
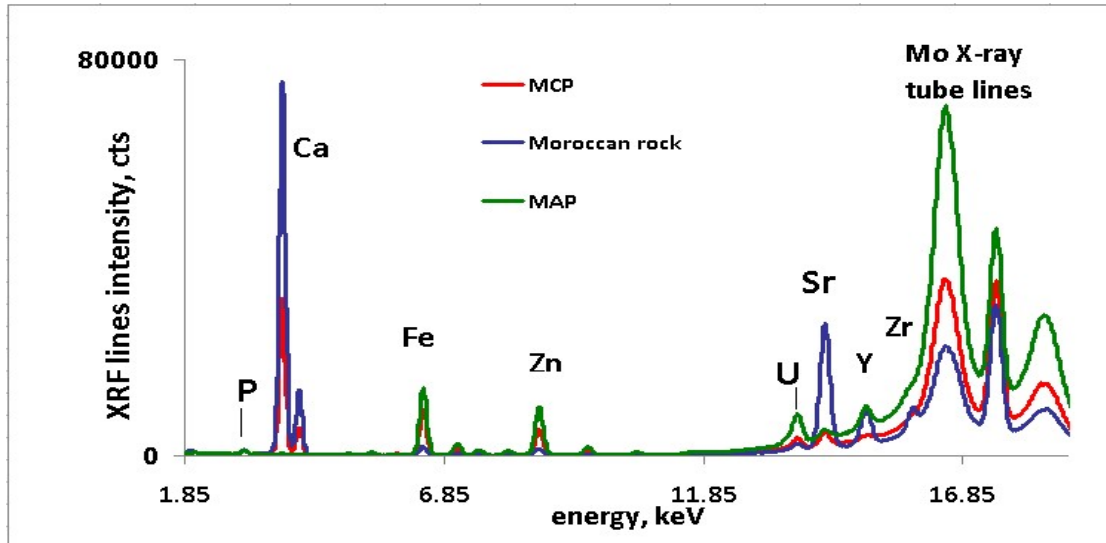


FIG.3. Concentration trend of uranium measured in residues after heap-leaching.

It is obvious from the Fig. 3 that analyser confidently distinguishes between different concentration levels. So it can serve as modern tool that enables to measure or monitor uranium traces in process residual materials.

## 2.2. Phosphate rock and fertilizers

Uranium can be found as one of the components in phosphate ores in the amount of 50–200 ppm [3]. The world U resources in phosphate rock are estimated as  $9 \times 10^6$  tonnes [4]. In production U is left produced fertilizer as a radioactive contaminant that is clearly seen from Fig. 4 below.



*FIG. 4. Spectra of phosphate rock, MCP and MAP. Parameters of measurement: Mo X-ray tube voltage 39 kV, current 100  $\mu$ A, 100  $\mu$ m thick Mo filter on tube, measurement time 600 s.*

Figure 4 shows the spectra of Moroccan phosphate rock and phosphate fertilizers mono-calcium phosphate (MCP) and mono-ammonium phosphate (MAP) produced from the named rock. U lines are identified in all these materials even in 5-minute measurements.

During laboratory application study the DL of U determination in phosphate rock was quantitatively estimated in line with the procedure 40CFR part 136 as 30 ppm in the range of concentration 50–300 ppm.

Estimated accuracy of U measurement was  $\leq 10$  ppm ( $2\sigma$ ). This level of quantification allows analyser to make sorting of raw phosphate rock or monitoring of uranium level in commercial fertilizers on the industrial conveyor.

## 2.3. Zircon and rutile heavy mineral sands

In 2009, Baltic Scientific Instruments and Richard Bay Minerals engineers carried out CON-X02 conveyor analyser application test at Richard Bay Minerals heavy mineral sand separation plant.

The target elements of these applications were Zr and Ti, but capability of analyser to detect and estimate the level of minor elements (U and Th) was also proven. The spectrum of the mineral sand after separation from silica containing rutile as major compound and zircon as a minor one is shown on Fig. 5.

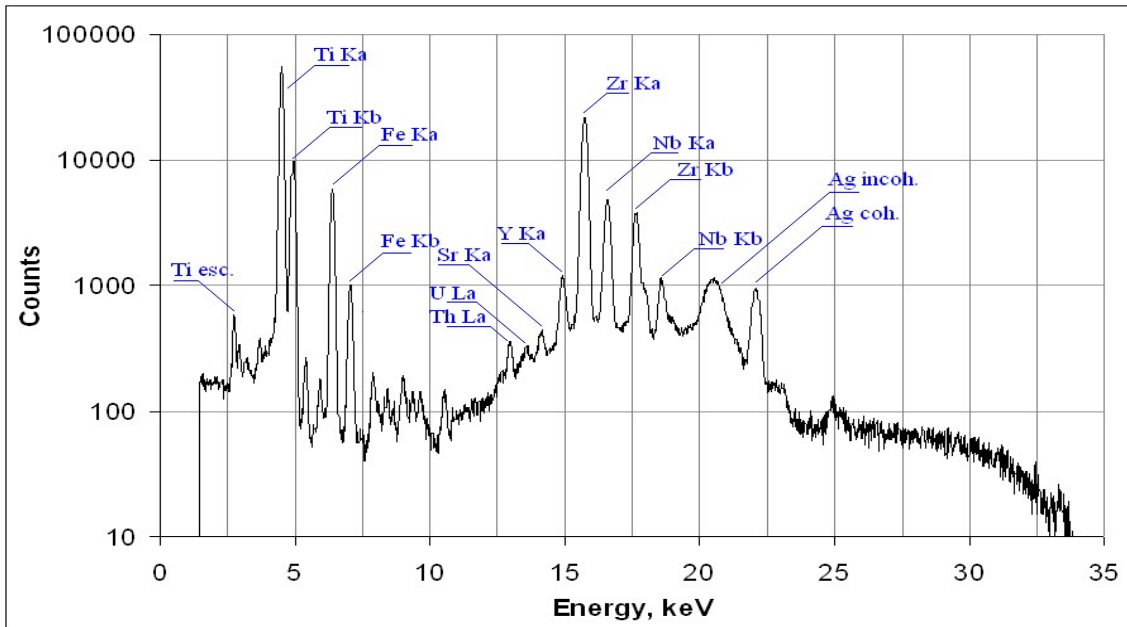


*FIG. 5. Spectrum of the heavy mineral sand after separation from silica. Parameters of measurement: Ag X-ray tube voltage 39 kV, current 100  $\mu$ A, 50  $\mu$ m thick Rh filter of primary radiation, measurement time 300 s, distance between sample and detector 50 mm.*

After 5-minute measurement, U and Th XRF lines are clearly visible in the rutile sample mostly consisting of the  $TiO_2$  sand and containing uranium at the level of 100 ppm. Normally concentration range of U in raw heavy mineral sands is 10–350 ppm [5] depending on type of main component.

CON-X02 and 03 analyser modifications are equipped with SDD detector. Its excellent energy resolution and throughput significantly improves signal-to-noise ratio at a fixed measurement time, which, in turn, enhances the instruments sensitivity to trace element measurement including U and Th.

DL proven for this study is 60 ppm; accuracy was  $\leq 15\%$  relative.

#### 2.4. Analysis of uranium as a minor element of monazite ore

Currently economically viable U ores contain 0.05–0.07 % of uranium oxide ( $U_3O_8$ ) [2].

This means that even before beneficiation uranium ores normally contain higher amount of U than in cases described above and analysis of U concentration becomes more fast, accurate and reliable. For example, average U concentration in monazite ore is  $\sim 0.2\%$  whereas Th content is as high as 4–7%.

The XRF spectrum of monazite ore is shown on Fig. 6.

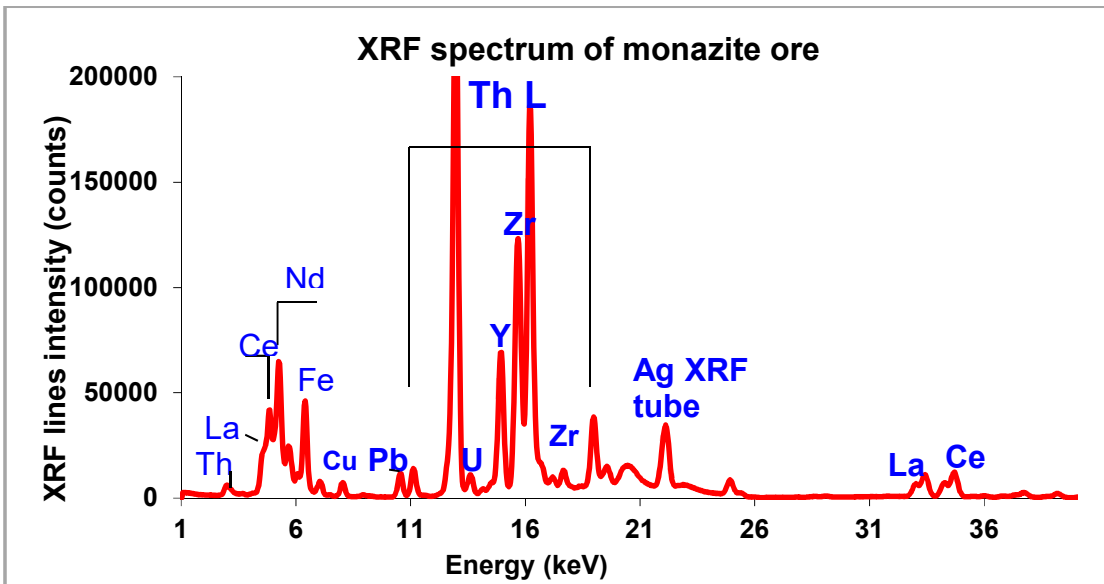


FIG. 6. Spectrum of monazite ore. Parameters of measurement: Ag X-ray tube voltage 45 kV, current 100  $\mu$ A, 100  $\mu$ m thick Ag filter, time of measurement 600 s.

In this application X-ray tube voltage was increased to 45 kV to enhance excitation of rear-earth elements K-lines (La, Ce, Pr, Nd etc.). High resolution provided by SDD detector enables uranium La line to be clearly seen alongside the significantly more intense Th lines. Their partial overlap does not significantly influence on accuracy and precision of analysis due to well developed algorithm of spectral deconvolution in the software. Despite strong neighboring Th lines high-quality analytical parameters are achieved. Uranium MDL calculated from spectral data is approximately 30 ppm and precision is approximately 25 ppm (at  $2\sigma$  level).

## 2.5. Analysis of uranium as a major element

Measurement of U content in rich uranium ores is also possible. At high U concentrations two ways of measurements can be used: direct uranium determination from its XRF spectral lines intensity (Fig. 7) or on the basis of the intensities of the main admixture elements. The combination of the both methods can be implemented in the software providing high accuracy which is typically less than 1% relative for high U contents.

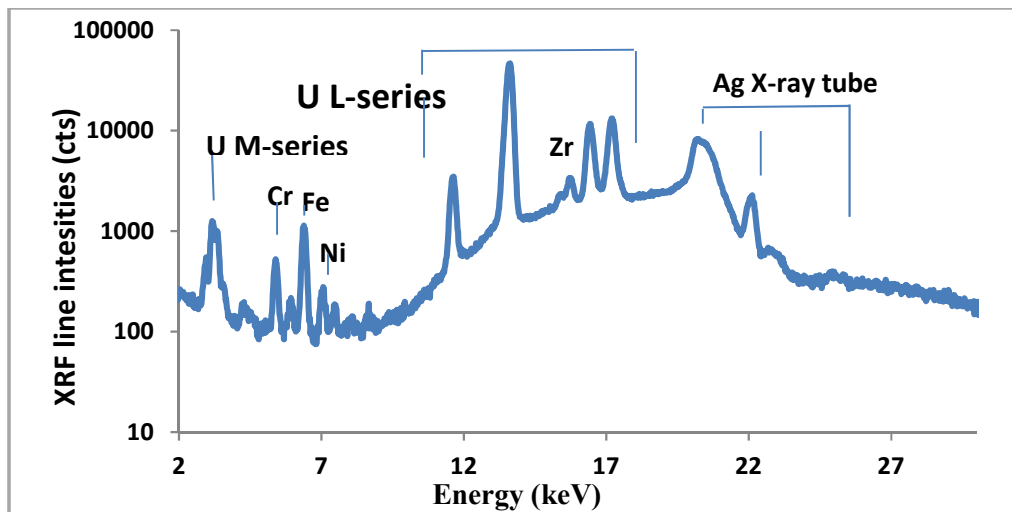


FIG. 7. Spectrum of  $U_3O_8$  on the Teflon substrate. Parameters of measurement: Ag X-ray tube voltage 39 kV, current 100  $\mu$ A, measurement time 600 s, distance between sample and detector 50 mm.

### 3. CONCLUSIONS

The XRF industrial on-line analyser CON-X series is applicable to measure uranium content in various mining and processing materials on the conveyor such as ores, minerals, process streams and residues in real time. Quantitative and semi-quantitative analysis can be implemented in the wide range of uranium concentrations from 100 ppm to more than 80%.

At low concentrations (less than 1%) its MDL for 5–10-minute measurements is on the level of 30–50 ppm even in the most adverse events (e.g. presence of Rb in commensurate concentrations such as in uranium ore residues after heap-leaching or strong neighboring of Th such as in monazite ore).

At higher uranium contents (in the rich uranium ores or concentrated products) relative accuracy of uranium determination with CON-X analyser is high and is estimated at less than 1% relative.

Introduction of industrial on-line XRF analysers CON-X series into uranium mining and process practice is the way to bring ‘a stand-alone small version of laboratory’ into uranium production thus optimizing the yield of U and making great monetary savings by reducing the consumption of energy, raw materials, chemicals, water and labour costs in mines and plants.

### REFERENCES

- [1] BALTIC SCIENTIFIC INSTRUMENTS, On-line XRF Conveyor Analyzer CON-X <http://bsi.lv/en/products/xrf-analyzers/-line-xrf-conveyor-analyzer-con-x/> (viewed June 2016).
- [2] WORLD NUCLEAR ASSOCIATION, World Uranium Mining (2011), <http://www.world-nuclear.org/info/inf23.html>.
- [3] INTERNATIONAL ATOMIC ENERGY AGENCY, World Distribution of Uranium Deposits (UDEPO) with Uranium Deposits Classification, IAEA-TECDOC-1629, IAEA, Vienna (2009).
- [4] RAGHEB, M., Uranium resources in phosphate rocks (2013, 2017) <http://mragheb.com/NPRE%20402%20ME%20405%20Nuclear%20Power%20Engineering/Uranium%20Resources%20in%20Phosphate%20Rocks.pdf>.
- [5] WORLD NUCLEAR ASSOCIATION, Mineral Sands, Naturally Occurring Radioactive Materials, Appendix 1 (2014), <http://www.world-nuclear.org/info/inf30a.html>.

# **QUANTITATIVE ANALYSIS OF THORIUM CONTAINING MATERIALS USING INDUSTRIAL XRF ANALYSER**

E. HASIKOVA, A. SOKOLOV, V. TITOV  
Baltic Scientific Instruments,  
Riga, Latvia

## **Abstract**

The potential applicability of X-ray fluorescence (XRF) industrial conveyor analyser CON-X series is discussed for thorium (Th) quantitative or semi-quantitative on-line measurement in different types of Th-bearing materials. Laboratory study of several minerals (heavy mineral sands and carbonate rocks as unconventional Th resources; monazite concentrate as Th-associated resources and uranium ore residues after heap-leaching as a waste product) was performed and analyser was tested for on-line quantitative measurements of Th contents along with other major and minor components. The Th concentration range in raw heavy mineral sand is 50–600 ppm; its minimal detection limit (MDL) at this level is estimated at 25–50 ppm in 5-minute measurements depending on the type of material. On-site test of the CON-X analyser for continuous analysis of thorium traces along with other elements in zircon sand showed that accuracy of Th measurements is within 20% relative. When Th content is higher than 1% as in the concentrate of monazite ore (5–8 % ThO<sub>2</sub>) accuracy of Th determination is within 1% relative.

## **1. INTRODUCTION**

Thorium (Th) as nuclear fuel is clean and safe and offers significant advantages over uranium. The technology for several types of thorium reactors is proven but still must be developed on a commercial scale. Examples of experimental Th reactors are in UK and India. Currently India is leading in Th-based nuclear reactors [1, 2]. In the case of commercialization of thorium nuclear reactors, thorium raw materials will be on demand [3]. With this, mining and processing companies producing Th and rare earth elements will require prompt and reliable methods and instrumentation for Th quantitative on-line analysis. X-ray fluorescence (XRF) is a method that can be used for the analysis of thorium raw materials [4].

Baltic Scientific Instruments develops and manufactures highly sensitive and accurate uranium and thorium (U and Th) XRF industrial on-line analysers for mining operators, prospectors and processing plants [5]. The expected minimal detection limit (MDL) for Th analysis is 25–50 ppm (depending on the type of matrix) which we have already achieved in our laboratory application studies.

Potential applicability of X-ray fluorescence industrial analyser CON-X series for on-line measurement of Th in different types of Th-bearing materials is discussed here.

Results of the laboratory study of several minerals are described below, namely; zircon and rutile heavy mineral sands, phosphate rock and carbonate minerals as unconventional Th resources; monazite concentrate as Th associated resources and uranium ore residues after heap-leaching as waste product. The analyser was tested for simulated on-line measurements of Th content along with other major and minor components.

Depending upon the type of process or application several versions of industrial analysers can be offered. Industrial on-line analysers CON-X series are based on the non-destructive XRF technology and one version of the analyser is mounted directly above a conveyor belt to measure and analyse crushed ore flows or another solid material in real time. Another on-stream version of the analyser measures solution or slurry flows between the process units to enable the production of high grade leaching solution or solid phase.

Drill core U and Th analyser is under development that is capable to follow the drilling equipment and make precise measurement and Th grade analysis on-site. Accurate knowledge of Th content in ore or rock may potentially optimize the yield of Th production process and gives great monetary savings by reducing the consumption of energy, raw materials, chemicals and water in mines and plants.

Figure 1 demonstrates CON-X02 analyser operating on the industrial conveyor.



*FIG.1. XRF industrial on-line analyser CON-X02 in operation on the industrial conveyor: measurement of chromite ore.*

## 2. ANALYSIS OF TH AS TRACE ELEMENT

### 2.1. Zircon heavy mineral sand

CON-X on-line analyser is able to measure Th content in real time even if Th is only moderately concentrated compared to the average crust composition.

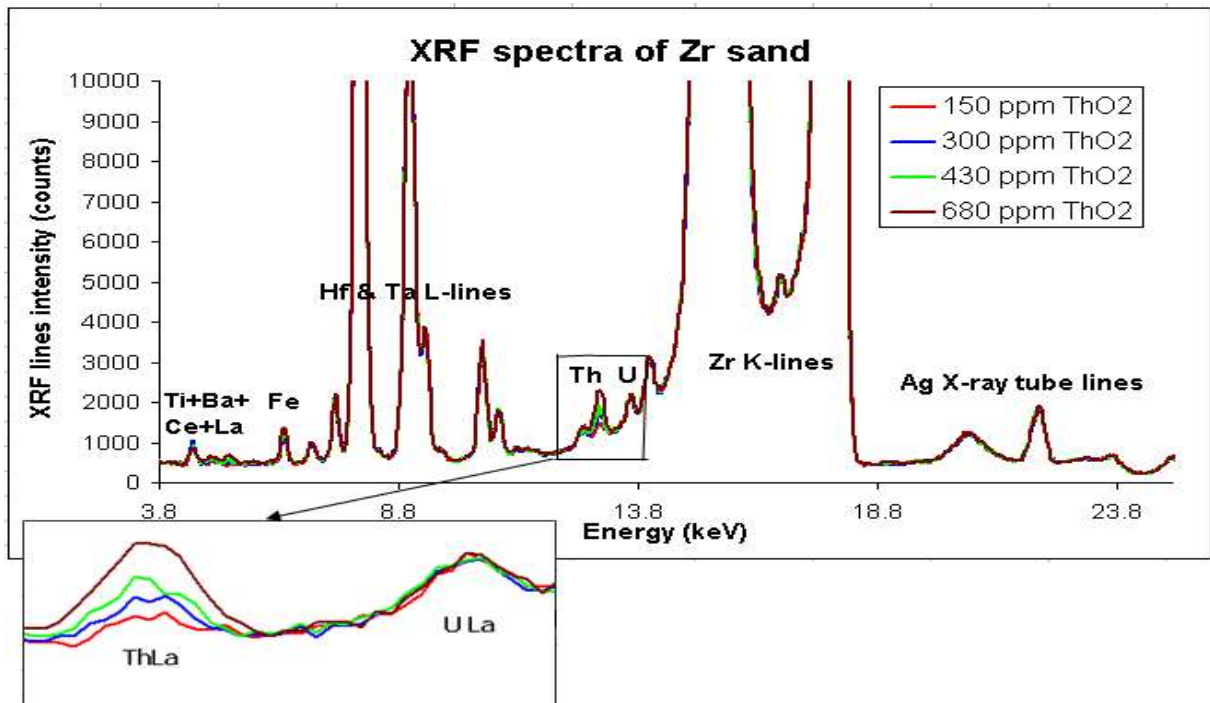


FIG. 2. Overview of the spectra of zircon mineral sand. Parameters of measurement: Ag X-ray tube voltage 36 kV, current 100  $\mu$ A, 60  $\mu$ m thick Ag filter of primary radiation, measurement time 600 s.

Th concentration range in raw heavy mineral sand is 50–500 ppm [6]. Zircon sand ( $ZrSiO_4$ ) is one of the constituents of heavy mineral sands. XRF spectra of zircon sand containing traces of ThO<sub>2</sub> are shown on Fig. 2. After 10-minute measurements a Th L $\alpha$  line is clearly visible.

CON-X analyser was calibrated at Baltic Scientific Instruments XRF application laboratory with zircon sand samples provided from mining operator and spiked in the laboratory with known amounts of Th-containing material. Linear calibration curve where Th L $\alpha$  line intensities were plotted vs. ThO<sub>2</sub> concentrations alongside with screen shot of Th concentration trend measured in zircon sand samples are shown on the Figs 3 and 4. Linear fit correlation is high enough ( $R^2 = 0.98$ ).

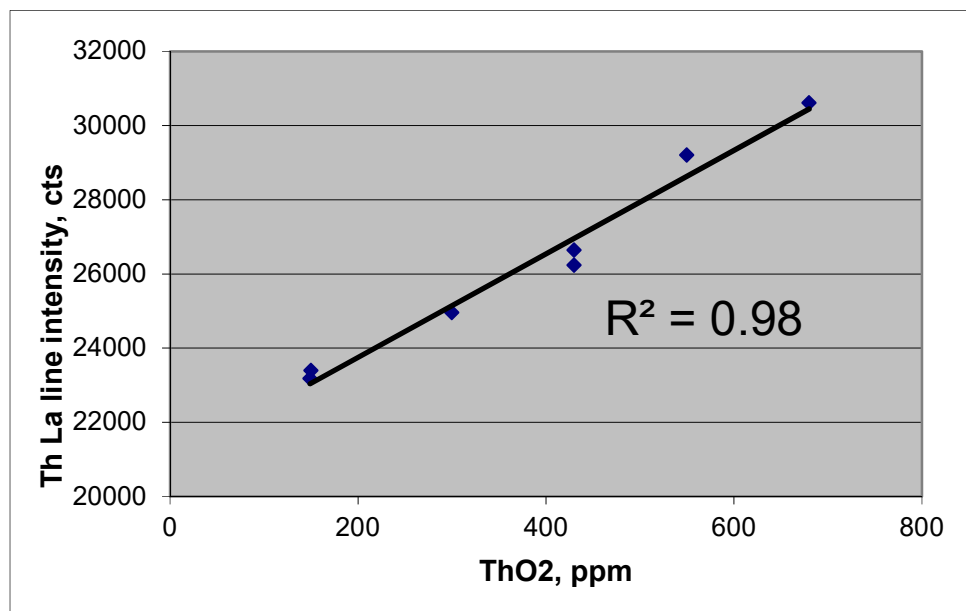
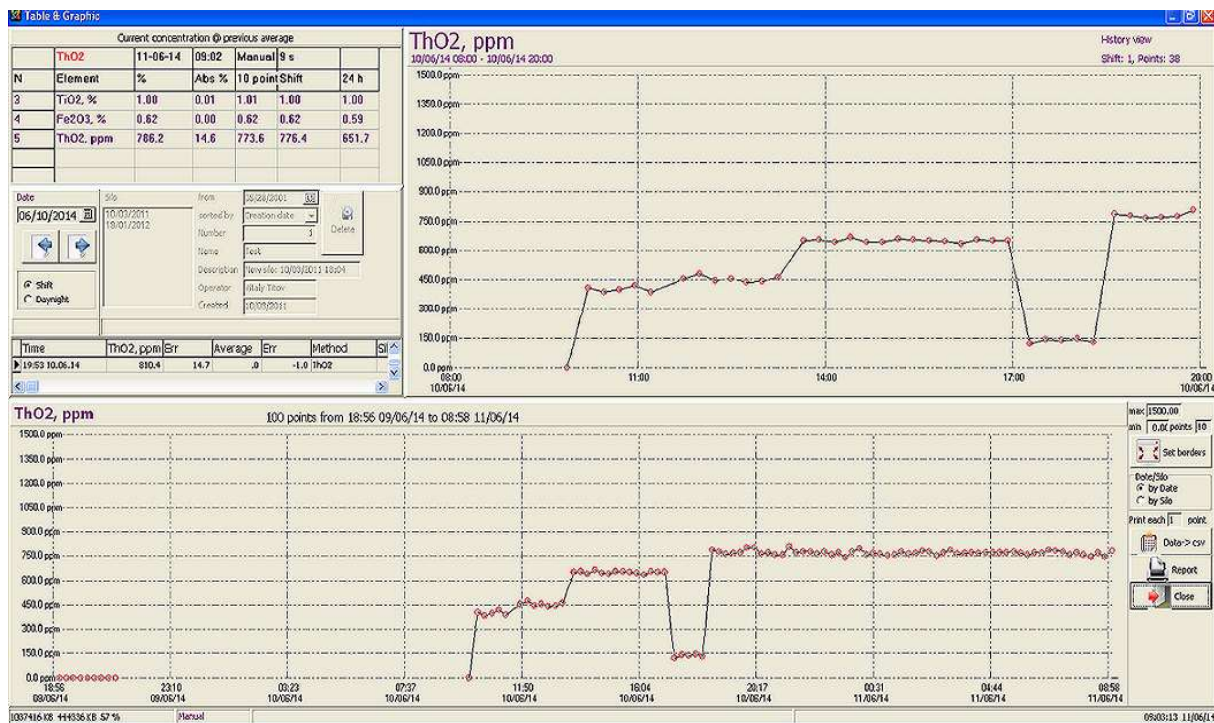


FIG.3. Thorium calibration curve.



*FIG.4. Concentration trend of thorium measured in spiked with ThO<sub>2</sub> samples of zircon sand.*

Th MDL is estimated at 25–50 ppm in 5–10-minute measurements depending on the type of the material and interfering elements. Statistical precision is estimated at 25 ppm.

Industrial tests of the CON-X analyser for continuous analysis of heavy mineral zircon and rutile sands were conducted at heavy mineral sand separation plant. The analyser was installed above the conveyor after separation of silica. Along with positive results for titanium and zirconium determination (target elements), test has shown reliable correlation of Th and U on-line measurements with laboratory results. CON-X and plant laboratory shift and all-day average measurements were compared. Difference between them was shown to be within 20% relative.

## 2.2. Other minerals

Precise and accurate determination of Th and U at trace levels in geochemical materials (granite, calcite, ankerite, phosphate rock and others) is essential for many geochemical and geophysical studies. Although XRF only provides data with the precision comparable to dilution mass spectroscopy and neutron activation analysis at Th concentrations > 10 ppm, it has the advantage also to determine many other useful elements [7]. Spectra of various geological materials scanned with CON-X analyser are shown on Fig. 5.

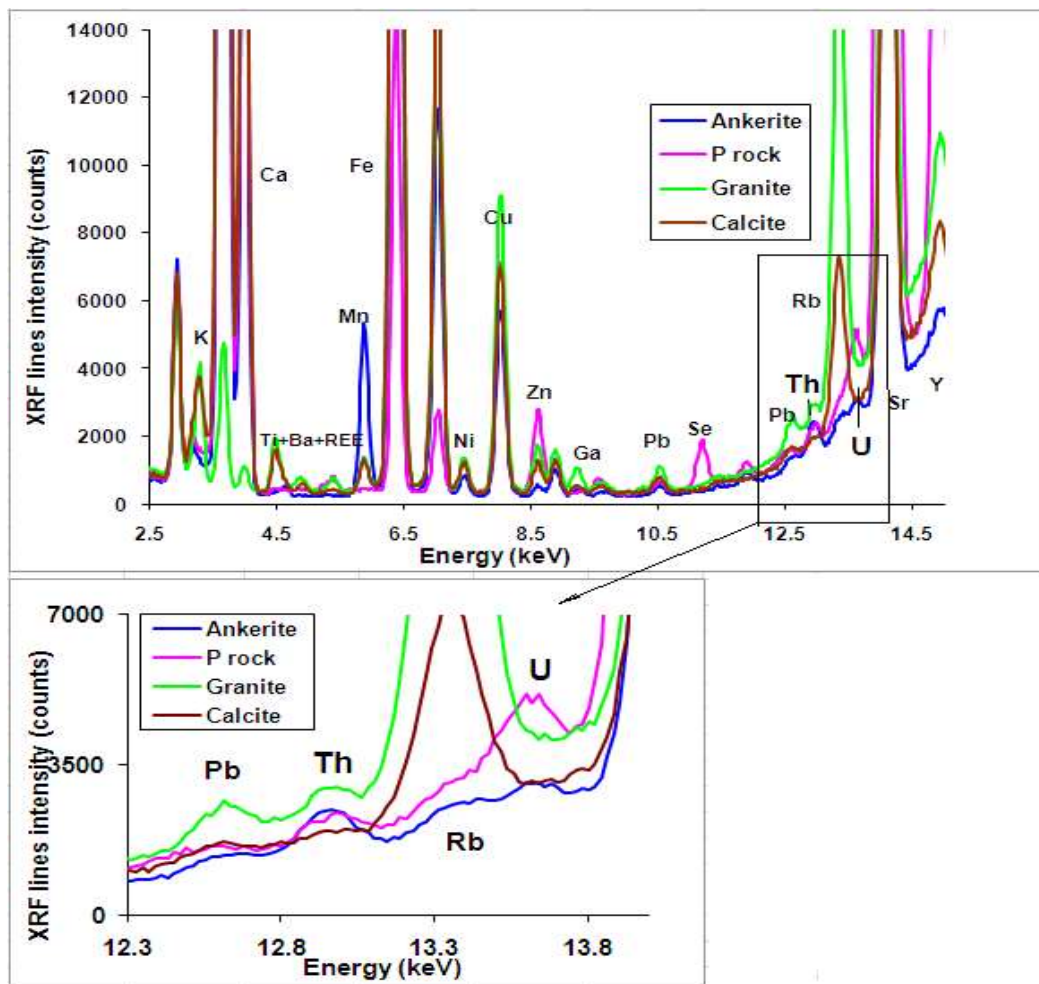


FIG. 5. Overview of the spectra of geological samples (indicated in legend). Parameters of measurement: Ag X-ray tube voltage 36 kV, current 500  $\mu$ A, 60  $\mu$ m thick Ag filter of primary radiation, measurement time 900 s.

The Th XRF line is clearly identified in all mineral products indicated on Fig. 5 in 15 min. measurements. Granite typically contains 10–40 ppm of Th. Provided that Th concentration in the measured granite sample is on the level of 40 ppm Th MDL in 15 min. measurements is estimated at 20 ppm.

CON-X analyser may be applied as a core drill analyser in a version of ‘mobile laboratory’. Geochemical studies may benefit from on-site core analysis in field mapping with a transportable XRF unit. For example, it can help in rapid decision-making on where to drill next.

### 3. ANALYSIS OF TH-ASSOCIATED MATERIALS

The amount of Th in monazite ore may be as high as 4–7%wt. XRF spectrum of such monazite ore is shown in the Fig. 6.

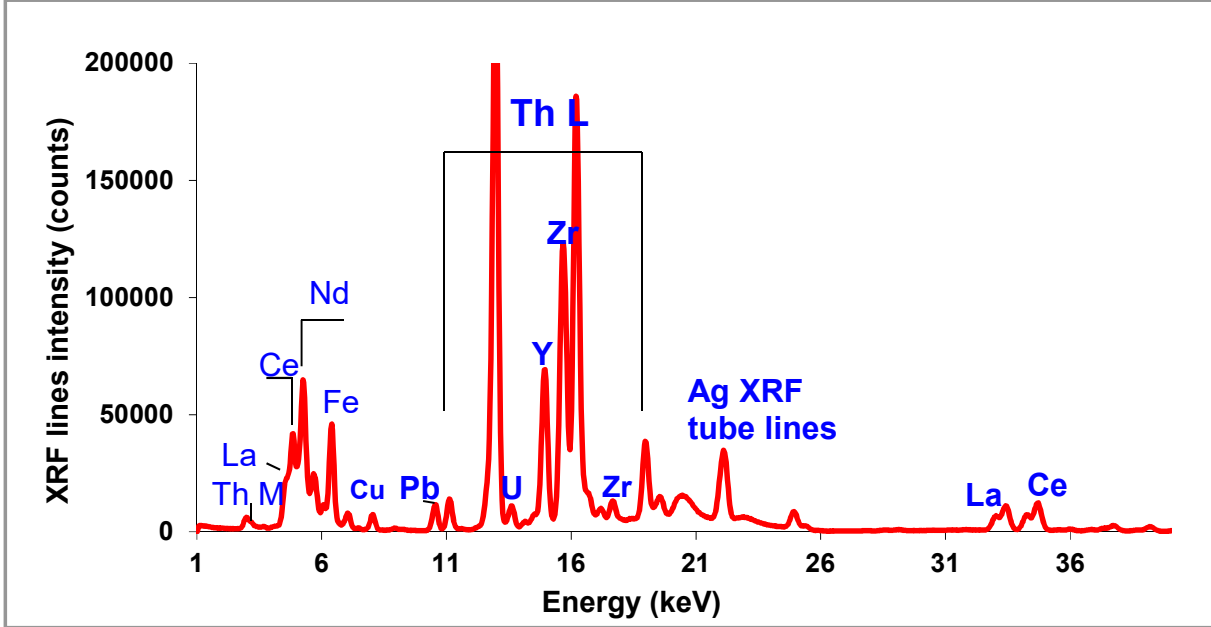


FIG. 6. Overview of the spectrum of monazite ore. Parameters of measurement: Ag X-ray tube voltage 45 kV, current 100  $\mu$ A, 100  $\mu$ m thick Ag filter of primary radiation, measurement time 600 s.

In this study high voltage of X-ray tube excitation was used to enhance the high energy detection efficiency to the level needed for the analysis of the rare-earth elements (La, Ce, Pr, Nd, etc.) using their K-series lines. High energy resolution of the silicon drift detector allows detecting uranium XRF lines (at  $\sim 0.2\%$ ) alongside with the significantly more intense Th lines. Their partial overlap does not significantly affect the precision due to spectral deconvolution algorithm used in the software.

MDLs of U and Th estimated from spectral intensities are on the level of 20 ppm both for Th and U.

#### 4. ANALYSIS OF TH IN WASTE PRODUCTS

Uranium ore residues after heap-leaching contain Th in different concentrations (see Fig. 7):

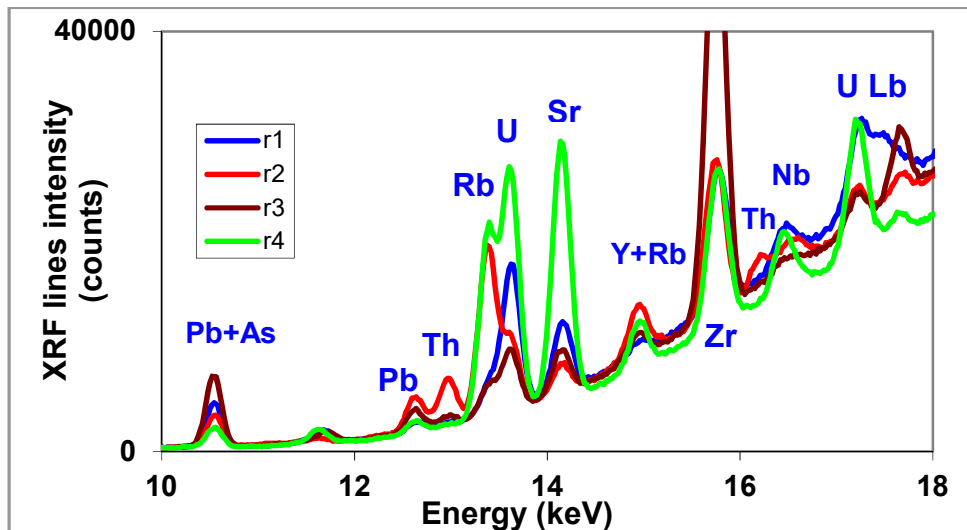


FIG. 7. Overview of the spectra of uranium ore residues. Parameters of measurement: Ag X-ray tube voltage 36 kV, current 500  $\mu$ A, 100  $\mu$ m thick Ag filter of primary radiation, measurement time 600 s.

In this potential application the on-line XRF conveyor analyser CON-X can serve as a tool controlling and estimating the effectiveness heap-leaching process thus giving quick response for unwanted increase of Th and U in residue. It also can be very useful in estimation of environmental impact by measuring concentrations of radioactive and rare-earth elements going to the dumps.

## 5. CONCLUSIONS

The XRF industrial on-line analyser CON-X series is potentially applicable to measure Th content in various geological, mining and processing materials such as ores and rocks, minerals, process streams and residues in real time. Quantitative and semi-quantitative analysis can be implemented in the wide range of uranium concentrations from less than 100 ppm to a 10% level.

At low concentrations (less than 0.1%) its MDL for 5–10-minute measurements is estimated at 20–50 ppm even in presence of interfering lead, rubidium and uranium (e.g. Rb at higher concentrations like in uranium ore residues after heap-leaching and in carbonate rocks). Accuracy at trace level is evaluated at 20–30% relative.

At higher Th contents (like in monazite ore concentrate) the relative accuracy of thorium determination with CON-X analyser is high and is estimated at less than 1% relative.

At this time to discuss the introduction of industrial on-line XRF analysers CON-X series into thorium mining and process control is a bit premature due to a number of legal restrictions and market situation. Moreover, thorium fuel cycle still is not brought to commercialization.

However, thorium prospects for future use in nuclear power plants as a nuclear fuel are the subject of wide scientific and public discussion [2, 3]. With the development of thorium industry, we propose a way to bring ‘a stand-alone small version of laboratory’ into thorium production thus optimizing the yield of thorium and making great monetary savings by reducing the consumption of energy, raw materials, chemicals, water and labour costs in mines and plants.

Although preliminary on-site test is recommended in order to address system feasibility at a large scale, provided results show that industrial conveyor XRF analyser CON-X series can be effectively used for analytical control of mining and processing streams of Th-bearing materials.

## REFERENCES

- [1] INTERNATIONAL ATOMIC ENERGY AGENCY, Role of Thorium to Supplement Fuel Cycle of Future Nuclear Energy Systems, IAEA Nuclear Energy Series NF-N-2.4, IAEA, Vienna (2012).
- [2] BARTEL, F., TULSIDAS, H., “Thorium. Occurrences, geological deposits and resources”, IAEA International Symposium on Uranium Raw Materials for Nuclear Energy, URAM 2014, 2014, Vienna, IAEA, Vienna (these proceedings).
- [3] KENNEDY, J., “Creating a multi-national development platform: Thorium energy and rare earth value chain”, IAEA International Symposium on Uranium Raw Materials for Nuclear Energy (URAM 2014), 2014, Vienna, IAEA, Vienna (these proceedings).
- [4] TSUJI, K., INJUK, J., VAN GRIEKEN, R., (Eds), X-ray Spectrometry: Recent Technological Advances, Wiley, Chichester (2004).
- [5] BALTIC SCIENTIFIC INSTRUMENTS, On-line XRF Conveyor Analyzer CON-X <http://bsi.lv/en/products/xrf-analyzers/-line-xrf-conveyor-analyzer-con-x/> (viewed June 2016).
- [6] WORLD NUCLEAR ASSOCIATION, Mineral Sands, Naturally Occurring Radioactive Materials, Appendix 1 (2014), <http://www.world-nuclear.org/info/inf30a.html>.

- [7] HART, R.J., REID, D.L., STUCKLESS, J.S., WELKE, H.J., Comparison of three techniques for the determination of uranium and thorium in rocks, *Chemical Geology* **29** (1980) 345–350.

# BRAZILIAN URANIUM PRODUCTION AND DEMAND: SCENARIOS FOR THE NEAR FUTURE

R.A.S. VILLEGRAS\*, L.A. GOMIERO\*\*

\*Laboratório de Poços de Caldas/  
Comissão Nacional de Energia Nuclear  
Poços de Caldas

\*\*Indústrias Nucleares do Brasil S.A.  
Caetité

Brazil

## Abstract

The Brazilian government announced some years ago plans to improve its nuclear program. As a result of this decision, a new nuclear power plant is already being built and there are studies dealing with, among other activities, the building of up to four new ones until the end of 2030. Such increase of the country's uranium demand significantly affects the Brazilian state companies that are in charge of the nuclear fuel cycle, as well as the nuclear authority of the country. This paper aims to describe the scenarios predicted to impact the Brazilian nuclear industry for the next years and the related institutions plans to meet the country's needs in terms of uranium exploration and production.

## 1. INTRODUCTION

Brazil's main sources of electrical energy have been, for many years, hydro and thermal (mainly gas burning rather than coal) electrical generation. For instance, in 2011 the hydroelectric source accounted for about 75% of the electrical energy generated in the country [1] (Fig. 1). This situation configures a scenario very different from the rest of the world where, in the same year, hydroelectric generation supplied only 16% of the electrical energy demand. Obviously, in a country with such hydro power potential, there is no will in Brazil to change this situation in a dramatic way.

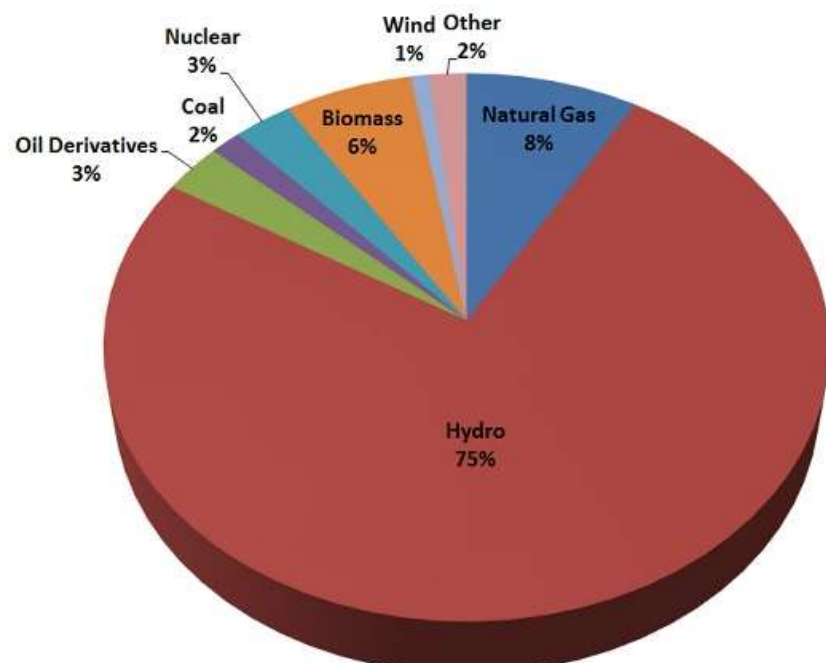


FIG. 3 Distribution of electric energy sources in Brazil (2012).

Even though to have more than 80% of its electrical energy produced from renewable sources can be considered a comfortable situation, since 2001 there have been a lot of discussion about it. That year there was a rainfall shortage, the production capacity of the hydroelectrical power plants was compromised and the citizens were required to lower their electrical energy consumption. In 2014, there was a probability of this happening again, as the country faced the same situation regarding the lack of rain. Summarizing, the hydroelectrical potential makes the country a unique case, but, on the other hand, there is a dependence on localization and on the amount of the annual precipitation. Taking this into account, the Brazilian government intends to diversify the country's energy matrix as much as reasonably possible and have been financing projects dealing with alternative renewable energy sources (like biomass and biodiesel). Additionally, at the end of 2007, plans regarding the expansion of country's nuclear program were announced.

This paper shows an overview of the Brazilian nuclear program, what has been planned for the near future and how these plans affect the institutions and companies in charge of the nuclear fuel cycle in Brazil, as well as its regulation.

## 2. THE BRAZILIAN NUCLEAR PROGRAM

Until the beginning of the 1950s, the Brazilian interests in the nuclear area were restricted to purely academic and theoretical studies. Right after then, the government started to design the regulation policy of the sector by establishing strategic uranium reserves, controlling of radioactive ore mining and began to support the development of nuclear activities.

The so called Brazilian Nuclear Program had its beginning by the 1970s, always pointing to the peaceful use of the nuclear power — actually, the Brazilian Constitution of 1988 states that. Nowadays, Brazil's program is large, comprising a wide range of nuclear applications. About 3000 facilities in the country are using radioactive sources in several activities in industry, health and research. In the last year, over 2.3 million patients used radiopharmaceuticals at more than 300 hospitals, with a growth in the annual demand of about 10% in the last ten years. All those activities are regulated by Comissão Nacional de Energia Nuclear—CNEN (in English, National Commission of Nuclear Energy), which is the regulatory body and also runs the main nuclear research facilities in the country, among other activities.

Concerning the nuclear fuel cycle, two state companies play a major role in the uranium production and electrical energy generation. Nowadays, Brazil has two nuclear power plants (Fig. 2): Angra I and Angra II, located in Rio de Janeiro state in the southeast part of the country, the most economically developed region. With these two plants, nuclear generated electric energy comprised only 3% of the Brazilian energy matrix in 2011.



FIG. 4. Angra I (right) and Angra II nuclear power plants.

Eletronuclear is the operator of both nuclear power plants. Table I shows some figures about Angra I and II capacity.

TABLE I. DATA ABOUT ANGRA I AND II NPPS

| Fact                                   | Angra I | Angra II |
|--|---------|----------|
| Beginning of commercial operation      | 1985    | 2001     |
| Capacity                               | 657 MW  | 1350 MW  |
| Number of fuel elements                | 121     | 193      |
| Average U demand (t of $U_3O_8$ /year) | 154     | 246      |
| Average U demand (t of U/year)         | ~131    | ~209     |

Indústrias Nucleares do Brasil (INB, in English Nuclear Industries of Brazil) is the operator of the steps that comprise the nuclear fuel cycle before the electrical energy generation. The company's two main facilities are the Unidade de Concentrado de Urânio – URA (Uranium Concentrate Facility, Fig. 3) and Fábrica de Combustível Nuclear – FCN (Nuclear Fuel Factory).



FIG. 5. INB's Uranium Concentrate Facility (URA)

The URA facility is located at the so called Uraniferous Province of Lagoa Real, localized in Bahia state in the northeast region of the country. This region has been explored for uranium since the 1970s and at the time of writing was the only production site in Brazil (at that time, also in South America). Besides mining, the complex comprises a chemical plant where the uranium concentrate is produced by means of heap leaching and then a solvent extraction step.

Nowadays, URA facility has a production capacity of 400 tonnes of  $U_3O_8$  [~340 t U] per year, enough to supply the internal demand. FCN is located in Rio de Janeiro state and consists of two sub-facilities. The first one is in charge of manufacturing the  $UO_2$  pellets and the other assembles the nuclear fuel elements.

The country already has the necessary know-how and technological development to run the two nuclear fuel cycle steps that are currently done abroad. This fact brings the country to a very restricted group of similarly capable countries. Only a few countries possess the technology of the whole nuclear fuel cycle and have large uranium resources.

### 3. NEAR FUTURE SCENARIOS AND PLANS

Although the use of medical and industrial radioactive applications has been growing as a result of the development of the country as a whole, the last significant movement of the nuclear fuel cycle was the construction and startup of the uranium mining and production site, URA, ten years ago.

The announcements made by the Brazilian government by the end of 2007 regarding its will to expand the nuclear program were focused, mainly, in four points:

- 1) Investment in hiring and development of human resources, not only for the companies involved but also for the regulatory body;
- 2) Building of up to 9 new nuclear power plants;
- 3) Investments in the operators of the nuclear fuel cycle to have all steps carried out in Brazil;
- 4) Restructuring of the regulatory body, with possible creation of an independent agency for regulation.

Obviously, this government decision brings new horizons and challenges to both state companies directly involved, as well to the regulatory body. The first consequence that could be seen was the beginning of construction of Angra III nuclear power plant (Fig. 4). By July 2009, Eletronuclear had all the licenses of the regulatory bodies involved, including CNEN, IBAMA (in English, Brazilian Institute of Environment) and from the municipality. Angra III is to be built in the same place where the existing plants are located and is going to be exactly the same as its predecessor, Angra II, adding 1350 MW more to the complex capacity. At the time of writing, the new NPP was expected to be operational by 2016–2017.



FIG. 6. Angra III NPP construction works.

Angra III building, however, is included in a greater plan of expansion of the country's nuclear electric generation capacity. By 2009, Eletronuclear and other related governmental bodies started the technical studies that will identify some options of areas where a nuclear centre can be built in the northeast region of the country. The main directive of these studies is that the sites to be selected must fulfil all the characteristics of a place able to receive up to 6 nuclear power plants, in order to optimize costs of building and operation and allow future expansions. Table II shows scenarios that have been defined about the building of new nuclear power plants.

TABLE II. SCENARIOS PREDICTED FOR NUCLEAR POWER GENERATION EXPANSION

| Scenario     | Years                |                        |                              |                               | Total   |
|--------------|----------------------|------------------------|------------------------------|-------------------------------|---------|
|              | 2016–2017*           | 2018–2022              | 2023–2026                    | 2027–2030                     |         |
| Reference    | 1350 MW<br>Angra III | 1000 MW<br>NE 1        | 1000 MW<br>NE 2              | 2000 MW<br>SE 4 + SE 5        | 5350 MW |
|              |                      |                        |                              |                               |         |
| Intermediary | 1350 MW<br>Angra III | 1000 MW<br>NE 1        | 2000 MW<br>NE 2 + NE 3       | 3000 MW<br>SE 4 + SE 5 + SE 4 | 7350 MW |
|              |                      |                        |                              |                               |         |
| High         | 1350 MW<br>Angra III | 2000 MW<br>NE 1 + NE 2 | 3000 MW<br>SE 4 + SE 5 + NE3 | 3000 MW<br>SE 4 + SE 5 + SE 4 | 9350 MW |
|              |                      |                        |                              |                               |         |

\*Although these are the dates originally predicted, delays in the construction have postponed Angra III start up to 2018 or later.

Taking in account the reference scenario, a large growth in the uranium internal demand, without precedents in the history of the Brazilian nuclear program, is obviously expected. Table III shows the expected demand, for a period of 60 years, of each nuclear power plant existing and to be built, as predicted in the Plano Nacional de Energia 2030 (PNE, in English, National Energy Plan 2030) [2]. PNE is a huge study that was published by the Brazilian government, which discusses plans, goals and State's directives related to the electrical energy production in the country until 2030.

TABLE III. EXPECTED URANIUM DEMAND OVER 60 YEARS

| Nuclear power plant | Tonnes of U <sub>3</sub> O <sub>8</sub> | Tonnes of U |
|---------------------|---|-------------|
| Angra I             | 4 800                                   | ~4 070      |
| Angra II            | 16 000                                  | ~13 600     |
| Angra III           | 19 200                                  | ~16 300     |
| NPP 1*              | 15 000                                  | ~12 700     |
| NPP 2*              | 15 000                                  | ~12 700     |
| NPP 3*              | 15 000                                  | ~12 700     |
| NPP4*               | 15 000                                  | ~12 700     |
| Total*              | 100 000                                 | ~84 800     |

\* To be built

Brazilian uranium reserves are enough to supply the nuclear program and the future plans. Two deposits are considered the main ones, as depicted in Fig. 5.

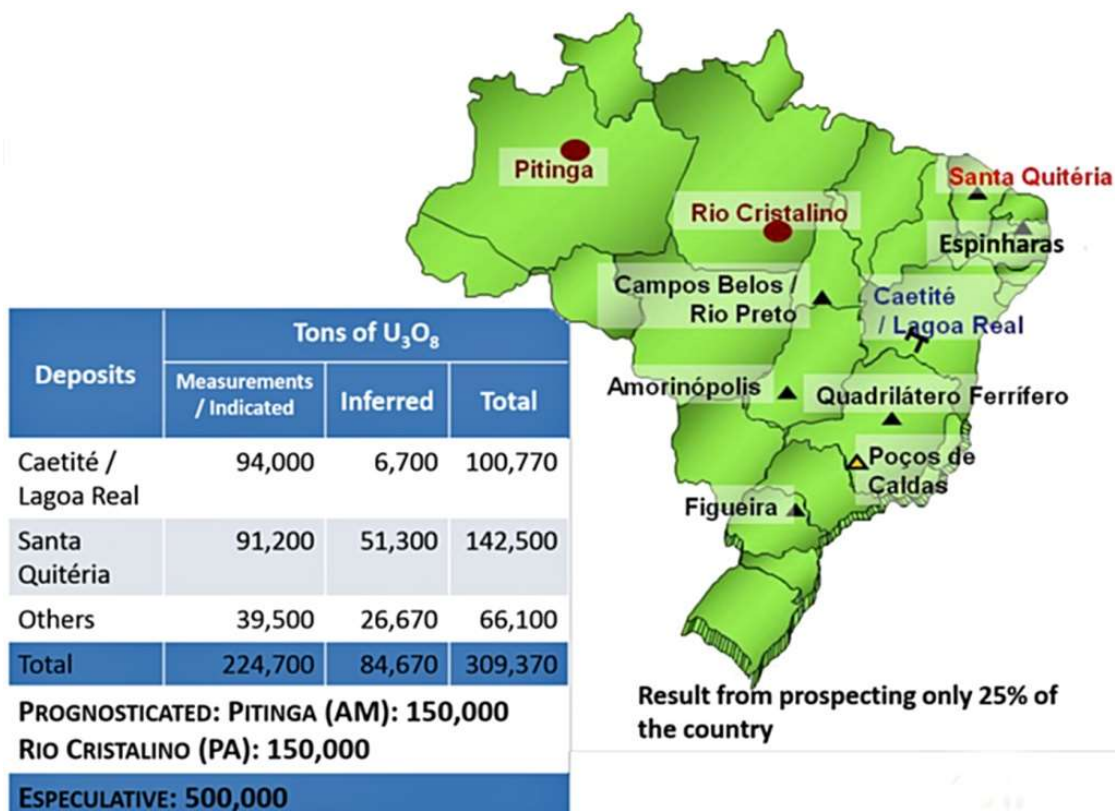


FIG. 7. Brazilian uranium reserves.

INB is working on the expansion of its activities to supply the uranium needed by the new nuclear power plants and to have all of the nuclear fuel cycle steps being done in Brazil. At the present time, the uranium ore concentrate produced in the country is sent abroad for conversion to UF<sub>6</sub> and subsequent enrichment. The construction of a conversion facility is at the initial project phase. The company already owns the technology needed, developed by the Brazilian Navy years ago.

The main focus, however, is the building of an isotopic enrichment facility. The Brazilian technology was also developed by the Navy and is based on gas ultracentrifugation. The facility will be built in independent stages and the company plans to be able to enrich all the uranium in the near future.

Concerning uranium mining and ore concentrate production, INB efforts are focused in two projects: URA activities expansion and the association with a private company to explore the phosphate associated uranium deposit located at Santa Quitéria in the state of Ceará.

URA is reaching 15 years of operation at the Uraniferous Province of Lagoa Real. At this time, there is only one anomaly being exploited in a region with more than 30 uranium anomalies, comprising about 100 000 tonnes of U<sub>3</sub>O<sub>8</sub> [~85 000 t U]. The Cachoeira mine is in process of conversion from open pit to underground mining, providing the continuity of operation for at least five more years. There are plans for immediate exploitation of two other anomalies. Exploration activities, nearly stopped since the 1980s, are now being carried out in the area in order to reassess the regional potential for uranium [3].

Several changes are being planned to URA's chemical plant. The most important one will be the change from the heap leaching process to tank agitated leaching. With this modification the uranium recovery will improve from the current 77% to at least 93%, expanding the annual production capacity to approximately 550 tonnes U<sub>3</sub>O<sub>8</sub> [~470 t U] per year. The agitated leaching facility is expected to be operational by mid-2018 but, there are already plans to double the initial capacity, allowing the plant,

together with the expansion of the solvent extraction area, to produce 1100 tonnes of U<sub>3</sub>O<sub>8</sub>/year [~930 t U/year].

The Santa Quitéria project is an association made by INB with a private company to explore a uranium deposit, which holds about 80 000 tonnes of U<sub>3</sub>O<sub>8</sub> [~68 000 t U] associated with 9 million tonnes of P<sub>2</sub>O<sub>5</sub>, with an average grade of 0.1% for uranium and 11% for phosphate [4]. The deposit is located in the central part of Ceará State, 45 km southeast from Santa Quitéria town. The project is very supported by the state and local municipality government, as it brings development to a very poor region.

The contract between the two parties was signed in 2010 and both companies together are now finalizing the chemical process adjustment studies and the licensing process. Once fully operational, the facility will be able to reach an annual production of up to 1500 tonnes of U<sub>3</sub>O<sub>8</sub> [~1300 t U] per year and is going to provide not only the amount of uranium concentrate needed as predicted in the reference scenario, but also assure, in terms of uranium supply, the intermediary and high scenarios.

#### 4. FINAL CONSIDERATIONS

The Brazilian government is aware of the social and economic problems that can arise from a lack of electric energy, especially in a developing country with large dependence on only one energy source. Taking this in account and also trying to lead a movement for reduction of CO<sub>2</sub> emissions (the target is to reduce 39% of the emissions until 2020), the government decided to support renewable energy initiatives and nuclear energy as options for ready and very clean energy sources.

As described in the previous sections, the Brazilian Nuclear Program now can be considered in an ascendant curve of importance and development within the next 20 years and beyond. The government intends to raise the share of nuclear generated electric energy in the energy matrix of the country to about 5% or, at least, keep the current share (3%) even with the building of new hydro generation electrical power plants. The construction of nuclear power plants and the opening of a mining enterprise in the northeast part of the country may be an opportunity to bring more development to its poorest region. On the other hand, the building of more nuclear power plants in the southeast reinforces the availability and confidence of the electric energy supplying system to the most industrialized region of the country.

Brazil has enough uranium to supply its needs, even in the case of the high scenario, and both companies directly involved with the nuclear fuel cycle in the country have the necessary know-how to reach the targets defined by the government. The country may be proud of having the technology to operate all the steps of the nuclear fuel cycle related to uranium processing, being such a level of technological development compared to the ones reached by the big private companies that are major players in the international uranium market.

#### ACKNOWLEDGEMENTS

The authors would like to thank CNEN, INB and IAEA for the support.

#### REFERENCES

- [1] EMPRESA DE PESQUISA ENERGÉTICA, Balanço Energético Nacional 2012 — Ano base 2011: Resultados Preliminares, EPE, Rio de Janeiro (2012) in Portugues.
- [2] EMPRESA DE PESQUISA ENERGÉTICA, Programa Nacional de Energia 2030, EPE, Rio de Janeiro (2007) in Portugues.
- [3] MATTOS, E.C., VILLEGRAS, R.A.S, Exploration and mining activities in the uranium province of Lagoa Real, 3<sup>rd</sup> International Conference on Uranium, (Proc. Int. Conf. Saskatoon, 2010), Vol. I, Metallurgical Society of Canada, Saskatoon (2010) 153–159.
- [4] DAHLKAMP, F.J., Uranium Deposits of the World USA and Latin America, Springer, New York (2010).

# **URANIUM MINING AND EXTRACTION INDUSTRIES, ENVIRONMENTAL IMPACTS AND MITIGATION TECHNIQUES**

A.A. GADALLA, M.M. EL-FAWAL  
Egyptian Nuclear and Radiological Regulatory Authority (ENRRA)  
Cairo, Egypt

## **Abstract**

The rapid growth in global energy demand is driving an expected expansion in the use of nuclear energy worldwide. This expansion in nuclear energy, increased interests in uranium exploration, with the potential for more uranium mining operations worldwide. On the other hand, uranium mining and extraction processes are accompanied by the production of huge amounts of residual wastes in the form of waste rocks. Within the framework of nuclear safety and radiation control in Egypt, radiological dose assessments were conducted in some phosphate and uranium mines. This paper reviews, discusses and evaluates different aspects of the environmental hazards of phosphate ores waste rocks as well as mill tailings produced during phosphate mining processes. In Abu-Tartur mine, one of the biggest underground phosphate mines in Egypt, airborne radioactivity, radon ( $^{222}\text{Rn}$ ) and its short-lived decay products (progenies) and thoron ( $^{220}\text{Rn}$ ), were measured in selected locations along the mine. The environmental gamma and workers dose equivalent rate were measured inside and outside the mine using thermo-luminescence dosimeters. Radiological safety measures are suggested to control the occupational exposures, and to mitigate these hazards are reviewed, discussed and evaluated.

## **1. INTRODUCTION**

In the nuclear fuel cycle, the initial stages or processes; mining and milling of uranium ores as well as in phosphate mining operations, huge volumes of residual materials or wastes in the form of waste rocks are generated. Since only uranium is extracted, all other elements (daughters) of the uranium decay chains remain in the tailings at their original activities. In addition, small residual amounts of uranium are left in the tailings, depending on the efficiency of the extraction process used. Radionuclides contained in uranium tailings may emit 20 to 100 times as much gamma-radiation as natural background levels on deposit surfaces. Gamma radiation levels decrease rapidly with distance from the pile. The radium-226 in tailings continuously decays to the radioactive gas radon-222, the decay products of which can cause lung cancer. Some of this radon escapes from the interior of the pile. Radon releases may be a hazard that continues after uranium mines are shut down.

## **2. NUCLEAR MATERIALS AND FUEL CYCLE CAPABILITIES IN EGYPT**

Uranium resources in Egypt could be classified as: vein-type (Gebal (G.) El-Missikat), (G. El Sella) and (Abu Rusheid Area); metamorphosed sandstone-type (Sikait area); shear zones in calc-alkaline granite and inter-mountain basin (G. Gattar); surficial type U-deposit in sedimentary rocks (Abu Zeneima). The Egyptian Nuclear Materials Authority (NMA) had undertaken various technical co-operation projects with the IAEA on uranium exploration since 1989. Before 1996, the exploration works resulted in the discovery of some low-grade U-occurrences which related to various geologic formations such as; vein-type (G. El-Missikat), metasomatized granites (G. Um Ara), shear zones in calc-alkaline granite and inter-mountain basin (G. Gattar) and surficial type U-deposit in sedimentary rocks (Abu Zeneima, Sinai). After the 1996, NMA exploration activities for uranium resources were focusing on the South-Eastern Desert of Egypt, these works resulted in the discovery of three U-resources. These resources (from south to north) include vein-types (G. El-Sella and Abu Rusheid area) and metamorphosed sandstone-type (Sikait area) [1]. Egypt has placed an emphasis on extracting uranium from phosphates as opposed to mining uranium itself. Egypt's assured phosphate reserves of 700 million t (Abu-Tartur phosphate mine) contain 40 000 t of uranium at average concentrations of 60 ppm [1]. Figure 1 displays some uranium occurrence locations in Egypt.

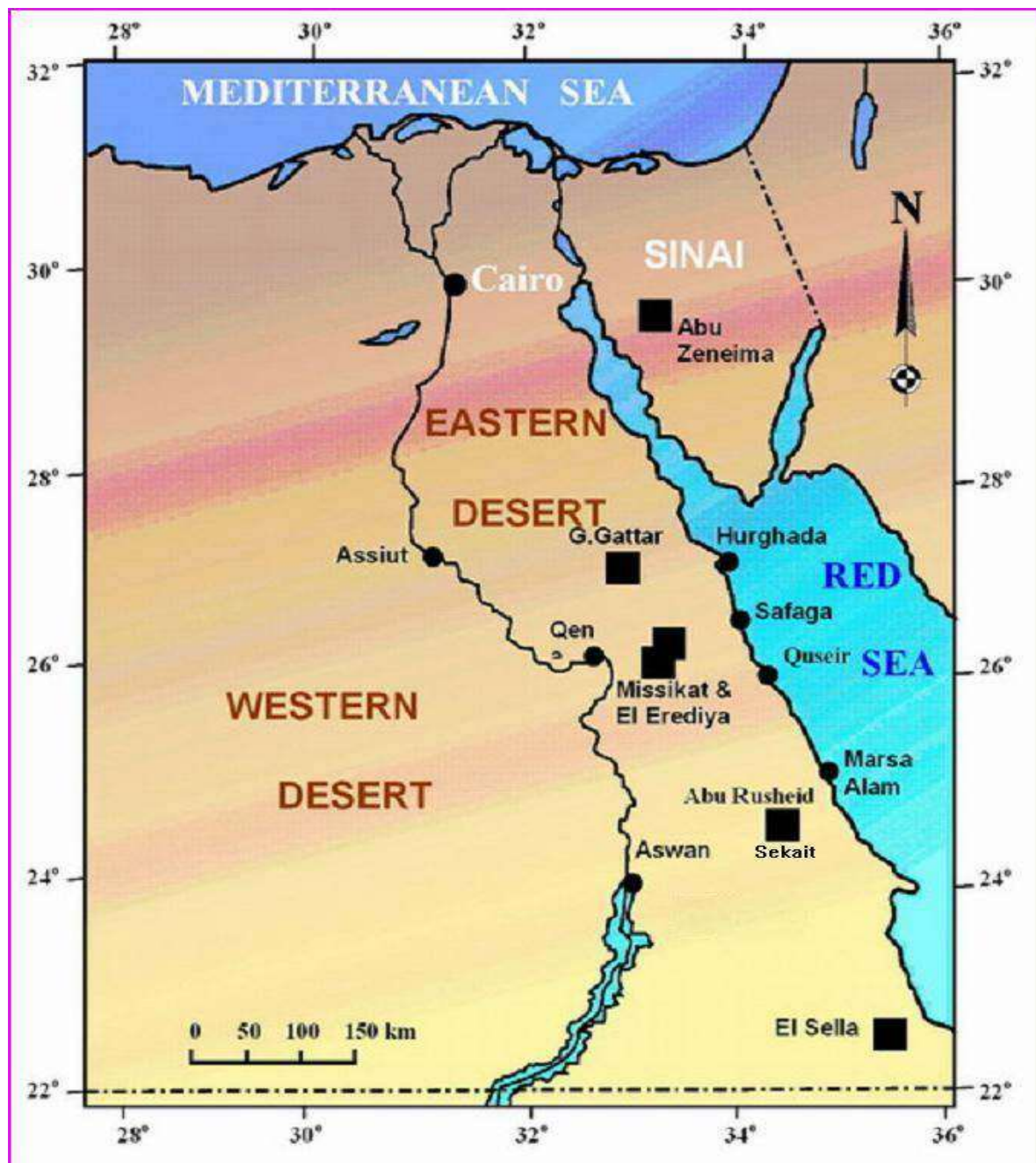
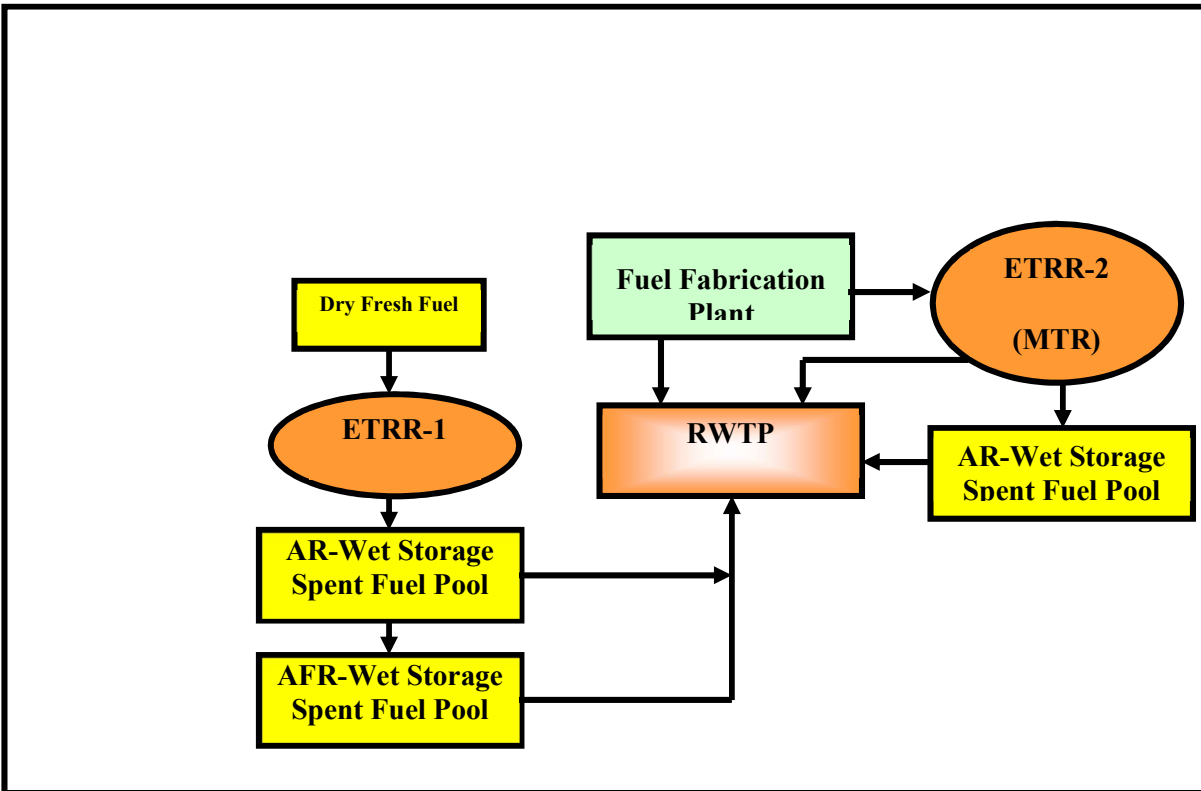


FIG.1. Uranium occurrence locations in Egypt [1].

Egypt has a simple research reactor fuel cycle as shown in Fig. 2. It consists of two research reactors, one fuel manufacturing pilot plant (FMPP), research reactor spent fuel pools and radioactive waste treatment plant used for low and intermediate level wastes. These facilities are located at Inshass Nuclear Research Centre near Cairo. The Egyptian FMPP was designed mainly for producing MTR-type fuel elements required for the Egyptian Second Research Reactor, ETRR-2, as well as other plates or elements for external clients with the same type and enrichment percentage.



*FIG. 2. Research reactors nuclear fuel cycle in Egypt.*

### 3. PHOSPHATE DEPOSITS AS UNCONVENTIONAL U-RESOURCE

Phosphate rock (phosphorite) is a marine sedimentary rock which contains 18–40% P<sub>2</sub>O<sub>5</sub>, as well as some uranium and all its decay products, often 70 to 200 ppm U, and sometimes up to 800 ppm. The main mineral in the phosphate rock is apatite, and most commonly fluorapatite.

Phosphate ores contain significant amounts of natural radioactive elements, specially <sup>238</sup>U and descendants, depending on its geographical and geological origin, up to 300 ppm for uranium.

About 20% of US uranium was extracted from central Florida's phosphate deposits to the mid-1990s, as a by-product, but it then became uneconomic. From 1981 to 1992, USA production averaged just over 1000 tU per year. Sedimentary and igneous phosphate ores are used as raw material for the production of phosphoric acid and consequently fertilizers<sup>28</sup>.

#### 3.1. Phosphate resources and mining in Egypt

Phosphate resources and mines in Egypt are widely distributed in many localities on the Red Sea coast, the Nile Valley and the Western Desert. According to WNA estimations (June 2014<sup>44</sup>), Egypt has reserves of 100 Mt phosphates containing 40 000 tU. The deposits in the first two districts are relatively rich in phosphate and exploited at several mines, but those of the western desert are of low grade except at the underground Abu-Tartor mine. The current reserve estimate in the exhaustively investigated area there is in the order of a billion tonnes of phosphate ore and the planned annual production is 4–5 million tonnes of ore rock and 2.2 million tonnes of wet rock [2]. The ore rocks are crushed, sieved, and transported to beneficiation plant to produce the wet rock. The wet rocks are stocked in large open piles for sale or transport to a phosphate chemical plant. There are two mechanical ventilation stations, one

<sup>28</sup> World Nuclear Association, <http://www.world-nuclear.org/>

for the east side and another one for the west side. Auxiliary air pumps are used for ventilation of the side tunnels during construction of the side tunnels and long wall retreats (ore rock cutting). As a safety measure, temperature, humidity and air flow rates in the working places inside the mine tunnels are measured and recorded on a routine basis. Average temperature ranges from 18 to 46°C, with 18 to 56% humidity, and 7–21 m<sup>3</sup>/s air flow rates were recorded [2].

### 3.2. Radiological impacts and risks for workers

In addition to the  $\alpha$  particle activity of uranium ore dust inhaled during phosphate and uranium ore mining processes, the radionuclides present in the ore are primarily  $\gamma$  ray emitters; 83% of the energy comes from <sup>214</sup>Bi and 12% from <sup>214</sup>Pb. Both of these are short lived descendants of <sup>222</sup>Rn. Typically, at the middle of a drift in a 0.1% uranium ore body, the dose rate is about 5  $\mu$ Gy/h. A risk of exceeding the annual limit of 50 mSv exists when the ore grade exceeds 0.5% [2]. A second radiological risk comes from the inhalation of ore dust, which can be accumulated in the lungs. These dust particles contain long life  $\alpha$  emitters: <sup>238</sup>U, <sup>234</sup>U, <sup>230</sup>Th, <sup>226</sup>Ra and <sup>210</sup>Po. Most of the radioactive atoms contained in the inhaled radioactive dust are eliminated biologically before they are able to disintegrate and release their energy. Nevertheless, the annual degree of contamination may become critical when the stopes are extremely dusty, and when the ore grade exceeds 0.5% U [2]. The risk from dust may become the principal hazard in open pits especially in dry climates or in ore treatment mills, in particular in the crushing and grinding processes.

A third radiological risk comes from the inhalation of radon and its daughter products. Radon, a short lived  $\alpha$  particle emitter, is a noble gas capable of migrating in rocks. The inhalation of radon is not a risk in itself because it does not remain in the lungs. It is either exhaled or it is distributed throughout the body via the circulation of blood, if it has entered the pulmonary tissues. However, when <sup>222</sup>Rn disintegrates, it generates short lived solid daughter products (<sup>218</sup>P, <sup>214</sup>Pb, <sup>214</sup>Bi). These isotopes, once fixed on mining aerosols, may settle in the lungs and emit their disintegration energy. Gaseous effluents from mine exhaust fans may be the origin of local sources of <sup>222</sup>Rn, this is because radioactive dust emission is generally negligible owing to precautions already taken in the mine [2, 3].

Of the three risk factors contributing to the annual average dose (as a sum of these three risks), the risk from radon represents 50 to 75% of the total risk for the underground mining of vein type ores. For the highly mechanized underground mining of sedimentary type ores, the risk from dust is in order of 50%, while the risk from the other two factors being about 25% each. The same distribution of risk factors is experienced in open pit mining and ore treatment mills [2].

Large-scale production of phosphoric acid results in the redistribution of huge amounts of natural radioactivity. The distribution of naturally-occurring uranium, radon, and other radioactive elements, depends on the type of rocks from which they originate and the processes which concentrate them. Rock phosphate contains high level of uranium-235 and radium-226. In the production of fertilizer, recycling of by product phosphogypsum as a building material causes lung exposure to public member about 15 times higher than normal levels. Personnel engage in handling, packing and transport of fertilizer receive additional external gamma exposure at dose rates up to 0.8 Gy/h [2].

## 4. RADIOLOGICAL SAFETY MEASURES AND MITIGATION TECHNIQUES

Radiation monitoring of workers involved in phosphate mining and processing activities is essential. In spite of the fact that monitoring itself does not improve working conditions, but demonstrates if additional operational radiation protection measures should be considered. Open pits phosphate mines are major emitters of gaseous effluents and radioactive dusts. These are not easily monitored and are of variable intensity owing to varying atmospheric conditions and to varying mining techniques. The operators must be equipped with dust masks or some other form of protection for these types of works so as to minimize dust inhalation. Liquid effluents, as in underground mines, can be treated and monitored. Airborne sources are mainly radioactive dusts, such as ore dusts at the beginning of the ore treatment cycle. The major part of these dusts is removed by industrial gas cleaner sand mine exhaust

fans. To mitigate these impacts, the processing wastes should be recycled to the greatest possible extent and liquid effluent sources of  $^{226}\text{Ra}$  and  $^{238}\text{U}$  can be adequately treated and monitored before discharge.

In Abu Tartor Mine, there are two mechanical ventilation stations, one for the east side and another one for the west side. Auxiliary air pumps are used for ventilation of the side tunnels during construction of the side tunnels and long wall retreats (ore rock cutting). As a safety measure, temperature, humidity and air flow rates in the working places inside the mine tunnels are measured and recorded on a routine basis. Average temperature ranges from 18 to 46°C, with 18 to 56% humidity, and 7–21 m<sup>3</sup>/s air flow rates were recorded [2].

## 5. RADIOLOGICAL DOSE ASSESSMENT FROM PHOSPHATE MINING IN EGYPT

Mining of phosphate rocks are major sources of heavy metals that enter the environment. Phosphate mining wastes can cause environmental hazards as they contain significantly toxic elements, such as Th, U, REE, As, Cd, V, Sb, Zn, Cr, Ni, Cu, etc., depending on the origin of the phosphate deposit, the mining method, and the beneficiation technology used. Several studies and research works have been carried out to investigate the environmental radiological impacts of phosphate mining industries in Egypt [2–7]. The natural radioactivity concentrations of  $^{226}\text{Ra}$  ( $^{238}\text{U}$ ) series,  $^{232}\text{Th}$  series and  $^{40}\text{K}$  were measured using a gamma-ray spectrometer (NaI (Tl) 3" × 3") for environmental samples collected from the Eastern Desert (G. Anz, G. Duwi), Western Desert (G. Abu Tartur) and Nile Valley (G. Saria, G. Abu Saboun, G. Owina) in Upper Egypt. A typical concentration of  $^{238}\text{U}$  in sedimentary phosphate deposits is 121 mg/ kg (1500 Bq/ kg) with a range of 30–260 mg /kg (372–3224 Bq/kg). The uranium contents of some Egyptian phosphate rocks in the Red Sea coast and several Nile valley sites are in the ranges of 19–142 mg/ kg (235–1761 Bq/ kg) and 48–185 mg /kg (595–2294 Bq/kg), respectively [3]. The average  $^{238}\text{U}$  content in Abu-Tartor phosphate rock is about 32.9 mg/ kg (408 Bq/kg) [2]. The primary potential environmental radiation problem is associated with phosphate rock mining and processing concerns, mining spoils and processing waste products. The activities of uranium isotopes;  $^{238}\text{U}$ ,  $^{235}\text{U}$  and  $^{234}\text{U}$  as well as  $^{210}\text{Pb}$  were measured using an alpha spectrometer and a low-background proportional gas counting system, respectively, after radiochemical separation. The activities of  $^{226}\text{Ra}$ ,  $^{232}\text{Th}$  series and  $^{40}\text{K}$  are between (14.9 ± 0.8 and 302.4 ± 15.2), (2.6 ± 1.0 and 154.9 ± 7.8) and (10.0 ± 0.5 and 368.4 ± 18.4) Bq/ kg, respectively [4–7]. Abu Tartor phosphate deposit was found to have lower activity than many others phosphate sedimentary deposits, with its average total annual dose being only 114.6 µSv/y. This value is about 11.46% of the 1.0 mSv/y recommended by the International Commission on Radiological Protection (ICRP–60, 1990 [8]) as the maximum annual dose to the public [5, 6]. The radioactivity levels in the surrounding region and the calculated exposure dose (nGy/h) are considered as a pre-operational baseline to estimate the possible radiological impacts due to mining, processing and future phosphate industrial activities.

## 6. CONCLUSIONS

Egypt has reasonable phosphate deposits in several locations in the Eastern and Western Deserts. These phosphate resources could be one of the important unconventional U–resources for the manufacture of nuclear fuel for future nuclear power program in Egypt. Several research studies and research works have been conducted in Egypt to investigate the radiological environmental impacts, health hazards and dose assessment for workers in phosphate mines in Egypt. The present study reviews and discusses the country capabilities regarding nuclear materials and fuel cycles activities in Egypt. Radiological health hazards from uranium and phosphate mines for workers have been reviewed and discussed. Studies and research activities concerning environmental impact and dose assessment in phosphate mining industries in Egypt have been reviewed, discussed and evaluated in the light of the available data, international standards and regulations controlling public and workers radiation exposure and doses during mining activities either in open-pit or underground phosphate mining industries in Egypt.

## REFERENCES

- [1] HOWARI, F.M., GOODEL, P., SALMAN, A., "Uranium Resources in the Middle East", paper presented at IAEA Int. Symp. on Uranium Raw Material for the Nuclear Fuel Cycle: Exploration, Mining, Production, Supply and Demand, Economics and Environmental Issues (URAM-2009), Vienna, 2009.
- [2] AHMED, S.S., "Environmental Issues in the Extraction of Phosphate Ore from Abu-Tartour Mine, Egypt", paper presented at the 1st Int. Mining Congress and Exhibition of Turkey — IMCET 2003, Antalya, 2003.
- [3] ABBADY, A.G.E., UOSIF, M.A.M., EL-TAHER, A., Natural radioactivity and dose assessment for phosphate rocks from Wadi El-Mashash and El-Mahamid Mines, Egypt, *J. Envir. Radioact.* **84** (2005) 65–78.
- [4] OTHMAN, I., AL-HUSHARI, M., RAJA, G., Radiation level in phosphate mining activities, *Radiat. Prot. Dosimet.* **45** 1–4 (1992) 197–201.
- [5] KHATER, A.E.M., HIGGY, R., PIMPL, M., Radiological impacts of natural radioactivities in Abu-Tartur phosphate deposit, *J. Envir. Radioact.* **55** (2001) 255–267.
- [6] KHATER, A.E.M., HUSSEIN, M.A., HUSSEIN, M.I., Occupational exposure of phosphate mine workers: airborne radioactivity measurements and dose assessment, *J. Envir. Radioact.* **75** (2004) 47–57.
- [7] BIGU, J., HUSSEIN, M.I., HUSSEIN, A.Z., Radioactivity measurements in Egyptian phosphate mines and their significance in the occupational exposure of mine workers, *J. Envir. Radioact.* **47** (2000) 229–243.
- [8] INTERNATIONAL COMMISSION ON RADIOLOGICAL PROTECTION, 1990 Recommendations of the International Commission on Radiological Protection. ICRP Publication 60. Ann. ICRP (1991).

# **ENVIRONMENTAL MONITORING DATA REVIEW OF A URANIUM ORE PROCESSING FACILITY IN ARGENTINA**

J.P. BONETTO

Gerencia de Apoyo Científico Técnico,  
Autoridad Regulatoria Nuclear,  
Ciudad Autónoma de Buenos Aires, Argentina

## **Abstract**

A former uranium ore processing facility in Argentina is currently undergoing the last steps of environmental restoration. The operator has been performing post-closure environmental monitoring, while the Argentine Nuclear Regulatory Authority (ARN) has been carrying out its own independent radiological environmental monitoring for verification purposes. A detailed revision of ARN's monitoring plan for uranium mining and milling facilities has been undergoing since 2013, starting with this particular site. Results obtained from long-time sampling locations (some of them currently unused) have created datasets with outliers and below detection-limit values which need to be analysed in order to decide if these sampling-points are useful, or new ones should be proposed. In this paper, the methodology and statistical tests used for analysing and comparing these datasets is presented, and conclusions are drawn for keeping or discarding sampling-points in future monitoring plans.

## **1. INTRODUCTION**

The Autoridad Regulatoria Nuclear of Argentina (ARN) is the institution in charge of the regulation and control of the nuclear activity with regard to radiological and nuclear safety, physical protection and nuclear non-proliferation issues. Among its various activities, when appropriate, it carries out an independent radiological environmental monitoring of nuclear fuel cycle facilities for verification purposes. The facilities are required to carry out their own environmental monitoring.

A revision of the ARN's environmental monitoring plans for U mining and/or processing facilities was undertaken last year, starting with one particular U ore processing facility, which was already closed by the time ARN was created in 1997, and is currently undergoing restoration activities. Environmental monitoring had been carried out throughout the facility's operation, and was adjusted after the facility's closure. This post-closure monitoring plan was adopted by the ARN and is currently the object of revision. It involves groundwater, surface water and sediment sampling outside the limits of the facility for U and  $^{226}\text{Ra}$  determinations.  $^{222}\text{Rn}$  concentration in air is also measured but it is not included in the present review.

Laboratory results from this and other facilities are collected to construct a database, where each sampling-point has a dataset of historical results. This data is ultimately used to assess the environmental impact of a facility. However, this data can also be used to evaluate if the monitoring plan is adequate for that objective, for example, by comparing datasets from the different sampling-points, and rejecting those which are redundant or do not provide useful information. The need for extra sampling-points could also be addressed through such comparisons. The main objective in the review of the monitoring plan for this unnamed facility is the selection of appropriate sampling points, so that a comparison of their datasets needs to be carried out.

Environmental data have characteristics such as infrequent but regular presence of outliers, positive skewness which commonly causes non-normal distribution of the data, and presence of left-censored data (values below detection limits, also referred to as non-detects) [1]. Outliers are lower or higher than usual observations (values), which can either result from a measurement or a transcription error (incorrect value) or be correct values. If incorrect, the outliers should be removed unless they can be corrected. If the outliers are correct values, they can represent either random low-probability natural variability or observations coming from a population different from the one under study. This last case

could represent an impacted sampling-point in environmental datasets, where the outliers provide the most useful information. Therefore, in some cases, outliers should not be removed. Tests for outlier detection are only helpful for identifying those unusual values: then, each outlying observation needs to be investigated separately to reach a decision whether to remove it or not [2]. The presence of left-censored data also poses particular difficulties. Using the detection limit value (or a fraction of it) as a substitute for the censored data is not adequate, and there are some statistical techniques available that make use of this special data [3].

The data obtained from this facility's monitoring presents most of the above-mentioned characteristics, so its interpretation is not easily done at first sight and appropriate statistical methods should be used, such as non-parametrical tests. The purpose of this work is to present a simple but adequate methodology for the review of environmental datasets, in order to help with the selection of the most appropriate sampling-points for the environmental monitoring plan of this U processing facility.

## 2. METHODOLOGY

### 2.1. Statistical tests

Datasets with ARN results up to 2013 were used. Pre-ARN traceable results from 1994 to 1997 were also included. Some of the sampling-points started being used later within that span of time, while some others stopped being sampled before its ending, but their datasets were used all the same, provided the number of results was adequate.

The statistical software ProUCL vs. 5.0.00 from US EPA was used for the data review and for all tests. It was chosen because of its free availability, and because it allows to run non-parametrical hypotheses tests with left-censored data [4].

Data review included testing to know the probability distribution of the datasets and to detect possible outliers [5]. A Shapiro-Wilk goodness-of-fit test ( $\alpha = 0.05$ ) was performed to check if the datasets follow a normal distribution. In the case of left-censored datasets, the same test was performed for the positive values only, plus the regression on order statistics (ROS) method available in the software was used to assign an imputed value for each non-detection, and then perform the test [4]. Dixon's test for outlier detection was performed on each dataset. Upon removal of outliers (when appropriate), the dataset would be re-tested for normality. For all datasets, the mean and median were calculated. For left-censored datasets, the nonparametric Kaplan-Meier estimation method was also used to estimate the population means [2].

Downstream sampling-points were considered as possibly impacted by the facility and were compared against upstream sampling-points, which were considered as background. These population comparisons were carried out employing two-sample hypotheses testing approaches [2]. Student's two-sample *t* test for equal variances, and its Satterthwaite version for unequal variances, was used when both datasets presented normal distribution. When at least one of both datasets did not follow a normal distribution, the nonparametric Wilcoxon-Mann-Whitney test was used. When at least one of both datasets presented left-censored data, the nonparametric Gehan and Tarone-Ware tests were used.

For all these comparisons, Form 1 of the tests was used, meaning the null hypothesis stated was "Downstream population mean/median  $\leq$  Upstream population mean/median", the alternative hypothesis being "Downstream population mean/median  $>$  Upstream population mean/median". Confidence coefficient was set at 90% ( $\alpha=0.10$ ) for increased test power.

When outliers were detected, tests were repeated with and without those outliers present in the datasets, in order to verify the influence of the outlier and, eventually, confirm the test conclusion. As with the lowered confidence coefficient, a Type II error (accepting the null hypothesis when it should have been rejected) was considered more serious than a Type I error.

A Two-tailed form for these tests (Form 3) was used when the sample-points could not be considered upstream or downstream (considering also groundwater flow from west to east). The null hypothesis stated for this form of the tests was “Mean/median of population 1 = mean/media of population 2”, and the confidence coefficient was set also at 90% ( $\alpha=0.10$ ).

## 2.2. Sampling plan

For the present review only the most relevant sampling-points were analysed, therefore a simplified version of the current monitoring plan is presented in this paper. It comprises surface water and sediment (where available) sampling from four streams that run eastwards (here referred to as streams 1, 2, 3 and 4). Streams 1 and 2 lie approximately 14 and 8 km, respectively, north of the facility, and are sampled both upstream (as a background point) and downstream (as a possibly impacted point) of the facility. Stream 3 is a small creek that also runs north of the facility, but near its source it lies 500 m from its northern boundary, thus receiving surface runoff from the area. In this case, two downstream points (a and b) are sampled for stream 3, each after an identifiable runoff course discharge. The runoff course that discharges before point b is also sampled before entering the stream. Stream 4 lies 10 km south of the facility, and is sampled only upstream. Eventually, streams 1 and 3 join stream 2 before it finally discharges into a wetland some 30 km west of the facility. Stream 4 also discharges into the same wetland. Being a receptacle for these surface-water courses, as well as for groundwater, surface water and sediments have also been sampled from this wetland. Groundwater is also sampled from 7 shallow wells (up to 5 m deep), all downstream from the facility. Three of them (here referred to as W1, W2, W3) have been built exclusively for sampling and are situated some 200 m to the east of the facility, in a neighbouring field. A fourth well close to these three is also sampled, but presents higher values, and does not need any statistical test to show its relevance to the monitoring plan. Wells W4 to W7 lie 1, 2, 4 and 11 km, respectively, away from the facility on an approximately straight-line heading towards the previously mentioned wetland. The samples are taken yearly, and are brought to the ARN laboratories for U and  $^{226}\text{Ra}$  determination.

Statistical tests were performed in datasets from 17 sampling-points. A brief description with the abbreviation of the sampling-points and their approximate location are presented in Table I and in Fig. 1, respectively.

TABLE I. BRIEF DESCRIPTION, ABBREVIATIONS AND ANALYSES CARRIED OUT FOR EACH SAMPLING-POINT

| Sampling-point |                          | Abbreviation | Media sampled and radionuclide analysed          |
|----------------|--------------------------|--------------|--|
| Stream 1       | Upstream                 | 1U           | U in water, U and $^{226}\text{Ra}$ in sediments |
|                | Downstream               | 1D           | U in water, U and $^{226}\text{Ra}$ in sediments |
| Stream 2       | Upstream                 | 2U           | U in water, U and $^{226}\text{Ra}$ in sediments |
|                | Downstream               | 2D           | U in water, U and $^{226}\text{Ra}$ in sediments |
| Stream 3       | Upstream                 | 3U           | U in water, U and $^{226}\text{Ra}$ in sediments |
|                | Downstream a             | 3Da          | U in water, U and $^{226}\text{Ra}$ in sediments |
|                | Downstream b             | 3Db          | U in water, U and $^{226}\text{Ra}$ in sediments |
| Runoff         | Before entering stream 3 | R            | U in water, U and $^{226}\text{Ra}$ in sediments |
| Stream 4       | Upstream                 | 4U           | U in water, U and $^{226}\text{Ra}$ in sediments |
| Wetland        |                          | Wtl          | U in water, U and $^{226}\text{Ra}$ in sediments |
| Well 1         |                          | W1           | U in water                                       |
| Well 2         |                          | W2           | U in water                                       |
| Well 3         |                          | W3           | U in water                                       |
| Well 4         |                          | W4           | U in water                                       |
| Well 5         |                          | W5           | U in water                                       |
| Well 6         |                          | W6           | U in water                                       |
| Well 7         |                          | W7           | U in water                                       |

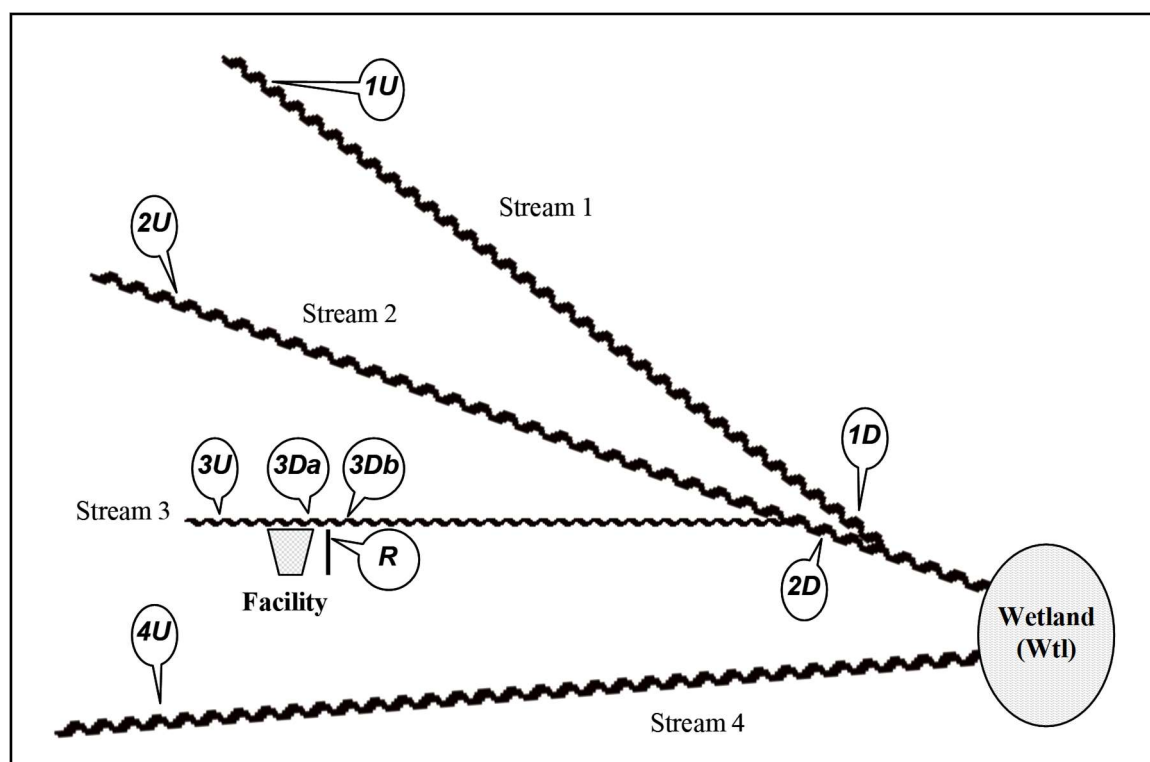


FIG. 1. Approximate location of sampling-points relative to the facility.

### 3. RESULTS

#### 3.1. U in water

Outliers (higher than usual values) were detected and removed from datasets *2D*, *3Da*, *3Db*, and *Wtl*. They could not be attributed to measurement or transcription errors. Instead, they were considered correct results not belonging to the population of interest, which could represent an impact from the facility. Removal was decided due to their extremely high values which could affect further tests. They particularly affected normality in the first two of the mentioned databases. Two outliers were also detected and removed from dataset *4U*. In this case, removal was decided to make sure the dataset represents a background population.

In the case of groundwater, outliers were detected and removed from datasets *W3*, *W4*, *W6* and *W7*, on the same grounds as mentioned above. Only dataset *W7* already followed a normal distribution prior to the outlier removal. Some general statistics from these datasets is presented in Table II.

TABLE II. SOME GENERAL STATISTICS FOR U IN WATER DATASETS

| Sampling-point | Number of results <sup>a</sup> | Non-detects | Mean ( $\mu\text{g/L}$ ) | Median ( $\mu\text{g/L}$ ) | KM Mean <sup>b</sup> ( $\mu\text{g/L}$ ) | Distribution <sup>c</sup> |
|----------------|--------------------------------|-------------|--------------------------|----------------------------|--|---------------------------|
| 1U             | 10                             | 4           | 2.6                      | 2.6                        | 2.6                                      | Normal                    |
| 1D             | 4                              | 0           | 7.0                      | 6.7                        | na                                       | Normal                    |
| 2U             | 10                             | 4           | 2.1                      | 2.1                        | 2.1                                      | Normal                    |
| 2D             | 18 (2)                         | 2           | 7.2                      | 6.3                        | 6.8                                      | Normal                    |
| 3U             | 16                             | 4           | 3.2                      | 3.4                        | 3.2                                      | Normal                    |
| 3Da            | 15 (1)                         | 4           | 3.3                      | 3.4                        | 3.3                                      | Normal                    |
| 3Db            | 20 (1)                         | 3           | 5.3                      | 5.0                        | 5.0                                      | Not normal                |
| R              | 11                             | 0           | 41.5                     | 48.0                       | na                                       | Normal                    |
| 4U             | 18 (2)                         | 4           | 1.2                      | 1.1                        | 1.2                                      | Not normal                |
| Wtl            | 14 (1)                         | 0           | 9.2                      | 6.0                        | na                                       | Not normal                |
| W1             | 7                              | 3           | 10.1                     | 10.6                       | 7.7                                      | Normal                    |
| W2             | 12                             | 3           | 8.2                      | 7.8                        | 7.1                                      | Normal                    |
| W3             | 16 (2)                         | 2           | 7.3                      | 6.8                        | 6.7                                      | Normal                    |
| W4             | 18 (1)                         | 0           | 7.8                      | 8.0                        | na                                       | Normal                    |
| W5             | 13                             | 0           | 7.1                      | 7.2                        | na                                       | Normal                    |
| W6             | 18 (1)                         | 3           | 2.9                      | 2.7                        | 2.9                                      | Normal                    |
| W7             | 18 (2)                         | 3           | 2.1                      | 1.8                        | 2.1                                      | Normal                    |

<sup>a</sup> Number of results with removed outliers, where applicable. Number of removed outliers in brackets.

<sup>b</sup> Nonparametric Kaplan-Meier method for mean estimation in the presence of non-detects only.

<sup>c</sup> Distribution followed by the dataset after outlier removal.

na = not applicable

### 3.2. U in sediments

Outliers were detected and removed from some of the datasets, as presented in Table III. These again could not be attributed to measurement or transcription errors, so each case was studied separately. One outlier in dataset *3U* was removed to ensure it keeps representing a background population, although the dataset presented a normal distribution even before the outlier was removed. An outlier was also removed from dataset *R*, for being an extremely high value. This caused the dataset to change from an approximately normal to a normal distribution. Up to three outliers were also detected in dataset *3Db*, but in this case, they were not removed, as they were not so extreme values, and such an amount of outlying observations was considered to represent an influence of the facility instead of a random natural variability. Also, their removal would not cause the dataset to follow a normal distribution. Some general statistics from these datasets is presented in Table III.

TABLE III. SOME GENERAL STATISTICS FOR U IN SEDIMENTS DATASETS

| Sampling-point | Number <sup>a</sup> of results | Non-detects | Mean (µg/g) | Median (µg/g) | KM Mean <sup>b</sup> (µg/g) | Distribution |
|----------------|--------------------------------|-------------|-------------|---------------|-----------------------------|--------------|
| 1U             | 7                              | 1           | 3.2         | 2.9           | 2.8                         | Normal       |
| 1D             | 7                              | 0           | 2.6         | 2.6           | na                          | Normal       |
| 2U             | 9                              | 2           | 2.4         | 2.3           | 1.9                         | Normal       |
| 2D             | 18                             | 0           | 2.2         | 2.2           | na                          | Not normal   |
| 3U             | 8 (1)                          | 0           | 1.6         | 1.5           | na                          | Normal       |
| 3Da            | 6                              | 2           | 1.9         | 2.0           | 1.7                         | Normal       |
| 3Db            | 16                             | 0           | 4.2         | 2.8           | na                          | Not normal   |
| R              | 8 (1)                          | 1           | 12.8        | 10.5          | 11.4                        | Normal       |
| 4U             | 9                              | 1           | 1.5         | 1.5           | 1.4                         | Normal       |
| Wtl            | 13                             | 0           | 2.3         | 2.1           | na                          | Normal       |

<sup>a</sup> Number of results with removed outliers, where applicable. Number of removed outliers in brackets.

<sup>b</sup> Nonparametric Kaplan-Meier method for mean estimation in the presence of non-detects only.

<sup>c</sup> Distribution followed by the dataset after outlier removal.

na = not applicable.

### 3.3. $^{226}\text{Ra}$ in water and in sediments

Slightly under 90% of all the  $^{226}\text{Ra}$  in water results were non-detects. Wells *W1*, *W2* and *W3* were the only sampling-points presenting results above the detection limits. A few outliers were detected but not removed, since they were not extreme values and the datasets already followed a normal distribution with them. General statistics for these datasets are presented in Table IV.

TABLE IV. SOME GENERAL STATISTICS FOR  $^{226}\text{Ra}$  IN WATER DATASETS

| Sampling-point | Number of results | Non-detects | Mean (mBq/L) | Median (mBq/L) | Distribution |
|----------------|-------------------|-------------|--------------|----------------|--------------|
| W1             | 7                 | 0           | 101.4        | 87.1           | Normal       |
| W2             | 11                | 0           | 48.4         | 49.8           | Normal       |
| W3             | 17                | 0           | 19.4         | 17.8           | Normal       |

Regarding  $^{226}\text{Ra}$  in sediments, outliers were detected and removed from some of the datasets, as presented in Table V. Dataset *IU* presented one outlier, which was removed to ensure the dataset represents a background population. Datasets *3Db* and *R* presented extremely high outliers which distorted the normal distribution, so they were removed. Their presence, however, again could imply a facility's impact. An outlier was detected in dataset *1D*, but it was not removed, since it was not an extreme value and the dataset already followed a normal distribution. Some general statistics from these datasets is presented in Table V.

TABLE V. SOME GENERAL STATISTICS FOR  $^{226}\text{Ra}$  IN SEDIMENTS DATASETS

| Sampling-point | Number of results <sup>a</sup> | Non-detects | Mean (mBq/g) | Median (mBq/g) | KM Mean <sup>b</sup> (mBq/g) | Distribution <sup>c</sup> |
|----------------|--------------------------------|-------------|--------------|----------------|------------------------------|---------------------------|
| 1U             | 8 (1)                          | 0           | 35.7         | 34.7           | na                           | Normal                    |
| 1D             | 9                              | 0           | 34.7         | 34.1           | na                           | Normal                    |
| 2U             | 9                              | 1           | 33.2         | 31.8           | 31.2                         | Normal                    |
| 2D             | 17                             | 2           | 36.2         | 33.3           | 33.8                         | Normal                    |
| 3U             | 11                             | 4           | 31.8         | 30.7           | 28.6                         | Normal                    |
| 3Da            | 5                              | 0           | 27.1         | 27.8           | na                           | Normal                    |
| 3Db            | 16 (2)                         | 3           | 43.2         | 40.6           | 38.6                         | Normal                    |
| R              | 9 (1)                          | 0           | 35.6         | 35.3           | na                           | Normal                    |
| 4U             | 8                              | 1           | 42.0         | 44.0           | 38.9                         | Normal                    |
| Wtl            | 10                             | 0           | 30.4         | 29.1           | na                           | Normal                    |

<sup>a</sup> Number of results with removed outliers, where applicable. Number of removed outliers in brackets.

<sup>b</sup> Nonparametric Kaplan-Meier method for mean estimation in the presence of non-detects only.

<sup>c</sup> Distribution followed by the dataset after outlier removal.

na = not applicable

### 3.4. Comparisons between sampling-points

Conclusions from the comparisons between upstream and downstream datasets as well as between upstream datasets and the wetland (as the final downstream sampling-point for all the streams) are presented in Table VI.

TABLE VI. CONCLUSIONS AND P-VALUES FROM DATASET COMPARISONS WITH DIFFERENT STATISTICAL TESTS

| Stream sampled       | Media sampled and radionuclide analysed | Statistical conclusion         | p-Value ( $\alpha = 0.1$ ) <sup>a</sup> |
|----------------------|---|--------------------------------|---|
| Stream 1             | U in water                              | Downstream > Upstream          | 0.002 G – 2.8E-4 TW                     |
|                      | U in sediment                           | Downstream $\leq$ Upstream     | 0.592 T                                 |
|                      | $^{226}\text{Ra}$ in sediment           | Downstream $\leq$ Upstream     | 0.573 S                                 |
| Stream 1 and Wetland | U in water                              | Wetland > Upstream             | 0.002 G – 0.003 TW                      |
|                      | U in sediment                           | Wetland $\leq$ Upstream        | 0.697 G – 0.698 TW                      |
|                      | $^{226}\text{Ra}$ in sediment           | Wetland $\leq$ Upstream        | 0.959 S                                 |
| Stream 2             | U in water                              | Downstream > Upstream          | 0.002 G – 0.003 TW                      |
|                      | U in sediment                           | Downstream $\leq$ Upstream     | 0.359 G – 0.349 TW                      |
|                      | $^{226}\text{Ra}$ in sediment           | Downstream $\leq$ Upstream     | 0.363 G – 0.445 TW                      |
| Stream 2 and Wetland | U in water                              | Wetland > Upstream             | 5.5E-4 G – 9.1 E-4 TW                   |
|                      | U in sediment                           | Wetland $\leq$ Upstream        | 0.296 G – 0.339 TW                      |
|                      | $^{226}\text{Ra}$ in sediment           | Wetland $\leq$ Upstream        | 0.533 G – 0.448 TW                      |
| Stream 3             | U in water                              | Downstream a $\leq$ Upstream   | 0.463 G – 0.369 TW                      |
|                      | U in sediment                           | Downstream a $\leq$ Upstream   | 0.500 G – 0.657 TW                      |
|                      | $^{226}\text{Ra}$ in sediment           | Downstream a $\leq$ Upstream   | 0.523 G – 0.395 TW                      |
| Stream 3             | U in water                              | Downstream b > Upstream        | 0.024 G – 0.056 TW                      |
|                      | U in sediment                           | Downstream b > Upstream        | 0.002 WMW                               |
|                      | $^{226}\text{Ra}$ in sediment           | Downstream b > Upstream        | 0.069 G – 0.095 TW                      |
| Stream 3 and Runoff  | U in water                              | Downst. b >or $\leq$ Downst. a | 0.039 G – 0.130 TW                      |
|                      | U in sediment                           | Downst. b > Downst. a          | 0.014 G – 0.016 TW                      |
|                      | $^{226}\text{Ra}$ in sediment           | Downst. b >or $\leq$ Downst. a | 0.056 G – 0.120 TW                      |
|                      | U in water                              | Runoff > Downstream a          | 5.3E-5 G – 5.0E-5 TW                    |
|                      | U in sediment                           | Runoff > Downstream a          | 0.010 G – 0.011 TW                      |
|                      | $^{226}\text{Ra}$ in sediment           | Runoff > Downstream a          | 0.020 T                                 |
|                      | U in water                              | Runoff > Downstream b          | 1.2E-4 G – 1.6E-5 TW                    |
| Stream 3 and wetland | U in sediment                           | Runoff > Downstream b          | 0.020 WMW                               |
|                      | $^{226}\text{Ra}$ in sediment           | Runoff <= Downstream b         | 0.649 WMW                               |
|                      | U in water                              | Wetland > Upstream             | 0.002 G – 0.004 TW                      |
| Stream 4 and wetland | U in sediment                           | Wetland $\leq$ Upstream        | 0.186 T                                 |
|                      | $^{226}\text{Ra}$ in sediment           | Wetland $\leq$ Upstream        | 0.286 G – 0.179 TW                      |
|                      | U in water                              | Wetland > Upstream             | 1.7E-5 G – 1.7E-6 TW                    |
| Stream 4 and wetland | U in sediment                           | Wetland > Upstream             | 0.038 G – 0.042 TW                      |
|                      | $^{226}\text{Ra}$ in sediment           | Wetland $\leq$ Upstream        | 0.909 G – 0.806 TW                      |

<sup>a</sup> G = Gehan test; TW = Tarone-Ware test; T = Student's *t* test; S = Welch-Satterthwaite's *t* test;  
WMW = Wilkinson-Mann-Whitney test.

Uranium in ground-water datasets from sampling wells were also compared using the same tests as for streams. Comparisons among W1, W2, W3, however, were carried out using the two-tailed form, since the wells are located near each other and their means are similar. Comparisons among W4, W5, W6 and W7, as well as comparisons between W1, W3 and W5, W4, were carried out using form 1. The conclusions from these comparisons are presented in Table VII, showing which wells have statistical higher media values.

TABLE VII. RESULTS OF COMPARISONS BETWEEN U IN WATER DATASETS FROM GROUNDWATER SAMPLING WELLS

| Dataset                       | W1    | = | W2    | = | W3    | = | W4                 | = | W5        | > | W6        | > | W7    |
|-------------------------------|-------|---|-------|---|-------|---|--------------------|---|-----------|---|-----------|---|-------|
| p-values for Gehan test       | 0.854 |   | 0.804 |   | 0.924 |   | 0.245 <sup>a</sup> |   | 0.000 076 |   | 0.009     |   |       |
| p-values for Tarone-Ware test |       |   | 0.879 |   | 0.734 |   | 0.962              |   | na        |   | 0.000 013 |   | 0.005 |

<sup>a</sup> For this comparison, only the parametric Welch-Satterthwaite's *t* test was used, since both datasets presented no non-detects and followed a normal distribution.

W1, W2 and W3 were the only sampling-points presenting enough above detection limit  $^{226}\text{Ra}$  in water values to be tested. They were compared using the Form 1 of the Welch-Satterthwaite's *t* test. Results are presented in Table. VIII.

Since detection limits were over one order of magnitude below the means of these datasets, it is assumed that the other wells have significantly lower  $^{226}\text{Ra}$  concentration.

TABLE VIII. RESULTS OF COMPARISONS BETWEEN  $^{226}\text{RA}$  IN WATER DATASETS FROM GROUNDWATER SAMPLING WELLS

| Dataset  | W1 | > | W2    | > | W3    |
|--|----|---|-------|---|-------|
| p-values for Welch-Satterthwaite's <i>t</i> test |    |   | 0.010 |   | 0.001 |

It is important to point out that all the above comparisons were also carried out including the outlying values initially removed from the datasets (as well as removing the outliers that were detected but not removed), reaching similar conclusions.

#### 4. CONCLUSIONS AND RECOMMENDATIONS

Even though some statistical differences between upstream and downstream values may suggest a possible influence from the facility, it must be pointed out that the highest mean values obtained from the reviewed databases fall well within the natural values for U and  $^{226}\text{Ra}$  in soils and in drinking water reported by UNSCEAR [6]. Also, water results from the reviewed sample-points are lower than the guidance level values for U and Ra in drinking water provided by the World Health Organization [7].

The tests presented here provide more conclusive information regarding the usefulness of sampling-points, particularly when the presence of outliers and left-censored data make it difficult to draw conclusions from raw data at first sight. Care needs to be taken to comply with all testing assumptions in order to obtain reliable results.

Stream 3 and the runoff course discharging into it have shown to provide the most useful information. More sampling-points should be added to this stream and any other runoff discharging into it.

Upstream and downstream comparisons presented the same conclusions for streams 1 and 2. There seems to be no need for sampling both of them, and at least one of them should be replaced by a closer stream, if possible.

Stream 4 should be sampled also downstream before deciding its usefulness as a sampling point.

The wetland should be kept as a sampling-point, but other streams discharging into it and not related to the facility should also be sampled before they reach it.

Wells near the facility are important, and newer neighbouring wells should be sampled, if possible. If any, W3 seems to be the least important of the three. Some of the farthest wells (W6 or W7) could also be discarded.

The results presented here cannot be used for evaluating environmental impact. The conclusions obtained from this work are intended to be used for further improvement of the ARN's monitoring plan.

## ACKNOWLEDGEMENTS

The author thanks Miguel Palacios, Soledad Acosta, Ana Grinman, Julia Mondini, Daniel Giustina and other former personnel of the U and Ra measurement laboratories.

## REFERENCES

- [1] HELSEL, D.R., HIRSCH, R.M., Statistical Methods in Water Resources, Studies in Environmental Science **49**, Elsevier, Amsterdam (1992).
- [2] SINGH A., SINGH A.K., ProUCL version 5.0.00 Technical Guide, EPA/600/R-07/41, Washington (2013).
- [3] HELSEL D.R., Nondetects and Data Analysis: Statistics for Censored Environmental Data, Statistics in practice, John Wiley & Sons, New Jersey (2005).
- [4] SINGH A, MAICHLE R., ProUCL version 5.0.00 User Guide, EPA/600/R-07/041, Washington (2013).
- [5] UNITED STATES ENVIRONMENTAL PROTECTION AGENCY, Data Quality Assessment: Statistical Methods for Practitioners, EPA/240/B-06/003, Washington (2006).
- [6] UNITED NATIONS SCIENTIFIC COMMITTEE ON THE EFFECTS OF ATOMIC RADIATION, Sources and Effects of Ionizing Radiation. Volume I: Report to the General Assembly with Scientific Annexes. Annex B: Exposures of the Public and Workers from Various Sources of Radiation, UNSCEAR 2008 Report, UN, New York (2008) (CD ROM).
- [7] WORLD HEALTH ORGANIZATION, Guidelines for Drinking-Water Quality, 4th edition, WHO, Geneva (2011).

# STUDIES OF THE URANIUM PYROCHLORE MINERAL BETAFLITE $[(\text{Ca},\text{U})_2(\text{Nb},\text{Ti},\text{Ta})_2\text{O}_7]$

S.A. MCMASTER, R. RAM, J. TARDIO, S.K. BHARGAVA  
Centre for Advanced Materials and Industrial Chemistry,  
School of Applied Sciences, RMIT University,  
Melbourne, Victoria  
Australia

## Abstract

Refractory uranium minerals are gaining increased attention as future sources of nuclear fuel to keep up with the world's growing demand for energy. One such mineral is the uranium pyrochlore betafite. Two betafite-containing samples were characterised using XPS, XRD and multi acid digestion / ICP-MS. XPS results showed the U oxidation state of the surficial uranium in both samples was predominantly  $\text{U}^{6+}$ , although some  $\text{U}^{5+}$  was detected. XRD analysis showed the betafite in the samples was amorphous, although after heating at  $1100^\circ\text{C}$  for 2 hours strong matches for both betafite and rutile were obtained for both samples. Dissolution studies showed similar trends for both samples, although the extent of dissolution for the betafite from the Ambatofotsky region in Madagascar was significantly greater in each experiment than that from Silver Crater Mine, Bancroft, Canada. This was most likely due to a higher amount of  $\text{U}^{6+}$  present in this sample. Heat-treating showed a higher rate of dissolution over the initial 100 min. of the dissolution test in both samples before the rate slowed over the remainder of the experiment. Unheated samples showed relatively consistent rates of dissolution over the duration of the experiments.

## 1. INTRODUCTION

Several uranium minerals are targeted in different ore bodies to produce the uranium that is used to generate electricity. To date, the most widely targeted uranium minerals have been uraninite ( $\text{UO}_2$ ) or pitchblende ( $\text{U}_3\text{O}_8$ ) due to their comparatively high concentration in most ore bodies and the ease with which uranium can be extracted out of these minerals [1]. As the use of nuclear power generation increases, the demand for uranium is struggling to keep up due to depletion of the high grade uraninite containing ore bodies mined previously. This has led to a focus on refractory uranium minerals as a uranium source to keep up with the growing demand for nuclear fuel [2]. One such uranium mineral which is receiving increasing attention is the uranium pyrochlore mineral betafite  $[(\text{Ca},\text{U})_2(\text{Nb},\text{Ti},\text{Ta})_2\text{O}_7]$ . Betafite is currently processed in various ore bodies around the world including Rössing uranium mine in Namibia (where betafite accounts for 5% of the total uranium in the deposit) [3]. Developments to target betafite as a source of uranium are rare due to the tendency of this mineral being difficult to leach under similar conditions used to leach minerals such as uraninite [4]. With the forecasted increases in demand for nuclear fuel, studies on characterisation and dissolution studies on uranium minerals such as betafite are becoming increasingly important.

Betafite is a pyrochlore group mineral with the structure  $\text{A}_2\text{B}_2\text{O}_6(\text{OH})_x$  and is a cubic derivative of the fluorite type structure where  $A = \text{Na}, \text{K}, \text{Ca}, \text{Sr}, \text{Sn}, \text{Ba}, \text{Pb}, \text{Bi}, \text{REE}, \text{U}$  and  $B = \text{Ti}, \text{Nb}, \text{Ti}, \text{Zr}, \text{Al}$  [5–7]. Pyrochlore group minerals are classified into 3 different subgroups on the dominant metal B site composition; Pyrochlore is the Nb dominate subgroup, microlite the Ta dominate and betafite is characterized by  $[\Sigma 2\text{Ti}_B > (\text{Nb}_B + \text{Ta}_B)]$  and  $\text{U}_A > 20\%$  [6, 8]. Uranium rich betafite samples have been demonstrated to be almost always metamict due to alpha radiation damage [6, 9, 10] although Ca-rich betafite samples reported on by Câmara et al. (2004) were shown to be non-metamict [11]. Lumpkin and Ewing (1996) [7] report XRD analysis of high purity natural betafites and determines that the high-water content in the samples could help to stabilize the mineral structure. This work also demonstrates the recrystallization of metamict betafite occurs at  $\sim 800^\circ\text{C}$ .

Lumpkin and Ewing (1996) [7] show extensive secondary alteration included predominantly A site cations Na, Ca and U leaching and hydration of the structure. This can lead to up to 20–30% of the

uranium initially occurring in the structure to be lost due to secondary alteration [7]. This work also predicts the mechanism of alteration in natural betafite samples. Initially cationic migration of A site metals Ca and Na to form pyrochlore  $[(\text{Ca},\text{Na})_2\text{Nb}_2\text{O}_7]$  and microlite  $[(\text{Ca},\text{Na})_2\text{Ta}_2\text{O}_7]$ . This changes the U:Nb:Ta ratio which in turn destabilizes the mineral. Further alteration of the remaining products forms uranypyrochlore  $[(\text{U},\text{Ca})_2\text{Nb}_2\text{O}_7]$ , liandratite ( $\text{UNb}_2\text{O}_8$ ) and rutile depending on the stoichiometry of the betafite initially [7].

Dissolution of natural betafites has been studied by McMaster et al. (2012) [12]. In this work, the influence of several parameters on betafite leaching were investigated. The results of this study show betafite is difficult to leach under mild conditions with ~5% of the uranium leached over a 24-hour period using similar acid, iron, redox potential and temperature conditions to that used in industrial minerals processing facilities [12]. Eyal et al. (1986) [13] present alkali dissolution studies on a natural betafite sample. In this work, successive leaches conducted under mild alkaline condition over a period of 50–100 days were completed to investigate the effect of the metamictisation on natural betafites. The results of this study show regions of the sample where alpha radiation damage was more prominent led to a higher rate of dissolution in these regions. Annealing the sample was demonstrated to produce a lower rate of dissolution in these previously metamictized regions of the sample.

In this study, characterisation of two natural betafite samples from different localities was conducted. The dissolution of these betafite samples was also investigated over a range of conditions.

## 2. MATERIALS AND METHODOLOGY

### 2.1. Materials

The two natural betafite mineral samples studied were sourced from Melbourne Museum and from an online mineral dealer. The Melbourne Museum sample, received in the form of a whole rock, weighed ~10 g. The sample was originally collected from the Ambatofotsky region in Madagascar and is referred to as BAM throughout the manuscript. The sample from the online mineral dealer received in the form of a whole rock weighed a total of ~8.1 g. The sample was originally collected from Silver Crater Mine, Bancroft, Canada and is referred to as BSC throughout the manuscript.

The following chemicals were used as received: sulphuric acid [ $\text{H}_2\text{SO}_4$ ] (98% AR grade, Merck Ltd), nitric acid [ $\text{HNO}_3$ ] (70% AR grade, Merck Ltd), hydrochloric acid [ $\text{HCl}$ ] (33% AR grade, Merck Ltd), hydrofluoric acid [ $\text{HF}$ ] (50% AR grade, Ajax Chemicals), 30% hydrogen peroxide [ $\text{H}_2\text{O}_2$ ] (30% AR grade, Merck Ltd), ferric sulphate  $[\text{Fe}_2(\text{SO}_4)_3 \cdot 5\text{H}_2\text{O}]$  (Lab Reagent, Ajax Chemicals), ferrous sulphate  $[\text{FeSO}_4 \cdot 7\text{H}_2\text{O}]$  (AnalalRChem-Supply Ltd), MilliQ water was used in the preparation of all solutions.

### 2.2. X-ray photoelectron spectroscopy (XPS)

The betafite samples were prepared by pressing powdered sample at 7 tonnes under vacuum for 5 minutes using a hydraulic press. This pressed sample was mounted for analysis using carbon tape. XPS measurements were conducted on a Thermo Scientific K Alpha XPS instrument. A low energy flood gun was used to remove charge build up on the sample surface. Al  $\text{K}\alpha$  (1486.6 eV) x-ray source was used with constant analyser pass energy of 150 eV with a spot size of 55  $\mu\text{m}$ . Forty sweeps at scan rates of 80 seconds each were completed for the main elements associated with betafite (U,Ca,Nb,Ti,Ta). The binding energies were calibrated by fixing the C 1s binding peak to 385.0 eV.

### 2.3. Elemental analysis (ICP-MS)

Fifty milligrams of the natural betafites was weighed out into a Teflon vessel and 4 mL of concentrated HCl was slowly added, the reaction was then left to subside. Two millilitres of concentrated  $\text{HNO}_3$  was then added and again the reaction was left to subside after which 2 ml of concentrated  $\text{H}_2\text{SO}_4$  and 3 mL of concentrated HF were added. The Teflon vessel was then heated to 160°C to dry the sample. A further 1 mL of concentrated  $\text{H}_2\text{SO}_4$  was added and the sample was heated again at 160°C to complete dryness. Once dry the powder was transferred to a BOMB pressure vessel and 1 mL of concentrated  $\text{HNO}_3$  and

two drops of H<sub>2</sub>O<sub>2</sub> were added and the reaction was left to subside. The further 19 mL of 2% HNO<sub>3</sub> was added and the vessel was then placed in an oven at 250°C for 5 hours. The ICP–MS sample was then made up by performing a dilution of the sample which was then acidified. ICP-MS analysis was completed using an Agilent HP 7700 series ICP–MS which was calibrated using a commercial multi element environmental standard.

#### **2.4. High temperature X-ray diffraction (HT-XRD)**

Heat treating was completed by taking approximately 0.2 g of finely crushed powdered sample and placing it in a platinum lined alumina boat before heating in a temperature programmed Laybec tube furnace. The samples were heat treated by heating to 1100 °C at a heat ramp rate of 20 °C/min. The furnace was held at 1100 °C for 2 hrs before being cooled to room temperature for XRD analysis. XRD analysis was completed using a Bruker D8 Advanced X-Ray Diffractometer using a CuK $\alpha$  radiation source. A 1° divergence slit was used to analyse between 2θ range 5–90° with a step size of 0.02° and 2s/step.

#### **2.5. Dissolution studies**

Dissolution studies were completed by adding the 250 mL of the desired sulphuric acid concentration to a 250 ml 3 neck flask. The solution was agitated by using an overhead mechanical stirrer and heated to the required temperature using a heating mantle. Once at temperature, the desired amount of ferric and ferrous sulphate was added to create the required redox potential (ORP). The solution was allowed to equilibrate for 10 min. then 50.0 mg of < 75 μm natural betafite was added. The time upon addition of sample was determined to be 0 min. and solution samples were collected at pre-determined intervals throughout the experiment.

Analysis of the diluted leach solutions taken was conducted on an Agilent HP 7700 series ICP–MS the instrument was calibrated using a commercially purchased uranium standard. The error in measurement on the instrument was calculated to be ± 3%.

### **3. RESULTS AND DISCUSSION**

#### **3.1. Characterisation studies**

##### *3.1.1. X-Ray diffraction analysis of natural betafites*

The XRD patterns presented in Figure 1 shows diffraction data for unheated and heat treated betafite BAM sample. The unheated pattern shows the as received sample is predominantly amorphous, though several broad weak intensity peaks can be observed which were matched to anatase (TiO<sub>2</sub>) (ICDD-PDF 078-2486). The heat treated (1100°C) sample was shown to contain a significant amount of rutile due a phase transition between anatase and rutile as well as the recrystallisation of amorphous anatase. The high concentration of rutile in the heat treated sample is consistent with results observed previously for annealed betafite samples [13–15]. Crystalline betafite was also identified in the heat treated sample demonstrating that all betafite in the unheated sample was amorphous due to metamictisation.

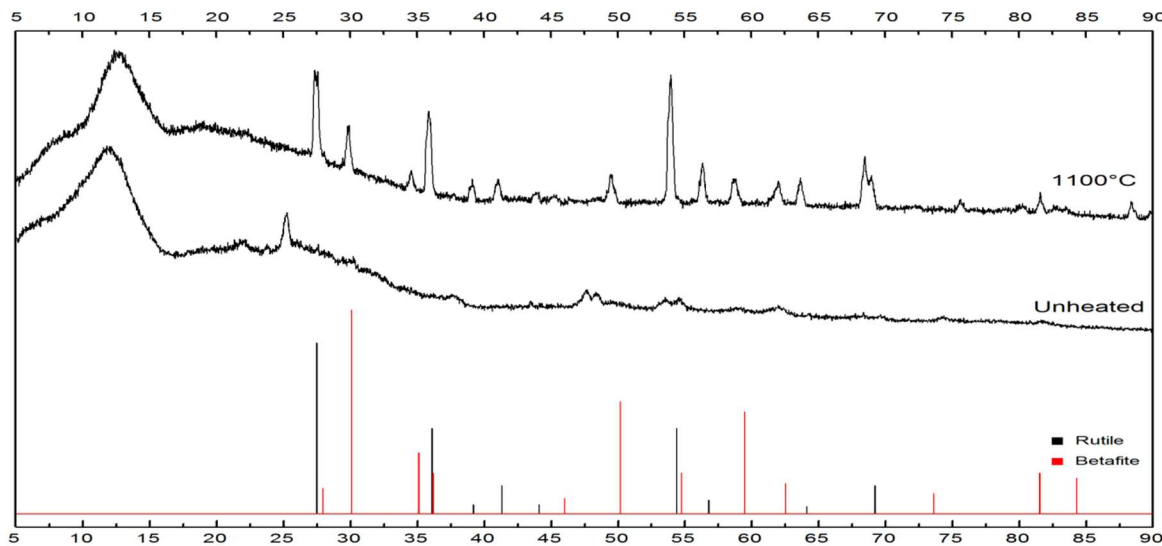


FIG. 1. XRD pattern of unheated (middle) and heat treated (top) natural betafite BAM. Database matches of ICDD JCPDS XRD database matches included for comparison. Betafite  $[(U,Ca)_2(Nb,Ti,Ta)_2O_7.xH_2O]$  (PDF 008-0300) (Red), Rutile  $[TiO_2]$  (PDF 034-0180) (Black).

The XRD patterns presented in Fig. 2 show unheated and heat treated betafite BSC. Analysis of the XRD pattern obtained for the unheated sample shows the sample is almost completely amorphous. Two broad weak peaks were shown to be present at 32 and 50 degrees 2theta, these peaks match the 2 major anatase peaks though due to the weak intensity of these peaks a definite match for anatase could not be obtained. When the sample was heated to 1100°C a strong match for betafite was obtained. The heated sample also contained a minor amount of rutile though this was significantly less than was shown to be present in the BAM sample based on the intensity of the rutile diffraction lines obtained.

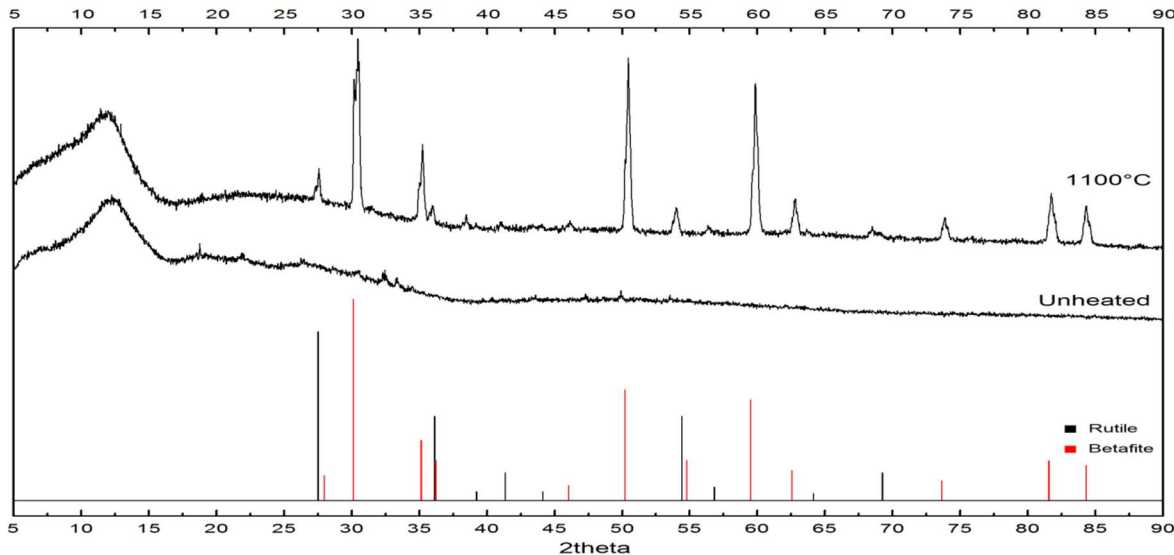


FIG. 2. XRD pattern of unheated (middle) and heat treated (top) natural betafite BSC. Database matches of ICDD JCPDS XRD database matches included for comparison. Betafite  $[(U,Ca)_2(Nb,Ti,Ta)_2O_7.xH_2O]$  (PDF 008-0300) (Red), Rutile  $[TiO_2]$  (PDF 034-0180) (Black).

### 3.1.2. Multi-acid digestion/ICP-MS analysis of natural betafites

Multi acid digestion/ICP-MS analysis of the natural samples BAM and BSC was completed to determine the bulk elemental composition of the samples (Table I). The results for the BAM sample show all the elements generally associated with betafite. This sample also showed appreciable quantities of sodium (4.4%) aluminium (9.1%) and iron (2.1%). Hogarth (1977) [6] reports that metals such as sodium have a similar atomic radius to calcium and can therefore generally substitute into the A site of the betafite structure. Additionally, aluminium and iron have similar atomic radii to Ti and can therefore be incorporated into the B site of the betafite structure ( $A_2B_2O_6OH$ ) [6].

Bulk elemental composition analysis of BSC shows similar elemental composition to that of the previous sample. This sample was shown to not contain any metals that can substitute into the A site such as calcium, sodium or potassium. Lumpkin and Ewing (1996) [7] report that metals such as A site cations such as Ca, Na and K are more likely to become removed from the betafite structure via natural weathering processes while the crystal structure remains similar [7]. This could also explain why the U oxidation state differs between BAM and BSC which is discussed in detail in the next section (Figs 3 and 4).

TABLE I. MULTI ACID DIGESTION – ICP-MS ANALYSIS OF NATURAL BETAFLITE SAMPLES BAM AND BSC

| <i>Bulk %<br/>Composition</i> | <i>Sample</i> |        |
|-------------------------------|---------------|--------|
| Element                       | BAM           | BSC    |
| Sodium                        | 4.41          | < 0.04 |
| Magnesium                     | 0.98          | < 0.04 |
| Aluminium                     | 9.14          | 9.70   |
| Potassium                     | 0.68          | < 0.04 |
| Calcium                       | 2.52          | < 0.04 |
| Titanium                      | 11.96         | 13.06  |
| Iron                          | 2.11          | < 0.04 |
| Copper                        | < 0.04        | 0.20   |
| Zinc                          | 0.81          | 0.12   |
| Niobium                       | 17.74         | 26.10  |
| Barium                        | 0.24          | 0.22   |
| Tantalum                      | 2.05          | 3.15   |
| Lead                          | 0.87          | 0.15   |
| Thorium                       | 0.91          | 0.57   |
| Uranium                       | 21.92         | 21.58  |
| Total                         | 76.35         | 74.85  |

### 3.1.3. X-ray photoelectron spectroscopy (XPS) of natural betafites

The oxidation state of surficial uranium in the natural betafite samples was determined via XPS. The data shown in Figure 3 shows two intense peaks located at ~381 and 392 eV, these are attributed to the

excitation states  $\text{U}4\text{f}_{7/2}$  and  $\text{U}4\text{f}_{5/2}$  respectively. Deconvolution of the  $\text{U}4\text{f}_{5/2}$  excitation peak reveals 3 peaks, 2 of weak intensity at 390.88 and 391.48 eV, as well as a more intense peak at 392.48 eV. Chadwick (1973) demonstrates that as the oxidation state of uranium increases the binding energy (BE) of the deconvoluted  $\text{U}4\text{f}$  peaks also increases by approximately 1.7 eV between  $\text{U}^{4+}$  and  $\text{U}^{6+}$  [16]. The deconvoluted peaks can also be used to determine the U oxidation state by calculating the Binding Energy (BE) difference between the deconvoluted peaks and higher energy  $\text{U}4\text{f}_{5/2}$  satellite peaks which occur at  $> 395$  eV. This difference indicates the U oxidation state present in the sample. For  $\text{U}^{4+}$  species the BE difference is between 6-7 eV, for  $\text{U}^{5+}$  between 7.7–8.5 eV, and two peaks at ~4 and 10 eV for  $\text{U}^{6+}$ . Satellite peaks occur for both  $\text{U}4\text{f}_{7/2}$  and  $\text{U}4\text{f}_{5/2}$  peaks but due to overlap of the  $\text{U}4\text{f}_{7/2}$  satellite peaks and the  $\text{U}4\text{f}_{5/2}$  excitation peak the  $\text{U}4\text{f}_{7/2}$  satellite peaks are generally not used for analysis of oxidation states. The spectrum presented in Fig. 3 shows two small satellite peaks at 396.68 and 402.48 eV. Since the gap between the deconvoluted peak at 390.88 eV and the satellite peak at 396.68 was 5.8 eV this peak was assigned to  $\text{U}^{4+}$ . The difference between the peak at 392.48 eV and the highest binding energy of 402.48 eV was shown to be 10.0 eV. For this reason, it was assumed that the peak at 396.68 eV was made up of 2 peaks, one being assigned to a  $\text{U}^{4+}$  satellite peak, the other peak assigned to  $\text{U}^{6+}$  satellite peak. The smallest deconvoluted  $\text{U}4\text{f}_{5/2}$  peak at 391.48 eV was assigned to  $\text{U}^{5+}$  since the BE is in between the  $\text{U}^{4+}$  and  $\text{U}^{6+}$  deconvoluted peaks. Due to the small magnitude of the deconvoluted  $\text{U}^{5+}$  peak the satellite peak which is expected to occur between 7.7 and 8.5 eV higher (~401 eV) could not be seen in the spectra.

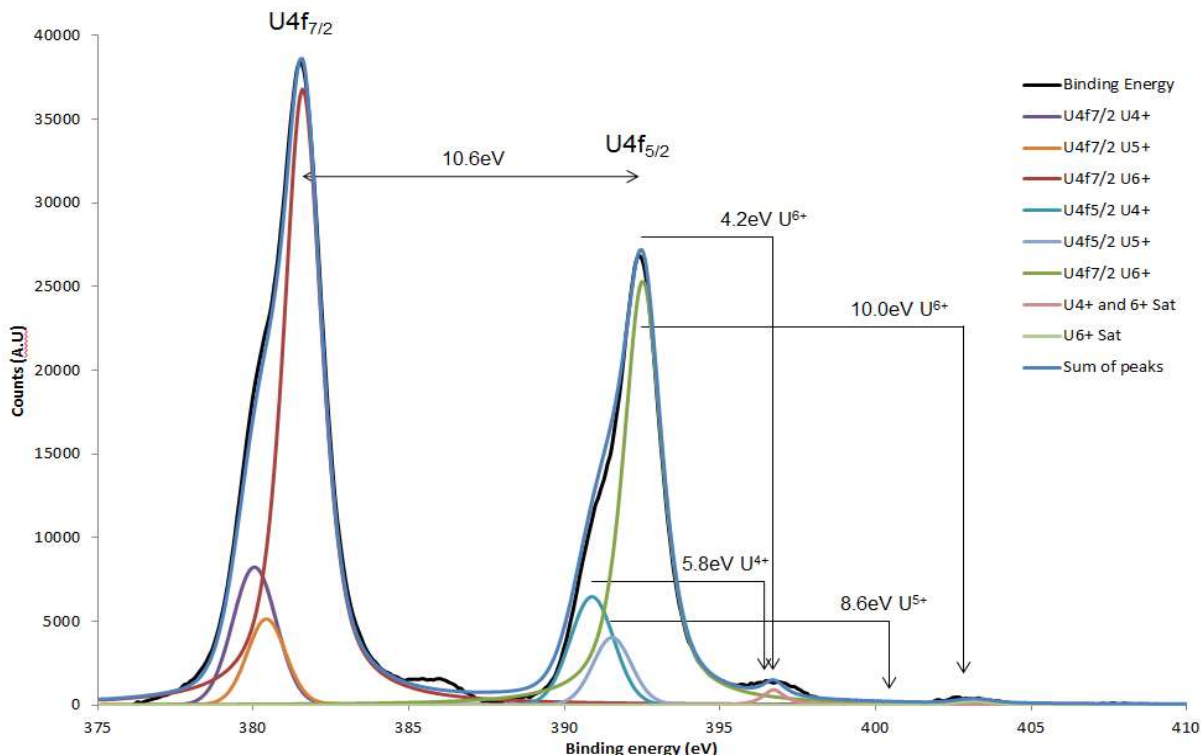


FIG. 3. XPS Spectra of  $\text{U}4\text{f}$  orbital of natural betaafite BAM.

XPS spectra of  $\text{U}4\text{f}$  orbital in the natural betaafite sample BSC shows 2 intense peaks at 381 and 392 eV which are due to  $\text{U}4\text{f}_{7/2}$  and  $\text{U}4\text{f}_{5/2}$  excitation states respectively (Fig. 4). Deconvolution of the  $\text{U}4\text{f}_{5/2}$  reveals 2 excitation peaks at 391.08 and 392.28 eV. Analysis of the  $\text{U}4\text{f}_{5/2}$  satellite peak shows 3 weak intensity peaks at 396.28, 399.68 and 402.98 eV. The binding energy difference between the lower energy deconvoluted  $\text{U}4\text{f}_{5/2}$  and the middle satellite peaks was calculated to be 8.6 eV and therefore assigned to  $\text{U}^{5+}$  oxidation state. The energy difference between the remaining 2 satellite peaks had a BE difference of 4.0 and 10.7 eV from the higher energy deconvoluted  $\text{U}4\text{f}_{5/2}$  and were therefore assigned

to  $\text{U}^{6+}$ . A weak intensity peak at 407.08 eV which is too high to be a satellite peak of the  $\text{U}4\text{f}_{5/2}$  excitation state was assigned to  $\text{Cd}3\text{d}_{5/2}$  excitation state which was shown by Gulino *et al* to have a similar binding energy [17].

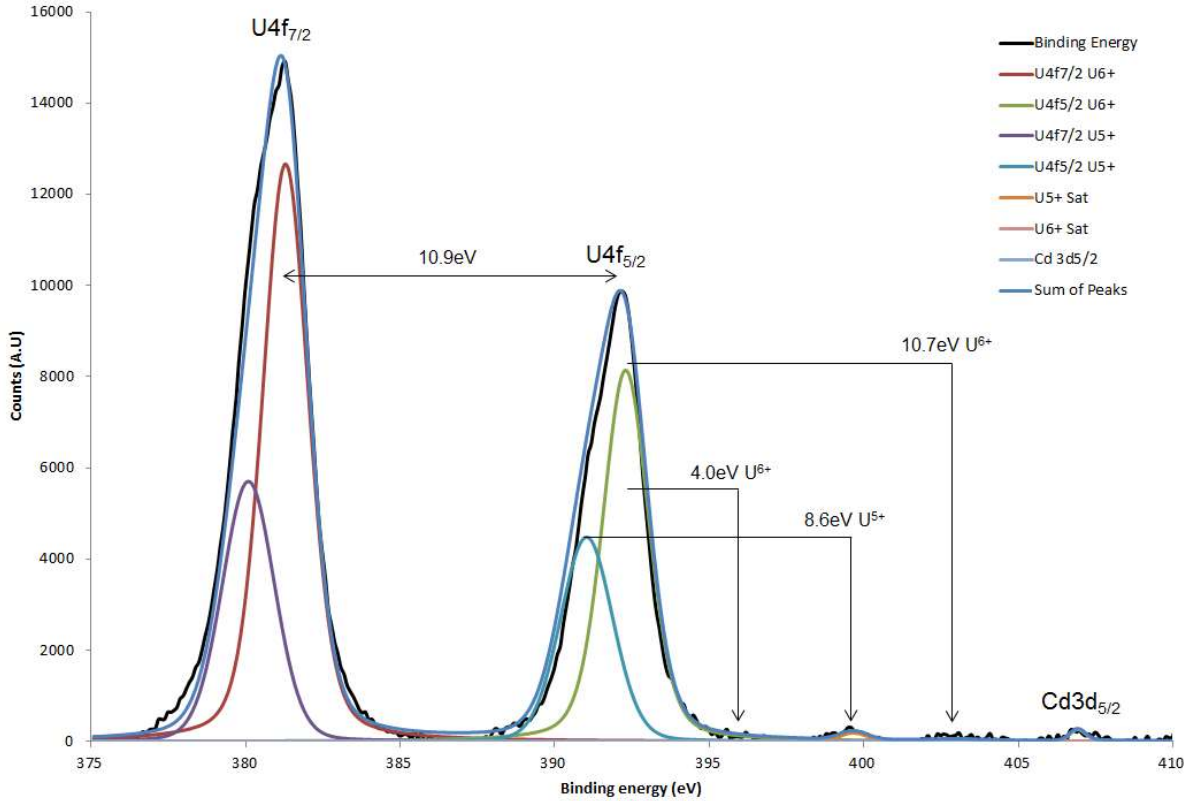


FIG. 4. XPS Spectra of  $\text{U}4\text{f}$  orbital of natural betafite BSC.

### 3.2. Dissolution studies of natural betafites

#### 3.2.1. Influence of $[\text{H}_2\text{SO}_4]$ on dissolution of natural betafites

Four experiments were conducted to study the influence of sulphuric acid concentration on natural betafite dissolution. The results presented in Figure 5 show as the concentration of acid is increased the rate of dissolution also increases. In the first 2 mins of each experiment  $\sim 2.0\%$  of the uranium from the natural sample was found to have dissolved at each acid concentration used, whereas after this period the rate of dissolution varied significantly for the different acid concentrations used. This initial rapid dissolution within the first 15 min for all tests is possibly due to surface  $\text{U}^{6+}$  being present from the weathering process and hence dissolving instantaneously. The highest sulphuric acid concentration used was 100 g/L (1.02 M), this lead to 57.7% uranium dissolved from BAM after 6 hours.

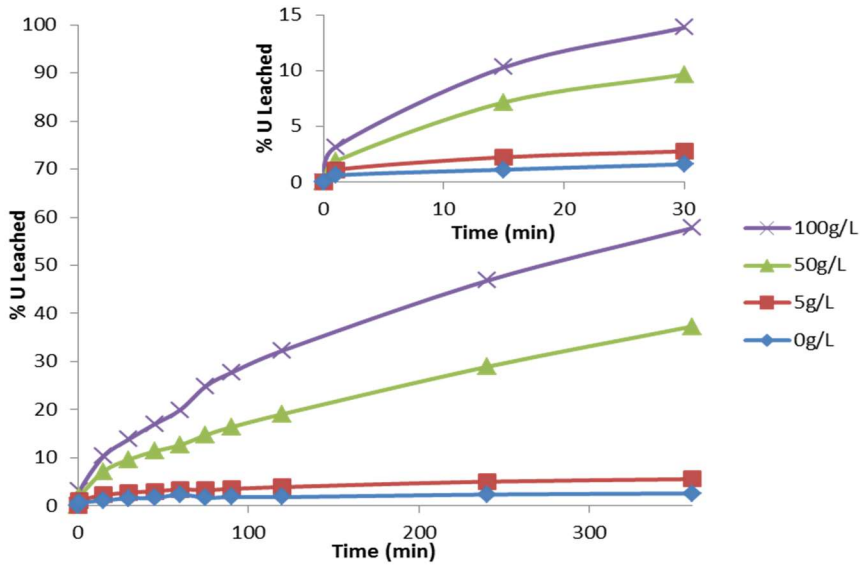


FIG. 5. Influence of  $[H_2SO_4]$  on uranium dissolution from natural betafite BAM. Temperature:  $35^\circ C$ ,  $[Fe]_{TOT}$ : 3 g/L, Redox Potential: 510 mV vs. Ag/AgCl.

The dissolution data presented in Fig. 6 shows the influence of sulphuric acid on uranium dissolution from BSC. The most notable difference between BAM and BSC is the comparative rates of dissolution between the two samples. At the highest acid concentration used (100 g/L) only  $\sim 4.7\%$  of the uranium was dissolved out of the sample. This significant difference in dissolution between BSC and BAM could be due the higher amount of  $U^{6+}$  characterised in BAM has led to a more rapidly rate of U dissolution.

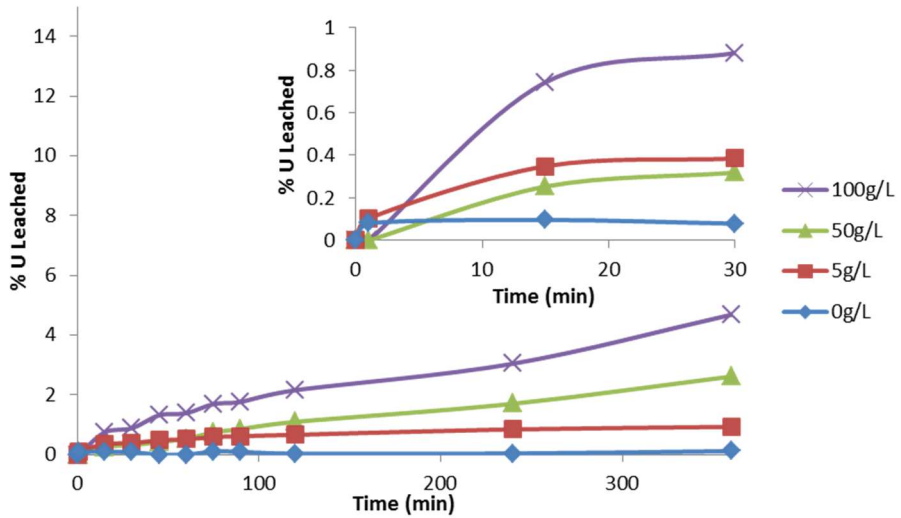


FIG. 6. Influence of  $[H_2SO_4]$  on uranium dissolution from natural betafite BSC. Temperature:  $35^\circ C$ ,  $[Fe]_{TOT}$ : 3 g/L, Redox Potential: 510 mV vs. Ag/AgCl.

### 3.2.2. Influence of temperature on U dissolution of natural betafites

The influence of temperature on uranium dissolution from BAM was studied between  $35$  and  $95^\circ C$ . The results presented in Fig. 7 show as the temperature increases, the rate of uranium dissolution also increases over the temperature range studied. In each experiment the dissolution rate decreased over the duration of the test. The highest temperature experiment conducted was at  $95^\circ C$ , this yielded  $\sim 35\%$  of the uranium dissolved out of the BAM sample after 360 minutes. Rate constants were calculated for use in determining the activation energies using the Arrhenius equation. The activation energy for

dissolution of uranium from BAM was calculated to be 32.4 kJ/Mol. Activation energies of other natural uranium mineral samples include 30.3 kJ/Mol for brannerite [18] and 33 kJ/Mol for Th-uraninite [19].

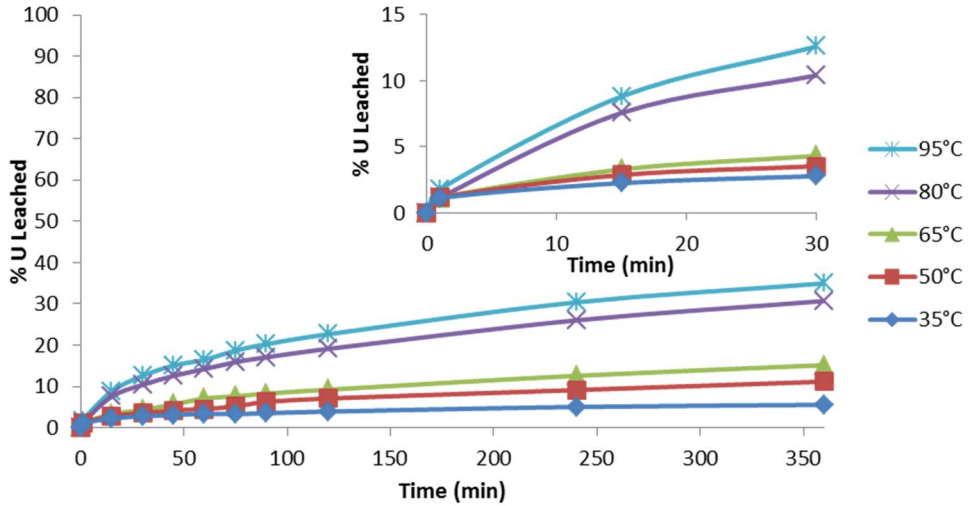


FIG. 7. Influence of temperature on uranium dissolution from natural betafite BAM.  $[H_2SO_4]$ : 5 g/L,  $[Fe]_{TOT}$ : 3 g/L, Redox Potential: 510 mV vs. Ag/AgCl.

The influence of temperature on uranium dissolution from BSC shown in Fig. 8 demonstrates similar trends to the BAM temperature experiments shown previously. Two major differences when studying the influence of temperature on both BAM and BSC samples is the extent of dissolution for BSC is significantly lower than BAM and the dissolution rate of BSC stays at a similar rate throughout the duration of the experiments whereas the rate for BAM decreases as the time increases. At 95°C only 9.1% of the uranium from the sample was leached out after 360 mins. This difference in the extent of dissolution between BAM and BSC could be due to the factors discussed previously. The activation energy for uranium dissolution from BSC was calculated using the Arrhenius equation to be 40.9 kJ/Mol. This activation energy was slightly higher than the BAM sample but still comparable to other uranium minerals [18, 19].

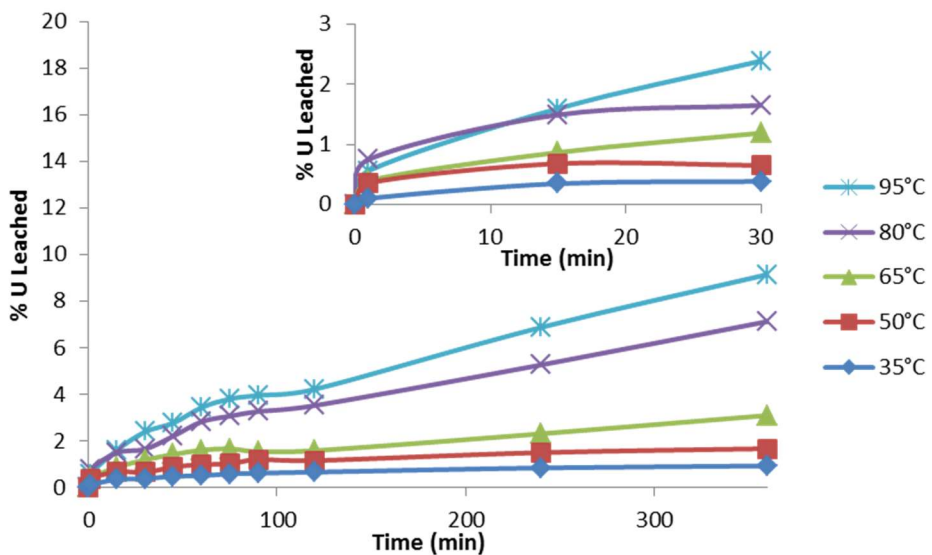


FIG. 8. Influence of temperature on uranium dissolution from natural betafite BSC.  $[H_2SO_4]$ : 5 g/L,  $[Fe]_{TOT}$ : 3 g/L, Redox Potential: 510 mV vs. Ag/AgCl.

### 3.2.3. Influence of heat treating on U dissolution of natural betafites

Comparisons between dissolution of uranium from unheated and heated BAM was conducted at two sulphuric acid concentrations; 0 g/L and 50 g/L. These experiments were designed to show the effect of metamictization on uranium dissolution of the natural samples. The dissolution results presented in Fig. 9 show two significantly different dissolution curves occur between when the sample is unheated and heated. In the unheated sample the dissolution rate stays constant throughout the experiment whereas in the heated sample the rate slows significantly after 120 mins. The two experiments conducted with no acid show more dissolution occurs when the sample is heated. This could be due to the annealing process alters the structure of the betafite so a higher amount of  $U^{6+}$  is accessible to be leached. This would explain why the rate decreases as the experiment progresses. Comparison between the unheated and heated 50 g/L  $H_2SO_4$  experiments show the initial rate is significantly higher over the initial 120 mins in the heated sample. After this point the dissolution rate slows considerably. This could be due to the aforementioned reasons; more  $U^{6+}$  could be found in the heated sample, or a structural transformation has led to the leachable uranium being more accessible to the leach solution. The decrease in rate after this point is most likely to be due to the heat treating leading to recrystallization of the betafite and hence the stronger mineral structure needing more energy to breakup and dissolve the uranium from the mineral.

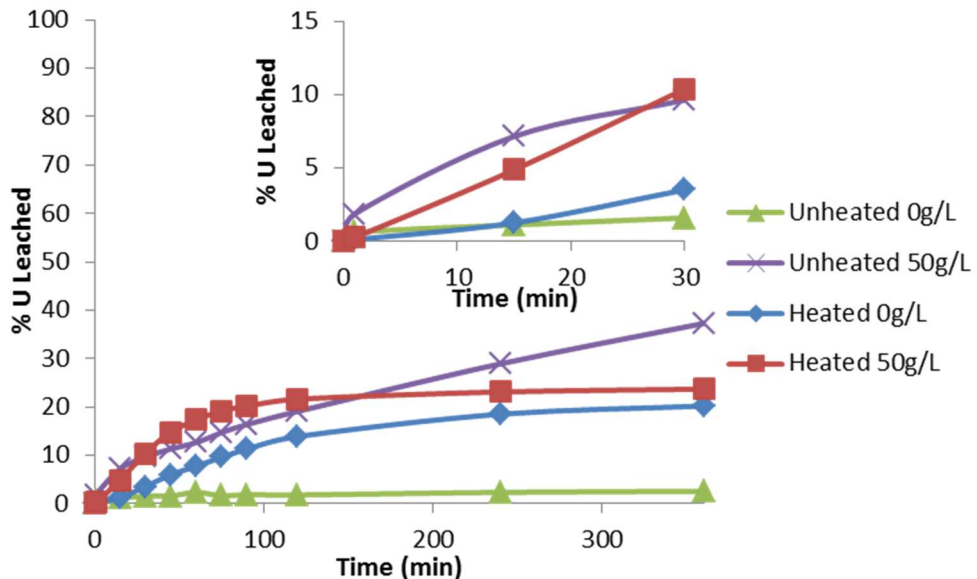


FIG. 9. Influence of heat treating on uranium dissolution from natural betafite BAM. Temperature: 35°C,  $[H_2SO_4]$ : 5 g/L,  $[Fe]_{tot}$ : 3 g/L, Redox Potential: 510 mV vs. Ag/AgCl.

Similar trends are present in BSC as were shown previously in BAM when studying the influence of heat treating. The results presented in Fig. 10 shows a higher amount of uranium was dissolved in the heated sample than the unheated sample when no sulphuric acid was added. As described previously a higher amount of  $U^{6+}$  could be present or the  $U^{6+}$  could more exposed to be leached. Comparison between the heated and unheated BSC dissolution curves when 50 g/L  $H_2SO_4$  was added shows a significantly higher dissolution rate in the heated sample over the initial 30 mins. After this point, the rate slows for the remainder of the 360-min experiment. This initial fast rate over the first 30 minutes is due to the reasons explained previously, but is shown to be more prominent due to the compounding effect of the high acid concentration. The dissolution rate of the heated sample is slower than the unheated sample after the initial spike for the first 30 mins. Again, this influence is attributed to the stronger mineral structure gained from annealing the heated sample leading to more energy needed to dissolve uranium from the mineral.

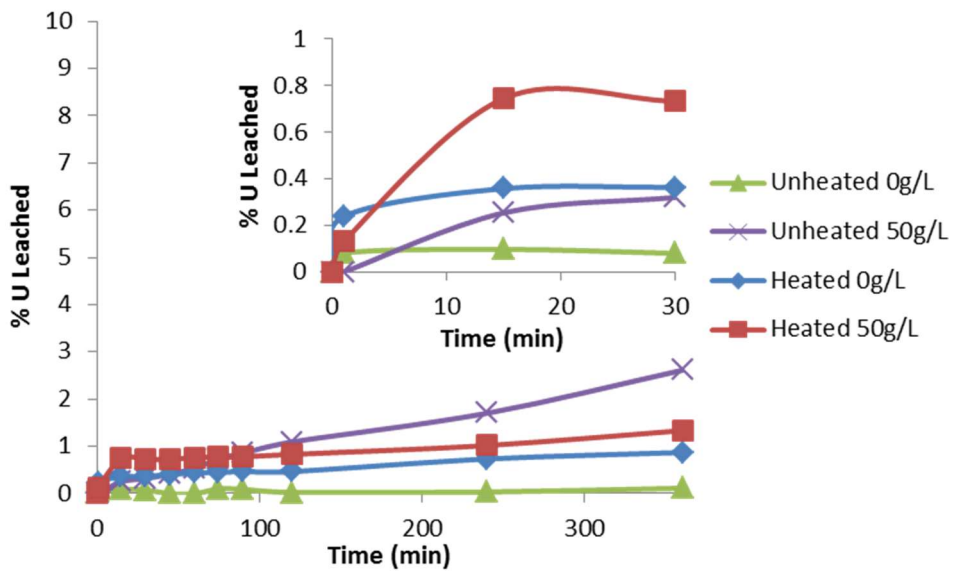


FIG. 10. Influence of heat treating on uranium dissolution from natural betafite BSC. Temperature: 35°C,  $[H_2SO_4]$ : 5 g/L,  $[Fe]_{TOT}$ : 3 g/L, Redox Potential: 510 mV vs. Ag/AgCl.

## ACKNOWLEDGEMENTS

Financial support from RMIT University is acknowledged. The authors would also like acknowledge D. Henry of Melbourne Museum for generously providing the BAM sample used in this study. SM acknowledges C. Plummer and A. Raynor for the assistance throughout the project.

## REFERENCES

- [1] POWNCEBY, M.I., JOHNSON, C., Geometallurgy of Australian uranium deposits, *Ore Geol. Rev.* **56** (2014) 25–44.
- [2] CHARALAMBOUS, F.A., RAM, R., MCMASTER, S., TARDIO, J., BHARGAVA, S.K., An investigation on the dissolution of synthetic brannerite ( $UTi_2O_6$ ), *Hydrometallurgy* **139** (2013) 1–8.
- [3] BERNING, G., COOKE, R., HIEMSTRA, S.A., HOFFMAN, U., The Rossing uranium deposit, South West Africa, *Econ. Geol.* **71** (1976) 351–368.
- [4] ABRAHAM, I.M., Geology and spatial distribution of uranium mineralization in the SK anomaly area, Rössing area, Namibia, Master's Thesis, University of the Witwatersrand (2009).
- [5] HOGARTH, D.D., A study of pyrochlore and betafite, *Can. Mineral.* **6** (1961) 611–633.
- [6] HOGARTH, D.D., Classification and nomenclature of the pyrochlore group, *Am. Mineral.* **62** (1977) 403–410.
- [7] LUMPKIN, G.R., EWING, R.C., Geochemical alteration of pyrochlore group minerals: Betafite subgroup, *Am. Mineral.* **81** (1996) 1237–1248.
- [8] YAROSHEVSKII, A.A., BAGDASAROV, Y.A., Geochemical diversity of minerals of the Pyrochlore group, *Geochem Int* **46** (2008) 1245–1266.
- [9] BURNS, P.C., FINCH, R., “Crystal chemistry of uranium”, *Uranium: Mineralogy, Geochemistry and the Environment* (RIBBE, P.H., Ed.), Mineralogical Society of America, Blacksburg, VA (1999) 23–90.
- [10] LUMPKIN, G.R., EWING, R.C., Alpha-decay damage in minerals of the pyrochlore group, *Phys. Chem. Mineral.* **16** (1988) 2–20.
- [11] CÁMARA, F., WILLIAMS, C.T., DELLA VENTURA, G., OBERTI, R., CAPRILLI, E., Non-metamict betafite from Le Carcarelle (Vico volcanic complex, Italy): Occurrence and crystal structure, *Mineral. Mag.* **68** (2004) 939–950.

- [12] McMASTER, S., RAM, R., CHARALAMBOUS, F., TARDIO, J., BHARGAVA, S., "Characterisation and dissolution studies on the uranium mineral betafite", Proc. Chemeca 2012: Quality of Life Through Chemical Engineering, Engineers Australia, Wellington, New Zealand (2012) 612–622.
- [13] EYAL, Y., LUMPKIN, G.R., EWING, R.C., "Alpha-recoil effect on the dissolution of betafite rapid natural annealing of radiation damage within a metamict phase", Materials Research Society Symposia Proceedings **50** (1986) 379–386.
- [14] McMASTER, S., RAM, R., CHARALAMBOUS, F., TARDIO, J., BHARGAVA, S., "Characterisation studies on natural and heat treated betafite", Proc. Chemeca 2013: Challenging Tomorrow, Engineers Australia, Brisbane, (2013) 529–535.
- [15] GEISLER, T., SEYDOUXGUILLAUME, A., POEML, P., GOLLASCHINDLER, U., BERNDT, J., WIRTH, R., POLLOK, K., JANSSEN, A., PUTNIS, A., Experimental hydrothermal alteration of crystalline and radiation-damaged pyrochlore, *J. Nuclear Materials* **344** (2005) 17–23.
- [16] CHADWICK, D., Uranium 4f binding energies studied by X-ray photoelectron spectroscopy, *Chem. Phys. Lett.* **21** (1973) 291–294.
- [17] GULINO, A., CASTELLI, F., DAPPORTO, P., ROSSI, P., FRAGALÀ, I., Synthesis and characterization of thin films of cadmium oxide, *Chemistry of Materials* **14** (2002) 704–709.
- [18] GOGOLEVA, E.M., The leaching kinetics of brannerite ore in sulfate solutions with iron(III), *J. Radioanal. Nucl. Chem.* **293** (2012) 185–191.
- [19] HEISBOURG, G., HUBERT, S., DACHEUX, N., RITT, J., The kinetics of dissolution of  $\text{Th}_{1-x}\text{U}_x\text{O}_2$  solid solutions in nitric media, *J. Nuclear Materials* **321** (2003) 141–151.

# **THE PROSPECTS FOR THE APPLICATION OF THE NEW GENERATION NEUTRON LOGGING SYSTEM DEVELOPED BY RUSBURMASH INC. (RUSSIAN FEDERATION) FOR HANDLING GEOTECHNICAL ISSUES AT SANDSTONE-HOSTED URANIUM DEPOSITS**

V.G. MARTYNNENKO, A.R. MINOSYANTS, S.N. FEDYANIN

Rusburmash Inc.,

Moscow, Russian Federation

## **Abstract**

In 2011–2013 Rusburmash Inc. was developing an AINK-49 new-generation hardware system for fission neutron logging. The work was completed using the financing provided by and upon the Technical Assignment from Atomredmetzoloto JSC as part of a Research and Development Plan. The system was developed with the involvement of the leading Russian scientific and manufacturing companies in this field.

## **1. INTRODUCTION**

The relevance of the system is based on the fact that Rusburmash Inc. is one of the leading Russian companies involved in the exploration and preparation of sandstone-hosted uranium deposits for ISL (in situ leaching) mining.

The peculiarity of these deposits consists in the complex radiological environment which is additionally subjected to complex and uncontrolled production-induced changes in the process of leaching. In such conditions the application of prompt fission neutron (PFN) logging has a promising outlook that has no alternative for operation in the conditions of altered ore as a result of production. This method is designed for the direct determination of uranium mass fraction within the drillhole environment. It is based on creating a neutron flux using an impulse neutron generator and recording of secondary neutrons produced in the natural environment under the influence from the generated neutrons.

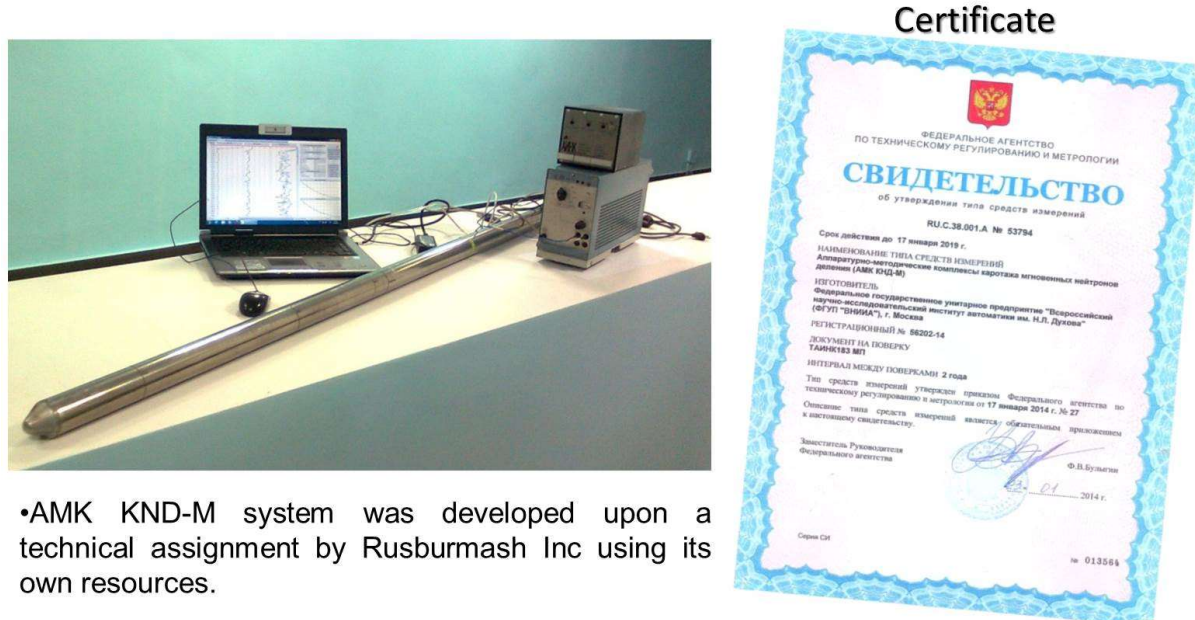
In addition to PFN logging the developed system features impulse neutron-neutron logging technique using thermal neutrons. This allows determination of ore in-situ moisture content and considerably increases the reliability of uranium mass fraction determination owing to the precise account of the moisture content. Availability of a pulsed neutron-neutron logging channel makes it possible to assess the coefficient of ore clay content, to reliably and reasonably define sub-economic ore types by permeability.

The system has a range of advantages compared to similar tools. Application of new neutron generators increased the output of the neutron flux, increased the life of the generator up to 250 hours and reduced the downhole tool diameter to 49 mm. This significantly broadens the scope of the equipment application due to the possibility of using it in small diameter holes (60 mm) and cased holes. Logging speed can be increased to 60 m/hour (instead of 30–45 m/hour) as well as significantly reduce operational costs.

The hardware complex provides reliable results in a complex radiological environment including the areas subject to alteration due to ISL operations. Therefore, in addition to handling exploration issues, the complex can become widely used in the operational and mined-out ISL sites to monitor the leaching process, to provide on-going control of the applied ISL process flowsheet performance, to assess uranium in-situ recovery performance and recovery level from the production-induced areas of uranium re-deposition.

In the period from 2011 to 2013, Rusburmash Inc successfully developed AINK-49 — a new generation hardware system for Prompt Fission Neutron (PFN) logging (Fig. 1). The system and measurement procedure were developed together with the Russian leading scientific and manufacturing companies:

The All-Russian Research Institute of Automatics (VNIIA, main developer), Federal State Unitary Research & Production Enterprise Geologorazvedka (metrological assurance and measurement procedure) and VNIIgeosystem State Research Center (mathematical modelling, software-interpretative support).



- AMK KND-M system was developed upon a technical assignment by Rusburmash Inc using its own resources.
- The instrumentation is certified and included in the State Register of Measuring Equipment.

*FIG. 1. AINK-49 new generation hardware system.*

The instrumentation is certified and included in the State Register of Measuring Equipment. The following leading companies have expressed interest in the PFN implementation: Uranium One, Areva, Navoi Mining and Metallurgical Complex (Uzbekistan) and many others.

Rusburmash is a leading Russian company engaged in the exploration and preparation of sandstone-hosted uranium deposits for in-situ leaching mining (ISL). Deep insight into disequilibrium issues associated with the development of uranium deposits motivated us to create a unique integrated logging system.

Generally, gamma logging is the main method of uranium deposits exploration. It is an indirect method based primarily on measuring the gamma radiation from the radium group elements (Fig. 2). Uranium mass fraction in gamma logging is determined based on the radioactive equilibrium factor (REF) between uranium and radium. Thus,  $REF = Gr_{Ra}/Gr_U$ , where  $Gr_{Ra}$  is expressed in the units of uranium in equilibrium. For the ore where U and Ra are in equilibrium REF is 1.

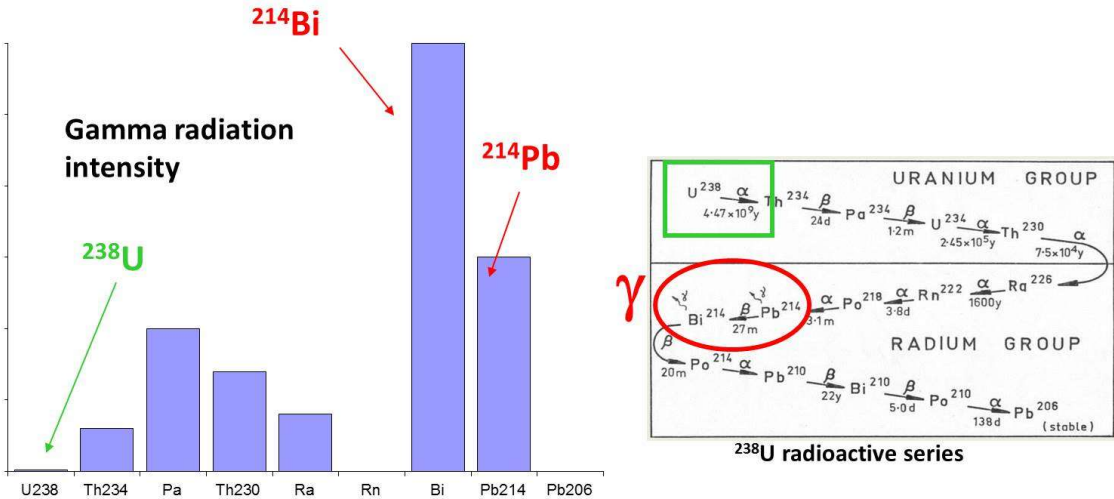


FIG. 2. Problem of U quantitative determination based on gamma logging data.

Sandstone-hosted uranium deposits are characterized by a complex radiological setting due to the radioactive disequilibrium between U and Ra. That said, the disequilibrium factor can vary over a wide range (Fig. 3) and this variation may be due to the geology and morphology of the deposit, its geochemical and lithological zonality and other factors (Fig. 4).

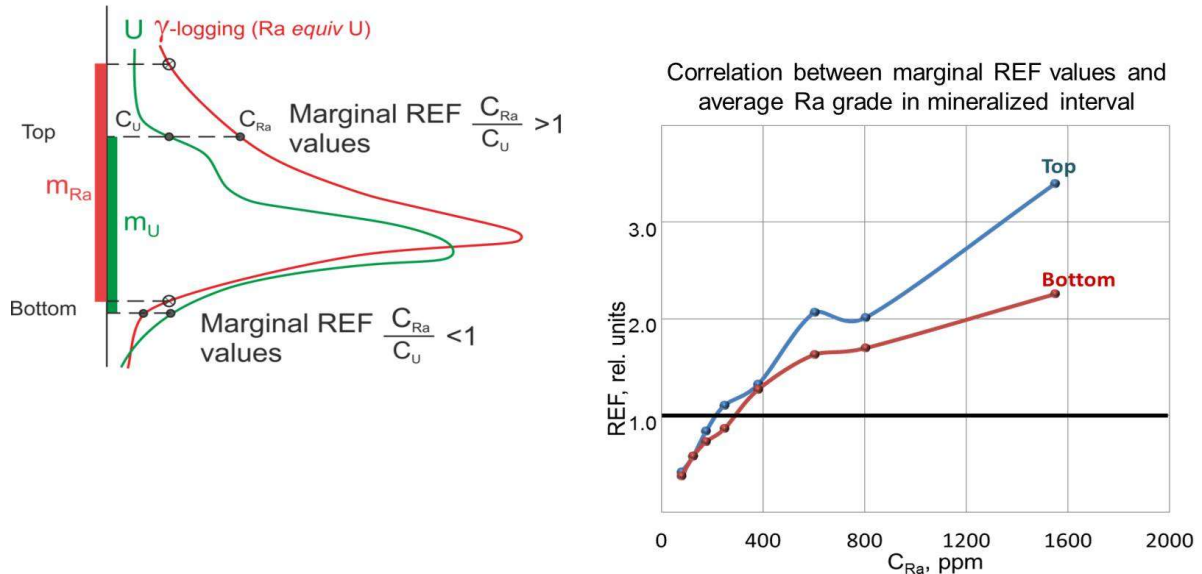


FIG. 3. Marginal REF values.

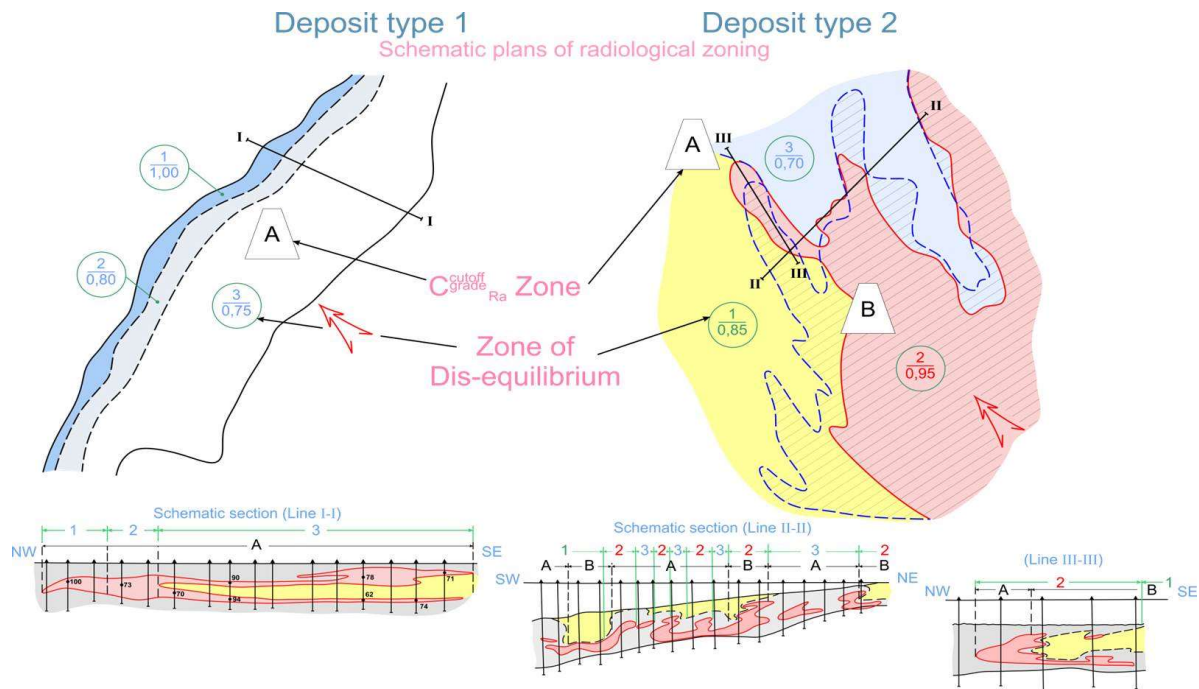


FIG. 4. Examples of zonality in the distribution of the Radioactive Equilibrium Factor between U and Ra.

Failure to take into account zonal variations in REF both over the deposit area and in section results in gamma logging (GL) data unreliability. Therefore, the application of gamma logging to estimate uranium resources at the exploration stage requires a preliminary study of ore radiological characteristics (Fig. 5).

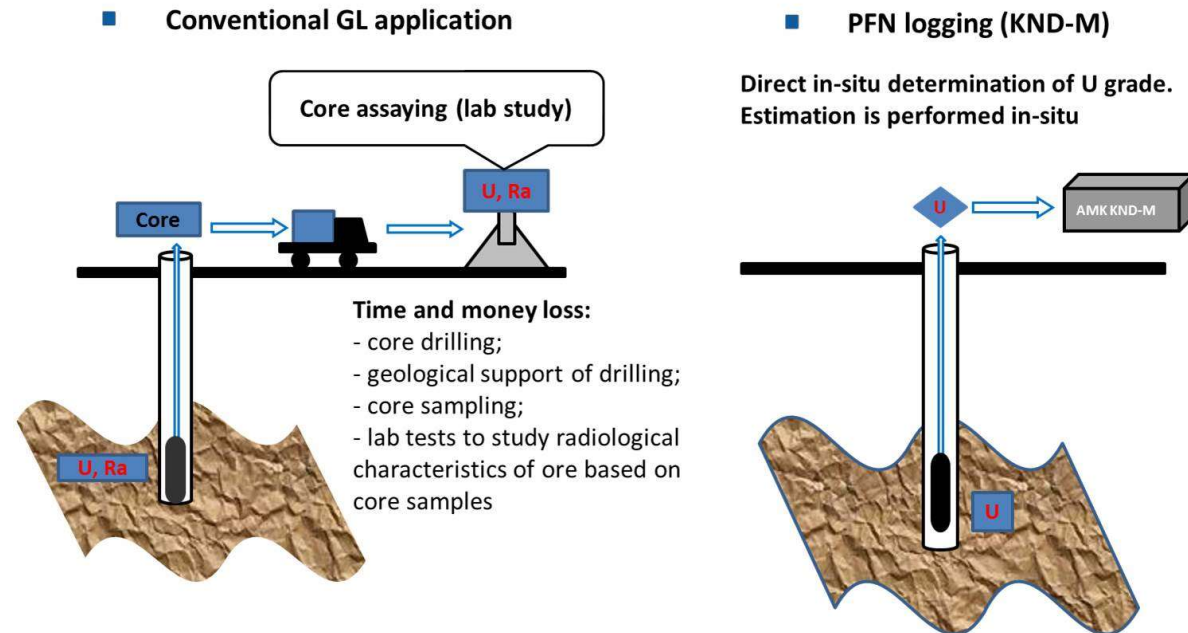


FIG. 5. Contrast of conventional gamma and PFN logging.

And this will naturally involve:

- Expensive core drilling for all exploratory holes;
- Geological support of drilling;
- A set of laboratory studies.

All of this increase labour intensity and reduce the effectiveness.

Prompt Fission Neutron (PFN) logging is a direct method for in-situ determination of U grade in a hole. For this reason, PFN logging represents a promising outlook for the exploration of uranium deposits where the radiological setting is rather complex. PFN logging allows considerable reduction in the amount of core drilling and associated activities. Core drilling in this case is applied not to study radiological characteristics of ore but only to verify PFN results.

Another promising application for PFN logging stems from the need for a rapid method that allows solution of uranium mining related issues.

The applicability comes from the fact that during ISL the productive interval undergoes complex and uncontrollable technogenic changes (Fig. 6). In such conditions the application of PFN logging is practically the only option.

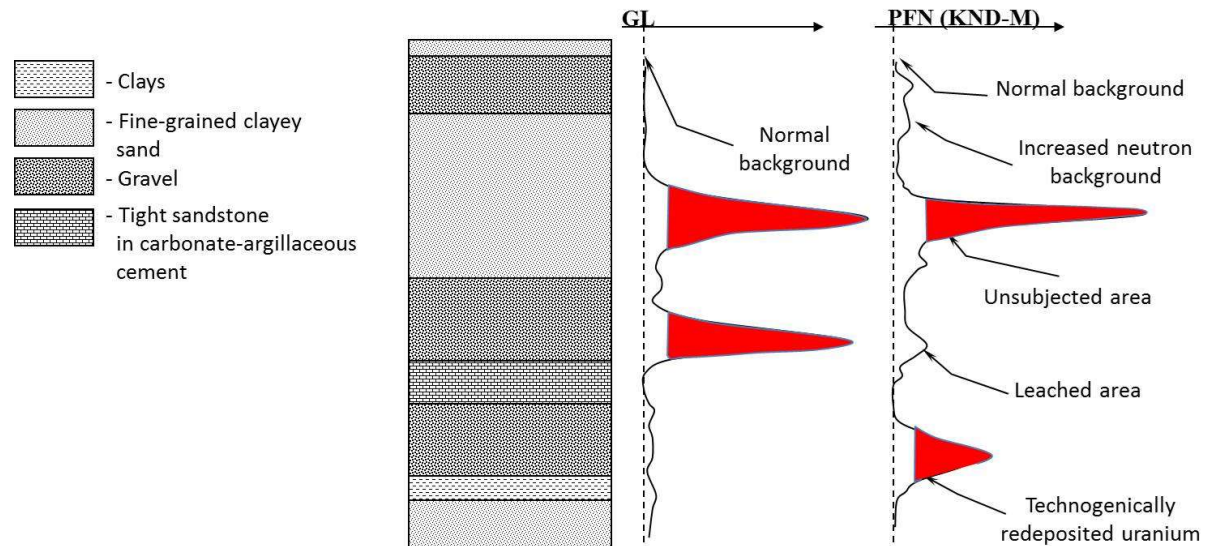


*FIG. 6. Comparison between GL and PFN results for the running ISL site.*

Thus, PFN logging main advantages are as follows:

- Immediate results for in-situ determination of mineralised intervals estimation parameters;
- Considerable reduction in the amount of core drilling, geological support and analytical study as against conventional gl;
- The possibility to control ISL process;
- The possibility to estimate residual productivity and technogenic-morphological alteration of ore bodies, and identify areas of production-induced redeposition of uranium in the productive horizon.

The effectiveness of the method as applied in areas where ISL mining was formally completed is confirmed by the fact that in 2000 in the Navoi MMC alone PFN data helped to bring at least 5 well fields back into operation. Additional uranium production from the deposits amounted to 3000 tonnes.

The PFN logging method is designed for direct determination of uranium mass fraction within the drillhole environment (Fig. 7). It is based on producing a 14 MeV neutron flux using an impulse neutron generator and recording of secondary neutrons —  $^{235}\text{U}$  prompt fission neutrons which occur in natural environment under the effect from the generated neutrons. The measured density of the prompt fission neutron flux is proportional to the content of natural uranium ( $\text{U}_{\text{natr}}$ ) in the radiation-exposed volume.

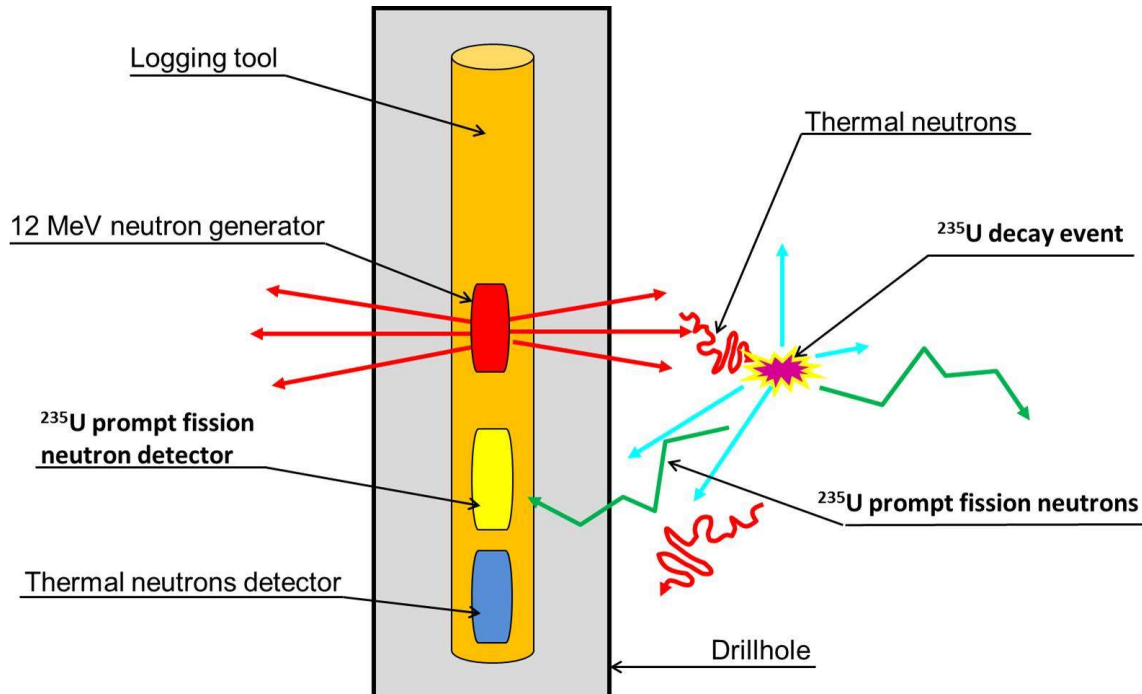


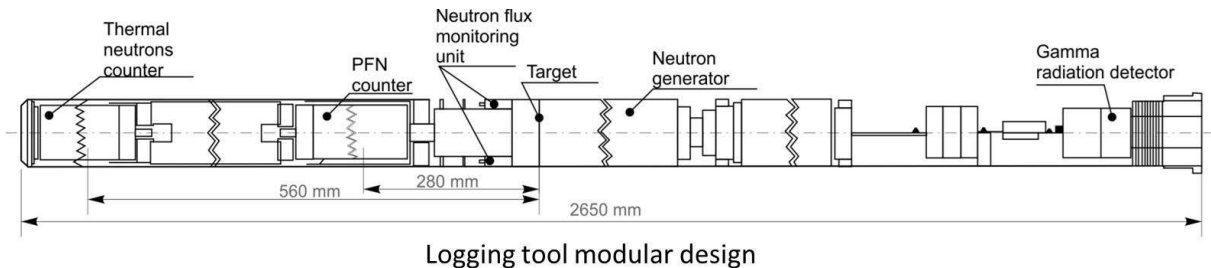
FIG. 7. PFN logging method.

The practice of using the PFN hardware system demonstrated that the application of the neutron flux detector often results in unacceptable errors in the determination of uranium grades due to inaccurate account of rock neutron properties.

A thermal neutrons detector was added to the AINK-49 logging tool to eliminate these errors. This detector implements Impulse Neutron-Neutron Logging (INNL) which records the density of thermal neutrons. INNL data contain information on neutron-absorption properties of the environment, hydrogen content (including moisture) and litho-geochemical characteristics of rock. Borehole logs lithological differentiation is performed based on average lifetime of  $\tau_n$  thermal neutrons.

Thus, the developed AINK-49 hardware system combining PFN logging and INNL not only allows improving the accuracy of determining uranium mass fraction owing to accurate account of moisture but also provides a possibility to assess the clayiness index of ore, i.e. to reliably and adequately define the rock which is impermeable for leaching solutions (sub-economic mineralisation).

The INNL unit was not the only successful solution in the AINK-49 design. There were some other technical challenges successfully resolved during its development (Fig. 8).



Neutron tubes with extended life

Neutron generator ING-12-50-100BT

*FIG. 8. Design.*

- Two configurations of neutron tubes developed with increased service life and neutron yield;
- New design of the neutron generator and neutron flux monitoring hardware developed.

AINK-49 basic specifications (Table I) suggest that as compared to its analogues the system has a range of advantages (Table II).

TABLE I. AMK KND-M BASIC TECHNICAL SPECIFICATIONS

|   |  |                        |
|---|--|------------------------|
| 1 | U mass fraction measurement range                    | 0.003 to 1.000%        |
| 2 | Pulse neutron generator average life time, hours     | 250 (min.)             |
| 3 | Neutron flux towards the end of life time, neutron/s | $1 \times 10^8$ (min.) |
| 4 | Logging tool outer diameter, mm                      | 49                     |
| 5 | Logging tool length, mm                              | 3000 (max.)            |
| 6 | Speed of logging, m/hr                               | 60 (min.)              |

TABLE II. AMK KND-M VS. ANALOGUES

| Company/<br>Institution              | Developer | Tool         | Pulse<br>neutron<br>generator<br>lifetime,<br>hours | Tool<br>diameter,<br>mm | Logging<br>speed, m hr | Definable<br>parameters                       |
|--------------------------------------|-----------|--------------|---|-------------------------|------------------------|---|
| Los Alamos<br>National<br>Laboratory | USA       | PFN          | 250   | 76                      | 30                     | U (PFN)                                       |
| VNII GIS                             | Russia    | KND-53       | 30  | 53                      | 30                     | U (PFN)<br>equiv-Ra (GL)                      |
| VNIIA                                | Russia    | AINK-60      | 30  | 60                      | 45                     | U (PFN)<br>equiv-Ra (GL)                      |
| VNIIA                                | Russia    | AMK<br>KND-M | 250   | 49                      | 60                     | U (PFN),<br>equiv-Ra (GL),<br>Moisture (INNL) |

These include:

- Fairly long operational life of the pulsed neutron generator (as against KND-53 and AINK-60);
- Relatively small diameter of the logging tool (as against PFN, AINK-60) and high speed of logging (compared to all the analogues);
- Higher reliability of uranium grade determination due to the account of ore neutron characteristics, especially moisture (as against PFN, KND-53, AINK-60).

In November 2013, AINK-49 pilot-scale tests were performed at uranium deposits in Russia and Kazakhstan. Figure 9 shows the comparison for the results of the standard set of logging (gamma-ray and resistivity logging) and AINK-49 (PFN channel and  $\tau_n$ ) for one of the holes characterized by a quite complex radiological setting.

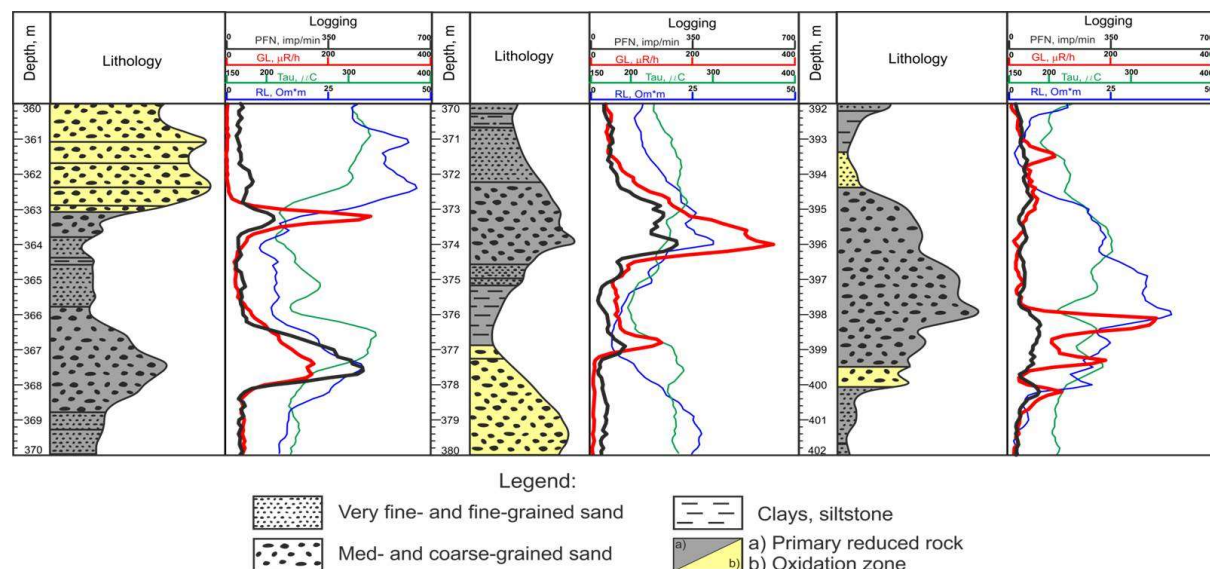


FIG. 9. Comparison between a standard set of GL and AINK-49 (PFN,  $\tau_n$ ).

The log for this hole demonstrates:

- Variations in disequilibrium both towards radium abundance and deficiency (the left side of the column);
- An area of the productive level with ore in equilibrium (the centre of the column);
- Practically uranium-barren radium anomalies (the right side of the column).

This comparison also demonstrates that thermal neutrons ( $\tau_n$ ) lifetime correlates well with the lithology of the rock sequence.  $T_n$  value within the intervals of impermeable rock (clay, siltstone) with a thickness of maximum 30–40 cm does not exceed 200  $\mu\text{s}$  on average. For permeable rock and ore, the value of this parameter varies within a range of 220–310  $\mu\text{s}$ .

Figure 10 shows the defined parameters of the mineralised interval of a hole as compared between GL, AINK-49 and core sampling. As you can see, the relative discrepancy between the metre-percent determined by AINK-49 and core sampling does not exceed 4%, whereas the discrepancy for GL is about 28%.

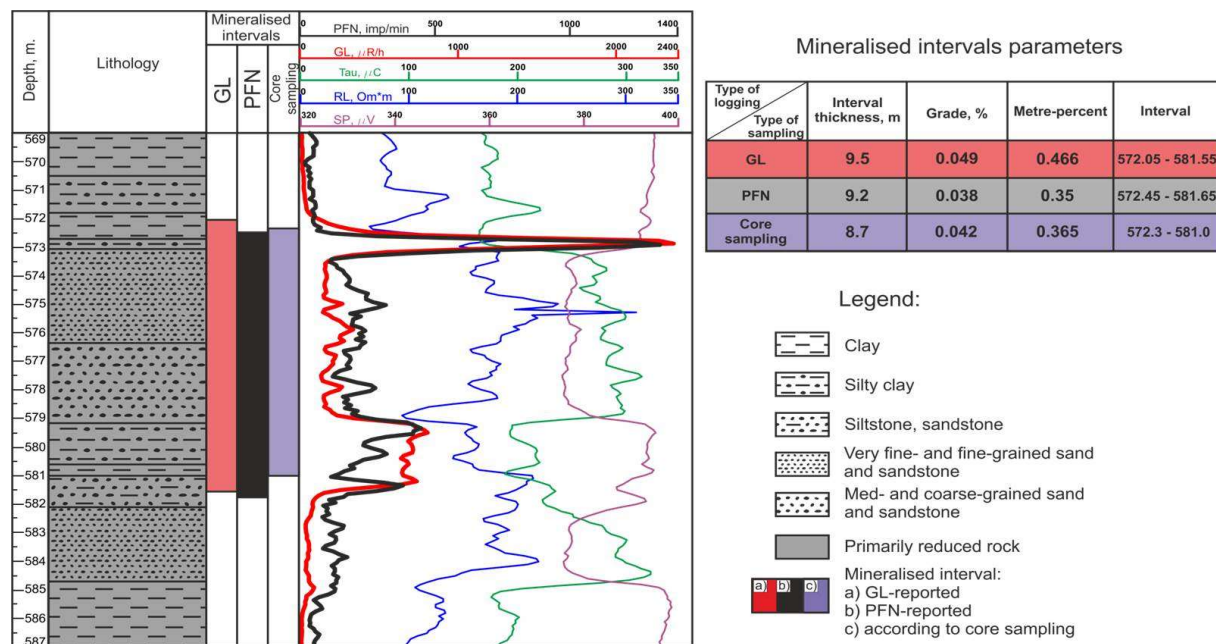


FIG. 10. GL and PFN data interpretation results vs core sampling.

It is obvious that AINK-49 hardware system provides reliable results to handle exploration issues in a complex radiological setting.

Considering the available experience in the application of neutron logging equipment in areas affected and modified by ISL and the PFN hardware system technical capabilities, we can distinguish other no less important and promising outlooks for its application in the existing ISL enterprises, such as:

- Monitoring of the leaching process and ongoing control of the applied ISL flowsheet effectiveness;
- Assessment of residual productivity in recovered areas to control uranium in-situ recovery;
- Identification and evaluation of technogenic uranium redeposition zones and production-induced morphological alteration of ore bodies to consider possible additional in-situ uranium recovery.

## BIBLIOGRAPHY

KHAIKOVITCH, I.M., MATS, N.A., GANICHEV, G.I., Metody yaderno-geofysicheskogo karotazha na mestorozhdeniyakh urana (research and practice edition), FGUNPP Geologorazvedka, St. Petersburg (2007). (in Russian).

MIRONOV, A.I., GANICHEV, G.I., MAKAROV, N.A., KHAIKOVICH, I.M., Instruktsiya po karotazhu metodom mgnovennykh neutronov deleniya pri izuchenii uranovykh mestorozhdeniy gidrogennogo tipa, Mingeo USSR, NPO Rudgeophysika, Moscow (1986). (in Russian)

POLYACHENKO, A.L., "O razvitiu karotazha na uran po mgnovennym neutronam deleniya: Protativnye generator neutronov I tekhnologii na ikh osnove", Proc. of the Scientific and Technical Int. Conf. (2012), VNIIA named after Dukhov N.L., Moscow (2012). (in Russian).

POLYACHENKO, A.L., POLYACHENKO, L.B., Abstracts of Papers. O povyshenii geologicheskoy informativnosti karotazha na uran po mgnovennym neutronam deleniya s dvukhzondovoy apparaturoy KND-M. Abstracts of the third international symposium Uran: geology, resources, production. Rosnedra Federeal Agency, Rosatom State Corporation, Rossiyskaya akademiya nauk, Moscow (2013). (in Russian).

SHIMELEVICH, YU.S., KANTOR, S.A., POLYACHENKO, A.L., Fizicheskiye osnovy impulsnykh neutronnykh metodov issledovaniya skvazhin, Izdatelstvo Nedra, Moscow (1976). (in Russian)

# PROSPECTS FOR INCREASING URANIUM RESOURCES IN THE KHIAGDA ORE FIELD, RUSSIAN FEDERATION

A.A. NOVGORODTSEV\*, V.G. MARTYNENKO\*,  
A.V. GLADYSHEV\*\*

\* Rusburmash Inc,  
Moscow

\*\* JSC Khiagda,  
Republic of Buryatia

Russian Federation

## Abstract

The Khiagda ore field uranium deposits are located in the Republic of Buryatia, Russian Federation. This paper discusses the prospects for increasing uranium resources at that site.

## 1. INTRODUCTION

The Khiagda ore field uranium deposits are located in the Republic of Buryatia, on the Amalat Plateau formed by Neogene basalts (Fig. 1). The slopes of the Baisykhon dividing uplift are incised by short (4 to 16 km) lateral tributaries of the Amalat and Atalanga palaeorivers. The palaeovalley network is filled with terrigenous-volcanogenic units of the Miocene Dzhilinda Formation (N1dz) buried under a thick cover of plateau basalts [1].

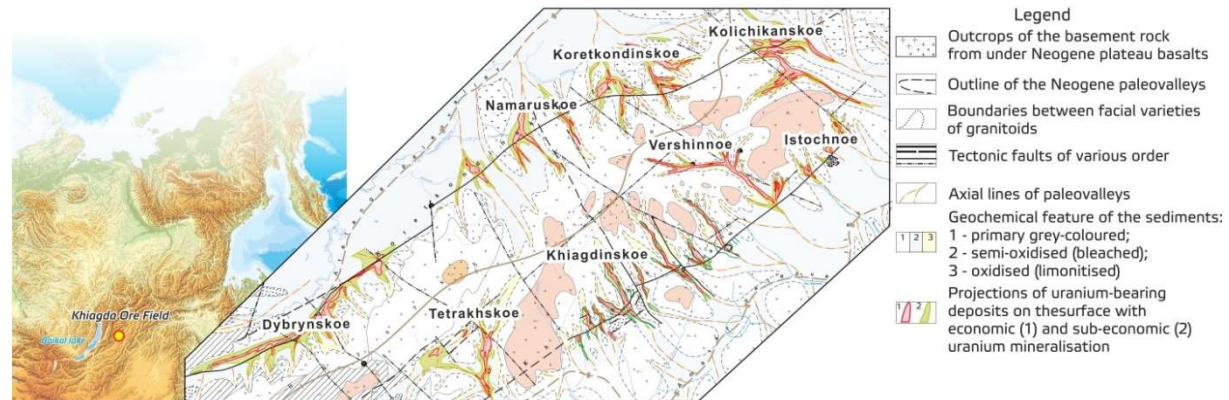


FIG. 1. Schematic geological map of the Khiagda ore field (based on the data by Rusburmash Inc).

The upheaval of the Baisykhon Uplift in the Neogene caused the penetration of the hydrodynamic flow of oxygenous uranium-bearing water into the sedimentary rock mass and formation of the subsoil/tabular oxidation zone (STOZ) on the boundary of which there formed uranium mineralisation (Fig. 2) [2].

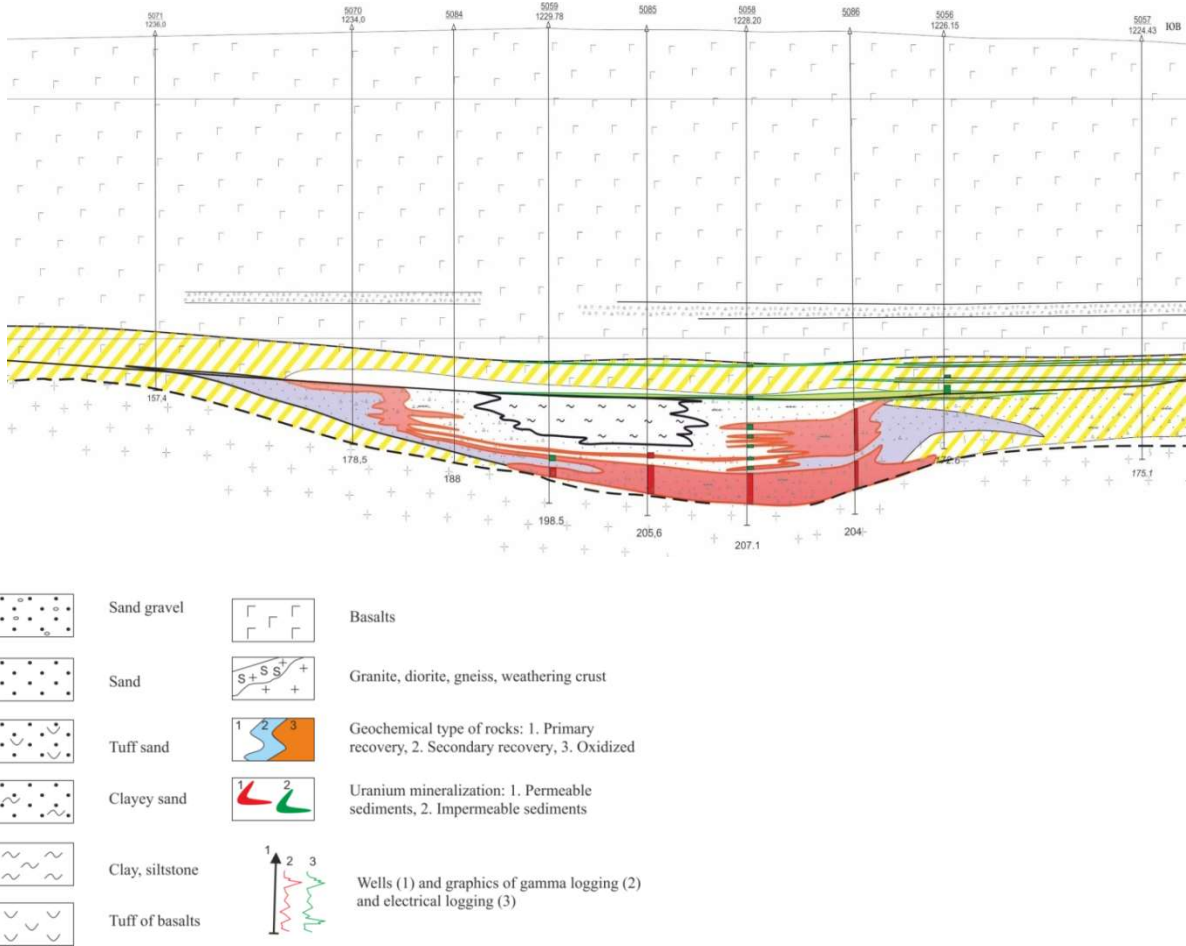


FIG. 2. The Kolichikanskoe deposit. Section along line No. 117.

## 2. RECENT INFORMATION AND INTERPRETATION

The new data obtained from geological exploration activities and mining of the ore field deposits allow for the following confident statements:

- The current position of the Khiagda field uranium mineralization is controlled by the STOZ pinching-out boundary (Fig. 3);
- The STOZ underwent partial gley reduction which is accompanied by the removal of soluble iron (Fig. 4) [3, 4];
- The development of the STOZ within the Khiagda ore field takes place from the Baisykh Uplift in the sides of the Atalanga and Amalat palaeovalleys. In plan view, it has a continuous complex bay-like morphology of the pinch-out;
- The oxidation zone and uranium mineralisation is developing in all permeable assemblages of rocks (Fig. 5) [5]:
- In the weathering crust of granites and in the disintegrated fractured portion of granites of the Palaeozoic basement [2];
- In the sedimentary, volcanogenic-sedimentary and volcanogenic deposits of the Neogene Dzhilinda Formation [2, 4];

- The STOZ pinching-out within the Khiagda ore field and associated uranium mineralisation have currently been studied in detail only in the basal portions of the sedimentary deposits of the Lower and Upper Members of the Lower Dzhilinda Formation. This has been done in the upper reaches of the revealed principal palaeotributaries of the Atalanga and Amalat stem palaeovalleys, within the areas of the STOZ pinching-out near the thalwegs of the palaeotributaries. No detail study of the pinching-out of the oxidation zone that retreats to the sides in the lower reaches of the palaeotributaries and the sides of the stem palaeovalleys or in the upper layers of sedimentary deposits has been performed. The pinching-out of the STOZ and associated mineralisation occurring in the volcanic-sedimentary deposits of the Dzhilinda Formation ( $n1dz2$ ) within the Khiagda ore field has been intersected by single lines of holes drilled in some of the deposits.

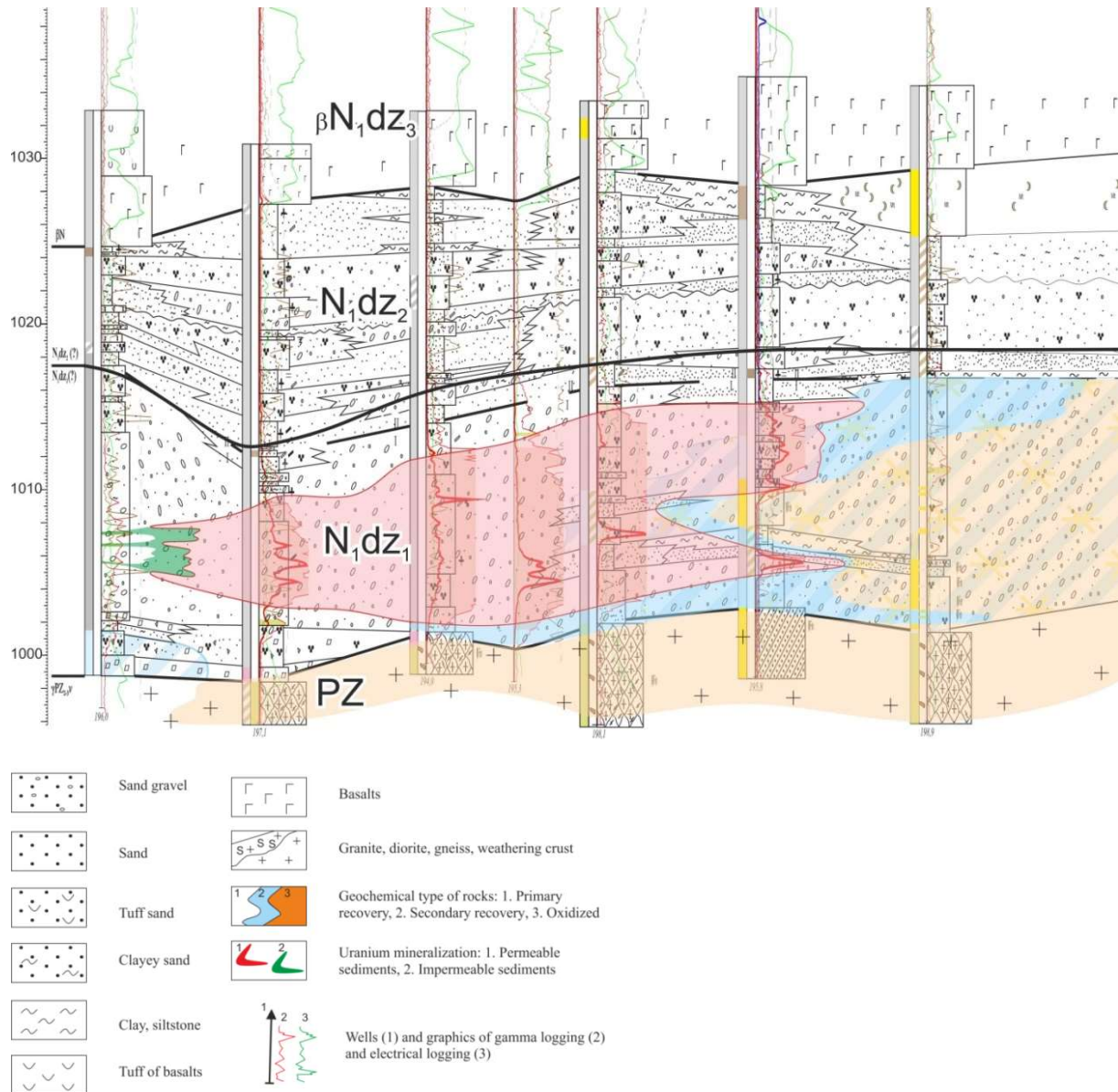


FIG. 3. The Dybrynskoe deposit. Section along line No. 850.

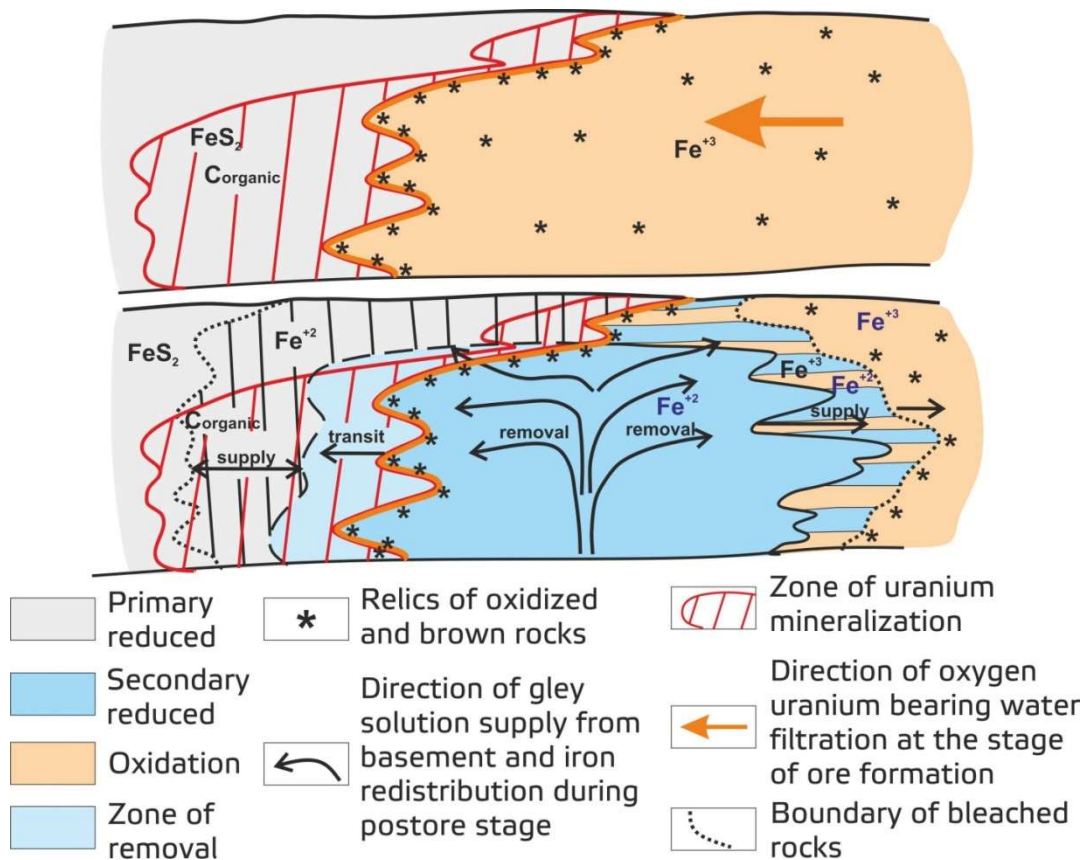


FIG. 48. Schematic cross section of formation of uranium mineralisation and post-ore redistribution of Fe within the Khiagda deposits.

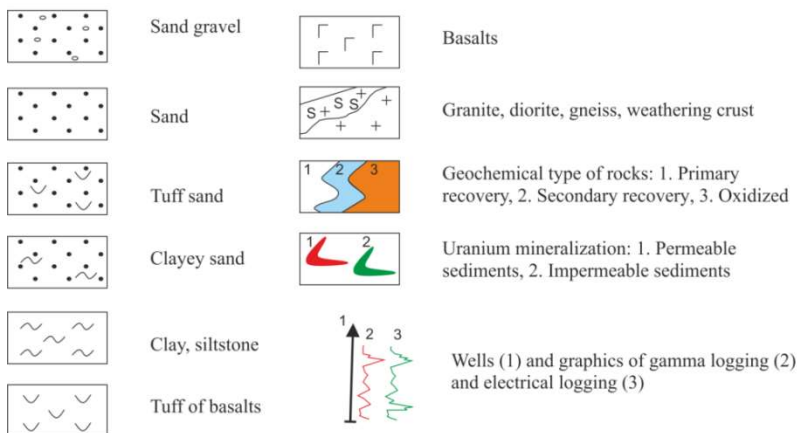
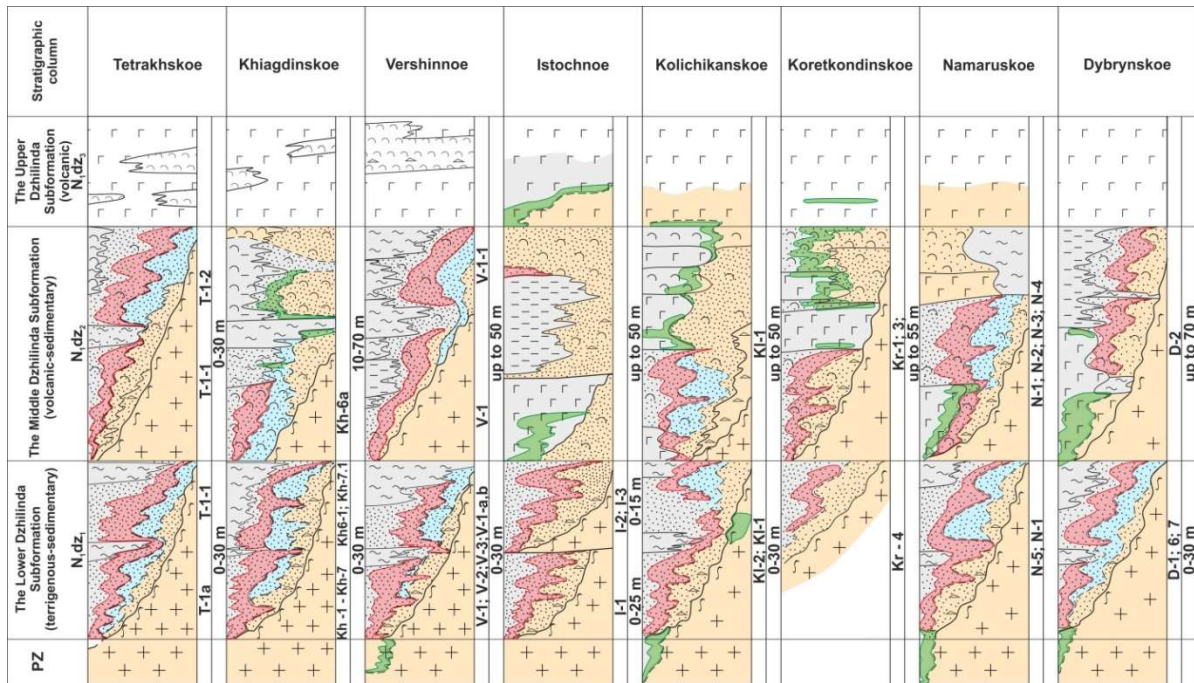


FIG. 5. A comparative schematic section of the Dzhilinda Formation of the Khiagda ore field.

The pinching-out of the STOZ and associated mineralisation occurring in the volcanic-sedimentary deposits of the Dzhilinda Formation (N1dz2) within the Khiagda ore field has been intersected by single lines of holes drilled in some of the deposits (Fig. 6).

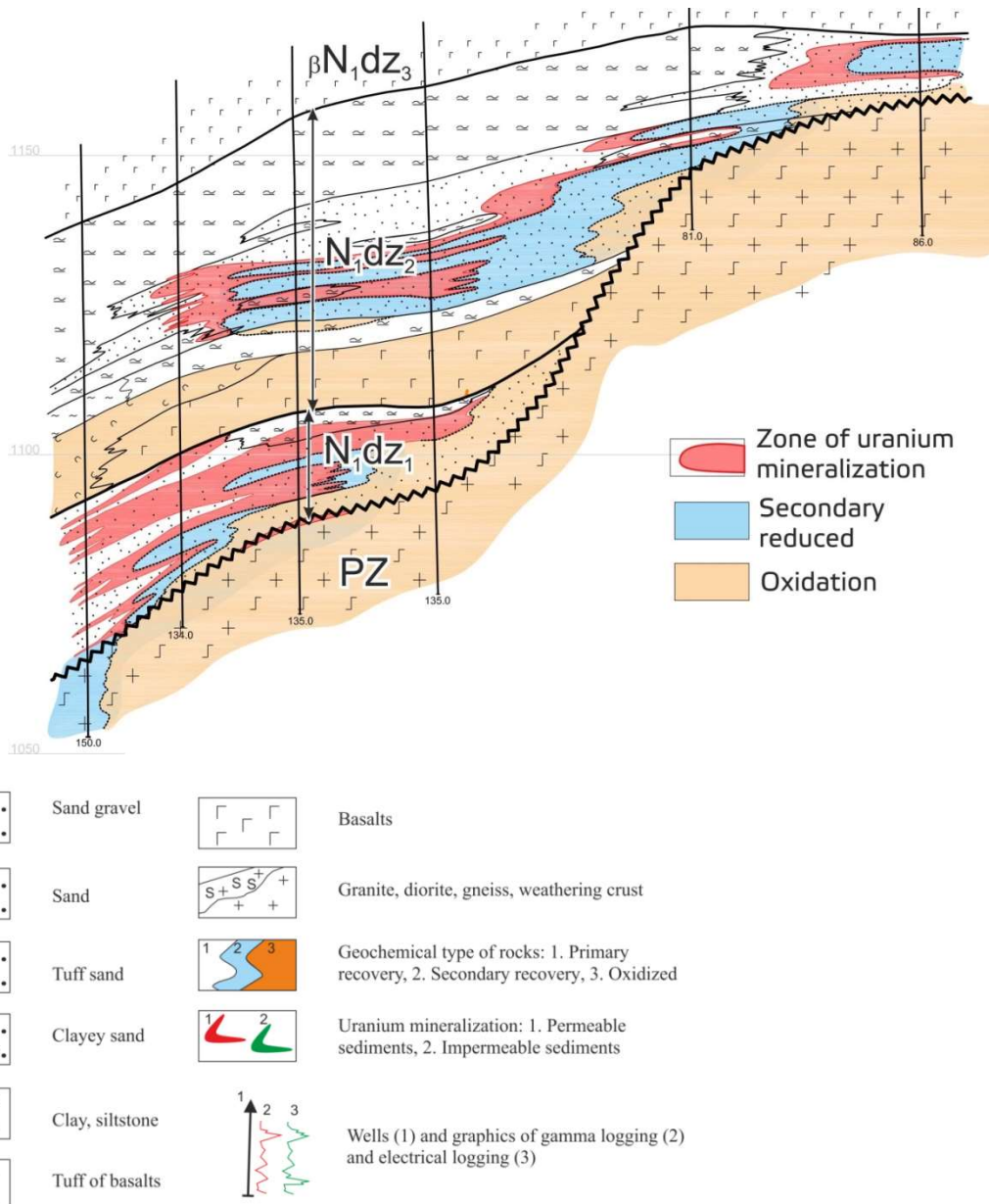


FIG. 6. The Dybrynskoe deposit. Section along line No. 164.

A focused study of this ore-bearing level within the area of the entire ore field will reveal multi-layer mineralisation associated with the pinching-out of the STOZ not only in the upper reaches of the palaeotributaries but also in the sides of the Amalat, Atalanga stem palaeovalleys (Fig. 7).

### Legend

The Lower Dzhilinda Fm oxidation zone pinchout boundaries and associated uranium mineralisation:

-  in the sedimentary subformation N<sub>1</sub>dz<sub>1</sub>
-  in the volcanogenic-sedimentary subformation N<sub>1</sub>dz<sub>2</sub>

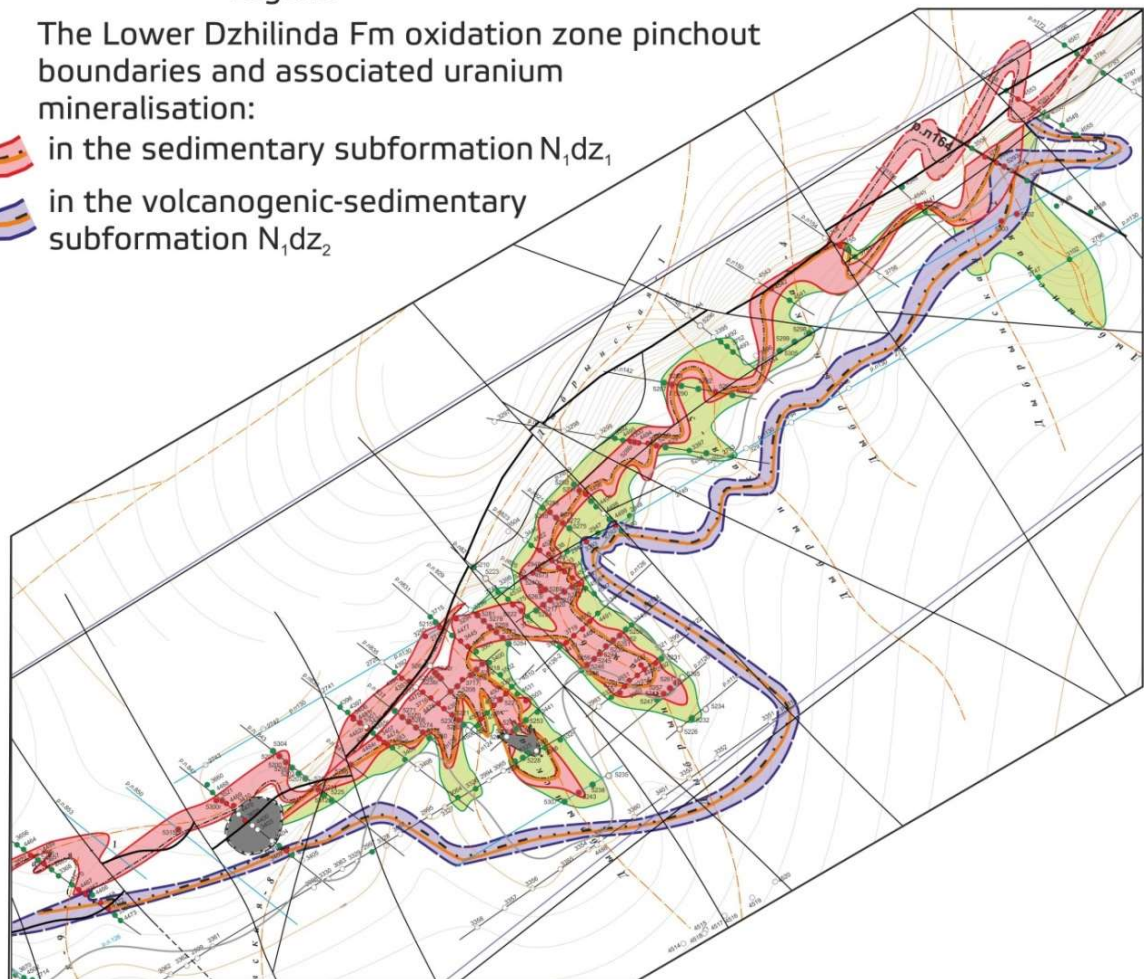


FIG. 7. The Dybrynskoe deposit. Uranium mineralization map.

A detailed study of these areas will allow a significant increase in uranium resources in the deposits most proximate to those explored and mined (Fig. 8) [2, 4, 6].

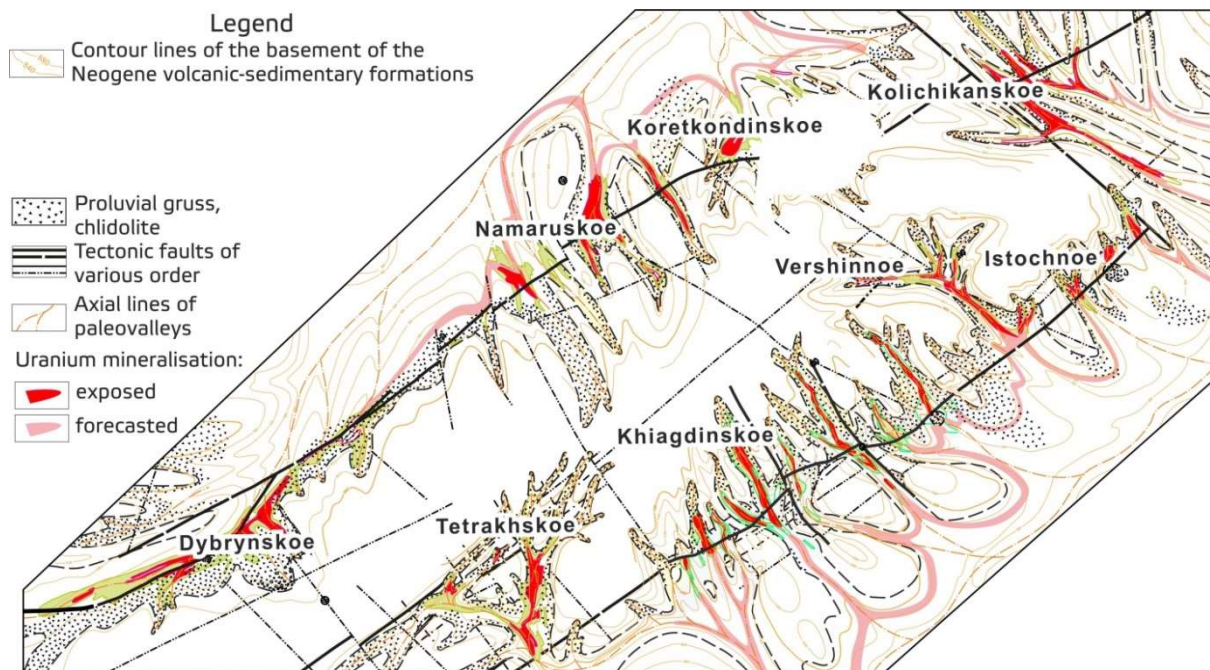


FIG. 8. Forecast map of uranium mineralisation of the lower Dzhilinda subformation.

## REFERENCES

- [1] MASHKOVTSOV, G.A., KONSTANTINOV, A.K., MIGUTA, A.K., SHUMILIN, M.V., SHCHETOCHKIN, V.N., Uran rossiyskih nedr, VIMS, Moscow (2010). (in Russian).
- [2] NOVGORODTSEV, A.A., MARTYNENKO, V.G., GLADYSHEV, A.V., Perspektivy uvelicheniya resursnogo potenciala Khiagdinskogo rudnogo polya, Uran: geologiya, resursy, proizvodstvo: Tezisy III mezhdunarod. Simpoziuma, Abstracts 3rd Internat. Symp. Uranium: Geology, Resources and Production, VIMS, Moscow (2013). (in Russian).
- [3] KOCHKIN, B.T., TARASOV, N.N., VELICHKIN, V.I., NESTEROVA, M.V., NOVGORODTSEV, A.A., SHULIK, L.S., Iron redistribution during postore stage at uranium deposits of the Khiagda ore field, Vitim District, Geol. Ore Deposits **56** 2 (2014) 113–127.
- [4] KOCHKIN, B.T., NOVGORODTSEV, A.A., TARASOV, N.N., MARTYNENKO, V.G., Morphology of orebodies and genesis of uranium deposits in the Khiagda ore field, Geol. Ore Deposits **56** 6 (2014) 479–492.
- [5] MAXIMOVA, M.F., SHMAROVICH, U.M., Plastovo-infiltratsionnoe rudoobrazovanie, Nedra, Moscow (1993). (in Russian).
- [6] KHALEZOV, A.B., Metodicheskie rekomendatsii. Prognozirovaniye, poiski I otsenka uranovykh mestorozhdeniy v paleoruslakh, Moscow (1999). (in Russian).

# USING HIGH TEMPERATURE REACTORS FOR ENERGY NEUTRAL MINERAL DEVELOPMENT PROCESSES, A PROPOSED IAEA COORDINATED RESEARCH PROJECT

N. HANEKLAUS<sup>\*†</sup>, F. REITSMA<sup>\*</sup>, H. TULSIDAS<sup>\*</sup>,  
B. TYOBEKA<sup>\*\*</sup>, E. SCHNUG<sup>\*\*\*</sup>, H.-J. ALLELEIN<sup>+</sup>,  
B. BIRKY<sup>++</sup>, P.F. PETERSON<sup>+++</sup>, G. DYCK<sup>\*</sup>, T. KOSHY<sup>\*</sup>

<sup>\*</sup> International Atomic Energy Agency,  
Vienna, Austria

<sup>\*\*</sup> National Nuclear Regulator,  
Centurion, Republic of South Africa

<sup>\*\*\*</sup> Technical University Braunschweig,  
Braunschweig, Germany

<sup>+</sup> Forschungszentrum Jülich/RWTH Aachen,  
Jülich, Germany/Aachen, Germany

<sup>++</sup> Florida Industrial and Phosphate Research Institute,  
Bartow, FL, United States of America

<sup>+++</sup> University of California,  
Berkeley, CA, United States of America

## Abstract

Today, uranium mined from various regions is the predominant reactor fuel of the present generation of Nuclear Power Plants (NPPs). The anticipated growth in nuclear energy may require introducing uranium and thorium from unconventional resources (e.g. phosphates, coal ash, sea water and rare earth ores) as a future fuel. In parallel, the demand for mineral commodities is growing and high-grade, easily extractable resources are being depleted. This shifts the global production to low-grade, or in certain cases unconventional mineral resources, the production of which is constrained by large-scale energy availability. Implemented and upcoming regulations dictate that the energy to develop these low-grade resources should be generated with reduced environmental footprint compared to present (mostly fossil fuelled) techniques. This paper introduces a Coordinated Research Project (CRP), bringing together mineral development and energy experts, aiming to understand how nuclear reactors, specifically High Temperature Reactors (HTRs), as a greenhouse-gas-lean energy source with little environmental footprint may be used to power energy-intensive mineral development processes. These minerals and processing technologies come with (phosphate rock-, copper-, gold-, rare earth ore) or without (aluminum-, titanium processing) the possibility to recover accompanying uranium or thorium that could be used to power the HTRs employed or other NPPs.

## 1. INTRODUCTION

The nuclear power industry expects significant growth in the future that will translate to additional nuclear fuel demand. The World Nuclear Association predicts a 48% increase in uranium demand from 2013–2023 [1]. The increasing demand may encourage exploitation of presently regarded unconventional uranium resources and alternative raw materials such as thorium. Both uranium and thorium can be found as accompanying impurities in several ores (e.g. phosphate, copper, gold, and rare earth ores [2]) that are processed on a large scale in various countries. With increasing demands for mineral commodities, low-grade resources, i.e. resources with a larger ratio of impurities or unwanted gangue materials, presently considered uneconomic to process, will have to be developed.

Processing lower grade mineral resources is associated with increasing energy requirements [3] and larger amounts of tailings. In contrast, environmental concerns (e.g. CO<sub>2</sub> emissions, water and land usage, waste treatment, etc.) are becoming more important in the mineral processing industry leading to planned or already imposed legislations regarding the use of cleaner energy sources as well as increased responsibilities to beneficiate/process tailings or waste materials (e.g. phosphate fertilizer producers in China will have to find a use for at least 25% of their main waste product phosphogypsum by 2025 [4]). Moreover, countries enforce or incent minimum standards of processing or refining raw materials before exporting them in order to keep the additional revenues (e.g. the government of Indonesia issued a regulation in January 2014 that bans the export of raw minerals that have not been domestically processed [5]).

The Nuclear Fuel Cycle and Materials Section of the Division of Nuclear Fuel Cycle and Waste Technology (NEFW) and the Nuclear Power Technology Development Section (NPTDS) of the Division of Nuclear Power (NENP) of the International Atomic Energy Agency (IAEA) are actively promoting research to examine whether or not HTRs are suitable to provide process heat and/or electricity to power mineral development processing. If recovered, the accompanying uranium/thorium could be used as nuclear reactor fuel for the greenhouse-gas-lean energy source employed or other NPPs. Figure 1 provides a brief schematic overview of the described system showing a High Temperature Gas-cooled Reactor (HTGR) as a representative HTR.

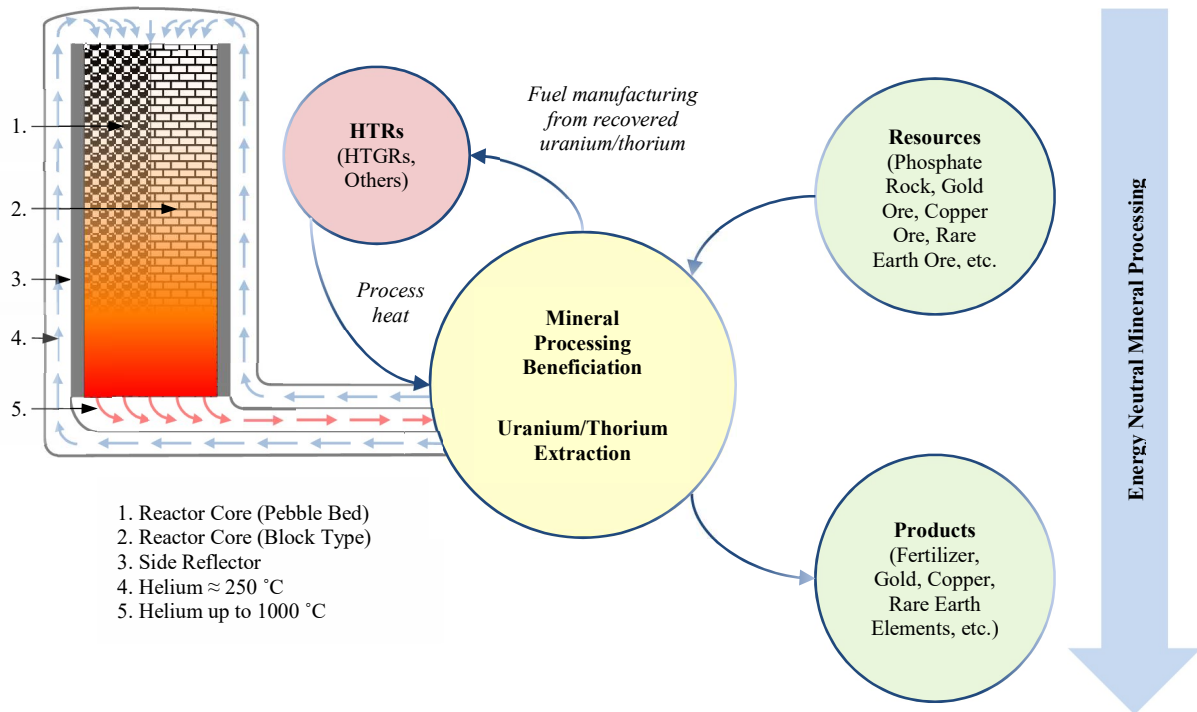


FIG. 1. Schematic overview of the envisaged coupled system.

Several HTGR designs with pebble bed or block type reactor core, using uranium and/or thorium as nuclear reactor fuel are available today (e.g. [6–8]) and could provide large amounts of reliable energy with little environmental footprint. Other HTR concepts such as the Fluoride-salt-cooled High-temperature Reactor (FHR) [9], the Compact High Temperature Reactor (CHTR) [10] or several fast reactor designs that reach the high outlet temperatures needed (minimum 600°C [11]) are presently under development and may be added to this list in the near future.

A new CRP: “Uranium — Thorium fuelled HTGR applications for energy neutral sustainable comprehensive extraction and mineral product development” — Code: T11006, jointly organized by

NEFW and NPTDS within the framework of the IAEA [12, 13] will conduct research and techno-economic feasibility studies on the combination of the following aspects: (1) the use of unconventional uranium (and thorium) resources as future nuclear reactor fuel; (2) the use of thermal processing to extract minerals and by-products in mining and mineral development processes; and (3) the study of the sustainability of these two processes, individually or combined with the utilization of HTRs as the electricity/process heat source. The CRP further intends to generate basic data on the availability and characteristics of such low-grade mineral resources and their impurities. Finally, the possibility of ‘energy neutral’ value addition in mineral development projects by using the recovered uranium/thorium as reactor fuel for the HTRs deployed to power the process as well as licensing such a coupled system will be evaluated.

## 2. PLANNED SCOPE OF THE COORDINATED RESEARCH PROJECT

### 2.1. Overview

The CRP is designed to be an interdisciplinary project in which experts from different fields can connect and interact with one another. In particular three different fields of research will be recognized: (1) Resources, raw materials and products; (2) mineral development processes; and (3) HTRs. It is believed that these fields influence one another (e.g. future/domestically available resources will determine the necessary beneficiation/processing techniques with different associated energy requirements to develop the ores) and may therefore not be regarded independently but in a comprehensive approach. Figure 2 indicates the interconnection of the different areas of research in the CRP.

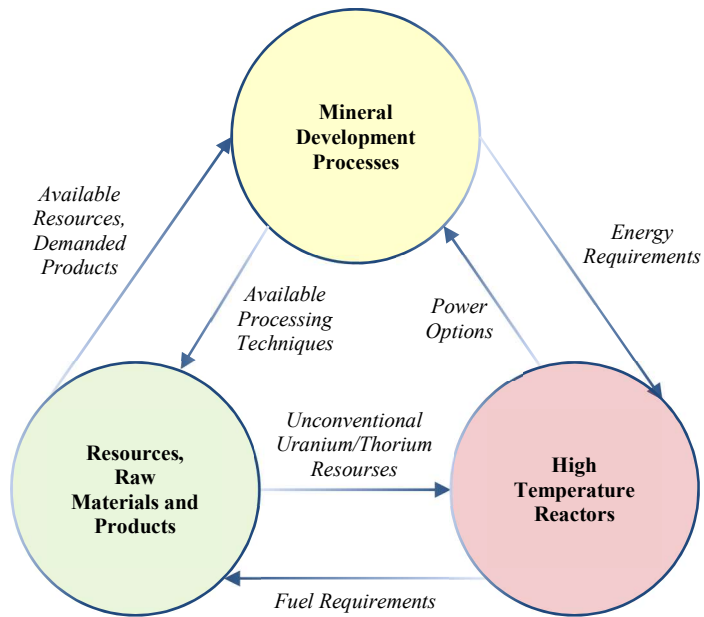


*FIG. 2: Interconnection between the research areas of the coordinated research project (CRP).*

### 2.2. Resources, raw materials and products

The CRP may differentiate between primary resources for mineral processing (e.g. phosphate rock, rare earth ores, etc.) and secondary resources to be used as unconventional raw materials for nuclear reactor fuel (uranium/thorium).

Basic data on available primary resources for present and future raw materials as well as products resulting from these raw materials will be analysed as part of the CRP. It is, for instance, foreseen to analyse available phosphate rock resources and their impurities (uranium/thorium but also others such as cadmium that may limit the ores usage as fertilizer raw material) in selected locations to determine the possibility for additional energy intensive beneficiation and/or thermal processing techniques that allow development of low-grade ores and production of higher purity end products.

Furthermore, the compositions of tailings and/or other mining waste will be analysed to determine whether or not treating these materials while recovering valuable impurities such as Rare Earth Elements (REE) can be technically and economically feasible, or is only desirable from an environmental and resource-conserving point of view.

### **2.3. Mineral development processes**

Although first estimates were conducted regarding phosphate rock processing [14], the CRP in accordance with the participating experts aims to consider various mineral development processes that may profit from using HTRs as a power source.

Various mineral development processes can, for instance, benefit from the use of so-called ‘thermal processing’. This is particularly beneficial for: (1) low-grade deposits that cannot be treated using the presently dominant chemical processing techniques; (2) the extraction of high-purity end products; and (3) the separation of high value or unwanted impurities (e.g. uranium, thorium, REE, etc.) that could be used/sold, and when extracted would result in cleaner final products. Compared to presently more economical chemical processing methods, the considerably lower waste products may make thermal processing attractive from an environmental point of view.

Experts from different mineral development processes shall provide detailed information on the energy requirements (including load variations, load availability and load reliability) of their respective processes so that HTR designers may develop suitable solutions to power the proposed processes. This analysis may include the amount of electricity and/or process heat, the type of carrier as well as the carriers technical characteristics such as average and maximum temperature, pressure, flow rate, etc. Detailed modelling, such as of required steam flows, is foreseen to understand whether or not HTRs are capable of powering certain mineral development processes.

In a similar way, other requirements that may comprise siting (on/off power grid, availability of cooling water, etc.), expected plant life time, acceptable tritium content in the final products, and more will be evaluated and discussed.

Furthermore, investigations regarding innovative processing techniques that are presently not considered due to economic or other reasons (e.g. limited availability of power at certain remote locations) but might become feasible if a HTR is employed (e.g. thermal processing of low-grade phosphate rock [15]) are foreseen in the CRP. This also includes investigations regarding innovative processing techniques of tailings or other waste material that is associated with the present and/or future processing techniques and could find new use as a raw material for different applications (e.g. processing of phosphogypsum in a combined phosphate fertilizer/sulphuric acid plant [16]).

### **2.4. High temperature reactors**

Developers of different HTR designs are encouraged to participate in the CRP. The IAEA aims to provide a platform where mineral development processing experts and HTR developers may connect and discuss mutual interests. In accordance with its statute [17] the IAEA supports a technology-neutral (i.e. independent of reactor technology) approach that will consider different HTR technologies and different HTR designs. First brief requirements that should be fulfilled by HTR developers can be found in [18].

### **3. DESIRED OUTCOME OF THE COORDINATED RESEARCH PROJECT**

Generally, the CRP aims to investigate whether or not mineral processing using HTRs, including ‘energy neutral’ fuel recovery, is technically and economically feasible. To do so the IAEA will facilitate technical interaction between mineral development processing experts and HTR developers and coordinate their joint research efforts. Specific case studies where both groups can study the same integrated system are encouraged. The case studies will take place under the umbrella of the IAEA CRP.

By the end of the four-year project the studies will be published in an IAEA technical document. The document will provide information and guidance to IAEA Member States interested in the technology and may illustrate technical and economical possibilities as well as limits of using HTRs for (“energy neutral”) mineral development processing.

It is assumed that Member States may contribute to selected areas of the CRP’s scope due to non-availability of expertise in all the technical areas. This is to be expected in a multi-disciplinary CRP where different expertise, typically not to be found in one organization, is required.

### **4. CONCLUSIONS**

In the future, we may need to extract nuclear fuel and minerals from the same unconventional resources to make nuclear fuel and low-grade ore processing feasible and cost-effective. These processes have a reduced environmental footprint only if greenhouse-gas-lean energy sources are applied for comprehensive extraction of all valuable commodities for the entire life of the project. Nuclear power, and specifically HTRs, is a promising technology that can produce the vast amounts of energy required for energy intensive mineral development processing reliably, at potentially low costs, with few emissions, and little land use compared to alternative power sources. Using HTRs is especially beneficial if enough uranium/thorium can be extracted from the primary ores to fuel the reactors used on site, or an equivalent or more amount in NPPs elsewhere.

Although promising, further investigations as part of this proposed IAEA CRP are required to judge whether or not using HTRs to power mineral development processing is technically and economically feasible.

### **ACKNOWLEDGEMENTS**

The authors would like to express their gratitude to those who have already submitted proposals to the IAEA. Any remaining errors, omissions, or inconsistencies are the authors’ alone.

### **REFERENCES**

- [1] WORLD NUCLEAR ASSOCIATION, Uranium Markets (2014) <http://www.world-nuclear.org/info/nuclear-fuel-cycle/uranium-resources/uranium-markets/>
- [2] GUPTA, C., SINGH, H., Uranium Resource Processing — Secondary Resources, Springer, (2003).
- [3] GUPTA C., Chemical Metallurgy — Principles and Practice, WILEY—VCH, Weinheim (2003).
- [4] ZHANG, P., Comprehensive Recovery & Sustainable Development of Phosphate Resources, Presentation to the Int. Symp. on Innovation and Technology in the Phosphate Industry (SYMPHOS 2013), Agadir, Morocco (2013).
- [5] SANTOSO, F.G., In Indonesia, Processing Minerals for Export now Mandatory (2014), <http://blog.ssek.com/index.php/2014/03/in-indonesia-processing-minerals-for-export-now-mandatory>.
- [6] INSTITUTE OF NUCLEAR AND NEW ENERGY TECHNOLOGY — TSINGHUA UNIVERSITY (2014), <http://www.inet.tsinghua.edu.cn/publish/inet/index.html>.

- [7] JAPANESE ATOMIC ENERGY AGENCY, High Temperature Engineering Test Reactor (2014), <http://httr.jaea.go.jp/index.html>.
- [8] STEENKAMPSKRAAL THORIUM LIMITED, Reactor Project, Th-100 (2014), <http://www.thorium100.com/>
- [9] UNIVERSITY OF CALIFORNIA, Fluoride-salt-cooled High-temperature Reactor research (2014), <http://fhr.nuc.berkeley.edu/>
- [10] DULERA, I.V., SINHA, R.K., Indian High Temperature Reactor Programme: An Overview, BARC Newsletter **315** (Sep.–Oct. 2010).
- [11] INTERNATIONAL ATOMIC ENERGY AGENCY, Status of Innovative Fast Reactor Designs and Concepts — A Supplement to the IAEA Advanced Reactor Information System (ARIS), IAEA, Vienna (2013).
- [12] INTERNATIONAL ATOMIC ENERGY AGENCY, Coordinated Research Activities — All CRPs open for proposals, IAEA, Vienna (2014), <http://cra.iaea.org/cra/explore-crps/all-opened-for-proposals.html>.
- [13] INTERNATIONAL ATOMIC ENERGY AGENCY, Nuclear Power Newsletter, News from the Division of Nuclear Power **11** 2 (2014) 9.
- [14] HANEKLAUS, N., SCHNUG, E., TULSIDAS, H., TYOBELKA, B., Using high temperature gas-cooled reactors for greenhouse gas reduction and energy neutral production of phosphate fertilizers, Annals of Nuclear Energy **75** (2015) 275–282.
- [15] HANEKLAUS, N., SCHNUG, E., TULSIDAS, H., REITSMA, F., “Using high temperature gas-cooled reactors for low grade phosphate rock processing”, Proc. SPS 2014, Montpellier, France (2014).
- [16] HANEKLAUS, N., SCHNUG, E., TULSIDAS, H., REITSMA, F., “Using high temperature reactors for energy neutral phosphate fertilizer and phosphogypsum processing, Uranium-Past and Future Challenges” (Proc. International Conference 2014: Uranium Mining and Hydrogeology VII, Freiberg, Saxony, Germany, 21–25 September 2014) (MERKEL, B.J., ARAB, A., Eds), Springer (2015) 785–792.
- [17] INTERNATIONAL ATOMIC ENERGY AGENCY, The Statute of the IAEA, IAEA, Vienna (1956), <http://www.iaea.org/About/statute.html>.
- [18] HANEKLAUS, N., REITSMA, F., TULSIDAS, H., “High temperature reactors for a proposed IAEA coordinated research project on energy neutral mineral development processes” (*submitted*), Proc. of HTR 2014, Weihai, China (2014).

# **RESEARCH ON URANIUM AND THORIUM ELEMENTS EXPLORATION THROUGH THE STUDY OF PETROGRAPHY, PETROLOGY AND GEOPHYSICAL METHOD IN SAGHAND AREA (CENTRAL IRAN) ISLAMIC REPUBLIC OF IRAN**

J. IRANMANESH, V. FATTABI, S. RAZIANI

Atomic Energy Organization of Iran,  
Tehran, Islamic Republic of Iran

## **Abstract**

This study is a research on uranium and thorium exploration by use of the petrography, petrology and radiometric data in the Saghand area, Central Iran plateau. The lithologies of this area comprise of granite and metasomatized granite. As a result of metasomatic process, uranium and thorium bearing minerals such as davidite and alanite were formed. Sericitization and albitization are the main alterations detected in the study area and thorium mineralization is more common in albitization. By investigation of the chemical classification, non-radioactive specimens, rock types include: diorite and granodiorite, while radioactive specimens consist of gabbroic rocks (basalt). According to the magma source graphs, these rocks formed by calc-alkaline series magma. A scintillometer and spectrometer (MGS-150) were used for radiometric data acquisition. 1001 data points have been obtained from 11 profiles and total counts for, K, U, and Th were measured. After primary data processing, data logarithms were calculated for normalizing, and the radiometric data show that uranium and thorium enrichment is more than potassium, while thorium and uranium enrichment are approximately equal. After data integration, two probable anomalies were determined in northwest and northeast parts of the study area.

## **1. INTRODUCTION**

Consumption of thorium in non-energy applications occurs mainly in chemical catalysts, lighting, and welding electrodes. Worldwide thorium consumption is very small and is estimated at a few hundred tonnes annually. The production of thorium from rare earth bearing minerals continues to create an oversupply of thorium. Because of the cost of disposal of thorium bearing products, non-radioactive substitutes are being developed, resulting in depressed demand for thorium [1].

Thorium can be used as a nuclear fuel, through breeding to  $^{233}\text{U}$ . Several reactor concepts based on thorium fuel cycles are under consideration, but much development work is still required before the thorium fuel cycles can be commercialized [2].

## **2. GEOLOGY OF THE STUDY AREA**

The study area is located in Yazd state, central Iran plateau. Oldest lithological units in this area include metamorphic rocks such as gneisses, mica schist, amphibolites and migmatites, which form Iranian metamorphic bedrocks of Precambrian age. The youngest rocks in this area are Zarigan granites. Older lithological units are affected by Precambrian metamorphism. The intrusion of the Zarigan granite affected all of the rocks in the study area. The final phase of Zarigan granite leads to albitization in the area. Because of the metasomatism in the area we can see amphibolization in the granitic rocks which are placed adjacent to the radioactive anomalies.

## **3. PETROGRAPHY AND MINERALOGY**

During the field work we choose 16 samples from radioactive and non-radioactive areas for petrography and mineralogical studies. After preparing the thin sections they were examined by microscope. In Figure 1, the rock is metasomatised granite with granular texture. Amphibole minerals are tremolite and actinolite. Carbonate minerals and other minerals like sphene are formed in fractions as viens.

In Figs 2–7 albites have a coarse grain to amorphous texture and are mostly altered. Carbonate minerals are less and are formed in fractions as veins. Chlorite minerals are more and are formed in the fractions.

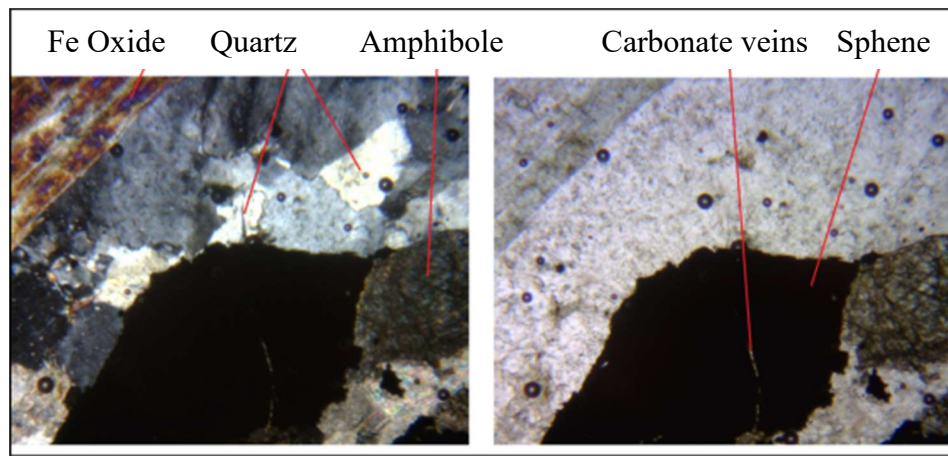


FIG. 1. Thin section of radioactive sample RS-LA-2 magnification  $50\times$  ppl and cpl<sup>29</sup>.

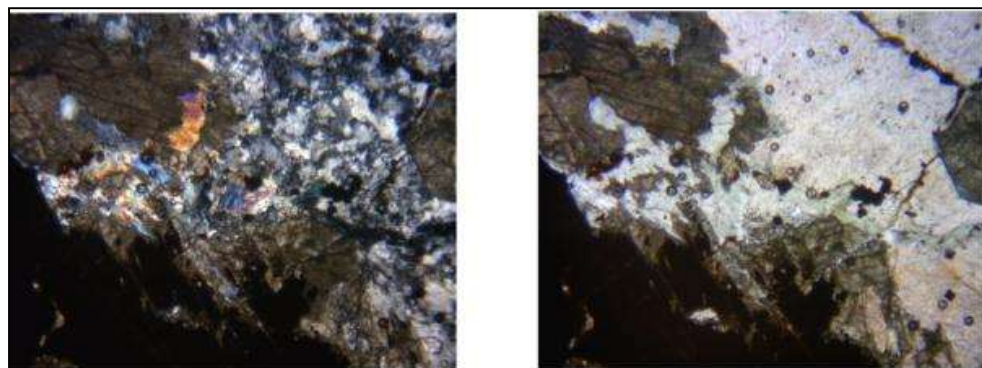


FIG. 2. Thin section of radioactive RS-LA-4, magnification  $50\times$  ppl and cpl.

<sup>29</sup> Plain polarized light, ppl and crossed polarized light, clp.

Alanite, biotite and phlogopite are shown in Figs 3–5.

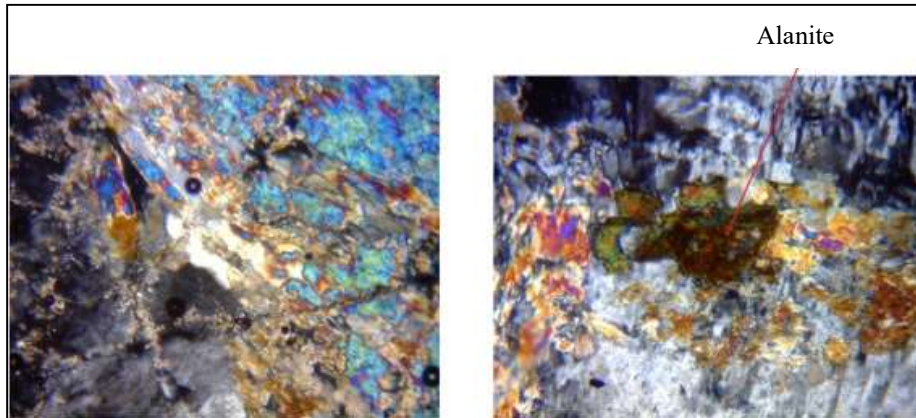


FIG. 3. Section of radioactive sample RS-LA-6, magnification  $100 \times$  both of the pictures are in cpl light but in the right picture the extinction of the alanite is shown.

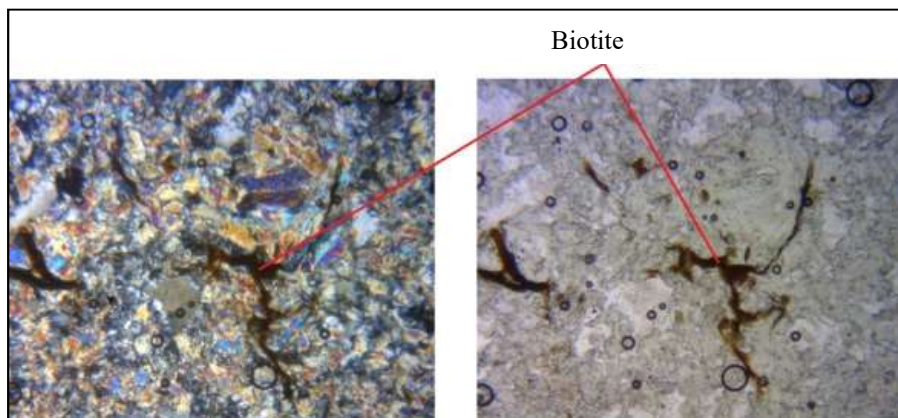
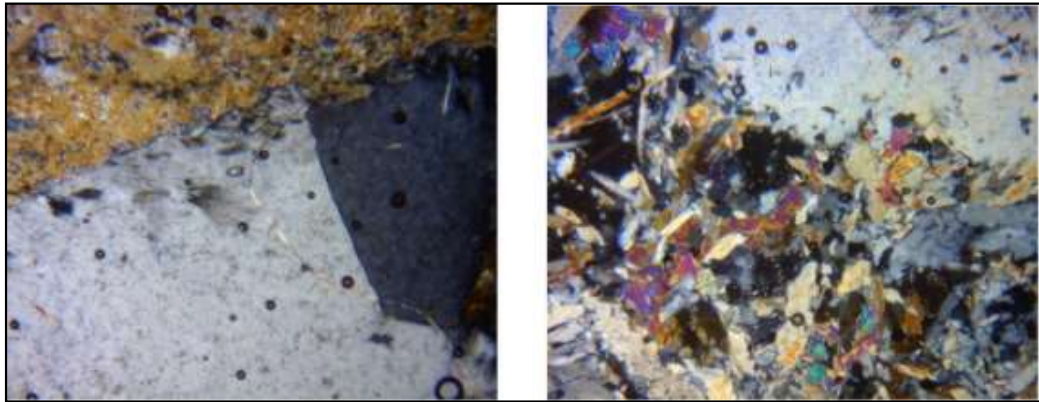


FIG. 4. Thin section of non-radioactive sample RS-L-4 with  $50\times$  magnification ppl and cpl.



FIG. 5. Thin section of non-radioactive sample RS-L-9 magnification  $50 \times$  cpl light.

There are two pictures of granite thin section, one of them radioactive with granular texture and coarse grain and the other is non-radioactive sample with fine grain granite texture (Fig. 6).



*FIG. 6. Left picture regards to radioactive sample RS-LA-1 in the ppl and magnification 50×, right picture regards to non-radioactive sample RS-L-1 cpl and magnification 50×.*

#### 4. RADIOMETRY

Data readings were taken at 11 profiles, then 91 data from each profile. The total data read is 1001 scintillometer and spectrometer readings concurrently measured. The statistical properties of the data are presented in TABLE I.

TABLE I. STATISTICAL INFORMATION TAKEN FROM RADIOMETRIC DATA

| Reading num.             | cps   | TC (ePPM) | K (%)  | U (ePPM) | Th (ePPM) |
|--------------------------|-------|-----------|--------|----------|-----------|
| Number of values         | 1001  | 1001      | 1001   | 1001     | 1001      |
| Number of missing values | 0     | 0         | 0      | 0        | 0         |
| Minimum                  | 40    | 2         | 0.0003 | 4.098    | 1.306     |
| Maximum                  | 6000  | 471.6     | 30.02  | 162.7    | 452.3     |
| Mean                     | 127   | 23.24     | 1.03   | 14.97    | 11.56     |
| Median                   | 80    | 19.17     | 0.0696 | 13.18    | 8.614     |
| First quartile           | 80    | 16.32     | 0.0356 | 8.521    | 6.345     |
| Third quartile           | 100   | 21        | 0.109  | 15.68    | 12.04     |
| Standard deviation       | 339   | 27.82     | 4.18   | 14.22    | 18.72     |
| Skew                     | 14.09 | 10.40     | 4.925  | 6.067    | 15.3      |
| Kurtosis                 | 224.5 | 136.1     | 24.39  | 46.48    | 321.9     |

In addition, data relating to a number of hot spots are presented in Table II.

TABLE II. RECORDED DATA OF HOT-SPOT SAMPLES  $\geq$  1000 CPS

| Reading num. | cps  | TC (ePPM) | K (%)   | U (ePPM) | Th (ePPM) |
|--------------|------|-----------|---------|----------|-----------|
| 89.RS.0742   | 6000 | 441.3     | 3.132   | 95.97    | 59.50     |
| 89.RS.0744   | 6000 | 471.6     | 19.70   | 99.69    | 452.3     |
| 89.RS.0653   | 5000 | 274.3     | 0.0853  | 144.9    | 97.55     |
| 89.RS.0975   | 2500 | 241.7     | 4.773   | 160.2    | 120.1     |
| 89.RS.0956   | 1700 | 249.5     | 6.397   | 162.7    | 106.6     |
| 89.RS.0557   | 1500 | 165.03    | 0.02303 | 108.737  | 80.41     |
| 89.RS.0871   | 1500 | 103.08    | 0.0931  | 48.2425  | 137.4     |
| 89.RS.0986   | 1100 | 60.6      | 0.1845  | 41.2795  | 42.871    |
| 89.RS.0494   | 1000 | 93.51     | 0.0009  | 122.998  | 7.589     |
| 89.RS.0901   | 1000 | 209.67    | 2.3559  | 139.111  | 139.282   |
| 89.RS.0905   | 1000 | 141.9     | 2.6855  | 103.215  | 68.484    |

Before mapping the contour, it helps to have information on the correlation of the variables. Therefore, linear regression lines fitted to the data can be analysed via a ‘scatter plot’. Figs 7 and 8 present the correlations of relevant variables. As can be seen in Fig. 7, the slope of the linear regression equation between uranium and thorium is close to a value of one (with some outliers). This means that the concentration of uranium and thorium are virtually identical in many cases. Therefore, it is not unexpected that the contours plotted for these two variables almost overlap (Fig. 10). Furthermore, as seen in Fig. 8, the amount of uranium and thorium in most cases several times the amount of potassium. Based on population isolated using Surfer and ArcGIS software and a kriging interpolation method, contour maps of the variables cps, uranium, thorium and potassium are obtained (Fig. 9).

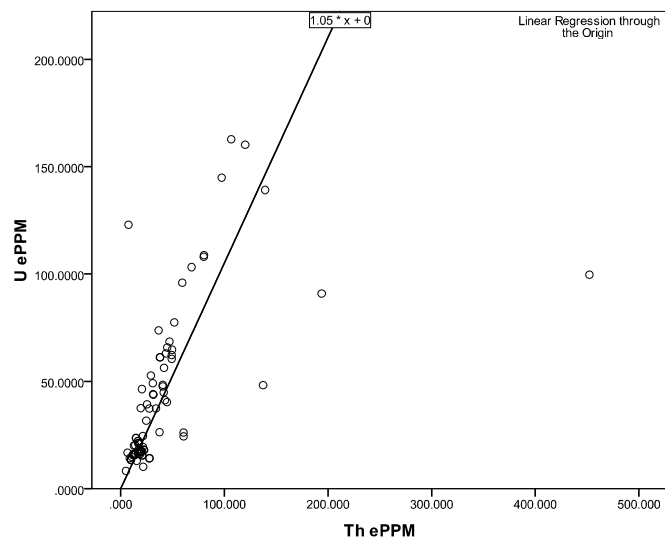
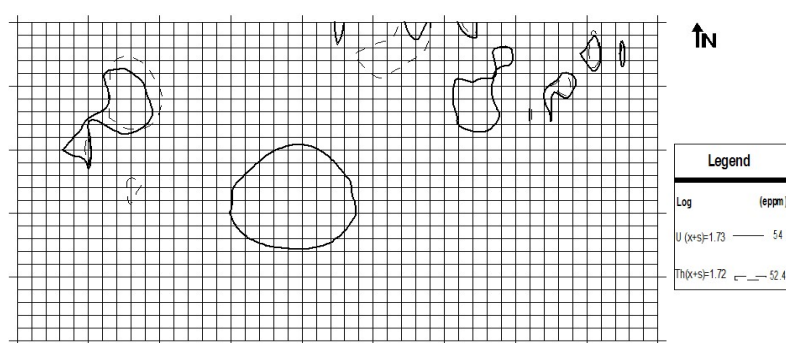
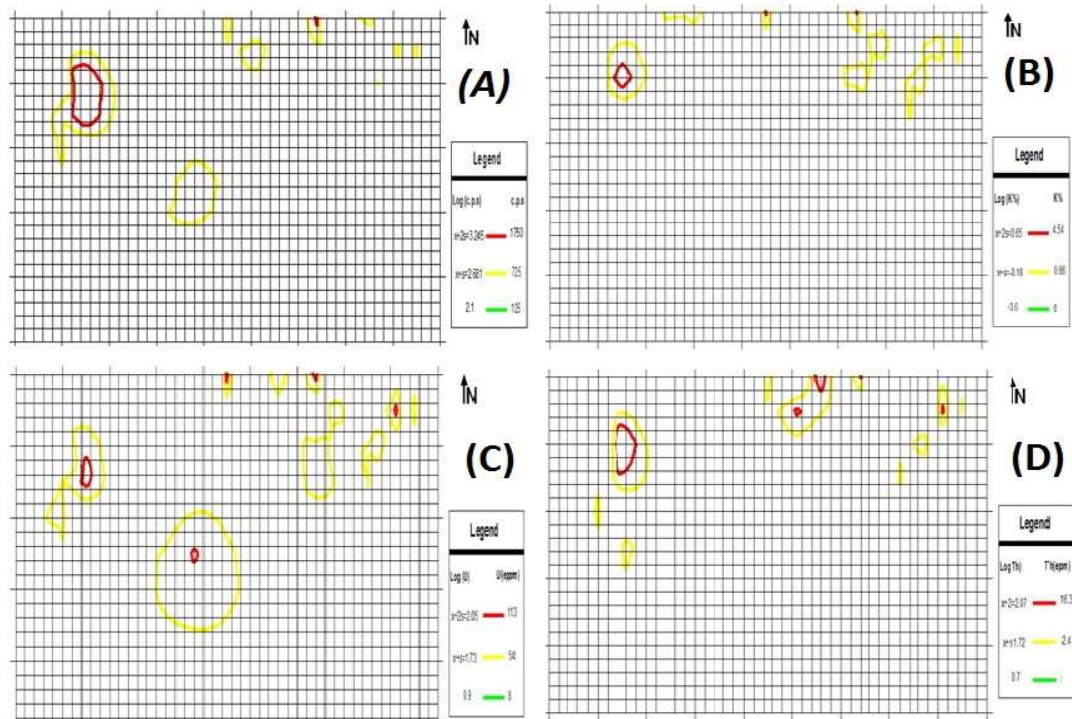
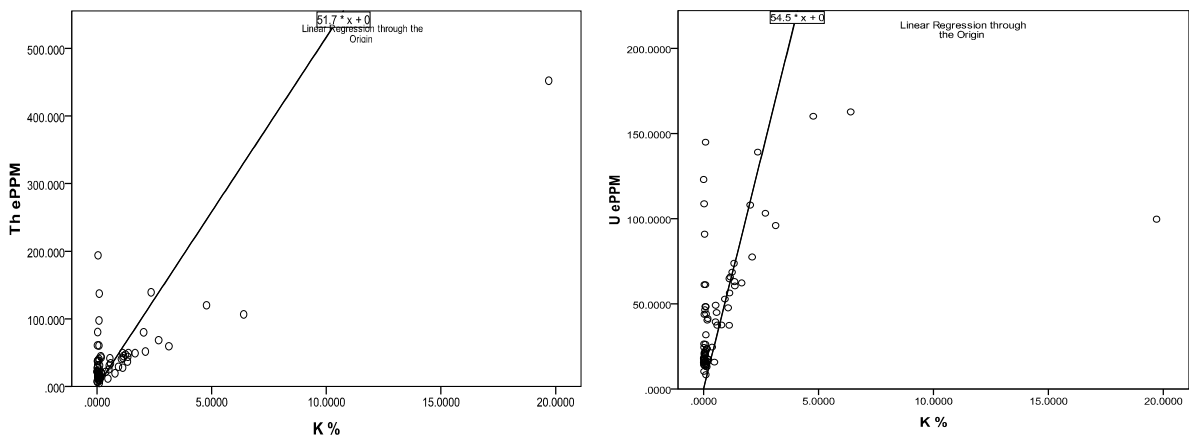


FIG. 7. Correlations between variables uranium and thorium.



As can be seen in the northwest corner and the northern limit concentration of radioactive sites have been studied. The focus of the centre is routinely observed in most of the trenches dug in the side of the road is a hill.

## 5. CHEMICAL CLASSIFICATION

There are two graphs for chemical classification of plutonic rocks. One of them is introduced by Cox et.al [3] and Middlemost [4]. After ground radiometric, 47 litho-geochemical samples were chosen to be analysed by XRF. After analysing the samples, the results of this analysis were plotted on the Cox and Middlemost graphs by the use of GCD software (Fig. 11).

Fig. 11 (A) shows that rock types of these 47 samples are almost diorite and granodiorite. Regards to the mineralogy rock type of high radioactivity areas are almost gabbro, produced by metasomatism processing on the granodiorite and diorites.

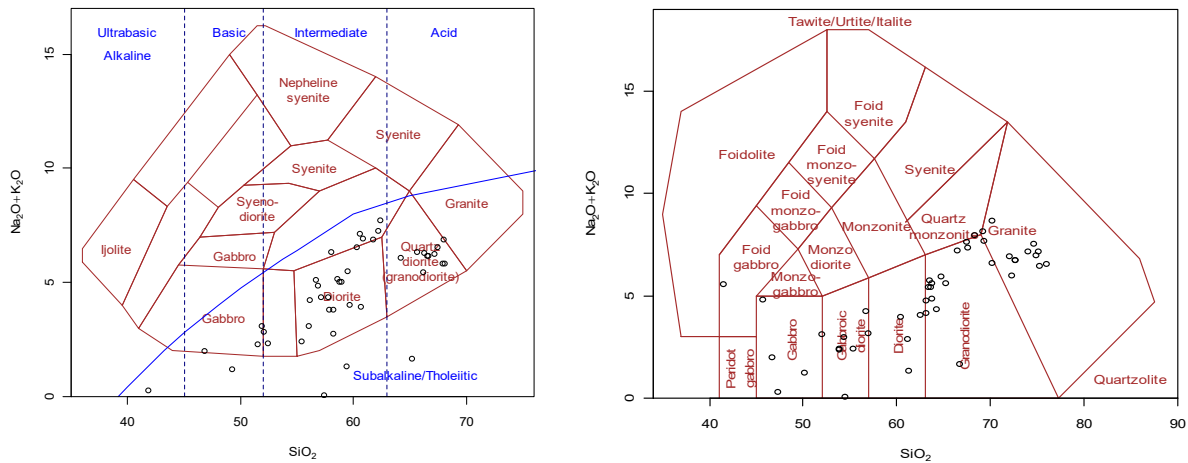


FIG. 11. A) Plotted samples on a Cox graph [3]; B) on a Middlemost graph [4].

## 6. MAGMA SERIES

One of common graphs for magma source identifying is AFM triangle graph, where A =  $\text{Na}_2\text{O} + \text{K}_2\text{O}$ , F =  $\text{FeO} + \text{Fe}_2\text{O}_3$  and M =  $\text{MgO}$ . The boundary of tholeiite series and calc-alkaline series are detected by several authors, but that of Irvine and Baragar [5] is more common. The 47 analysed samples are plotted on an AFM graph in Fig. 12 and show that the magma source for the most of samples are calc-alkaline and some of them are from the tholeiite series source, i.e. the magma has two sources.

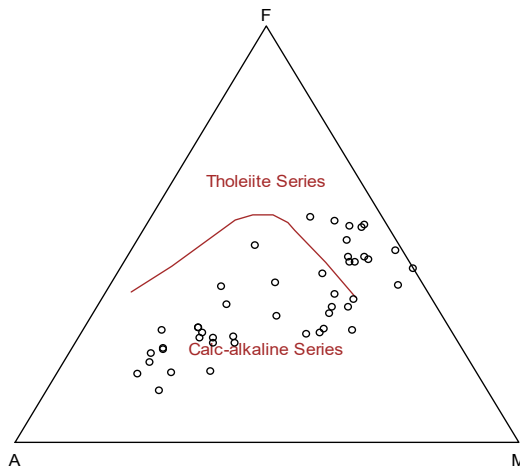


FIG. 12. Plotted samples on the AFM graph (after [5]).

Tholeiite magmas will make basalt, dolerite, diabase and ultramafics [6]. In the other side calc-alkaline series will make (gabbro-basalt, diorite-andesite, monzonite-latite, tonalite- dacite, granodiorite-rhyodacite and granite-rhyolite).

Results of the chemical classification and AFM graph are combined and showed in the TABLE III. According to TABLE III radioactive samples are gabbro (and its volcanic pair basalt) and their magma is from calc-alkaline series which are coloured yellow in the table.

TABLE III. ROCK TYPE AND MAGMA SERIES OF LITHO-GEOCHEMICAL SAMPLES

| Sample | SiO <sub>2</sub> | Na <sub>2</sub> O | K <sub>2</sub> O | CPS   | Middlemost.plut    | AFM                  |
|--------|------------------|-------------------|------------------|-------|--------------------|----------------------|
| RS.01  | 66.649           | 5.892             | 0.251            | 100   | 'granite'          | calc-alkaline series |
| RS.02  | 66.551           | 5.91              | 0.2249           | 200   | 'granite'          | calc-alkaline series |
| RS.03  | 59.503           | 5.316             | 0.136            | 150   | 'granodiorite'     | calc-alkaline series |
| RS.04  | 67.919           | 5.73              | 0.096            | 150   | 'granite'          | calc-alkaline series |
| RS.05  | 52.491           | 0.866             | 1.463            | 2000  | 'gabbroic diorite' | tholeiite series     |
| RS.06  | 60.879           | 6.649             | 0.237            | 150   | 'granodiorite'     | calc-alkaline series |
| RS.07  | 62.228           | 6.666             | 0.574            | 150   | 'granite'          | calc-alkaline series |
| RS.08  | 66.201           | 5.271             | 0.17             | 170   | 'granite'          | calc-alkaline series |
| RS.09  | 68.02            | 6.78              | 0.076            | 180   | 'granite'          | calc-alkaline series |
| RS.10  | 46.865           | 1.605             | 0.37             | 1600  | 'gabbro'           | tholeiite series     |
| RS.11  | 57.49            | 0.009             | 0.021            | 350   | 'diorite'          | tholeiite series     |
| RS.12  | 58.112           | 0.102             | 0.166            | 900   | 'diorite'          | tholeiite series     |
| RS.13  | 90.829           | 10.13             | 1.9506           | 12000 | 'foid gabbro'      | calc-alkaline series |
| RS.14  | 65.695           | 6.184             | 0.119            | 180   | 'granite'          | calc-alkaline series |
| RS.15  | 51.593           | 2.164             | 0.097            | 130   | 'gabbroic diorite' | tholeiite series     |
| RS.16  | 56.921           | 4.43              | 0.425            | 120   | 'granodiorite'     | calc-alkaline series |
| RS.17  | 60.309           | 5.888             | 0.648            | 120   | 'granodiorite'     | calc-alkaline series |
| RS.18  | 41.867           | 0.19              | 0.06             | 110   | 'gabbro'           | tholeiite series     |
| RS.19  | 56.221           | 3.942             | 0.262            | 160   | 'diorite'          | tholeiite series     |
| RS.20  | 59.394           | 1.124             | 0.156            | 170   | 'granodiorite'     | tholeiite series     |
| RS.21  | 61.816           | 6.732             | 0.113            | 120   | 'granite'          | calc-alkaline series |
| RS.22  | 62.4             | 7.604             | 0.087            | 180   | 'granite'          | calc-alkaline series |
| RS.23  | 51.897           | 2.823             | 0.266            | 5000  | 'gabbroic diorite' | tholeiite series     |
| RS.24  | 67.238           | 6.151             | 0.08             | 140   | 'granite'          | calc-alkaline series |
| RS.25  | 66.321           | 6.222             | 0.066            | 180   | 'granite'          | calc-alkaline series |
| RS.26  | 58.603           | 4.67              | 0.46             | 120   | 'granodiorite'     | calc-alkaline series |
| RS.27  | 57.22            | 4.07              | 0.27             | 110   | 'granodiorite'     | calc-alkaline series |
| RS.28  | 59.687           | 3.913             | 0.101            | 110   | 'granodiorite'     | calc-alkaline series |
| RS.29  | 64.21            | 5.962             | 0.079            | 120   | 'granite'          | calc-alkaline series |
| RS.30  | 67.507           | 6.409             | 0.101            | 120   | 'granite'          | calc-alkaline series |
| RS.31  | 58.796           | 4.852             | 0.169            | 160   | 'granodiorite'     | calc-alkaline series |
| RS.32  | 58.257           | 2.592             | 0.127            | 130   | 'granodiorite'     | tholeiite series     |
| RS.33  | 57.91            | 3.637             | 0.144            | 140   | 'granodiorite'     | calc-alkaline series |
| RS.34  | 58.252           | 3.439             | 0.36             | 160   | 'diorite'          | calc-alkaline series |
| RS.35  | 60.583           | 6.974             | 0.141            | 450   | 'granite'          | calc-alkaline series |
| RS.36  | 31.542           | 3.062             | 0.26             | 120   | 'gabbro'           | calc-alkaline series |
| RS.37  | 68.122           | 5.639             | 0.176            | 160   | 'granite'          | calc-alkaline series |
| RS.38  | 58.087           | 6.033             | 0.267            | 350   | 'granodiorite'     | calc-alkaline series |
| RS.39  | 49.333           | 1.11              | 0.069            | 1600  | 'gabbroic diorite' | tholeiite series     |
| RS.40  | 57.771           | 4.065             | 0.275            | 210   | 'granodiorite'     | calc-alkaline series |
| RS.41  | 58.97            | 4.481             | 0.529            | 150   | 'granodiorite'     | calc-alkaline series |
| RS.42  | 60.685           | 3.767             | 0.156            | 180   | 'granodiorite'     | calc-alkaline series |
| RS.43  | 55.48            | 2.019             | 0.386            | 280   | 'diorite'          | tholeiite series     |
| RS.44  | 56.103           | 2.738             | 0.339            | 320   | 'diorite'          | tholeiite series     |
| RS.45  | 65.221           | 1.43              | 0.187            | 450   | 'granodiorite'     | tholeiite series     |
| RS.46  | 52.149           | 2.294             | 0.536            | 170   | 'diorite'          | tholeiite series     |
| RS.47  | 56.701           | 4.874             | 0.234            | 190   | 'granodiorite'     | calc-alkaline series |

## 7. CONCLUSIONS

- 1) Petrographic studies show which radioactive minerals are almost alanite. Most of amphiboles include tremolite and actinolite. In addition, there are quartz, sphene, albite, rutile and carbonates as main minerals. No opaque minerals were identified in radioactive specimens;
- 2) Albite minerals occur in radioactive specimens. This shows that radioactive element mineralization happened with albitization. Radiometry readings near the albite veins confirm that radioactive element mineralization happened with albitization;
- 3) The area rock types are granite and metasomatized granite, but radioactive specimens are mostly metasomatized granite, which confirms other reports about Saghand mineralization area;
- 4) In the studying area we have common sericitic alteration which is the result of K-feldspar alteration;
- 5) The slope of the linear regression equation between uranium and thorium is close to 1, i.e. the concentrations of uranium and thorium in the samples are almost identical. Therefore, not unexpected that the contours plotted for these two variables are almost overlap;
- 6) Uranium and thorium enrichment is more than potassium, while uranium and thorium enrichment looks equal;
- 7) According to field observation and radiometry contour maps, radioactive anomalies are located in northwest and northeast parts of study area;
- 8) With regards to chemical classification graphs, general rock types are diorite and granodiorite, and radioactive specimens are gabbro (or basalt) and they are from a calc-alkaline magma.

## REFERENCES

- [1] HEDRICK, J.B., Thorium, USGS Mineral Year Book 2006, United States Geological Survey (2007).
- [2] ORGANISATION FOR ECONOMIC CO-OPERATION AND DEVELOPMENT NUCLEAR ENERGY AGENCY/ INTERNATIONAL ATOMIC ENERGY AGENCY, Uranium 2007: Resources, Production and Demand, OECD, Paris (2008).
- [3] COX, K.G., BELL, J.D., PANKHURST, R.J., The Interpretation of Igneous Rocks. George Allen and Unwin, London (1979).
- [4] MIDDLEMOST, E.A.K., Naming materials in the magma/igneous rock system. Earth Science Reviews **37** 3-4 (1994) 215–224.
- [5] IRVINE, T., BARAGAR, W., A guide to the chemical classification of the common volcanic rocks. Canadian J. Earth Sciences **8** 5 (1971) 523–548.
- [6] KELLEY, K.A., PLANK, T., FARR, L., LUDDEN, J., STAUDIGEL, H., Subduction cycling of U, Th, and Pb, Earth and Planetary Science Letters **234** 3 (2005) 369–383.

# **ENVIRONMENTAL GEOLOGICAL STUDIES OF THORIUM AND OTHER RADIOACTIVE ELEMENTS IN THE NARIGAN AREA (CENTRAL IRAN) ISLAMIC REPUBLIC OF IRAN**

J. IRANMANESH, M. RAZAEI, A. NOOHI  
Nuclear Science and Technology Research Institute,  
Atomic Energy Organization of Iran,  
Tehran, Islamic Republic of Iran

## **Abstract**

The study area is located in the Bafg-Saqand metallogenetic zone of Yazd Province in the Central Iran structural zone. Lithologically, the stratigraphic units of the Narigan area include the Rizzo limestone formations, Narigan granite, quartz-porphyry and metasomatic granites. The study area has higher concentrations of radioactive elements and some elements exceeding health standards. These elements are potentially mobile and may migrate from the soil into plant tissues via root absorption and thence to animals, where the emitted radiation could also put animals at risk. Environmental studies were undertaken in this research area in order to determine the biodiversity of plants in the Narigan area. Soil and plant root samples were also taken. The amounts of radioactive elements were analysed by gamma-ray spectrometry with hyper-purity germanium detectors (HPGe). Data obtained from analysis of these plants shows that most samples had elevated concentrations of the radioactive elements  $^{226}\text{Ra}$ ,  $^{137}\text{Cs}$ ,  $^{40}\text{K}$ ,  $^{238}\text{U}$  and  $^{232}\text{Th}$ , and can be considered as a potential environmental risk. The radionuclide study of plant and laboratory XRF studies of soil samples show that the roots of the plant *Astragalus* can be a geobotanical reference material for the two elements U and Th in the Narigan region.

## **1. INTRODUCTION**

In recent years, public participation and environmental groups in most national and international institutions and organizations insist on the need to maintain and introduce protection of the environment in the context of religious and moral issues. The design and implementation of an effective environmental management system must consider the culture and religion of the people living in the area for which the program is to develop [1]. In this, rocks and geological formations in the first cycle of the biosphere, and sometimes active processes or characteristics of its inherent regional geology and rock formations are considered [2]. Human interference in nature that may cause environmental damage includes activities such as exploration, extraction and mineral processing, construction, and industrial activity [3]. Where soils contain high levels of radioactive elements such as U and Th, these may be able to migrate into plant tissue through root absorption and move to animals. The importance of possible environmental contamination resulting from the mobility and concentration of radioactive elements in natural ecosystems should include a consideration that exploration, extraction and processing of these materials may increase this migration. This study is to evaluate the environmental setting of the Narigan area (Central Iran) and investigate the concentrations and possible health effects of radioactive elements such as K, Th, U there.

In the Narigan area, due to the natural contamination of the initial (normal) environment and thus the likelihood of transmission of radioactive materials, an evaluation of environmental cycles is needed in order to determine the extent of radioactive contamination of the area's natural and dynamic processes in the life cycle. This is important considering the dry and fragile ecosystems, as the risk of irreversible damage to the environment is increased in these climates.

## **2. GEOGRAPHICAL LOCATION, TOPOGRAPHY AND GEOMORPHOLOGY**

The Narigan area is located in the geopolitical subdivisions of the Bafg district in the northeast part of Yazd province in central Iran with an area of approximately 138 km<sup>2</sup>. The Narigan area, in terms of topography, has land with gentle ups and downs, an elevation of 1700 to 1900 m above sea level and a relatively dry to desertic climate with hot, dry periods, and half-yearly wet and cold periods [4]. Much

of the area had good crops and tree cover, where conditions allow and particularly where it is a low alluvial zone. The area is limited by the Dolomite Mountains to the north and to the south by a limestone wall. Between these two mountains the topography is relatively gentle hills state mainly made of granite. In the central part of the basin, the seasonal river Cyrus Abad passes east – west through granite hills. Also the Bafg district (including the Narigan area) is part of the tectonic situation in the central zone of tectonic processes such as faulting, including numerous strike-slip faults (e.g. Kuhbanan, and Nayb and Doruneh) enclosed with geologic regimes. Mining, geographical and geomorphological interests and resources, together with railways connecting the region across the country, support the growth and development of the mining industry in the province, especially for the city of Bafg.

### 3. GEOLOGICAL SETTING

Narigan is part of the metallogenic belt Bafg-Saqand tectonic division of Iran in the Central Iran structural zone. The total area has Precambrian basement rocks. In terms of volume volcanic rocks of alkaline intrusions are quite dominant, which can be seen from the volcanic rocks in central Iran Koshk series (the Bafg), tuffs and alkaline ryolite Esfordi Volcanic rock formations belong to the Rizzo, Dose and Tashk and intrusive Narigan and Zarigan [4]. Based on the stratigraphic position and time of the geological formations in central Iran, and in most other parts of Iran, one can say that in the Narigan area the central volcanic-sedimentary layers of limestone and dolomite belong to the Pre-Cambrian to Late Cambrian. The general stratigraphy of the area has Narigan members 4 and 5 of the Saqand and Rizzo series as well as a granite pluton [5]. In the Narigan overall tectonic zone and the general area of mining Bafg – Saqand rocks have, since their formation, been under different tectonic processes of Cambrian compressive and tensile fracturing. The active tectonic fault zone and mineralized Bafg — Saqand lithology have controlled and directed the creation the anomalies of radioactive and other elements.

### 4. MATERIALS AND METHODS

First, in order to assess the environmental and radioecology of the Narigan area, the initial concentrations (normal) of radioactive material and the biological environment of the area were sampled. All samples were analysed by XRF and then by mineralogical characteristics, and samples were subjected to XRD study. Simultaneous interpretation of geological, ecological and environmental assessment work was done for the region in which the species identification and the determination of the radioactive elements contained (biogeochemistry) were done. Analysis were examined with a gamma ray spectrometer system containing a hyper-purity germanium detector (HPGe).

#### 4.1. Contamination of soil and plants

Contamination of plants is not the main way in which the environment is affected. How and how much these contaminants can have adverse effects on the health of the plants, and the entire life cycle, is another matter and scope. Discussing it could even require consideration of the topics of nutrition science, crop protection, biology, ecology and environmental herbal aspects, geochemical reservoirs, the relevant ecological compartments (including air, water and types of plants). The absorption and transport of radioactive elements such as uranium (U) and thorium (Th) have been the focus of several standards developed to allow these elements in soil, water, air, and plants to be interpreted by the various organizations involved with issues of public health and environmental protection and nuclear safety. The main purpose of the soil sampling in the Narigan area was to determine the radioactive content of the soils (Table I) and undertake an environmental risk assessment based on available health and environmental standards. In this regard, a total of 15 soil samples were taken regularly during geological surveys. One of the parameters that determine the priority areas for soil sampling location was perspective where radiation levels were measured both before and after sampling. During field operations measurements were performed by a scintillometer. Next, sampling was done in the Narigan area, and the subsequent analyses interpreted regarding the correlation between the amount and type of radioactive elements in soil and plants and considering biogeochemical and geobotanical processes.

TABLE I. SOIL SAMPLES TAKEN FROM THE BASE AND ROOT ZONE AND THEIR CONTENT OF RADIOACTIVE ELEMENTS

| Sample n°    | U<br>( ppm ) | U<br>(Bq/ Kg) | Th<br>( ppm ) | Th<br>( Bq/ Kg) | C.P.S<br>SUR | C.P.S<br>SIN | C.P.S<br>BAC 50 |
|--------------|--------------|---------------|---------------|-----------------|--------------|--------------|-----------------|
| NA.Soil.0001 | 21           | 530.88        | 3             | 12.18           | 70 – 100     | 70 – 100     | 75              |
| NA.Soil.0002 | 1            | 25.28         | 2             | 8.12            | 130          | 130          | 60              |
| NA.Soil.0003 | 5            | 126.40        | 58            | 235.45          | 300          | 300          | 95              |
| NA.Soil.0004 | 4            | 101.12        | 20            | 81.18           | 250          | 200          | 65              |
| NA.Soil.0005 | 75           | 1896          | 12            | 48.71           | 200 – 500    | 200 – 500    | 120             |
| NA.Soil.0006 | 23           | 581.440       | 9             | 36.52           | 200 – 500    | 300          | 80              |
| NA.Soil.0007 | 13           | 328.64        | 4             | 16.23           | 230 – 250    | 230 – 250    | 80              |
| NA.Soil.0008 | 6            | 151.68        | 9             | 36.52           | 40 – 50      | 40 – 50      | 60              |
| NA.Soil.0009 | 39           | 985.92        | 5             | 20.28           | 300          | 600          | 95              |
| NA.Soil.0010 | 15           | 379.20        | 5             | 20.28           | 170          | 250          | 90              |
| NA.Soil.0011 | 26           | 658.28        | 6             | 24.34           | 180          | 250          | 90              |
| NA.Soil.0012 | 9            | 227.52        | 14            | 56.825          | 75           | 75           | 60              |
| NA.Soil.0013 | 11           | 278.08        | 3             | 12.18           | 130          | 100          | 60              |
| NA.Soil.0014 | 19           | 480.32        | 2             | 8.12            | 230 – 240    | 300          | 90              |
| NA.Soil.0015 | 25           | 632           | 1             | 4.06            | 300 – 700    | 300 – 700    | 85              |

Key: C.P.S SUR (Counts Per Second, Surface); C.P.S SIN (Counts Per Second, Sinkhole); C.P.S BAC (Counts Per Second, Background).

#### 4.2. Methods used to analyse soils and roots

First of all, soil samples for XRF sample preparation and came in pill form (such as preparing soil samples) and samples for all major oxides (major elements) were analysed by XRF (Table II). In order to understand the mineralogical characteristics of the samples, all samples were analysed by X-ray diffraction (XRD). Results indicate that quartz, calcite, and the clay mineral clinochlore constitute the most important mineralogical components. Minor amounts of the minerals biotite, albite, haematite and gypsum were also detected.

TABLE. II. MAJOR OXIDES BY XRF ANALYSIS OF SOIL FROM THE NARIGAN AREA

| Sample n° | SiO <sub>2</sub> | Al <sub>2</sub> O <sub>3</sub> | Fe <sub>2</sub> O <sub>3</sub> | CaO   | Na <sub>2</sub> O | MgO   | K <sub>2</sub> O | TiO <sub>2</sub> | MnO  | P <sub>2</sub> O <sub>5</sub> | SO <sub>3</sub> | LOI   | Total  |
|-----------|------------------|--------------------------------|--------------------------------|-------|-------------------|-------|------------------|------------------|------|-------------------------------|-----------------|-------|--------|
| NA. 0001  | 9.85             | 2.3                            | 23.17                          | 19.49 | 0.11              | 3.30  | 0.23             | 0.22             | 0.31 | 0.15                          | 25.75           | 14.72 | 98.60  |
| NA. 0002  | 42.25            | 8.44                           | 15.01                          | 12.10 | 490.              | 5.67  | 1.74             | 0.33             | 0.26 | 0.10                          | 0.15            | 12.97 | 97.76  |
| NA. 0003  | 47.95            | 7.03                           | 12.22                          | 10.80 | 0.50              | 10.87 | 0.88             | 0.60             | 0.31 | 1.63                          | 0.00            | 7.12  | 99.91  |
| NA. 0004  | 52.15            | 7.75                           | 6.30                           | 13.80 | 1.36              | 6.90  | 2.18             | 0.93             | 0.24 | 0.58                          | 0.03            | 7.86  | 100.08 |
| NA. 0005  | 34.90            | 8.33                           | 13.90                          | 10.73 | 0.24              | 7.36  | 1.21             | 0.55             | 0.06 | 0.12                          | 9.82            | 12.54 | 99.76  |
| NA. 0006  | 56.36            | 10.28                          | 7.61                           | 8.21  | 0.84              | 5.45  | 1.79             | 0.63             | 0.09 | 0.15                          | 0.47            | 7.8   | 99.68  |
| NA. 0007  | 50.97            | 10.16                          | 4.18                           | 7.72  | 1.11              | 3.07  | 2.10             | 0.53             | 0.02 | 0.12                          | 8.52            | 12.08 | 100.58 |
| NA. 0008  | 39.43            | 6.57                           | 3.48                           | 23.84 | 1.00              | 2.04  | 1.32             | 0.40             | 0.07 | 0.26                          | 0.12            | 20.72 | 99.25  |
| NA. 0009  | 59.43            | 12.82                          | 5.13                           | 6.74  | 1.21              | 2.78  | 3.34             | 0.90             | 0.03 | 0.20                          | 0.22            | 6.85  | 99.65  |
| NA. 0010  | 52.60            | 11.98                          | 6.63                           | 10.04 | 0.66              | 3.30  | 2.59             | 0.70             | 0.08 | 0.12                          | 1.71            | 8.81  | 99.22  |
| NA. 0011  | 56.11            | 13.90                          | 6.44                           | 7.33  | 0.78              | 3.34  | 2.96             | 0.75             | 0.06 | 0.12                          | 0.05            | 7.94  | 99.78  |
| NA. 0012  | 48.40            | 7.5                            | 9.71                           | 13.65 | 1.00              | 5.02  | 1.62             | 0.54             | 0.11 | 0.13                          | 2.08            | 10.18 | 99.94  |
| NA. 0013  | 48.57            | 9.23                           | 4.68                           | 11.66 | 2.53              | 2.75  | 2.36             | 0.75             | 0.09 | 0.14                          | 0.61            | 15.97 | 99.34  |
| NA. 0014  | 48.94            | 14.19                          | 7.15                           | 6.13  | 0.87              | 2.42  | 3.61             | 0.74             | 0.02 | 0.13                          | 4.72            | 10.15 | 99.07  |
| NA. 0015  | 48.24            | 10.05                          | 8.15                           | 10.47 | 0.55              | 4.41  | 1.63             | 0.59             | 0.08 | 0.15                          | 3.61            | 11.31 | 99.24  |

## 5. STUDY OF PLANT BIODIVERSITY

Arid regions such as the Narigan area show a heterogeneous plant distribution and components are based on ecosystems. The Bafg area and a lot of the Iranian plateau are, in terms of classification of plant growth (botany), a part of the Iranian–Turanian region. The Iranian–Turanian botanical region is divided into three parts; mountain, plain and desert. The Narigan area is part of the Iranian–Turanian desert. In the areas of less than 100 mm average annual rainfall severe drought is caused and plant communities show a highly fragmented and often non-woody vegetation cover. The root systems of plants are a very deep (for water), or shallow and wide [6]. Species in terms of importance include *Alhagi persarum*, *Tamarix ramsiessima* subsp. *euryptera*, *Pistacia atlantica*, *Amygdalus scoparia* and *Astragalus*; two types are shown in Fig. 1.

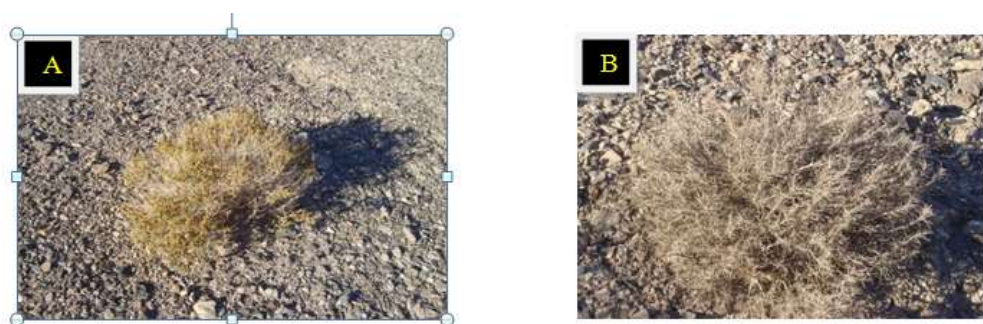


FIG. 1. *Salsola rigida* (A) and *Astragalus* plant; (B) at Narigan.

## 6. BIOGEOCHEMICAL AND GEOBOTANICAL METHODS AND THE CONTAMINATION OF PLANTS

### 6.1. Biogeochemical methods

A key biogeochemical method for examining environmental problems is inorganic analytical testing and interpretation of the benchmark area plants [7]. Many studies have shown that regarding the concentration of trace elements by plants, several factors are effective. Some of these factors include the type and age of the plant or specific organ samples, the soil type and drainage conditions, soil pH (with effect on the mobility of elements), and depth of roots [8, 9] (see Table III). During sampling biogeochemical aspects should take into serious consideration, and the influence of plant age and organ samples (according to the results of various studies in the world) is important. Reviews are biogeochemical with chemical analysis of plant material from their humus. Because plants absorb different nutrients from the soil and air, absorption through the roots or leaves can be made. Active root absorption of trace elements can be fast or slow. In some plants, elements such as Se, Pb, Th and U are often selectively (preferentially) absorbed by active absorption. Thus the availability of a sufficient condition for trace element for plant to absorb an element, but also in terms of plant physiology it may form trace element anomalies (relative to the specific plant). Overall, the evaluation of plants for environmental contamination has many complexities and problems. In studies on the absorption of uranium (U, Th) at uranium-contaminated sites by native plants [10, 11] and fruit and vegetable areas [12] involving various plants and migration of uranium in soil, the plants generally have a positive effect.

TABLE III. CHEMICAL CHARACTERISTICS – PHYSICAL SOIL BIOGEOCHEMISTRY

| pH   | Organic matter (%) | CEC (cmol+ Kg) | clay (<0.001 mm) (%) |
|------|--------------------|----------------|----------------------|
| 4.71 | 0.31               | 0.94           | 12.5                 |

### 6.2. Radionuclide measurements in plants

For the analysis of environmental radionuclides in the Narigan area and to be consistent with geology exploration, geophysical and geochemical studies that have been done in the past, 15 plant and soil samples were taken. The analysis was carried out on soil samples by the XRF device. It was found that some samples contained higher concentration of the major oxide K<sub>2</sub>O as well as trace elements, Th and U. Samples for analysis by a gamma-ray spectrometry system containing a hyper-purity germanium detector (HPGe) were prepared. Weighed samples were placed oven for 24 hours at 85° to dry and then were weighed again. Samples were ground in a mortar, with thorough cleaning between samples, and placed in special containers called Marynly. The radionuclides content of the sample (in terms of emitted gamma radionuclides) was determined from placing the prepared samples in each of the aforementioned devices (Table IV).

TABLE IV. LIST OF PLANT SAMPLES TAKEN AND ANALYSIS OF PLANT SAMPLES CONTAINING RADIOACTIVE NARIGAN REGION BY HPGE DEVICES

| Sample code | Specific sample                   | Sample location/anomaly | Radionuclide Bq/kg |                   |                   |                   |
|-------------|-----------------------------------|-------------------------|--------------------|-------------------|-------------------|-------------------|
|             |                                   |                         | <sup>40</sup> K    | <sup>137</sup> Cs | <sup>226</sup> Ra | <sup>232</sup> Th |
| N.001       | Cycle                             | 3/2                     | 10±158             | –                 | 2±7               | 15±2              |
| N.002       | Buhse                             | 4                       | 14±150             | –                 | 3±16              | 2±13              |
| N.003       | Buhse subs.<br><i>peurypterum</i> | 3/2                     | 214.10             | 71/0              | –                 | –                 |
| N.004       | <i>Salsola rigida</i>             | 3/3                     | 01+2.15            | 00+3.94           | 01+1.03           | 01+2.68           |
| N.005       | <i>Scoriola arentialis</i>        | 3/3                     | 02+1.13            | 00+1.47           | 00+3.45           | 01+1.01           |
| N.006       | <i>Scoriola arentialis</i>        | 1/5                     | 02+3.62            | 02+3.33           | 01+1.89           | 00+8.08           |
| N.007       | <i>Scoriola arentialis</i>        | 1/5                     | 24±245             | –                 | 2±10              | 2±10              |
| N.008       | <i>Astragalus</i>                 | 5/2                     | 02+1.92            | 00+4.81           | 02+1.01           | 01+1.93           |
| N.009       | <i>Salsola rigida</i>             | /-4                     | 313.42             | LLD               | –                 | –                 |
| N.0010      | <i>Salsola rigida</i>             | /-4                     | 313.42             | LLD               | –                 | –                 |
| N.0011      | <i>Punica granatum</i>            | –                       | –                  | –                 | –                 | –                 |
| N.0012      | Buhse subsp.<br><i>eurypterum</i> | /-4                     | –                  | LLD               | –                 | –                 |
| N.0013      | <i>Salsola rigida</i>             | /-4                     | 14±154             | –                 | 5±34              | –                 |
| N.0014      | <i>Scoriola arentialis</i>        | /-4                     | 204.90             | 1.40              | –                 | –                 |
| N.0015      | <i>Tamarix gallica</i>            | /-4                     | 14±91              | –                 | 4±27              | –                 |

### 6.3. Geobotanical methods

In addition to biogeochemistry, geobotany is another branch of science that can be based on some plants being used as an index of abundance of certain elements in the environment. The science includes trying to identify plants that have high concentrations of certain elements in one region or the whole world. Thus, we can see that the mass of an element represents the plant or the plant nutrients present at that point. For example, species of *Astragalus* are abundant in the environment [13]. Conversely, the absence of a plant in the study area (which we expect to exist) could also partly be due to the presence of an element or elements at concentrations which are high enough to be poisonous to the plant. Scientific geobotany also considers plant morphological and physiological effects that may assist with certain mineral exploration and environmental aims. In terms of radioactive elements such as Ra, Th, U this is true.

The presence of U can increase the number of abnormal chromosomes in the nucleus of plant cells and cause plants to produce fruit with unusual shapes. Ra and Th in low concentrations can accelerate plant growth, and at high concentrations, give rise to distortions in the bud and unusual plants that are stunted. This is shown in many local and some global reference plants [14]. These plants of geobotanical interest include particularly the most common gramineous (non-woody stems) types, some of which are high in ash content. Sometimes factors associated with mineral deposit provide an element to a plant that can be used as indicators for other elements. The present study investigated the scope of the preliminary geobotany of the Narigan region and showed that the *Astragalus* plant growth distributed in a certain region is correlated to the distribution of radioactivity U and Th in the same. The main habitat of the

plant occurs in the south and south boundaries of radiological anomaly IV (granite outcrop areas Narigan) has radiation level higher than other parts of the region.

## 7. CONCLUSIONS

- 1) Based on mineral exploration in Iran so far, the most significant deposits of uranium and thorium found are located in Central Iran structural zone. Detailed studies of geology, geography and geobotany on the zone that has been made. In most regions where the geological nature, climate and geography are the same, the appropriate regional Narigan radioecology and environmental studies can be used as the template for the production of knowledge in this field;
- 2) Radiometry and spectrometry studies have found that amongst rock units in Narigan the highest radioactivity is shown by the Narigan Granite. The U and Th radioactivity that can be found in these rocks have means of 20 ppm;
- 3) The Narigan area of Yazd province, despite being a desert with dehydration and fragmentation of vegetation, considering the vegetation diversity of the region, like other regions of Iranian – Turanian botanical region the Narigan area shows an extra-ordinary diversity of plant and animal species. Therefore, the Narigan area is a protected area of the Department of Environment and Natural Resources, and a pasture grazing is qualified by the appointed Department of Town and Country Planning;
- 4) Narigan area precipitation is low and surface water, due to climatic conditions, is very rare in the desert. From the point of view of the environment for mining activities (particularly mining of radioactive elements) this is a positive factor (the possibility of transmission of contamination to other areas is less);
- 5) So far, studies of geology and mining in various regions of the central region Narigan have been made, but unfortunately the amount and variety of ecological and environmental research in this area is very limited;
- 6) According to the study area at Narigan high radiation levels exist on the surface of the soil samples. Therefore, the amount of radioactivity that could be an actual or potential hazard to human health, animals and plants in the area should be considered;
- 7) Different elements, including radioactive elements, are capable of migration and absorption by plants, animals and humans. Therefore, each of these geochemical reservoirs (rocks, soils, plants, etc) should be monitored and evaluated for the ongoing contamination of radioactive elements and their data will be drawn from the scientific reports on the development programmes;
- 8) According to XRD analyses conducted, it became clear that a large variety of minerals are present in Narigan area soils including quartz, calcite, clinochlore, bazanit, gypsum, halite, magnetite, biotite, actinolite, albite, phlogopite and dolomite. Based on mineralogical and geological evidence of U and Th mineralization and mineral deposits of the Narigan area (and almost every other area) are of hydrothermal origin;
- 9) According to a survey conducted on Narigan area plant biogeochemistry, which has been done by HPGe system, it was found that most plants in this area with large amounts of radioactive elements, including Cs, Th, Ra and K. As these plants are consumed by animals and humans it could have dangerous health consequences in the present or the future.

## REFERENCES

- [1] OUGHTON, D.H., STRAND, P., The Oslo consensus conference on protection of the environment, *J. Environmental Radioactivity* **74** (2004) 7–17.
- [2] KRONFELD, J., GODFREY-SMITH, D.I., JOHANNESSEN, D., Uranium series isotopes in the Avon Valley Nova Scotia, *J. Environmental Radioactivity* **73** 3 (2004) 335–352.
- [3] MOORE, F., HORMOZI., B. YAGHOBPOOR M., A., Mineral Resources from the Economic and Environmental Viewpoint, Special Publication, Iran (1996) 71–31.
- [4] KASMAEE, M., Iran's climatic zoning, housing and residential environments, Building and Housing Research Center **151** (1993).
- [5] DUQUENE, L., VANDENHOVE, H., TACK, F., VAN DER AVOORT, E., VAN HEES, M., WANNIJN, J., Plant induced changes in soil chemistry do not explain differences in uranium transfer, *J. Environmental Radioactivity* **90** 1 (2006) 1–14.
- [6] SAMANI, B., Geology and exploration of radioactive anomalies in Narigan, Internal Rep. **356**, The Atomic Energy Organization of Iran (1996) 1–31.
- [7] LAND DEVELOPMENT CONSULTANTS, Design criteria urban green spaces, No. **203**, Management and Planning, Department of Technical and Design Criteria (2001) 30-50.
- [8] OULD-SADA, Z., CARINI, F., MITCHELL, N.G., A model testing study for the transfer of radioactivity to fruit, *J. Environ. Radioactivity* **70** (2003) 207–221.
- [9] JIANJUN SHI, JIANGFENG GUO, Distribution and migration of  $^{95}\text{Zn}$  in a tea plant/soil system, *J. Environ. Radioactivity* **87** (2006) 170–174.
- [10] PANDE, S. K., DESHMUKH, A. N., SHRIVASTAVA, P.K., The significance of the dormant stage in the growth-cycle of deciduous plants for biogeochemical uranium prospecting, India, *J. Geochem. Exploration* **46** (1993) 365–374.
- [11] IBRAHIM, S.A., WHICKER, F.W., Comparative uptake of U and Th by native plants at a U production site, *Health Physics* **54** 4 (1998) 413-419.
- [12] SARIC, M. R., STOJANOVIC, M., MILAN, B., 1995. Uranium in plant species grown on natural barren soil, *J. Plant Nutrition* **18** (1995) 1509-1518.
- [13] EBBS, S.D., BRADY, D.J., KOCHIAN, L.V., Role of U speciation in the uptake and the translocation of uranium by plants, *J. Experimental Botany* **49** 324 (1998) 1138-1190.
- [14] SIEGEL, F.R., Applied Geochemistry, Wiley, New York (1974).

# MEASUREMENT OF $^{226}\text{Ra}$ AND $^{228}\text{Ra}$ IN BRAZILIAN AND ISRAELI PHOSPHATES

A.C. AVELAR<sup>\*,\*\*</sup>, W.M. FERREIRA<sup>\*</sup>, M.A.B.C. MENEZES<sup>\*\*</sup>

<sup>\*</sup> DZOO, School of Veterinary Medicine,  
Universidade Federal de Minas Gerais (UFMG),

<sup>\*\*</sup> Laboratory of Neutron Activation,  
Reactor and Irradiation Service,  
Centre of Nuclear Technology Development (CDTN/CNEN),

Pampulha, Belo Horizonte, Brazil

## Abstract

Phosphoric acid has been considered an alternative source of uranium for decades. This paper presents an overview for both phosphate and uranium data to facilitate discussions of the viability of their potential synergic co-operation. The paper describes the results of gamma spectrometric measurements of the natural radionuclides  $^{226}\text{Ra}$  and  $^{228}\text{Ra}$  in rock phosphates used in Brazilian agriculture. Three Brazilian and an Israeli phosphate (imported and used in Brazilian agriculture) were analysed and compared with international criteria. Specific activities of  $^{226}\text{Ra}$  (from the uranium decay series) and  $^{228}\text{Ra}$  (from the thorium decay series) were taken into consideration to evaluate their radioactivity. Results indicate that some of phosphates are non-negligible sources of radioactivity (it is worth noting the activity of  $^{226}\text{Ra}$  in the Israeli phosphate) which could pose a risk for some workers who inadvertently manipulate phosphate and its dusts with their bare hands and without any respiratory protection equipment (RPE). Conversely, rock phosphates exhibiting higher  $^{226}\text{Ra}$  activity concentration are the prime candidates for a successful uranium production from phosphates.

## 1. INTRODUCTION

From 1960s onwards, phosphoric acid has been considered an alternative source of uranium [1]. Worldwide, some experimental techniques of uranium recovery from phosphates have been developed: precipitation, liquid membrane, solvent extraction and ion exchange. Those techniques can be used in varying combinations. At commercial scale, two extraction technologies of uranium from phosphoric acid stand out: solvent extraction (SX) and ion exchange [2].

Israel has a long and successful history of extracting uranium from phosphate ores of the Negev desert, as officially reported by the United Nations in 1982 [3]. Perhaps because of French restrictions on Israel's supply of uranium in the 1960s, Israelis developed their own method of extracting uranium from domestic phosphate rocks from Negev [3].

Currently, in most of countries, commercial recovering of uranium from phosphoric acid is considered marginal. New feasible approaches for the recovery of uranium from phosphoric acid, uranium market behavior, scarcity of fossil resources and new rules to limit carbon dioxide emissions from coal-fired power plants, could change this tendency in the medium to long-term [2, 4]. The IAEA plays an important role, leading efforts to incentive technologies and initiatives for uranium production from phosphates and unconventional sources [2].

After a period of 12 years of constant rising prices, starting in 1995 when it was as low as US \$10/lb, in 2007 the uranium oxide spot price reached a peak of US \$137/lb [5]. The Fukushima-Daiichi NPP accident in Japan and Germany's decision to phase out its remaining nuclear plants, among other factors, have influenced markets, resulting in an ongoing slump in uranium oxide prices for the last three years; at the time of writing uranium oxide is under US \$40/lb as December 2014 [5].

In the other hand, rock phosphate ranks as the second commodity (coal and hydrocarbons excluded) in terms of gross tonnage and volume of international trade. Phosphate prices — a key input to the production of most agricultural commodities such soy, maize, and animal feed — experienced a nine-fold increase between 2006 and 2008. At the time of writing the escalation of phosphate prices was easing [6]. Rock phosphate price reached a historical high price of US \$430 per metric tonne f.a.s. (free alongside ship) in August 2008, declined to US \$90 in July 2009 and smoothly reached US \$108 in June 2014 **Error! Reference source not found.**. At the time of writing about 90% of world phosphate production was utilized by the fertilizer industry to manufacture fertilizers, with the remainder being used to manufacture of animal feeds, detergents and chemicals. Rock phosphate is the major source of phosphorus in agriculture and livestock [4].

Price scenarios towards 2024 for phosphates are mixed. Potential game changers include geopolitical instability and conflicts in Middle East and North Africa (regions producing most of world phosphate) and stronger than expected phosphate demand growth by emerging countries, especially China, where commercialization of agriculture is still keeping pace, which could put upward pressure on fertilizer prices. Counterbalancing, if more phosphate plants are built and/or put into operation in China, USA, Brazil, Israel and North Africa, or the world demand moderates, prices of phosphate could assuage [4].

Further to phosphorus and calcium, phosphate ore is also source of some hazardous elements, such: arsenic, cadmium, thorium and uranium and including a variety of radioisotopes as well. This radioactivity is released in the environment, contributing to the background **Error! Reference source not found.**. The International Atomic Energy Agency and European Union Council have changed the profile of radiation protection, increasing the regulatory awareness of NORM (Naturally Occurring Radioactive Material) **Error! Reference source not found.**. Like in NORM facilities, phosphate and fertilizer industries have been identified in terms of their scope as industries requiring further attention due to the radioactivity associated to their products and processes. Data from studies show that workers involved in phosphate-associated activities could be internally exposed to some radionuclides by inhalation and ingestion of phosphate dust in unprotected operations (e.g. in the absence of respiratory protective equipment) **Error! Reference source not found.**. Some studies considering phosphate facilities worldwide point out to the mean annual effective doses in these industries were found to be very similar: in Florida in the range 0.081–0.171 mSv for workers in dry product areas; in Huelva, Spain, the annual effective dose was found to be in the range 0.076–0.134 mSv; in Poland, the mean annual effective dose was found to be 0.10 mSv **Error! Reference source not found.**.

## 2. PROJECT OVERVIEW

Three Brazilian industrial phosphates (nominated POL, FST and FSS) and an Israeli rock phosphate (nominated IPR, imported and used in Brazilian agriculture; this product is currently one of the most commercialized fertilizer in Brazil due its low price) were analysed. The specific activities of  $^{226}\text{Ra}$  (from the uranium decay series) and  $^{228}\text{Ra}$  (from the thorium decay series) were taken into consideration to ensure an adequate risk assessment.

The specific activities of  $^{226}\text{Ra}$  and  $^{228}\text{Ra}$  were determined by high-resolution gamma spectroscopy with HPGe (hyper pure germanium detector) and Genie 2000® software from Canberra® in the Centre of Nuclear Technology Development (CDTN/CNEN). The concentration of  $^{226}\text{Ra}$  was measured using the 186.2 keV energy peak, the concentration of  $^{228}\text{Ra}$  through  $^{228}\text{Ac}$ . The measurement system was calibrated using a set of standard samples from IAEA. The measured samples were crushed and sieved to a grain (98% at least) size as small as 200 Tyler mesh. Stable mass was achieved grinding, drying at 105°C and mixing each material.

### 3. RESULTS

TABLE I. ACTIVITY CONCENTRATION OF  $^{226}\text{Ra}$  AND  $^{228}\text{Ra}$  IN THE STUDIED PHOSPHATES

| Phosphate, %, country                           | $^{226}\text{Ra}$ [Bq.g $^{-1}$ ] | $^{228}\text{Ra}$ [Bq.g $^{-1}$ ] |
|---|-----------------------------------|-----------------------------------|
| POL, 46% P <sub>2</sub> O <sub>5</sub> , Brazil | 0.14 ± 0.04                       | 0.40 ± 0.10                       |
| FST, 45% P <sub>2</sub> O <sub>5</sub> , Brazil | 0.02 ± 0.01                       | 0.60 ± 0.10                       |
| FSS, 19% P <sub>2</sub> O <sub>5</sub> , Brazil | 0.50 ± 0.10                       | 0.50 ± 0.10                       |
| IPR, 31% P <sub>2</sub> O <sub>5</sub> , Israel | 1.60 ± 0.20                       | 0.80 ± 0.30                       |

POL, FST and FSS = Brazilian industrial phosphates, IPR = Phosphate rock from Israel. n=3

### 4. DISCUSSION

Consensus seems to be emerging from activity concentrations under 1 Bq.g $^{-1}$  for uranium and thorium series as criteria for determining whether exposure due to the given material should be excluded from regulatory consideration, i.e., to obtain clearance or be labelled as NORM material **Error! Reference source not found.**. Thereto, materials with activity concentrations above these levels, where the Israeli phosphate fits in, a national or international regulatory body needs to decide on a case-by-case basis if it should be included in the system of control **Error! Reference source not found.**.

Workforce in facilities where occur mining and/or processing of phosphates, or handle phosphate products in farmland activities, have a greater chance of taking in more radionuclides and been more exposed to the gamma radiation from dusts than the rest of the public. Previous studies demonstrated that activity concentration, exhalation rate and absorbed dose due the presence of  $^{226}\text{Ra}$  in phosphates were found to increase substantially with the use of phosphate fertilizers in India **Error! Reference source not found.**<sup>13</sup>.

Conversely, these rock phosphates exhibiting higher  $^{226}\text{Ra}$  activity concentration are most suited candidates for a sucessful uranium production from phosphates, since there is a direct correlation between the occurrence of uranium, in particular the plentiful  $^{238}\text{U}$ , and the occurrence of its daughter  $^{226}\text{Ra}$  **Error! Reference source not found.**

Although the appropriate application of phosphates contributes significantly towards sustainable agricultural intensification, some phosphates contain considerable radioactivity, which may result in an increment in the agricultural workforce's exposure to radiation.

The monitoring and control of the production of phosphate fertilizers should be considered for regulation as a practice. The most practical regulatory option for fertilizer activities seems the establishment of an exemption or a radioactivity limit for notification **Error! Reference source not found.**. The literature suggests that annual doses received by workers of this industry are below 1 mSv in most of cases. Furthermore, there are no significant exposure pathways to members of the public **Error! Reference source not found.**

As pointed out by IAEA **Error! Reference source not found.**, every effort should be made at international level to reduce the exposure to  $^{226}\text{Ra}$  in operations involving several industries including phosphate. Particularly, it should be avoided any unprotected handling of rock phosphates (some of them with high concentration of  $^{226}\text{Ra}$ , as shown in this study) in farmland activities.

Moreover, in terms of IAEA safety standards, the radiation protection process should recommend action to: (a) reduce the doses received by exposed individuals or groups of individuals; (b) avert doses to individuals or groups of individuals that are likely to arise in the future; and (c) prevent or reduce environmental impacts from the radionuclides present in any radioactive material **Error! Reference source not found..**

## ACKNOWLEDGEMENTS

This project is partially supported by: The Ministry of Science and Technology of Brazil via CNPq, FAPEMIG and the Ministry of Education via CAPES/Universidade Federal de Minas Gerais. We appreciate every effort from CDTN/CNEN during A.C. Avelar's Post-Doc internship at the institute in order to carry-out the nuclear analyses.

## REFERENCES

- [1] INTERNATIONAL ATOMIC ENERGY AGENCY, Uranium Extraction Technology, IAEA-TRS-359, IAEA, Vienna (1993).
- [2] UxP Uranium Extraction from Phosphoric Acid? UxP Newsletter: Special Edition, UxP Network News, Aleff Group, London, UK (2013), Available at:  
[http://www.uxponline.com/resources/file/pdf/meet/uxp2013/UXP\\_NewsletterProgressReport0.3November2009-June2012.pdf](http://www.uxponline.com/resources/file/pdf/meet/uxp2013/UXP_NewsletterProgressReport0.3November2009-June2012.pdf).
- [3] UNITED NATIONS, Study on Israeli Nuclear Armament, A/36/431, New York (1982)  
<https://www.un.org/disarmament/publications/studyseries/no-6/>.
- [4] WORLD BANK, Commodity markets outlook 2014 (January 2014).
- [5] INVESTMENTMINE, Historical Uranium Prices and Price Chart Available (8 December 2014), <http://www.infomine.com/investment/metal-prices/uranium-oxide/all/>.
- [6] PHOSPHATES: MARKET RESEARCH REPORT PHOSPHATES, Market Publishers, London (2012).
- [7] FOOD AND AGRICULTURE ORGANIZATION AND INTERNATIONAL ATOMIC ENERGY AGENCY, Use of phosphate rocks for sustainable agriculture, FAO Fertilizer and Plant Nutrition Bulletin **13**, Rome (2004).
- [8] INDEX MUNDI WEBSITE Commodity Prices, Phosphate (2014),  
<http://www.indexmundi.com/commodities/?commodity=rock-phosphate>.
- [9] KANT, K., UPADHYAY, B., SONKAWADE, R.G, CHAKARVARTI, S.K., Radiological risk assessment of use of phosphate fertilizers in soil, Iran. J. Radiat. Res. **4** (2006) 63–70.
- [10] ADAM, A.A., ELTAYEB, M.A.H., Uranium abundance in some Sudanese phosphate ores, J. Argent. Chem. Soc. **97** 2 (2009) 166–177.
- [11] MANGINI, A., SONNTAG, C., BERTSCH, G., MÜLLER, E., Evidence for a higher natural uranium content in world rivers, Nature **278** (1979) 337–339.
- [12] ATSDR — Agency for Toxic Substances and Disease Registry of United States. Toxicological profile for uranium, U.S. Department of Health and Human Services, Washington (1999).
- [13] INTERNATIONAL ATOMIC ENERGY AGENCY, Radiation protection and management of NORM residues in the phosphate industry, Safety Reports Series No. **78**, IAEA, Vienna (2013).
- [14] INTERNATIONAL ATOMIC ENERGY AGENCY, NORM IV — Naturally occurring radioactive materials, Proceedings of an International Conference held in Szczyrk, Poland, 17–21 May 2004, IAEA-TECDOC-1472, IAEA, Vienna (2005).
- [15] HOFFMANN W., KRANEFELD A., SCHMITZ-FEUERHAKE I.,  $^{226}\text{Ra}$  contaminated drinking water: hypothesis on an exposure pathway in a population with elevated childhood leukemia, Environ. Health Perspect. **101** (1993) 113–115.
- [16] U.S. ENVIRONMENTAL PROTECTION AGENCY, Radionuclide Basics: Radium, <https://www.epa.gov/radiation/radionuclide-basics-radium>.

# A NEWLY DEVELOPED ACCELERATOR FOR FUTURE POSSIBLE APPLICATIONS — TO CONVERT THORIUM TO URANIUM-233

T. KAMEI, Y. KOKUBO  
Kyoto Neutronics Co. Ltd.,  
Kyoto, Japan

## Abstract

For a sustainable society, low-carbon energy sources and automobiles are required. Renewable energy such as wind-mills and solar power are used to provide low-carbon energy. Electric and hybrid vehicles are expected as low-carbon automobiles. Essential raw materials to fabricate these machineries are rare-earth elements (REE). REE supply has security issues due to monopoly concerns. Radioactive thorium always accompanies REE in nature and causes difficulty for wide production. Thorium can be used as nuclear fuel, but is merely fertile; an additional supply of fissile material is necessary to use it as a nuclear fuel. The available implementation capacity of thorium, by using plutonium from the uranium fuel cycle, is 392 GWe at 2050. This capacity requires only 76 000 tonnes of thorium, compared to a total amount of thorium occurring as a potential by-product of REE extraction of 444 000 tonnes. Thus, a new accelerator neutron source is developed to utilize thorium. The authors adopt low-energy and high-intensity accelerator using D-Be reaction and SiC device, ‘TRANS’ (Tandem Repeat Accelerator Neutron Source). TRANS can be operated in parallel mode to increase neutron yield. Here the concept of TRANS is described and its applications such as thorium fuel and Mo-99 production introduced.

## 1. INTRODUCTION

Constructing a sustainable society is one of the most important political subjects in recent years. Though there are many requirements for sustainability, it is widely recognized that reducing anthropogenic emission of CO<sub>2</sub> is a key from a view of preventing global warming. Half of the anthropogenic CO<sub>2</sub> is emitted from energy sector and the most part comes from fossil fuel power plant [1]. Since low-carbon energy is needed, renewable energies such as solar power or wind-mills are implemented. In addition to these energies, nuclear power is also recommended as low-carbon energy source as mentioned in the fifth assessment report of IPCC [2].

The second largest CO<sub>2</sub> emission comes from transportation sector. Its 70% is shared by road transportation [3, 4]. Therefore, the development of electric vehicle (EV) and hybrid vehicle (HV) are being progressed. For these low-carbon automobiles, rare-earth elements (REE) are necessary [3]. REE is used as a material of permanent magnets which are a part of electric motors. At the same time, REE is indispensable for permanent magnet of the dynamo of wind-mills. For photovoltaic cells, REE is used as transparent electrode. Annual world supply amount of REE is about 130 000 tonnes and 97% depends on China which is subject of resource security [5, 6]. These surroundings reveal that stable supply of REE which is indispensable both for renewable energy and low-carbon automobiles is necessary for constructing sustainable society.

REE exists enough from a resource view and can be confirmed not only in China but also in the North America, South America, Australia and CIS (Commonwealth of Independent States – an association of former Soviet Union republics) and so on. But REE is not supplied in great quantities from any country except China, partly because radioactive thorium always accompanies REE in natural deposits. Though thorium is fertile material, thorium is not able to be used directly as a nuclear fuel due to its lack of fissionable isotope. Therefore, separated thorium at a rare-earth refinery plant becomes merely part of radioactive waste as long as it is not used. The USA’s Molycorp stopped rare-earth mining business in early 2000s because market competitiveness could not be kept including thorium care in the production cost, although their Mountain Pass REE mine reopened in 2013. Recently, Australia’s Lynas opened a rare-earth plant in Malaysia with a financial support from JOGMEC (Japan Oil, Gas and Metals National Corporation), notwithstanding some obstructions from within Malaysia due to concerns against thorium

and other radioactivity in waste products [5]. These surroundings of REE clearly indicate that sustainable society cannot be achieved if thorium is not adequately taken care [8–10].

There are two ways to utilize thorium as nuclear fuel. The first is to supply external fissile material. The second is to provide an external neutron source. The first author has examined simulation of available implementation capacity of thorium fuel cycle which is started by external supply of plutonium from spent uranium fuel [11, 12]. It was not considered in these evaluations to use enriched uranium for starting the use of thorium because it is used for uranium fuel cycle itself. By the collaboration between uranium fuel cycle and thorium, about 392 GWe of thorium nuclear power can be implemented around at 2050. It should be noted here that required amount of thorium for this implementation capacity will be about 76 000 tonnes while accumulated amount of thorium separated during refinery process of rare-earth will reach to 444 000 tonnes. This means that the utilization of plutonium from spent uranium fuel is not enough to fully consuming potentially separated thorium and that as a result the storage of the excess amount of thorium becomes a concern.

Therefore, it is necessary to explore a way to flexibly using thorium which is independent from uranium fuel cycle, such as external neutron source. The authors have proposed a way based on the use of accelerator **Error! Reference source not found.**. We are now developing a prototype of new accelerator and we report here its recent progress including application for thorium nuclear fuel.

## 2. OUTLINE OF ACCELERATOR NEUTRON SOURCE ‘TRANS’

It is necessary to add fissionable material which is not contained in the natural composition of thorium for converting it as nuclear fuel. Thorium-232 transmutes to fissionable uranium-233 by absorption of neutron via thorium-233 and protoactinium-233. That is to say, an external neutron source enables natural thorium to be converted to nuclear fuel. Radioactive isotopes cannot be practically used for this purpose due to their small neutron yield (for example, Cf-252  $8.6 \times 10^4$  n/s). Fission neutron can be of course used for converting thorium because the process is essentially same to the conversion of uranium-238 to plutonium-239. There are many examples of this such as Shippingport nuclear power plant **Error! Reference source not found.**. However, the fission reaction itself needs neutrons to sustaining it and there are not enough neutrons for converting thorium. Fusion neutrons are also a candidate for thorium conversion but neutron yield is not enough comparing to fission reaction. Spallation reaction source using high-energy accelerator is expected because of its large production of neutrons [15–17].

Many kinds of accelerator have been developed in the past long years. Though purpose of this paper is not to review these accelerators, it should be mentioned here that conventional accelerators are not necessarily suitable for the sake of producing thorium nuclear fuel. Many accelerators will be needed for converting thorium to nuclear fuel because large amount of thorium, a few thousand tonnes annually, occurs as a potential byproduct of REE refining process. Therefore, such accelerator should satisfy requirements of low-manufacturing cost, low-operation cost and high-reliability. Low manufacturing cost can be achieved by using low-cost material and by adopting entry-level manufacturing technology. High conversion ratio of input energy to acceleration energy enables low-operation costs because consumption of electricity can be reduced. High-reliability mainly depends on the reliabilities of components used for the system. In addition, since the accelerator is used for generating neutrons, not only the amount of neutron yield but also the energy of neutrons should be considered. It is required to enable generation of neutrons having adequately low energy, because high-energy neutron often produces unnecessary nuclear reactions which make the process difficult to handle. Based on these discussions, the authors have designed a new large intensity accelerator neutron source which satisfies both low-cost and high-reliability by adopting low-acceleration energy of charged particle. This is named ‘TRANS’ (Tandem Repeat Accelerator Neutron Source). A schematic diagram of TRANS is illustrated in Figure 1.

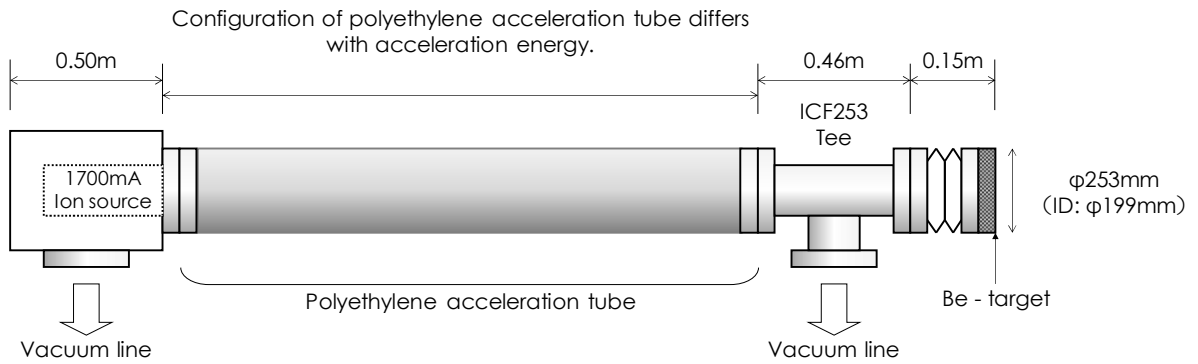


*FIG. 1. Schematic diagram of TRANS and acceleration mechanism.*

Positive deuteron ions and beryllium are used as charged particle and bombarding target of TRANS, respectively. Though there are other candidates of combination of charged particle and target such as proton and lithium, we adopted the combination of deuteron and beryllium for generating relatively large amount of neutron at low-acceleration energy [18] and for avoiding high chemical reactivity of lithium.

Extracted deuteron ion from ion-source is accelerated by electrode charged to negative potential. The potential of electrode can be shifted from negative to positive at very high frequency by adopting SiC (silicon carbide) semiconductor switch. Switching speed is shorter than 40 ns from 10% to 90% of departure and destination values. Once deuteron ion beam reaches to this electrode, its potential is shifted from negative to positive. Then the positive ion is again accelerated to higher acceleration energy. Potential of one electrode is, for example, set to 160 kV. Thus, if three electrodes are used in axial direction, charged particle is accelerated to 480 kV in total. Acceleration energy of deuteron ion is low up to a few MeV to keep neutron energy generated from beryllium target. One of our designs for thorium fuel production adopts 960 keV of acceleration energy. Production cost of accelerator tends to increase with acceleration energy. Therefore, our new accelerator can achieve low cost.

Operation cost can be evaluated as acceleration efficiency which is determined by a ratio between the input energy (consumption of electricity) and the output energy of accelerated charged particle. The acceleration efficiency of widely used RF-LINAC is only about 5% because of low efficiency of the Klystron tube, which is based on conventional vacuum tube technology. The SiC semiconductor device which is used for TRANS has very small resistivity and very high speed repetition frequency. Therefore, the device has very little loss of energy even though it is operated at large voltage and large current. As a result, acceleration efficiency of TRANS reaches to about 60%. Available voltage of one SiC device is 1.2 kV and hundreds of these devices are connected both in parallel and series for enabling a switching module to drive hundreds of kV (Patent application number: 2014-038129).

All circuits are configured by solid-state devices thus they have very high reliability comparing to vacuum tube. In addition, this switching module can be easily improved by the improvement of the device such as increasing of available voltage. If one switching module becomes to drive larger voltage, total length of accelerator can be shortened. Total cost can be also reduced because number of required devices becomes small. One acceleration tube of TRANS is called as ‘barrel’. The specification of single-barreled TRANS is shown in Table I.

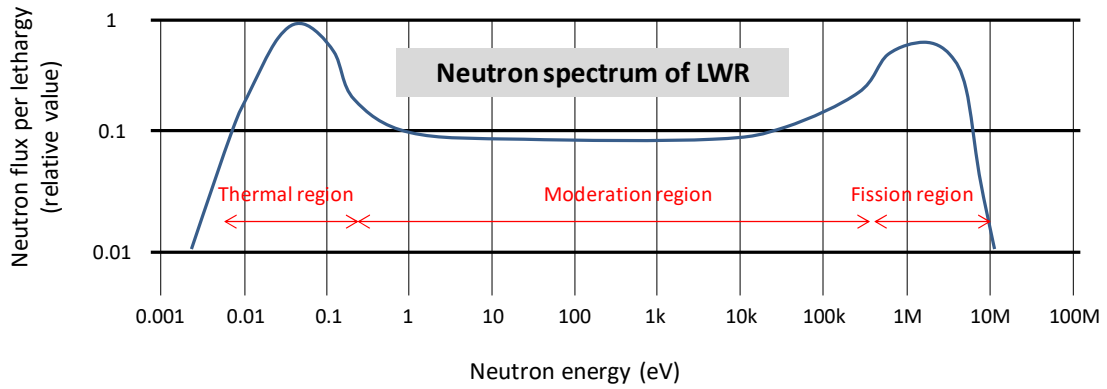
TABLE I. SPECIFICATIONS OF TRANS SERIES

|                                  | Items                       | TRANS-960C               | TRANS-480C               | TRANS-200C               |
|----------------------------------|-----------------------------|--------------------------|--------------------------|--------------------------|
| TRANS specification              | Acceleration energy         | 960keV                   | 480keV                   | 200keV                   |
|                                  | Acceleration current (Max)  | 100mA                    | 150mA                    | 120mA                    |
|                                  | Beam power (Max)            | 96kW                     | 72kW                     | 24kW                     |
| Acceleration tube                | Neutorn yield (Max)         | $3.2 \times 10^{12}$ n/s | $8.7 \times 10^{11}$ n/s | $1.1 \times 10^{10}$ n/s |
|                                  | Number of acceleration tube | 4 (T1~T4)                | 3 (T1~T3)                | 1 (T1)                   |
|                                  | Pulse width of ion beam     | 40ns                     | 40ns                     | 40ns                     |
|                                  | Beam extraction current     | 1000mA                   | 1000mA                   | 1000mA                   |
| High voltage pulse generator     | Length                      | 2495mm+ $\alpha$         | 1430mm+ $\alpha$         | 475mm+ $\alpha$          |
|                                  | Number of pulse generator   | 4                        | 3                        | 1                        |
|                                  | Rated voltage               | 240kV                    | 160kV                    | 200kV                    |
|                                  | Offset voltage              | -120kV                   | -80kV                    | -100kV                   |
| Pulse repetition frequency (Max) |                             | 2MHz                     | 2MHz                     | 2MHz                     |

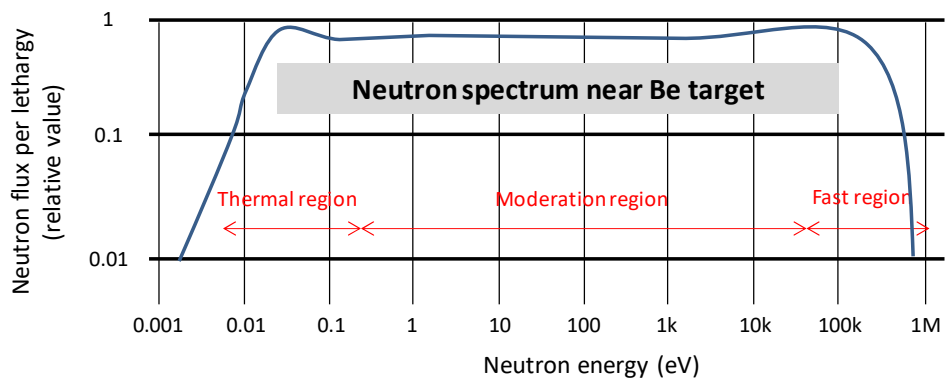
If the neutron yield of single-barreled TRANS is small for some application, TRANS can operate at multi-barreled mode for enhancing the neutron generation amount. The low manufacturing and operation costs enable multiple operation of accelerators. The other remarkable advantage of multi-barreled TRANS is that the configuration can form spatial distribution of neutron source. Spallation neutron source is normally only a point source. TRANS can form a line-source, a plate-source with different intensity of neutron for each barrel (Patent number: JP 5575963).

### 3. APPLICATION OF TRANS FOR THORIUM NUCLEAR FUEL “NTD-TH (THORIUM)”

If pure silicon is irradiated by neutrons, some part of Si-30 transmutes to radioactive Si-31. Then this Si-31 transmutes to stable P-31 (phosphorus). As a result, n-type semiconductor can be formed by this irradiation. This method is called as ‘NTD’ (Neutron Transmutation Doping) for adding small amount of impurity **Error! Reference source not found.**. NTD-Silicon is commercially used because homogeneous doping is available. The authors are developing a new method adopting this NTD for producing thorium fuel which is called as ‘NTD-Th (thorium)’. To say, Th-232 transmutes finally to U-233 via Th-233 and Pa-233. As mentioned above, conversion of thorium to U-233 by neutron irradiation has been demonstrated such as at the Shippingport nuclear power plant. However, as long as light water reactor is used for irradiation, conversion efficiency is not high because fission neutrons are immediately moderated due to the water and thus resonance absorption cannot be used. On the other hand, TRANS enables a flat neutron spectrum because it can adopt any moderation material instead of water. Fig. 2 shows an example of neutron spectrum of TRANS using lead as moderator. As a result, the resonance absorption region (Fig. 3) can be used to enhance conversion ratio of thorium to uranium-233.



(a) LWR



(b) TRANS

*FIG. 29. Neutron spectrum of LWR and TRANS.*

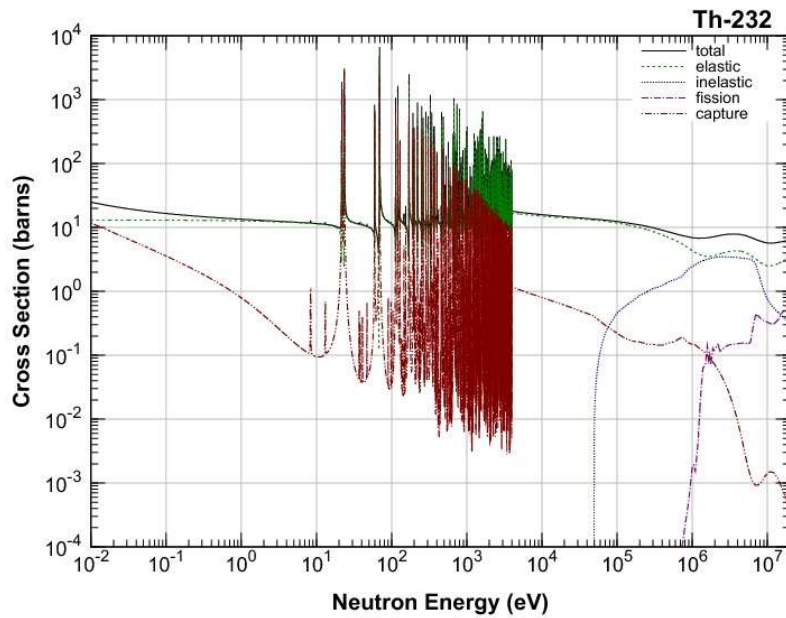


*FIG. 3. Absorption cross-section of thorium (JENDL-4.0).*

The configuration of TRANS for NTD-Th is shown in Fig. 4. The moderator is Pb (lead) and the irradiation target is made of thorium metal. Once the thorium is irradiated, it is converted to such as an oxide or fluoride for supply to an ordinary LWR, HTGR (High temperature gas-cooled reactor) and advanced MSR (molten-salt reactor) (Patent number: JP 5614821).

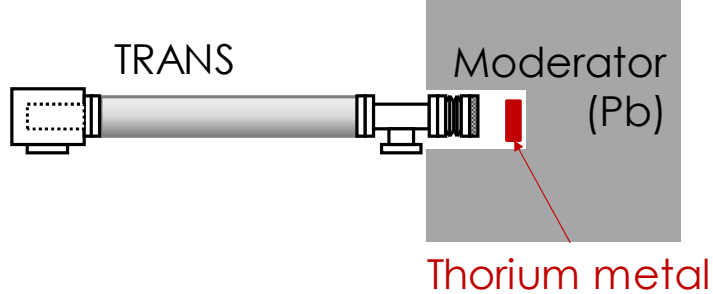


*FIG. 4. Configuration of TRANS for NTD-Th.*

One of the differences between NTD-Silicon and NTD-Th is the existence of intermediate element from the original material to the destination material. For the case of NTD-Th, Pa-233 between thorium and U-233 behaves as obstacle for high conversion ratio of thorium. This is mainly because of relatively long half-life of Pa-233 of about 27 days (c.f. the half-life of Th-233 of about 22 minutes). In addition, Pa-233 has a relatively large neutron absorption cross-section to be Pa-234. Pa-234 decays to U-234 which is not a fissionable isotope. Thus, the neutron irradiation time of thorium should be as short as possible to avoid production of U-234. In our process of NTD-Th, thorium is at first irradiated by neutrons, for example, for 10 days. Then this irradiated thorium is removed from irradiation area to await conversion of Pa-233 to U-233. The production amount of U-233 is shown in Table II. Assuming that 3% of an initially loaded 100 tonnes of LWR thorium fuel is uranium-233, 2500 8-barreled TRANS are needed for preparing thorium fuel. This calculation is still in a preliminary phase and detailed evaluation will be studied by using PHITS code **Error! Reference source not found.** for optimization of irradiation system. The composition of uranium isotope obtained by NTD-Th is shown in Table III. The composition of uranium in equilibrium fuel in MSBR (Molten-Salt Breeder Reactor) is also shown as reference here **Error! Reference source not found..**

TABLE II. PRODUCTION AMOUNT OF U-233

| Number of barrel | Amout [g/year] |
|------------------|----------------|
| Single           | 150            |
| 4                | 600            |
| 8                | 1200           |

TABLE III. COMPOSITION OF URANIUM ISOTOPE OBTAINED FROM NTD-TH AND MSBR

| Nuclide          | Ratio (NTD-Th)       | Ratio (MSBR) |
|------------------|----------------------|--------------|
| $^{232}\text{U}$ | 0% (Less than 1 ppb) | 20~80 ppm    |
| $^{233}\text{U}$ | 99.87%               | 64.5%        |
| $^{234}\text{U}$ | 0.13%                | 23.2%        |
| $^{235}\text{U}$ | 0%                   | 6.0%         |
| $^{236}\text{U}$ | 0%                   | 6.3%         |

As can be seen from Table III, the production amount of U-232 is extremely small based on the method of NTD-Th. This is because the neutron spectrum of TRANS at low acceleration energy does not contain high-energy neutrons. There are three paths of  $(n, 2n)$  reaction to produce U-232 as indicated in Fig. 5. All of these paths happen only by neutrons having energy higher than about 5.7 MeV. TRANS does not generate high energy neutrons. On the other hand, a fission reaction produces high-energy neutron thus production amount of U-232 becomes large.

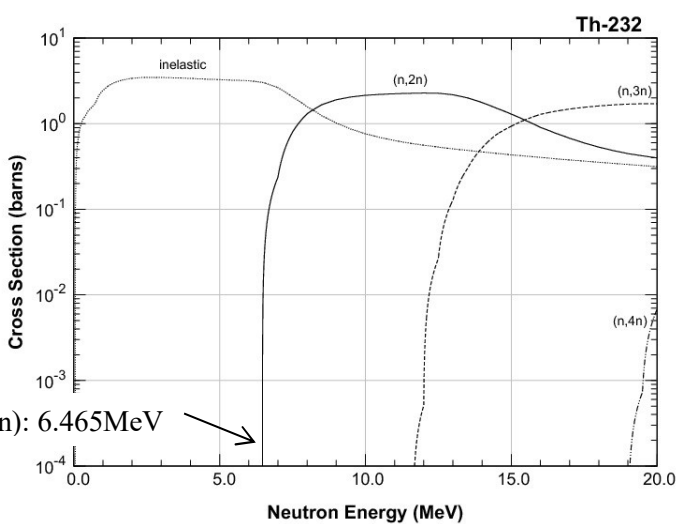
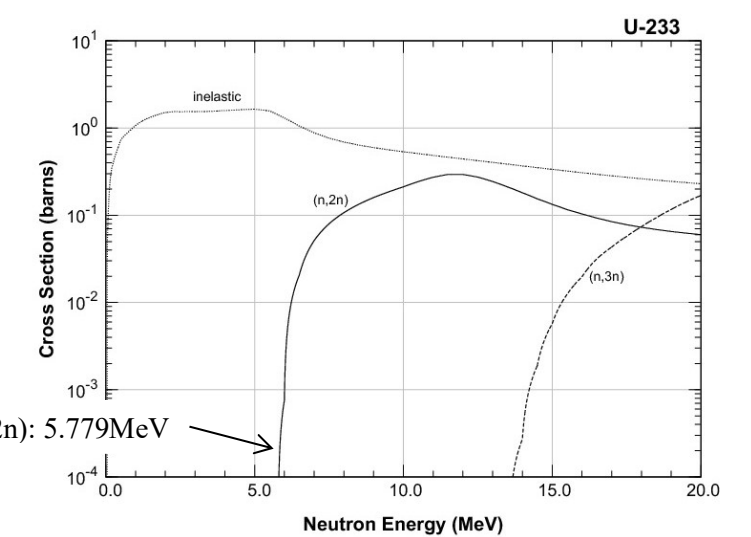
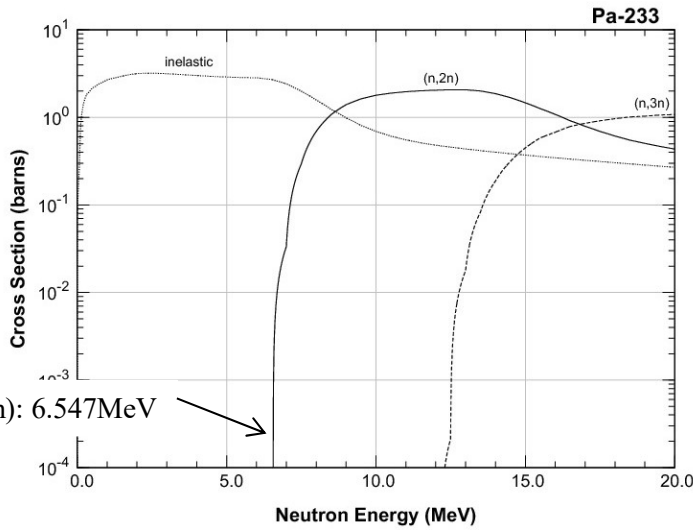
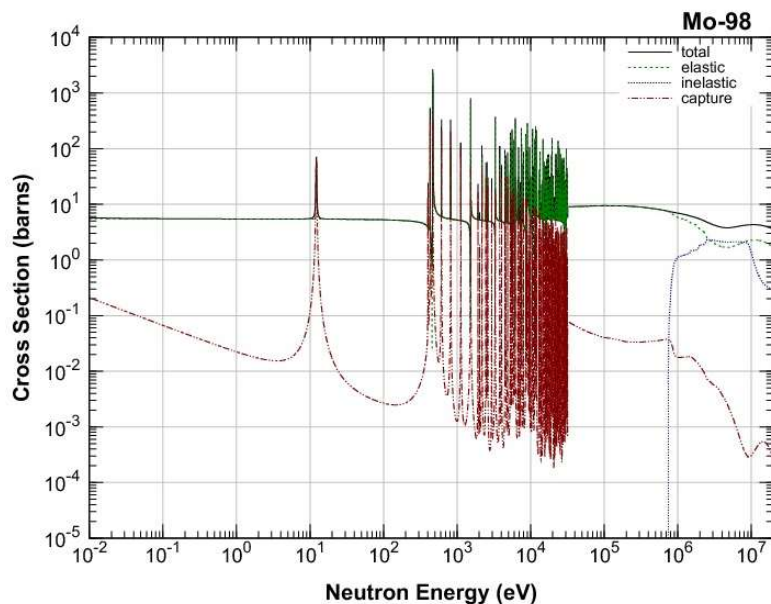


FIG. 5. Three paths to produce U-232 and neutron absorption cross-section [JENDL-4.0].

It is often said that existence of U-232 in the thorium fuel cycle enhances nuclear proliferation resistivity **Error! Reference source not found.**. This is because its daughter nuclide (thallium-208) emits strong gamma rays. At the same time, this gamma activity also makes it difficult to fabricate thorium-uranium-233 fuel if the uranium-233 is obtained after irradiation of thorium in LWR. The U-233 obtained by NTD-Th can be used for fuel fabrication because its accompanying gamma activity is very little. There are several ways to improve nuclear proliferation resistivity such as blending of natural uranium. Accelerator driven system adopting TRANS is also one of the attractive methods to utilize thorium with high nuclear proliferation resistivity because U-232 is formed inside of reactor core containing fast neutron generated by fission reactions.

The principle of NTD-Th can be applied for medical isotope production such as Mo-99 (molybdenum). Natural Mo contains about 24% of Mo-98. Mo-98 transmutes to Mo-99 by absorption of a neutron. However, the absorption cross-section of thermal neutron is small, being 0.13 barns. Therefore, the conversion ratio of Mo-98 to Mo-99 is very low as long as natural Mo is irradiated in ordinary LWRs because fission neutrons are immediately moderated to thermal energy. As described above, TRANS can form a flat neutron spectrum by using suitable moderator instead of water. Since resonance absorption region of Mo-98 can be utilized (Fig. 6), the total absorption cross-section becomes 6.5 barn, 50 times larger than ordinary irradiation method of Mo-98 in LWR.

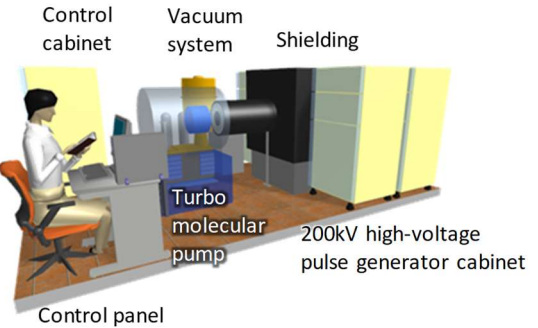
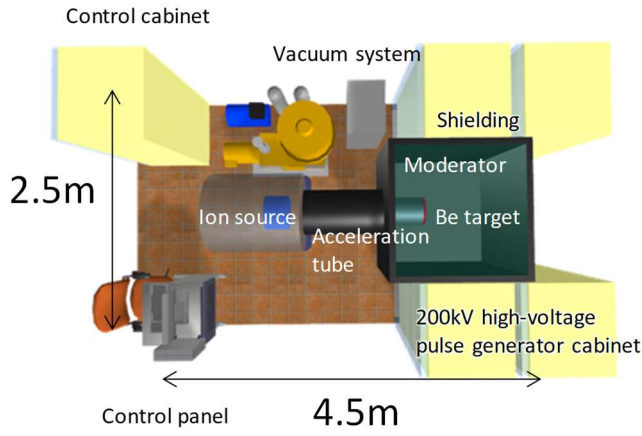


*FIG. 6. Absorption cross-section of Mo-98 [JENDL-4.0].*

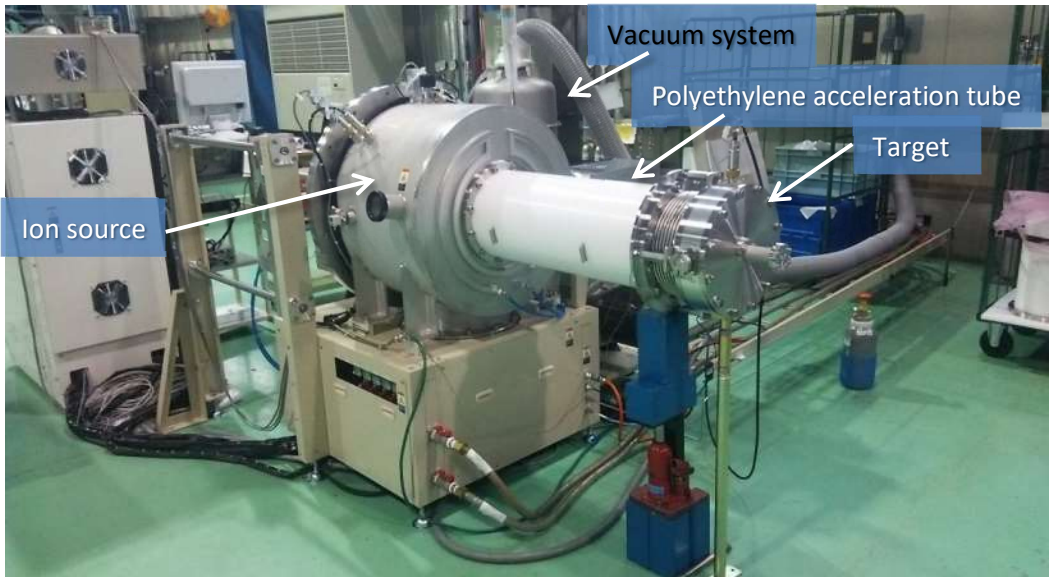
We are now fabricating prototype of TRANS-200C (Fig. 7) and will demonstrate Mo-99 production using natural Mo under collaboration with KAKEN in February 2015. The results will also be used to evaluate our concept of NTD-Th.

#### 4. SUMMARY

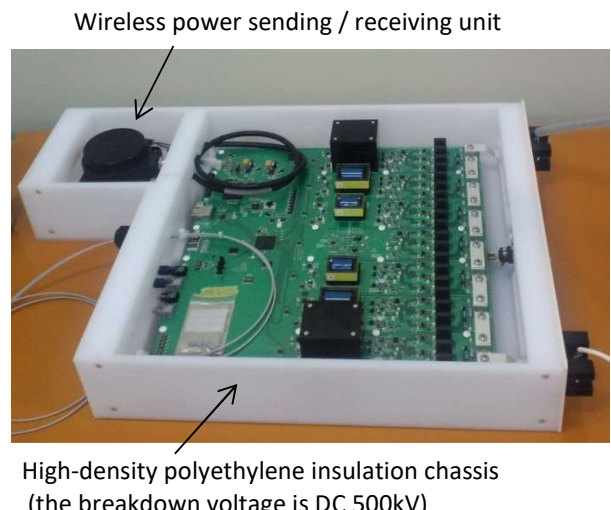
A new concept of accelerator neutron source named TRANS is now under development for the purpose of thorium nuclear fuel production. TRANS can generate large amounts of neutrons at low manufacturing and operation cost. Thorium-uranium-233 alloy (NTD-Th) can be produced with very little contamination of U-232 by adopting a low acceleration energy. Preliminary calculations show that about 1.2 kg of U-233 can be produced by an 8-barreled TRANS in a year. This evaluation will be done in detail by using PHITS code in near future. The prototype of TRANS will be used for producing Mo-99 in February 2015 also for evaluation of NTD-Th. NTD-Th adopting TRANS is expected to bring a way to solve the problem of thorium which would have a significant role for constructing sustainable society.



(b) Schematic of side view



(d) SiC high-voltage pulse generator cabinet



(e) 8kV/240A-peak SiC switching module

FIG. 7. TRANS-200C (prototype).

## REFERENCES

- [1] INTERNATIONAL ENERGY AGENCY, World energy outlook, (2009).
- [2] INTERGOVERNMENTAL PANEL ON CLIMATE CHANGE, Fifth Assessment Report (2014).
- [3] INTERNATIONAL ATOMIC ENERGY AGENCY, CO<sub>2</sub> Emissions from Fuel Combustion 1971–2005, IAEA, Vienna (2007).
- [4] NISHIKAWA, Y., Resource development the potential for thorium in power generation, Mining Journal (2 August 2013) 15.
- [5] NISHIKAWA, Y., Another nuclear renaissance, Mining Journal (6 May 2011) 15.
- [6] HUMPHRIES, M., Rare Earth Elements: The Global Supply Chain, Congressional Research Service (16 December 2013).
- [7] WADA, Y., A Radioactive Thorium Pollution Case in Malaysia: Asian Rare Earth Incident Revisited, Rare Earth Symposium, University of Queensland, Brisbane, Australia (31 May 2013), <http://www.csrm.uq.edu.au/docs/Yoshi.pdf>
- [8] KAMEI, T., Preliminary study of development of the organization of rare-earth exportation countries (OREEC), Journal of Sustainable Development of Energy, Water and Environment Systems **1** 1 (2013) 1–13.
- [9] KAMEI, T., Study of nuclear environment & material strategy, Nuclear Safety and Simulation **2** 4 (2011) 338–348.
- [10] KAMEI, T., A study of functions of “The bank (thorium energy bank)”, Nuclear Safety and Simulation **4** 1(2013) 67–71.
- [11] KAMEI, T., HAKAMI, S., Evaluation of implementation of thorium fuel cycle with LWR and MSR, Progress in Nuclear Energy **53** 7 (2011) 820–824.
- [12] KAMEI, T., Symbiotic energy demand and supply system based on collaboration between rare-earth and thorium utilization, Nuclear Safety and Simulation **2** 2 (2011) 178–190.
- [13] KOKUBO, Y., KAMEI, T., “Conceptual design of thorium-fuelled mitrailleuse accelerator-driven subcritical reactor using D-Be neutron source”, Proceedings of the PHYSOR2012, Knoxville, TX, USA, 15–20 April 2012 (2012).
- [14] CLAYTON, J.C. “The shippingport pressurized water reactor and light water breeder reactor”, 25th Central Region Meeting American Chemical Society, Pittsburg (1993), [http://www.iaea.org/inis/collection/NCLCollectionStore/\\_Public/25/025/25025940.pdf](http://www.iaea.org/inis/collection/NCLCollectionStore/_Public/25/025/25025940.pdf)
- [15] RUBBIA, C., “Status of the energy amplifier concept”, Proc. 2nd International Conference on Accelerator-driven Transmutation Technologies and Applications **1** (1997) 35–51.
- [16] MANSANI, L., ARTIOLI, C., SCHIKORR, M., RIMPAULT, G., ANGULO, C., DE BRUYN, D., The European Lead-cooled EFIT Plant: An industrial-scale accelerator-driven system for minor actinide transmutation: I, Nuclear Technology **180** 2 (2012) 241–263.
- [17] MASON, T. E., ABERNATHY, D., ANDERSON, I., ANKNER, J., EGAMI, T., EHLERS, G., ZHAO, J., The Spallation Neutron source in Oak Ridge: a powerful tool for materials research, Physica B: Condensed Matter **385** (2006) 955–960.
- [18] HAWKESWORTH, M.R., Neutron radiography: equipment and methods, Atomic Energy Review **15** 2 (1977) 169–220.
- [19] TANENBAUM, M., MILLS, A. D., Preparation of uniform resistivity n-type silicon by nuclear transmutation, J. Electrochem. Soc. **108** 2 (1961) 171–176
- [20] SATO, T., NIITA, K., MATSUDA, N., HASHIMOTO, S., IWAMOTO, Y., NODA, S., OGAWA, T., IWASE, H., NAKASHIMA, H., FUKAHORI, T., OKUMURA, K., KAI, T., CHIBA, S., FURUTA, T., SIHVER, L., Particle and heavy ion transport code system, PHITS, version 2.52. Journal of Nuclear Science and Technology **50** 9 (2013) 913–923.
- [21] ROSENTHAL, M. W., HAUBENREICH, P. N., MCCOY, H. E., MCNEESE, L. E., Recent progress in molten-salt reactor development, Atomic Energy Review **9** 3 (1971) 601–650.
- [22] KANG, J., VON HIPPEL, F. H., U-232 and the proliferation-resistance of U-233 in spent fuel, Science & Global Security **9** 1 (2001) 1–32.

# **CHALLENGES OF DEVELOPMENT OF REGULATORY CONTROL FOR URANIUM MINING IN DEVELOPING COUNTRIES TO ACHIEVE REGULATORY COMPLIANCE — TANZANIAN EXPERIENCE**

A. KILEO, D. MWALONGO, A. MWAIPOPO,  
S. MDOE, I. MKILAHA  
Tanzania Atomic Energy Commission,  
Arusha, Tanzania

## **Abstract**

Managing radiation and waste in uranium mining is of paramount importance for the protection of occupational workers, the public and the environment. Responsibilities of the parties which are involved in this part of Nuclear Fuel Cycle are outlined in the legislation and regulations governing the uranium prospecting, mining and processing. The Tanzania Atomic Energy Commission, as regulator for nuclear science and technology applications, has developed the legislations for exploration, construction, mining and milling, packaging and transport of yellow cake and finally decommissioning of uranium mine sites in Tanzania. This paper outlines the challenges in developing these legislations to meet the international standards, particularly in the area of radiation protection. The paper also reviews and analyses gaps and shortcomings, currently being addressed, for safe and sustainable uranium mining in United Republic of Tanzania.

## **1. INTRODUCTION**

Uranium is a naturally occurring element with an average concentration of 2.8 parts per million in the earth's crust. It is mostly used as fuel for nuclear power plants; a small fraction is used for production of medical isotopes, marine propulsion as well as developing nuclear weapons. Through a system of safeguards, the IAEA in collaboration with Member States works to make sure that uranium is used for safe and peaceful purposes. Uranium exploration activities carried in Tanzania since 1970s, and continued from 2007, have indicated potentially economically viable uranium mines in different parts of the country including Manyoni in Singida, Bahi in Dodoma and the Mkulu River in Ruvuma (Nyota). A summary of the established resources is given in Table I which includes the grades.

TABLE I. URANIUM RESOURCES OF TANZANIA<sup>30</sup>

| Deposit name                 | Resources (tU) | Grade (%U) | Estimated in | Type      | Sub-type         | Operator               |
|------------------------------|----------------|------------|--------------|-----------|------------------|------------------------|
| Likuyu North                 | 2308           | 0.020      | 2011         | Sandstone | Tabular          | Uranex NL              |
| Manyoni District-Zone A      | 1771           | 0.0127     | 2008         | Surficial | Lacustrine-playa | Uranex NL              |
| Manyoni District-Zone C 1    | 6122           | 0.0125     | 2011         | Surficial | Lacustrine-playa | Uranex NL              |
| Manyoni District-Zone C West | 347            | 0.0119     | 2011         | Surficial | Lacustrine-playa | Uranex NL              |
| Manyoni District-Zone E      | 2079           | 0.0110     | 2011         | Surficial | Lacustrine-playa | Uranex NL              |
| Manyoni District-Zone F      | 462            | 0.0119     | 2011         | Surficial | Lacustrine-playa | Uranex NL              |
| Manyoni District-Zone G      | 655            | 0.0127     | 2011         | Surficial | Lacustrine-playa | Uranex NL              |
| Mtonya                       | 770            | 0.022      | 2013         | Sandstone | Tabular          | Uranium Resources Inc. |
| Nyota                        | 45600          | 0.025      | 2011         | Sandstone | Tabular          | Mantra/ Uranium One    |

<sup>30</sup> Source: IAEA UDEPO database, extracted 2013.

In 2007, Tanzania recognized that any uranium mining needs to be taken care of by competent regulatory authority at each step due to national and international concern on safety and security. The International Atomic Energy Agency (IAEA), in collaboration with other national and international organizations, provided recommendations for uranium production in order to safeguard people and environment against radiation effects. Various national and regional IAEA Technical Cooperation projects were initiated since 2007 to upgrade regulatory knowledge and infrastructure in the specific area of uranium mining and processing in developing IAEA member states, particularly in Africa. In Tanzania, overall regulation of uranium mining is expected to be carried out by the Tanzania Atomic Energy Commission (TAEC), in accordance with the national regulations, international agreements and conventions for efficient and safe uranium production to be used for social economical purposes. Given that uranium mining in Tanzania is new, legislations specifically for uranium mining was formed. This legislation covered the exploration, construction, mining and milling, packaging and transport, waste management and decommissioning. The regulatory regime of uranium mining in Tanzania has adapted most of its regulatory infrastructure from that of Australia and developed them over time to time, starting from the Atomic Act of 2003 [1], the Protection from Ionizing Radiation Regulations of 2004 [2] and regulations for Packaging and Transport of Radioactive Materials [3]. The Radioactive Waste Management for the Protection of Human Health and Environment Regulation 1999 [4] and Radiation Safety in the Mining of Radioactive Minerals Ore Regulation 2011 [5] were developed, as well as the Mining (Radioactive Minerals) Regulations 2010 [6]. Each of them plays its role in safety and protection of people and the environment from the effect of radiation and associated waste generated from uranium mining. These legislations are categorized in two major areas:

- Those specifically for uranium mining such as Mining (Radioactive Minerals) Regulations [6] and Radiation Safety in Mining of Radioactive Minerals Regulation 2011 [5];
- Those generally for radiation protection for application of ionizing radiation like the Atomic Energy Act [1], Protection from Ionizing Radiation Regulation [2].

Note that originally legislation for the control of ionizing radiation in the United Republic of Tanzania was first enacted in 1983 through the protection from “Radiation Act, No. 5 of 1983” which was enacted in 1999.

In this study the current status of uranium mining and the regulatory infrastructure in Tanzania is explained and challenges and the gaps are identified. Recommendations for addressing the shortfalls and some enhancement are made in order to achieve good practice for uranium mining in Tanzania and comply with the international standard and conventions.

Figure 1 shows the basic elements of the regulatory framework. From the figure it is apparent that the regulatory framework relies on the enabling legislation, which in this case is the Atomic Energy Act no. 7 of 2003 [1]. However, owing to the fact that during the development of the Act there uranium mining was not anticipated, this act would need revision to take into account a series of new requirements.

## Elements of the Regulatory Framework

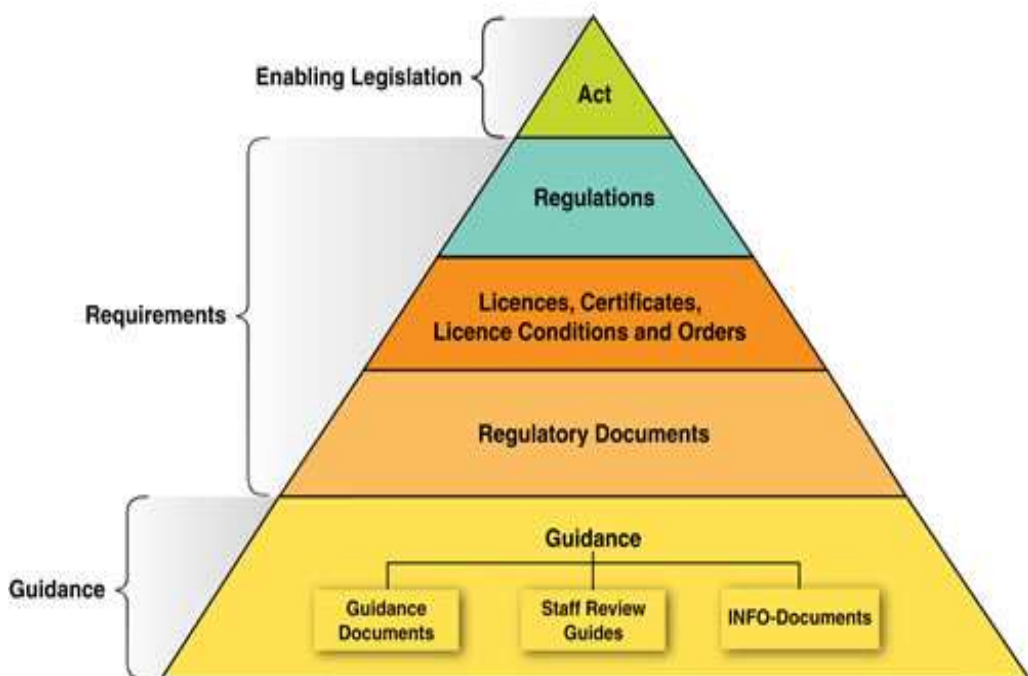


*FIG.1. Key elements of regulatory frameworks (adapted from IAEA presentations).*

In this paper it is the concepts of the other main elements that will be analysed and presented so as to accommodate the uranium mining. However, the key steps that were adopted by the United Republic of Tanzania (URT) in developing regulatory systems for uranium mining involved:

- a) *Knowledge acquisition*: In this case, a system for educating staff in the area was undertaken and accommodated in the programmes that existed while new ones were established. The main goals included developing capabilities to regulate the safe and secured uranium mining in Tanzania;
- b) *Developing regulatory framework*: In this step, experiences were drawn from other States and other established standards and procedures to develop this needed framework;
- c) *Creating awareness among regulators*: In this case, different regulators are sensitized so that the knowledge and experiences of uranium mining are shared;
- d) *Inviting stakeholders and key organizations to assess the regulatory approach*: After a framework is drawn, contract such international organizations to assess and advise on any improvements so that we can ensure safe and secured uranium mining;
- e) *Improve the regulatory framework*: At this stage an improvement strategy was to be taken to ensure safe and secured uranium mining.

Presented in this paper is an undertaken of the above strategic activities as a means of sharing experiences. In carrying out this, there are some shortfalls that followed and were tackled as they appeared. These included:

- Ignorance on the needs and requirements of uranium mining;
- Rigidness in accepting new approaches especially on some regulators who thought uranium mining could be treated like any other mine;
- Anti-uranium mining activists who mislead most of the ordinary public in falling to misconceptions.

## 2. URANIUM MINING

While large scale commercial mining commenced many years ago, mining of uranium is yet to commence in Tanzania and hence is a new sub-industry of mining compared to other types of minerals. The study indicates that nuclear technology applications in the area of medicine, research and industrials are equally at infancy stage in Tanzania, but due to safety and security requirement for uranium, TAEC, in collaboration with other stakeholders, has set different statutes that regulate and control all activities associated with uranium exploration, development, mining, decommissioning, waste management and transportation of yellow cake in the URT.

In Tanzania, uranium exploration is regulated by different authorities. TAEC is the engine for regulatory control in this industry responsible for overall protection of people and environment from hazards of radiation generated from the uranium mining. It was established by the Tanzania Atomic Energy Act No. 7 of 2003 [1] after the repeal of the former Protection from Radiation Act No 5 of 1983 which formed the National Radiation Commission.

Other regulatory authorities are the Ministry of Energy and Minerals (MEM) which is responsible for authorization of prospecting and licensing of the mining activities, the National Environmental Management Council (NEMC) which has duty to protect the environment. Each of these imposes its power to regulate the industry for safety, security and social economic development of the uranium mining in the United Republic of Tanzania. The development of the regulatory infrastructure of the uranium mining in Tanzania has covered the exploration, development and construction, mining and milling, transportation and waste management and decommissioning (Fig. 2). In this study we are going to look the regulatory regime for each phase and analyse regulatory challenges based on the international standards.

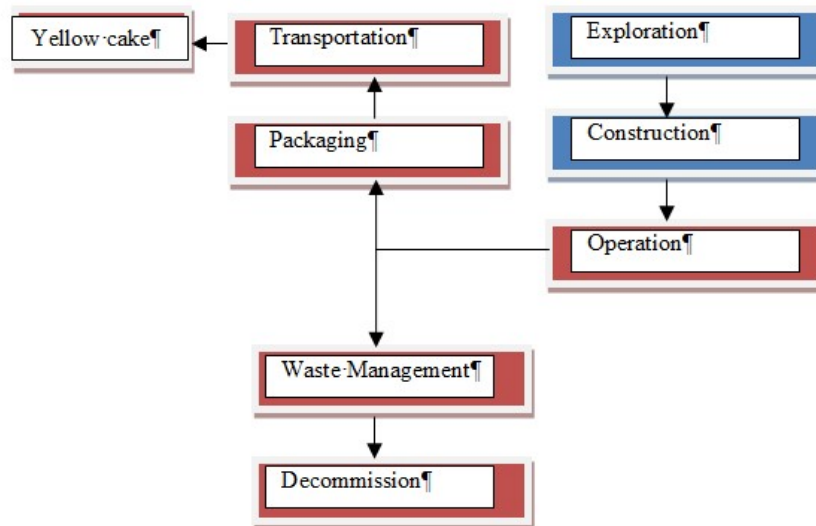


FIG. 2 Uranium production life cycle activities for application in Tanzania.

## 3. REGULATORY FRAMEWORK FOR URANIUM MINING

### 3.1. Exploration

Uranium exploration started in Uluguru Mountains in 1953. At that time there were no controls for exploration by Regulatory Authority, although no uranium mines were established. The rise in price for uranium triggered exploration activities in 2007, when deposits with potentially economically viable uranium were discovered and regulatory control of this sector started. Despite the number of regulators being many, the steps of regulation remain the same. These are described herein.

### *3.1.1. Prospecting licenses*

The MEM has jurisdiction over all mining activities including the uranium mining where the prospecting license in URT is offered by the Ministry for any company intending to do mineral exploration in Tanzania, according to Section 6 of the Mining Act, 2010 [2], whereby ‘no person shall, on or in URT prospect for minerals or carry on mining operations except under the authority of a mineral right granted or deemed to have been granted, under this Act’. Also under Section 1 of the regulation for radioactive minerals [2] its prohibited to prospect unless granted license form MEM, TAEC, NEMC and other authorities. In 2003 the government through MEM, TAEC and NEMC licensed Mantra and Uranium One for exploration of uranium in Bahi, Mkuju and Manyoni. The Mkuju River project under Mantra has shown potentially economically recoverable ore bodies which prompted Mantra to move towards development and construction of the mine site which require approval from the TAEC.

### *3.1.2. Environmental impact assessment*

The regulatory authorities before approving or licensing, the facility, conducts pre-authorization assessment establish that the facility is not likely to cause significant adverse environmental effects, or should such effects exist, steps to address them be implemented to mitigate the effects [7]. Uranium One (Mantra Tanzania Ltd) submitted the Environmental Assessment Report to TAEC as well as to NEMC and MEM for review.

The environmental aspects of uranium mining in Tanzania is regulated by the three authorities; TAEC under section 44 [1] and the Ministry of Energy and Minerals in consultation with the NEMC to carry out a review. This involves the establishment of a system for determination and control of radiation exposures associated with naturally occurring radioactive materials including mining and processing activities.

## **3.2. Development and construction**

Site evaluation construction and preparation stage is the second in uranium mining where by the regulatory authority assess the design, the license is provided when the operator meets the requirement as provided in regulation. Principally, MEM and NEMC have been licensing and authorizing such other mines like gold, diamonds, tanzanite and the like without taking the staged approach. Therefore, with uranium mining, it is necessary to have this stepwise authorization. This includes the mine development and operation, milling, packaging and transportation. The planned regulatory regime will involve staged authorization which will consider development, operation decommissioning and wastes management.

## **3.3. Uranium mining and milling**

Recovering uranium oxide at Mkuju River Uranium Mine Project, with uranium mineralization near the surface, will involve the use of open pit techniques to extract the uranium ore and process the mined uranium ore by means of various techniques including in-situ leaching [8]. Emphasis here is on radiation safety, safeguards and waste management. Regulatory framework developed offers a chance of the authorization.

## **3.4. Uranium transportation**

The Atomic Energy Act of 2003 Part two section 3 of the regulation [2] it is stated that, a person shall not acquire, store, transport, import or export radioactive minerals unless he obtains a permit granted by the Minister by filling in a specific form for such activity. Uranium oxide concentrate, or yellowcake, is transported from the mines to conversion plants in 200-litre drums packed into normal shipping containers. No radiation protection is required beyond having the steel drums secured and clean and kept in the shipping containers, thus it is licensee’s responsibility to make sure that the containers that transporting the yellow cake are certified by the regulatory authority.

### **3.5. Waste management**

Uranium mines and mill tailings may cause environmental pollution, hence the need for regulatory control. The soil and groundwater at and around the uranium mining and milling site may also experience similar pollution which needs regulatory intervention. The waste resulting from the uranium mining will be regulated by national and international law, policies and regulations. The regulations [2] stipulates that the holder shall make sure that the disposal of any radioactive mineral is done in a manner which shall not cause any harm or damage to any person, animal or the environment.

The radioactive materials contamination is explained in Section 6 of the regulations [2]. A holder shall store the contaminated equipment and materials in a secured and fenced off area and shall ensure that at all times the area has appropriate warning signs indicating the levels of radioactive hazards that are possible in the premises and site and that signs are displayed in conspicuous locations. Table II shows all the regulatory entities as stipulated in their relevant laws and regulations. However, in realizing the major role that TAEC has to play in uranium mining in Tanzania, a number of actions were planned and undertaken as per Table III below. Most of these activities were undertaken beyond the Commission involving major stakeholders including other regulators.

### **3.6. Decommissioning**

Decommissioning is the post-operation phase of the uranium mining which involve the decontamination and dismantling of the facility to ensure permanently safety of people and environment now and in the future. Important aspects like the competent regulatory infrastructure, national policy for environment, funding mechanism, strategy for stakeholder involvement has been mentioned to be an obstacle for safe uranium mining decommissioning if they are not adhered to [9, 10]. TAEC is revising the existing regulations to accommodate these aspects.

TABLE II. REGULATORY BODIES AND THEIR RESPONSIBILITIES

| Institution                               | Responsibilities                                  | Phase   | Remarks  |
|---|---|---|--|
| Tanzania Atomic Energy Commission         | Occupational, public and environmental protection | Exploration, development, mining and milling, packaging and transportation              | Other regulatory authorities are also involved in each stage |
| Ministry of Energy and Minerals           | Authorize prospecting                             | Prospecting, exploration, development, mining and milling, packaging and transportation | Other regulatory authorities are also involved in each stage |
| National Environmental Management Council | Environmental protection                          | Exploration, development, mining and milling, packaging and transportation              | Other regulatory authorities are also involved in each stage |
| Occupational and Safety Authority         | Occupational protection                           | Exploration, development, mining and milling, packaging and transportation              | Tanzania Atomic Energy Commission is also involved           |
| Surface and Marine Transport Authority    | Road safety                                       | Transportation  | Tanzania Atomic Energy Commission is also involved           |

TABLE III. PREPARATORY STAGES OF REGULATORY ACTIONS FOR URANIUM MINING

| Nº | Stage          | Risks   | Action                   | Status  |
|----|----------------|---|--------------------------|---|
| 1  | Exploration    | Naturally Occurring Radioactive Materials (NORMs) risks | Regulations on NORMs     | Development   |
| 2  | Development    | Limited time of exposure                                | Procedures and licensing | Regulations developed, Procedures under development |
| 3  | Mining         | Long-term exposures and dusts                           | Procedures and licensing | Regulations developed, Procedures under development |
| 4  | Milling        | Exposure and dusts                                      | Procedures and licensing | Regulations developed, Procedures under development |
| 5  | Transportation | Radiation risks   | Procedures and licensing | Regulations developed, Procedures under development |

#### 4. URANIUM MINING REGULATION GOOD PRACTICE

Although there are overlapping mandates within the Government agencies, collaboration between them has reduced most of the problems. This aspect also featured during the IAEA UPSAT (Uranium Production Site Appraisal Team) mission [11] and some suggestions for harmonization made.

##### 4.1. Challenges

There are four major challenges in regulatory infrastructure development in Tanzania for uranium mining:

- Inadequate regulations;
- Inadequate resources;
- Overlapping mandates;
- Inadequate specific experience.

These are discussed in turn below, and recommendations are included in the final sections.

###### 4.1.1. *Inadequate regulations*

There are different sections which impose the enforcement in the legislations through penalties, imprisonment or both, yet these penalties and enforcement have not been described in occupational workers, safety, general public and the environment. For example, Section 5 [2] states “A holder shall ensure that a person shall not carry work involving Radioactive materials unless they have passed a medical examination and they shall be given a similar examination every time the physician deems it necessary”, this currently has no enforcement. A system for implementation and enforcement is needed

###### 4.1.2. *Inadequate resources*

Uranium mining, as stated earlier, is a new industry in Tanzania, and there is a significant skill gap and equipment shortcomings that need to be attended for efficient and effective regulatory control. Whilst on the one hand the proponents are well trained with good experience in the industry, on the other hand the regulator is new in this industry (whilst already competent in industrial and medical radiation protection). Since the industry requires competent regulatory authorities to regulate uranium mining

activities, human capital development as well as suitable equipment are required for the regulatory authorities be effective.

#### *4.1.3. Overlapping mandates*

In developing the Tanzania Atomic Energy Commission's regulations for uranium production cycle, reference was made to international guidelines especially the International Basic Safety Standards for Protection against Ionizing Radiation and for the Safety of Radioactive Sources (BSS), published by the IAEA as Safety Series No. 115 in 1996 and updated in 2011 [12]. The uranium mining sub sector is regulated by different Government authorities, each mandated to impose its power and responsibility for aspects of safety and security. Coordination is required to minimise overlap and avoid gaps, and ensure government resources are responsibly used.

#### *4.1.4. Inadequate specific experience*

Whilst the TAEC was established 1983 it has experience in medical, and industrial application, uranium mining is new therefore it and the other regulators lack specific experience in the uranium industry specifically.

### 5. DISCUSSION

Following various discussions and meetings as well as the UPSAT mission, an analysis was carried out to indicate how important it is to have an effective regulatory framework for the uranium mining and milling in Tanzania. The challenges and recommendations were drawn and advanced to the Central Government for further guidance. The following affirmative actions have been decided and a direction given so that:

- All the relevant laws and regulations need be reviewed to accommodate the decision to have TAEC the leading regulator in the activities of mining of radioactive ores;
- A stakeholders meeting to discuss the recommendations on this review called and a consensus reached;
- All the laws and regulations be amended accordingly to accommodate the above.

All these processes have commenced, with a team doing the necessary revision and once completed a meeting will be called. During these steps, the International community will be taken on board through the involvement of the IAEA.

Indeed, following this decision, TAEC, in collaboration with IAEA and other key stakeholders, have an important role of ensuring that the regulatory infrastructure for uranium exploration, development, mining, milling, transport and the management of radioactive waste are undertaken according to international good standards.

### 6. RECOMMENDATIONS

- The TAEC has a duty to develop the policy, update regulations, prepare a code of practice for safe uranium mining; other regulatory authority should seek advice from the Commission in its areas of expertise;
- Additional capacity building for regulators, training for nuclear law, uranium mining and processing is required;
- An outreach program for occupational, public and environmental exposure is required to offset the negative perceptions of uranium mining;
- There should be strong enforcement provisions and penalties for non-compliance in this area due to its sensitivity;
- The overlapping mandates between the Government authorities can be eliminated or avoided through establishing a top level steering committee to harmonize the uranium subsector through the following activities:

- Sharing of information and resources;
- Jointly developing monitoring and inspection programs;
- Developing means to resolve possible disputes among the authorities.

## ACKNOWLEDGEMENTS

The authors would like to thank International Atomic Energy Agency (IAEA), for their support through different projects specifically the UPSAT mission.

## REFERENCES

- [1] UNITED REPUBLIC OF TANZANIA, The Atomic Energy Act, No. 7 of 2003 (2003).
- [2] UNITED REPUBLIC OF TANZANIA, Atomic Energy (Protection from Ionizing Radiation) Regulations (2004).
- [3] UNITED REPUBLIC OF TANZANIA, The Packaging and Transport of Radioactive Materials Regulations (2011).
- [4] UNITED REPUBLIC OF TANZANIA, Radioactive Waste Management for the Protection of Human Health and Environment Regulation (1999).
- [5] UNITED REPUBLIC OF TANZANIA, Radiation Safety in the Mining and Processing of Radioactive Ores Regulation (2011).
- [6] UNITED REPUBLIC OF TANZANIA, Mining Act (Radioactive Minerals) Regulation (2010).
- [7] INTERNATIONAL ATOMIC ENERGY AGENCY, Establishment of Uranium Mining and Processing Operations in the Context of Sustainable Development, IAEA Nuclear Energy Series NF-T-1.1, IAEA, Vienna (2009).
- [8] BOYTSOV, A., STANDER, S., MARTYNENKO, V., “The outlook on potential uranium ISL mining at Nyota Deposit (Tanzania)”, Proc. Int. Symp. Uranium Raw Material for the Nuclear Fuel Cycle: Exploration, Mining, Production, Supply and Demand, Economics and Environmental Issues (URAM-2014), Vienna, 2014, IAEA Vienna (this volume).
- [9] FRANKLIN M., FERNANDES H., Identifying and overcoming the constraints that prevent the full implementation of decommissioning and remediation programs in uranium mining sites, *J. Environ. Radioactivity* **119** (2013) 48–54.
- [10] World Nuclear Association. Safe Decommissioning of Civil Nuclear Industry Sites. (September 2006), <http://www.world-nuclear.org/WNA/Publications/WNA-Position-Statements/Safe-Decommissioning-of-Civil-Nuclear-Industry-Sites/> [Accessed January 2015].
- [11] TULSIDAS, H., Mining Uranium; With an eye on ‘sustainable’ mining, Tanzania hosts Uranium Production Site Appraisal Team, IAEA Fuel Cycle and Waste Newsletter **9** 2 (Sept. 2013) 11, ([http://www.iaea.org/OurWork/ST/NE/NEFW/Technical-Areas/NFC/documents/uranium/Tulsidas\\_2013\\_UPSAT\\_Tanzania.pdf](http://www.iaea.org/OurWork/ST/NE/NEFW/Technical-Areas/NFC/documents/uranium/Tulsidas_2013_UPSAT_Tanzania.pdf)) [Accessed April 2015].
- [12] INTERNATIONAL ATOMIC ENERGY AGENCY, Radiation Protection and Safety of Radiation Sources: International Basic Safety Standards (Interim Edition), General Safety Requirements Part 3 (IAEA GSR–Part 3), IAEA, Vienna (2011).

# **DEVELOPMENTS IN THE MODELING APPROACH FOR RADIOLOGICAL SAFETY ASSESSMENT OF U-238 SERIES RADIONUCLIDES IN WASTE DISPOSAL**

D. PÉREZ-SÁNCHEZ\*, M. THORNE\*\*

\* CIEMAT,  
Departamento de Medio Ambiente,  
Madrid, Spain

\*\* MTA Limited, Hamsterley,  
Bishop Auckland, Durham,  
United Kingdom

## **Abstract**

The migration of radionuclides in the U-238 decay series in soils and their uptake by plants is of interest in various contexts, including the disposal of radioactive waste and the remediation of former sites of uranium mining and milling. In order to investigate the likely patterns of behaviour of U-238 series radionuclides being transported through the soil column, a detailed soil-plant model originally developed for studying the redox behaviour of radionuclides in soil-plant systems has been adapted to make it applicable to the U-238 series. Hydrological conditions are a primary factor, both in respect of the overall advective flow deeper in the soil, which controls the rate of migration, and in the influence of seasonally changing flow directions closer to the soil surface, which can result in the accumulation of radionuclides at specific depths irrespective of changes in sorption between the oxic and anoxic regions of the soil. However, such changes in sorption can also be significant in controlling the degree of accumulation that occurs. This importance of seasonally varying factors in controlling radionuclide transport in soils even in very long-term simulations is a strong argument against the use of annually averaged parameters in long-term assessment models.

## **1. INTRODUCTION**

Human and environmental radiation exposures from sites or areas contaminated with radioactive substances need to be quantified as part of the risk assessment process and for developing long-term remediation strategies. In most radiological assessment models, simplistic, empirical ratios are used to simulate contaminant transfers between environmental compartments. These are favoured because they facilitate modelling. Their use, however, significantly increases the uncertainty of model predictions, because they do not account for the underlying processes that govern spatial and temporal variations in radionuclide concentrations. In relation to more explicit, process-based modelling, representation of the migration of radionuclides in the U-238 decay series in soils and their uptake by plants is of interest in various contexts, including the disposal of radioactive wastes and the remediation of former sites of uranium mining and milling.

The structures of models used to assess doses in the biosphere for long-term waste disposal assessments have not changed significantly in the last few years. Several aspects of the model representations of the biosphere are currently being debated in international forums, and these aspects would benefit from further investigation. The potential topics of interest include biogeochemical zonation of radionuclides in the sub-surface, caused by changes in the redox characteristics in response to a variable water table. It has been proposed that traditional model structures are not able to represent this aspect of the system adequately.

Many models for transfer of radionuclides from soil to plants adopt a simple well-mixed approximation for soils and equilibrium transfer factors for uptake by plants. Such models are inadequate to represent the redistribution of radionuclides in soils and uptake by plants for short-term releases or when the characteristics of the system change with time. About twenty years ago, a new generation of multi-

compartmental models was developed to address these issues [1–3]. However, these models remained multi-compartmental in nature and did not explicitly represent the physical processes that are taking place. More recently, physically based models based on use of the advection-dispersion equation for transfers in soils and Michaelis-Menton kinetics for uptake by plant roots have been developed [4]. However, such models require much more extensive data than are needed for the more conventional assessment models and their range of applicability is not yet well-established.

Major improvements are needed to make models more process-based and capable of simulating the kinetics of contaminant transfers. A major challenge is to identify where the greatest advantages can be gained in reducing model uncertainty and understanding variability, developing criteria to identify if further research is required for parameterize dynamic-mechanistic models, and identifying the level of model complexity needed for specific exposure scenarios. The soil to plant interactions are a key part of modelling doses arising via the foodchain, they are common to all dose assessment models. In the past decade there has been divergence with models results showing a range of alternative treatments of soil to plants systems modelling approach. The trend has been to balance the detailed descriptions of transport sub-models in soil and surface waters with more detailed representations of the uptake by crops.

This paper reviews the processes that need to be represented in order to simulate the behavior of U–238 series radionuclides in long-term assessment models for soil-plant system for radioactive waste disposal [5], and proposes a model structure and associated mathematical model that can be used to investigate the potential impacts of seasonally variable conditions on the calculated radionuclide concentrations in soils and plants. This work looks also at the potential for the inclusion of spatio-temporal variability in models for long-term dose assessments.

## 2. MATERIALS AND METHODS

### 2.1. Modelling approach

The model was originally constructed to represent selenium transport and accumulation in soils and therefore takes into account variation in sorption as a function of water saturation and radionuclide transport in soils with local redox-sensitive behaviour in each of the layers [1]. As used here, this newly developed model was reconfigured and run for U–238 and Ra–226 only for Mediterranean conditions considering long-term issues [7]. The model adopts a 1D vertical compartment model (Fig.1) for soil that could represent flow through a full solution of Richards equation, however, as details of flow in the unsaturated zone are not needed a mass balance approach can be adopted in which precipitation inputs are balanced against losses by evaporation, transpiration and drainage, and any increase/decrease in storage in the soil.

In the model the evolution of the water content of each of the vertical compartments is computed by mass balance, taking account of precipitation and irrigation input ( $P$ ), evapotranspirative losses ( $E_i$ ), flows between horizontal layers ( $I_{i, i+1}$  and  $I_{i+1, i}$ , with the special case to groundwater (G) at the base of the model) and sub-horizontal drainage ( $H_i$ ).

The water content,  $Q_i$  of each of the vertical compartments is computed by mass balance, taking account of precipitation input ( $P$ ), evapotranspirative losses ( $E_i$ ), flows between horizontal layers ( $I_{i,i+1}$  and  $I_{i+1,i}$ , with the special case to groundwater ( $G$ ) at the base of the model) and subhorizontal drainage ( $H_i$ ). The mass balance equations can be written:

$$\begin{aligned}\frac{dQ_1}{dt} &= P + I_{2,1} - E_1 - I_{2,1} - H_1 \\ \frac{dQ_i}{dt} &= I_{i-1,i} - E_i - I_{i,i+1} - H_i \quad i = 2, 10 \\ \frac{dQ_{10}}{dt} &= I_{9,10} - E_{10} - I_{9,10} - H_{10}\end{aligned}\tag{1}$$

Quantities are considered for unit area so that  $Q_i$  has units of m and  $dQ_i/dt$  has units of m y<sup>-1</sup>. In practice, the equations as written apply only to under-saturated layers. When a layer is saturated, its water content cannot increase, and the corresponding equation becomes a balance equation (flow in equals flow out).

For dose calculations, the model includes also the plant uptake and cropping losses and the radionuclide is readily available to plants by root uptake and can be lost from the soil-plant system by cropping, also the radionuclide present in plant residues returned to soil will be mainly in organic form and will be released from organic material by mineralisation reactions over timescales. The results of the model give the hydrological behaviour for different soil layer and also the amount of radionuclide for all the compartments considered and the plant concentration according with density root distribution.

The mathematical structure of the model is essentially identical to that described previously in [8] and the model was implemented in the AMBER 5.4 simulation system **Error! Reference source not found.** that provides a simple method for encoding decay chains of any length. This meant that extending from the single-member decay to the full decay chain for U-238. Shorter-lived progeny of these radionuclides, notably the several generations of short-lived progeny of Rn-222, are considered to be present in secular equilibrium with their most immediate ancestor in the modelled chain.

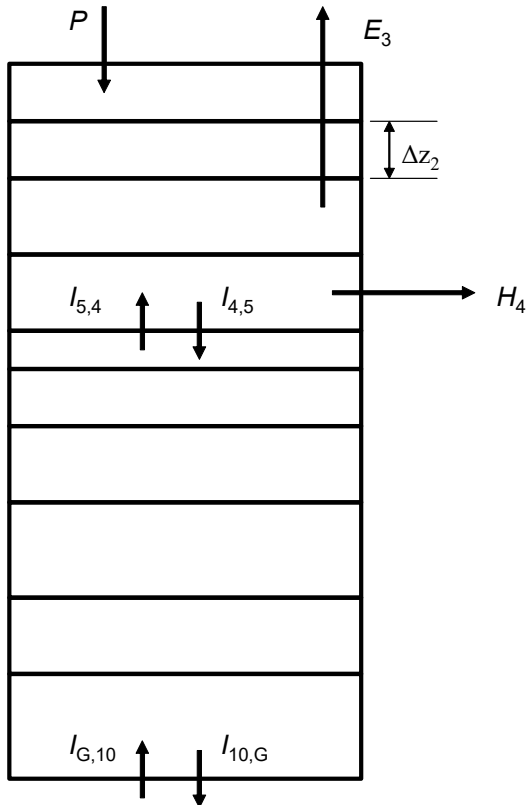


FIG. 1. CIEMAT's vertical compartment model for near-surface flow and transport modelling.

### 3. RESULTS AND DISCUSSION

For the waste management strategy is important to consider the near-surface water tables are of concern. A key concern in Spain is the variation of the water table height and the CIEMAT model implements a time-varying water table. Ten layers in the soil model are modelled and the water content of the individual layers therefore varied in time on a temporal scale of months. The model employed here by CIEMAT has been specifically developed to address the problem and to evaluate redox sensitivities of selenium [1]. The model has been revised to allow results for U-238 and Ra-226 (including daughters) to be calculated. This is the basis for the calculation for uranium and radium included in the results show above.

The example calculations carried out here focus on irrigated agricultural systems and compare the pathways by which crops can become contaminated as a result of irrigation with contaminated groundwater: namely by root uptake or direct foliar interception of contaminated irrigation water. Essentially, the model has been tested in a scenario for which they had largely been designed (representation of radionuclides transport and accumulation under temperate agricultural conditions) as well as scenarios which differed in important respects of hydrological regime and irrigation demand. The intention was to identify the modelling differences and, with contributions from a simple model used before, to discuss alternative approaches. A simple agricultural system has been described using a common basis (irrigation of cereals on a sandy, well-drained soil). Climatological data was taken from Spanish Mediterranean conditions.

Calculations were performed for a simulation period of 10 000 years. For the first 100 years of that period, model results were output at a time interval of 0.05 years, so that the detailed intra-annual variability could be observed. For the period from 100 to 10 000 years, results were output each mid-year because this gives representative concentrations. In the first set of calculations, U-238 was specified as the radionuclide present in irrigation water and due to, the long-lived nature of U-234, the in-growth of progeny is of limited importance when U-238 is added to soil in irrigation water.

Therefore, it was of interest to run the model for Ra-226, for which in-growth of Pb-210 and Po-210 occurs on a timescale of a few years.

Figs 2 and 3 provide a closer look at the results from the model for the irrigation scenario at temperate conditions. In Fig. 1, the top soil concentration is shown as a function of time, for the first ten years from the commencement of irrigation. With its lower distribution-coefficient ( $K_d$ ), the interannual variation for U-238 shows a series of peaks and troughs on an increasing trend with steady state established over a period of around ten years. For the more strongly sorbing Ra-226 there is an increase during the irrigation period, as with the Uranium, but the accumulated material is unaffected by varying water fluxes in the soil because of the high sorption. Concentration of Ra-226 stays constant during this period. For the less strongly sorbed uranium there is a loss during this period.

In Fig. 3, compared to the results for a simple one-compartment model the Ra-226 behaves in a fairly straightforward way on the long-term, the high  $K_d$  dominating over the variability caused by the fluctuating water table depth. The results show accumulation to similar levels in the upper soil. The single compartment results are higher but this can be accounted for by the distribution in the remainder of the 10-layer column.

The effect of the variable water table appears to be enhanced leaching of low  $K_d$ -species (U-238 here). The long-term equilibrium value for U-238 in the model is around one-and-a-half orders of magnitude lower than the simple interpretation of the case. Here the interannual variation is more pronounced, though not easily represented on the log-axis.

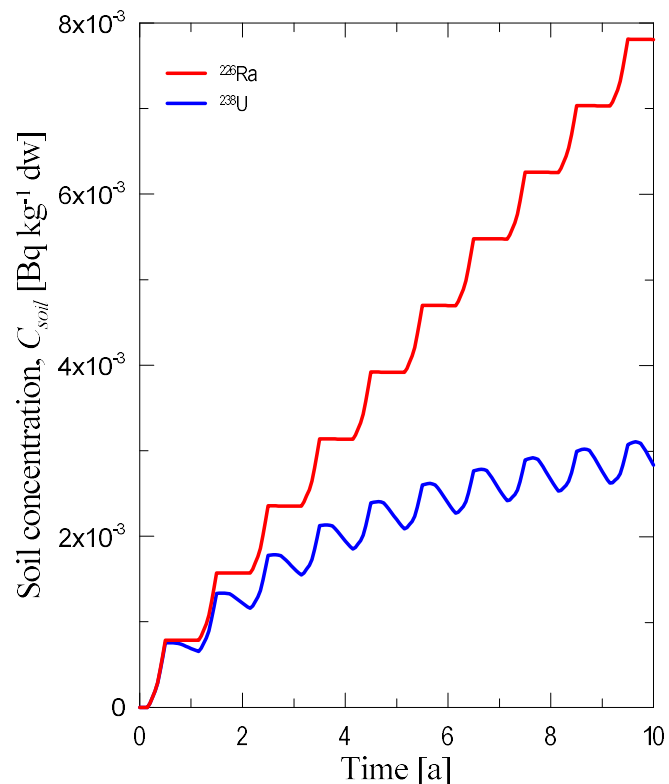
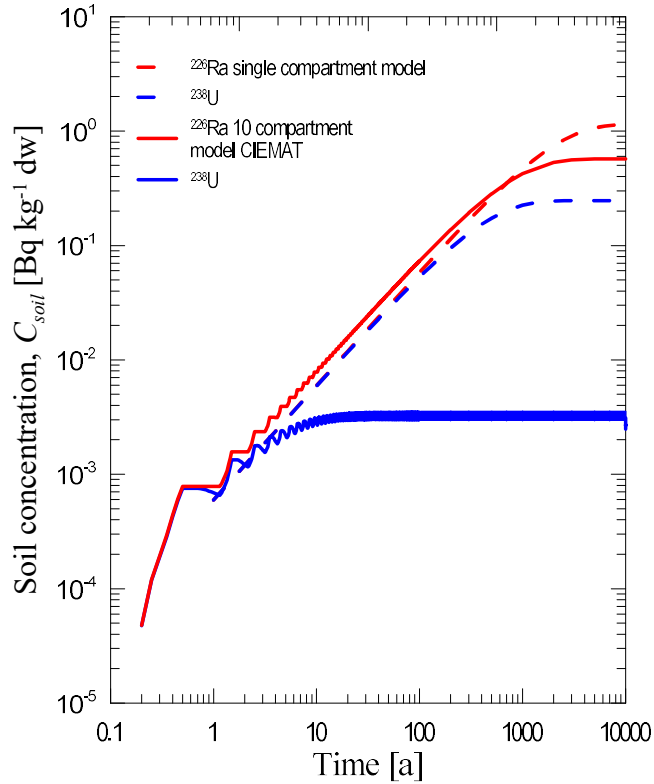


FIG. 2. Comparison of the results from the CIEMAT model with variable water table height and those for a single compartment model. Interannual variation in the concentration of the top 0.1 m of soil as a result of fluctuating water table for the first ten years after the start of irrigation.



*FIG. 3. Comparison of the results from the CIEMAT model with variable water table height and those for a single compartment model Long term accumulation in the upper soil over a period of 10 ka.*

#### 4. CONCLUSIONS

The model approach, constitute a powerfull tool for exploring the behaivour of radionculides in the soil-plant systems under different hydrological regimes. Describe key processes and variables controlling radionuclide transfers. The model is of interest because it is a multi-layer compartment model that makes use of monthly water balance figures to simulate the movement of the water table height and thereby to generate the water fluxes between and moisture content in ten equispaced soil layers as a function of time during each year **Error! Reference source not found.**. These fluxes are then used to drive radionuclides transport for U–238 and Ra–226 (with daughters).

Use of models more directly based on underlying processes also has implications for experiments which are likely to become more complex, as additional supplementary information will be required to characterise those processes and field studies (where multi-element analyses of samples will be important in determining the behaviour of contaminants and nutrients in relation to each other).

It is considered that this model will find application both in safety assessments relating to the disposal of radioactive wastes and in programmes relating to the clean-up of sites contaminated with Naturally Occurring Radioactive Materials (NORM) and U–mining remediation. Currently, the model is being applied in studies relating to the near-surface disposal of low-level radioactive wastes, taking into account both the transport of U–238 series radionuclides in groundwater and potential human intrusion resulting in the contamination of surface soils.

#### ACKNOWLEDGEMENTS

This work has been financially supported by the Empresa Nacional de Residuos Radiactivos (ENRESA) under agreement CIEMAT/ENRESA. However, the opinions expressed are those of the authors and do not necessarily represent those of the funding organizations. The authors would also like to thank Ryk Klos and Shulan Xu for their ideas and technical discussions on the subject.

## REFERENCES

- [1] THORNE, M.C., AND COUGHTREY, P.J., Dynamic models for radionuclide transport in soils, plants and domestic animals (COUGHTREY, P.J., BELL, J.N.B, ROBERTS, T.M., Eds), Ecological Aspects of Radionuclide Release, Blackwell Scientific Publications, Oxford, (1983).
- [2] NAIR, S., GROGAN, H.A., MINSKI, M.J., BELL, J.N.B., Models for the prediction of doses from the ingestion of terrestrial foods (COUGHTREY, P.J., BELL, J.N.B, ROBERTS, T.M., Eds), Ecological Aspects of Radionuclide Release, Blackwell Scientific Publications, Oxford (1983).
- [3] BROWN, J., SIMMONDS, J.R., FARMLAND: A dynamic model for the transfer of radionuclides through terrestrial foodchains, National Radiological Protection Board Report NRPB-R-273, UK (1995).
- [4] WHEATER, H.S., BELL, J.N.B., BUTLER, A.P., JACKSON, B.M., CICIANI, L., ASHWORTH, D.J., SHAW, G.G., Biosphere Implications of Deep Disposal of Nuclear Waste: The Upwards Migration of Radionuclides in Vegetated Soils, Imperial College Press, London (2007).
- [5] MITCHELL, N., PÉREZ-SÁNCHEZ, D., THORNE, M.C., A review of the behaviour of U-238 series radionuclides in soils and plants, *J. Radiological Protection* **33** (2013) R17–R48.
- [6] PEREZ-SANCHEZ, D., THORNE, M.C., LIMER, L.M.C., A mathematical model for the behaviour of Se-79 in soils and plants that takes account of seasonal variations in soil hydrology, *J. Radiological Protection* **32** (2012) 11–37.
- [7] PÉREZ-SÁNCHEZ, D., THORNE, M.C., Modelling the behaviour of uranium-series radionuclides in soils and plants taking into account seasonal variations in soil hydrology, *J. Environmental Radioactivity* **131** (2014) 19–30.
- [8] PÉREZ-SÁNCHEZ, D., AND THORNE, M. C., An Investigation into the Upward Transport of Uranium-series Radionuclides in Soils and Uptake by Plants, *J. Radiological Protection* **34** (2014) 545–573.
- [9] QUINTESSA, AMBER 5.4 Reference Guide, Quintessa Limited, Henley-on-Thames, UK (2010).
- [10] KLOS, R. LIMER, L., SHAW, G., PÉREZ-SÁNCHEZ, D., AND XU, S., Advanced spatio-temporal modelling in long-term radiological assessment models—radionuclides in the soil column, *J. Radiological Protection* **34** (2014) 31–50.

# **STEADY-STATE FLUID FLOW AS A COMPLEMENTARY DRIVER OF MINERALIZATION AND REDISTRIBUTION AT UNCONFORMITY-TYPE URANIUM DEPOSITS IN THE ATHABASCA BASIN, SASKATCHEWAN, CANADA**

G. RUHRMANN  
Private Consulting Firm,  
Wachtberg, Germany

## **Abstract**

Seismic pumping has been proposed as a driving force for fluid mixing and attendant U–precipitation near the Lower Proterozoic unconformity in the Athabasca Basin. Related strain-fluid modelling shows that multiple seismic pulses were necessary to generate the observed ore masses by tapping kilometre-scale U-reservoirs. 3D flow modelling presented here covers the intermittent seismically calm periods during which fluid flow was driven by other mechanisms. The results from a simulation of steady-state flow in a typical unconformity-related deposit setting suggest the formation of fluid-fluid, fluid-rock and fluid-ore interaction zones near an incompletely sealed structure. The contrast of hydraulic conductivity of the structure and that of wall rocks determines the vertical position of potential reaction zones relative to the unconformity. Highly permeable structures result in reaction zones below, while smaller contrast leads to reaction zones above the unconformity without having to invoke respective dilatant and compressive seisms. Basinal fluids driven by regional gradients entering mineralized structures may have caused uranium mobilization and in reaction with reducing basement rocks, reprecipitation along the structure.

## **1. INTRODUCTION**

It is a general consensus that the oldest mineralization event (approximately 1590 Ma) in the Athabasca Basin and subsequent remobilization and resetting of radiometric ages correlate with far-field, continent-wide tectonic events [1]. On a local scale, numerical modelling [2, 3] shows that faulting in a dilational regime may have driven oxidized uraniferous basinal fluids into reducing basement environment. In a compressional setting, basement fluids would have been injected into Athabasca Group rocks thereby precipitating uranium out of oxidizing basinal fluids. The results of transient modelling of porosity and permeability development during a faulting event [4] suggested that multiple seismic pulses were necessary to generate the observed ore masses by tapping kilometre-scale reservoirs [5].

The fluid flow model based on steady-state conditions presented here rests on the following premises:

- Regional flow in the basin during interseismic phases is quasi-steady state driven by one or several forces including sediment compaction, clay dehydration, meteoric infiltration and salinity or temperature-caused density differentials. Large-scale, i.e. several times larger than deposit size, thermal convection cells were shown to be reasonable in >5 km thick basin fill above a 30-km thick crust [6]. Numerical modelling of the fluid pressure regime suggests that fluid overpressure in a moderate range may have contributed to the flow of oxidizing fluids in the basal part of the basin [7];
- Each faulting episode disturbs temporarily the regional flow, which recovers within a certain time span [8]. The length of the recovery period is controlled by gradient, permeability and storativity of the fault material and wall rock, and may persist only tens to hundreds of years [9];
- The length of time between major faulting events followed by a recovery period is sufficiently long for steady-state conditions to re-establish;
- Repeated rupturing in active faults results in increased fracture porosity of fault zones [5];

- Accordingly, fault zones may provide conduits for steady-state fluid flow between recurrent faulting events.

The model presented here does not take into consideration the effects of gases or differential fluid densities.

## 2. APPROACH

Steady-state groundwater flow was investigated using a generic numerical flow model of a typical unconformity-related uranium deposit configuration in the Athabasca Basin. The model consists of an assemblage of basement rocks overlain by sedimentary rocks of the Athabasca Group and intersected by a strike-slip or reverse fault. The model was portrayed by MODFLOW-96, a computer program that numerically solves the three-dimensional groundwater flow equation for a porous medium using a finite-difference method [10–14]. The data input and post-processing of results were facilitated by the use of PMWIN [15, 16], version 8.0.34 (2011), an integrated graphical user interface for MODFLOW [17]. The current package of PMWIN and the visualization software is copyrighted by SIMCORE SOFTWARE.

The model consists of more than 50 000 active cells in 26 layers. The cell size ranges from  $5 \times 5$  m in fault zones to  $100 \times 100$  m in the surrounding wider area. Figure 1 depicts the model dimensions and Figure 2 the vertical discretization across the centre of the fault.

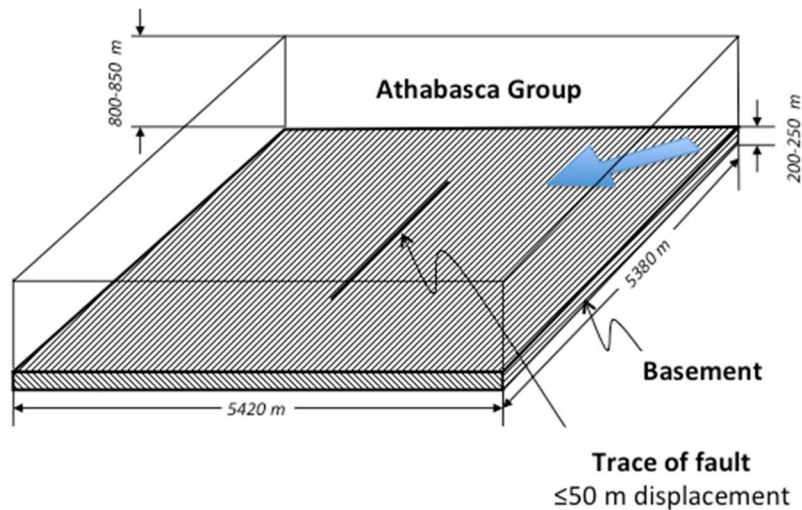


FIG. 1. Model dimensions. The arrow indicates the general direction of regional flow.

The basement and Athabasca Group rocks are treated as a continuum, i.e. spatially defined values of hydraulic conductivity and porosity were assigned. This approach is valid as long as the microfracture and fissure spacing is sufficiently dense that the fractured medium acts in a hydraulic fashion similar to granular porous medium [18]. The fault was simulated by assigning a hydraulic conductivity larger than that of the neighbouring medium. Table I provides an overview of parameters used and their sources [18] and [19].

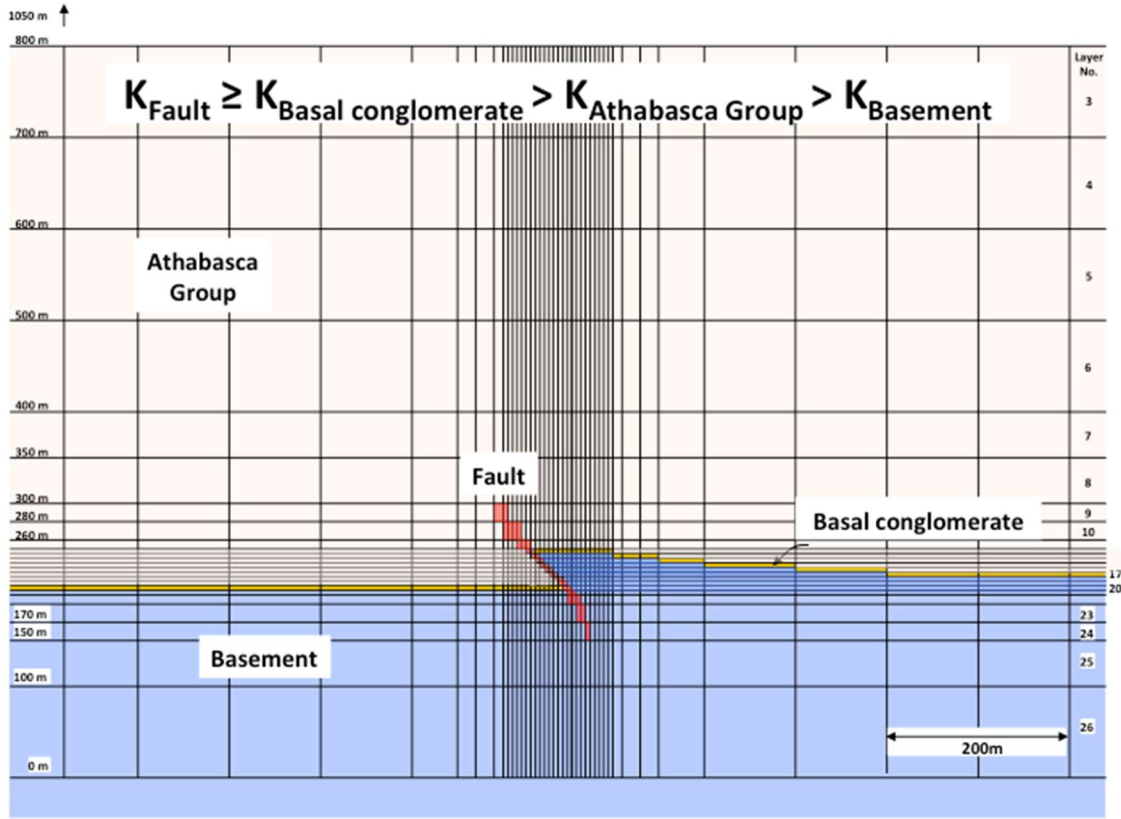


FIG. 2. Vertical discretization across the centre of the reverse model fault.

Advection flow modelling was performed with PMPATH [20], version 8.0.31, a particle tracking program based on MODPATH (Pollock, 1988 [21]) that reads the model data file and simulation results from MODFLOW.

TABLE I. HYDRAULIC FLOW MODEL PARAMETERS

|   | Ref.             | Sand and sandstone  | Conglomerate            | Lithified basal conglomerate/fanglomerate | Crystalline rock                         | Structure                                |
|---|------------------|---|-------------------------|---|--|--|
|   | [18]             | $1 \times 10^{-10}$ to $1 \times 10^{-2}$   | $1 \times 10^{-3}$ to 1 | n.d.                                      | $1 \times 10^{-8}$ to $1 \times 10^{-4}$ | n.d.                                     |
| Saturated horizontal hydraulic conductivity (m/s) | mean values [19] | $7.3 \times 10^{-6}$  | n.d.                    | n.d.                                      | $3.6 \times 10^{-7}$                     | n.d.                                     |
|   | Model input      | $1 \times 10^{-6}$  | n.a.                    | $1 \times 10^{-5}$                        | $1 \times 10^{-7}$                       | $1 \times 10^{-3}$ to $1 \times 10^{-5}$ |
| Saturated vertical hydraulic conductivity (m/s)   | Model input      | $1 \times 10^{-8}$ to $1 \times 10^{-7}$  | n.a.                    | $1 \times 10^{-6}$ to $1 \times 10^{-5}$  |  | Isotropic conditions                     |
| Transmissivity (m <sup>2</sup> /s)                | Model input      | Calculated by the model software (hydraulic conductivity × thickness of confined, saturated layers)         |                         |   |  |  |
| Boundary condition                                |                  | Constant head cells along the model boundary in all layers provide a gradient of 1 % across the model block |                         |   |  |  |

n.d. = no data, n.a. = not applicable

The boundary conditions are defined by constant head cells that control a gradient across the model block. The gradient was oriented at an oblique angle to the structure. No initial vertical gradients were set. A regional gradient of 1% was selected out of a range of approximately 0.2% to 2% determined from data on: (a) regional advective flow velocities ranging from 1 m/a to 10 m/a [22] and several metres per year thermal convection rates [6]; (b) an effective porosity of 5%; and (c) an assumed hydraulic conductivity of  $1 \times 10^{-6}$  m/s for sandstone.

MT3DMS, a modular three-dimensional transport modelling tool [23] was utilized for the simulation of advection and dispersion of fluids containing 500 µg/L U [24] originating from a structure-hosted mineralized body. MT3DMS allows the input of mass loading. The multispecies capabilities were not utilized. MT3DMS establishes the transport flow field on the basis of the output head and cell-by-cell flow data computed by MODFLOW. MT3DMS has the capability of modelling changes in the concentrations of groundwater solutes due to advection, dispersion, diffusion, and some chemical reactions including equilibrium-controlled linear or non-linear sorption, and first-order irreversible or reversible kinetic reactions. Due to the generic character of the model presented here the sorption function was not used.

The solution algorithm is based on ‘Upstream Finite Difference Method’, which tracks particles moving through the active flow field. A transport step-size of one day was used, which meets the applicable criteria at given velocities and grid discretization (Courant number = 0.75 and Peclet number < 2 in the high resolution zones of the model block). As a solver, a ‘Generalized Conjugate Gradient Solver’ was implemented. This configuration produces results that serve as a first approximation considering the general uncertainty of the input parameters.

Solute transport was simulated as advection modified by dispersion and diffusion in order to circumscribe the extent of a hydrogeochemical plume in groundwater stemming from mobilized ore and alteration products. The dispersion and diffusion parameters were gathered from various literature [18, 25, 26]. All parameters are summarized in Table II.

TABLE II. MODEL INPUT DATA RELEVANT TO ADVECTION AND SOLUTE TRANSPORT

|   |                             | Sand and sandstone | Conglomerate   | Diagenetically altered basal conglomerate  | Crystalline rock  | Structure   |
|---|-----------------------------|--------------------|--|--|---|---|
| Porosity (%)  | [18]                        | 5–30               | 25–40  | n.d.   | 0–10  | n.d.  |
| Effective porosity (%)  | [22]<br>Model input         | n.d.<br>5          | n.d.<br>n.a.   | n.d.<br>5  | n.d.<br>1   | 1–5<br>10   |
| Uranium concentration in fluids near mineralization ( $\mu\text{g/L}$ ) | [24]<br>[22]<br>Model input |                    |  | 0.3–530<br>4–12<br>500   |   |   |
| Mechanical dispersion coefficient (m)                                   | [18]<br>[25]<br>Model input |                    | As linear velocities are expected to be around $3 \times 10^{-7}$ m/s to $4 \times 10^{-7}$ m/s [6, 22], molecular diffusion is likely to contribute to dispersion |  | Longitudinal<br>1<br>n.a.<br>1<br>Transverse<br>0.1<br>n.a.<br>0.1<br>0.1 | 1<br>1  |
| Effective molecular diffusion ( $\text{m}^2/\text{s}$ )                 | [18]<br>[26]<br>Model input |                    |  | $1 \times 10^{-11}$ to $1 \times 10^{-10}$ for non-reactive species in clay<br>$2.6 \times 10^{-12}$ to $1.2 \times 10^{-11}$ for U species dissolved from $\text{UO}_2$ in bentonite<br>$5 \times 10^{-11}$ |   | $5 \times 10^{-11}$<br>$5 \times 10^{-11}$<br>$5 \times 10^{-11}$ |
| Boundary condition  |                             |                    | Constant-concentration cells (1 $\mu\text{g/L}$ ) on upstream boundaries   |  |   |   |

n.d. = no data, n.a. = not applicable

### 3. MODELLING RESULTS

#### *Robustness of model*

The variation of hydraulic conductivities within the ranges given in Table I shows the modelling results to be robust.

#### *Effects of a structure on the regional flow pattern*

Figure 3 illustrates the flow patterns that result from the effects of a structure on an otherwise undisturbed flow field in the basin fill and in basement rocks.

An open structure modifies the regional flow pattern (blue arrow = general flow direction) by deforming equipotential lines (a) and causing low pressure and high velocities in its vicinity as indicated by closely spaced stream lines (b, f).

Flow patterns generated by the model confirm earlier proposals [27, 28]. Blue = higher U-concentration, green = lower U-concentration released from a source in the potential mixing zone depicted in (e).

Basinal fluids (red) enter basement rocks (d, f) and basement fluids (blue) enter rocks above the unconformity (u/c) shown in yellow (b, e, f).

Both basin- and basement-hosted U-sources are available to being scavenged near open faults by steady-state flow of oxidizing fluids (d, f). This is consistent with the findings in the Millennium U-deposit [29].

*Location of potential reaction zones*

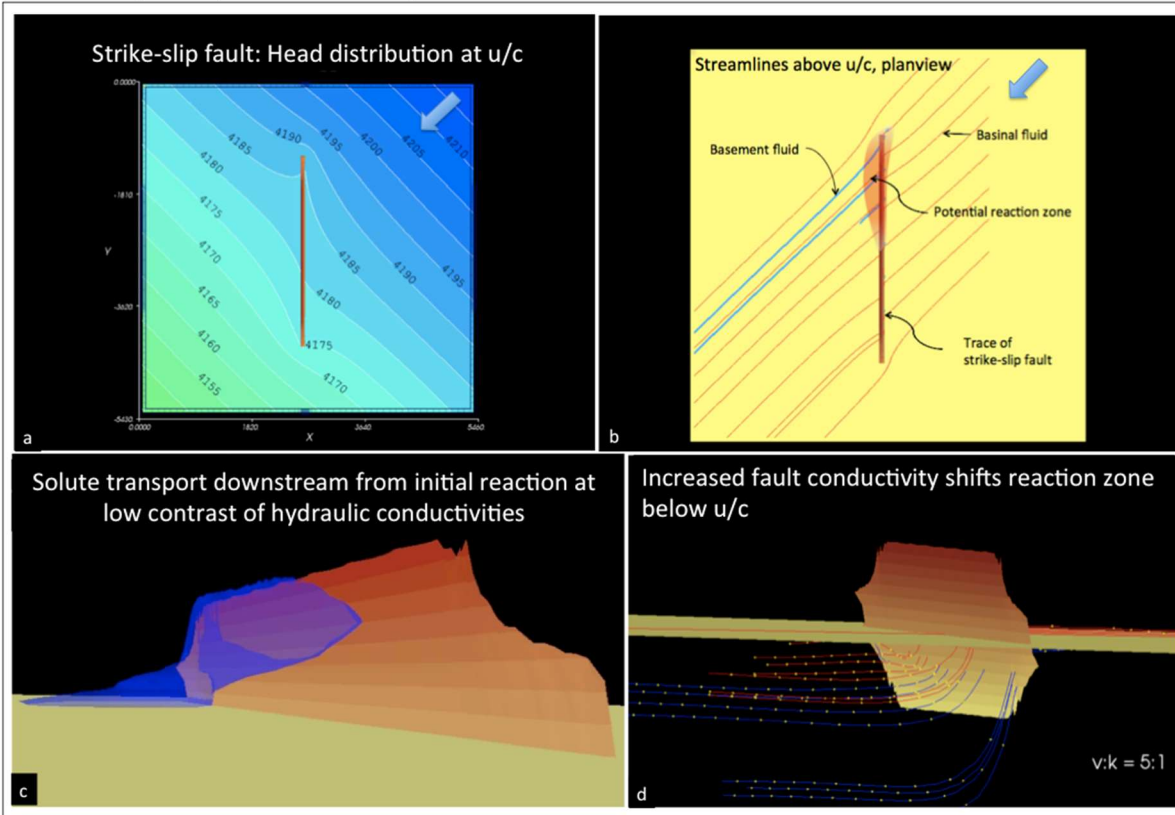
Fluid flow patterns under steady-state flow conditions suggest the presence of reaction zones in the basement (d, f), where uranium bearing basinal fluids enter a reducing basement environment. Reaction zones are likely to form also at the unconformity and in the sandstone (e), where the parallel orientation of adjacent basin and basement-derived high-velocity streamlines suggest turbulent flow conditions amenable to mixing, attendant reduction and precipitation of tetravalent uranium. This is consistent with the observed distribution of mineralization. The localization of mixing zones above, at or below the unconformity depends on the conductivity contrast between structure and wall rock. The mixing zones form at greater depth with increasing conductivity contrast (d versus b).

*Mobilization of mineralized and reactive solutes*

Basinal fluids entering mineralized structures cause the redistribution of existing U-mineralization (c, g, h) and in reaction with basement fluids, the re-precipitation along the structure (e).

The distribution of solutes shown in (c), (g) and (h) would explain the localization of alteration haloes caused downstream of mineralization by uranium depleted solutions reacting with wall rock.

Strike-slip fault, no vertical displacement



Reverse fault, vertical displacement  $\leq 40$  m

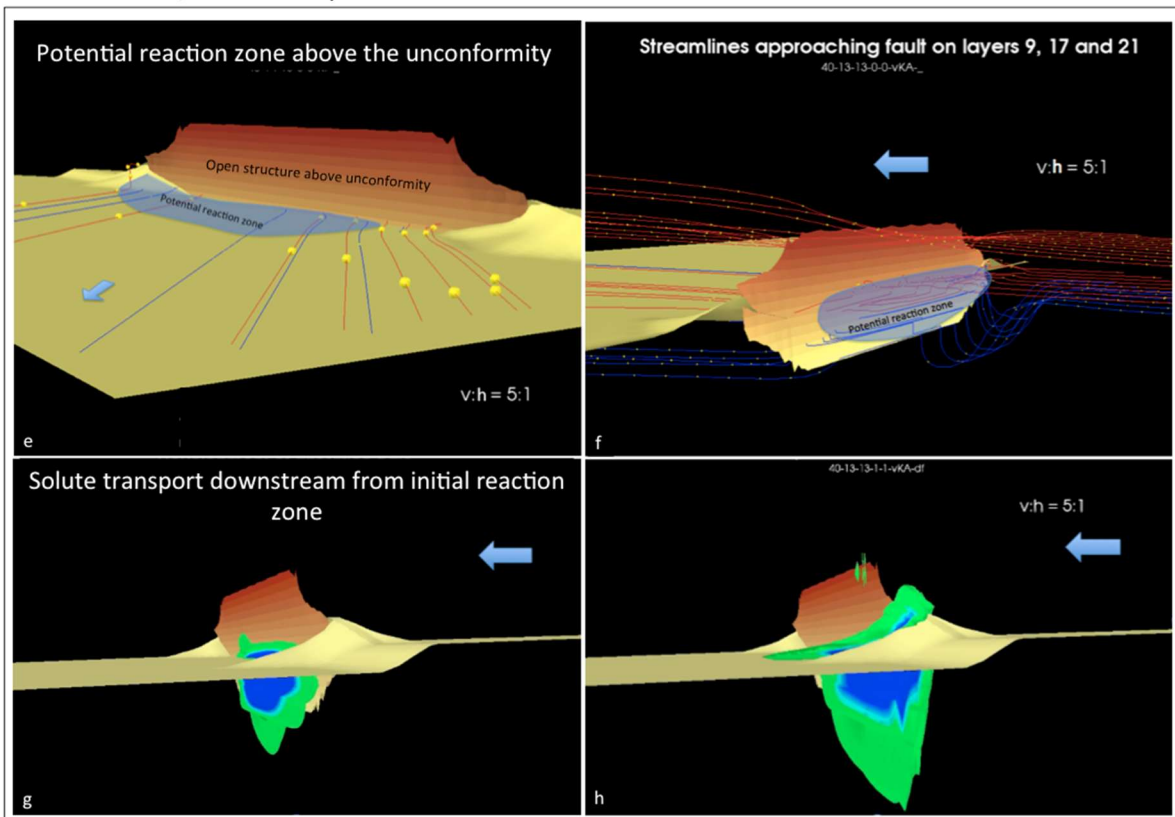


FIG. 3. Modelling results.

#### 4. CONCLUSIONS

The fluid flow patterns under steady-state flow conditions determine the location of potential mixing zones and locales of mineralization and alteration in the basement, at the unconformity and in the Athabasca Group. The modelling results indicate that the localization is a function of the hydraulic conductivity of a structure relative to the surrounding rocks.

U-sources in the basement as described for instance for the Millennium U-deposit [29] could be located within the range of scavenging fluids crossing the unconformity in the upstream area of an orebody. Conversely, oxidizing basinal fluids entering a mineralized structure may have caused the resorption of U-mineralization, observed in the field as ‘worm rock’, and in reaction with basement fluids, the reprecipitation along the structure. Conceptual flow paths previously depicted [27, 28] can be confirmed by steady-state numerical simulation.

The generic model presented here may be converted to deposit-specific flow models by quantifying the range of most likely gradients, hydraulic conductivities, flow velocities, location and volumes of catchment spaces in the basin fill and basement rocks. Transport parameters could be modified to match the results from mass balance calculations of deposits in the Athabasca Basin as performed for instance at the Shea deposit [22]. The integration of flow-relevant information from geological, geochemical, geophysical and structural models as presented in [22, 30–32] into this flow model could further the understanding of unconformity-related uranium deposits.

#### ACKNOWLEDGEMENTS

The author would like to express his sincere appreciation to the late F.-J. Dahlkamp, who reviewed a previous version of the paper and who pointed out essential metallogenetic aspects. Scott Donald scrutinized the modelling technique and provided valuable advice. K. Lehnert-Thiel and B. Boldt-Leppin are thanked for their helpful comments and suggestions. I. Annesley brought up recent developments in modelling genetic processes and was always available for constructive discussions. Last but not least, H. Föhse improved the present version of the paper by giving valuable editorial hints.

#### REFERENCES

- [1] ALEXANDRE, P., KYSER, K., THOMAS, D., POLITO, P., MARLAT, J., Geochronology of unconformity-related uranium deposits in the Athabasca Basin, Saskatchewan, Canada, and their integration in the evolution of the basin. *Mineralium Deposita* **44** (2009) 41–59.
- [2] JEБRAK, M., FAURE, S., “Modelling of paleostress in unconformity-related uranium deposits” (CUNEY, M., Ed.), Proc Int. Conf. Uranium Geochem 2003 – Uranium deposits – Natural Analogs - Environment, Nancy, France (2003) 187–188.
- [3] SCHAUFS, P., ORD, A., ANNESLEY, I., MADORE, C., QUIRT, D., THOMAS, D., PORTELLA, P., A comparison of the McArthur River and Cigar Lake unconformity-related uranium deposits, Saskatchewan, Canada: insight from deformation — fluid flow models, Structure, Tectonics and Ore Mineralization Processes, (Contributions of the Economic Geology Research Unit **64** (James Cook University, Townsville, Australia) (2005).
- [4] SHELDON, H.A., ORD, A., Evolution of porosity, permeability and fluid pressure in dilatant faults post-failure: implications for fluid flow and mineralization, *Geofluids* **5** (1997) 272–288.
- [5] MATTHÄI, S.K., ROBERTS, S.G., Transient versus continuous fluid flow in seismically active faults: An investigation by electrical analogue and numerical modelling (JAMTVEIT B., YARDLEY, B., Eds), *Fluid Flow and Transport in Rocks — Mechanisms and effects*, Springer (1997) 263–295.
- [6] RAFFENSPERGER, J.P., GARVEN, G., The formation of unconformity-type uranium ore deposits 1, Coupled groundwater flow and heat transport modeling, *American J. Science* **295** (1995) 581–636.

- [7] CHI, G., BOSMAN, S., CARD, C., Numerical modeling of fluid pressure regime in the Athabasca basin and implications for fluid flow models related to the unconformity-type uranium mineralization, *Journal of Geochemical Exploration* **125** (2013) 8–19.
- [8] CUI, T., YANG, J., SAMSON, W., Formation of unconformity-related uranium deposits: perspectives from numerical modeling, *GeoCanada 2010 – Working with the Earth*, Calgary, Alberta, Canada (2010).
- [9] MATTHÄI, S.K., FISCHER, G., Quantitative modeling of fault-fluid-discharge and fault-dilation-induced fluid-pressure variations in the seismogenic zone, *Geology* **24** 2 (1996) 183–186.
- [10] MCDONALD, M.G., HARBAUGH, A.W., A modular three-dimensional finite-difference ground-water flow model: Report prepared by U.S. Department of the Interior, U.S. Geological Survey, National Center, Reston, VA (1984).
- [11] MCDONALD, M.G., HARBAUGH, A.W., A modular three-dimensional finite-difference ground-water flow model: Technical report, U.S. Geol. Survey, Reston, VA (1988).
- [12] MCDONALD, M.G., HARBAUGH, A.W., A modular three-dimensional finite-difference ground-water flow model: U.S. Geological Survey, Techniques of Water-Resources Investigations, Book 6, Chapter A1 (1988).
- [13] HARBAUGH, A.W., MCDONALD, M.G., User's Documentation for MODFLOW-96, an update to the U.S. Geological Survey modular finite-difference groundwater flow model: U.S. Geological Survey Open File Report **96-485** (1996).
- [14] HARBAUGH, A.W., MCDONALD, M.G., Programmer's Documentation for MODFLOW-96, an update to the U.S. Geological Survey modular finite-difference groundwater flow model: U.S. Geological Survey Open File Report **96-486** (1996).
- [15] CHIANG W.-H. KINZELBACH W., 3D-Groundwater Modeling with PMWIN: First Edition, Springer Berlin Heidelberg New York (2001).
- [16] CHIANG, W.H., 3D-Groundwater Modeling with PMWIN. A simulation system for modeling groundwater flow and transport processes: Second Edition, Springer Berlin Heidelberg New York (2005).
- [17] CHIANG, W.H., KINZELBACH, W., 3D-Groundwater Modeling with PMWIN A Simulation System for Modeling Groundwater Flow and Transport Processes (2nd ed.), Springer Verlag (2005).
- [18] FREEZE, R.A., CHERRY, J.A., *Groundwater*, Prentice-Hall, Inc., Englewood Cliffs, N.J. (1979).
- [19] UNLAND, W., HOLL, N., Dewatering of planned Key Lake open pits in northern Saskatchewan, *CIM Bulletin* **73** 818 (1980) 91–99.
- [20] CHIANG, W.H., KINZELBACH, W., PMPATH. An advective transport model for Processing Modflow and Modpath: Geological Survey of Hamburg, Germany (1994).
- [21] POLLOCK, D.W., Semianalytical computation of path lines for finite difference models, *Ground Water* **26** 6 (1988) 743–750.
- [22] LE CARLIER DE VESLUD, C., CUNEAy, M., LORILLEUX, G., ROYER, J.J., JÉBRAK, M., 3D modeling of uranium-bearing solution collapse breccia in Proterozoic sandstones (Athabasca Basin, Canada) – Metallogenetic interpretations. *Computers and Geosciences* **35** (2009) 92–107.
- [23] ZHENG, C., WANG, P.P., MT3DMS: A modular three-dimensional multispecies model for simulation of advection, dispersion and chemical reactions of contaminants in groundwater systems: Documentation and Users Guide, Contract Report SERDP-99-1, U.S. Army Engineer Research and Development Center, Vicksburg, MS (1999).
- [24] RICHARD, A., PETTKE, T., CATHELINEAU, M., BOIRON, M.C., MERCADIER, J., CUNEAy, M., DEROME, D., Brine–rock interaction in the Athabasca basement (McArthur River U deposit, Canada): consequences for fluid chemistry and uranium uptake: *Terra Nova* **22** 4 (2010) 303–308.
- [25] KONIKOW, L.F., The secret to successful solute-transport modeling, *Groundwater* **49** 2 (2011) 144–159.
- [26] MOORE, S.M., SHACKELFORD, C.D., “Uranium diffusion in soils and rocks”, Proc. Tailings and Mine Waste 2011, Vancouver, BC (2011).

- [27] WHEATLEY, K., MURPHY, J., LEPPIN, M., CUTTS, C., CLIMIE, J.A., “Advances in the genetic model and exploration techniques for unconformity type uranium deposits in the Athabasca Basin” (ASHTON, K.E., HARPER, C.T., Eds.), Proc. MinExpo ’96 Symposium — Advances in Saskatchewan Geology and Mineral Exploration, Saskatchewan Geological Society, Special Publication No. **14** (1996) 126–136.
- [28] ALEXANDRE, P., KYSER, K., POLITO, P., THOMAS, D., Alteration Mineralogy and isotope geochemistry of Paleoproterozoic basement-hosted unconformity-type uranium deposits in the Athabasca Basin, Canada: *Economic Geology* **100** (2005) 1547–1563.
- [29] FAYEK, M., CAMACHO, A., BESHEARS, C., JIRICKA, D., HALABURDA, J., Two sources of uranium at the Millennium uranium deposit, Athabasca Basin, Saskatchewan, Canada, *GeoCanada 2010*, Calgary (2010).
- [30] SKIRROW, R.G., JAIRETH, S., HUSTON, D.L., BASTRAKOV, E.N., SCHOFIELD, A., VAN DER WIELEN, S.E., BARNICOAT, A.C., Uranium mineral systems: Processes, exploration criteria and a new deposit framework, *Geoscience Australia Record* **2009/20** (2009).
- [31] POTMA, W., FISHER, L., SCHAUBS, P., CLEVERLEY, J., CORBEL, S., LAU, I., PHANG, C., HOUGH, R., JSU – ERA Ranger Mineral System Project Final Report. CSIRO National Research Flagships, Minerals Down Under, Northern Territory Geological Survey, *Record 2012-004* (2012).
- [32] ANNESLEY, I.R., REILKOFF, B., TAKACS, E., HAJNAL, Z., PANDIT, B., “A Regional Multi-scale 3D Geological Model of the Eastern Sub-Athabasca Basement, Canada: Implications for vectoring towards unconformity-type uranium deposits”, IAEA-CN-216, International Symposium on Uranium Raw Material for the Nuclear Fuel Cycle: Exploration, Mining, Production, Supply and Demand, Economics and Environmental Issues (URAM-2014), IAEA, Vienna (2014) Abstact 086.

# **REGULATORY ISSUES FOR SAFETY AND ENVIRONMENTAL ON URANIUM MINING AND MILLING IN ROMANIA**

L. POP

Safeguards, Physical Protection and Mining Unit,  
National Commission for Nuclear Activities Control,  
Bucharest, Romania

## **Abstract**

The safe deployment of nuclear activities in Romania is provided by Law 111/1996, republished and completed by Law 193/2003 and Law 378/2013. The competent national authority in the nuclear field, which has responsibilities of regulation, authorization and control as stipulated in this Law, is the National Commission for Nuclear Activities Control (CNCAN). According to article 2b) provisions of the nuclear Law shall apply to design, possession, siting, construction-assembly, commissioning, operation, conservation and decommissioning of the mining and milling facilities for uranium and thorium ores and of the waste management facilities of the waste resulted from the mining and milling of uranium and thorium ores.

## **1. INTRODUCTION**

Based on the provisions of Law 111/1996 CNCAN has issued a series of Radiological Safety Norms and Guidelines for Uranium and Thorium Ores. The provisions of these norms provide elementary safety standards for the health protection of both workers and the general public against the dangers arising from ionizing radiation. In the same vein the specific regulations and guidelines contain detailed provisions on: the content of radiation protection program, conditions for release in the environment of liquid and gaseous effluents, monitoring and surveillance programs of the radioactivity of the environment factors, long term stability of dumps and tailing ponds, decommissioning of uranium production facilities, and so on.

## **2. DESCRIPTION OF REGULATORY ISSUES FOR URANIUM MINING AND MILLING**

### **2.1. Radiological safety norms on operational radiation protection in mining and milling of uranium**

The applicable field and content:

- Requirements regarding the dose limits and optimization for professional exposure of workers and general population, involved in mining and milling uranium and thorium ores;
- Responsibility of legal constituted persons that develop mining and milling activities;
- Requirements regarding the content of radiation protection programme, respectively: responsibilities sharing, radioactive sources management, areas under control and areas under survey, doses monitoring (external exposure, radon and decay products, radioactive dust), dose recording;
- Requirements regarding health survey for workers;
- Conditions for release in the environment of liquid and gaseous effluents;
- Requirements regarding environmental monitoring programme and Thorium Ores.

**2.2. Radiological safety norms on decommissioning of uranium and thorium ores mining and milling facilities- criteria for release from CNCAN authorization regime for use in other purposes of buildings, materials, facilities dumps and lands contaminated by mining and milling of uranium and thorium ores**

The applicable field and content:

- Requirements for mining and milling facilities decommissioning;
- The content of detailed radiological assessment;
- The content of technical detailed decommissioning plan;
- The contents of a final radiological report;
- Criteria for release metal scrap;
- Criteria for release for industrial use of areas contaminated by uranium mining;
- Criteria for release for forest and agricultural purposes and public gardens of areas contaminated by uranium mining;
- Criteria concerning the safeguard and use of mine dumps;
- Criteria for release for further commercial or industrial use of buildings used for commercial or industrial purposes and the disposal of building debris from uranium and thorium mining and milling;
- Criteria for release for general use or reusable equipment from uranium and thorium mining and milling.

**2.3. Radiological safety norms on the management of the uranium and thorium mining and milling radioactive waste**

The applicable field and content:

- Responsibility of legal constituted persons that develop radioactive wastes management activities;
- Radioactive wastes management strategy;
- Safety requirements for management facilities of radioactive wastes from uranium and thorium ores mining and milling;
- Safety assessment for radioactive waste management facilities.

**2.4. Radiological safety norms – authorization procedures for uranium and thorium mining and milling, nuclear raw materials processing and nuclear fuel production activities**

The applicable field and content:

- Authorization regime (Registration and Authorization);
- Authorization phases;
- The content of authorization file, requirements for content of technical authorization documentation.

**3. CONCLUSIONS**

With regards to uranium mining and milling, the Romanian legislation takes into account three objectives to:

- Ensure that the workers, the public and the environment are protected against the radiological hazard resulting from the exploitation of the uranium mining and milling industries;

- Provide protection during the period of exploitation and after the closure of uranium mines or milling facilities;
- Ensure that wastes (dumps) resulting from the operating of uranium mines and tailing ponds resulting of uranium ore milling are treated as radioactive waste.

## BIBLIOGRAPHY

(in Romanian)

THE PARLIAMENT OF ROMANIA, Law 111/1996, republished and completed by Law 193/2003 and 378/2013, Bucharest.

NATIONAL COMMISSION FOR NUCLEAR ACTIVITIES CONTROL, Radiological Safety Norms on Operational Radiation Protection in Mining and Milling of Uranium, NMR- 01, approved by CNCAN President Order 127/27.05.2002 and published in MO Part. I, No 677/12.09.2002, Bucharest.

NATIONAL COMMISSION FOR NUCLEAR ACTIVITIES CONTROL, Radiological Safety Norms on Decommissioning of Uranium and Thorium Ores Mining and Milling Facilities, NMR-03, approved by CNCAN President Order 207/24.11.2003 and published in MO, Part I, No 734/28.08.2006, Bucharest.

NATIONAL COMMISSION FOR NUCLEAR ACTIVITIES CONTROL, Radiological Safety Norms on the Management of the Uranium and Thorium Mining and Milling Radioactive Waste, NMR-02, approved by CNCAN President Order 192/26.09.2002 and published in MO, Part I, No 867/02.12.2002, Bucharest.

NATIONAL COMMISSION FOR NUCLEAR ACTIVITIES CONTROL, Radiological Safety Norms – Authorization Procedures for Uranium and Thorium Mining and Milling, Nuclear Raw Materials Processing and Nuclear Fuel Production Activities, approved by CNCAN President Order 171/24.11.2003 and published in MO, Part I, No 530/14.06.2004, Bucharest.

# FURTHER NEW ACTIVITIES AT URANIUM DEPOSIT ROZNA

F. TOMAN, P. VINKLER  
DIAMO State Enterprise, Division GEAM,  
Dolni Rozinka, Czech Republic

## Abstract

Mining of uranium ore has been running at the Czech Rožná deposit for 56 years, since 1957. Extraction of uranium ore is currently performed in the mining field of blind shaft R7S. Top slicing and caving under the artificial roof method is used for the extraction. Uranium ore is treated at a chemical treatment plant (a mill) situated in the close vicinity to the mine. Milling is carried out under a closed cycle of process water. Due to the positive annual precipitation-evaporation balance, the surplus of process water in tailing ponds has to be purified by evaporation and membrane processes before discharging into a river. New activities are being sought and carried out uranium production gradually decreases. Geological exploration works for a construction of an underground gas storage were started three years ago, and new horizontal galleries were driven and 100 m long exploratory holes drilled. Sampling of rocks for geochemical, geomechanical and petrographic tests were carried out. So far 1264.9 m of exploration galleries and 1130 m of exploration holes have been made. Additional geological exploration works for construction of underground research workplace started in 2013 near the Bukov1 shaft.

## 1. INTRODUCTION

The DIAMO state enterprise implements the governmental, environmental remediation program of the uranium, other mineral ores and, partially, of the coal mining in the Czech Republic. It undertakes environmental remediation of the other industrial impacts from the past. This enterprise also ensures production of uranium concentrate for the nuclear energy sector as only one the producer in the central Europe in division GEAM Dolní Rožinka. Mining has been running at Rožná deposit for 57 years, since 1957. Extraction of uranium ore is currently performed in the mining field of blind shaft R7S. The mine and nearby mill at Dolní Rožinka are located approximately 130 km south-south-east of Prague.

The general advance of mining at the deposit is from top to bottom. It means that at first subsurface parts of the deposit were extracted (uranium mineralization was found at depths as shallow as 2.0–2.5 m below the surface). Gradually mining operations proceeded into increasing depths, and at present most works are done by conventional underground methods at depths ranging from 950 to 1200 m below the surface (24th level). From the beginning of exploitation to the year 2014, altogether 16 million tonnes of ore with an average U content of 0.116 kg per tonne were processed, which represented more than 18 thousand tonnes of uranium.

Uranium ore mined from the Rožná deposit is treated at the nearby Dolní Rožinka chemical treatment plant (a mill). In the mill, uranium is extracted from the crushed and uranium extracted from the ground — up ore by alkaline leaching. A resin-in-pulp process is used for separation of uranium leached from the ground ore. The final product of the milling is ammonium diuranate,  $(\text{NH}_4)_2\text{U}_2\text{O}_7$ , which is exported to nuclear conversion facilities abroad.

Milling is carried out under the condition of the closed cycle of technology (process) water. Due to the positive annual precipitation-evaporation balance, a surplus of technology water in tailing ponds has to be purified before discharging into a river. The water in the tailing ponds has high salinity — about 33 g/L. It is a complicated chemical system including a lot of inorganic and organic compounds, where the predominant contaminant is sodium sulphate. Evaporation and membrane processes (electrodialysis and reverse osmosis) are used to purify the water. The final products of the water treatment are cleaned water, discharged into the river in volume about 420 m<sup>3</sup>/year, and over 8000 tonnes of anhydrous sodium sulphate that is sold for washing powder production and to the glass or paper industries.

DIAMO's GEAM Division at Dolní Rožínka has currently about 1000 employees and is the second largest employer in the district. After the eventual termination of mining it is supposed that more than 700 workers will be made redundant. It will be in region where unemployment exceeds 12%. That is why a great effort of the division management is devoted to preparation of new job opportunities at the mill and mine.

## 2. NEW ACTIVITIES AT GEAM DOLNÍ ROŽÍNKA

### 2.1. New activities at the mill

More than 190 workers are employed at the mill. After the termination of the mining more than 75% of them would be made redundant. These people have long-term experience with hydrometallurgical processes and they are specialists for various technologies. That is why the following activities at the mill are being prepared for them:

- Participation in the Competence Centre for Effective and Ecological Mining of Mineral Resources – the main target is monitoring and designing technologies for the separation of REE (rare earth elements) from the mined ore, tailings or stockpiled waste rock;
- Laboratory and pilot testing of membrane technologies (electro-deionisation with bipolar electrodialysis membranes);
- People at mill have long term experiences with electrodialysis and reverse osmosis apparatus and the mill has a lot of water streams with various salinities and compositions which are suitable for pilot plant testing or apparatus checking;
- Design of technological solutions in the field of mine water treatment — staff from the mill participated at construction of 2 of the largest mine or technological water treatment plants in the Czech Republic;
- Disposal of waste products after sorption of uranium from waters;
- Machinery manufacturing and assembly of technological units.

### 2.2. New activities at the Rožná I mine

The mine Rožná has about 500 workers. They are able to work at various underground constructions like galleries, underground gas storages, underground research workplaces, etc. There are started two great constructions close to mine Rožná I — underground gas storage and an underground research workplace.

#### 2.2.1. *Underground gas storage*

Geological exploration works for construction of underground gas storage were started on 21<sup>st</sup> level of shaft R7S in 2010.

Planned parameters of the gas storage are:

- Total rock excavation – 380 000 m<sup>3</sup>;
- Estimated construction time – 8 years;
- Maximum gas pressure – 20 MPa;
- Total volume in storage – 100 million m<sup>3</sup>;
- Situated in migmatite rock body with rock compressive strength of up to 170 Mpa.

So far, 1265 m exploration drifts and 1130 m boreholes have been made. An isometric scheme of underground gas storage is given in Fig. 1.

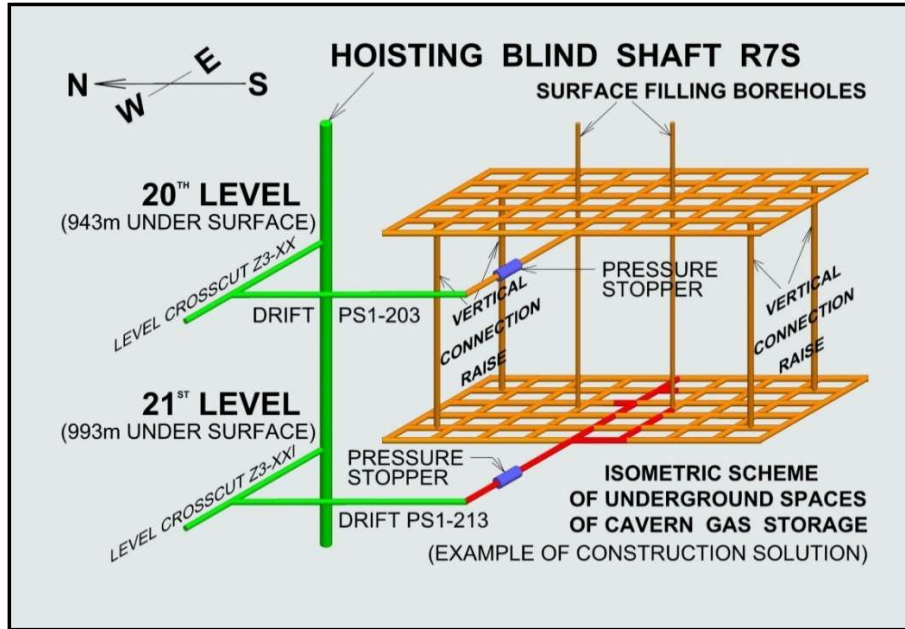


*FIG. 1. Isometric scheme of underground gas storage – presumed design.*

## 2.2.2. Underground research workplace

The main aim of this workplace is to determine and verify geological conditions for specific intervention into Earth's crust. The main targets are:

- Characterization of the rock mass at depth 500–900 m;
- Characterization of rock;
- Developing methods and acquisition of their using for characterization of rock at depths suitable for deep geological disposal of radioactive waste.

This construction started on 12<sup>th</sup> level near the shaft Bukov 1 in 2013. The total length will be 417 m with an average profile of 9.2 m<sup>2</sup>. The depth is 524 m under the surface. So far 270 m of drifts have been made. Work is driven in biotite gneisses with a rock compressive strength up to 150 MPa. An isometric scheme of underground research workplace is given in Fig. 2.

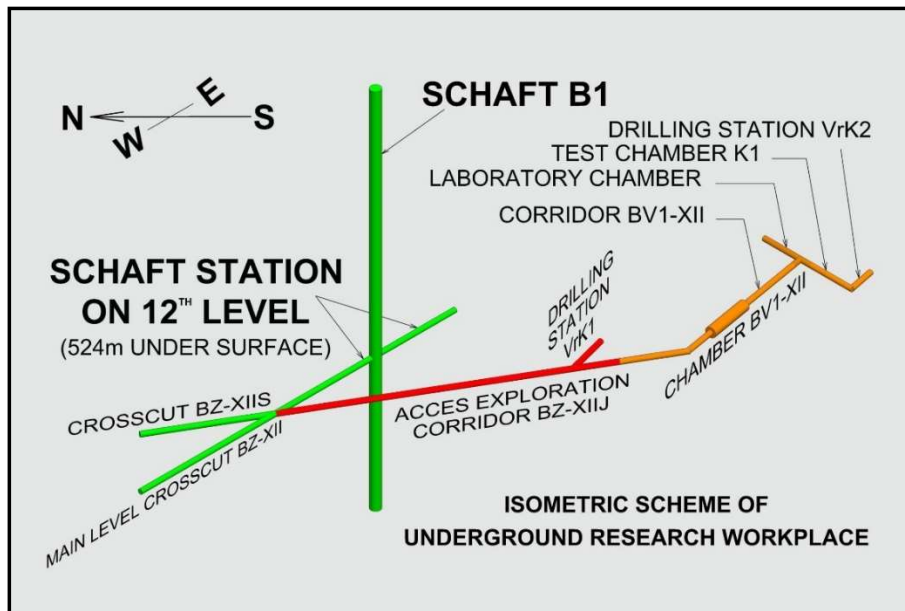


FIG. 2. Isometric scheme of underground research workplace.

### 3. CONCLUSION

New activities are searched and carried out with consequence of gradual decreasing of uranium production. The mining and milling of uranium ore at Rožná deposit is coming to end. It is assumed that it will be possible to keep mining and milling until the end of 2016. The main target and also benefit of the new activities is the using of skilled human resources in the mine Rožná I and made available underground locations. The most important benefit of the new activities is maintaining employment, because GEAM Dolní Rožínka Division of DIAMO is significant employer in the Bystricko region of the Czech Republic.

### BIBLIOGRAPHY

DIAMO state enterprise, <http://www.diamo.cz/en/>.

HAHNE, R. SCHOPPE, M. PAUL, M. SLEZAK, J. MERKEL, B., Water balance and hydrogeological modeling in the case of the TPF Rozna/ Czech Republic, Uranium in the Aquatic Environment, Springer Berlin Heidelberg (2002) 719–726.

KŘÍBEK, B., ŽÁK, K., DOBĚŠ, P., LEICHMANN, J., PUDILOVÁ, M., RENÉ, M., SCHARM, B., SCHARMOVÁ, m. HÁJEK, A., HOLECZY, D., HEIN, U.F., LEHMANN, B., The Rožná uranium deposit (Bohemian Massif, Czech Republic): shear zone-hosted, late Variscan and post-Variscan hydrothermal mineralization, Mineralium Deposita 44 1 (2009) 99–128.

TOMAN, F., Membrane processes at branch plant GEAM Dolní Rožínka, Bulletin No. 8, Czech membrane section at Czech chemical engineering society (1998) (in Czech).

TOMAN, F., MAREK M., “Membrane processes in a water treatment at the uranium chemical mill”, MELPRO 2014 Membrane and Electromembrane Processes, Prague, 2014, Book of Abstracts (2014) 154.

TOMAN, F., JEŽOVA, V., Uranium ore mill at Dolni Rozinka: 40 years of operation, Uhli-Rudy-Geologicky Pruzkum 14 10 (2007) 12–14 (in Czech, English abstract).

# THE CHARACTERISTICS OF URANIUM OXIDE SINTERED PELLETS FROM PHOSPHATE FERTILIZER WASTE AS A POTENTIAL RESOURCE OF URANIUM

A. MUCHSIN, R. LANGENATI, G.K. SURYAMAN

Nuclear Fuel Fabrication Division,  
Center for Nuclear Fuel Technology,  
National Nuclear Energy Agency,  
Kawasan PUSPIPTEK, Serpong, Banten, Indonesia

## Abstract

Indonesia's energy demand is increasing rapidly. To meet its electrical energy needs, the government seeks to increase the use of potential energy sources in synergy (an energy mix of fossil and non-fossil fuels). The non-fossil energy sources considered are hydroelectric, geothermal, biofuel, microhydro, biomass, solar, wind and nuclear power. According to the National Energy Management Blueprint 2005–2025, the role of nuclear energy is about 2% of the electricity total. Efforts are being made to support the program, including strengthening the domestication option of nuclear fuel industry and enhancing the sustainability of its supply. Therefore, the availability of domestic uranium resources becomes important. Results of previous study indicate that the uranium content in phosphate fertilizer waste ranged from 70–100 ppm in a solution of phosphoric acid. From this source up to 55.5 t/a of yellow cake could be obtained from fertilizer waste. This study reveals that UO<sub>2</sub> powder from phosphate fertilizer waste could be used to make UO<sub>2</sub> sintered pellets which meet the specifications of nuclear fuel. The use of uranium from phosphate fertilizer waste would not only enhance the availability of uranium in Indonesia but also addresses environmental issues.

## 1. INTRODUCTION

The electricity demand has a tendency to increase every year. In Indonesia, electricity has an important role. Electricity not only enhances the quality of life in Indonesia but also drives the national development. However, there are still many regions in Indonesia which are not electrified. This condition drives the Indonesian government to electrify more regions in Indonesia, especially rural areas. Currently Indonesia's sources for electricity mostly come from coal, oil and water. To fulfil the electricity demand in Indonesia, the government has to find and use other resources to generate power. Indonesia has many resources of both fossil and non-fossil energy. Fossil resources such as oil, natural gas and coal are available in Indonesia. On the other hand, there are also non-fossil resources such as water, geothermal, biofuel, biomass, solar energy, wind energy (including on the large, mini and micro scales) and nuclear. Nuclear energy is one of the options to fulfil the electricity demand in Indonesia. It can be built on a large scale [1]. According to the National Energy Management Blueprint 2005–2025, the role of nuclear energy is about 2% of the total national electrical energy. Efforts have been made to support the program. Some of the efforts are strengthening the domestication option of nuclear fuel industry and enhancing the sustainability of the nuclear fuel supply. Therefore, the availability of uranium resources becomes important.

The uranium materials can be obtained from mining and milling of uranium ore. According to Indonesia Nuclear Energy Outlook 2014, Indonesia's total uranium reserves is recorded at 63 000 tonnes U<sub>3</sub>O<sub>8</sub> [2] (~53 000 tU). In Indonesia, uranium could not only be obtained from uranium mining and milling, but also from phosphate fertilizer waste. The Petrokimia Gresik company is one of the phosphate fertilizer producers in Indonesia. Wastes produced by this company contain uranium, which could be used as raw material for nuclear fuel. According to previous research, the uranium content in Petrokimia Gresik waste is around 70–100 ppm [3]. Due to massive production of this factory, within a year, the amount of yellow cake which could be obtained from this factory is around 55.5 tonnes. The phosphate waste could become the source of dangerous pollution for the environment if it is released to the environment without processing it first. The utilization of UO<sub>2</sub> powder from phosphate fertilizer waste would not only enhance the availability of uranium in Indonesia but also address environmental issues associated with the phosphate waste itself.

The National Nuclear Energy Agency (BATAN), as a government institution whose duties are research and development in utilization of nuclear energy, has to become the source of information and give a contribution especially to the uranium supply for the power plan issues. Therefore, BATAN does many research projects about nuclear fuel. Part of the research that has been done regards the conversion of yellow cake to UO<sub>2</sub> powder. Previous research showed that the yellowcake which comes from phosphate fertilizer waste could be converted to UO<sub>2</sub> powder. The quality of UO<sub>2</sub> powder from the converted phosphate waste yellow cake is not much different with UO<sub>2</sub> powder from commercial yellow cake [4]. It is the aim of this paper to examine the characteristics of sintered pellets from converted UO<sub>2</sub> powder from yellow cake of phosphate fertilizer waste and assess its prospects to become a resource of uranium for nuclear fuel. The characteristic of the sintered pellets that is emphasized is part of its physical properties, in this case pellet density.

## 2. METHODOLOGY

The converted UO<sub>2</sub> powder from yellow cake obtained from Petrokimia Gresik company phosphate fertilizer waste was characterized for its chemical and physical characteristics. The UO<sub>2</sub> powder was produced using an ammonium diuranate process. The characterized physical properties of UO<sub>2</sub> powder are tap and bulk density. The characterized chemical properties are the O/U ratio and the impurity content in UO<sub>2</sub> powder. The O/U ratio was characterized using a gravimetric method while the impurity content was analysed using Atomic Absorption Spectrometry. The UO<sub>2</sub> powder was then compacted with 3 MP pressure and the density of green pellets was calculated using a metrology method. The standard used for the UO<sub>2</sub> powder was the operational quality control method of nuclear fuel laboratory at Experimental Fuel Element Installation [4].

A sintering process was done for 16 green pellets from converted UO<sub>2</sub> powder using a Degussa chamber for 3 hours in temperature of 1700 °C with a hydrogen atmosphere. The observations of the sintered pellets are visual inspection, sintered pellet density, microhardness and microstructure of sintered pellet. A metrology method was used for density measurements, and an optical microscope was used for the observation of sintered pellets microstructure. The standards used for the quality control of the sintered pellet are ASTM C753 [5] and ASTM C776 [6].

## 3. DISCUSSION

The conversion process of yellow cake to UO<sub>2</sub> sintered pellets is shown in Figure 1.

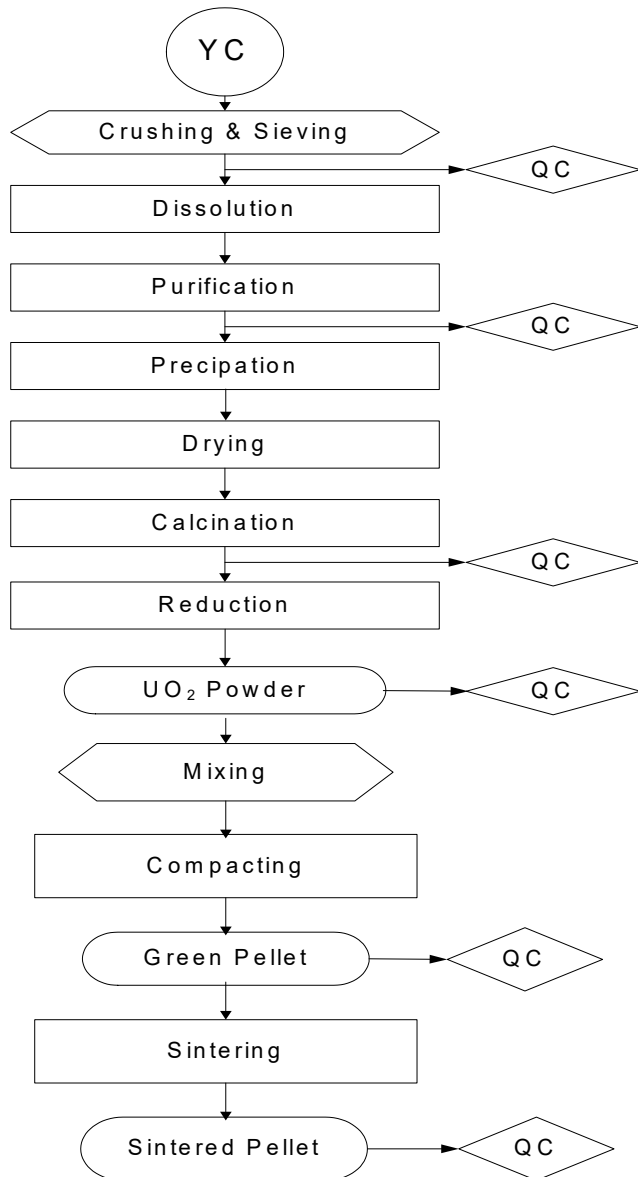


*FIG. 1. Process flow diagram.*

The conversion process of yellow cake to  $\text{UO}_2$  powder has been done in the previous research. This paper is the continuation of the previous research. In this paper, the converted  $\text{UO}_2$  powder is compacted and sintered. The sintered pellet is then characterized.

### 3.1. $\text{UO}_2$ powder characteristics

The characterization of  $\text{UO}_2$  powder included its physical and chemical characteristics, being tap density, bulk density, O/U ratio and impurity content. The results of tap density, bulk density and O/U ratios are shown in Table I.

TABLE I. TAP DENSITY, BULK DENSITY AND O/U RATIO OF UO<sub>2</sub> POWDER

| No | Type of characterization | Specification (g/cm <sup>3</sup> ) | Measurement results (g/cm <sup>3</sup> ) |
|----|--------------------------|------------------------------------|--|
| 1  | Bulk density             | 1.5 ± 0.2                          | 1.0600                                   |
| 2  | Tap density              | 2.0                                | 1.8361                                   |
| 3  | O/U ratio                | 2.00 – 2.13                        | 2.06 ± 0.0081                            |

It can be seen from Table I that the tap and bulk density of UO<sub>2</sub> powder is slightly under the specification while the O/U ratio has already met the specification. The green pellets of the compacted powder have a good visual appearance. There are no defects on the surface of the pellets. To overcome the low value of tap and bulk density of the powder, powder preparation could be done before UO<sub>2</sub> powder is compacted. The processes for powder preparation include the pre-pressing, crushing and granulating. By doing the powder preparation before compacting process, it is expected that the powder density would be better and the powder compaction process would be easier.

The impurity content characterization is very important. The impurity content in powder shows the purity of the powder. The powder is claimed to be nuclear grade if the impurities are below the specification limit. The impurity content of UO<sub>2</sub> powder from converted phosphate fertilizer yellow cake is shown in Table II.

TABLE II. IMPURITY CONTENT IN UO<sub>2</sub> POWDER

| Impurity | Measurement result (ppm) | Specification limit(ppm) |
|----------|--------------------------|--------------------------|
| Cd       | 0.11                     | 0.2                      |
| Cr       | 9.827                    | 100                      |
| Cu       | 22.98                    | 20                       |
| Ca       | 92.87                    | 50                       |
| Fe       | 99.46                    | 100                      |
| Mg       | 33.14                    | 50                       |
| Mo       | 5.05                     | 50                       |
| Mn       | 78.82                    | 10                       |
| Si       | 242.52                   | 60                       |
| Ni       | 3.23                     | 30                       |
| Al       | 107.11                   | 50                       |
| Co       | 2.20                     | 75                       |
| Pb       | 1.01                     | 60                       |
| Zn       | 32.66                    | 100                      |
| V        | 2.98                     | 5                        |
| Sn       | 26.27                    | 50                       |

Table II shows that most of the impurities of the powder are below the specification except for Cu, Ca, Mn, Si, Al and Sn. Those impurities which are still above the specification could be reduced by increasing the efficiency of purification process. This can be done with optimization of the process parameters.

### 3.2. Sintered pellets characteristics

Characterization of  $UO_2$  sintered pellets were done for all pellets. Those characterizations are pellet density, O/U ratio, visual inspection, microhardness and microstructure. Density measurement was done by using metrology method. The purpose of visual inspection is to check the sintered pellet integrity. The pellet integrity indicates the strength of the pellets when they are loaded into the fuel rod and to ensure adequate fuel performance of those pellets. The visual inspection consists of the observation of surface crack, chips and other defects at the pellet surface [5]. The cleanliness of the sintered pellets is also become attention at the visual inspection.

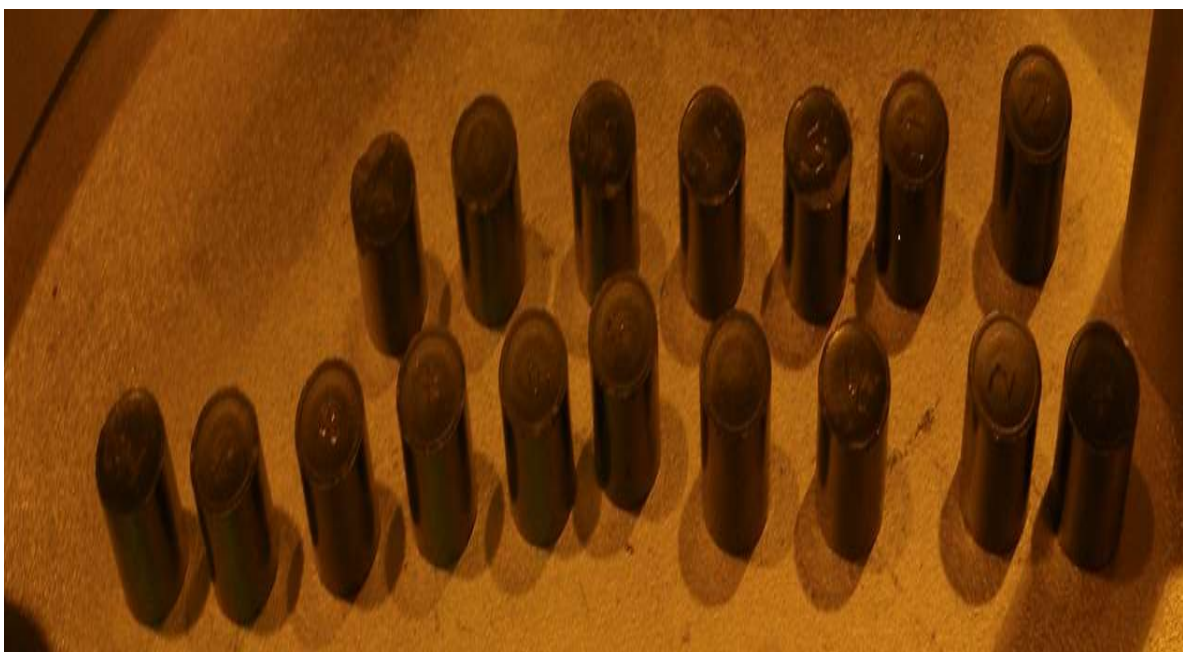


FIG. 2.  $UO_2$  sintered pellets.

The result of density measurements and visual inspection of the pellets are shown in Table III.

TABLE III. GREEN PELLETS DENSITY, SINTERED PELLETS DENSITY AND VISUAL INSPECTION RESULTS

| No.     | Density (g/cc) |                 | Visual inspection result<br>(cracks, chips & cleanliness) |
|---------|----------------|-----------------|---|
|         | Green pellet   | Sintered pellet |   |
| 1       | 5.23           | 9.95            | No cracks or chips, clean surface                         |
| 2       | 6.01           | 9.87            | No cracks or chips, clean surface                         |
| 3       | 5.08           | 9.91            | No cracks or chips, clean surface                         |
| 4       | 5.30           | 10.00           | No cracks or chips, clean surface                         |
| 5       | 5.09           | 9.90            | No cracks or chips, clean surface                         |
| 6       | 5.09           | 9.93            | No cracks or chips, clean surface                         |
| 7       | 5.27           | 9.88            | No cracks or chips, clean surface                         |
| 8       | 5.23           | 9.93            | No cracks or chips, clean surface                         |
| 9       | 5.19           | 9.92            | No cracks or chips, clean surface                         |
| 10      | 5.20           | 9.93            | No cracks or chips, clean surface                         |
| 11      | 5.23           | 9.91            | No cracks or chips, clean surface                         |
| 12      | 5.18           | 9.91            | No cracks or chips, clean surface                         |
| 13      | 5.17           | 9.85            | No cracks or chips, clean surface                         |
| 14      | 5.13           | 9.94            | No cracks or chips, clean surface                         |
| 15      | 5.16           | 9.89            | No cracks or chips, clean surface                         |
| 16      | 5.17           | 9.94            | No cracks or chips, clean surface                         |
| Average | 5.23           | 9.91            |   |

It is shown in Table III that the density of sintered pellets has an average density of 9.91 g/cc or 90.42% of the Theoretical Density (TD = 10.96 g/cc). The density specification of sintered pellets is not less than 94% of TD [6]. These results indicate that the sintered pellets do not meet the requirement because the sintered density is low. It could happen because the powder which is used to make a pellet is too porous. The morphology and characteristic of the powder are influenced by the conversion process, especially at the purification, precipitation, calcination and reduction processes. Therefore, process optimization becomes very important.

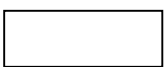
Visual inspection of all pellets shows that all pellets have no crack and chips at the surface. The cleanliness of all pellets is good. No macroscopic inclusions were found. The average O/U ratio of sintered pellets was 2.0003.

The O/U ratio value of sintered pellets is slightly lower than the O/U ratio of UO<sub>2</sub> powder. This phenomenon indicates that during the sintering process, reduction and oxidation process happened. Those processes make the O/U ratio of the sintered pellets more ideal and meet the requirement better.

The observation of sintered pellets microhardness was done at several positions. First position is near the edge of the sintered pellet (A) and the second position is around the centre of the pellet (B). The result of microhardness testing is shown in Table IV. The microhardness in A position is higher in B

position. This could be the indication that there are differences in microstructure of sintered pellets in A and B position.

TABLE IV. UO<sub>2</sub>SINTERED PELLET MICROHARDNESS AT 2 POSITIONS

| A   | Hardness (VHN) | B  | Hardness (VHN) |
|---|----------------|--|----------------|
|  | 657.8          |  | 634.2          |

The sintered pellet microstructure is shown in Fig. 3. In position A, the microstructure is more homogeneous than the microstructure in B position. In B position, some pores exist in several positions. These pores could lower the microhardness. This phenomenon could be the cause of microhardness in B position is lower than in A position. Pores have an important role in sintered pellets. The function of pores is to accommodate fission products from the radiation process in the nuclear reactor.

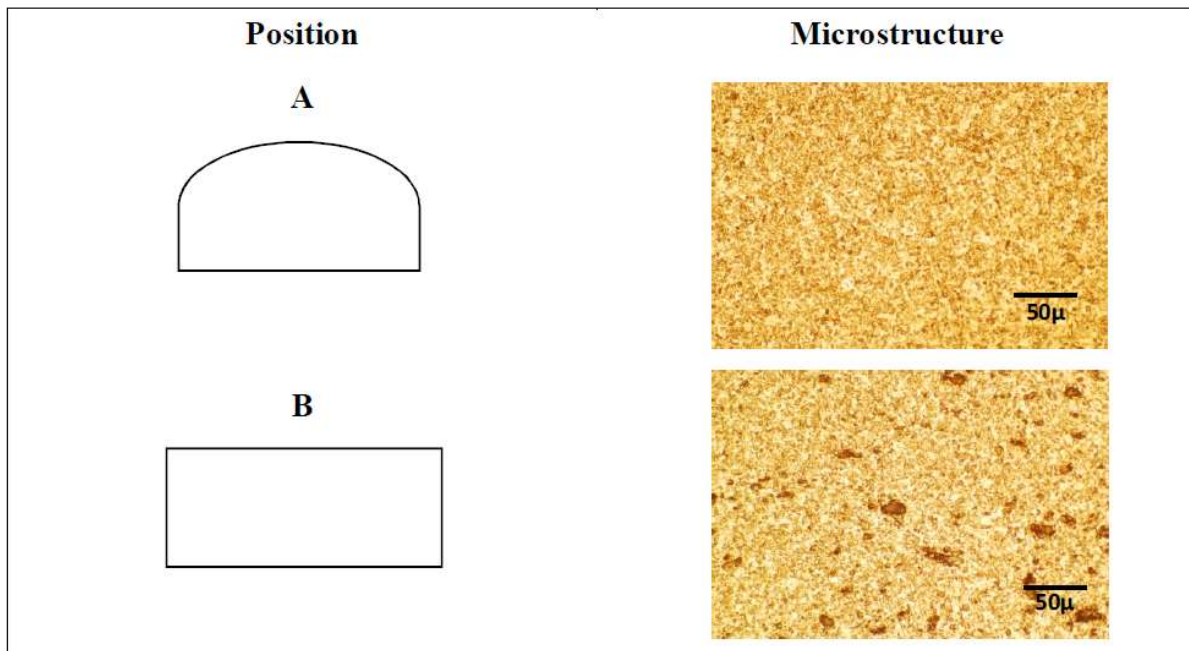


FIG. 3. The microstructure of UO<sub>2</sub> sintered pellets.

#### 4. CONCLUSION

The UO<sub>2</sub> powder from yellow cake derived from phosphate fertilizer waste has been successfully turned into UO<sub>2</sub> sintered pellets. The characterization results from the sintered pellets shows that most of the required specification has been met, but there are still needs to be some improvement in the purity of the powder and sintered pellet density. This can be done by parameter optimization of the purification process. To improve the sintered pellet density, powder conditioning before final pressing could be done. The processes which included in powder conditioning are pre-pressing, crushing and granulating. Yellow cake from phosphate fertilizer waste has a good potential to become a raw material for nuclear fuel and become the uranium back-up source in the future for Indonesia.

## REFERENCES

- [1] SUGIYONO, A. “Indonesia electricity outlook 2010-2030: Prospect of new and renewable energy utilization”, Proc. 5<sup>th</sup> Nat. Conf. Jakarta, 2012, BATAN, Jakarta (2012) 87–94.
- [2] BATAN, Indonesia Nuclear Energy Outlook, BATAN, Jakarta (2014).
- [3] RIZA, F. NURI, H. L., ARIEF, E. R., “Uranium processing become yellow cake”, Proc. 12<sup>th</sup> Conf. Yogyakarta, BATAN, Yogyakarta (2006) 164–174.
- [4] SURYAMAN, G.K., TOROWATI, MUTIARA, LANGENATI, R., Comparison of Chemical and Physical Properties of UO<sub>2</sub> Powder Yellow Cake Conversion of Phosphate Fertilizer Waste and Commercial Yellow Cake, Jurnal Teknologi Bahan Nuklir **9**. Serpong, Indonesia (2013) 77–83 (in Indonesian, English abstract).
- [5] ASTM STANDARD C776-06, Standard Specification for Sintered Uranium Dioxide Pellets, ASTM International, West Conshohocken, PA, USA (2011).
- [6] ASTM STANDARD C753-04, Standard Specification for Nuclear-Grade, Sinterable Uranium Dioxide Powder, ASTM International, West Conshohocken, PA, USA (2009).

# **STUDY OF GEOLOGICAL DETAILS TOWARDS FEASIBILITY OF URANIUM PROJECT: INDIAN CASE STUDIES**

A.K. SARANGI, K.S.V. KUMAR  
Uranium Corporation of India Ltd,  
Singhbhum East, Jharkhand, India

## **Abstract**

Appropriate technical evaluation of geological details at early stage of exploration is the key to minimising the lead-time between discovery and production, and has a major influence on economic viability of the deposits. Indian uranium deposits are of medium-tonnage and low-grade occurring in dissimilar geological provinces. Detailed studies of geological characteristics of these deposits are very vital to the proper selection of technology and subsequent successful operation. The method of mining is influenced by the ore body depth, size, grade, configuration, hostrock and adjoining strata characteristics, hydrological condition and other factors. The ore processing technology is also subjective to mineralogical characteristics of the ore. In order to draw the flowsheet, determine process parameters and selection of reagents, a comprehensive study on identification of minerals and their probable metallurgical characteristics, general physical relationship between various minerals, mineral liberation size etc is of great significance. The technology for disposal of tailings is also influenced by geological/geo-hydrological characteristics.

## **1. INTRODUCTION**

Appropriate technical evaluation of geological details from early stage of exploration and during different stages of feasibility studies is very vital for successful commissioning and operation of uranium mining and processing projects. The feasibility study, apart from determining the economic viability, must accurately and completely describe the process details considering the factors those influence the technology and parameters. Considering the significance of the steps associated with preparation of feasibility report and to minimise the risks associated with each stage of decision making, feasibility studies are normally carried out in sequence. The conceptual study (or scoping study) generally starts with early stage of exploration as the geological details emerge, the pre-feasibility study may include test work and analysis based on specific information on the deposit and the feasibility study must conclude on the process with sufficient degree of confirmatory note to enable to take the vital decision on investment on the project.

The key to successful operation of Indian uranium deposits lies in outlining a pre-development strategy as the exploration advances to different stages. This phase called ‘exploratory mining’ — which starts with detailed exploration and ends with approval of the project — is very critical for early commissioning of the project. The activities during this period include collection of representative drill core samples during exploration, laboratory studies, geo-technical studies and determination of geo-mechanical properties of ore and waste rock, etc. Later, the ore lenses are accessed through limited entry or entries. Developments along the ore body helps in better understanding of the configuration of the lenses. Studies for strata control in case of underground mining are carried out towards deciding the mining (e.g. stoping) method. Large ore samples generated during the process helps in detailed pilot plant studies and operation of the plant on continuous mode while fine-tuning all process related steps. The period of exploratory mining is further utilised in locating and planning infrastructure needs, preparation of different reports for regulatory clearances and generating public opinion in favour of uranium mining.

Collection and analysis of appropriate geological details supporting the requirement of conceptual study (or scoping study), pre-feasibility study and feasibility study play an important role. All Indian uranium deposits have gone through an extensive phase of exploratory mining, generating large volumes of data which are of immense value to the operators during the life of the mines and plants.

## 2. SIGNIFICANCE OF GEOLOGICAL DETAILS FOR URANIUM MINING AND PROCESSING

Detailed studies of geological characteristics of uranium deposits are very vital to the proper selection of technology and subsequent successful operation.

Uranium mining is generally done in any of the three ways — underground mining, open pit mining and in-situ leaching. A study on ore deposit type may provide useful guide to the proposed exploration programme. It may also provide some clue to probable continuity, grade distribution, disequilibrium factor, uniformity in grade and width and other characteristics of the mineralisation. A broad understanding on possible mining technologies may be inferred from the study of ore deposit types. It is essential to establish the correlation between uranium content and radioactivity at a very early stage of exploration, as radiometric counters are used to measure the uranium content.

Assessment of uranium resources at appropriate stage of exploration is vital for decision on subsequent stages of exploration and intensity of activities. The estimations based on different cut-off criteria are more meaningful during conceptual / pre-feasibility studies. However, the decision on final cut-off grade and thickness is required to be taken during pre-feasibility study. Reporting of the presence of by-products may help in deciding the ultimate cut-off values. It needs to be emphasized that the resource estimation is based on only limited information during exploration and different categories of resources (measured, indicated and inferred) provide different level of confidence.

Ore reserve estimation during pre-feasibility / feasibility stage is the most fundamental to any mining project. It needs to be fully understood that the entire resources are never available for commercial mining operations. Ore reserve is the economically mineable part of a resource (measured and indicated) demonstrated by at least a pre-feasibility study. This study must include adequate information on mining, processing, metallurgical, economic and other relevant factors (called ‘modifying factors’) demonstrating economic extraction.

The mining methods — underground and open pit are influenced by the ore body depth, size, grade, configuration, host rock, adjoining strata characteristics, hydrological condition, etc. All this information emerge from extensive surface exploration over the entire deposit area. Consideration of competency of host rock and strata above and below the mineralisation are important for mine planning and outlining the mine layout. Study of Rock Quality Designation (RQD), joint quality / spacing / filling material and hydrological conditions / water inflow helps in assessment of geo-mechanical properties of the rock mass. Adequate number of representative ore and waste rock samples are required to be collected for laboratory analysis of compressive strength, tensile strength, internal angle of friction and other rock properties for design of stopes and support pattern in case of underground mining. These tests are also required to derive pit slopes, preferred location for haulage roads and other features in case of open pit mining. Study on presence of faults, folds, joints and other physical features, and their continuity, also play important role while finalising the mine layout.

Study on hydrogeology of the area helps in deciding the dewatering / pumping system of the mine. Sometimes a detailed analysis on hydrogeology of the area is required for environmental study.

The ore processing technology is also subjective to mineralogical characteristics of the ore. In order to draw the flowsheet, determine process parameters and selection of reagents, a comprehensive study on complete analysis of ore / host rock, identification of minerals and their probable metallurgical characteristics, general physical relationship between various minerals, mineral liberation size etc are of great significance. These tests are required to be carried out on all the representative borehole core samples to establish uniformity of characteristics. In case of wide fluctuations of the key characteristics, limited mining is required to be undertaken to obtain adequate ore samples from different metallurgical domains and establish the appropriate flowsheet. Sometimes, the tests are required to be repeated many times to derive the preferred route.

Studies on bond index, determining the amenability of ore to conventional treatment methods, feed size, requirement of acid / alkali and other reagents, recovery under different pH, emf, retention time and temperature etc. are of significance towards finalising the flowsheet before its validation in pilot plant studies.

The technology for disposal of tailings is also influenced by geological / geo-hydrological characteristics. Presence of natural barrier (hills) around the proposed site, general geology of the area with regard to presence of major faults and joints, porosity / permeability of the underlying strata, proximity to mineralised zone etc are of primary consideration for any meaningful assessment of tailings disposal site. Disposal of tailings in open pit is though the most preferred mechanism, it may not always become feasible because of chosen mining method.

### 3. INDIAN URANIUM INDUSTRY

Indian nuclear industry is nourished by indigenous production and import of uranium under India specific agreements to meet its nuclear fuel requirement. However, it has been aptly realised that use of indigenous uranium is very vital towards long-term energy security of the country. Therefore, maximising the uranium production from indigenous resources is considered a critical task in country's nuclear power programme.

Uranium production of India is now met from two ore processing plants (Jaduguda and Turamdihi) located in the state of Jharkhand in Eastern part of the country. These plants are fed by ore from six underground mines (Jaduguda, Bhatin, Narwapahar, Turamdihi, Bagjata and Mohuldih) and one opencast mine (Banduhurang). In addition, one large underground mine and processing plant (Tummalapalle) is under construction in the state of Andhra Pradesh in Southern part of the country. The planned expansion of indigenous nuclear power programme calls for opening of new mines and setting up process plants for meeting the timely fuel requirement. Accordingly, few more ore mining and processing projects are envisaged in different parts of the country.

Appropriate technical evaluation of geological details at early stage of exploration is the key to minimising the lead-time between discovery and production. This has a major influence on economic viability of the deposits.

Indian uranium deposits are of low grade, small in size occurring in dissimilar geological provinces. The key to successful operation of Indian uranium deposits lies in outlining a pre-development strategy as the exploration advances to different stages. This phase called 'exploratory mining' — which starts with detailed exploration and ends with approval of the project, is very critical for successful commissioning of the project. The activities during this period include collection of representative drill core samples during exploration, laboratory studies, geo-technical studies and determination of geo-mechanical properties of ore and waste rock, etc. Later, the ore lenses are accessed through limited entry or entries. Developments along the ore body helps in better understanding of the configuration of the lenses. Studies for strata control in case of underground mining are carried out for deciding the mining (stoping) method. Large ore samples generated during the process of such developments help in detailed pilot plant studies and operation of the pilot plant on continuous mode while fine-tuning all process related steps. The period of exploratory mining is further utilised in locating and planning infrastructure needs, preparation of different reports for regulatory clearances and generating public opinion in favour of uranium mining.

All Indian uranium deposits have gone through such an exploratory mining phase, generating large volume of data which are of immense value to the operators during the life of the mines and plants.

### 4. INDIAN CASE STUDIES

In Singhbhum Shear Zone (SSZ) in Jharkhand, the ore deposits are located along the shear zone. The ore lenses extend as thin veins with moderate dip ( $\sim 40^\circ$ ) from surface following the lithological contacts. Detailed studies of geological details like dip, strike, width, inclination, rock quality etc have helped in

planning mine entries. Vertical or inclined shafts are planned at the centre of the ore mass preferably in thin and lean zones, thereby minimizing underground transportation cost and limiting the in-situ ore loss. Decline entries at Narwapahar, Turamdihi, Bagjata and Mohuldih are planned after proper assessment of the country rock, inclination of the orebody, joint characteristics, water bearing strata etc. Development headings have been planned and method of extraction (stoping) are selected after consideration of width and dip of the lodes. Selection of cut-and-fill method of stoping has helped in disposal of appreciable quantity of uranium tailings in underground. Use of ramp entry into the stopes has helped to dispose waste rock within the stopes. Assessment of rock quality on the basis of geological discontinuities at desired places has helped in design of artificial support facilitating maximum ore recovery. At Banduhurang, low-grade near surface orebody has been carefully developed as an opencast mine after due consideration and optimization of techno-economic factors like stripping ratio, uranium content, leachability, cost of the product etc. Application of software in modelling the orebody has helped to fine-tune the mining scheme with different options before start of the mining activities.

The similarity in ore characteristics (siliceous host rock) in Singhbhum region has helped to adopt identical flowsheet in both Jaduguda and Turamdihi plants. However, the difference in work index of ore of different mines has necessitated adopting different grinding parameters. Other steps like acid leaching, ion exchange and product precipitation etc are common for both the plants. Recovery of by-products in both the plants is subject to change in the mix of feed from different mines.

At Tummalapalle in Cuddapah basin of Andhra Pradesh, two parallel ore zones in carbonate host rock show consistent dip of  $15^{\circ}$  extending for a strike length of 6.6 km. In order to minimise the cost of production and dilution through optimum level of mechanization and maximize the ore recovery, decline entry at  $9^{\circ}$  gradient has been developed along the orebody following the apparent dip. The advance strike drives (ASDs) are developed in the strike direction. Size of the panels, ore extraction and size of rib pillars are planned on the basis of competency of host and wall rocks, width of orebody and parting between two lodes. A poor rock strata unexpectedly encountered in the roof of the hanging wall lode has hindered the planned progress. Efforts to modify the development sequence through a trial stope are in progress.

Because of the carbonate host rock, extensive laboratory and pilot plant studies have been done in finalising the alkaline leaching process. The fine grained nature of minerals within competent host rock has necessitated leaching under high pressure-temperature conditions. The final product will precipitate as sodium diuranate (SDU).

At Gogi in Karnataka, fracture controlled mineralisation in limestone and granitic host rock warrants extensive pre-mining investigations. After the surface exploration, the on-going exploratory mining has provided a better understanding on orebody configuration. The mining scheme is being worked out. The representative ore samples are under pilot plant studies for finalization of suitable flowsheet.

## 5. CONCLUSION

In spite of many technological challenges associated with development of Indian uranium deposits (because of their adverse characteristics), the uranium industry of the country has recorded magnificent growth supporting the indigenous fuel need. The key to successful operation of these deposits lies in extensive investigation of various geological properties and their detailed analysis towards selection of appropriate technology. Use of modern techniques like application of integrated software in simulating the mine layout is being routinely followed. Assimilation of global technology with indigenous know-how, standardization of working modules and equipment, continuous improvement in working practices etc have provided desired benefits. The industry's best practices have created a newer benchmark in comparable industries of the country.

## ACKNOWLEDGEMENTS

Authors wish to thank Chairman and Managing Director of Uranium Corporation of India Ltd for encouragement and permission to publish this paper. Contributions from the colleagues are also thankfully acknowledged.

## BIBLIOGRAPHY

- BELL, D.H., Some operating concerns in carbonate leaching, *CIM Bull.* **72** (1979) 177–180.
- BIENIAWSKI, Z.T., *Engineering Rock Mass Classifications: A Complete Manual for Engineers and Geologists in Mining, Civil, and Petroleum Engineering*, John Wiley & Sons, (1989) 251 pp.
- CUNHEY, M., The extreme diversity of uranium deposits, *Mineralium Deposita* **44** (2009) 3–9.
- DESMUKH, D.J., *Elements of Mining Technology* **2** (1988) 520 pp.
- GOW, W.A., RITCEY, G.M., The treatment of Canadian uranium ores: A Review, *CIM Bull.* **62** (1969) 1330–1339.
- INTERNATIONAL ATOMIC ENERGY AGENCY, Guidebook on the development of projects for uranium mining and ore processing, IAEA-TECDOC-595, IAEA, Vienna (1991).
- GUPTA, R., SARANGI, A. K., Emerging Trend of Uranium Mining: The Indian Scenario, Uranium Production and Raw Materials for the Nuclear Fuel Cycle – Supply and Demand, Economics, the Environment and Energy Security (Proc. Int. Symp., Vienna, 2005) IAEA, Vienna (2006) 47–56.
- LAMBERG, P., “Particles—the bridge between geology and metallurgy” (Proc. Conf. Mineral Engineering, Lulea, Sweden) (2011) 8–9.
- POOL, T.C., “Technology and the Uranium industry”, The Uranium Production Cycle and the Environment, C&S Papers Series No. 10/P, IAEA Vienna (2002) 261–271.
- RADIVOJEVIC, M., REHREN, T., PERNICKA, E., SLJIVAR, D., BRAUNS, M., BORIC, D., On the origins of extractive metallurgy: new evidence from Europe, *J. Archaeological Sci.* **37** 11 (2010) 2775–2787.
- SARANGI, A.K., Grade Control in Jaduguda Uranium Mine, Jharkhand, *Trans. Mining, Geological and Metallurgical Institute of India (MGMI)* **99** 1–2 (2003) 73–79.
- SCHWEITZER, J.K., JOHNSON, R. A., Geotechnical classification of deep and ultradeep Witwatersrand mining areas, South Africa, *Mineralium Deposita*, **32** 4 (1997) 335–348.
- SORENSEN, E., JENSEN, E., “Uranium extraction by continuous carbonate leaching in a pipe autoclave”, Advances in Uranium Ore Processing and Recovery from Non-Conventional Resources, Proc. Panel Proc. Series, IAEA, Vienna (1985) 41–51.
- STANTON, R.L., *Ore Petrology*, McGraw Hill, New York (1972) 714 pp.

# **ORE GENESIS OF GOGI URANIUM DEPOSIT IN BHIMA BASIN, YADGIR DISTRICT, KARNATAKA, INDIA**

M.K. KOTHARI\*, A.K. RAI\*\*, P.S. PARIHAR\*\*

\* Atomic Minerals Directorate for Exploration and Research,  
Department of Atomic Energy, Bangalore,

\*\* Atomic Minerals Directorate for Exploration and Research,  
Department of Atomic Energy, Hyderabad,

India

## **Abstract**

Gogi Uranium Deposit in Yadgir district, Karnataka, India, is located in the middle of the 40 km long E-W trending Kurlagere–Gundahalli fault in the southern margin of the Neoproterozoic Bhima basin. Uranium mineralization is hosted by brecciated limestone and basement granite, occurring in the form of fracture fillings veins and veinlets in tectonised zone along the reverse Kurlagere–Gundahalli fault. The mineralization is intimately associated with sulphides and low rank bituminous organic matter. The discrete uranium phases in both the host rocks are mainly coffinite and pitchblende, with minor amounts of U–Ti complex in granite. It is envisaged that the uranium from fertile granite was remobilised during deformation and transported as soluble carbonate complexes in the hydrothermal fluid. The spatial and textural relationship of sulphides and organic matter with uranium phases suggest that they have formed earlier and provided a strong reducing environment for the precipitation of uranium from hydrothermal fluids. The mode of occurrence, mineral assemblage, textural relationship, paragenetic sequence coupled with compositional characteristics suggest that the uranium deposit at Gogi is a fracture controlled polyphase, epithermal vein type uranium mineralization.

## **1. INTRODUCTION**

Proterozoic basins are the prime targets for high grade and large tonnage uranium deposits in the world. In India there are fourteen Proterozoic basins popularly known as ‘Purana basins’ which are under active exploration since 1980s [1]. The Bhima basin is located on the northern margin of the Western Dharwar Craton in Southern India. The investigations in Bhima basin commenced in 1996 which brought to light surface uranium occurrences in fracture zones along the basin margin. The concerted exploration efforts in Bhima basin achieved medium grade uranium deposit at Gogi along Kurlagere–Gundahalli fault [2, 3]. The present paper deals with petrography, mineral chemistry, control of uranium mineralization and ore genesis of Gogi uranium deposit.

## **2. REGIONAL GEOLOGY**

The Neoproterozoic Bhima basin is youngest and smallest Proterozoic basin in India covering about 5200 sq km (Fig. 1), located on the northeastern margin of the Dharwar craton in parts of Karnataka and Andhra Pradesh. The northern and western extension of this basin is concealed under the Late Cretaceous–Palaeocene Deccan traps. The southern and eastern part of the basin is unconformably overlying the basement crystalline rocks, which comprises of Peninsular gneisses, enclaves of greenstones /schist belts in the Peninsular gneisses and intrusive pink and grey granitoids of Closepet equivalent (~2.5 Ga). A number of basic dykes traverse the crystalline terrain. The Bhima group comprises dominantly limestone and subordinate shale with thin arenite and conglomerate at the base [4]. The average stratigraphic thickness of the Bhima sediments is about 300 m as observed from surface and sub-surface data. Age of the Bhima basin deduced from biota and litho-stratigraphy points to Vendian /Neoproterozoic age (< 625 – > 550 Ma) [5].

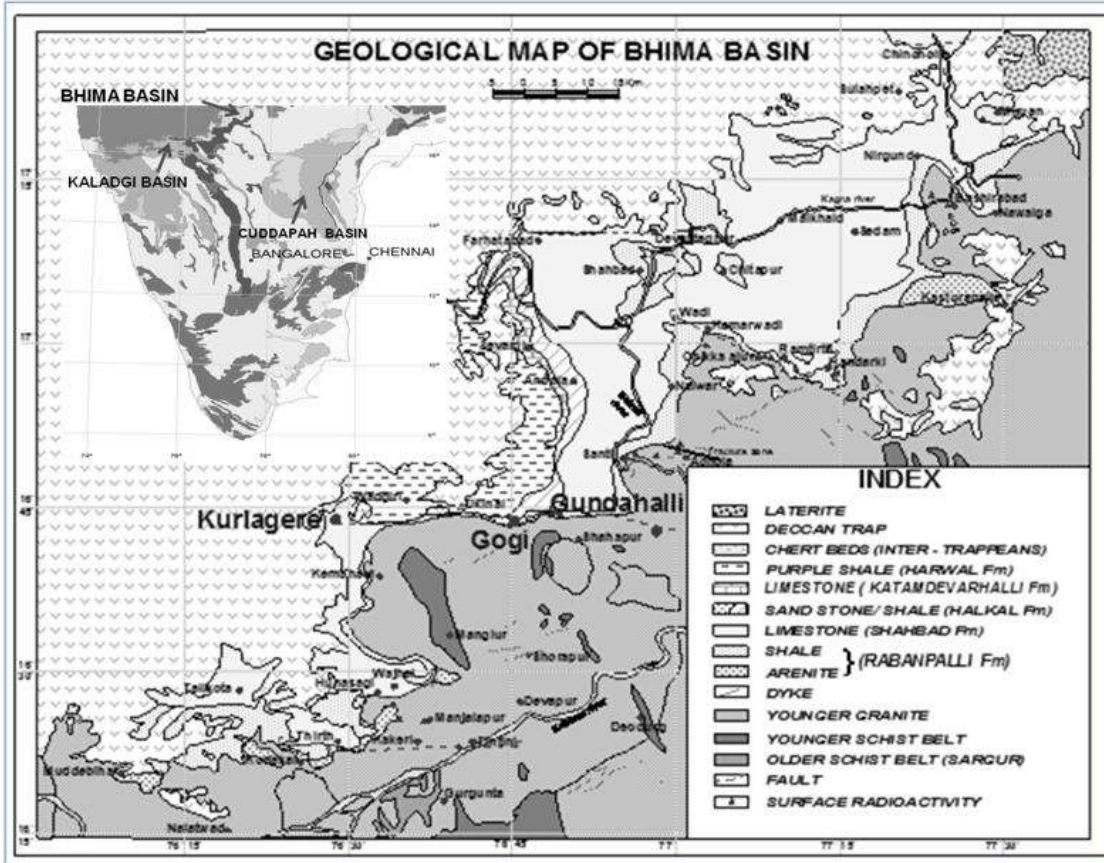
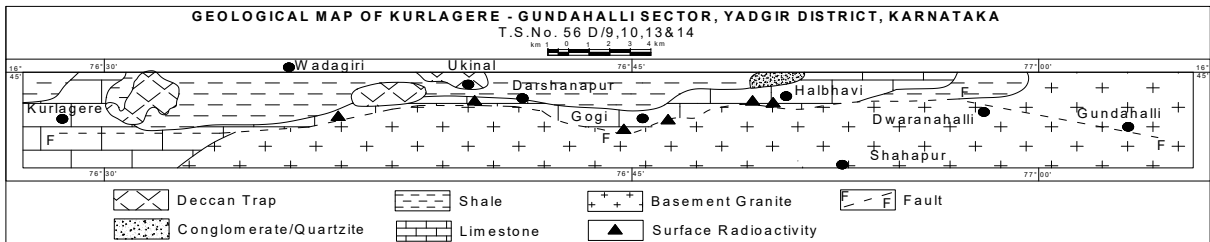


FIG. 1. Geological map of Bhima basin, Karnataka and Andhra Pradesh, India.

The sediments of the Bhima group are horizontally disposed retaining their original depositional imprints such as bedding planes, cross stratification and form stratified layer over one another indicating quiescent condition of depositional environment. The sediments are devoid of significant imprints of tectonism and metamorphism. The basin is dissected by prominent E–W and NW–SE trending faults besides a number of smaller N–S and NE–SW trending cross faults. The major E–W faults are Tirth–Tintini fault and Wajhal fault in southern part, Kurlagere–Gundahalli fault in central part and Farhatabad fault in northern part of the basin. The NW–SE trending Wadi fault is located in the north-eastern part of the basin (Fig. 1). Moderate to intense deformation is observed in the vicinity of the faults resulting in steep dips, intense brecciation isoclinal and recumbent folding and thrusting. The width of the tectonised zones across the faults varies widely with maximum of 500 m along Kurlagere–Gundahalli fault. These faults have been recognised as normal faults with major strike slip component [6]. Detail surface and subsurface investigation by Atomic Minerals Directorate for Exploration and Research (AMD) has established the reverse nature of Kurlagere–Gundahalli and Wadi faults.

### 3. LOCAL GEOLOGICAL SETUP

Gogi uranium deposit is located at the middle of E–W trending Kurlagere–Gundahalli fault that runs over 40 km from Kurlagere in the west to Gundahalli in the east (Fig. 2), and takes a swing at Gogi due to NE–SW cross fault. The area exposes basement granite followed by Shahabad limestone with minor glauconitic shale and arenite. The tectonised zone is characterised by intense brecciation in both limestone and granite with clasts and fragments of granite, basic rock, limestone and shale embedded in grey limestone. The beds are sub-vertical due south near the fault and progressively become horizontal away from the tectonised zone. Kurlagere–Gundahalli fault is a reverse fault with moderate dips forming ‘nose like’ structure (Fig. 3) in the Gogi area and becomes sub-vertical to vertical in the west (Ukinal–Darshanapur area) and in the east (Halbhavi area).



*FIG. 2. Geological map of Kurlagere–Gundahalli sector, Yadgir district, Karnataka, India.*

#### 4. MINERALIZATION

Uranium mineralization in Gogi area is hosted in brecciated limestone closer to the sediment basement contact along Kurlagere–Gundahalli fault. Subsurface exploration brought to light significant mineralization in brecciated limestone and sheared basement granite within the tectonised zone [4, 7]. The mineralization extends over 800 m × 200 m area, where a total of 3619 tU (4268 t of  $U_3O_8$ ) with average grade 0.14% U (0.17%  $U_3O_8$ ) has been established [8].

Uranium mineralization in limestone occurs as two distinct lodes viz., (i) Hangwall lode and (ii) Footwall lode. The moderate to steeply dipping hangwall lode occurs close to the upper granite shale tectonised contact, the sub horizontal footwall lode occurs immediately above the lower shale granite contact. At places both hangwall and footwall lodes are merged forming a thick ore zone in the ‘nose like’ structure (Fig. 3) [9].

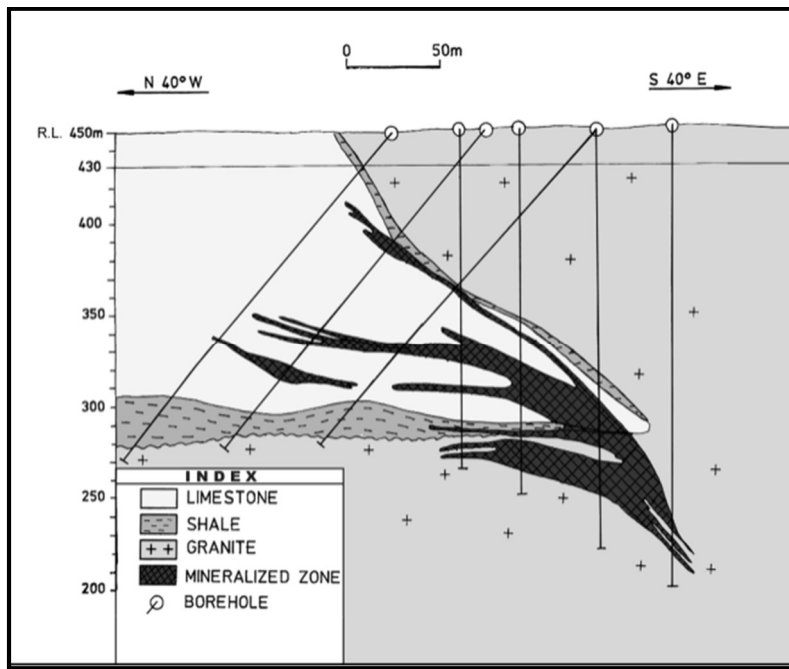


*FIG. 3. Transverse section of Gogi Uranium Deposit, Yadgir District, Karnataka, India, after [9].*

#### 5. PETROGRAPHY OF MINERALIZED LIMESTONE

The impure limestone hosting uranium mineralization is light to dark grey in colour, fine grained and compact. The rock is mainly composed of primary micritic calcite (size < 4 microns) which often results into secondary sparry calcite on diagenetic alteration. The rock contains quartz, chalcedony, chert, feldspar, barite, chlorite, glauconite, dolomite, limonite, clay and sulphides and organic matter as

impurities. Stylolites present at places indicate the consequences of deep burial and development of pressure solutions. The brecciation observed in limestone is due to deformation. The fractures in the rocks are sealed by sparry calcite, chert, barite and sulphides. Low rank bituminous organic matter is noticed along the fractures occurring as large globular aggregates with variable reflectivity and it is of migratory nature, transported by the circulating fluids [7] (see Fig. 16).

The ore minerals in limestone are dominantly pyrite and minor marcasite, galena, chalcocite, pyrolusite, arsenopyrite, nicolite and cobaltite. Pyrite occurs in different morphology and textural varieties viz., frambooidal pyrite, eudedral pyrite, lumpy pyrite, reticulate pyrite, botryoidal pyrite, oolitic pyrite (Figs 4–9), porous pyrite and zoned pyrite [10]. Frambooidal pyrite occurs as spheroidal to sub spheroidal agglomerates of equidimensional and equimorphic microcrystal varying in size from 5  $\mu\text{m}$  to 75  $\mu\text{m}$ . Agglomerations of frambooids have led to formation of porous pyrite, which later recrystallised to form pitted or porous euhedral pyrite [11]. Euhedral pyrite varies in size from < 0.2 mm to >1 mm, whereas lumpy pyrite occurs as veins upto 5 to 6 cm thickness, formed by infiltration of hydrothermal solution into the brecciated zones. Colloidal pyrite occurring as botryoidal and oolitic forms in association with chert formed by primary precipitation suggesting physico-chemical condition of ore formation [12, 13]. The colloidal pyrite suggests a low temperature condition below 80°C.

Galena occurs as euhedral to subhedral grains in association with pyrite, pitchblende and coffinite (Fig. 10) and also as inclusion in pitchblende and coffinite. Chalcocite, arsenopyrite, nicolite and cobaltite are occurring in association with pyrite and marcasite in veins (Fig. 11). Pyrolusite is present as bands in limestone.

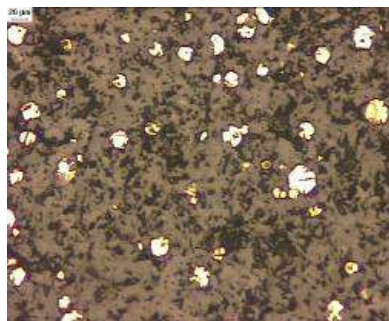


FIG. 4. Frambooidal pyrite in limestone, 10 $\times$ , RL, IN.

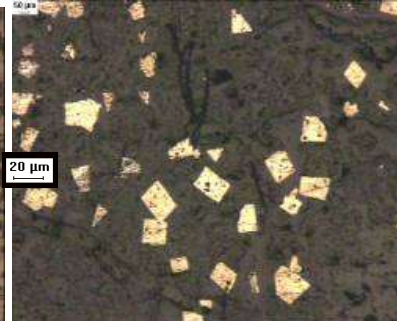


FIG. 5. Euhedral pyrite in micritic limestone. 5 $\times$ , RL, IN.



FIG. 6. Lumpy pyrite in micritic limestone. 5 $\times$ , RL, IN.

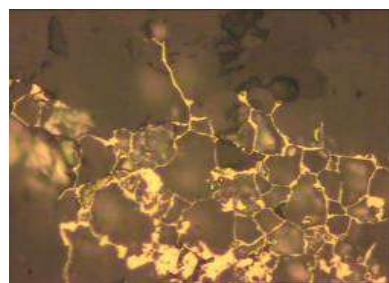


FIG. 7. Reticulate pyrite in micritic limestone, 50 $\times$ , RL, IN.

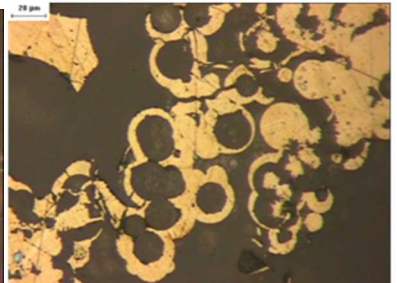


FIG. 8. Botryoidal pyrite in micritic limestone 20 $\times$ , RL, IN.



FIG. 9. Oolitic pyrite in micritic limestone. 50 $\times$ , RL, IN.

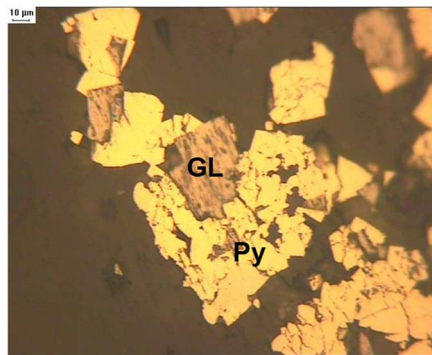


FIG. 10. Galena (GL) being replaced by pyrite (Py). 50 $\times$ , RL, IN.

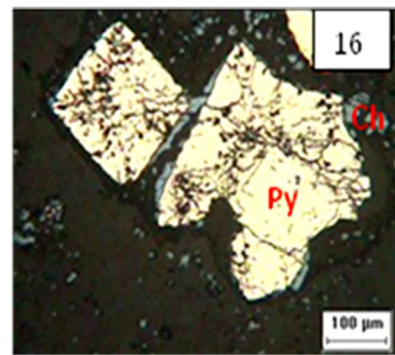


FIG. 11. Chalcocite (Ch) surrounding pyrite (Py). 50 $\times$ , RL, IN.

Major uranium minerals identified in the limestone are coffinite and pitchblende. These minerals are mainly present as veins and veinlets (Figs 12–14) in association with sulphides and organic matters. Pitchblende is of two generation viz., earlier one is rimmed by coffinite and the later one occurs as replacing coffinite within the carbonaceous matter as well as along the fractures of coarse grained pyrite (Figs 16, 17). The mutual replacement of coffinite and pitchblende results in meshwork formation (Fig. 18). Pitchblende is observed in association with frambooidal pyrite varying in size from 10  $\mu\text{m}$  to 50  $\mu\text{m}$  (Fig. 15). Besides, the discrete phases of uranium minerals, uranium is adsorbed on limonite and clay.

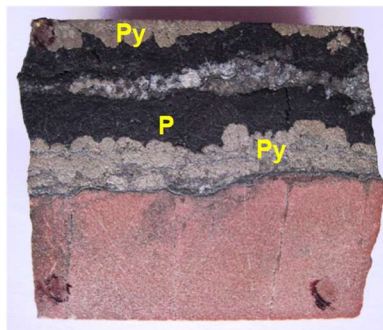


FIG. 12. Pitchblende (P) and pyrite (Py) vein in limestone (Polished core slab).



FIG. 13. Corresponding alpha tracks on C.N. 85 Film.

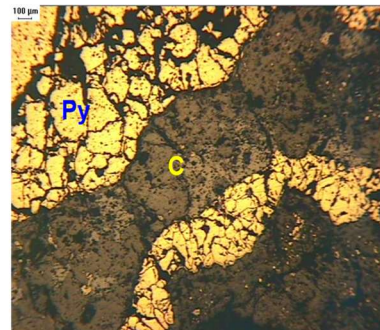


FIG. 14. Coffinite (C) band between pyrite (Py) bands. 5 $\times$ , RL, IN.

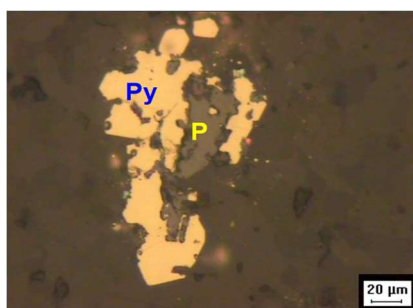


FIG. 15. Pitchblende (P) association with frambooidal pyrite (Py), 50 $\times$ , IN, RL.

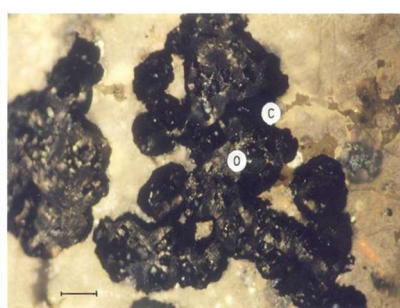


FIG. 16. Organic matter (O) rimmed with Sulphides (fine grains of high reflectivity and coffinite. 20 $\times$ , IN, RL, Bar: 0.25mm.



FIG. 17. Coffinite (C) in association with organic matter (O), 2 $\times$ , RL, XN.

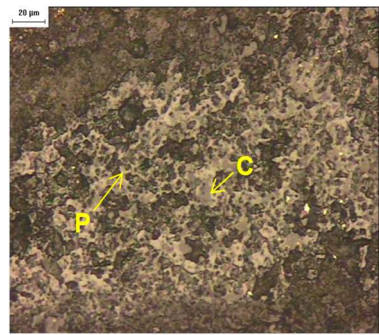


FIG. 18. Meshwork of Pitchblende (P) and coffinite (C), 20 $\times$ , RL, IN.

## 6. PETROGRAPHY OF MINERALIZED GRANITE

Petrographically the basement granite is deformed biotite ( $\pm$  hornblende) granite, granodiorite with cataclastic texture (Fig. 19). It comprises quartz, microcline, perthite, orthoclase and plagioclase as major minerals and chloritised biotite, minor hornblende, accessories zircon, monazite, apatite, allanite and sphene observed as minor minerals. The ore minerals mainly include sulphides comprising pyrite, chalcopyrite, arsenopyrite and galena as veins and disseminated specks, besides ilmenite as disseminated grains and specular haematite along fractures and grain boundaries.

The rock has undergone brittle to ductile deformation. Development of fractures, grain size reduction, brecciation and cataclasitisation represent the brittle phenomena. Subgrain rotation, grain boundary migration, undulose extinction and ribbon formation in quartz grains shows the signatures of ductile deformation. The mild to intense alterations are manifested by sericitisation, chloritization, epidotisation and hematitisation. At places fluorite is present as vein in association with chlorite and opaques.

The uranium minerals are mainly coffinite minor uraninite and pitchblende with subordinate U–Ti complex (Figs 20–22). Uraninite is present as discrete grains whereas coffinite and pitchblende occur as vein, veinlets and fracture fillings with pitchblende replaced by coffinite and U–Ti complex at places. Oxidation of  $\text{Fe}^{+2}$  to  $\text{Fe}^{+3}$  in chlorite and higher concentration of silica might have led to the precipitation of coffinite. At places coffinite is botryoidal in nature, which indicates its low temperature of formation. Pitchblende occurs as veinlets in association with quartz, pyrite, fluorite and chlorite. U–Ti complex is reddish brown present in intergranular spaces and fractures. Uranium is also adsorbed on clay, chlorite and limonite.



FIG. 19. Porphyroblast of feldspar (P) surround by quartz ribbons, in cataclasite grainte 2 $\times$ , TL, XN.

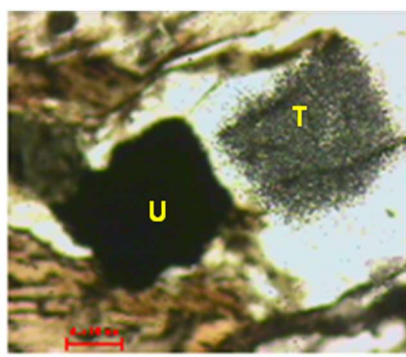


FIG. 20. Uraninite (U) with tracks (T) in granite, 5 $\times$ , TL, XN bar 0.135mm.



FIG. 21. Pitchblende (P) along fractures in quartz grains, 50 $\times$ , RL, IN.

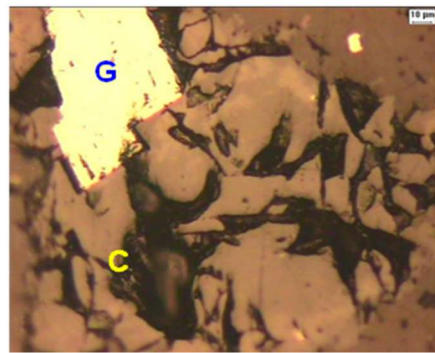


FIG. 22. Botryoidal Coffinite (C) with galena (G), 20 $\times$ , RL, IN.

## 7. MINERAL PARAGENESIS

Based on the textural relationship among various gangue and ore minerals, a paragenetic sequence is established (Table I). It comprises 3 stages i.e. pre-ore, ore and post-ore stage. The pre-ore stage comprises precipitation of calcite and chert which constitute the dominant carbonate and silicate phases of brecciated siliceous limestone and quartz, feldspar, biotite and chlorite in granite. The ore stage comprises a) the major U phases viz. two generations of pitchblende with intervening coffinite. b) sulphides are mainly prior to the precipitation of uranium minerals and is dominated by pyrite, chalcopyrite and galena, c) organic matter and clay, the formation of which started prior to major U phases. The post-ore stage is noticed by veins of calcite and quartz.

TABLE I. PARAGENETIC SEQUENCE OF THE MINERALS AT GOGI AREA

| Mineral                      | Pre ore | Ore   | Post ore |
|------------------------------|---------|-------|----------|
| <b>Minerals in limestone</b> |         |       |          |
| Calcite (Primary)            | -----   |       |          |
| Calcite (Secondary)          | -----   |       | -----    |
| Dolomite                     | ---     |       |          |
| Barite                       | -----   |       |          |
| Chert                        | -----   |       |          |
| <b>Minerals in granite</b>   |         |       |          |
| Quartz (Primary)             | -----   |       |          |
| Quartz (Secondary)           |         | ----- |          |
| Feldspar                     | -----   |       |          |
| Biotite                      | -----   |       |          |
| Chlorite                     |         | ----- |          |
| Zircon and Monazite          | -----   |       |          |



| <b>Sulphides</b>        |       |       |       |
|-------------------------|-------|-------|-------|
| Pyrite                  | ----- | ----- | ----- |
| Euhedral                |       | ----- |       |
| Framboidal              | ----- | ----- |       |
| Reticulate              |       |       | ---   |
| Colloidal               |       |       | ----- |
| Chalcopyrite            |       | ----  |       |
| Galena                  |       | ---   |       |
| Arsenopyrite            | ----- |       |       |
| Nicolite and Cobaltite  | ----- |       |       |
| Chalcocite              | ----- |       |       |
| <b>Uranium minerals</b> |       |       |       |
| Coffinite               | ---   |       |       |
| Pichblende              | ----  | ----- |       |
| U-Ti complex            |       | ----  |       |
| Adsorbed U on           |       | ---   |       |
| Organic matter          |       |       |       |
| Adsorbed U on Clay      |       | ----  |       |
| <b>Organic matter</b>   |       |       |       |

## 8. GEOCHEMISTRY OF MINERALIZED LIMESTONE

Major and minor oxide data (Table II) of mineralized limestone of Shahabad Formation reveal the followings:

- 1) CaO content varies from 18–53% in general with very little MgO (0.5–1.68%) indicating the carbonate mineral as calcite;
- 2) Few samples analysed low CaO (< 20%) with high SiO<sub>2</sub> (upto 60%) manifest the presence of chert and can be designated as cherty limestone;
- 3) High LOI upto 39.25% may be due to presence of organic matter, clay and carbonate minerals;
- 4) Other minor impurities include Al<sub>2</sub>O<sub>3</sub> (1.2–6.58%), K<sub>2</sub>O (0.2–2.05%), Na<sub>2</sub>O (0.13–0.8%), FeO (0.28–1.72%), Fe<sub>2</sub>O<sub>3</sub> (0.3–4.34%) suggests mineralogy as clays, limonite and iron sulphides;
- 5) Examination of trace element data (Table III) reveals uranium ore has positive correlation with Co, Ni, Pb and V (Fig. 23);
- 6) Samples with higher content of uranium are also enriched in V, Co, Ni, Mo, Cu, Ag and Pb;
- 7) Positive correlation of Pb with Uranium suggests Pb in the ore is mainly radiogenic.

TABLE II. MAJOR OXIDES (WT%) OF MINERALIZED LIMESTONE

| Sl No | SiO <sub>2</sub> | Al <sub>2</sub> O <sub>3</sub> | Fe <sub>2</sub> O <sub>3</sub> | FeO  | CaO   | MgO  | Na <sub>2</sub> O | K <sub>2</sub> O | P <sub>2</sub> O <sub>5</sub> | TiO <sub>2</sub> | MnO  | LOI   |
|-------|------------------|--------------------------------|--------------------------------|------|-------|------|-------------------|------------------|-------------------------------|------------------|------|-------|
| 1     | 39.67            | 1.71                           | 1.17                           | 0.65 | 30.74 | 0.50 | 0.35              | 0.30             | 0.45                          | <0.01            | 0.06 | 23.44 |
| 2     | 37.73            | 2.34                           | 2.10                           | 1.69 | 31.15 | 1.01 | 0.31              | 0.35             | 0.45                          | <0.01            | 0.05 | 21.98 |
| 3     | 30.34            | 2.34                           | 3.24                           | 1.15 | 33.90 | 1.04 | 0.39              | 0.55             | 0.50                          | <0.01            | 0.01 | 25.64 |
| 4     | 41.58            | 2.13                           | 1.24                           | 0.68 | 28.43 | 0.82 | 0.39              | 0.20             | 0.34                          | <0.01            | 0.06 | 22.18 |
| 5     | 8.10             | 1.43                           | 3.19                           | 1.62 | 52.58 | 0.54 | 0.25              | 0.68             | 0.22                          | <0.01            | 0.06 | 29.36 |
| 6     | 31.28            | 3.48                           | 2.41                           | 1.72 | 32.47 | 1.46 | 0.46              | 0.65             | 0.46                          | <0.01            | 0.06 | 24.62 |
| 7     | 35.96            | 2.30                           | 1.59                           | 1.33 | 31.75 | 1.04 | 0.46              | 0.50             | 0.38                          | <0.01            | 0.06 | 23.66 |
| 8     | 38.86            | 1.95                           | 1.81                           | 0.57 | 30.24 | 0.62 | 0.39              | 0.45             | 0.39                          | <0.01            | 0.06 | 23.66 |
| 9     | 36.00            | 5.77                           | 2.04                           | 0.68 | 27.29 | 1.35 | 0.23              | 1.85             | 1.12                          | <0.01            | 0.07 | 22.44 |
| 10    | 33.09            | 1.70                           | 1.51                           | 1.26 | 35.21 | 1.30 | 0.23              | 0.40             | 0.34                          | <0.01            | 0.06 | 24.96 |
| 11    | 44.35            | 2.24                           | 1.86                           | 1.04 | 29.54 | 0.73 | 0.39              | 0.40             | 0.40                          | <0.01            | 0.06 | 18.00 |
| 12    | 38.53            | 4.67                           | 1.40                           | 0.90 | 27.47 | 1.38 | 0.26              | 1.51             | 1.14                          | 0.30             | 0.08 | 22.30 |
| 13    | 61.84            | 4.99                           | 1.24                           | 1.62 | 11.26 | 1.22 | 0.19              | 1.51             | 1.10                          | 1.19             | 0.04 | 11.86 |
| 14    | 69.15            | 3.79                           | 2.53                           | 1.62 | 6.83  | 1.20 | 0.14              | 0.99             | 0.51                          | 0.48             | 0.02 | 8.78  |
| 15    | 77.05            | 1.30                           | 0.99                           | 1.35 | 6.32  | 0.46 | 0.13              | 0.26             | 0.32                          | 1.00             | 0.02 | 7.40  |
| 16    | 59.87            | 2.25                           | 1.04                           | 0.72 | 17.88 | 0.64 | 0.13              | 0.67             | 0.61                          | 0.32             | 0.06 | 15.20 |
| 17    | 46.03            | 3.33                           | 1.76                           | 0.90 | 22.97 | 1.02 | 0.29              | 1.06             | 0.99                          | 0.35             | 0.08 | 18.86 |
| 18    | 33.98            | 3.37                           | 1.42                           | 0.63 | 29.8  | 0.89 | 0.35              | 0.96             | 0.98                          | 0.30             | 0.08 | 25.20 |
| 19    | 64.41            | 2.48                           | 11.16                          | 0.90 | 5.23  | 0.82 | 0.13              | 0.61             | 0.32                          | 0.43             | 0.02 | 10.22 |
| 20    | 39.32            | 3.69                           | 2.11                           | 1.17 | 25.10 | 1.05 | 0.35              | 1.06             | 0.88                          | 0.43             | 0.07 | 22.78 |
| 21    | 74.68            | 4.15                           | 3.98                           | 0.90 | 4.13  | 1.15 | 0.11              | 1.19             | 0.61                          | 0.48             | 0.02 | 6.36  |
| 22    | 48.20            | 6.58                           | 2.22                           | 0.99 | 19.24 | 1.68 | 0.29              | 1.76             | 1.70                          | 0.50             | 0.05 | 14.86 |
| 23    | 35.76            | 5.73                           | 1.86                           | 0.90 | 30.44 | 1.48 | 0.35              | 2.05             | 1.57                          | 0.40             | 0.07 | 19.54 |
| 24    | 12.84            | 2.65                           | 1.14                           | 0.56 | 43.72 | 1.30 | 0.26              | 0.78             | 0.36                          | 0.14             | 0.18 | 33.75 |
| 25    | 10.50            | 2.45                           | 1.70                           | 0.50 | 49.40 | 1.05 | 0.5               | 0.66             | 0.35                          | 0.16             | 0.2  | 33.15 |
| 26    | 18.28            | 3.18                           | 0.78                           | 0.65 | 41.64 | 1.36 | 0.28              | 0.9              | 0.32                          | 0.12             | 0.18 | 32.50 |
| 27    | 6.22             | 1.35                           | 0.30                           | 0.36 | 50.66 | 0.56 | 0.68              | 0.32             | 0.22                          | 0.02             | 0.10 | 37.50 |
| 28    | 17.70            | 3.48                           | 0.68                           | 0.68 | 38.86 | 1.30 | 0.46              | 0.94             | 0.42                          | 0.16             | 0.15 | 32.50 |
| 29    | 9.54             | 2.08                           | 0.54                           | 0.42 | 46.50 | 1.00 | 0.50              | 0.55             | 0.08                          | 0.06             | 0.18 | 39.25 |
| 30    | 18.10            | 3.56                           | 0.58                           | 0.56 | 39.56 | 1.16 | 0.48              | 1.06             | 0.12                          | 0.08             | 0.16 | 32.80 |
| 31    | 17.70            | 3.60                           | 0.60                           | 0.56 | 40.95 | 1.18 | 0.36              | 1.06             | 0.10                          | 0.16             | 0.16 | 32.00 |
| 32    | 10.00            | 2.12                           | 0.52                           | 0.38 | 47.18 | 0.84 | 0.45              | 0.60             | 0.08                          | 0.04             | 0.15 | 37.75 |
| 33    | 7.30             | 1.44                           | 2.46                           | 0.38 | 46.50 | 0.68 | 0.44              | 0.40             | 0.04                          | 0.12             | 0.16 | 37.35 |
| 34    | 10.76            | 2.08                           | 0.70                           | 0.54 | 46.50 | 0.86 | 0.45              | 0.60             | 0.04                          | 0.08             | 0.16 | 37.15 |
| 35    | 19.42            | 1.20                           | 4.34                           | 0.46 | 38.86 | 0.60 | 0.24              | 0.38             | 0.05                          | 0.20             | 0.16 | 31.65 |
| 36    | 8.08             | 1.40                           | 0.98                           | 0.28 | 48.58 | 0.82 | 0.44              | 0.44             | 0.06                          | 0.14             | 0.22 | 37.20 |
| 37    | 8.55             | 1.64                           | 0.70                           | 0.32 | 49.26 | 0.90 | 0.78              | 0.44             | 0.08                          | 0.06             | 0.20 | 37.55 |

Analytical technique: SiO<sub>2</sub>, TiO<sub>2</sub> and P<sub>2</sub>O<sub>5</sub> by UV–VIS Spectrophotometry; Al<sub>2</sub>O<sub>3</sub> by ICP–AES; Fe<sub>2</sub>O<sub>3</sub>, MnO, MgO and CaO by AAS; FeO by Titrimetry; Na<sub>2</sub>O and K<sub>2</sub>O by Flame photometry; LOI by Gravimetry

TABLE III. TRACE ELEMENTS (PPM) OF URANIFEROUS LIMESTONE

| Sl No | Cu  | Ni  | Co  | Pb    | Zn  | Cr  | V    | Ag | Mo  | $U_3O_8$ (T) (%) |
|-------|-----|-----|-----|-------|-----|-----|------|----|-----|------------------|
| 1     | 60  | <25 | <25 | 1586  | <25 | 47  | NA   | NA | NA  | 0.522            |
| 2     | 73  | <25 | <25 | 63    | <25 | 40  | NA   | NA | NA  | 0.076            |
| 3     | <25 | <25 | <25 | 66    | <25 | 60  | NA   | NA | NA  | 0.073            |
| 4     | 90  | 45  | 23  | 453   | 43  | 250 | NA   | NA | NA  | 0.662            |
| 5     | 188 | 38  | 35  | 620   | 58  | 146 | NA   | NA | NA  | 0.956            |
| 6     | 61  | 24  | 27  | 501   | 22  | 320 | NA   | NA | NA  | 0.735            |
| 7     | 23  | 38  | 51  | 84    | 21  | 102 | NA   | NA | NA  | 0.081            |
| 8     | 32  | 48  | 23  | 28    | 26  | 47  | NA   | NA | NA  | 0.025            |
| 9     | 49  | 76  | 39  | 174   | 27  | 29  | NA   | NA | NA  | 0.130            |
| 10    | 165 | 120 | 43  | 425   | 100 | 95  | NA   | NA | NA  | 0.538            |
| 11    | 58  | 48  | 35  | 550   | 45  | 126 | NA   | NA | NA  | 0.712            |
| 12    | 70  | 52  | 51  | 383   | 64  | 105 | NA   | NA | NA  | 0.521            |
| 13    | 52  | 41  | 43  | 111   | 20  | 48  | NA   | NA | NA  | 0.120            |
| 14    | 78  | 17  | 28  | 40    | NA  | <25 | 58   | <2 | <5  | 0.013            |
| 15    | 74  | 19  | 26  | 30    | NA  | <25 | 99   | <2 | <5  | 0.030            |
| 16    | 52  | 18  | 13  | 53    | NA  | <25 | 86   | <2 | <5  | 0.037            |
| 17    | 14  | 11  | 14  | 61    | NA  | <25 | 131  | <2 | <5  | 0.044            |
| 18    | 34  | 10  | <10 | 79    | NA  | <25 | 103  | <2 | <5  | 0.041            |
| 19    | 20  | 15  | 11  | 53    | NA  | <25 | 77   | <2 | <5  | 0.026            |
| 20    | 15  | 9   | 29  | 115   | NA  | <25 | 101  | <2 | <5  | 0.057            |
| 21    | 21  | 10  | 24  | 38    | NA  | <25 | 130  | <2 | <5  | 0.034            |
| 22    | 47  | 26  | 37  | 54    | NA  | 45  | 153  | <2 | <5  | 0.027            |
| 23    | 32  | 10  | 11  | 47    | NA  | <25 | 217  | <2 | <5  | 0.026            |
| 24    | 36  | 9   | 17  | 84    | NA  | 72  | 137  | <2 | <5  | 0.041            |
| 25    | 45  | 11  | 26  | 114   | NA  | 29  | 152  | <2 | <5  | 0.061            |
| 26    | 41  | 11  | 24  | 67    | NA  | 66  | 185  | <2 | <5  | 0.031            |
| 27    | 17  | 12  | 13  | 213   | NA  | <25 | 310  | <2 | <5  | 0.099            |
| 28    | 15  | 14  | 11  | 193   | NA  | <25 | 332  | <2 | <5  | 0.094            |
| 29    | 11  | 10  | 11  | 72    | NA  | <25 | 197  | <2 | <5  | 0.039            |
| 30    | 12  | 22  | 30  | 210   | NA  | <25 | 422  | 3  | 63  | 0.213            |
| 31    | 32  | 20  | 42  | 517   | NA  | <25 | 383  | 10 | 46  | 0.390            |
| 32    | 28  | 21  | 25  | 345   | NA  | <25 | 241  | 5  | 81  | 0.218            |
| 33    | 14  | 14  | 15  | 181   | NA  | <25 | 103  | <2 | 42  | 0.063            |
| 34    | 20  | 19  | 25  | 294   | NA  | <25 | 160  | <2 | <5  | 0.154            |
| 35    | 91  | 36  | 47  | 463   | NA  | <25 | 494  | 7  | 131 | 0.422            |
| 36    | 76  | 36  | 44  | 578   | NA  | <25 | 522  | 8  | 82  | 0.313            |
| 37    | 20  | 28  | 31  | 401   | NA  | <25 | 443  | 6  | 106 | 0.246            |
| 38    | 84  | 43  | 82  | 866   | NA  | 61  | 506  | 37 | 228 | 0.687            |
| 39    | 105 | 77  | 105 | 695   | NA  | 433 | 1143 | 31 | <5  | 0.588            |
| 40    | 36  | 36  | 129 | >1000 | NA  | 48  | 539  | 62 | 721 | 1.678            |
| 41    | 35  | 40  | 60  | 478   | NA  | 149 | 843  | 6  | <5  | 0.443            |

Analytical techniques:  $U_3O_8$  by Pellet flourimetry, trace elements by flame-AAS / ICP-AES

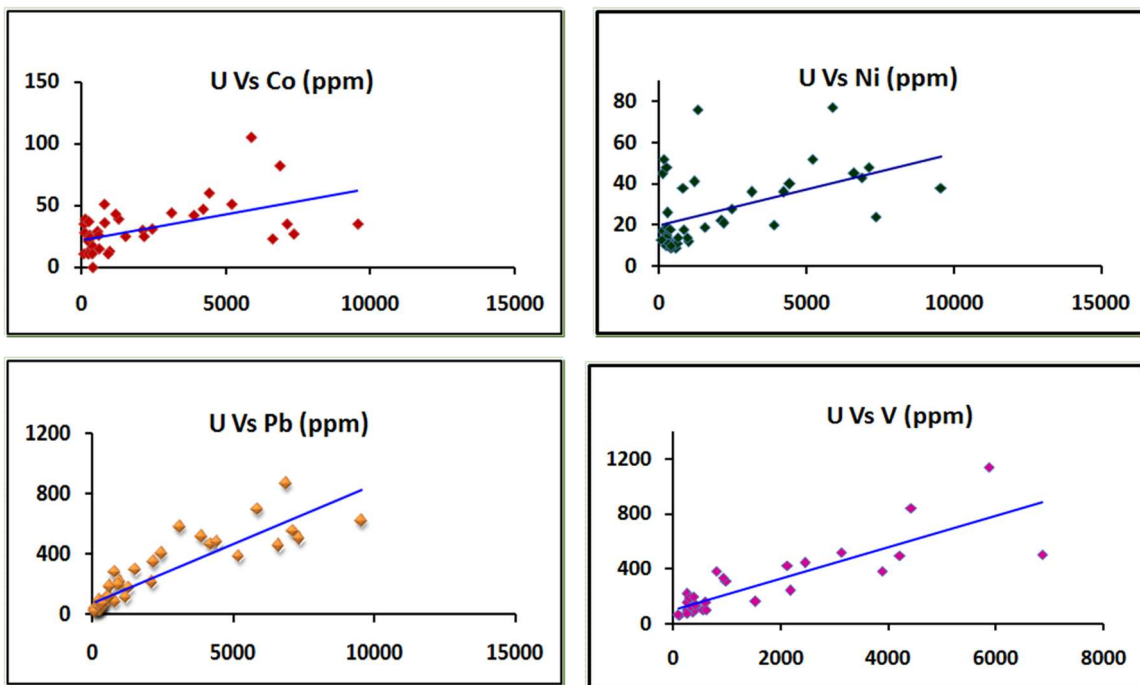


FIG. 23. Binary plots showing correlation of Uranium verses Ni, Co, Pb and V.

## 9. MINERAL CHEMISTRY

Electron Probe Micro Analysis (EPMA) has identified pitchblende, coffinite and U-Ti complex as the radioactive mineral phases both in uraniferous limestone and granite from Gogi area (Table IV). A critical examination of data reveals the following.

### Pitchblende

- Pitchblende in limestone has high  $\text{UO}_2$  (average 83.9%),  $\text{PbO}$  (average 6.3%),  $\text{Y}_2\text{O}_3$  (average 0.13%) and  $\text{FeO}$  (average 1.04%) followed by low contents of  $\text{SiO}_2$  (average 2.73%) and  $\text{Ln}_2\text{O}_3$  (average 0.5%) with negligible  $\text{ThO}_2$  (average 0.04%) in comparison to the pitchblende in granite;
- The silica content in pitchblende of granite varies from 5.4 to 10.2% with average being 7.3% indicating the process of coffinitisation of pitchblende;
- The range of  $\text{UO}_2$  content in pitchblende from both granite and limestone is similar (~80%). But the  $\text{PbO}$  content is low in limestone than granite showing redistribution due to remobilisation of Pb on a much higher scale in granite;
- The total REE ( $\text{Ln}_2\text{O}_3$ ) content in pitchblende is low 0.20 to 0.96 % (in limestone) and 0.22 to 3.36% (in granite). The LREE and HREE pattern in both granite and limestone is similar;
- The pre-coffinite pitchblende is marked by high  $\text{PbO}$  (10.3%) and the post-coffinite pitchblende has low  $\text{PbO}$  (5%).

### Coffinite

- The coffinite in limestone is marked by high  $\text{UO}_2$  (average 77.9%),  $\text{PbO}$  (average 3.2%),  $\text{FeO}$  (average 0.62%) and low  $\text{SiO}_2$  (average 10.3%),  $\text{Ln}_2\text{O}_3$  (average 0.28%) with negligible  $\text{ThO}_2$  in comparison to that in granite;

- The REO (Total) content in coffinite ranges from 0.08 to 0.61% in limestone and 0.22 to 8.18% in coffinite occurring in granite.

### **U-Ti complex**

- It is present only in granite and marked by wide variation in the contents of U, Ti and Si (10–44%) suggesting that it is a complex of U, Ti and Si rather than brannerite, which has restricted range of composition;
- The U-Ti complex is characterised by low ThO<sub>2</sub> (average 0.4%) with negligible PbO in comparison to pitchblende and coffinite;
- The REO (Total) content in U-Ti complex in granite varies from 1.12 to 3.80%.

### **Sulphides**

Pyrite is the major sulphide phase with minor galena and chalcopyrite. The sulphur isotope study of pyrite from core samples of mineralized limestone reveals large variation in the value of  $\delta^{34}\text{S}$  from -13.9 to + 25.3‰ indicating both biogenic as well as hydrothermal source of sulphur [14].

### **Carbonaceous matter**

The organic matter from the mineralized limestone is heterogeneous in composition. The samples (n=6) have been analysed by Electron Micro Probe technique with UO<sub>2</sub> content varying from 0.00 to 14.87% and negligible ThO<sub>2</sub>. The other impurities are SiO<sub>2</sub>(0.06–14.61%), Al<sub>2</sub>O<sub>3</sub> (0.02–4.96%), FeO (0.00–1.61%) and CaO (0.00–5.3%).

### **Ore genetic model**

Geological field observations, petrography, mineral chemistry vis-à-vis geochemical attributes of Gogi uranium deposit point out multi-phase ore genesis event that encompasses various episodes from source level to the development of the deposit. The fertile Closepet equivalent younger granite (~2.5 Ga) in the basement acted as a source of uranium. The regional geotherm is raised by later intrusive basic dykes in the basement helping in dislodging uranium from the discrete uranium phases and refractory minerals. The Bhima sediments deposited over an eroded-peneplained basement during Meso to Neoproterozoic (1.6 to 0.6 Ga) period.

Post sedimentation faulting proximal to the unconformity plane, facilitated the formation of hydrothermal fluids which segregated and scavenged major amount of uranium from fertile granite. Multistage sequential structural events led to the growth of fracture system which provided the ideal conduits for the migration of mineralized solutions. Uranium has been transported as soluble carbonate complexes in the hydrothermal fluid along fractures and precipitated in the reduction zone rich in organic matter and sulphides. Distinct generations of uranium minerals, various types of pyrites, wide range of  $\delta^{34}\text{S}$  also support a multistage development of the polymetallic deposit in Gogi area.

TABLE IV. CHEMICAL ANALYSIS (IN WT%: RANGE AND AVERAGE) OF THE URANIUM PHASE IN THE LIMESTONE AND GRANITE

|                                | PITCHBLENDE        |              |                    |              | COFFINITE           |              |                    |              | U-Ti Complex<br>Granite |              |
|--------------------------------|--------------------|--------------|--------------------|--------------|---------------------|--------------|--------------------|--------------|-------------------------|--------------|
|                                | Limestone          |              | Granite            |              | Granite             |              | Limestone          |              |                         |              |
|                                | Range (n=9)        | Average      | Range (n=14)       | Average      | Range (n=20)        | Average      | Range (n=16)       | Average      | Range (n=6)             | Average      |
| SiO <sub>2</sub>               | 1.65-4.39          | 2.73         | 5.39-10.18         | 7.28         | 11.07-20.90         | 15.64        | 6.02-16.21         | 10.34        | 6.06-15.99              | 8.36         |
| TiO <sub>2</sub>               | N.D                | N.D          | 0.08-2.42          | 0.57         | 0.090-3.03          | 0.58         | N.D                | N.D          | 19.64-63.96             | 42.00        |
| Al <sub>2</sub> O <sub>3</sub> | 0.090-1.21         | 0.53         | 0.50-0.85          | 0.63         | 0.70-2.08           | 1.20         | 0.61-3.47          | 1.81         | 1.50-1.67               | 1.55         |
| FeO                            | 0.41-4.14          | 1.04         | 0.08-0.36          | 0.24         | 0.00-0.41           | 0.11         | 0.26-1.21          | 0.62         | 0.88-2.80               | 1.86         |
| MnO                            | 0.070-0.15         | 0.10         | N.D                | N.D          | N.D                 | N.D          | 0.00-0.12          | 0.060        | N.D                     | N.D          |
| MgO                            | N.D                | N.D          | 0.050-0.19         | 0.13         | 0.050-0.31          | 0.13         | N.D                | N.D          | 0.060-0.12              | 0.09         |
| CaO                            | 1.22-2.43          | 1.64         | 1.01-3.24          | 2.32         | 0.95-2.56           | 1.45         | 1.86-2.75          | 2.21         | 0.73-1.62               | 1.81         |
| Na <sub>2</sub> O              | 0.090-0.22         | 0.13         | N.D                | N.D          | N.D                 | N.D          | 0.14-0.39          | 0.28         | N.D                     | N.D          |
| P <sub>2</sub> O <sub>5</sub>  | 0.12-0.33          | 0.23         | 0.010 - 0.28       | 0.08         | 0.13-1.03           | 0.52         | 0.26-0.85          | 0.53         | 0.14-0.50               | 0.32         |
| UO <sub>2</sub>                | 79.37-87.22        | 83.91        | 74.56-82.78        | 80.24        | 64.18-78.60         | 71.47        | 70.68-84.65        | 77.93        | 23.17-53.91             | 41.35        |
| ThO <sub>2</sub>               | 0.00-0.09          | 0.040        | 0.00-0.16          | 0.040        | 0.00-0.20           | 0.060        | 0.00-0.10          | 0.020        | 0.030-1.03              | 0.37         |
| PbO                            | 3.88-6.98          | 6.28         | 0.090-8.63         | 2.48         | 0.00-5.02           | 1.27         | 0.65-12.16         | 3.20         | 0.00-0.07               | 0.040        |
| La <sub>2</sub> O <sub>3</sub> | 0.00-0.10          | 0.050        | 0.00-0.58          | 0.29         | 0.00-0.33           | 0.15         | 0.00-0.12          | 0.030        | 0.01-0.22               | 0.11         |
| Ce <sub>2</sub> O <sub>3</sub> | 0.10-0.37          | 0.22         | 0.11-2.14          | 1.17         | 0.080-2.76          | 1.54         | 0.00-0.12          | 0.050        | 0.00-1.43               | 0.56         |
| Pr <sub>2</sub> O <sub>3</sub> | 0.00-0.21          | 0.030        | 0.00-0.26          | 0.040        | 0.00-0.55           | 0.21         | 0.00-0.09          | 0.030        | 0.11-0.27               | 0.20         |
| Nd <sub>2</sub> O <sub>3</sub> | 0.00-0.33          | 0.13         | 0.00-0.68          | 0.25         | 0.00-2.48           | 0.92         | 0.00-0.24          | 0.050        | 0.63-1.36               | 1.06         |
| Sm <sub>2</sub> O <sub>3</sub> | N.D                | N.D          | 0.00-0.36          | 0.10         | 0.00-0.65           | 0.18         | N.D                | N.D          | 0.00-0.45               | 0.14         |
| Gd <sub>2</sub> O <sub>3</sub> | N.D                | N.D          | 0.00-0.39          | 0.12         | 0.00-0.55           | 0.14         | N.D                | N.D          | 0.00-0.39               | 0.22         |
| Er <sub>2</sub> O <sub>3</sub> | 0.00-0.34          | 0.10         | N.D                | N.D          | N.D                 | N.D          | 0.00-0.52          | 0.12         | N.D                     | N.D          |
| Yb <sub>2</sub> O <sub>3</sub> | N.D                | N.D          | 0.00-0.15          | 0.090        | 0.00-0.40           | 0.14         | N.D                | N.D          | 0.00-0.22               | 0.090        |
| Y <sub>2</sub> O <sub>3</sub>  | 0.020-0.24         | 0.13         | 0.00-0.25          | 0.030        | 0.00-1.11           | 0.52         | 0.00-0.050         | 0.010        | 0.060-0.56              | 0.33         |
| <b>Total</b>                   | <b>95.51-99.57</b> | <b>97.28</b> | <b>92.43-98.96</b> | <b>96.09</b> | <b>92.07-100.92</b> | <b>96.23</b> | <b>94.65-99.77</b> | <b>97.30</b> | <b>96.90-101.69</b>     | <b>99.94</b> |
| Ln <sub>2</sub> O <sub>3</sub> | 0.20-0.96          | 0.51         | 0.22-3.36          | 2.05         | 0.22-8.18           | 3.80         | 0.08-0.61          | 0.28         | 1.12-3.80               | 2.39         |

Analytical technique: Electron Micro Probe technique by Cameca SX-50

## 10. DISCUSSION

The uranium mineralization in brecciated limestone and granite occurs as fracture fillings veins and veinlets confined to the structurally weak regions of the fault zones. The main uranium phases are coffinite and pitchblende with minor amounts of U-Ti complex in granite. Pitchblende is both pre- and post coffinite. The earlier pitchblende is partially replaced by coffinite and later replaces the coffinite. Coffinite precipitates when silica concentration is high in solution ( $> 60$  ppm) at temperature of 200° to 300°C in weakly alkaline (pH-7.2 to 10.5) and reducing condition [15]. Both pitchblende and coffinite are characterised by negligible ThO<sub>2</sub> and low REE content indicating low temperature of formation.

Uranium minerals are associated with low rank bituminous and migratory type organic matter and sulphides. The organic matter from the mineralized limestone is heterogeneous in composition with high UO<sub>2</sub> content due to its reducing property. The sulphides are dominated by pyrite with minor chalcopyrite, galena and marcasite occurring as veins and veinlets in the brecciated limestone and granites. Pyrite occurs in different morphology and textural varieties viz., frambooidal pyrite, porous pyrite, idiomorphic pyrite, lumpy pyrite (in veins), zoned pyrite, botryoidal pyrite, oolitic pyrite and reticulate pyrite. Textural relationship between organic matter and sulphides with uranium phases indicate that they are earlier providing reducing environment for precipitation of uranium from the uranium bearing hydrothermal solutions.

The mode of occurrence of major mineral assemblage, negligible ThO<sub>2</sub> and low REE content and their spatial association and textural relationship with organic matter and pyrite indicate that the mineralization is hydrothermal vein type. Presence of mineralization in both limestone and granite further corroborate their hydrothermal origin. Mineralized zone is also characterised by hydrothermal wall rock alterations viz: chloritisation, carbonatisation and argillitisation. The sulphur isotope study of pyrite reveals large variation in the value of  $\delta^{34}\text{S}$  from -13.9 to + 25.3‰ indicating both biogenic as well as hydrothermal source of sulphur.

The mineral assemblage of the mineralized limestone depicts that the probable range of Eh and pH for the uranium mineralization is -0.2 to -0.3V and 7 to 8 respectively (Table V) [16]. The temperature range for the mineral formation is 80° to 200°C. The low temperature condition is further corroborated by the presence of frambooidal pyrite, negligible Th and REE content in pitchblende and coffinite.

TABLE V. MINERAL ASSEMBLAGE AND ASSOCIATED EH AND PH CONDITIONS (AFTER [16])

| Mineral     | Eh(V)         | pH         |
|-------------|---------------|------------|
| Calcite     | +0.1 to -0.35 | > 7.8      |
| Chert       | -0.2 to -0.35 | 7 to 7.8   |
| Pyrite      | -0.2 to -0.35 | <7 to 7.8  |
| Marcasite   | -0.2 to -0.35 | <5         |
| Pitchblende | -0.25 to 0.6  | 0.25 to 11 |
| Coffinite   | -0.2 to -0.35 | 7 to 7.8   |

The basement granite is fertile having anomalous uranium content (average 29 ppm) in labile state which is further supported by high uranium content (upto 308 ppb) in water samples collected from granitic terrain [17]. The labile uranium from fertile granite remobilised during dyke activity in the basement and by ductile-brittle deformation. The uranium transported as soluble carbonate complexes in the hydrothermal fluid as indicated by the occurrence of calcite veinlets in the mineralized zone cutting the host rock. The U carbonate complexes is best formed under alkaline (pH > 7.5) and oxidizing (Eh > 0.2V) conditions at low temperature [18]. The uranium precipitated in carbonaceous matter and sulphide

rich reduced zone. The first phase is pitchblende that with increasing silica concentration got coiffinitised resulting in the formation of coiffinite. The coiffinite at later stage got replaced by pitchblende under reduced silica concentration. Thus, the mineralization is of more than one phase.

The interpreted paragenetic sequence of minerals at Gogi is set out in Table I. Detailed analytical data are given in Tabs II – IV.

## 11. CONCLUSION

The hydrothermal mineralization at Gogi is formed at alkaline (pH of 7 to 8) and reducing (Eh of -0.2 to -0.3 V) conditions at low temperature (< 200°C) as evident from the mineral chemistry and mineral assemblage. The mode of occurrence of ore minerals, textural relationship between ore and gangue minerals and paragenetic sequence suggest that uranium deposit at Gogi is a fracture controlled, polyphase, epithermal vein type formed by circulating fluids operating in upper crustal environment.

## ACKNOWLEDGEMENTS

The authors are thankful to the colleagues actively engaged in exploration at Gogi uranium deposit for discussions and valuable suggestions. We also thank to our colleagues in various laboratories for analytical support.

## REFERENCES

- [1] SINHA. R.M., SAXENA, V. P., Cuddapah Basin: A potential storehouse for Uranium Deposits, Nuclear India **37** (2003) 9–11.
- [2] ACHAR, K.K., PANDIT, S.A., NATARAJAN, V., KUMAR, MARY K., DWIVEDY, K.K., “Uranium mineralization in the Neoproterozoic Bhima basin, Karnataka, India”, Recent Developments in Uranium Resources, Production and Demand, IAEA, Vienna, (1997) 1–22.
- [3] PANDIT, S.A., NATARAJAN, V., BHAT, GANESH, DHANA RAJU, R., SWARNKAR, B.M., BANERJEE, D.C., “Neoproterozoic Bhima Basin as a potential target for uranium exploration – a case study from Gogi area, Gulbarga District, Karnataka, India”, Field Workshop on Integrated Evaluation of the Kaladgi and Bhima Basins, Geol. Soc. India, Bangalore, Abstract volume (KALE, V.S., SAWKAR, R.H., Compilers) (1999) 58–60.
- [4] KALE, V.S., MUHOLKAR, A.V., PHANSALKAR, V.G., PESHWA, V.V., Stratigraphy of the Bhima Group, Jour. Palaeont. Soc. India **35** (1990) 91–103.
- [5] PANDIT, S.A., NATARAJAN, V., DHANA RAJU, R., Exploration for uranium in the Bhima Basin in parts of Karnataka, India, Exploration and Research for Atomic Minerals **14** (2002) 59–78.
- [6] JAYAPRAKASH, A.V., “Evolutionary history of Bhima Basin”, Field Workshop on Integrated Evaluation of the Kaladgi and Bhima Basins, Geol. Soc. India, Bangalore, Abstract Volume (KALE, V.S., R SAWKAR, H., Compilers), (1999) 23–28.
- [7] DHANA RAJU, R., KUMAR, MARY K., BABU E.V.S.S.K., PANDIT, S.A., Uranium mineralization in the Neoproterozoic Bhima Basin at Gogi and near Ukinil: An Ore Petrological study, Journal of Geological Society of India **59** (2002) 299–321.
- [8] PANDIT, S. A., PANNEERSELVAM, A., CHAVAN, S. J., NATARAJAN, V., BIRUA, M.K., VERGHESE, S.K., JAIN, A.K., Unpublished Ore Reserve Report of Gogi Uranium Deposit (internal report) AMD (2006).
- [9] PANNEERSELVAM, A., Unpublished Annual Report (internal report), Bhima Basin Investigations, AMD (2004).
- [10] SIKTA PATNAIK, HEDGE G. N., PANNEERSELVAM A. JAIN, A.K., VERMA, M.B., RAI, A.K., Textural characterization of pyrite from Gogi uranium deposit, Bhima basin, Yadgir district, Karnataka: Implication for ore genesis, The Indian Mineralogist **45** 1 (2011) 121–129.
- [11] KOHN, M. J., RICIPUTI, L.R., STAKES, D., ORANGE, D.L., Sulfur isotope variability in biogenic pyrite: Reflections of heterogeneous bacterial colonization? American Mineralogist **83** (1998) 1454–1468.

- [12] FOLEY, N., AYUSO, R.A., SEAL II, R. Remnant colloform pyrite at the haile gold deposit, South Carolina: A textural key to genesis, *Economic Geology* **96** (2001) 891–902.
- [13] BARRIE, C.D., BOYCE, A.J., BOYLE, A.P., WILLIAMS, P.J., BLAKE, K., OGAWARA, T., AKAI, J., PRIOR., D.J., Growth controls in colloform pyrite, *American Mineralogist* **94** 4 (2009) 415-429.
- [14] OHMOTO, H., Stable Isootope Geochemistry of Ore Deposits, in stable isotopes in high temperature geological processes, *Mineral Society America* (1986) 491–560.
- [15] DE VOTO RICHARD, H., Uranium geology & exploration, Colorado School of Mines, Golden Colorado, (1978) 10.
- [16] KRUMBEIN, H.C., GARRELS, R.M., Origin and classification of chemical sediments in terms of pH and oxidation-reduction potentials, *J. Geology* **60** (1952) 1–33.
- [17] PANEERSELVAM, A., Unpublished Annual Report (internal report), Bhima Basin Investigations, AMD (2009).
- [18] NASH, J.T., GRANGER, H.C., ADAMS, S.S., Geology and concepts of genesis of important types of uranium deposits. *Economic Geology* **75** (1981) 63–116.

# ESTIMATION OF URANIUM CONCENTRATION IN BUILDING STONES USED IN JORDANIAN BUILDINGS

H.H. SALEH

Department of Physics,  
Al-Hussein Bin Talal University,  
Ma'an, Jordan

## Abstract

Materials derived from rock and soil such as building stones contain mainly natural various quantities of uranium (U) that may cause a biological risk to human beings. The aim of this work was to determine the concentrations and isotopic compositions of uranium in Jordanian natural building stones samples for radiation protection purposes. The collected building stone samples include four types used mainly in the Jordanian buildings were analysed using inductively coupled plasma-mass spectrometry ICP-MS. Gamma spectrometry was used to obtain the relative concentrations ratios of  $^{235}\text{U}/^{238}\text{U}$ .

## 1. INTRODUCTION

Radiation exposure due to Uranium isotopes ( $^{235}\text{U}$  and  $^{238}\text{U}$ ) and other radionuclides in building materials can be divided into external and internal exposure. The external exposure is caused by direct gamma radiation. An inhabitant living in an apartment block made of concrete receives an annual effective dose of about 0.25 mSv (excess to the dose received outdoors). Enhanced or elevated levels of natural radionuclides in building materials may cause doses in the order of several mSv  $\text{a}^{-1}$  [1–3].

The internal exposure is caused by the inhalation of radon ( $^{222}\text{Rn}$ ), thoron ( $^{220}\text{Rn}$ ) and their short lived decay products. Radon is part of the radioactive decay series of uranium, which is present in building materials. Because radon is an inert gas, it can move rather freely through porous media such as building materials, although usually only a fraction of that produced in the material reaches the surface and enters the indoor air. The most important source of indoor radon is the underlying soil but in some cases the building materials may be an important source. In most cases the main part of indoor radon on the upper floors of a building originates from building materials. Typical excess indoor radon concentration due to building materials is about 10–20 Bq  $\text{m}^{-3}$ , but in some zones and in rare cases it may rise up to greater than 1000 Bq  $\text{m}^{-3}$  [4–6].

In literature, many studies interested in estimation the natural radioactive nuclides due to building materials in Jordan and its health risk [7–10].

Uranium is one of the naturally occurring elements that can be found in most rocks and soils as well as in surface and ground water in different quantities. Also, the  $^{235}\text{U}/^{238}\text{U}$  ratio could be a good indicator of the origin and the activities associated with any uranium containing samples. Different techniques were used to obtain Uranium isotopes and so this ratio of various materials [11–15]. Inductively coupled plasma-mass spectrometry ICP-MS in addition to gamma spectrometry are powerful non-destructive techniques used for direct determination of the U concentration, also, the measurement time by ICP-MS is shorter than that taken by alpha spectrometry [11].

The main object of this work is to determine the  $^{235}\text{U}/^{238}\text{U}$  ratio for some stone samples used in Jordanian buildings.

## 2. MATERIALS PREPARATION

Ajlun, Ma'an, Desert and Samic stones are the main types of artificial stone used in buildings interfaces in Jordan. Stone samples were collected from these types and taken to the Jordan Atomic Energy Commission (JAEC) laboratories. There, the samples were dried up in an oven at 130°C for 10 hours,

then milled to powder in many stages of  $125\mu\text{m}$  radius as a primary preparation for all of the measurements. The samples were divided to two parts for further preparation for each spectroscopy. The samples were divided into two parts for each spectroscopy; further simple preparation was required for ICP-MS technique, while gamma spectrometry is a direct measurement.

### 3. RESULTS AND DISCUSSION

Using the ICP-MS technique one can make a direct determination of the U concentration and other chemical nuclides found in the samples. Figure 1 shows the concentration of all chemical elements found.

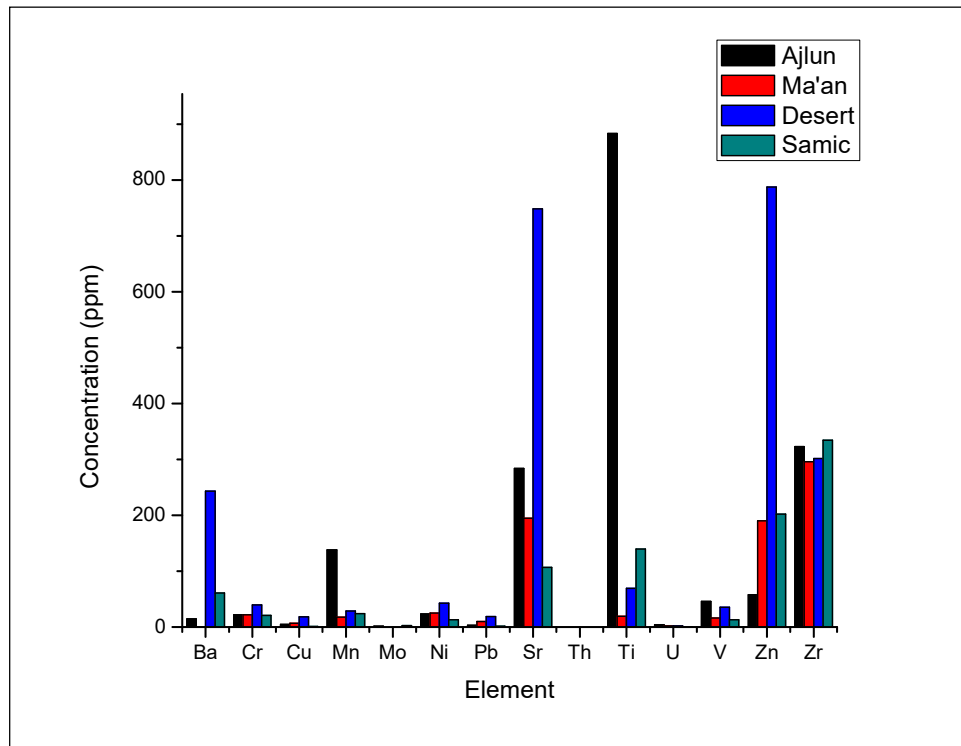


FIG.1. Concentrations of elements in stone samples using the ICP-MS technique.

The different element concentrations are interpreted as reflecting the geological origin of each stone and its original elemental composition. U concentrations were very low and ranged between  $(0.477 \pm 0.057)$  ppm in Samic stones to  $(4.092 \pm 0.413)$  ppm in Ajlun stones. Table I presents the average uranium concentrations in ores and rocks.

TABLE I. AVERAGE URANIUM CONCENTRATIONS IN ORES, ROCKS AND WATERS (PPM).

| Material                 | Concentration, ppm U<br>(reference) |
|--------------------------|-------------------------------------|
| Average granite          | 4.4 [16]                            |
| Average volcanic rock    | 20–200 [17]                         |
| Average basaltic rock    | 0.8 [16]                            |
| Average sedimentary rock | 2 [17]                              |
| Average sandstone        | 0.45 [18]                           |
| Average limestone        | 2.2 [18]                            |
| Average igneous rock     | 2.7 [18]                            |
| Average black shale      | 50–250 [17]                         |
| Average earth's crust    | 2.8 [17]                            |

In Jordan, many studies interested in Uranium concentration in rocks. Moh'd and Powell [19] found that the average uranium values is 14 ppm through a study of the northwest Jordanian rocks in the range < 1–70 ppm while the phosphatic rocks show a higher range (52–70 ppm) which is in agreement with our presented results.

Using gamma spectrometry, the specific activity of each radionuclide can be calculated using the relation;

$$A = \frac{N_{net}}{(\varepsilon)(t)(m)(f)} \quad (Bq/kg) \quad (1)$$

where;

$A$ ; activity concentration of the radionuclide.

$N_{net}$ ; the net counts into the photo peak region.

$\varepsilon$ : detector efficiency at this energy.

$t$ : counting time in sec.

$m$ : sample mass.

$f$ : branching ratio.

The specific activity of  $^{235}\text{U}$  and  $^{238}\text{U}$  were calculated and the ratio between their concentrations are reported in Table II below.

TABLE II. CALCULATED  $^{235}\text{U}$  SPECIFIC ACTIVITY,  $^{238}\text{U}$  SPECIFIC ACTIVITY AND  $^{235}\text{U}/^{238}\text{U}$  RATIO IN SAMPLES USING GAMMA SPECTROMETRY TECHNIQUE

|                                 | Stone type |       |        |       |
|---------------------------------|------------|-------|--------|-------|
|                                 | Ajlun      | Ma'an | Desert | Samic |
| $^{235}\text{U}$ (Bq/kg)        | 1.8        | 1.4   | 1.4    | 0.69  |
| $^{238}\text{U}$ (Bq/kg)        | 13.3       | 18.0  | 9.07   | 16.1  |
| $^{235}\text{U}/^{238}\text{U}$ | 0.135      | 0.078 | 0.154  | 0.043 |

The lowest ratio was found in Samic stones while the highest ratio was for the Desert stones. Furthermore, the ratios are different which means that it can be used as indicator of the stone origin.

#### 4. CONCLUSIONS

Using ICP-MS and gamma spectrometry, U concentrations and  $^{235}\text{U}/^{238}\text{U}$  ratios were measured in four of the main stone types used in Jordanian building interfaces. The measured (U) concentrations were ranged from  $(0.477 \pm 0.057)$  ppm to  $(4.09 \pm 0.41)$  ppm and all of their values were less than the world average of 2.8 ppm except that for Ajlun stones. The mineral content of each type can be the main cause of this concentration range and it interprets the slight rise of (U) concentrations in Ajlun stones over the associated average value in the earth's crust.

The obtained  $^{235}\text{U}/^{238}\text{U}$  ratios from gamma spectrometry do not exceed (0.15) and also can be an indicator of the stone mineral content because of their distinct values.

#### ACKNOWLEDGEMENTS

The author gratefully acknowledges the Jordan Atomic Energy Commission (JAEC) for permission to use their laboratories and JAEC staff for their assistance and technical support given in physical and chemical sample preparations.

#### REFERENCES

- [1] ALNOUR, I. A., WAGIRAN, H., IBRAHIM, N., HAMZAH, S., ELIAS, M. S., LAILI, Z., OMAR, M., Assessment of natural radioactivity levels in rocks and their relationships with the geological structure of Johor state, Malaysia. Radiat. Prot Dosimetry **158** 2 (2014) 201–207.
- [2] CMSI, Report on Concrete Block and Bricks Manufacturing, The Construction and Material Science Institute, RSS, Amman (2002).
- [3] INTERNATIONAL ATOMIC ENERGY AGENCY, Natural and induced radioactivity in food, IAEA-TECDOC-1287, IAEA, Vienna (2002).
- [4] JAEGER, R.G., BLIZARD, E.P., CHILTON, A.B., GROTHUIS, M., HÖNIG, A., JAEGER, T.A., EISENLOHR, H.H., Engineering compendium on radiation shielding, Shielding Fundamentals and Methods 1, Springer-Verlag, Berlin (1968).
- [5] ZUBAIR, M., VERMA, D., AZAM, A., ROY, S., Natural radioactivity and radiological hazard assessment of soil using gamma-ray spectrometry, Radiat. Prot. Dosimetry **155** 4 (2013) 467–473.
- [6] EUROPEAN COMMISSION, Enhanced radioactivity of building materials, European Commission, Radiation protection **96**, Luxembourg (1999).

- [7] AHMAD, A., HUSSEIN, A., ASLAM, Radiation doses in Jordanian dwellings due to natural radioactivity in construction materials and soil, *J. Environ. Radio.* **41** 2 (1998) 127–136.
- [8] KHATIBEH, A.J.A.H., MA'LY, A., AHMAD, N., Natural Radioactivity in Jordanian Construction Materials, *Radiat. Prot. Dosimetry* **69** 2 (1997) 143–147.
- [9] AHMAD, N., KHATIBEH, A. J. A. H., MA'LY, A., KENAWY, M. A., Measurement of natural radioactivity in Jordanian sand, *Radiat. Measurements* **28** 1-6 (1997) 341–344.
- [10] AL-JUNDI, J., SALAH, W., BAWA'ANEH, M. S., AFANEH, F., Exposure to radiation from the natural radioactivity in Jordanian building materials, *Radiat. Prot. Dosimetry* **118** 1 (2006) 93–96.
- [11] TAGAMI, K., UCHIDA, S., Rapid uranium preconcentration and separation method from fresh water samples for total U and  $^{235}\text{U}/^{238}\text{U}$  isotope ratio measurements by ICP-MS, *Analytica Chimica Acta* **592** (2007) 101–105.
- [12] SENFTLE, F. E., STIEFF, L., CUTTITTA, F., KURODA, P. K., Comparison of the isotopic abundance of  $\text{U}^{235}$  and  $\text{U}^{238}$  and the radium activity ratios in Colorado Plateau uranium ores, *Geochimica et Cosmochimica Acta* **11** 3 (1957) 189–193.
- [13] ROSSI, G., MOL, M., Isotopic analysis of uranium by an optical spectral method - III: Determination of  $\text{U}^{235}/\text{U}^{238}$  ratios with a hollow-cathode source and a direct-reading attachment. *Spectrochimica Acta Part B: Atomic Spectroscopy* **24** 7 (1969) 389-390, E1-E2, 391–398.
- [14] SMITH, B.W., QUENTMEIER, A., BOLSHOV, M., NIEMAX, K., Measurement of uranium isotope ratios in solid samples using laser ablation and diode laser-excited atomic fluorescence spectrometry, *Spectrochimica Acta Part B: Atomic Spectroscopy* **54** 6 (1999) 943–958.
- [15] GRAY, P. J., ZHANG, L., XU, H., MCDIARMID, M., SQUIBB, K., CENTENO, J. A., Determination of  $^{236}\text{U}/^{238}\text{U}$  and  $^{235}\text{U}/^{238}\text{U}$  isotope ratios in human urine by inductively coupled plasma mass spectrometry, *Microchemical Journal* **105** (2012) 94–100.
- [16] BROWNLOW, A.H., *Geochemistry*, Prentice-Hall, Englewood Cliffs, NJ (1979).
- [17] HARRIS, R.C., Distribution of uranium in rocks and radon levels in water in the San Carlos – Safford – Duncan nonpoint – Source managenent zone, Arizona Geological Survey Open-File Report 96–28, Tucson, AZ (1996), [http://repository.azgs.az.gov/sites/default/files/dlio/files/2010/u14/ofr\\_96\\_28.pdf](http://repository.azgs.az.gov/sites/default/files/dlio/files/2010/u14/ofr_96_28.pdf).
- [18] TUREKIAN, K., WEDEPOHL, K., Distribution of the Elements in Some Major Units of the Earth's Crust, *Geological Society American Bulletin* **72** 2 (1961) 175–192.
- [19] MOH'D, B. K., POWELL, J. H., Uranium distribution in the Upper Cretaceous-Tertiary Belqa Group, Yarmouk Valley, northwest Jordan, *J. Earth and Environmental Sciences* **3** 1 (2010) 49–62.



# **APPROACHES TO MASTERING THE URANIUM POTENTIAL OF CAMEROON**

P.J. CHAKAM TAGHEU, A. SIMO  
National Radiation Protection Agency (NRPA),  
Yaounde, Cameroon

## **Abstract**

Several mineral deposits have been discovered in Cameroon including, gold, alluvial diamonds, iron, bauxite and uranium which are still in the exploration stage. Although Cameroon has not yet launched a nuclear programme, the development of its uranium resource is considered as a key factor to boost the national economy. Many uranium occurrences have been discovered in Cameroon, particularly in Kitongo, Salaki, Mayo Nielse and Teubang in the Northern region, Ngombas near Lolodorf in the Southern region and Bagangté in the western region. Cameroon government programme to estimate the national uranium potential includes: (i) geological mapping; and (ii) assessing of the uranium resource through drilling. The results of these studies may provide a better understanding of the national uranium potential. This paper aims to point out the constraints in assessing the uranium potential of Cameroon and proposes measures that could enable the enhancement of the production possibilities.

## **1. INTRODUCTION**

The African continent hosts important mineral resources that represent approximately 30% of the world reserves and resources. Recently, Africa has been contributing about 20% of world uranium production. Based on the diversity of actors concerned and the importance of the resulting good and services, African mining incomes are important for the world economy. However, despite the favorable geological and mining contexts, these resources generally are less valorized due to certain constraints. In the case of Cameroon, the weak understanding of the mining potential and mastering of the uranium production cycle, indispensable for the elaboration of the sound national development strategies, is a great concern. Geologic mapping and data on the mining potential of Cameroon still have to be improved. Geologists reveal that more than 50% of the territory remains unexplored. among the objectives of the government, there is the promotion of geologic and mining research.

This paper sketches some problems inhibiting the mastering for the mining cycle in general and more specifically that of uranium in Cameroon and proposes solutions.

## **2. SOME ASPECTS OF URANIUM POTENTIAL IN CAMEROON**

Uranium occurrences and deposits have been identified at Kitongo, Salaki, Mayo Nielse and Teubang in the Northern Cameroon and in Ngombas near Lolodorf in Southern Cameroon, at Bagangté in Western Cameroon.

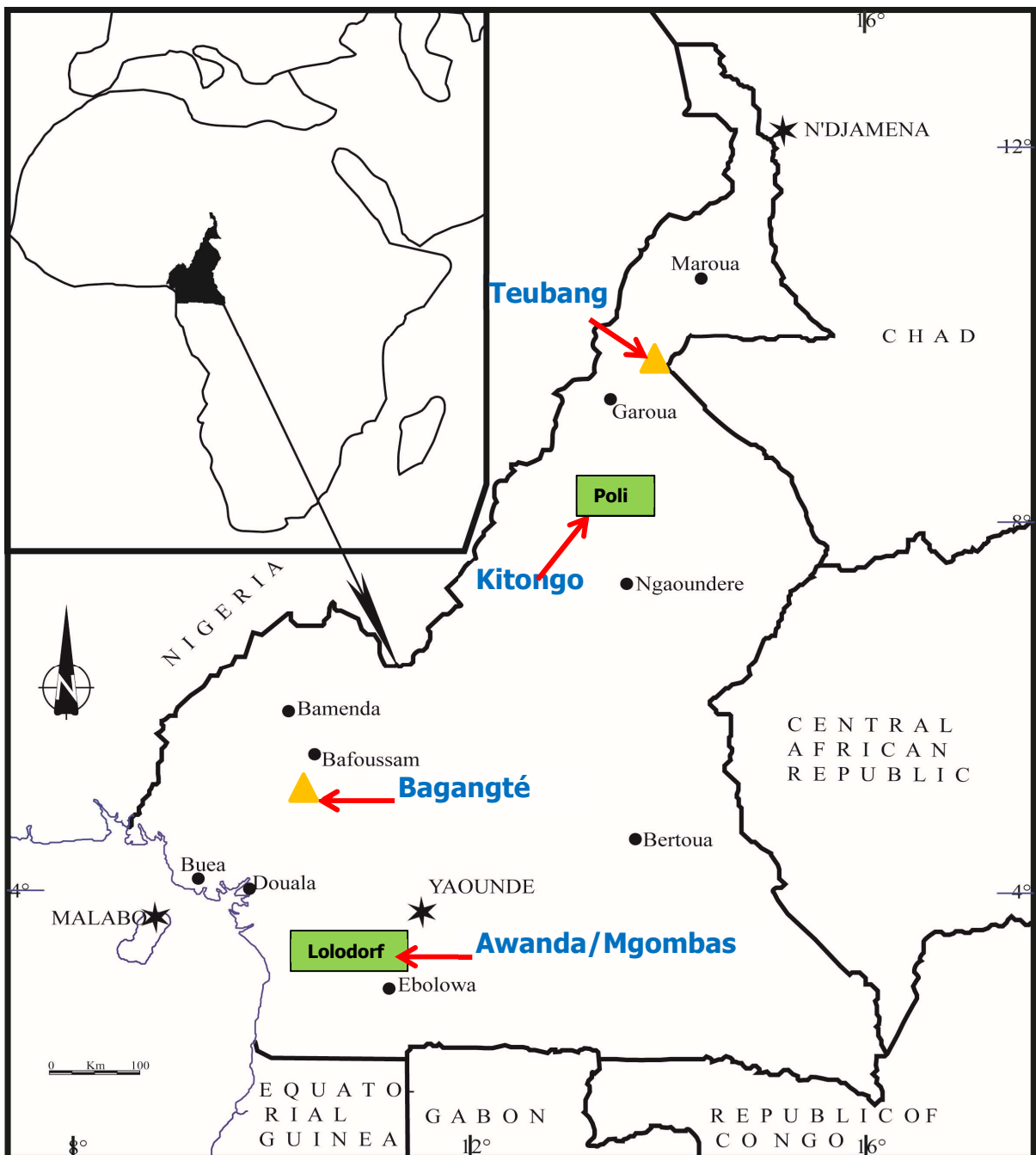


FIG. 1. Location of uranium deposits in Cameroon.

- At Kitongo, uranium mineralization is hosted in granitic rocks that include interleaved sequences of metavolcanic and metasedimentary rock of the commonly termed Poli Group [1]. These rocks underwent a two-stage of albitization and the second albitization that has overprinted the first one, which is more effective at fault intersections. The most promising uraniferous bodies are intimately related to intersections between the ductile ENE-trending faults and the brittle conjugate faults postdating the shearing event;
- The geology of Salaki is characterized by an intrusion of metadiorite including large enclaves at the scale of layers of meta-basalts and metavolcanoclastites. The superimposition of metabasalt is generally marked by alternation of massif basalts, andesitic basalts, and dolerites. However, uranium mineralization is held within mylonitic section irrespective to the lithology affected by the tectonites [2];
- The Teubang region includes a Pan-African Neoproterozoic metamorphic basement overlain by non-metamorphic Palaeozoic and Cretaceous units. Alluvium is found along streams dissecting

the region with most anomalies related to sub-concordant alaskitic granitoid intrusions all of which are late Pan-African ages. These are represented by NS-directed basic to intermediate orthogenesis (660–620 Ma) enclosed within older metasedimentary and metavolcanoclastic units and exhibit a regional metamorphic gradient evolving westwards from low grade schist to migmatites and anatetic intrusions [3];

- At Ngombas near Lolodorf (southern Cameroon), uranium mineralization is held by Th-enriched alkali syenite. Structural features of the syenites suggest that it is a syntectonic emplacement. It is composed of sheet-like intrusions stretched parallel to regional tectonic trends characterizing an oblique thrust zone at the front zone of the Yaoundé pan-African nape systems. The origin of the uranium mineralization in the syenite appears to be complex; it is generally linked with fine grain mesocratic rocks described here as xenoliths. Minimum uranium concentrations recorded in all tectonic settings range between 221 and 351 ppm, while the maximum values range between 1135 and 1548 ppm) [4].

### 3. CHALLENGES IN URANIUM EXPLORATION AND DEVELOPMENT

Since 1950, exploration activities related to uranium, including ground borne and airborne radiometric surveys, geologic studies, drilling, have been supervised and conducted in Cameroon by several mining companies and organizations such as the CEA (Paris), IAEA, Utah Development Company (UDC), German Federal Institute for Geosciences and Natural Resources (BGR), the Canadian Agency for International Development CAID, Mega Uranium and other Junior Mining Companies.

Although the work dome has been substantial, the results have not lead to quantification of uranium resource in the country and its feasibility studies. Difficulties encountered during the implementation of this programme were due to: (i) nature or state of data (obsolete or nonexistent); (ii) insufficient survey over the whole national territory notably due to the inaccessibility to the potential mining sites; (iii) inexistence of documentation centres and information system on geo-scientific data; (iv) lack of effective analytical laboratories and geo-scientific society; (v) lack of qualified human resource in the domain of uranium exploration; and (vi) thick overburden of large surface of the country. To address these challenges, the Government of Cameroon has initiated a project described below.

### 4. PROJECT FOR CAPACITY BUILDING IN THE MINING SECTOR

The Project for capacity building in the mining sector (2012–2017) is mainly focused on the capacity building to boost the mining sector. This project aims at ameliorating: (i) the effectiveness and transparency in the management of the mining sector; and (ii) the framework for sustainable development. One of the three components of the project deals with the access to mineral resources and management of mining operations.

The objective is to ameliorate the knowledge and the access to mineral resource as well as the management of extractive activities. It is comprised of a geology programme, a support to the management of mining rights and mining activities, actions to reinforce the transparency and mining royalty.

It is under this project that airborne geophysical survey of targeted zones has been initiated in six out of ten administrative regions in Cameroon. This operation will cover a surface of 160 000 km<sup>2</sup> and enable the exploration of about 70% of the country, leading to the production of thirteen new geologic maps as against one existing at present.

### 5. CONCLUSION

Cameroon, in general, appears to be a country which could contribute to the world uranium production. However, the insufficiency of data on actual uranium potential hampers this vision. Ongoing efforts to better master the mining potential in Cameroon are indeed notable, but still not enough to solve the uranium production constraints.

In this context, the current programme of the IAEA to assist member states for a better understanding of the geology of uranium is a good opportunity to share related international experiences and knowledge at the country level. We consider that it is necessary to:

- Strengthen technical capacity of stakeholders involved in the geology of uranium;
- Constitute a reliable database of uranium geology (including updated maps at appropriate scales) as supporting tool for efficient decision of private investors;
- Support research programmes dedicated to uranium in universities and research institutes;
- Encourage the transfer of exploration and mining technology to the nationals.

## REFERENCES

- [1] KOUSKE, A.P., SUH, C.E., GHOGOMU, R.T., NGAKO, V., Na-metasomatism and uranium mineralization during a two-stage albitization at Kitongo, Northern Cameroon: structural and geochemical evidence, *Int. J. Geosciences* **3** (2012) 258–279.
- [2] MEGA URANIUM CORPORATION CAMEROON PLC, The exploration activities in the Salaki concession, year end report (2011).
- [3] MEGA URANIUM CORPORATION CAMEROON PLC, the exploration activities in the Teubang concession, year end report (2011).
- [4] MEGA URANIUM CORPORATION CAMEROON PLC, the exploration activities in the Lolodorf concession, year end report (2011).

# URANIUM DEPOSITS OF MADAGASCAR

L.H. RANDRIAMANANJARA  
Ministry of Strategic Resources,  
Directorate of Mines,  
Antananarivo, Madagascar

## Abstract

Madagascar has a high potential for uranium in the crystalline basement and sedimentary formations. The Government of the Republic of Madagascar has been promoting a comprehensive national policy, aiming at the major goal of poverty reduction through economic growth. In order to realize this policy, it was recognized that the promotion of mining activities is crucial, with focus on the large-scale mining development by introduction of foreign direct capital investment. The first discovery of uranium in Madagascar was in the lacustrine basin of Antsirabe located in the central part of the country. Generally, the uranium mineralization is found within five formations and different deposit types: (i) pegmatites (central part of Madagascar; Itasy, Antsirabe, Mandoto regions), locally called uranium pegmatite; (ii) the pyroxenites mineralized with urano-thorianite (Fort-Dauphin area, South Eastern); (iii) uraninite-bearing granites (Ankazobe); (iv) the neogene lacustrine basin of Antsirabe, with autunite (central part); and (v) the Isalo formation of Mahajanga and Moramanga basin, locally called uranium sandstones (carnotite bearing).

## 1. INTRODUCTION

Uranium potential of Madagascar mainly seen in the crystalline basement and in the sedimentary formations, both discovered by Henri Besairie since 1928. Different companies are carrying out exploration in these potential areas of Madagascar. The higher value of uranium is reported from in the southern part of the country. Uranium potential of the whole country is examined by regional surveys and currently detailed exploration is carried out in most favourable areas in the south of the country.

## 2. GEOLOGY OF MADAGASCAR

With an area of over 590 000 km<sup>2</sup>, Madagascar's geology mainly consists of a Precambrian basement of metamorphic and intrusive rocks [1]. The architecture of the basement of Madagascar is still poorly understood. The current studies seek to define potential areas for uranium mineralization by identifying the different tectono-metamorphic units by favourable lithological, structural, metamorphic, and geochronological characteristics. The basement complex is bounded in the west by series of monoclines spread over a narrow strip of the eastern coastal basin in three wide basins of Ambilobe, Majunga and Morondava, all which have shared the same geological history. The younger sedimentary formations are cut by Albo-Cenomanian dykes or lacoliths and the effusive Turonian to Santonian, Tertiary and Quaternary rocks.

Madagascar was part of the Gondwana super continent and was positioned between India, Antarctica and was adjacent to the present landmass of Tanzania, Kenya and Somalia in Africa. As a result of the breaking up of this super continent, which was initiated by the Permo-Triassic rifting, the failed rifts created the Karoo sedimentary corridor that continued up to the Turonian time, when India separated from Madagascar.

Madagascar has two main of geological entities [1]:

- Two thirds of the land mass is constituted by the Precambrian crystalline formations (the crystalline basement) composed of four domains and four sub-domains: Antananarivo and Tsaratanana (Neoarchean), Ikalamavony (Ikalamavony and Dabolava Suite), Bemarivo (Palaeoproterozoic) and Vohibory domain (oceanic arc/forearc) and Antongil–Masora (Mesoarchean) which is divided into Antogil sub-domain and Masora sub-domain, Anosy–Androyen divided into Anosy sub-domain and Androyen sub-domain;

- A third of the land mass is formed of the Phanerozoic, non-methamorphosed sedimentary formations (the sedimentary cover).

The main geological structures delineated in Madagascar are [1]:

- The Angavo–Ifanadiana shear zones;
- The Bongolava–Ranotsara structure (after gamma spectrometry and magnetic data);
- Three shear zones in the south (Ampanihy–Voronkafotra and Tranomaro).

### 3. HISTORICAL WORK

A summary of uranium exploration efforts in Madagascar is shown in Table I. The first uranium discoveries were made in 1909. During 1947 to 1969, small production was carried out by the French CEA (Commissariat à l'énergie atomique).

TABLE I. A BRIEF CHRONOLOGY OF URANIUM EXPLORATION AND MINING IN MADAGASCAR

| Date            | Activities   | Organization  |
|-----------------|--|---|
| 1909            | The first uranium discovery (uranocircite) in the central part in the Neogene lake basin of Antsirabe  | Private Company   |
| 1947            | Uranothorianite discovery in the south-eastern part of Madagascar  | Geological Survey of Madagascar<br>French CEA   |
| 1947–1969       | <p>Intensive activities are carried out in uranium zones:</p> <ul style="list-style-type: none"> <li>• Central part (Antsirabe): field checking of airborne data;</li> <li>• South eastern part (Tranomaro): geological prospection and airborne geophysical;</li> <li>• Western part (Folakara, Makay): geological prospection; airborne geophysical surveys.</li> </ul> <p>Mining in:</p> <ul style="list-style-type: none"> <li>• Pegmatite and lake basin of Antsirabe zone;</li> <li>• Uranothorianite deposits of Fort Dauphin zone: 39 large mines and 17 small mines.</li> </ul> |   |
| 1976–2000       | <p>Resumption of uranium exploration program in partnership with:</p> <ul style="list-style-type: none"> <li>• IAEA (1976–1984): geophysical airborne survey, geological prospecting, drilling works in the uranothorianite deposits of Fort Dauphin zone (180 holes of total depth of 7460 m);</li> <li>• UNDP (1978–1980): geological and geophysical prospecting in Antsirabe and Folakara (western part);</li> <li>• COGEMA (1999–2000): exploration works in the western part (Morondava and Mahajanga Basins).</li> </ul>  | Military Office of Industry Strategic (Malagasy public enterprise OMNIS <sup>31</sup> ) |
| 2004–2009       | Uranium exploration  | OMNIS in partnership with various foreign Companies (14 Companies)                      |
| 2009 to present | Uranium exploration  | OMNIS in partnership with a few foreign Companies                                       |

<sup>31</sup> Office des mines nationales et des industries stratégiques

## 4. URANIUM DEPOSITS

The major uraniferous areas in Madagascar are located in the:

- Central part of Madagascar, in the Itasy, Antsirabe and Mandoto regions;
- Southeastern Madagascar, in the Fort Dauphin–Tranomaro region;
- Morondava basin (Makay and Folakara regions).

Main host rocks for the uranium mineralization are pegmatites, pyroxenites and lacustrine sediments. Brief descriptions of the main localities are given below.

### 4.1. Pegmatites of Antsirabe

This sector is located in the central part of Madagascar, in Betafo region. The Betafo town is located 190 km from Antananarivo crossing the Antsirabe prefecture, served by National Road n° 7.

There are four principal geological unities:

- Crystalline basement;
- Eruptive rocks and granites;
- Recent volcanic rocks;
- Superficial formations.

### 4.2. Vavavato formations

The massive located in north of Betafo constitutes a huge granite mass with lined migmatites which clearly separates the old base. Granite has special characters with basic rocks enclaves more or less transformed and its association with the rich in migmatites intercalated and intrusions and basic (amphibolites, pyroxenite, diorites, gabbros, norites). The border contains massive uranium pegmatites affected by intensive tectonic activity, thus forming steep valley sides. Important features seen in this area include:

- Straight valleys, generally silt bearing associated by flat grained white quartz;
- Post fault of granite intrusion affecting the whole area with general trend of N20°E.

There are three types of pegmatites, all essentially potassic are identified in this area:

- Pegmatites within granites;
- Pegmatites within gabbros;
- Pegmatites within crystalline basement.

Pegmatites within granites have round pieces of quartz with biotite sheets concentrated within weathered zones, generally accompanied by haematite and magnetite. The pegmatites contain locally small grains of betafite, euxenite, columbite, orangite, garnet, pyrite and rarely amethyst. In general radioactive values range from 18 to 50 cps (counts per second).

Pegmatites within gabbros are seen on the surface by straight veins of white milky quartz which are from 50 to 200 m of length, localised in fractures of north south strike. They are found up to 7 m in depth and have a dip of 70° E. Magnetite is present in zoned pegmatites, characterized by euxenite crystal generally associated of betafite, beryl or oxide iron. Radioactivity is of the order of 30 to 50 cps. A general estimation of a zoned pegmatite of Antovontany or Ankazo gives a mineralised volume estimate of 4000 m<sup>3</sup>, with an average radioactivity is 40 to 50 cps.

Pegmatites within the crystalline basement are localised in the fractures zones, represented by migmatite gneiss complex with frequent intercalations of feldspar amphibolite. The Karahara pegmatites record values of 100 to 700 cps.

The principal uranium minerals are:

- Betafite:  $(\text{Ca}, \text{Na}, \text{U})_2 (\text{Ti}, \text{Nb}, \text{Ta})_2 \text{O}_6 (\text{OH})$ ;
- Euxenite:  $(\text{Y}, \text{Ca}, \text{Ce}) (\text{Nb}, \text{Ta}, \text{Ti})_2 \text{O}_6$ ;
- Samarskite:  $(\text{Y}, \text{Fe}^{3+}, \text{Fe}^{2+}, \text{U}, \text{Th}, \text{Ca})_2 (\text{Nb}, \text{Ta})_2 \text{O}_8$ ;
- Fergusonite:  $\text{RE Nb O}_4$  (where RE = rare earth).

#### 4.3. Pyroxenites of Tranomaro Area

The area is located about 800 km from Antananarivo to the South of Madagascar, in Toliara province, served by National Road N7 until Ihosy and secondary road n° 13 from Ihosy to Tranomaro.

The area is exposed by the Tolagnao Ampanihy unit of Proterozoic age (2600–2500 Ma), characterized by leptynites with an abundance of werneritite, pyroxenite, sometimes amphibolite, cipolins and marble formations of sedimentary origin that have undergone an intense degree of metamorphism (granulite facies).

The principal uranium mineral is uranothorianite  $(\text{Th}, \text{U})\text{O}_2$ . Mineralization is presented in the form of lenticular and irregular clusters of uranothorianite in lenses of pyroxenite of green, dark green, blackish grey colour and/or amphibolites of dark brown colour generally in association with mica schists (phlogopites), gneisses, anorthosites and marbles.

Recent analyses gave 480–500 Ma age for uranothorianite. Two main stages of metasomatism are recognized in the Tranomaro region: aluminous diopside + carbonated-scapolite (meionite)  $\pm$  titanite  $\pm$  spinel  $\pm$  wollastonite  $\pm$  corundum  $\pm$  uranothorianite developed during stage 1 at 5 kbar and 850°C (temperature estimated by the stability of nearly pure meionite); F-phlogopite, F-pargasite  $\pm$  uranothorianite  $\pm$  REE-rich hibonite  $(\text{CaAl}_{12}\text{O}_9)$  developed during stage 2 at 800°C, 3 kbar [2]. Stage 1 is dated by U–Pb zircon at 565 Ma [3]. Stage 2 may be related to the giant monazite mineralization in the nearby Anosyan Mountains, which is dated at 545 Ma [4].

Pyroxenites are sometimes dissected by seams or dykes of basalte or dolerite of Cretaceous but which do not appear to have affected the mineralization. Spinel and the corundum are very frequent in the uranothorianite deposits in certain sectors. The principal uranium mineral is uranothorianite. The dimension of the lenses of uranothorianite varies in length of a few to hundreds of metres (up to 300 m). Uranothorianite has cubic forms, with dimensions of a few tens of micron to a few millimetres and even of centimetre size.

#### 4.4. Lacustrine basin Vinaninkarena Zone-Antsirabe

The uraniferous zone of Vinaninkarena is located about 12 km in the south of Antsirabe. The uraniferous zone is with the contact of crystalline basement, in the south of the old lake. The presence of hydrothermal sources has played a role in uranium precipitation. This model shows that the uranium source is from the erosion and transport of niobotantalates minerals of pegmatites, mixing with lake water with significant concentration in the Southern zone where the lake was gradually emptied.

The mineralized sediments are fluvio-lacustrine, located in a Plio-Pleistocene basin, formed by subsidence faults. The mineralized lenses have dimensions from a few decimetres to a maximum of 3 m. Uranocircite and uranium phosphate (autunite) occur in form of impregnations often distinguishable to the naked eye in sub-horizontal lenses of clay and consolidated sandstone.

The principal uranium minerals are:

- Autunite:  $(\text{PO}_4)_2 \text{Ca}(\text{UO}_2)_2 \cdot 8\text{H}_2\text{O}$ ;
- Uranocircite:  $\text{Ba}(\text{UO}_2)_2(\text{PO}_4)_2 \cdot 12\text{H}_2\text{O}$ ;
- Gummite: mixed oxides of hydrated uranium, with impurities.

The major uraniferous pegmatites are identified by a central massive quartz core in deeply lateritized terrain. They consist of microcline and quartz, with or without accessory biotite, muscovite, black tourmaline, beryl, almandine and apatite [5]. There are two contrasting sub-types, (i) pegmatites with columbium-tantalum-complex, rare-element minerals carrying uranium and thorium and (ii) deposits rich in beryl and muscovite.

## 5. URANIUM IN THE SEDIMENTARY BASINS

### 5.1. Folakara Area

Folakara area is accessible by National Road n° 1, situated in the western part of Madagascar about 500 km in the west of Antananarivo. The Folakara Basin consists of Karroo sediments mainly of marine origin, rather than continental sediments usually seen in the Karroo of eastern Africa.

Geological formations belong to the Isalo Group which is divided into (from bottom to top):

- Isalo I: continental arkosic coarse grained to fined grained deltaic sandstone;
- Isalo II: Intercalations of coarse grained to fined grained sandstone and thick purple to green and gypseferous black shale beds, with marine influence at the bottom.

The geological structure is monocline with a dip between 3° and 15° W and NW. The uranium ores are met in Isalo II, composed of alternating coarse cross-bedded sandstone yellow, red and sometimes striped red clay (lutite). The stratigraphic sequence is composed of fluvio-deltaic sediments.

Uranium mineralization is essentially carnotite and secondary francevillite, in the continental series of Isalo II. This mineralization is associated with organic matter with pieces of silicified wood and minor pyrite and pyrolusite acting as reducing agents. All carnotite mineralization are located near the base of the Isalo II in Amboloando sandstone and less extensive in Ankaramenabe sandstone. The mineralization has an irregular form; it is characterized by lenses of uranium vanadate, subhorizontal irregular shape, with dimensions of several tens of kilometres. The mineralized layers are discontinuous.

In the Morafenobe area, after some drilling was carried out recording values the content up to 0.17 % of  $\text{UO}_2$ . The principal uranium minerals are carnotite,  $(\text{VO}_4)_2(\text{UO}_2)_2\text{K}_2 \cdot 3\text{H}_2\text{O}$  and francevillite,  $(\text{Ba},\text{Pb})(\text{UO}_2)_2(\text{VO}_4)_2 \cdot 5\text{H}_2\text{O}$ .

### 5.2. Makay Area

The sector is situated in the Morondava basin, about 500 km in the south-west of Antananarivo, served by the national road RN7 Antananarivo–Malaimbandy and by minor roads, only approachable during the dry season from Malaimbandy.

The Makay zone is strongly tectonised. Submeridional structures from near base, controlled the sedimentation basin, which is NNE–SSW divided horsts and grabens and dissected by NE structures.

The abundance of faults indicates the presence structural traps. Indications of hydrocarbon are seen in the middle and lower Sakamena, which could have acted as a reducing environment for uranium.

CEA's stratigraphic studies indicated oxidized sandstones in the Isalo II. The occurrence of oxidized sandstone in contact with a reducing potential (hydrocarbons) in the Sakamena or Sakoa sediments may have favoured uranium mineralization.

The Sakoa formations from bottom to top are:

- Tillites and black schists series;
- Coal layers;
- Red layers;
- Limestones.

Uranium potential primarily is in the reduced carboniferous layers and black schist. The Sakamena formations are characterized by sandstones and red colour schist. Middle and bottom part Sakamena are reducing due to the presence of abundant organic material and graphite. They constitute, along with the presence of hydrocarbons, a great reduction potential which can trap uranium in solution.

The Isalo I formation consists of fluvial feldspathic sandstones and coarse grained subangular, therefore high porosity and no presence of clay. Sandstones have the characteristics of a good uranium host rock and have a very large volume. The Isalo II formation is distinguished by facies of fine clays and coarse massifs. Uranium potential of Isalo II is of the same order as the Isalo I.

## 6. EXPLORATION

A summary of uranium exploration done in Madagascar is give in Table II.

TABLE II. BRIEF SUMMARY OF EXPLORATION CARRIED OUT IN MADAGASCAR

| Uraniferous areas                         | Exploration works  |
|---|--|
| Pyroxenite of Tranomaro–Fort Dauphin zone | <p>Works carried out CEA:</p> <ul style="list-style-type: none"> <li>– Cartography: scale maps of 1/500; 1/1 000;</li> <li>– Trenches, pits;</li> <li>– Uranothorianite mining: 39 larger mines and 17 small mines.</li> </ul> <p>Works carried out OMNIS:</p> <ul style="list-style-type: none"> <li>– Drilling: 180 holes with total depth of 7450 m;</li> <li>– Airborne prospecting (gamma spectrometer and magnetometer);</li> <li>– Cartography: scale maps of 1/200; 1/500; 1/1 000; 1/10 000; 1/20 000; 1/100 000;</li> <li>– Trenches, pits.</li> </ul> |
| Antsirabe lake basin                      | <p>Works carried out OMNIS:</p> <ul style="list-style-type: none"> <li>– Drilling: 127 holes with total depth of 3950 m;</li> <li>– Cartography: scale maps of 1/10 000; 1/100 000;</li> <li>– Pits.</li> </ul>  |
| Folakara sedimentary basin                | <ul style="list-style-type: none"> <li>– Drilling works (CEA): 1215 holes with total depth of 54 000 m;</li> <li>– Drilling works (OMNIS): 28 holes with total depth of 1950 m;</li> <li>– Trenches, pits (OMNIS).</li> </ul>  |

### 6.1. Exploration in the Morondava Basin

Historic exploration in the Morondova Basin is highlighted below:

- 1958 to 1963, the CEA prospected the sedimentary rocks of the Karoo Supergroup in the Morondava Basin in western Madagascar, beginning exploration work in the Folakara and Makay districts. Most of the work was completed in the Folakara District, where the CEA utilized airborne radiometrics, delineating a number of airborne radiometric anomalies. These airborne anomalies were followed up using various ground surveys (i.e. ground radiometric surveys), geochemistry, geophysics (seismic) and drilling (stratigraphic and definition). Several of the radioactive anomalies yielded positive results and were investigated further by drilling.

No profitable uranium deposits were outlined and the CEA abandoned all exploration activities in the Folakara District by 1963;

- 1958 to 1962, the CEA carried out exploration work in the Makay District, located centrally in the Morondava Basin. Most of the work was limited to airborne radiometric surveys and some ground observations. In 1963, the CEA stopped prospecting for uranium in Madagascar;
- 1976 to 1982, OMNIS, a Madagascar Government organization, carried out a number of ground surveys in the Folakara District under a UNDP and IAEA supported programme. The final report recommended focusing exploration activities in the Makay area (more than 95% of UMC permits) which had several untested airborne radiometric anomalies and was therefore considered more promising;
- 1982 to 1984, the French group Minatome S.A., a part of the Compagnie Générale des Matières Nucléaires ('COGEMA')/AREVA Group, was attracted by the uranium potential of the Karoo Supergroup in the Folakara and Makay districts and proceeded to re-evaluate the potential of these areas;
- 1999 to 2000: COGEMA, a wholly owned subsidiary of CEA, carried out limited geological studies and exploration activity in the southern part of the Morondava Basin. In 2000, COGEMA abandoned all exploration efforts in Madagascar.

## 7. CONCLUSION

Apart from the potential areas identified earlier, recent geochemical surveys by the Japan International Cooperation Agency (JICA) team and Ministry of Mines in southern part of Madagascar recorded high values of uranium. The maximum value recorded was 590 ppm and the minimum value 0.3 ppm. The southern part of Madagascar is recognized with the high potential for uranium.

## REFERENCES

- [1] BESAIRIE, H., *Précis de géologie malgache*, Annales géol. Madagascar **36**, Impr. nationale, Tananarive (1973) pp141.
- [2] RAKOTONDRAZAFY, M.A.F., MOINE, B., CUNNEY, M., Mode of formation of hibonite ( $\text{CaAl}_{12}\text{O}_{19}$ ) within the U-Th skarns from the granulites of S-E Madagascar. *Contrib. Mineral. Petrol.* **123** (1996) 90–201.
- [3] ANDRIAMAROFAHATRA, J., DE LA BOISSE, H., NICOLLET, C., Datation U–Pb sur monazites et zircons du dernier épisode tectono-métamorphique granulitique majeur dans le Sud-Est de Madagascar. *C. R. Acad. Sci. Paris.* **310** 2 (1990) 1643–1648.
- [4] PAQUETTE, J.-L., NÉDÉLEC, A., MOINE, B., RAKOTONDRAZAFY, M., U–Pb, single zircon Pb-evaporation, and Sm–Nd isotopic study of a granulite domain in SE Madagascar. *J. Geol.* **102** 5 (1994) 523–538.
- [5] BOURRET, W., Uranium-bearing pegmatites of the Antsirabe-Kitsamby district, Madagascar, *Ore Geology Reviews* **3** 1–3 (1988) 177–191.

# BOTTLE ROLL TEST FOR TEMREZLI URANIUM ORE

K. ÇETIN, A.A. İSBİR TURAN, E. ÜÇGÜL, M.Y. ALBAYRAK  
General Directorate of Mineral Research and Exploration,  
Ankara, Turkey

## Abstract

The new leach test procedure which is held in General Directorate of Mineral Research and Exploration (MTA) of Turkey is mostly suitable for determining metal extraction conditions and recovery values in uranium containing ore bodies. The tests were conducted with samples taken from Temrezli Uranium Ore located in approximately 200 km east of Turkey's capital, Ankara. Mining rights of Temrezli Ore were 100% Anatolia Energy Ltd controlled at the time of writing. The resource estimate includes an indicated mineral resource of 5410 t U<sub>3</sub>O<sub>8</sub> at an average grade of 1426 ppm (~4590 tU at ~1210 ppm U) and an additional inferred resource of 3300 t U<sub>3</sub>O<sub>8</sub> averaging 904 ppm (~2800 tU at ~767 ppm U). In accordance with the demand from Anatolia Energy bottle roll leach tests have been initiated in MTA laboratories to investigate the recovery values of low-grade uranium ore under in-situ leach conditions. Bottle roll leaching tests are performed on pulverized samples with representative lixiviant solution at ambient pressure and provide an initial evaluation of ore leachability with a rough estimate of recovery value. At the end of the tests by using 2 g/L NaHCO<sub>3</sub> and 0.2 g/L H<sub>2</sub>O<sub>2</sub> up to 84.6% of uranium recovery was obtained after 12 days agitation leach study.

## 1. INTRODUCTION

The element uranium is very widely presented throughout the crust of the earth. Mostly all types of rocks contain some amount of uranium. Uranium is also present in ground water, river water and seawater. On the other hand, the common commercial source of uranium is rocks, though it may also be extracted from seawater. Uranium ions normally occur in tetravalent or hexavalent form in nature, but they are more easily soluble in acidic water in the hexavalent state. Metallic uranium is highly reactive, chemically, so it can be leached in acidic or alkaline environment [1]. The properties of uranium, particularly its solubility, ease of transport and precipitation, and have led to the formation of ore deposits of a number of types in a variety of geological settings. Many uranium ore types call for the application of conventional mining methods like open pit mining or underground mining and subsequent extraction by hydro-metallurgical process. But, sometimes the occurrence of uranium in sandstone provide an opportunity to recover the metal in an innovative method of extraction called In-Situ Recovery (ISR, also called In-Situ Leaching, ISL), provided some necessary geological and geo-technical conditions are met [2, 3]. Certain geological and hydrological criteria must also be met before an ore body/deposit is considered suitable for in-situ leaching. The ore should occur in a generally horizontal bed underlain and overlain by a relatively impermeable stratum. The host rock should have a good permeability. The ore must be located below the water table. The direction and velocity of regional water flow must be known. The uranium minerals in the ore body must be amenable to proposed dissolution process preferably with carbonate solutions or relatively mild reagents. The ore should occur at favourable depth. The ore body should be of sufficient size and grade to justify the cost of production. Under favourable geological-hydrogeological conditions, the process of in-situ leaching is carried out by injecting the suitable mining solution into the ore body through injection holes. The solution is allowed to pass / flow through the ore body for desired period dissolving the desired metal content and the pregnant solution is then recovered through production well by pumping. The pumped out solution passes through a normal hydrometallurgical route in which uranium is separated.

Abzalov [3] reported that sandstone uranium deposits represent uranium concentrations formed by low-temperature hydrothermal processes, usually of diagenetic to epigenetic origin. The deposits are commonly hosted in arkosic sandstone and are therefore referred to as sandstone-type uranium [3]. Furthermore, there is a very important technical report about ISR that was published by IAEA in 2001, a manual of acid in situ leach uranium mining technology [4]. This report includes the observations of ISR leaching in acidic media especially using geological and hydrogeological data. In another technical report of IAEA, it is about recent developments in uranium resources and production with emphasis on

in situ leach mining [5]. The report especially contains new projects about uranium mining, ISR mining, licensing, heap leaching and restoration.

There is another technical report that was published by the government of Western Australia, Department of Mining and Petroleum in 2013. This report includes the general properties of uranium element and uranium mining and the environment, mining media, mining techniques for possible application in Western Australia [6]. An important review about uranium mining was written by Edwards and Oliver [7]. They reported that acid leaching is predominant process for uranium, usually with sulphuric acid because of its relatively low cost and wide availability. They discussed alkaline ISR and give the general schematic process of acidic and alkaline leaching.

The bottle roll leach test is a relatively inexpensive method for measuring the ability of the mineral species present in the sample to dissolve when subjected to mining solution and provides an upper limit of uranium recovery percentages. The recovery percentages determined with this method may not be realized in an operational scale due to reduced formation contact as a result of factors such as imperfect well field pattern, permeability, cementation and aquifer heterogeneity. Other factors such as time and economics may also reduce the recovery percentage and therefore results must be carefully interpreted [8].

Bottle roll tests are performed on pulverized samples with representative lixiviant solution at ambient pressure and provide an initial evaluation of the leachability of the ore and a rough estimate of recovery percentages. In essence, this method verifies the presence of uranium minerals amenable to remobilization. It is limited by the fact that it does not measure or duplicate in situ properties (permeability, porosity, etc.) of the host formation and therefore provides an optimistic estimate of recovery percentages [9]. The Temrezli in-situ recovery (ISR) Uranium Project (the Project) is an advanced exploration-stage uranium recovery project located in Turkey approximately 200 km east of Turkey's capital, Ankara. The Project lies in the central Anatolian uranium district which is considered to be one of Turkey's most significant and richest uranium districts. The Project area is located in a sparsely populated agricultural area near the small villages of Akoluk, Mehmetbeyli, and Temrezli. The nearest large town is Sorgun, approximately 10 km to the north. The Project is controlled 100% by Anatolia Energy Ltd. (Anatolia) through its wholly-owned Turkish subsidiary Adur Madencilik Ltd. Şti. (Adur). The resource estimate includes an indicated mineral resource of 5410 tonnes U<sub>3</sub>O<sub>8</sub> at an average grade of 1.426 ppm (~4590 tU at ~1210 ppm U) and an additional inferred resource of 3300 tonnes of U<sub>3</sub>O<sub>8</sub> at an average grade of 904 ppm (~2800 tU at ~767 ppm U) [9].

The Temrezli deposits and related uranium occurrences are found within a fairly young sedimentary basin that lies atop a Cretaceous granitic batholith within the Kırşehir massif in Central Anatolia. Mineralization within the Project area occurs within a sedimentary sequence of semi-continuous layers grading from conglomerates and coarse, medium, and fine sandstones, to clay and limestone [9].

It was reported that quartz and K-feldspar make up the bulk of the sample (45.2% and 23.5%). Clay minerals (primarily kaolinite) and calcite each make up almost 10 percent of the sample. Plagioclase, pyrite, and other minor minerals make up the rest of the sample [9]. The uranium minerals comprise approximately 1.5% (by mass) of the sample. Most of these are complex phases composed of extremely fine grained uranium minerals that are mostly found along the grain boundaries of the host rock minerals. Although a few relatively discrete phases could be discriminated, most of the uranium bearing occurrences was too fine grained to accurately identify the mineral species. It appears that a large proportion of the uranium may be hosted by secondary Ca-bearing species such as uranophane, becquerelite and haiweeite. Small amounts of uraninite (and/or more hydrated uranium oxides) and coffinite (and/or more hydrated species like soddyite) may also be present. A very small proportion of the uranium was found to contain Ti and it is possible that refractory brannerite is present [10].

## 2. EXPERIMENTAL

### 2.1. Chemicals and sample preparation

$\text{NaHCO}_3$  (Merck),  $\text{CO}_2$  (g), 30%  $\text{H}_2\text{O}_2$  (Merck); chemicals are used in analytical grade, pH meter (ORION) is used to control the pH of the leaching mixture (see Fig. 1), TCLP (Toxicity Characteristic Leaching Procedure) extraction device is used for shaking the bottles for 20 h, centrifuge system is used to separate the solid and the liquid parts of the leaching mixture, vacuum filtration is used for this purpose, too. An agitator is used for bottle roll tests; a splitter is used to divide the optimum grain size of the ore sample [11].



FIG. 1. Adding chemicals to leach vessels.

Split sandstone cores typically recovered from deposits targeted for ISR operations are manually crushed and blended without reducing grain sizes or drying. The process of splitting and weighting the leach vessel charge should be conducted quickly to minimize air oxidation of  $\text{U}^{4+}$  to  $\text{U}^{6+}$ . If manual crushing of the core sample is not possible (concreted samples), it may be necessary to achieve this step using a jaw crusher or equivalent. Following crushing, blending of the material should be as thorough as possible without drying or excessive air exposure. Subsamples of the material are collected for chemical head analysis, calculation of moisture content, the bottle roll test and one part of these is separated as witness sample [12, 13].

### 2.2. Materials and methods

These bottle roll leach tests are intended to demonstrate that the host ore uranium mineralization is capable of being solubilized using conventional in-situ recovery (ISR) chemistry. The lixiviate solution is prepared using 2.0 g/L  $\text{NaHCO}_3$  as the source of the carbonate complexing agent (formation of uranyl dicarbonate (UDC) and uranyl tricarbonate ion (UTC)). 0.5 g/L to 1.0 g/L  $\text{H}_2\text{O}_2$  is added as the uranium oxidizing agent as the tests are conducted at ambient pressure. pH adjustment is conducted by saturating the ore/solution slurry with gaseous carbon dioxide. pH control is critical to prevent potential calcium carbonate (calcite,  $\text{CaCO}_3$ ) precipitation within the wells and orebody. The pH should generally be held below 7.5. These project specific limits should be applied to the leach testing to provide the most representative results.

In order to allow for head space in the leach container, 500 or 600 g dry sample is added to the reaction vessel. One pore volume of the selected 500–600 g core sample should, at 30% porosity, equal 60–72 mL. 300–360 mL of lixiviate is added to the 200–240  $\text{cm}^3$  core samples and the reaction vessel is rotated on the roller table.

Using a solid gravity (SG) of  $2.5 \text{ g/cm}^3$  and porosity of 30% (these are average data for sandstone),  
 1 Pore Volume (PV) =  $600\text{-gram charge} / 2.5 \text{ SG} \times 0.30 \text{ porosity} = 72 \text{ mL}$   
 $5\text{PV} = 5 \times 72 = 360 \text{ mL lixiviate}$

The leaching procedure for Bottle Roll Tests, as applied to Temrezli uranium ore, is shown in Fig. 2.

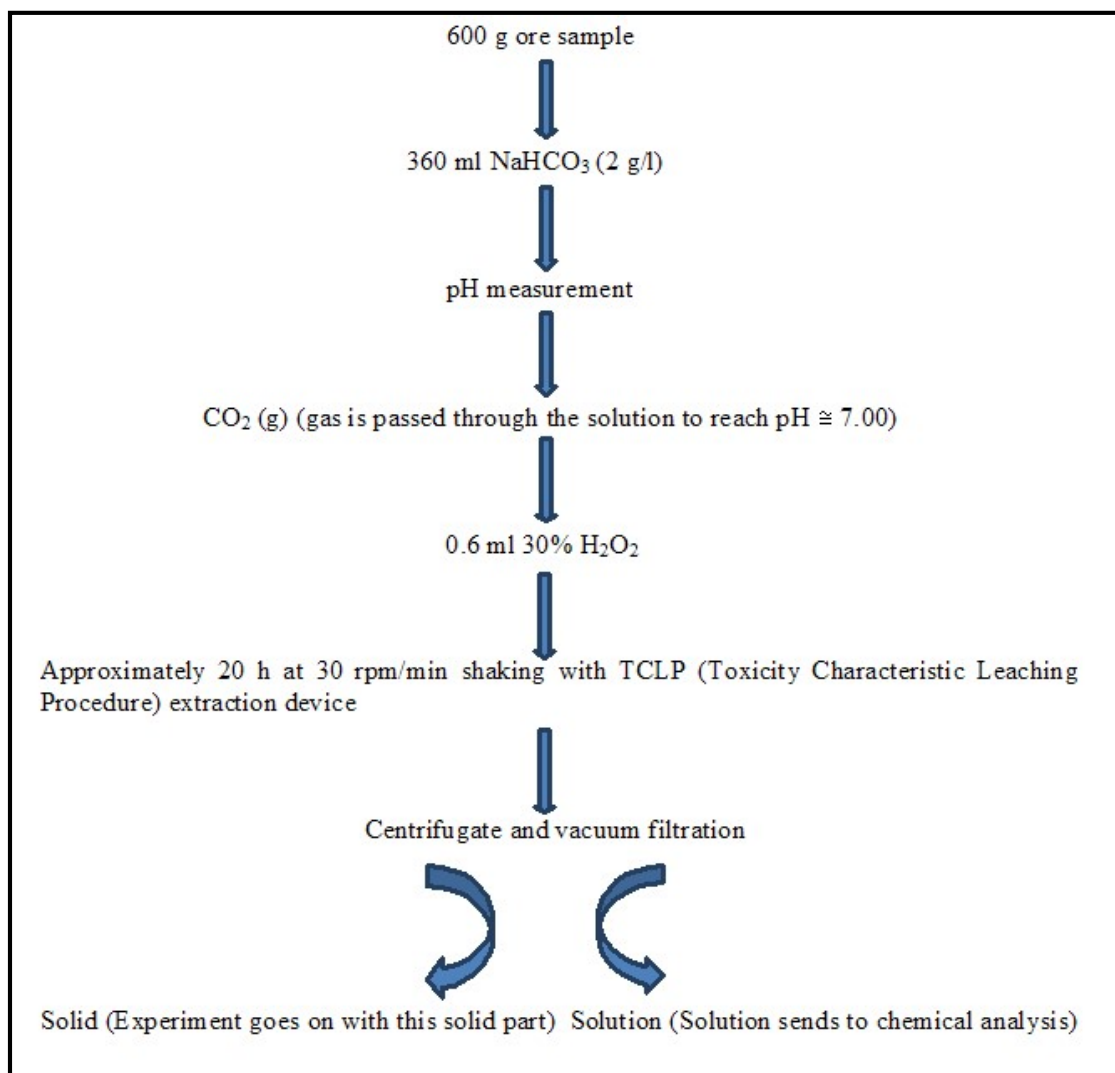


FIG. 2. Procedure for bottle roll test of uranium.

Due to this leaching procedure, following the initial 20 h leach period, the entire lixiviate charges are extracted using a combination of high speed centrifugation and, if necessary, vacuum filtration. Analysis for uranium and the client's preferred suite of elements can be conducted on a periodic or daily basis. A clean charge of lixiviate is added to the solids which remain in the extraction vessels.  $\text{H}_2\text{O}_2$  (hydrogen peroxide) is added to refortify lixiviate to the desired  $\text{H}_2\text{O}_2$  concentration, pH is adjusted with  $\text{CO}_2$  and vessel rotation is continued for at least 5 additional 20-hour periods (30 PV). The recovered core (tails) is dried, ground and analysed for uranium for mass balance purposes both on a whole sample basis and on grain size distribution basis if the client so desires. For accurate 'heads' uranium determinations, the mass uranium recovered by solution extraction should be added to either the sum of the fractionated 'tails' or the total tails.



FIG. 3. Bottle roll leach test apparatus.

### 3. RESULTS AND DISCUSSION

The test was conducted with two samples ALT 1A and ALT 1B. The steps of the test procedure were followed as given above. All samples were taken from the beginning to the end of the test were sent to analytical laboratories for chemical analysis. The chemical analyses were conducted by ICP–OES (Inductively Coupled Plasma Optical Emission Spectroscopy).

Initial core analysis was prepared for uranium and other elements as requested by client (Table I).

TABLE I. CHEMICAL ANALYSIS OF CORE SAMPLE

| pH  | Ca<br>mg/kg | Mg<br>mg/kg | Na<br>mg/kg | P<br>mg/kg | Fe<br>mg/kg | As<br>mg/kg | Mo<br>mg/kg | Se<br>mg/kg | S<br>mg/kg | U<br>mg/kg | V<br>mg/kg |
|-----|-------------|-------------|-------------|------------|-------------|-------------|-------------|-------------|------------|------------|------------|
| 7.7 | 5200        | 1000        | 80          | 250        | 11500       | < 20        | < 20        | < 20        | 8000       | 432        | 20         |

#### 3.1. Agitation leach study results for ALT 1A

Bottle roll test continued during twelve days with two samples. The test were repeated each day according to the test procedure until desired number of pore volumes have been achieved. The results are as given below (Tables II–IV).

TABLE II. LEACHATE VOLUME AND URANIUM WERE RECOVERED DURING TWELVE DAYS

| Number of days | Pore volume (PV) | Feed lixiviate pH | Extraction fluid pH | Volume recovered L | U mg/L | U mg   |
|----------------|------------------|-------------------|---------------------|--------------------|--------|--------|
| 1              | 1-5              | 6.94              | 6.96                | 0.280              | 67     | 18.76  |
| 2              | 6-10             | 7.00              | 6.90                | 0.319              | 90     | 28.71  |
| 3              | 11-15            | 7.01              | 6.95                | 0.331              | 70     | 23.17  |
| 4              | 16-20            | 7.01              | 6.95                | 0.320              | 81     | 25.92  |
| 5              | 21-25            | 7.01              | 6.97                | 0.330              | 90     | 29.70  |
| 6              | 26-30            | 7.00              | 6.99                | 0.309              | 89     | 27.50  |
| 7              | 31-35            | 6.96              | 7.01                | 0.327              | 70     | 22.89  |
| 8              | 36-40            | 6.94              | 6.94                | 0.330              | 65     | 21.45  |
| 9              | 41-45            | 6.96              | 7.01                | 0.336              | 55     | 18.48  |
| 10             | 46-50            | 6.95              | 7.00                | 0.336              | 47     | 15.79  |
| 11             | 51-55            | 7.00              | 7.02                | 0.323              | 43     | 13.89  |
| 12             | 56-60            | 6.99              | 6.99                | 0.316              | 35     | 11.06  |
| Total          |                  |                   |                     | 3.857              |        | 257.32 |

TABLE III. CHEMICAL ANALYSIS OF THE RECOVERY FLUID

| pH<br>leachate | Elec cond<br>umho/cm | Alk<br>mg/L | HCO <sub>3</sub><br>mg/L | Ca<br>mg/L | Mg<br>mg/L | Na<br>mg/L | P<br>mg/L | Fe<br>mg/L | S<br>mg/L | SO <sub>4</sub><br>mg/L | U<br>mg/L | V<br>mg/L |
|----------------|----------------------|-------------|--------------------------|------------|------------|------------|-----------|------------|-----------|-------------------------|-----------|-----------|
| 8.02           | 2230                 | 1030        | 1260                     | 150        | 34         | 390        | <0.2      | <0.2       | 280       | 840                     | 67        | <0.2      |
| 7.94           | 2260                 | 1095        | 1340                     | 25         | 22         | 416        | <0.2      | <0.2       | 240       | 720                     | 90        | <0.2      |
| 8.02           | 2170                 | 1245        | 1520                     | 16         | 15         | 435        | <0.2      | <0.2       | 170       | 510                     | 70        | <0.2      |
| 8.07           | 2270                 | 1263        | 1540                     | 15         | 12         | 440        | <0.2      | <0.2       | 200       | 600                     | 81        | <0.2      |
| 8.27           | 2340                 | 1283        | 1570                     | 13         | 10         | 451        | <0.2      | <0.2       | 214       | 642                     | 90        | <0.2      |
| 8.65           | 2420                 | 1343        | 1640                     | 10         | 9          | 450        | <0.2      | <0.2       | 234       | 702                     | 89        | <0.2      |
| 8.39           | 2530                 | 1280        | 1560                     | 22         | 10         | 760        | <0.2      | <0.2       | 217       | 651                     | 70        | <0.2      |
| 8.40           | 2500                 | 1330        | 1620                     | 18         | 9          | 755        | <0.2      | <0.2       | 203       | 609                     | 65        | <0.2      |
| 8.65           | 2480                 | 1435        | 1750                     | 29         | 8          | 774        | <0.2      | <0.2       | 169       | 507                     | 55        | <0.2      |
| 8.66           | 2440                 | 1433        | 1750                     | 11         | 7          | 788        | <0.2      | <0.2       | 155       | 465                     | 47        | <0.2      |
| 8.71           | 2520                 | 1435        | 1750                     | 28         | 7          | 806        | <0.2      | <0.2       | 179       | 537                     | 43        | <0.2      |
| 8.77           | 2580                 | 1475        | 1800                     | 9          | 7          | 839        | <0.2      | <0.2       | 179       | 537                     | 35        | <0.2      |

TABLE IV. CHEMICAL ANALYSIS OF THE TAIL

| pH   | Ca mg/kg | Mg mg/kg | Na mg/kg | P mg/kg | Fe mg/kg | As mg/kg | Mo mg/kg | Se mg/kg | S mg/kg | U mg/kg | V mg/kg |
|------|----------|----------|----------|---------|----------|----------|----------|----------|---------|---------|---------|
| 8.47 | 5000     | 1200     | 900      | 200     | 11000    | <20      | <20      | <20      | 7500    | 84      | <20     |

The total uranium leached is 257.3 mg at the end of the test. The feed mass is 598.7 g and the tail mass 556.7 g. According to head and tail chemical analysis, 84.6% uranium was recovered.

### 3.2. Agitation leach study results for ALT 1B

Results for ALT 1B tests are given in Tables V–VII.

TABLE V. LEACHATE VOLUME AND URANIUM WERE RECOVERED DURING TWELVE DAYS

| Number of days | Pore volume (PV) | Feed lixiviate pH | Extraction fluid pH | Volume recovered L | U mg/L | U mg          |
|----------------|------------------|-------------------|---------------------|--------------------|--------|---------------|
| 1              | 1–5              | 6.94              | 7.00                | 0.281              | 60     | 16.88         |
| 2              | 6–10             | 7.00              | 6.99                | 0.336              | 53     | 17.81         |
| 3              | 11–15            | 7.01              | 7.02                | 0.281              | 66     | 18.55         |
| 4              | 16–20            | 7.01              | 7.00                | 0.307              | 77     | 23.64         |
| 5              | 21–25            | 7.01              | 7.01                | 0.318              | 91     | 28.94         |
| 6              | 26–30            | 7.00              | 7.03                | 0.268              | 101    | 27.07         |
| 7              | 31–35            | 6.96              | 7.00                | 0.302              | 85     | 25.67         |
| 8              | 36–40            | 6.94              | 6.94                | 0.274              | 78     | 21.37         |
| 9              | 41–45            | 6.96              | 6.99                | 0.288              | 65     | 18.72         |
| 10             | 46–50            | 6.95              | 6.99                | 0.278              | 62     | 17.24         |
| 11             | 51–55            | 7.00              | 7.01                | 0.255              | 51     | 13.01         |
| 12             | 56–60            | 6.99              | 6.99                | 0.268              | 46     | 12.33         |
| <b>Total</b>   |                  |                   |                     | <b>3.456</b>       |        | <b>241.21</b> |

TABLE VI. CHEMICAL ANALYSIS OF THE RECOVERY FLUID

| pH<br>leachate | Elec Cond<br>umho/cm | Alk<br>mg/L | HCO <sub>3</sub><br>mg/L | Ca<br>mg/L | Mg<br>mg/L | Na<br>mg/L | P<br>mg/L | Fe<br>mg/L | S<br>mg/L | SO <sub>4</sub><br>mg/L | U<br>mg/L | V<br>mg/L |
|----------------|----------------------|-------------|--------------------------|------------|------------|------------|-----------|------------|-----------|-------------------------|-----------|-----------|
| 7.95           | 2190                 | 1040        | 1270                     | 140        | 35         | 380        | <0.2      | <0.2       | 275       | 825                     | 60        | <0.2      |
| 7.65           | 2150                 | 1095        | 1340                     | 18         | 22         | 412        | <0.2      | <0.2       | 230       | 690                     | 53        | <0.2      |
| 8.14           | 2340                 | 1360        | 1660                     | 22         | 17         | 436        | <0.2      | <0.2       | 210       | 630                     | 66        | <0.2      |
| 8.28           | 2470                 | 1480        | 1810                     | 20         | 14         | 449        | <0.2      | <0.2       | 214       | 642                     | 77        | <0.2      |
| 8.44           | 2630                 | 1565        | 1910                     | 55         | 13         | 453        | <0.2      | <0.2       | 225       | 675                     | 91        | <0.2      |
| 8.50           | 2640                 | 1523        | 1860                     | 50         | 11         | 460        | <0.2      | <0.2       | 256       | 768                     | 101       | <0.2      |
| 8.50           | 2760                 | 1575        | 1920                     | 42         | 12         | 862        | <0.2      | <0.2       | 208       | 624                     | 85        | <0.2      |
| 8.51           | 2860                 | 1630        | 1990                     | 52         | 11         | 383        | <0.2      | <0.2       | 188       | 564                     | 78        | <0.2      |
| 8.57           | 2880                 | 1713        | 2090                     | 44         | 10         | 395        | <0.2      | <0.2       | 169       | 507                     | 65        | <0.2      |
| 8.65           | 2970                 | 1797        | 2190                     | 40         | 10         | 427        | <0.2      | <0.2       | 165       | 495                     | 62        | <0.2      |
| 8.69           | 3010                 | 1805        | 2200                     | 36         | 9          | 950        | <0.2      | <0.2       | 160       | 480                     | 51        | <0.2      |
| 8.76           | 3140                 | 1942        | 2370                     | 10         | 8          | 980        | <0.2      | <0.2       | 155       | 465                     | 46        | <0.2      |

TABLE VII. CHEMICAL ANALYSIS OF THE TAIL

| pH   | Ca<br>mg/kg | Mg<br>mg/kg | Na<br>mg/kg | P<br>mg/kg | Fe<br>mg/kg | As<br>mg/kg | Mo<br>mg/kg | Se<br>mg/kg | S<br>mg/kg | U<br>mg/kg | V<br>mg/kg |
|------|-------------|-------------|-------------|------------|-------------|-------------|-------------|-------------|------------|------------|------------|
| 8.26 | 5000        | 1200        | 900         | 200        | 11000       | <20         | <20         | <20         | 7500       | 110        | <20        |

A graphical comparison of the uranium extraction results from the tests on ALT 1A and ALT 2A is given in Fig. 4.

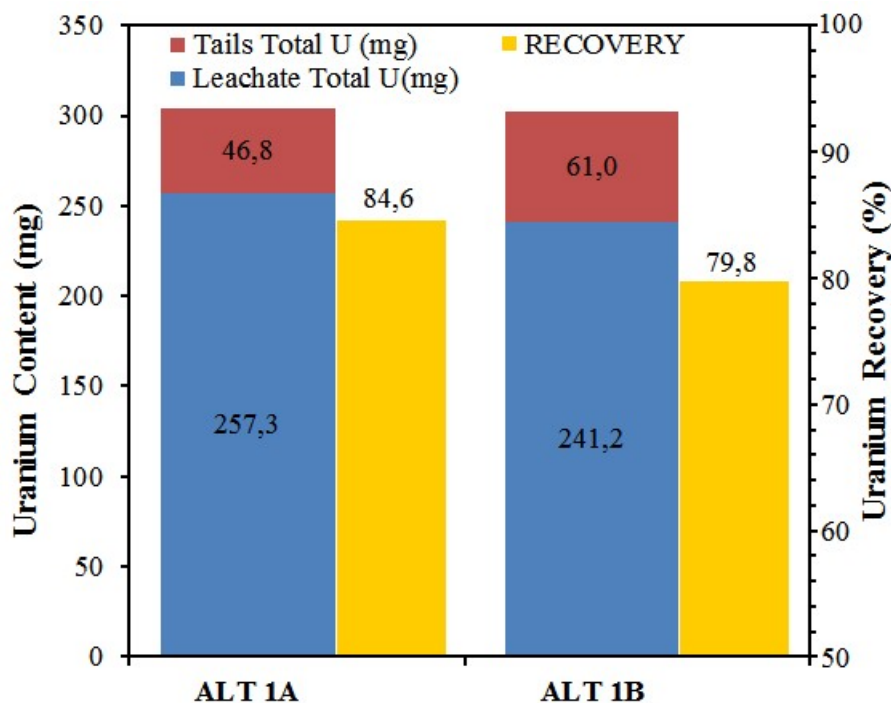


FIG. 4. Uranium recovery of ALT 1A and ALT 1B according to uranium contents of their tails and recovery fluids.

#### 4. CONCLUSIONS

The bottle roll tests showed uranium recoveries of 84.6% and 79.8%. Results also suggest that only small percentages of vanadium minerals were mobilized during leaching. Furthermore, vanadium concentrations within the tested samples were very low. Additionally, the precipitation of Ca (as  $\text{CaCO}_3$ ) is not unusual for alkaline ISR operations. Therefore, mobilization of vanadium and other metals is not anticipated to be a significant operational issue.

The tests may be combined with column leach test to provide approximate in-situ conditions (permeability, porosity and pressure). However, the bottle roll test is an indication of an ore's reaction rate and the potential uranium resource recovery.

#### REFERENCES

- [1] SREENIVAS, T., RAJAN, K.C., Studies on the separation of dissolved uranium from alkaline carbonate leach slurries by resin-in-pulp process, Separation and Purification Technology **112** (2013) 54–60.
- [2] SARANGHI, A.K., BERI K.K., “Uranium mining by in-situ leaching”, Proc. Technology Management for Mining for Mining Processing and Environment, IIT, Kharagpur, India (2000).
- [3] ABZALOV, M.Z., Sandstone-hosted uranium deposits amenable for exploitation by in situ leaching technologies, Applied Earth Science: Transactions of the Institutions of Mining and Metallurgy: Section B **121** 2 (2012) 55–64.
- [4] INTERNATIONAL ATOMIC ENERGY AGENCY, Manual of Acid In Situ Leach Uranium Mining Technology, IAEA-TECDOC-1239, IAEA, Vienna (2001).
- [5] INTERNATIONAL ATOMIC ENERGY AGENCY, Recent Developments in Uranium Resources and Production with Emphasis on In Situ Leach Mining, IAEA-TECDOC-1396, IAEA, Vienna (2004).

- [6] DEPARTMENT OF MINES AND PETROLEUM, Guide to Uranium in Western Australia, Government of Western Australia, East Perth, Western Australia (2013).
- [7] EDWARDS, C.R., OLIVER, A.J., Uranium Processing Overview, *JOM* **52** 9 (2000) 12–20.
- [8] YÖRÜKOĞLU, K., Hammadde olarak uranyum ve Türkiye Uranyum Potansiyeli (Uranium as Raw Materials and The Potential of Uranium in Turkey), *Mimar ve Mühendis Dergisi* (Architect and Engineer Journal) **75** (2014) 40–41 (in Turkish).
- [9] PERTEL, D., ANNETT, R., Mineral Estimate, Aldridge Uranium Ltd., Temrezli Uranium Deposit, Central Anatolia, CSA Global Resource Industry/Consultants, West Perth, WA, Australia (2011).
- [10] ÜÇGÜL E., İSBİR TURAN A.A., ÇETİN K., Uranyum cevheri için döner silindir hazneli liç testi (Bottle roll leaching test for uranium ore), *MTA Doğal Kaynaklar ve Ekonomi Bülteni* (MTA Natural Resources and Economy Bulletin) **17** (2014) 21–25 (in Turkish).
- [11] WWC Engineering, Temrezli ISR Uranium Project Preliminary Economic Assessment, (2013).
- [12] CLARK, D.L., HOBART, D.E., NEU, M.P., Actinide carbonate complexes and their importance in actinide environmental chemistry, *Chem. Rev.* **95** 1 (1995) 25–48.
- [13] METS (Mineral Engineering Technical Services, Pty Ltd), Temrezli Uranium Project Bottle Roll Test Results, Internal draft report, prepared by METS for Anatolia Energy (2011).

# **URANIUM IN SOUTH AFRICA: EXPLORATION AND SUPPLY CAPACITY**

A.O. KENAN, E. CHIRENJE  
Council for Geoscience,  
Pretoria, South Africa

## **Abstract**

The major uranium deposits types are quartz-pebble conglomerate of the Central Rand Group (Witwatersrand Supergroup) and the Dominion Group, sandstone of the Karoo Uranium Province, surficial deposits of the Namaqualand region, as well as coal and carbonaceous shale of the Springbok Flats Basin. Recent exploration activities (both greenfields and near-mine) have increased the resource potentials of these deposits. South Africa's Council for Geoscience is currently conducting high resolution magnetic and radiometric surveys in the Namaqualand region beyond the known uranium mineralization. Witwatersrand Basin is the only deposit where uranium mining is active at present in South Africa. Total uranium production in 2013 was 531 t. However, with production expected to increase in the Witwatersrand Basin, production is expected to reach 700 t U by the end of 2015. Furthermore, with uranium production envisaged to begin in the Karoo Uranium Province, Namaqualand region and the Springbok Flats Basin; uranium production may exceed 1000 t U by the year 2020.

## **1. INTRODUCTION**

There are four major uranium deposits in South Africa, which are the Witwatersrand Basin (quartz-pebble conglomerate-hosted deposit), the Karoo Uranium Province (sandstone-hosted deposit), the Springbok Flats Basin (coal- and carbonaceous shale-hosted deposit) and Namaqualand surficial deposit (Fig. 1). The Witwatersrand Basin is located in the central parts of South Africa, and extends into Gauteng, Mpumalanga, North West and Free State provinces with an area of more than 30 000 km<sup>2</sup>. The Karoo Uranium Province is located in the south-western part of South Africa, while the Springbok Flats Basin is located in the northern part of South Africa. The Namaqualand surficial deposit is located in the north-western part of South Africa.

Uranium has been produced in South Africa since 1952. The highest uranium production in the country was attained in the early 1980s where uranium production exceeded 6 000 tonnes of uranium. Since then, uranium production has steadily declined and reached 531 tonnes of uranium in 2013. It is envisaged that uranium production will increase in the near future. The South African government approved the Integrated Resources Plan 2010 that will enable the increase in nuclear energy capacity from the current 1.8 GWe to 9.6 GWe by the year 2030. The current nuclear energy capacity requires about 294 tonnes of uranium per annum (tUpa), and the expected expansion will require a total of 1536 tUpa. The government remains committed to nuclear energy capacity expansion, even though there are delays in the expansion progress. In addition, the global nuclear energy capacity is envisaged to expand significantly due to countries like China, Russia and India committing to nuclear energy expansion. It is on this backdrop that it is expected that uranium demand will increase in the future, and hence have a positive effect in the uranium prices which will bring the deposits currently being investigated into production.

## **2. URANIUM DEPOSITS**

There are eight known uranium deposits in South Africa, which are: quartz-pebble conglomerate, sandstone, coal, carbonaceous shale, surficial, intrusive, granite-related, and phosphorite deposits. However, the major uranium deposits, which contribute to the nation's resource inventory, are quartz-pebble conglomerate, sandstone, coal, carbonaceous shale, and surficial deposits (Fig. 1 modified from [1]).

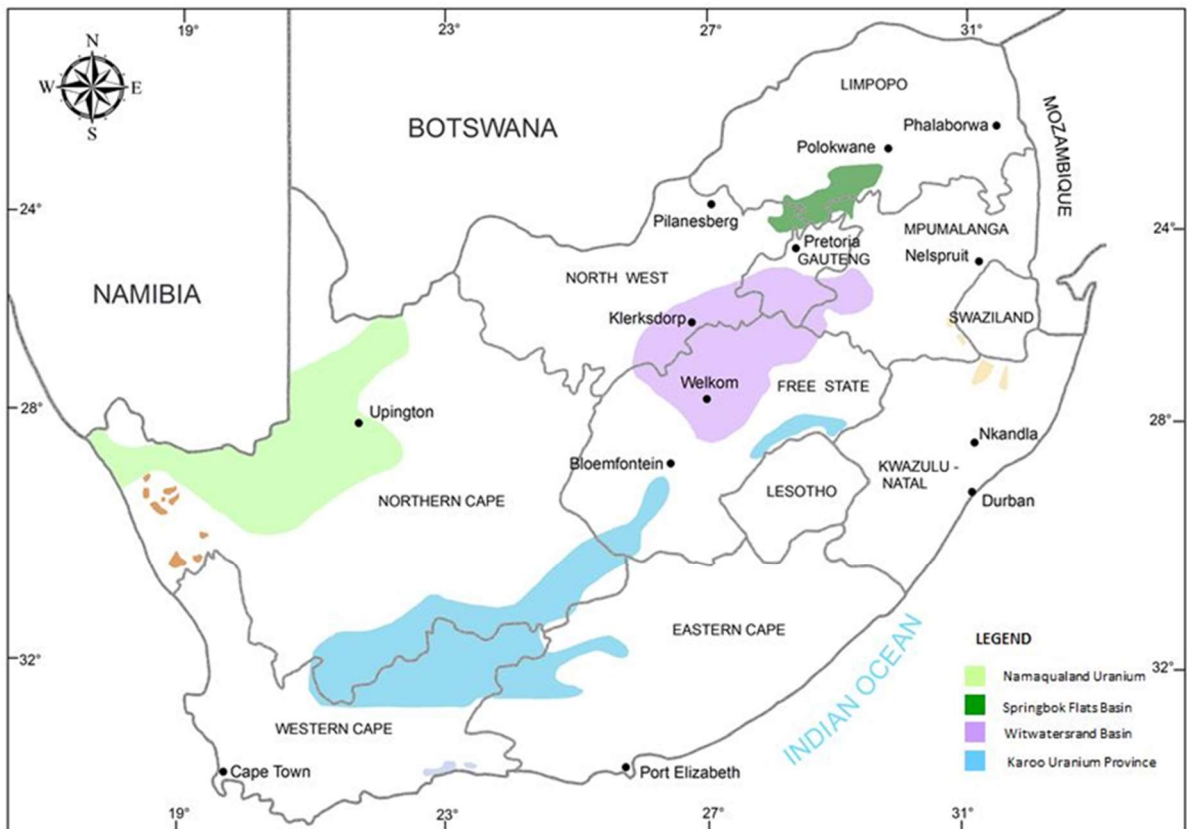


FIG 1. Map showing major uranium deposits in South Africa (Modified from [1]).

The Witwatersrand Basin consists of the economically important Witwatersrand Supergroup and the Dominion Group. The Dominion Group is disconformably overlain by the Witwatersrand Supergroup, and consists of a basal sedimentary horizon which contains two important uranium-bearing quartz-pebble conglomerates known as the Upper and the Lower Reefs. These basal sedimentary sequences represent the earliest sedimentation in the region of about 2800 Ma [2].

The Witwatersrand Supergroup is stratigraphically divided into Central Rand Group and West Rand Group. Economically, the Central Rand Group is the most important in terms of both gold and uranium resources. The Witwatersrand Basin represents a fluvial fan, or a fan delta, composed of many cycles of sedimentation. Uranium mineralization occurs in, or adjacent to, bands of quartz-pebble conglomerate which are preferentially developed at, or near, the base of each cycle of sedimentation where it is frequently associated with carbon of biogenic origin [1]. Rich concentrations of gold, uraninite and other detrital heavy minerals are associated with kerogen, particularly on major scour surfaces. The kerogen is believed to be syngenetic and derived from prokaryotic microbial mats. The only primary uranium mineral is uraninite, which is found to be extremely well sorted. Other uranium minerals include coffinite, and minor amounts of authigenic brannerite [1–3].

The Springbok Flat Basin hosts both the coal-hosted uranium deposit as well as the carbonaceous shale-hosted uranium deposit. The Springbok Flats Basin is fault-bounded graben, and trends northeast-southwest for about 190 km. According to [1], uranium is concentrated in coal and carbonaceous shale in the upper part of the ‘Coal Zone’ over a vertical interval of 1 m, within which there is a 0.1 m thick enriched zone. The uranium is disseminated in the coal and carbonaceous shale, with uranium phases having grain sizes of less than 20 microns. It is suggested that the uranium carriers were coffinite, oyamalite, auerlite, and solid solutions between coffinite and xenotime. A high proportion of uranium is probably held in organo-metallic compounds. The uranium in the basin is thought to have originated

from granites of the Bushveld Complex and surround and underlie much of the Springbok Flats basin. Highest concentrations of uranium occur in the vicinity of granitic palaeoridges and beneath coarse-grained, pebbly sandstones of the Late Triassic Molteno Formation, where it discordantly overlies the ‘Coal Zone’. Since uranium is confined to the uppermost part of the ‘Coal Zone’, it probably formed epigenetically from oxidized ore fluids that migrated from both the granitic palaeoridges and adjacent hinterland, as well as from Molteno Formation sediments, which contained abundant granitic detritus.

Uranium in the main Karoo Basin (Karoo Uranium Province) occurs in the sandstones of the Beaufort Group (Upper Carboniferous to Jurassic) and specifically within the Adelaide Subgroup (lower Beaufort Group) in the south-western parts of the Karoo Basin. The Karoo Uranium Province includes a small satellite area located to the north of Lesotho, in central parts of South Africa. Adelaide Subgroup consists mainly of sandstone and mudstone, and to a minor extent mudstone-pebble conglomerate. The Beaufort Group sediments were deposited on a vast alluvial plain, in which abundant mudrock represents floodplain and lacustrine deposits whilst the sandstone packages represent fluvial channel deposits. The majority of uranium-bearing sandstones are fine-grained in the main Karoo Uranium Province, and coarse-grained in the small satellite area in the north of the Karoo Uranium Province. There are two types of sandstones that host uranium mineralization in the Karoo Uranium Province as proposed by reference [4] these are laminated sandstone and carbonate-cemented sandstone. The uranium mineralization in the laminated sandstones occurs in the basal parts of the sandstone body and contains high values of both uranium and molybdenum. The uranium ore body in the laminated sandstones is generally tabular in shape. Uranium mineralization in the carbonate-cemented sandstones occurs at both the basal parts and elevated parts of the sandstone body, with uranium mineralization hosted by pods and lenses of fine-grained sandstone cemented by carbonate. In both the laminated sandstone and carbonate-cemented sandstone, uranium mineralization is restricted within areas that have presence of carbonaceous materials. The primary uranium minerals are coffinite and uraninite as well as secondary uranium minerals (uranophane, beta-uranophane, and carnotite) formed by recent oxidation.

According to [1], surficial deposits in the Namaqualand region can be subdivided into four types; lacustrine, fluvial, pedogenic and ferruginous mudrock. Currently, the most economically important surficial uranium deposit is the lacustrine type of the Henkries deposit. According to [5], lacustrine deposits in the Namaqualand region occur over pans in which the pans have either a purely internal drainage character with only an inlet, or are situated within drainages having both the inlets and outlets. Pan sediments in the Namaqualand region consists of salt, gypsiferous clay, massive gypsum, clay, sand and diatomaceous earth. The principal uranium mineral in these deposits is carnotite. However, other uranium minerals occur in minor amounts such as uraninite and urano-organic complexes. Fluvial deposits are located within sediments filling ancient valleys, with cementing material being dominated by calcite. Carnotite is the only identified uranium mineral in the fluvial deposit and is normally associated with calcrete or gypcrete cement [6]. The Tertiary to Recent surficial sediments of the Namaqualand region, filling palaeo-drainage channels, is mainly confined to the river courses with the main ones being the Koa and Sout. The valley-fill material was deposited under much lower gradients, especially on the Bushmanland Plateau, and the thicknesses are, consequently, of the order of only a few metres. Towards the Orange River, however, the sediments attain thicknesses in excess of 300 m. In the Koa River valley, the sediments tend to be upward-fining, having boulders and gravels near the base and well-sorted Aeolian sand higher in the sequence, some of which were probably reworked by fluvial action [5]. According to [5], the warping along the Griqualand-Transvaal axis has caused reduction in gradients, and in some areas, the gradients have been reduced to zero or even reversed causing ponding and the formation of pans. A typical example in this context of uranium distribution is Geelyloer. Cross-cutting dunes have formed, for example, at Dirkskop and Kamasoas in the Koa River valley. Humid climatic conditions, associated with increased Pleistocene glaciation, caused the formation of perennial lakes. Organic matter which accumulated in those lakes has been preserved as black organic-rich clays, peats, and diatomaceous deposits, for example the occurrences at Henkries and Kannikwa [7].

### 3. EXPLORATION

Exploration for uranium in the Witwatersrand Basin started in 1944. Currently, near-mine exploration in the Witwatersrand Basin is conducted primarily for gold, to increase the life of the operating mines within the basin. Drilling has been ongoing in the extensions of the Great Noligwa mining lease to determine the extent of remnant blocks of the Vaal Reef. Exploration targets have also been identified within the Kopanang mining lease and adjacent areas. On-going exploration and resource development work in the Cooke operations has highlighted numerous potential uranium resource extensions.

Uranium was discovered in the Karoo sandstones during oil exploration in 1967 by Southern Oil Exploration Corporation. Since 2005, more than 630 000 m of drilling has been completed and geophysically logged and additional 15 000 m of historic boreholes are available. The shallow nature of the mineralization and resources are potentially amenable to open pit mining. It has been proposed that alkaline leaching will be used for processing of ore, and production may start in 2016 [8].

Uranium was discovered in the Springbok Flats Basin in 1976 during exploration for coal in the basin. A pre-feasibility study was completed in 2012 in the Settlers area, and a bankable feasibility study is currently on-going.

The surficial deposits in the Namaqualand region were discovered in 1975 as a result of airborne radiometric surveys. Exploration began again in 2008, of which drilling was conducted and uranium re-evaluation was done with most of mineralization occurring within 20 m from the surface [9].

### 4. GEOPHYSICAL EXPLORATION

Regional geophysical data is available for the Springbok Flats (Figs 2 and 3). The data shows a number of regional structures related to faulting resulting in uranium mineralization being deeper or shallow in response. Mineralization is too deep to be detected by airborne radiometric total counts but, however, the total counts image clearly shows the outline of the basin owing to the contrasting Bushveld Lebowa Granite Suite surrounding the basin. The granites are believed to be the source of uranium in the coals and shales. The Department of Science and Technology of South Africa has provided funds to carry out downhole geophysics in the basin through partnership with exploration and mining industries that can offer access to boreholes data. Currently, there are on-going studies aimed at generating a three-dimensional geophysical model of the Springbok Flats Basin.

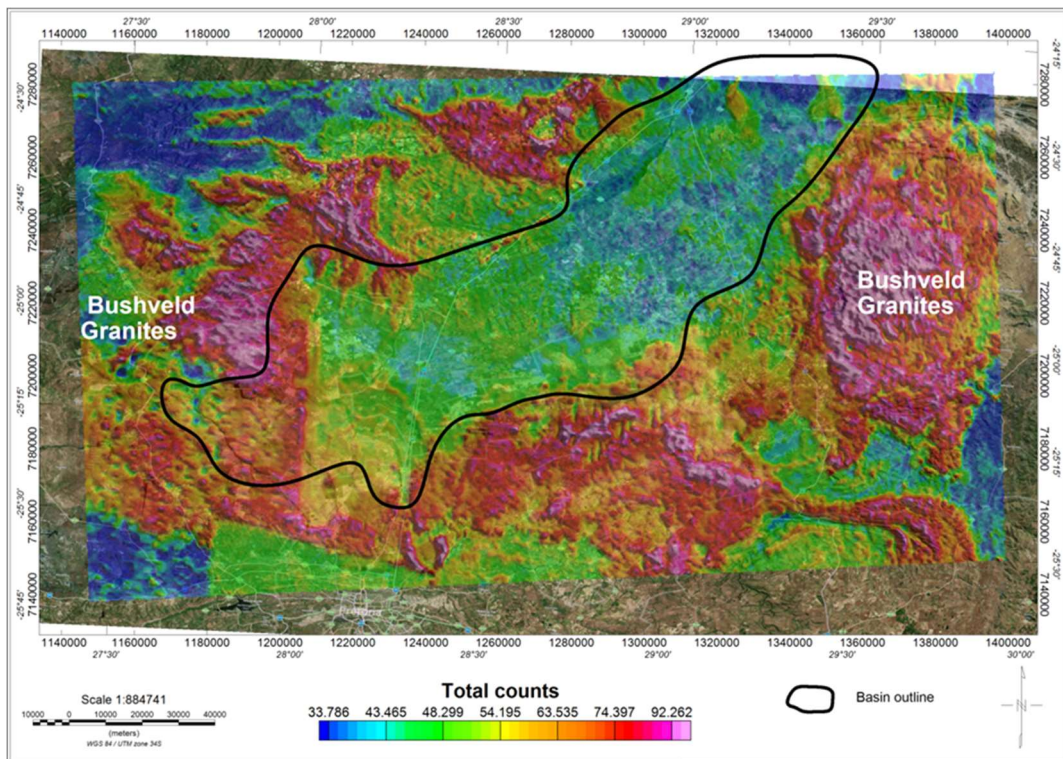


*FIG 2. Regional radiometric map showing the locality of the Springbok Flats Basin and interpreted structures [10]<sup>32</sup>.*

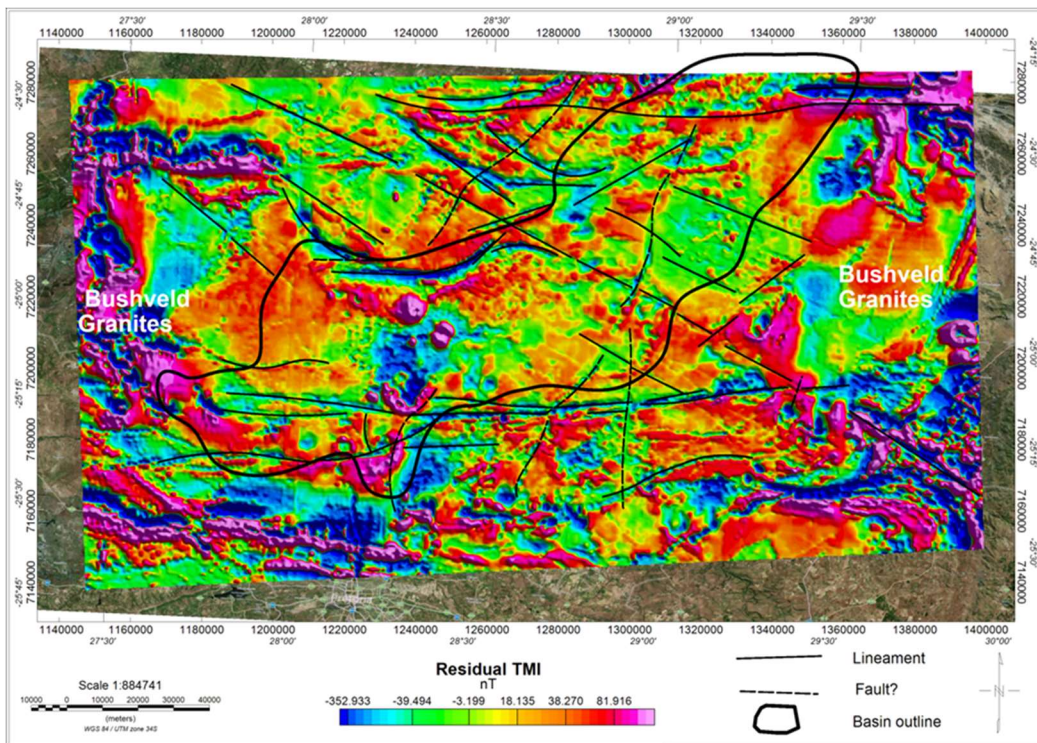


*FIG 3. Regional magnetic map showing the locality of the Springbok Flats Basin and interpreted structures [10].*

<sup>32</sup> Figs 2–7 are copyright to Council for Geoscience, Petoria, South Africa, and are reproduced here with permission.

In Namaqualand, a high resolution airborne magnetic and radiometric survey was recently completed at 200 m line spacing and 80 m altitude over a selected block (Figs 4 and 5) covering approximately 300 000-line km. These new data will be used for the generation of new mineral targets including uranium.

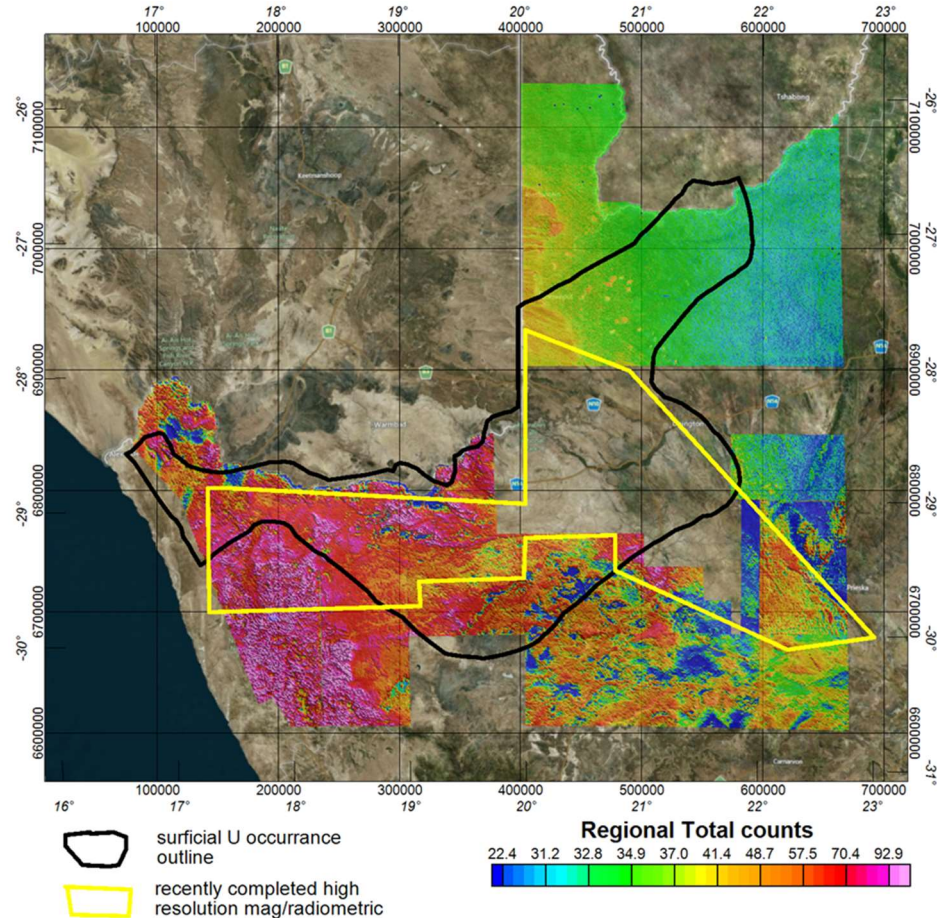


*FIG 4. Illustration of the recently flown high resolution radiometrics block (yellow) overlain on existing regional radiometric data map [10].*

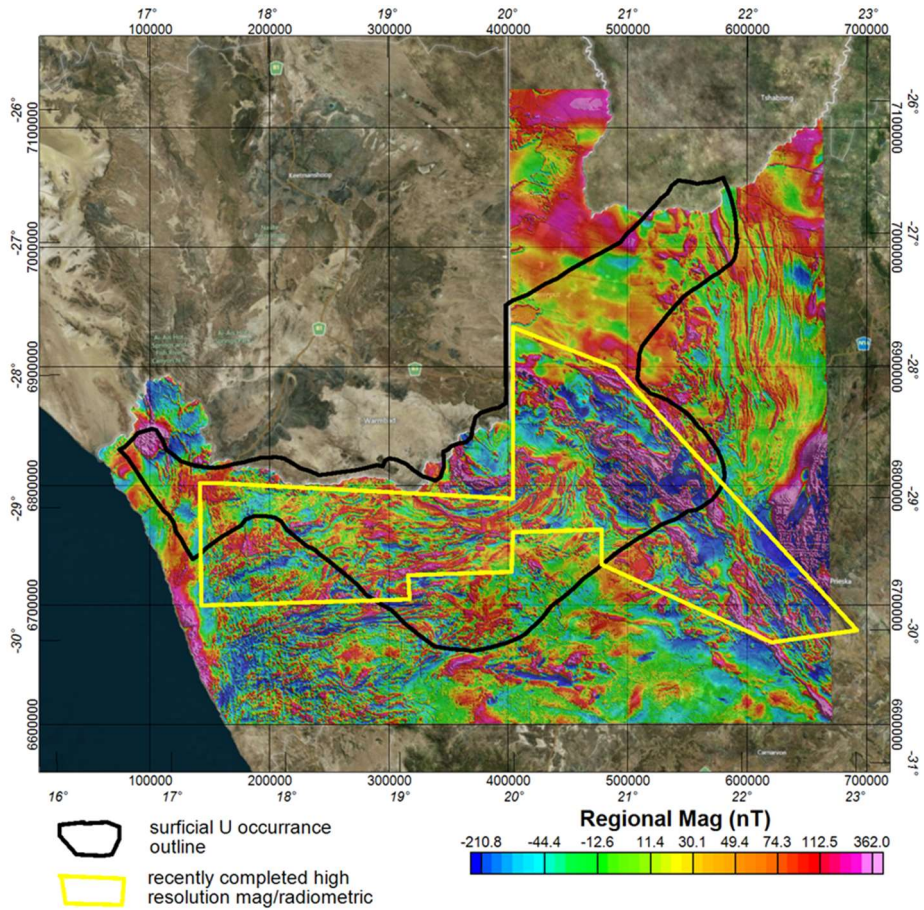


*FIG 5. Illustration of the recently flown high resolution magnetics block (yellow) overlain on existing regional magnetic data map [10].*

## 5. RESOURCES

The total contained in-situ uranium resources in South Africa is about 679 310 t U<sub>3</sub>O<sub>8</sub> (which is equivalent to about 1820 million troy pounds (Mlb) U<sub>3</sub>O<sub>8</sub> or 576 055 tU) as summarized in Table I. The largest proportion of South Africa's identified in-situ uranium resources (about 84%) are hosted by the quartz-pebble conglomerate of the Witwatersrand Basin and their associated tailings. About 12% of the nation's in-situ resources are hosted by coal and carbonaceous shale of the Springbok Flats Basin, 4% in the sandstones of the Karoo Uranium Province, and less than 1% in the Namaqualand surficial deposits (Fig. 6).

TABLE I. IN-SITU CONTAINED URANIUM RESOURCES IN SOUTH AFRICA

| Deposit  | Measured resources                              |  | Indicated resources                          |  | Inferred resources                           |  | Total resources per deposit                  |  |
|--|---|--|--|--|--|--|--|--|
|  | Metric tonnes,<br>$\text{U}_3\text{O}_8$<br>(U) | Million troy pounds,<br>$\text{U}_3\text{O}_8$ | Metric tonnes,<br>$\text{U}_3\text{O}_8$ (U) | Million troy pounds,<br>$\text{U}_3\text{O}_8$ | Metric tonnes,<br>$\text{U}_3\text{O}_8$ (U) | Million troy pounds,<br>$\text{U}_3\text{O}_8$ | Metric tonnes,<br>$\text{U}_3\text{O}_8$ (U) | Million troy pounds,<br>$\text{U}_3\text{O}_8$ |
| Witwatersrand Basin (palaeo-quartz pebble conglomerate)            | 47 523<br>(40 300)                              | 127  | 219 607<br>(186 227)                         | 588  | 300 855<br>(255 125)                         | 806  | 567 985<br>(481 651)                         | 1 521  |
| Karoo Uranium Province (sandstone)                                 | 0 (0)   | 0  | 9 936<br>(8 426)                             | 27   | 15 881<br>(13 467)                           | 43   | 25 817<br>(21 893)                           | 69   |
| Springbok Flat Basin (carbonaceous shale and coal)                 | 0 (0)   | 0  | 0 (0)  | 0  | 83 462<br>(70 776)                           | 224  | 83 462<br>(70 776)                           | 224  |
| Namaqualand Surficial Deposit (clay, diatomaceous earth, calcrete) | 415<br>(352)                                    | 1  | 937<br>(795)                                 | 3  | 694<br>(589)                                 | 2  | 2 046<br>(1 735)                             | 6  |
| Total resources  | 47 938<br>(40 651)                              | 128  | 230 480<br>(195 447)                         | 617  | 400 892<br>(339 956)                         | 1 074  | 679 310<br>(576 055)                         | 1 820  |

\*Totals tonnages may differ from sum of the individual deposits' tonnages due to rounding.

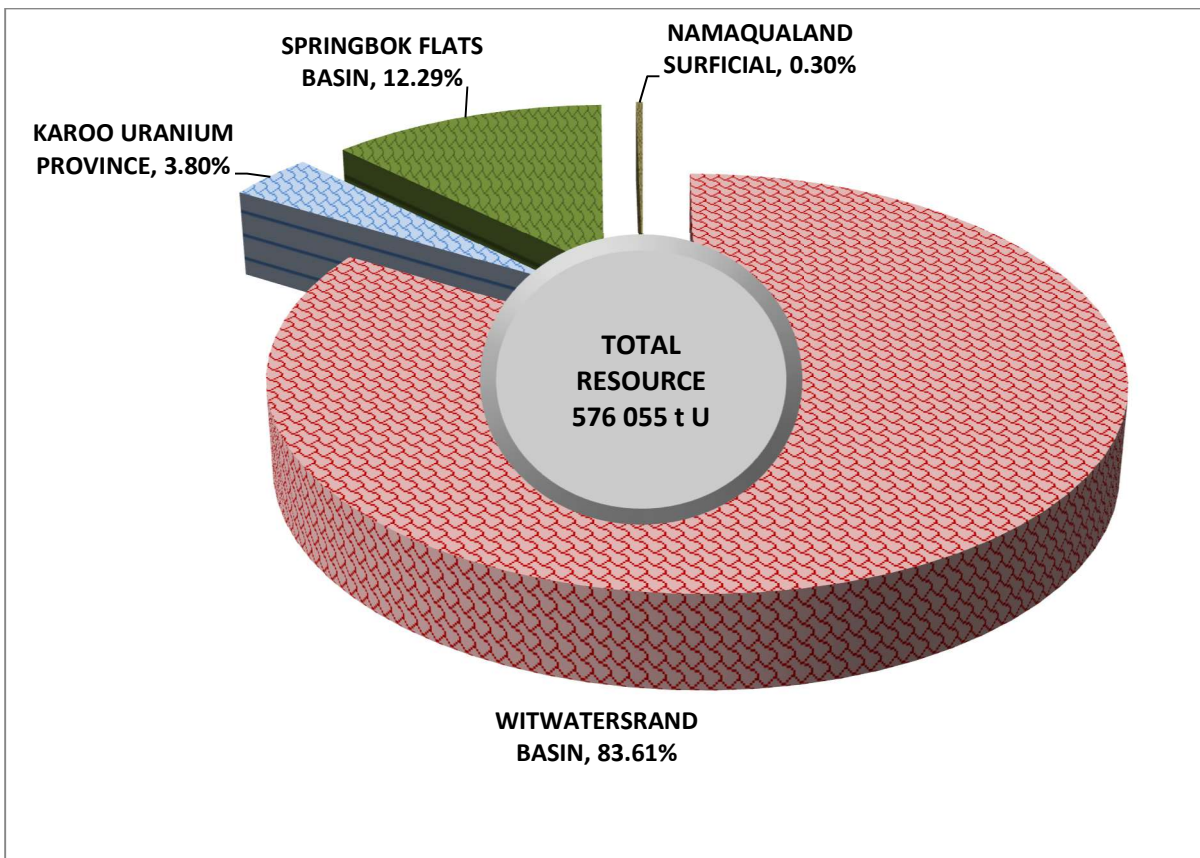


FIG 6. Proportions of South Africa's uranium resources in the major deposits.

## 6. PRODUCTION

The majority of South Africa's uranium production (Fig. 7) has, historically, come from the Witwatersrand Basin as by-product of gold, with less significant uranium quantities coming from the Palabora carbonatite deposit as by-product of copper. Uranium production from Palabora carbonatite ceased in 2001.

Uranium in the Witwatersrand Basin is currently produced in the Vaal River (near the town of Orkney) and Cooke operations (near the town of Carletonville). In the Vaal River operations, the reef materials from Moab Khotsong, Great Noligwa and Kopanang are processed in the Noligwa gold plant/South Uranium plant circuit [11]. The ore materials from the Cooke operations are treated at Cooke 4 (formerly known as Ezulwini) gold and uranium plants. A conventional acid leaching, ion exchange, solvent extraction and ammonium diuranate precipitation process is followed. The ore is treated in the uranium plant before being passed to the gold plant. This so-called 'reverse leaching' process enables better gold recoveries. The ammonium diuranate slurry is shipped to Nuclear Fuels Corporation of South Africa (NUFCOR) in tankers where it is calcined to uranium oxide ( $\text{U}_3\text{O}_8$ ) and sold on the international market. In 2013, uranium production increased by 14% to 531 tU compared to 2012, due to improvements of mine-call factor and decrease of safety-related stoppages.

It was expected that by the end of 2014 uranium processing at Mine Waste Solution (MWS), located in Stilfontein (which is about 16 km east of Klerksdorp), will begin. Other uranium supply potentials in the Witwatersrand Basin include the Dominion Reef mine (currently stopped uranium production), mines in the Free State Goldfield, as well as tailings facilities scattered throughout the Witwatersrand Basin. In addition, the deposits in the Karoo Uranium Province, Springbok Flats Basin, and Namaqualand surficial deposits represent future potential uranium suppliers. Therefore, uranium production in South Africa is expected to increase in the future, if uranium price becomes favourable to

producers. Currently, it is expected that uranium production will increase to 700 tU for the year 2015 due to start of production from the Cooke operations, and expected production at MWS.

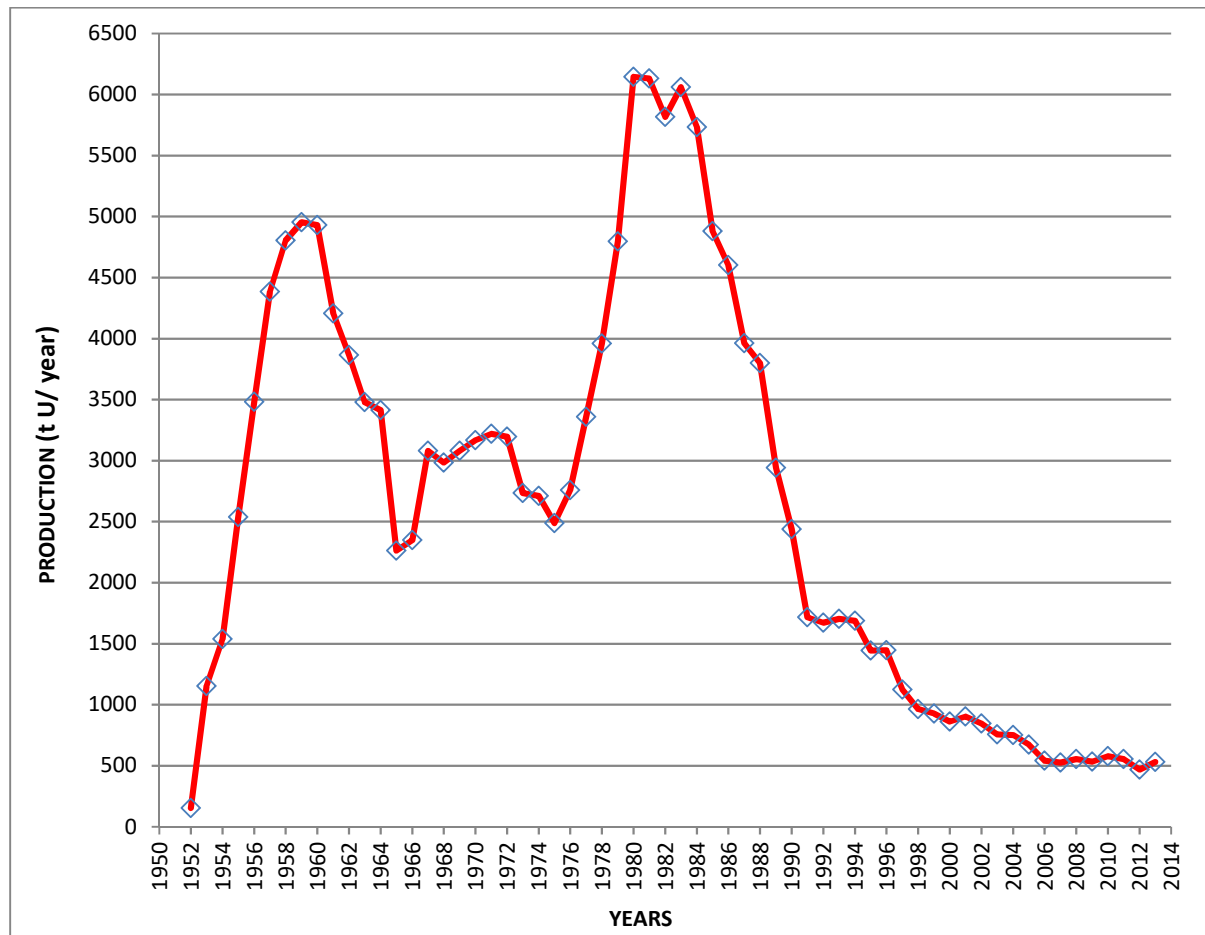


FIG 7. Graph showing historical production of uranium in South Africa.

## 7. CONCLUSION

South Africa's uranium production is forecast to rise to 700 tonnes per year by the end of 2015, due to expected increase in the production from the Witwatersrand Basin as production begins in the Cooke operations and also other mining companies seeking to re-mine the tailings which contain considerable amounts of low-grade uranium.

Karoo Uranium Province, Springbok Flats Basin, and Henkries deposits are expected to start production before the year 2020, which would increase South Africa's uranium output to over 1000 tU.

## ACKNOWLEDGEMENTS

The authors gratefully acknowledge the following organisations and companies for providing data and information: the Council for Geoscience, the Department of Mineral Resources, AngloGold Ashanti Limited, Peninsula Energy Limited, Harmony Gold Limited, HolGoun Uranium and Power Limited, Gold One International Limited, Sibanye Gold Limited, and Witwatersrand Consolidated Gold Resources Limited.

## REFERENCES

- [1] COLE, D.I. "Uranium", The mineral resources of South Africa (WILSON, M.G.C., ANHAEUSSER, C.R., Eds), Sixth edition, Council for Geoscience, Pretoria, South Africa (1998) 642–658.
- [2] MCCARTHY, T.S., "The Witwatersrand Supergroup", The Geology of South Africa (JOHNSON, M.R., ANHAEUSSER, C.R., THOMAS, R.J., Eds), Geological Society of South Africa, Johannesburg/Council for Geoscience, Pretoria (2006) 155–186.
- [3] ROB, L.J., ROB, V.M., "Gold in the Witwatersrand Basin", The Mineral Resources of South Africa (WILSON, M.G.C., ANHAEUSSER, C.R., Eds), Sixth edition, Council for Geoscience, Pretoria, South Africa (1998) 294–349.
- [4] COLE, D.I., WIPPLINGER, P.E., Sedimentology and molybdenum potential of the Beaufort in the main Karoo Basin, South Africa. Memoir, Council for Geoscience (South Africa) **80** (2001).
- [5] HAMBLETON-JONES, B.B., LEVIN, M., WAGENER, G.F., "Uraniferous surficial deposits in Southern Africa", Mineral Deposits of Southern Africa, II (ANHAEUSSER, C.R., MASKE, S., Eds), Geological Society of South Africa, Johannesburg (1986) 2269–2287.
- [6] CARLISLE, D., Possible variations on the calcrete-gypcrete uranium model. U.S. Dept. Energy, GJBX-53 (80) Grand Junction, CO (1980).
- [7] LEVIN, M., 1978. Uranium occurrences in the Gordonia and Kuruman Districts, PER-37, Atomic Energy Board, South Africa, Pelindaba (1978).
- [8] PENINSULA ENERGY, Annual Report 2013 (Accessed 5/5/2014), <http://www.pel.net.au>.
- [9] Xtract Resources., 2013 Investor Presentation (Accessed 20/1/2014), <http://www.xtractresources.com/presentations.htm>.
- [10] COUNCIL FOR GEOSCIENCE (South Africa) geophysics data archives, 2014.
- [11] ANGLOGOLD ASHANTI, Annual Report 2013 (Accessed 20/5/2014), <http://www.anglogold.co.za>.

# **GEOCHEMICAL MODEL ON URANIUM MINERALIZATIONS IN THE RHYOLITE-GRANITE COMPLEX IN THE JABAL EGHEI AREA, LIBYA**

J. KOVAČEVIĆ

Geological Survey of Serbia,

M. B. RADENKOVIĆ

University of Belgrade,

Vinca Institute of Nuclear Sciences,

Š.S. MILJANIĆ

University of Belgrade,

Faculty of Physical Chemistry,

Belgrade, Serbia

M. B. TEREESH, S. TURKI

Tajoura Nuclear Research Centre,

Tripoli, Libya

## **Abstract**

The geological investigations of the Tibesti Massif and its surroundings undertaken by the Industrial Research Center of Libya, commissioned detailed geologic maps of rhyolite-granitoide rocks in the Jabal Eghei area. The radiological survey of the terrain, followed by gamma-spectrometry and ICP-MS analysis, resulted with discovery of two significant uranium mineralizations located in the central area of about 60 square kilometres. Uranium concentrations in these mineralizations were found to range from approximately  $50 \text{ mg kg}^{-1}$  to more than  $600 \text{ mg kg}^{-1}$ . Additional geochemical analysis has shown that these mineralizations are accompanied by increased contents of silver, arsenic, molybdenum, mercury and lead. Here is presented a simplified generic model for uranium mineralization in the Jabal Eghei region. Uranium was mobilized from main primary sources mostly through cold solutions and deposited in contact zones with rhyolites. Uranium mineralization is spatially and genetically related to the volcanic complexes and the spatial position of the postorogen magmatism, which is the lithologic control factor of the mineralization position. The main ore material was pitchblende, although the presence of uranite, coffinite and uranium titanite could not be excluded. A full explanation of the genesis of these mineralizations could be obtained after detailed geological investigations.

## **1. INTRODUCTION**

During geological mapping in the Jabal-Eghei Kangara Massif, Libya, enhanced levels of naturally occurring radioactivity were detected. [1]. More detailed studies on composition, geological structure, magmatism, mineralization control factors, geochemical and geophysical characteristics [2, 3] as well as radiological and radiation spectrometry analysis done within this research [4] have revealed the enhanced radioactivity originates in rhyolite-granitoide rocks with two significant uranium anomalies. The investigated area is located in the south-eastern Libya and is part of the Tibesti Mountains, the largest massif in the Sahara. Situated at altitudes between 720 m and 1120 m, the area is, in morphological sense a rocky desert, composed of granitoid rocks mostly flattened by eolian erosion, with prominent ridges of quartzite, gneiss or scarn. In its central part the main feature is a rhyolite mass shown in Figure 1.



*FIG. 1. The rhyolite-granite rocks in the Jabal Eghei area, Libya.*

Two significant uranium mineralizations were identified in rhyolites and a few at the edges, cutting through granite rocks. Mineralization in the central area is mostly hosted by silifited rhyolites and the others, near the granite-rhyolite contact zone, characterized by the presence of the silicified breccia rocks [4].

## 2. MATERIALS AND METHODS

A radiometric survey was conducted on the entire massif area of about 60 km<sup>2</sup> over granitoid rocks, using either a GR-110 scintillation counter or a GR-130 mini-spec portable gamma spectrometer (NaI detector), both by Exploranium, Canada. A total of 110 samples of different geological composition were collected and subjected to laboratory analysis. After the secular radioactive equilibrium has been reached in ground, sieved and homogenized samples, standard gamma spectrometry method was performed using Canberra HPGe gamma spectrometry system, with relative efficiency of 23% and a resolution of 1.8 keV at 1332.5 keV <sup>60</sup>Co line. Calibration was done using CSR soil material spiked with <sup>22</sup>Na, <sup>57</sup>Co, <sup>60</sup>Co, <sup>89</sup>Y, <sup>133</sup>Ba and <sup>137</sup>Cs (MIX-OMH-SZ, National Office of Measures, Budapest) in the Marinelli beaker geometry. Besides gamma spectrometry, ICP MS analysis had been done for about 40 elements contents and non-destructive ED XRF analysis for total concentrations determination. Geochemical analysis was combined with microscopic observation of geological preparation for more details on the geological structures and associations present in investigated area.

## 3. RESULTS AND DISCUSSION

Sample analyses have shown high uranium contents in the rhyolites. Concentrations values determined by ICP-MS technique ranged from 50 mg kg<sup>-1</sup> to more than 600 mg kg<sup>-1</sup> as discussed in [5]. Specific activities of <sup>238</sup>U obtained by gamma spectrometry were in the range of 82 to 7477 Bq kg<sup>-1</sup>, with lowest values characteristic for silified rhyolite. Activity concentrations of the main terrestrial radioisotopes ranged from 22 to 5256 Bq kg<sup>-1</sup> for <sup>226</sup>Ra, from 11 to 221 Bq kg<sup>-1</sup> for <sup>232</sup>Th and from 132.0 to 2304 Bq kg<sup>-1</sup> for <sup>40</sup>K.[6]. Thorium concentrations of 30–70 ppm detected near to the granitoid-rhyolite zone may not be considered as significant. Chemical analysis indicated uranium mineralizations to be accompanied with high contents of other elements such as silver, arsenic, molybdenum, mercury and lead.

The formation of uranium mineralizations is directly related to its geochemical properties and behavior in different geological media and they are spatially and genetically connected to the granitoid rocks cut through by rhyolites. In the initial phase uranium was probably bonded mostly to petrogenetic minerals

of granitoids (feldspar and biotite). Although with low concentration, the total amount of uranium was large. Besides uranium traces in petrogenetic minerals of magmatic rocks, it may appear also as independent minerals or cationic substitutes in the accessory minerals of granitoid complexes and vulconites. It may be supposed that complexes of uranyl-ion with  $\text{KAsO}_4^{2-}$  and  $\text{SiO}_3^{2-}$  were formed in water at pH between 4 and 7.5. In presence of  $\text{Na}^+$ ,  $\text{K}^+$ ,  $\text{Ca}^{2+}$ ,  $\text{Mg}^{2+}$  and  $\text{Fe}^{2+}$ , the solubility of such complexes decreased leading to formation of more favorable conditions for uranium mineralization. Some of formed minerals were insoluble (such as compounds with  $\text{PO}_4^{3-}$ ,  $\text{AsO}_4^{3-}$  and  $\text{SiO}_2$ ), thus they appear accompanied with uranium at a location, while others were easily released into solution [7].

Based on the geological and structural characteristics of the area, locations of uranium mineralizations and results of the geochemical analyses, it could be concluded that a hydrothermal stage occurred in their formation. The main primary sources of uranium mineralization are granitoids. Uranium is mobilized from petrogenetic minerals of granitoids (feldspar and biotite) mostly through cold solutions and deposited in favorable environment such as contact zones with rhyolites, fault structures filled with clay, ferrous oxides and other minerals [8]. Typical rhyolite rock with flow streams found in the investigated area is shown in Figure 2. During the phase of magma differentiation, uranium concentration in feldspar was low but in micas (biotite basically) it could be a few times than in magmatic rocks. The chemical stability of uranium compounds is highly dependent on pH and Eh values, temperature and the nature of ore-bearing fluids. Under certain conditions, 40% of total uranium could be mobilized. Regarding the genesis of the uranium deposits, connection between mineralization and tecto-magmatic (tecto-volcanic) structures, or more specifically, effusive, volcanic and sub-volcanic structures could be assumed and the possibility of volcanic uranium mineralization should not be excluded as it is spatially and genetically related to the volcanic complexes (rhyolites).



*FIG. 2. Typical rhyolite rock with flow streams [4] (reproduced with permission).*

The spatial position of the postorogen magmatism, which is at the same time lithologic control factor for mineralization position, is controlled by the location of deep fault zone cross sections. The forms of ore bodies depend on the structural and lithologic control factor and here in the first described anomaly, it is probably in the form of pillar (column). The main ore material was pitchblende, although the presence of uraninite, coffinite and uranium titanite could not be excluded. A full explanation of the genesis of these uranium mineralizations could be obtained from detailed geological investigations.

#### ACKNOWLEDGEMENTS

Authors are grateful to Industrial Research Centre and Nuclear Research Centre in Tajoura, the Geological Survey of Serbia, the Vinca Institute of Nuclear Sciences and the Faculty of Physical

Chemistry, University in Belgrade for support and collaboration in this joint research project. It is partly supported by the Ministry of Education and Science of Republic of Serbia within the project No. 43009.

## REFERENCES

- [1] TOLJIĆ, M., KOVAČEVIĆ, J., Geological map of Libya 1:250,000; Sheet Wadi Eghei NF 34-1, in General Report (Mineral raw materials), Industrial Research Center, Tripoli, Libya and the Geological Institute of Serbia, Belgrade (2010).
- [2] EL-MAKHROUF, A.A., Geology, petrology, geochemistry, and geochronology of Eghei (Nugay) batholith alkali rich granites, NE Tibesti, Libya, Doctoral Dissertation, University of North Carolina at Chapel Hill, Chapel Hill, NC (1984).
- [3] EL-MAKHROUF, A.A., Tectonic interpretation of Jabal Eghei area and its regional application to Tibesti orogenic belt, south central Libya (SPLAJ), *J. African Earth Sci (and the Middle East)* **7** 7–8 (1988) 945–967.
- [4] TEREESH, M.B., Radioactivity of the Rhyolite-granitoide rocks in the Jabal Eghi area of Southern Libya, PhD Thesis, Belgrade University, Serbia (2013).
- [5] KOVAČEVIĆ, J., TEREESH, B.M., RADENKOVIĆ, M.B., MILJANIĆ, Š.S., Discovery of uranium mineralizations in the rhyolite–granite complex in the Jabal Eghei area of southern Libya, *J. Serb. Chem. Soc.* **78** 5 (2013) 741–758.
- [6] TEREESH, M.B., RADENKOVIC, M.B., KOVACEVIC, J., MILJANIC, S. S., Terrestrial radioactivity of the Jabal Eghei area in southern Libya and assesment of the associated environmental risks, *J. Radiat. Prot. Dosim.* **153** 4 (2013) 475–484.
- [7] ROMBERGER S.M., Transport and deposition of uranium in hydrothermal systems at temperatures up to 300 °C, in Geological implications, in Uranium geochemistry, minera-logy, geology, exploration and resources, (DE VIVO, B., Ed.), The Institution of Mining and Metallurgy, London, UK (1984) 12–17.
- [8] MOREAU M., L'uranium et les granitoides—essai d'interpretation (in French), in Geology, mining, and extractive processing of uranium, (JONES, M.J., Ed.), The Institution of Mining and Metallurgy, London, UK (1977) 83–102.

# DADAG URANIUM DEPOSIT IN CENTRAL ANATOLIA, TURKEY

I.H. ÜNAL

General Directorate of Mineral Research and Exploration,  
Ankara, Turkey

## Abstract

Production of energy in Turkey is largely provided by natural gas and coal thermal power plants and electricity consumption increases rapidly. There is insufficient domestic reserve to supply all power plant fuel needs, meaning Turkey has to import natural gas and coal, resulting in a foreign trade deficit. The government prefers to use domestic energy resources (uranium, thorium and lignite) to fuel power plants. Nuclear energy is the best choice to close the gap of energy and the foreign trade deficit of Turkey; therefore, Nuclear Power Plants are going to be constructed to close the energy gap. Uranium and thorium reserves were found by General Directorate of Mineral Research and Exploration over the last 40 years, with resources amounting to ~9000 t  $U_3O_8$  [~7600 t U]. In the past, pilot yellow cake production was successfully completed but uranium pellets and fuel bars were not produced. The General Directorate initiated a new exploration program in Central Anatolia, finding the Dadag deposit in 2012 with follow-up in 2013. The grade ranges between 100–900 ppm in the Early Eocene aged Kubaca unit (limestone, sandstone and bituminous shale). Further drilling, detailed geological mapping, 3-D modeling, geophysical investigations and resource calculations continue in 2014.

## 1. BACKGROUND AND INTRODUCTION

Consumption of electricity increases very rapidly in Turkey. Production of energy is largely provided with natural gas and coal thermal power plants. There is not sufficient domestic reserve to supply all fuel needs for power plants. Because of this, Turkey has to import natural gas and coal to produce electricity. This situation contributes to a foreign trade deficit. In addition, the cost of imported fuels increases. The government prefers to use domestic resources, which are uranium, thorium and low grade lignite to supply fuels for power plants. Nuclear energy is seen as the best choice to close gap of energy and the foreign trade deficit of Turkey. Therefore, the first Nuclear Power Plant (NPP) construction has been initiated in Mersin. The other NPPs are planned to be constructed to close the energy gap.

The exploration of radioactive elements in Turkey has been continued for forty years. Almost all of the uranium and thorium reserves were found by General Directorate of Mineral Research and Exploration. Geoscientists discovered approximately 9000 t  $U_3O_8$  [~7600 tU] resources in Turkey. In the past, pilot yellow cake production was successfully completed but there was no production of later-stage products for nuclear energy, such as uranium pellets and fuel bars.

Nowadays exploration of radioactive elements is more important than in the past. As a result, General Directorate of Mineral Research and Exploration prepared a new exploration program in Central Anatolia. After the geological, geophysical and geochemical applications, the Dadag deposit was found in 2012. In the project, approximately 6000 m diamond core drilling, hundreds of surface rock sampling and thousands of surface geophysical anomaly points were completed in 2013. According to geochemistry results of rock samples from cores and trenches, the grade ranges between 100–900 ppm. Core samples were taken with the help of down hole geophysical methods which were gamma ray log and natural gamma ray spectrometry method. Anomalous curves are observed in Early Eocene aged Kubaca unit which consists of limestone, sandstone and bituminous shale. Reserve calculation has been continued for this uranium reserve. Exploration facilities which are 10 000 m diamond core drilling, detailed geological mapping 3-D modeling and geophysical investigations are going to continue in 2014.

## 2. GEOLOGY AND LOCATION OF STUDY AREA

The Dadag (Dadağ) uranium deposit is located in the Central Anatolia area of Turkey [1]. It is 280 km far away from the capital city Ankara (Fig. 1).

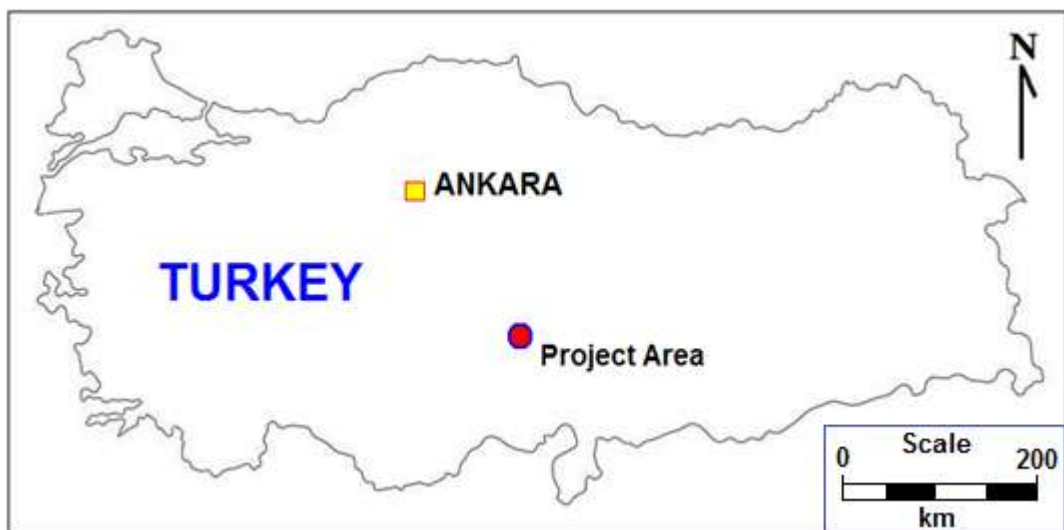


FIG. 1. Location map of project area.

Marble sequences in Tamadağ formation and Kaman Group, which are Palaeozoic aged phyllite, schist and calc-schist, are the oldest geologic units in study area. The Early Lutetian aged Ayhan Formation overlies these. It consists of river, lacustrine and coastal sedimentary rocks which are sandstone, mudstone, siltstone, conglomerate and claystone. The names of geologic units, from older to younger, are Saytepe, Esefin, Kubaca, İlicek and Lalelik. The Oligocene aged Kızılıöz formation overlies the Ayhan formation [2]. It consists of conglomerate, sandstone, siltstone, mudstone and is a braided fluvial deposit. The Yüksekli Formation which overlies it consists of lacustrine environment of Upper-Miocene Pliocene aged (Fig. 2).

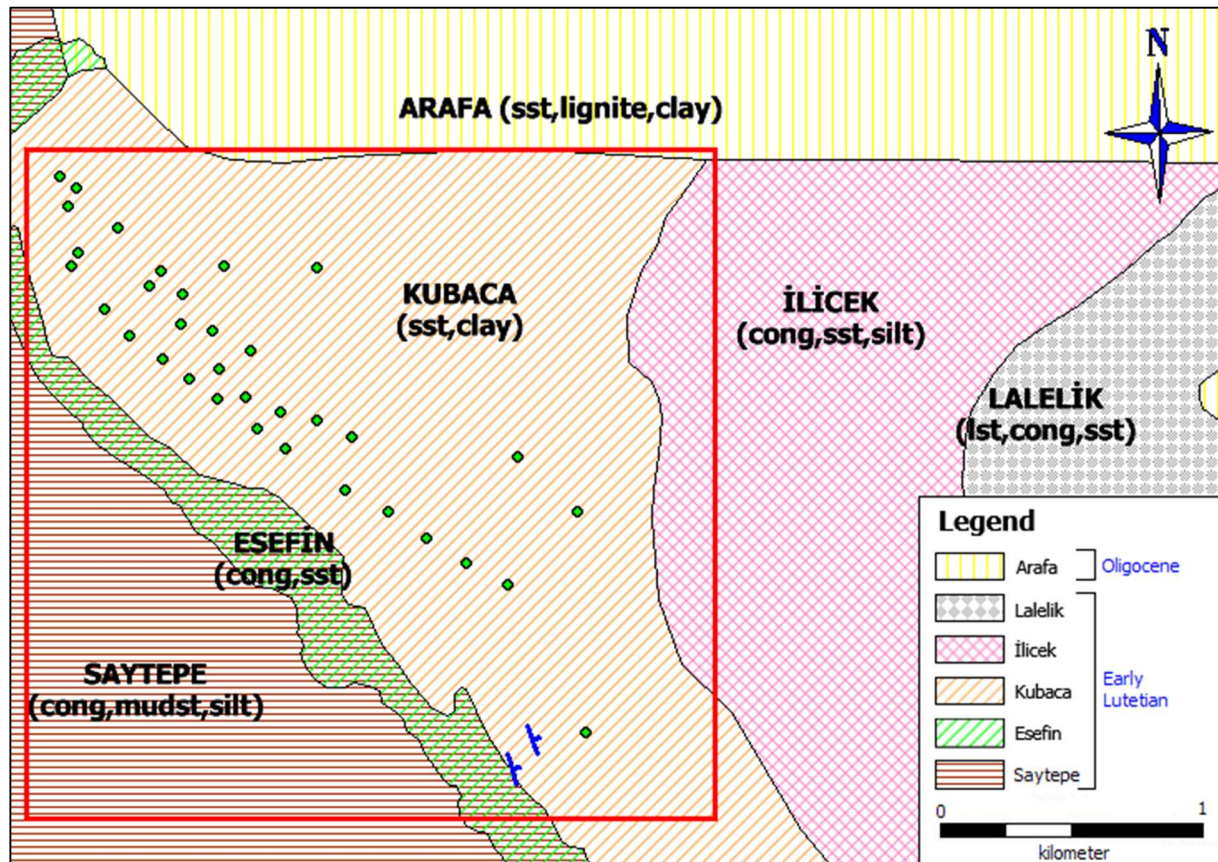


FIG. 2. Geology map of project area (modified from [2]).

### 3. EXPLORATION

Uçakçıoğlu (1987) and Çetintürk (1992) [3, 4] measured radioactive anomalies in this study area. Detailed geological mapping, geochemical sampling and ground-surface geophysical investigations were combined with these old data. After that, geophysical anomalies demonstrates that trend of uranium deposit has a direction towards to NW-SE. Drill hole locations were chosen on this trend. Its dimensions are approximately 2 km long and 600 m wide (Fig. 3).

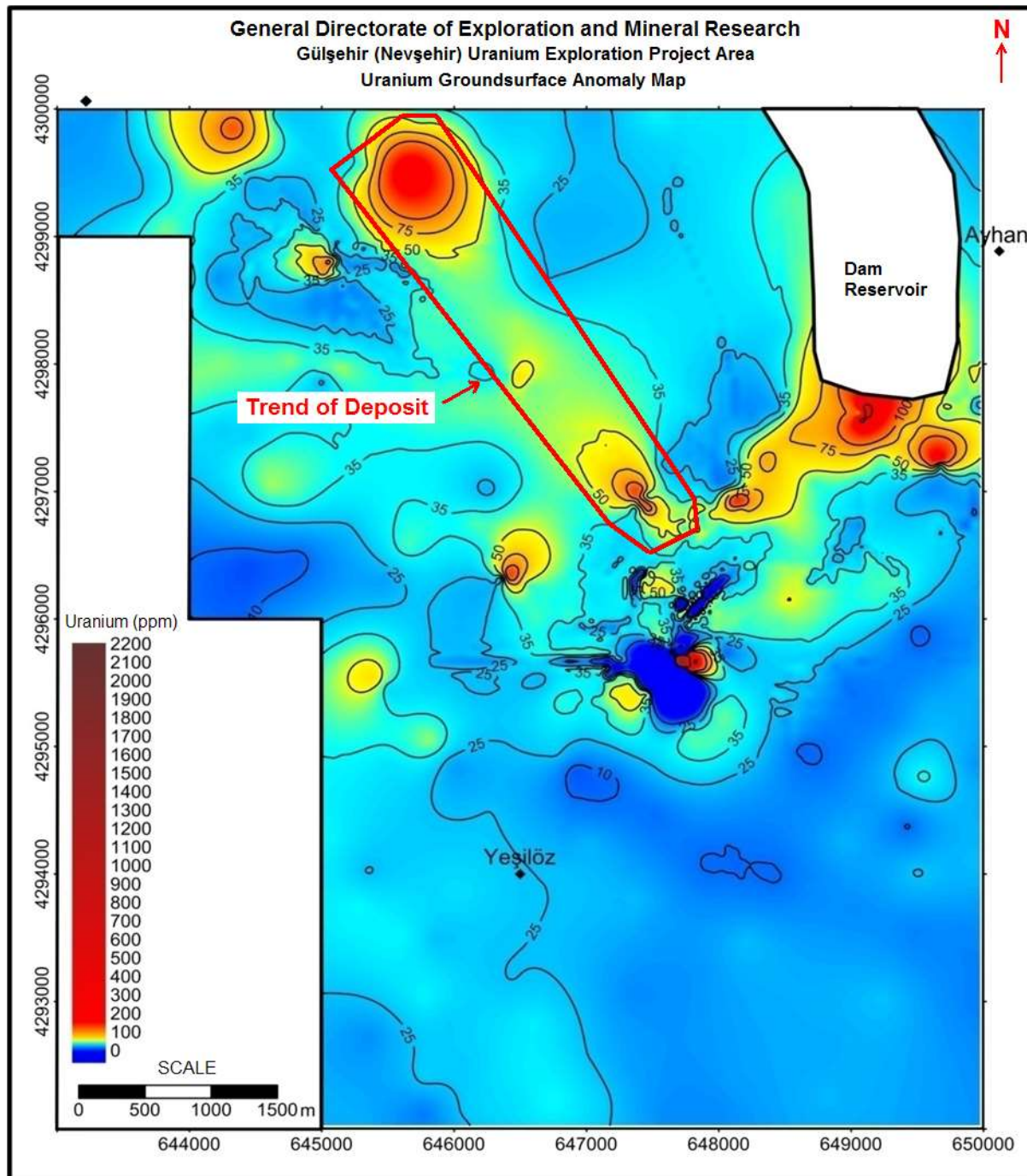


FIG. 3. Uranium ground surface anomaly map (modified from [1]).

In the project area, 34 diamond core drill holes were completed on NW–SE trend with the starting point of Kubaca Hill. Uranium, thorium and potassium anomaly logs were measured with the help of natural and spectral gamma ray downhole geophysical methods. Anomalies were measured in the Kubaca unit, which contains siltstone, sandstone, claystone and mudstone (Fig. 4).



FIG. 4. Core photograph of Kubaca Unit in GD-7 drill hole (photograph by author).

Geochemical, mineralogical and petrological samples were taken from cores and outcrops where the gamma-ray anomalies were measured. ICP-MS, XRD and XRF analysis for uranium and thorium elements were completed [1]. In some drill holes, downhole logs detected 3 different anomalous layers. Uranium enrichment is a possibility for roll-front type mineralization. In addition, a sulphurous gas release area was found. A trench study was completed, uranium mineralization was observed and anomalies measured (Fig. 5).



FIG. 5. Uranium mineralized zone photograph in trench study (photograph by author).

According to ICP–MS tests, the maximum uranium value is 955 ppm and thorium value is 29 ppm. Some significant geochemical results were given in Table I.

TABLE I. SIGNIFICANT GEOCHEMISTRY RESULTS FROM CORE SAMPLES

| Drill hole name | Depth       | Uranium (ppm) | Thorium (ppm) |
|-----------------|-------------|---------------|---------------|
| GD-3            | 89.20–90.00 | 881           | 12            |
| GD-5            | 117.4–117.8 | 566           | 29            |
| GD-7            | 118.2–119.0 | 642           | 12            |
| GD-7            | 119.0–119.8 | 955           | 26            |
| GD-9            | 111.8–112.3 | 789           | 6             |
| GD-13           | 165.8–166.6 | 698           | 5             |
| GD-32           | 130.6–131.2 | 636           | 8             |
| GD-32           | 135.4–135.9 | 553           | 8             |
| GD-33           | 137.1–138.1 | 667           | 18            |
| GD-38           | 144.9–145.6 | 563           | 6             |

Distances between drill hole locations are approximately 60 m. To calculated prereserve of deposit parameters were defined. Affected area was selected as the area of circle which has 60 m radius ( $2826 \text{ m}^2$ ). Thickness is the length of uranium sample interval. Grade is the uranium value obtained from ICP–MS tests. Density was taken as  $2 \text{ kg/m}^3$ . The formula is given below (Fig. 6).

$$Reserve = \sum \frac{\text{Thickness} \times \text{Grade} \times \text{Area} \times \text{Density}}{100}$$

FIG. 6. Reserve calculation formula.

Total uranium reserves were calculated in two different levels, the first is 150–249 ppm (71.7 tU) and second is 250–955 ppm (106.4 tU). The total reserve is 178.1 tU.

#### 4. CONCLUSION

Detailed exploration facilities are going to continue in 2014 in Dadağ Uranium deposit. Second stage 10 000 m drilling program, new geochemical studies and geophysical investigations are going to be very significant to increase reserve of uranium deposit.

## **REFERENCES**

- [1] AKSOY, M., SEZEN, E., ÜNAL, İ.H., Exploration Studies Report of Nevşehir-Avanos Uranium Licences, Ankara, Turkey (2013).
- [2] ATABEY, E., TAHRAN, N., YUSUFOĞLU, H., CANPOLAT, M., Geology of Area between Hacıbektaş, Gülsün and Nevşehir, MTA Report, Ankara, Turkey (1988).
- [3] ÇETINTÜRK, İ., Uranium Exploration of Kırşehir- Kayseri-Nevşehir-Niğde, Ankara, Turkey (1992).
- [4] UÇAKÇIOĞLU, S., Uranium Exploration Report of Nevşehir-Gülsün, MTA Rep. No. 8453, Ankara, Turkey (1987).